DOT/FAA/TC-22/11

Federal Aviation Administration
William J. Hughes Technical Center
Aviation Research Division
Atlantic City International Airport
New Jersey 08405

Lightning Protection of Aircraft Handbook

November 2022

Final report

U.S. Department of Transportation
Federal Aviation Administration

NOTICE

This report is available at the Federal Aviation Administration William J. Hughes Technical Center's Full-Text Technical Reports page: actlibrary.tc.faa.gov in Adobe Acrobat portable document format (PDF).

Technical Report Documentation Page

Form DOT F 1700.7 (8-72) Reproduction of completed page authorized

1. Report No.	2. Government Accession No.	3. Recipient's Catalog No.
DOT/FAA/TC-22/11		

4. Title and Subtitle	5. Report Date
LIGHTNING PROTECTION OF AIRCRAFT HANDBOOK	November 2022
	6. Performing Organization Code

7. Author(s)	8. Performing Organization Report No.
Franklin A. Fisher and J. Anderson Plumer	DOT/FAA/TC-22/11

9. Performing Organization Name and Address	10. Work Unit No. (TRAIS)
Lightning Technologies, an NTS Company 10 Downing Industrial Parkway Pittsfield, MA 01201 USA	11. Contract or Grant No. 692M15-20-C-00009

12. Sponsoring Agency Name and Address	13. Type of Report and Period Covered
Policy & Innovation Division AIR-600 Aviation Safety, FAA Seattle Headquarters 2200 S 216th St Des Moines, WA 98198	14. Sponsoring Agency Code AIR-600

15. Supplementary Notes

The Federal Aviation Administration William J. Hughes Technical Center Research Division, COR was Lynn Pham.

16. Abstract

This handbook edition is an update of the DOT/FAA/CT-89/22 Aircraft Lightning Protection Handbook to include major advances and updates of standards and other criteria used for protection design and verification testing of airframes and systems. The handbook will assist aircraft design, manufacturing, and certification organizations in understanding the effects of lightning strikes on aircraft, and in protecting aircraft against the physical and induced effects that lightning may cause on aircraft structures and systems.

The edition keeps the original 18 chapters with the first half dealing with the lightning environment, and the physical ('direct') effects of lightning, and the second half dealing with induced ('indirect') effects of lightning. Chapter 1 deals with the nature of high voltage electrical sparks and arcs and with related processes of electric charge formation, ionization, and spark propagation in air. Chapter 2 provides an elementary description of cloud electrification and lightning strike formation and follows with statistics of cloud-to-earth lightning parameters from which the aircraft lightning design and test standards have been derived. Chapter 3 and Chapter 4 introduce the reader to the basic mechanisms of naturally occurring and aircraft initiated lightning strikes. Chapter 5 reviews the history of aircraft lightning protection regulations and standards and introduces the latest versions of them. Chapter 6 and Chapter 7 contain the basic elements of protection design for the airframe, fuel tanks, and fuel system components. Chapters 8 through 17 focus on protection of electrical and avionic systems against induced effects. Chapter 18 presents an overview of test methods used to verify the ability of equipment to tolerate lightning-induced transients and the ability of complete systems to tolerate those transients, particularly when applied in the multiple stroke and multiple burst waveform sets.

17. Key Words	18. Distribution Statement
Lightning protection, lightning safety, carbon fiber composite, physical effects, induced effects, fuel vapor ignition, fuel system protection, simulation, aircraft certification, electromagnetic field, induced current, induced voltages, electromagnetic shielding	This document is available to the U.S. public through the National Technical Information Service (NTIS), Springfield, Virginia 22161. This document is also available from the Federal Aviation Administration William J. Hughes Technical Center at actlibrary.tc.faa.gov.

19. Security Classif. (of this report)	20. Security Classif. (of this page)	21. No. of Pages	22. Price
Unclassified	Unclassified	517	

CONTENTS

INTRODUCTION

This book will assist design engineers in understanding the effects of lightning strikes on aircraft, and in protecting aircraft against the physical and induced effects that lightning may cause on aircraft structures and systems. It will also be of use by those engaged in reviews of designs, test, and analysis data for the purpose of finding compliance with applicable airworthiness regulations. This book is also intended for use by those involved in design of aircraft engines, avionics and other aircraft systems and equipment, aircraft operations, and investigation of possible lightning related incidents and accidents.

This is the third edition of *Lightning Protection of Aircraft*, which was first written at the request of the US Federal Aviation Administration (FAA) and published in 1989. The first edition was originally intended to be an update of a reference book of the same title by F. A. Fisher and J. A. Plumer, which was published in 1976 by the US National Aeronautics and Space Administration as NASA RP-1008. Expanded, hardbound versions of the first edition were published in 1990 and 2004 by Lightning Technologies, Inc. (LTI). The 1990 and 2004 editions have been used for many years as an FAA handbook and both editions have been the textbook for classes on lightning protection of aircraft and avionics offered by LTI.

This third edition is an update of the 2004 edition, keeping the original eighteen chapters and much of the original text since much of the classic work in the science of lightning protection of aircraft was accomplished in the pre-2000 period. Much of this original work, which was supported by various government agencies concerned with the safety of aircraft, has been referenced throughout this book. References to and results of additional work that has been conducted since 2004 have been added, where appropriate, to several chapters, but no attempt has been made to provide an exhaustive review of all of the work accomplished since 2004.

Since 2004, major advances and updates of standards and other criteria used as the bases for protection design and verification testing of airframes and systems have occurred, and these are described and referenced throughout this edition. These advances and updates have been made by SAE Committee AE2 and European Organization for Civil Aviation Equipment (EUROCAE) Working Group 31, who are the technical committees responsible for keeping abreast of advancements in the science of lightning phenomenology and effects on aircraft, and the methods of simulation of the physical and induced effects on aircraft through testing and analysis. These committees provide technical inputs to the airworthiness certification requirements, and related advisory material published by the aircraft certifying authorities in the United States, Europe, and other countries. These requirements and advisory material are updated periodically by the authorities as advancements are made in the understanding of the aircraft lightning environment, and the ways this environment interacts with new aircraft structural materials and systems. Since the late 1980's, the SAE and EUROCAE committees have worked closely together so that the airworthiness requirements, standards, and certification test methods are the same for aircraft being designed and certified in the US and Europe. This book makes frequent reference to documents published by the SAE and EUROCAE committees but does not duplicate the material in them. The user of this book is encouraged to obtain and have ready access to those documents.

This handbook is organized along the same general lines as the last edition, with the first half dealing with the lightning environment, and the physical ('direct') effects of lightning, and the second half dealing with induced ('indirect') effects of lightning. More specifically:

Chapter 1 - *An Introduction to High Voltage Phenomena* deals with the nature of high voltage electrical sparks and arcs and with related processes of electric charge formation, ionization, and spark propagation in air. All of these are factors that affect the way that lightning leaders attach to an aircraft and the way that the hot return stroke arc affects the surface to which it attaches. The material introduces practices and terms used for many years in the electric power industry, but which are not commonly studied by those dealing with aircraft. These terms and practices have, however, affected the tests and practices used to evaluate the effects of lightning on aircraft.

Chapter 2 - *The Lightning Environment* provides an elementary description of cloud electrification and lightning strike formation and follows with statistics of cloud-to-earth lightning parameters from which the aircraft lightning design and test standards have been derived. The user of this book is urged to study these two introductory chapters before proceeding with later sections of the book. The treatment of these topics is on an elementary level and is aided by simple illustrations, which should enable those with only a limited background in electricity to proceed to an adequate understanding of important principles.

Chapter 3 - *Aircraft Lightning Attachment Phenomena* and Chapter 4 - *Lightning Effects on Aircraft* introduce the reader to the basic mechanisms of naturally occurring and

aircraft initiated lightning strikes. The flight conditions when strikes have most frequently occurred, and the types of effects these strikes may have on the aircraft. The distinction between the physical effects (traditionally referred to as "direct effects') and the induced effects that appear in aircraft wiring and impact electronic equipment (traditionally referred to as 'indirect effects') is made here and these new terms continue to be used throughout the text since they are more descriptive of these two categories.

Chapter 5 - *The Certification Process* reviews the history of aircraft lightning protection regulations and standards and introduces the latest versions of these; most notably, the standards for the lightning environment, zoning and testing that have been published and updated by SAE and EUROCAE since 1999. Since further updates of these criteria are expected the user of this book should always obtain the most recently published versions of each of the requirements and standards documents referenced in this book. The regulations related to protection against lightning are presented and the supporting advisory circulars and other guidance documents are cited as to purpose but not repeated here. It is not the purpose of this book to repeat material that is published in other documents that are readily available to the reader.

Chapter 6 – *Protection Against Physical Effects*, and Chapter 7 - *Fuel System Protection* contain the basic elements of protection design for the airframe, fuel tanks, and fuel system components. The methods presented here are basic approaches, and many variations on these, too numerous to describe in this book, have been successfully used. The reader is cautioned that all candidate designs should be tested, especially those that do not have a successful history of prior use. Fuel vapor ignition remains one of the most serious lightning hazards and should be given careful attention in any design and certification program. It is not possible to verify adequacy of fuel system protection without lightning testing of fuel tanks and systems.

Chapters 8 through 17 focus on protection of electrical and avionic systems against induced effects. As with all aspects of electromagnetic interference and control, the prevention of damage and interference from lightning becomes more and more critical as aircraft evolve. Most of the navigation and control functions aboard modern aircraft place a computer between the pilot and the control surfaces or engines, often without mechanical backup. This makes it essential that the computer and control equipment be designed to prevent damage or upsets by lightning. Control of these induced effects requires coordination between those who design the airframe and its interconnecting wiring, those who design avionic systems, and those who oversee the certification process. Part of the overall control process requires the selection of transient design levels and application of suitable test standards and practices.

Chapter 8 - *Introduction to Induced Effects* introduces the subject of induced effects and briefly summarizes the subjects covered in more detail in later chapters.

Chapter 9 - *Elementary Aspects of Induced Effects* covers the basic physics common to the subsequent chapters.

Chapter 10 - *The External Electromagnetic Field Environment* covers the external electromagnetic field environment.

Chapter 11 - *The Internal Fields Coupled by Diffusion and Redistribution* and Chapter 12 - *The Internal Fields Coupled Through Apertures* describe how electromagnetic fields appear inside the airframe, and ways to estimate the magnitudes of these internal fields. These four chapters 9, 10, 11 and 12 are the most analytically oriented of the book.

Chapter 13 - *Full Vehicle Testing* describes the methods available for measuring the transient voltages and currents induced by lightning in aircraft electrical wiring. These are known as "full vehicle" tests and are usually applied at reduced amplitudes so as not to damage the tested airplane.

Chapter 14 - *Response of Aircraft Wiring* discusses some of the practical problems of calculating the response of aircraft wiring to electromagnetic fields and provides some examples of how basic principles can be used to estimate the magnitudes of induced transients in simple circuits.

Chapter - 15 *Shielding* reviews the physics of shielding effectiveness and discusses this important protection approach of shielding of aircraft wiring. This chapter also emphasizes the features that must be included in shield designs that are necessary to realize maximum effectiveness from shields.

Chapter 16 - *Design to Minimize Induced Effects* discusses some of the policy matters relating to control of induced effects, tasks that must be undertaken by those responsible for setting overall design practices. Principally these relate to shielding and grounding practices to be followed, and to transient design level specifications to be imposed on vendors.

Chapter 17 - *Circuit Design* discusses some aspects of circuit design, principally those relating to surge protective devices and methods of analyzing the damage effects of surge voltages and components on electronic devices.

Control of lightning induced effects by analysis can only be carried so far; proof of tolerance of induced effects is most likely to come about by performing tests on individual items of equipment and on interconnected systems. Chapter 18 - *Test Techniques for Evaluation of Induced Effects* presents an overview of test methods used to verify the ability of equipment to tolerate lightning-induced transients and the ability of complete systems to tolerate those transients, particularly when applied in the multiple stroke and multiple burst waveform sets. These test methods have recently been incorporated in new or updated lightning test standards. A few comments on personnel safety are also included, since lightning tests involve the generating and applying very high voltages and currents - far exceeding the levels employed in most electrical test laboratories. They also far exceed lethal levels and have proven fatal to inexperienced operators. Lightning tests to evaluate or verify either physical or induced effects should be performed only by personnel experienced in this technology.

Note that for numbers in thousands or more, spaces are used instead of commas or periods to separate groups of three numbers (e.g., 1 000). The intention is for a cleaner look and to avoid the possible confusion internationally between meanings of periods and commas used in these numbers.

Finally, this edition includes corrections of some errors that were found in earlier editions. It is hoped that all have been found and corrected, but we offer apologies for any that may remain.

Andy Plumer
Lightning Technologies, an NTS Company
23 February 2022

ACKNOWLEDGEMENTS

The authors appreciate the encouragement and support of the US Federal Aviation Administration (FAA) and of Ms. Lynn Pham of the FAA Technical Center and of Lightning Technologies, an NTS Company for preparation of this edition.

We also wish to thank the following colleagues from SAE Committee AE2 for their careful reviews of the manuscript and corrections of technical errors: Josh Bakk, Jim Harrington, Larry Hebert, Howard Jordan, Keisuke Kawamura, Richard Olson, and Brock Milford. The authors also wish to thank Dave Walen for his encouragement to prepare this new edition. Original contributions to the chapters dealing with the results of research in intracloud lightning employing storm penetration aircraft were provided by Dr. Rodney A. Perala and Terry Rudolph of Electro Magnetic Applications Inc. Additional thanks are expressed to the following people for their contributions:

The members of EUROCAE Working Group 31 and SAE Committee AE2 who prepared the updated lightning environment and test standards referenced throughout this book.

Lynn Pham and Edward Weinstein of the FAA Technical Center as well as Robert Steinle and Cindy Ashforth of the FAA AIR-600 Policy and Innovation Division, who reviewed the manuscript and references for accuracy.

Shawna L. Shea of Lightning Technologies, who prepared the manuscript as it was being written up to the final edition with attention to all of the details.

Edward J. Rupke of Lightning Technologies who prepared some of the original illustrations.

Kenneth G. Wiles of Lightning Technologies who contributed to the chapters on testing for the induced effects of lightning.

Acronyms and Abbreviations

(This list includes abbreviations and groups of initials peculiar to the subject matter of this text, in addition to many standard acronyms.)

AC	Advisory Circular
ac	Alternating Current
ADF	Automatic Direction Finding
AEHP	Atmospheric Electrical Hazards Program
AE-2	The Lightning Committee of the SAE
ANSI	American National Standards Institute
ARP	Aerospace Recommended Practice
ATC	Air Traffic Control
ATL	Actual Transient Level
AWG	American Wire Gauge
BIL	Basic Insulation Level
CDCCL	Critical Design Configuration Control Limitation
CFC	Carbon Fiber Composite
CFRP	Carbon Fiber Reinforced Plastic (same as CFC)
CFR	Code of Federal Regulations
CW	Continuous Wave
DC	Direct Current
DoD	Department of Defense
DSO	Digitizing Storage Oscilloscope
EASA	European Aviation Safety Agency
EMC	Electromagnetic Compatibility
EMF	Expanded Metal Foil
EMI	Electromagnetic Interference
EMP	Electromagnetic Pulse
ETDL	Equipment Transient Design Level
EUROCAE	The European Organization for Civil Aviation Equipment
EUT	Equipment under Test
FAA	Federal Aviation Administration
FADEC	Full Authority Digital Engine Control System
FAR	Federal Aviation Regulation
FQIS	Full Quantity Indicating System
FQMS	Full Quantity Measurement System
FVT	Full Vehicle Test
GFRP	Glass Fiber Reinforced Plastic
GMT	Greenwich Mean Time
GRN	Ground Return Network
HIRF	High Intensity Radiated Fields

IEEE	Institute of Electrical and Electronic Engineers
IFR	Instrument Flight Rules
ITO	Indium Tin Oxide
IWWF	Interwoven Wire Fabric
JSC	Johnson Space Center
LTA	Lightning Transient Analysis
LTI	Lightning Technologies, Inc.
LTRI	Lightning and Transients Research Institute
MB	Multiple Burst
MOV	Metal Oxide Varistors
MS	Multiple Stroke
NACA	National Advisory Committee for Aeronautics
NASA	National Aeronautics and Space Administration
NATO	North Atlantic Treaty Organization
NAV	Navigation
NEMP	Nuclear Electromagnetic Pulse
NLR	Non-linear Resistor
NTSB	National Transportation Safety Board
OAS	Overall Shield
RF	Radio Frequency
RTCA	Radio Technical Commission for Aeronautics
SAE	SAE International
SE	Shielding Effectiveness
SWC	Surge Withstand Capability
TCL	Transient Control Level
TG	Transient Generator
UD	Unidirectional
UHF	Ultra-high Frequency
US	United States
USAF	United States Air Force
VHF	Very High Frequency
WWF	Woven Wire Fabric
2D	Two-dimensional
3D	Three-dimensional

Chapter 1

AN INTRODUCTION TO HIGH VOLTAGE PHENOMENA

1.1 Introduction

Lightning is a high voltage and high current phenomenon and those who would deal in protection against its effects should have some basic understanding of the physics involved. This chapter is intended to introduce the reader to the general physical nature of electrical sparks and arcs, and to provide some data on the voltages necessary to initiate sparks. Partly, the material is provided to introduce the subject of lightning phenomena and partly to illustrate some of the factors that must be considered during tests to simulate the effects of lightning. An understanding of high voltage phenomena is also important when discussing when and where aircraft are struck by lightning and an understanding of high current arc phenomena is important when designing aircraft surfaces to withstand the effects of lightning.

The literature on high voltage phenomena is vast and no attempt will be made to give a comprehensive review. Most of the works are to be found in publications aimed at the electric power industry. Some specific works that deal with the subject will be cited, but since the following material is only a review, no attempt will be made to cite references for each point discussed.

1.2 Initial Ionization Effects

In the study of gas discharges, it is customary to divide the phenomena into two general types: those that are, and those that are not self-sustaining. Complete breakdown of a gas, or the formation of a spark between two electrodes, is a transition from a non-self-sustaining discharge to one of several types of self-sustaining discharge. Usually, this transition occurs with explosive suddenness. To illustrate some of the phenomena involved, consider Fig. 1.1, which shows how the current between two electrodes immersed in a gas depends on the voltage between the electrodes. In the space between the electrodes, there is an electric field, *E,* whose magnitude is proportional to the applied voltage, and inversely proportional to the distance between the electrodes.

Under the influence of light and other radiation, such as X-rays, cosmic rays or radioactive decay, electrons are emitted from the negative electrode (or cathode). Electrons may also be released in the gas by the radiation. At low levels of voltage, or electric field, all the electrons drift towards the positive electrode, or anode, and are collected. For a considerable range of voltages (region 2 of Fig. 1.1 (b)) the current remains constant, but the discharge is not yet self-sustaining, since the current would cease if the ionizing illumination of the cathode were removed.

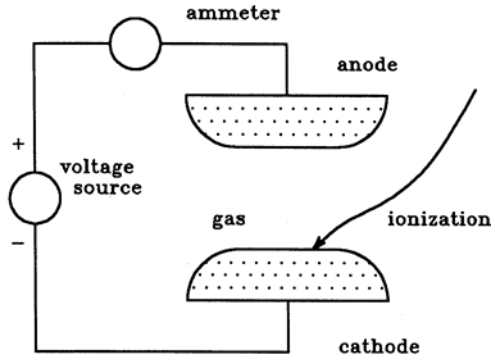

(a) electrode configuration

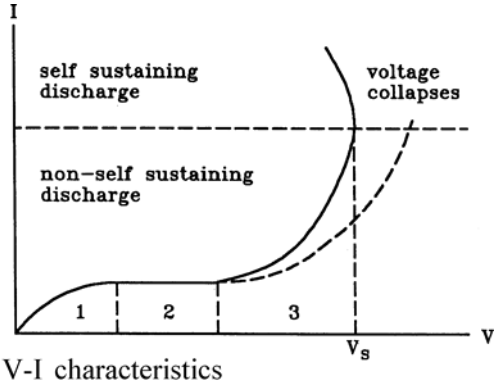

(b) V-I characteristics

Fig. 1.1 Current-voltage relations in pre-spark regions.

If the voltage is increased into region 3 of Fig. 1.1(b), some of the electrons emitted from the cathode begin to collide with gas molecules with sufficient force to knock electrons free. Where there was one electron, there are now two electrons free. Where there was one electron, there are now two electrons, plus one, positively charged ion. Both electrons then move, under the influence of the field, and strike more gas molecules, liberating more electrons. This chain reaction generates an electron avalanche. This discharge is still not self-sustaining; however, since if the source of ionization were removed, the current would cease. The total number of electrons produced by the acceleration of a group of electrons is

$$N^- = n_0^- e^{\alpha d} \qquad (1.1)$$

where N^- is the final number of electrons, n_0^- is the number of initial electrons and d is the distance traversed.

The quantity α is called Thompson's first ionization coefficient and indicates the number of electrons produced by a single electron traveling a distance of 1 cm. α depends on the density of the gas and on the strength of the electric field. The electric field determines how much the electrons are accelerated, and the gas density determines how far an electron can move before it collides with a gas molecule and liberates another electron. It follows that an electron avalanche proceeds faster in dense than in rarified gas. The molecules from which electrons are liberated are left with a positive charge and are thus accelerated in a direction, but the mass of the ions is much more than the mass of the electrons, so they move much more slowly. If the voltage is increased into region 3 of Fig. 1.1 (b), the current begins to depart from the simple exponential law of Eq. 1.1. Thompson ascribed the increased current to ionization resulting from the motion of the positively charged molecules, and considered the total current to have two components, one due to the motion of electrons, Eq. 1.1, and one due to the motion of the positively charged particles and governed by a similar relationship.

$$N^+ = n_0^+ e^{\beta d} \qquad (1.2)$$

Where N^+ is the final number of positively charged particles, n_0^+ is the initial number and d is the distance traversed.

The quantity β was designated Thompson's second ionization coefficient. It is now known that ionization by positive ions is insufficient to account for the increased current in region 3 of Fig. 1.1 (b). Instead, the number of electrons is regarded as

$$N = \frac{n_0 e^{\alpha d}}{1 - T e^{\alpha d - 1}} \qquad (1.3)$$

where the coefficient, T, is the generalized secondary ionization coefficient, which includes the process considered by Thompson, but also other processes, such as the action of positive ions, photons, and metastable atoms at the cathode. Finally, at the sparking voltage, V_s, the gap breaks down and the voltage collapses. A criterion for breakdown (or the achievement of a self-sustaining discharge) is that

$$T\left(e^{\alpha d - 1}\right) \geq 0 \qquad (1.4)$$

If Eq. 1.4 is true and if the initial source of ionization is removed, then the current continues to increase to a value limited only by the impedance of the external circuit.

Eqs. 1.3 and 1.4 include the effect of an attachment coefficient, η, since there are factors that act to capture electrons. The ionization and attachment coefficients are shown in Fig. 1.2. Below 25 kV/cm, the attachment coefficient is greater than the ionization coefficient, hence

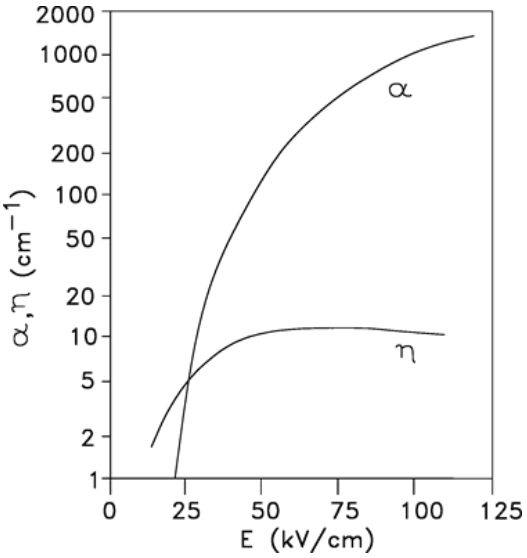

Fig. 1.2 Ionization and attachment coefficient.

an avalanche cannot develop in a field less than 25 kV/cm. (This curve relates to standard sea-level atmospheric conditions. Effects of non-standard conditions are discussed in §1.5.5).

1.3 Streamer Effects

Eq. 1.4 is seldom used as a practical criterion for gas breakdown conditions since the actual process of gas breakdown is much more complex and random that this simple equation implies. Actual breakdown is, instead, ascribed to the growth of a streamer that leads to ionization in the gas. The development of this streamer is separate from any processes taking place at the electrode. Whether the streamer leads to a complete breakdown between two electrodes or is confined to the localized discharges called corona depends to a considerable extent on how the electric field is distributed across the entire gap. The localized corona discharge will be considered first. It occurs when only the region around the electrode is highly stressed; that is to a sufficiently high electric field (25-30 kV/cm).

1.4 Corona

Corona (Fig. 1.3) is a glow discharge that forms around conductors when the surface voltage gradient (rate of change of voltage with distance normal to the surface) at the electrode exceeds a critical level, about 30 kV/cm in air at sea level atmospheric pressure. Corona can also form on objects electrically bonded to the earth that are exposed to a high electric field from a remote source such as a high voltage power line or a charged thunderstorm cloud.

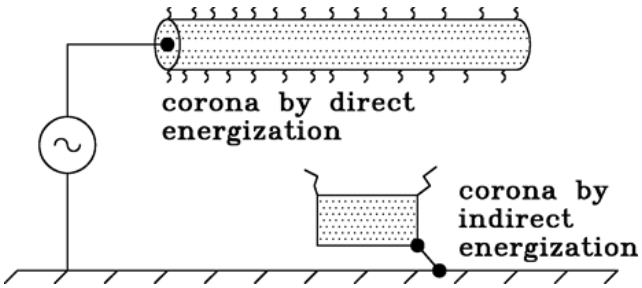

Fig. 1.3 Corona

Corona also forms on the masts of ships and on the extremities of aircraft. Then the phenomenon is commonly called St. Elmo's fire. Corona is a localized discharge, but can be the precursor to complete breakdown, and can be a prolific source of interference in radio receivers.

1.4.1 Negative Corona Processes

The negative corona process occurs when the electrode upon which the corona forms is subjected to a sufficiently large negative electric field (a negative field being defined as one in which an electron in the space around the electrode is forced away from the electrode, Fig. 1.4). A common situation involves the electrode being connected to the negative terminal of a power supply while the positive terminal is grounded. The negative electrode need not be directly connected to a power source; however, the electric field may be created by induction from other charged electrodes. Consideration of where the other electrodes are located is rather academic, since the important matter is that an electric field exists in the immediate vicinity of the conductor upon which corona forms.

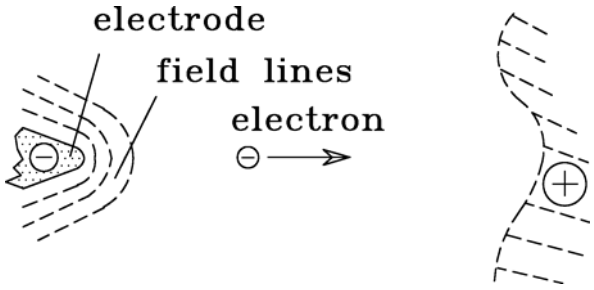

Fig. 1.4 Motion of an electron in a negative field.

Because of some initial ionization process, an electron is liberated in the gap. Under the influence of the electric field the electron is repelled away from the electrode. As it is repelled, it collides with the gas molecules and a flood of other electrons is triggered by the avalanche process described in §1.1. This leaves a cloud of mixed positive and negative charge, Fig. 1.5 (a). The electric field forces the electrons away from the space where the avalanche is formed and so the slower and more immobile positive ions are left behind, as shown in Fig. 1.5 (b). The electrons immediately attach to neutral ions, usually oxygen, and form negative ions.

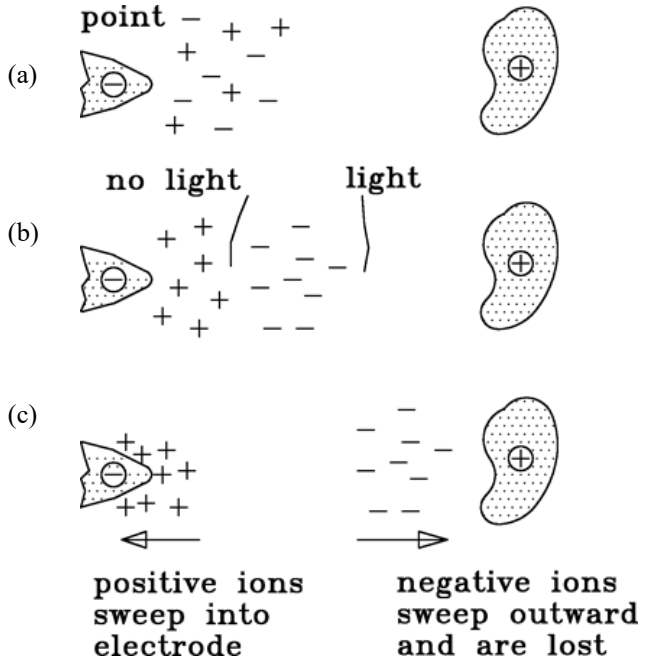

Fig. 1.5 Motion of Ions for negative corona.

The electric field in the gas depends on all the charge that is on the electrode and the charge that is in the space around the electrode. In the space beyond the positive ions, the electric field is in the sum of that produced by the negative charge on the electrode and the positive charge in the space adjacent to the electrode. The result is that the electric field in the space beyond the positive ions is reduced and the ionization process stops until the positive ions have been swept into the cathode and the negative ions have been moved away from the cathode and into the surrounding space, possibly being collected by the anode if it is nearby.

After the charges have been swept away, 1.5 (c), the process may repeat, by if the electric field at the tip of the cloud of positive ions is not sufficient to cause further ionizing collisions, the streamers will not extend further into the gap. This condition exists in divergent fields, those in which the stress is localized, such as surrounding the sharp pointed electrode shown in Fig. 1.6 (a).

In a uniform field, such as that between the two flat electrodes shown in Fig. 1.6 (b), whenever the electric field at the electrode reaches a critical gradient, the same critical gradient is present all the way across the gap.

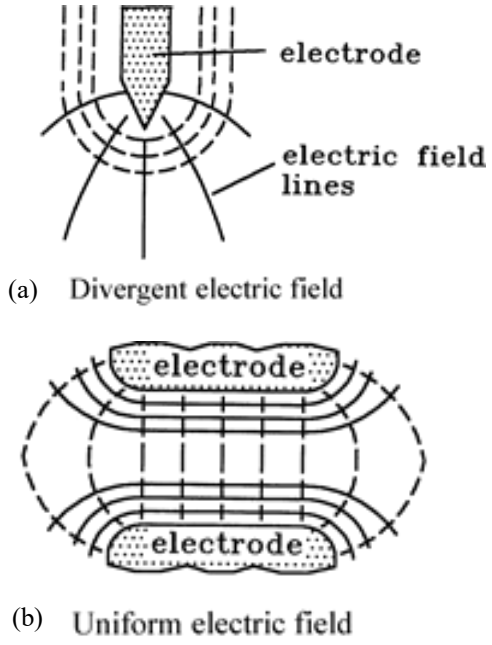

Fig. 1.6 Divergent and uniform electric fields.

As a result, the corona does not remain localized, but invariably grows and leads to complete breakdown.

The critical gradient at which corona is initiated is about 30 kV/cm at sea level conditions although this gradient does depend somewhat on the physical size and shape of the electrodes. In a more rarified gas, the critical gradient would be lower than 30 kV/cm, the governing factor being the density of the gas. Reference data relating density (pressure and temperature) to altitude is available in standard handbooks [1.1]. At an altitude of 3 048 m (10 000 ft.), the critical gradient would be about 22 kV/cm. Corona is visible because light is emitted at the tip of the discharge as ions are bombarded and the collisions raise the impacted atoms to a high energy state. Later, the excited atoms may revert to their normal lower energy state and, as they do, the excess energy is radiated as electromagnetic waves, some of the radiation occurring in the visible band and appearing as light. The light ceases as soon as the bombardment stops, and the charged ions are swept away. The charge itself is not visible. The visible light that is emitted is predominantly blue. It is also rich in ultraviolet and can be photographed much more readily through a quartz lens than a conventional glass lens.

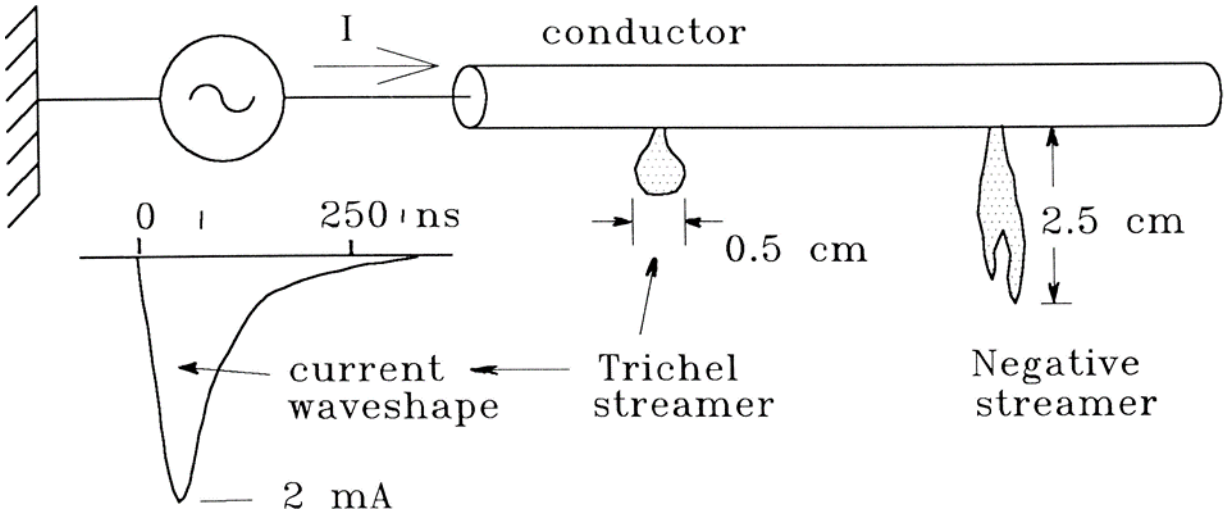

Fig. 1.7 Negative Corona.

The negative corona process may manifest itself as a train of individual pulses, called Trichel pulses after an early investigator of the phenomenon. It may also manifest itself as a pulseless glow or as a negative streamer. Trichel streamers extend about 1 cm away from the electrode and each one produces a current pulse of amplitude varying from 1 x 10^{-8} A at point electrodes to 2 x 10^{-2} A at large electrodes. Examples of the physical and electrical nature of negative corona pulses are shown in Fig. 1.7.

The discharge propagates for up to 20 ns (20 x 10^{-9} *s*), before being choked off by the space charge. Current rise times are between 25 and 50 ns, and half-values are attained in about twice that time. Because the pulses are short, they can lead to radio frequency (RF) interference over a very wide band of frequencies. If the field strength increases, the rate at which the Trichel pulses are formed also increases. The maximum frequency of the pulses has been reported as 2 kHz for an 8-mm sphere and 3 MHz for a 30-degree conical point. After the Trichel pulses reach their maximum frequency, a pulseless glow forms around the electrode. Under these conditions, the discharge current becomes essentially direct current (DC) and ceases to emit RF interference. As the electric field is increased even further, negative streamers appear and extend out from the electrode several centimeters. The current consists of pulses superimposed on a quasi-state current. The rise times of the pulses are on the order of 0.5 μs (0.5 x 10^{-6} s).

1.4.2 Positive Corona Processes

Positive corona occurs when the electric field at the surface of the electrode is positive, either because the electrode is energized with positive voltage or because it is grounded and in the electric field produced by an electrode energized with negative voltage. Positive corona has many of the same characteristics as negative corona, but the electrons and positive ions are accelerated in the opposite direction. The mechanism is illustrated on Fig. 1.8. The amplitude of the current pulses is generally much larger than with negative corona, but the pulses do not occur with as high a repetition rate. The initial electron is drawn

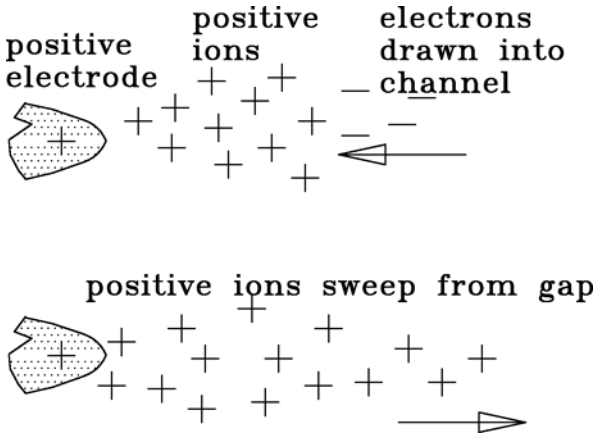

Fig. 1.8 Motion of ions for positive corona.

towards the positive electrode and the positive ions formed by collision are repelled away from the positive electrode. The field strength at the surface of the electrode diminishes and the discharge stops until the charged particles are swept from the space around the electrode. The electric field beyond the cloud of positive ions is enhanced because it responds both the positive space charge acts to lower the intensity of the field produced by the negative charge on the electrode. This enhanced field helps a positive streamer to propagate farther than a negative streamer would.

Positive corona takes three distinct forms: onset pulses, Hermstein's glow, and positive streamers. Onset pulses appear as streamers in a stem with some branching, and a high repetition rate gives the corona a brush like appearance. From an 8-mm sphere, current amplitudes have been measured at 0.25 A. Mean rise time is 30 ns and mean decay time is about 100 ns.

The maximum repetition rate is about 200 Hz for large electrodes and 2 000 Hz for point electrodes. The somewhat longer rise and decay times might imply that the pulses produce less radio interference than negative corona pulses, but the higher amplitude of the current pulses makes the absolute interference levels higher.

As the voltage increases, the corona glow forms an ionizing layer (Hermstein's glow) and the discharge current consists of small ripples at a frequency of up to 2 x 10^6 Hz, super-imposed on a quasi-DC current. As the voltage is increased still further, the streamers extend still further, propagating at velocities ranging from 20 to 2 000 m/μs.

Sketches of positive corona and its current waveforms are shown in Fig. 1.9.

1.5 Breakdown Processes in Air Gaps

It is a common misconception that the breakdown strength of air is about 30 kV/cm or 3 MV/m. That figure is indeed about the electric field gradient at which corona begins to form and it is the intrinsic breakdown strength of short air gaps contained between electrodes carefully contoured to eliminate any regions where the local electric field strength is greater than 30 kV/cm. Such electrodes are usually found only in laboratories. With practical gap geometries, and particularly with gap geometries greater than a few centimeters in extent, it is much more realistic to assume the average breakdown strength of air under lightning conditions to be about 5 kV/cm or 500 kV/m. With longer duration waveforms, the average breakdown strength may be more on the order of 3 kV/cm.

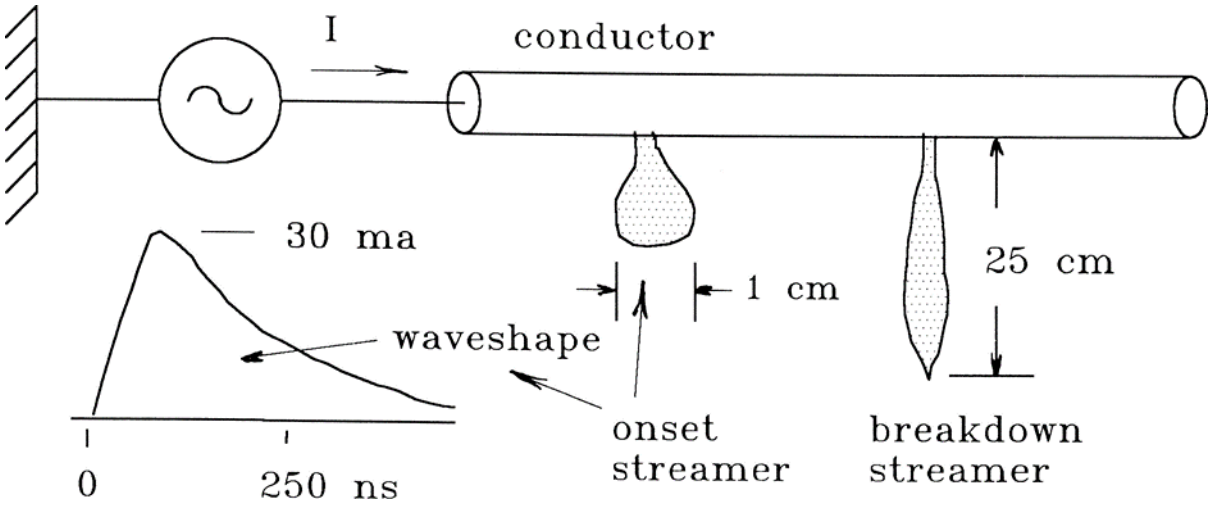

Fig. 1.9 Positive Corona.

With short duration pulses, the breakdown strength may be much more than 5 kV/cm, but such a condition usually means only that a developing breakdown has not had sufficient time to progress to final breakdown. With a large gap, such as found around an aircraft in flight, any place the macroscopic electric field has a gradient greater than 400-500 kV/m is a place where one can assume that a breakdown is in process or is about to be.

The following material illustrates why the breakdown strength of air has this surprisingly low value (to some). This section will discuss the conditions under which corona streamers can continue to grow until a gap is completely bridged. It will discuss the mechanism by which the streamers develop in a gap to which voltage is suddenly applied and will show how that process differs if the voltage is increased more gradually. It will also discuss the effect of variations in the rise and decay (or 'front') times of the applied voltage on the rate at which the breakdown progresses. This discussion concludes with an explanation of the volt-time or time-lag effect.

The basic aim of this section will be to provide tutorial material with an emphasis on physical understanding of electrical sparks used in testing, of lightning phenomena, and how lightning interacts with aircraft. It will deal only with air at near sea level atmospheric pressure and mainly with electrodes spaced so far apart that the field between them is far from uniform, and in which the metal of the electrodes and the vapor from them can play no significant part in the breakdown process.

Also, the section will focus on two general types of electrical discharge phenomena. The first is that which occurs when the electrodes are directly connected to a voltage source that supplies the energy necessary for the development of the spark and the electric field through which that spark propagates. The second is that in which the discharge originates from the exterior surface of an aircraft, and the energy necessary for the development of the spark must be extracted from a pre-existing electrical field. There are some differences between these two processes, which will be discussed in Chapter 3.

1.5.1 Types of Surge Voltage

When discussing the breakdown strength of air, it is common practice to refer to lightning voltage surges, switching voltage surges, and power frequency voltages. Breakdown strength of air gaps have their origin in the electric power field, to which most studies have been directed. For continuity, the terms will be retained here, although they are not particularly apt in relationship to aircraft.

Surges having front times measured in a few microseconds and decay times measured in a few tens of microseconds are commonly called lightning surges, since surges induced on power lines by lightning have such waveforms. Other mechanisms can, of course, also produce surges of such waveforms.

Switching surges, as their name implies, arise on power lines through the operation of switches and circuit breakers. They are characterized by front times measured in tens and hundreds of microseconds and decay times measured in hundreds and thousands of microseconds. Such times are also characteristic of the propagation of a lightning flash toward or away from an aircraft.

Power frequency voltages primarily relate to 50 or 60 Hz energization of transmission lines and will be given only passing consideration in the following material.

Nuclear effects, nuclear electromagnetic pulse (NEMP), may lead to surges measured in tens of nanoseconds, but they are beyond the scope of the following material.

A distinction must be made between the terms *surge* and *impulse*. Accepted practice uses *surge* to refer to a voltage produced at random by nature and *impulse* to refer to a voltage or current produced under controlled conditions in a laboratory. For even more precision, the terms *lightning impulse* and *switching impulse* are used.

1.5.2 Waveform Definitions

Voltages and currents tend to have different waveforms, both because of the nature of physical processes and because of the intrinsic behavior of testing machinery.

Voltage impulses

Voltage impulses used in high voltage testing and research most commonly have double exponential waveforms, as illustrated in Fig. 1.10(a). They are described approximately by an equation of the form

$$E = E_0(e^{-\alpha t} - e^{1\beta t}) \qquad (1.5)$$

Double exponential waveforms are used because they have the general characteristics of natural surges (fast front times and slower decay times) and can be produced by simple capacitor and resistor networks. Double exponential waveforms are characterized by their peak amplitude, front time and decay time, definitions of front and tail time being given by industry standards [1.2]. The virtual front time is taken to be 1.67 times the time interval between the 30% and 90% points. For many purposes, this virtual front time is a better characterization of the effects of the impulse than the time to actual peak because it also defines the effective rate-of-rise of the impulse. It is defined by the 30% and 90% points rather than the 10% and 90% used in electronic practice, because the initial turn-on of the impulse is often distorted by the characteristics of the impulse generator. This distortion is of little importance as regards the effect of the impulse, but it can lead to controversy as to when the impulse reaches its 10% point. Decay time is usually taken to be the time to decay to 50% of the peak amplitude. It is seldom characterized by the time to decay to 37% (e-folding time), both because the 50% point is easier to determine and because the shape of the impulse below 50% is seldom of importance in studies of breakdown characteristics.

A waveform commonly used in the electrical industry is 1.2 x 50 μs, for which $\alpha = 1.46 \times 10^4$ and $\beta = 2.475 \times 10^6$, where α and β are measured in seconds. The constants yield a wave with a 1.2 μs front, as defined by industry standards, not the time to absolute peak voltage.

A true double exponential waveform can only be produced by an ideal surge generator, that stores its energy either purely inductance or purely capacitance. For real generators, with both inductance and capacitance, a double exponential output is, at best, only an approximation of the actual output waveform. Capacitive surge generators optimized for high voltages usually have inductances sufficiently low that their outputs can be described quite well by double exponential equations.

Current Impulses:

Current impulses used for evaluating low impedance surge protective devices often have waveforms that cannot be described by double exponentials, mostly because the inductances of the generators used to produce the surges

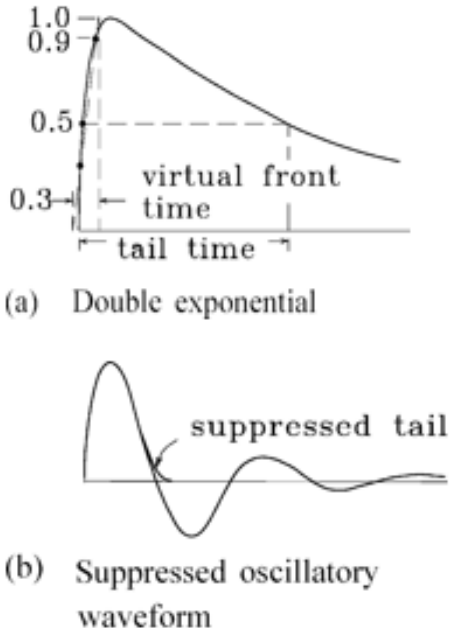

Fig. 1.10 Current waveforms for use in testing.

is not negligible. A common waveform is shown in Fig. 1.10(b) and is described approximately as

$$I = I_0 e^{-\alpha t} \sin(\omega t) \qquad (1.6)$$

Frequently, the nature of the device under test is such that only the first half cycle of the current is produced. A wave- form commonly used has an 8 μs front and a 20 μs tail. A wave having that ratio of front to tail time is not one that can be produced by a double exponential surge generator, though it is routinely produced by discharging an energy storage capacitor through an inductive circuit.

No special attempt should be made to relate the shape of surges used for testing insulation to the shape of the surges used for testing surge protective devices. The relationship has very little to do with the physical characteristics of lightning or of naturally occurring surges; it is mostly a historical matter reflecting the early development of the high voltage testing art and the incorporation of common practices into standards.

Also, one should not consider that these waveforms necessarily represent the shapes of natural lightning currents or the voltages produced by lightning.

They are intended to have the same general characteristics (fast fronts and longer tails) and have time scales typical of those produced by natural lightning, but they are only standardized waveforms used for testing.

1.5.3 Volt-Time Curves

Repeated applications of voltage do not always produce the same pattern of flashover and if the voltage is barely sufficient to cause breakdown of an air gap, some applications of voltage will cause breakdown and others will not. Breakdown is thus a statistical matter; if the voltage is low the probability of breakdown is low and if the voltage is high the probability is greater.

The breakdown voltage also depends strongly on waveform. In general, long duration voltage impulses cause breakdown of a gap at lower levels than short duration impulses. Short duration voltage impulses may be sufficient to initiate the breakdown process and to produce intense ionization (and in the process draw large currents from the voltage source) but may not last long enough to cause a complete breakdown. Also, the current drawn by the developing breakdown may be so large that a considerable amount of the voltage initially applied to the gap is lost in the impedance of the test circuit external to the gap. This loss of voltage may be sufficient to prevent the gap from breaking down.

Typical waveforms that could be observed during breakdown testing with lightning impulse waves are shown in Fig. 1.11. The shape of the voltage actually developed across the gap is shown by the heavy line, while the shape that the voltage would have had if it were not interrupted by the breakdown is shown dotted. This latter waveform is called the prospective voltage. Accepted terminology defines full waves as those that do not lead to breakdown, chopped waves or tail chopped waves as those causing breakdown after the voltage has begun to decay and steep front or front chopped waves as those that cause breakdown before the wave reaches its peak prospective voltage.

If repeated voltage impulses are applied at gradually decreasing amplitudes, there can be found an impulse amplitude below which no breakdowns occur. This amplitude is known as the *withstand* WS level. At amplitudes only

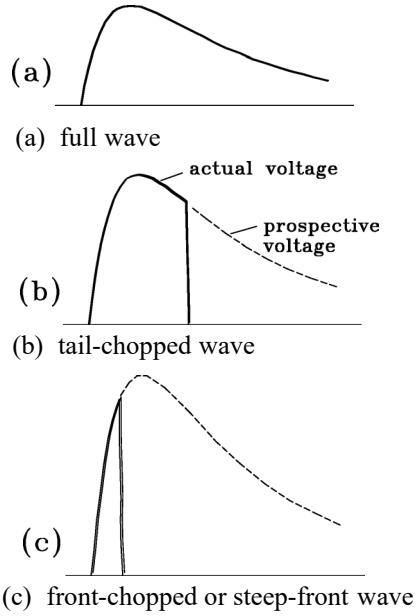

Fig. 1.11 Voltage waveforms.

slightly higher than the withstand WS level breakdowns sometimes (but not always) occur. If the voltage impulse amplitude is raised still further, a level is found where 50 percent of the impulses cause breakdown. This amplitude is known as the critical flashover CFO level. The critical flashover CFO level is sometimes designated U50, from the German Überspannung or overvoltage.

With short gaps, up to about 10 - 20 cm, breakdowns occur at the peak of the voltage waveform, but with a sufficiently long gap the breakdowns tend to occur after the voltage has reached its peak and started to decay. As voltages are increased, breakdowns occur at earlier times, sometimes well before the voltage has reached its peak prospective voltage. Plotting breakdown voltages as a function of time produces a volt-time or *time-lag* curve (Fig. 1.12). For breakdowns that occur after the voltage has begun to decay, the point plotted is the maximum voltage and the time at which breakdown occurs. Fig. 1.13 shows volt-time curves measured on various lengths of transmission line insulators. Note that the critical flashover voltage is about 550 kV/m and that much higher voltages are required to produce breakdown at short times. This suggests that breakdown is a process that does not take place instantaneously. Research indicates that this is so.

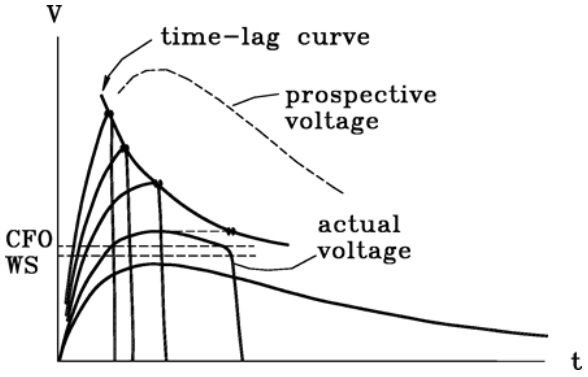

Fig. 1.12 Development of a volt-time or time-lag curve.

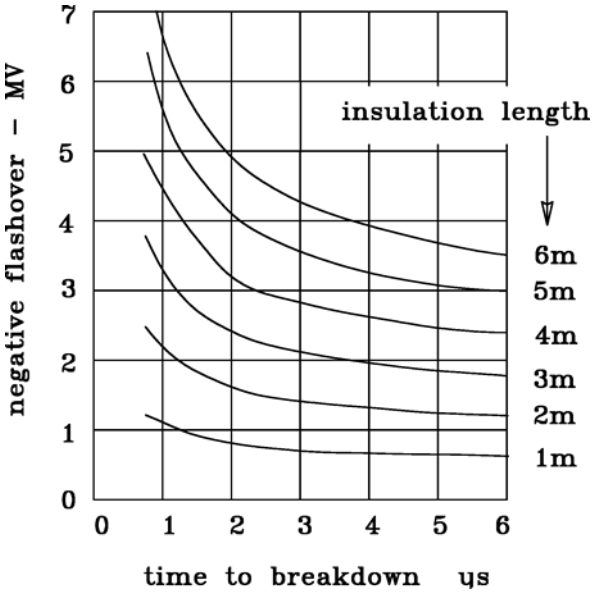

Fig. 1.13 Volt-time curves for transmission line insulators.

1.5.4 Streamer Development

The study of long air gaps with lengths greater than about 0.5m using streak cameras (or similar devices) has revealed that there are several distinct stages in the process. These are the formation of an initial corona, growth of a streamer and leader, and a final jump, which culminates in the development of a highly conducting channel across an air gap.

Initial corona

The initial burst of corona emerges from an energized electrode as soon as the electric field at some point on the electrode reaches about 30 kV/cm.

This usually takes place before the applied voltage has reached its maximum value. The corona forms in a small fraction of a microsecond and propagates away from the electrode very rapidly, at a velocity of several meters per microsecond (m/μs). This corona, however, does not go across the entire gap between the electrodes unless the electrodes are close together (perhaps 25 cm). If the voltage were removed, the corona would stop and there would be no breakdown.

Streamer

If the voltage is of sufficient magnitude and is maintained, a more intense and more localized discharge, called a streamer, develops out of this initial corona, and works its way towards the grounded electrode in a manner very similar to that of lightning, as described in Chapter 2. Initially, this streamer propagates at several centimeters per microsecond (cm/μs), much slower than the initial corona, and carries a current of about 100 A.

Leader

If the voltage is sufficient the streamer progresses further into the air gap and is fed charge via a spark that is called the leader. The voltage drop along a leader is rather small, about 2 kV/cm, making its resistance on the order of 20 ohms per cm. The leader is thus sufficiently conductive that it acts as an extension of the electrode and the result is that most of the applied voltage is impressed across the unbridged portion of the gap. As the leader progresses, the gradient across the unbridged portion of the gap increases and the leader progresses faster and carries more current.

Final Jump

When the corona ahead of the leader contacts the opposing electrode or a streamer that has originated from there, a more conductive channel begins to grow through the leader and eventually bridges the entire gap. This is called the final jump. At this stage, the entire gap is bridged by a highly conducting channel. As the channel carries more current it becomes hotter and more conductive, which allows it to carry more current and become hotter still. Eventually, the current becomes limited by the external laboratory generator circuit and the voltage across the gap collapses. This same situation exists in natural lightning. The air gap is much longer than any laboratory gap, but the corona-streamer-leader process is the same. That is why laboratory sparks can be used to simulate lightning attachments, for example, to aircraft nose radomes, or to models of airplanes to determine possible initial lightning attachment locations.

Electrode configurations

The characteristics of a breakdown are influenced by the type of electrode. Some common laboratory electrode configurations are shown in Fig. 1.14. The most easily studied geometries consist of an energized sphere or rod placed above a grounded plane, a sphere-plane, or rod-plane configuration. Another common geometry consists of two rods, one energized, and the other grounded. The breakdown process in such a rod-rod gap is more complicated than in a rod-plane gap, because the breakdown develops simultaneously from each rod, one of which is energized positive and other negative. Sphere-sphere electrodes are used in studies of uniform fields and can be used as standard electrodes for measurement of voltage. When high voltage tests are made to determine the points at which lightning might attach to an aircraft, the geometry approximates that of a rod to plane configuration.

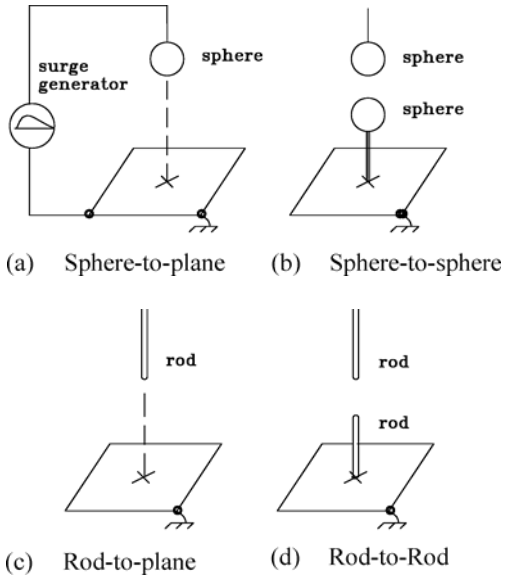

Fig. 1.14 Electrode configurations.

Methods of Observation:

Early studies of breakdown phenomena focused on the behavior of gaps exposed to lightning impulse voltages. One of the techniques used for the studies is shown in Fig. 1.15. The figure shows a test setup in which a positive polarity, 3 MV (megavolt or 3 x 10^6 volt) impulse was applied to a rod gap. A parallel rod-rod gap, outside the field of view of the camera, was used to remove the voltage before the breakdown in the gap under study had progressed to completion. By adjusting the length of the parallel gap, the phenomena in the gap under study could be observed at different stages in the development of the breakdown.

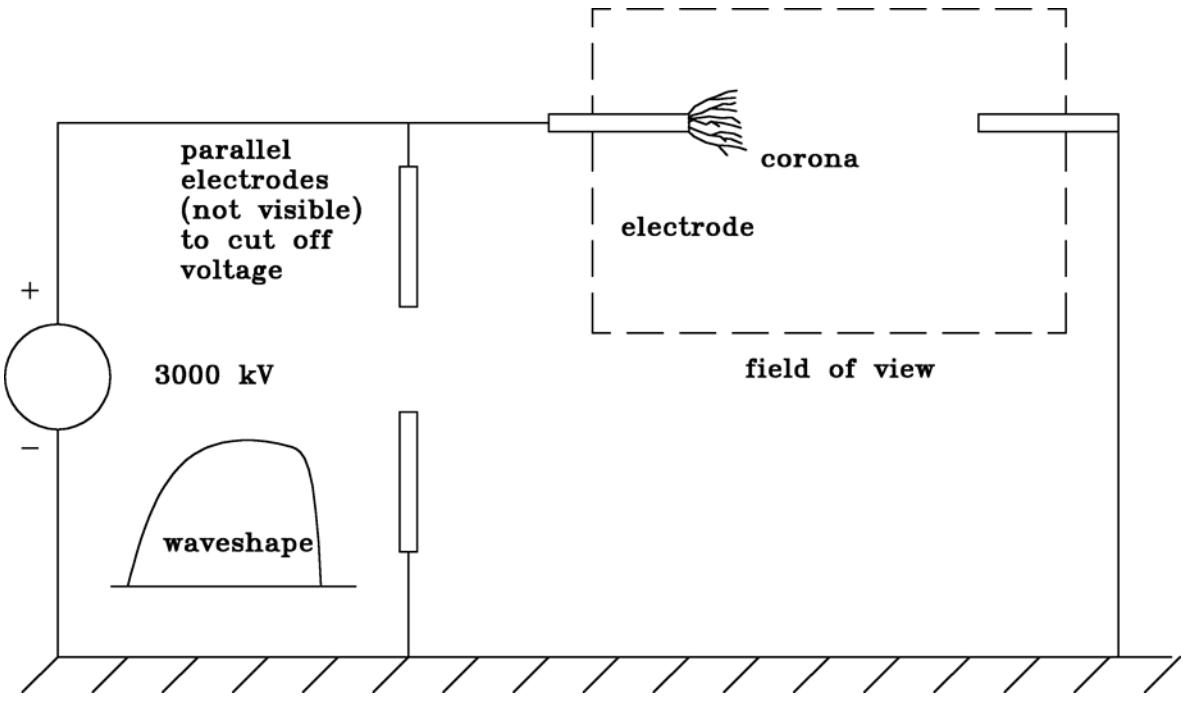

Fig. 1.15 Study of rod-rod breakdown.

A photograph of the early stages of breakdown (Fig. 1.16) shows a very extensive and diffuse set of tentacles extending from the impulse electrode. This is the first corona. The photograph was taken through a quartz lens, which passes more of the ultraviolet spectrum than a conventional glass lens. A photograph taken with a glass lens would show very little of the diffuse corona.

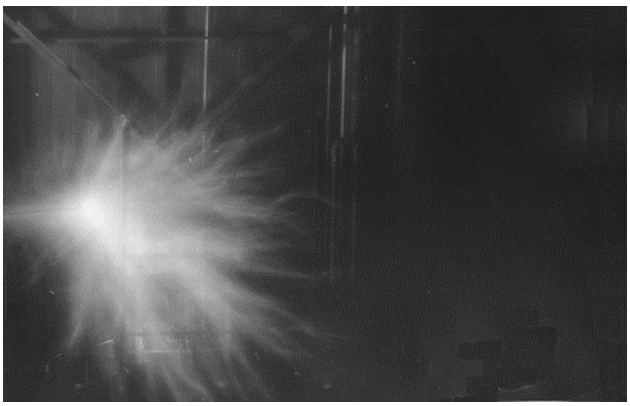

Fig. 1.16 Initial corona and streamers

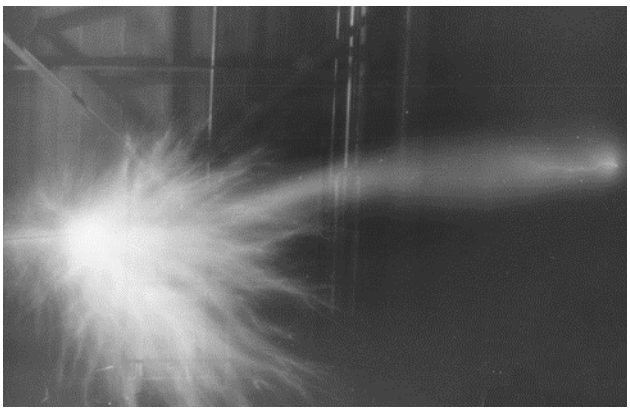

Fig. 1.17 Growth of a streamer.

When the parallel gap was made longer and the discharge allowed to progress to a later stage (Fig. 1.17), one portion of this corona bridged the entire gap, and a brighter and more conducting channel began to form around the lower (negative) electrode and progressed into the space bridged by the corona. This is called a streamer. Similar streamers develop at the upper (positive) electrode, but they are difficult to see through the corona. When the breakdown process was allowed to progress to completion, the breakdown channel was as shown of Fig. 1.18.

At the center of the gap can be seen the region where the downward and upward leaders joined. The direction of propagation of the leaders can be seen by the faint branches extending to the side of the main channel.

Streak camera

The technique of using a parallel gap to interrupt the developing breakdown is now seldom used; modern techniques make use of streak cameras. The basic principle of a streak camera is shown in Fig. 1.19. It essentially consists of moving the lens (mechanically or electronically) while the breakdown is in progress. The result is that the image recorded on the film is spread out and displayed as a function of time. If the lens is moved in discrete steps (framing mode), Fig. 1.19(a), a developing breakdown can be photographed as a series of instantaneous snapshots. More commonly, the lens is moved continuously (streak mode), Fig. 1.19(b), and the image is blurred. The luminous head of the leader appears on the photograph as a bright band gradually bridging the gap while other luminous processes show as a band behind the leader

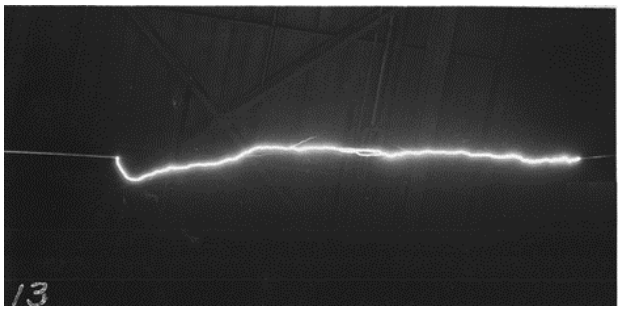

Fig. 1.18 Completed breakdown.

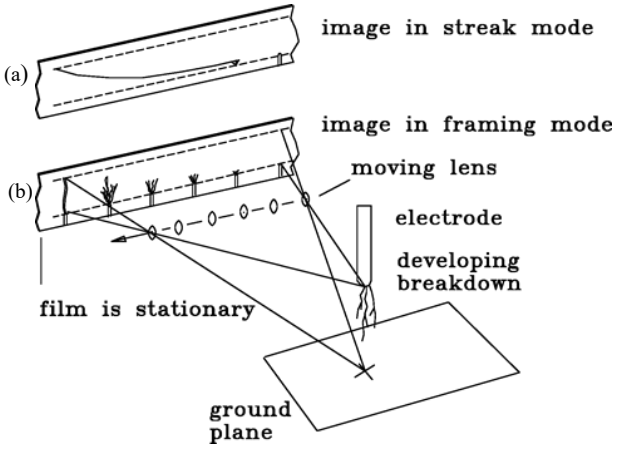

Fig. 1.19 Streak and framing cameras.

Boys camera:

An early camera, called the Boys camera, after the inventor, moved the lens mechanically and has been widely used to study the breakdown processes in lightning. Modern devices achieve the same effect electronically. An optical image is formed on an electron-emitting surface and the electrons from that surface are focused with an electron lens (magnetic or electrical) onto a phosphorescent screen, producing an image which can then be photographed with a conventional camera. Generally, an image intensifier section is used to amplify the image and make it possible to display phenomena that are only faintly luminous. The focused beam can be moved by deflection plates similar to those used in a cathode ray tube.

Switching impulses

Studies from about 1965 have mostly focused on the mechanism of breakdown that occurs when electrodes are exposed to switching impulses, since it has been found that such impulses cause flashovers at much lower voltages than lightning impulses do. Positive impulses produce breakdown at lower voltage than negative impulses and have been the most studied. Also, the studies have focused on the behavior with voltages just sufficient to cause breakdown and have not dealt with the breakdown process when the gap is subjected to over voltages. In this respect, the studies have differed from early studies of breakdown with lightning voltages, where the influence of excess voltage on the speed of breakdown has been important to design of insulation.

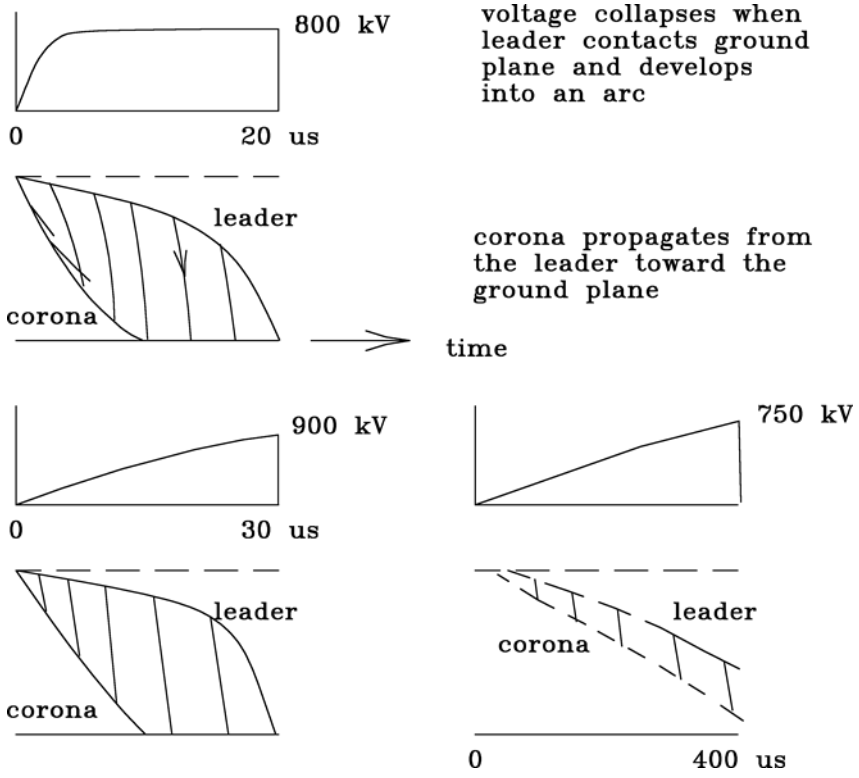

Voltage collapses when leader contacts ground plane and develops into an arc.

Corona propagates from the leader toward the ground plane.

Fig. 1.20 Influence of wavefront on the development of the leader.
Adapted from [1.3] and [1.4].

Fig. 1.20, adapted from Fig. 10 of [1.3] and from [1.4], shows sketches of what would be revealed when viewing, with a streak camera, the breakdown of a rod-plane gap when the rod is energized with positive polarity surges of the indicated waveform. Photographs showing the phenomena in more detail appear in [1.3]. For some rates of rise of voltage, the discharge proceeds smoothly toward the ground electrode. If the rate-of-rise is lower, the discharge becomes more discontinuous. In general, the corona propagates from the developing leader towards the ground plane, as evidenced by the slope of the image produced by the developing corona.

With negative polarities, the discharge is even more discontinuous. Discharges frequently take place in the air beyond the head of the leader and propagate both forwards, toward the grounded electrode, and backwards, toward the advancing leader. The sketch of Fig. 1.21 (adapted from Fig. 17 of [1.3] and from [1.5]) illustrates the phenomenon. Note that the curvature of the image due to the corona is opposite to that of Fig. 1.20. With this geometry, a leader, often called the 'junction leader' also grows from the grounded rod towards the leader from the rod to which voltage is applied

Studies also show that, with switching impulse waveforms, the critical breakdown voltage depends on the rise time of the voltage waveform, and that there is a specific front time that produces the minimum average breakdown voltage. This front time is in the range from 200 to 600 microseconds, but it depends on the length of the gap, being longer for longer gaps.

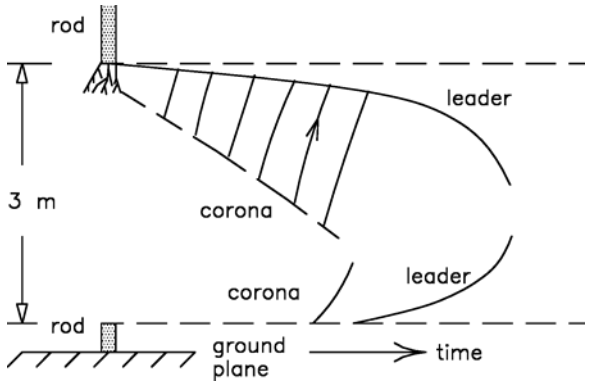

Fig. 1.21 Negative polarity sparkover of 3-meter, rod-to-rod gap with lower rod mounted on a ground plane. 1.5/1 000 microsecond wave adapted from [1.3] and [1.5].

The above is still a rather superficial description of the breakdown process and some more discussion is in order. Consider, first, the initial corona. As has been noted earlier, the initial corona forms as soon as the electric field at the energized electrode reaches a critical gradient of 30-33 kV/cm, and continues to propagate as long as the electric field is greater than about 25 kV/cm. If the gap is short, or if the field in the gap is uniform, the corona bridges the gap, leading to complete breakdown.

More commonly, the corona bridges only a portion of the gap, the extent of the corona depending on the distribution of electric field across the gap, as illustrated in Fig. 1.22. With a rod or pointed electrode, the critical gradient is reached at a lower voltage than if a more rounded electrode were used, but the highly stressed region around the electrode is smaller with a rod electrode than with a rounded electrode. The result is that, with a rod electrode, the initial corona forms at a relatively low voltage, does not extend very far into the gap, and the initial velocity of the leader is relatively low.

Around a larger electrode with a more rounded tip, the initial corona forms at a higher voltage, extends further into the gap and the initial velocity of the leader is greater. If the electrodes are sufficiently rounded, as with closely spaced spherical electrodes, the initial corona, when it forms, extends all the way to the other electrode and breakdown takes place in a fraction of a microsecond.

Streamer gradient

The rate at which the streamers extend themselves depends on the average gradient across the unbridged portion of the gap. As the leader works its way across the gap, placing more voltage on the unbridged portion of the gap, the average gradient across the unbridged portion increases with time and the velocity of the streamer increases. In general, the streamers continue to propagate as long as the average gradient in the unbridged portion is about 5 kV/cm or greater. If the gradient is greater than 5 kV/cm, the streamers propagate faster, but this requires injecting charge into the gap at a higher rate and, hence, more current must be drawn from the source feeding the breakdown. Frequently, the available current is limited, and the streamers propagate at a velocity that limits the gradient to about 5 kV/cm (500 kV/m). This critical gradient is essentially what determines the minimum breakdown voltage of large air gaps, since the leader velocity determines how long the voltage must be maintained

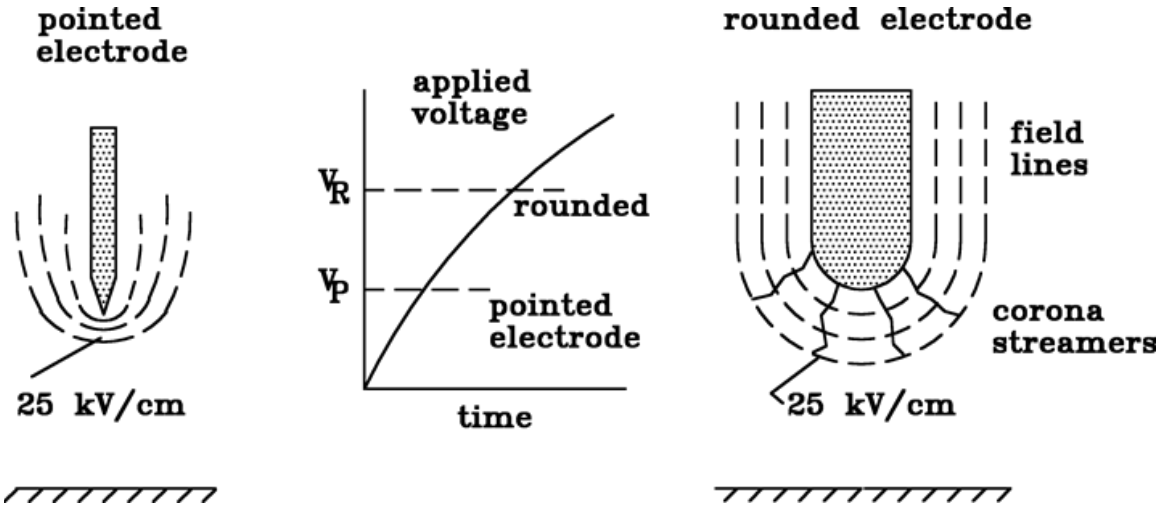

Fig. 1.22 Factors influencing initial corona.

to cause breakdown. An average leader velocity of 10 cm/μs implies that a 50 cm gap would require voltage to be maintained for 5 μs before the flashover would be complete. If a higher voltage were applied to the gap, the leader velocity would increase, and the breakdown would grow to completion in a shorter time.

1.5.5 Effects of Gas Density and Humidity

The flashover voltage of air gaps depends on atmospheric conditions. Usually, it is raised by an increase in air density or by an increase in humidity. An increase in air density (pressure and temperature both affect air density) decreases the mean free path of electrons and, consequently, decreases the likelihood that they will be accelerated to a sufficient velocity to produce secondary emission. Water molecules tend to absorb electrons and thus decrease their chance of participating in the formation of electron avalanches.

For uniform field conditions and gap distances of a few centimeters, the variation of breakdown voltage with pressure is governed by Paschen's Law, which states that the breakdown voltage depends on the product of gas pressure and gap length, according to the curve plotted in Fig. 1.23. For most conditions, breakdown strength decreases as pressure decreases, but there is a minimum pressure below which breakdown voltage begins to increase again.

The effect of pressure on breakdown voltage in large and non-uniform gaps is not easy to calculate and is best determined experimentally.

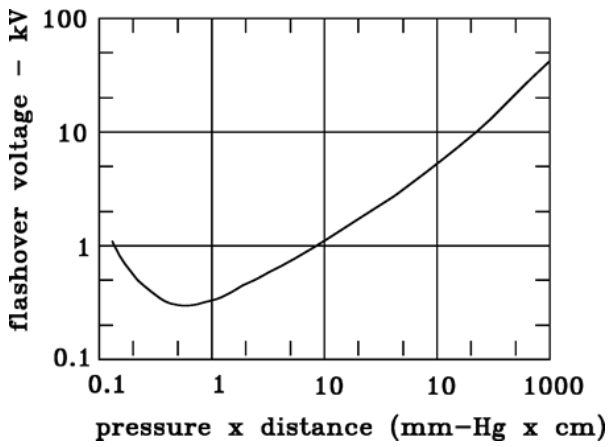

Fig. 1.23 Gap breakdown voltage [1.6]

Generally, published values for flashover voltage are corrected to standard conditions. In both Europe and the US these are

air pressure = 1 013 mb air
temperature = 0°C
moisture content = 11 gm/cubic meter.

In older US practice, these standard conditions were air pressure = 760 mm Hg, air temperature = 25°C and humidity = 15.5%. Correction factors have been developed for both air density and humidity. A discussion of those correction factors is beyond the scope of this chapter and not important to aircraft lightning interactions, but they can be found in the literature [1.7 - 1.8].

1.6 Gases Other Than Air

The common lifting gas helium used in lighter than air vehicles, has a nominal air breakdown voltage of 200 kV/m which is about 40% of that of air (500 kV/m under long rise voltages (Switching Impulse) or DC voltages, which are expected to standard conditions. This means that it is more likely for ionization to develop within a helium-filled envelope than in the air outside – an important consideration for lightning protection design of these air vehicles.

1.7 Properties of Arc

An electrical arc is a self-sustaining discharge that exists after has a low voltage rise and can conduct large currents. Its characteristics depend on the materials of the electrodes from which the arc forms and the composition of the gas in which the arc burns. This discussion will deal only with arcs in air at atmospheric pressure.

In the context of aircraft and lightning protection, arcs form most commonly in response to an initial breakdown brought about by excessive voltage applied to the gap between two electrodes. In other situations, such as electrical switches and circuit breakers, they may also form between current carrying electrodes that are initially in contact and then separated.

In the context of arcs as an ignition source within an aircraft fuel tank (Chapter 7) an electrical arc is what happens when current is transferred between electrodes (structural elements) in contact but without sufficient conducting cross-section to conduct the current without excessive heating, melting and outgassing of electrode products and arc plasma. This contrasts with electrical sparks, which have been described in this chapter in the context of long air gaps. In fuel tanks, sparks may also develop between parts that are separated, such as between fuel quantity probes and nearby structure elements.

If the arc is initiated by air breakdown of a gap, prior to that breakdown, the voltage between the electrodes is high and the current through the gap is very low. Once the breakdown occurs, an ionized region is formed in the gas between the electrodes and current flows through that ionized region. Fig. 1.24 is a plot of the distribution of potential between two electrodes. Note that most of the voltage drop (or *rise* – it is a matter of prospective) concentrated at the cathode and at the anode, while the voltage drop in the intervening air space is much more gradual. The energy released in the three regions is the product of the current and the voltage across that region.

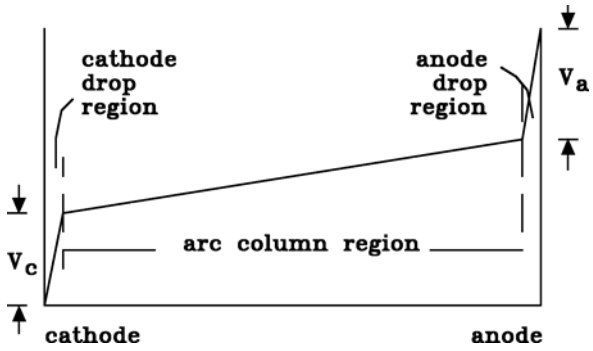

Fig. 1.24 Distribution of potential between spark-electrodes.

Arc temperature

The energy released in the ionized region of a freely burning arc is, under most conditions, sufficient to raise the temperature of the conducting path to between 5 000° K to 6 000° K. At these temperatures, the arc becomes such a good conductor that its current is limited only by the impedance of the external circuit. If a very high current is built up very rapidly, temperatures on the order of 20 000° K can be reached. This is what happens in the conductive channel of a lightning flash.

Arc voltage

As the arc attains these temperatures, the voltage along its axis collapses from an initial value of about 5 kV/cm to a value on the order of 10 V/cm. The increase of temperature, and the collapse of voltage, are not instantaneous, but can take place in a fraction of a microsecond. Development of a completely stable arc, however, may take many seconds or even minutes, because the conditions at the electrodes also influence the development of the arc.

Of the electrodes at the ends of an arc, the cathode (or negative electrode) is the one that most affects the properties of the arc, since it is at the cathode that the electrons, transported through the arc, are released. Before the arc forms, the cathode is cold, and electrons are pulled from the cathode when the voltage gradient at its surface approaches 30 kV/cm. After the arc forms, the cathode becomes heated, in places, to its boiling temperature and the electrons are pulled from the cathode by the electric field between the surface of the cathode and the adjacent column of ionized gas. For a freely burning arc, this voltage drop is approximately 10 volts and occurs over a very short distance between the cathode and the arc channel (probably on the order of 5 x 10^{-5} cm). Before steady state conditions are reached, this voltage may increase to several times this value.

The energy released at the surface of the cathode is given by the product of gap current and cathode voltage drop and, since the cathode drop region is very short, the energy released is readily transferred to the material from which the cathode is formed. Localized temperatures at the points from which the current emanates are always high enough to cause local boiling at the surface of the electrode, (approximately 3 400°K. for aluminum). This localized heating of an electrode arises from the cathode voltage drop; it has little to do with the temperature of the column of gas adjacent to the electrode.

Current density

On average, cathode current density is on the order of 5 000 A/cm^2 for iron or copper electrodes, at least for arc currents a few tens of amperes in amplitude. The current density may be higher for higher arc currents. The electrons are not emitted uniformly over the whole surface of the cathode; however, they are emitted from localized cathode spots. The current from any particular spot tends to be constant, and if the total current in the arc becomes too large to be supplied by one cathode spot, others form. The cathode spots rapidly move about and, if the arc is free to move, there is little damage to the surface of the cathode. Localized melting and boiling may occur, but the cathode spots move before the surface at any particular point becomes noticeably damaged.

Lightning flashes sweeping across bare, exterior aluminum surfaces of aircraft frequently produce only mottled blemishes on those surfaces. However, if the arc is constrained to stay in one point as when it has attached to a painted surface, then the heating continues in that area and more intense melting of metal or damage to carbon fiber reinforced composite surfaces may occur. Surface coatings, even a thin film of paint, may be enough to prevent the arc from moving freely and thus more damage may result from longer duration lightning channel attachments. These effects are discussed further in Chapters 4, 6 and 7.

Arc resistance

Care should be taken in discussing the “resistance" of an arc; since it is a quantity that really only applies for a particular current and for steady state conditions. Arc voltage as a function of current is the more useful quantity. As regards aircraft, arc voltage is important in three main contexts; the amount of damage done to a surface contacted by an arc, the length of arc which may be swept across an insulating surface before the voltage becomes sufficient to puncture the insulation (paint) and establish a new attachment location, and in the design of laboratory equipment with which to simulate lightning effects. All of these are discussed in more detail in later chapters.

An example of a voltage measurement taken across an arc burning in air is shown in Fig. 1.25. In this example, the voltage fluctuated with time as the high temperature carried the arc into the air and the arc length changed. Similar variations are noted if the conditions at the electrodes change, as during tests where the arc burns away the surface of the object under test.

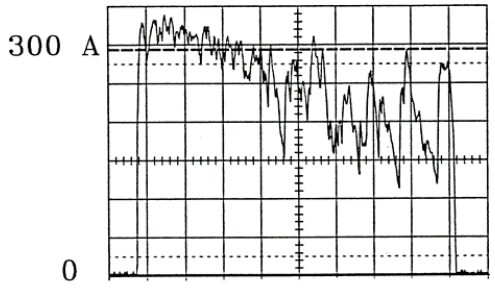

(a) Current

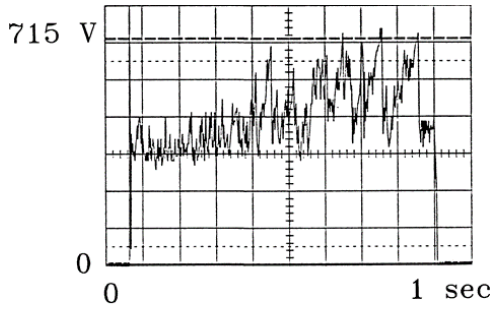

(b) Voltage

Fig. 1.25 Voltage and current of a 7-inch gap burning in air.

References

1.1 *Reference Data for Engineers: Radio, Electronics, Computer, and Communications, Seventh Edition*, Howard W. Sams and Co., Indianapolis, Indiana, 1985, pp. 48-4.

1.2 *IEEE Standard Techniques for High Voltage Testing, IEEE Std. 4-1978*, Institute of Electrical and Electronic Engineers, New York, 1978, pp. 47-55.

1.3 T. E. Allibone, The Long Spark, *Lightning, Volume 1, Physics of Lightning, R. H. Golde - Editor*, Academic Press, London and New York, 1977, Chapter 7, pp. 231-280.

1.4 G. N. Aleksandrov et al, "Peculiarities of the Electric Breakdown of Extremely Long Air Gaps," *Dokl. Akad. Nauk SSSR*, Vol 183, 1968, pp. 1048.

1.5 I. S. Stekolnikov, A. V. Shkilev, "The Development of a Long Spark and Lightning," *International Gas Discharge Conference, Montreux*, 1963, pp. 466-481.

1.6 *Transmission Line Reference Book, 345 kV and Above*, Electric Power Research Institute, Palo Alto, CA, 1982.

1.7 *IEEE Std. 4-1978*, pp. 23-26.

1.8 *Transmission Line Reference Book*, pp. 528-530.

Chapter 2

THE LIGHTNING ENVIRONMENT

2.1 Introduction

The lightning flash originates with the formation of electrical charge in clouds in the air. The most common producer of lightning is the *cumulonimbus cloud*, often called the "thundercloud". Other types of clouds, including smaller cumulus clouds and non-convective, stratiform clouds, can produce electric charges and lightning as well. Lightning has also occurred during sandstorms, snowstorms, and in the clouds over erupting volcanos. On rare occasions, lightning has even been reported to occur in clear air, although this phenomenon is most likely caused by conventional clouds beyond the observer's field of vision. Lightning originating in sandstorms and volcanic eruptions is usually not of serious concern to aircraft, but lightning associated with other non-thunderstorm cloud conditions may present problems because it is apt to occur when it is unexpected. Pilot's reports of lightning strikes to aircraft often state that they were struck under conditions far from known thunderstorms, where a lightning strike would not be expected.

The most common types of lightning are those involving a cloud and the earth, called *cloud-to-earth* lightning, and lightning between charge centers within the same cloud, called *intracloud* lightning. This latter is sometimes erroneously called intercloud or cloud-to-cloud lightning. True cloud-to-cloud lightning between isolated cloud centers is possible; however, what appears to be cloud-to-cloud lightning is often a spectacular manifestation of *intracloud* discharges. While aircraft may be involved with any of the three types of lightning, *cloud-to-earth* and *intracloud* lightning flashes are the most common types.

Much of the data presented in this chapter is related to lightning flashes to earth, since there is less data available on the electrical characteristics of intracloud flashes or flashes to aircraft (which may include both intracloud and cloud-to-earth flashes.) There are several reasons for this, the major one being that most research on lightning has centered on cloud-to-earth lightning and most of our understanding of lightning comes from the study of *cloud-to-earth* lightning.

There have been several studies involving aircraft flown into storms in order to better study intracloud lightning. These studies have shed considerable light on the nature of intracloud lightning and have shown that aircraft can trigger a lightning flash and that these aircraft-triggered flashes originate from the aircraft. The triggering mechanism and the nature of lightning flashes triggered by and originated at an aircraft are discussed in Chapter 3.

Despite its importance to aircraft operation, there is simply much less information on the characteristics of *intracloud* lightning than on those of c*loud-to-earth* lightning. *Intracloud* lightning, unlike *cloud-to-earth* lightning, is largely hidden from direct observation and so is much more difficult to study. Conducting research on the characteristics of lightning is often a labor of love, requiring both extensive apparatus and extreme patience. Observing lightning from a fixed, ground-based station is much easier and cheaper than observing lightning from a moving aircraft. Also, most of the funding for research on lightning has come, directly or indirectly, from those who are concerned with the effects of lightning on electric power transmission and distribution lines, which are affected only by *cloud-to-earth* strikes.

Cloud-to-earth strikes are, nevertheless, important for aircraft as well, since aircraft are struck by *cloud-to-earth* lightning and there is considerable evidence that currents in *cloud-to-earth* flashes are more severe than *intracloud* flashes. Most of the test specifications and test practices relating to aircraft and lightning have been derived, directly or indirectly, from studies of *cloud-to-earth* lightning. Finally, the ground facilities that support aircraft are only exposed to *cloud-to-earth* lightning. This book does not specifically deal with ground support facilities, but such facilities obviously must be protected from lightning to fulfill their support role for flying aircraft.

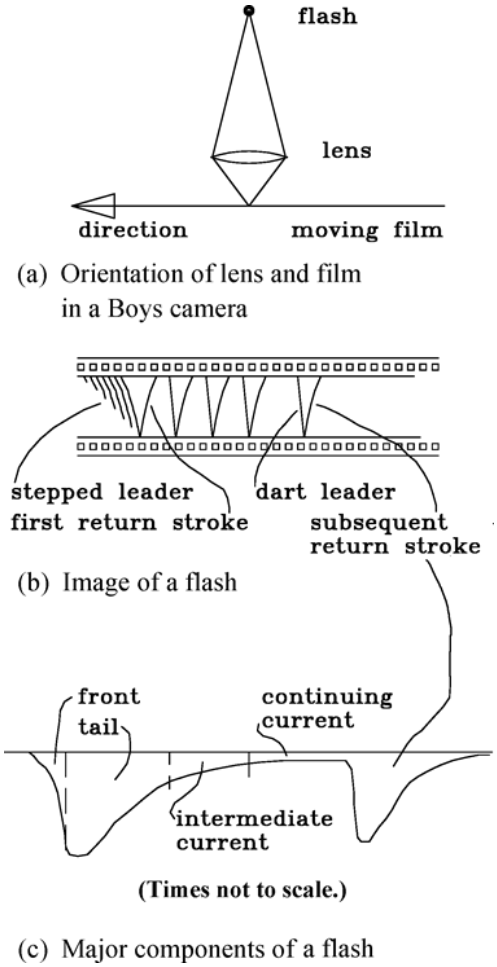

Fig. 2.1 Generalized nature of negative, cloud-to-earth lightning.

To introduce the terms that will be discussed in the following sections, consider Fig. 2.1, which is a sketch of a typical cloud-to-earth lightning flash using a camera with a continuously moving film (a Boys camera, as discussed in §1.5.4). The image on the film would appear as shown on Fig. 2.1(b) and the current measured at ground level would appear as shown in Fig. 2.1(c). A leader starts at the cloud and works its way, in steps, toward the earth. When it nears the earth's surface, a streamer forms upwards, from the earth, toward the descending leader. Streamers are not very luminous and can seldom be seen by the naked eye.

Eventually, the two join and there occurs a very bright flash, due to the very rapid flow, or discharge, of charge from the leader into the earth. This is commonly known as the *first return stroke*.

The term *return stroke* was assigned because of the rapid propagation of the bright flash up the leader, recorded by the fast streak camera. The term is a misnomer because in fact the charge moves downward, not upward in the stroke process. Since *return stroke* is used frequently in the literature, it will be retained occasionally in this book. However, it will be replaced with simply *stroke* in most applications.

Thus, the term *return stroke* is, perhaps, unfortunate. Return strokes will be referred to, from here on, simply as *first strokes, or strokes*. After the leader is discharged by the first stroke, the remaining charge in the cloud flows to earth in the remaining electric arc, referred to now as the *lightning channel*. This continued discharge is referred to as the *intermediate* and *continuing current*. After all the charge in the original charge cloud region has been conducted to earth, the upper ends of the original lightning channel may extend into other nearby regions, which produce a dart leader to recharge the original channel. This charge then immediately discharges to the earth in a subsequent stroke. The pattern of *dart leader - subsequent stroke - continuing current* - may repeat several times.

The *first strokes* are characterized by four time intervals; a current rise time (or *front)* lasting for a few microseconds or less, a decay time (or *tail),* lasting for tens of microseconds, *an intermediate current*, lasting for a few milliseconds and a *continuing current*, that may have a total duration of a second or more. The intermediate current and continuing currents may not always occur and sometimes there may only be one stroke.

Each of these aspects of the flash is discussed in the following sections. For a more complete discussion of the mechanism of the lightning discharge, the reader is referred to the literature, of which [2.1 - 2.4] are probably the most complete. Each of them contains extensive bibliographies which this chapter will not attempt to review.

2.2 Generation of the Lightning Flash

The lightning flash originates with the generation of charge, after which the lightning flash develops by the streamer mechanism discussed in Chapter 1.

2.2.1 Generation of the Charge

The exact mechanism(s) by which electrical charge develops in clouds is still unknown, but there is little doubt that the energy that produces lightning in the traditional cumulonimbus cloud is provided by warm air rising upwards into a developing cloud (Fig. 2.2). As the air rises it becomes cooler and, at the dew point, the excess water vapor condenses into water droplets, forming a cloud. By the time the air has risen high enough for the temperature to drop to -40° C, the water vapor it contains has frozen to ice. At lower elevations, there may still be many super cooled water drops that are not frozen, even though the temperature is lower than the freezing point. In this super cooled region, ice crystals and hailstones form.

According to one theory [2.5], the cloud becomes electrically charged by the following process:

Some of the ice crystals which have formed coalesce into hailstones. These hailstones fall through the cloud gathering additional supercooled water droplets. As droplets freeze onto a hailstone, small splinters of ice chip off. Apparently, these splinters carry away a positive electrical charge, leaving the hailstone with a net negative charge. The vertical wind currents in the cloud carry the ice splinters into the upper part of the cloud, while the hailstone, being heavier, falls until it reaches warmer air, where some portion of it melts and the remainder continues to earth. Thus, the upper part of the cloud takes on a charge that is predominantly positive while the lower regions take on a charge that is predominantly negative.

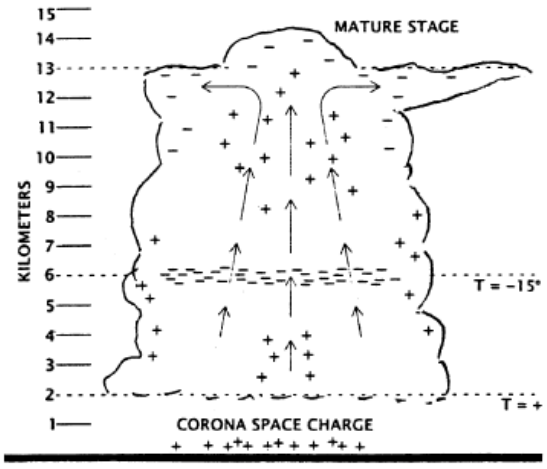

Fig. 2.2 Generalized diagram showing distribution of air currents and electrical charge in a typical cumulonimbus cloud [2.12].

Other theories [2.5 - 2.11] have been proposed to account for the electrification of the cloud. All of them are based on experimentally observed evidence that the charge in the top of the cloud is positive, while the lower portion of the cloud contains negative charge. Most of the early work on the distribution of charge in clouds was based on indirect evidence from the changes in the electric field at ground level as lightning flashes take place. Such measurements can give ambiguous results, particularly if the electric field changes are observed at only one location, a matter discussed further in [2.3]. Direct measurement of charges by aircraft or instrumented balloons are more reliable. These airborne observations indicate that the top of the cloud does have a positive charge, that the middle regions of the cloud have negative charge, and that there are also pockets of positive charge near the base of the cloud. Some observations [2.12] suggest that the negative charge is distributed in a layer approximately 1 000 ft. thick, rather than being more or less evenly distributed through the lower portions of the cloud. Fig. 2.2 shows how the charge in a typical cloud might be distributed.

The air currents and the electrical charges tend to be contained in localized cells and the cloud as a whole is composed of several cells. A typical cloud might have the cell structure shown in Fig. 2.3 [2.13]. The electrical charge contained within a cell might appear as shown in Fig. 2.4 [2.11]. The temperature at the main negative charge center is about -5 °C and at the auxiliary pocket of positive charge below it, about 0 °C. The main positive charge center in the upper cloud is about 15 °C colder than its negative counterpart.

The lifetime of a typical cell is about 30 minutes. In its mature state, the cell as a whole has a potential, with respect to the earth, of 10^8 to 10^9 volts. It has a total stored charge of several hundred coulombs, with potential differences between positive and negative charge pockets, again, on the order of 10^8 to 10^9 volts.

2.2.2 Electric Fields Produced by Change

As a charged cloud passes over a given point on the earth, an electric charge is induced on the surface of the earth, under the cloud, and the average electric field at the earth's surface changes from its fair weather value of about 300 volts per meter, positive, to as high as several

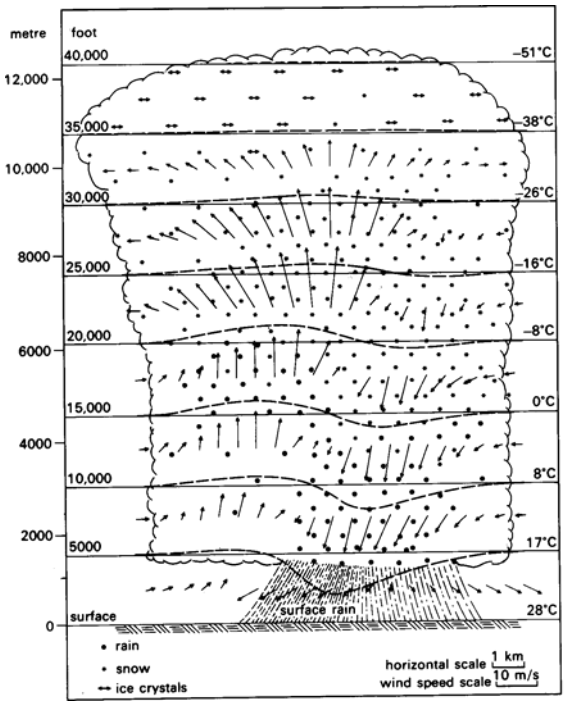

Fig. 2.3 An idealized cross section through a thunderstorm cell in its mature stage [2.13].

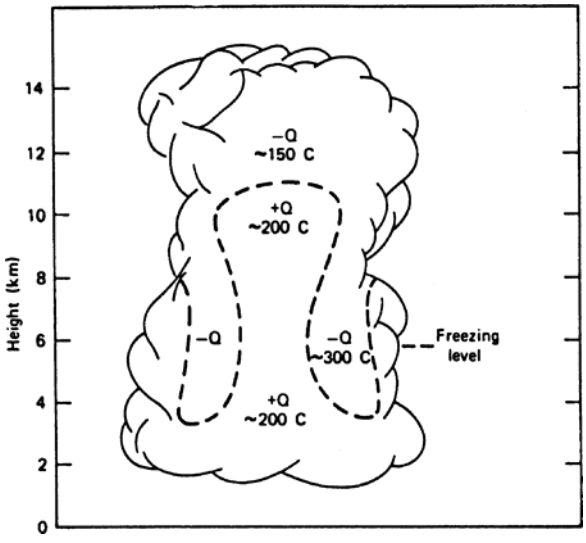

Fig. 2.4 Estimated charge distribution in a mature thundercloud [2.11].

thousand volts per meter, negative. These polarity conventions are illustrated in Fig. 2.5. Generally, when a cloud is overhead, the field at ground level is negative, but when a localized positive region is overhead, the field may be positive. The potential gradient is concentrated around sharp protruding points on the earth's surface and can exceed the breakdown strength of the air, which has a nominal value of 30kV/cm at sea level conditions, and less at higher altitudes.

When the breakdown strength of the air is exceeded, current into the air increases sharply and a bluish electrical discharge called corona forms around sharp, conductive objects electrically bonded to the earth. This discharge is the St. Elmo's fire discussed in Chapter 1. The magnitude of the current from a single discharge point may range from 1 or 2 microamperes (μA) to as high as 400 μA. This field-induced corona is generally less intense than the corona observed on energized conductors and discussed in Chapter 1. The presence of St. Elmo's fire should be taken as signifying a dangerous condition to an exposed observer on the ground, such as a mountain climber on an exposed ridge. It is not necessarily an indicator that lightning is imminent, however, since it only reflects the state of the electric field at the earth's surface, not at the base of the clouds where lightning usually originates.

The emanation of corona from objects on the earth's surface is only possible when the electric field is highly localized and does not extend over a sufficient distance for streamers to propagate. An important reason for this is that the shapes of conductive objects from which corona emanates are such that the electric field is locally enhanced. In addition, the charges injected into the air by the corona accumulate, forming a space charge.

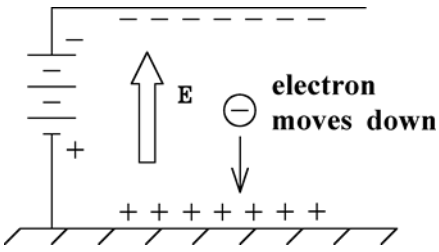

Fig. 2.5 Polarity considerations.

Theoretically, this space charge may reduce the resultant electric field at the earth's surface, so that a developing breakdown in the air 'sees' a more uniform electric field than would a microscopic observer at the earth's surface.

2.2.3 Development of the Leader

At some stage in the electrification of the cloud, a discharge towards the earth takes place. It starts as a slow-moving column of ionized air called the pilot streamer. After the pilot streamer has moved perhaps 30 to 50 m, a more intense discharge, called the stepped leader, takes place. This discharge lowers additional negative charge into the region around the pilot streamer, 'recharges' it and allows it to continue for another 30 to 50 meters, after which the cycle repeats. A discharge propagating in this manner is called a streamer discharge; its development was discussed in Chapter 1 and is illustrated further in Fig. 2.6.

Since the initial development of the leader takes place in the charged cloud, the developing streamer branches and begins to collect charge from its surroundings in the cloud. Because it collects charge in this way, the streamer may be viewed as connected to the cloud and at the same potential as the cloud. As the head of the leader moves farther into the un-ionized air, charge flows down from the charged regions of the cloud, along the partially conducting filament and toward the head of the leader, thus tending to keep all parts of the leader at a very high potential. The amount of charge lowered into the leader ranges from about 2 x 10^{-4} to 20 x 10^{-4} coulombs per meter of length. Therefore, a leader 5 km long would have stored within it a charge of 1 to 10 coulombs.

The leader, as postulated by Wagner [2.14], is illustrated in Fig. 2.7. The head of the leader may have a larger diameter than the rest of the leader, although this is difficult to prove by photographs. The head of the leader is usually visible because of the optical radiation associated with the extension of the electron avalanches, but once the growth ceases, the radiation stops; consequently, the corona sheath surrounding the central conducting filament ceases to be visible. Since the potential of the leader is very high, there is a high radial electric field throughout the leader's length; high enough to exceed the breakdown strength of the air. Thus, secondary streamers branch out radially away from the central filament, until the field strength at their tips falls to about 30 kV/cm.

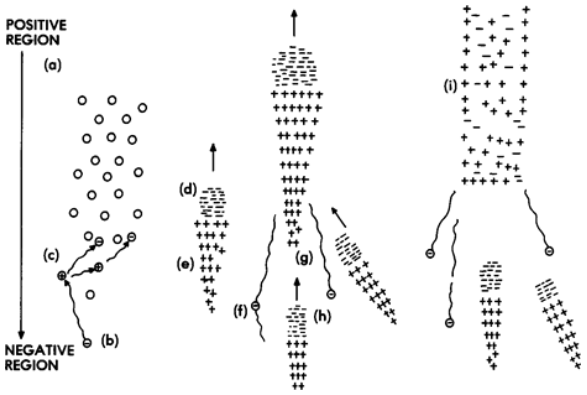

Fig. 2.6 Stages in the development of a lightning leader.

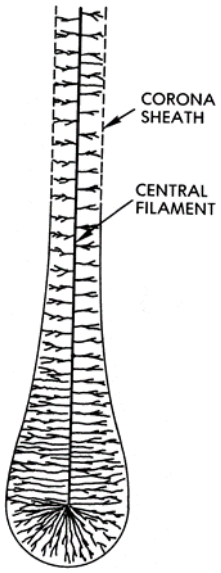

Fig. 2.7 The lightning leader as postulated by Wagner [2.14].

Diameter of the leader

It can be shown that the electric field strength at the edge of a cylinder containing a charge, q_o, per unit length is

$$E_r = \frac{1.8\,x\,10^{10} q_0}{r} \qquad (2.1)$$

From this and the above breakdown strength of air, it can be deduced that the radius of the leader ranges from 1.2 to 12 meters. At higher elevations, the breakdown strength of air is less; hence the leader radius may be larger.

Photographs of actual lightning leaders have been taken with a Boys camera, a specialized camera in which the film moves relative to the camera lens. Fig. 2.1 illustrates the principle of operation of a Boy's camera and Fig. 2.8 [2.15] is an actual Boys camera photograph. The leader originates at the top, left-hand corner of the picture and lengthens as time increases. The bright line at the right-hand end of the picture is produced by the first stroke, discussed in §2.2.5.

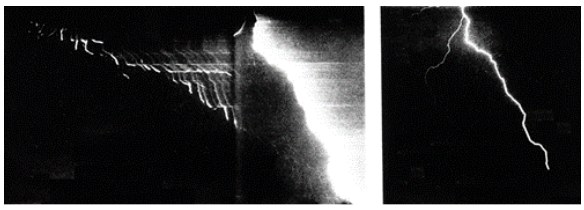

(a) Boys camera photograph (b)Conventional Photograph

Fig. 2.8 Boys camera photograph of a lightning leader.

Leader velocity and current

From photographs such as Fig. 2.8, it has been learned that the leader advances at about 1 x 10^5 to 2 x 10^5 m/s, or 0.03% to 0.06% of the speed of light [2.16]. In order for a charge of 2 to 20 x 10^{-4} coulombs to be deposited by a leader advancing at the rate of 1 x 10^5 m/s, the average current in the leader, i_l, must be 20 to 200 A. A current of this magnitude could be carried only in a highly conducting arc, assumed to be the central conducting filament of the leader. Such an arc would have a diameter on the order of a few millimeters and an axial voltage gradient, g_l, of about 5 x 10^3 V/m. A leader 4 km long must therefore have a voltage drop along its length of 2 x 10^7 V. The longitudinal resistance, R_l, of the conducting filament would then be in the range of 40 to 400 ohms per meter (Ω/m).

It should be noted that leaders sometimes start from something on the earth. If an airplane were to be flying over a tower it may be susceptible to a strike in such conditions, with the leader continuing to progress toward the sky. This happens most frequently from tall buildings or towers, or from buildings or towers located atop hills. Generally, one can tell from the direction of the branching of the lightning flash whether the leader started at the cloud or at the ground: if the branching is downward (Fig. 2.9(a)) the leader originated at the cloud; if the branching is upward, (Fig. 2.9(b)), the leader originated from the earth.

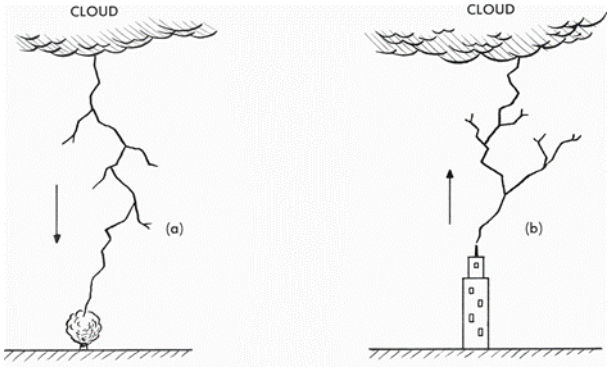

Fig. 2.9 Leader direction as determined from direction of branching.

2.2.4 Transition from Leader to Stroke

As the negatively charged stepped leader approaches the earth, positive charge accumulates in the earth underneath it or, more accurately, negative charge is repelled away from the region under the leader. Eventually, the electric field strength around objects on the earth becomes sufficiently high that a streamer starts at the earth's surface and works its way toward the downward approaching leader.

This seems to occur when the average voltage gradient between the leader and the earth's surface reaches about 5.5 kV/cm (550 kV/m). When the leaders from the cloud and from the earth meet, the conducting filament in the center of each streamer provides a low impedance path so that the charge stored in the head of the lightning leader can flow easily to earth. As the current in the central filament increases from its initial amplitude of a few tens of amperes to much higher values, the filament gets hotter, its diameter expands and its longitudinal voltage gradient decreases. In other words, it becomes an even better conductor, which, in turn, allows even more current to flow in the arc. As the charge in the lower part of the leader flows rapidly to earth, the heavily conducting arc reaches higher into the charged leader channel as it conducts charge to earth. The upper extremity of the region in which the leader discharge is taking place moves upwards, toward the cloud, at a rate of roughly 10^8 m/s (or one third the velocity of light) until it reaches the cloud. This heavily conducting region, called the first stroke, produces the intense flash normally associated with the lightning stroke.

Some stages in the development of the first stroke are shown in Fig. 2.10 [2.14]. Fig. 2.11 shows an oscillogram of an actual lightning current as measured at the earth's surface. The figure also shows two subsequent stroke current waveforms, which are discussed in §2.2.7.

The point at which the downward and upward-going leaders meet (sometimes called the *junction* or *switch point*) can be recognized on photographs as a point where the channel seems to split. Fig. 2.12 shows an example in a photograph of an actual lightning flash and Fig. 1.18 showed an example observed during laboratory testing.

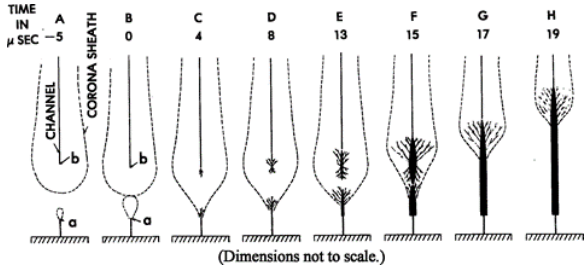

Fig. 2.10 States in the development of the first stroke [2.14]

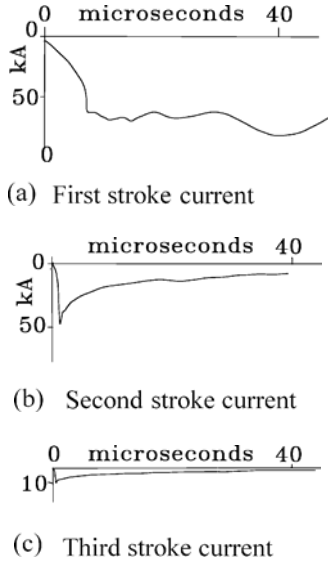

Fig. 2.11 Example of multiple stroke (MS) lightning current waveshapes [2.25].

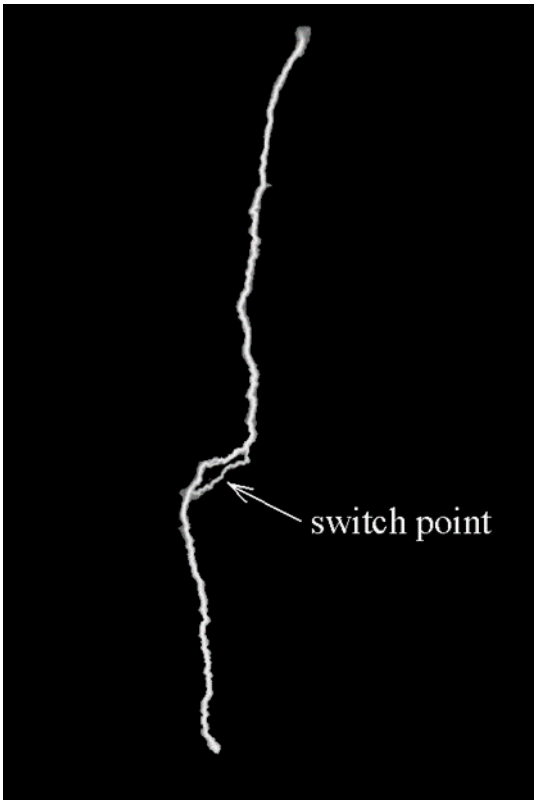

Fig. 2.12 Junction of downward and upward streamers in a simulated lightning flash.

The branch of a downward leader which first induces a junction leader from the earth effectively determines where, on the earth, the flash will ultimately terminate. The distance between the lightning leader and the ground (or grounded object) at the instant when the upward leader from earth is first initiated is called the striking distance. Analysis of the striking distance is important in the protection of objects on the earth's surface [2.17 - 2.19].

2.2.5 Further Development of the First Stroke

The high currents associated with lightning (~10 kA to ~250 kA) are produced as the first stroke drains the charge in the leader channel. The amplitude of the current is determined by the velocity with which this first stroke propagates, together with the amount of charge in the leader channel. The rate of charge flow from the leader channel to the earth is given by the current, *I*, in Eq. 2.2.

$$I = \frac{dq}{dt} \qquad (2.2)$$

Let *v* be the velocity of the first stroke and *q* be the amount of charge deposited per unit length, *dl*, along the leader channel. Since

$$V = \frac{dl}{dt} \qquad (2.3)$$

it follows that

$$i = qv \qquad (2.4)$$

As a numerical example let

$$v = \frac{10^8 m}{s} \text{ and } q = 10x10^{-4}\text{C/m}$$

Then

$$I = 10 \text{ x } 10^{-4} \text{ x } 10^8$$
$$= 10 \text{ x } 10^4$$
$$= 100\,000 \text{ A}$$

The velocity of the first stroke is not constant from one stroke to the next but, rather, it seems to vary with the peak amplitude of the current in the stroke. The relationship between current amplitude and velocity may be deduced either from theoretical concepts or from experiments. The relationship derived by Wagner [2.21] is shown in Fig. 2.13. Considerations of the first stroke velocity are primarily of importance in studying the time history of the electric field produced by the lightning flash. Measurements of electric field produced by remote lightning flashes have been used to estimate the amplitudes of those flashes.

There is evidence that the velocity of the first stroke decreases as it propagates up the channel. This suggests that, for a given flash, the peak current at altitude is less than the peak amplitude measured at the earth's surface. Also, since the stroke current represents the discharge of charge stored in the leader, the time duration of the stroke current should be less at finite altitudes, through which only a portion of the leader change passes, than at the earth's surface, through which all of the leader charge passes. The velocity may also affect the surge impedance of the lightning channel, and thus the way that the stroke current interacts with a conductor, such as an aircraft.

Factors affecting first stroke velocity

The velocity of propagation of the first stroke is less than the speed of light for two basic reasons. The first involves the longitudinal resistance of the first stroke channel. Some of the factors associated with this longitudinal resistance are shown in Fig. 2.14. Central to the phenomenon is the fact that the current in the lightning channel must increase rapidly from the ~200 ampere current associated with the initial development of the leader to a current of perhaps ~10 kA to ~250 kA, as the first stroke becomes fully developed. It is a characteristic of an arc channel that the current density remains nearly constant. If the current through the arc is increased, the arc channel expands in diameter. The channel cannot expand instantaneously however, since energy must be put into the channel to cause it to heat up sufficiently to force it to expand. Accordingly, if the current through the arc channel is suddenly increased, as in Fig. 2.14(a), the longitudinal voltage gradient of the channel must similarly increase.

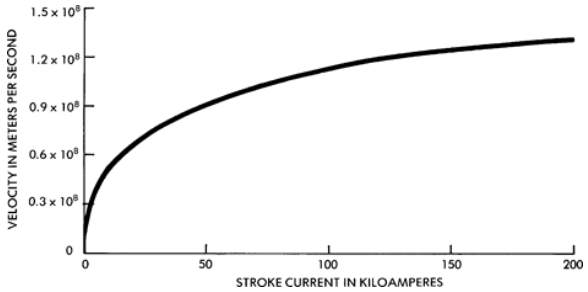

Fig. 2.13 Relation between stroke current and stroke velocity [2.21].

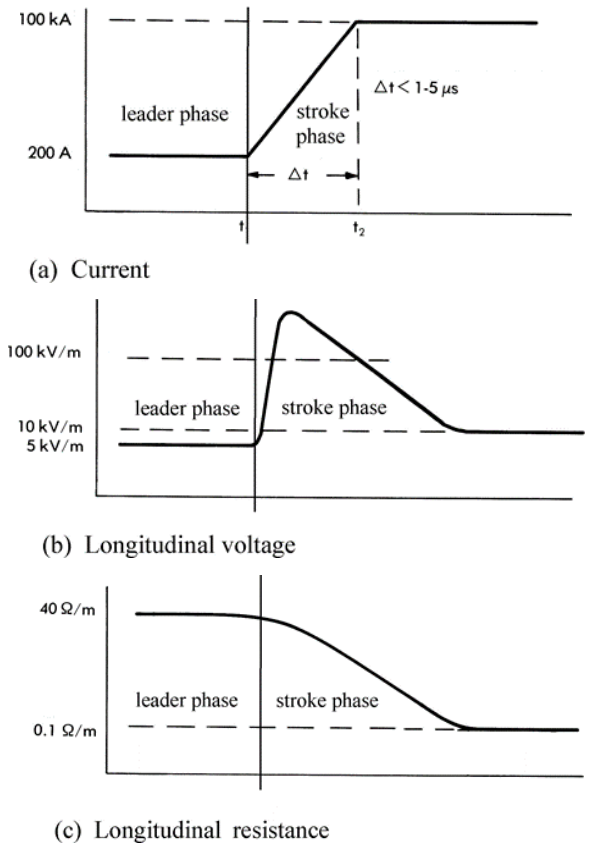

Fig. 2.14 Phenomena associated with the passage of the stroke.

Since the rate at which energy is injected into the channel is the product of the current and the longitudinal voltage gradient, the increased longitudinal voltage gradient may be taken as the mechanism forcing the arc channel to get hot enough to expand to the diameter required to carry the high currents.

It is not known what the maximum longitudinal voltage gradient would be in a lightning channel, but it is known from studies of arcs in laboratories that the gradient can fall to values as low as 100 kV/m in a fraction of a microsecond. Presumably, therefore, the channel should expand to its final diameter in a few microseconds and the longitudinal voltage gradient should simultaneously decay to between 5 and 10 kV/m. The longitudinal resistance of the channel should, therefore, fall from an initial value of about 40 Ω/m to a small fraction of an ohm per meter during the same time period. Note that this collapse of the longitudinal resistance of the lightning channel is not instantaneous. The initial resistance of the leader is high enough to retard the development of the leader discharge (the upward-propagating stroke) and hence reduce its velocity of propagation below that of the speed of light.

There is little data available to substantiate the estimates given above. This is unfortunate, since a knowledge of the voltage along a lightning channel would be a key element in determining the behavior of a lightning channel attachment on the surfaces of aircraft in flight (a subject discussed in Chapter 3). Some estimates of channel voltages have been made based on an assumed inductance of 1 μH/m, a value estimated from a conductor over a ground plane.

Another factor that contributes to the reduction of return stroke velocity below the speed of light is illustrated in Fig. 2.15 (a). A growing streamer leaves a column of electrical charge, several meters in diameter, in its wake. At the center of that column is a highly conductive core, only a few millimeters in diameter, which ultimately becomes the leader. This conductive core expands to a few centimeters' diameter during the return stroke. The inductance of the lightning channel during the first stroke is determined by the diameter of this highly conductive central core, while the capacitance of the channel is determined by the diameter of the column of electrical charge. The lightning leader may then be modeled as shown in Fig. 2.15(b), in which a highly conductive central conductor is fastened onto a series of radiating sparks. (The figure shows the leader in a horizontal position, whereas a vertical presentation would be more realistic).

(a) Distributed charge surrounding a highly conductive central core.

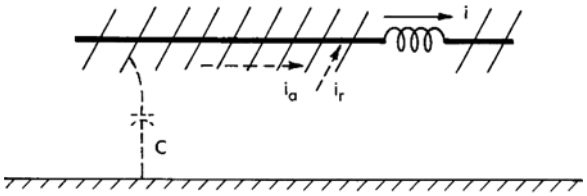

(b) Highly conductive central core fastened onto a series of projecting splines.

Fig. 2.15 Effect of corona cloud on the propagation velocity of a lightning leader.

A better analogy might be to view the lightning flash as a piece of tinsel rope for decorating a Christmas tree: a central piece of string is surrounded by a tube of fine filaments projecting radially away from the central core. In either case, the radial filaments can carry a radial current, i_r, but cannot carry an axial current, i_a. Accordingly, the lightning first stroke has both a high capacitance and a high inductance per unit of length. In this respect it differs from a solid conductor of large diameter which, while possessing a high capacitance per unit length, simultaneously possesses a low inductance per unit length. It follows that the surge impedance (also known as characteristic impedance) is governed by the ratio of inductance to capacitance, is high while the velocity of propagation, governed by the product of inductance and capacitance, is less than that of the speed of light.

Impedance of the Channel

Wagner [2.21] concludes that the surge impedance of the lightning channel is of the order of 3 000 ohms for return strokes of large amplitude (~100 kA). This large impedance is probably due to the resistance associated with the collection of charge at the upper end of the lightning channel. This current-limiting effect is probably most prevalent during the rise of the first stroke current.

After the charge has been collected and the current in the channel has attained its final value, the longitudinal resistance becomes quite small, and the impedance is determined primarily by the inductance and capacitance of the lightning channel at that time. The surge impedance of the lightning channel is, then, essentially the same as if it were a hypothetical conductor suspended in air, remote from any returning current path. Such an impedance might be on the order of 500 ohms.

Current Waveforms

Since the 1920s, large numbers of natural lightning current waveforms have been recorded at the earth's surface. Thus, the characteristic waveforms of natural lightning currents are well-known to science. These revelations can be attributed principally to the work of Berger [2.15 - 2.16]. Typical waveforms detailing the front of the initial first stroke are shown in Figs. 2.16 and 2.17 [2.22 - 2.23]. Fig. 2.17 shows the currents on two different time scales, one to indicate the shape of the front of the stroke current and one to indicate the shape of the stroke current decay, known as the *tail*. In all cases, the current is seen to have a concave front, the current initially rising slowly, but then increasing to a maximum current rate of change just before peak amplitude is reached.

It has been speculated that the initial, slowly changing portion of these current oscillograms represents the growth of an upward going leader from the instrumented tower within which the measurements were taken. The attainment of maximum di/dt, just prior to the peak of the current pulse, is typical of a natural lightning stroke. These waveforms also support the notion that subsequent strokes in a lightning flash, even measured at the earth's surface, exhibit front times considerably faster than the rise time of the initial stroke in the flash. (Subsequent strokes are discussed in §2.2.7.)

The true front time of the stroke, as it passes a point remote from the earth's surface, has probably never been measured. However, one can assume that it is similar to front times measured at the earth's surface. Measurements recorded onboard instrumented aircraft have included the front times of lightning currents, but many of these pertain to flashes that were triggered by the presence of the aircraft. In addition, many of those flashes seem to have been more representative of intracloud flashes, than of cloud to earth flashes.

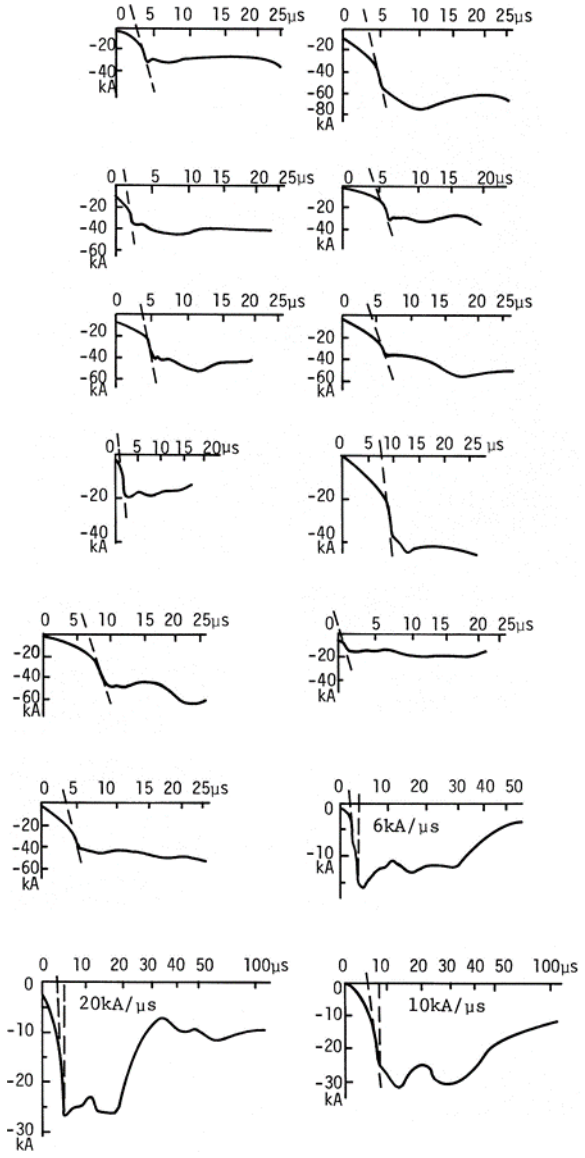

Fig. 2.16 Wavefronts of lightning stroke currents as measured by Berger [2.16].

2.2.6 Further Development of the Lightning Flash

The decay of the first stroke current, after the charge has been drained from the leader, happens at a lower rate than the rise to peak. Oscillograms showing typical decay times are shown in Fig. 2.17. This figure displays the current on

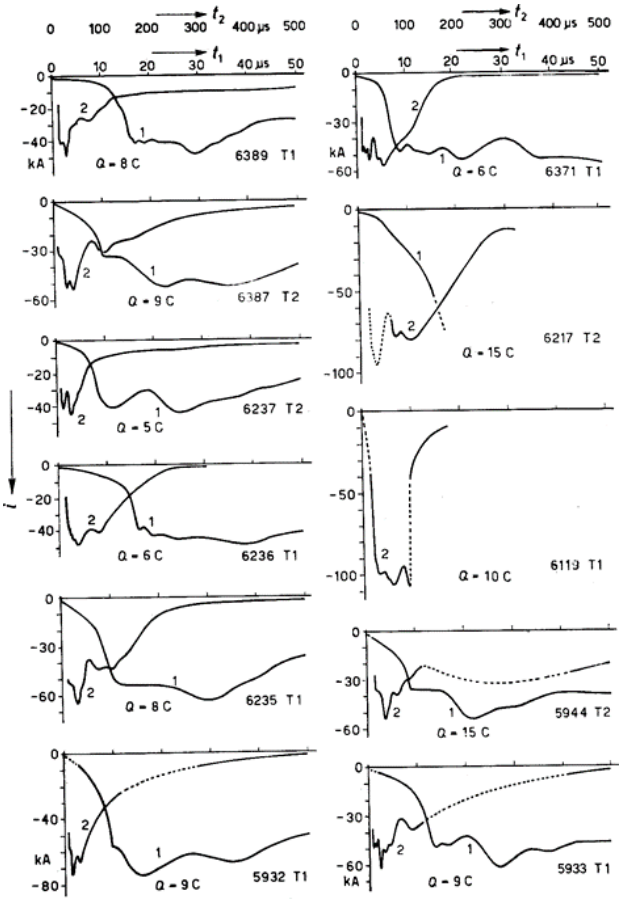

Fig. 2.17 Current oscillograms from single strokes of first downward flashes [2.16].
t_1 Fast time scale 0 – 50 µs
t_2 Slow time scale 0 – 500 µs

two different time scales, emphasizing the front and the tail. Some of the oscillograms showing the front are the same as those shown in Fig. 2.16.

As the first stroke propagates toward the cloud, it may encounter other branches of the leader, as shown in Fig. 2.18. As it passes these branches, the charge stored in them feed into the developing lightning stroke and momentarily increase the current. Therefore, one cannot assume that the amount of charge (and therefore the current) in the first stroke decreases linearly with distance up the channel from earth.

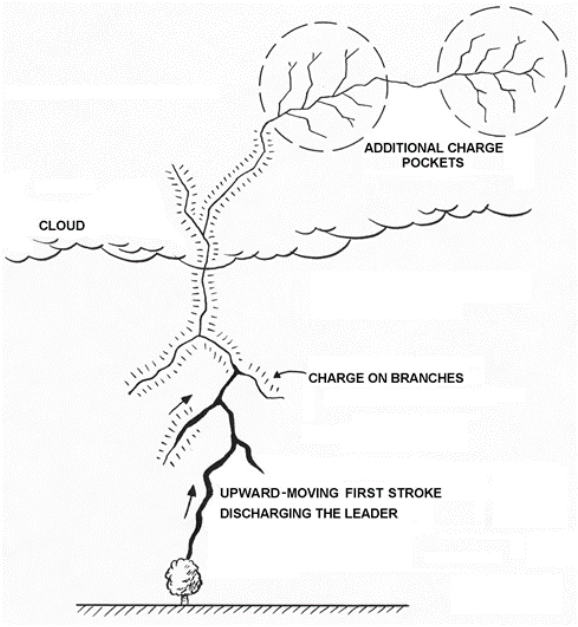

Fig. 2.18 Further development of the flash.

By the time the stroke reaches the cloud, all the leader charge has been conducted to earth in the first stroke. Our understanding of what takes place within a thundercloud has been hampered by our inability to see into the interiors of clouds. Nevertheless, some of the phenomena can be inferred from measurements of electrical radiation produced by the developing flash and from the usual behavior of the flash after the initial stroke has passed. As the stroke reaches into the cloud, it appears to encounter a much more heavily branched leader than it did in the air below the cloud. The stroke can thus tap the charge diffused through a large volume of the cloud, rather than only the charge in the more localized leader. It must be during this period that the *intermediate current* is developed.

As the discharge continues to spread through the cloud, over a period measured in large fractions of a second, currents of several hundred amperes continue to flow in the lightning flash. These are referred to as *continuing currents*. As one may expect, there is no clear-cut demarcation between the tail of the stroke and the intermediate current, or between the end of the intermediate current and the start of the continuing current. In fact, intermediate currents can occur at a variety of different times during a lightning flash

.

2.2.7 Subsequent Strokes

The growing discharged region within the cloud eventually reaches into a different cell of the cloud or, at least, into a region where there is another localized body of electrical charge. This 'recharges' the lightning channel, producing subsequent strokes, as are shown in Fig. 2.11 (b, c). These subsequent strokes follow the first stroke too rapidly to allow for any significant diffusion of the ionized gas comprising the channel. Thus, the recharging process occurs smoothly, not through the step-by-step process by which the initial leader forms in non-ionized air. Accordingly, the recharged leader is called a *dart leader* instead of a *stepped leader,* and follows the same path taken by the initial leader and channel. Unlike the initial stepped leader, the dart leader is seldom branched. When the dart leader reaches the earth's surface, another stroke occurs, as the dart leader discharges. This is called a subsequent stroke. The amplitude of this stroke is again high since the current comes from an intensely ionized channel close to the earth. While the amplitude is usually not as high as that of the first stroke, the current rises to peak more rapidly than that of the first stroke, presumably because the upward leader from the earth does not have to propagate into virgin air.

Two oscillograms of actual subsequent strokes are shown in Fig. 2.11 (b and c). Anderson and Eriksson [2.24] averaged the results of many different recordings and derived the composite picture of the front of first and subsequent strokes shown in Fig. 2.19.

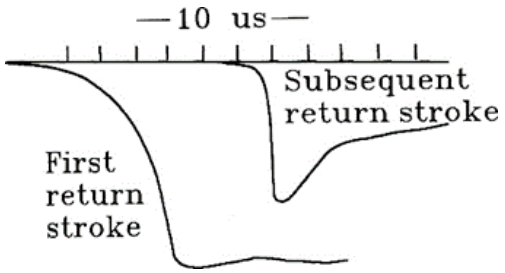

Fig. 2.19 Drawings of first and subsequent strokes. Adapted from [2.24].

2.2.8 Lightning Polarity and Direction

The direction of current flow in a lightning flash is sometimes a source of confusion. While the first stroke process, which produces the high currents, thunder, and the highest intensity light, does, in fact, start near the earth and grow upward into the ionized channel, that process usually lowers negative charge from the thundercloud down to the earth (except in the rarer cases of positive flashes). With the intent of clarifying matters, the statement is sometimes made that lightning strikes upward and not downward. This is at least partially true; the first stroke process that produces the high peak currents, thunder, and the highest intensity light, in fact does start near the earth and grows upward into the ionized channel previously established by the stepped leader, thus tapping the charge in the stepped leader. The stepped leader, nevertheless, originates at the cloud and lowers electrons into the leader channel, from whence they ultimately flow into the earth. The source of charge is, after all, in the cloud.

A pedagogical analogy can be made between a lightning stroke and a line of cars waiting at a traffic light. The junction of the upward and downward leaders is when the light turns green. At this instant, the car in front of the line begins to move, then the second car, then the third, and gradually the motion propagates backward, up the line of traffic until the entire traffic stream is in motion. Since the motion of the electric charges in the stroke produces light (because the accelerating charges heat the surrounding air and excite electrons in gas molecules with which they collide), the traffic analogy might be made more visually effective if one imagines that it is night-time and that the drivers of the cars are instructed to switch their headlights on as they start to move. Although, when viewed from a veranda of a tall building nearby, the illumination on the street below appears to propagate backward as the cars begin to move, each individual car moves forward. Similarly, a lightning stroke lowers charge to the earth, but the light it produces moves upward from the earth, because it is near the earth that the charges first begin to move.

Flashes originating at the earth's surface

When tall buildings or mountain tops are involved in a lightning flash, the growth of the lightning channel often originates at the earth's surface, that is, the stepped leader starts at a point on the tall structure and propagates upward, into the cloud. Such flashes seem to be triggered by the high electric field concentrated around the top of the building or mountain. They may be recognized by the upward direction of branching, as mentioned earlier, and shown in Fig. 2.9(b). Most commonly, this type of flash is induced by a negatively charged cloud, or at least by a cloud having an excess of negative charge in its lower regions so that the step leader carries positive charge upwards into the cloud. This type of flash starts off with a relatively low continuing current and lacks the original high current stroke typical of flashes in which the leader originates at the cloud. Subsequent strokes, if they occur, are like those found in flashes that originate at the cloud. Flashes of this type can also be triggered artificially by launching, from the earth, a small rocket trailing a wire attached to the earth.

Positive flashes

Roughly 10% of all lightning flashes lower positive charge to the earth (or, more accurately, transport electrons from the earth to the cloud) and are accordingly called positive flashes. As with negative flashes, they may either involve a leader that initially propagates from the cloud towards the earth or a leader that initially propagates from the earth towards the cloud. Positive flashes are responsible for the highest peak currents and charge contents ever recorded. Examples of current waveforms from some of these strong positive flashes are shown in Fig. 2.20 [2.23]. They usually consist of only one, high current stroke and lack the restrike phase typical of flashes of negative polarity. It has been found that lightning flashes that occur in the winter because of charge in low altitude clouds, sometimes accompanied by snow, are of positive polarity and of exceptional severity. There is also some evidence that these very high amplitude, positive flashes occur when positive charge from the top of a thundercloud is transported close to the earth before the charge has had a chance to flow off into the ionosphere. Aircraft operating in these regions, such as for example along the west coast of Japan, have experienced unusually extensive physical damage from positive flashes in that region.

2.3 Intracloud Flashes

Intracloud flashes occur between discreet charge centers within the same cloud. A distinguishing characteristic of intracloud flashes is that they seem to lack the intense first stroke phase typical of flashes to the earth, or at least

the electromagnetic radiation they produce suggests that this is so. Discreet charge centers may be involved in cloud-to-earth flashes as well, however, making it difficult for an airborne observer to tell whether an intracloud or cloud-to-earth flash has occurred.

In temperate regions, about two-thirds of all lightning flashes are intracloud flashes. In tropical regions, where cloud bases are generally higher above the earth, this ratio is higher.

Aircraft may be able to *trigger* lightning by flying through a heavily charged region of a cloud. In these instances, the lightning flash originates at the aircraft, and leaders propagate away from the aircraft in opposite directions. These are called bi-directional leaders, and they are propelled by electric fields that exist between regions of positive and negative charge in the cloud(s). There is no consensus as to whether this takes place routinely with commercial aircraft, but aircraft initiated flashes have definitely been observed with research aircraft that are flown into thunderstorms seeking to intercept lightning and measure its characteristics. The flashes that have been initiated seem to have more of the characteristics associated with intracloud lightning than with those associated with cloud-to-earth lightning.

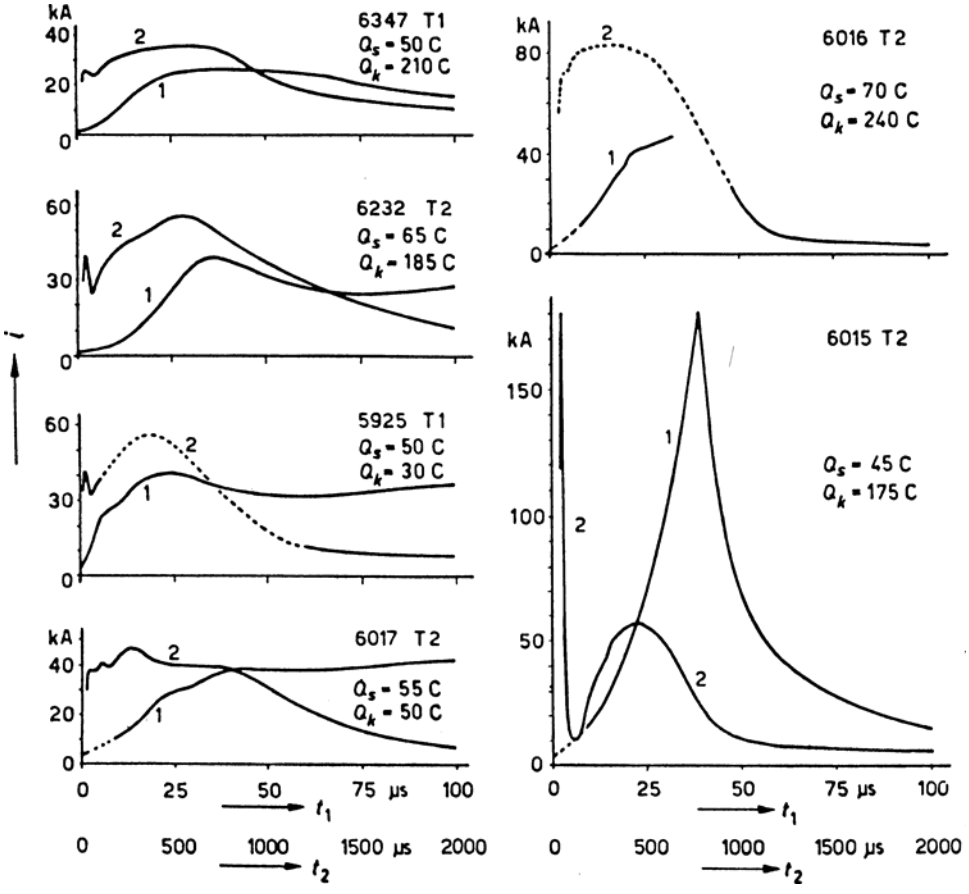

Fig. 2.20 Examples of strong, positive strokes [2.23]
t_1 Fast time scale 0 – 100 µs
t_2 Slow time scale 0 – 200 µs

Q_s = electric charge (in coulombs) within 2 µs of the origin.
Q_k = electric charge (in coulombs) in the continuing current after 200 µs.

In particular, the flashes that have been initiated by the aircraft have lacked a high amplitude strokes. These strikes more often have been populated by short-duration pulses of current whose amplitudes have usually been less than 50 kA and time durations of less than 20 μs. The question of aircraft-initiated lightning is discussed further in Chapter 3.

2.4 Superstrokes

From time to time, lightning flashes occur that seem to be far more powerful than normal. Some of the evidence of these so-called *superstrokes* is anecdotal, and derived merely by the examination of damage, such as conductors twisted by magnetic forces or glass shattered over wide areas. Other evidence comes from the observations of orbiting satellites, deployed to watch for evidence of nuclear explosions in the earth's atmosphere. All that is known of these superstrokes is that they exist and that they are rare. The satellite observations seem to indicate that superstrokes involve the upper portions of clouds. It has been observed that winter storms in parts of Japan, or other areas near seacoasts in the northern latitudes, sometimes produce lightning flashes of exceptional severity. This can probably be attributed to cold air masses flowing from land over warmer ocean areas, since these flashes are usually observed near seacoasts. They are especially prevalent over western seacoasts that experience cold, easterly air flows over warmer ocean areas. Superstrokes occur most frequently during the winter, when the freezing level in the clouds occurs at relatively low altitudes. Statistical data on these superstrokes is sparse, but efforts are underway to collect effects data for superstrokes that could be compared with experimentally generated lightning effects, to ascertain their amplitudes and charge transfers. Data from ground-based lightning detection and warning systems, operated by national weather reporting services in countries were these events are most frequently reported, are also being reviewed to determine statistics of the high amplitude events. There is no evidence that these superstrokes have interacted with aircraft or caused exceptional damage.

2.5 Statistical Information on Earth Flashes

Lightning flashes are quite variable from one to another. Peak currents, total duration, waveforms, number of strokes in the flash, charge transferred, etc., may all vary over wide limits, and only in general terms can one find a correlation between different parameters.

Data on the characteristics of lightning are best presented in statistical terms, the mode that will be used in the following sections.

One point that needs to be emphasized is that virtually all the data on lightning comes from measurements made at the earth's surface. These measurements are probably influenced by the growth of an upward leader from the measurement location, which is usually a tall tower, sometimes positioned atop a mountain or tall building. Some measurements have been made of the amplitude and waveforms of lightning currents passing through aircraft. Most of these are of leader currents and other current pulses (which might be termed strokes) having lower peak currents and longer times to crest than those observed at the earth's surface. Mostly, these differences can be explained by the fact that most of the flashes were initiated by the aircraft and were more characteristic of intracloud flashes than of cloud-to-earth flashes. In fact, very few of the flashes recorded by instrumented aircraft are believed to have been cloud-to-earth flashes. As noted earlier, intracloud flashes often lack the well-defined high-amplitude return stroke of cloud-to-earth flashes.

There exist two pre-eminent sets of statistical data on the characteristics of cloud-to-earth lightning; one made by Anderson and Erickson [2.24 - 2.25] and one by Cianos and Pierce [2.26]. Another summary was prepared in 2013 by the technical committees responsible for defining the lightning environments applicable to aircraft [2.27]. This summary included work of other researchers who studied downward and upward lightning flashes measured on towers and rocket triggered lightning.

2.5.1 The Anderson and Ericksson Data

Anderson and Ericksson [2.24 - 2.25] took measured waveform data from several measured lightning strikes (principally those recorded by Berger on Mt. San Salvatore) and derived several sets of statistical data. Fig. 2.21 gives the key to the data presented in Figs. 2.22 through 2.29. These figures show data for both initial and subsequent strokes. As speculated in §2.2.5, the data on rates of change of current (*di/dt*) may best represent the theoretical rate of change of current that should be applied in the formulation of aircraft protection and design certification standards. The data represents only negative cloud-to-earth flashes. Therefore, it should be noted that data in the <1% or >99% categories are not included, since the available data in these ranges was not statistically significant.

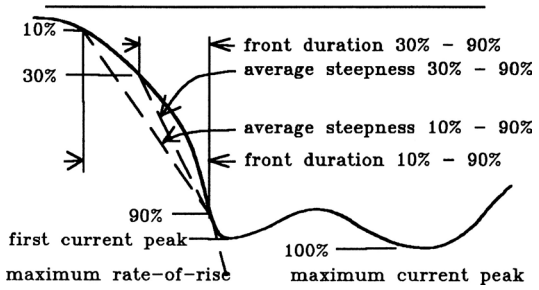

Fig. 2.21 Definition of waveform parameters. Adapted from [2.24].

Several important conclusions can be drawn from these sets of data:

1. First strokes statistically have a higher amplitude than subsequent strokes, but this is not true for all lightning flashes.

2. The second peak in the first stroke generally has the highest amplitude. This is probably due to charge from leader branches discharging into the main leader channel.

3. The rates of rise ('steepness') of subsequent strokes are statistically higher than those associated with first strokes.

4. On average, subsequent strokes reach 50% of the amplitudes of first strokes.

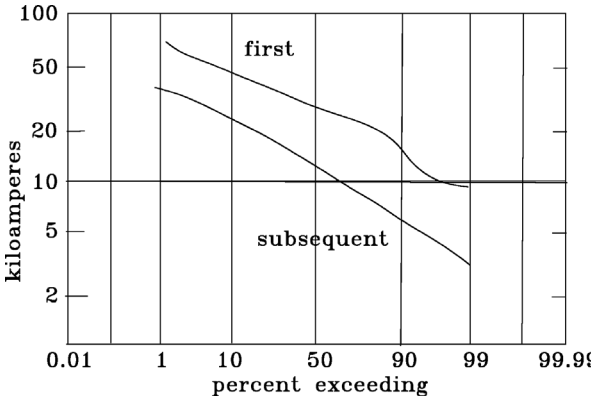

Fig 2.22 Amplitude of first current peak. Adapted from [2.24].

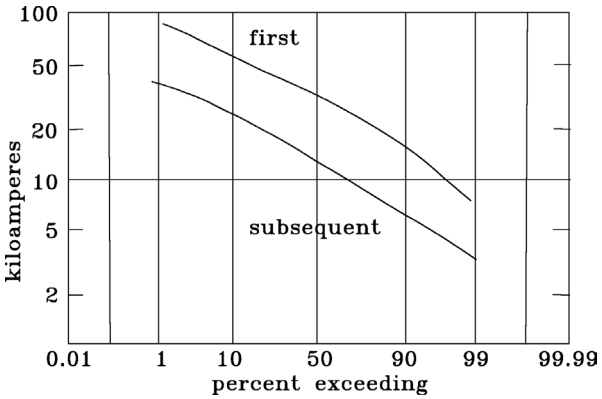

Fig 2.23 Amplitude of maximum current peak. Adapted from [2.24].

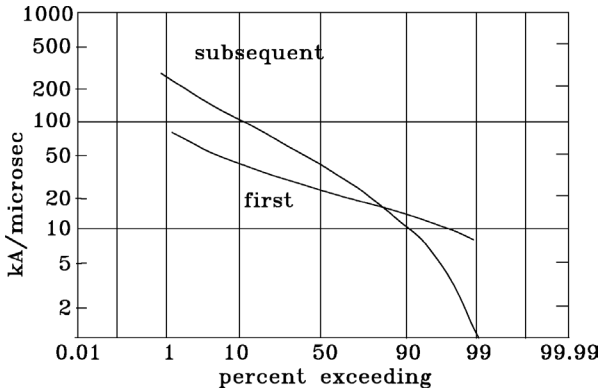

Fig 2.24 Maximum rate-of-rise. Adapted from [2.24].

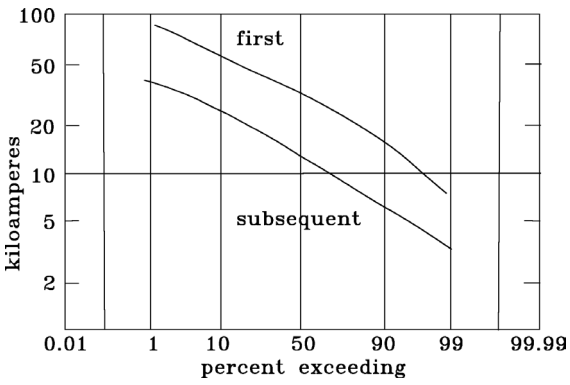

Fig 2.25 Average steepness at 30% - 90%. Adapted from [2.24].

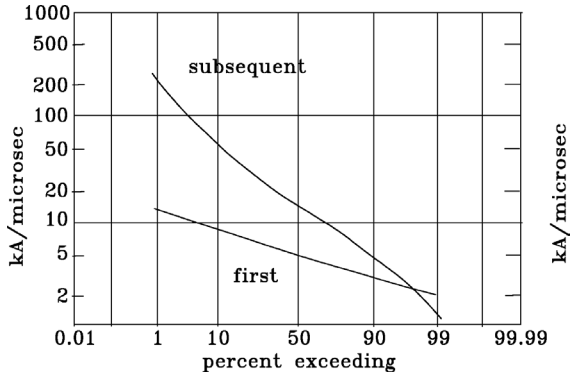

Fig 2.26 Average steepness at 10 - 90%.
Adapted from [2.24].

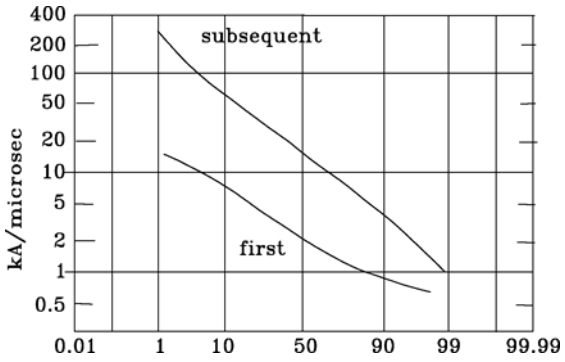

Fig 2.27 Average steepness at 10%.
Adapted from [2.24].

2.5.2 The Cianos and Pierce Data

Cianos and Pierce [2.26] observed that many of the statistical characteristics of lightning are nearly linear when plotted as log-normal distributions. They used this approach to present their own data, choosing the straight line that fit best. The following figures, summarizing their data, are reproduced from their report. These data were obtained from both positive and negative flashes, although, like the data from Anderson and Erickson, most of it pertains to negative flashes.

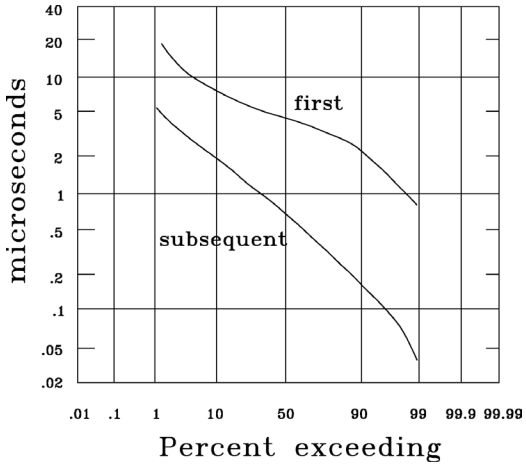

Fig 2.28 Front duration 10 - 90%. Adapted from [2.24].

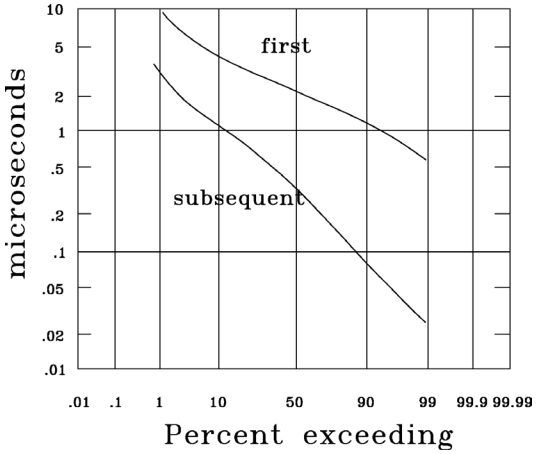

Fig 2.29 Front duration 30 - 90%. Adapted from [2.24].

Peak Currents

Fig. 2.30 presents statistics on the peak current amplitudes of lightning strokes. This is the parameter that determines the explosive, or shock wave effects of a lightning stroke. It is also related to the voltage developed across aircraft structural resistances and, hence, to the magnitudes of lightning-induced transients in aircraft electrical wiring

referenced to an airframe. It is also related to the maximum voltage developed across bonding resistances and, hence, to the possibility of arcing at structural interfaces.

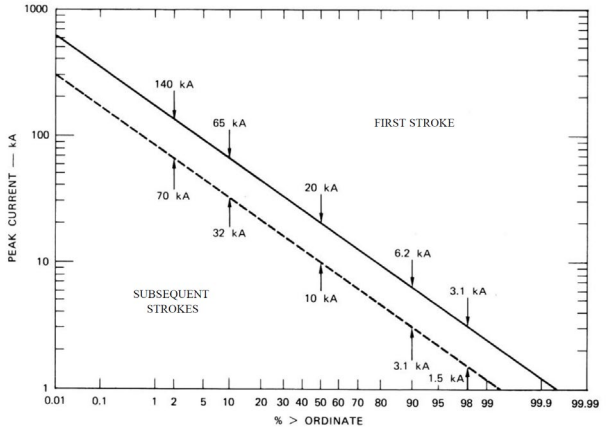

Fig. 2.30 Distribution of peak currents for first and subsequent strokes [2.26]

Parameters of lightning flashes summarized by Cianos and Pierce are found in Figs. 2.31 through 2.40. Key parameters are tabulated in Table 2.1.

The peak current amplitude of a lightning strokes is the parameter that determines the explosive, or shock wave effects of a lightning stroke. It is also related to the voltage developed across aircraft structural resistances and, hence, to the magnitudes of lightning-induced transients in aircraft electrical wiring installed in an airframe. It is also related to the maximum voltage developed across bonding resistances and, hence, to the possibility of arcing at structural interfaces.

Rates of change of current

The rate of change of a stroke current is subject to considerable interpretation since it is seldom practical to define the precise time at which the stroke starts or the precise time at which the peak amplitude is attained. Lightning strokes typically have a concave front, starting out slowly and then rising faster as the current gets higher. Thus, the effective rate-of-rise of a lightning stroke's current is not directly obtained by dividing the peak current by the front time. The rate-of-rise of lightning current is what determines how much voltage is magnetically induced in wire harnesses by the changing magnetic flux associated with the lightning stroke current.

Durations

The duration of a lightning stroke affects the severity with which metal structures may be deformed by magnetic forces. The duration of a stroke, which is measured in tens of microseconds, should not be confused with the duration of an entire lightning flash. A flash typically lasts for hundreds of milliseconds, or a large portion of a second.

There appears to be a connection between a flash's duration and the number of return strokes in the flash. Flash duration is also related to the time interval between strokes.

Charge transfer

Most of the charge is transferred by the continuing currents that flow between the strokes in the flash, rather than by the strokes themselves. In positive flashes, a much larger percentage of the charge is transferred in the stroke, as there is only one stroke in a positive flash. Both the time durations and the amplitudes of most positive flashes are larger than the corresponding measurements of negative strokes. Thus, it is primarily the amplitude and duration of the continuing currents that determine the thermal effects of a lightning flash.

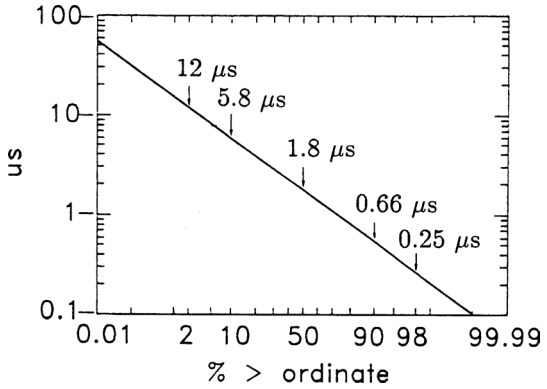

Fig 2.31 Time to first stroke current peak [2.26].

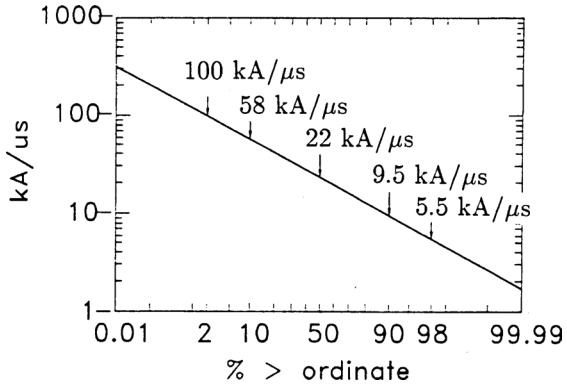

Fig 2.32 Rates of first stroke current rise [2.26].

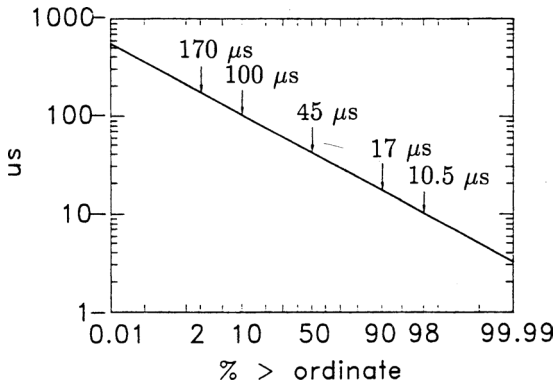

Fig. 2.33 First Stroke current, time to half value

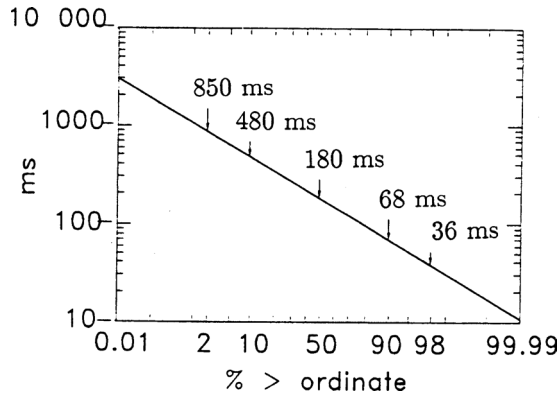

Fig 2.34 Duration of flashes to Earth [2.26].

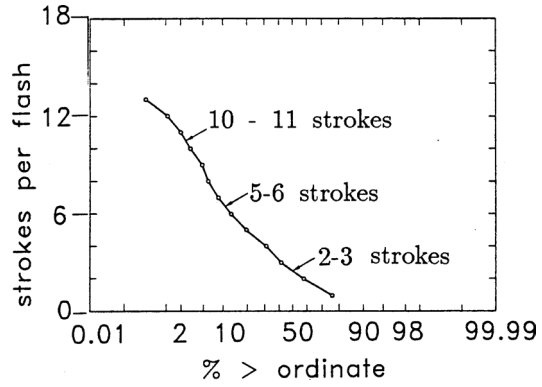

Fig 2.35 Number of strokes per flash [2.26].

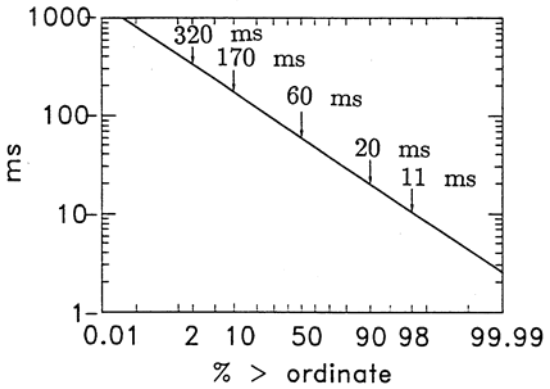

Fig 2.36 Time interval between strokes [2.26].

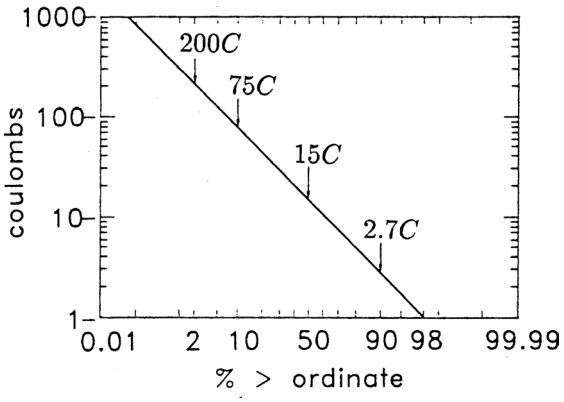

Fig 2.37 Charge per flash [2.26].

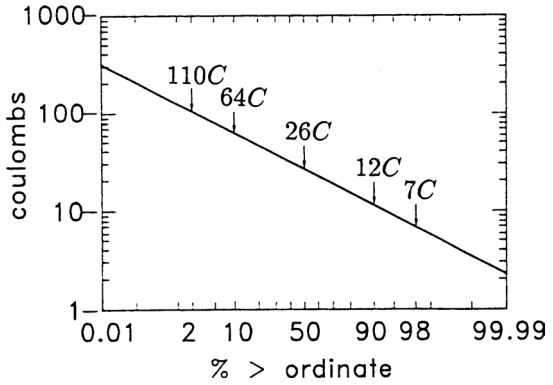

Fig 2.38 Charge in continuing current [2.26].

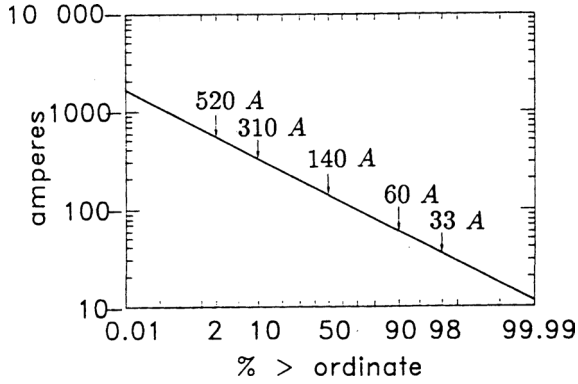

Fig 2.39 Amplitude of continuing current [2.26].

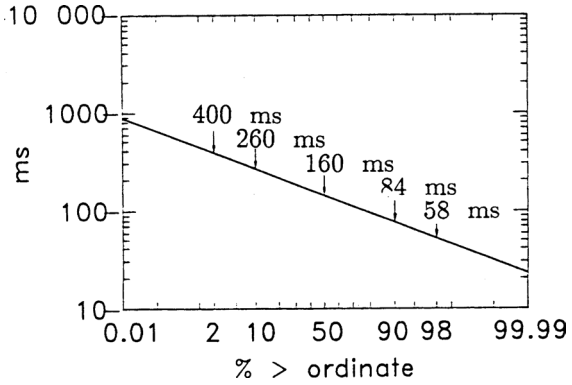

Fig 2.40 Duration of continuing current [2.26].

2.6 Summary of Data by Aircraft Lightning Standards Committees

A more recent summary of negative and positive lightning flash characteristics has been compiled by the technical committees responsible for formulating the lightning environment parameters applicable for aircraft lightning protection design and certification [2.27]. Tables 2.1 and 2.2 show the range of parameters from 95% probability (of that parameter being exceeded) to 5% probability, for negative and positive flashes. These tables are reproduced from [2.27]. Further details of each of the lightning parameters that are summarized in Tables 2.1 and 2.2 are provided in the appendix of [2.27].

Table 2.1 - Parameters for Negative Lightning Flashes Measured at Ground [2.27]

Parameters	Unit	Lightning Parameters 95%	Lightning Parameters 50%	Lightning Parameters 5%
Negative Flashes:				
Number of strokes		1 - 2	3 - 4	12
Time intervals between strokes	ms	12	47	180
Flash duration	ms	37	240	910
Charge in flash	C	1.4	16	98
Negative First Stroke:				
Peak current	kA	14	30	80
Peak rate-of-rise	kA/μs	5.5	12	32
Front duration[1]	μs	1.8	5.5	18
Stroke duration[2]	μs	30	75	200
Total charge[3]	C	1.1	5.2	24
Impulse charge	C	1.1	4.5	20
Action integral	A^2s	6×10^3	5.5×10^4	5.5×10^5
Negative Subsequent Strokes:				
Peak Current	kA	4.6	11	30
Peak rate-of-rise	kA/μs	20	37	200
Front duration[1]	μs	0.20	0.90	3.2
Stroke duration[2]	μs	8.3	31	110
Total charge[3]	C	0.30	1.6	12
Impulse charge	C	0.23	0.73	3.6
Action integral	A^2s	4.8×10^2	3.1×10^3	3.5×10^4
Continuing Current[4]:				
Amplitude	A	48	140	427
Duration	s	0.077	0.16	0.344
Charge	C	8	26	85

NOTE 1: The above lightning parameters do not necessarily occur together in one flash.

NOTE 2: The percentage figures represent percentiles, that is, the percentage of events having a greater amplitude than those given.

[1] 2 kA to Peak

[2] 2 kA to half peak (50%) value on tail

[3] Includes continuing current

NOTE 3: The values for 5% and 95% are interpolated from data in [2.26]

Table 2.2 - Parameters for Positive Lightning Flashes Measured at Ground [2.27]

Parameters	Unit	Lightning Parameters 95%	Lightning Parameters 50%	Lightning Parameters 5%
Positive Flashes:				
Flash duration	ms	14	85	500
Total charge[3]	C	20	80	350
Positive Stroke:				
Peak current	kA	4.6	35	250
Peak rate-of-rise	kA/μs	0.2	2.4	32
Front duration[1]	μs	3.5	22	200
Stroke Duration[2]	μs	25	230	2000
Impulse charge	C	2	16	150
Action integral	A^2s	2.5×10^4	6.5×10^5	1.5×10^7

NOTE 1: The above lightning parameters listed above do not necessarily occur together in one flash.

NOTE 2: The percentage figures represent percentiles, that is, the percentage of events having a greater amplitude than those given.

[1] 2 kA to Peak

[2] 2 kA to half peak (50%) value on tail

[3] Includes continuing current

NOTE 3: The values for 5% and 95% are interpolated from data in [2.26]

2.7 Engineering Models of Lightning Flashes

Pierce [2.26] gives several models of the current flowing in both typical and severe lightning flashes. These formed part of the basis for the lightning protection design for the space shuttle (Fig. 2.41, [2.28]). These models also influenced the lightning environment models presently used for the certification of aircraft. They are discussed in subsequent chapters. All of these are idealized models for purposes of design and analysis.

As such, they duplicate the effects of lightning, but the chance that any real lightning flash producing currents or combinations of currents of this exact shape is practically zero. The models shown in [2.26] are presented only for historical reference and should not be used as specifications for purposes of testing, since it may be very difficult and expensive for them to be produced in a testing laboratory. The external lightning environment applicable to protection design and certification of aircraft is discussed in Chapter 5.

2.8 Lightning Frequency of Occurrence

Thunderstorm days

For many years, weather bureau stations have recorded thunderstorm days (the number of days per year on which thunder is heard). This index, called the *isokeraunic level*, is shown for the continental United States (US) in Fig. 2.42. Similar data for the world is shown in Fig. 2.43 [2.29]. This information is of limited value, however, since no distinction is made between *cloud-to-cloud* discharges and *cloud-to-earth* and because there are no allowances made for variations in the durations of storms (A storm lasting an hour would be counted as heavily as one lasting several hours).

A better indicator of lightning frequency would be thunderstorm hours per year. Some weather bureau records are now being compiled from *thunderstorm hours*, rather than thunderstorm days, but not much of this data has yet been accumulated.

Despite its limitations, isokeraunic data is useful in assessing the likelihood of lightning strikes to earth-based objects. Pierce [2.26] has summarized some of the available data and concludes that if there were 25 thunderstorm days per year, there would be about 4 flashes to earth per year per km^2. The earth flash rate is not directly proportional to the isokeraunic level; it varies more as the square of the isokeraunic level. Anderson and Ericksson [2.24] also discuss the relationship between earth flash density and thunderstorm days.

It is important to note that thunderstorm days include both flashes among clouds and flashes to earth. There is some evidence that the proportion of flashes that go to earth is related to geographical latitude. It is believed that this relationship arises from variations in the average altitudes of clouds, which, in turn, have a bearing on the types of storms that form most frequently in each region. Pierce takes this factor into account in his discussion of the relationship between earth flash density and thunderstorm days. In general, the clouds in colder, higher latitudes are closer to earth than clouds in more temperate regions.

Flash counters

It would be better to measure the frequency of occurrence of lightning on counts of actual lightning flashes, rather than on counts of thunderstorms. Instruments are available to make such counts. One relatively simple type [2.30] detects the electric field changes produced by lightning and records, on an electromechanical counter, the number of times the field change exceeds a threshold value. By tuning the resonant frequency of the sensor, this device can be made to respond only to flashes within a certain geographical radius (usually about 30 km). These instruments can also be made to respond primarily to cloud-to-earth flashes and to reject field changes associated with intracloud flashes. Networks of such instruments have been deployed throughout the US, Europe, and South Africa.

The frequency with which lightning flashes strike a particular object on the earth depends strongly on the climactic and geographical conditions where the object is located and upon its height with respect to other objects nearby. Objects on the peaks of hills are more prone to being struck than objects in valleys. The probability that a given object will be struck also depends upon the 'lightning strike attraction area' covered by that object. For flat structures upon the earth, the strike attraction area is directly proportional to the area covered by the structure. If there is a protruding object on the earth, the strike attraction area depends upon the height of the object. With reasonable accuracy, it can be assumed that a structure of height h will intercept all flashes that would ordinarily strike the earth over a circle of radius 2h (see Fig. 2.44).

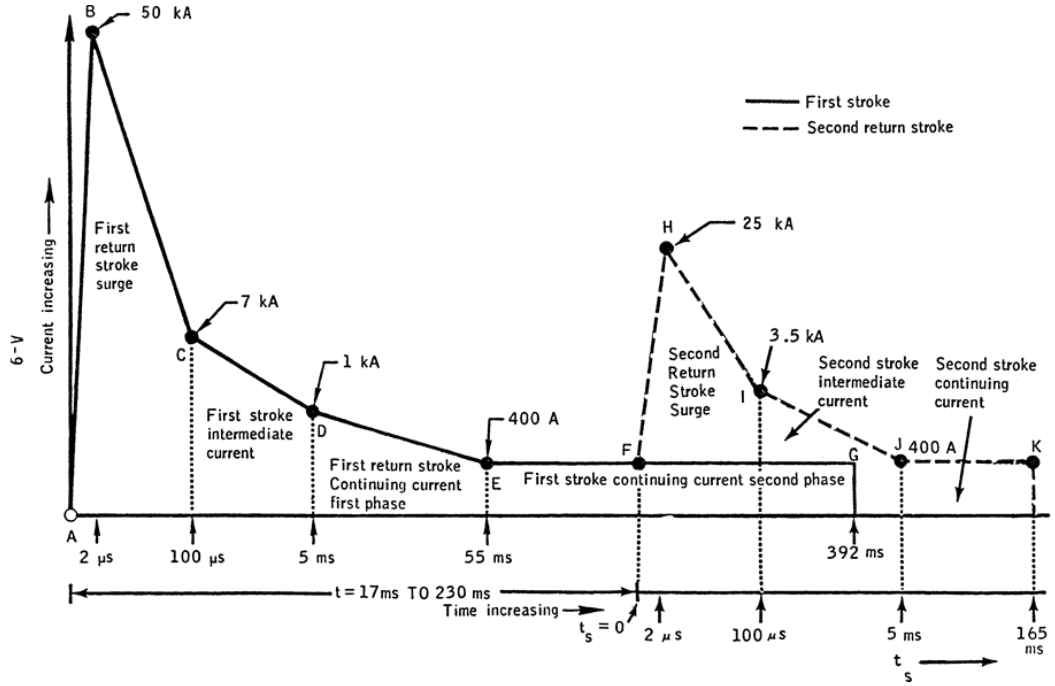

Fig. 2.41 The lightning model to which the space shuttle was designed [2. 28].

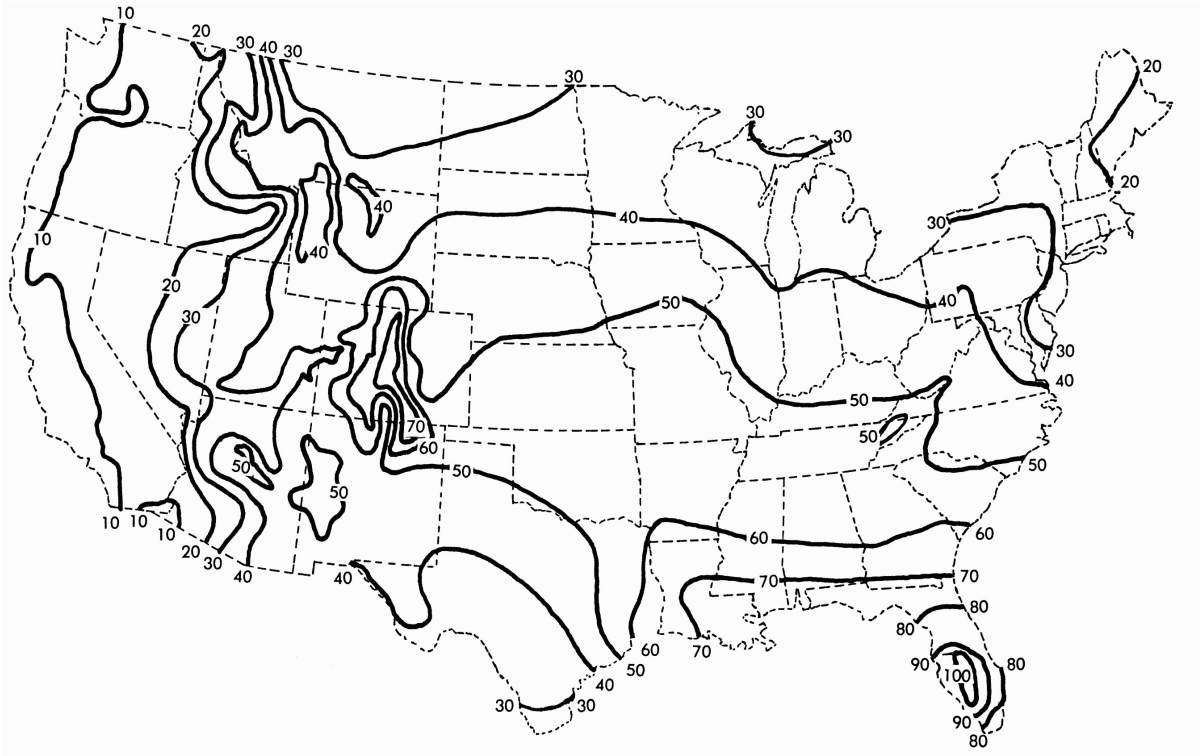

Fig. 2.42 Thunderstorm days (Isokeraunic Levels) within the continental United States.

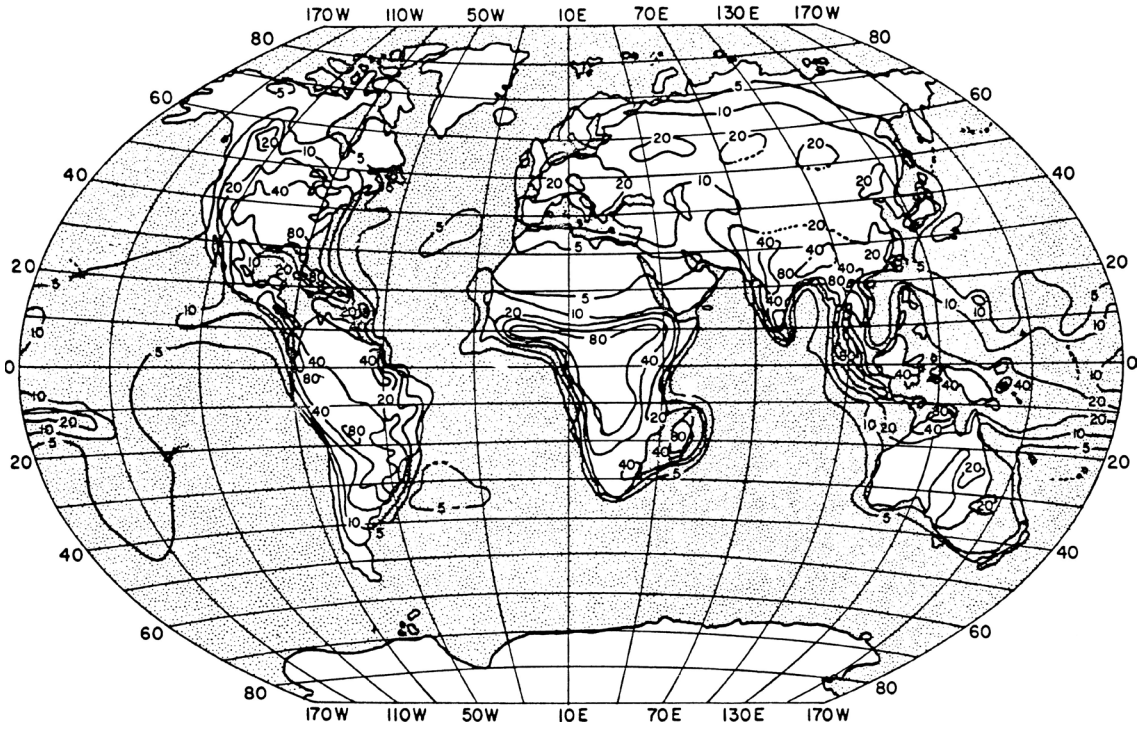

Fig. 2.43 Isokeraunic map of the world [2.29].

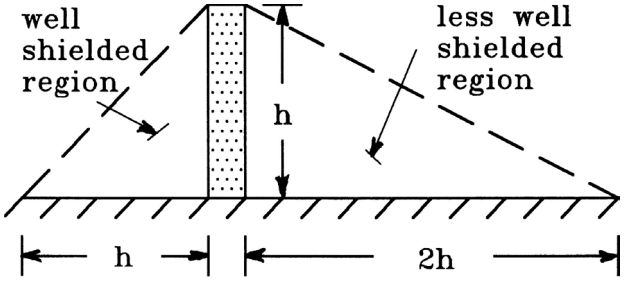

Fig. 2.44 Protected Areas

It is more difficult to predict how often a given aircraft will be struck in flight. Field experience seems to be the only reliable guide. Commercial aircraft in regularly scheduled service in the US are struck about once per year, frequently while in climb out to cruise altitudes, descent to landing, or holding patterns, and usually while flying at less than 20 000 ft. altitude. Transport aircraft are seldom struck while at cruising altitudes and cruising speeds. This is partly because thunderstorm areas and other electrified cloud regions can usually be avoided. Statistically, aircraft that are constrained to operate at low altitudes and along fixed corridors tend to be struck most often. Military aircraft tend to be struck less often than commercial aircraft, primarily because training flights are usually scheduled during good weather.

Lightning location

Another type of instrument [2.31 - 2.33] uses antennas to respond to both the electric and magnetic field changes produced by lightning, since by doing so one can determine the location of lightning flash producing the fields.

References

2.1 Lightning, Volume 1: Physics of Lightning, R. H.Golde - Editor, Academic Press, London and New York, 1977.Volume 2 of the series deals with lightning protection.

2.2 M. A. Uman, Lightning, McGraw Hill, New York, 1969.

2.3 M. A. Uman, The Lightning Discharge, Vol. 39 in International Geophysics Series, Academic Press, 1987.

2.4 The Earth's Electrical Environment, National Academy Press, Washington, DC, 1986.

2.5 Sir Basil Schonland, “Lightning and the Long Electric Spark, “Advancement of Science 19, November 1962, pp. 306-313.

2.6 C.T.R. Wilson, “Some Thunderstorm Problems,” Journal of the Franklin Institute. Vol. 208, 1, July 1929, pp. 1-12.

2.7 C.T.R. Wilson, “Investigations on Lightning Discharges on the Electrical Field of Thunderstorms,” *Proceedings of the Royal Society of London*, Series A, 221, 1920, pp. 73-115.

2.8 Sir George Simpson, “The Mechanism of a Thunderstorm,” *Proceedings of the Royal Society of London*, Series A, 114, 1927, pp. 376-99.

2.9 E.A. Evans and K.B. McEachron, “The Thunderstorm,” *General Electric Review*, September 1936, pp. 413-25.

2.10 G. C. Simpson, “Lightning," *Journal of the Institution of Electrical Engineers*, Vol 67, Nov. 1929, pp. 1269-82.

2.11 G.C. Simpson and F. J. Scrase, “The Distribution of Electricity in Thunderclouds," *Proceedings of the Royal Society of London*, Series A 161, 1937, pp. 3090-52.

2.12 E. R. Williams, “The Electrification of Thunderstorms," *Scientific American*, Nov. 1988, pp. 88-99.

2.13 R.H. Golde, *Lightning Protection*, Edward\newline Arnold, London, 1973.

2.14 C.F. Wagner and A.R. Hileman, “The Lightning Stroke-II,” *AIEE Transactions*, Vol 80, Part III, American Institute of Electrical Engineers, New York, New York (October 1961), pp. 622-42.

2.15 K. Berger and E. Vogelsanger, “Photographische Blitzuntersuchungen der Jahre 1955...l965 auf dem Monte SanSalvatore," *Bulletin des Schweizerischen Elektrotechnischen Vereins*, 14 (July 9, 1966), pp. 599-620.

2.16 K. Berger, “Novel Observations on Lightning Discharges: Results of Research on Mount San Salvatore,” *Journal of the Franklin Institute*, Vol. 283, 6 June 1967, pp. 478-525.

2.17 R. H. Golde, “The Lightning Conductor”, *Journal of the Franklin Institute*, June 1967, pp. 457.

2.18 R. H. Golde, “The Lightning Conductor", pp. 451- 478.

2.19 J.L. Marshall, *Lightning Protection*, John Wileyand Sons, New York, 1973.

2.20 C.F. Wagner, “Lightning and Transmission Lines,” *Journal of the Franklin Institute*, 283, 6 (June 1967): 558-594: 560, and C.F. Wagner, Stroke," *IEEE Transactions on Power Apparatus and Systems* Vol. 82, October 1963, pp. 609-17.

2.21 C.F. Wagner and A.R. Hileman, “Surge Impedance and its Application to the Lightning Stroke,” *AIEE Transactions*, Vol. 80, Part 3, February 1962, pp. 1011.

2.22 Berger, “Novel Observations,” op. cit., pp. 492.

2.23 Berger, “Novel Observations,” op. cit., pp. 494.

2.24 R. B. Anderson and A. J. Ericksson, “Lightning Parameters for Engineering Applications,” *ELEK 170, CIGRE Study Committee 33*, Suceava, Roumania, 25- 29 June 1979.

2.25 R. B. Anderson and A. J. Ericksson, “Lightning Parameters for Engineering Applications,” *Electra*, Vol.69, pp. 65-102.

2.26 N. Cianos and T. Pierce, A Ground-Lightning Environment for Engineering Use, *Technical Report 1*, prepared by the Stanford Research Institute for the McDonnell Douglas Astronautics Company, Huntington Beach, California, August, 1972.

2.27 Aircraft *Lightning Environment and Related Test Waveforms, SAE ARP 5412B,* Society of Automotive Engineers, Inc., Warrendale, PA USA, January 2013

2.28 *Space Shuttle Program Lightning Protection Criteria Document, JSC-07636, Revision A*, National Aeronautics and Space Administration, Lyndon B. Johnson Space Center, Houston, Texas (November 4, 1975), pp. A-5.

2.29 D. W. Bodle et al, *Characterization of the Electrical Environment*, University of Toronto Press, Toronto, Ontario, 1976, pp. 14.

2.30 Anderson and Ericksson, Electra op. cit.

2.31 E. P. Krider, R. C. Noggle, and M. A. Uman, “A Gated Wideband Magnetic Direction Finder for Lightning Return Strokes", *J. Geophys. Res.*, Vol. 82, 1976, pp. 951-960.

2.32 E. P. Krider, R. C. Noggle, A. E. Pifer, and D. L.Vance, “Lightning Direction Finding Systems for Forest Fire Detection”, *Bull. Am. Meteorol. Soc.*, Vol. 61, 1980, pp. 980-986.

2.33 R. E. Orville, R. B. Pyle, and R. W. Henderson, ``AnEast Coast Lightning Detection Network", *IEEE Trans. Power Systems*, Vol. PWRS-1, 1986, pp. 243-246.

Chapter 3

AIRCRAFT LIGHTNING ATTACHMENT PHENOMENA

3.1 Introduction

This chapter discusses the circumstances under which aircraft are struck by lightning and considers the question of whether aircraft trigger lightning or whether they just happen to be in the path of a naturally occurring flash. It also deals with how the lightning flash interacts with aircraft surfaces and defines lightning strike zones within which these surfaces fall. Methods for locating the zones on specific aircraft are discussed in Chapter 5.

Statistics on lightning strikes reported by aircraft operators seem to indicate that no aircraft is likely to receive more than one or two lightning strikes in a year, but that the geographical regions where aircraft operate, as well as the flight altitudes and operational restrictions regarding routes and traffic patterns, do influence the frequency of strike occurrences. The question also arises: "If lightning strikes do in fact occur infrequently, can they be avoided altogether?" Because some aircraft seem to experience more than their 'fair share' of lightning strikes, a related question also arises: "Why are some aircraft (apparently) more likely to be struck than others?"

To answer these questions, a considerable amount of research into the effects of such factors as aircraft size, flight altitude, weather conditions, air speed, engine exhaust, and even microwave radar emissions, on lightning strike formation have been undertaken over the years. Much of this research has been aimed at answering the question of whether or not an aircraft can, in fact, somehow, acquire enough electric charge to produce its own lightning strike or if it can trigger an impending flash from charge within a nearby cloud. While some of the findings are inconclusive, others have provided definite answers to some of these questions. This chapter summarizes what has been learned about the aircraft's influence on lightning strike occurrence and dispels some misconceptions about this phenomenon. It also examines how other factors, such as flight and weather conditions, effect the probability of lightning strikes to aircraft. In conclusion, this chapter emphasizes that lightning strikes to airplanes cannot be entirely avoided and that it is therefore important to incorporate lightning protection into all new aircraft designs.

The prevailing atmospheric and flight conditions at the times when aircraft have been struck by lightning have been of interest since the beginning of powered flight because lightning and other thunderstorm effects, such as turbulence and icing, are to be avoided if possible. To learn more about these conditions, several aircraft lightning strike incident reporting projects have been implemented. Beginning in 1938, the Subcommittee on Meteorological Problems of the National Advisory Committee for Aeronautics (NACA) prepared and distributed a sixteen-page questionnaire to airlines and the Armed Forces [3.1]. Pilots filled out these questionnaires after lightning strike incidents and forwarded them to the NACA subcommittee for analysis. The questionnaire was evidently too lengthy for widespread use and was discontinued by 1950. Nevertheless, the program provided important data for the first time on the prevailing meteorological conditions when strikes occurred and the resulting effects on the aircraft.

Following that, programs were conducted by the Lightning and Transients Research Institute (LTRI) [3.2], the Federal Aviation Administration (FAA) [3.3] and Plumer and Hourihan of General Electric, together with five United States (US) commercial airlines [3.4]. This latter project is known as the Airlines Lightning Strike Reporting Project. Anderson and Kroninger of South Africa [3.5], Perry of the British Civil Aviation Authority [3.6], and Trunov of the USSR National Research Institute for Civil Aviation [3.7] have also conducted studies. More recent data from the Airlines Lightning Strike Reporting Project has been reported by Lightning Technologies Inc. (LTI) [3.8].

Strike incidence data, based largely on turbojet or turboprop aircraft, is usually summarized according to the following categories:

1. Altitude.
2. Flight path; that is, climbing, level flight, or descent.
3. Meteorological conditions.
4. Outside air temperature
5. Lightning strike effects on the aircraft

Altitude, flight path, meteorological conditions, and air temperature are topics discussed in this chapter. Lightning strike effects on aircraft are discussed in Chapter 4.

3.2 Lightning Attachment Point Definitions

The lightning flash initially attaches to, or enters, the aircraft at one location and exits from another. Usually these attachment locations are extremities of the aircraft, such as the nose or a wing tip. For the purposes of this text, they will be called the *initial entry* and *initial exit points*. In the initial attachment process, 'junction leaders' originate from the aircraft and propagate into the air at a distance of perhaps 50 meters or more until they intercept the approaching lightning leader of a naturally-occurring flash. If the lightning event is 'triggered' by the presence of the airplane in the electric field produced by cloud electrification, then leaders originate from (more or less) opposite extremities of the airplane and propagate away from the airplane in opposite directions, toward the regions of opposite- polarity charge.

During the leader attachment process, and for the duration of the lightning channel's attachment to the airplane, current flows *into* one point on the aircraft and *out* of another. The 'entry' point may be either an anode or a cathode (that is, a spot where electrons are either entering or exiting the aircraft.) It is usually not possible to tell, from the visual evidence after the strike, whether a given attachment point was an anode or a cathode and usually this information would be of little practical importance. Instead, by convention, the marks left on aircraft skins by lightning attachment at forward or upper locations have usually been called *entry points* and those at aft or lower locations on the aircraft have been termed *exit points*.

Since most aircraft fly further than their own lengths within the lifetime of most flashes, the location of the entry point must change as the flash reattaches to other points aft of the initial entry point.

The location of the exit points may also change, particularly if the initial exit point is at a forward portion on the aircraft. Thus, for any one flash, there may be many entry or exit points. The following definitions are used:

lightning attachment point: Any point where the lightning flash attaches to the aircraft.

initial entry point: The point where the lightning leader first enters the aircraft (usually an extremity).

final entry point: The point where the lightning channel last enters the aircraft (usually a trailing edge).

initial exit point: The point where the lightning leader first `exits' from the aircraft (usually an extremity).

final exit point: The point where the lightning channel last exits from the aircraft (usually a trailing edge).

swept "flash" (or channel) points: points where the flash channel reattaches between the initial and final points, usually associated with the entry part of the flash channel.

3.3 Circumstances Under Which Aircraft are Struck

The following paragraphs summarize the important findings from the transport aircraft data gathering projects noted previously and describe the flight and weather conditions under which lightning strikes are most common. Knowledge of these conditions may help pilots and minimize future lightning strike incidents, but such incidents can never be entirely avoided, except by operating entirely in clear, "blue sky" conditions, far from clouds.

3.3.1 Altitude and Flight Path

Fig. 3.1 shows the altitudes at which aircraft are typically struck, according to the reporting projects discussed above. In the figure, these altitudes are juxtaposed with a side-elevation view of a typical cumulonimbus (thunder) cloud. The turbojet and turboprop data from the four summaries are in close agreement. For comparison, the data from the earlier piston aircraft survey of Newman [3.2] are also presented.

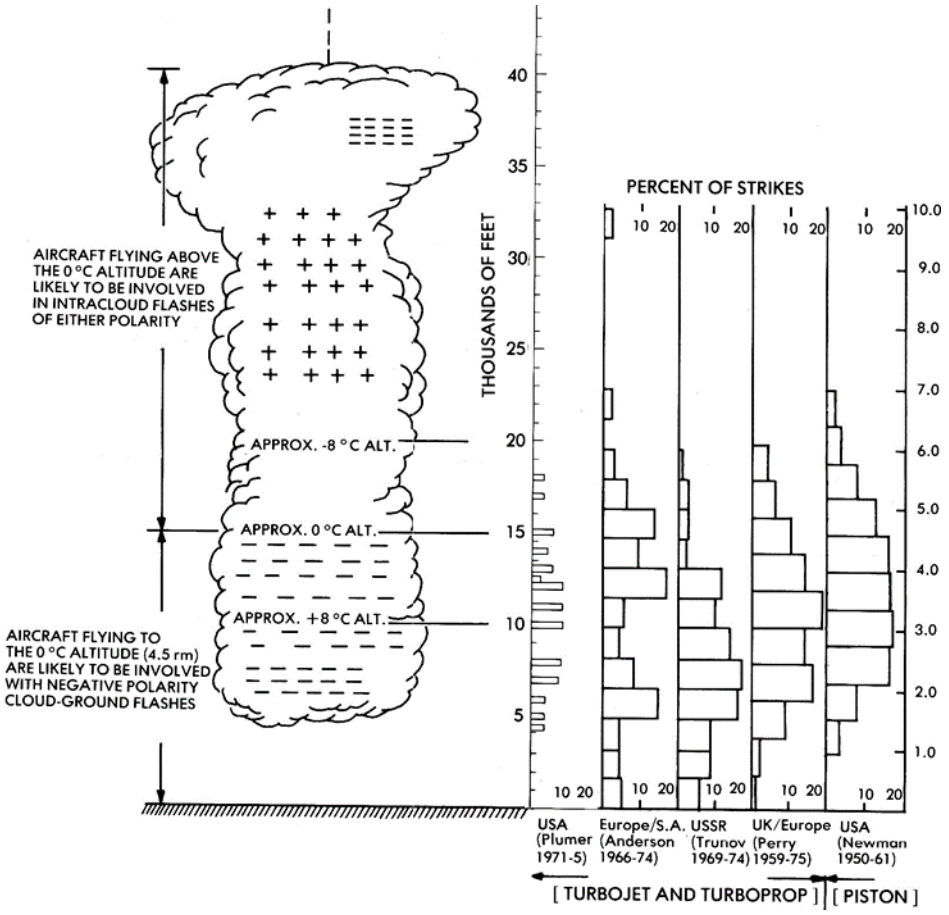

Fig. 3.1 Aircraft lightning strike incidents vs. altitude.

Cruise altitudes of 10 000 - 13 000 m (33 000 - 41 000 ft.) for turbo-jet powered aircraft are considerably higher (10 000 m) than those of earlier piston-powered aircraft, which flew at about 3 000 - 6 000 m (10 000 - 20 000 ft.); yet Fig. 3.1 shows the altitude distribution of lightning strike incidents to be nearly the same. This fact indicates (1) that there are more lightning flashes to be intercepted below about 6 096 m (20 000 ft.) than above this altitude, and (2) that jet aircraft are being struck at lower than cruise altitudes, that is: during climb, descent, or hold operations. Flight regime data obtained from the aircraft lightning strike reporting projects shown in Fig. 3.2 [3.8] confirm this.

If the strike altitudes shown in Fig. 3.1 are compared with the electrical charge distribution in the typical thundercloud, shown in this figure, it is evident that strikes occurring above about 3 048 m (10 000 ft.) are associated with intracloud flashes between positive and negative charge centers in the cloud (or between adjacent clouds), whereas

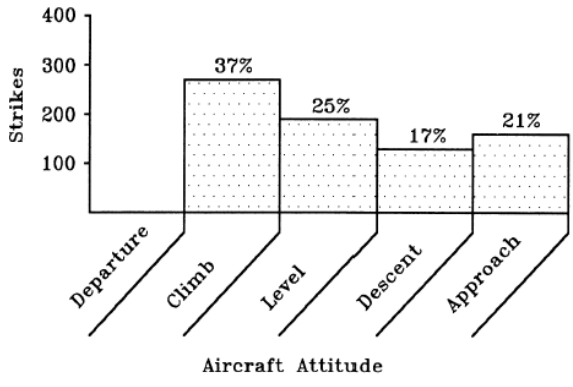

Fig. 3.2 Flight regime when struck.

some of the lightning strikes below about 3 048 m (10 000 ft.) probably result from cloud-to-ground flashes. Strike incidents occurring above 6 096 m (20 000 ft.) occur less frequently, because aircraft at these altitudes can more easily divert around thunderclouds and other cloud regions than can aircraft at lower altitudes.

3.3.2 Synoptic Meteorological Conditions

The data discussed thus far seems to imply that an aircraft must be within or beneath a cloud to receive a strike and, (since cloud electrification is often accompanied by, and possibly due to, some form of precipitation) that most strikes would occur when the aircraft is within a cloud, or in or near regions of precipitation. Strike incident reports show that precipitation (usually rain) is present when most lightning strikes occur, but other lightning strikes occur to aircraft in or beneath a cloud when there is no precipitation nearby, and even (much more rarely) to aircraft flying in clear air at a supposedly safe distance from a thundercloud. Commercial and military pilot training and established procedures instruct pilots to circumvent thunderclouds or regions of precipitation evident either visibly or on radar, but strikes to aircraft flying 25 miles from the nearest radar returns or precipitation have, nevertheless, been reported. Flight lore aside, there have been no confirmed reports of aircraft receiving the so-called "bolt from the blue" when operating in clear air a long distance from clouds. Significant amounts of atmospheric electric charge are always associated, if not with precipitation, at least with some form of cloud. Positive ions and electrons are associated with cloud particles, such as raindrops, snowflakes, ice crystals, and dust. There appears to be minimal charge in free air.

The weather conditions that prevailed during the time of reported strikes would, perhaps, be of the most interest to aircraft operators. Unfortunately, there is no universal data bank for this type of data, but several surveys have been conducted, including those of [3.2] through [3.8].

When turbojet-powered aircraft were introduced into widespread commercial service in the 1960s, a considerable amount of curiosity arose regarding the possible influences of jet exhaust, higher flight altitudes and (especially) higher airspeeds on lightning strike occurrences and the effects of strikes on these new airplanes. An important study, involving a more limited number of strikes, but containing more weather information than the broad-based surveys referenced above, is that of H.T. Harrison [3.9] of the synoptic meteorological conditions prevailing for 99 lightning-strike incidents occurring between July 1963 and June 1964.

Table 3.1 lists the synoptic weather-type and the percentage of strike incidents occurring in each weather type. Examples of the most predominant synoptic conditions are presented in Fig. 3.3(a) through 3.3(d).

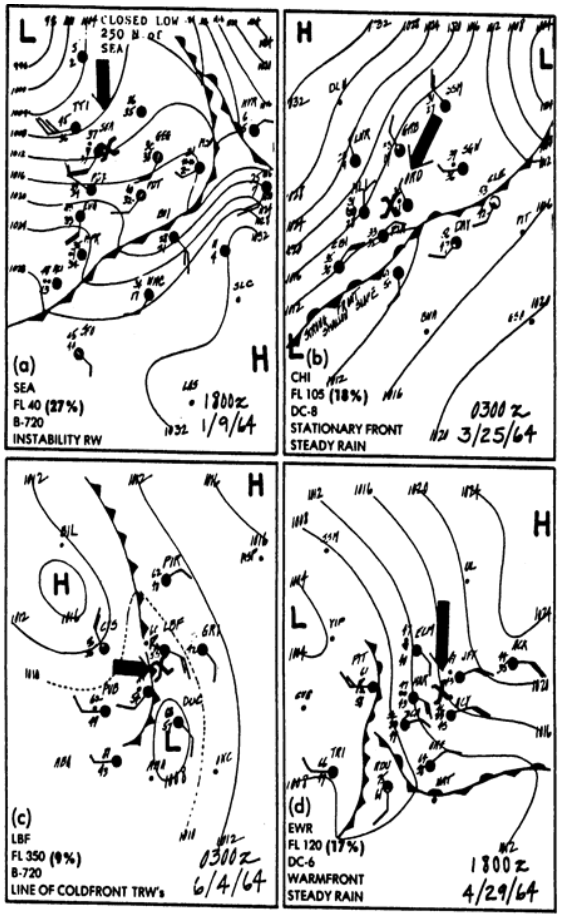

Fig. 3.3 Examples of most recent synoptic meteorological conditions when aircraft have been struck. Tips of arrows indication positions of aircraft when struck.

Harrison has drawn the conclusion that any condition that causes precipitation may also be expected to produce electrical discharges (lightning), although he adds that no strikes were reported in the middle of warm front winter storms. Data from the Airlines Lightning Strike Reporting Project, reported by Rasch et al [3.4] shows that lightning strikes to aircraft in the US and Europe occur most often during the spring and summer months, when frontal weather conditions that produce thunderstorms and other regions of convective activity are most prevalent.

Table 3.1
Synoptic Types Involved with
99 Electrical Discharges
July 1963 to June 1964

Synoptic Type	Percentage
Airmass instability	27
Stationary front	18
Cold front	17
Warm front	9
Squall line or instability line	9
Orographic	6
Cold LOW or filling LOW	5
Warm sector apex	3
Complex or intense LOW	3
Occluded front	1
Pacific surge	1

3.3.3 Immediate Environment at Time of Strike

Cloud electrification is generally believed to be associated with precipitation in freezing conditions, and to happen within or above the altitudes where freezing occurs within clouds. Such conditions occur where cold air-masses collide with warm air-masses that contain moist air.

It is also important to note that many strike incidents have been reported where no bona fide thunderstorms have been visually observed or displayed on ground-based or aircraft weather radars. Harrison [3.9], for example, reports that United Air Lines flight crews reported 99 cases of static discharges or lightning strikes in flight during the period of his survey. Correlation of these incidents with weather conditions prevailing in the vicinity and in the general area at the time of strike gave the results shown in Table 3.2.

Table 3.2
Percentage of Strike Incidents vs Reported Thunderstorms

Thunderstorms reported in vicinity	33%
Thunderstorms reported in general area	24%
No thunderstorms reported	43%

Figs. 3.4, 3.5, and 3.6 show the immediate environment of the aircraft at the times of the 881 strikes reported in [3.8]. In over 80% of the strikes reported, each aircraft was with in a cloud and was experiencing precipitation and some amount of turbulence. The reports of turbulence indicate convective activity.

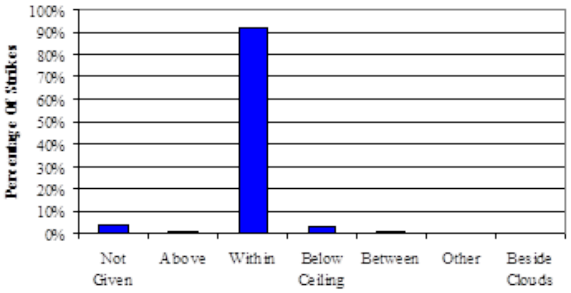

Fig. 3.4 Location with Respect to clouds Comparison (*Combined 1971-1987 and 1991-1999).*

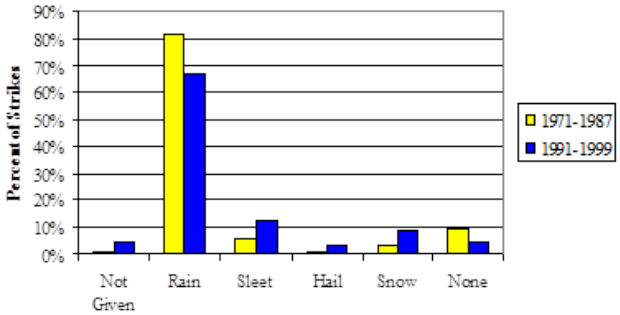

Fig. 3.5 Precipitation at time of aircraft lightning strikes.

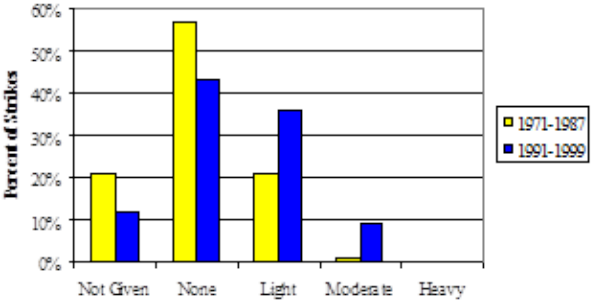

Fig. 3.6 Turbulence experienced when lightning strikes have occurred.

The incident reports above also show that most aircraft strikes have occurred when the aircraft is within ±10 degrees of the freezing point of water (0 °C). Fig. 3.7 [3.8] shows the distribution of lightning strikes to aircraft as a function of outside air temperature. Freezing temperatures (and below) are thought to be associated with the electrical charge separation process. Of course, strikes to aircraft at temperatures higher than +10 °C have occurred when the aircraft was beneath a cloud that was close to the ground, or when the aircraft was parked on the ground, where the temperature has been as high as +30 °C.

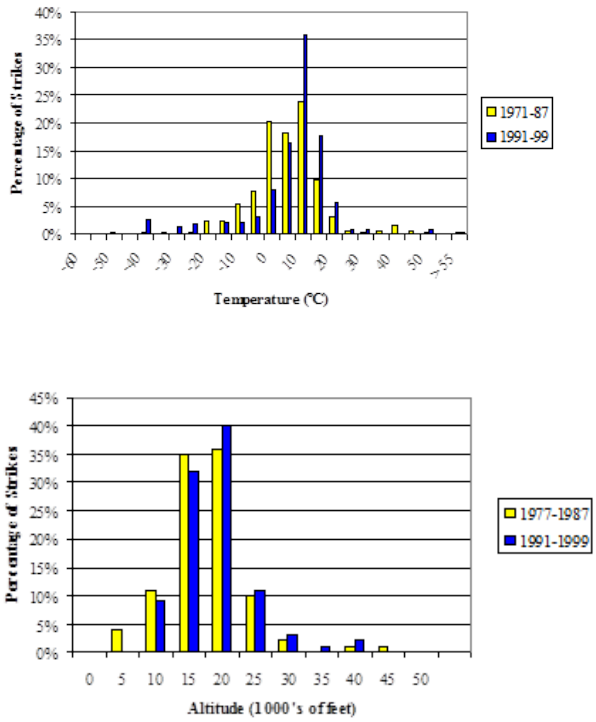

Fig. 3.7 Distribution of lightning strikes.

3.3.4 Thunderstorm Avoidance

Clearly, whenever it is possible to avoid the severe environments that thunderstorms present, it is desirable to do so, for, even if the aircraft is adequately protected against lightning effects, the turbulence caused by wind and precipitation in or near thunderstorms presents a serious hazard to safe flight. Consequently, the operating procedures of commercial airlines and other air carriers advise strongly against penetrating known thunderstorm conditions, or areas of heavy precipitation, icing, turbulence, and wind shear. Lightning flashes are associated with all of these conditions.

Thunderstorm indication

In attempts to avoid thunderstorm regions, pilots use several indicators:

1. Visual sighting of thunderclouds (cumulonimbus) in daytime and of lightning at night

2. Airborne radar patterns of heavy precipitation areas

3. Airborne lightning strike indicators, which sense electromagnetic radiation from distant flashes and present their range and bearing on cockpit displays.

4. Weather advisories, relayed by Air Traffic Control (ATC) or other weather services to aircrews, combined with specific guidance for thunderstorm avoidance.

Methods of avoidance

Methods of thunderstorm avoidance in common use are, in order of preference:

1. Circumnavigation of visible thunderstorm conditions, as indicated by visual observations and/or airborne weather radar displays. Ideally, these conditions should be kept at a distance of 25 miles or more, but traffic constraints often limit this distance.

2. Circumnavigation of areas of heavy precipitation indicated on airborne weather radar displays.

3. Flying over the tops of thunderclouds and other cloud formations.

The degree to which any of these measures is successful depends on the accuracy of the information received by the pilots and upon air route traffic control and flight schedule constraints.

Weather radar

Aside from visual observation, which has obvious limitations, the most common method of detecting thunderstorms is using airborne weather radar. Radar, however, cannot detect clouds themselves; it usually detects only liquid droplets. Unfortunately, aircraft radars do not see frozen precipitation as well as they see wet precipitation. So thunderstorm tops, which are composed of mostly low-reflectivity precipitation particles, are not seen well by aircraft radar. Thus, only the presence of wet precipitation in the cloud produces a radar echo. This limitation allows aircraft to experience occasional encounters with hail, and with lightning. A typical C-band airborne weather radar presentation of a thunderstorm (cumulonimbus) cloud with active precipitation and frequent lightning is shown in Fig. 3.8 [3.10]. The pictures were taken during an early research project carried out by Beckwith of United Air Lines to determine the weather detection capability of airborne radar. The photographs shown were taken during a United Air Lines flight from Chicago to Denver on August 3, 1960. Fig. 3.8 shows the northern end of a line of severe thunderstorms, developed from a cold front in Illinois. A detour to the North was planned and successfully executed with the aid of this radar presentation. The flight remained in clear and generally smooth air while making the detour. The strong echoes were easily detected with a slight upward tilt of the radar antenna, to eliminate ground clutter.

Considering the variable nature of the cloud conditions that produce electric charge and lightning strikes to airplanes, and the limited information available to pilots on their locations and severities, it is not surprising that there are varying opinions as to what detour distance is adequate to avoid turbulence and lightning. Primarily, a pilot is advised to use distances commensurate with the specific capability of the radar available.

Weather radar, however, is not a foolproof means of detecting and avoiding thunderstorms or other lightning strike conditions, because situations exist in which radar is not capable of distinguishing thunderstorm returns from the ground returns or ground clutter.

In this case, returns from the ground (ground clutter) obscured the return from the storm. However, if ground clutter does obscure a storm return at low flight altitudes and an aircraft is successful in avoiding all thunderstorms by the recommended distances of up to 25 miles, the severe turbulence associated with thunderstorms is usually also avoided. Nevertheless, lightning flashes may extend farther outward from the storm center than turbulence and, for this reason, lightning is not as easily avoided.

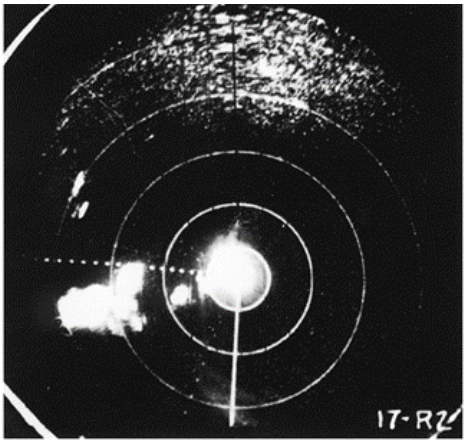

TIME: 0026Z
ALTITUDE: 28 000 FT.
RANGE MARKS: 10-MILE
ANT.: 1½° UP
HEADING: 255° TRUE
STRONG ECHOES HERE ARE THE N END OF A LINE OF THUNDERSTORMS WHICH WERE PRODUCING SEVERE WIND AND LIGHTNING DAMAGE BELOW. LESS THAN ONE HOUR EARLIER, HAILSTONES OF GOLF BALL SIZE WERE REPORTED IN THE AREA OF THE NEAREST LARGE ECHO. STORM PICTURED ON PHOTO 17-C2.

(a) Radar presentation

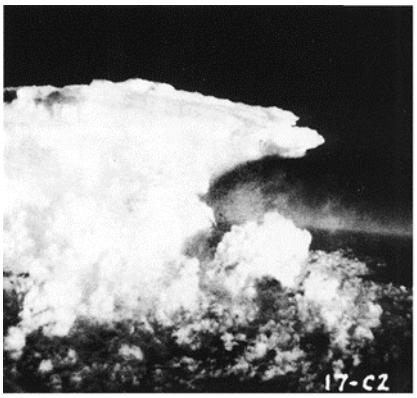

TIME: 0028Z
ALTITUDE: 28 000 FT.
SOUTH OF DUBUQUE, IOWA, LOOKING SE TO S AND W EDGE OF THUNDERSTORM LINE. THIS CUMULONIMBUS WAS BUILT TO AN ESTIMATED ALTITUDE OF 45 000 FEET. ECHO ON PHOTO 17-R2 CORRESPONDS TO THIS VISUAL.

(b) Visual appearance of storm

Fig. 3.8 Radar presentation and subsequent photograph of a thunderstorm.

Color radar

Many airborne weather displays use colors to distinguish between different intensities of precipitation, which are defined in terms of dBz. The boundaries between bands of different color are the colors mentioned above. A typical color-weather radar display is shown in Fig. 3.9 [3.11]. Some decaying thunderstorms, or other electrified cloud regions, may not present distinctive radar echoes. Such conditions sometimes become embedded in expanding anvils, stratiform or cirrus clouds, so as to render them invisible.

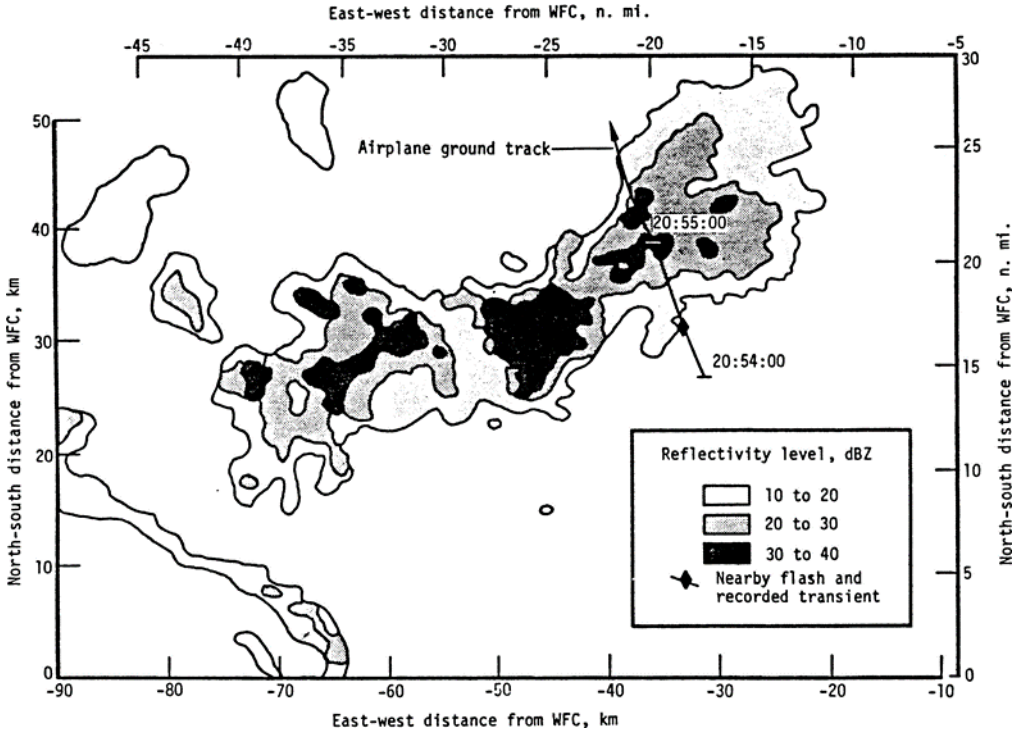

Fig. 3.9 Reflectivity contours at the time of a strike near to the F-106B. Flash 4, 20:54:21.9 GMT, July 22, 1980. Taken by NASA -Wallops SPANDAR radar at 20:56:51.5 GMT with a radar tilt angle = 0 °C.

In-flight measurements conducted by the Air Force and the US FAA and reported by Fitzgerald [3.12], indicate that thunderstorms in their early stages of dissipation have sufficient charge to cause some lightning discharges, if a means of streamer initiation becomes available. An aircraft entering such a region could constitute that means of initiation. Thus, in normal, instrument flight rules (IFR) operations in regions where an active thundercloud is merged with decaying thunderclouds and other cloudy areas, diverting from the normal course to avoid the active cloud may take the flight through a decaying area, where there is sufficient residual charge to produce a lightning strike after all.

Lightning warning instruments

From time to time, attempts have been made to develop an airborne instrument capable of warning pilots impending lightning strikes to their aircraft and providing information to the pilot for use in avoidance. Most of these attempts have involved installing a device, on an airplane, that senses when the ambient electric field around the airplane approaches the intensity at which a lightning strike is imminent [3.13]. Some of these sensors have been installed in research airplanes, and have been used to obtain data on electric field intensities prior to lightning strikes, but none of them have been developed sufficiently to provide practical advisories to pilots for strike avoidance. Because of the apparent wide variation in electric field intensities and orientations that may precede lightning strikes to aircraft, the development of a useful lightning strike avoidance system seems remote. The objective is thwarted by the difficulty of translating electric field data into advisory information in a short enough time to aid the pilot in an avoidance maneuver.

There *are* instruments that locate and plot the locations of lightning flashes as they occur, but that is a different story.

Perhaps the most effective warning of imminent strikes presently available to flight crews is electrostatic discharge (also known as *corona* or *St. Elmo's Fire*). This discharge is visible at night as a bluish glow at the aircraft's extremities. Static discharging also causes interference (instability) in low frequency automatic direction finding (ADF) indicators, and audible "hash" in high frequency (HF) communications receivers.

Pilot responses to lightning strikes (which may also be called static discharges or electrical discharges) vary. Typical answers by pilots of one airline [3.9] to the question "Do you have any recommendations for avoiding electrical discharges?" were as follows:

"From cruise speed, a reduction of 25% to 30% in airspeed will often allow the static buildup to stabilize at a lower maximum and dissipate rather than discharge. These build-ups are generally accompanied by a buzz-type static on VHF (very high frequency) and ADF (automatic direction finding) and a random swinging of the ADF needles though I have observed the ADF needles to hold a steady error of up to 90 ° as the static level stabilized at or near its peak, generally just prior to the discharge or beginning of dissipation."

"Climb or descend through the freezing level as quickly as possible."

"Avoid all precipitation. I know of no way to predict accurately where a discharge will occur."

"Slow down to minimum safe speed, change altitude to avoid temperature of -7 °C (20°F) to 2 °C (35 °F)."

"Not without excessive detour, both route and altitude."

"The static discharges I have encountered have built up at a rate which would preclude any avoidance tac - tics (3 to 15 seconds)."

"No, I have never known when to expect this until just prior to the discharge."

"No, not in the modern jets. Once the static begins the discharge follows very quickly."

"All information received at the ... training center applicable to static discharges and their avoidance has been completely accurate and helpful."

"No, hang on!'"

"Lead a clean life."

Thus, there is a wide divergence of pilot opinion regarding the best way to avoid lightning strikes. However, from this and many other sources, it is possible to list the conditions most often present just prior to experiencing a lightning strike, and the actions (if any) that most pilots take to reduce the possibility of receiving a strike.

A lightning strike is imminent when a combination of some of the symptoms which follow is present.

Conditions:

1. Flight through or in the vicinity of the following:
    - Unstable air.
    - Stationary front.
    - Cold front.
    - Warm front.
    - Squall line.
2. Within a cloud.
3. Icy types of precipitation.
4. Air temperature near 0ºC.
5. Progressive buildup of radio static.
6. St. Elmo's fire (when dark).
7. Experiencing turbulence.
8. Flying at altitudes between 1 500 m and 4 500 m (5 000 ft. and 15 000 ft.); most prevalent: 3 350 m (11 000 ft.)
9. Climbing or descending.

Actions:

1. Avoid areas of heavy precipitation.
2. Change altitude to avoid temperature near 0 °C.
3. Turn up cockpit lights.
4. Have one pilot keep eyes downward.

Since air traffic congestion often precludes circumvention of precipitation and since diversion often poses hazards, avoidance, while desirable, is neither a dependable nor an adequate means of protecting the aircraft against lightning strikes. The aircraft, therefore, must be designed to safely withstand lightning strike effects.

3.3.5 Frequency of Occurrence

Commercial Transport Aircraft

The numbers of lightning strikes actually experienced (as related to flight hours) by piston, turboprop, and pure jet aircraft from the 1950's through the mid 1970's are tabulated in Table 3.3. These numbers are based on the data reported by Newman [3.2] and Perry [3.6]. From this data, it follows that an average of one strike can be expected for each 3 000 hours of flight for any type of commercial transport aircraft. Experience since that time period, though not published, confirms the experience of Table 3.3.

Table 3.3 Incidence of Reported Lightning Strikes to Commercial Aircraft

	Newman (1950 – 1961)		Perry (1959 – 1974)		TOTALS		
	Strikes	Hours	Strikes	Hours	Strikes	Hours	No. hours per strike
Piston	808	2 000 000	–	–	808	2 000 000	2475
Turboprop	109	415 000	280	876 000	389	1 291 000	3320
Pure Jet	41	427 000	480	1 314 000	521	1 741 000	3340
ALL	958	2 842 000	760	2 190 000	1718	5 032 000	2930

Table 3.4 Incidence of Reported Lightning Strikes to US Air Force Aircraft

Aircraft type vs mean hours between lightning strikes						
	1965	1966	1967	1968	1969	Average per year
Bomber	55 500	48 000	47 900	73 000	28 000	50 480
Cargo	68 000	140 000	112 000	124 000	76 000	104 000
Fighter	141 000	105 000	112 000	65 000	73 000	99 200
Trainer	246 000	378 000	500 000	224 000	130 000	295 600

More recent experience seems to indicate that commercial aircraft operating in Europe receive more lightning strikes per year than similar airplanes operating in the continental US. This would be due to shorter average flight distances and times, which necessitate more flight time at intermediate altitudes, in contrast to the average flight distances and times in the US.

Military and general aviation aircraft

Unlike commercial airlines, military and general aviation aircraft are not usually constrained by regular flight schedules or congested traffic patterns around metropolitan airports. This distinction may contribute to the fact that these aircraft do not seem to experience as many lightning strikes as do commercial aircraft. This is evident in Table 3.4, which presents statistics from United States Air Force (USAF) experience for the years 1965 to 1969. However, USAF regulations do not require that lightning strike incidents be formally documented by flight crews unless a substantial amount of damage is done to the aircraft. Thus, many strikes to USAF aircraft undoubtedly go unreported.

Statistics such as those of Table 3.3, which apply to a broad category of aircraft and include data from a variety of different operators in varying geographic locations, may be misleading. For example, whereas Table 3.4 shows that there is an average of 99 000 flying hours between reportable lightning strikes to USAF fighter-type aircraft, the strike experience in Europe is known to be more frequent than strike experience in the US and in most other parts of the world. Weinstock and Shaeffer [3.14] reported 10.5 strikes per 10 000 hours for certain F-4 models flying in Europe. This rate is about 5 times greater than the world-wide exposure rate for these aircraft. A similar situation pertains to commercial aircraft operating in Europe, as indicated by Perry's summary of United Kingdom and European strike data [3.6], for example. This unusually high lightning-strike exposure seems to result both from a higher percentage of flights in cloud conditions, in comparison to flights in the US and, perhaps, more restricted flight patterns necessitated by higher traffic congestion in Europe.

Trends affecting strike rates

There are several trends in commercial and general aviation that are likely to increase the exposure of aircraft everywhere to lightning strikes in the future:

1. Increases in the use of 'hub and spoke' arrangement of commercial routes in the US, resulting in more time in descent, hold and climb patterns at intermediate altitudes.

2. Increases in numbers of small aircraft and rotorcraft equipped for IFR flight.

3.4 Aircraft Lightning Strike Mechanisms

In the following paragraphs, the electrical conditions that produce lightning are described, together with the mechanisms of lightning strike attachment to an aircraft. While it is not possible to anticipate or avoid these conditions all the time, it is important to understand the strike attachment process in order to properly assess the effects of lightning strikes on the aircraft.

3.4.1 Electric Field Effects

In a naturally occurring lightning strike situation, a stepped leader propagates outward from a cloud charge center. At that time, the ultimate destination of the flash, at an opposite charge center in the cloud or on the ground, is not yet determined. The difference of potential that exists between the stepped leader and the opposite charge(s) establishes an electrostatic force field between them, which can be graphically represented by imaginary lines of electrostatic force and equipotential surfaces, as shown in Fig. 3.10. The electric field intensity, commonly expressed in kilovolts per meter, is greatest where equipotential surfaces are closest together. This electric field is what ionizes the air to form the conductive path that becomes the lightning leader. Because the direction of electrostatic force is normal to the equipotential surfaces, and strongest where they are closest together, the leader is most likely to progress toward the most intense opposite polarity field regions.

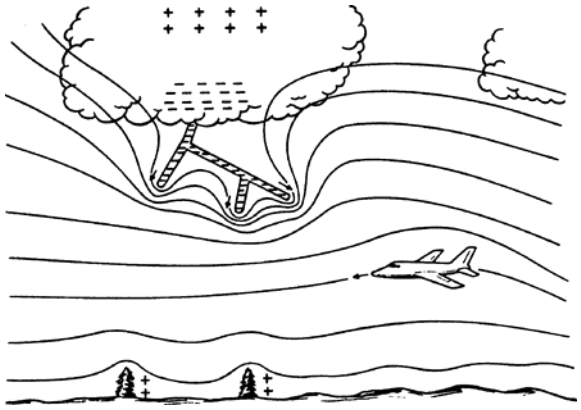

Fig. 3.10 Stepped leader approaching an aircraft.

If an aircraft happens to be in the vicinity, the aircraft will assume the electrical potential of its location. Since the aircraft is an electrical conductor, all of its surface is at the same potential and it, therefore, diverts and compresses adjacent equipotentials. This increases the electric field intensity at the aircraft's extremities and, especially, between the aircraft and other charged objects, particularly the advancing leader. If the aircraft is far away from the leader, its effect on the field near the leader is negligible; however, if the aircraft is within several tens or hundreds of meters from the leader, the electric field surrounding the aircraft intensifies and junction leaders originate at extremities of the aircraft and propagate in the direction of the original lightning leader. As this happens, the intervening field becomes even more intense, and the lightning and junction leaders continue to approach each other until they join. The junction usually occurs 50 (or so) meters from the aircraft extremity. At the same time, one or more leaders propagate(s) from an approximate opposite extremity of the aircraft, in the general direction of regions of opposite polarity charge (which could be at the earth or elsewhere in the cloud).

The highest electric fields around the aircraft occur at extremities, where the field's equipotential surfaces are compressed closest together, as shown in Fig. 3.11. Typically, these extremities are the nose, wing and empennage tips, propeller blades, or helicopter rotor blades. When the leader advances to the point where the field adjacent to an aircraft extremity is increased to about 30 kV/cm (at sea level pressure), the air ionizes and streamers form at these extremities, extending in the direction of the oncoming lightning leader.

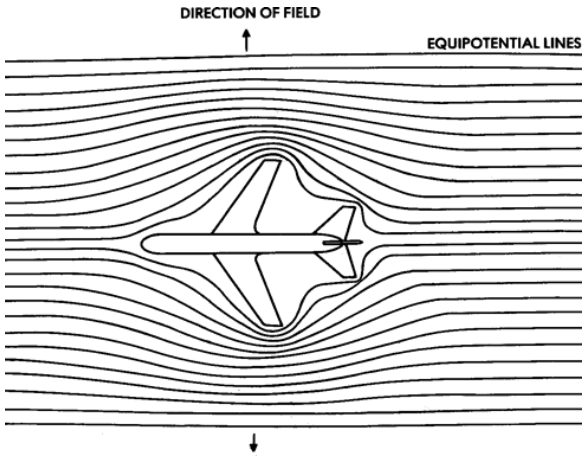

Fig. 3.11 Intensification of electric field around an aircraft.

3.4.2 Charge Stored on Aircraft

When the aircraft is attached to the leader, some charge (free electrons) flows onto the aircraft, but the amount of charge that can be taken on is very small compared to what is available from the lightning leader. The charge raises the aircraft to a high voltage and excessive charge causes the electric field around the aircraft to become so high that intense corona forms, which carries away the excess charge. If additional charge flows onto the aircraft, corona spreads to extremities of slightly larger curvature radius. A typical leader contains about 1 to 10 coulombs of electric charge. The capacitance of an aircraft (with respect to its surroundings) amount of charge that can be stored on an aircraft is limited by the corona inception voltage at the aircraft's extremities, which is about 50kV, resulting in electric field intensities at extremities with small radii of curvatures of around 20 – 30 kV/cm which is the corona inception field. Thus, the amount of charge that can be stored on an aircraft is:

$$Q = CV \qquad (3.1)$$

Or, for an aircraft whose capacitance is 500 pF,

$$Q = (500\ x\ 10^{-12}F)(50\ x\ 10^{3}V) \qquad (3.2)$$
$$= 25 \text{ x } 10^{-6} \text{ coulombs}$$

So there is no room for any significant portion of the leader's charge to be stored on an aircraft. Thus, the leader charge extends into the leader branch(es), exiting from the aircraft, which becomes merely an extension of the lightning channel on its way to an ultimate destination at a region of opposite polarity charge.

Once an oncoming lightning leader has attached to an aircraft, exit leader branches may continue to propagate from more than one opposite extremity of the aircraft at the same time. This constitutes a splitting of the developing lightning leader. The branches continue to propagate away from the aircraft, independently of one another, until one (or more) of them reaches its 'destination'. This process of attachment and continued propagation beyond an aircraft is illustrated in Fig. 3.12.

When the leader has reached its destination, and a continuous ionized channel between charge centers has been formed, the charge in the leaders discharges very rapidly to earth resulting in the stroke as described in Chapter 2. The stroke current resulting from discharging of the leader above the aircraft (the leader charge below the aircraft does

not discharge through the aircraft) and any subsequent stroke or continuing current components, must flow through the aircraft, which is now part of the conducting path between charge centers, as shown in Fig. 3.12(a). In the text that follows, this is called the lightning *channel.*

If another branch of the original leader reaches the ground before the branch that has involved the aircraft, the return stroke discharges the former branch, and all other branches, including the one involving the aircraft. This results in less stroke current going through the aircraft than would be the case in Fig. 3.12(a).

After the leader branches have discharged the branches that did not contact the earth die out as shown in Fig. 3.12(b). No continuing currents or subsequent strokes flow through the aircraft in such a case, and any damage to the aircraft is slight. A still photograph of a downward-branching flash after completion of the main channel is shown in Fig. 3.13. Several dying branches are evident in the photograph.

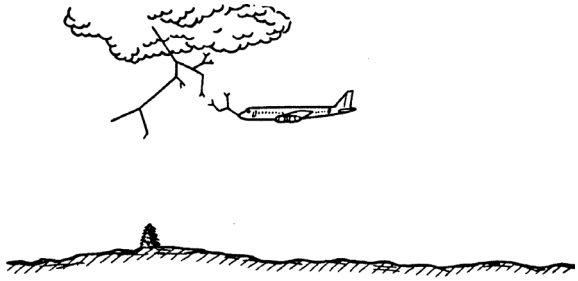

(a) Natural Leader approaching Aircraft . Junction Leader Responds from Aircraft

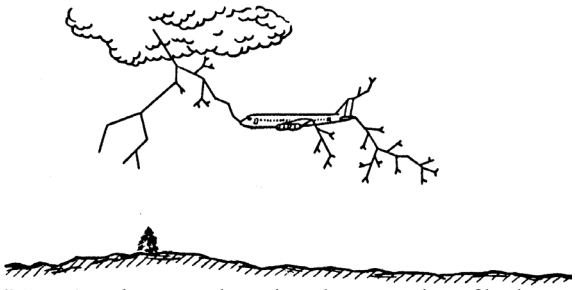

(b) Attachment and continued propagation of both branches of Natural Leader

Fig. 3.12 Stepped leader attachment to aircraft.

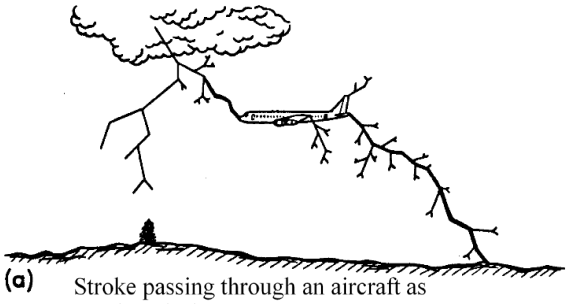

(a) Stroke passing through an aircraft as Leader Discharges

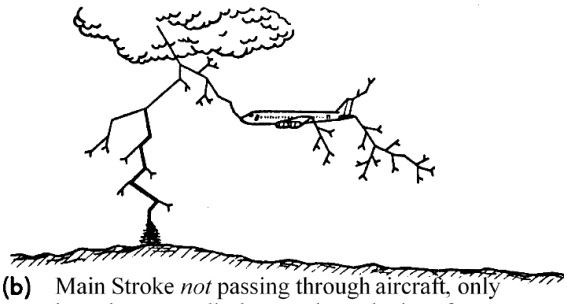

(b) Main Stroke *not* passing through aircraft, only branch current discharges through aircraft

Fig. 3.13 Stroke current paths.

3.4.3 Aircraft-Triggered Lightning

A question often asked is, "If an aircraft cannot produce a lightning flash from its own stored charge, can it trigger (i.e., initiate) a natural one?" In other words, "Would the lightning flash have occurred if the aircraft were not present?" A secondary question would be, "If aircraft do trigger lightning, does this influence the criteria to which aircraft must be designed?" The mechanism of aircraft triggered lightning is discussed in depth in §3.7 and the subject of design criteria is discussed in Chapter 5, but some preliminary discussion is in order.

There is clear evidence that lightning flashes have been triggered by research aircraft that were intentionally flown into clouds to observe lightning phenomena. These lightning strikes have originated at the aircraft, but it is not clear how often aircraft in normal service trigger lightning strikes. Studies have shown that a large percentage of lightning strikes to aircraft have evidently been triggered by and initiated at the aircraft.

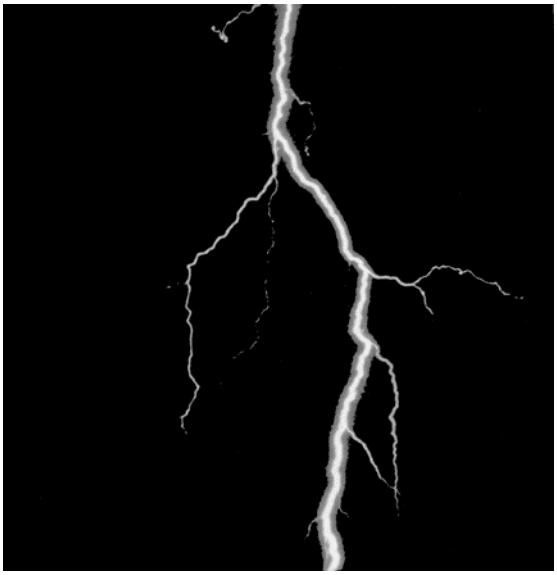

Fig. 3.14 Downward branching lightning flash.

Some of the lightning strikes to research aircraft have been observed by Doppler radar originating at the aircraft, with leaders propagating away from the aircraft in generally opposite directions. The triggered lightning currents measured on research aircraft have generally been of lower amplitude than typical cloud-to-ground lightning currents.

Nevertheless, these lower current amplitudes do not seem high enough to account for some of the physical damage observed on aircraft. Thus, some percentage of the reported strikes to aircraft must be of the cloud-to-earth variety.

There is ample evidence that aircraft and helicopters of all sizes trigger lightning strikes, but that evidence also suggests that larger aircraft trigger lightning more frequently than small airplanes [3.15]. This is because larger airplanes perturb a proportionately larger region of the ambient electric field.

The motion of an aircraft has little influence on the propagating leader because the aircraft's velocity (about 10^2 m/s) is much slower than that of the leader, which advances at a rate of 10^5 to 10^6 m/s. Thus, the aircraft appears stationary to the leader during the leader formation process.

Several other stimuli have been mentioned as possible causes of aircraft lightning strikes. These include engine exhaust and radiated electromagnetic energy, such as radar transmission.

Effect of engine exhaust on lightning attachment

There has been speculation that the hot exhaust gases from jet engines may contain enough ionized particles to attract or trigger a lightning flash to a jet aircraft. This speculation was heightened by the widely publicized launch of Apollo 12, which apparently triggered a lightning flash (or flashes) that twice struck the top of the vehicle, once when it had reached 1950 m (6 400 ft.) and again at 4 270 m (14 000 ft.). The flash(es) exited in the vehicle exhaust plume.

Studies by Nanevicz, Pierce, and Whitson [3.16] of incidents in which a rocket was rapidly introduced into an intense electric field, indicate that the exhaust plume is relatively electrically conductive in comparison to the surrounding air, making the effective, electrical length of the rocket longer than the rocket's actual physical length.

An empirical study by Pierce [3.15] of documented strikes to tall, grounded, and airborne conductors concluded that there must also be a potential discontinuity between an air vehicle and the adjacent atmosphere of up to

10^6 V before the lightning leader can be initiated from the vehicle. The study also concluded that the rapid discharge of hot ionized gas from a rocket engine may remove enough charge from the vehicle to increase its potential to 10^6 V or more with respect to its surroundings.

Shaeffer and Weinstock [3.14] have studied the conductivity of an aircraft jet-engine exhaust. In this case, ionized particles and free electrons in a jet exhaust originate in the combustion chamber as a result of chemical reactions taking place between the intake air and jet fuel. The ion concentration in a jet-engine's exhaust has been measured by Fowler [3.17] to be between 5 x 10^6 and 3 x 10^7 particles per cubic centimeter (p/cm^3). The free electron density that can be deduced from this is between 5 x 10^3 to 3 x 10^5 (p/cm^3). The electron density in luminous rocket exhaust has been calculated by Pierce [3.18] to be 10^{12} p/cm^3. This is comparable to the electron density in the tip of an advancing leader. Conversely, the free electron density in ambient air ranges from 10^2 to 10^3 p/cm^3. Evidently, jet-engine exhaust is only slightly more ionized than the ambient air, and much less so than rocket exhaust. Therefore, jet exhaust is not sufficiently conductive to initiate or attract a lightning leader. This conclusion is supported by aircraft lightning strike incident reports, which indicate that engine exhaust pipes are not often lightning attachment points unless they are already located at an aircraft extremity where the electric field would be intense from geometrical conditions alone.

There is also no evidence to suggest that jet aircraft are struck more frequently (i.e., per flight hour) than piston-engined aircraft. Overall, the ability of the jet aircraft to operate at higher altitudes and spend less time climbing and descending to airports has probably rendered the jet less susceptible than its piston-engined predecessor to lightning strikes, which occur predominantly at low or intermediate altitudes.

Some records do exist of strikes to jet engines, and, in some cases, these strikes have terminated inside the engine exhaust pipes, as illustrated in Fig. 3.15. These strikes are evidenced by spots of melted metal within 0.5 m (18 in) of the aft end of the exhaust pipe. Electronic engine instruments with sensors mounted on the engine have experienced damage from lightning induced effects associated with strikes to the nacelles or exhaust pipes. Apparently, there is either sufficient ionization in the exhaust (or the dielectric strength of the exhaust is sufficiently weakened) that a propagating leader may become diverted into the exhaust channel, or streamers may propagate outward from the exhaust pipe once the aircraft has been struck elsewhere by a leader.

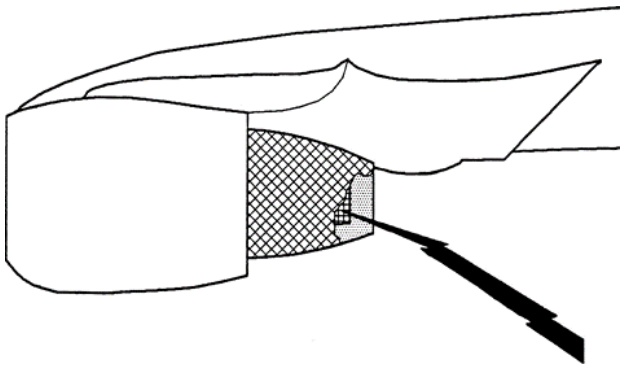

Fig. 3.15 Lightning flash terminating inside a jet engine exhaust tail pipe.

While the engine exhaust may divert or encourage an existing leader, it seems improbable that it could trigger a flash by itself, as a rocket plume can. Other strikes have terminated on the nacelles of wing and fuselage mounted engines, in the same manner as with other aircraft extremities. Viewed another way, if a jet engine did leave a trail of ionized exhaust behind it, then this must eventually cause an imbalance of electric charge between the aircraft and its surroundings, even in clear weather. As with P-static charging, such a condition would produce static discharges and corona from sharp extremities and cause interference in radio equipment. It is well established that this does not happen.

Effects of electromagnetic radiation

It has been suggested that an aircraft's radar may trigger aircraft initiated strikes or divert naturally occurring lightning strikes to an aircraft. This question was also investigated by Schaeffer and Weinstock [3.14], who showed that the transmitted power level of microwave radiation necessary to produce an electric field capable of ionizing air is about 6.7 x 10^6 watts, which is far greater than that available from aircraft radars.

Aircraft lightning strike incident reports also show no evidence of radar or other electromagnetic radiators having been involved in the lightning strike formation. There have been many strike incidents that resulted in radomes

being punctured, but these were clearly the result of the electric field associated with coronal and streamer activity originating inside the radome causing dielectric breakdown of the nonconductive radome wall. These punctures have occurred whether or not the radar was operating. The addition of diverter strips to the outside of the radome usually prevents these punctures, by enabling streamers and leaders to originate on the exterior of the radome.

3.5 Swept Channel Phenomena

After the aircraft has become part of a completed flash channel, the ensuing stroke and continuing currents that flow through the channel may persist for up to a second or more. Essentially, the channel remains in its original location, but the aircraft moves forward a significant distance during the life of the flash. Thus, whereas the initial entry and exit points are determined by the mechanisms previously described, there may be other lightning attachment points on the airframe that are determined by the motion of the aircraft through the relatively stationary flash channel. For example, when a forward extremity on a fighter aircraft, such as the pitot boom, becomes an initial attachment point, the aircraft's surface moves through the lightning channel and, thus, the channel appears to sweep back over the surface, as illustrated in Fig. 3.16. This occurrence is known as the swept flash (or 'swept stroke') phenomenon. The sweeping action can cause the lightning channel to attach and dwell for short periods at various surface locations along the line of flight, aft of initial leader attachment locations. The durations of these reattachments (known as the 'dwell times') depend on the type and thickness of surface finish. This sweeping mechanism usually prevents all the current in the lightning flash from being delivered to one spot on the aircraft surface, a phenomenon of particular importance in relation to the design and protection of fuel tanks.

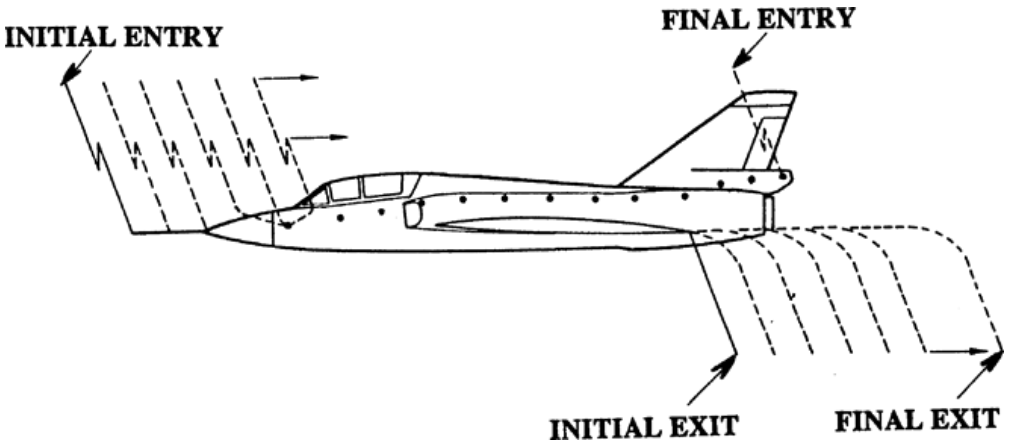

Fig. 3.16 Typical path of swept channel attachment points.

If part of the surface, such as the radome, is nonconductive, the flash may continue to dwell at the aft-most conductive attachment point (e.g., the aft end of the pitot boom) until another exposed, conductive surface (e.g., the fuselage) passes by; or the channel may puncture the nonconductive surface and reattach to a conductive object beneath it (e.g., the radar dish). Whether puncture or surface flashover occurs depends on the amplitude and rate-of-rise of the voltage stress created along the channel, as well as the voltage withstand strength of the nonconductive surface and any air gap separating it from the enclosed conductive objects. When the lightning arc has been swept back to one of the trailing edges, it may remain attached at that point for the remaining duration of the lightning flash. An initial attachment point at a trailing edge, of course, would not be subjected to any swept channel action. Instead, the lightning channel would be extended horizontally aft of the aircraft.

An aircraft's forward motion does not usually permit the aircraft to escape from the lightning channel once that channel has attached. This is because the potential difference between charge centers (cloud and earth or another cloud) is sufficient to maintain a very long channel, until the charges have neutralized each other and the flash dies.

3.6 Lightning Attachment Zones

Since there are some regions on an aircraft where lightning is unlikely to attach and others that are susceptible to attachment for only a small portion of the total flash duration, it is common practice to divide the surface of an aircraft into zones, according to expected components of the lightning flash and severity of effects.

3.6.1 Zone Definitions

As the mechanisms of aircraft lightning interaction have become better understood, definitions of lightning strike zones have evolved. For a long period of time, the zone definitions and location guidelines in Federal Aviation Administration (FAA) Advisory Circular *AC 20-53A* [3.19] were used. Then, in 1999, SAE published Aerospace Recommended Practice (ARP) 5414 [3.20], containing the following updated definitions of the lightning strike zones and methods of locating them:

Zone 1A: First stroke zone.

Zone 1B: First stroke zone with long hang-on.

Zone 1C: Transition zone for first return stroke.

Zone 2A: Swept-channel zone.

Zone 2B: Swept-channel zone with long hang-on.

Zone 3: Those surfaces not in *Zones 1A, 1B, 1C, 2A*, or *2B*, where attachment of the lightning channel is unlikely. Also, those portions of the aircraft that lie underneath or between the other zones and/or conduct substantial amounts of electrical current between direct or swept attachment points.

Zones are the means by which the external environment is applied to the aircraft. The locations of these zones on any aircraft are dependent on the aircraft's geometry and operational factors, and often vary from one aircraft to another. Therefore, a determination must be made for each aircraft configuration. Further discussion of the zone definitions and methods of locating the zones (with typical examples) are provided in Chapter 5.

3.7 Mechanism of Aircraft Triggered Lightning

Aircraft triggered lightning is defined as lightning that occurs because of the presence of an aircraft but that would not otherwise occur. A frequent theme in pilots' reports of lightning strikes to aircraft is that the aircraft was struck before there was any evidence of lightning activity in the area, and a belief commonly expressed is that the aircraft triggered the lightning flash, rather than the aircraft just being an inadvertent bystander through which a naturally occurring lightning flash chose to pass.

Evidence has accumulated that aircraft can indeed trigger lightning, and theories have been developed to explain the mechanism. It is well established that research aircraft intentionally flown into charged clouds have triggered flashes and that these flashes have originated at the aircraft. It is not as evident that aircraft flown under normal conditions and seeking to avoid lightning often trigger lightning flashes. Possibly, those aircraft are more often struck by a naturally propagating leader, as discussed in §3.4.3. To some extent, the matter may be academic. The important point is that aircraft are struck by lightning and that measures must be taken to protect them, whether or not the lightning is triggered by the aircraft.

The subject of aircraft triggered lightning first began to be seriously studied in the 1960's [3.21 - 3.25]. It was during this period that it was shown that lightning could be deliberately triggered by rockets with trailing wires [3.26]. Toward the end of the 1960's, Apollo 12 was struck by what was deemed to be a triggered lightning flash and studies [3.27 - 3.28] were undertaken to understand the conditions that could result in lightning being triggered by an aerospace vehicle.

In 1972, it was suggested [3.29] that in order for an airborne vehicle to trigger lightning, there must be an ambient electric field of at least 10 kV/m and the vehicle must span a potential difference, in that field, of about one million volts. Also in 1972, an interesting study was published which concluded that aircraft could trigger lightning and that static charge on the aircraft was an important factor [3.30].

A good review of this subject and bibliography was published in 1982 [3.31]. Even up to this date, however, there was some uncertainty and debate regarding the possibility of aircraft triggered lightning. This was due to a lack of definitive measurements of aircraft triggered lightning and the absence of any known physical models to explain it.

F-106B research aircraft

In 1981, a F-106B aircraft operated by the National Aeronautics and Space Administration (NASA) Langley Research Center, as part of the Storm Hazards Research Program, was outfitted as a research vehicle to be flown into clouds to collect data on the characteristics of lightning intercepted by aircraft. Starting in 1982 the ultra-high frequency (UHF)-band radar at the Wallops Flight Facility of the NASA Goddard Space Flight Center, was used to guide the F-106B through the upper regions of thunderstorms to increase the probability of the aircraft being struck by lightning [3.32].

Analysis of the radar echoes showed that nearly every echo from a lightning strike to the F-106B started directly above the aircraft's echo and propagated away from the aircraft. This certainly suggested that the lightning flashes were triggered by the F-106B and were not naturally occurring flashes. If they had been naturally occurring flashes, intercepted by the F-106B, an observer would have seen the echoes start some distance from the aircraft and propagate toward it, finally blending with the aircraft's echo at the same instant the strike was recorded by the aircraft. None of the lightning flashes showed this pattern. Many echoes were seen from naturally occurring intracloud flashes, but none of them ever struck the F-106B.

In addition to the radar echoes, analyses by Rudolph and Perala [3.33 - 3.35] using three-dimensional (3D) numerical models have predicted currents to arise from triggering that are very similar to those actually recorded by instruments on the vehicle. All of this evidence rather conclusively proves that the F-106B research aircraft has triggered lightning flashes.

There also has been other significant research into the mechanisms of triggered lightning. Work by Bicknell and Shelton [3.36 - 3.38], has been done on energy considerations, the role of positive corona streamers and precipitation particles electrode velocity by Nagai, Koide and Kinoshita [3.39], and other topics [3.40 - 3.42]. Experimental studies by Kasemir and Perkins [3.43] have included a scale model Space Shuttle Orbiter vehicle and an electrically floating cylinder by Labaune et al [3.44].

Mechanism of triggering

Triggered lightning occurs because the local electric field induces charge on the extremities of the aircraft. This charge then produces an electric field sufficient to cause air breakdown at places on the aircraft, corona (as discussed in Chapter 1) or St. Elmo's Fire (as discussed in Chapter 2). If the ambient electric field is sufficiently high, streamers then develop and propagate away from the aircraft, becoming bi-directional leaders.

The basic mechanism of propagation is similar to that described in Chapter 1 with one major difference. During breakdown of a gap subjected to an externally applied impulse, the energy required to establish the field into which the streamer propagates is produced by the externally applied impulse. The streamer may then continue to propagate by conducting charge along its channel and establishing a field at its tip sufficient to maintain propagation. The minimum electric field required, at the tip of a lightning leader, to maintain its propagation is approximately 500 kV/m at sea level.

The energy involved in aircraft triggered lightning is not stored on the aircraft but must come from a remote source. Electrical charge stored on the aircraft may certainly *contribute* to the initial breakdown, but it can never be enough, on its own, to sustain the propagation of lightning leaders. This is why, when streamers propagate away from the aircraft, they propagate in opposite directions; positive streamers in one direction and negative streamers in the other direction.

Prerequisites for triggering

For triggered lightning to form, the static electric field in which the aircraft is immersed must be large enough and oriented properly so that the locally enhanced fields somewhere on the aircraft exceed the local breakdown strength of the air. The largest enhancements of the field occur at sharp points or edges, particularly if those points and edges are oriented in the approximate direction of the ambient field. An aircraft in flight has many such sharp points and sharp edges, including propeller tips, wings and empennage tips. For distances of half a meter or so, these locally enhanced fields are likely to be higher than the ambient field by a factor of ten or more. Hence, it is considerably more likely that initial air breakdown and formation of a lightning channel will occur in the presence of an aircraft than in its absence.

The second requirement for triggered lightning is that the electric field be sufficiently high, and high over a sufficient distance that a streamer can form and propagate. The electric field conditions that produce only corona are

not sufficient; during thunderstorms corona forms on grounded objects all the time, but the corona does not develop into streamers or leaders because the electric field into which the corona grows is not sufficiently high. The research discussed in Chapter 1, on streamer development from electrodes subjected to externally applied impulses, shows that the streamers continue to propagate and develop into full-fledged lightning leaders if the average electric field in the gap exceeds about 500 kV/m, at sea level. At flight altitudes, the ambient field sufficient to support continued streamer propagation is somewhat less, due to lower air densities.

That research also showed that an average voltage gradient of 500 kV/m applied to an electrode gap always leads to breakdown if the voltage is maintained long enough. 500 kV/m is the value at sea level; 250 kV/m could be expected to cause breakdown at 6 000 m (20 000 ft.) altitude. Therefore, an electric field of several hundred kV/m represents conditions that are just on the edge of breakdown. Another is that breakdown is almost certain to occur whenever the field achieves the requisite minimum level since in time there will be a local break-down that will then be able to propagate. As a consequence, all triggered lightning flash situations should show similar properties.

3.7.1 Triggered Lightning Environment

The key factor in aircraft triggered lightning is the static electric field produced by thunderstorms. Such fields have been measured by several researchers using aircraft, rockets, balloons, and parachuted sondes (see Table 3.5). These measurements show that the requisite fields of 250 - 500 kV/m do occur in clouds. Higher values have also been reported [3.45]. Additional observations [3.46 - 3.47] report values also consistent with Table 3.5.

Table 3.5
Thunderstorm Electric Fields Measured
in Airborne Experiments

Investigator	Typical (V/m)	High Values Occasionally Observed	Measurement Type
Winn et al. (1974)	5- 8 x 10^4	2 x 10^5	Rockets
Winn et al. (1981)	—	1.4 x 10^5	Balloons
Rust, Kasemir	1.5 x 10^5	3.0 x 10^5	Aircraft
Kasemir and Perkins (1978)	1 x 10^5	2.8 x 10^5	Aircraft
Imyanitov et al. (1972)	1 x 10^5	2.5 x 10^5	Aircraft
Evans (1969)	—	2 x 10^5	Parachuted Sonde
Fitzgerald (1976)	2- 4 x 10^5	8 x 10^5	Aircraft

The simplified thunderstorm cell model [3.48] shown in Fig. 3.17 is used here to illustrate the conditions under which electric fields like those in Table 3.5 may be produced by a thundercloud. The illustration is based on data obtained by NASA using an F-106B research aircraft. The cell has a +40 Coulomb charge centered at 10 km (32 800 ft.) above ground, a -40 Coulomb charge centered at 5 km (16 400 ft.), and a +10 Coulomb charge centered at 2 km (6 000 ft.).

Calculation of the electric fields can be simplified by assuming point charges located in a vertical line with image charges in the ground. Contours of constant electric field from such an assemblage of charges are shown in Figs. 3.18 - 3.20. Because the calculations are based on point charges, the figures show an upper bound on the field but, in reality, the actual charges are distributed. The field outside the charged region may be calculated correctly by assuming point charges, but for points inside the charged region, the actual field would be smaller than indicated on the figures.

Fig. 3.18 is the most interesting for the purposes of investigating triggered lightning on the F-106B. If the aircraft is in essentially level flight, the horizontal field is the one most enhanced.

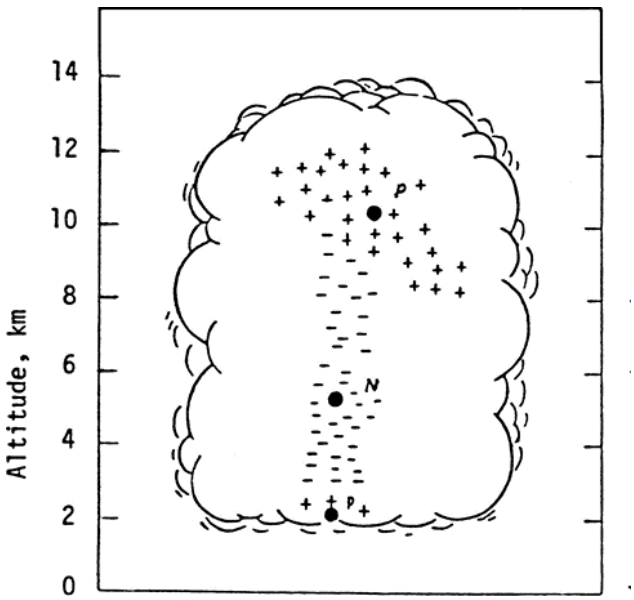

Fig. 3.17 Thunderstorm Charge Separation model.

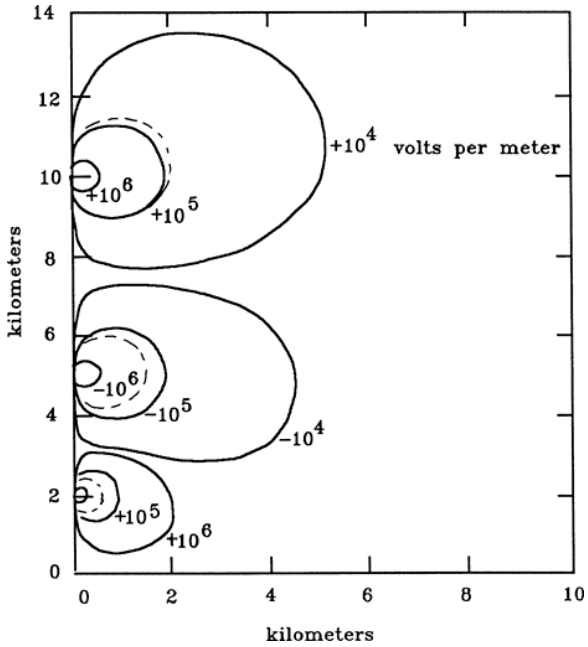

Fig. 3.18 Radical component of electric field [3.48].

Lightning can be triggered at any point in space at which the enhanced field around the aircraft exceeds the minimum breakdown strength of the air. Since this breakdown strength depends on altitude or, more exactly, on air density, a field that causes triggered lightning at a high altitude (10 km) may not do so at lower altitudes. Taking these factors into account, the dashed lines in Figs. 3.18 and 3.19 show the points in space at which an electric field of breakdown strength can be reached on the aircraft, assuming proper orientation. The calculations assume that the net aircraft charge is zero. If the aircraft were charged, the dashed lines could extend further away from the charge centers. Fig. 3.20 shows the total magnitude of the field.

The dashed lines thus indicate the regions inside which the F-106B, in level flight, could trigger lightning. At high altitudes, where the breakdown strength of air is low, triggering can occur up to two kilometers from the charge center. At the very low altitudes (2 km) where the breakdown strength of air is greater, the trigger region is only a few hundred meters across. In fact, because the charges are really distributed, and are not point sources, triggering at these low altitudes may not be possible.

3.7.2 The Response of Aircraft to Triggered Lightning

The basic electromagnetic response of an aircraft to a triggered lightning strike is illustrated in Fig. 3.21. This figure approximates a situation in which an F-106B aircraft flies directly toward a positive charge center. The aircraft becomes polarized in response to the ambient field. That is, electrons are pulled from the aft end, toward the nose.

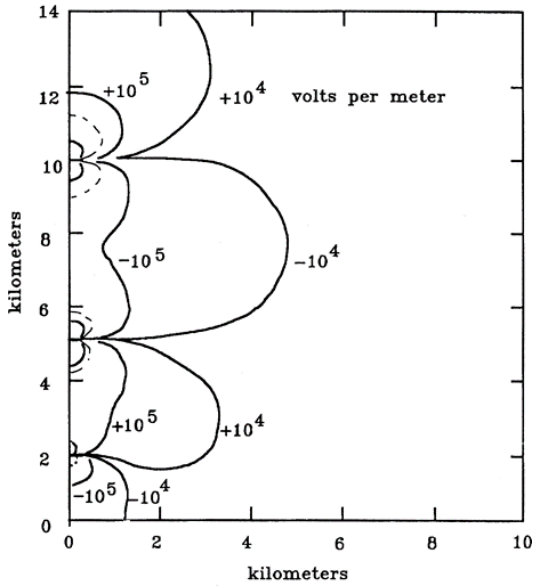

Fig. 3.19 Vertical component of electric field [3.48].

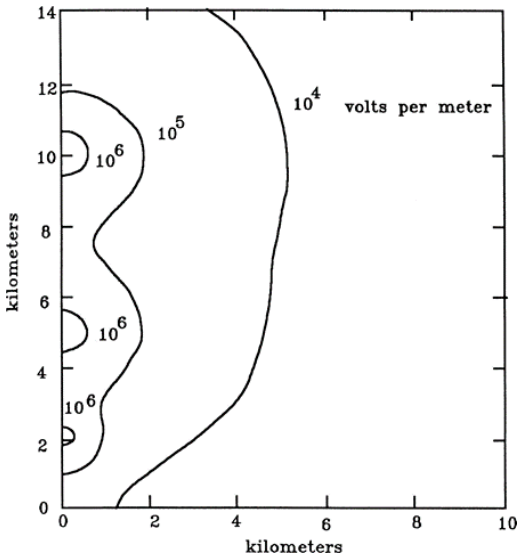

Fig. 3.20 Magnitude of total electric field [3.48].

Thus, the F-106B accumulates a negative charge (surplus of electrons) at its nose and a positive charge (deficiency of the electrons) at its tail, although the net charge on the aircraft remains unchanged. The field strength at all

points on the surface of the aircraft is the sum of the incident electric field and the field components produced by the induced charges. Thus, the field is enhanced by the presence of the aircraft. The electric field at the nose points toward the fuselage and the field at the tail points away from the fuselage. The polarities of the fields are as defined in §2.2.2. For the orientation shown, the enhanced field is largest at the nose of the aircraft.

As the aircraft flies towards the atmospheric charge regions, the electric fields at the surface of the aircraft slowly increase (that is, become more negative at one end and more positive at the other end). Eventually, the enhanced field at the nose becomes great enough to initiate a burst of corona; electrons at the nose flowing off into the air ahead of the nose. This tends to reduce the electric field at the nose (making it less negative) and may even prevent a discharge from occurring.

The flow of electrons from the nose can also be viewed as a flow of positive charge from the air onto the aircraft that leaves the aircraft with a net positive charge. This additional positive charge enhances the field at the aircraft's tail end, eventually producing another streamer there. That streamer may be viewed either as transferring positive charge into the air aft of the aircraft or as transferring negative charge from the air into the aircraft. Not every streamer at the nose is accompanied by a simultaneous streamer at the tail, but, ultimately, all the negative charge transferred into the air at the nose must be balanced by charge transferred into the aircraft from a discharge at the opposite extremity. The net result is either a single pulse of current flowing through the aircraft or, more commonly, two pulses of current, separated by several tens or hundreds of nanoseconds, one charging the aircraft and another discharging it. The differences between the shapes of these two pulses reflect differences in the mechanisms that produce them. One pulse resembles the negative discharges discussed in Chapter 1, while the other has the characteristics of a positive discharge.

As the discharges extend into the air, they continue to enhance the electric field at their tips and, provided the ambient field is sufficient, they continue to grow. The two oppositely directed streamers thus transfer electrical charge out of one portion of the air, through the aircraft and into another portion of the air. Fig. 3.18 illustrates the conditions under which a discharge would start at the nose and exit at the tail. Other discharge paths are also possible, depending on the orientation of the aircraft relative to the electric field. On the F-106B, most but not all of the discharges involved the nose boom. Exit points on the wing tips and tail were also common. On a larger aircraft, one might expect streamers to start at points other than the nose.

Current Waveforms

Lightning current flowing through an aircraft produces electromagnetic fields that can be measured by appropriate sensors. Sensors located as indicated in Fig. 3.21 would pick up the electric and magnetic fields (and their derivatives) with waveforms similar to those shown in the figure.

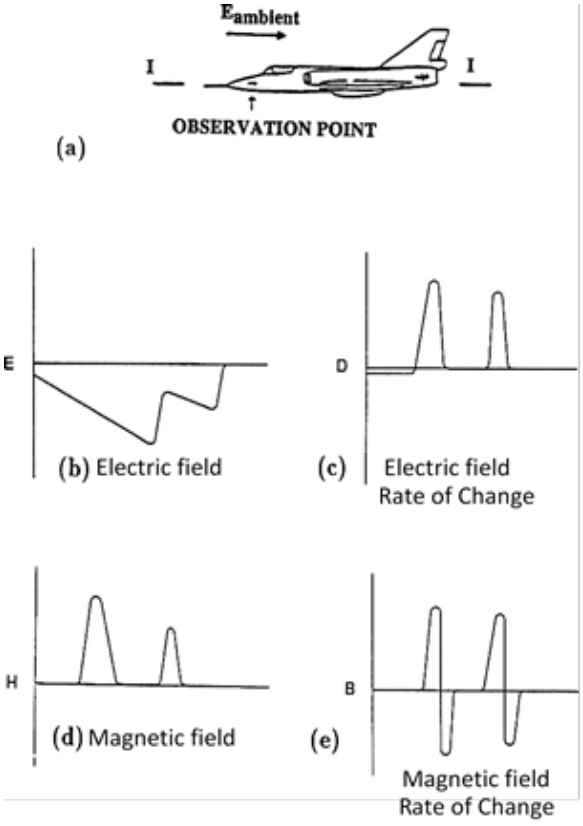

Fig. 3.21 Expected behavior of triggered lightning for nose-to-tail oriented electric field.

On the F-106B, only the D-dot and B-dot sensors had bandwidths wide enough to record the phenomena shown in Fig. 3.22. (D-dot corresponds to the rate of change of electric field and B-dot corresponds to the rate of change of magnetic field.) The plots in Fig. 3.22 are simplified so that they ignore the resonant response of the aircraft.

The actual data, of which Figs. 3.23 through 3.25 are examples, resembled Fig. 3.22 in their general features. Note that both single and double pulses were measured on the aircraft. Fig. 3.22 shows examples [3.33]. The initial air breakdown takes place in a fraction of a microsecond and has a high frequency content sufficient to excite traveling wave currents that propagate back and forth between the extremities of the aircraft. These traveling wave currents are important in that they may enhance the coupling of electric and magnetic fields to the wires in the aircraft.

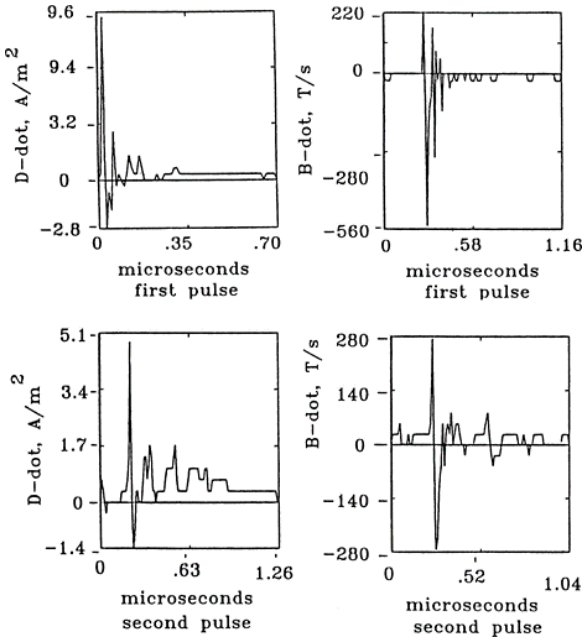

Fig. 3.22 In-flight D-dot and B-dot strike data.

There are other components of a triggered lightning flash to an airplane that can last as long as a second. For example, Fig. 3.23 shows the currents from three different flashes flowing in the tip of the F-106B vertical fin. Each of the flashes produced a continuing current of 80 amperes average amplitude, each lasting for about 0.3 seconds. Such amplitudes and durations are typical of the continuing current phases of flashes measured at ground level. The current was not steady but included many higher amplitude pulses superimposed on an underlying current. The recording channel with which the current of Fig. 3.23 was measured had a direct current (DC) response that allowed the continuing current to be recorded faithfully, but the frequency response extended only to 400 Hz, insufficient to resolve the amplitudes and waveforms of the individual pulses.

Fig. 3.24 shows the characteristics of another typical lightning flash. It displays the outputs from a number of different sensors as measured on a recorder with a bandwidth from 400 Hz to 100 kHz. It also shows the fin current recorded with a DC to 400 Hz bandwidth. Each pulse of current is associated with a change of the electric field (D-dot) and a burst of light from the channel of the flash.

The fin current of Fig. 3.24 was also recorded with a digital transient recorder that took samples every 40 nanoseconds. Fig. 3.25 shows details of the first pulse of current measured on the fin. The time of triggering is indicated in Fig. 3.25. Pulses of current occurred about every 50 μs, on average. The highest amplitude pulse was 18 kA. Lightning currents of this nature have not been measured at ground level.

The measured current waveform shown in Fig. 3.25 is important because it prompted the establishment of a multiple burst (MB) current test requirement for induced effects. This development is discussed further in Chapters 5 and 18.

Rates of Change

The rates of change of current and rates of change of electric field are both important parameters of a lightning flash. The standardized lightning environment, discussed in Chapter 5, is largely based on measurements taken at ground level of cloud-to-ground lightning, but the measurements taken on the F-106B [3.48], provide some examples of responses of aircraft subjected to triggered lightning flashes.

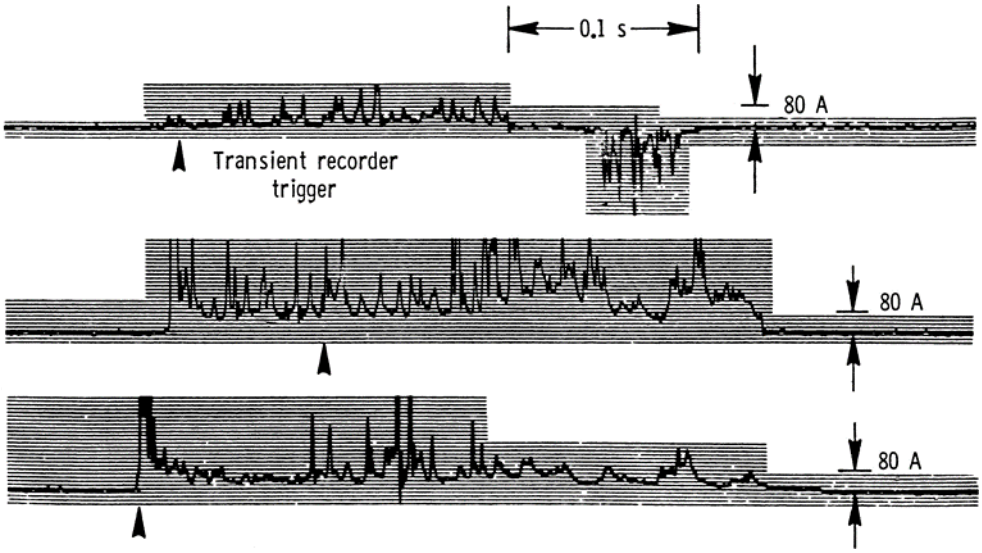

Fig. 3.23 Vertical fin currents [3.48].

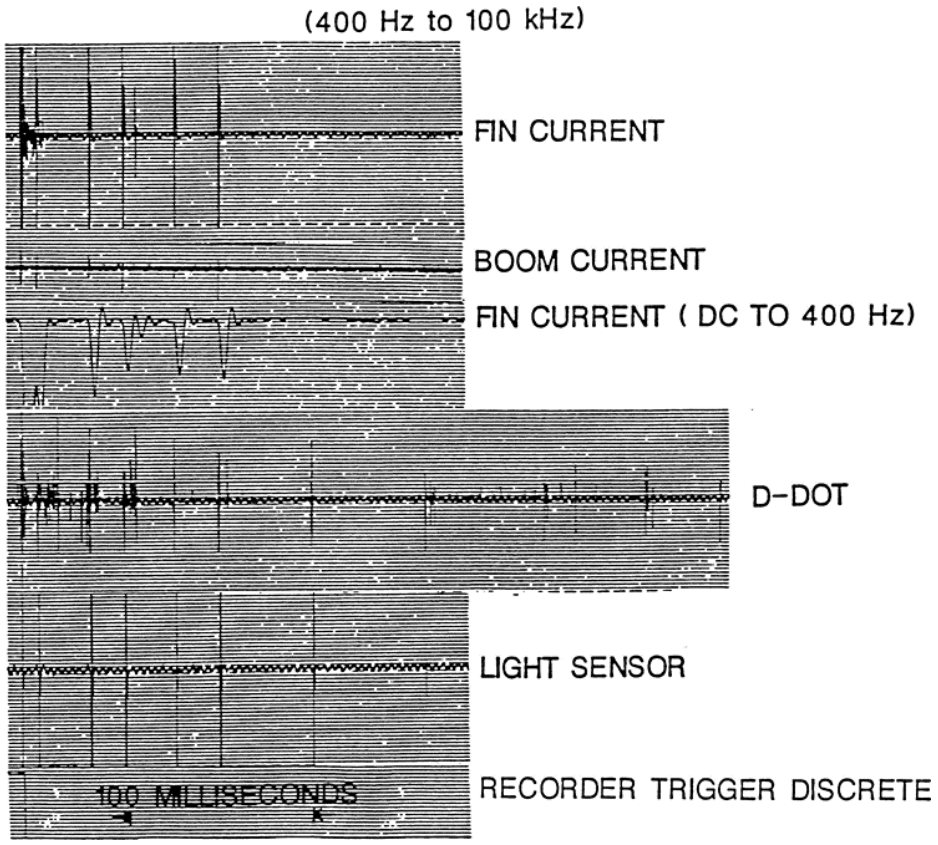

Fig. 3.24 Recordings made during the flash [3.48].

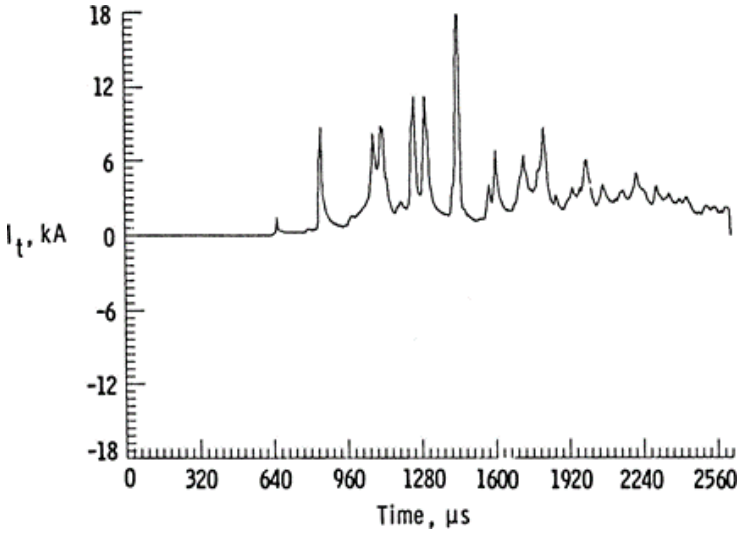

Fig. 3.25 Vertical fin current. A typical burst of pulses [3.48].

References

3.1 L. P. Harrison, "Lightning Discharge to Aircraft and Related Meteorological Conditions," *Technical Note 1001*, National Advisory Committee for Aeronautics, Washington, D.C., May 1946.

3.2 M. M. Newman and J. D. Robb, "Aircraft Protection from Atmospheric Electrical Hazards," *ASD Technical Report 61-493, or L and T Report 374*, Lightning and Transients Research Institute Minneapolis, Minnesota, December 1961.

3.3 "Lightning Strike Survey Report for the Period of January 1965 through December of 1966," *Federal Aviation Agency Report of the Conference on Fire Safety Measures for Aircraft Fuel Systems. Appendix II*, Department of Transportation, Washington D.C., December 1967.

3.4 B. I. Hourihan, "Data from the Airlines Lightning Strike Reporting Project," June 1971 to November 1974, *Summary Report GPR-75-004*, High Voltage Laboratory, Electromagnetics Unit, Corporate Research and Development, General Electric Company, Pittsfield, Massachusetts, March 1975.

3.5 R. B. Anderson and H. Kroninger, "Lightning Phenomena in the Aerospace Environment: Part II, Lightning Strikes to Aircraft," *Proceedings of the 1975 Conference on Lightning and Static Electricity*, December 1975.

3.6 J. A. Plumer and B. L. Perry, "An Analysis of Lightning Strikes in Airline Operation in the USA and Europe," *Proceedings of the 1975 Conference of Lightning and Static Electricity*, December 1975.

3.7 O. K. Trunov, "Conditions of Lightning Strikes in Air Transports and Certain General Lightning Protection Requirements," *Proceedings of the 1975 Conference on Lightning and Static Electricity*, December 1975.

3.8 J. Anderson Plumer, "Data from the Airlines Lightning Strike Reporting Project: Pilot Reports and Lightning Effects", Lightning Technologies, Inc., Pittsfield, Massachusetts, August 2001.

3.9 H. T. Harrison, "UAL Turbojet Experience with Electrical Discharges", *UAL Meteorological Circular No. 57*, United Air Lines, Chicago, Illinois, January 1, 1965.

3.10 W. B. Beckwith, "The Use of Weather Radar in Turbojet Operations", *UAL Meteorological Circular No. 53*, United Air Lines, Denver, Colorado, April 1, 1965.

3.11 T. H. Rudolph et al., "Investigations Into the Triggered Lightning Response of the F-106B Thunderstorm Research Aircraft," *NASA Contractor Report 3902*, June 1985.

3.12 D. R. Fitzgerald, "Probable Aircraft Triggering of Lightning in Certain Thunderstorms," *Monthly Weather Review*, December 1967, pp. 835-42.

3.13 G. A. M. Odam, "An Experimental Automatic Wide Range Instrument to Monitor the Electrostatic Field at the Surface of an Aircraft in Flight," *Technical Report 69218*, Royal Aircraft Establishment, Farnborough Hants, England, October 1961.

3.14 J. F. Shaeffer and G. L. Weinstock, "Aircraft Related Lightning Mechanisms", *Technical Report AFAL- TR-72-386*, prepared by the US Air Force Avionics Laboratory, Air Force Systems Command, Wright- Patterson Air Force Base, Ohio, January 1973.

3.15 E. T. Pierce, "Triggered Lightning and Some Unsuspected Lightning Hazards," *American Association for the Advancement of Science, 138 the Annual Meeting, 1971*, Stanford Research Institute, Menlo Park, California, January 1972.

3.16 J. E. Nanevicz, E. T. Pierce, and A. L. Whitson, "Atmospheric Electricity and the Apollo Series", *Note 18*, Stanford Research Institute, Menlo Park, California, June 1972.

3.17 R. T. Fowler, *Ion Collection by Electrostatic Probe in a Jet Exhaust*, graduate thesis, Air Force Institute of Technology, Wright-Patterson Air Force Base, Ohio, June 1970.

3.18 E. T. Pierce, "Atmospheric Electric and Meteorological Environment of Aircraft Incidents Involving Lightning Strikes", *Special Interim Report 1*, Stanford Research Institute, Menlo Park, California, October 1970.

3.19 "Protection of Aircraft Fuel Systems Against Lightning," *Federal Aviation Agency Advisory Circular AC 20-53*, Federal Aviation Administration, Department of Transportation, Washington, DC, October, 1967.

3.20 "Aircraft Lightning Zoning" Aerospace Recommended Practice ARP5414, SAE International, Warrendale, PA, December, 1999.

3.21 B. Vonnegut, "Electrical Behavior of an Aircraft in a Thunderstorm," Federal Aviation Admin., *Rep. FAA-ADS-36*, February 1965.

3.22 D. R. Fitzgerald, "Probable Aircraft Triggering of Lightning in Certain Thunderstorms," *Monthly Weather Review*, Vol. 95, pp. 835, 1967.

3.23 B. J. Petterson, and W. R. Wood, "Measurements of Lightning Strikes to Aircraft," Final Report to Fed. Aviation Admin. under Contracts FA65WA1-94 and FA66NF-AP-12, January 1968.

3.24 W. E. Cobb and F. H. Holitza, "A Note on Lightning Strikes to Aircraft," *Monthly Weather Review*, Vol. 96, No. 11, Nov., 1968.

3.25 D. R. Fitzgerald, "Aircraft and Rocket Triggered Natural Lightning Discharges," *Lightning and Static Electricity Conference*, December 1968.

3.26 M. M. Newman, J. R. Stahmann, J. D. Robb, E. A. Lewis, S. G. Martin and S. V Zinn, "Triggered Lightning Strokes at Very Close Range,"*J. Geophys*. Res., Vol. 72, p. 4761, 1967.

3.27 R. Godfrey, E. R. Mathews, and J. A. McDivitt, "Analysis of Apollo 12 Lightning Incident," *NASA (MSC) Rep. 01540*, February 1970.

3.28 M. Brook, C. R. Holmes, and C. B. Moore, "Lightning and Rockets: Some Implications of the Apollo 12 Lightning Event," Naval Research and Review, April 1970.

3.29 E. T. Pierce, "Triggered Lightning and Its Application to Rockets and Aircraft," 1972 *Lightning Conference Proceedings*, AFAL-TR-72-325.

3.30 J. F. Shaeffer, "Aircraft Initiation of Lightning," *1972 Lightning and Static Electricity Conf*., pp. 192-200, 12-15 December 1973.

3.31 D. W. Clifford, and H. W. Kasemir,"Triggered Lightning" *IEEE Trans. on Electromagnetic Compatibility*, Vol. EMC-24, No. 2, May 1983.

3.32 V. Mazur, B. D. Fisher, and J. C. Gerlach, "Conditions Conducive to Lightning Striking by an Aircraft in a Thunderstorm" *Proc. of the 8th Int. Aerospace and Ground Conf. on Lightning and Static Electricity*, Fort Worth, TX, DOT/FAA/CT-83-25, June 1983.

3.33 R. Rudolph, and R. A. Perala, "Linear and Nonlinear Interpretation of the Direct Strike Lightning Response of the NASA F-106B Thunderstorm Research Aircraft," *NASA CR-3746*,December 1983.

3.34 T. Rudolph, R. A. Perala, P. M. McKenna, and S. L. Parker, "Investigations into the Triggered Lightning Response of the F-106B Thunderstorm Research Aircraft," *NASA CR-3902*, June 1985.

3.35 T. H. Rudolph, R. A. Perala, C. C. Easterbrook and S. L. Parker, "Development and Application of Linear and Nonlinear Methods for Interpretation of Lightning Strikes to Inflight Aircraft," *NASA CR 3974*, 1986.

3.36 J. A. Bicknell, and R. W. Shelton, "The Energy Requirements of an Aircraft Triggered Discharge," *10th Int. Aerospace and Ground Conf.*, Paris, France, pp. 217-221, 1985.

3.37 J. A. Bicknell, and R. W. Shelton, "Some Possible Energy Requirements of a Corona Triggered Lightning Stroke," *VIIth Int. Conf. on Atmos. Electricity*, Albany, NY, pp. 438-440, June 3-8, 1984.

3.38 R. W. Shelton, and J. A. Bicknell, "Corona from Simulated Aircraft Surfaces and Their Contribution to the Triggered Discharge," *Int. Aerospace and Ground Conf. on Lightning and Static Electricity*, Dayton, Ohio, pp. 28-1 - 28-9, June 24-26, 1986.

3.39 Y. Nagai, T. Koide and K. Kinoshita, "Relations of the Flashover Voltage Versus the Velocity of the Moving Electrode," Abstract, pp. 23.1 - 23.8.

3.40 H. W. Kasemir, "Theoretical and Experimental Determination of Field, Charge and Current on an Aircraft Hit by Natural or Triggered Lightning," *Int. Aerospace and Ground Conf. on Lightning and Static Electricity*, Orlando, FL, pp. 2-1 2-10, June 24-26, 1984.

3.41 L. W. Parker, and H. W. Kasemir, "Predicted Aircraft Field Concentration Factors and their Relation to Triggered Lightning," *Int. Aerospace and Ground Conf. on Lightning and Static Electricity*, Dayton, Ohio, pp. 9-1 - 9-18, June 24-26, 1986.

3.42 R. W. Ziolkowski, and J. B. Grant, "The Mathematical and Physical Scaling of Triggered Lightning" *Report No. DE84002480 UCID-19655*, Lawrence Livermore Laboratory, December 1983.

3.43 H. W. Kasemir, and F. Perkins, "Lightning Trigger Field of the Orbiter," *Report No. CN 154148}, NOAA*, Boulder, Co., October 1978.

3.44 G. Labaune, et al., "Experimental Study of the Interaction Between an Arc and an Electrically Floating Structure," *Int. Aerospace and Ground Conf. on Lightning and Static Electricity*, Dayton, Ohio, pp. 27-1 - 27-9, June 24-26, 1986.

3.45 M. A. Uman, and E. P. Krider, "A Review of Natural Lightning: Experimental Data and Modeling," *IEEE Trans. on EMC*, Vol. EMC-24, No. 2, May 1983.

3.46 D. R. Fitzgerald, "Electric Field Structure of Large Thunderstorm Complexes in the Vicinity of Cape Canaveral," *Int. Conf. on Atmospheric Electricity*, June 3-8, 1984, Albany, N.Y., pp. 260-263.

3.47 J. R. Gayet, "Location of Lightning Strokes on Aircraft in Storm Field with Measured Electrical, Microphysical and Dynamical Properties," *10th Int. Aerospace & Ground Conf. on Lightning and Static Electricity*, Paris, France, 1985.

3.48 F. L. Pitts, L. D. Lee, R. A. Perala and T. H. Randolph "New Results of Quantification of Lightning/Aircraft Electrodynamics" *J. of Electromagnetics*, Vol. 7. 1987, pp. 451-485.

Chapter 4

THE EFFECTS OF LIGHTNING ON AIRCRAFT

4.1 Introduction

We had just taken off from Presque Isle, Maine, and had been in cruise power for 50 minutes, when a large thunderhead cumulus was observed directly on course. Lightning could be seen around the edges and inside the thunder head. All cockpit lights were on, and the instrument spotlight was full on, with the door open. I had just finished setting the power and fuel flows for each engine. As the ship approached the thunderhead, there was a noticeable drop in horsepower and the airplane lost from 180 MPH airspeed to 168 MPH, and continued to lose air speed due to power loss as we approached the thunderhead. A few seconds before the lightning bolt hit the airplane, all four engines were silent and the propellers were windmilling. Simultaneous with the flash of lightning, the engines surged with the original power. The lightning flash blinded the Captain and me so severely that we were unable to see for approximately eight minutes. I tried several times, during this interval, to read cockpit instruments but it was impossible. The First Officer was called from the rear to watch the cockpit. Of course, turbulent air currents inside the cumulus tossed the ship around to such an extent that, had the airplane not been on autopilot when the flash occurred and during the interval of blindness suffered by the cockpit occupants, the ship could have easily gone completely out of control. The Captain and I discussed the reason for all four engines cutting simultaneously prior to the lightning flash and could not explain it, except for the possibility of a magnetic potential around the cumulus affecting the primary or secondary circuit of all eight magnetos at the same time.

~ First Officer N.A. Pierson's experience on a flight from Presque Isle, Maine, to the Santa Maria Islands on July 9, 1945.

It was not long after the beginning of powered flight that aircraft began being struck by lightning, sometimes with catastrophic results. Early wooden aircraft with metal control cables and guy wires were not capable of conducting lightning stroke currents of tens of thousands of amperes or more. Wooden structural members, and even the steel control cables, exploded or caught fire. Even if severe structural damage did not occur, pilots were frequently shocked or burned by lightning currents entering their hands or feet via control pedals or the stick. Sometimes fuel tanks caught fire or exploded. These effects, coupled with the air turbulence and precipitation also associated with thunderstorms, quickly taught pilots to stay clear of stormy weather.

Early Research

With the advent of all-metal aircraft, lightning strikes became more tolerable, but thunderstorms continued to be treated with respect. Nonetheless, because a few accidents attributed to in-flight lightning strikes continued to happen, the Subcommittee of Aircraft Safety, Weather and Lightning Experts was formed by the National Advisory Committee for Aeronautics (NACA) in 1938 to study lightning effects on aircraft and determine what additional protective measures were needed. Dr. Karl B. McEachron, Director of Research at the General Electric High Voltage Laboratory, was a key member of this committee, and during its twelve-year existence he performed the first simulated lightning tests on aircraft parts. During and subsequent to this period, other organizations, such as the United Stated (US) National Bureau of Standards, the University of Minnesota, and the Lightning and Transients Research Institute (LTRI), and the aircraft manufacturing industry also began to conduct research into lightning effects on aircraft.

A major purpose of this chapter is to draw attention of aircraft designers to the many potential effects that lightning may cause to an aircraft, and so enable the lightning safety assessment to be conducted in a manner that will enable all potential safety hazards to be identified.

The chapter is organized to explain the physical effects (also known as *direct effects*) of lightning, and then the induced effects (also known as *indirect effects*) of lightning strikes to an airplane; the intent being to alert designers to possible hazards so that they can be avoided by design. Together these categories are intended to include all the effects of lightning on the aircraft. Examples of these effects from in-flight or laboratory test experience are presented. Lessons learned regarding each effect are also given.

Later chapters will address protection against each effect, and in so doing provide further explanations of the mechanisms responsible for each.

Physical effects

For a long time, the physical damage effects at the points of lightning attachment to the aircraft were the main concern of protection design. These included holes burned in metal skins, puncturing, or splintering of nonconductive structures, welding or roughening of moveable hinges and bearings, and rupture of bond straps, control cables and rods that conduct lightning currents during a strike. If the lightning attachment point was a wing tip light or antenna, the possibility that some of the lightning current might be conducted directly into the aircraft's electrical circuits was also of concern. Today, these and other physical damage effects are often called the *direct effects* of lightning. Since present day military and commercial aircraft fly Instrument Flight Rules (IFR) in many kinds of weather, protective measures against physical effects have been designed and incorporated into these aircraft so that hazardous consequences of lightning strikes are rare. Ignition of fuel vapors due to arcs and sparks inside fuel tanks are also known as physical (direct) effects.

Induced effects

Since the installation of electronic equipment (especially solid-state electronics) in aircraft, it has become apparent that lightning strikes may cause other effects to this equipment. For example, the operation of cockpit instruments and navigation equipment has been interfered with, and circuit breakers have opened in electric power distribution systems when aircraft have been struck by lightning. The causes of these effects are the electromagnetic fields, and the structural voltage rises associated with lightning currents flowing in the airframe. Even though metal skins provide a high degree of electromagnetic shielding, some of these fields penetrate directly through windows or seams and induce transient voltage surges in the aircraft's electrical wiring. The resistances of structural joints and of non-metallic (composite) structures permit voltages to occur between equipment locations in the aircraft. These surge voltages, in turn, may damage or upset electrical or electronic equipment.

In some cases, it is unclear which category a particular effect falls within. An example is a current in a hydraulic tube that causes arcing at anodized pipe fittings that results in a fluid leak, loss of pressure and loss of flight control. One might call this a direct effect, but the physics that results in current in the tube is the same as that which induces current in interconnecting wire harnesses. To avoid the risk of missing some effect of unknown origin, it is best not to put effects into broad categories, but instead to consider them by type of effect. This is the approach that we will follow in describing the typical lightning effects that are shown in this chapter.

In short, the recommendation is to consider all of them as *lightning effects*. If broad categories are desirable, it may be more appropriate to call them *physical effects* and *induced effects,* as we will do in this book.

Some of the lightning effects that we will describe in this chapter are usually benign and little needs to be done to eliminate them *(indeed, it is nearly impossible to get rid of all of the effects of lightning – a very severe environment due to its extremely high temperatures and strong overpressures, not to mention the very high electric currents and specific energies).*

A point to be remembered is that benign effects can also cause catastrophic consequences if they happen where and when the 'right' combination of other conditions are present.

Trends that can increase potential lightning hazards

Lightning-related accidents involving commercial aircraft are rare as compared with other causes, but there are two trends in aircraft design that threaten to aggravate the problem unless specific protective methods are incorporated in system equipment designs. The first of these is the increasing use of electronic systems to navigate and control the aircraft.

The second trend is the increasing use of glass or carbon-reinforced plastics in place of aluminum structures, a practice that reduces the electromagnetic shielding previously furnished by the highly conductive aluminum skin. This reduced shielding may greatly increase

the level of surges induced in interconnecting wiring not protected by other means. Because electronic systems were becoming increasingly depended upon for safety of flight, the National Aeronautics and Space Administration (NASA), the Federal Aviation Administration (FAA), and the Department of Defense (DoD) initiated research programs, beginning in 1967, to learn how to measure or predict the levels of lightning induced voltages and how to protect against them. A considerable amount of research has been conducted since then by government and industry organizations. This research has resulted in the development of techniques for quantifying lightning induced effects, for protecting equipment and systems from them and for verifying the adequacy of protection. Much of this work was focused on protection of electrical and avionic systems, but it applies equally to protection of hydraulics, mechanical flight and landing gear controls, air conditioning, and other aircraft systems.

Since the induced effects originate in the aircraft's electrical wiring, their consequences may show up anywhere within the aircraft, such as at equipment locations remote from the lightning flash attachments. The physical effects, on the other hand, occur most often at or near the points of lightning attachment, or within structures or fuel tanks that lie within lightning current paths between strike entry or exit points. This comparison is illustrated in Fig. 4.1. It should be expected that lightning currents engulf the entire airframe and much of the electrically conductive items installed within.

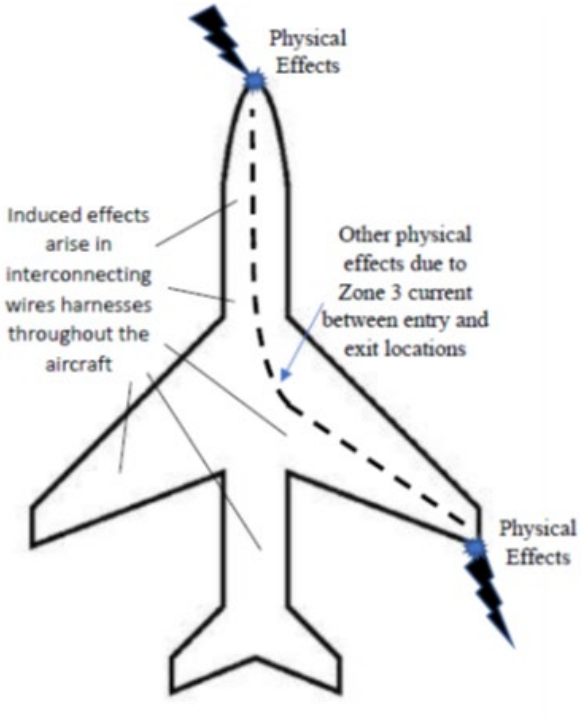

Fig. 4.1 Areas of physical and Induced Effects

4.2 Physical Effects on Metal Structures

Metal structures include the outer skins of the aircraft, together with internal metal framework, such as spars, ribs, and bulkheads. The aluminum of which most of these structures are made provides excellent electrical conductivity and, because lightning currents spread out and flow through the entire airframe between lightning entry and exit points, the current density at most places in the airframe is rarely sufficient to cause physical damage. Only if there is poor electrical bonding (contact) between structural elements in the current path is there likely to be some physical damage due to arcing between structural elements. On the other hand, where the current paths converge to the immediate vicinity of an entry or exit point, there may be a sufficient concentration of magnetic force and resistive heating to cause damage. Damage at these points is further compounded by intense heat and blast forces from the lightning channel. Individual discussions of these effects follow.

4.2.1 Pitting and Melt-through

If a lightning channel touches a metal surface for a sufficient time, the surface melts at the point of contact, called the *arc root*. Common evidence of this are the successive pit marks often seen along a fuselage or empennage, as shown in Fig. 4.2, or the holes burned in the trailing edges of wings or empennage tips, as shown in Fig. 4.3. Holes are typically melted in skins of 1 mm (0.046") thickness or less, except at trailing edges, where the lightning channel may hang on for a longer time and melt holes through much thicker skins. Since a melt-through does not happen instantaneously, the continuing currents are the lightning flash components most responsible for pitting and melt-through. The melt-through of skins is usually not a safety-of-flight problem unless the skins enclose an area containing a flammable material, such as some thermal blanket materials or the vapor in an integral fuel tank. Small holes of the sort melted by lightning do not allow enough air loss to reduce cabin pressure to dangerous levels.

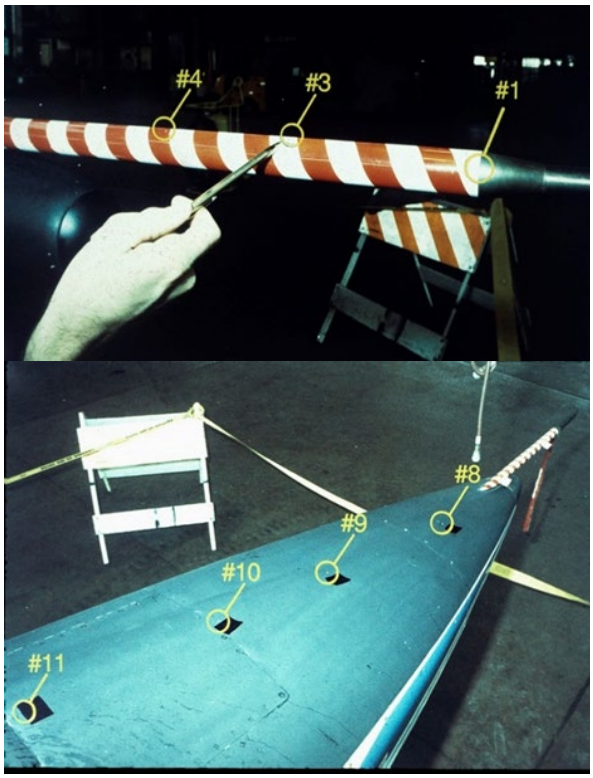

Fig. 4.2 Successive pit marks extending aft from pitot boom. Initial leader attachment was at tip of nose boom of this USAF T-38 trainer operated by NASA (NASA Photo)

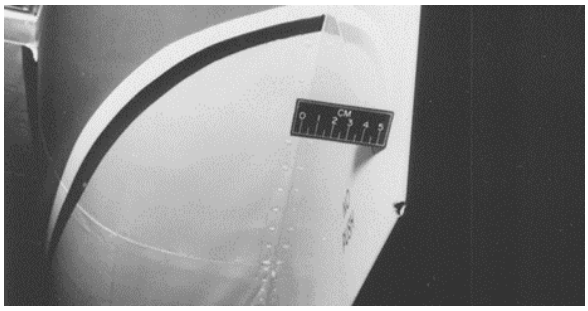

Fig. 4.3 Hole melted in trailing edge corner of ventral fin. (Andy Plumer photo)

Whether melt-through happens or not depends on the degree to which the lightning channel attaches to the metal surface in a concentrated or diffused (spread-out) manner. If the surface is an anode as in Fig. 4.4 there are not as many arc roots and the depth of melting is greater than if the attachment location is a cathode where there are many more arc roots and the energy dissipated at any one is much less, as shown in Fig. 4.5. Electrons are emitted from a cathode and received at an anode. These differences are apparent on unpainted metal surfaces. If the surface is painted, the paint will concentrate the current regardless of whether the surface is an anode or a cathode so that all the current enters (or exits) at one spot. Examples are shown in Figs. 4.6 and 4.7.

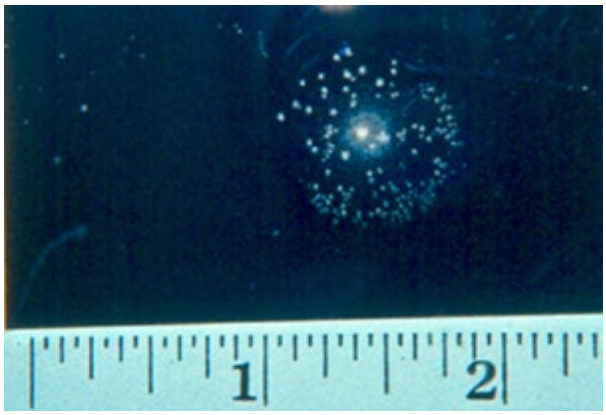

Fig. 4.4 Anode spot on unpainted aluminum surface. (Laboratory test result, Dimension in inches) (Lightning Technologies, Inc. photo)

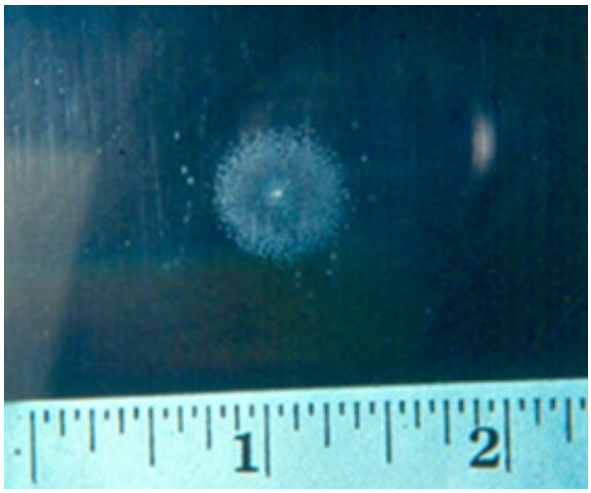

Fig. 4.5 Cathode spots on unpainted aluminum surface. (Laboratory test result. Dimensions in inches) (Lightning Technologies, Inc. photo)

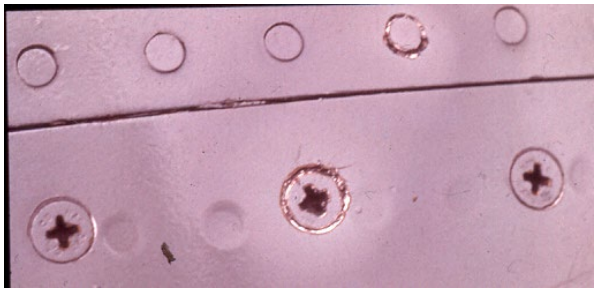

Fig. 4.6 Typical lightning attachments to rivet and fastener. Note the thermal "halo" in the surrounding paint and discoloration of paint aft (Left) of the strike point. (Andy Plumer photo)

A painted, flush mounted rivet will attract lightning reattachment as shown in Fig. 4.7. This is because there is a small intensification of the electric field at the rivet edge when a sweeping channel passes nearby.

Fig. 4.7 Lightning channel reattachment to painted flush rivet. Note the thermal "halo" in the surrounding pain and darkening of paint aft (left) of the strike point. (Andy Plumer photo)

Holes melted in aluminum skins that enclose fuel have allowed ignition and explosion of fuel vapors, and holes melted in other aluminum skins have allowed ignition of other flammable materials such as thermal blankets. Some strikes produce many melt spots, often but not always, at edges of rivets or fasteners. Examples are shown in Fig. 4.8. When the lightning channel happens to reattach to a rivet, the thermal mass of the rivet usually prevents a hole from being melted through the entire thickness of the skin. So does the usual presence of a sub-structural element to which the skin is fastened. But if the channel happens to re-attach at a spot where there is skin only, a hole is more likely. Some of each are shown in Fig. 4.8.

Fig. 4.8 Cluster of melted spots in painted aluminum fuselage skin. All are due to multiple reattachments in one strike. This cluster covers a region ~1 m in length along the lower fuselage of regional jet airplane. (Andy Plumer photo)

Hagenguth [4.1] found that the size of hole melted in an aluminum sheet of a given thickness could be approximated by the following two empirical expressions:

$$A = 0.93Q\,t^{-.09} \text{ for } 0 < t < 0.8 \text{ mm}$$

$$A = 0.81Q\,t^{-1.54} \text{ for } 0.8 < t < 4 \text{ mm}$$

where,

A = area of hole melted (square millimeters)
Q = charge (coulombs) delivered to the point by the arc
t = thickness of metal sheets (centimeters).

The rate of charge delivery for the above experiments was 200 A. This is similar to the amplitudes of the continuing currents in a lightning flash.

Further discussion of and design of protection against melt-throughs is discussed in Chapters 6 and 7.

1. The amount of electric charge delivered to a spot and the rate at which this is delivered are the important lightning characteristics that influence melting of holes.
2. Holes into integral fuel tanks or other fuel vapor areas can lead to explosion of vapors. Holes elsewhere may not be of immediate concern unless there are flammable materials nearby, or other vulnerable systems.
3. If left unrepaired for extended periods, holes may be the source of crack initiation.

4.2.2 Magnetic Forces

Metal skins or structures may be deformed because of the intense magnetic fields that accompany concentrated lightning currents near lightning attachment points. It is well known that when electric currents flow in the same direction through two or more parallel wires, mutual attractive forces act on the wires. If the structure near an attachment point is viewed, electrically, as being made up of many parallel conductors converging to the lightning attachment point, then as lightning current flows from the point, forces occur which tend to draw these conductors closer together. If a structure is not sufficiently rigid, pinching or crimping may occur, as shown in Fig. 4.9. The amount of damage produced is proportional to the square of the amplitude of the lightning stroke and is more or less proportional to the time duration of the stroke. Thus, the stroke currents, because of their high amplitudes, are the components of a lightning flash primarily responsible for magnetic force damage.

Fig. 4.9 Example of magnetic pinch effect at lightning attachment points.
(NASA Photo)

In addition to light-weight control surfaces, other items that may be damaged by magnetic forces include electrical bond straps in concentrated current paths, lightning diverter strips on non-metallic structures, antennas, air data probes, or any other object that may conduct concentrated lightning stroke currents. Magnetic force damage is usually not significant enough, by itself, to require abortion of flight, and may not even be detected until the aircraft is inspected following a strike. Bond straps that must conduct significant amounts of lightning current, such as across stabilizer trim actuators have been exposed to magnetic forces that have broken the straps or pulled them out of their attachment lugs. Guidelines for controlling magnetic force effects are contained in Chapter 6.

Lessons learned regarding magnetic forces include,

1. The possibility of magnetic forces is often overlooked. Examples are a bond strap that is designed with adequate cross-section which may break if the strap is installed with a bend, or two aluminum hydraulic tubes installed in parallel that may slam together and break if exposed to lightning currents. A hollow push rod to an elevator may be crushed if it must carry excessive current.

2. Some lightning test standards and test plans do not require that the test specimens be tested in a configuration with nearby conducting objects that represents the aircraft installation.

4.2.3 Pitting at Structural Interfaces

Wherever inadequate electrical contact exists between two mating surfaces, such as at control surface hinges, wheel bearings or door stops that must conduct lightning currents, melting and pitting of these surfaces may occur. Examples are at access door stops shown in Fig. 4.10. Current was transferred from the door to the fuselage via the door stops.

Other examples are the nose wheel axle and bearing shown in Fig. 4.11.

Fig. 4.10 Evidence of arcing at crew escape door stops during strike to door [4.2]

Fig. 4.11 Nose wheel axle and bearing after arcing due to lightning strike to nose wheel [4.2]

4.2.4 Resistive Heating

Another physical effect is the resistive heating of conductors exposed to lightning currents. When the resistivity of a conductor is too high, or its cross-sectional area too low for adequate current conduction, lightning currents may deposit appreciable energy in the conductor, raising its temperature excessively. Since the resistivity of most metals increases with temperature rise, a given current in a heated conductor deposits more energy than it would in an unheated, less resistant conductor. Most metal structural elements can tolerate lightning current with little change in temperature. The methodology for determining temperature rises in conductors of specific material or cross-sectional size is described in Chapter 6.

Resistive energy deposition is proportional to the integral of the square of the lightning stroke current whose time duration (usually less than 500 μs) is short enough that most of the energy is deposited in the conductor before it can be conducted or radiated away. This is called the *action integral* (also *specific energy*) of the current and is discussed more fully in Chapter 5. For any conductor, there is a lightning stroke current action integral value at which the conductor will melt and vaporize (see Fig. 4.12). Small diameter copper wires of the sizes commonly used to interconnect avionic equipment or supply power to small loads (AWG 20 and 22), often melt or vaporize when subjected to significant amounts of lightning current.

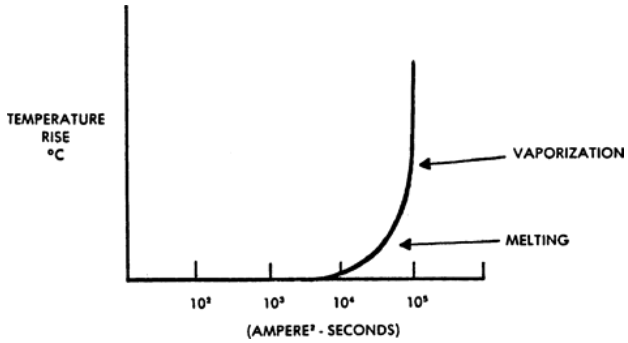

Fig 4.12 Action integral (A^2s) vs temperature rise in a metal conductor.

Examples of the damage produced by explosive vaporization of small-diameter conductors are shown in Figs. 4.13 and 4.14. The damage is usually most severe when the exploding conductor is within an enclosed area, such as the composite wing tips shown in Fig. 4.14. When the energy of an explosion is contained within an enclosure such as this, the pressure builds up until it is sufficient to rupture the enclosure. The chemical energy from the combustion of the wire is added to the energy deposited by the lightning current, increasing the total damage.

For carbon fiber reinforced plastic (CFRP) structures, the temperature rise is very significant due to the higher resistance of carbon as compared with most metals. However, this high temperature will melt and ignite resins before the carbon is vaporized so the carbon reinforced composite material is damaged in other ways as described in § 4.2.3.

Exposure of the wiring

Most aircraft electrical wiring is installed within conductive airframes, and thus is not exposed to significant amounts of the lightning current. There are some exceptions, however. For example, a wiring harness feeding a wingtip navigation (NAV) light might be installed on an unprotected, fiberglass wingtip. A lightning strike to the navigation light would vaporize the wire harness, causing an explosion as the lightning current path formed as a plasma inside the wingtip. Such an explosion can do extensive damage to the enclosing wingtip and surrounding structures. Fig. 4.13 is an example of this type of explosive damage to a radome that enclosed a small diameter wiring harness feeding a pitot heater. The shock-wave damage to the aluminum wings of a small airplane (shown in Fig. 4.14) occurred when the NAV light wire harness exploded inside the fiberglass wingtips. This strike entered one wing tip and exited from the other, so the effects at each tip were the same.

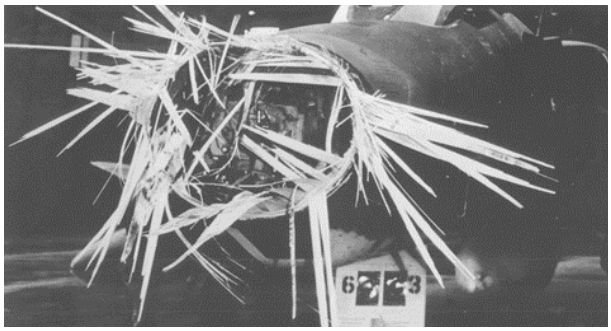

Fig. 4.13 Lightning damage to radome, probably caused by an exploding pitot tube ground wire. (USAF photo)

Fig. 4.14 illustrates the fact that effects of lightning currents at "entry" and "exit" locations are the same if the surface or structure materials at these locations are the same. It makes no difference whether the lightning has "entered" or "exited" at locations of similar design. The physical effects are the same.

The small single engine airplane of Fig. 4.14 experienced a severe cloud-to-earth strike that attached to both wing tip NAV lights. Since the wing tips were of fiber glass without lightning protection, the only path to the airplane was via the NAV light wire harnesses. These exploded, the fiberglass tips were blown away, and the physical damage to the aluminum outboard wing tips was due to the overpressure, momentarily contained within the fiberglass wing tips, from the exploding wire harness. Some of the lightning current commuted to the airframe via the tip ribs, but enough current was conducted into the aircraft electrical system via the remaining light harnesses to burn out all the electrically operated cockpit instruments and radios. The strike happened in daylight and the pilot managed to land safely at a nearby airport.

Exploding wire harnesses are one of the most common and damaging lightning effects. They have not, as far as is known, had catastrophic consequences because these harnesses are usually found in secondary structures that are not flight critical. There is no reason, however, to allow these situations to persist, because protection is easily applied, as will be described in Chapter 6. Such protection can also minimize the possibility of conducting lightning current surges into power distribution or avionic systems, or into control cables that might be damaged with catastrophic consequences.

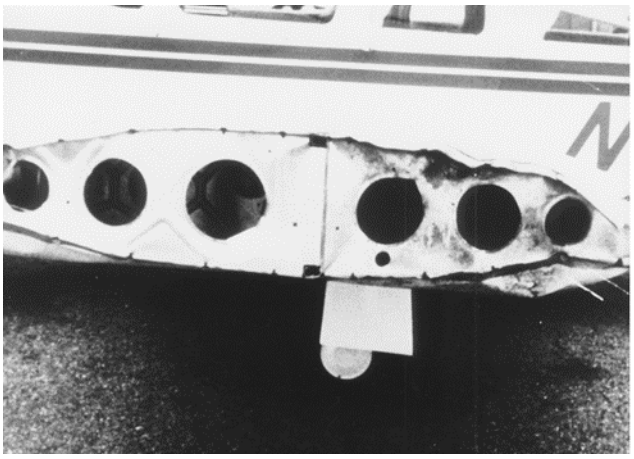

Left wing tip, showing overpressure damage to aluminum outer wing.

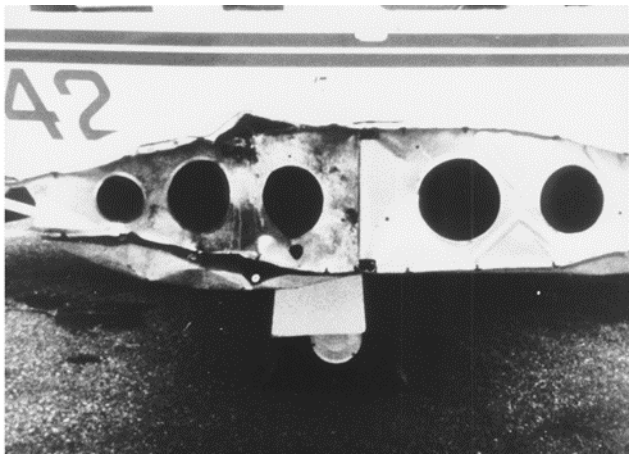

Right wing tip, showing overpressure damage to aluminum outer wing.

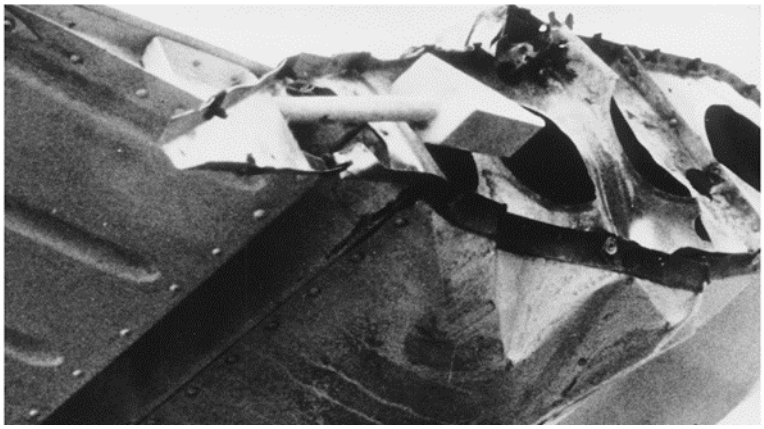

Close-up view of damaged right wing tip

Fig. 4.14 Damaged wingtip structures due to exploding navigation light wire harnesses. Flash entered at one wing tip and exited from the other. Both fiberglass wingtips were blown off the wingtips in flight.
(National Transportation Safety Board photo)

4.2.5 Shock Wave and Overpressure

When a lightning stroke current flows in an ionized leader channel, a large amount of energy is delivered to the channel in several hundred microseconds. This causes the channel to expand with supersonic speed. Its temperature has been measured by spectroscope techniques to be 30 000 °K and the channel pressure (during expansion) is about 10 to 15 atmospheres [4.3]. When the supersonic expansion is complete, the channel diameter is several centimeters, and the channel pressure is in equilibrium with the surrounding air. An example of the pressure wave from a stroke current of moderate amplitude is shown in Fig. 4.15. Later, the channel continues to expand more slowly to the equilibrium situation of a stable arc. The cylindrical shock wave propagates radially outward from the center of the channel and, if a hard surface intervenes, the kinetic energy in the shock wave is transformed into a pressure rise several times that of the shock wave. The overpressure close to the channel is very high.

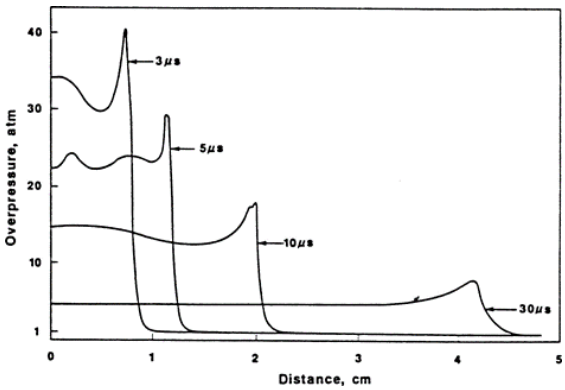

Fig. 4.15 Pressure vs. radius at four times dues to a 30 kA arc [2.14].

Depending on the distance of the channel from the aircraft surface, overpressures at that surface can be as high as several hundred atmospheres. The lightning channel does not have to contact a surface to inflict damage upon it but may simply be "swept" into close proximity to the surface as the aircraft flies through the lightning channel. A common example of this effect is a shattered cockpit windscreen, as illustrated in Fig. 4.16.

In some instances, the effects of the shock wave are sufficient to fracture the windscreen and allow lightning currents to enter the anti-ice heating element as discussed further in Chapter 6.

Fig. 4.16 Shattered exterior ply of cockpit windscreen [4.2].

Examples of shock wave implosion damage include cracked or shattered windshields and navigation light globes. Modern windshields, especially those aboard transport aircraft, are of laminated construction and of sufficient strength to withstand these shock waves without being completely broken. However, broken windshields resulting from a lightning strike are considered a possible cause of the crash of at least one propeller-driven aircraft [4.4].

4.2.6 Effects on Other Systems

All systems within an aircraft potentially experience lightning effects. Several of the more common examples are as follows.

Hydraulics

Hydraulic tubes share the lightning currents that are conducted through an airframe between lightning entry and exit locations. Where hydraulics are routed between the fuselage and one of the stabilizers, these currents may be in the 10s of kiloamperes because the tubes are often exposed to strong magnetic fields from lightning currents flowing in nearby torque tubes or other control mechanisms. In other words, the hydraulic tubes comprise a major current path between stabilizers and fuselage.

The tubes themselves are exposed to magnetic force effects which can cause mechanical failures, and the couplings are potentially exposed to electrical arcing, especially if they include nonconductive corrosion resistant surface finishes in the coupling interfaces. If arcing happens in the couplings, it is likely that fluid leaks develop, possibly resulting in loss of pressure and control function. Similarly, hydraulic power cylinders have lost pressure due to arcing between piston and cylinder. There have been several incidents of transport aircraft having lost elevator control function.

Guidance for protection of hydraulic systems is presented in Chapter 6.

Landing Gear

Landing gear are exposed to direct lightning strikes when extended, and when parked on the ground. Lightning strikes to nose gear seem to be the most common, but main gear have also been struck. The nose and main gear are in lightning strike *Zones 1B* and *3*, so must conduct all the currents in the lightning flash. Typical effects of these currents are:

1. Arcing between axle and bearing as was shown in Fig. 4.11.

2. Arcing among ball bearings, races, and surfaces.

3. Arcing damage to brake shoes.

4. Damage to tires. If tires are metal reinforced the stroke currents may go into the reinforcing strands and damage tire material in the process. Otherwise, the lightning currents flash harmlessly across the outside surfaces of the tires. The higher pressure inside the tires makes it more likely for ionization and flashover to happen on the outside surface of a tire than for this to occur on the inside.

5. Damage to electronic control systems due to high amplitude lightning currents in the wire harnesses from wheel-mounted sensors and actuators.

Cabin Interiors

When aircraft skins are struck by lightning there is a likelihood of melting of aluminum skins and cracking, of CFRP skins, so that items on the interior of these skins may be exposed to some of the effects of lightning.

Examples that have occurred are ignition of cabin insulation material and current entry into nearby wire harnesses. Other possibilities would appear to be:

1. Any effects of high temperatures (at or above the melting temperature of aluminum (660 °C) or the temperature of an electric arc (up to 20 000 °C) in the event that a hole is melted in the skin and items inside the skin are exposed to the lightning channel (arc).

2. The effects of composite resin burning due to contact of lightning with an unprotected composite skin. The lightning channel is capable of igniting resin in most composite skins.

3. Contact of deformed metal skins or cracked or broken fibers of a CFRP skin with nearby electrically conductive components or materials that would be damaged by electrical arcing. Such arcing can be an ignition source for flammable materials.

4. Lightning current conducted into the airplane due to a strike to an externally mounted electrical device, such as an antenna, air data probe, or light. (This effect is also to be addressed when designing the installations of externally-mounted items.)

5. Shock wave damage or dielectric breakdown and puncture or cabin windows, access panels, or doors that could expose personnel to safety hazards.

6. Strikes to drain tubes fabricated of electrically conductive materials that comprise a pathway for lightning currents to reach the interior of the aircraft. Such tubes may provide a path to devices or systems that are not considered susceptible to lightning effects.

4.3 Physical Effects on Highly Resistive Structures

Early aircraft of wood and fabric construction would probably have suffered more catastrophic damage from lightning strikes had it not been for the fact that these aircraft were rarely flown in weather conducive to lightning. The all-aluminum aircraft that followed, were able to fly in or near adverse weather and receive strikes but, because aluminum is an excellent electrical conductor, severe or catastrophic damage from lightning was rare. The use of separate (non-integral) fuel tanks may have aided this situation. Electronic systems (mostly radio transmitters) and receivers utilized vacuum tubes that are inherently more robust than the solid-state electronics used today, and many other functions now routinely performed by electronics were operated mechanically “by hand”.

However, today there is a trend, toward use of non- metallic materials in aircraft construction. These materials, which include glass fiber reinforced plastic (GFRP) and CFRP are being used because they offer cost and weight reductions.

Nonconductive Composites

Nonconductive composites include (GFRP) and some other reinforced plastics. Some of these materials have begun to replace aluminum in secondary structures, such as nose, wing and empennage tips, tail cones, wing-body fairings, and control surfaces and, in several instances, entire aircraft have been fabricated of nonconductive composites.

When nonconductive, composite material encloses a metal object, such as a radar antenna, the electric fields that exist during the strike attachment process can penetrate the composite surfaces and initiate streamers from the metal objects inside. Unless some conductive layer or other device is applied to stop the electric field penetration, these streamers may puncture the composite as they propagate outward to establish a lightning attachment. This puncture begins as a pinhole but if the stroke currents and their accompanying blast and shock waves soon follow, they inflict much more extensive damage. The process begins with streamer formation inside the composite, as shown in Fig. 4.17. If the field is present for a sufficient time, some of the field concentrates at the composite wall, producing a puncture.

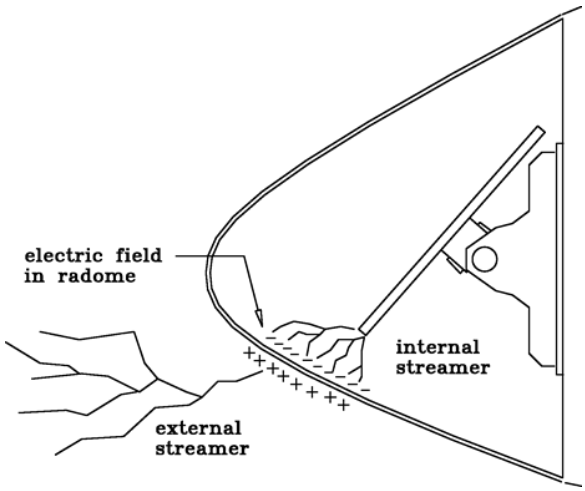

Fig. 4.17 Mechanism of puncture of a radome

An example of puncture damage on a fiberglass honeycomb radome is shown in Fig. 4.18. In this example, a streamer evidently propagated from the radar antenna, puncturing the fiberglass-honeycomb wall and rubber-erosion protection boot on its way to establish a lightning leader as part of the aircraft lightning strike process described in Chapter 3. The stroke current must have been responsible for most of this damage. If only a streamer punctures a radome, the result is less noticeable pinholes on the exterior surface and often a disbond of the inner surface of the composite sandwich. Examples of these effects are shown on Figs. 4.19 and 4.20.

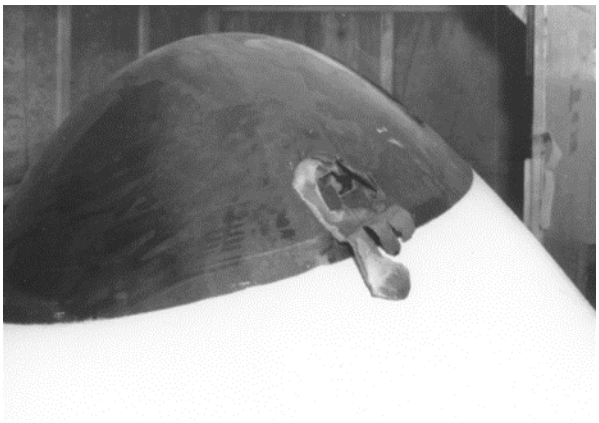

Fig. 4.18 Puncture of a fiberglass-honeycomb radome.

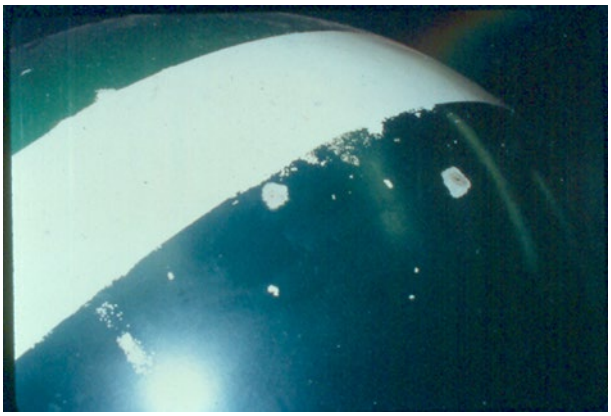

Fig. 4.19 Pinholes in radome due to streamers.

Fig. 4.20 Dis-bond of fiberglass sandwich inner surface due to streamer puncture.

The reason for the difference in responses of the exterior (Fig. 4.18) and interior (Fig. 4.20) surfaces is likely the difference in pressure between exterior and interior of the radome.

Means to protect radomes and other nonconductive composite structures are described in Chapter 6.

Conductive composites

Composites reinforced with carbon fibers do have electrical conductivity and, because of this, their behavior with respect to lightning is considerably different from that of nonconductive composites. CFRP are employed extensively both in secondary and primary structural applications. The resins include epoxy and polyester which are non-electrically conductive. Carbon Fiber Composite (CFC) laminates are also employed in many propellers and helicopter rotor blades, either as skins, reinforcing spars, or both. Sometimes an entire airframe has been fabricated of CFRP.

The electrical conductivity of CFRP laminates is in the reinforcing carbon fibers, so CFRP is not isotropic, but depends on the directions of these fibers in the laminates.

Most composites are comprised of multiple layers (plies) of either aligned fibers in one direction, or woven fabrics where fibers are in two directions. There are many configurations in use, tailored to mechanical loads and other structural requirements.

In a unidirectional (UD) laminate, the highest electrical conductivity is in the direction of the fibers. The conductivity perpendicular to the fiber direction is usually much less than the in-line conductivity. The electrical conductivity normal to the plane of the laminate (i.e., among separate plies) may vary from zero to a value much lower than the in-plane conductivities. This is due to the (usual) resin-rich areas between plies. Attempts to add conductivity by formulating an electrically conductive resin while maintaining necessary adhesive and mechanical properties have not been successful for aircraft applications.

There are also other forms of composites, employing chopped fibers in a random array throughout the volume of a structural item. These are found less often in aircraft applications.

The main lightning effects on CFRP materials are:

1. Overheating due to current in the carbon fibers. This is often called “ohmic heating”.

2. Cracking or fracturing of plies due to the shock wave radiating from the stroke currents.

3. Delamination of plies from one another as a result of either the overheating outgassing of resin within the composite, or the shock wave applying mechanical bending force to the laminate.

If the carbon fibers get very hot, this will melt, vaporize, and ignite the surrounding resin. Being stiffer than aluminum skins of equivalent thickness, CFRP skins may crack or fracture in response to impinging shock waves from lightning stroke currents, while most aluminum skins are sufficiently ductile that they can absorb this energy by deforming, but not usually rupturing. All these effects are due to the stroke currents in the lightning flash.

The volume resistivity of CFRP varies with density and direction of fibers as noted above, but may average about 6×10^{-3} ohm-cm in the plane of the fibers, whereas that of aluminum is about 3×10^{-6} ohm-cm. Thus, CFRP laminates must dissipate up to 2 000 times as much energy as aluminum skins when conducting the same amount of lightning current.

The intermediate and continuing currents amplitudes are much lower than the stroke currents do not have sufficient amplitude, nor do they emit overpressures that would produce effects similar to the stroke currents. These currents do cause burning away of the resin in CFRP surfaces, leaving the fibers in disarray.

The voltage rise due to current flow through the resistance of the CFRP contributes to the voltages and currents that are induced into the interconnecting wiring within the aircraft. This voltage also drives some of the lightning current into interior structural elements and systems, which would not otherwise experience such high current were they part of an all-aluminum aircraft. This effect and the means to protect against hazards associated with it are addressed in subsequent chapters.

Fig. 4.21 shows the back sides of two test panels, one of aluminum and one of unprotected CFRP, both of which had been subjected to the same simulated lightning test. The aluminum panel was only dented, but the CFC panel was broken.

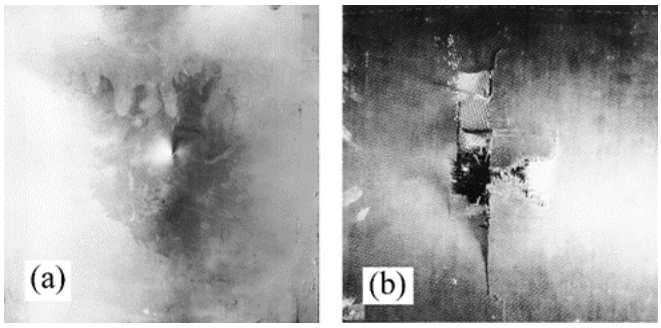

Fig. 4.21 Lightning effects to interior surfaces of aluminum and CFRP skins 1 mm (40 mils) thick
(a) Aluminum, showing deformation and a small melt-through
(b) CFRP, showing cracked and broken piles

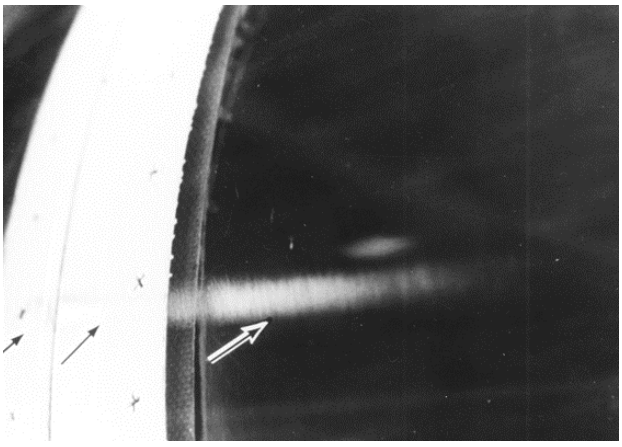

Fig. 4.22 Evidence of lightning attachment to canopy fastener and scorching of canopy. (USAF Photo)

Other plastics

Transparent acrylics or polycarbonate resins are often utilized for cabin windows, canopies, and lamp enclosures. These materials are usually found in locations where lightning may initially contact the airplane, or where lightning channels containing stroke currents may attach or "sweep" by. Most of the polycarbonates isotropic, are very good electrical insulators and do not experience puncture as readily as fiberglass reinforced plastics do. The electric field does penetrate these enclosures, inducing streamers from conducting objects inside, but the streamers are not usually able to puncture a polycarbonate, which have higher dielectric strengths.

Fighter pilots beneath polycarbonate canopies have often reported electric shocks indicative of streamering off their helmets. Fortunately, the streamer current levels (a few amperes) have not caused injuries because the streamers have not become part of the lightning leader (100's – 1 000's of amperes). Leaders originating outside of a canopy from a conductive frame may flash along its surface. This sometimes leaves scorched paths on the outer surfaces of canopies, as shown in Fig. 4.22. Scorches like this can sometimes be polished away, but, in other cases, it has been necessary to replace the canopy.

Effects on Personnel

The bright flashes from nearby lightning channels have been known to temporarily disorient pilots. When a strike occurs at night, a pilot may become blinded for up to 30 seconds by the bright flash. This is not as severe in daylight when the eye is not as sensitive.

The electric fields associated with the lightning strike attachment process or with the charge in a nearby lightning channel have induced currents in personnel exposed to such fields penetrating windows or GFRP surfaces of sufficient magnitude to cause electric shock. In at least one case, either electric shock or blindness caused a fighter pilot to lose control of his aircraft at low altitude, resulting in a fatal accident. When two pilots are available, usually only one of them is assigned to look through the windshield during flight conditions where lightning strikes are likely. The other pilot focuses on cockpit instruments so that the aircraft can continue to be flown safely.

Electric shock may also result from differences in potential among control handles and pedals that may happen if these items are not electrically bonded to an airframe that provides an equipotential reference during a lightning strike. A metal airframe does this quite naturally, but one fabricated largely of composites may require additional measures to control potential differences to safe levels.

The potential differences described above are due to structural voltages and electromagnetic fields that arise as lightning current flow through the airframe. These effects are described more fully in Chapters 8 through 12.

In addition to the physical effects described in the preceding paragraphs, replacement of metal skins with nonmetal materials removes the inherent protection against electromagnetic field penetration that is an important byproduct of aluminum skins. Unless specific protective measures are taken, electrical wiring and electronic components inside nonconductive skins are much more susceptible to the induced effects of lightning than are those inside metal skins.

4.4 Effects on Fuel Systems

Lightning interactions with aircraft fuel systems represent one of the most catastrophic potential hazards to flight safety. An electric arc conducting only one ampere of current is sufficient to ignite flammable hydrocarbon fuel vapor, yet lightning flashes may inject thousands of amperes of current into an aircraft and through structures containing flammable fuel vapors. Ignition or explosion of fuel vapors has usually resulted in a catastrophic failure condition from which the aircraft cannot recover.

There are several dozen civil and military aircraft accidents on record that have been attributed to lightning- related ignition of fuel vapors. Two examples are discussed in [4.5] and [4.6]. Although the exact source of ignition in each case remains obscure, the most likely possibility is that electrical arcing or sparking occurred at some structural joint or plumbing interface that was not intentionally designed to conduct electric currents. Some accidents have been attributed to lightning ignition of fuel vapors exiting from vent outlets, but this possibility has never been confirmed. The airstream flowing past a vent outlet dilutes the vapor so that it is no longer flammable.

Several other fuel tank explosions were the result of the melting of holes through metal skins. In two cases, aircraft experienced strikes to condensate drains, causing arcing at the interfaces between the drains and the tank skins. In addition to the physical effects described above, there are several instances in which induced effects have been responsible for the ignition of fuel [4.7]. Lightning induced voltages in aircraft electrical wiring are believed to have produced sparks at capacitance-type fuel probes inside the fuel tanks of several military aircraft, causing the fuel vapor to explode, in some cases leading to the loss of the aircraft. Capacitance-type fuel probe installations are usually designed to tolerate hundreds of volts without sparking, and laboratory tests have shown that the voltage required to spark a typical capacitance-type probe is many times greater than that induced in most fuel quantity indicating system (FQIS) circuits by lightning. However, several installations have had FQIS wiring installed within fixed leading or trailing edge regions that are not well shielded from lightning electromagnetic fields.

These fields have induced voltages much higher than those found in wire harnesses completely enclosed by an airframe.

The availability of improved test and instrumentation techniques along with numerical simulation codes has led to greater understanding of the processes of lightning current flow in fuel tank structures and into systems installed within the tanks. This has enabled more complete identification of potential ignition sources, allowing more effective protection designs to be made. This topic is discussed more fully in Chapter 7.

4.5 Direct Strike Effects on Electrical Systems

If an externally mounted electrical device, such as a navigation lamp or antenna, happens to be located where lightning attachments may occur, protective globes or fairings may shatter and permit some of the lightning current to be conducted directly into associated electrical wiring.

In the case of a wing tip navigation light, for example, lightning may shatter the protective globe and light bulb(s), allowing the lightning channel to attach to the lamp elements so that some of the lightning current enters the wire harness running from the lamp to the power source. Even if only a fraction of the total current enters these wires, they may be too small to conduct the current and may be melted or vaporized, as described in §4.2.4.

The accompanying voltage surge may cause breakdown of insulation or damage to other electrical equipment powered from the same source. At best, the struck circuit is disabled, and, at worst, other equipment powered from the same source is also disabled, perhaps impairing flight safety. There have been many examples of this effect, involving both military and civilian aircraft. The externally mounted hardware most frequently involved includes navigation lights, antennas, windshield heaters, and air data probe heaters and, in earlier days, the trailing long-wire antennas that were deployed in flight for high frequency radio communications. The latter were quite susceptible to lightning strikes and, since the antenna wires were too small to conduct the lightning currents, they were frequently burned away. The high frequency radio sets feeding these antennas were often damaged, and cockpit fires were not uncommon.

Example of damage

When the lightning channel attaches to an external electrical device (such as a wingtip light) mounted on a nonconductive portion of an airframe, the lightning current is forced to flow through the device's wire harness to get to the airframe. The damage from such an incident can be extensive. An example of this type of damage occurred to a small aircraft as shown in Fig. 4.23. This aircraft had fiberglass wingtips which were not protected from lightning. Each tip contained a fuel tank. The details of this incident, described below, will be used to illustrate several possible lightning effects.

The aircraft was flying at about 900 m (3 000 ft.) in light rain and moderate turbulence when it was struck by lightning. The pilots had seen other lightning flashes in the vicinity before their aircraft was struck, and embedded thunderstorms had been forecast enroute, but there had been no storm cells visible on the air traffic control (ATC) radar being used to vector the aircraft (which had no weather radar of its own).

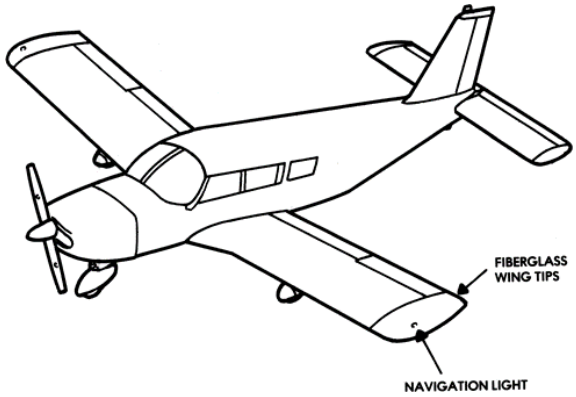

Fig. 4.23 Small aircraft with fiberglass wing tips.

The lightning strike entered one wing tip and exited from the other. It sounded to the pilot like a rifle going off in the cabin, and the cabin immediately filled with smoke. The full list of effects from this strike is given below.

1. The No.1 very high frequency (VHF) communication set was burned out.
2. Seventy-five percent of the circuit breakers were tripped, of which only 50% could be reset later.
3. The left wing tip tank-fuel quantity indicator was disabled.
4. The right main tank-fuel quantity indicator was badly damaged.
5. Several instrument lights were burned out.
6. The navigation light switch and all the external lights were burned out.

Despite these effects the pilot was able to land the aircraft at a nearby airport. Subsequent inspection showed extensive damage to the right- and left-wing tips and to their electrical wiring. The lightning attachment points, and physical effects are pictured in Fig. 4.24(a) through (f) and are represented by a diagram in Fig. 4.25.

Sequence of events

The physical evidence suggests that the flash included two or more strokes, separated by a few milliseconds of continuing current. Assuming, for purposes of explanation, that the original lightning flash "entered" the right wing tip and "exited" from the left wing tip, the probable sequence of events was as follows:

The initial point of lightning entry was the right wing tip navigation light housing, Fig. 4.24(a). Current from this stroke entered the housing ground wire and exploded both sections of it on the way to the right outboard aluminum rib. (This is evidenced by the absence of these wires and the blackened interior shown in Fig. 4.24(b)). Current was conducted through the airframe to the left outboard rib and out the tank-sender unit ground wire to the sender unit, the base of which is shown in Fig. 4.24(c). From there, the current followed the filler gap ground braid and exited the aircraft at the filler cap, Fig. 4.24(d). The current exploded the sender-unit ground wire but not the heavier filler-cap ground braid, which was only frayed. Sparks undoubtedly occurred inside the fuel tank along the ground braid and between the filler cap and its receptacle, but the aviation-gasoline fuel vapor in the ullage of the half-full tanks was probably too rich to support ignition.

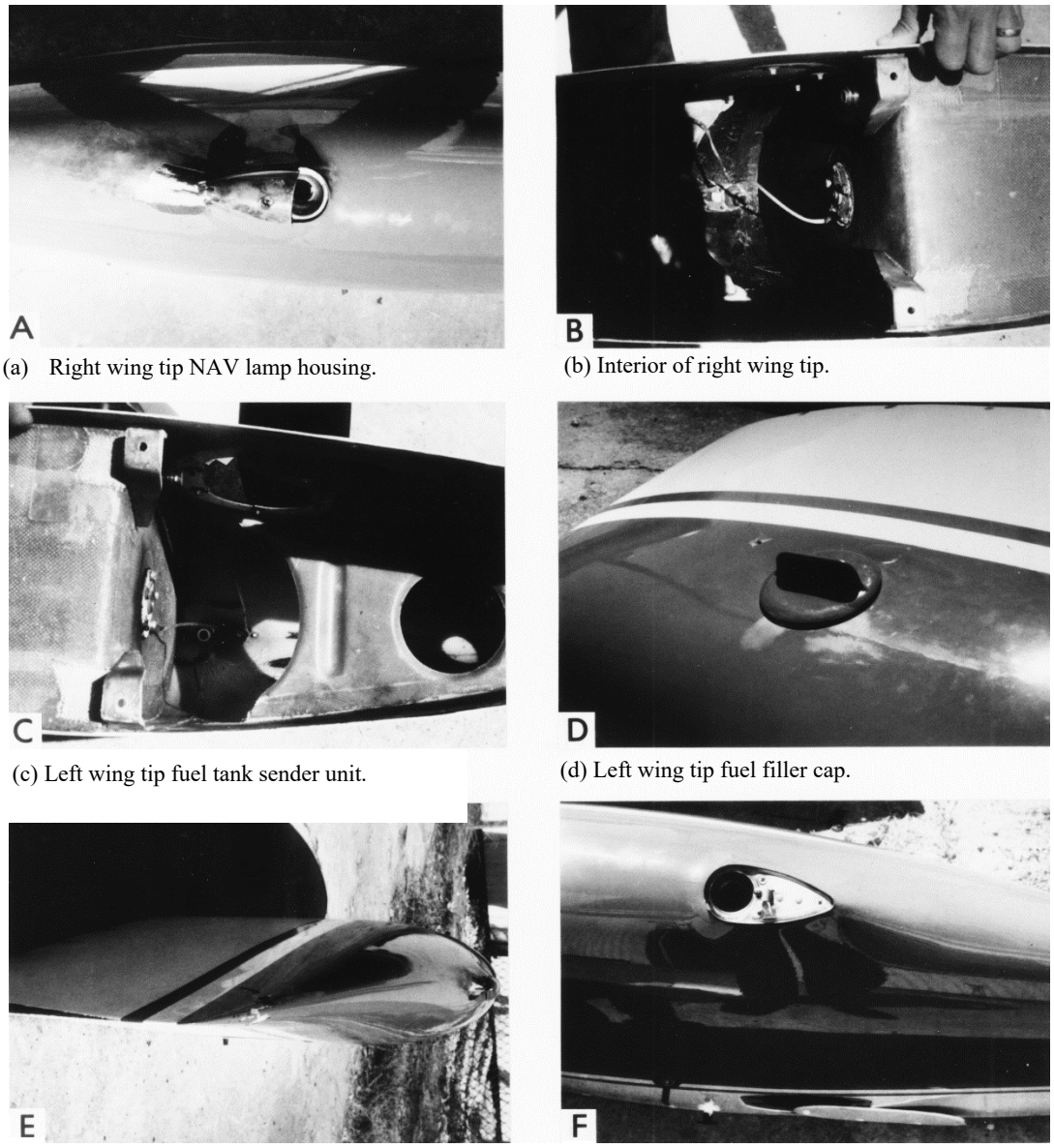

(a) Right wing tip NAV lamp housing.

(b) Interior of right wing tip.

(c) Left wing tip fuel tank sender unit.

(d) Left wing tip fuel filler cap.

(e) Right wing tip and puncture at trailing edge.

(f) Left wing tip lamp housing.

Fig. 4.24 Attachment points and direct effects on GFRP wing tips

Blast forces from stroke No.1, at the right navigation light housing, also shattered the lamp globe and bulb, as shown in Fig. 4.24(a). This shattering allowed a portion of the first stroke current to enter the right navigation light power wire, exploding it between the lamp and the outer rib, where the current jumped to the rib and continued through the rest of the airframe to the left sender unit ground wire.

Lightning current flowing in the navigation-lamp power wire elevated its voltage to several thousand volts with respect to the airframe, a voltage high enough to break down the insulation at the outer rib feed through point, as shown in Fig. 4.25. Until breakdown occurred here, a few microseconds after the first stroke began, the wire was at a sufficiently high voltage to break down the insulation between itself and the neighboring sender wire. This breakdown occurred along the full length of the wire, inside the right wing. The portion of the current that arced into the sender wire caused a large voltage to build up across the inductance of the right wing tip fuel-gauge magnet, to which this wire was connected. This voltage, in turn, sparked over the gap between the gauge terminal and the nearest grounded housing wall, the arcing badly damaging the gauge unit. While the navigation light power wire was also exploded, it is probable that this did not occur until the second stroke.

Since the aircraft was moving forward, the entry and exit points of the second stroke were farther aft on both wing tips than those of the first stroke. Since no other metal components were present aft of the first stroke entry point on the right wing tip, the second stroke punctured a hole in the fiberglass trailing edge and contacted the metal outboard rib, as shown in Fig. 4.24(e). As shown in Fig. 4.25, current from this stroke proceeded through the airframe to the left wing tip, where, by this time, the stroke had swept aft, adjacent to the navigation lamp (Fig. 4.24(f)). From this point, the stroke current exited. Current from stroke No.2 thus probably arced between the left outer rib to the navigation lamp power wire (the ground wire having been vaporized by the first stroke) and followed the lamp power wire to the lamp housing. The power wire was vaporized by the current from the second stroke.

Both left and right navigation lamp power wires were connected in the cabin and to both the 12 VDC bus and the tail light. The voltage and current surges which entered the lamp power wires inboard of the outer rib feedthrough were also conducted to the tail light (burning it out) and to the 12 VDC bus. The surge voltage on the bus was, of course, immediately imposed on all the electrical equipment powered from this bus. This included all of the electrical equipment in this aircraft. Arcing undoubtedly occurred in several components, creating short circuits on power systems that tripped multiple circuit breakers. Because circuit breakers react much too slowly to prevent passage of a lightning surge, at least one piece of equipment (the No.1 VHF communication set) and several instrument lamps were burned out before the circuits were interrupted.

The absence of explosive damage to the GFRP wing tips that contained the wire harnesses meant that the intensities of the stroke currents in this flash were considerably lower than the currents that produced the extensive damage seen on the aircraft in Fig. 4.14. Nevertheless, this strike produced considerable damage of another sort throughout this airplane.

Similar incidents

There have been many incidents similar to that described above in [4.8 - 4.9] and, together, these have stimulated the development of design and verification methods [4.10] for general aviation aircraft with fiberglass components.

The incident described above is an example of how a change in materials can increase the vulnerability not only of the airframe but also of other systems that, in years past, had the inherent protection of conventional aluminum skins. The lightweight lamp and sender unit electrical wires would have been quite adequate for an installation in which a metal skin was available to carry away lightning currents, but they were woefully inadequate when used unmodified inside a plastic wing tip, where they became the only available conducting path for lightning currents trying to enter the airframe.

A lesson to be learned from this incident is that omission of lightning protection for seemingly non-critical systems such as external lights can allow lightning to play havoc throughout much more critical systems in an aircraft.

Guidance for protection of lights and other exterior-mounted devices is provided in Chapter 6.

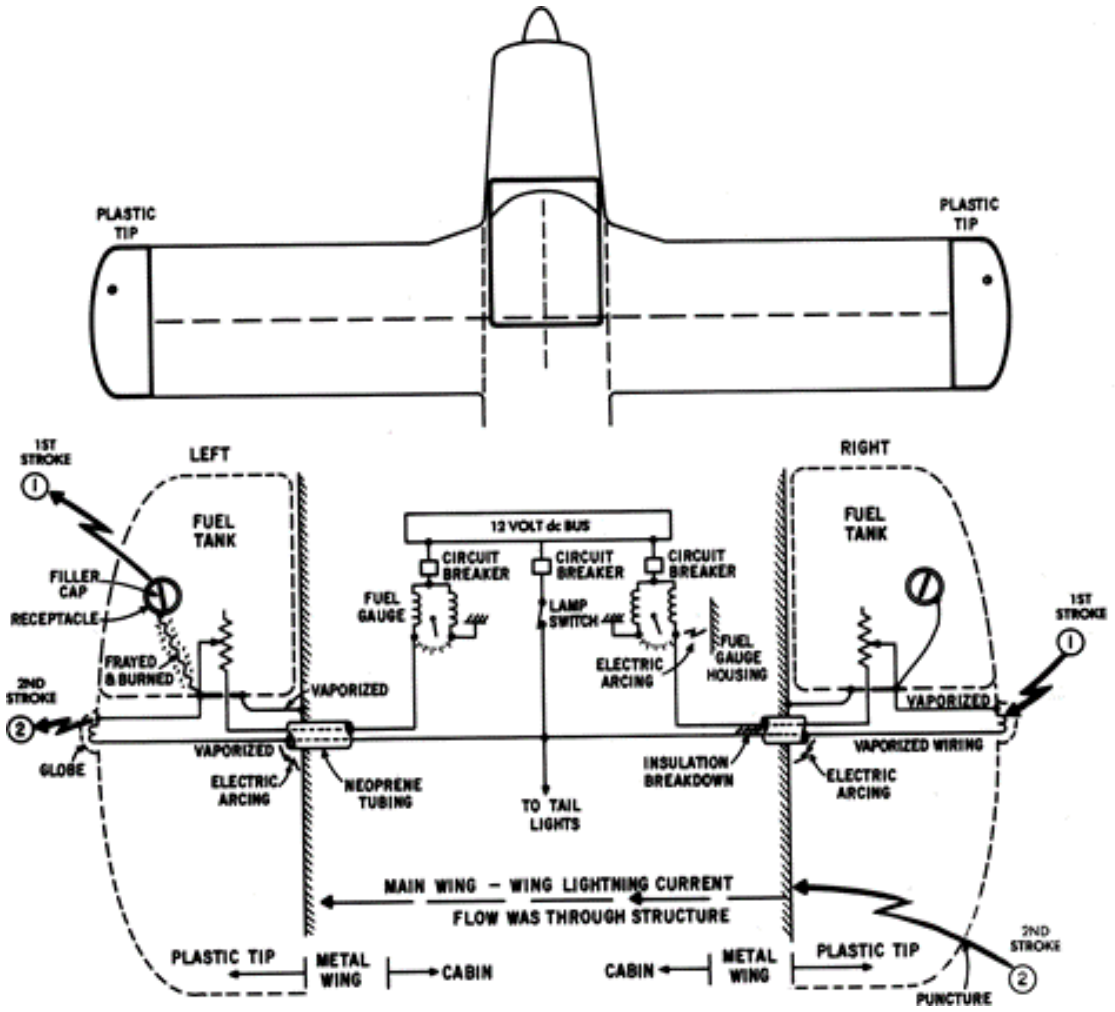

Fig. 4.25 Diagram of Lightning paths and effects in small aircraft of Fig. 4.24.

4.6 Effects on Propulsion Systems

Reciprocating engines

The effects of lightning upon reciprocating engines as used for small airplanes seem to have been limited to pitting metal parts in bearings and gearboxes and of metal blades or burning of small holes in metal spinners, as shown in Figs. 4.26 and 4.27. When a lightning channel attaches to a propeller blade, the current must flow through the blade and through engine shaft bearings, into the engine block and from there to the engine mounts and the airframe. These are usually massive enough to carry these currents with no harmful effects. The exception would be the front bearings. No reports of lightning-related damage to aft engine bearings or internal parts are known. Engine manufacturers usually stipulate that the bearings be inspected and replaced (if necessary) within a specified number of flight hours following the strike. Propeller pitch controls do not seem to have been adversely affected by lightning strikes to blades, but these are also inspected together with bearings following a strike.

Fig. 4.26 Lightning strike damage to a metal propeller blade. This blade "cut through" the lightning channel after first being struck on its tip. The channel reattached to the inboard surface of the blade before the channel reattached further aft on the airplane. (NASA photo)

Fig. 4.27 Holes in aluminum spinner due to lightning attachments. (NASA photo).

Turboprop engines

There have been no reports of power loss in turboprop engines because of lightning strikes. Possible damage to gearbox and bearings is a concern like reciprocating engines.

Propellers and prop pitch controls

Effects of strikes to metal blades are usually limited to small pits. Wooden propellers, especially those lacking metal leading edges, would probably suffer more damage, but such propellers are seldom used on aircraft that fly in weather conditions where lightning strikes are likely to occur.

The spinner of Fig. 4.27 is on the same airplane as the blade of Fig. 4.26. The holes indicate intermediate or continuing current effects but not stroke current. The initial lightning attachment to this aircraft was probably at one of the metal blade tips, and the stroke current may have entered one of the blades. Effects of stroke currents on metal surfaces are not always evident.

Turbojet engines

Anecdotal lightning strike incident reports indicate that lightning effects on turbojet engines are limited to (mostly) temporary disruptions of engine operation. Flameouts, compressor stalls, and rollbacks (reduction in turbine speed) have been reported after lightning strikes to aircraft with fuselage mounted turbojet engines. This type includes both military aircraft with internally mounted engines and fuselage air intakes, and aircraft with engines externally mounted to the fuselage. These are exposed to sweeping lightning channels that appear momentarily in front of engine inlets.

There have been no recorded attempts to duplicate engine flameouts or stalls with simulated lightning in a ground test, however, it is generally believed that these events result from disruption of the inlet air by the high temperature and/or shock wave associated with the lightning channel sweeping aft along a fuselage and passing close in front of an engine inlet. Heavy rain that is frequent in thunderstorms may also be a factor.

A stroke current and the accompanying shock wave is considered sufficient to disrupt engine operation. The steep temperature gradient surrounding the lightning channel is also important since it would be detected by the pressure and temperature sensor in the engine inlet and would influence control system operation. These effects have been reported as occurring more often on smaller military or business jet aircraft than on larger transport aircraft,

probably due to a greater disruption by the lightning channel to a smaller volume of inlet air. Thus, smaller diameter engines are probably more susceptible to disrupted inlet air than are larger diameter engines.

Wing mounted turbofan engines

There have been only a few anecdotal reports of lightning effects on wing-mounted turbojet engines, since these are usually large engines, whose inlet air flow is unlikely to be noticeably disrupted by the shock wave from a lightning flash. If a lightning channel sweeping along a fuselage surface appears in front of a wing-mounted engine it is likely that it would reattach to the inlet lip and "sweep" aft along the fan cowl exterior surface and not enter the engine inlet.

There has been no evidence of a lightning channel having been 'sucked into' a wing mounted engine inlet or attaching to fan blades although this possibility has been considered by engine manufacturers who have occasionally conducted lightning tests of fan blades, and incorporated protective measures where necessary.

Operational aspects

Lightning strikes have been known to produce several different effects upon jet engines, ranging from stalls or rollbacks to complete flameouts, as noted above. In one recorded instance, it was not possible for the flight crew to re-start either engine. The plane crashed and there were no survivors.

Operators of aircraft with engines or inlets close to the fuselage should anticipate possible loss of power in the event of a lightning strike and should be prepared to take quick corrective action. Usual guidelines are to keep engine igniters on during flights through areas of precipitation. Flight through areas of heavy precipitation should be avoided.

Turbine stalls

Collected lightning strike incident reports indicate that lightning effects on turbojet engines are limited to temporary disruptions of engine operation. Flameouts, compressor stalls, and rollbacks (reduction in turbine rpm) have been reported after lightning strikes to aircraft with fuselage mounted engines. (This type includes both aircraft with internally mounted engines and fuselage air intakes, and aircraft with engines externally mounted on the fuselage.)

There have been no attempts to duplicate engine flameouts or stalls with simulated lightning in a ground test, and there has been no other qualitative analysis of the interference mechanism; however, it is generally believed that these events result from disruption of the inlet air by the shock wave associated with the lightning channel sweeping aft along a fuselage. This channel may indeed pass close in front of an engine intake, and if a restrike occurs, the accompanying shock wave is considered sufficient to disrupt engine operation. The steep temperature gradient surrounding the lightning channel may also be important. These effects have been reported as occurring more often on smaller military or business jet aircraft than on larger transport aircraft. Thus, smaller engines are probably more susceptible to disrupted inlet air than are their larger counterparts.

Operational aspects

Lightning strikes have been known to produce several different effects upon jet engines, ranging from stalls or roll- backs to complete flameouts. However, in most cases it has been possible to restart or recover the engine to full power while still in flight. Perhaps because of this, together with the impracticality of a laboratory simulation, there has been no published research into the problem. Nevertheless, operators of aircraft with engines or inlets close to the fuselage should anticipate possible loss of power in the event of a lightning strike and should be prepared to take quick corrective action.

There have been only a few reports of lightning effects on wing-mounted turbojet engines, since these are usually large engines, whose inlet air flow is unlikely to be noticeably disrupted by the shock wave from a lightning flash.

Helicopter Rotor Blades

Main and tail rotor blades of helicopters are the most frequent lightning strike locations and often experience physical damage. Since the blades are usually fabricated of combinations of materials, usually including a spar made of metal or CFRP, a trailing edge comprised of GFRP or CFRP skins stiffened with paper honeycomb, and a leading-edge erosion surface often made of titanium or nickel. The composite skins usually enclose the spar and may extend beneath the erosion strip.

For lightning protection, the composite skins are usually covered with a metal mesh. A typical arrangement is shown in Fig. 4.28.

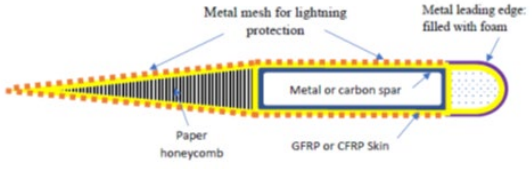

Fig. 4.28 Cross-section of typical helicopter rotor blade.

A problem with designs like this is that when lightning strikes the tip of the blade, all the electrically conductive elements want to share in conducting the current to the hub, not just the designated lightning protection metal mesh. For this to happen safely, all the metal parts need to be electrically bonded together. If this is not done, the potential differences (voltages) that arise between the parts will cause dielectric breakdown and arcing among the parts. Unfortunately, the arcing may cause effects that can lead to cracking of the spar, or other effects than may result in catastrophic failure of the blade, as happened in one accident involving a helicopter in flight. One of the rotor blades separated due to a spar crack caused by a lightning strike to the same blade several years before. This crack had progressed to failure of the spar and the blade [4.10]. The accident investigation found that the crack had originated from effects of an electric arc through an insulating material at the interface between the blade leading edge and the spar. Superficial effects of the lightning strike had been repaired years before, but evidence of this internal acing had not been discovered.

Lessons learned from this accident include:

1. Lightning effects may potentially occur anywhere throughout the aircraft between possible lightning entry and exit locations. The safety assessments conducted during the aircraft design and certification phases are depended on to identify all possible effects and their locations throughout the aircraft. Results of these safety assessments should be used to establish continued airworthiness requirements and inspections, especially following lightning strikes. It is never sufficient to deal only with superficially visible lightning effects.

2. Electrical insulation, as well as electrical bonding, are important features of aircraft lightning protection. It is fundamentally easier to maintain bonding than it is to maintain effectiveness of insulation. Dielectric breakdown the size of a pinhole destroys the effectiveness of an entire insulation layer, as does a pinprick to a child's balloon. An imperfection in electrical bonding is usually tolerable as long as the remainder of the bond remains effective. This is not so regarding insulation.

3. Unless a complex, flight-critical structure, like a helicopter rotor blade, can be fully inspected following a lightning strike, it should be removed from service and replaced with a new blade.

4. Some effects of lightning currents, such as marks left by electric arcing at interior locations in the current path, are often not recognizable by personnel at remote service shops or inspection stations. Unless such persons have received specific instruction as to where to look and what to look for, the evidence may not be noticed. Non-destructive inspection or non-destructive testing methods may be ineffective in detecting effects like arc marks or dielectric punctures caused by lightning

Physical effects of a strike to a tail rotor are shown in Fig. 4.29.

Fig. 4.29 Effects of lightning strike to a tail rotor (US Coast Guard Photo)

The composite shell of this blade was destroyed by a strike apparently entering the trailing edge of this blade near the tip. The metal spar remained intact. Details of these effects are not available but inadequate protection was provided to the composite shell. This incident was survivable, and the helicopter made a successful landing.

Lessons learned

A possible lesson learned from this incident is that the effects on any blade depend on where the lightning current is introduced to the blade. Lightning certification tests should consider all possible lightning attachment locations, and, if it is not abundantly clear that a possible location on the blade and the current paths from it are well protected, it should be included in the test procedure. Unfortunately, this often means that more than one test specimen has to be provided, adding considerable cost to the process, but avoiding the greater costs of repair or of an accident in the future.

4.7 Induced Effects

Even if a lightning flash does not make direct contact with an aircraft's electrical wiring, strikes to the airframe are capable of inducing voltage and current transients in internal wiring.

Upset or damage of electrical equipment by these induced transients has been considered an *indirect effect,* however it is perhaps more correct to call them induced

effects since they are described by first principles of electromagnetics which include the process of induction by changing magnetic fields associated with the lightning currents.

Induced effects must be considered along with physical effects in assessing the total susceptibility of aircraft to lightning. Flight critical systems, such as the full authority digital engine control (FADEC) system illustrated in Fig. 4.30, are potentially susceptible to induced effects, and careful attention must be given to protection design and verification. Fig. 4.30 shows in fundamental terms the origin of induced effects in interconnecting wiring.

Magnetically induced voltages

The mechanism whereby lightning currents magnetically induce voltages in aircraft electrical circuits is illustrated in Fig. 4.30. As lightning current flows through an aircraft, strong magnetic fields are produced, which surround the conductive airframe and change rapidly with the fast- changing lightning stroke currents. Some of this magnetic flux may leak inside the aircraft through apertures, such as windows, composite fairings, seams, or joints.

Other fields may arise inside the aircraft, when lightning current diffuses to the inside surfaces of skins. In either case, these internal fields pass through aircraft electrical circuits and induce voltages in them proportional to the Sikorsky.

Structural voltage rises

Lightning currents in structures comprised of metal or CFRP will produce voltages due to Ohm's law that are proportional to the material resistances and the magnitudes of lightning currents in them. In low-resistance materials such as aluminum these voltages are low, but in CFRP structures whose resistivities are much higher, these IR voltages can be significant. The resistances of joints in either kind of structures may also be significant.

Magnetically induced and structural IR voltages occur simultaneously in nearly all wiring within an aircraft during a lightning strike, so the potential exists for multiple effects on avionic systems. For example, four channels of quad-redundant digital flight control system might all be damaged at the same time, if protection against induced effects is not incorporated. Safe operations of such systems in the lightning environment cannot be achieved by relying only on redundant systems.

Systems of concern

Systems of greatest concern regarding lightning-induced effects include the following.

1. FADEC systems.
2. Full authority electronic flight control (i.e., Fly-by-wire) systems.
3. Supervisory control systems capable of initiating control inputs that could endanger flight safety.

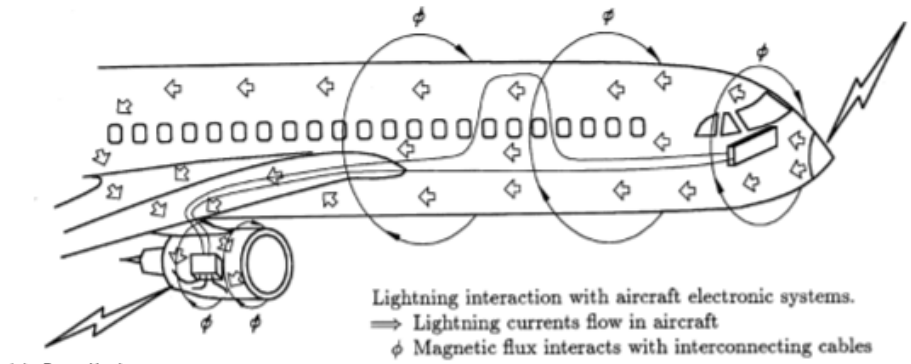

(a) Installation

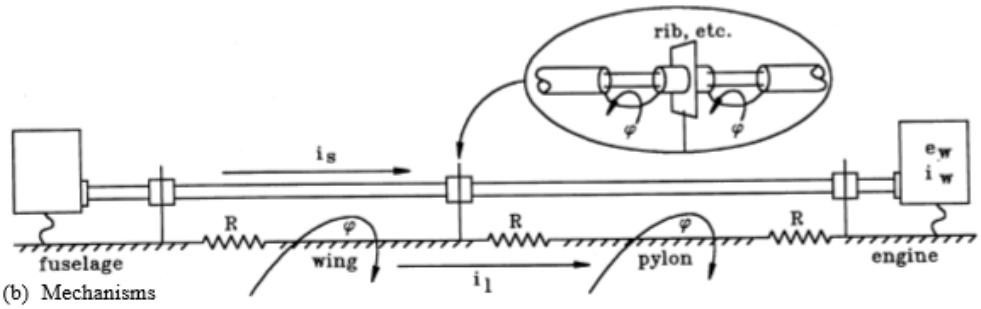

(b) Mechanisms

$$e_s = i_R + \frac{d\varphi}{d\tau}$$

$$i_s = \frac{1}{L_s}\int e_s(\tau)\,d\tau$$

$$e_w = i_s R_s$$

$$i_w = \frac{1}{L_w}\int e_w(\tau)\,dr$$

where

i_l = Lightning current in airframe
R = Structural resistance of airframe
φ = Magnetic flux
e_s = Shield external voltage
i_s = Shield current
e_w = Shielded wire voltage
i_w = Shielded wire current

Fig. 4.30 Origins of induced effects in aircraft electrical/electronic systems.

Aircraft experience

Until the advent of solid-state electronics in aircraft, induced effects from external environments, such as lightning and precipitation static electricity, were not a serious problem, and received relatively little attention. Vacuum tube electronics are inherently more tolerant of induced voltages since they operate at high voltages themselves, and readily recover after a surge voltage causes a flashover among electrodes enclosed in a vacuum. Also, their applications were mostly limited to communication and navigation functions, and not flight controls.

In contrast, solid state electronic circuit elements operate at low voltages, and when exposed to induced voltages originating in interconnecting wiring, they often cause breakdown of solid-state junctions which do not recover when the overvoltage is removed. This is most likely in large scale integrated circuit devices, in which there is very little mass in which to dissipate energy.

When solid-state digital electronics became widespread in the 1980s they were employed in equipment performing the more critical functions, including flight and engine controls. At first these were supervisory roles where the control function remained manual, and the electronics were employed to optimize performance. Later the electronics were made responsible for the entire control function. These "full authority" systems have no mechanical backup. An example of an accident caused by induced effects and another example of an incident where the aircraft was recoverable are summarized below.

On February 8, 1988, a SA 227-AC Metro III was on a scheduled flight from Hanover to Dusseldorf with 19 passengers and two crewmembers on board. During initial approach, approximately seven nautical miles from the threshold, the aircraft entered a thunderstorm region. First, the electrical power supply failed. Then, two minutes later, the aircraft was thrown into an uncontrolled descent whereupon it disintegrated in the air and all the occupants were killed. In the concluding investigation report, the investigation commission established that an electrical failure, caused by lightning, had rendered the landing flaps and horizontal stabilizer trim inoperable, and that this had been the primary contributor to the accident. An especially dramatic factor in this incident was the fact that damage to the electrical system's diodes had thwarted all attempts by the crew to restore the power supply.

Although both the manufacturer of the airplane and the certification authority assessed total electrical failure of the power supply because of a lightning strike to be improbable, a subsequent case has nevertheless occurred.

In this second incident, the exemplary behavior of the crew (as well as their observance of a safety recommendation that had been issued by the investigation commission after the previous accident) prevented another fatal accident. During the climb of an SA 227 Metro III from 14 000 ft., under IFR conditions, the airplane was struck by lightning. According to the report of the crew, suddenly, the entire electric power system failed. The pilot-in-command immediately took over the controls, as recommended in the airline's flight operating manual in such cases. Since the switches for operating the power supply were located directly in front of the left seat, the pilot-in-command immediately had to return control of the aircraft to the co-pilot again. They managed to maintain safe flight, using the built-in, third artificial horizon. The pilot-in-command, in the left seat, was thus free to focus his attention on the restoration of the electrical system, which required strict observance of a procedure involving the manipulation of battery and generator switches in a particular order. The "crew coordination" in the cockpit worked out well and the aircraft and its occupants were saved.

It is worth noting that the pilot-in-command was familiar with the procedure for restoring the electric power system and knew that an accident could be prevented if that procedure were precisely followed. The pilot's awareness of the procedure can be attributed, in part, to a safety recommendation (inspired by the previous lightning-attributed power failure) that resulted in "Total Electrical Failure" (described above) being incorporated into the SA 227 Metro III's flight manual.

Since these incidents, the diodes that had interfered with the restoration of the power system were removed from all SA 227 Metro IIIs, in accordance with a safety recommendation issued by the Accident Investigation Bureau.

Trends

While, historically, induced effects have not been a major safety hazard, there are four trends in aircraft design and operations which could increase the vulnerability of aircraft to these effects. These trends include the following:

1. Increasing use of composite structures in place of aluminum.
2. Further miniaturization of solid-state electronics.
3. Greater dependence on electronics to perform flight critical functions.
4. Greater congestion in terminal airways, requiring more frequent flight through adverse weather conditions at altitudes where lightning strikes frequently occur.
5. Fully or highly integrated cockpit instruments and displays.
6. Electronic flight instrumentation systems.
7. Aircraft electric power control and distribution systems.
8. Electrical/avionic systems that include externally mounted apparatus, such as air data probes, heaters, actuators, and antennas.

Consequences

One of the consequences of these trends is that protective measures, which in older generation, metal aircraft largely 'come for free', must in the future be explicitly provided. Such provisions can have an adverse effect on aircraft weight and program cost.

Nearby lightning effects

What if a lightning flash passed close to but did not contact the aircraft? The changing electromagnetic field produced by that flash might upset electronic systems in the aircraft.

However, there are no scenarios that can be imagined in which the effects of a nearby lightning flash on systems within an aircraft would be more severe than would the effects produced by a flash that directly contacts and is conducted through the aircraft. One can imagine that the nearby flash might be a very severe one, with higher amplitude stroke currents and other characteristics than are included in the standards (see Chapter 5) for design and certification of the aircraft. But if this were the case, the electric charge contained in the nearby lightning leader would have to be large and so produce an electric field that would have this nearby flash attaching to the aircraft in the first place. The higher the charge that is brought towards an aircraft by a lightning leader, the longer the striking distance between the aircraft and the leader. Thus, the induced effects that are of concern and that must be addressed for protection design and certification are those that arise from direct contact of the aircraft with the lightning flash and conduction of the lightning flash currents.

Relation to electromagnetic interference (EMI) and electromagnetic compatibility (EMC)

Induced effects of lightning are part of the broad subject of EMI and EMC. However, the EMI and EMC standards in industry-wide use do not deal with the effects of lightning. A major difference is that lightning induced transients are best characterized as a time domain phenomenon, while classical EMI/EMC are defined in the frequency domain. Susceptibility to excessive voltages or currents and susceptibility to narrow band interference or emission are not the same thing, and protection against one usually does not imply protection against the other. The standards that deal with lightning effects on aircraft are described in Chapter 5.

References

4.1 J.H. Hagenguth *Lightning Stroke Damage to Aircraft* Transactions of the American Institute of Electrical Engineers 1949, Vol. 68, No. 2, pp. 1036-1046.

4.2 R. L. McDowell (Galaxy Scientific Corp.) J.A. Plumer (Lightning Technologies, Inc.) *Data from the Airlines Lightning Strike Reporting Project: Pilot Reports and Lightning effects* Lightning Technologies, Inc. report LT-01-1942.

4.3 M.A. Uman, *Lightning*, McGraw-Hill, New York, 1969, pp.230.

4.4 *Report of the Investigation of an Accident Involving Aircraft of U.S. Registry, NC 21798, Which Occurred near Lovettsville, Virginia, on August 31, 1940*, Civil Aeronautics Board, Washington, D.C., 1941.

4.5 *Aircraft Accident Report: Boeing 707-121, N709-PA, Pan American World Airways, Inc., near Elkton, Maryland, December 8, 1963*, File No. 1-0015, Civil Aeronautics Board, Washington, D.C., 25 February 1965.

4.6 *Aircraft Accident Report: TWA Lockheed 1649A near Milan, Italy*, File No. 1-0045, Civil Aeronautics Board, Washington, D.C. (November 1960). English translation of report by Italian Board of Inquiry.

4.7 J. A. Plumer, "Lightning Induced Voltages in Electrical Circuits Associated with Aircraft Fuel Systems," *Report of Second Conference on Fuel System Fire Safety*, 6 and 7 May 1970, Federal Aviation Administration, Washington, D.C. (1970), pp.171-92. Don Flagg, "Night Flight," *Aero Magazine*, January/February 1972, pp. 18-21.

4.8 Page Shamberger, "Learning About Flying the Hard Way," Air Progress, February 1971, pp. 64.

4.9 *AGATE Lightning Direct Effect Handbook*, General Aviation Program Office, MS 261, NASA Langley Research Center, Hamption, Virginia 23681-0001.

4.10 Aircraft Accident Report 1/2005 - Sikorsky S-76A+, G-BJVX, 16 July 2002. Published 10 December 2014.

Chapter 5

THE CERTIFICATION PROCESS

5.1 Introduction

The purpose of this chapter is to describe the aircraft lightning protection requirements set forth by the United States (US) Federal Aviation Administration (FAA) and similar certifying authorities in other countries, and to discuss the several steps that can be taken by applicants to comply with these requirements. In most cases, the FAA regulations will be cited as examples, since FAA regulations are similar to those in effect in most other countries, especially as regards lightning protection. The material in this chapter includes descriptions of performance requirements, standards, specifications, and procedural steps. It does not include design data or methodology, which are the subject of the succeeding chapters. It is recommended that those responsible for design and certification be familiar with the material in this chapter before proceeding with a lightning design program, as the success and efficiency of an overall design depends considerably on the steps that are followed to achieve the design.

Aircraft lightning protection requirements and related standards have evolved, over the years, to keep pace with increases in knowledge of lightning and its effects on aircraft, as well as changing aircraft structural materials and systems. Before this, the aircraft protection requirements focused on one or two potential hazards, such as fuel tanks and antennas and other external "points of entry", while largely ignoring other hazards, such as internal arc and spark sources or induced effects on electrical and avionic systems which had not become evident at the time.

The requirements and standards are being updated occasionally to reflect improved understanding of the natural lightning environment and its effects on aircraft and the emergence of new aircraft design technologies, such as electronic control systems and advanced composite airframes. This progress appears well positioned to adapt to future trends as well, via on-going technology review and standards-writing activities among industry and regulatory agency groups. The lightning protection design and certification process has been aided by a proliferation of technical literature on aircraft lightning interaction mechanisms, protection techniques and verification methods. Some of this material is summarized in this chapter, with references.

5.2 FAA Lightning Protection Regulations

Since lightning represents a possible safety hazard whose consequences may extend to loss of the aircraft and the lives of those aboard, the fundamental goal of aircraft lightning protection is to prevent catastrophic accidents and to enable the aircraft to continue flying safely after a lightning strike and be able to land at a suitable airport. It is not required that the aircraft survive a strike without damage which requires repairs, although this is often an additional goal of lightning protection since the costs of repair and downtime can be substantial.

Regulations and Advisory Circulars (ACs)

Lightning protection requirements have been included in the collection of Federal Aviation Regulations (FARs) published in Title 14 (Aeronautics and Space) of the US Code of Federal Regulations (CFRs). Suggested means of showing compliance with these regulations are published by the FAA in Advisory Circulars (ACs). These FAA CFRs deal with the aircraft as a whole and, more specifically, with the fuel system and other systems performing what have historically been regarded as 'critical' and 'essential' functions. 'Critical' functions are those that are necessary for continued safe flight and landing of an aircraft or helicopter. 'Essential' functions are others, like communication or navigation, which, if lost, place the aircraft in greater danger but do not immediately result in a plane crash. Specific lightning protection regulations for each category of aircraft and rotorcraft are listed in Table 5.1. The intent of these regulations is highlighted in this chapter. The full texts of each regulation are available from the FAA website. Corresponding regulations of other certifying authorities are available from their websites.

Table 5.1 – Federal Aviation Regulations (FARs) Pertaining to Lightning Protection as of April 2020

	Vehicle Type and Regulations			
	Aircraft		**Rotorcraft**	
	Normal Category	**Transport Category**	**Normal Category**	**Transport Category**
Airframe	*Subpart D – Design and Construction* §23.2335 Amdt. 23-64 (2017)	*Subpart C - Structure* §25.581 Amdt. 25-23 (1970)	*Subpart D – Design and Construction* §27.610 Amdt. 27-46 (2011)	Subpart D – Design and Construction §29.610 Amdt. 29-53 (2011)
Fuel System	*Subpart E – Powerplant* §23.2430(a)(2) Amdt. 23-64 (2017)	*Subpart E – Powerplant* §25.954 Amdt. 25-146 (2018)	*Subpart E – Powerplant* §27.954 Amdt. 27-23 (1988)	*Subpart E – Powerplant* §29.954 Amdt. 29-26 (1988)
Electrical and Avionic Systems	*Subpart F – Equipment* §23.2515 Amdt. 23-64 (2017)	*Subpart F – Equipment* §25.1316 Amdt. 25-134 (2011)	*Subpart F – Equipment* §27.1316 Amdt. 27-46 (2011)	*Subpart F – Equipment* §29.1316 Amdt. 29-53 (2011)
Engine Control Systems	*Subpart B – Design and Construction; General* §33.28 Amdt. 33-26 (2008)			
Propellers	*Subpart C – Tests and Inspections* §35.38 Amdt. 35-8 (2008)			

These regulations state a performance requirement but include neither guidelines for achieving compliance nor specific technical design requirements. In this manner, the CFRs allow the designer a maximum amount of flexibility. The FAA requires verification that the design for a new aircraft complies with the CFRs and that the design does, in fact, provide the necessary protection. This verification is usually achieved by laboratory tests, but can sometimes be accomplished through analysis, demonstrations of similarity of the candidate design(s) with designs that have been incorporated in previously certified airplanes, or some combination of these methods.

Lightning protection requirements are included in the CFRs for Transport Category Aircraft (Part 25), Normal Category Aircraft (Part 23, which are hereinafter referred to as “General Aviation" aircraft) and for both categories of Rotorcraft (Parts 27 and 29). These are functional requirements and are therefore comparatively brief. They do not attempt to define the intensity of the lightning environment, the frequency of expected lightning strike occurrences or the locations where strikes are likely to enter or exit an aircraft, neither do they specify lightning test pass/fail criteria, such as acceptable amounts of physical damage to structures or acceptable levels of interference with electronic systems. These details are to be proposed by the applicant (using published guidance for certification of a new aircraft or modification of a previously certified aircraft) and reviewed and approved (or modified) by the certifying authority as complying with the regulation.

Descriptions of the lightning environment for design and certification purposes, and of the way this environment should be applied to an aircraft, are presented in several documents published by SAE and Radio Technical Commission for Aeronautics (RTCA), in the US, and by European Organization for Civil Aviation Equipment (EUROCAE), in Europe. This topic is also discussed in Chapter 5, § 5.5 of this handbook. The CFR Part 25 regulations are cited as examples in the following discussion.

5.2.1 Protecting the Airframe

The basic lightning protection regulation for airframes and all aircraft systems except those specifically addressed by another regulation is the same for all categories of aircraft and appears in the CFRs, using transport (Part 25) category airplanes as an example is as follows:

FAA 14 CFR § 25.581 Lightning Protection

(a) The airplane must be protected against catastrophic effects from lightning.

(b) For metallic components, compliance with paragraph (a) of this section may be shown by—

(1) Bonding the components properly to the airframe: or

(2) Designing the components so that a strike will not damage the airplane

(c) For nonmetallic components, compliance with paragraph (a) of this section may be shown by—

Designing the components to minimize the effect of a strike; or

(1) Incorporating acceptable means of diverting the resulting electrical current so as not to endanger the airplane.

Amdt. 25-23 (1970)

This is usually considered the 'top level' regulation. Similar 'top level' regulations are found in the CFRs dealing with Normal Category (Part 23) and Rotorcraft (Parts 27 and 29). These regulations state that compliance can be shown either by **bonding** components to the airframe or by **designing** components so that a strike will not endanger the airframe. In this context, the term "bonding" means electrical continuity between components that is adequate for conducting lightning currents.

At the time this basic regulation was adopted (1970) it was widely believed that hazardous lightning effects were limited to the external structure or to components directly exposed to lightning strikes. It was believed that protection from these effects could be achieved by ensuring that components and structures directly exposed to lightning strikes were adequately bonded to the main airframe. Examples of these components and structures were flight control surfaces, air data probes, empennage tips and other components located at extremities of the aircraft where lightning strikes most frequently occur. Adequate bonding would prevent damage to the hinges, fasteners and other means of attaching these components to the airframe.

Bonding resistance

Unfortunately, this emphasis on bonding has led some designers to conclude that bonding, by itself, provides adequate lightning protection for an aircraft and that little else needs to be done. To them, a lightning-protected aircraft means a 'bonded' aircraft. Verification of this 'bonded' status has, in turn, been signified by attainment of a specified electrical resistance among the 'bonded' components. The industry has adapted various bonding resistance limits for this purpose, among them the US military specification *US MIL-B-5087B* [5.1], which requires that components that could be subjected to lightning currents be interconnected with a 'bonding' resistance not exceeding 2.5 milliohms. This is supposed to be achieved by ensuring metal-to-metal contact between parts and is intended to be verified by a direct current (DC) resistance measurement.

Criteria like the 2.5 milliohm bonding specification have taken on an importance all of their own, occasionally to the neglect of the real purpose of lightning protection design, which is to prevent hazardous lightning effects. While electrical continuity among the metal parts of an aircraft is important, there are many other features of a successful protection design that are of equal importance.

Effects within the aircraft

The focus of 14 CFR 25.581 on the bonding and externally mounted components has, perhaps, led designers to give inadequate attention to lightning effects occurring *within* the airframe. These internal effects, which will be referred to henceforth as *induced effects*, arise either directly, from current flow between internal structural members, or indirectly, from changing magnetic and electric fields interacting with electrical systems. Induced effects have been the cause of several catastrophic accidents, brought about by electrical arcing among essential electronic components. More detailed discussions of these effects, and related protection methods, are found in the following chapters.

The emphasis of 14 CFR 25.581 on the external aspects of lightning protection does not, of course, excuse the designer from actively identifying and addressing all potentially hazardous lightning effects. The first sentence of 14 CFR 25.581 is the important overall requirement:

The airframe must be protected against catastrophic effects of lightning.

Methods of protection design into the aircraft are described in Chapter 6 and methods of compliance are provided in SAE Aerospace Recommended Practice (ARP) 5577 [5.2]. Compliance in accordance with an SAE ARP is authorized by FAA AC 20-155A [5.3] which authorizes guidance in several ARPs for lightning protection compliance purposes.

5.2.2 Protecting the Fuel System

The emphasis of CFR 25.581 on the *external* aspects of lightning protection, and the fact that several catastrophic accidents were directly attributed to lightning-related ignition sources *within* fuel tanks, led to the addition of 14 CFR 25.954, which focuses specific attention on aircraft fuel systems, as follows:

§ 25.954 Lightning Protection

(a) For purposes of this section—

(1) A critical lightning strike is a lightning strike that attaches to the airplane in a location that, when combined with the failure of any design feature or structure, could create an ignition source.

(2) A fuel system includes any component within either the fuel tank structure or the fuel tank systems, and any airplane structure or system components that penetrate, connect to, or are located within a fuel tank.

(b) The design and installation of a fuel system must prevent catastrophic fuel vapor ignition due to lightning and its effects, including:

(1) Direct lightning strikes to areas having a high probability of stroke attachment

(2) Swept lightning strokes to areas where swept strokes are highly probable; and

(3) Lightning-induced or conducted electrical transients.

(c) To comply with paragraph (b) of this section, catastrophic fuel vapor ignition must be extremely improbable, taking into account flammability, critical lightning strikes, and failures within the fuel system.

(d) To protect design features that prevent catastrophic fuel vapor ignition caused by lightning, the type design must include critical design configuration control limitations (CDCCLs) identifying those features and providing information to protect them. To ensure the continued effectiveness of those design features, the type design must also include inspection and test procedures, intervals between repetitive inspections and tests, and mandatory replacement times for those design features used in demonstrating compliance to paragraph (b) of this section. The applicant must include the information required by this paragraph in the Airworthiness Limitations section of the Instructions for Continued Airworthiness required by §25.1529.

[Doc. No. FAA-2014-1027, Amdt. 25-146, 83 FR 47556, Sept. 20, 2018]

It will be noted that this regulation addresses the fuel tanks and the components located within the tank and requires no catastrophic fuel vapor ignition from direct or swept lightning strikes or the electrical transients induced by lightning strikes. Also, in subparagraph c, catastrophic ignition of fuel vapors is to be extremely improbable, considering flammability, critical lightning strikes, and failures within the fuel system. This extends the regulation to consider anticipated failures that may occur in the fuel system during manufacture and in subsequent service. It also requires that inspection and test procedures be developed and included in the instructions for continued airworthiness so that the effectiveness of lightning protection measures is assured throughout the life of the airplane. Methods of protection design are provided in Chapter 7. Means of compliance are provided in FAA AC 25.954-1 [5.4].

The lightning protection regulations for Fuel Systems for General Aviation Aircraft (Part 23) and Rotorcraft (Parts 27 and 29), are also shown in Table 5.1. Here, the emphasis is on eliminating fuel-vapor ignition sources due to the lightning strike attachment to exterior surfaces of the aircraft, and there is no focus on ignition sources due to current inside the fuel tanks, but the first sentence states the important overall requirement:

> *The fuel system must be designed and arranged to prevent the ignition of fuel vapor...*

Acceptable means of compliance with these regulations are described in AC 20-53C [5.5]. Compliance does not require that fault tolerance be demonstrated or that CDCCLs related to the fuel system lightning protection have to be provided.

5.2.3 Protecting Other Systems

Until the 1990's, none of the CFRs dealt specifically with lightning protection of other systems, such as the flight control, propulsion, electrical and avionic systems. Instead, the general safety regulations for equipment, systems, and installations aboard the aircraft, stated in *CFR 25.1309* for transport aircraft, require that catastrophic hazards resulting from any foreseeable operating condition, be shown by probability analysis not to happen more than once in a billion flight hours. Demonstrating compliance of protection designs with this was impractical since reliable probabilities of lightning strike frequencies, intensities, strike locations, and effects do not exist. There were no accepted methodologies for calculating the probability of occurrence of a particular lightning hazard, or of the failure of a specific protection design to lightning.

Although CFR 25.1309 makes no specific mention of lightning as a "foreseeable operating condition", this regulation was often applied as applicable to lightning protection since it includes "critical environmental conditions." Since the publication by FAA and other airworthiness authorities of CFR 25.1316 (and similar prescriptive requirements for the other categories) lightning protection designs have not been required to comply with CFR 25.1309 for protection effectiveness.

5.2.4 Protecting Electrical and Avionics Systems

Recognizing the increasing role of electronic controls in the operation of the aircraft, the FAA initiated a rule-making project to add a CFR dealing specifically with lightning protection of flight critical and flight essential electrical and avionics systems and equipment. This regulation, *CFR 25.1316* [5.6] requires that these systems and equipment continue to perform their intended functions or be recoverable in a timely fashion (that is, remain functional) following an in-flight lightning strike. The regulation applicable to Part 25 airplanes is reproduced here.

> ***§25.1316 Electrical and electronic system lightning protection.***
>
> *(a) Each electrical and electronic system that performs a function, for which failure would prevent the continued safe flight and landing of the airplane, must be designed and installed so that—*
>
> *(1) The function is not adversely affected during and after the time the airplane is exposed to lightning; and*
>
> *(2) The system automatically recovers normal operation of that function in a timely manner after the airplane is exposed to lightning.*
>
> *(b) Each electrical and electronic system that performs a function, for which failure would reduce the capability of the airplane or the ability of the flight crew to respond to an adverse operating condition, must be designed and installed so that the function recovers normal operation in a timely manner after the airplane is exposed to lightning.*
>
> *[Doc. No. FAA-2010-0224, Amdt. 25-134, 76 FR 33135, June 8, 2011]*

Similar regulations exist for the other three categories of airplanes.

5.3 Other Aircraft Lightning Protection Requirements

The US Department of Defense (DoD) has promulgated requirements for lightning protection of military aircraft and rotorcraft. The basic requirements document is *US MIL STD 464C* [5.7], which requires that the "system" shall meet its operational performance requirements the physical and induced effects of lightning. This standard also includes the lightning environment that is applicable to the systems.

In this context, "system" can be the aircraft, or certain onboard systems that perform operational functions.

Generally, the DoD lightning protection requirements in [5.7] are the same as those in the regulations pertaining to civil aircraft and helicopters. Verification test standards are less well defined as they are in the SAE standards applicable to civil aircraft. The term "aerospace vehicle" re-

fers to fixed wing aircraft, rotorcraft, and missile "systems", as well as to major systems such as engines, external fuel tanks, and weapons.

Non-US aircraft

Aircraft of non-US manufacture are usually certified by appropriate agencies of the country of origin, although these aircraft must also meet US CFRs if they are to be operated in the US. The converse is true for US manufactured aircraft which are to operate in other countries. Compliance with the various requirements is facilitated by bi-lateral agreements among nations, and by use of foreign regulations. For example, Certification Specifications are regulations from the European Aviation Safety Agency (EASA), mutually agreed upon by participating nations. The certifying authority for the country to which application for certification has been made has the responsibility of 'validating' the original certification data. That is; the first country to which application has been made 'certifies', and the other countries 'validate'.

The lightning protection requirements are similar in all sets of regulations, although the applicability and degree of enforcement has varied somewhat. There is a high degree of cooperation among aircraft lightning protection specialists worldwide and further progress in international standardization of lightning protection requirements and standards is likely to occur.

5.4 Summary of US FAA Lightning Protection Requirements

The basic requirement is that

> *the aircraft must be protected against catastrophic effects of lightning,*

as stated in CFR 25.581. This applies to the airframe, plus all of the systems and components necessary to allow the aircraft to continue safe flight and landing.

The CFRs state only the functional requirements, and in the most general and broad terms. Translation of these terms to specific technical design goals is left to the manufacturer of the aircraft or system, with review and approval authority vested in the US FAA and the certifying authorities in other nations. The lightning environment for protection design and certification purposes is described in §5.5, and the steps necessary to complete the lightning protection and certification tasks are described in §5.6.

5.5 The Lightning Environment for Design and Verification

Before describing the specified lightning environment for aircraft, some discussion is in order as to how it evolved.

5.5.1 Early Lightning Standards

The first industry to experience lightning problems, and to establish the need for standardization of a lightning environment for design and test purposes, was the electric utility industry. Shortly after overhead power transmission and distribution lines became widespread, it was apparent that lightning would be a severe problem. Power transformers, generators, motors, and switching devices experienced damage from voltage and current surges due to lightning strikes to the power lines. Research programs to quantify natural lightning electrical characteristics were initiated by utility companies and equipment manufacturers such as General Electric Company and Westinghouse Electric Company.

Shortly thereafter, standards emerged that defined the lightning surge voltage and current levels that must be withstood by power system apparatus. Extensive laboratory test facilities were constructed to verify the ability of equipment to tolerate these standards. As power transmission voltages increased and associated equipment became more sophisticated, improvements were necessary in lightning protection technology and the need for better information on the natural lightning environment grew. As a result, an extensive amount of research into lightning phenomenology and its effects on electric power systems and apparatus was carried out during the period 1920 to 1960.

Insulation coordination

This research led to a comprehensive philosophy, called insulation coordination, dealing with the lightning protection of electric power equipment. It incorporated standardized voltage levels to which equipment should be designed, standardized levels and procedures for proof tests on equipment and standards for the performance of protective equipment, such as lightning and surge arresters. All equipment associated with electric power transmission and distribution facilities is designed, tested, and protected in accordance with these industry wide lightning standards. The result is that, whereas thousands of lightning strikes occur daily to electric utility systems, very few power outages are now attributable to lightning.

Early research on aircraft

Lightning standards for aircraft emerged later. The Lovettsville, Virginia accident, described in Chapter 4, prompted research into the possible effects of lightning on aircraft and several of the utility laboratories were called upon to provide test facilities and lightning expertise. During the next 17 years, several other accidents, involving ignition of fuel vapors, were thought to have resulted from lightning strikes. Additional research and testing programs were prompted by these accidents. Most of this work was conducted at the General Electric Company High Voltage Laboratory in Pittsfield, Massachusetts and the National Bureau of Standards High Voltage Laboratory near Gaithersburg, Maryland, under sponsorship of aircraft manufacturers, the Civil Aeronautics Board, and the National Advisory Committee for Aeronautics (NACA), the predecessor of US National Aeronautics and Space Administration (NASA).

Original airplane standards

The first airplane lightning protection design and test standards were published by the US FAA in its AC 25-136B [5.8] and by the US DoD in military standard US MIL-B-5087B [5.1]. Both documents appeared in the mid 1950's. US FAA AC 25-136B [5.8], reprinted somewhat later as US FAA AC 20-53 [5.9], dealt exclusively with lightning protection of airplane fuel systems. US MIL-B-5087B dealt exclusively with providing electrical bonding in airplane structures and apparatus. These were the areas of greatest concern at the time.

Defined lightning threat

AC 20-53 and MIL-B-5087B each defined the lightning threat as a 200 kiloampere peak current with a unipolar waveform, a rate-of-rise of 100 kA/μs and a decay time to 50% of peak amplitude of about 50 μs. This represented a severe first stroke in a cloud-to-earth flash. US FAA AC 20-53 also defined an intermediate and continuing current component, but US MIL-B-5087B included only the first stroke in its defined environment.

Both documents required tests of critical components, such as fuel tank skins, access panels, filler caps, antenna installations, and other "points of entry" on the aircraft. Little attention was given to the effects of currents conducted through interior structures or systems, or to induced effects of lightning on electrical and avionics systems. These latter effects were not well understood during this period.

5.5.2 Experience with Early Aircraft Standards

Most of the early aircraft lightning protection design activities were focused on protection against the induced or physical damage effects of lightning, such as deformation of lightweight metal structures, melting of holes through fuel tank skins, puncture of dielectric surfaces, such as radomes and canopies, and prevention of electrical arcing at structural interfaces in fuel tanks. The required testing was carried out by existing utility manufacturer laboratories, such as General Electric and Westinghouse, and by several small specialty organizations such as Lightning and Transients Research Institute (LTRI). The stroke currents required by the specifications were produced by charged capacitor banks discharged through wave shaping impedances into the test specimens.

Unipolar current waveforms

However, it was not possible to obtain the unipolar wave- forms specified in US FAA AC 20-53 and US MIL-B-5087B with the existing capacitor banks, even those available at the largest electrical equipment manufacturers laboratories. The reason for this was that the specified unipolar current required an over-damped test circuit including an excessive amount of resistance. The resistance usually limited the peak current to amplitudes of 70 kA and below, and most of the energy originally stored in the capacitor bank was dissipated in test circuit resistance, instead of in the test specimen. The performance of test equipment, and some of the tradeoffs between generator size and waveform, are discussed further in §18.4.

Oscillatory current waveforms

Since the specified over-damped waveform could not be readily produced, laboratories, instead, provided a damped sinusoid waveform. This made it possible to achieve the required 200 kA peak current amplitude with less resistance. Unfortunately, the frequencies and time durations of the damped sinusoid currents used for aircraft testing varied from laboratory to laboratory, because their test equipment had been built for purposes other than testing aircraft equipment and because there was no standardized definition for a damped sinusoid test current.

Three typical damped sinusoids, all with 200 kA peak amplitudes, are illustrated in Fig. 5.1. Note the significant difference in overall time duration and energy associated with each waveform. Clearly, the amount of damage that would be inflicted on a test specimen by a quickly damped

current waveform is much less than that inflicted by a slowly damped current waveform. This situation illustrates a significant shortcoming of the early lightning test standards. This shortcoming became especially apparent with the emergence of advanced composite structures, which are more sensitive to the effects of energy dissipation than conventional aluminum structures were. Standards now define the Action Integral (Specific Energy) of the current wave as well as the peak amplitude. Action Integral is discussed further in §5.5.3.

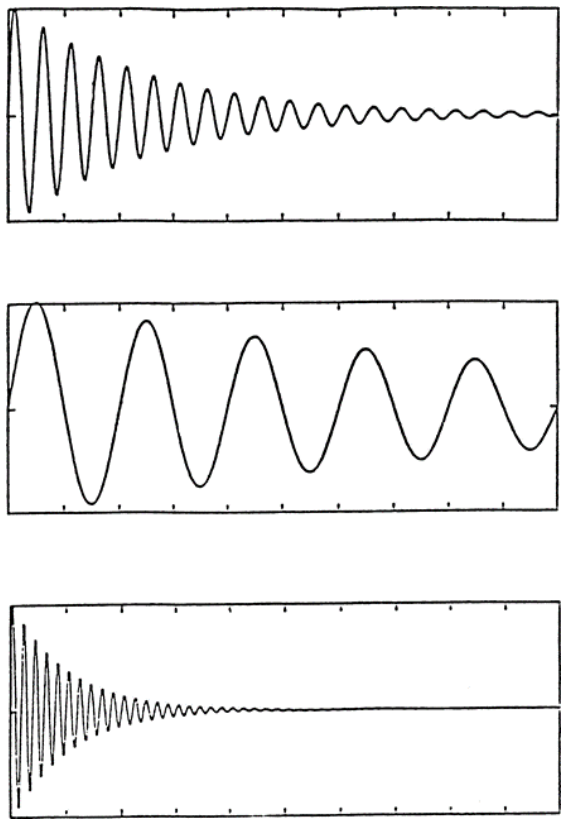

Fig. 5.1 Three typical damped sinusoid test currents prior to SAE standard.

Lightning strike zones

An additional shortcoming of the early airplane lightning standards was the complete absence, in US MIL-B-5087B, and poor definition, in US FAA AC 20-53, of lightning strike zones. Strike zones are how the lightning environment is applied to specific airplane surfaces and structures. The original zone definitions did not distinguish between surfaces that were trailing edges and those that were leading edges (or frontal surfaces), even though the durations of lightning attachments to these types of surfaces are significantly different.

It is well known, for example, that lightning currents commonly melt holes in trailing edges, where the flash may hang on for prolonged periods, whereas holes are infrequent in frontal or side surfaces of an aircraft.

Test methods and induced effects

Finally, the early standards failed to define acceptable test methods, and did not address induced effects on aircraft electrical and electronic systems. Lightning related accidents continued to occur, even to aircraft protected in accordance with US FAA AC 20-53 and US MIL-B-5087B.

5.5.3 SAE/EUROCAE Lightning Committees

Recognizing the above deficiencies, the US FAA and US DoD, in 1972, requested that the US SAE committee on electromagnetic compatibility (SAE AE-4) form a subcommittee to develop improved aircraft lightning protection design and test standards. This new subcommittee included lightning phenomenologists and specialists in aircraft lightning protection design and testing. The committee was designated special task F of SAE AE-4 and was later given the permanent designations SAE AE-4L (lightning) and, finally, AE-2. This committee has functioned continuously since 1972 and has become the US focal point for development and standardization of aircraft lightning protection requirements.

In 1988, a similar committee was organized in Europe under the EUROCAE, and designated EUROCAE Working Group 31 (Lightning). One of the purposes of this committee was to provide a venue for communicating concerns of European regulatory authorities and the air- craft industry to the US committee, and (especially) for harmonizing future lightning-related airworthiness certification requirements, environmental definitions and test standards. Since then, the SAE and EUROCAE lightning committees have worked closely together and have published US and European versions of documents pertaining to the lightning environment, aircraft lightning zoning, certification procedures for aircraft protection designs that address lightning physical and induced effects, aircraft-certification test procedures and aircraft-equipment test procedures. The two committees continue to work closely together to update the lightning-related requirements, advisory and test standards documents.

Current components A, B, C, and D

The first task accomplished by the SAE lightning committee was to develop a standard lightning environment for design and test purposes, synthesized from the available natural lightning data. The result was first published, in 1975, as a committee report entitled, *Lightning Test Waveforms*

and Techniques for Aerospace Vehicles and Hardware [5.10]. This report included a standard severe lightning flash current waveform comprised of four current components, designated A, B, C and D (illustrated in Fig. 5.2) and a set of test methods for utilizing the standardized currents.

One of the important sources of natural lightning data drawn upon by the SAE Committee in formulating this standard was the compendium of world-wide cloud-to-earth lightning data published by Cianos and Pierce [5.11].

Component A is a synthesis of both negative and positive cloud-to-earth stroke parameters. The 200 kA amplitude is typical of a severe (but not the most severe) positive flash stroke (positive flashes typically have only one stroke, followed by continuing current). The peak rate-of-rise of 140 kA/μs, is typical of a subsequent stroke in a negative flash, which usually contains more than one stroke. The subsequent strokes in the negative flashes have higher rates of change than the first strokes. The action integral (specific energy) of the 200 kA Component A, at 2×10^6 A^2s (or joules/ohm) is higher than recorded for negative first stokes but lower than recorded for severe positive strokes, which are believed to reach up to 15×10^6 A^2s (or joules/ohm) on rare occasions. The aircraft lightning environment standards do not take account of these high action integral strokes, which are believed to occur in less than 5% of the positive cloud-to-earth flashes. Since positive flashes comprise only ~10% of the worldwide lightning strikes to earth, the stroke currents that exceed 2×10^6 A^2s (or joules/ohm) might be expected to occur in only $^1/_2$ of one percent of all cloud-to-earth lightning flashes. Complete records of positive lightning currents are few, however, so the statistics noted above may not be representative of the real environment.

The physical damage to aircraft structures, including arcing among structural joints in fuel tanks, was more dependent upon peak current amplitude and overall time duration than upon the actual waveform of stroke currents, and generation of a unidirectional (UD), 200 kA first stroke current was not likely to become practical (at least for laboratories conducting aircraft lightning development and certification tests). Thus updated lightning environment standards permitted the use of either UD or damped sinusoid currents, as long as their peak amplitudes, Action Integrals (specific energies), and overall time durations conformed to the specifications of the idealized, unipolar stroke current. Subsequent studies undertaken by the US SAE committee showed that physical damage, while not related to specific waveform, is indeed related to these parameters.

Action integral (specific energy)

The action integral (or specific energy) of a current pulse, is the time integral of the square of the current and represents the ability of the current to deposit energy in a resistive object. The units of the action integral are traditionally given in A^2s (ampere-squared seconds), although it is more descriptive and equally correct to express the units of the action integral as J/Ω (joules per ohm). It is helpful to think of this as joules of damaging energy deposited per ohm of resistance of an article into which the current is injected.

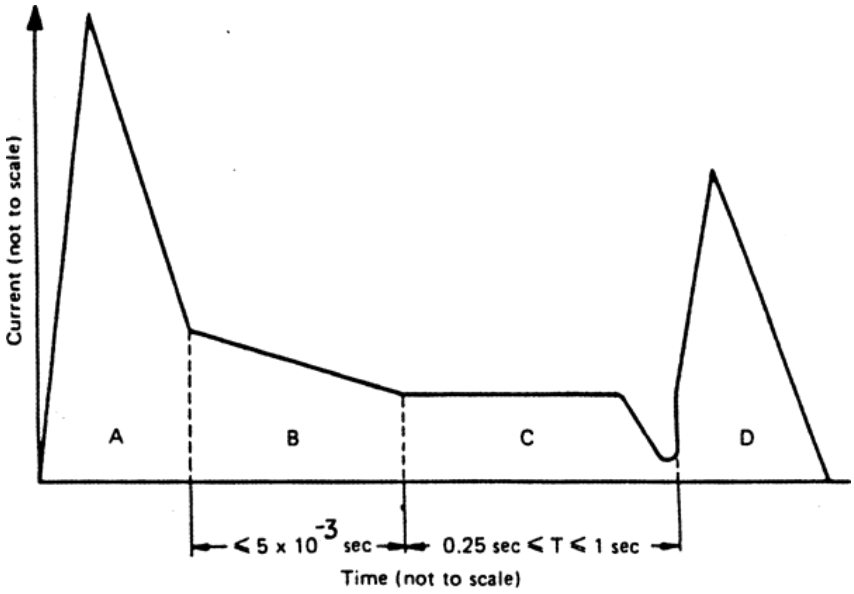

Fig. 5.2 SAE Lightning flash current components.

The action integral is derived from the definition of electric power as the product of voltage and current. (Eq. 5.1)

$$P = VI \qquad (5.1)$$

By an Ohm's law substitution of $V = IR$, one obtains Eq. 5.2:

$$P = (IR)I = I^2R \qquad (5.2)$$

Thus, P can represent the rate at which the electrical energy of a lightning stroke current, I, is converted to heat in the resistance, R, of a piece of aircraft structure. To express this as a thermal power dissipation per unit resistance, P is divided by R, yielding Eq. 5.3.

$$\frac{P}{R} = I^2 \qquad (5.3)$$

Finally, to obtain the total energy converted to heat per ohm of resistance by a lightning stroke whose waveform is given by the function $I(t)$, one must take the integral, with respect to time, of the I^2 in Eq. 5.3, where $I^2 = [I(t)]^2$. This yields Eq. 5.4, which is called the *Action Integral (AI)* or *specific energy* of the stroke.

$$AI = \int_{t_0}^{t_f} i^2(t)dt \quad A^2s \qquad (5.4)$$

For the interval of integration (t_o to t_f), one chooses a convenient time interval that includes the lightning stroke event in its entirety. Other details of the standard lightning environment are described in § 5.5.4.

Research programs

The advent of full authority control systems employing sensitive micro-electronics prompted a change in focus toward aspects of the aircraft lightning environment related to the characteristics of intracloud lightning strikes frequently encountered by aircraft. The amplitudes and action integrals (specific energies) of the currents in these strikes were believed to be less than those associated with C-G flashes. This belief was based upon the more limited extent of the physical damage experienced by aircraft receiving strikes at altitudes above 3 048 m (10 000 ft). Other aspects of intra-cloud lightning flashes, such as peak rates of change of current and multiplicity of current pulses, were of concern. There was also interest in obtaining a better understanding of the ways that lightning electric arcs ('lightning channels') interact with aircraft structural shapes and, thus, the application of the lightning environment to specific locations and surfaces of the aircraft.

Several flight research programs were implemented, beginning in 1980, to study the intracloud and cloud-to-cloud lightning environments. In these programs, which were sponsored by NASA, the USAF, US FAA, and the French research agency Office National d'Etudes et de Recherches

Aerospatiale (ONERA), aircraft were instrumented with devices capable of sensing and recording electrical parameters of in-flight lightning strikes. The results of these programs, which are briefly reviewed in Chapter 3, have been widely published and several aspects of the intracloud lightning environment such as the multiple burst (MB) waveform set have been incorporated in the aircraft lightning standards.

5.5.4 The Standardized Environment

The most recent standardized lightning environment is defined in SAE ARP 5412B [5.12] and EUROCAE ED 84 [5.13], has been in use since 1997 for aircraft design and certification purposes and has been recognized by the US FAA and European EASA for these purposes. FAA implements this and other SAE ARPs for certification purposes via AC 20-155A [5.3]. This environment is a combination of individual waveforms representing characteristics of natural lightning flashes described in Chapter 2:

- Electric fields (presented as test voltages) that appear at the surfaces of airplanes when lightning is about to strike, or after an initial strike has happened and the plane is flying through the lightning channel.
- Currents, that represent the strokes, intermediate and continuing currents that exist in most cloud-to-earth flashes of either polarity
- Currents that represent the pulses that exist in intracloud flashes

Voltages (Electric Fields)

There are three voltage waveforms (*A, C, D*) representing electric field environments at the exterior surfaces of airplanes and waveform (B) that is used for dielectric strength testing of internal components.

Waveform A – Derivative Voltage Waveform

Voltage Waveform A (Fig. 5.3) represents the voltage that may occur along a lightning channel when it is conducting a fast-changing stroke current. This waveform is applicable for testing dielectric surfaces exposed to swept lightning leaders and channels. The voltage rises toward its peak at a rate of 1 000 kV/µs until flashover takes place in the air gap between a test electrode and a test specimen surface.

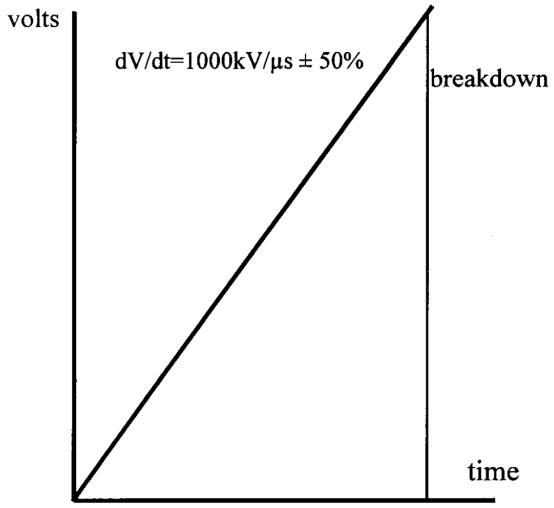

Fig. 5.3 – Voltage Waveform A

Voltage Waveform B – Impulse Dielectric Test Voltage

Voltage Waveform B is not part of the standard external lightning environment but is a standard used for qualifying insulating materials. Its rise and decay times are as shown in Fig. 5.4. This is known in the electric power industry as the "Lightning Impulse" voltage, so called because it represents the voltage applied to power transmission line insulation when a lightning stroke current enters the line.

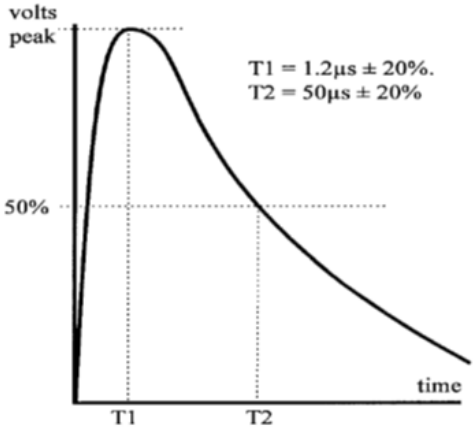

Fig. 5.4 – Voltage Waveform B

Voltage Waveform C – Scale Model Test Voltage

Voltage Waveform C (Fig. 5.5) rises to its peak in 2 µs and is often used for testing scale models of airplanes to locate initial lightning attachment regions. The flashover time is to be at two microseconds. This is equivalent to 60 µs if the scale of the airplane model is 1/30.

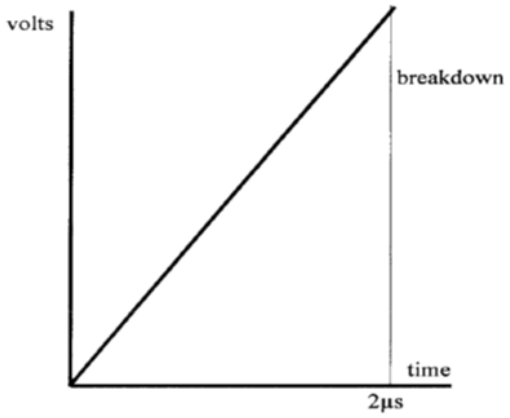

Fig. 5.5 – Voltage Waveform C

Voltage Waveform D – Initial Leader Attachment Voltage

Voltage Waveform D (Fig. 5.6) rises to its peak in a longer time; between 50 and 250 µs, during which interval a flashover occurs to the test specimen. This waveform is believed to more closely represent the electric field that is present at an aircraft surface during initial lightning leader attachment. In the electric power industry, this is called the "Switching Impulse" voltage, so called since it appears across power transmission line insulation when a switch is opened while the line is conducting current.

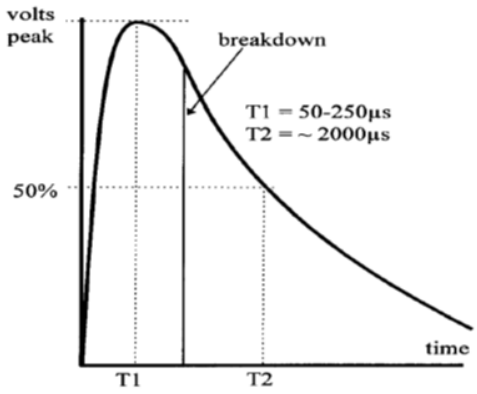

Fig. 5.6 – Voltage Waveform D

Currents

There are four standard current *components* (*A, B, C, D*) that are applied to represent the effects of cloud-to-ground lightning flashes, and another, *Component H*, that represents additional effects of intracloud flashes. These are applied, as appropriate, to the lightning strike zone(s) in which an aircraft surface, structure or given system is located. Together, these components constitute the external lightning current environment. They are defined as follows:

Component A – First Stroke Current

Component A shown in Fig. 5.7 has a peak amplitude of 200 kA, an action integral (specific energy) of 2 x 10^6 A^2s and a quad-exponential waveform. This waveform represents a first stroke in a positive cloud-to-ground flash of 200 000 amperes at a rate-of-rise of 1 x 10^{11} A/s at $t = 0.5$ µs. It has a peak rat of rise of 1.4 x 10^{11} A/s at $t = 0$. *Component A* is a synthesis of the of rise parameters of a negative first stroke and the high amplitude and action integral of a positive stroke. These parameters are not expected to be found together in nature, but by combining them in *Component A* one stroke current can be applied to represent the important aspects of severe (But not the most severe) parameters of both positive and negative C-G flashes. The effects of *Component A* are shock wave and heating, together with generation of induced effects in aircraft wiring that is installed within resistive structures that are exposed to this current.

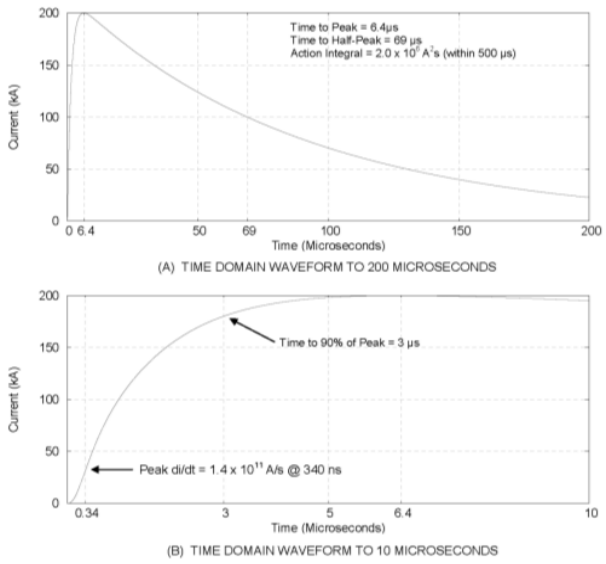

Fig. 5.7 – *Component A*, First Stroke Current

It may be noted that neither the peak current amplitude nor the action integral of *Component A* is the maximum recorded in nature. Nevertheless, the combination of parameters included in *Component A* represents a sufficiently severe environment for the safety of the aircraft to be assured. Historically, there has been no consistent correlation between lightning related accidents and the (apparent) intensity of the lightning flash that hit the aircraft. Most of the accidents have been due, instead, to design deficiencies.

Transition Zone First Stroke

The intensity of the first stroke in a cloud-to-earth flash at flight altitude may be less than that of the same stroke current at the earth's surface, because some of the charge that is conveyed to earth in the stroke current at the bottom of the flash will have passed through an airplane at flight altitude as part of the leader, prior to initiation of the leader discharge by the first stroke. Therefore, a reduced amplitude version of *Component A*, called *Component* A_H, has been defined for application to surfaces of an aircraft exposed to a stroke current swept aft from potential initial leader attachment locations during the time the leader takes to reach the earth and initiate the first stroke. These surfaces are in Zone 1C. This current has a peak amplitude of 150 kA and action integral of 0.8 x 10^6 A^2s. *Component* A_H is also defined in [5.12] and [5.13].

Component B – Intermediate Current

Component B has an average amplitude of 2 kA and a charge transfer of 10 coulomb. For analysis, a quad exponential current waveform should be used. This represents the transition phase between stroke and continuing currents in the lightning flash, and momentary increases in continuing current. The major effect of Component B is melting of metal surfaces and burning (pyrolysis) of composite resins. The analysis version of Component B is shown in Fig. 5.8.

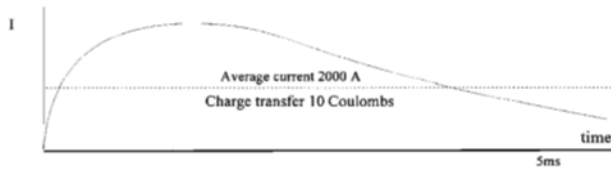

Fig. 5.8 – *Component B*, intermediate current

Component C – Continuing Current

Component C is a DC waveform delivering 200 coulombs of charge at a rate of between 200 A and 800 A, in a time period of between 0.25 s and 1 s. Rates of 200 A, 400 A and 800 A are authorized, for corresponding time durations to yield 200 coulombs. For analysis purposes, a rectangular waveform of 400 A for a period of 0.5 second should be utilized. The primary effect of this waveform is melting of metal structures due to the high temperature of the lightning channel and the long time durations. The 400 A version waveform is shown in Fig. 5.9.

Similarly, other combinations of average current amplitude and time duration are allowed to deliver the 200 Coulomb charge transfer defined for *Component C*, as long as this charge is delivered within two seconds.

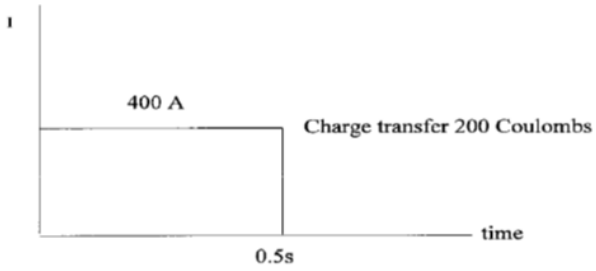

Fig. 5.9 – *Component C*, Continuing current

Component D - Subsequent Stroke Current

Component D has a peak amplitude of 100 kA, an action integral (specific energy) of 0.25 x 10^6 A^2s and a quad-exponential waveform. It has a maximum rate-of-rise of 1.4 x 10^{11} A/s at $t = 0^+$ which is the same as that of Component A. This waveform represents a severe subsequent stroke in a multiple stroke (MS) flash, which in fact may be the highest amplitude stroke in such a flash. Component D also represents the first negative stroke in the *MS* waveform set shown in Fig. 5.10, since the MS waveform set represents only negative C-G flashes, in which the first stroke should be 100 kA. *Component D* is shown in Fig. 5.10.

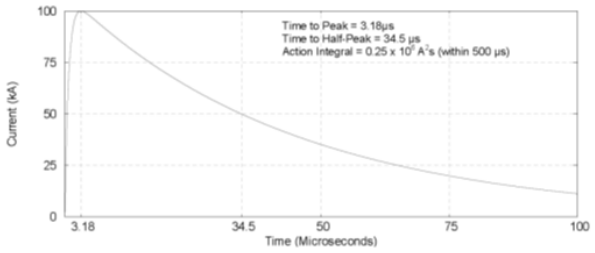

Fig. 5.10 – *Component D*, subsequent stroke current

For lightning physical effects testing purposes, damped sinusoid versions of *Components A*, A_H and *D* are allowed as long as the test currents reach the same peak current, and deliver the same action integrals within the specified 500 μs time intervals.

Component H – Intracloud Lightning Pulse Current

Component H represents one of the many pulses that appear in the intracloud flashes that strike airplanes at higher altitudes (10 000 ft. – 30 000 ft.) and which do not contact the ground. It is of interest because it has high rate of change at t = 0^+ of 200 kA/μs. Its amplitude is 10 kA

which represents a severe version. Component H is shown in Fig. 5.11.

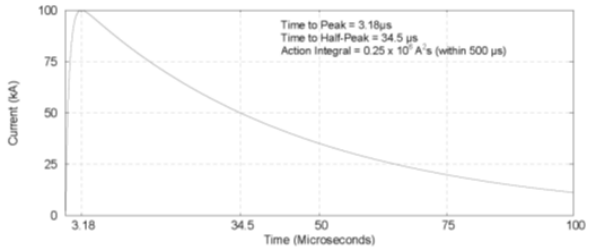

Fig. 5.11 - *Component H*, Intracloud Current Pulse

The effect of *Component H* is the potentially high voltage induced in interconnecting wiring of electrical and avionic systems due to fast changing magnetic fields associated with *Component H*. The *Component H* pulses appear in bursts of similar pulses that are believed to be associated with leaders stepping away from an aircraft that has initiated a lightning flash. In the standard MB environment there are three bursts of 20 Component H pulses in each burst. There are only minor physical effects from *Component H* since the amplitude and time duration are small compared with the current components in the C-G flashes.

Multiple Stroke (MS) Waveform Set

The MS waveform set is applied to represent the presence of subsequent strokes in the same lightning channel that is in contact with the aircraft. These induce electrical transients in interconnecting wiring which can affect the performance of avionic systems. The standard MS waveform is defined as a Current Component D followed by 13 randomly spaced subsequent strokes of peak amplitude of 50 000 amperes each. These subsequent stroke waveforms, known as Component D/2, are simply a Component D at 1/2 its defined amplitude. Multiple, randomly spaced transient pulses have been known to cause upset of digital systems.

The MS waveform set is illustrated in Fig. 5.12. The 13 subsequent strokes occur randomly over a period of 1.5 seconds according to the following constraints.

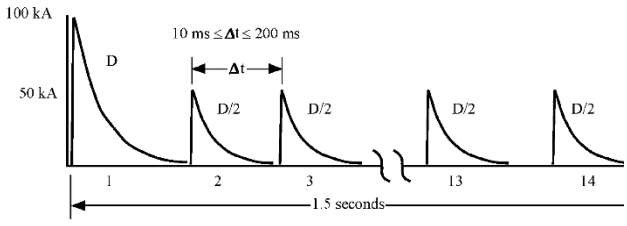

Fig. 5.12 – MS Waveform Set

- The minimum time between subsequent strokes is 10 ms.
- The maximum time between subsequent strokes is 200 ms.
- This range of times spans the intervals between strokes that have been recorded in negative C-G flashes.

Whereas *Component D* has been defined as a severe subsequent stroke for evaluation of lightning effects, it is used in the MS environment to represent a severe first stroke in a negative cloud-to-earth flash. As discussed in Chapter 2, negative first strokes rarely exceed 100 kA, so *Component D* is appropriate.

MB Waveform Set

The standard waveform for simulating the MB environment consists of repetitive Component H waveforms in 3 sets of 20 pulses each, as illustrated in Fig. 5.13.

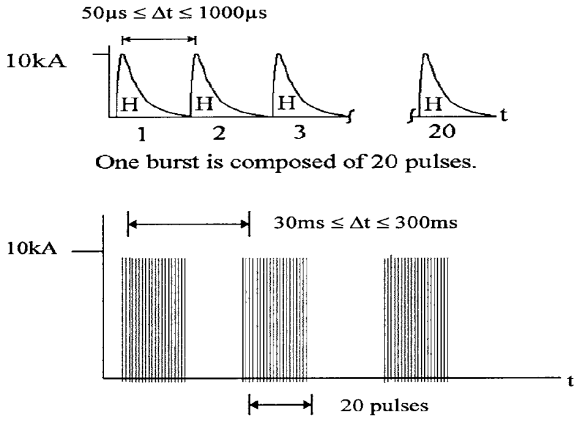

Fig. 5.13 – MB Waveform Set

The minimum time between individual *Component H* pulses within a burst is 50 µs and the maximum is 1 000 µs. This spans the range of intervals recorded between pulses in a typical burst.

The timing of the individual bursts is subject to the following constraints:

- The minimum time between bursts is 30 ms.
- The maximum time between bursts is 300 ms.

This range of times spans the intervals between strokes that have been recorded in intracloud strikes to instrumented aircraft. The MB waveform set is also applied to evaluate possibilities of avionic system upset.

For testing of avionic systems with the MS and MB waveform sets, the corresponding induced voltages and currents in interconnecting wiring are first determined and these are then applied as waveform sets to interconnected and operating systems to assess possibilities for system functional upset.

Available test current waveforms that meet the important parameters (peak current, action integral, time duration and charge transfer) are also described in SAE ARP 5412B [5.12] and EUROCAE ED-84 [5.13]. Frequency spectra of current Components A, A_H, D and H are also provided in for use by those who wish to translate the lightning environment into an equivalent Fourier frequency domain.

Of course, the lightning currents are not continuous sinusoid signals and should not be visualized as such. Sometimes, continuous wave (CW) currents at frequencies within the equivalent spectra, instead of pulse currents at the defined waveforms, are injected into airplanes for the purpose of measuring induced transients in aircraft wiring. This requires inverse transformation of CW signals into the time domain to determine the responses of measured circuits to the defined time-domain current components. Some cursory comparisons of CW and time domain pulse current tests of airplanes have been published, but exhaustive comparisons are not available.

Test Waveforms

The idealized lightning environment waveforms summarized here and described in the standards [5.13 - 5.14] are appropriate for analysis, but they are sometimes difficult to apply to full-scale components or vehicles in a test program. This is because it may become prohibitively costly to develop and operate current generators that can deliver the severe environments, especially to large vehicles such as a transport aircraft wing. Therefore, the approach for testing frequently involves the use of waveforms other than the idealized stroke current waveforms of Figs. 5.7 and 5.10. However, these alternate currents must yield physical effects or other test results that are the same as if caused by the idealized currents. For testing of systems exposed to induced effects, the test results must be readily extrapolated or scaled to those which would be obtained if the vehicle were tested with the idealized waveforms. Additional discussion of test waveforms and methods is found in subsequent chapters.

5.5.5 Zoning and Application of the Current Components

Current *Components A, B, C, D* and *H* together comprise the important characteristics of a severe natural lightning flash current although not all the components may attach everywhere on the aircraft. The process for assigning the current components is through zoning of the aircraft surfaces and structures and is discussed in the following paragraphs.

Lightning Strike Zone Definitions

The zone definitions are based on the following principles:

1. There are surfaces likely to experience initial leader attachment and the first stroke in the flash. These are usually extremities with low radii of curvature where electric fields may be concentrated, such as the nose area, tail cone, wing, and empennage tips.

2. There are other surfaces that are not likely to experience initial leader attachment and first strokes but are likely to experience subsequent strokes in negative C-G flashes. These include fuselage surfaces aft of initial leader attachment regions such as most of the fuselage in a traditional design.

3. There are other surfaces that are not likely to experience any lightning attachment but are having to conduct lightning currents between possible entry and exit locations. These are often wing surfaces inboard of wing tip extremities. Unless the wings are steeply swept, leaders and channels will not sweep along wing surfaces inboard of wing tip areas.

With these principles in mind, the following zones have been defined in [5.15 - 5.16]:

Zone 1A – First stroke zone

All the areas of the aircraft surfaces where a first stroke is likely during lightning channel attachment with a low expectation of flash hang-on.

Zone 1C - Transition zone for first return stroke

All the areas of the aircraft surfaces where a first stroke of reduced amplitude is likely during lightning channel attachment with a low expectation of flash hang-on.

Zone 1C also includes the first stroke, but one that is assumed to strike an aircraft at flight altitudes between 1 524 and 3 048 m (5 000 and 10 000 ft.), where the intensity of a severe return stroke is expected to be lower than

at the earth by the amount of charge that has been conducted through the aircraft during the leader phase. Whereas a lightning leader almost always attaches to the forward-most extremity of a nose, continued movement of the aircraft may sweep the leader channel alongside the fuselage (or an engine nacelle) for a certain distance prior to completion of the flash and arrival of the first stroke (which is represented in the *Zone 1A* and *1C* environments).

Zone 1B - First stroke zone with long hang-on

All the areas of the aircraft surfaces where a first stroke is likely during lightning channel attachment with a high expectation of flash hang-on.

Zone 2A - Swept stroke zone

All the areas of the aircraft surfaces where subsequent stroke is likely to be swept with a low expectation of flash hang-on.

Zone 3

Those surfaces not in Zones 1A, 1B, 1C, 2A, or 2B, where any attachment of the lightning channel is unlikely, and those portions of the aircraft that lie beneath or between the other zones and/or conduct substantial amount of electrical current between direct or swept stroke attachment points.

The standard for locating lightning strike zones on an aircraft is SAE ARP 5414B and EUROCAE ED 91A [5.14 and 5.15]. The contents of this standard are not repeated here so the reader should consult this standard when locating the lightning zones on a particular aircraft. Instead, some considerations that are not presented in the standard are discussed here.

The process begins with location of places where a lightning leader can originate. These are the initial entry and exit locations for the current components. This is often accomplished by high voltage strike attachment testing of scale models of the aircraft, or by numerical simulation of electric field concentrations at the aircraft extremities. Sometimes the initial leader attachment points may be identified by inspection if the aircraft geometry is like previously zoned aircraft whose initial strike zones have been established by model test. The leader situation is as shown in Fig. 5.14. By re-orienting the model to expose it to electric fields from different directions, all the possible leader attachments can be located.

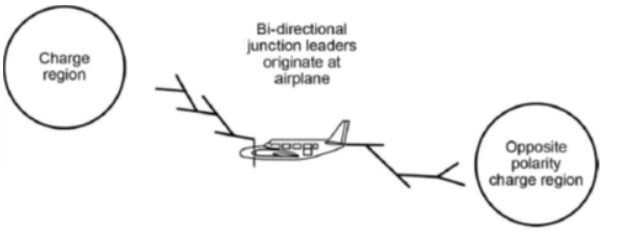

Fig. 5.14 – Initial leader attachments at an aircraft [5.14].

The process continues by locating other surfaces that can be exposed to “sweeping” lightning leaders or channels. Since a fixed wing aircraft is moving forward while in flight it will fly through the lightning leader and then the channel so that the leader or channel will reattach to other surfaces further aft of the initial attach point. If, as is usual, one of the initial leader attachment points is at a trailing edge, then the leader and channel will simply extend itself so that it remains in contact with the aircraft. This situation is shown in Fig. 5.15.

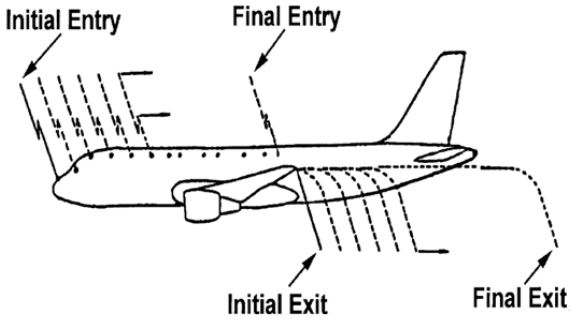

Fig. 5.15 – Flight of the aircraft through the channel

Thus, there are many places on aircraft surfaces that may be exposed to lightning strikes. They originate at extremities where the electric fields are strongest, but reattach to flat surfaces aft of initial leader attach locations.

Some of the questions have arisen concerning establishment of zone locations and boundaries. For example, an aircraft nose and a wing-mounted engine inlet have always been considered to be in *Zone 1A* (surfaces that experience the first stroke but with a low probability of flash hang-on). The possible rearward extent of this zone is established as follows:

The situation is shown in Fig. 5.16. The leader sweep distance, d, depends on the aircraft velocity, v_{ac}, the leader velocity, v_l, and the altitude, h, above ground, since the first stroke is not discharged until the leader has reached its ultimate destination at the earth, as shown in Eq. 5.5.

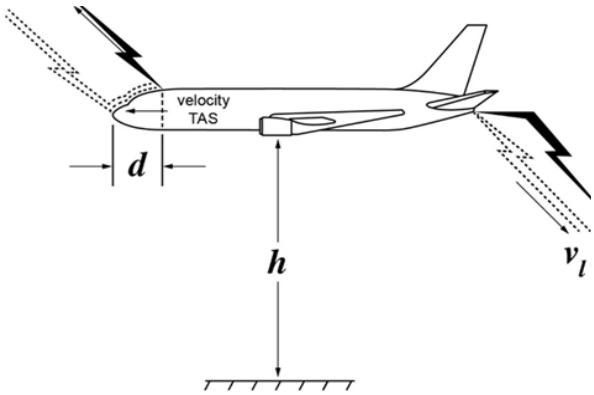

Fig. 5.16 – Leader sweep prior to first stroke arrival [5.14].

$$d = h\frac{v_{ac}}{v_l} \qquad (5.5)$$

Rearward extent of Zone 1A

In the past, the rearward extent of *Zone 1A* has been of little interest because most fuselage and engine nacelle structures have had aluminum skins that easily withstood *Zone 1A* lightning currents. Replacement of aluminum skins with advanced composites, however, makes this aspect of lightning strike zone location take on much greater importance. Analysis and inspections of lightning strike evidence on the surfaces of aircraft struck in flight shows that first return strokes of cloud-to-earth flashes may arrive at an aircraft several meters aft of initial leader attachments. The altitude and speed of the aircraft are important factors in establishing how far aft of initial leader attachments (to forward extremities) the first stroke currents may arrive. These factors apply, of course, only to cloud-to-earth flashes. The time at which the leader reaches the earth may be assumed to be the same as when the return stroke reaches the aircraft because, once initiated, the stroke (often called the 'return stroke') travels back up the channel almost instantaneously (at about one-third the speed of light). Thus, the leader speed is a significant parameter influencing leader sweep along an aircraft surface.

Leader velocity

The velocity of a typical cloud-to-ground lightning leader has been determined by high-speed photography and reported by many researchers as being between 1 and 1.5 x 10^5 m/s, Schonland, Malan, and Collens [5.16]. For example, reported in 1935 that the average velocities of 24 stepped leaders of negative polarity ranged from 1 x 10^5 to 13 x 10^5 m/s. Orville and Berger [5.17] measured a mean velocity of 2.5 x 10^5 m/s for an upward-progressing positive leader from a tower on Monte San Salvatore in 1965. Uman [5.18] reports a typical average stepped leader velocity as 1.5 x 10^5 m/s and more recently Fieux et al [5.19] have estimated leader velocities ranging from 0.2 x 10^5 m/s to 1 x 10^5 m/s. Elsewhere in the literature, one finds the values of 1 x 10^5 m/s or 1.5 x 10^5 m/s quoted most widely. It is appropriate, therefore, to utilize velocities in this range for v_l in Eq. 5.5.

If a typical leader traveling at an average speed of 1.5 x 10^5 meters per second were to strike the nose of an aircraft traveling 250 knots (134 m/s) at an altitude of 1 500 meters (5 000 ft.), the aircraft would have moved about,

$$d = \frac{(134 m/s)(1\,500\ m)}{1.5\ x\ 10^5\ m/s} = 1.3\ m \qquad (5.6)$$

by the time the stroke current arrived at the aircraft. The assumption should be that the leader would have reattached to a spot 1.3 m aft of its initial attachment location and at that moment the first stroke will arrive.

In this way the aft extension of *Zone 1A* is determined. In fact, in the zoning standard it is assumed that the full amplitude of the first stroke *Component A* is only valid up to 5 000 ft. Above this altitude the assumption is that some of the leader charge that is discharged by the first stroke has already passed through the aircraft at the low rate of the leader current, by the time the leader reaches the earth, and the stroke happens. Between 1 524 and 3 048 m (5 000 and 10 000 ft.) the amplitude of the first stroke is reduced to Component A_H, a reduced amplitude version of Component A. The amplitude of *Component* A_H is 150 kA and its action integral is 0.8 x 10^6 A^2.s. Such a current will inflict less than half of the thermal effects of Component A, whose action integral is 2 x 10^6 A^2s. The surfaces where first stroke Component A_H is found are in *Zone 1C*.

Above 1 524 m (5 000 ft.) and up to 3 048 m (10 000 ft.) the applicable first stroke is *Component A_H*. Since aircraft must operate from the ground up to cruise altitude, Component A is applicable in the first 1.3 m aft of leader attachment, and *Component A_H* is applicable 1.3 m further aft, by Eq. 5.5. The 1.3 m distances are due to the assumed airspeed of 250 knots, which is the maximum allowed up to 3 048 m (10 000 ft.) in many areas of the world. The result is shown in Fig. 5.17.

Zone 2A, within which only subsequent strokes are applicable, follows Zone 1C.

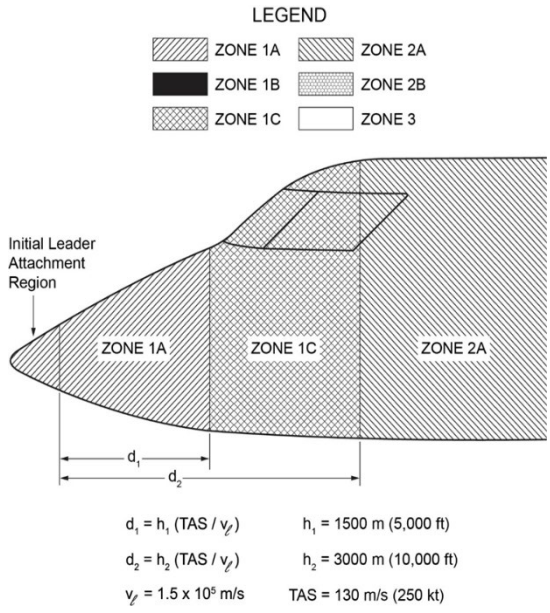

Fig. 5.17 – Zones 1A, 1C and part of 2A [5.14].

Note that the entire nose radome is shown as being the initial leader attachment region, since the electric field is intensified about the group of radome lightning diverters, and also the sharp edge of the forward bulkhead.

The analyses above are based on a cloud-to-earth lightning flash situation. A similar mechanism would exist for cloud-to-cloud discharges, but less is known about them. Since cloud-to-earth flashes are generally believed to present the most serious environment, the analyses in this section will continue to represent the cloud-to-earth case.

This analysis is simplistic and assumes that the leader takes a straight path between the aircraft and the earth, at a dependable velocity, which certainly does not always happen. Most of the possible variations probably extend the transit times and possible leader sweep distances, but there is no practical way to account for these variations in a way suitable for inclusion in the standard for zoning of aircraft. The guidelines that follow cover most of the in-flight lightning strike experience, but not all of it.

Further extent of zones

In order to account for tortuosity of the lightning channel as it "sweeps" along the aircraft surfaces, the zones are extended laterally a distance of 0.5 m onto adjoining wing and empennage surfaces.

As previously discussed, the surfaces aft of Zones 1A and 1C are in Zone 2A. Trailing edges behind Zone 2A are in Zone 1B (if the trailing edge is a possible leader attachment location) or Zone 2B (if the trailing edge is not an initial leader attachment location).

Zone 3 includes surfaces not within the other zones. It also includes all of the structures between possible lightning strike entry and exit locations. This means that nearly all the airframe is in Zone 3 and must conduct the lightning current components. Fig. 5.18 shows the zones on a complete aircraft.

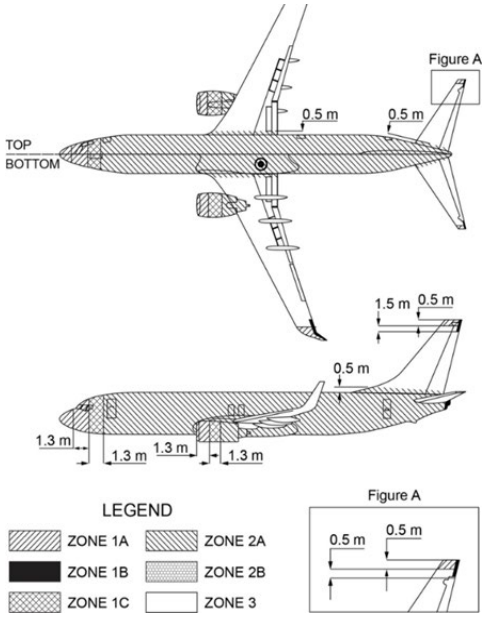

Fig. 5.18 – Lightning zones on a transport aircraft [5.14]

Since an aircraft can travel its full length (~80 m) in the lifetime (i.e., 1 s) of a C-G flash its full fuselage and empennage are exposed to reattachments of a lightning channel that originates at the nose (in 1 s it travels 130 m at 250 kts). This is not shown in the example of Fig. 5.18. A more correct example would be that in Fig. 5.19.

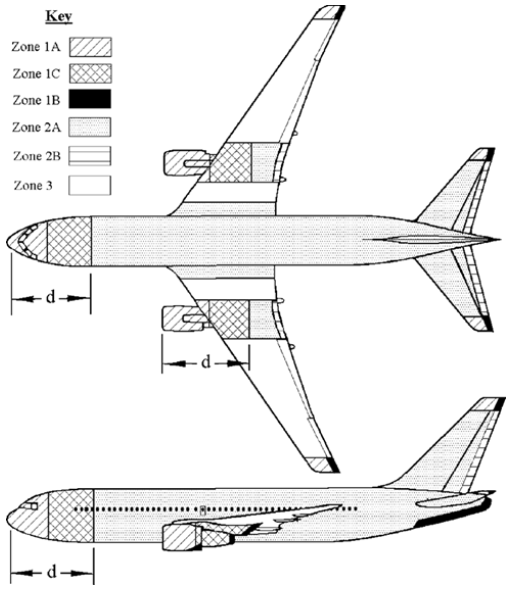

Fig. 5.19 – Large transport aircraft with more realistic zoning of empennage surfaces

More detailed illustrations of lightning strike zones on wing tips and winglets are shown in Fig. 5.20 [5.14].

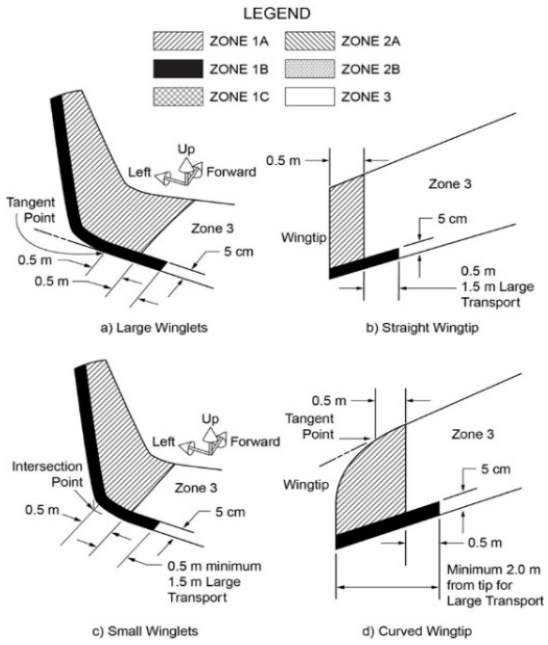

Fig. 5.20 – Lightning zones on winglets and wing tip

The significance of either of the lightning strike zones is that skins, structures and other objects located in these zones must be designed to tolerate the effects of direct or swept lightning strike attachments. In Fig. 5.20, for example, the integral fuel tank skins aft of the nacelles were required to be thick enough to withstand swept lightning strike currents, whereas skins in Zone 3 would perhaps not have to be this thick.

Swept channel zones

Over the years, the terms *swept stroke* and s*wept stroke zone* have become synonymous with Zone 2A, and the terms direct strike and direct strike zone have meant Zone 1A and 1B.

The term ‘swept channel’ refers to the continued sweeping of a lightning channel over the surface of the aircraft after the first stroke has occurred. Subsequent strokes may occur in the swept channel, and this is why the term ‘swept stroke’ has often been used.

Strokes, however, are not lightning arcs, but rather pulses of current, which, being of very short duration, are not likely to reattach to points aft of where they first enter the aircraft’s surface. So, the term ‘swept stroke’, though historically popular, may be misinterpreted to imply that the stroke attachment spot is somehow being swept. It is the lightning channel that is “swept” by the motion of the aircraft through it.

Currents applicable in each zone

The lightning currents to be expected in each zone are found in Table 5.2.

For conventional aluminum skins, the line of demarcation between Zone 1A, 1C, and 2A is of little practical importance, because most aluminum skins can withstand even the first return stroke (*Current Component A*) with little damage.

When the area of interest includes more than one zone, the protection assessment shall be performed utilizing the zone or zones with the most severe environment. The zones determine the lightning environment applicable to the aircraft surfaces, and to structures and systems within the aircraft. Zoning is used to determine the lightning current entry/exit path(s) through the aircraft and to locate the path(s) that represent(s) the most severe threat to the structure or system under investigation. The current components listed in Table 5.2 are applied for evaluation of physical effects and to verify adequacy of protection designs.

Table 5.2 Current Components Applicable in Each Zone[1]

Current Component:	A	A_H	D	B	C*	C
Zone:						
1A	√			√	√	
1B	√		√	√		√
1C		√		√	√	
2A			√	√	√	
2B			√	√		√
3 Conduction	√		√	√		√
3 Arc entry[2]	A/5			√	√	

Note 1: Applicable via arc entry except for Zone 3 conduction
Note 2: Applicable only to transport aircraft fuel tank surfaces in Zone 3

The order of application of current components is to have the initial stroke current component (A, A_H, D, A/5) applied first, followed by the intermediate (B) and continuing currents (C*, C). Only surfaces in Zone 1B are to receive a second stroke, Component D.

Composite structures

If the skin or structure aft of a leading-edge attachment area is made of composites, or other poorly conducting materials, the rearward extent of Zone 1A and also of 1C becomes of more critical importance. Some carbon fiber composite skins can tolerate the effects produced by the Zone 2A currents, which include subsequent stroke Component D, without requiring additional protection. However the first stroke (Component A) assigned to Zone 1A surfaces can deliver eight times more energy than the current (Component D) included in Zone *2A*, and the resulting damage can be extensive unless protective coatings or other methods have been applied.

The significance of the 'B' designation can be seen in the currents specified for Zones 1A and 1B. Due to the short hang-on time for an initial strike to a Zone 1A surface, only current components A, B and C* are applied, but all the current components are experienced by trailing edge surfaces in Zone 1B.

Most protective measures add weight and increase cost. Thus, the decision as to whether to apply protection or not, (or even whether a composite skin should be utilized in the first place), may depend directly on the designation of the lightning strike zones, and especially on a realistic determination of the rearward extent of Zone 1A and Zone 1C.

Further discussion of distance traveled vs. flight conditions

From Fig. 5.16 it is evident that the distance, *d*, that the aircraft travels between the time of leader attachment and return stroke arrival is dependent on the aircraft's velocity and altitude, in addition to the leader velocity. Fig. 5.21 is a plot of Eq. 5.5 for three different values of v_{ac}. It shows the range of distances, *d*, that an aircraft flying at a given velocity may move with respect to the lightning leader channel (i.e., the leader sweep distance) prior to the arrival of the first stroke. This range of distances considers the full range of flight altitudes and velocities within which aircraft are most likely to operate.

From Fig. 5.21 (and Fig. 5.16) it may be seen that an aircraft cruising at 250 knots (288 mph, 130 m/s) airspeed, at an altitude of 3 048 m (10 000 ft.), would travel 2.6 meters. During the time it would take a lightning leader traveling 1.5×10^5 m/s to reach the earth and initiate the return stroke. This is a significant portion of the fuselage length of some small jet aircraft, or an entire engine nacelle on a large transport aircraft. This implies that all of these surfaces could be exposed to the first stoke of a lightning flash, represented by Component A (or Component A_H). Since the first stroke is considered a part of the Zone 1A or Zone 1C environment, surfaces of the aircraft that are exposed to the swept leader channel are within these zones.

On the other hand, a propeller driven aircraft whose flight envelope extends only to a speed of 170 knots (87 m/s, 196 mph) and an altitude of 1 829 m (6 000 ft. .) would travel only 1.06 m before the arrival of the first stroke. Aircraft surfaces aft of the leader channel sweep distance would experience only the subsequent strokes, represented by Component D, and the intermediate and continuing currents, Components B and C*, assigned to Zone 2A.

High speed aircraft

Since many of today's military aircraft are designed to operate at high speeds, a large portion of their surfaces aft of initial leader attachment points would, by the results of Figs. 5.21, might be considered within either Zone 1A or 1C up to an altitude of 3 km (10 000 ft.). Whether or not extension of Zones 1A and 1C aft of the 1.3 m and 2.6 m distances illustrated previously is applicable depends on whether the aircraft may operate at speeds above 250 knots if higher speeds are to be operated.

This possibility was first recognized when the first 'all composite' aircraft was being designed and was described in [5.20]. The significance of this rearward extension of Zone 1A has been academic for conventional aluminum structures because most aluminum skins do not suffer catastrophic damage from the lightning environment of Zones 1A and 1C. This is not the case for composites unless adequate protection is provided.

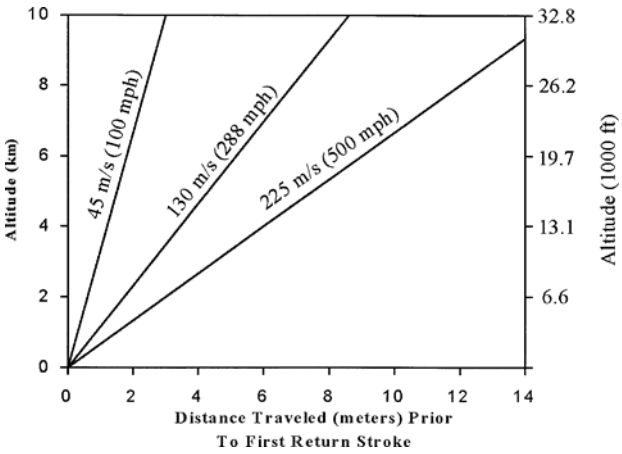

Fig. 5.21 - Distance traveled prior to arrival of return stroke for leader velocity = 1.5 x 10^5 m/s.

When considering Fig. 5.21 it should be remembered that most C-G flashes are expected to originate from 3 km (10 000 ft.) and below. Thus, the airplanes operating above this altitude would not normally encounter C-G flashes where Components A and A_h are applicable. Experience has shown effects of severe stroke currents on surfaces of commercial transport and general aviation aircraft well aft of the 2.6 m leader extension predicted by Eq. 5.6 and Figs. 5.17 and 5.18. These airplanes were struck at altitudes of 3 km (10 000 ft.) and below where the airplanes were traveling at airspeeds of 250 knots or below. These must have been due to non-traditional flashes that took longer, more tortuous routes to ground.

Skins and structures made of advanced composites are likely to suffer greater damage from the first return stroke (Component A or A_H), defined for Zones 1A and 1C, than from the subsequent stroke (Component D), defined for Zone 2A. This can be attributed to the higher action integrals involved (2.0 x 10^6 A^2s for Component A or 0.8 x 10^6 A^2s for Component A_H) versus 0.25 x 10^6 A^2s for Component D.

Several factors reduce the likelihood of experiencing the first strokes in cloud-to-earth flashes at the altitude and velocity limits of the aircraft's flight envelope to acceptable risk levels:

Most strikes occur at lower altitudes. Experience shows that most lightning strikes occur when the aircraft is flying at altitudes between 1.5 km (5 000 ft.) and 6 km (20 000 ft.), as discussed in Chapter 3. Most of the cloud-to-earth strikes are believed to occur when the aircraft is below 3 km (10 000 ft). At these altitudes, an aircraft's velocity is often less than at higher altitudes. Statutes in many countries require that aircraft operating below 3 km (10 000 ft.) not exceed 250 knots.

Most severe strokes occur at lower altitudes. Most strokes that have caused severe physical effects on aircraft have occurred at altitudes of 6 km or less, and many of these have been at altitudes below 1.5 km. In most of the cases of severe damage or loss of the aircraft, the strike occurred at 1.5 km (5 000 ft.) or below. These first strokes are more commonly represented by the Zone 1A environment. In a very few cases, evidence of a severe stroke has been reported occurred at cruise altitudes of between 10 and 12 km. The nature of the lightning currents responsible for this damage is not known, but they may be associated with positive polarity charges which exist in the tops of cumulonimbus clouds at high altitudes.

It is logical that most of the severe strokes occur closest to the earth, because these strokes result from discharges of a cloud-to-earth leader system that is above the aircraft and experiences more of the leader charge in the first stroke than would an aircraft in a leader that is mostly between the aircraft and the ground.

Strikes at flight altitudes may not be cloud-to-earth. The preceding discussion addresses leader propagation between a cloud and the ground. It is probable that many of the strikes involving aircraft at cruise altitudes above 6 km do not involve the ground but propagate, instead, between upper-level charge centers in or among the clouds. Less is known about the formation of these intracloud flashes, but it is probable that their leader propagation times are shorter than those of the cloud-to-ground flashes that originate at high altitudes. These factors reduce the probability of significant stroke currents appearing at aircraft in flight altitudes above 3 km (10 000 ft.) but probably do not eliminate this possibility. Flashes originating in the upper reaches of thunderstorm clouds have occasionally been observed propagating all the way to ground. Such flashes transfer large amounts of positive charge.

Methodology for zone location

Guidance for location of lightning strike zones on an aircraft is provided in [5.14]. Based on the considerations described above, the following procedures can be used to locate the lightning strike zones on a specific aircraft.

1. All aircraft extremities such as the nose, wing and empennage tips, tail cone, wing-mounted engine nacelles and other significant projections, should be regarded as initial leader attachment locations. Forward extremities should be considered to be in Zone 1A and trailing edge extremities should be in Zone 1B, in accordance with the zone definitions. If there are uncertainties regarding possible initial leader attachment locations, scale models may be tested with high voltages to see where leaders may originate. The standard for the model test is SAE ARP 5416A [5.21].

2. In-flight experience and laboratory tests of scale models of aircraft have shown that the leading edges of large, straight wings and the brow areas above cockpits of transport category aircraft may also receive initial leader attachments, but not as frequently as aircraft extremities. These attachments are thought to be more likely to result from a naturally occurring leader approaching the aircraft than from an aircraft-initiated leader, and they are akin to the lightning strikes known to attach, now and then, to the flat roofs of large buildings. There is reason to believe that the stroke currents following such attachments are lower in intensity than the strokes associated with Zones 1A, 1C or 2A. The electric field due to a smaller leader charge allows an advancing leader to meander closer to building rooftops before inducing junction leaders from more prominent locations. In such cases, the rearward extension of susceptibility to lightning attachment would continue aft.

If lightning effects to such surfaces could produce a catastrophic effect, a reduced intensity lightning environment has been defined for application to flat surfaces aft of fuel tank skins. This is comprised of:

- A stroke current that is represented by Component A/5 (40 000 A at 0.08 x 10^6 A^2s)
- Followed by *Component B*
- Followed by *Component C**, if the surface is not subject to channel hang-on, or *Component C* if the surface is a trailing edge where lightning channel hang-on is likely.

3. Since all aircraft spend some time flying at altitudes below 3 km (10 000 ft.), the minimum rearward extension of first stroke Zones 1A/1C on a particular aircraft should be determined from Eq. 5.6 or Fig. 5.15.

4. Since nearly all aircraft can travel more than their entire length in the one or two second lifetime of a lightning flash, the remainder of the surfaces aft of Zone 1A/1C should be considered within Zone 2A. Trailing surfaces should be considered in Zone 1B or 2B, depending on whether they are also initial leader attachment areas or not. Surfaces 0.5 m (18 in) to either side of Zone 1A/1C and *2A* surfaces (located as described above) should be included within that same lightning strike zone. This takes account of the small lateral movements of the sweeping channel that occur when the aircraft is turning, or when there is turbulent airflow alongside an aircraft surface.

5. Surfaces of the vehicle for which there is a low possibility of direct contact with the lightning arc channel, and that lie between the zones described above, should be designated Zone 3. Structures that lie beneath and between all the surface zones are also within Zone 3. Zone 3 areas may conduct all the lightning currents that enter or exit from Zones 1A or 1B.

Small protrusions

The zoning standard recommends that small protrusions from surfaces are also in the zone of those same surfaces and not exposed to more intense lightning strokes than is assigned to their zone unless their height above the surface is more than 10% of the distance between the protrusion and the nearest boundary with a strike zone where more intense strokes are expected. This arbitrary rule has seemed to be effective. A common example is a blade antenna in Zone 2A. If this does not extend into the airstream more than 10% of its distance from the boundary with Zone 1C, it remains in Zone 2A, but if this antenna extends outward more than 10% of this distance, it is to be assigned Zone 1C.

Zoning of rotorcraft

Due to the wide range of airspeeds associated with rotorcraft, and the fact that they have moving rotors, there is a correspondingly wide range of possibilities for initial swept leader attachments to helicopter main and tail rotor blades. Therefore, it is best to regard all of the upper surfaces and edges of main rotor blades, and all surfaces and edges of tail rotor blades, of a helicopter as belonging to Zone 1A, even though the zoning standard shows rotor blades as having more limited Zone 1A and 1B surfaces. It is usually the upper surfaces of blades that get struck but all surfaces should have the same protection. Lightning channels are known to be tortuous and can swirl around the edges of wing tips and blades, such that they can reattach to opposite surfaces.

Some operators have stated that their helicopters are more likely to be struck while parked on the ground. Thus, unless blades can be inspected prior to flight, it is prudent to consider the upper surfaces of blades as in Zone 1B. The zoning standard considers only the in-flight situation.

If the helicopter does not have skids or fixed landing gear, most of the lower surfaces would be in Zone 1B, again since the helicopter may be in hover mode when struck. If skids or fixed, extended landing gear are present, those would be the items exposed to direct strikes and the lower surfaces would be protected from strikes by their presence.

An example of a helicopter zoned without skids or fixed landing gear is shown in Fig. 5.22.

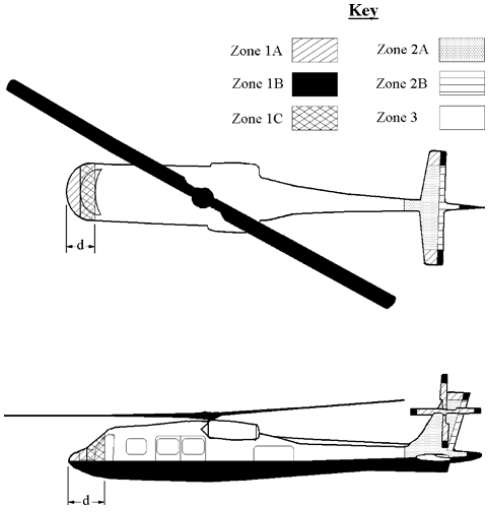

Fig. 5.22 – Lightning Zones of helicopter without fixed landing gear or skids.

Once the lightning strike zones have been established, they should be documented on a drawing of the aircraft or rotorcraft, with boundaries identified by appropriate station numbers or another suitable notation. It is usually appropriate for the applicant to review the zone drawings with cognizant certifying engineers to obtain concurrence, as the zones form the basis for certification of the designs that follow.

Further guidance on zone location methodology is contained in [5.15 - 5.16].

5.6 Steps in Design and Certification

Experience has shown that the most successful lightning protection design and certification programs have been achieved when the work was conducted in a logical series of steps.

In this context, 'successful' means achieving a satisfactory protection design that complies with the regulations and has a minimum impact on overall weight and cost.

The details and order of these steps may vary somewhat from one program to another, but most programs include the following basic steps:

Step a – Locate the lightning strike zones on the aircraft

Determine the aircraft surfaces, or zones, where lightning strike attachment to the aircraft is probable, and the portions of the airframe through which lightning currents must flow between these attachment points.

Step b – Establish the lightning environment

Identify the components of the lightning environment that are applicable to surfaces of the aircraft in each zone.

Steps a and b have been discussed in § 5.5.5.

Step c – Perform the Lightning Hazard Assessment

Determine the aircraft structure, systems and components safety classifications and make hazard assessments (safety assessments) to review the aircraft and its systems and components to identify lightning effects and potential hazards.

Safety assessments are necessary for certification of an aircraft including all its systems and components. The procedures for conducting these assessments are provided in

the guidance documents applicable to the airframe as a whole and each major system of the aircraft. The aircraft parts and applicable guidance documents are as follows:

Guidance Documents

A number of documents published by the certifying agencies (FAA, EASA) are available to assist in the certification process. For example, FAA has published ACs that explain the process of lightning safety assessments and showing compliance with various regulations. Those pertaining to lightning protection are listed below.

Airframe and all systems except those addressed by other standards: SAE ARP 5577 [5.2].

Fuel Tanks and System: FAA AC 20-53C [5.5], FAA AC 25.954-1 [5.4], SAE ARP 6205 [5.22].

Electrical and Avionic Systems: FAA AC 20-136B [5.8].

Engines: FAA AC 33.28-1 [5.23].

The result of the safety assessments described for each area listed above is identification of the functions required for safe flight and the structures, systems and equipment that perform these functions. This categorizes systems into lightning criticality categories as follows: Level A – Catastrophic, Level B – Hazardous, Level C – Major, Level D – Minor, and level E – No safety affect. Somewhat similar categories are available for structures. These definitions are found in FAA's system design and analysis regulations such as FAA AC 25.1309-1A [5.24].

Also, the locations of the structural elements, system component installations and interconnecting wiring associated with these systems, will be identified, so that the interactions of the lightning environment with these items can be addressed successfully.

Important considerations

The specific procedures for the assessments described in the above references should be referred to for the applicable systems. These are not repeated here. Instead, we provide some important factors that should always be considered when conducting the safety assessments. Sometimes one or more of these have been overlooked, resulting in incomplete assessments and protection.

1. **Whole aircraft effects.** Lightning currents flow throughout the entire aircraft so the potential effects are not limited to the immediate vicinity of lightning entry or exit points. Especially for fuel and electrical/avionic systems which occupy much of the volume of an aircraft, all parts of the system are exposed to lightning effects. For example, electrical arcing due to current flow among fastened lightning effects have been observed large distances from the strike entry or exit locations. This is due to the flow of current between these locations. For the same reason, induced voltages and currents should be assumed to be coupled to interconnecting wiring throughout the wiring installations of electrical/avionic systems.

2. **Multiple strikes in a flight**. When considering the effects of lightning it should be remembered that aircraft may experience more than one strike in a single flight. Neither airworthiness regulations nor advisory material state how many strikes may be expected, or must be protected against, in the same flight. It is well known that aircraft frequently experience more than one strike during a flight. Protection designs such as "one-shot" voltage suppressors or diverter strips that tolerate only one strike and are intended to be replaced after a strike should be avoided. In principle, protection features and devices should be designed to perform their intended functions for the expected life of the aircraft. Doing so will minimize the need for periodic inspection and maintenance activities and the risk of failures if a protection device is not functional.

3. **MSs or bursts.** Within each strike there are usually MSs or bursts of pulses as described in Chapter 2. Care needs to be taken to assure that these multiple effects are considered. Test standards for electrical and avionics systems include MS and burst tests, but standards for testing fuel tanks, systems and structures do not. The safety assessments should ask the question of whether a first strike might degrade protection features so that a second or third strike may overcome the remaining protection.

4. **Limitation of assessments to examples in guidance documents**. The guidance documents listed above provide examples of areas to be reviewed. An example is the list in § 4.3 of SAE ARP 5577 [5.2]. This is not intended to be all-inclusive. There are usually additional structures, systems, or components whose potential for hazardous responses to lightning need to be evaluated. Certification managers or authorities should not accept assessments whose scope is limited to the lists in the guidance documents without challenging the assessors to look beyond those examples.

5. **Lightning strikes do not happen in fair weather.** This means that the lightning assessments should consider the need for system functionalities at the

times and flight regimes when lightning is most likely. As noted in Chapter 3, strikes happen when the aircraft is in visual flight rules flight, during precipitation (often icing), in turbulence, and during climb and descent. Pilot workloads are likely to be high, and multiple systems are needed. The safety assessments need to consider these likelihoods. This broadens the scope of the assessments.

6. **The aircraft safety assessment should be consulted.** Results of the aircraft safety assessment should be reviewed before beginning the lightning safety assessments. The aircraft assessment will show the structures and systems that are needed for safe flight. Do not be surprised if a system that may potentially fail due to a lightning effect has not been included on the list of systems whose failures may prove catastrophic to the aircraft. Those conducting the aircraft assessment may have not been aware of a potential lightning effect.

Step d – Establish protection criteria

Decide on the amounts of physical damage that will be acceptable for structures, and the degrees of upset and/or damage that will be acceptable for systems that perform the functions necessary for safe flight, as well as protection requirements for other systems, such as flight control and the fuel system.

Step e – Design lightning protection

Design lightning protection measures for each of the structures, systems, and/or equipment in need of protection. In some cases, the lightning protection is inherent in the design of the structure or system. In others the protection features must be added. Since the regulations require protection against catastrophic events, there may be lightning damage or other effects that are in compliance with the regulations yet imply an economic burden on the airplane owner or operator. Decisions are then made regarding how much additional protection to be applied to minimize this damage. Methods of protection design are included in Chapters 6 through 17 for various types of structures and systems.

Step f – Verify protection adequacy

Verify the adequacy of the protection designs by one of the following methods:

a. Showing sufficient similarity of design details relevant to lightning susceptibility with previously proven designs

b. Performing simulated lightning tests

c. Performing acceptable analyses.

d. Some combination of the above methods.

For electrical and avionic system certification, margins between system and equipment voltage and current tolerance levels and actual levels determined by analysis or test usually need to be shown. These margins account for experimental error and analytical uncertainty.

More specific versions of the above set of steps are in use for design and certification of fuel systems, electrical and avionic systems, structures and other systems are presented in the aforementioned advisory documents. These are discussed further in the applicable chapters of this book.

References

5.1 *Bonding, Electrical and Lightning Protection, for Aerospace Systems*, US Military Specification MIL- B-5087B, 15 October 1964.

5.2 *Aircraft Direct Effects Certification* SAE ARP 5577, 26 March 2008.

5.3 *Industry Documents to Support Aircraft Lightning Protection Certification* FAA AC 20-155A, 16 July 2013.

5.4 *Transport Airplane Fuel System Lightning Protection* FAA AC 25.954-1, 24 Sept 2018.

5.5 *Protection of Aircraft Fuel Systems Against Fuel Vapor Ignition Caused by Lightning* FAA AC 20-53C, 24 Sept 2018.

5.6 *Electrical and Electronic System Lightning Protection* 14 CFR 25.1316.

5.7 *Department of Defense Interface Standard: Electromagnetic Environmental Effects Requirements for Systems* MIL-STD-464C, 01 December 2010.

5.8 *Aircraft Electrical and Electronic System Lightning Protection* FAA AC 20-136B, 7 September 2011.

5.9 *Protection of Aircraft Fuel Systems against lightning* FAA AC 20-53, 10 November 1965.

5.10 *Lightning Test Waveforms and Techniques for Aerospace Vehicles and Hardware,* Report of SAE Committee AE4, Special Task F, 5 May 1976.

5.11 N. Cianos and E. T. Pierce, A Ground Lightning Environment for Engineering Use, Technical Report 1Stanford Research Institute for McDonnell Douglas Astronautics Company, Huntington Beach, CA, August 1972.

5.12 *Aircraft Lightning Environment and Related Test Waveforms,* SAE ARP 5412B, 11 January 2013.

5.13 *Aircraft Lightning Environment and Related Test Waveforms Standard* EUROCAE ED 84, Paris, 2013.

5.14 *Aircraft Lightning Zoning* SAE ARP 5414B, 5 December 2018.

5.15 Aircraft Lightning Zoning Standard EUROCAE ED 91A, Paris, 10 January 2019.

5.16 B. F. J. Schonland, D. J. Malan and H. Collens, *Progressive Lightning: II*, *Proceedings of the Royal Society of London*, Vol. 152, 1935, pp. 595-625.

5.17 R. E. Orville and K. Berger, "Spectroscopic and Electric Current Measurements of Lightning at the Monte San Salvatore Observatory in Lugano, Switzerland", *Proceedings of the Fifth International Conference on Atmospheric Electricity*, Garmish-Partenkirchen, Germany, 2-7 September 1974.

5.18 M. A. Uman, "Spark Simulation of Natural Lightning," *1972 Lightning and Static Electricity Conference*, 12-15 December 1972, pp. 5-13.

5.19 R. P. Fieux et al, *Research on Electrically Triggered Lightning in France,* IEEE Trans. On Power Apparatus and Systems, Vol. PAS-97, No. 3, May/June 1978, pp. 725-733.

5.20 J. A. Plumer, "Further Thoughts on Lightning Strike Zones for Aircraft," Supplement to *Lightning Technology,* NASA Conference Publication 2128, FAA-RD-80-30.

5.21 *Aircraft Lightning Test Methods* SAE ARP 5416A, 7 January 2013.

5.22 *Transport Airplane Fuel Systems Lightning Protection SAE* ARP 6205.

5.23 *Compliance Criteria for 14 CFR 33.28 Aircraft Engines, Electrical and Electronic Control Systems* FAA AC 33.28-1.

5.24 *System Design and Analysis* FAA AC 25.1309-1A.

Chapter 6

PROTECTION AGAINST PHYSICAL DAMAGE

It was not easy, however, to escape from Crete, since Minos kept all his ships under military guard, and now offered a large reward for his apprehension. But Daedalus made a pair of wings for himself, and another for Icarus, the quill feathers of which were threaded together, but the smaller ones held in place by wax. Having tied on Icarus' pair for him, he said with tears in his eyes: "My son, be warned! Neither soar too high, lest the sun melt the wax; nor sweep too low, lest the feathers be wetted by the sea!" Then he slipped his arms into his own pair of wings and they flew off. "Follow me closely," he cried, "do not set your own course."

As they sped away from the island in a northeasterly direction, flapping their wings, the fishermen, shepherds, and ploughmen who gazed upward mistook them for gods. They had left Naxos, Delos, and Paros behind them on the left hand, and were leaving Lebynthos and Colymne behind on the right, when Icarus disobeyed his father's instructions and began soaring towards the sun, rejoicing in the lift of his great sweeping wings. Presently, when Daedalus looked over his shoulder, he could no longer see Icarus; but scattered feathers floated on the waves below. The heat of the sun had melted the wax, and Icarus had fallen into the sea and drowned. Daedalus circled around, until the corpse rose to the surface, and then carried it to the nearby island now called Icaria, where he buried it.

Robert Graves, The Greek Myths I (Baltimore: Penguin Books, 1955):312-13.

6.1 Lightning Physical Effects on Metal Skins and Structures

The physical effects of lightning on metal structures were described in Chapter 4 and include the following:

1. Melting or shock wave effects at lightning attachment points on metal surfaces.
2. Temperature rises in metal conductors due to lightning currents.
3. Magnetic force effects.
4. Acoustic shock effects.
5. Arcing at structural bonds, hinges, and joints.
6. Ignition of flammable vapors within fuel tanks.

Whether the melting of holes or the creation of a hot spot in a particular area constitutes a hazard or not depends on what is enclosed by the metal skin. In some places, ignition of flammable materials, such as thermal insulation blankets that may be in contact or in close proximity to inner surfaces of airplane skins, is a concern. In other places, where no flammable materials or vapors are in direct contact with the metal skins, the designer must be concerned only with preventing the formation of holes that could degrade structural strength and lead to eventual structural failure. Usually holes melted by lightning attachments are not large enough to allow noticeable loss of cabin pressure.

Corrosion at a spot where lightning had attached is probably the most likely form of structural degradation. However, such corrosion sources do not appear instantaneously and are likely to be identified and repaired long before corrosion and stress propagations set in.

Important factors

Lightning strikes usually produce very little damage where they attach to a metal surface, since relatively little energy is released at lightning attachment points. The energy that *is* released at an attachment point is the product of the lightning current and the cathode or anode voltage drop at the end of the lightning channel (known as the arc root). This drop is a few tens of volts. Thus, a 400-ampere continuing current releases power at the rate of 12 kW if the cathode (or anode) drop is 30 volts. The dwell time of the lightning attachment at any single spot is very short so the energy dissipation is minimal. The electrical resistance of aluminum is so small that temperature rises near strike points are not sufficient to cause melting.

Since the lightning channel is an electrical arc, it can be very hot (30 000 °C), but only the root of the arc contacts the surface to which the channel attaches. Since the arc is surrounded by air, any energy released in it is free to escape into the air. Contact of the lightning arc with a metal surface causes the metal to melt in the manner of an electric arc welder electrode momentarily attaching to a metal surface.

Lightning current can produce spectacular damage then it flows through an arc that is confined within a region where the pressure may exceed atmospheric pressure. This situation is encountered when a lightning arc forms within a nose radome or other nonconductive structural enclosure. Since the voltage necessary to sustain an electric arc increases with pressure, the power associated with such an arc (V x I) is higher than it would be in ambient air, and so is the energy it releases. The confinement of overpressure, which lasts until the enclosure ruptures, often inflicts substantial damage on the structure that encloses the arc. An exception to this general statement is covered in §6.1.2.

Assuming that the lightning channel is not confined, the damage it produces at a particular attachment point on a metal skin is largely determined by how long the lightning channel remains attached to this spot. If the channel sweeps swiftly across an unpainted aluminum skin, for example, the damage might consist merely of minor pitting of the skin's exterior surface. However, the channel attachment spot is not usually completely free to move. Conventional paints and primers on metal surfaces (and similar paints combined with resins and smoothing agents on the surfaces of composite skins in Zones 1A or 2A) cause the lightning channel to dwell for longer periods at attachment points. This increases the probability of melt-through at those points, on metal surfaces, and increases the probability of thermal damage to composite surfaces. Damage to composite surfaces caused by lightning continuing currents is usually minimal.

The damage to metal and composite surfaces may be summarized as follows:

Damage to metal skins

- Attachment of lightning *stroke currents* to metal skins rarely leads to melt-through, since the time durations of stroke currents are too short.

- Attachment of lightning *intermediate and continuing currents* to metal surfaces produces melting, which may include complete melt-through.

Fig. 6.1 shows an example of small pit marks left by a lightning flash on the nose of a research airplane.

At trailing edges, in *Zones 1B* or *2B*, the lightning channel may remain attached for longer periods, melting away ('eroding') larger amounts of metal. This is usually not hazardous, and it is neither practical nor necessary to protect against erosion of metal or erosion of holes in trailing edges.

Protection design should be focused on preventing metal skins from melting through or composite skins from being punctured in areas where such damage would endanger safety of flight. Holes in aircraft skins that do not endanger safety of flight may be permitted. The conditions under which safety of flight might be endangered from hole formation are:

1. When the hole is melted through the skin of a fuel tank or some other enclosure containing flammable materials, so that these materials are allowed to come into contact with the lightning channel.

2. When the hole causes depressurization.

3. When the hole sufficiently degrades the mechanical strength of a primary aircraft structure or other component (such as a helicopter rotor blade), to cause catastrophic failure of such structure or component, either immediately or at some future time.

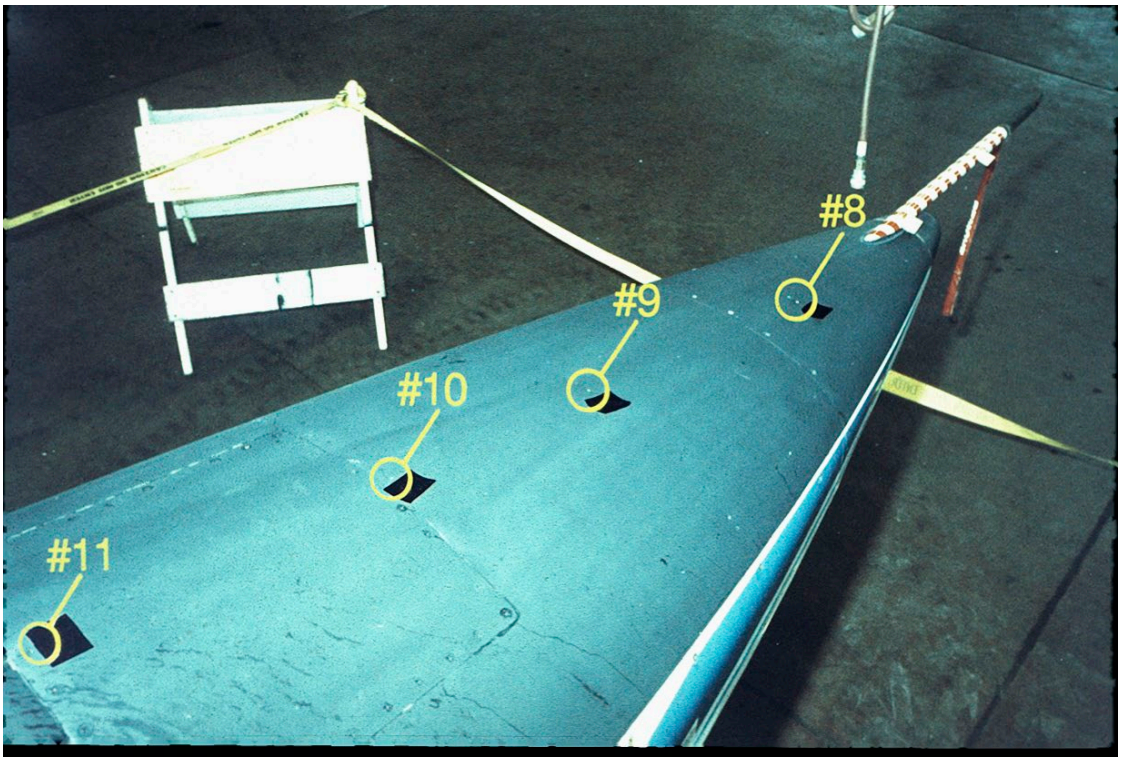

Fig. 6.1 Melted spots left on painted metal surface by lightning strike to nose boom. Spots are approximately 300 mm (12 in) apart (NASA Photo).

There have been reports of holes melted in pressurized fuselages by swept lightning channel reattachments, but the holes were far too small (less than 10 mm in diameter) to allow significant depressurization of a conventional airplane cockpit or cabin area. Since trailing edge areas are not pressurized, the larger holes melted by longer duration currents hanging on to trailing edges have not posed a depressurization problem. Nevertheless, the possibility of such an event should be considered in any design that involves pressurization of or containment of fuel within trailing edge sections.

Melting and charge transfer

Experiments to determine the relationship between lightning charge transfer and melt-through hole-size in sheet metals have shown that the volume of metal melted away at a lightning attachment point is closely related to the charge carried into the point by the lightning current, provided that the time duration of the lightning attachment is in the range from 10 - 2 000 milliseconds and that the rate of charge delivery is within the range associated with lightning intermediate and continuing currents (200 - 2 000 A). Effects such as melt-through are also dependent upon the type of metal involved and its thickness.

Hole size vs charge transfer

Quantitative relationships between electric arcs and typical aircraft skin metals were reported in 1949 by Hagenguth [6.1], who made laboratory measurements of the amount of continuing current and charge transfer necessary to melt holes of various sizes in typical metal skins. He found that a nearly linear relationship exists between the amount of charge (Q) delivered to an arc attachment point and the amount of metal melted away from it when the charge was delivered at the rates typical of lightning continuing currents (200 - 400 A).

Results of his laboratory tests are presented in Fig. 6.2. These results have been used to estimate the amounts of charge transferred to spots on aircraft surfaces that have received natural lightning strikes.

Melt-through thresholds

Brick [6.2], Oh and Schneider [6.3] made tests to determine the minimum amounts of charge and current required to melt through aluminum and titanium skins of various thicknesses. This data can be used to project the minimum lightning conditions that might ignite flammable fuel vapors in contact with the inner surfaces of integral fuel tank skins. Brick and Schneider also showed that the melting effects depended on current amplitude as well as on the amount of charge transferred to the lightning arc attachment spot. Whereas Hagenguth had shown that over 22 coulombs, when delivered by a current of 200 A, were necessary to melt completely through 2 mm (0.080 in) aluminum skins, Brick, Oh, and Schneider showed that only about 10 C, when delivered by a higher amplitude current of about 500 A, was enough to melt completely through such a skin. In laboratory tests, as little as 2 C, when delivered by about 130 A, melted a hole completely through a 1 mm (0.040 in) aluminum skin.

Oh and Schneider's melt-through thresholds for these and other skin thicknesses are shown in Fig. 6.3. The close proximity of their test electrode to the skins (2.4 to 4.8 mm) might have restricted natural movement of the arc on the surface of the skin and been responsible for their low Coulomb ignition thresholds. However, this restriction resembles the conditions prevalent when the exterior surface of an aircraft skin is painted.

Additional data

Work by Kester, Gerstein, and Plumer [6.4] with an L-shaped electrode spaced 6.4 mm (0.25 in) above the skin, permitting greater arc movement due to the horizontal electrode, showed that 20 coulombs or more, when delivered at 130 A, are required to melt through a 1 mm thick aluminum skin. Their data is presented in Fig. 6.4. However, the magnetic interactions associated with currents in the L-shaped electrode might have forced unnatural movement of the arc, resulting in an optimistic result. Since movement of a natural lightning arc is neither restricted nor forced by any electrode, it is probable that the aluminum melt-through threshold data shown in Fig. 6.3 are conservative, while those shown in Fig. 6.4 might be optimistic. This is especially true when the surface of the metal is bare and movement of the lightning arc is not restricted by paint or other surface finishes. Other work [6.5] has generally corroborated the results of Figs. 6.2 and 6.3.

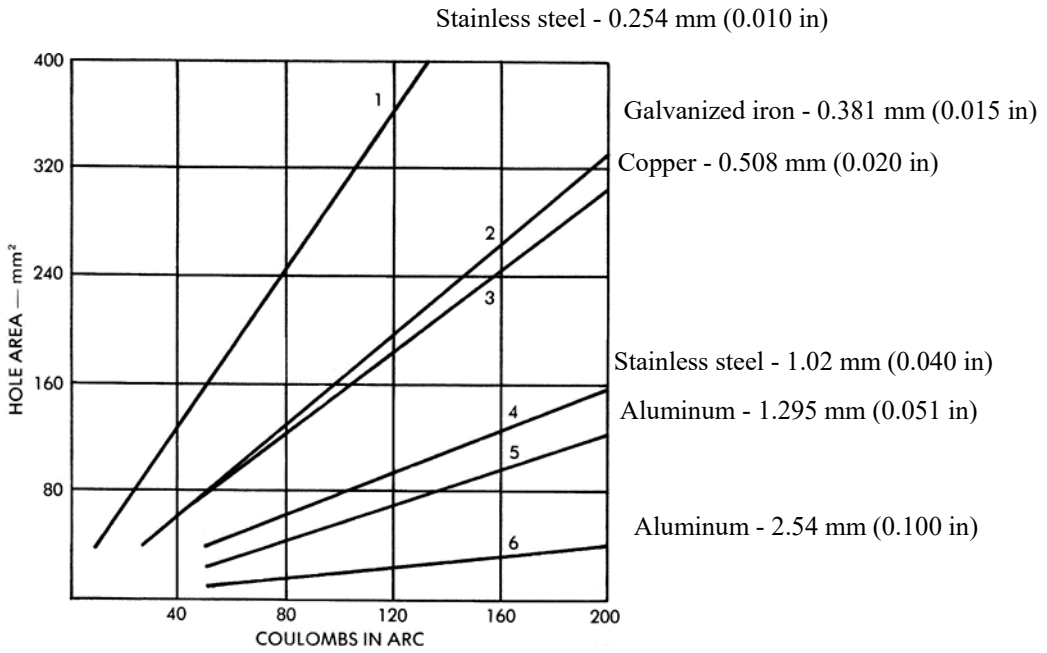

Fig. 6.2 Sizes of holes melted in metal sheets by continuing currents [6.1]

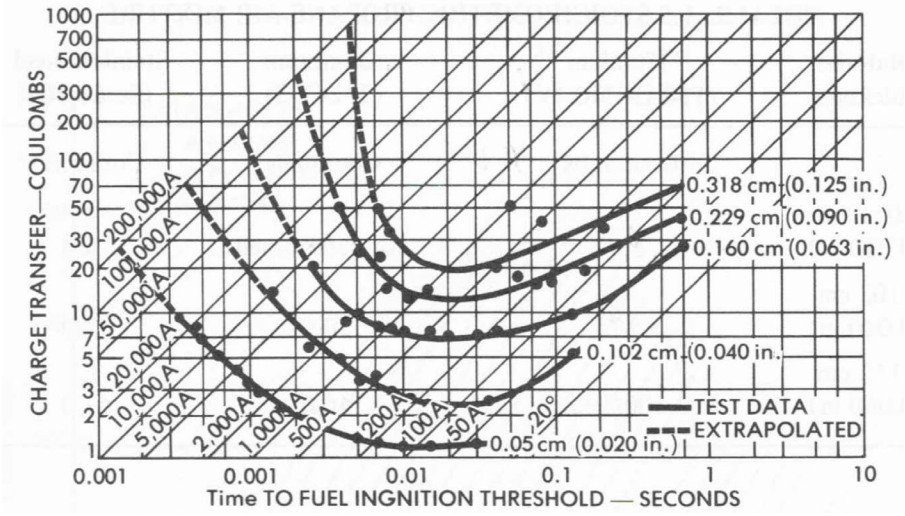

a. Aluminum skins - 2024 T3

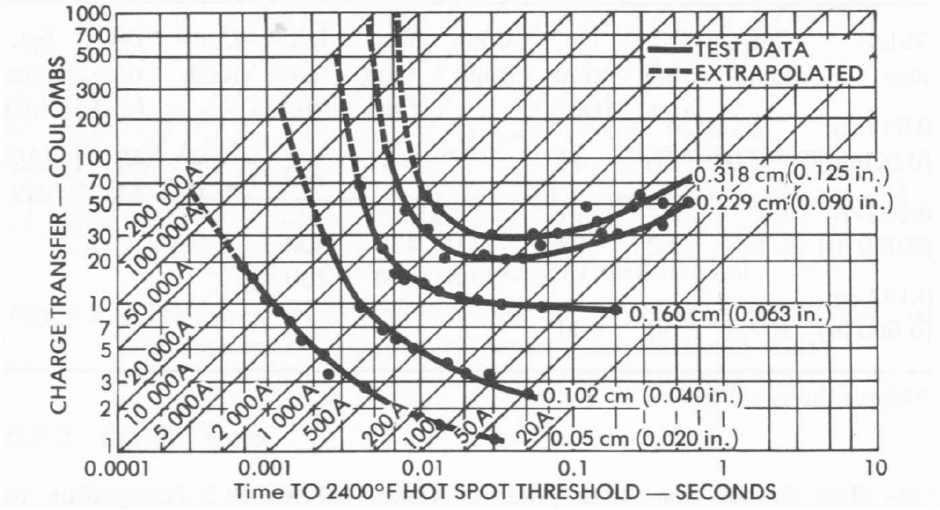

b. Titanium skins

Fig. 6.3 Fuel Vapor Ignition Thresholds for Metal Skins [6.2 - 6.3]

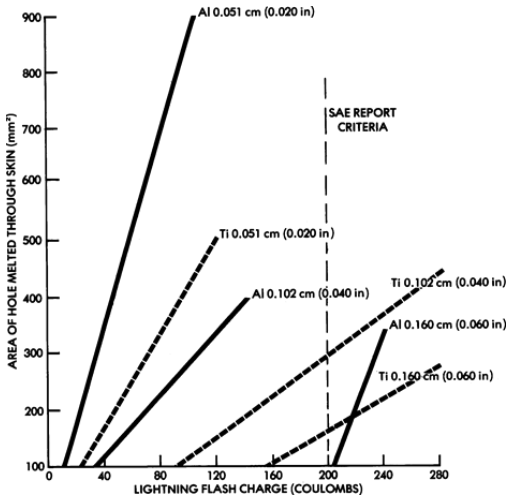

Fig. 6.4 Areas of holes melted through aluminum and titanium skins

Influence of paints

Because the electrical insulating properties of most paints, they tend to make lightning channels remain attached to the surface of the aircraft at one spot by extending the distance that the channel has to stretch before sufficient voltage is developed along the channel from an existing attachment spot to the next one to puncture the paint and establish a subsequent attachment. Also, paint tends to concentrate the electric arc attachment to a small area of metal surface, increasing the thermal effects at that area.

Influence of pressure

All the data on melt-through of metal surfaces discussed above was taken from experiments on test panels in ambient conditions, that is, with equal pressure on both sides of the panels. However, some aircraft surfaces are pressurized, which has been shown to blow melted metal away from a hole and expose interior materials to the hot electric arc. Thus, when metal surfaces are pressurized during melt-through tests, the minimum charge transfer at which a hole appears decreases as compared with an unpressurized surface.

A lightning arc may heat the surface to its melting point, but if there is no pressure, surface tension prevents the molten metal from flowing away and leaving a hole. A very modest amount of pressure, however, suffices to push the molten metal away and leave a hole. Some tests have shown that if a gauge pressure of 34.5 kPa (5 psig) is applied to one side of a 2.3 mm (0.090 in) aluminum skin, holes can be melted in the skin by a 23 C discharge. With no pressure applied, 66 C is required to produce a hole of equivalent size. Skin metals should be tested under pressure if the skin encloses a hazardous substance that may lead to a catastrophic effect.

Trailing edges

The structural integrity of trailing edge closeout members, or other load-bearing parts, may be degraded if a significant portion of metal is melted away from them by lightning arcs hanging-on for prolonged periods of time. For design purposes, the charge transferred under the defined lightning environment should be assumed to be 200 C, in accordance with [6.6]. Figs. 6.2 and 6.4 estimate the amount of metal that would be melted away by 200 C of continuing current charge entering a lightning hang-on point in Zones 1B or 2B.

Protection methods against melted holes

Some of the considerations governing protection of metal surfaces are illustrated in Fig. 6.5.

Protection by increasing skin thickness

The most direct way to prevent melt-through is to provide skins of sufficient thickness to withstand the effects of lightning attachment without complete melt-through. The specific thickness required to achieve this depends on the expected lightning channel dwell time. For most painted metal skins the dwell time will be less than 50 ms.

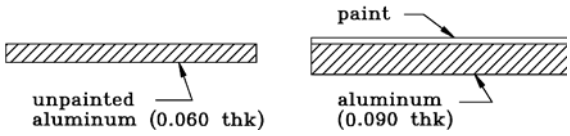

(a) Increasing skin thickness

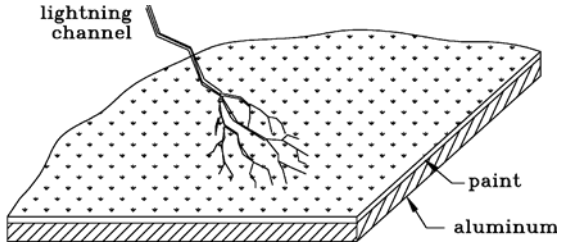

(b) Arc root dispersion

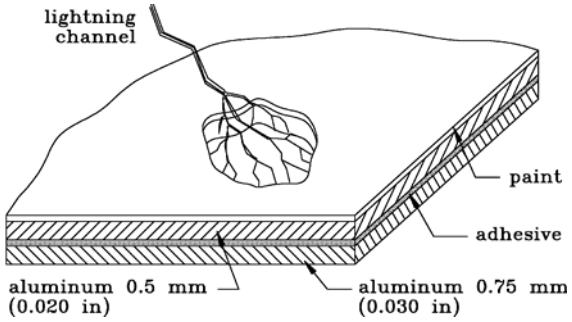

(c) Laminated skins

Fig. 6.5 Methods of protection against melt-through.

For unpainted aluminum skins (polished or anodized) in locations where the dwell times are not expected to exceed 5 ms, only Current Component B needs to be withstood. Based on Fig. 6.3(a), this requires a skin at least 1.5 mm (0.060 in) thick.

For painted skins in Zones 1A, 1C and 2A, channel dwell times should be assumed to be 20 ms for typical paint thicknesses not exceeding 0.25 mm (0.010 in). This requires the skin to be between 2.0 and 3.0 mm (0.080 and 0.120 in) thick. These are the most common criteria for preventing melt-through of aluminum skins.

Protection by arc root dispersion

Arc root dispersion is a protective benefit that arises from the treatment of an exterior surface with an electrically 'bumpy' finish. The bumps create local intensifications of the electric field close to the surface, which cause the arc root to divide into multiple paths, rather than remaining concentrated in one place. Fine wire screens, expanded metal foils (EMFs), and paint primers filled with chopped metal fibers have been effective in laboratory tests. Unfortunately, metal-filled paints require excessive maintenance and, therefore, are not presently in wide use. EMFs are the most common means of achieving arc root dispersion.

If lightning can be divided into multiple current filaments as it enters an aircraft's skin, so that attachments (arc roots) occur at multiple points on the surface of the skin, the energy dissipated where each individual current filament attaches to the skin is reduced by $1/n^2$, where n is the number of current filaments. Thus, the total dissipated energy (and resulting damage) is reduced from what it would have been had all the current entered the surface at a single spot. The action integral associated with each filament of current would be

$$\int I^2 dt(each\ filament) = \frac{\int I^2 dt(total)}{n^2} \qquad (6.1)$$

This implies that the damage to an airplane skin can be minimized using surface treatments that encourage *arc root dispersion.* The $1/n^2$ damage reduction implied by Eq. 6.1 is, of course, only true for damage effects that are proportional to action integral. There are other energy transfer mechanisms associated with electric arc attachment to conductive surfaces that are *not* dependent on (or at least not directly related to) action integral.

Laboratory tests have confirmed that thermal and shock wave damage to metal and carbon fiber composite (CFC) skins is greatly reduced when provisions are made to encourage arc root dispersion.

Protection with multiple layers

A third method for protecting metal skins is to laminate them with a protective layer of thin metal applied with a nonconductive adhesive (most structural adhesives are nonconductive). Laboratory testing has shown that the melting activity is usually limited to the exterior layer of metal, and that the inner layer remains undamaged. This principle is illustrated in Fig. 6.5(c). The outer layer melts away but, as it does so, the arc remains attached to the edges of the hole melted in the outer layer and does not reattach to the exposed inner layer. In effect, the outer layer of metal is sacrificed to protect the inner layer.

For example, an exterior layer of 0.5 mm (0.020 in) aluminum bonded to an inner layer of 0.75 mm (0.030 in) aluminum can withstand the same lightning environment as a single sheet of 2 mm (0.080 in) aluminum. Since melting of holes in metal skins is of so much concern to protection of fuel systems, these studies are covered further in Chapter 7.

6.1.1 Protection against Resistive Heating

As current passes through the resistance of a conductor, it generates heat within the conductor. This is sometimes called *ohmic heating*. Resistive heating of aluminum aircraft skins and structural members by lightning current rarely produces temperatures high enough to be of concern because the lightning current is distributed widely throughout the skins and structures, the current densities are low, and the cross-sectional areas are nearly always more than sufficient to conduct the current without noticeable heating. However, conductors with small cross-sections, such as wiring harnesses and steel control cables, can be damaged by resistive heating if significant amounts of the lightning current flow in them. A particularly important problem arises if a conductor is heated to its melting temperature, because then it can explode, causing very severe damage.

Some of the factors that affect heating and melting of various metals are listed in Table 6.1.

Table 6.1
Typical Physical and Electrical Properties of Common Metals

	Aluminum	**Copper**	**Titanium**	**Stainless Steel (304)**	**Magnesium**	**Silver**
Resistivity, ρ Ω-cm	2.8 x 10^{-6}	1.72 x 10^{-6}	42 x 10^{-6}	72 x 10^{-6}	4.45 x 10^{-6}	1.59 x 10^{-6}
Temperature coefficient of resistance, λ (1/ °C)	0.00429	0.00393	0.0035	0.001	0.0165	0.0041
Thermal coefficient, (1/ °C)	0.254 x 10^{-4}	0.164 x 10^{-4}	0.085 x 10^{-4}	0.120 x 10^{-4}	0.025 x 10^{-4}	0.019 x 10^{-4}
Specific heat, *c* cal/gm· °C	0.215	0.092	0.124	0.120	0.245	0.056
Density, D (g/cm^3)	2.70	8.89	4.51	7.90	1.74	10.49
Melting point (°C)	660	1 084	1 670	1 150	650	962

Calculating temperature rise

The temperature rise in a current-carrying conductor is:

$$\Delta T = \frac{0.2389\rho}{cDA^2}\int i(t)^2 dt \qquad (6.2)$$

where

i = the current through the conductor in amperes

t = time in seconds

c = the specific heat of the conductor in cal/g·°C

D = the density of the conductor in g/cm^3

ρ = the resistivity of the conductor in Ω-cm

A = the cross-sectional area of the conductor in cm^2.

Temperature rise is directly proportional to the action integral (specific energy) of the lightning current and inversely proportional to the square of the cross-sectional area of the conductor. The equation is expressed in terms of unit length. Energy is deposited uniformly along the length of the conductor, producing a uniform temperature rise along its length.

As it stands, however, Eq. 6.2 has two shortcomings:

1. It assumes there is no heat loss from radiation.
2. It assumes that resistance does not change with temperature.

Since little energy can be lost through radiation during the short duration of a lightning stroke current, shortcoming number one has a negligible effect on the accuracy of the predicted temperature rise. Resistance does depend on temperature, however (shortcoming number two). Since resistance also affects the amount of electrical energy that can be deposited in the conductor, it is important to account for this dependency. This can be achieved by expressing resistivity as a function of temperature,

$$\rho = \rho_{20}[1 + \lambda\Delta T] \qquad (6.3)$$

where,

ρ_{20} = resistivity at 20 °C

λ = temperature coefficient of resistivity.

Incorporating Eq. 6.3 into Eq. 6.2 gives:

$$\Delta T = \frac{0.2389\rho_{20}[1+\lambda\Delta T]}{cDA^2}\int i(t)^2 dt \qquad (6.4)$$

Since everything but ΔT in Eq. 6.4 is a constant, the equation can be simplified by combining the conductor dimensions, material properties and specified action integral into a single constant, k, as in the following expression:

$$\Delta T = k[1 + \lambda\Delta T] \qquad (6.5)$$

or, rearranged,

$$\Delta T = k/[1 - k\lambda] \qquad (6.6)$$

Eq. 6.6 shows calculated temperature rises for various metals as functions of the action integral of the current.

Physical and electrical properties needed in Eqs. 6.4 and 6.6 for common structural metals and electrical conductors are provided in Table 6.1. This table also includes the melting points of the metals.

Because of their high amplitudes, the stroke currents have the highest action integrals and will produce higher temperatures, when flowing through resistance, than do the other components of the lightning flash. For design purposes, the action integrals associated with current waveform Components A and D should be used for determining temperature rise in conductors exposed to these currents, depending on the lightning strike zone in which the particular conductor is located. In most cases the lightning stroke currents are shared among many structural elements so temperature rises among primary structural elements are negligible. There are discrete locations, usually on secondary structures or externally-mounted apparatus, where significant portions of lightning currents have to be conducted on their way to primary structures. An example follows.

Example:

The choice of the standardized lightning current component on which to base the protection design for a particular system depends upon the lightning strike zone(s) in which that system resides. Consider, for example, a navigation light that is mounted on a plastic vertical fin cap and 'grounded' to the airframe via two bond straps, as shown in Fig. 6.6. In this example, two parallel conductors are available to share the current, but since the action integral in each conductor will be reduced by the square of the number of conductors, the action integrals in each of the two conductors

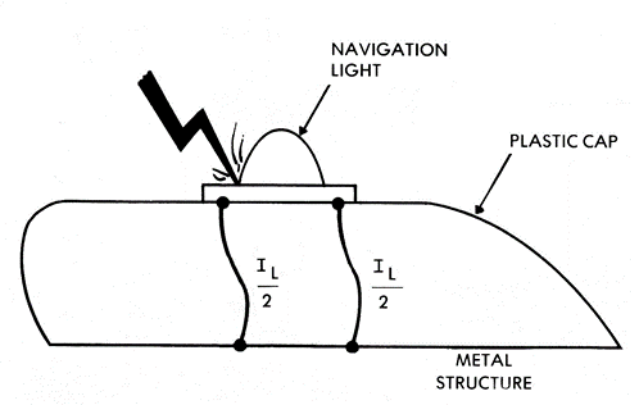

Fig. 6.6 Bond straps for navigation light

will be one fourth of the total action integral of the lightning channel.

If this light is located in Zone 1B, then its pair of bond straps must be able to conduct the total flash current. If it is assumed that the lightning channel will not touch the bond straps, the design criterion for these straps is that, together they must be able to safely carry Components A and D, which have a total action integral of 2.25 x $10^6 A^2s$. Individually, however, each strap only needs to withstand one fourth of that total action integral, or about 0.56 x $10^6 A^2s$ in each strap. This assumes that the lightning stroke current would be shared equally by the two bond straps, a valid assumption if the physical characteristics and lengths of each strap are the same.

If the straps were made of copper wires with cross- sectional areas of 0.1 cm^2 the temperature rise produced by 0.56 x 10^6 A^2s. in each strap would be determined from Eq. 6.6, using the physical and electrical properties for copper given in Table 6.1. Solving first for k,

$$k = \frac{0.2389\ x\ 1.72\ x\ 10^{-6} x\ 0.56\ x\ 10^6}{(0.092\ x\ 8.89\ x\ 0.1^2)} = 28.13°C \qquad (6.7)$$

This would be the temperature rise if the resistivity remained constant, but the resistivity actually increases with temperature. Therefore, Eq. 6.6 must be used as follows to calculate the actual rise:

$$\Delta T = \frac{28.1}{1-0.00393\ x\ 28.1} = 31.6°\ C \qquad (6.8)$$

A conductor with a 0.1cm^2 cross-sectional area is about the same size as an AWG No. 7 wire. Since a 32 °C temperature rise would not damage the wire, Eq. 6.8 shows that two bonding straps or wires of this cross-sectional area would provide adequate protection for this navigation light and its wiring. If one of the wires were to work loose, however, all of the current would have to pass through only one

wire and the action integral would be 2.25 x 10^6 A^2s. This would produce a temperature rise of over 200 ˚C.

It is most important to consider resistive temperature rise in cases where all, or a large fraction, of the lightning stroke current will be carried in a single conductor. Examples include radome diverter bars, bonding straps (or jumpers), conduits or cable shields, ground wires passing through plastic radomes or wing tips, and certain hydraulic or control lines that might be exposed to lightning strike currents.

Temperature rises calculated as described above must be added to the initial, ambient temperature of the conductor to determine the final temperature. If Eqs. 6.5 – 6.8 are used to calculate final temperatures higher than several hundred ˚C, errors will accrue due to certain physical property changes at higher temperatures not considered by this equation. As a 'rule of thumb', it is best to optimize conductor specifications to limit temperature rises to 40 ˚C. This minimizes distortion, elongation, and changes in temper.

Fig. 6.7 presents computed temperature rises for conductors made of the metals described in Table 6.1, due to lightning stroke currents whose action integrals are those of stroke current Components A and D, as well as the combination of A and D, and a higher action integral of 3 x 10^6 A^2s.

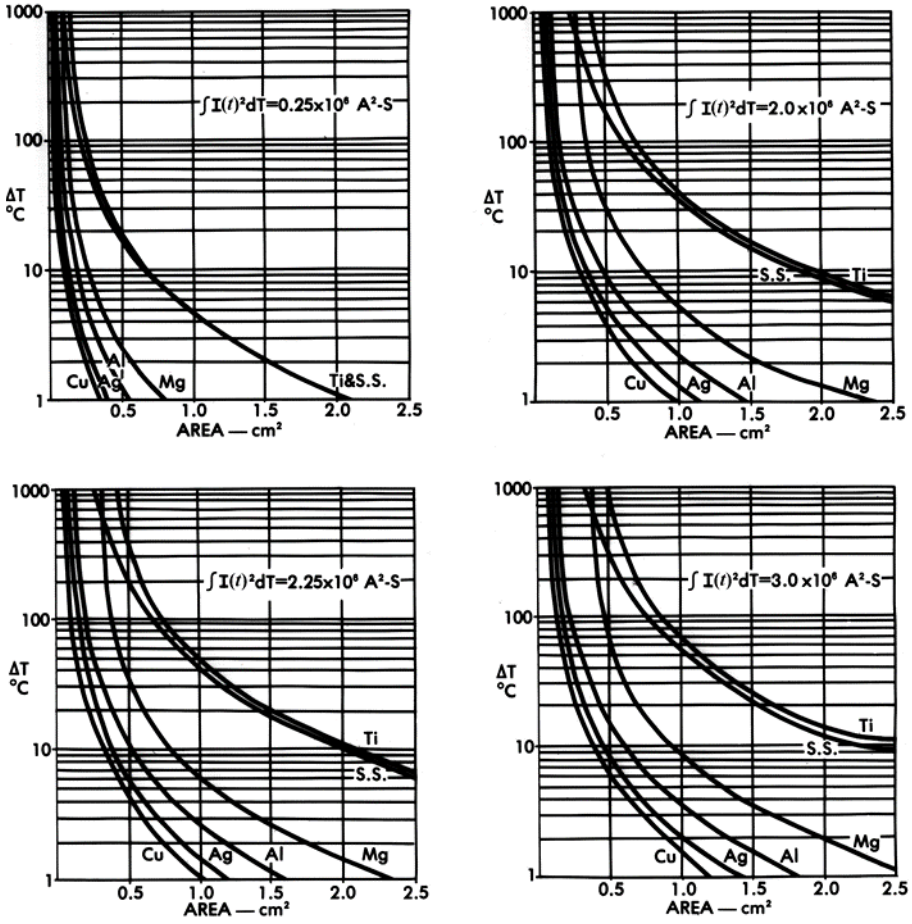

Fig. 6.7 Temperature rises due to stroke currents in conductors

Thermal elongation

Most metals expand when their temperatures rise. This does not pose any problems for conductors such as flexible bond straps that can deflect when expanded, but if conductors expected to carry high currents are held rigidly in place, large thermal stresses may arise and the conductors may buckle, or become dislodged from their mounts. Examples of conductors prone to this type of damage include lightning diverter straps, ground conductors and the pitot probe air-tube shown in Fig. 6.8.

By virtue of its location at the nose of the aircraft, the pitot probe is in Zone 1A and, thus, must be capable of conducting stroke currents of 2 x 10^6 A^2s. to the airframe. The air tubes, if made of metal, would have to have a large enough cross-section to carry the lightning current and withstand the resulting resistive heating, thermal elongation and magnetic force effects of the lightning current. This means they probably would be larger than needed just to transmit pitot air pressures to the flight instruments. It is best, therefore, to make these tubes out of a non-conductive plastic and provide a separate metal conductor to carry lightning current from the probe to the airframe. Based on the computation of Eq. 6.8, an AWG No. 7 or larger copper wire would suffice. A stranded wire would be better than a solid one because it can flex with temperature changes.

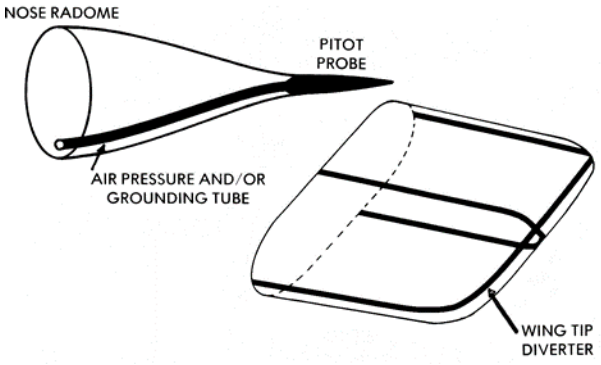

Fig. 6.8 Examples of rigidly held lightning current conductors

Example of thermal elongation calculation

If the air tube in the radome shown in Fig. 6.8 were made of copper, had an outside diameter of 0.476 cm (3/16 in) and a wall thickness of 0.124 cm (0.049 in), its cross-sectional area would be 0.138 cm^2 (0.021 in^2). A stroke current with action integral of 2 x 10^6 A^2s would raise the temperature of a conductor of these dimensions by 67 °C.

The amount of thermal expansion to be expected along any dimension of a part is dependent on the temperature rise and the thermal coefficient of linear expansion of the metal, according to the following relationship:

$$\Delta L = L\alpha\Delta T \qquad (6.9)$$

where α is the coefficient of expansion and L is the length of concern. Of course, all dimensions of a homogeneous material elongate proportionately, and this may affect fittings and clamps. The most significant expansion would probably be along the length of the conductor.

Based on the coefficient of linear expansion for copper given in Table 6.1, 0.164 x 10^{-4} (1/°C), and on the assumption that the tube has a length, L, of 2 meters when 'cold', a 67 °C temperature rise would cause an elongation of

$$\Delta L = 2\ x\ 0.164\ x\ 10^{-4} x\ 67$$
$$= 2.198 \times 10^{-3}\ \text{m} = 2.2\ \text{mm} \qquad (6.10)$$

This amount of expansion may be well within the limits established by normal environmental temperature cycling, but other situations might exist where the thermal expansion caused by lightning current could be a concern. Any conductor that might carry lightning current should be examined to see whether thermal elongation might be a problem.

Exploding wires

Temperature rise is most likely to be excessive in cases where lightning current is carried by only a single, undersized conductor, such as a bond strap or a steel control cable. In such cases, the action integral of the lightning current and the resistance of the conductor may both be high enough to allow enough energy to be deposited in the

conductor to raise the conductor's temperature to the melting or vaporization points. Since the resistance of most metal conductors increases with temperature, an even higher amount of energy is deposited in the conductor as its temperature rises, and this, in turn, increases the temperature even further. If the action integral is high enough, the conductor may melt and perhaps even explode. The explosion of a wire can cause severe damage, since the chemical energy associated with combustion of the vaporized wire is added to the electrical energy produced by passage of the lightning current. An example of damage to a radome that was probably the result of an exploding wire is shown in Fig. 4.13.

If a wire explodes before all of a stroke current charge has been discharged, the balance of the charge continues in the form of an electric arc. If this arc exists in a confined space it can produce even more overpressure (shock wave) than it would were it in an unenclosed space because as the surrounding pressure increases more voltage is required to sustain the arc, meaning that power increases. The overpressure increases as the power dissipated by the arc increases. All of this means that arcs within enclosed spaces may cause more than anticipated damage to surrounding structures. The implication is that care should be taken to prevent enclosed conductors from exploding, and prevent non-metallic skins from being punctured by a lightning strike.

An example of damage from an exploding wire within an enclosure is the explosion of the unprotected, composite wing tip shown in Fig. 4.14. In that example, the navigation light harness was the only conductor available to carry lightning current from the lamp assembly to the airframe. It exploded, destroying the wing tip and deforming the upper and lower surfaces of the wing. This incident could have been prevented by providing an alternate, external path for the lightning current.

6.1.2 Protection against Magnetic Force Effects

When several conductors in parallel carry lightning current each one is acted upon by a magnetic force due to the current in the other conductor(s). The basic situation is illustrated in Fig. 6.9. Based on Ampere's Law, the mutual force per unit length between the wires is

$$\frac{dP_{1,2}}{dl_s} = \frac{\mu I_1 I_2}{D} \qquad (6.11)$$

where

μ = absolute permeability of air (4π x 10^{-7} H/m)

$P_{1,2}$ = force on conductors per unit length (N/m)

D = distance between conductors (m)

$I_{1,2}$ = current in conductors (A)

These forces pull the conductors together when the currents in them are in the same direction and push the conductors apart when the currents are in opposite directions.

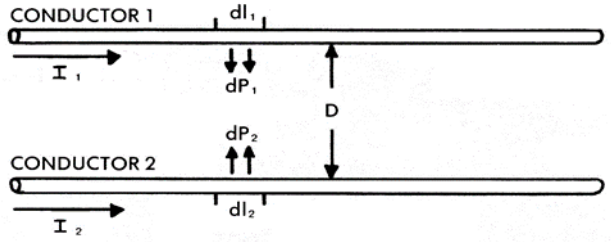

Fig. 6.9 Magnetic forces between parallel current-carrying conductors.

In either case, the magnetic forces are strongest where the conductors are closest together. An example of this situation on an airplane might be found in a military aircraft radome-mounted pitot system, in which two metal air pressure tubes are provided to convey both static and dynamic air pressure to the flight instruments. If these tubes were mounted 2 cm apart and half of the Zone 1 lightning current (200 kA) were carried in each, the peak magnetic force on each conductor would be, by Eq. 6.11,

$$\frac{dP_{1,2}}{dl_{1,2}} = \frac{2 \times 10^{-7} \times 100 \times 10^{3} \times 100 \times 10^{3}}{2 \times 10^{-2}} \qquad (6.12)$$

$$= 100\,000 \text{ N / m}$$

$$= 6\,854 \text{ lb / ft of length}$$

This peak force, of course, would exist only at the instant when the lightning current was at its peak, but it is sufficient to do extensive damage to arrangements of conductors sharing lightning currents. If all the current is in a single tube, the magnetic force surrounding such a tube can be sufficient to crush the tube. It is usually much easier to determine magnetic force effects by tests of candidate installations than be calculations, and the test results are more likely to be realistic.

The foregoing discussion has assumed that the lightning stroke current as the important parameter. The continuing current phase of a lightning flash does not give rise to a high effective force because I^2, and therefore the peak force, is too low.

Studies of or tests on components likely to be damaged by magnetic forces should be performed with simulated lightning currents having amplitudes and action integrals similar to those of Components A or D, depending on the lightning zone in which the installation is located.

Examples of magnetic force effects

Secondary airframe structures and control surfaces sometimes become badly damaged by magnetic force effects. The wing tip trailing edge shown in Fig. 4.3 is an example. The upper and lower surfaces of this wing were made of 0.71 mm (0.028 in) and 0.80 mm (0.031 in) aluminum, respectively. These are thin metal skins that easily deform. In situations like this it is best to evaluate the effects by lightning test of the control surface, bond straps, or other arrangement of conductors that are exposed to large percentages of lightning stroke currents.

Repulsive forces

The preceding example illustrates a situation in which the magnetic forces are attractive; that is, when the parallel currents are in the same direction. There are situations in which lightning currents through adjacent conductors, or in adjacent legs of the same conductor, are in opposite directions. This produces magnetic forces that act to separate the conductors.

An example would be the force exerted on metal conductors (such as pitot air tubes) mounted along the inside surface of a military aircraft radome wall, when a lightning channel sweeps along the outside surface of the wall (see Fig. 6.10(a)). Such a force can inflict severe damage on the air tubes and radome wall, as the tubes are ripped away from the wall. This problem might be reduced by installing segmented diverters to the outside of the radome. The diverters would allow the flash to reattach more frequently, as illustrated in Fig. 6.10(b), minimizing the length of reverse current flow and resulting magnetic force effects.

Protection designs should be lightning tested to verify their adequacy since magnetic force effects are not readily determined by analysis. The test setup should be arranged to simulate the sweeping action of the lightning channel. This can be done by positioning the high current test electrode parallel to the surface of the radome, as if it were a sweeping channel.

Magnetic forces on bond straps

Another common example of a situation in which lightning currents in opposite directions give rise to repulsive forces is the bent bond strap shown in Fig. 6.11(a). Even if the strap has a cross-sectional area sufficient to conduct the current, if it forms a bend of more than about 45 degrees (Fig. 6.11(b)) it may break if it is subjected to major portions of the stroke current. Whenever possible, such straps should be installed with gentle bends, as shown in Fig. 6.11(a). It is not always possible to install a bond strap with gentle bends, since slack must usually be included in the strap to permit the bonded assemblies to be removed or for access or maintenance. In these situations, alternative means of providing electrical conductivity between assemblies should be considered. Bond straps are most frequently used to provide paths for static charges that accumulate on the aircraft and/or the bonded assembly during flight in precipitation. Frequently, the hinges or fasteners that join assemblies can provide adequate current paths for static charges, and for lightning currents, so that bond straps are not necessary. The reliability of such alternate paths should be confirmed by measurements of electrical continuity through the alternate path.

When lightning stroke currents flow in bond straps, there is often sufficient inductive voltage developed along the bond strap to cause flashover(s) of air gaps or other insulation between the bonded assemblies. When this happens, some of the lightning current flows across these gaps. This is also the case with hinge bearings lubricated with plastic bushings, which do not offer conductivity across the hinge. The bond strap will allow sufficient voltage to be built up across the bushing to cause flashover.

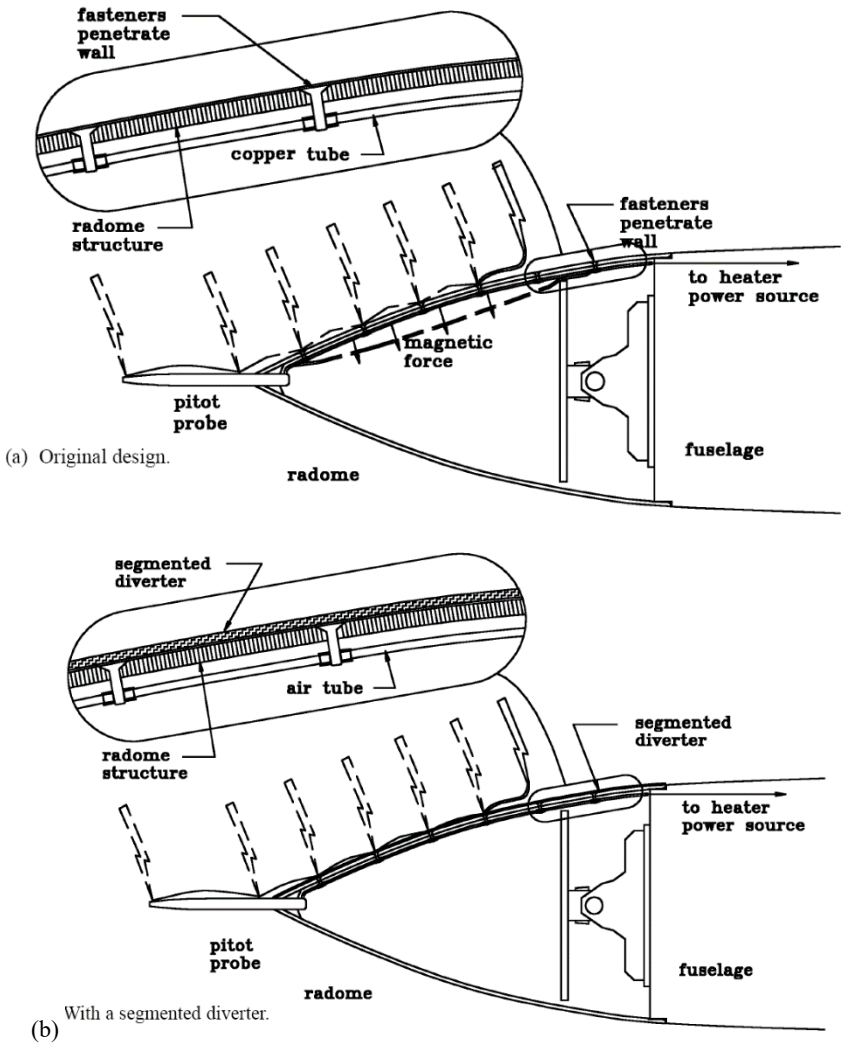

(a) Original design.

(b) With a segmented diverter.

Fig. 6.10 Magnetic forces.

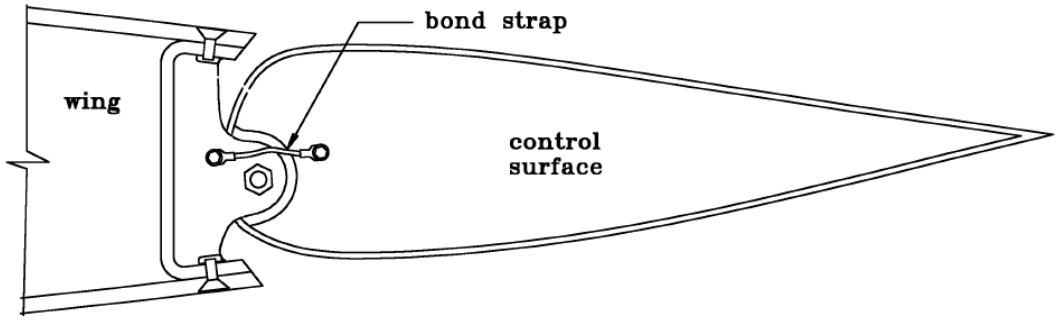

(a) Minimal magnetic forces but impractical for the function

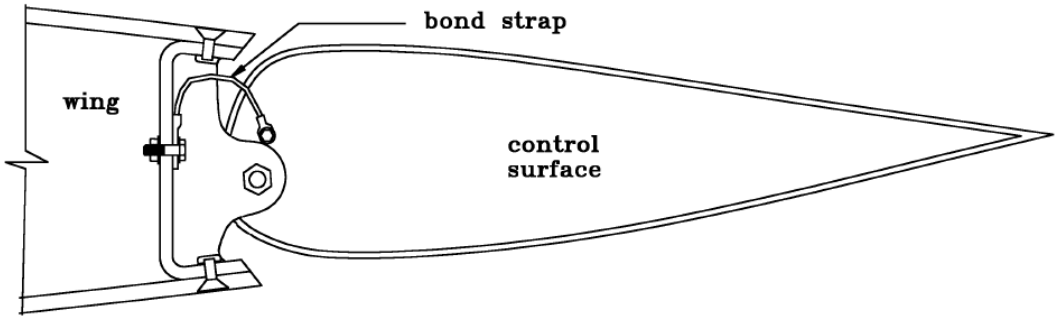

(b) Practical to implement but exposed to magnetic forces

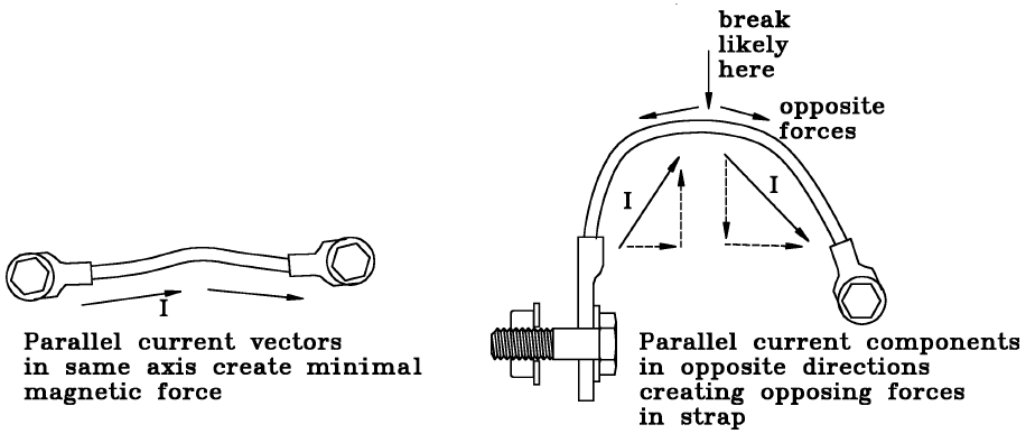

(c) Origin of forces

Fig. 6.11 Example of magnetic forces on a bond strap

Inductive voltages along bond straps can be minimized by keeping bond straps as straight and short as possible. Some other recommendations regarding the design of bond straps intended to carry lightning currents are presented in Fig. 6.12. The basic rules to follow are:

1. Use conductors with sufficient cross-sectional area to carry the intended lightning current action integral without excessive temperature rise (i.e., <40 °C).

2. Keep bond straps as short as possible, consistent with requirements for flexibility and strain relief.

3 Avoid bends of more than 45 degrees, or other features that result in a reversal of the current direction.

4. Avoid all sharp bends.

5. If two or more parallel straps are used, separate them sufficiently (usually by 30 cm or more) to minimize magnetic force effects due to parallel current flow.

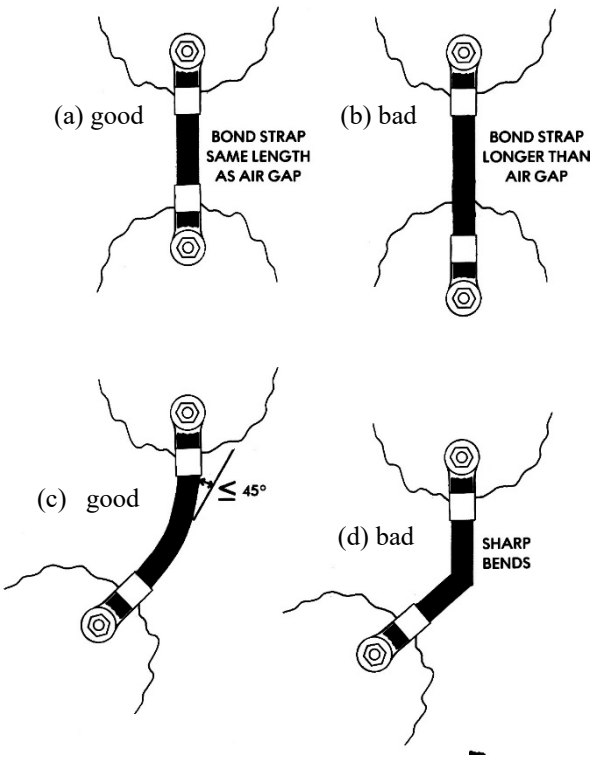

Fig. 6.12 Design of bonding straps ('jumpers').

The rules above should be followed for all light-weight conductors, such as metal air tubes or hydraulic lines that must carry significant portions of the lightning current. Installations should be tested to verify their adequacy.

Consequences of magnetic damage

Because of weight restrictions, the strength and rigidity of some metal components typically found at extremities of an airframe (such as wingtips, flaps, and ailerons) may not be sufficient to resist deformation by magnetic forces from the lightning currents concentrated in these locations. Such deformations do not normally impair safety of flight, but they may require expensive repairs or replacement. Normally, only severe lightning currents cause this deformation. Reinforcement of these components to prevent magnetic deformation must be justified on economic grounds.

Since it often difficult to predict magnetic force effects by mathematical analysis for all but the most elemental geometries, laboratory tests are likely to provide the most straightforward and economical means of determining whether magnetic force effects are likely to damage a particular structure.

6.1.3 Protection against Acoustic Shock

A lightning stroke supplies energy to its channel almost instantaneously, after which a cylindrical pressure wave propagates away from the channel, initially at supersonic speeds. Calculations by Hill [6.7] and summarized by Uman [6.8] (Fig. 6.13 [6.9]) suggest that the initial overpressure produced by a 30 kA stroke is about 30 atmospheres at a radial distance of 1 cm from the channel and 3 atmospheres at a distance of 4 cm. A summary of work on overpressures compiled by Uman and shown in Fig. 6.14, suggests that at distances of a few tens of centimeters, the overpressure might be about 0.05 atmospheres. The subject of pressure waves from high current arcs is discussed in considerable detail by Uman in [6.8], which contains several additional references.

The acoustic pressure wave associated with a return stroke in a channel sweeping across a windshield has been known to crack windshields and, in laboratory tests with simulated lightning arcs, has produced cracks in carbon fiber reinforced plastic (CFRP), also known as CFC up to 6 mm (0.236 in) thick. Whether cracking occurs or not also depends upon the stiffness and degree of reinforcement provided by frames and stiffeners in the airframe structure.

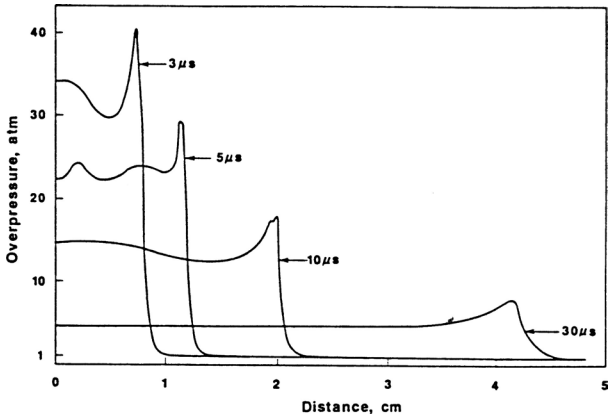

Fig. 6.13 Pressure vs. radius at four times following development of a 30 kA arc [6.7- 6.8]. Double exponential waveshape with $\alpha = 3 \times 10^4\ sec^{-1}$ and $\beta = 3 \times 10^5\ sec^{-1}$.

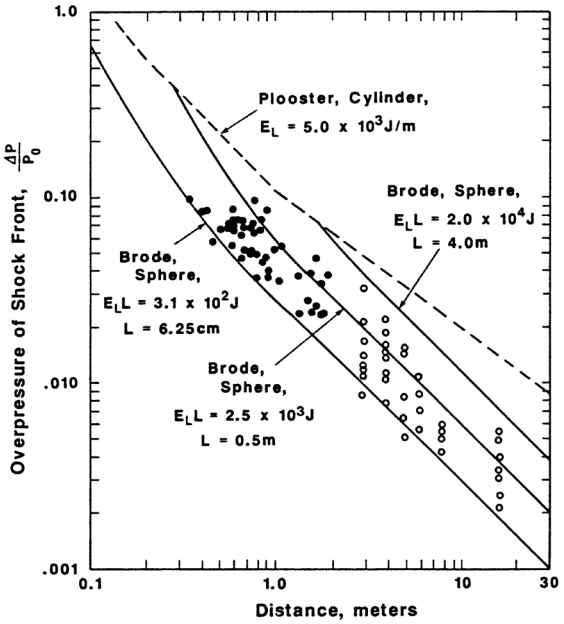

Fig. 6.14 Shock wave overpressure as a function of distance from a 4-m laboratory spark [6.8].

Very stiff structures can be broken by the shock wave since they cannot bend to absorb the shock. More flexible, unreinforced materials can deform without cracking or breaking. The importance of lightning shock wave effects is sometimes overlooked by designers and laboratory test specialists, who fail to account for or adequately evaluate these effects.

Shock Waves in Lightning Testing

One area where acoustic shock waves must be considered is during laboratory testing in which high currents are injected into a test sample from a metal electrode close to the item under test. Gap spacings between the electrode and the test surface are usually limited to between 20 and 50 mm by the voltage limitations of the test generators. An acoustic wave could be partially confined by the electrode as shown in Fig. 6.15(a) and cause unnatural damage to the surface under test. To ensure that this does not happen, the end of the electrode can be encased in a sphere of insulating material, as in Fig. 6.15(b). This forces the origin of the arc on the electrode to be at right angles to the surface under test. Shock waves originating at the electrode are not directed toward the test surface and, since the surface of the insulated electrode nearest the test surface is spherical, shock waves originating at the surface under test are dispersed and not reflected by the electrode.

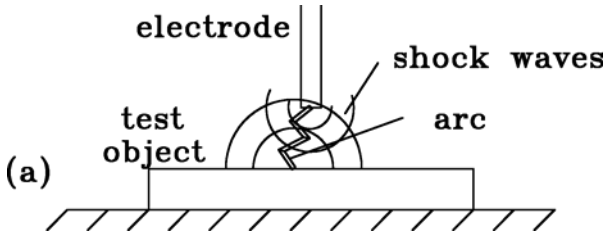

(a) Pressure waves confined by a metal electrode.

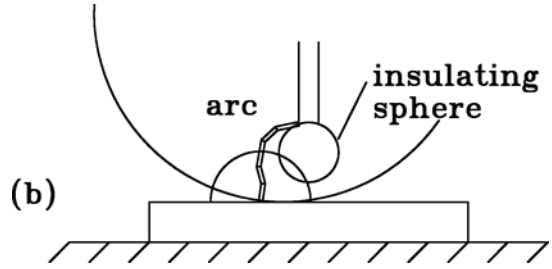

(b) Insulating sphere so arc is not beneath electrode

Fig. 6.15 Shock waves encountered during laboratory testing with high currents.

The electrode arrangement of Fig. 6.15(b) is called an *arc jet diverting electrode* and is in wide use in laboratory testing of aircraft materials and components. This avoids excessive damage that is not typical of lightning effects.

6.1.4 Arcing across Bonds, Hinges, and Joints

Riveted joints

There is some incompatibility between the construction practices best for lightning protection and those best for control of corrosion. Ideally, for lightning protection, joints in metal structures should include some metal-to-metal contact between the surfaces being joined. This requires that parts be joined before paints or sealers are applied. Corrosion control, on the other hand, generally requires that metal surfaces be coated with non-conducting finishes or sealants before the rivets are installed. Usually it also requires that the rivets and the rivet holes be coated or sealed. Joints prepared in this way present an insulative barrier through which lightning current must arc as it passes through the joint. In general, arcing within joints is undesirable because it weakens the joint and may introduce corrosion or other long-term deleterious effects.

In some applications, the insulating films associated with corrosion protective coatings have not resulted in major lightning arcing problems. Often, the insulating films are broken during installation, providing incidental conductive paths. The large number of fasteners required to meet mechanical requirements tends to ensure that many parallel conducting paths are established, thus greatly limiting the arc damage at any one fastener.

However, there are some situations where lightning current through a riveted joint can present some hazards. One is when the space behind the riveted joint contains flammable fluids or flammable vapors. Any possibility of arcing in such a joint should be regarded as a hazard. Fuel tanks are the most common example of this situation on aircraft and, because of the potential hazards, this subject is given special attention in Chapter 7.

Lightning channels frequently attach to individual rivets or fasteners, like those shown in Fig. 6.16. In such cases, the struck fastener may carry a larger portion of the lightning current than its neighbors. If the skin is aluminum, the current in the struck fastener may be only 10% to 30% higher than the current in neighboring fasteners, but if the skin is CFC, the struck fastener experiences significantly more current than the other fasteners in the same row. In this latter case, there is a significant possibility of arcing at the struck fastener. Therefore, nuts or nut plates of fasteners installed in CFC skins usually have to be provided with a sealant barrier or other means to prevent arcing or arc products from contacting fuel vapors if the fasteners are in a fuel tank.

Design guidelines

Most airframe structural interfaces are located in Zone 3 and are therefore expected to conduct some portion of the lightning current when the airplane experiences a lightning strike. Some fasteners are also installed in strike zones where individual fasteners may be struck, so they experience higher currents. Most riveted or fastened interfaces in an airplanes primary structure can be made to tolerate lightning current without significant damage to the fasteners or surrounding holes by ensuring that individual fasteners are not required to carry more than 5 kA of Component A stroke current. Current densities in most aircraft structures meet this guideline automatically because of the large numbers of fasteners used in those structures. In some cases, rivets or fasteners must tolerate stroke currents higher than 5 kA, and this may be verified by test. Of course, current conduction capability depends upon fastener size so the capabilities of specific fastener types and sizes should be evaluated by lightning tests.

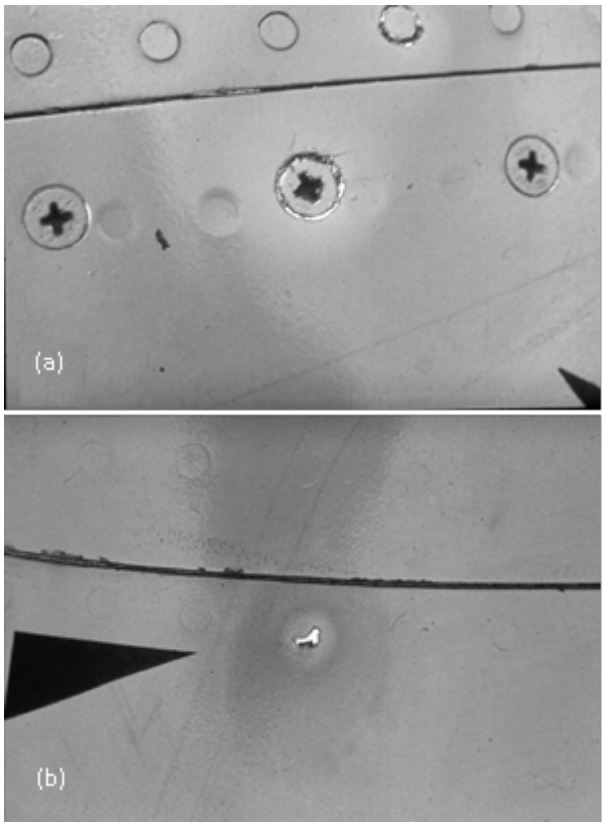

Fig. 6.16 Three fasteners (a) and one rivet (b) after in-flight lightning attachment.

Some structures whose rivets (or fasteners) are more likely to carry excessive lightning current are:

1. Secondary structures, such as flight control surfaces, that are in lightning strike zones, wing tips, and tail cones that are attached to primary structure by small numbers of fasteners.

2. The primary structures of very light aircraft (those of gross weight less than about 1 800 kg (4 000 lbs.) and employing comparatively few fasteners. This includes small, recreational, and utility aircraft.

3. Primary structures that utilize adhesive bonds in place of rivets or fasteners.

Secondary Structures

Fig. 6.17 shows an example of typical lightning damage to a secondary aircraft structure. This figure shows damage to the aluminum vertical stabilizer and cap of a small aircraft caused by an in-flight lightning strike, described by the pilots as "very loud." The aluminum cap was joined to the fin with 16 removable fasteners. The dark soot on the upper end of the rudder is evidence of intense arcing. A combination of arc pressure and magnetic forces deformed the surrounding structure. This kind of damage is typical of what can be expected in a Zone 1B location. The amplitude of the flash is, of course, unknown.

Often secondary structures, such as wing tips, tail cones, wheel well doors and flight control surfaces, do not have enough fasteners to transfer lightning currents without significant damage to the fasteners and surrounding structural material. Sometimes twisting or bending from magnetic forces is added to the damage from arcing at the fasteners. In many cases, this damage does not present a hazard to safety of flight. In the long run, repairing these types of structures after a strike may be less trouble than trying to build protection into them. Some examples of secondary structures on small aircraft where lightning currents might be expected to flow through a small number of fasteners are shown in Fig. 6.18. The lightning safety assessment will show if (and how much) damage may result in a hazard to safe flight, in which cases protection to minimize the damage is necessary.

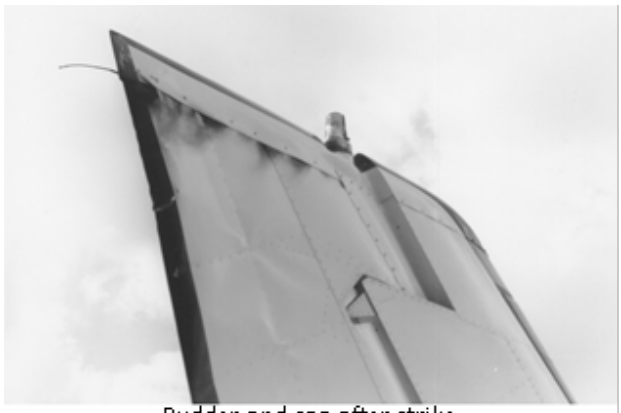

(a) Rudder and cap after strike.

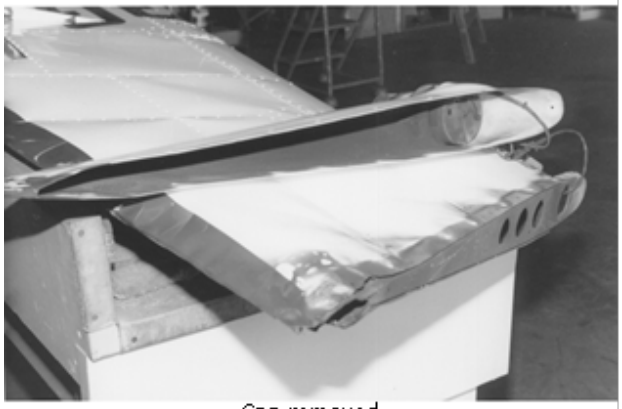

(b) Cap removed.

Fig 6.17 Lightning damage to rudder of a small aircraft

Adhesive bonds

Structural adhesives are being used more commonly in addition to (or instead of) rivets in some aircraft structural joints. These adhesives reduce manufacturing costs and, when used in fuel tanks, are less prone to leaking. Adhesive joints also distribute mechanical loads more uniformly than mechanically fastened joints. Unfortunately, nearly all these adhesives are electrical insulators and, by virtue of their uniform application throughout joints, effectively insulate one part from another. This forces lightning and other electrical currents to spark through the adhesive at random locations within the joints or at the edges of the adhesive bonds.

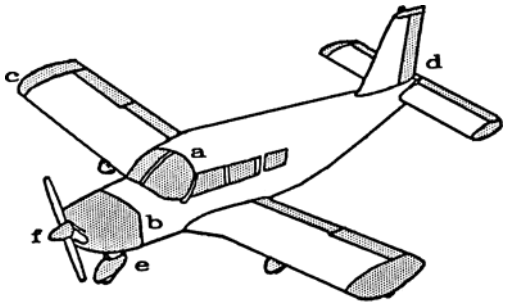

Fig 6.18 Examples of secondary structures and control surfaces where lightning may cause damage.

An example of where arcing may occur is illustrated in Fig. 6.19. This sparking may occur anywhere that the adhesive is in a possible lightning current path, unless alternative paths are available via fasteners, or other means, such as fasteners.

In order to ensure uniform coating, some adhesives are carried by thin fiberglass cloths, rather than being brushed or sprayed on to the joint surfaces. The carrier cloth forces a minimum separation of about 0.1 mm (0.005 in) between the parts, virtually guaranteeing that no electrical contact can exist between the bonded parts. When adhesives are brushed or flowed on, without carriers, the adhesive layer is typically between 0.05 and 0.1 mm (0.002 and 0.004 in) thick. This is still thick enough to act as an insulator, although some incidental surface-to-surface contacts may exist.

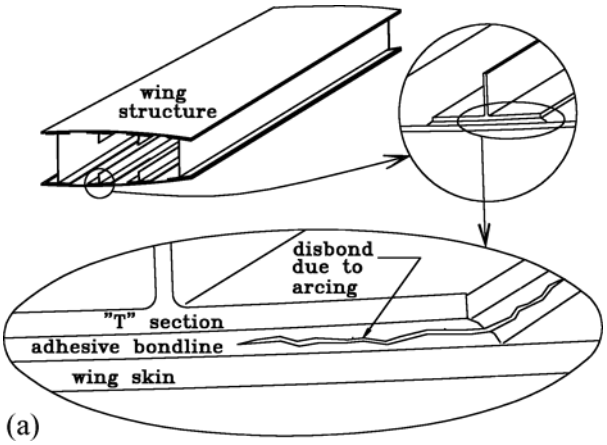

Fig 6.19 Arcing at adhesively bonded joints.

Arcing may occur at these spots, and this arcing may be intense since the current densities in the arcs may be high.

Adhesive bonds that interrupt the main lightning path through an aircraft's structure are of greatest concern because they are almost certain to allow sparking.

Adhesive bonds that fasten internal stiffeners or frames to electrically conductive skins are of less concern (except within fuel tanks) because these bonds do not interrupt the primary current path through the airframe. The intensity of the sparking in these bonds is typically much lower. Fig. 6.19 shows examples of adhesive bonds at structural joints where current paths through rivets are not available.

Hinges and bearings

Hinges or bearings that are located where lightning currents might pass through them (such as at control surfaces in *Zones 1B or 2B*) must be able to safely conduct those currents without impairment of their function, such as by pitting or welding of hinge parts. Otherwise, suitable means must be provided to carry the lightning current around the hinge or bearing. Tests and field experience are the only real guides as to whether the hinge might be excessively damaged.

Problems and considerations regarding the rotating bearings of propulsion systems are discussed in §6.7, but experience indicates that pitting and welding damage to slowly rotating joints is only likely to occur when a hinge or bearing has a single point of contact through which most of the lightning current must pass. In laboratory tests, welding of poorly joined metal surfaces has occurred, but the welding has seldom been so severe that the joint could not be broken apart by hand, or by normal control force. Hinges with multiple points of mechanical contact, such as the piano hinge illustrated in Fig. 6.20, can safely conduct lightning currents with pitting or erosion so minor that they present no real hazard. This is because they provide multiple points of contact.

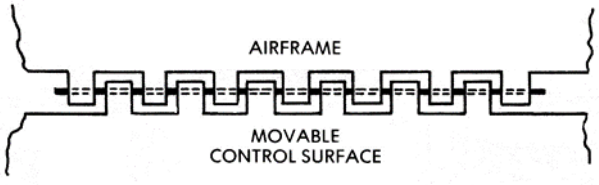

Fig 6.20 Piano type hinge provides multiple conduction paths

The hinges and bearings used for aircraft control surfaces are usually substantial enough that they require no special protection. Lightning current could, conceivably, weld movable parts together, but the weld-points would be small enough that the actuators could easily free the joint.

If tests indicate that excessive damage to a control-surface hinge or bearing might occur, additional conductivity should be provided. The most effective way to achieve this is to provide additional areas of contact in the hinge itself, or else to consider hinges whose design provides more inherent conductivity. Fluid lubricants usually provide adequate electrical conductivity. Even though the lubricant itself is nonconductive, there are usually random points of contact in the bearing.

Bonding jumpers on hinges

Flexible bonding straps or 'jumpers', of the type shown in Fig. 6.11, are often installed across aircraft control-surface hinges. In many cases, these jumpers do not really reduce the hinge current at all. The reason for this is that lightning current from the early portion of a stroke, during which the amplitude is changing rapidly, tends to follow the path of least inductance, rather than the path of least resistance. The paths provided by the jumpers are almost always longer and more inductive than paths directly through the hinges.

This has been demonstrated by Stahmann [6.10], who found that bonding jumpers made little or no difference in the amount of superficial pitting that occurred on typical piano type hinges on control surfaces or landing gear doors, even when the direct current (DC) resistance through the hinge was as high as several ohms. No binding or other adverse consequences were found to result from the pitting that occurred in Stahmann's tests of piano-type hinges and ball joints.

Bond straps across hinges are sometimes required to prevent the electromagnetic interference (EMI) that arises when precipitation static charges must be conducted through hinges with loose or resistive contact. The low currents associated with precipitation static are sometimes unable to follow the interrupted paths afforded by hinges without minute sparking. If bond straps are applied for this purpose, they should be installed according to the guidelines given in Fig. 6.12.

To be sure of the ability of a particular hinge design to safely conduct lightning currents, tests in which simulated lightning currents are conducted through a prototype hinge, should be performed. The test currents applicable for the zone in which the hinge is located should be used. If excessive pitting, binding, or welding occurs, additional conductivity may be needed.

6.1.5 Joint and Bonding Resistance

Electrical bonding (in contrast to adhesive bonding) is the term used to describe the means by which electrical continuity is established between elements of a circuit or between two or more conductive objects. For example, in a lightning protection design for an airplane, bonding can refer to the electrical connections between adjacent structural members, between lightning diverters on a nose radome and the fuselage, or between equipment cable shields and local, structural grounds.

It is a common misconception that adequate bonding between components of a lightning protection system can be determined solely on the basis of the DC resistance of the bond. This misconception may originate, in part, from a now discontinued U.S. military standard, *MIL-B-5087, Bonding, Electrical, and lightning Protection for Aerospace Systems* [6.11], which, essentially, requires that:

The component must carry the lightning current without risk of damaging flight controls, producing sparking, or voltages in excess of 500 volts.

Such a voltage did not present much of a hazard to the electro-mechanical and vacuum tube components in use when *MIL-B-5087B* was formulated. For a 200 kA lightning stroke current conducted through an airframe, the 500 volt criterion essentially implied that the end-to-end resistance not be greater than 2.5 milliohms. What is sometimes read into the specification is that, for lightning purposes, *all* joints must have a resistance of 2.5 milliohms or less. Combined with the term "sparking" in the specification, one can interpret 2.5 milliohms as the DC resistance necessary to prevent sparking. That does not appear to have been the intent of this specification, nor is it correct. No resistance specification, by itself, can assure that arcing or sparking at a joint will not occur.

Whatever may have been the original intent of those who drafted *MIL-B-5087B* (and predecessor versions), the 2.5 milliohm criterion has become so engrained in aircraft-industry design lore as to become an article of faith. In particular, a belief has developed that any joint that has a DC resistance of 2.5 milliohms or less is, by virtue of *MIL-B-5087B*, 'good' and therefore satisfactory for all purposes, including lightning. A corollary to this belief (myth is a better term) is that designers need be concerned *only* with demonstrating that a joint has a resistance of 2.5 milliohms or less. If the bonding for the lightning protection of an airplane were based upon such a simplistic premise, the results could be disastrous.

The ability of a bond to conduct high currents without sparking or burning is really determined by contact materials, shapes and surface areas, treatments of mating surfaces, and contact pressure (as manifested, for example, by torque on a fastener). These happen also to be the factors that influence bond resistance, but there are many conditions that can result in a designated bond resistance, yet not all would conduct current adequately.

A desire to have a bonding resistance number that may be utilized for manufacturing quality control purposes is understandable, but this resistance, whatever it is, should be determined by measuring the DC resistances of joints that have successfully performed the functions required of them. Once established in this manner, the DC resistance may be used, together with visual inspection and tightness criteria, as a quality control standard. Bond straps whose current carrying ability is not sufficient, due to inadequate cross-section or excessive bends can break or explode when exposed to high stroke currents, resulting in excessive overpressure, which, when contained within an enclosure, may cause substantial damage, as illustrated in Figs. 6.21 and 6.22.

Fig 6.21 Result of exploded wire harness through fiberglass wing tip (gone) between navigation lamp and aluminum wing

Fig 6.22 Result of inadequate bonding between navigation lamp and aluminum wing tip

The only way to ascertain that a bond is adequate to safely conduct a required current is to test it with this current. Many joints that have been proven capable of carrying lightning current have demonstrated resistances much lower than 2.5 milliohms, but some joints have produced spark showers even though their DC resistances were less than 2.5 milliohms. Other joints with resistances higher than 2.5 milliohms have also successfully conducted lightning currents. An example is shown in Fig. 6.23. The pipe joint in this photograph had a resistance of 0.53 milliohms, by virtue of the bonding jumper shown, yet a test at 100 kA produced intensive arcing. Currents of less than this amplitude also produced arcing. The inductance of the jumper (i.e., 'bond strap') was too high for the strap to conduct much of the current, so most of it passed through the fasteners, arcing at the various metal-to-metal interfaces in the joint. The adequacy of any joint or fastener configuration for safely carrying lightning current must be determined by laboratory test at current levels representative of the full, specified lightning environment. No DC resistance analysis procedures exist that can reliably predict when arcing will occur at a particular joint or whether the installation of a bond jumper would prevent such arcing.

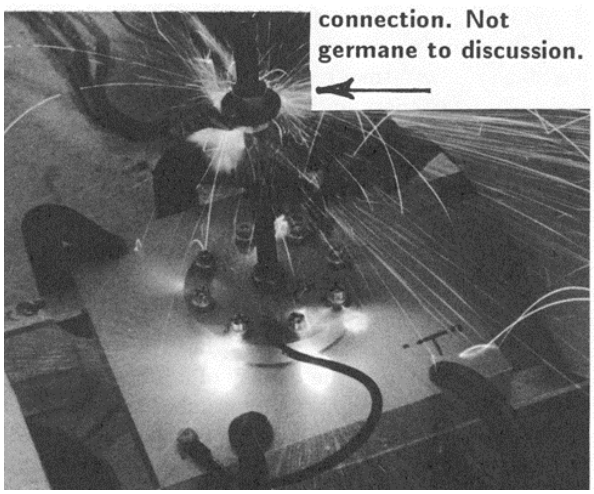

Fig. 6.23 Test of pipe joint with bond strap

6.2 Nonconductive Composites

The basic types of nonconductive material used on aircraft include fiber-reinforced plastics, such as aramid fiber and fiberglass, and non-filled resins, such as polycarbonates and acrylics. Nonconductive composites, such as fiberglass, are used to make many of the secondary structures on airplanes, including radomes, wing and empennage tips, fairings, and fins. These materials are also used as primary structures in small aircraft and as fuselage skins in some helicopters. Polycarbonates, acrylics, and glass are used for

canopies and windshields, where optical transparency is required, as discussed in §6.4. Radomes require special attention because they are, of necessity, made from nonconductive material and cannot be protected by metallizing their exterior surfaces, and because they are typically mounted on extremities of the aircraft where they are likely to become initial lightning attachment locations.

Nonconductive composites come as solid laminates whose fibers can be in one direction, as in unidirectional (UD) plies, or in multiple directions, usually woven, as in bi-directional plies. Ply directions can vary, using notations of 0/90 or +/- 45 degrees to indicate fiber directions. Groups of fibers make up the yarns that are then woven into a fabric.

Laminates are made up of multiple fabric plies of resin-impregnated fibers ranging from two to more than fifty plies. Sometimes these laminates enclose a core made of foam or honeycomb and the whole is cured, usually under vacuum and at elevated temperatures to achieve a strong, stiff structural material. Sometimes the resin is cured at room temperature.

Electrically conductive composites (carbon fiber composites) are addressed in §6.5.

6.2.1 Lightning Effects on Nonconductive Composites

Since electric fields can penetrate surfaces made from nonconductive composites, streamer and junction leader activity may originate from conductive objects beneath the non- conductive skins and may puncture these skins. Thus, lightning flashes may attach to the enclosed metal objects. A puncture by a junction leader usually begins as a tiny pin-hole. If a lightning stroke also passes current through this hole, the hole becomes much larger, often causing significant damage to the surrounding material (see Chapter 4). Radomes are particularly prone to this kind of damage. A photograph of a radome damaged by puncture is shown in Fig. 4.18.

Punctures of nonconductive composites can be prevented by installing conductors or diverters to intercept lightning flashes and divert them to nearby metal structure. Since the design of such conductors requires some understanding of the mechanism of puncture, an overview of that subject follows.

6.2.2 Mechanisms of Damage to Nonconductive Composites

There are two ways in which lightning can interact with a nonconductive composite: by puncture or by surface flashover. The latter is a preferable outcome since it seldom causes significant damage to the structure; only singeing and discoloration of the exterior surface finish. Whether puncture or flashover occurs is governed by the intensity and orientation of the electric field penetrating the composite laminate, and the dielectric strength of this laminate. The basic electrical ionization process is reviewed in Chapter 1. The mechanism of attachment to an aircraft is reviewed in Chapter 3. As noted in those sections, high electric fields produce corona and streamers which propagate outward from the aircraft. Fig. 6.24 illustrates how this process occurs within a nose radome. Whether the streamers from the aircraft are induced by the rapidly changing electric field of an approaching lightning leader or whether they grow in response to a quasistatic electric field is rather academic; the point is that the streamers and leaders do develop.

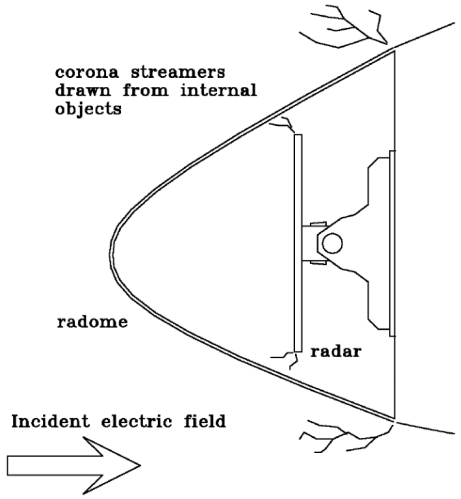

(a) Internal and external streamers.

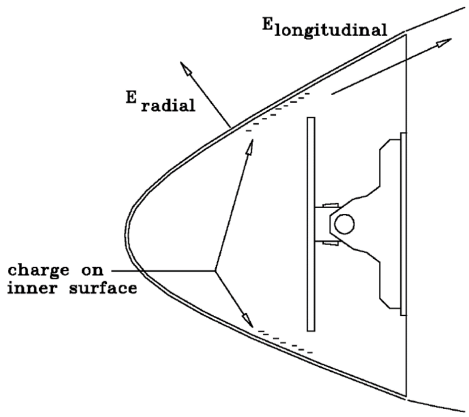

(b) Charges and electric fields produced by internal streamers.

Fig. 6.24 Streamers and charges induced by an incident electric field

Although we refer to these materials as 'nonconductive' actually, electric charge is able to migrate over the surface of a radome, given sufficient time. The surface resistance of the fiberglass typically used to make wing tips and other fairings ranges from 10^{12} to 10^{14} ohms per square, while the anti-static paints often applied to radomes have surface resistances of about 10^6 to 10^7 ohms per square. These resistances are low enough to yield relaxation times of 10 to 100 milliseconds. (Relaxation time is a measure of how long it takes electrical charge to move onto or off of a 'nonconductive' surface.)

This means that, in response to a slowly changing external electric field, charges do migrate from neighboring conductive structures on to the radome. These charges reduce the electric field intensity at conductive object (e.g., a radar antenna) within the radome but increase the field intensity through the radome wall, sometimes resulting in small pinhole punctures.

If the internal electric field becomes high enough, electrical streamers form from metal objects inside the nonconductive structure and propagate outward until they come into contact with the internal surface of the skin. There, they deposit electric charge, as shown in Fig. 6.24. One can imagine that these streamers 'spray' electric charge onto the interior surface of the composite, somewhat as an airbrush would spray paint.

The electric charge on the inner surface produces an electric field (Fig. 6.24(b)) having a component directed longitudinally along the inner surface and another component directed radially, out through the skin.

Because the dielectric constant of the skin is higher than that of the air, the electric field in the composite skin material is lower than the electric field in the air. What happens next involves some complex interactions between the development of the internal and external streamers and the dielectric strength of the composite. There are two possibilities: external flashover, and puncture.

External flashover

One possibility is that external streamers from adjacent metal structure may develop fast enough to suppress the internal streamers. A streamer develops from a metal surface when the electric field at that surface becomes sufficiently high.

As the streamer propagates away from the surface, the field at its tip remains high (which is why it propagates), but the streamer acts like a conductor and tends to reduce the electric field at points behind it, as shown in Fig. 6.25, where the internal field has begun to decline due to external streamer formation.

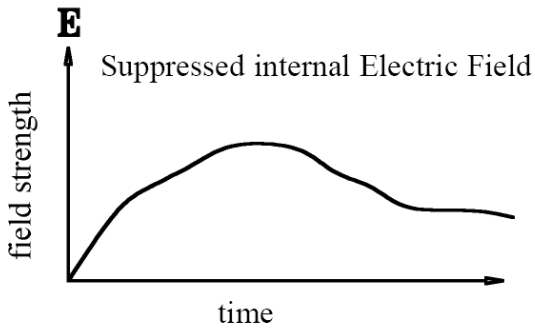

Fig. 6.25 Suppression of electric field by streamers.

This reduction robs internal streamers of the electric field they need to continue propagating. If the longitudinal surface electric field is reduced enough, the other internal streamers will cease to grow and the external streamer that is furthest extended will, so to speak, 'win the race' and provide the path for the lightning flash. A photograph of an external streamer intercepting an approaching leader is shown in Fig. 6.26. This photograph was taken during a laboratory test, in which the source of opposite polarity charge was, of necessity, positioned close to the radome being tested. In a natural lightning strike to an aircraft in flight, the streamer and junction leader that originate from the radome propagate many meters away from the airplane before coming into contact with the approaching lightning leader, or indeed, starting an aircraft-lightning flash (see Chapter 3).

It is impractical to simulate this completely in a laboratory test, but what can be done is to put the opposite polarity charge on a large, flat plate that represents an equipotential plane in the electric field about the radome, and position this plate several meters from the radome to produce an electric field environment that is similar to that which would exist when the airplane is flying in an electric field.

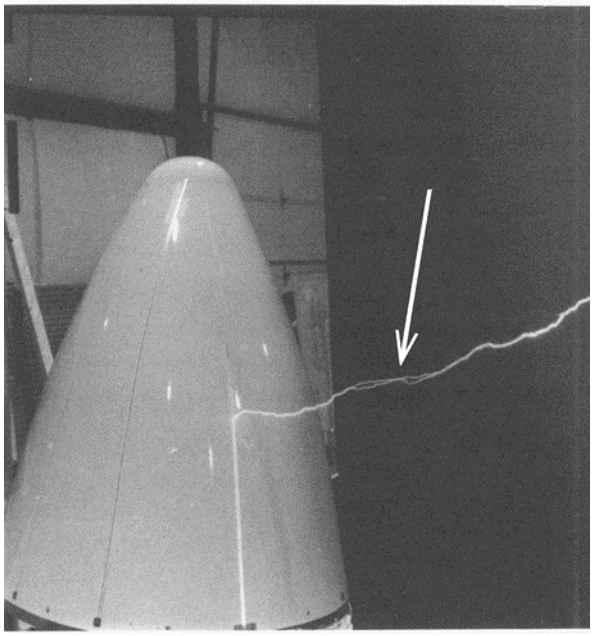

Fig. 6.26 Simulated lightning attachment tests of a nose radome. Arrow points to intersection of approaching and induced streamers

In Fig. 6.26 the junction leader has originated from a fastener at the base of the radome and propagated outward along a segmented diverter and into the air in the direction of the field presented by charge in the leader that has come from an electrode some distance from the radome.

Puncture

The other possibility is that corona may form on the outer surface of the composite and propagate out into the air in the form of an external streamer, as shown in Fig. 6.27. This external streamer deposits a charge on the outer surface of the radome that is of opposite in polarity to the charge being deposited on the interior surface. If these two opposite charge layers continue to build up, the electric field between the layers may become high enough to puncture the composite. Once puncture occurs, a spark is formed and current is free to pass through the composite material.

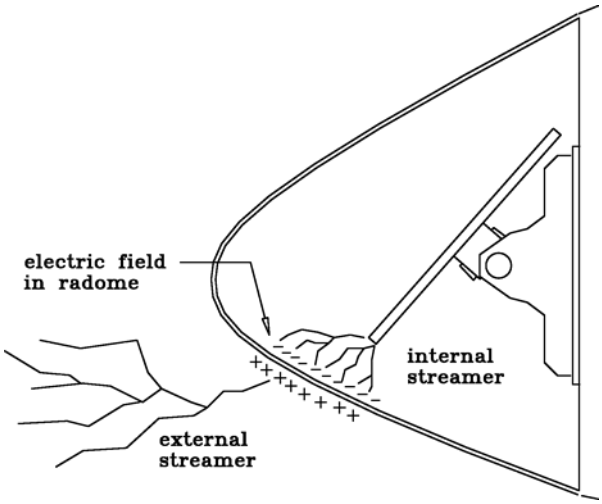

Fig. 6.27 Mechanism of puncture of a radome

If the lightning channel is completed elsewhere, this puncture may only produce a small pinhole in the composite, but if the lightning channel is completed by junction with the external streamer from the composite, the lightning stroke current passes through the skin. The shock wave produced by this sudden, high current is enough to severely damage the composite. A photograph of a radome exhibiting this type of damage is shown in Fig. 4.18.

Composite materials are more susceptible to puncture than homogeneous materials, because composites contain many insulating boundaries among the reinforcing fibers. Electric fields concentrate across these boundaries and ionization can take place within the resin or along the boundaries. Also, some composites may contain microscopic air pockets or voids where ionization may also occur.

The reinforcing honeycomb or foam reinforcing layer also contains air cells which ionize at lower field intensities than do solid dielectrics. The voltage required to puncture a given thickness of fiberglass or aramid fiber reinforced resin composite is much less than that necessary to puncture homogeneous material, such as polycarbonate resin, that is not reinforced by fibers. The measure of the ability of a nonconductive material to resist puncture is its dielectric strength, which is the maximum electric field a given thickness of the material can withstand without puncture. Homogeneous materials, such as acrylic and polycarbonate sheets, have very high dielectric strengths.

Protection of nonconductive composites

Whether or not a structure needs to be protected against lightning depends both on its function and on the consequences of damage. If damage would not create a serious hazard, then protection may not be required. For example, if the loss of a small tail cone or empennage tip would not endanger the aircraft, then these structures could be left unprotected and simply repaired or replaced in the event of a lightning strike. High costs and prolonged down-times associated with the repair or replacement of damaged items can be another reason to require lightning protection for certain items, even if they are not necessary for safe flight. The loss of a nose radome during Instrument Flight Rules (IFR) conditions, however, may not be acceptable, since this might lead to the radar becoming disabled. Also, debris from a broken radome could be ingested into a fuselage or wing-mounted engine, with the potential of damage to the engine, or collide with other more critical parts. For this latter reason especially, nose radomes are usually provided with lightning protection.

There are two basic ways of providing protection for nonconductive composites. One employs solid metal (usually aluminum) or segmented type diverter strips or bars on the exterior surface. These provide preferential places from which streamers and junction leaders may develop, while allowing the rest of the skin to be transparent to electromagnetic waves. (This is the approach used for protecting radomes and some antenna fairings.) The second method is to apply an electrically conductive material over the exterior of the structure. This provides the most effective lightning protection and should be employed whenever possible. It also provides improved protection of enclosed systems against the magnetic and electric fields associated with lightning. Of course, this latter method cannot be used on radomes, which must be radio frequency (RF) transparent.

6.2.3 Protection with Diverters

There are two types of diverters: solid and segmented. If properly applied, either type significantly reduces the number of lightning related punctures (of a radome for example), but they are not 100% effective. Occasional punctures of protected radomes do, nevertheless, occur. Application of diverters will be discussed with particular emphasis on radomes, because that is where they are most commonly used, but the discussion is equally applicable to any insulating structure made from nonconductive composites.

Unprotected radomes are punctured partly because of the low dielectric strength of most radome walls and partly because, to serve its purpose, the radar antenna must protrude beyond any surrounding metal structure. This, in turn, means that the electric field is concentrated around the metal structure of the radar antenna and that electrical streamers can most easily form from this extremity.

Solid diverters

Solid diverters are continuous metal bars placed on the outside of a nonconductive skin to provide preferential streamer and junction-leader origination points. The intention is that streamers that propagate from the diverter will intercept a lightning flash and safely conduct lightning currents to an adjacent, conductive structure. Solid diverters also provide some electrostatic shielding from the external electric field for objects under the skin they are protecting. Thus, they tend to inhibit the growth of streamers from these internal objects. Fig. 6.28 shows solid diverters mounted on the outside of a radome.

Solid diverters should be designed to conduct, without damage, the lightning current of the lightning strike zone in which the part is located, typically 200 kA (2×10^6 A^2s) for diverters on a nose radome in *Zone 1A*. Solid diverters are usually made of aluminum bars with rectangular cross sections large enough to permit conduction of the current without excessive temperature rise. For mechanical reasons, and to prevent the holes for the fasteners holding the diverters in place from unduly reducing the cross-sectional area, most solid diverters have cross-sectional areas of about 0.5 cm^2 (0.08 in^2). Some are larger. A common design is 3.2 mm (0.125 in) thick by 12.7 mm (0.50 in) wide, but thicknesses of up to 6.4 mm (0.25 in) have been used. These diverters are usually attached to the skin with screws, spaced approximately 15 cm (6 in) apart. It is important that the diverters be securely fastened to the skin to prevent them from coming lose, through exposure to rain erosion and lightning magnetic force effects.

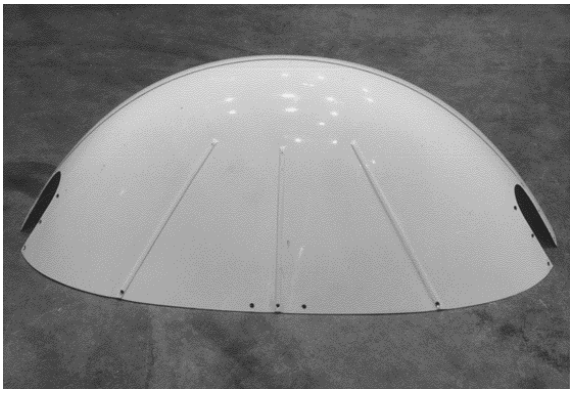

Fig. 6.28 Solid metal diverters on a radome.

In sandwich type skins with foam or honeycomb cores, the mounting fasteners for solid diverters are often surrounded by plastic inserts that prevent moisture from entering the core of the protected composite structure.

If solid diverters are installed on an exterior surface, they may cause some drag. This can be minimized by orienting the bars parallel to the airstream, by shaping the cross section of the bars aerodynamically, or by embedding the diverters into the external surfaces of the skins.

Solid diverters should only be imbedded into a composite skin if their cross-sections are large enough to conduct the lightning stroke current without damage. Otherwise, the mechanical energy associated with the destruction of an imbedded solid diverter strip by lightning could cut the radome in which the strip is imbedded along the entire length of the strip. Other disadvantages of imbedding solid diverters in a composite lay-up include tooling and manufacturing problems and stress concentrations along the grooves that must be provided to accommodate the strip within the lay-up.

Internal diverters

An alternative sometimes considered is to mount solid diverters on the inside surface of a radome with metal fasteners (sometimes called studs) that protrude through the radome wall and serve as lightning attachment points (see Fig. 6.29).

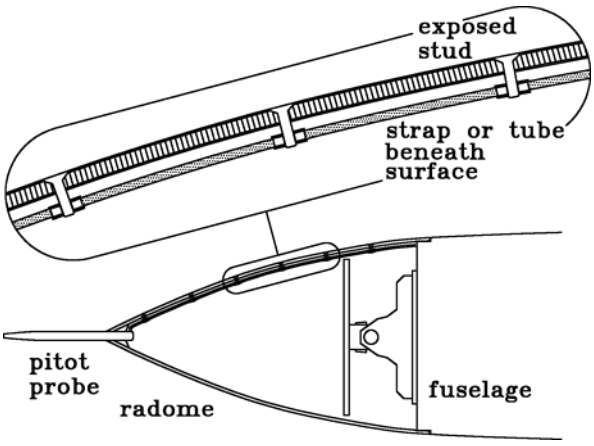

Fig. 6.29 Solid Internal diverter strip with protruding studs.

Although this type of diverter installation may reduce the aerodynamic drag created by external mounting, it does not take advantage of the insulation capability of the dielectric wall, and internal side flashes can result. In addition, magnetic forces due to lightning flashes sweeping from one stud to the next may tear the diverter away from the radome wall. (See §6.2.3)

In general, the thicker the radome wall, the greater the permissible spacing between studs. In many cases, 30 cm (1 ft.) is close enough, but each individual case must be evaluated by lightning strike attachment tests. Appropriate test procedures are discussed in §6.8.

Foil sttrips

Thin foil strips, usually made of aluminum 0.08 to 0.40 mm (0.003 to 0.015 in) thick, have occasionally been used in the past, but these usually provide protection against only one strike because they may melt or vaporize.

When this occurs, the strips leave an ionized channel through which subsequent currents in the same flash can travel, but protection is lost for later strikes (which sometimes may occur during the same flight). Also, the exploding strip may damage the composite material to which it is attached. For these reasons, foil strips are not recommended for certifiable designs and there is no further discussion of them in this text.

Segmented diverters

Solid diverter bars tend to interfere with radar transmission, limiting their usefulness in protecting radomes. To overcome this limitation, segmented diverters (sometimes called 'button strips') were developed [6.12 - 6.15]. These consist of a series of thin, conductive segments, often interconnected by a resistive paint to provide a path for static charges and to prevent sparking between segments due to static charge accumulations on the radome during flight through precipitation. The segments are fastened to a thin, fiberglass strip, which can be cemented to the surface being protected. The only fastener required is the one that connects one end of the diverter to the airframe. Some typical segmented diverters are shown in Fig. 6.30.

Segmented diverters do not provide a metal path to carry lightning current. Instead, they provide many small air gaps that ionize when a high electric field is applied.

Since the small gaps are close together, the resulting ionization is nearly continuous and thus provides a conductive path for lightning leaders and flash currents. The segmented diverters thus guide, rather than conduct, the flash across the protected surface. The structure and ionization process of segmented diverters are shown in Fig. 6.31.

Segmented diverters have been used on many radomes. The field experience indicates that, for most applications, they are almost as effective as solid metal diverters.

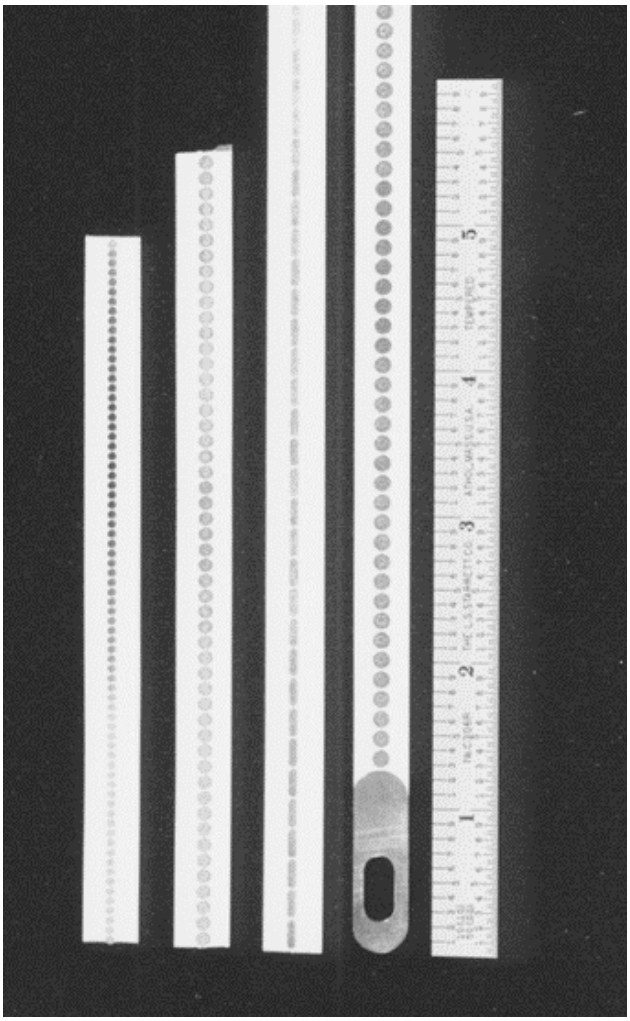

Fig 6.30 Segmented diverters. Scale in inches.

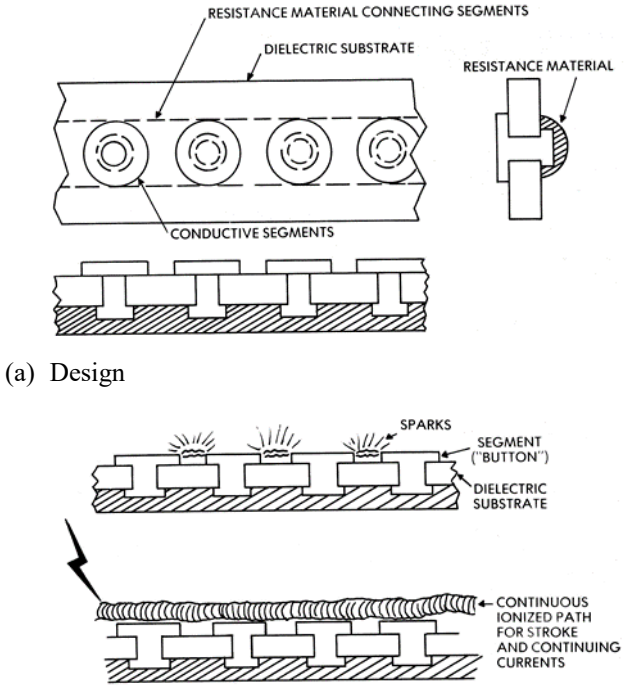

(a) Design

(b) Breakdown and conduction process

Fig 6.31 Design and breakdown process in segmented diverters.

Ionization

In order for segmented diverters to ionize, there must be an electric field tangent to the diverter. This is provided by charge in the approaching lightning leader, or by ambient electric fields that precede an aircraft-initiated strike.

Some segmented diverters have a resistive paint applied along the back surface that connects the segments together through a high resistance that allows static charges to flow away from the segments and prevents sparking among the segments which may radiate.

Effect of internal conductors on segmented diverters

Conductors beneath the surface being protected can affect the performance of segmented diverters. A conductor immediately beneath the diverter may reduce or re-orient the electric field and inhibit ionization of the diverter. Even if the diverter does ionize, the ionization voltage rise along it may be sufficient to puncture the composite wall beneath the diverter and allow the lightning arc to attach to the internal conductor. This can also happen when electrical conductors are placed on or near the inside surface of a radome. Positioning such conductors away from the radome wall may prevent these punctures.

Spacing between segmented diverters

The maximum spacing between segmented diverters, and the minimum permissible spacing to underlying conductors is dependent, among other things, upon the amount of voltage required to ionize the segmented diverter strips.

Ideally, the ionization voltage (electric field strength might be a better term) should be lower than that required to ionize a path along the bare surface of the radome and also much lower than that required to puncture the radome. Laboratory tests have shown the ionization levels of several strip designs to be in the range of 20 to 50 kV per meter. This is much less than the 350 to 500 kV per meter required to ionize the air across an insulating surface.

Breakdown voltages of segmented diverters

The ionization of segmented diverters is a highly nonlinear process, and the total, end-to-end voltage required to produce ionization may change very little with variations in the length of the strip. Ionization probably proceeds from the ends of the strip in a self-propagating manner, similar to the propagation of leaders, discussed in chapters 1 and 2. The performance of segmented diverters has been exhaustively studied. The results of these studies show that strip ionization is completed within one microsecond of the time that it starts and that, once the strip is fully ionized, the individual sparks contact each-other and become one, long spark, which 'lifts off' of the diverter and exists in the air immediately above it. On a moving aircraft, the arc quickly 'peels away' from the position above the segmented diverter, and the lightning current flows directly to the fastener that connects the diverter strip to the airframe.

Laboratory comparisons of various segmented diverter designs by themselves are usually not capable of evaluating the protection effectiveness of a candidate diverter type. Laboratory testing of complete, nonconductive structures (i.e. radomes) with candidate diverter types and arrangements, including simulation of the conducting objects inside the radome, is the best way to evaluate candidate designs.

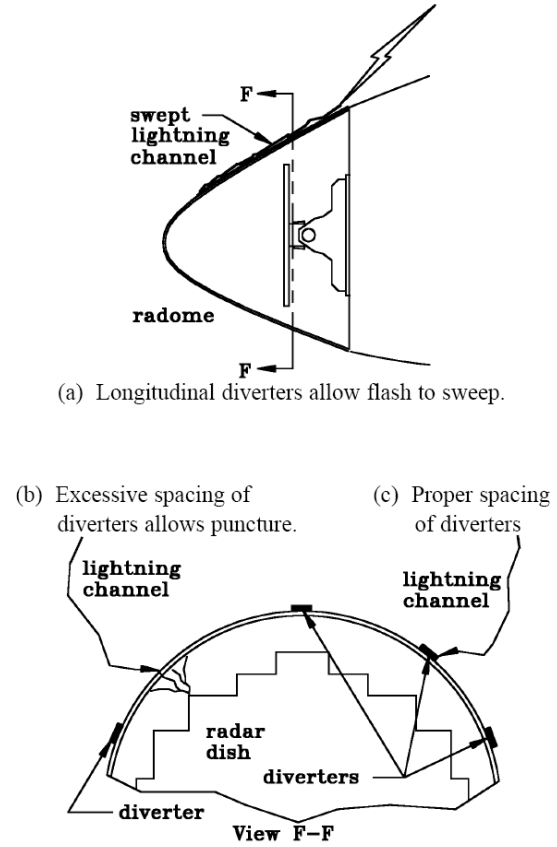

Fig. 6.32 Diverters on a radome.

Application of diverters

Proper application of all types of diverter involves ensuring that there is never enough voltage and time to allow puncture of the nonconductive composite being protected. Even if the diverters have been successfully arranged to prevent punctures by electric fields during the initial lightning attachment process, there is still the possibility that voltage developed along the impedance of the ionized channel alongside a segmented diverter could be sufficient to puncture the composite and allow lightning attachment to conductive objects inside. Diverters should neither be too far from enclosed conductors nor too close to them. Typical diverter spacings on transport airplane radomes range from 30 cm (12 in) to 60 cm (24 in). Other application guidelines are:

1. As much as possible, orient the diverters in the direction of the airstream, along the surface of the radome, as shown in Fig. 6.32(a). This minimizes the possibility of rain erosion damage to the diverters. In addition, this orientation usually coincides with the direction of maximum electric field intensity. It also allows lightning channels to sweep alongside a diverter, rather than across the less well protected surfaces between diverters.

2. Provide an adequate number of diverters and keep the paths they provide to conductive structure as short as possible. This might require some diverters to be oriented perpendicular to the line of flight, especially on large, wide radomes or antenna fairings mounted to fuselage top or bottom surfaces.

3. Use enough diverters to provide lightning strikes from all possible directions with a preferred path to flash across the surface of the skin, rather than puncturing the skin and striking the objects under the skin.

4. The spacing of either type of diverter depends on the dielectric strength of the skin material, the proximity of conducting objects behind the skin, and the length of the diverters. There are no 'cookbook' tables or analytical tools with which to determine the necessary spacing for particular configurations. Spacing of diverters should be decided based on tests of actual radomes or antenna fairings with diverters taped temporarily in place in a 'cut and try' process. Flat panel specimens of the nonconductive composite skin may also be used for spacing tests. If flat panel tests are used, a final verification test should be conducted on a complete radome or fairing. A typical flat panel test setup is shown in Fig. 6.33.

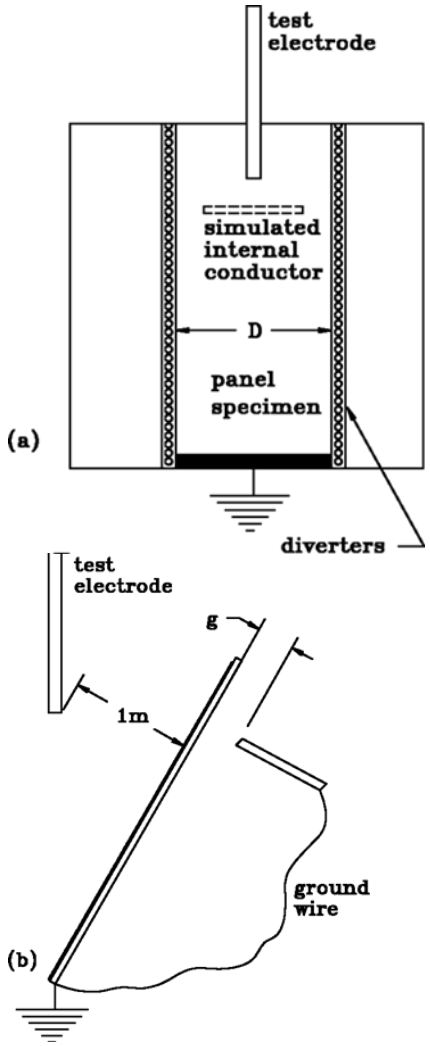

Fig. 6.33 Test of flat panel to determine diverter spacing.

5. Be sure that the current along the diverter does not produce enough voltage rise along the impedance of the metal diverter or the impedance of the electric arc alongside a segmented diverter to puncture the radome wall and allow lightning to attach to internal conductors (see Fig. 6.34). The voltage rise is due primarily to the inductance, *L*, of the diverter or arc, and, may be estimated by assuming *L* to be 1 µH/m for most diverters, and assuming *dI*/*dt* to be 100 000 A/µs (1 x 10^{11} A/s), the peak rate-of-rise of the first and subsequent strokes in the standard lightning environment (*Components A* and *D*). This voltage is a short duration 'spike', which is the time derivative of *Component A* (or *D*).

6. It must be compared with the breakdown voltage (and time) of the composite skin and the air gap between the interior surface of the skin and conductive objects inside. This can be determined by a high voltage test of the skin and air gap combination.

If this is not practical, the design can be verified by a high current test of a typical diverter installation, but this approach is more difficult since it requires producing test currents with the specified rate-of-rise.

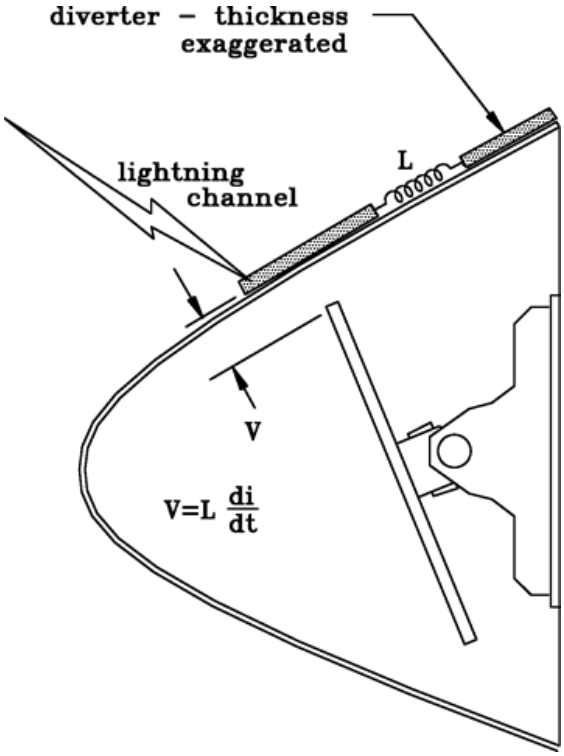

Fig 6.34 Inductive voltage developed along a diverter.

7. Fasten the diverter strips or bars securely to the skin. Solid diverters are mechanically fastened about every 15 cm (6 in). Segmented diverters are adhesively bonded directly to the composite skin.

   At the aft end of either type of diverter, provide a suitable path to carry the lightning current to the conducting airframe structure. This can consist of a single fastener or a fastener and spacer combination, as illustrated in Fig. 6.35. In either case, the arrangement should be capable of conducting currents appropriate for the zone in which the diverters are located.

8. Provide an appropriate finish. This may be a paint on solid diverters, but the individual segments of segmented diverters, and the gaps between them, must not be covered with primers or paints. If covered with paint, these diverters will not ionize and thus will not function.

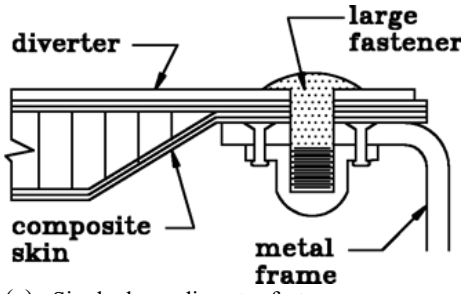

(a) Single, large diameter fastener

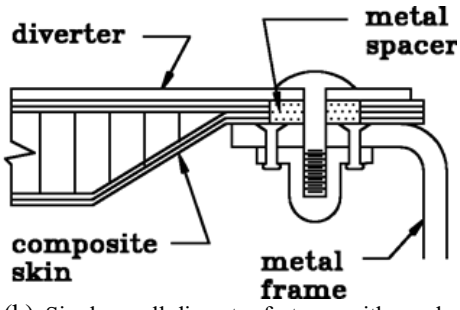

(b) Single small diameter fastener with conductive spacer.

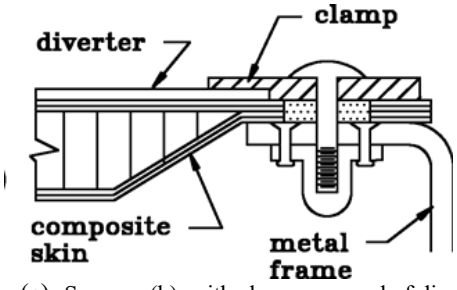

(c) Same as (b), with clamp over end of diverter

Fig. 6.35 Methods of grounding diverters.

9. The ability of a complete diverter arrangement to intercept strikes and prevent puncture should be verified by high voltage-strike attachment tests. The adequacy of mechanical and electrical fastening and grounding designs should be verified by high current tests. Both the high voltage and high current tests should be conducted on full-scale hardware, duplicating that to be used in production. The tests should be conducted in accordance with § 5.1.2 of Reference [6.16].

10. The intent of Guideline 3 is to assure that enough diverters are used to prevent punctures resulting from initial lightning leader attachments. Guideline 4 extends this criterion for protection against swept channels, and Guideline 5 is aimed at preventing punctures resulting from inductive voltages that arise when lightning currents flow in or along the diverter.

Guideline 6 is aimed at assuring that the diverter remains physically attached and adequately bonded to the airframe when it is called upon to conduct or guide high currents.

In applying these guidelines, it is helpful to know the voltage needed to puncture nonconductive, composite skins (i.e., radome walls) or to produce flashover across an external surface. The voltage required to puncture a particular composite skin is determined by material type and thickness, as well as lay-up patterns, sandwich core materials, fillers, and surface finishes. The voltage required to produce a flashover through air averages about 500 kV/m at sea level. It is less than this at flight altitudes, where the outside air pressure is less. Voltages necessary for initiating surface flashovers are usually somewhat less than this, averaging 350 - 400 kV/m. Once initiated, surfaces may flashover large distances without much additional voltage, if the voltage is sustained for a sufficient duration. If the voltage is of short duration, such as the inductive voltage produced by current along a diverter, then the required breakdown stress is higher, perhaps 1 000 kV/m. The influence of gap length and duration of voltage was also discussed in §1.5.3 and §1.6.2. Coordinating spacing between diverters with the dielectric strength of the surface being protected usually requires tests, the principles of which are shown in Figs. 6.33 and 6.36. The test methods are described in § 5.1.3 of Reference [6.16].

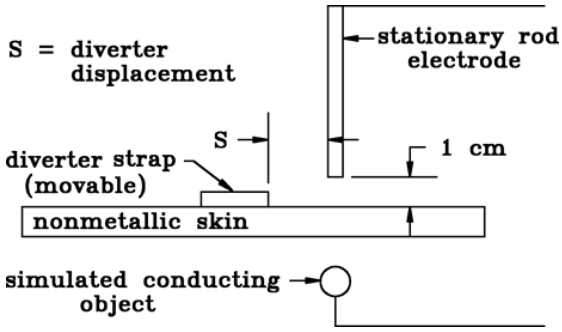

Fig. 6.36 Experimental determination of maximum diverter displacement distance.

6.2.4 Protection with Conductive Coatings

Where electromagnetic transparency is not required, conductive materials can be applied to nonconductive surfaces to conduct lightning currents to the airframe. Materials that can be used for this purpose include arc or flame sprayed metals, woven wire fabrics (WWFs), solid metal foils, EMFs, aluminized fiberglass, nickel plated aramid fiber and metal loaded paints. Some of these systems can also be used to protect conductive CFC materials, as described in §6.4.

Arc or flame sprayed metals

Arc-sprayed and flame-sprayed metals are solid metal coatings applied by spraying molten metal onto the surface to be protected, or into a mold into which the composite skin will be laid up. Their thicknesses range from 0.1 to 0.2 mm (0.004 to 0.008 in) and the metal most commonly used is aluminum. Other metals are occasionally used when galvanic incompatibility is of concern. During application, the molten metal solidifies on the exterior surface of the composite, producing a hard, stiff, and conductive layer that is capable of conducting lightning currents with very little damage, except at the arc attachment spots, where small amounts of the metal are usually melted away. The sprayed metal can be painted with traditional surface primers and paints, but the paint intensifies damage at strike attachment points. Arc or flame sprayed metal coatings applied to existing surfaces have a somewhat rough finish that may require smoothing. This can be overcome by spraying the metal into the mold, before the composite plies are laid in and the part is cured. This produces a metal finish that is smooth from the start.

The advantages of the arc or flame-sprayed metals include good protection for all lightning strike zones and the ability to cover complex shapes that may be difficult to cover with wire fabrics or EMFs. Their disadvantages include cost, weight, and difficulty getting the sprayed metal to release readily from the mold. A significant disadvantage is the tendency for the arc sprayed coating to crack if the underlying skin flexes, which is likely on many places around an airplane. For this reason, this approach has not been frequently used. The weight of the sprayed aluminum is usually in the range of 250 - 350 g/m^2 (0.05 - 0.06 lbs/ft^2).

Woven wire fabrics (WWFs)

Metal fabrics woven from small diameter wires of aluminum, copper or other metals can provide very effective protection for nonconductive surfaces. Quinlivan, Kuo and Brick [6.17], and King [6.18] investigated WWFs and metal foils primarily as protection for CFC materials, but their findings apply to the protection of nonconductive composites as well. The metal fabrics most commonly applied are woven of aluminum wires spaced 40 to 80 wires per cm (100 or 200 wires per inch). Wire diameters range from 0.05 to 0.1 mm (0.002 to 0.004 in). These fabrics are identical to filter screens commonly used in the chemical and water processing industries. The protection effectiveness comes from the electrical conductivity of the wires, and also from the arc root dispersion that was described in § 6.2.2 due to the fabrics that offer an electrically uneven surface where multiple electric field enhancements cause multiple punctures and arc roots, each of which carry only small fractions of the total lightning current. The result is less physical damage, but a somewhat larger diameter of paint removal and erosion of the fabric as compared with the narrower and deeper damage to painted solid metal surfaces.

WWFs do not drape well over surfaces with compound curvatures, and this is especially true of tightly woven fabrics. They must be cut and lapped to fit. Wire fabrics can readily be co-cured in a composite laminate since the resin can flow between the individual wire strands. WWFs can also be cemented onto a previously manufactured surface, although care should be taken not to let excessive adhesive build up over the fabric.

The advantages of wire fabrics include their ability to co-cure with the composite laminate, very effective protection for all strike zones, flexibility, and light weight (typically 0.15 to 0.2 kg/m^2 (0.03 to 0.04 lbs/ft^2)). WWFs also provide the underlying composite surface with some protection against particle erosion.

A disadvantage of WWFs, as noted above, is the difficulty associated with forming them over com- pound curves. It is sometimes necessary to cut the fabric into gores and lap it to fit.

Solid metal foil

Solid metal foils of 0.025 mm (0.001 in) thickness or greater have sometimes been cemented over nonconductive, composite surfaces to provide a conductive layer. Metal foils have an electrically smoother finish than woven fabrics and EMFs, however. This means that solid metal foils do not encourage arc root dispersion, a beneficial effect that reduces energy densities at individual arc attachments. Also, a substantial amount of foil is usually melted away at lightning attachment points, although the nonconductive composite underneath is not usually damaged. The amount of metal foil melted away by a strike is related to the intensity of the lightning current and to the thickness of the foil, but there are no significant differences between the performances of different types of metals. Most applications of solid metal foils in the past have used aluminum foil.

Manufacturing concerns have limited the use of metal foil for lightning protection purposes. Metal foils, like metal fabrics, do not form smoothly over compound curvatures. To prevent wrinkling, the foils must be cut and spliced, which requires seams that can arc and delaminate,

even at low current levels. In addition, the absence of minute holes in the solid foils, through which resin may flow in the manufacturing process, sometimes makes it difficult to achieve a sufficient adhesive bond between the foil and the composite surface. Un-bonded areas may allow the foil to become delaminated and they also collect moisture, which can cause corrosion.

Because of these difficulties, solid metal foils are rarely used to protect composite materials. They have sometimes been used to protect thin metal skins from melt-through. In such applications, the foils have been adhesively bonded to exterior metal surfaces. When contacted by lightning arcs, the foil melts away and the lightning arc remains attached to the edges of holes melted in the foils. This seems to prevent arc attachment to the underlying metal skin. Usually, these applications have been retrofits to existing aircraft wing skins containing fuel, not part of a new aircraft design. Such retrofits must be tested because flight experience is limited. The use of solid metal foil to prevent melt-through of metal skins is not recommended for new aircraft designs.

Perforated metal foils

Perforated metal foil is fabricated by punching or cutting processes in which metal foil is perforated. The result has the appearance of a screen made from a single piece of metal. They have better conductivity than metal fabrics, which depend upon contacts between individual wires to provide conductivity. Depending upon the shape and frequency of perforations, they have better conformability to complex surfaces than solid metal foil or WWFs.

Expanded metal foils (EMFs)

EMF is fabricated by a milling process in which metal foil is perforated and then stretched. The result has the appearance of a WWF, but it is formed from a single piece of metal, and thus has better conductivity than metal fabrics, which depend on contact between individual wires to provide conductivity.

The protection effectiveness of perforated and EMFs is very good for all lightning strike zones. In most cases, the protection effectiveness of EMFs is better than that afforded by WWFs and flame sprayed metals having comparable weights per unit surface area.

EMFs can be formed more easily over compound curves than WWFs, because they can be stretched somewhat. They can also be bonded to composite laminates in a manner comparable to WWFs. Like WWFs, EMFs promote arc root dispersion. Thus, much less expanded foil is burned away at a strike attachment point than would an equal thickness of solid foil.

Since the 1990s, EMFs have become the popular method for protecting composites, both non-conductive and conductive. Several suppliers have aggressively, and successfully, promoted EMFs for protection of composite skins. The weight of EMF ranges from 100 to 600 g/m^2 (0.02 to 0.12 lb/ft^2).

Aluminum and copper expanded foils are used most commonly. The aluminum is used on fiberglass and aramid fiber reinforced composites. The copper is used on carbon-reinforced composites (see §6.4.4) where the possibility of corrosion prevents the use of aluminum. Aluminum generally provides the best lightning protection per unit weight, although its advantage over copper is not great.

The protective effectiveness of EMFs (and also woven wire meshes) depends significantly on the thickness of exterior surface finishes. The general relationship between protection effectiveness and surface-finish thickness is described by Fig. 6.37.

Aluminized fiberglass

Glass fibers can be coated with aluminum, usually by depositing metal vapor on the surfaces of the glass fibers. The result is a glass fiber fabric with significant electrical conductivity. An individual aluminum-coated glass fiber has a nominal resistance of 2 ohms/cm of length. A virtue of this material is that it can be co-cured with the rest of a fiberglass laminate, although the aluminum-coated fabric does not have the same mechanical properties as the glass-only fabric.

Individual coated glass fibers have been reported to carry 50 A for 1 μs, 5 A for 1 ms and 0.3 ampere continuously. This relatively high current-carrying capability is the result of good thermal coupling between the aluminum and the glass. The glass provides a heat sink, enabling the aluminum-coated fiber to carry twice the current that could be carried by the aluminum by itself.

At the point of lightning strike attachment to a structure made of aluminized fiberglass, some volume of the aluminum is explosively vaporized, the area affected depending on the magnitude of the lightning current and the amount of aluminum on the coated fibers. If the aluminum coated

fiberglass material is covered with fillers or paints, the expanding gases at lightning attachment points are contained and more of their explosive force is directed into the underlying composite skin being protected. The amount of additional damage from this mechanism is related to the thickness of coating, as illustrated in Fig. 6.37.

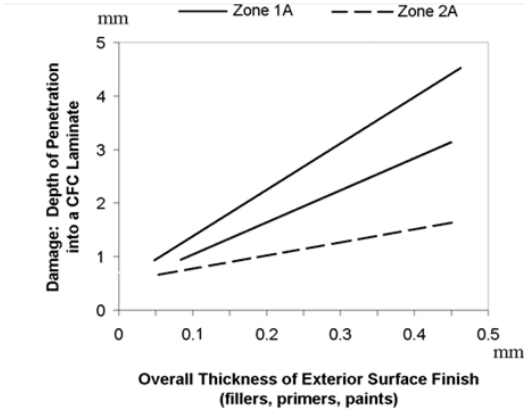

Fig. 6.37 General relationship of depth of damage into a CFC laminate vs. thickness of surface finishes. (The performance of a particular laminate and surface finish must be evaluated by test). Note the range of depths due to Zone 1A currents.

Increased damage caused by confinement of arc products by paint coatings is not only a problem with aluminized fiberglass; it occurs, to some extent, with any painted material. Confinement does, however, seem to promote more extensive damage to aluminized fiberglass than to either WWFs or EMFs.

Metal loaded paints

Adding metal particles, such as copper or aluminum, to a paint provides a surface that has a certain amount of conductivity and has some ability to provide lightning protection. The protection is marginal, however, because the metal particles make only random contact with each other, which gives the coating a much lower conductivity than an equivalent film of pure metal.

No practical thickness of metal loaded paint is sufficient to conduct a full lightning current. Rather, the paint acts primarily to guide a flashover across the coated sur- face. The lightning current is then carried more in the resulting arc than in the coating of conductive paint, in a manner like that associated with segmented diverters.

Conductive paint films are least effective if they are applied on a conductive composite such as CFC, or a metal surface. In these applications, the lightning current usually finds a path directly *through* the paint to the conductive composite. When this happens, the conductive paint behaves similarly to a nonconductive paint, concentrating the lightning arc root and compressing the shock wave forces until the paint is burned away.

Conductive paint has the advantage that it can be applied to an existing surface, even one of complex shape. Copper paints have been the most widely used an early application of copper loaded paint has been for the protection of helicopter rotor blades or fixed wing aircraft propeller blades fabricated of nonconductive composites, however the possibility of particle erosion is a threat to conductive paints and these are no longer used in these blade applications. Metal loaded paints have been less successful on blades with metal spars or embedded de-ice heater wires inside them, because sufficient voltage builds up along the resistance of the conductive paint to force puncture and lightning current attachment to the spar or wires inside the blade. The mechanism of this puncture is illustrated in Fig. 6.38.

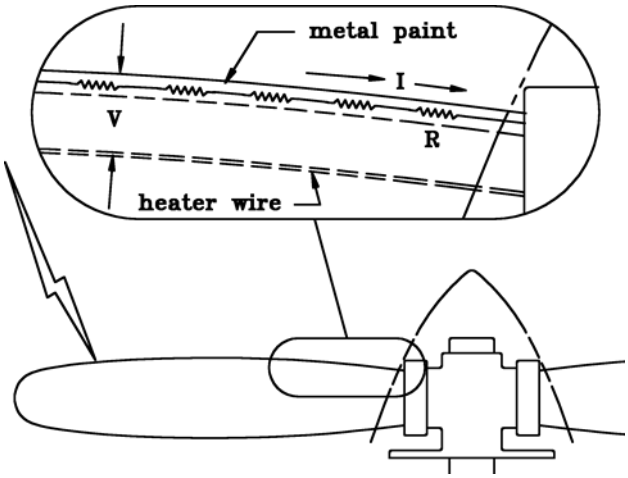

Fig. 6.38 Voltages developed over a metal loaded paint surface due to the resistance of the conductive paint.

Conductive paints are the least desirable of lightning protection methods, partly because of the voltage buildup problem but also because they tend to erode away in many applications when exposed to intense rain or hail. It is usually not possible to get sufficient conductive particles into a paint for it to offer adequate current conduction capabilities without burning away due to current flow.

6.3 Windshields, Canopies and Windows

Cockpit windshields, canopies, and cabin windows are often located in direct and/or swept lightning channel attachment regions (*Zones 1A/1C* or *2A)*. Rupturing of windshields due to lightning strikes has not been frequent; the most frequent effect instead having been shattering of exterior glass plies or deformation of acrylic layers. Windshields that are strong enough to withstand bird strike tests can usually also tolerate lightning strikes. But at least one plane crash in the 1930s has been attributed to a ruptured windshield [6.19]. There are several aspects of windshield and canopy designs that can make them susceptible to damage, and designers should verify that lightning effects will not cause safety of flight hazards. The fact that some new windshield laminate configurations have flown for some number of flight hours without having experienced damage due to lightning is not sufficient justification for them to be certified on the basis of successful flight experience. Certification of windshields should be based on lightning tests, or demonstration of similarities of the candidate windshield design to a previously certified design. Similarity assessments should assure that the shape and contour of new windshields is the same as those of originally certified windshields since these factors, together with construction details influence susceptibilities of windshields to lightning environments.

Electrically-heated windshields

Windows and windshields are fabricated from glass, acrylics, and polycarbonates, or some combination of these materials. All these materials have higher dielectric strengths than nonconductive composites. However, windshield laminates can be punctured by the electric fields associated with lightning channels being swept across the windshield surfaces. These fields terminate on the electrical heating elements embedded in windshield laminates. Sections 5.1.2 and 5.2.2 of Reference [6.16] describe how candidate windshield laminates should be tested to verify ability to resist puncture due to electric fields associated with a sweeping lightning leader, and to tolerate the shock wave associated with a lightning stroke current in a channel that is swept across a windshield surface.

Electrical heating elements embedded within laminated windshields are used to clear icing and fogging. Typical configurations are shown in Fig. 6.39. Heating elements are either fine metal wires or metal films, powered from either 28 volt DC or 115 volt ac systems. Since the wires are of small diameter and arranged in zig-zag patterns, an electric field becomes concentrated at the wires.

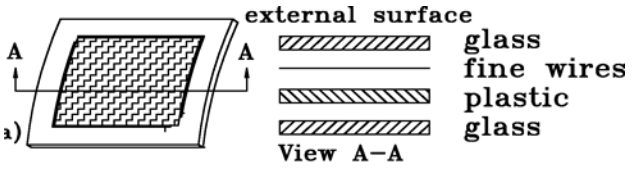

(a) Fine metal wires in a zig-zag pattern

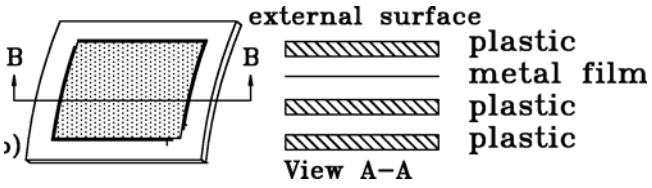

(b)Metal film in acrylic or polycarbonate sandwich.

Fig. 6.39 Electrically-heated windshields.

Other potential hazards that could result from puncture of the outer ply of the windshield are illustrated in Fig. 6.40. The first is the confined shock wave. This is always sufficient to shatter the exterior ply and sometimes sufficient to shatter the inner ply as well. If that happens, particles may be blown directly into the cockpit and into a pilot's face.

Another potential hazard is direct conduction of very high surge currents into the aircraft's electric power distribution system, accompanied by damaging other electrical loads powered from the same source.

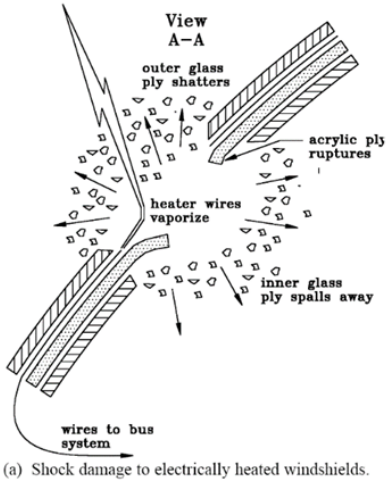

(a) Shock damage to electrically heated windshields.

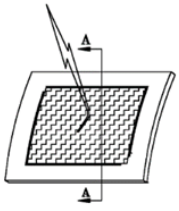

(b) Surge current into power system.

Fig. 6.40 Lightning damage to electrically heated windshields.

Protection methods

One method of eliminating the problems described above is to de-ice the windshield with hot air instead of electrical heating elements. Removing the heating elements eliminates the most frequent cause of windshield puncture and eliminates the conducted surge problem.

The following approaches can be followed to reduce or eliminate the hazards associated with electrical heating elements.

1. Utilize a tough center ply of acrylic or polycarbonate resin. These materials are usually resilient and tolerant of shock wave or impact damage, preventing complete rupture of the windshield.

   Some specifications require that windshield structures be able to survive the impact of a 4 lb. bird at a relative velocity of 200 knots. Such windshields have sometimes been capable of tolerating the effects of *Zone 1A/1C* punctures of their outer ply without rupture of the acrylic ply.

2. Utilize a metal film heating element instead of fine embedded wires. The films are less likely to promote puncture of the outer ply since they offer less electric field stress concentration than do the wires.

3. Employ surge suppression devices on the power distribution circuits or busses that feed electrical windshield de-icing systems.

These devices should be rated to limit surge voltages to the system transient control level (TCL), as defined in Chapter 5, while safely conducting substantial currents to airframe ground. Fig. 6.41 shows options for installation of surge suppressors. Information on surge suppression devices is given in Chapter 17. Metal oxide varistor (MOV) type devices and some Zener diodes have proven capable of conducting up to 10's of kiloamperes of stroke current and should be used for protection of windshield heater power feed and control circuits. These should always be separated from power distribution busses by circuit breakers in case of device failure, which often apply short circuits to ground.

Since the integrity of windshields, canopies and other aircraft windows is usually necessary for continued safe flight, candidate windshield and window designs should be tested. Appropriate lightning test methods are described in §5.1.2 and §5.2.2 of Reference [6.16].

The protection methods described above are applicable to side windows and frontal windshields, although frontal windshields have been most commonly damaged by lightning.

Canopies rarely employ de-icing elements and are most often made from polycarbonate resins, which have very high dielectric strengths. This is also true of side windows.

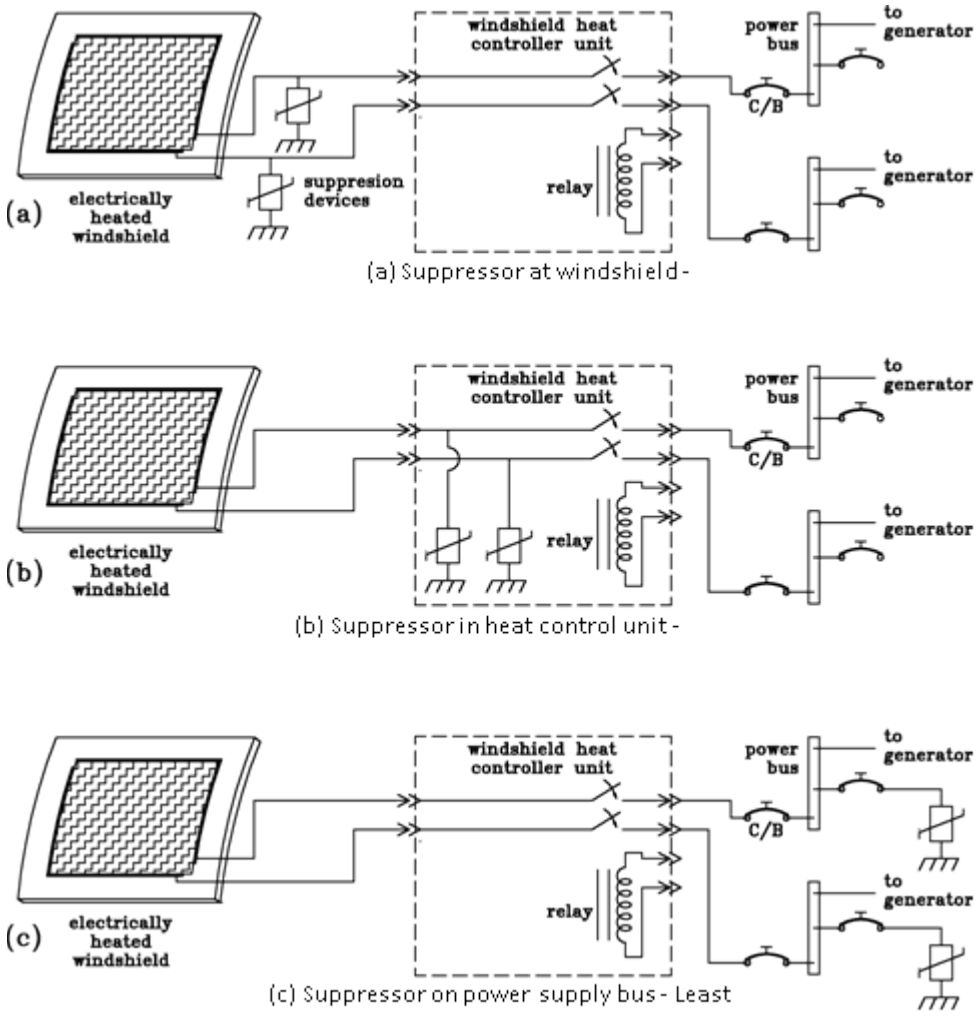

Fig. 6.41 Surge protection of windshield heater circuits.

Sometimes metal films are deposited on the interiors of bubble type canopies to shield the pilot from strong electric fields that would otherwise cause electric shocks. These films have not been known to promote puncture of canopies fabricated of polycarbonate resins. They are not employed on cockpit windows since some shielding against electric fields is already provided by embedded heater elements.

Anti-static coatings

Electrical charges that accumulate on frontal windshields and canopies due to triboelectric charging from ice crystals can be bled away by electrically conductive films. To remain optically transparent, these films must be very thin and, thus, their electrical conductivity is not sufficient to conduct lightning currents. Neither have they appeared to influence lightning susceptibilities of the windshields to which they have been applied.

The most common coating in present use is Indium Tin oxide (ITO), which is preferred for its durability against rain erosion.

Flash blindness

If a lightning strike occurs at night in front of a windshield, the bright flash can temporarily blind a pilot who is looking out the window at the moment when a lightning strike occurs in front of the aircraft. This blindness can make it difficult or impossible for the pilot to read instruments for a minute or two following the flash. Several accidents have been caused by instances of flash blindness that occurred when an aircraft was on a final approach to an airport or in IFR conditions and only one pilot was flying the aircraft.

No windshield treatment has been found that can prevent flash blindness without impairing normal visibility. Thus, when there are two pilots, one of them should focus on the instruments and avoid looking out the windshield during conditions that might lead to a lightning strike. Cockpit instrument lights and display intensities should also be kept at maximum brightness.

6.4 Electrically Conductive Composites

Electrically conductive composites include resins reinforced with various arrangements of carbon fibers or yarns, and other resins reinforced with boron filaments. CFC, also known as graphite-epoxy composites, are by far the most common, due to their high strength to weight property. Some boron composites are in use, but all of these were designed prior to 1980 because the economic and structural advantages of CFC have precluded the use of boron in modern designs. Therefore, the protection designs described in this section deal with CFC.

Damage to carbon fiber composites

- Lightning stroke currents heat carbon yarns sufficiently to melt and vaporize the surrounding resin. This is known as ‘pyrolysis’ of the resin. Stroke currents also produce shock wave damage that can fracture carbon laminates in the vicinity of the stroke cur- rent attachment locations. This happens near strike attachment locations and also in composite structures that are conducting high current densities.

- Lightning intermediate and continuing currents rarely produce significant effects on carbon composites, since these currents tend to move around and re- attach to loose carbon filaments at the edges of areas damaged by stroke current. Otherwise, most carbon composite structures are capable to conducting these current without excessive temperature rises that could melt resins.

6.4.1 Electrical Properties of CFC

While lightning protection of conventional all-metal aircraft is mostly a matter of attention to detail and does not usually have much impact on the cost or weight of the final product, lightning protection for aircraft whose structures consist largely of CFC’s must be integral to the overall design of the aircraft from the very beginning and may have a significant impact on the final cost and weight of the airplane.

The electrical property most important for lightning protection of CFC is its resistivity. This same parameter is also expressed as conductivity. The units are as follows:

Resistivity is commonly represented by the Greek letter ρ (rho). The SI unit of electrical resistivity is the ohmmeter ($\Omega \cdot m$). For example, if a 1 m × 1 m × 1 m solid cube of material has sheet contacts on two opposite faces, and the resistance between these contacts is 1 Ω, then the resistivity of the material is 1 $\Omega \cdot m$. It is a measure of the opposition of the material to electric current flow.

The converse of resistivity is conductivity, the ability of a material to conduct electricity, for which the symbol is the Greek letter σ (sigma), The SI unit of electrical conductivity is siemens per meter (S/m). Numerically, the value of conductivity is the reciprocal of resistivity.

From this point on, the discussion will be about resistivity. The reasons for this selection are that resistivity is directly related to electrical energy dissipation in the material, and in turn, to physical damage inflicted by lightning currents. Also, resistivity is an important parameter in the coupling of lightning energy into aircraft electrical and electronic systems.

Since carbon fiber reinforced composites are not isotropic, the values of resistivity depend on the direction of current flow in the composite. Nearly all any current is in the carbon fibers, so the resistivity is always the lowest in the direction(s) of the fibers.

CFC as used in aircraft construction is usually in the form of multiple flat layers of either UD fibers, or groups of fibers called yarns or tows, always in a single direction, or woven arrangements of yarns or tows that form cloth plies, as in a woven cloth fabric. In these latter configurations, there are fibers in at least two directions. Often, woven plies are arranged in two or more directions, identified by the common notations "0/90" (zero degree and ninety-degree woven ply) and "+45/-45" (actually this is electrically the same as the "0/90" except that the ply is rotated 45 degrees with respect to the "0/90" ply). The reasons for these arrangements are to accommodate mechanical loads, and to improve damage tolerances, especially from impacts of objects (and lightning strikes). Usually, the directions of the fibers in the plies are identified by coordinates x, y, and z as shown in Fig. 6.42.

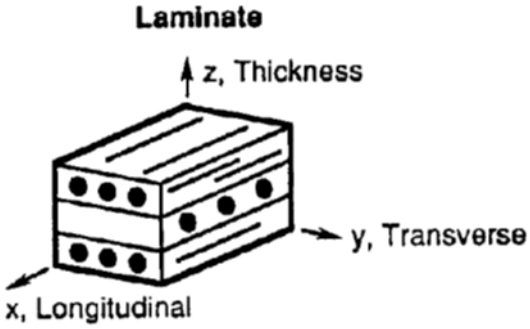

Fig. 6.42 Directions of carbon plies.
(From Composite Material Handbook-17 Rev G)

The resins that surround the carbon fibers are almost always non-electrically conductive. In fact, being mostly polycarbonates, they are good electrical insulators. This means that unless current densities are high enough to produce voltages that can ionize (break down) the resin, the currents remain only in the carbon fibers and the resistivity of the laminate is therefore dependent on the fiber directions.

Resistivity must therefore be measured and expressed in the direction(s) of interest. A CFC laminate that is a combination of many 0/90 and +45/-45 degree woven fabrics is likely to have similar resistivities in all directions within the plane of the plies, usually called the x-y plane. A typical resistivity of such a laminate in the x-y plane is,

$$\rho = 6 \times 10^{-3} \text{ ohm-cm}$$

This is an electrical conductivity of $1/\rho$, or,

$$\sigma = 1.67 \times 10^{3} \text{ siemens per cm}$$

The dimensional unit "cm" is used in these examples because airplane material dimensions are most commonly expressed in small units, and the numbers are more easily visualized in small units.

The reader is cautioned not to confuse the *volume* resistivity with *surface* resistivity. The two are not closely related and the latter parameter is not useful in assessments of lightning effects on CFC structures or enclosed systems.

Neither is volume resistivity to be confused with the actual resistance between any two locations on or within a CFC structure. Resistances across CFC structural components can be determined by the familiar method of conducting an electric current between the locations of interest and measuring the voltage rise between those locations. The resistance is the voltage divided by the current. When the current and voltage are directed between other pairs of locations, it is likely that the computed resistances will differ, since the amounts of carbon fibers extending between these other locations will be different.

In most aircraft applications the resistances of interest will be in the longitudinal directions of the CFC, rather than in the cross-sections. These cross-section resistances are likely to be much higher than the longitudinal resistances since there are usually no carbon fibers in the cross sectional (i.e., "z") direction. Conduction in the z direction depends on there being sufficient voltage among plies to establish conductive paths among plies. Usually this requires breakdown of the resin. If currents among plies become sufficient, the interlaminate arcs that exist between plies develop sufficient temperature and pressure to cause delamination and/or rupture of plies.

If conduction of lightning currents through laminate cross-sections is needed, alternate provisions to allow this, mainly via fasteners, must be provided. The situation just described is shown in Fig. 6.43. For prevention of fastener corrosion there is sometimes a layer of nonconductive primer or sealant around the fasteners. This inhibits conduction of lightning currents except where there are incidental contacts of fasteners with carbon fibers. At higher current densities, such as exist near lightning strike locations, sufficient voltage may exist between fasteners and holes to

cause dielectric breakdown of these nonconductive materials, allowing current transfer to the fasteners via arcing. In situations where there are many fasteners the intensities of this arcing will be minimal, and any physical effects may not be noticed. The higher the current density (i.e., current per fastener) the more noticeable will be the effects of the arcing, to the point where there will be rings of blackened paint around the fastener heads as shown in Fig. 6.44.

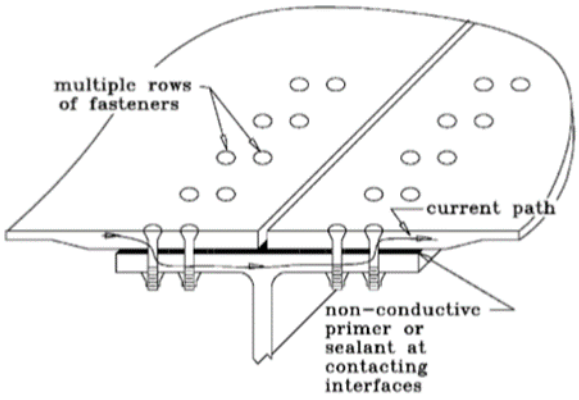

Fig. 6.43 Current conduction via fasteners

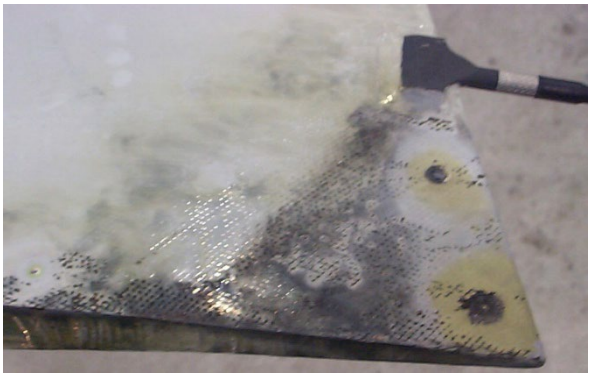

Fig. 6.44 Evidence of arcing around fasteners in CFC

6.4.2 Electrical Properties of Resins and Adhesives

For purposes of considering lightning current behavior throughout CFC laminates, the resins can be considered non-conducting. The structural adhesives used to join CFC and other composites behave in a similar manner. These materials do not follow ohms law and only become electrically conductive when sufficient electric field is applied across their thicknesses to change the electrical properties from those of insulators to breakdowns of their molecular structures in the form of an electrical spark. This is called *dielectric breakdown.*

There have been attempts to provide some electrical conductivity to resins (and adhesives) and thereby allow electric currents to be conducted among carbon fibers and yarns and among plies. However, the structural properties of these resins are degraded and no longer desirable for use in composites. Similar attempts have been made for structural adhesives but without much success. The approach has been to incorporate conductive additives, and these have adversely affected mechanical properties making the composites and the structures that are adhesively bonded together with these conductive products not satisfactory for their intended purposes.

The CFC structural materials are therefore an interesting combination of conductors and insulators, so that users of these materials need to be aware of these properties and design so that lightning and other electric currents can be safely conducted by them or diverter around them so that they are not damaged by these currents.

6.4.3 Damage Mechanisms of CFC

Electric currents and potential differences (voltages) can damage CFC in several ways. These include:

- Ohmic heating and pyrolysis of resins
- Dielectric breakdown of resin among yarns and plies
- Ignition and burning of resins due to lightning arc attachment
- Shock wave effects due to lightning arc attachment

Ohmic heating happens due to the conduction of currents in the carbon fibers resulting in heating of the fibers and surrounding resins. As noted in § 6.5.1 the fibers are resistive and so will get hot as current flows in them. Carbon sublimes at a temperature of about 5 500 °C (9 800 °F) which is far higher than the melting temperatures of most resins (hundreds of degrees) so the filaments used in CFC will remain intact although they become disarrayed when the surrounding resin melts or burns. When this happens, the electrical continuities of filaments may be interrupted, and the original mechanical strength of the CFC laminate will have been degraded or lost altogether. A photograph of a "popsicle stick" laminate after conducting excessive current is shown in Fig. 4.10. The stroke currents, Components A, A_H and D are most likely to cause ohmic heating.

The current densities that result in resin melting are usually higher than is typical for most CFC applications in airplanes that conduct Zone 3 currents of hundreds of A/cm^2 but these high current densities may often be pre-

sent near lightning strike attachment locations, for example on wing tips, winglets, and other Zone 1A/B locations where local current densities are high (kiloamperes/cm^2). Protection features like EMFs can reduce current densities to non-damaging levels.

Dielectric breakdown happens when voltages among yarns and plies are sufficiently high to cause ionization of the resin. This is typically in the range of 16 - 32 kV/mm (400 - 800 V/mil). Dielectric breakdown of CFC resins also will not happen unless the local current density is high, as near a lightning strike entry location. When it does happen, the result is sometimes interlaminar pressure buildup and delamination, depending on the amount of current that is transferred among carbon plies. The most likely opportunity for dielectric breakdown is when there are yarns or tows of carbon filaments conduction different amounts of current in multiple directions. Whether this happens or not usually depends on how laminates are fastened together, and whether or not attention has been paid to making sure that all plies are electrically connected together via fasteners that penetrate complete laminates.

Ignition and burning of resins is due to the high current densities that surround lightning arc attachments to CFC surfaces. An electric arc conducting stroke currents reaches temperatures around 30 000 °C (54 000 °F) which easily melts and ignites resins by heat radiating from the arc and by overheating of the carbon fibers. The result of this leaves the carbon fibers in disarray and sometimes a hole completely through the laminate. The stroke currents, Components A, A_H and D are most likely to cause ohmic heating. Fig. 6.45(a) illustrates effects of ignition and burning of unprotected CFC skins. Due to the low thermal conductivity of CFC carbon fibers and resins the ignition and burning of CFC may only be several plies deep, leaving the remainder of a laminate intact. This was the case in Fig. 6.45(a) where only the shock wave effects, and no melting or burning, are evident on the interior surface of this 4-ply CFC laminate, Fig. 6.45(b). This damage is inflicted at or near points of lightning attachment and is caused primarily by stroke currents. Thus, this type of damage can occur in all zones, with the exception of *Zone 3*.

The extent of the damage depends upon the type and thickness of the CFC skins involved, the thickness of finishes and paints, and the intensity of the lightning strike. Experience has shown that the amount of surface damage produced by a lightning flash is closely related to the action integrals (specific energies) of the current components in the flash.

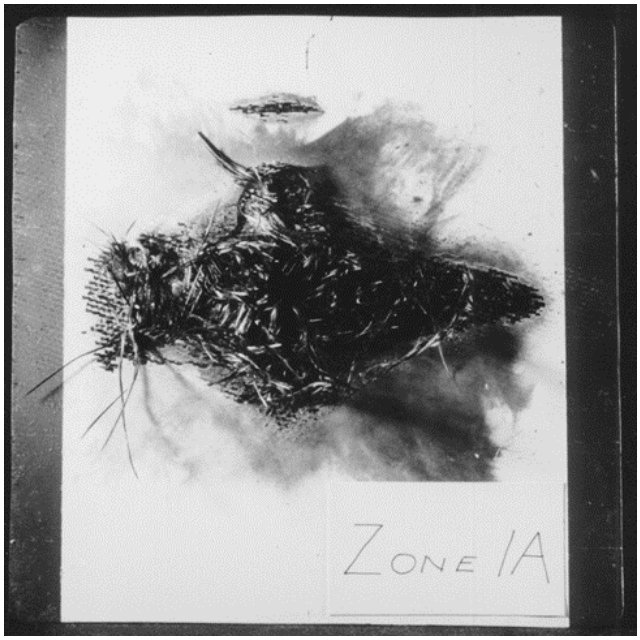

(a) *Front side, showing thermal effects.*

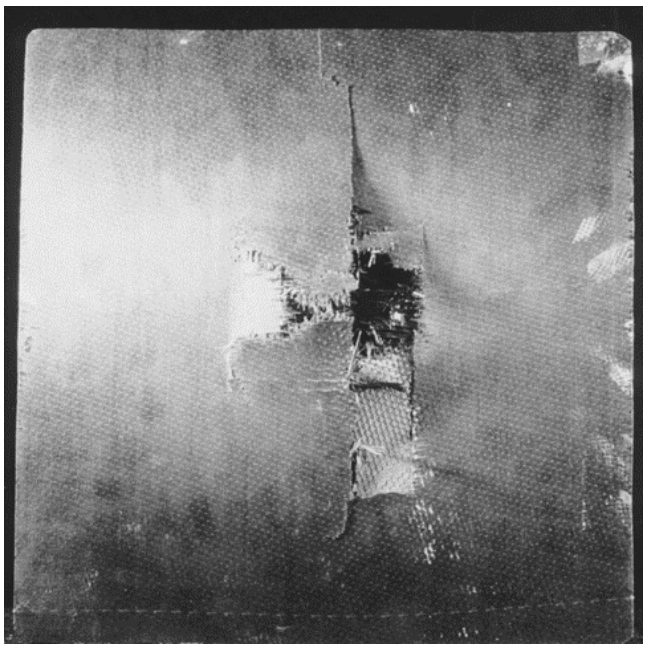

(b) Interior Surface, showing shock wave effects.

Fig. 6.45 Extent of damage to a painted CFC skin.

.

Shock wave effects are due to impact on CFC surfaces of nearby shock waves emanating from lightning arcs that have attached to a nearby CFC surface. Since CFC plies are brittle, and do not sustain localized bending, they are more likely to break, as is illustrated in Fig. 6.45(b).

Shock waves are most intense where all of a stroke current has been injected to a single spot on a painted CFC surface. In contrast, if the surface is not painted (or coated with other resin-rich layers or primers that are electrically insulating and do not readily allow multiple electrical contacts) all or most of a stroke current is concentrated at a single spot (arc root) where both the thermal and shock wave effects are maximized. This was the case in Fig. 6.45.

In addition to the concentration of arc roots, paints and other nonconductive surface finishes have also been found to 'blanket' the shock wave originating at arc attachments and thus apply more pressure to the CFC surface than would exist if no covering were present. For sure the surface finish is quickly blows or burned away by the electric arc, but not before it has had an opportunity to intensify the shock wave impact on the CFC. The extent of shock wave damage has also been closely related to the action integral (specific energy).

6.4.4 Protection of CFC Skins

As described in Chapters 4 and §6.5 there are several ways that lightning strikes can damage CFC skins. Protection approaches should consider each.

Design objectives

Most solid CFC laminates used as aircraft skins have thicknesses ranging from 2 plies (0.5 mm, 0.02 in) to 20 plies (5 mm, 0.20 in). The thinner skins are usually used in sandwich constructions where there are two such skins (face sheets), and thicker laminates are employed as single, solid skins. CFC skins comprised of woven fabrics of any of these thicknesses can usually conduct lightning currents away from lightning attachment points without physical damage, but this should be verified by laboratory lightning current test. Skins that are comprised of UD plies may conduct without damage in the direction of the fibers, but there may be internal arcing if the current must flow in other directions due to lightning attachment locations and overall flow patterns. CFC skins that are not in lightning strike zones 1A, 1B, 1C or 2A and 2B where direct strikes are expected may not need protection against the localized damage from lightning strikes, but these will almost always need to be able to conduct lightning currents. This requires that a means be provided to transfer currents from adjoining structures into and out of the CFC laminates. The most common method has been to use structural fasteners, since these can make electrical contact with all plies in a laminate, and multiple face sheets in sandwich panels.

CFC surfaces in Zone 3 do not normally need lightning protection unless there is a potentially catastrophic consequence of some failure condition that might happen as a result of an unexpected lightning strike to a surface in Zone 3. CFC structures that are in Zone 3 (as most aircraft structures anywhere on the aircraft normally are) do need to be capable of safely conducting Zone 3 lightning currents. This sometimes necessitates that additional electrical conduction capability be added to Zone 3 CFC structures. This can be done by providing alternate conductors within the airplane that are in parallel with the CFC structures.

The protection design objectives for CFC structures therefore as follows:

1. Prevent hazardous damage (i.e. puncture, cracking, loss of mechanical strength) at and near possible strike attachment points in *Zones 1A, 1C, 2A, 1B* and *2B.*

2. Provide adequate lightning current paths among parts, to prevent damage at joints. In CFC fuel tanks, this objective must be accomplished without arcing or sparking, which could ignite fuel vapors. (Design methods for arc and spark suppression are discussed in Chapter 7.)

3. Lightning physical effects protection designs for CFC structures must be coordinated with other electrical requirements, such as EMI control, power system grounding, and lightning induced effects protection design.

Whether protection is required or not depends on the structural purpose of the CFC skin structures, and the consequences of damage. If this damage represents a flight safety hazard, as may occur if a pressure hull is punctured or a control surface is delaminated, protection must be applied to comply with the applicable certification requirements. Otherwise, the decision about whether to apply protection depends on cost-of-ownership aspects. For these cases, a decision may be made not to protect, unless physical damage to the part would give rise to excessive repair and downtime costs.

Some examples of CFC skins that usually do require protection for airworthiness certification, and some that do not, are listed below:

CFC skins and/or structures that may need protection.

- Primary structures including fuselage pressure-hulls, wings, empennage structures.
- Engine nacelles and pylons.
- Flight control surfaces.
- Leading edge devices.
- Actuator housings.
- Fuel tank skins and structures.

CFC skins that may not need protection.

- Tail cones
- Wing and empennage tips
- Winglets
- Wing-body fairings
- Some ventral and dorsal fins
- Some access doors

The nuisance factor and costs of repairs and downtimes associated with lightning damage to some of the non-flight-critical structures listed above sometimes may prompt decisions to protect some of these items and, as will be shown, effective protection can be provided with minimum impact on cost and weight. It may be embarrassing, for example, for airline passengers to see a winglet that is not looking very nice, upon disembarking (or worse yet) embarking for a flight after the unprotected CFC winglet has been struck by lightning.

Methods for protecting CFC skins and application considerations are discussed in the following sections.

The basic protection benefits provided, in varying degrees, by each of the following methods include:

1. Improved electrical conductivity, so that a portion of the lightning current flows in the protective layer and not in the CFC.

2. Arc root dispersion, so that lightning currents enter skins at a multiplicity of points over a wider area, instead of at a single point.

3. Uniform transfer of lightning currents into and out of CFC laminates so that electrical stress and damage at individual fasteners, holes, and plies is minimized.

The following are some of the lightning protection methods that have proven in laboratory testing and in-service experience to be effective.

Woven wire fabrics (WWFs)

WWFs can be used to protect exterior surfaces of CFC skins. One layer of this fabric can be resin-bonded to the exterior of the CFC laminate during the original cure process, so that the metal fabric is in direct contact with the carbon fibers. Plain and satin woven cloth has been the most successful.

The woven cloth of 80 – 200 wires per inch (30 – 80 wires per cm) has been most successfully applied and the wire sizes have been 0.002 – 0.004 inch (0.05 – 0.1 mm) diameter. These wire fabrics are similar to filter screens used in the chemical industry.

The most common metals have been aluminum or copper. Aluminum may corrode when in contact with carbon and copper is three times as heavy as aluminum. In the WWF form (also called "wire mesh") the weights range from 0.025 lb/ft^2 – 0.05 lb/ft^2 (120 gm/m^2 – 240 gm/m^2) depending on the metal, wire size, and density of wires.

To address the corrosion problem of aluminum wires a thin barrier of fiberglass cloth is sometimes incorporated between the metal fabric and the CFC. Wires plated with a corrosion-resistant finish such as enamel have also been used so that the wire fabric may be co-cured together with the carbon laminate, thereby allowing intimate contact between the aluminum wires and the carbon. Copper has also been used instead of aluminum and is preferred by designers of large transport airplanes since it is less likely to corrode in the presence of carbon.

Accelerated salt spray tests have shown that aluminum fabrics cured and encapsulated with resins and coated with paint do not corrode, although corrosion may occur at penetrations, such as window openings, where moisture can get to the edges of protected CFC laminates. Other metals, such as tin, phosphor, bronze, and stainless steel, are more compatible with CFC and are sometimes preferred from a corrosion standpoint, but their lightning protection effectiveness is less than that of aluminum fabrics. Among the various metals, aluminum has shown the best protection effectiveness, although copper mesh of similar wire size and density has also provided adequate protection.

WWFs provide both improved conductivity and arc root dispersion. Protective effectiveness is very good, even on thin (2 - 4 plies) CFC skins. The arc root dispersion effect, illustrated for interwoven wire fabric (IWWF) in Fig. 6.46, is also promoted by WWFs and EMFs because all these

treatments provide a rough, conductive surface that promotes electric field stress concentration and puncture at many points during the strike attachment process. Physical damage at attachment points is normally limited to erosion of a small area of the fabric.

WWFs should be laid up in the skin mold, together with any barrier ply and the CFC. The wire fabric must be the outermost ply of the laminate.

A disadvantage of WWFs is that they are not as easily draped and formed around complex surfaces as are the EMF that are described below. Thus the wire fabrics are used most frequently on two-dimensional (2D) structures like helicopter rotor blades, where the fabrics are most easily utilized.

The WWFs are available with or without pre-impregnated resins so that they can be included together with the carbon plies in molded structures.

Expanded metal foils (EMFs)

EMFs can also be used to protect CFC skins. These have similar appearances to the WWFs but are made by stretching a perforated layer of solid foil to change the perforations into diamond-shaped openings. The have current conduction and protection effectiveness characteristics similar to those of WWFs. They should be co-cured with the CFC laminate, using resin pre-impregnated CFC fabric to bond and encapsulate them. Because the EMFs are all one piece of metal they are somewhat more conductive than are the WWFs.

It will be noticed that the percentages of open areas of the EMFs are significantly greater than the among the open areas of woven wire meshes since a weave leaves little open space whereas the stretching process used in fabricating the EMFs necessarily results in finite open areas where there is no metal. This open space characteristic is the main difference in the lightning protection performance between WWFs and EMFs. The open spaces accentuate the electric field concentration at the nodes between the strands. The idea is illustrated in Fig. 6.46.

Weights and thicknesses of aluminum and copper EMFs are shown in Table 6.4.

Table 6.4 – Ranges of Specifications of Expanded Metal Foils (EMFs)

Material	Weight	Thickness	Open Area
Aluminum	0.01 lb/ft^2	0.002 inch	50%
	(60 g/m^2)	(0.05 mm)	
	to	to	
	0.03 lb/ft^2	0.006 inch	60%
	(180 g/m^2)	(0.15 mm)	
Copper	0.015 lb/ft^2	0.004 inch	80%
	(75 g/m^2)	(0.10 mm)	
	to	to	
	0.04 lb/ft^2	0.005 inch	70%
	(200 g/m^2)	(0.12 mm)	

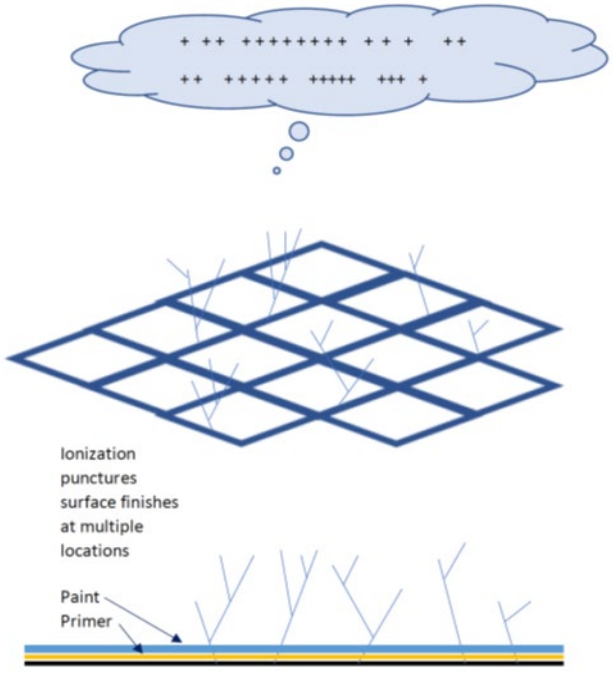

Fig. 6.46 Multiple electric field concentrations and ionizations at nodes in EMFs promote arc root dispersion. Isometric and cross-section views.

The ionizations at the discrete conductors in the EMF may penetrate the exterior surface finishes and enable a lightning leader or channel to attach to the EMF at multiple locations, thereby reducing current amplitudes and action integrals (specific energies) and physical effects at any individual spot. These are called arc roots. The result is multiple arc roots but minimal effects at each one. The effect is to minimize impact to the underlying CFC laminate. The EMF is much lighter in weight than would be a metal foil of similar thickness.

The source of the electric field in Fig. 6.47 could be an external source such as a nearby cloud that is electrically charged, an approaching lightning leader, or the charge in a lightning channel that is sweeping alongside the surface looking for a new place to attach to the aircraft surface.

The surface resistivity of a typical, 200 g/m^2 (0.040 lb/ft2) copper mesh that has been used to protect carbon laminates in aircraft applications is ~0.6 milliohms per square. This is useful for computations of temperature rise in copper mesh, using Eqs. 6.4 through 6.8.

Aluminum and copper EMFs provide the most effective lightning protection and are popular because they also offer some electromagnetic shielding.

The weight penalty associated with the use of EMFs is somewhat greater (depending on specific thicknesses) than that associated with WWFs, but the foils provide somewhat better electromagnetic shielding do than the meshes because they provide better electrical bonding to mechanical fasteners and hard metal surfaces do. Expanded foils are sometimes used where protection against both physical and induced effects is desired.

Interwoven wires

CFC fabric is available with small diameter metal wires woven together with the carbon yarns in both wove and weft directions. Typical configurations employ from 8 to 24 wires per inch (3 to 9 wires per cm). The wires have diameters ranging from 0.003 to 0.005 in (0.08 to 0.12 mm). The periodic appearance of the wires at the fabric surface intensifies the electric field at a multiplicity of locations, encouraging arc root dispersion. This approach is applicable only for protection of CFC laminates, since there are not enough wires to conduct the full lightning current and most of it must be conducted in the CFC laminate. The role of the interwoven wires is to ease the conduction of lightning current into the CFC by the mechanism of arc root dispersion. A typical CFC laminate containing an exterior ply with interwoven wires is illustrated in Fig. 6.47 [6.20]. This figure shows, in exaggerated form, the yarns in the top ply, which is intended to be the exterior ply, exposed to lightning strikes. The electric field intensifies where these wires appear at the surface of the laminate, causing the multiple lightning attachment points. The effect is similar to that illustrated in Fig. 6.46 for the EMF.

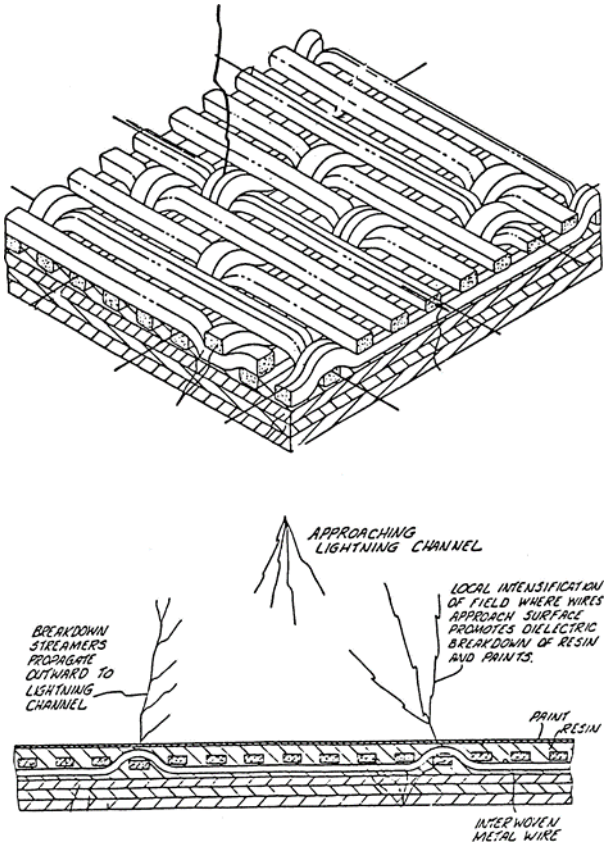

Fig. 6.47 CFC laminate with interwoven wires [6.20]

Fig. 6.48 is a photograph of a typical unpainted CFC laminate surface, showing the interwoven wires. Only the surface ply has the wires. It is not necessary to include wires in any other plies. Doing so may cause delamination. Simulated lightning stroke currents enter a wider area of surface, as illustrated in Fig. 6.50, and usually vaporize the exposed portions of the wires, typically over a surface area 4 - 8 in (10 - 20 cm) in diameter. In most cases, this damage is limited to the outermost ply, which contains the wires. The exposed portions of the wires are vaporized, giving the surface a speckled appearance and often delaminating the outer ply over a similar area.

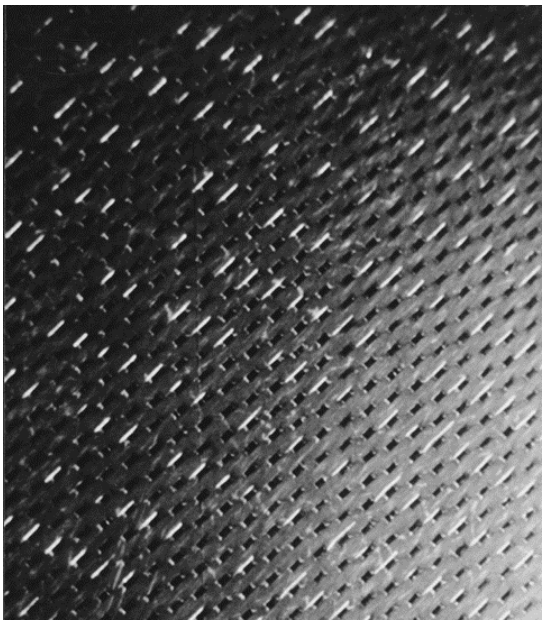

Fig. 6.48 Unpainted CFC laminate with interwoven wires. Wires are in both directions.

The weight penalty associated with using interwoven wires is very small, only about 5% of that associated with using WWFs or EMFs. Also, the wires do not affect the strength of the CFC plies to which they are added, so the interwoven wire ply is also a structural ply.

Fig. 6.49 shows a four-ply CFC skin panel 1 mm (0.040 in) thick that has been subjected to a *Zone 1A* lightning test. The damage is limited to the outermost CFC ply.

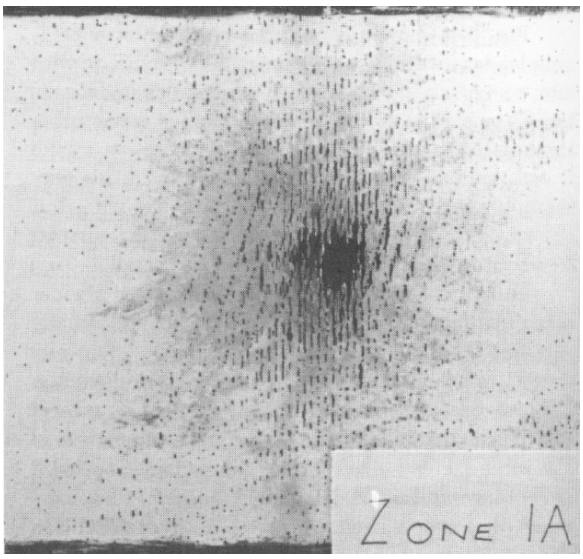

Fig. 6.49 Damage to protected CFC panel 1 mm (0.040 in) thick. *Zone 1A* stroke, 190 kA, 2 x $10^6 A^2 \cdot s$. No effects are visible on reverse surface.

Fig. 6.50 shows the behavior of a simulated lightning leader attaching to a painted CFC laminate with interwoven wires. Each of the current filaments attaches to a wire at the laminate surface, puncturing the paint. An individual attachment point on a wire is pictured in Fig. 6.51. The resin shown in this photograph has been punctured, exposing the wire, but the wire was not damaged because the test current, representative of a lightning leader, was small.

The interwoven wires do not have to conduct much of the lightning current. Instead, they ease the flow of current into the carbon, which, in most applications, is of sufficient cross section to safely conduct the lightning current without assistance. Thus, fabrics and foils used for protecting carbon skins may usually be of lighter weight than those employed to protect fiberglass skins.

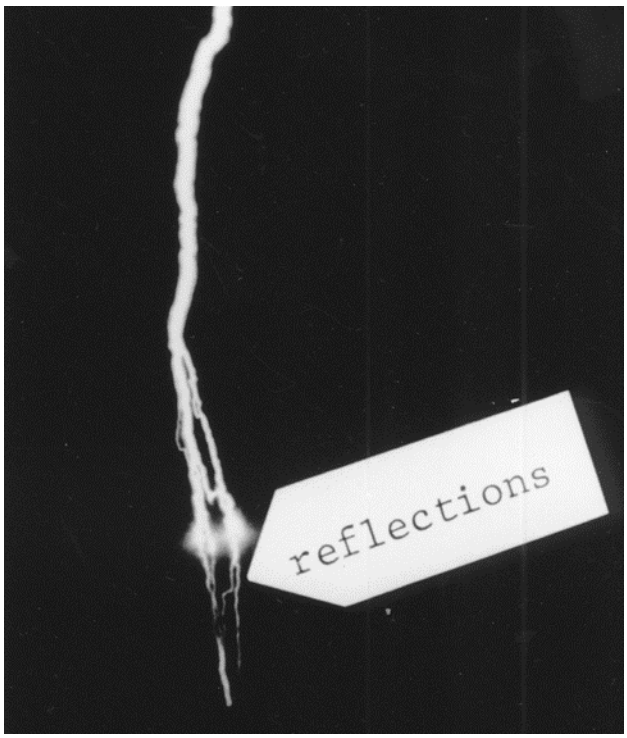

Fig. 6.50 Simulated lightning leader attaching to a painted CFC laminate containing interwoven wires. Each current filament attaches to a wire.

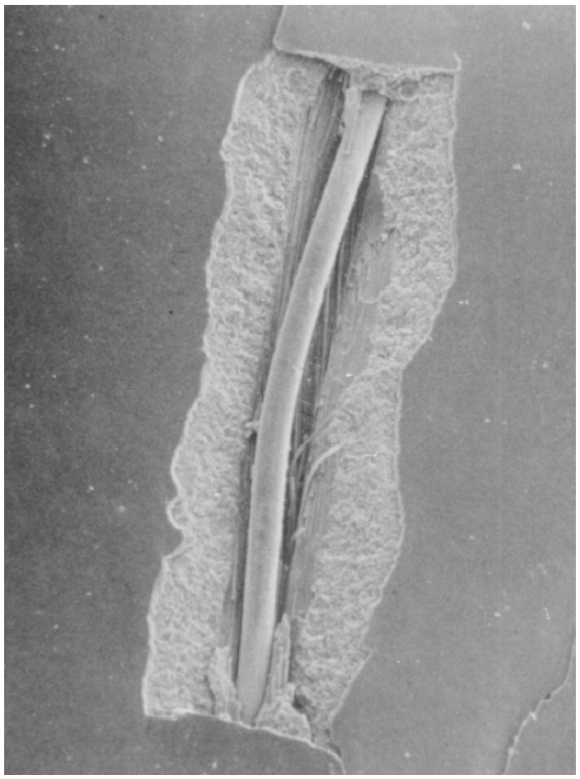

Fig. 6.51 Typical arc root at interwoven wire. 35X magnification.

Metal coated CFC

CFC yarns and cloths are available with nickel electro-plated or electro-deposited on them to increase their electrical conductivity. The metal is typically several microns thick, but usually all fibers in a yarn or ply of cloth are coated, yielding a significant reduction in resistance.

The mechanical strength of coated CFC plies is somewhat inferior to that of plies made with uncoated CFC. For this reason, the coated ply cannot always be counted as a structural ply, and an additional layer of structural CFC may have to be added to the laminate, increasing weight. As with metal fabrics and foils, only one ply of metal coated CFC material should be used, and it must be the outermost ply.

The lightning protection effectiveness of metal coated CFC is not as good as that of WWFs and expanded foils. It does permit some damage to occur to the coated ply and to one or two underlying carbon plies. This method is not often used since the EMFs and the interwoven wires became available.

6.4.5 Protection of CFC Joints and Splices

In addition to damage at attachment points, lightning currents can also cause damage at the places where they flow from one piece of CFC to another, as at interfaces with adjoining skin panels or with substructures such as ribs and spars. Two basic methods of joining composites are in use:

Adhesive bonding

Adhesives are frequently used at structural joints and seams, either alone or in combination with mechanical fasteners. Since nearly all adhesives are electrically non- conductive, they present a barrier to current flow and force lightning currents to flow in fasteners and other places where CFC or other conductive parts of the structure come in contact. If no such paths exist, the adhesive bond must be made sufficiently conductive to permit current transfer.

Specific ways to provide electrical conductivity across adhesive joints and bond straps include:

1. Doping of adhesive with electrically conductive particles.

2. Insertion of a conductive scrim into the bond.

Doped adhesives

Adhesives doped with electrically conductive particles are commercially available, but the conductive particles are usually steel, silver or aluminum and their main purpose is thermal, rather than electrical conduction. Few of these adhesives can meet the demanding requirements of airframes. Tests [6.21] have shown that such adhesives can conduct up to about 100 A per cm^2 (645 A per in^2) without loss of mechanical strength. However, these adhesives are not as strong as nonconductive adhesives and are therefore not often used in primary structural applications. The use of aluminum particles in a CFC structure also raises galvanic compatibility concerns. If the adhesive is not sufficiently conductive to transfer lightning currents, the current arcs through the adhesive, dis-bonding the joint.

Conductive scrim

The conductivity of an adhesively bonded structural joint can be improved if a conductive scrim is incorporated into the joint. This method has proved successful in

some applications. The scrim contacts both surfaces of the joint, while allowing the adhesive to flow between the conductive yarns of the scrim. Typical configurations are shown in Fig. 6.52. The most common scrim is a single, loosely woven layer of carbon fiber cloth.

Galvanically compatible metal fabrics have also been used. In either case, anticipated current densities must be low enough that arcing will not occur at the points of contact between the scrim and CFC parts being joined. Such arcing would cause pressure-buildup within the bond and possible dis-bonding.

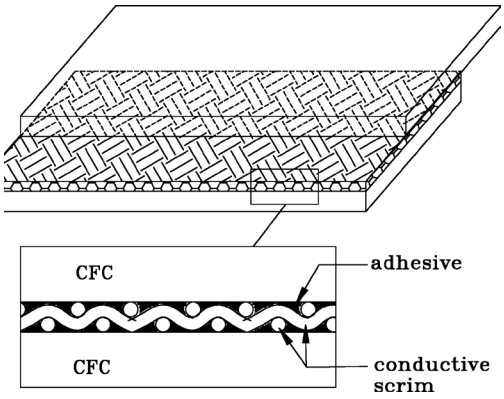

(a) Basic Concept.

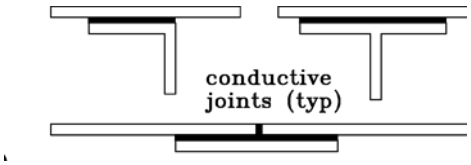

(b) Examples.

Fig. 6.52 Adhesive joint with conductive scrim.

Bolted and riveted joints

The other method of joining composite materials is with riveted or bolted joints, in which the bolts, or rivets, or other mechanical fasteners are employed to hold two members together. Mechanical fasteners (whose composition is dictated by the simple fact that no other materials have yet been developed with sufficient strength) also vicariously provide electrical conductivity between the parts that they join.

Although mechanically fastened joints do provide electrically conductive paths, the contact area between the fastener and the composite is usually limited to the surface under the fastener head or nut. There may be contact between the holes in the parts being joined and the shanks of the fasteners, but this contact is sometimes incidental. Some fasteners are available with metal inserts that provide electrical contact among all plies in the fastened laminates. These inserts are made of galvanically compatible metals or surface finishes to inhibit corrosion. The insert must be interference-fit to make electrical contacts with carbon yarns in the individual plies which adds a step to the manufacturing process.

In some situations, the fasteners themselves can be interference-fit but this may apply excessive pressure against the hole, resulting in cracking or local delamination of the laminate. The inserts can be made of metals that are not as hard as the fasteners would be, thus applying less stress to the interfacing laminates. The fastener pulls tight against the insert countersink.

Most of the electrical contact is between the fastener head and the countersunk holes in the laminates. Washers or fastener heads that overlap the exterior surface of the CFC, or the protection layer (if there is one) are also used to improve electrical conductivity. Even so, tests have shown that significant arcing can take place around fastener heads, especially when the lightning attachment point is near or at the fastener. In such cases, the fastener current density is high. As discussed in Chapter 7, arcing at a fastener can be a matter of concern when the fastener protrudes into a fuel tank.

Methods of either eliminating this arcing or isolating it from fuel vapors are described in Chapter 7. The amount of arcing that commonly takes place adjacent to a fastener head or inside fastener holes usually does not significantly damage CFC laminates or weaken the fasteners. The number of fasteners or rivets employed in most designs is usually sufficient to conduct most *Zone 3* lightning currents.

Loss of strength at joints

Work has been done to evaluate the degree of strength loss caused by lightning currents in composite joints. Schneider, Hendricks, and Takashima [6.22] have studied the effects of lightning currents on typical bonded and bolted joints of graphite composites, and their preliminary findings show that bonded joints suffer more damage from lightning currents than bolted joints do. Other, similar tests [6.22] have produced similar results.

Candidate bond and joint designs should be tested with anticipated current densities to verify that these joints can tolerate the design-level currents without loss of mechanical strength. Guidelines for performing such tests are contained in § 5.2.3 of [6.16].

6.4.5 Application Considerations

Other aspects of lightning protection design for CFC skins involve optimizing cloth or tape lay-up patterns (as well as ply seams) for maximum current carrying capability, use of mechanical fasteners for electrical bonding and defining repair techniques that preserve the integrity of lightning protection. Brief discussions of each of these topics follow.

Lay-up patterns

Experience has shown that woven cloth fabrics are more tolerant of lightning strike effects than laminates made of UD tapes. The interweaving of carbon yarns in the woven cloth restricts the propagation of damage from blast and shock wave effects, and the cloth plies also have more uniform electrical conductivity in the plane of the laminate.

UD tapes, on the other hand, tend to unwind along their lengths over significant distances from a lightning attachment point, causing damage to propagate over greater distances from the strike point than is typical with woven cloths. Also, electrical conductivity tends to be somewhat better parallel to the tapes and poorer perpendicular to the tapes. This causes lightning currents (and resulting damage) to penetrate deeper into a laminate as it seeks conductive paths in all directions. The interwoven wire protection method is not applicable to tape laminates, since the wires can be provided only in the direction of the tape.

If tapes are needed for mechanical strength, it is best to include cloth plies as the inner and outer surfaces of the laminate. The exterior surface cloths may contain interwoven wires, as described earlier, for lightning protection purposes. The other methods of protecting CFC laminates may be applied as well.

Appliqués

In an effort to address some of the maintenance and longevity problems associated with aircraft paints, colored fluoropolymer foil appliqués, with EMFs integrated to them, have been manufactured and tested as a substitute for conventionally painted EMFs co-cured to composite surfaces. Initial lightning tests have shown that these appliqués can provide about the same degree of protection for CFC laminates as co-cured EMFs beneath conventional paint finishes [6.23]. The advantage of the appliqués has been that they are easy to apply and that they can be removed or replaced without damaging the layer of CFC beneath them. Damage to EMF during repair has been a problem with conventional paint finishes. Flight experience is limited, so the long-term durability of expanded foil appliqués has not been evaluated as of this printing.

Ply seams

Seams are necessary in CFC cloth lay-ups, where the edges of pieces of cloth meet. As long as the seams of all plies do not coincide, there is usually adequate electrical conductivity throughout the laminate. Ply seams are typically simple butt joints and, thus, electric currents are forced to flow through adjacent plies to get across seams.

Seams in some lightning protective layers may need to be spliced or bridged, in some manner, to allow current transfer and minimize arcing. Protective layers that require splicing include wire fabrics and expanded foils. Splices can be either separate pieces of the fabric or foil applied over the seam, or they can be overlaps. Two common designs are illustrated in Fig. 6.53. In either case, the amount of overlap necessary to transfer currents depends on the expected lightning current density. Overlaps of 1 cm (0.5 in) have been found capable of transferring currents of 2.5 kA per cm (1 kA/in) across overlaps or splices along the length of a seam without dis-bonding or excessive arcing. However, the adjoining pieces, must be co-cured with the underlying laminate and they must be in good physical contact with each other. Larger overlaps of up to about 5 cm (2 in) are usually necessary at joints exposed to higher current densities, such as occur at wingtips, empennage tips or other structures in which lightning currents are high.

Splices and overlaps that are secondarily bonded with a layer of adhesive are not nearly as conductive as co-cured splices, because the adhesive forms an insulating barrier between the conductive layers, allowing arcing to occur within ply bonds. If secondary bonds must be used, adhesives should be non-supported (i.e., without carriers) and of minimum thickness. The vacuum bagging and curing of structures containing spliced protection plies should be conducted in a manner that encourages the maximum possible metal-to-metal contact in the splice.

Splices at manufacturing joints

Splices in protection layers that extend across manufacturing joints in large structures may need to have larger overlaps if they are to be the only means of transferring current across such a joint. Most candidate joint designs should be tested to verify that current transfer does, in fact, occur in the designated splice plies or plates, rather than in an alternate manner that involves arcing and dis-bonding, which would degrade mechanical strength.

Seams in interwoven wire and metallized fabrics

Splices are not usually needed in laminates protected with interwoven wires or metallized fabrics, because these protection methods depend on the bulk CFC laminate to conduct the lightning current. Thus, the edges of interwoven wire and WWF protection plies may be simply butted together and co-cured with the rest of the laminate.

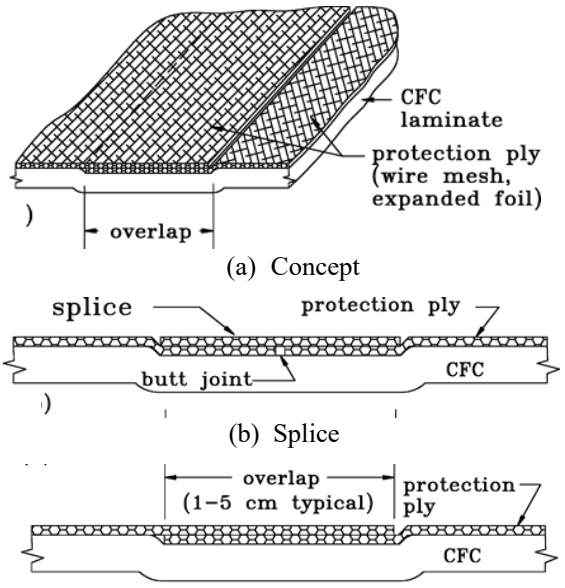

(a) Concept

(b) Splice

(c) Overlap

Fig. 6.53 Typical configurations of splices in protective plies.

Electrical bonding to fastener

It is frequently necessary to make electrical bonds between protection layers and metal fasteners in order to transfer current between adjoining parts or substructures. This can be done either by direct conduction between a CFC laminate and its fastener in the fastener hole, or by installing the fasteners in overlapping washers (sometimes called dimpled washers) or metal doubler plates. These concepts are illustrated in Fig. 6.54.

It is rarely possible to extend protection plies or layers into countersunk fastener holes because the protection ply is usually supposed to be co-cured with the laminate and therefore the holes must be drilled afterwards. Good conductivity can be achieved if the fasteners are drawn tightly into countersinks and sealant barriers are minimized so that the fastener-heads make the best possible electrical contact with the cross section of CFC within the countersinks (see Fig. 6.54(a)).

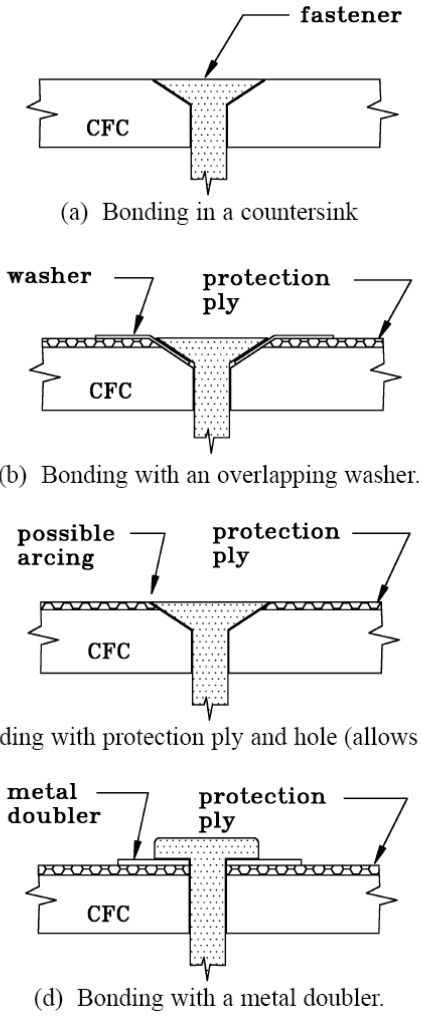

(a) Bonding in a countersink

(b) Bonding with an overlapping washer.

(c) Bonding with protection ply and hole (allows arcing).

(d) Bonding with a metal doubler.

Fig. 6.54 Electrical bonding via fasteners

Protection plies can be electrically bonded to the fastener through overlapping washers or a metal doubler plate, as shown in Fig. 6.54(b). These methods are sometimes used when the protection layer is also intended to afford electromagnetic shielding for onboard systems, although overlapping washers are not always necessary for such applications. A typical application is the avionics bay access door illustrated in Fig. 6.55. Good electromagnetic shielding requires that the protection ply be bonded to surrounding structure on all edges, as shown. This bonding is provided by the removable fasteners and by the piano-type hinge along the fourth edge.

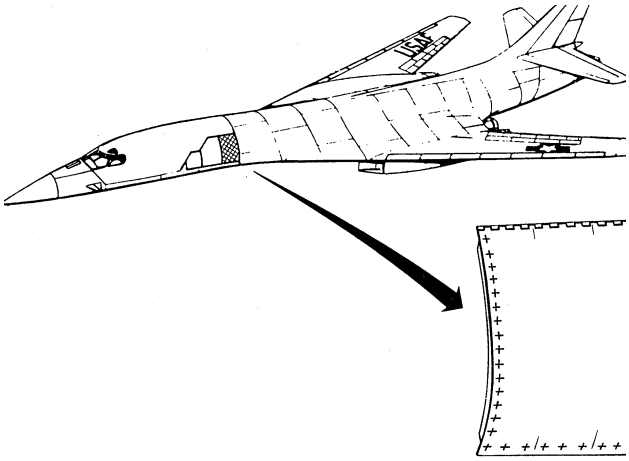

Fig. 6.55 Access door attached to surrounding skin via multiple removable fasteners and piano hinge

Repairs of Lightning Damage to CFC skins

Repairs to thin CFC skins

There is no practical way to repair actual lightning damage so the area that has been damaged must be removed so that new skin material can be inserted and attached to the surrounding undamaged skins. The repair example that follows in Fig. 6.56 applies to thin, 20 - 80 mil thick (1 mm - 2 mm) CFC skins where the lightning damage has penetrated completely (or nearly completely) through the skin. Such skins are usually found in secondary structures of large transport airplanes or in primary structures of small airplanes and helicopters.

The first task with repairing this damage is to locate the extent of the damage. Superficial damage can be seen, but other damage, usually among lightning strike damage to CFC skins is to locate the area that has been damaged so that this can be removed and replaced. Fig. 6.56(a) shows an area of visible lightning damage surrounded by a larger area of invisible damage to inner plies, indicated by the callout and dashed line. This invisible damage needs to be located by ultrasonic scans, or other non-destructive means so that it can be removed along with the visible damage. The famous "tap test" can be used for an initial look but should not be depended upon by itself to locate all of the invisible damage.

A circular area that includes all of the invisible damage is then cut out from the skin so that a new circular laminate of the same construction as the damaged one can be inserted in place of the removed damage area.

After the new circular laminate is put in place a larger, rectangular laminate is installed over the circular plug on the interior surface of the laminate. Both the circular plug and rectangular laminate are secondarily bonded in place. The interior view of this is shown in Fig. 6.56(c).

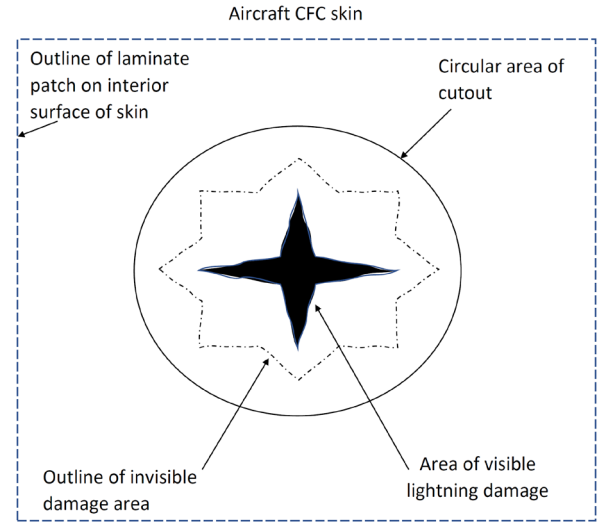

(a) Exterior view showing areas of lightning damage

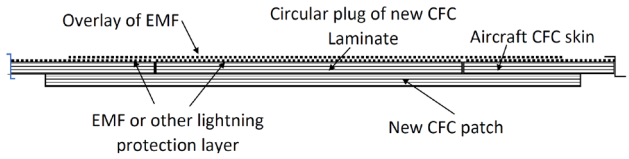

(b) Edge view showing CFC skin, circular CFC plug, CFC patch and EMF

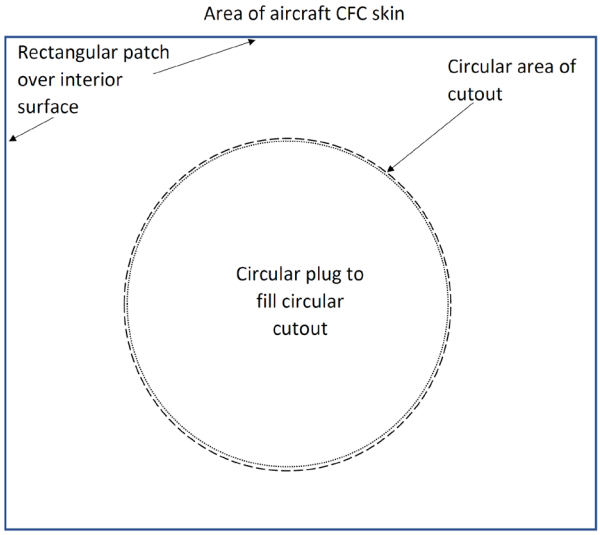

(c) Interior view showing rectangular patch over circular plug

Fig. 6.56 Concept for repair of lightning damaged thin CFC skins

Fig. 6.56(b) is an edge view of the repair including an additional layer of EMF (or other lightning protection layer) that has been secondarily bonded to the existing protection layer. Further discussion of this protection repair is presented in the following paragraphs. The protection layers are not shown on Figs. 6.56(a) or (c).

The process for making a repair of this nature would be as follows:

1. Locate the visible and invisible areas of lightning damage.

2. Cut out the damage areas. Usually, a circular cutaway will be relieve mechanical stress at corners but the cutaway detail should be determined by structural specialists.

3. Fabricate a plug of similar laminate to closely fit the cutout. Also fabricate a square or rectangular patch of similar laminate, or other laminate depending upon structural needs. The circular plug should have the lightning protection layer co-cured with its laminate. The patch should not have a lightning protection layer.

4. Install the plug and the patch as shown in Fig. 6.56(b) and (c). These may be adhesively bonded together. Vacuum bagging should be used where practical to achieve a strong mechanical bond between the patch, plug, and surrounding aircraft skin. It is not necessary to achieve electrical bonds among these three laminates. Future lightning strikes to the repaired area will be conducted via the EMF splice ply to surrounding skin (see steps 6 and 7).

5. It is likely that the damaged area is in lightning strike zone 1A, 1C, or 2A. The lightning protection features should be restored to original design or equivalent. The following steps explain how this may be done.

6. It is not feasible to directly bond the plug electrically to the surrounding aircraft skin. This must be done by providing an overlay (splice layer) of EMF that may be adhesively and electrically bonded to EMF layers that have been co-cured to the CFC laminates in the plug and the surrounding aircraft skin. Satisfactory electrical bonds can usually be achieved by removing surface finishes from the surrounding skin down to bare metal, and by having the plug EMF unfinished so that it is also bare metal. The overlay can be adhered to the plug and skin with a thin layer of resin or adhesive that penetrates the holes in the EMF layers but does not leave an adhesive film between the two EMF layers. Achievement of a tight mechanical bond may be helped by vacuum bagging the new joints.

7. In some situations, it is advisable for both structural and electrical purposes to add fasteners between the laminate patch and the surrounding skin. This may be necessary for repairs to Zone 1A or 1C skins where lightning currents are highest. Fasteners can improve electrical bonding and current transfer from the repaired area to surrounding skin and improve mechanical strength of the bond. Fasteners will allow some of the lightning current to flow past the repair via the CFC patch. The types and amounts of fasteners should be coordinated with structures specialists.

8. If the repair is to be incorporated in a primary structure skin, its effectiveness should be confirmed by lightning test of a specimen of the repair installed in a sample of the airplane skin. The tests should be conducted as described in § 5.2.1 of [6.16] for the lightning strike zone that the repair will be installed within.

Repairs to thick CFC skins

Lightning strike damage to CFC skins that are greater than 80 mils (2 mm) thick may sometimes be accomplished without removal of the entire area of skin. If the thermal and shock wave effects have not penetrated completely through such a skin, the damaged plies may sometimes be removed and replaced, one-by-one to refill a damaged area with new plies. The idea is shown in Fig. 6.57.

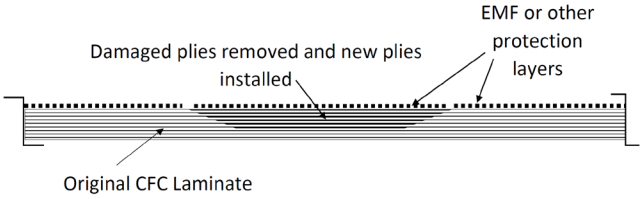

Fig. 6.57 Repair of thick CFC skins

In the example of Fig. 6.56, the areas of visible and invisible damage would be identified as in the earlier example, and the areas of damaged plies would be removed by grinding through undamaged plies outboard of the damage area. Then the exposed surfaces would be cleaned, and new CFC plies cut and fitted and adhesively bonded to the cleaned-out area. No attempt should be made to make electrical bonds between the new and existing plies. A layer of EMF or other lightning protection material would be applied to the outermost new

CFC ply. The surface finishes on the surrounding original laminate surface should be removed down to the original EMF, leaving this EMF and the new EMF on the repair with bare metal surfaces.

An overlapping layer of EMF layer should then be secondarily bonded to the EMFs on the repair and surrounding areas so that an electrical bond is achieved. As with any repair, a sample of the repair should be prepared on a piece of similar CFC laminate for lightning testing in accordance with § 5.2.1 of [6.16] to confirm the adequacy of the repair method.

Appropriate structural tests should be applied to any type of repair to verify that the repaired article is able to tolerate required mechanical loads.

Note that the repair guidance provided in this chapter should not be used by itself to make repairs. Further details need to be provided to assure that the repaired skins meet structural requirements. For further information refer to Composite Material Handbook-17 or Commercial Aircraft Composite Repair Committee.

6.5 Physical Effects on Propulsion Systems

Engine cowlings or nacelles made from composite materials may be damaged by lightning attachment. Unless these structures are provided with protection, they may be punctured, and lightning currents may attach to engine components within. Lightning effects of this type are identical to those described previously for other exposed composite structures. Punctures and direct lightning attachments to fuel lines, electric wire harnesses and bleed air or other pressurized tubes or pipes may cause fires or other hazards. The induced effects associated with strong magnetic fields surrounding lightning currents in piston engine blocks or turbine engine cores may damage electronic engine controls or engine instruments. The induced effects of lightning and protection methods are described in Chapters 8 through 17. The effects discussed here are those related to strikes to propellers and rotor blades, gear boxes, and the occasional engine flameouts experienced by gas turbine engines during lightning strikes.

6.5.1 Propellers

Aircraft propellers are frequent targets for lightning strikes. The fact that propellers are usually located in *Zones 1A* or 1B makes them susceptible to initial leader attachment and (often) first stroke attachment as well, (see Fig. 6.58) but blades in a pusher configuration are in *Zone 1B* and are susceptible to all components of the lightning environment.

The strokes of a lightning flash, due to their short durations, probably strike only one blade at a time. Even the duration of the intermediate current may be short enough that it also involves only one blade. However, the propeller does rotate fast enough that continuing current jumps from one blade to another, entering all of the blades.

A lightning flash to an aluminum propeller does little apparent damage, but such blades must be carefully inspected and repaired following a strike, since even small pits and melted spots may become stress concentration points. It is not correct to assume that lightning strikes occur always to the blade tip areas.

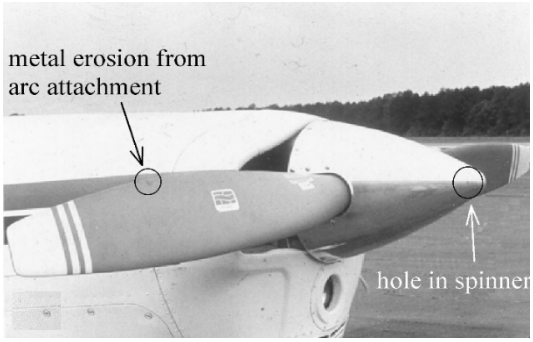

(a) Point of Initial leader attachment to spinner

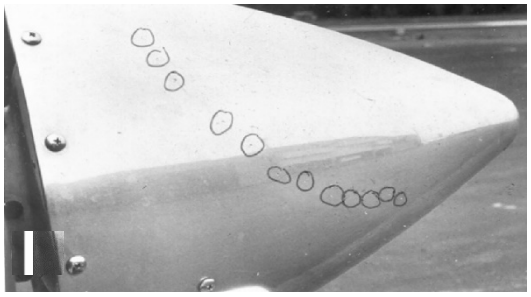

(b) Swept leader effects on spinner

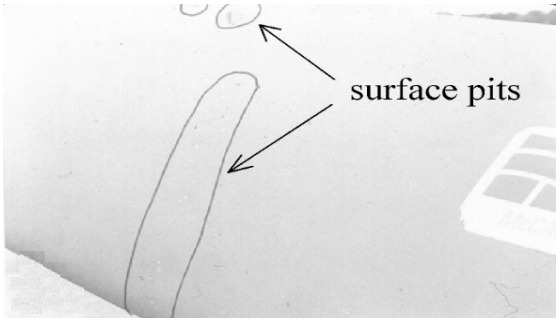

(c) Close-up of effects on blade

Fig. 6.58 Propeller spinner and blade strike.

The entire surface of the blade is exposed to lightning channels that may reattach randomly at any spot on a rotating blade. It has sometimes been assumed that the tips of blades, usually inboard to 18 inches from a tip, are susceptible to direct strikes by stroke currents, but experience shows that this is not a correct assumption.

While lightning leaders often attach to blade tips, the combination of the aircraft's forward motion and blade rotation renders all surfaces of the blades potentially susceptible to contact with a lightning channel. All of the current that enters propeller blades must also pass through the propeller hub, gearbox, and the engine.

Propellers made of fiberglass and CFC are more susceptible to damage from lightning than aluminum propellers, especially if they contain any internal conductive parts. A lightning flash can puncture to internal conductors, such as spars, causing complete destruction, since the blade is under high stress during an in-flight lightning strike.

Lightning current that attaches to a propeller's electric de-ice heater element could be conducted into the heater power source, damaging other equipment powered from the same source, in the same manner as a strike to a heated windshield. Protection techniques for composite propeller blades are the same as for some other composite structures described in §6.2.4, and include the use of woven wire meshes and EMFs. Often a metal leading edge rain erosion strip can be integrated into a blade's lightning protection design to conduct lightning flash currents.

A typical CFC propeller blade has a short, metal spar enclosed within CFC skin laminates and a foam filler. Because of mechanical stress concerns, mechanical fasteners are rarely used in blade manufacture. Instead, blade laminates are attached together by adhesive bonds. Usually the CFC laminates are not connected electrically to the metal spar until these elements join at the blade hub. Even at the hub, there is usually no intentional electrical contact between CFC laminates and metal parts, so lightning currents arc across small gaps, usually with no more than cosmetic effects on exterior finishes if these arcs are made to occur on exterior surfaces. The CFC laminates are commonly protected by EMF. A common mistake has been to assume that lightning strikes will only attach to the outer 0.5 m (18 in) of a blade. In fact, a tradition has evolved to protect only these surfaces from *Zone 1A* or *1B* lightning currents. Actually, the *entire* surfaces of composite propeller blades must be protected from these lightning environments if catastrophic effects are to be avoided.

It is always necessary to verify adequacy of propeller protection designs by lightning tests of the blade.

All surfaces of a blade should be assumed to be within Zone 1A and the blade interior structure is within Zone 2.

6.5.2 Helicopter Rotor Blades

In general, helicopter rotor blades are similar to the propeller blades of fixed-wing aircraft in their lightning strike exposure. The main difference is the larger size of the rotor blades and, therefore, a greater likelihood that helicopter rotor blades will be struck by lightning. The same considerations discussed in §6.6.1 for propeller blades, apply. Many helicopter main and tail rotor blades are constructed of CFC laminates enclosing a shorter metal spar surrounded by a foam filler.

The entire top surface and some of the bottom surface areas of main rotor blades are susceptible to *Zone 1A* lightning attachments when the blade is rotating. Since helicopters are frequently parked out of doors and their rotors receive lightning strikes when the main rotor is not moving, one should assume that any spot on the upper surfaces of helicopter main rotor blades is susceptible to initial leader attachment and to all of the currents that follow in the flash, thus *Zone 1B*. Airworthiness regulations seem (surprisingly) to require only that aircraft *in flight* be protected from catastrophic lightning effects, even though a helicopter rotor blade damaged by a strike while parked on the ground may fail in a subsequent flight. Helicopter operating procedures generally call for some inspection of the blades prior to takeoff but, while helicopter operators are skilled pilots, they do not necessarily know how to recognize lightning effects on rotor blades.

There have been several accidents with fatalities [6.24-6.25] caused by lightning strikes to rotor blades. In one case, a blade was struck, and superficial damage was repaired, but unknown interior effects due to arcing among internal components were not detected and this blade was returned to service. A second lightning strike to the same blade resulted in separation of the outer part of this blade due to the first- and second strike effects combined with flight loads, resulting in fatal crash of the helicopter [6.25]. Unless reliable means are employed to detect all internal lightning effects, a blade once damaged by lightning should never be returned to service. The best use of such a blade would be careful dissection to locate and understand any internal effects, followed by the scrapyard.

Other lightning effects may damage blade de-icing heater blankets and tip lights. All these possibilities mandate that helicopter rotor blades (both tail rotor blades and the main rotor) be designed so that all their surfaces are protected from hazardous lightning effects. It is never sufficient to assume that only the outboard surfaces of helicopter rotor blades (main and tail) are exposed to severe lightning strikes.

6.5.3 Gear Boxes

Lightning currents entering propellers or rotor blades must enter the airframe through the gears and bearings supporting the propeller or rotor shaft. The conduction of these currents through the bearings, which are supported on insulating lubricant films, usually causes some pitting of the bearing surfaces. This does not appear to be a major problem, since there are no known records of any catastrophic failures of bearings associated with lightning strikes. Airplane engine manufacturers, however, have always recommended that gear boxes and bearings be disassembled and inspected after a strike. This usually leads to the replacement of the bearing since it is not possible to differentiate between arc pitting and wear. There does not appear to be any way of avoiding such pitting, since lightning current that enters a propeller blade must always go through the bearing. There are no practical ways of diverting these currents away from the bearings. Bond straps may be considered, but the impedances of bond straps that must be much smaller in cross-section than engine bearings means that a large percentage of any lightning current will always flow across the bearings.

Instead, the helicopter gearbox chip-detector systems are depended upon to indicate the conditions of bearings and gears.

6.5.4 Turbine Engines

Small turbine engines, especially those mounted on the fuselage, have experienced flameouts, turbine stalls, or rollbacks that coincided with the appearance of lightning flashes in front of the engine inlet. The phenomenon is thought to be caused by the lightning channel interrupting the air flow at the engine air inlet. Numerous cases of power loss under similar circumstances have been reported [6.26] and, in one instance, both engines of a small business jet aircraft sustained a flameout. Other damage to the engine or nacelle is generally not observed following these incidents. No protective measures are known, other than ensuring that pilots are aware of the possibility and are practiced in restart procedures. One procedure has been to keep igniters turned on during flights in weather conditions conducive to rain showers and lightning strikes.

References

6.1 J. H. Hagenguth, "Lightning Stroke Damage to Aircraft," AIEE Transactions 68, American Institute of Electrical Engineers, New York, 1949, pp. 9-11.

6.2 R. O. Brick, "A Method for Establishing Lightning Resistance and Skin Thickness Requirements for Aircraft," *1968 Lightning and Static Electricity Conference*, December 1968, pp. 295-317.

6.3 R. O. Brick, L. L. Oh and S. D. Schneider, "The Effects of Lightning Attachment Phenomena on Aircraft Design," *1970 Lightning and Static Electricity Conference*, December 1970, pp. 139- 156.

6.4 F. L. Kester, J. A. Plumer and M. Gerstein, "A Study of Aircraft Fire Hazards Related to Natural Electrical Phenomena," *NASA CR1076*, June 1968.

6.5 J. Philpott, "Factors Affecting Puncture of Aluminum Alloy by Simulated *Lightning," Lightning and Static Electricity Conference Papers*, December 1972.

6.6 *Protection of Airplane Fuel Systems Against Fuel Vapor Ignition Due to Lightning*, FAA AC 20-53A, Federal Aviation Administration, Washington, D.C., 12 April 1985.

6.7 R. D. Hill, "Channel Heating in Return Stroke Lightning" *J. Geophys. Res.*, Vol 76, 1971, pp. 637-645.

6.8 M. A. Uman, *The Lightning Discharge*, International Geophysics Series, Volume 39, Academic Press, Orlando, 1987, pp. 293-303.

6.9 Paul T. Hacker, "Lightning Damage to a General Aviation Aircraft Description and Analysis" *NASA TN D-7775*, National Aeronautics and Space Administration, Lewis Research Center, Cleveland, Ohio, September 1974, pp. 49.

6.10 J. R. Stahmann, "Control Surfaces and Door Hinge Bonding Effectiveness in Modern Aircraft" *Proceedings of the 1972 Lightning and Static Electricity Conference*, 1215 December 1972, pp. 527-534.

6.11 *Bonding, Electrical, and Lightning Protection for Aerospace Systems*, MIL-B-5087B (ASG), 15 October 1964.

6.12 M. P. Amason, G. J. Cassell, J. T. Kung, "Aircraft Applications of Segmented Strip Lightning Protection Systems", *Proceedings of the 1975 Conference on Lightning and Static Electricity*, 14-17 April 1975, at Culham Laboratory, England.

6.13 S. A. Moorefield, J. B. Stryon, and L. C. Hoots, "Manufacturing Methods for Advanced Radome Production," *Interim Technical Report 6*, prepared by the Brunswick Corporation for the Air Force Materials Laboratory, Air Force Systems Command, United States Air Force, Wright Patterson Air Force Base, Ohio, November 1975, pp. 32-40.

6.14 Amason, Cassell, and Kung, "Aircraft Applications of Segmented Strip Lightning Protection", pp. 9.

6.15 D. A. Conti and R. H. J. Cary, "Radome Protection Techniques", *Proceedings of the 1975 Conference on Lightning and Static Electricity*, 14-17 April 1975, at Culham Laboratory, England.

6.16 Aircraft lightning Test Methods, *SAE Aerospace Recommended Practice* (ARP) *5416A/EUROCAE ED 105A.*

6.17 J. T. Quinlivan, C. J. Kuo, and R. O. Brick, "Coatings for Lightning Protection of Structural Reinforced Plastics", *AFML-TR-70-303 pt. I*, Air Force Materials Laboratory, Nonmetallic Materials Division, Air Force Systems Command, Wright- Patterson Air Force Base, Ohio, March 1971.

6.18 R. O. Brick, C. H. King, and J. T. Quinli-van, "Coatings for Protection of Structural Reinforced Plastics", *AFML-TR-70-303 Pt. II*, Air Force Materials Laboratory, Nonmetallic Materials Division, Elastomers and Coatings Branch, AFML/LNE, Wright-Patterson Air Force Base, Ohio 1972.

6.19 *Report on the Investigation of an Accident Involving Aircraft of U.S. Registry NC 21789, Which Occurred Lear Lovettsville, Virginia, on August 31, 1940*, Civil Aeronautics Board, Washington, D. C., 1941.

6.20 McClenahan et al. U.S. Patent Number 4,448,838, May 1984.

6.21 J. E. Pryzby and J. A. Plumer "Lightning Protection Guidelines and Test Data for Adhesively Bonded Aircraft Structures," *NASA Contractor Report 3762*, Jan. 1984.

6.22 S. D. Schneider, C. L. Hendricks, and S. Takashima, "Vulnerability/Survivability of Composite Structures-Lightning Strike", D6-42673-3, prepared by the Boeing Commercial Airplane Company for the Air Force Flight Dynamics Laboratory, Aeronautical Systems Division, Wright-Patterson Air Force Base, Ohio, April 1976.

6.23 Sayyid A. Nadimi, Michael N. Shaw, Bobby A. Collins, Terrence G. Vargo, and Andrew Dalgleish, "Evaluation of a Fluoropolymer Appliqué for Lightning Protection of Aircraft", *International Conference on Lightning and Static Electricity (ICOLSE), 2003 paper I03-20.*

6.24 UK AAIB Accident Report EW/C95/1/1 Aerospatiale AS332/L of 19 Jan 1995.

6.25 UK AAIB Accident Report EW/C2002/07/04 Sikorsky S76A of 16 July 2002.

6.26 D. Newton, *Severe Weather Flying,* McGraw-Hill, New York, 1983, pp. 65.

Chapter 7

FUEL SYSTEM PROTECTION

7.1 Introduction

The design of adequate lightning protection for aircraft fuel systems is one of the most important lightning protection tasks. Airworthiness certification requirements stress fuel system safety because this system has been responsible for most of the lightning-related aircraft accidents. Elements of the fuel system are typically spread through-out much of an aircraft and occupy a significant amount of its volume. They include the fuel tanks themselves, associated vents, drains, access panels, transfer plumbing, and electrical controls and instrumentation. Careful attention must be paid to all these elements if adequate protection is to be achieved.

7.2 Ignition Sources and Fuel Flammability

The main objective of fuel system lightning protection is to keep the ignition of fuel from destroying the aircraft during a strike. This goal is quite challenging because thousands of amperes of current must be transferred through the airframe when the aircraft is struck by lightning and a tiny spark of less than one ampere may release sufficient energy inside a fuel tank to ignite the fuel vapor and initiate a fire or an explosion.

Prevention of fuel ignition hazards from lightning must be accomplished by one or more of the following approaches:

1. **Containment:** Designing the structure to contain the over-pressure from an explosion without rupturing.

2. **Inerting:** Controlling the atmosphere in the fuel system to ensure that it cannot support combustion.

3. **Foaming:** Filling the fuel system with a material that prevents a flame from propagating.

4. **Eliminating ignition sources:** Designing the fuel tank structures and system components and installations so that lightning does not produce any ignition sources

The following paragraphs discuss potential lightning related, fuel vapor ignition-sources and methods of eliminating them. Whereas the other approaches listed above have been successful; in specific situations, they incur weight and cost penalties that have made them prohibitive for widespread use. Additionally, some commercial aircraft regulations require elimination of ignition sources, regardless of other protection approaches, such as inerting systems. Several important studies relating to fuels and the mechanism of ignition are reviewed in the following pages. These discussions provide guidelines for effective protection of fuel systems.

Laboratory studies involving simulated lightning strikes to fuel tanks, or portions of an airframe containing fuel tanks, have demonstrated several possible ignition mechanisms. These mechanisms can be divided into two broad categories: thermal ignition sources and electrical ignition sources.

Thermal ignition sources

1. Hot spots on the interior surfaces of metal or composite fuel tank skins, due to lightning attachment to exterior surfaces.

2. Hot parts, such as electrical wires, ground braids, or tubes, raised to elevated temperatures by the conduction of high densities of lightning current.

For hot spots to ignite fuel vapor, their temperatures must usually exceed 800 °C (1 500 °F) for a period of one second or more. Some metals, such as aluminum, melt through before their interior surfaces reach the short-term ignition point of the fuel. The autoignition temperatures published in fuel tank safety guidance documentation reflect long term exposure of the fuel to the temperatures and should not be confused with the short term autoignition temperatures discussed in this chapter regarding lightning waveforms.

Electrical ignition sources

Electrical Sparks: Electrical sparks are ionizations of the air between conductive elements that are isolated from one another. These ionizations are caused by potential differences (electric fields) arising from lightning currents in the airframe, or from changing magnetic fields. A spark occurs when a sufficiently high electric field creates an ionized, electrically conductive channel across a small gap in air or other mixtures of gases. Whether or not a spark happens depends on the strength of the electric field (voltage) between the conductive elements, and conditions of the gases. The amount of voltage required to form a spark

in air depends on the length of the gap, the shapes of the electrodes involved, and the air pressure and humidity. At sea level a potential difference of ~30 kV is needed to create a spark in air as sea level between conductive elements one cm apart that produce a non-uniform electric field. The minimum potential difference necessary to cause a spark in air is about 300 V, across very small air gaps. When caused by lightning currents flowing in an airframe, the sparks are of only a few microseconds duration, but this is sufficient time to release sufficient energy to ignite a flammable vapor. Locations where sparks may happen can be between fuel measurement system (FMS) probes and nearby tank structures, and between other elements when sufficient voltage exists. In metal tanks there are few if any locations where sufficient voltages exist to form sparks. In tanks fabricated of Carbon Fiber Composite (CFC) where the structure IR voltage is much higher, there may be several places where sparks might exist during lightning stroke current flow in the tank structure.

Electrical Arcs. Electric arcs are the formation of vaporized metals or other materials and sometimes ionized air or other gases due to the melting of the contact surfaces between conductive parts. This happens when the current density through the contacting surfaces exceeds their current carrying capability, which usually causes molten and/or burning material to be ejected from the contact area.

An arc can also be initiated by two electrodes initially in contact and drawn apart as the contacting surfaces are melted and a gap is form, allowing an arc to be "drawn" between them. Arcs have also been called 'thermal sparks', but this name is confusing since all sparks are 'thermal' and emit sufficient heat to ignite fuel vapors. Thus, sparks are related to voltages and arcs are related to currents.

Arcing and sparking within the fuel vapor space of a fuel tank is one of the primary concerns of the fuel tank protection designer. The distinction between arcing and sparking is worth reviewing. Arcs occur when current flows through the interface between two conductive objects that make inadequate or intermittent electrical contact. Such a condition may exist at the interface of a fastener with structure (as at an access door) or between two structural components (such as a spar and rib). A spark, on the other hand, can only exist where two structural elements are isolated from each other, such as between a spar and wing skin that are bonded together by an electrically nonconductive adhesive. Current through a fuel tank may result in a difference of potential between these structures, causing a spark to jump across the bond line. In most tank designs, sparks are less likely than arcs.

While the mechanisms described above have been postulated as the probable cause of the in-flight fuel tank explosions associated with lightning strikes, the exact location or source of ignition has not been positively identified in many of these accidents, since evidence left by an arc or spark is difficult to identify, especially in the midst of charred debris left by the post-ignition explosion and sub-sequent fire damage. A spark with sufficient energy to ignite fuel vapor may be too small to leave any residual evidence of its occurrence, such as pitting on a metal surface. Ignition could also occur outside the fuel system, for example, at a fuel vent outlet, from which a flame could propagate through vent pipes to the inside.

Fuel Flammability

Fuel cannot ignite until some of it has become vaporized and mixed in a combustible ratio with oxygen or air. Thus, the flammability of the vapor in a fuel tank varies according to the concentration of evaporated fuel in the available air. Reducing the fuel-to-air ratio below the lower flammability limit produces a mixture that is too lean to burn. Likewise, if the fuel-to-air ratio is too high, the mixture will be above the upper flammability limit and too rich to burn. Between these limits, there is a range of mixtures that will ignite and burn. These limits define a flammability envelope, within which a fuel and air mixture will burn.

When only equilibrium conditions are considered, the particular fuel-to-air ratio that can exist in a tank is determined by the temperature of the fuel and the altitude of the aircraft. The temperature determines the vapor pressure, and thus the quantity and composition of the fuel vapor as smaller hydrocarbons will vaporize at lower temperatures, and the altitude determines the quantity of air. The combination of temperature and altitude determines whether the vapor in the ullage (the space above the liquid fuel from which fuel has been drained) of a fuel tank is flammable or nonflammable.

Research concerning fuel vapors and their flammability characteristics has included laboratory investigations of fuel vapors, both in laboratory-type containers and in aircraft fuel tanks during actual flight. The findings of some of this research are discussed below.

Nestor's study

One of the most comprehensive laboratory studies is that of Nestor [7.1], who paid particular attention to the behavior of fuels in aircraft tanks and flight environments. He found wide variations in the amount of fuel that can exist in the vaporized state as a result of the wide variety of temperatures, pressures, and motions associated with flight.

Flammability envelopes. The relationship of temperature and altitude to tank vapor flammability is illustrated by the flammability envelope. A typical flammability envelope is shown in Fig. 7.1 [7.2].

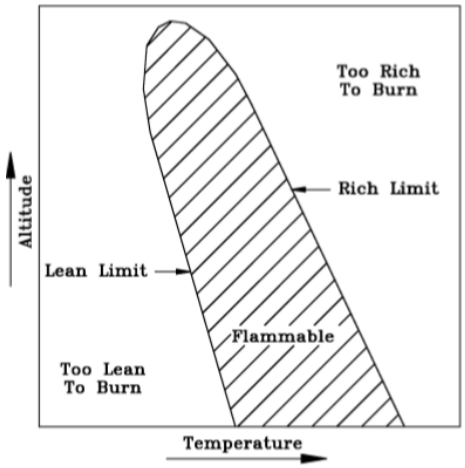

Fig. 7.1 Typical flammability envelope of an aircraft fuel [7.2].

Types of fuel

Almost all aircraft with reciprocating engines use 100 octane aviation gasoline ("Avgas"). Turbine engine fuels, however, come in two broad categories based on their distillation curves: aviation kerosene and wide-cut fuels. The aviation kerosene includes Jet A, Jet A-1, and JP-5. The wide-cut fuels, which have a higher percentage of smaller, more volatiles components, include Jet B and JP-4. Turbine powered commercial aircraft in the United States and in some other countries are fueled with aviation kerosene. The United States Air Force (USAF) converted to JP-8, starting with its European partners, and finishing in the US in the mid-1990s. The US Navy has used JP-5 for aircraft carrier operations because this fuel has a high flashpoint and is less likely to produce a flammable vapor, when stored aboard ship, than the wide-cut fuels, which evaporate flammable vapor concentrations at lower temperatures.

The flammability limits for aviation gasoline and the turbine fuels are presented in Fig. 7.2 [7.3]. As shown in this figure, the lean limit for the aviation kerosenes at sea level ranges from 40 °C to 60 °C and the rich limit ranges from 85 °C to 105 °C. For the wide-cut fuels, the lean and rich limits at sea level are about -30 °C and 10 °C, respectively. For aviation gasoline, the lean limit is approximately -40 °C and the rich limit about -5 °C.

The volatility of each of the above fuels is related to its vapor pressure. Fuels with higher vapor pressures, such as JP-4, release sufficient vapor at lower temperatures to form a flammable mixture, thus lowering the left boundary of the flammability envelope because it contains more, smaller, hydrocarbons. Fuels with lower vapor pressures, such as JP-5, must be at a higher temperature to release sufficient vapor to form an ignitable mixture.

The flammability of a fuel as a function of its temperature can be visualized by considering one of the standard test methods for flash point, ASTM D56, which determines the minimum temperature of the liquid fuel required to create a flammable mixture at 1 atmosphere. In this test, a small amount of fuel is contained in a closed cup with a sliding lid opening. The fuel is heated via a gas burner in a water bath and the temperature of both the water and fuel are measured. As the temperature of the fuel is increased, the tip of a flame situated above the lid is brought in contact with the fuel vapor as the sliding lid is opened, exposing a mixture of the fuel vapor and surrounding air to the flame. As the temperature of the increases the amount of fuel vapor increases until the mixture reaches the lower flammability limit and ignites.

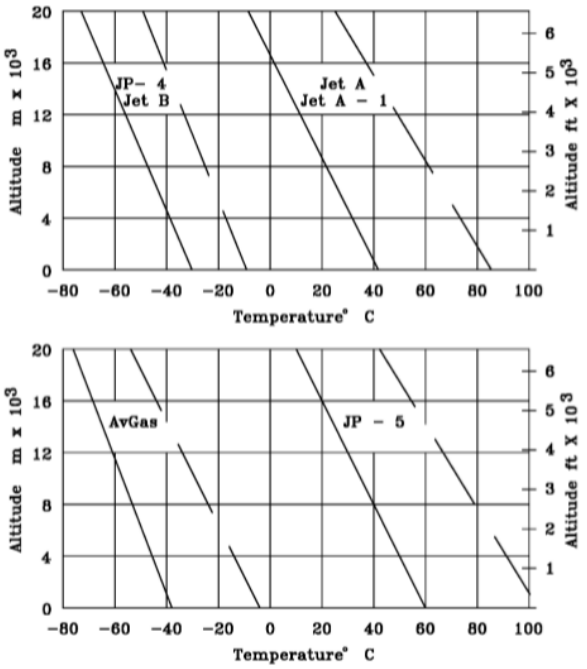

Fig. 7.2 Flammability limits for typical aircraft fuels as a function of altitude and temperature [7.4].

Some other related aspects relating to fuel vapor flammability are discussed in the following paragraphs.

Dissolved oxygen

Oxygen that is dissolved in fuel during ground pumping and filtration processes is carried into the tank during refueling operations. At flight altitudes, where the ambient pressure is lower, some of this oxygen comes out of the fuel and increases the oxygen content of the fuel vapor in the tank ullage. The ignition of oxygen-enriched fuel vapor requires less spark energy than the ignition of unenriched vapor. The influence of oxygen enrichment on the ignition sensitivity of fuel vapors is shown later in this chapter.

Inerting

A number of methods have been developed to inert the ullage in aircraft fuel tanks to preclude ignition and or keep flame fronts from enlarging and spreading if there were a source of ignition. These involve filling the fuel tank ullage with a non-flammable atmosphere, for example by displacing the fuel vapor and air mixture in the ullage by nitrogen enriched air such that the oxygen concentration is below the concentration that will support ignition or continued combustion. Gases including helium, carbon dioxide, and halons, when added to the atmosphere in the tank ullage in varying amounts will create an inert mixture [7.5]. Nitrogen inerting systems utilizing onboard nitrogen storage were developed and flight tested on the USAF C-141 and C-135 aircraft [7.6] among others.

Extinguishing

Extinguishing involves detecting a flame and rapidly filling the tank with an inert gas, such as halogen, that extinguishes the flame. Historically, halogens have been used for this purpose.

Mixing of fuels

There are several important factors that may alter the flammability limits of the vapor inside an aircraft fuel tank from those shown in Fig. 7.2. One of these is the mixing of one type of fuel with another. Fig. 7.3 [7.4] shows, for example, the flammability limits determined by Nestor of a mixture comprised of 85% Jet A and 15% Jet B fuels. Such a mixture might form in an aircraft that initially fueled with Jet B then subsequently refueled with Jet A. The lean limit of the flammability envelope of the resulting mixture in the tank would be 'lower' (further to the left in the graph in Fig. 7.3) than if the tanks had contained 100% Jet A fuel. If this happens, the resulting envelope encompasses the altitudes and temperatures where most lightning strikes to aircraft have occurred.

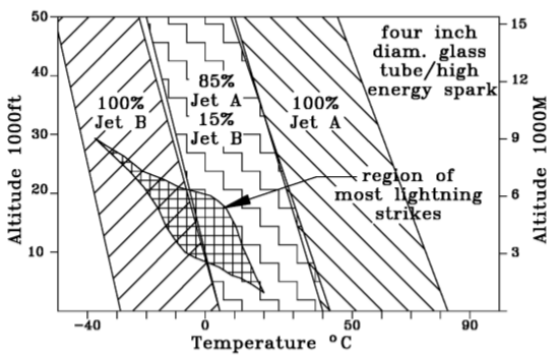

Fig. 7.3 Flammability envelope of the fuel blend 85% Jet A/15% Jet B, and altitude/temperature region of most lightning strikes [7.4].

Agitation

Agitation is another way that the flammability envelopes might be altered from those shown in Fig. 7.2, for the envelopes are valid only when the mixture is stabilized. Agitation of fuel, or spray from a pump or pressurized fuel line, can extend the flammability envelopes in Figs. 7.2 and 7.3 to the left, into colder temperatures. Thus, while Figs. 7.2 and 7.3 indicate that the vapor-air mixture in the tanks of an aircraft fueled with Jet A would be too lean to support combustion for the conditions under which most lightning strikes occur, there can be no assurance that this is always so, since the fuel could become agitated during flight.

Foams

The use of reticulated foams in fuel tanks to prevent the propagation of a flame front has been shown to be very successful in some applications. The foams usually add little weight and displace less than 3% of the fuel volume in the tank. The foam cools and slows the speed of the flame, causing it to die from oxygen starvation. Unfortunately, some of the foams accumulate enough static charge (from the friction of fuel flowing through them during refueling) to produce sparks that ignite fuel vapors [7.6]. Each time such an ignition occurs, some of the foam can be lost. After many hours of flight, the foam eventually burns away to the extent that it no longer provides protection. A conductive foam has been developed that significantly reduces the likelihood of internally generated sparks. Foams have been employed for protection against gunfire in military airplanes but have not, reportedly, been used in commercial transport airplanes.

Extinguishing systems have been incorporated in the design of several fighter aircraft to provide protection against fuel ignition due to enemy gunfire.

Ignition thresholds

Lewis and Von Elbe [7.7], in studies made in the 1950's and 1960's for the US Bureau of Mines, found that the minimum ignition energy of most light hydrocarbon fuels (methane, propane, pentane, butane, hexane, heptane, etc.) was 220 microjoules, a value which is the basis for the present 200 microjoule criteria for a fuel vapor ignition source threshold. It is however, important to note that no mixture of those gases in standard air at room temperature and atmospheric pressure is ignitable with a 200 microjoule spark.

Investigations by Crouch [7.8] to determine minimum ignition thresholds of the hydro-carbon fuels commonly found in aircraft fuel tanks, have shown that the 200 microjoule criterion would not always cause an ignition.

The test data, for a 1.2 stoichiometric mixture of propane with 20% oxygen, is plotted Fig. 7.4. Tests were made with sparks of several energy levels. The horizontal lines represent the range of probability for each energy level. Energy levels at which no ignitions occurred (0%) are plotted as horizontal lines between the left vertical axis and the probability that would have resulted had one more test produced an ignition. Levels with all ignitions (100%) are plotted between the right vertical axis and the probability that would have resulted had one more test produced no ignition.

In Crouch's experiments, the probability of ignition was increased by raising the oxygen content of the mixture. Crouch found that a 200-microjoule spark would ignite a 30% oxygen mixture between 70% and 80% of the time as shown in Fig. 7.4.

Apparently, if a 200-microjoule spark energy is to be used as a pass/fail threshold for sparking in candidate fuel systems, then tests should be conducted using an enriched oxygen test mixture. If a standard 1.2 stoichiometric mixture were used with a fuel vapor that was 20% oxygen, sparks of less than 700 to 800 microjoules would be unlikely to be detected. 'Detection', in this case, means that the test mixture is ignited.

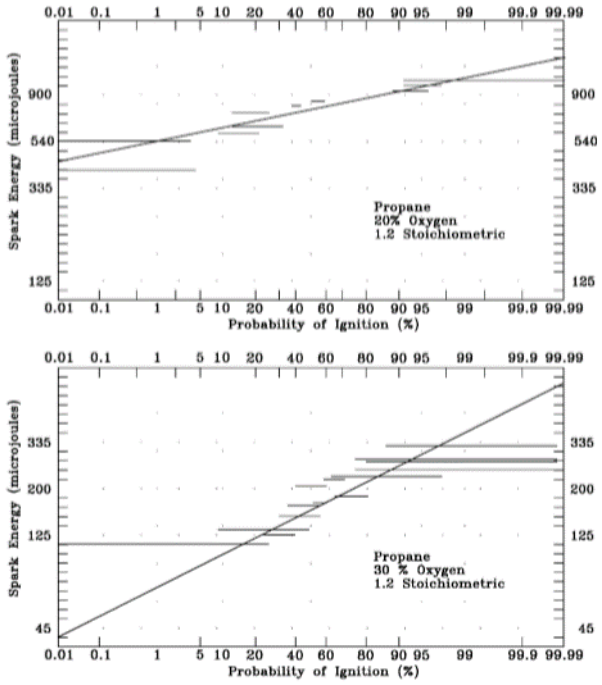

Fig. 7.4 Probability of ignition versus spark energy.
(a) Propane, 20% oxygen, 1.2 stoichiometric.
(b) Propane, 30% oxygen, 1.2 stoichiometric.

Although a 700 to 800 microjoule spark energy level is 3.5 to 4 times the criterion presently in use, it is still extremely low compared to the many joules of energy that can be released in a lightning-related arc. It is easy to see how even a small portion of the energy available from lightning currents in structures containing fuel can cause fuel vapor ignition and a consequent safety of flight hazard.

Current-time threshold

While the minimum energy concept helps greatly in evaluating the hazard from sparks, the lightning environment is described in terms of current waveforms, rather than in terms of energy.

Translation of aircraft structural current elements that flow in small arcs into energies, or even specific energies, is a formidable task, as would be the task of measuring energies dissipated in small arcs. Attempts have been made to evaluate the probability of ignition in terms of current in an arc, but a review of that data indicates that it does

not appear to be reliable and that evaluations in terms of current (magnitude and waveform), rather than energy, are too simplistic to be useful. Fig. 7.5 shows the results of one set of experiments [7.9], but these results are likely to be unique to the electrode configuration used in these experiments.

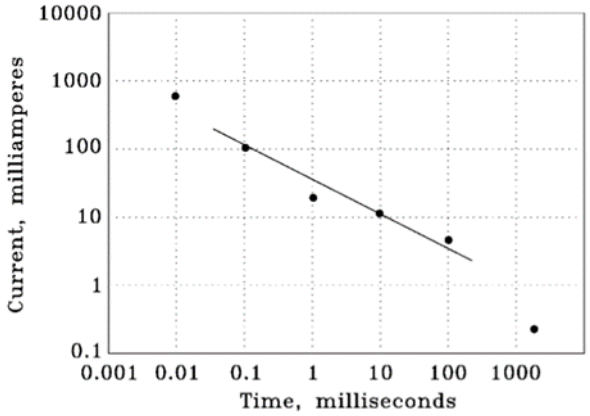

Fig. 7.5 Ignition current due to an arc as a function of pulse duration [7.9]

It is sufficient to recognize the importance of carefully controlling the lightning currents flowing in fuel tank structures and the induced effects of the lightning currents, since even very small percentages of the total lightning current might produce incendiary arcs or sparks. The following subsections describe some of the potential ignition sources that exist in aircraft fuel systems and the methods of preventing them. Ignition sources in the exteriors of fuel tank walls are addressed first, followed by other sources that may exist inside fuel tanks.

7.3 Protection Design

The user of protection design methods described in this handbook should note that the FAA regulation for protection of transport aircraft fuel systems, reviewed in §5.2.2 requires that catastrophic failures of protection designs be less probable than once in 10^{-9} flight hours, and that fault tolerance be provided against protection failures due to manufacturing escapes, service environments and maintenance activities. Some examples of possible failures and fault tolerant designs are included in the guidance that follows; however, no attempt is made to provide an exhaustive list of examples. Further guidance for this failure analysis, fault tolerant design process and continued airworthiness procedures is found in FAA Advisory Circular 25.954-1 [5.4] and SAE ARP 6205 [5.22]. Designers of helicopters and small airplanes do not have to meet this fault tolerance requirement, but continued airworthiness is essential for all fuel system lightning protection designs.

7.3.1 Fuel System Vent System Protection

The temperature of a lightning channel far exceeds that required to ignite a flammable fuel-air mixture; therefore, any direct contact of the lightning flash with such a mixture must be considered an ignition source. Since fuel tank vents are the primary means by which a flammable fuel vapor can be exposed to the outside of an aircraft, a considerable amount of research has been undertaken to evaluate the possibilities of lightning ignition of fuel vent vapors.

Basic Vent Outlet Studies

One of the first fuel vent studies was conducted for the US National Aeronautics and Space Administration (NASA) by Lockheed-California Company and the Lightning and Transients Research Institute (LTRI) in 1963 [7.10]. In that program, fuel-air concentrations in the vicinity of aircraft vent outlets of several configurations were measured and mapped under various conditions of tank vapor fuel-air ratio and effluent velocity. The tests were performed in a wind tunnel producing an airflow of up to 100 knots. Mast vents discharged into wakes and into free air streams were tested, as well as flush vents discharging into boundary layers, as shown in Fig. 7.6 [7.10].

The study showed that a vent discharging into a free air stream provides the greatest dilution of fuel vapor and thus has the smallest flammable region of the vent configurations tested, but it also showed that flammable mixtures could exist in the immediate vicinity of each type of vent outlet.

Dilution profiles

A typical mixture concentration profile for the area aft of a flush vent outlet is shown in Fig. 7.7 [7.11]. Dilution of the original effluent by air to 30% or less of the initial concentration might well lean it out of the flammability envelope, depending on its original fuel-air concentration. Thus, dilution to a nonflammable mixture probably occurs at a distance of one vent diameter or more from the vent outlet. This finding suggests that a lightning strike or associated streamer must occur very near to the edge of a vent outlet for an ignition to occur.

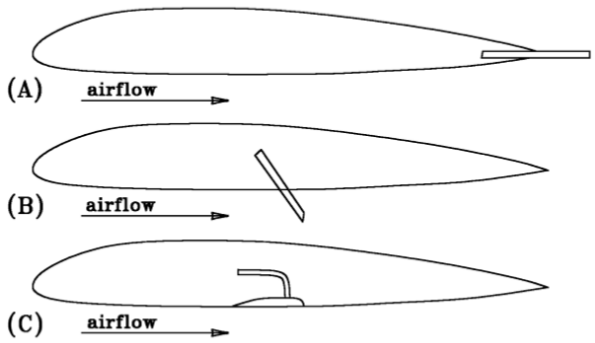

Fig. 7.6 Three general classes of fuel vent exit.
(A, B) Mast or extended outlets.
(C) Flush vent outlet.

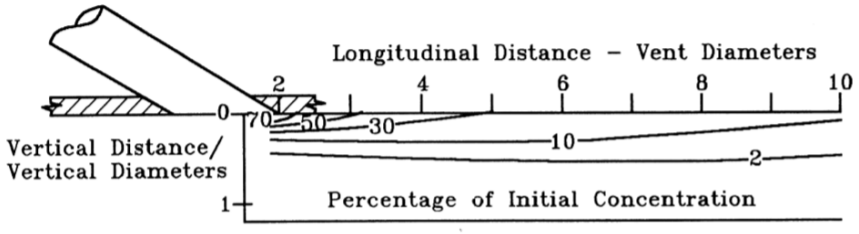

Fig. 7.7 Typical profile of vent effluent in air stream aft of a flush vent outlet.
-Profiles vary according to boundary layer thickness and velocities of effluent and air stream.
-Boundary layer thickness = 0.50 vent diameters
-Vent exit velocity = 0.1 times free stream velocity.

Flame arrestors

The above prediction was confirmed in the second part of the 1963 Lockheed - LTRI study [7.12]. During these tests, lightning strikes were applied to flush vent outlets from which flammable fuel-air mixtures were exiting into a 100-knot airstream. The tests were performed with and without flame arrestors installed. These flame arrestors were being evaluated as possible protective devices.

They consisted of a parallel bundle of small diameter metal tubes inserted into the vent line near the vent outlet, as pictured in Fig. 7.8(a). An alternate construction utilized a series of baffles extending into the fuel vapor flow, as shown in Fig. 7.8(b). The objective, in either case, was for the tubes or baffles to cool the flame enough to extinguish it.

The test results showed that it was only possible to ignite the vent effluent in the 100-knot airflow when the lightning arc was delivered directly to the lip of the vent outlet. Arcs delivered to points as close as 25 mm (1 in) away did not ignite the effluent. The results also showed that flames ignited by the strikes to the outlet could propagate inward through the flame arrestors when they were installed near the vent outlet. While the flame arresters did extinguish some flames ignited at the outlet, they did not stop all such flames. Evidently, the intense blast pressures of the lightning arc forced the flame through the arrester.

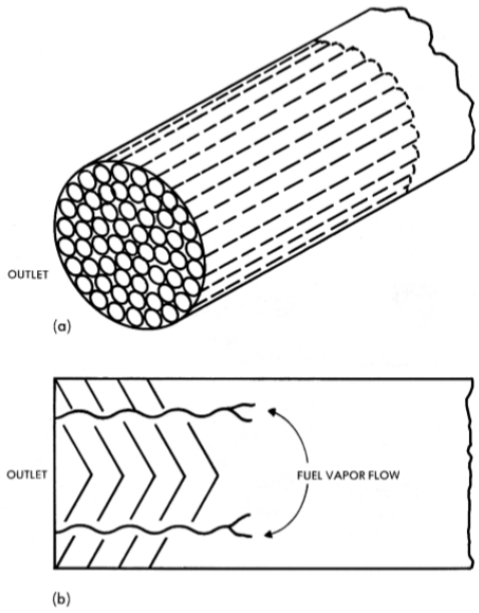

Fig. 7.8 Flame arrestor configuration
(a) Tubular construction.
(b) Baffle construction.

FAA/Atlantic Research studies

The crash of a Boeing 707 aircraft near Elkton, Maryland, on December 8, 1963, after being struck by lightning [7.12], prompted another investigation into the possibility of lightning-initiated fuel tank vent fires. This investigation, sponsored by the FAA, was undertaken by Bolta and others of the Atlantic Research Corporation with the support of Newman and others of the LTRI [7.13]. The work focused on the Boeing 707 wing tank and vent system, with the objective of determining the conditions under which ignition of fuel vent effluent allows flames to propagate back through the vent duct and surge tank and from there into the reserve tank. Another objective was the evaluation of various protective measures, including flame arresters and flame extinguishing systems.

Unlike the earlier Lockheed program, the vent was tested in still air, the rationale being that, if an ignitable effluent is assumed to be at the outlet, attachment of the lightning arc to the lip of the vent outlet would ignite the vent efflux no matter what the airflow condition was. The ignitable mixture was a 1.15 stoichiometric mixture of propane and air.

Thermocouples were installed along the vent line to determine the time at which a flame passed by, to enable calculation of flame front velocities. It was important to know these velocities because the operation of an automatic extinguishing system that was being designed at the time depended on the elapse of sufficient time between the initial sensing of a flame at a vent outlet and the activation of an extinguisher in the surge tank located about 1 m (3.3 ft.) down the vent line.

The simulated lightning tests confirmed that a strike must occur close to the vent outlet for ignition to occur.

Flame velocities

Average flame velocities of up to 45 m/s were recorded between the vent outlet and the surge tank when simulated lightning strokes of 175 kA and 1.5 x 10^6 A^2s were applied during the tests described above. These tests simulated a severe stroke current, such as might be experienced at a vent outlet located in Zones 1A, 1C or 1B.

Other tests were performed with the high current directed to the desired spot through a 100 mm (4 in) wide aluminum foil tape, which exploded as the current passed through it. The resulting flames reached higher velocities of up to 126 m/s (413 ft/s), but the exploding tape may have caused the higher flame speeds, creating conditions more severe than occur during a natural lightning strike attachment, where an arc alone is the ignition source.

When lower amplitude currents of 44 kA and only 0.001 x 10^6 A^2s were applied, ignitions still occurred, but the highest average flame velocity was 17.4 m/s (57.1 ft/s), which indicates that the intensity (and resulting shock wave) of the lightning current is one of the factors that affects the flame velocity. The 44 kA current was described by Bolta as a "high-voltage" discharge [7.13] because it was applied with a Marx-type, high voltage generator. The ignitions occurred as soon as the 13 cm (5.1 in) or 30 cm (11.8 in) air gap between the discharge electrode and vent outlet flashed over. The current level affects the velocity of the flame front, but the energy required to cause the ignition is delivered at the start of the current.

Flame arrestor performance

Various flame arresters were tested, including some made from corrugated aluminum and stainless steel, a ceramic material, and various copper screens. None of them could stop a flame ignited by a simulated stroke current when installed near the outlet of the vent line. Arresters wound from corrugated stainless steel 12.7 mm (0.5 in) or 25.4 mm (1 in) deep did stop flames when installed about 1 m (3.3 ft.) upstream from the vent outlet near the surge tank as shown in Fig. 7.9 [7.14], even when the flames travelled in the vent tube at average speeds as high as 122 m/s (400 ft/s). Other arresters, made of screens and ceramics, did not stop flames ignited by the simulated strokes.

A flame suppression system developed by Fenwal, Inc. [7.15] for industrial applications was also tested in this program. This system consisted of a fast-acting sensor for detecting the presence of a flame and a set of canisters containing a quantity of liquid suppressing agent for release into the surge tank by an electric detonator.

When the sensor detected the light of the flame, it sent a signal to the detonator, which dispersed the extinguishant into the tank within a few milliseconds, before the flame had reached the tank.

This system effectively suppressed flames that traveled slowly enough, 30 m/s (100 ft/s) or less, to give the system time (18 ms) to react, but it did not stop flames that had gone past the surge tank by the time the extinguishant was released. In the latter case, the extinguishant might still have put out the fire in the surge tank, but the flame front, on its way through interconnecting vent lines to the fuel tanks, would have passed out of the reach of the extinguishant

The Atlantic Research-LTRI program also included an investigation of arc plasma propagation into the vent line, but this was inconclusive because of instrumentation difficulties.

Effect of ice on flame arrestor performance

The effect of ice formation on the performance of a flame arrester was also considered [7.16], resulting in the conclusion that unacceptable icing would occur only when the worst combination of atmospheric and flight conditions existed. This conclusion was based on analysis only and should be verified by flight tests. Aircraft icing, however, is known to have been underway when some lightning strikes have been reported, so the effects of ice on any lightning protection feature should be considered.

Airflow velocity effects at vent outlets

In the Atlantic Research-LTRI and Lockheed programs discussed above, it was assumed that lightning could attach to the lip of a vent outlet. However, no attempt was made, in either program, to establish whether or not this assumption was likely for an aircraft in flight or, if it were correct, how often it would occur.

Neither the Elkton B-707 aircraft [7.12] nor any other aircraft known to have been struck by lightning has ever shown any physical evidence of lightning attachment directly to a fuel-system vent outlet. The outlet in the B-707, while located near the wing tip, is not located at the very tip of the wing where lightning attachments occur most often. It is therefore unlikely that flush-mounted vents, such as those on the B-707 or other aircraft, would receive direct (i.e. initial) strikes.

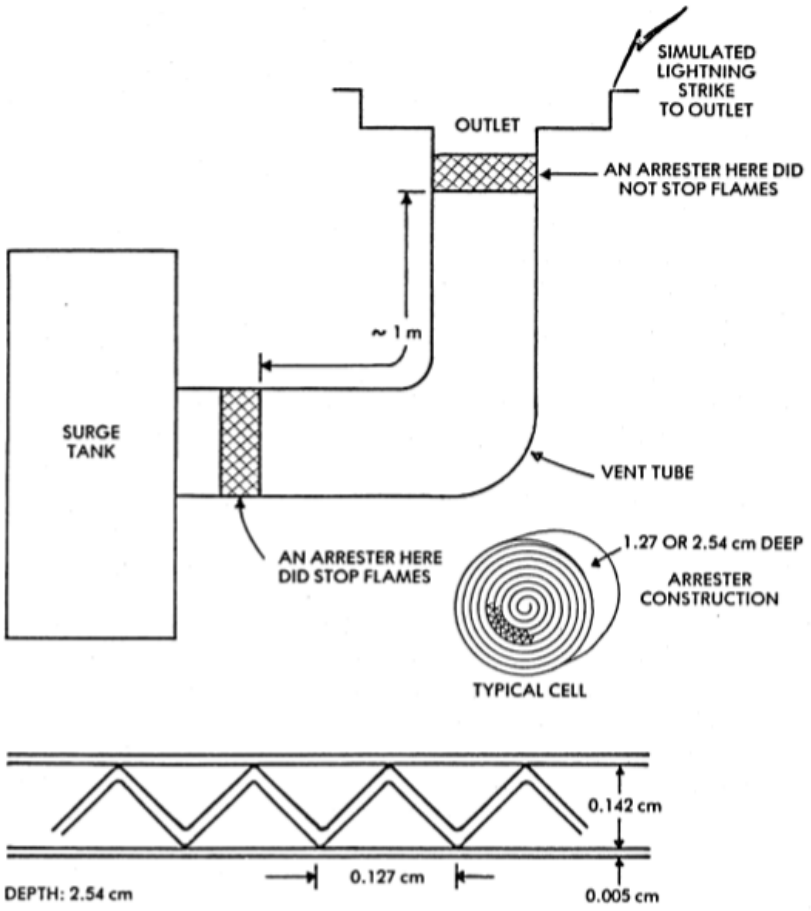

Fig. 7.9 Successful flame arrestor installation in simulated vent tube of a transport aircraft.

The question then arises as to whether a lightning flash channel could sweep across a vent outlet from another attachment point and ignite the effluent. Answers to this question were sought by Newman and others, who undertook an experimental program [7.17] between 1966 and 1967. In this program, simulated lightning strikes were delivered to a B-707 wing tip and vent assembly were used as a lightning test specimen to learn more about the possibility of fuel vapor ignition by this mechanism. This study also explored the degree to which air flowing past the vent outlet at realistic speeds would make ignition unlikely, even if a sweeping lightning channel did attach to the outlet.

The results showed that ignition of fuel vapor at a vent outlet is unlikely, even if a sweeping lightning channel did attach to the outlet.

In earlier programs [7.10, 7.13], ignitions had been obtained nearly 100% of the time when the vent outlets were in still air, but Newman found that ignition of a 1.5 stoichiometric propane-air mixture by a 48 kA, 0.009 x 10^6 A^2s direct strike occurred only once in 34 shots with a 90-knot (46 m/s, 150 ft/s) airflow over the outlet. No ignitions occurred out of 200 shots with the vent outlet immersed in a 200 knot (100 m/s, 330 ft/s) airflow. When strokes of longer duration were swept across the vent outlet by the 90-knot airflow, the effluent was ignited 11 times out of 15 tests, but when the velocity of the airflow was increased to 200 knots, only 2 ignitions occurred in 46 tests.

Nearly all of Newman's tests were performed under the most vulnerable effluent condition, which was found to be a 1.5 m/s (5 ft/s) flow out of the vent outlet, such as might exist when an aircraft is climbing. Since more than half of all reported lightning strikes occur when the aircraft is either in level flight or descending, and since most aircraft climb at well over 90 knots, the probability of an in-flight ignition from a direct strike to a vent outlet must be very unlikely. Newman's investigation did show that a channel

sweeping across the vent outlet might have a greater chance (2 in 46) of igniting an effluent, even under climb conditions at the more realistic speed of 250 knots.

This result demonstrates the importance of locating vent outlets away from both initial strike and swept channel zones on the aircraft. Most civil aircraft are limited by air traffic control (ATC) regulations to speeds of 250 knots at flight altitudes below 3 048 m (10 000 ft). This emphasizes the importance of proper zoning of the aircraft, and especially the regions where initial lightning strikes are likely.

Explosive Ignitions in vent systems

In the program described above, Newman and his colleagues conducted a test [7.18] in which a strike to the vent outlet produced indications of unusually high flame velocities and severe deformation of the vent outlet, indicating much higher pressures than normal. They cite a similar case in another program, in which flame velocities more than 300 m/s (1 000 ft/s) were measured. The implication of these findings is serious, because an arrester or surge tank protection system capable of extinguishing the lower velocity flames may not be able to stop flames traveling as fast as 300 m/s.

Kester's study

Kester and others [7.19] attempted to reproduce these high flame velocities in a 14 cm (5.5 in) simulated vent tube, but did not measure flame velocities higher than 20 m/s (65 ft/s) in this system, even when severe, 180 kA, 1.0 x 10^6 A^2s strokes were applied. These velocities were comparable to those measured in the Atlantic Research-LTRI program of 1964.

Kester and his colleagues also reported one explosive ignition when a stroke of 195 kA was delivered to the vent outlet. It was found that the 195 kA stroke current had induced a voltage in instrument wiring that was high enough to break down the insulation around several pressure probes inside the vent line. The vent outlet and parts of the surge tank were badly deformed, even though they were made of 6.4 mm (0.25 in) steel. Again, much higher than usual pressures were indicated.

The explosion in the Kester program serves as a warning that a similar explosion might arise from the presence of multiple ignition sources in an actual fuel system, unless care is taken to design the system so that it is free of such sources. It is not unreasonable to expect simultaneous arcing at multiple locations when lightning current flows through a fuel tank structure that has not been designed and verified to be free of arc sources. The same is true of spark sources at, for example, multiple fuel quantity probes, if adequate protection is not provided.

Gillis' study

The question of whether these explosive ignitions could occur in actual fuel tank vent systems was of such importance that the FAA undertook yet another study of flame propagation in vent systems.

The work, conducted by Gillis [7.20], expanded upon earlier research by including the study of flame behavior in the long vent lines leading inboard from the surge tanks (in wingtip areas) to the wing and center tanks of a typical transport aircraft vent system [7.21]. Gillis did not use simulated lightning arcs for an ignition source but, instead, discharged 100 J of electrical energy into a spark plug at the vent outlet. This is much less energy than would be released by a lightning arc of the same length. Nevertheless, Gillis recorded flames [7.22] that had accelerated to 300 m/s (1 000 ft/s) far inboard when the simulated aircraft-fuel vent system was in climb condition.

The total number of authentic tests performed by Gillis was 13, of which 11 resulted in flame velocities of 150 m/s (500 ft/s) or higher. The propagation of such high-speed flame fronts is perhaps best explained in Gillis' own words [7.23]:

> "When an explosive gas is confined in a channel and ignited, the flow induced by the thermal expansion of the gas in the combustion wave is restricted by the channel wall. Consequently, the flow attains much higher velocities than under conditions of free expansion in an open flame, and flame and flow commonly augment each other by a feedback mechanism as follows: stream turbulence, however slight it may be initially, produces a wrinkling of the combustion wave surface; the resulting increase of surface increases the amount of gas burning per unit time, namely, the flow of gas in the channel; this in turn produces more turbulence and hence, increased wrinkling of the wave, and so on, so that the progress of the combustion wave becomes non-steady and self-accelerating. In addition, the burning velocity increases as the unburned gas ahead of the flame is preheated and precompressed by the compression waves that are generated by the mass acceleration in the combustion wave. The compression wave is initially a comparatively weak pressure wave, which is overtaken and reinforced during its travel by numerous other pressure waves originating in the combustion zone.
>
> The coalescence of these pressure waves into a strong shock front in a configuration which is deadended can result in a reflection of the shock wave back toward the combustion zone. The effect of the

passage of this reflected shock wave through the combustion wave is similar to the effect of a sudden release of pressure by a rupture of a diaphragm. A rarefaction wave propagates backward into the unburned gas and a jet of unburned gas develops which penetrates deeply into the burned gas. The shear between burned and unburned gas in this flow configuration produces extreme turbulence so that a sudden large increase in the burning rate occurs."

The study showed that a vent discharging into a free air stream provides the greatest dilution of fuel vapor and thus has the smallest flammable region of the vent configurations tested, but it also showed that flammable mixtures could exist in the immediate vicinity of each type of vent outlet.

In three of the 13 tests mentioned above, localized pressures were developed of sufficient intensity to distort 1 to 1.5 m (3 to 5 ft.) sections of the rectangular vent duct. A subsequent hydrostatic pressure test of a 1 m (3.3 ft.) section of similar duct showed that a pressure of approximately 475 psig was required to produce similar distortion. This pressure exceeds the structural limitations of typical aircraft fuel tank and vent structures.

Gillis concluded that the surge tank located just inboard of the vent outlet was a factor contributing to the high flame speeds because, when a flame reaches it from the vent outlet, the pressure permitted to build up in it serves as a force to drive flames rapidly down the vent lines towards the fuel tanks. This creates turbulence in these ducts which further accelerates flames down the ducts.

Gillis' work demonstrates that flames can travel at sonic velocities in typical transport aircraft vent systems, producing damaging overpressures. Flame arrestors have been developed that are capable of stopping flames ignited at vent outlets, but their effectiveness is very much related to their installations in specific vent systems so lightning testing of them in such installations, and with typical aviation fuel vapors, is necessary to confirm their ability to quench lightning-ignited flames.

The research just summarized demonstrates the importance of eliminating any source of ignition within a fuel vent system, or elsewhere within the fuel tanks and system.

Summary and recommendations regarding vent System protection

Table 7.1 summarizes the ignition and flame velocity results for each of the research programs just discussed. A few important conclusions and protection considerations can be drawn from the research.

1. Although there has been no positive evidence that a lightning strike has ever ignited a vent effluent on a transport type aircraft in flight, several in-flight explosions have occurred following strike attachments within a meter or so of vent outlets. This suggests that other ignition sources, not associated with the vent outlets, may have been the cause of some accidents.

2. For ignition to occur at a vent outlet, a lightning channel must attach directly to, or within a few centimeters of, the edge of the outlet. Ignition may also occur from a flash which has swept back over a vent outlet from an initial attachment point elsewhere on the aircraft. This would indicate that it is desirable to locate vent outlets in areas not subject to direct or swept flash attachments. Guidance for locating direct attachment and swept flash zones has been provided in Chapter 5.

3. Flame arresters of the corrugated steel type shown in Fig. 7.9 have been the most effective in stopping flames. Flame arrester performance is most satisfactory when the arrester is located some distance away from the vent outlet, so that blast forces from the lightning arc will not propel flames through the arrester.

4. An arrestor located anywhere in the vent system can become clogged with ice. The probability of this should be evaluated, preferably by in-flight tests under the expected environmental conditions. Electrical de-icing devices may have to be added to the vent system if icing is possible.

5. Ninety-degree bends in the vent tubes should be avoided because they expand the turbulence and surface area associated with propagating flames and thereby increase the velocity of propagation. Instead, straight or smoothly curved ducts should be used because they minimize the possibility of explosive flame propagation.

6. The best way to protect a fuel vent outlet is to locate it in a Zone 3 surface. It is preferable to use a recessed or flush outlet instead of a protruding tube outlet because the latter could become a source of corona or streamering that might promote lightning attachment.

Table 7.1
Summary of Results of Lightning-initiated Flame Propagations

Program	Amplitude (kA)	Action Integral ($10^6 A^2 s$)	Airstream Velocity (knots)	Attachment Point	Results
1963 Lockheed LTRI	100	0.069	100 (50 m/s)	lip of vent outlet	100% ignitions and flames propagation with and without flame arrester installed at vent outlet.
1964 Atlantic Research LTRI (Bolta, et al)	175	1.5	0	lip of vent	100% ignitions and flame propagation up to 45 m/s, and at 126 m/s when ignited by an exploding foil. Flame arrestor stopped these flames when installed 1 meter upstream from outlet.
1964 Atlantic Research LTRI (Bolta, et al)	44	0.001	0	lip of vent outlet	100% ignitions and flames propagating up to 17.4 m/s (no arrestor).
1966 LTRI (Newman, et al)	48	0.009	90 (46 m/s)	lip of vent outlet	1 ignition and flame propagation out of 34 direct strokes to vent outlet (no arrestor.)
1966 LTRI (Newman, et al)	48	0.009	200 (100 m/s)	lip of vent outlet	0 ignitions out of 200 direct strokes to vent outlet.
1966 LTRI (Newman, et al)	58	0.172	90 (45 m/s)	swept access outlet	11 ignitions out of 15 swept strokes across vent outlet.
1966 LTRI (Newman, et al)	58	0.172	200 (100 m/s)	swept access outlet	2 ignitions out of 46 swept strokes across vent inlet.
1966 LTRI (Newman, et al)	58	0.172	250 (130 m/s)	swept access outlet	No ignitions out of 2 swept strokes across vent outlet.
1966 Dynamic Science-GE (Kester, et al)	195	1.0	0	lip of vent outlet	100% ignitions and flames propagating up to 20 m/s.
1969 Fenwal	100 J spark		0	lip of vent outlet	11 ignitions and flame velocities over 150 m/s in 13 authentic tests. Several at sonic velocity (300 m/s).

Strokes to vent outlets only. No ignitions were obtained from strokes away from vent outlet.

The most successful location for a flame arrestor installation seems to be at the surge tank end of the vent outlet tube, as shown in Fig. 7.9. Whatever location(s) are being considered for location of a flame arrestor should be evaluated for effectiveness with lightning tests of the candidate arrestor installed in a physically correct mockup of the installation in the vent system from the outlet to the surge tank (or other fuel tank if a surge tank is not present) since the installation has a significant influence on the performance of the arrestor. Guidance for performance of lightning tests is in SAE ARP 5416A [5.21].

Flame arrestors are utilized for purposes other than lightning protection. One potential hazard that results from the installation of flame arresters is arcing at the flexible vent tube couplings at either side of the arrester, due to lightning currents in the tube. (Arrestors are often in locations where they could share substantial amounts of Zone 3 lightning current with surrounding structure.). This topic is discussed in §3.7.

7.3.2 Fuel Jettison and Drain Pipes

Some aircraft are equipped with a means of dumping or jettisoning fuel overboard, often through a pipe extending into the airstream from a fuel tank, as shown in Fig. 7.10. Such pipes are susceptible to lightning attachment if they are in lightning strike Zones 1B and 2B and, if the pipes extend sufficiently far from aircraft surfaces in Zone 3, they may also attract lightning strikes. There is usually an electrically operated valve installed in the pipe. Since this valve is normally closed, it is unlikely that a flame could travel past it into the fuel tank. However, if this pipe were struck by lightning while fuel was being jettisoned, it is very unlikely that flames could propagate through the pipe into the tank because the fuel jettison pipe is filled with fuel when it is in operation, and there is no vapor available through which a flame could propagate. It is more likely that lightning would ignite the jettisoned fuel spray, and the resulting fire may damage other areas of the aircraft.

Another ignition hazard is posed by the formation of electrical arcs produced by the passage of lightning currents across poor electrical bonds between fuel pipes and fuel tanks or between bulkhead fittings and their fasteners. This danger is increased by the presence of the electrically insulating, corrosion protection sealants commonly applied around fasteners. These sealants sometimes force lightning currents to arc through them in the fastener holes, and the arc products may blow out of the holes, past the fasteners, and into the fuel vapor area.

Electrical bonding jumpers installed across such joints, as illustrated in Fig. 7.11(a), may be adequate to equalize the static charge differentials that sometimes develop in fuel systems, but their inductance is usually too high to prevent lightning current from arcing at fastener head or nut interfaces.

One way to alleviate this problem would be to ensure that there is bare metal on the mating surfaces of the pipe flange and tank, such that some, at least, of these mating surfaces are free of corrosion-resistant finishes or sealants (see Fig. 7.11(b)). The advantage to this approach is that it lets the current flow in the shortest physical path. However, this approach is often incompatible with leakproof and corrosion protection design practices. A second approach would be to provide conductive paths for lightning currents through the fasteners, but to coat the exterior surfaces of the fastener heads or nuts inside the tank with a tough, resilient, fuel tank sealant so that any arcing that occurs at the fasteners would be isolated from the fuel vapors. Guidelines for the use of fuel tank sealant are found in §7.3.5 and §7.3.6.

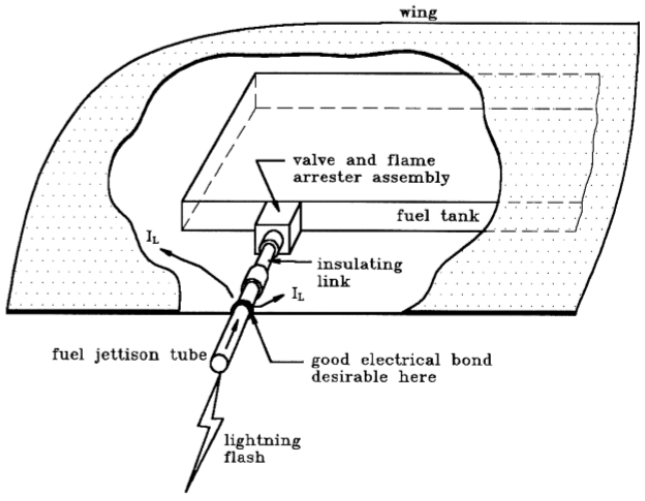

Fig. 7.10 Protection for a fuel jettison pipe.

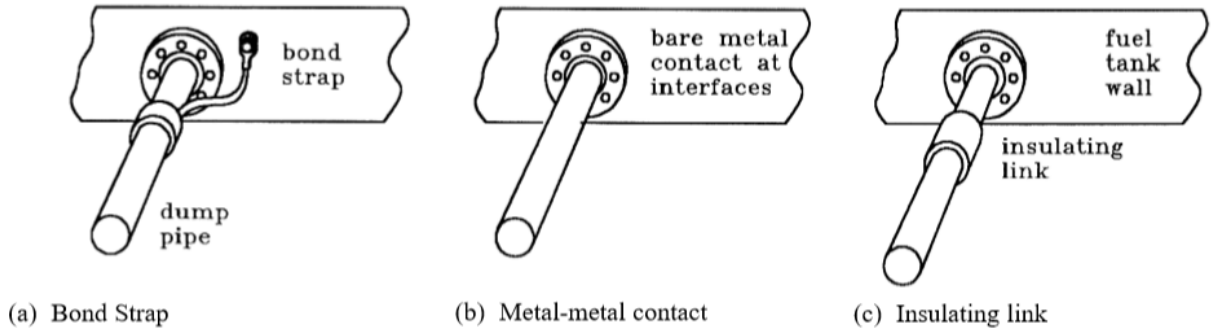

Fig. 7.11 Interface of fuel jettison pipe to fuel tank

Pipe joints should be tested with simulated lightning currents to assure that arcing does not occur.

This testing should be conducted using the test currents and test methods recommended in applicable standards [7.24] for the particular lightning strike zone in which the jettison or drain pipe is located.

Another solution to the problem of arcing at jettison pipe bulkhead interfaces would be to interrupt the current path to the fuel tank, by inserting an electrically nonconductive section of pipe as shown in Fig. 7.11(c). This insulating section, sometimes called an *isolator* would divert any lightning currents entering the jettison pipe to the airframe, thereby eliminating the possibility of sparking at the fuel tank/skin interface. Additional examples of the use of nonconductive pipe sections are discussed in §7.3.7.

7.3.3 Integral Fuel Tank Skins

Integral tanks skins are those in which fuel is in direct contact with the inner surface of the outside skin of the aircraft. Tanks of this type are commonly found in the wings of transport and general aviation aircraft, and also in the wings and fuselages of modern military fighter aircraft. External fuel tanks of the type carried on pylons or wing tips are also of the integral type. Most fuel tanks within rotorcraft are of the bladder type, and many such tanks are located beneath surfaces which are in Zone 3 due to the position of the rotor blades overhead.

If integral tank skins are located in lightning attachment zones, measures must be taken to ensure that a lightning channel attachment on the exterior surface would not melt through the skin or get the inside surface hot enough to ignite the fuel vapor. Integral skins are usually part of the primary structure of an aircraft that is exposed also to lightning currents being conducted between possible lightning entry and exit locations.

Factors that must be considered include the type and thickness of the metal skin, its surface finish, and how long a lightning flash is likely to dwell at a particular spot on the skin. Other factors are structural fasteners and other joints across which the currents must flow.

Melt-through of metal skins

A lightning arc will melt through a typical aluminum skin before the inside surface of the skin becomes hot enough to ignite the fuel vapor. The melting temperature of aluminum (~660 °C) is lower than the short time ignition temperature of most hydrocarbon fuel vapors. Experiments by Crouch [7.25], using propane, pentane, and JP-4 fuels, showed that ignitions would not occur until the hot spot ignition source temperature reached 900 °C. Thus, fuels within an aluminum integral tank would not be ignited unless a hole were melted completely through the skin and the fuel vapor was exposed to the extremely high temperature of the lightning arc (more than 30 000 °C).

On the other hand, the melting temperature of titanium is 1 700 ºC and that of stainless steel is 1 400 ºC. Both melting points are higher than the fuel ignition temperature. While titanium and stainless-steel skins are more resistant to lightning melt through, they would not need to be melted completely through for ignition to occur.

The amount of lightning current required to erode or melt holes in metal aircraft skins has long been of interest. First, for the purpose of estimating how much lightning current actually was involved in the damage sustained by aircraft in flight and, second, for determining the minimum skin thickness required to prevent melt-through of an integral fuel tank skin.

Review of Basic Skin Melt-through Studies

Research on the sizes of holes melted through metal skins of various thicknesses by lightning currents was discussed in Chapter 6 regarding the effects of lightning on structures. Whereas for structural integrity it is important to know the *size* of the holes that might be melted, in regard to fuel systems it is more important to know the minimum amount of *charge* that could ignite the fuel vapor. For fuel systems with aluminum integral tank skins, this means knowing the amount of charge necessary to melt even the smallest hole in the skin.

Melt-through thresholds of aluminum skins

Brick, in 1968 [6.2], and Oh and Schneider, in 1972 [7.26], performed experiments to determine the amount of charge and current required to melt through aluminum and titanium skins of various thicknesses and ignite a flammable vapor on the other side. These experimenters reported that melt-through depended heavily on current amplitude as well as on dwell time, and thus charge conducted into the dwell spot. While earlier work had shown that over 22 °C, when delivered by a current of 200 A, were necessary to melt through 2.06 mm (0.080 in) aluminum skins, the work of Brick, Oh, and Schneider showed that only about 10 °C, when delivered by about 500 A, was enough to melt completely through the same thickness of aluminum skin. In their laboratory tests, as little as 2 C, when delivered by about 130 A, melted a hole completely through 1.0 mm (0.040 in) of aluminum. Their results have been corroborated by others since.

Oh and Schneider's melt-through thresholds for these and other skin thicknesses are shown in Fig. 7.12 (shown also as Fig. 6.3 in Chapter 6) [7.26]. The proximity of their test electrode to the skins, 2.4 to 4.8 mm (0.1 to 0.2 in), may have restricted natural movement of the arc on the surface of the skin, forcing all of the charge to enter at the same spot, thus yielding low coulomb ignition thresholds. Most surface finishes will also restrict movement of the electric arc and thus concentrate most of the current and charge transfer at a single spot.

Work by Kester, Gerstein, and Plumer [7.27] with an L-shaped electrode spaced 6.4 mm (0.25 in) from the skin, permitted some arc movement along the horizontal surface of the electrode and the surface beneath, showing that this arc movement necessitated 20 C delivered at a rate of 130 A to melt through a 1.0 mm (0.040 in) aluminum skin. Magnetic fields generated by currents parallel to the skin might have also caused the arc to move. This would be an artifact of the laboratory test arrangement. Since a natural lightning arc is neither restricted nor forced by an electrode, it is probable that the true aluminum melt-through threshold lies between these two extremes, at least for unpainted surfaces. On the other hand, the electrical insulating properties of most paints tend to confine the arc to one point, concentrating the heating effects on a smaller volume of metal. This tends to decrease the amount of current and charge required to melt completely through.

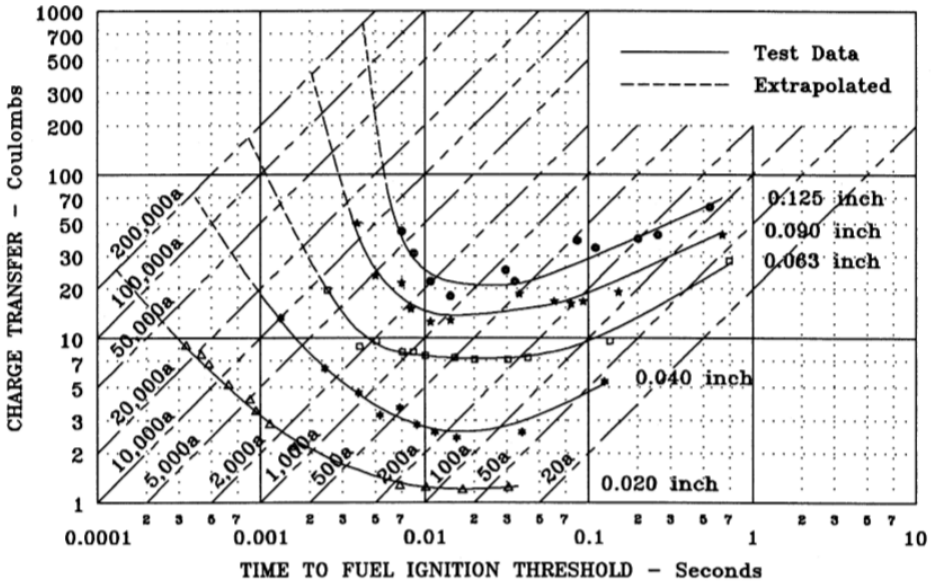

Fig. 7.12 Melt-through and ignition thresholds for aluminum skins (2024 T3) [7.26].

Pressure effects

All of the referenced data reported on melt-through of fuel tank skins was obtained from experiments performed on test panels in ambient conditions, that is, with equal pressure on both sides of the panels. Some aircraft fuel systems maintain a small positive air pressure in their tanks. Military fighter aircraft maintain a positive tank pressure to sustain fuel flow during extreme maneuvers. Many fuel vent systems use ram air inlets (called 'NACA scoops') that provide some positive pressure inside the tank. It has been demonstrated that pressure inside a fuel tank on which melt-through tests are being conducted can make a difference in the amount of charge necessary to melt a hole. A lightning arc may heat the surface of a fuel tank skin to a temperature at which the metal is nearly molten, but if there is no pressure inside the tank, surface tension prevents the molten metal from flowing away and leaving a hole. A modest amount of pressure, however, suffices to push the molten metal away and leave a hole. Some unpublished test results showed that, with a gauge pressure of 34.5 kPa (5 psig), holes could be melted in a 2.3 mm (0.090 in) aluminum skin by a 23 C discharge. With no pressure, 66 C was required to produce a hole.

The influence of positive internal tank pressure is usually not considered in certification tests of airplane fuel systems, which are typically conducted on tank structure and system test specimens at laboratory ambient air pressure. If it is expected that the fuel tank will have some positive pressure within it, the tests should be conducted with this same pressure applied. This may require that specimens of fuel tank skins be mounted to a test chamber that can be pressurized. The melt-through threshold data described in the previous paragraphs was obtained from tests of unpressurized skin samples, in laboratory ambient temperature and pressure conditions.

Ignition thresholds of titanium skins

Titanium skins are found on integral fuel tanks of some supersonic aircraft.

Oh and Schneider have similarly determined the coulomb transfer ignition thresholds of titanium skin materials of various thicknesses, as shown in Fig. 7.13 [7.26]. Oh and Schneider and other researchers have confirmed that, since the melting point of titanium is higher than the fuel ignition temperature, it is not necessary for a hole to be melted completely through a titanium tank skin for ignition to occur. All that is necessary for there to be an ignition source is that a hot spot of sufficient temperature be formed on the inside surface of the tank skin. The lower thermal conductivity of titanium prevents rapid heat transfer away from the arc attachment point and accounts for the fact that coulomb ignition thresholds for titanium skins are generally lower than those for aluminum skins.

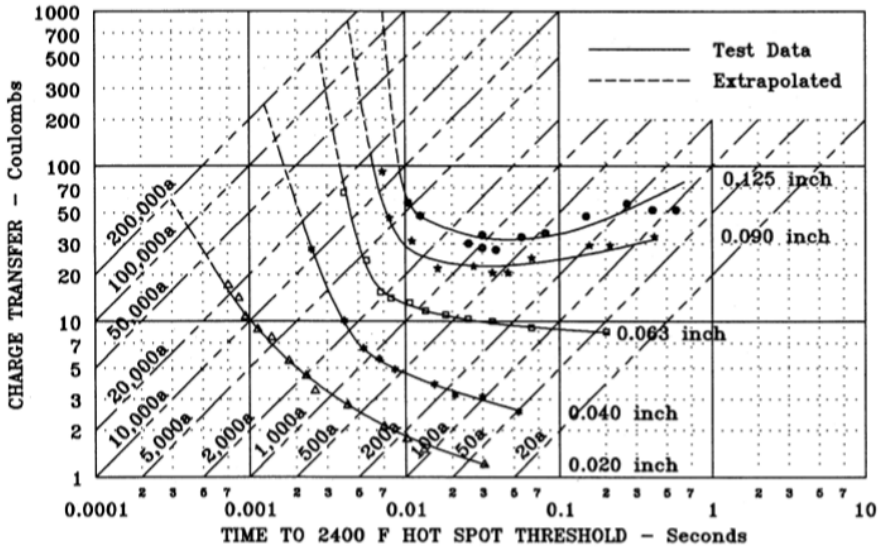

Fig. 7.13 Hot spot ignition thresholds for titanium skins (6AL4V) [7.26].

Ignition thresholds of CFC skins

There are several mechanisms by which vapor inside a CFC tank may be ignited. These include the following:

- Ohmic heating of the carbon fibers, resulting in vaporization and burning of the resin where it is in contact with fuel vapors
- The shock wave accompanying high peak currents, such as Current Components A and D, can crack and sometimes punch completely through CFC skins.

These effects can make large holes in CFC skins, providing large areas of exposure of fuel vapors to the lightning arc. Even breakage of a few carbon yarns may produce arcing of sufficient intensity to ignite fuel vapors. It is not possible for incendiary hot spots to form on a CFC skin because the resins in a CFC melt at ~350°C, which is too low a temperature to ignite fuel vapors. In most cases, CFC skins are punched through from shock wave effects before the resin on the interior ply melts or burns.

Analytical studies by Lee and Su are described in [7.28]. Tests conducted by Schulte [7.29] with Zone 2A currents applied to 3.18 mm (0.125 in) aluminum and CFC panels showed that, for the same applied test conditions, temperatures of 100 °C to 150 ºC were reached on the interior surfaces of CFC panels, while aluminum panels of the same thickness reached temperatures of 160 °C to 200 ºC. Panels of 6.35 mm (0.25 in) thickness reached temperatures of 70 °C and 80 ºC respectively. The major difference was noted in the time to reach peak temperature. The temperatures of the CFC panels responded 100 times more slowly than the aluminum, taking seconds to reach peak temperature. Aluminum panels reached their peak temperatures in tens of milliseconds. Fig. 7.14 gives a summary of the data, displaying the time and temperature profiles for aluminum and CFC fuel tank skins of various thicknesses. These tests were conducted in a wind tunnel air stream of between 65 and 150 miles per hour (29 - 67 m/s), which blew the test current arc across the surface of the test specimen. All of Components D and B would have entered the test panel surfaces at the first arc attachment spot, but some of the Component C* currents, which were applied at an average amplitude of 400 A for 60 ms, reattached to other points downwind of the initial attachment point and thus did not contribute to the original hot spot formation. It would have been better had these tests been conducted in still air, since the Zone 2A current components are defined on the basis that all three components enter a moving aircraft surface at the same point.

Wahlgren [7.30] also investigated hot spot temperatures, but the temperatures reported are questionable because they exceed those required for resin pyrolysis.

The panels tested by Schulte [7.29] were comparatively thick, such as might be found on inboard sections of transport or fighter type aircraft wings, and the tests applied a Zone 2A environment, not the more damaging Zone 1A/1C lightning environment. The latter environment includes Component A, which has an action integral eight times greater than that of Component D, applicable in Zone 2A. Thus, hot spot temperatures for CFC skins in Zone 1A (or 1C) might be higher than those recorded by Schulte.

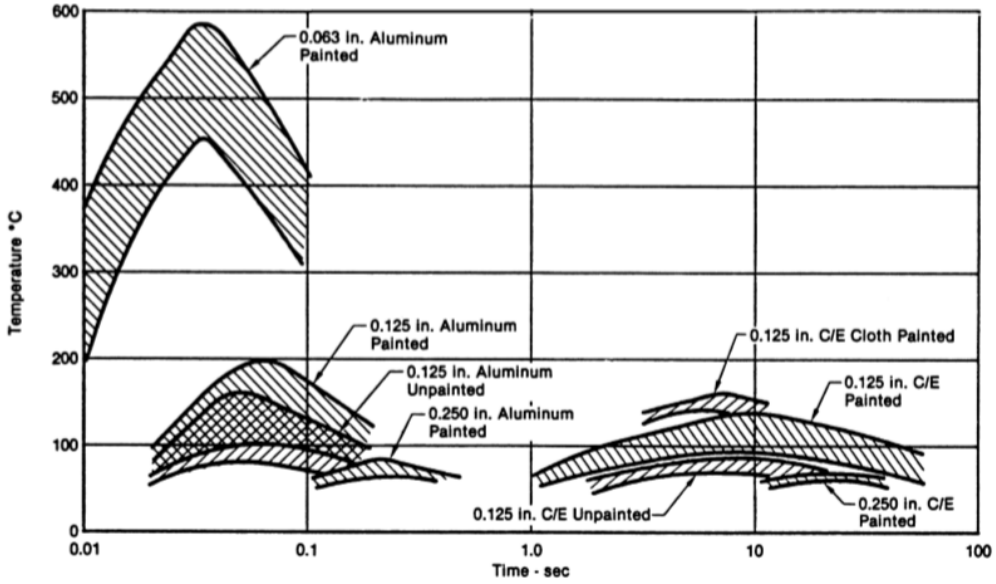

Fig. 7.14 Hot spot temperature and time to reach peak temperature Zone 2A currents applied to aluminum and carbon fiber composite (CFC, also known as C/E) in a wind stream [7.29].

Hot spot data for thinner CFC skins was obtained in experiments conducted by Olsen et al [7.31] under a variety of conditions. They did not record inner surface hot spot temperatures but, instead, recorded whether a flammable fuel vapor on the interior surface of the skin from the test current arc was ignited or not. A summary of their results, for CFC skins 1.0 mm (0.040 in) and 1.14 mm (0.045 in) thick is presented in Table 7.2. The authors noted that the ignitions may not have been caused by hot spots per se, but by glowing hot fibers of graphite, either loose in the system or released by pyrolyzed resin.

The Olsen data show that paint intensifies lightning effects, allowing ignitions to occur following lower amounts of charge transfer. This is due to the current and shock wave concentration effects of the paint, which are described in Chapter 6. The Olsen data show that painted CFC skins can tolerate larger amounts of charge transfer, by a factor of two or more, than can aluminum skins of the same thickness. The data applies for Zone 2B, where the stroke current is Component D. Tests at Zone 2A levels did not cause any ignitions. Tests on skins of this thickness with Component A usually punched a hole that exposed combustible vapors to the arc plasma, causing an ignition.

Thus, to assess the possibilities of fuel vapor ignition, designers need to know the lightning strike zones within which protective skins are located, and the expected dwell times of the lightning channel. For example, a dwell time not longer than 5 ms, accompanied by a charge transfer of 10 coulombs, is expected on an unpainted or thinly painted skin. If this skin is at least 1 mm thick, there is virtually no possibility of fuel vapor on the opposite side being ignited. However, a thicker paint finish (i.e., 0.25 mm (0.01 in)), or equivalent combination of surface resin, filler, and paint, would increase the dwell time to 20 ms and the charge transfer of 16 coulombs. This includes current Component B (10 coulombs) followed by Component C* (~ 400 A for 15 ms = 6 coulombs), a charge transfer that approaches the ignition threshold of 22 coulombs reported in [7.32]. In such a case, the candidate skin and surface finish combinations should be tested to verify that there is no possibility of igniting fuel vapor.

The Olsen tests, and most similar test programs, were conducted at room temperature. The Schulte data showed that the airstream had a significant cooling effect on aluminum but a much smaller effect on CFC.

Table 7.2
Zone 2B Test Results for Ignition Thresholds

Test Panel	Thickness (in)	Prepreg form	Ply orientation (deg)	Finish	Coulombs required for ignition
1-1	0.045	Tape	$[0/\pm45/90]_S$	Unpainted	50 to 60
1-2	0.045	Tape	$[0/\pm45/90]_S$	Painted	35 to 45
4-1	0.040	Fabric	$[0/90]_3$	Unpainted	37 to 40
4-2	0.040	Fabric	$[0/90]_3$	Painted	22 to 25
7-1	0.040	Fabric	$[\pm45]_3$	Unpainted	33
7-2	0.040	Fabric	$[\pm45]_3$	Painted	22 to 25
7-3	0.040	Fabric	$[\pm45]_3$	Painted	24-29
0.063 Al	0.063	Aluminum	N/A	Unpainted	6 to 9

This is to be expected due to the much higher thermal conductivity of aluminum as compared with that of CFC. Since the rate of cooling varies with air temperature, it is probably not practical to consider the effect of cooling as a parameter in lightning protection designs, although there may be some designs whose response to lightning is influenced by temperature. Absent such influence, standard temperature conditions, 20 °C (68 °F) should be utilized for design and testing purposes.

Lightning channel dwell times on skin surfaces

The two proceeding sections provide useful data for determining the probability that an aluminum skin will melt through or the probability that a hot spot on a titanium or CFC skin will ignite fuel vapor. This data is based on assumed known values for the amplitude of the current at the lightning attachment point in question and the amount of time the lightning channel dwells at that point (the 'dwell time').

The swept channel mechanism, discussed in Chapter 3, is illustrated in Fig. 7.15. A knowledge of dwell times in swept flash zones is of great importance because integral fuel tank skins are often found in these zones.

Early versions of regulatory documents, such as US FAA AC 20-53 [7.33], specified that aluminum skins in lightning strike zones should be at least 2.0 mm (0.080 in) thick to withstand melt-through. In the past, when the structural requirements for large transport aircraft were such that skins had to be at least 2.0 mm thick for structural purposes, the lightning protection against melt-through was achieved without additional means. The advent of newer alloys of aluminum, and of other structural materials, whose behavior is less well understood, means that tests to confirm safe tolerance of the lightning environment should be included to confirm absence of ignition sources.

In some more recent designs, thinner skins have been able to meet the structural requirements. This saves weight and cost, provided that the lightning protection requirement can be met with a skin thinner than 2.0 mm. To determine the actual skin thickness required to resist melt-through or hot spot formation, it is necessary to know the maximum possible lightning channel dwell time for the intended skin surface treatment. Dwell time information has been obtained from a combination of laboratory tests that simulated the 'sweeping' of the lightning flash channel over typical surfaces, and measured data from natural lightning strikes to aircraft.

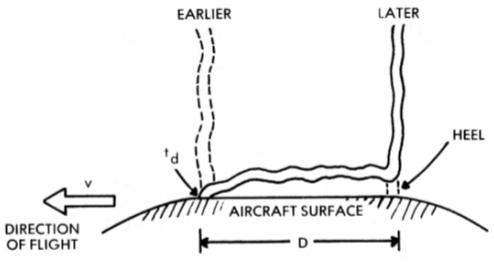

Fig. 7.15 Swept channel reattachment.

Brick, Oh, and Schneider's work

Brick, Oh, and Schneider [7.34] studied the dwell times of 400 A, decaying arcs (channels) that were blown by the exhaust from a wind tunnel over the surfaces of aluminum and titanium skin panels. The panels were given a variety of treatments to study the effect of surface treatment on dwell time. The wind speeds were varied between 67 m/s (150 mph) and 112 m/s (250 mph), to represent the air speeds of typical aircraft. The test current was representative of the continuing current portion of the lightning flash and delivered an average charge of about 0.2 coulombs per millisecond of dwell time. This represents a typical continuing current of ~200 A. *(Note that the terms "arc" and "channel" are used interchangeably. Technically, an "arc" may be considered what is produced in laboratory simulations, and the "channel" is the ionized air that conducts the currents in natural lightning.)*

The researchers reported that the arcs dwelled for 2 ms or less on uncoated surfaces of both metals, and for 4.8 ms on an anodized aluminum surface. These dwell times are within the 5 ms time period of current Component B. Thus, the 2 ms dwell time would have allowed a charge of 4 coulombs to enter a single spot, whereas the 4.8 ms dwell would have permitted 10 coulombs (nearly the total charge of Component B) to enter the spot. Of course, the amount of charge entering the attachment point would be determined by the amplitude of the lightning current in the flash at the time of its attachment to that point. In testing, the current components are usually applied in order from highest amplitude to lowest amplitude. In nature, the components can come in any order. To ensure that the worst case is tested, the effects of currents of various amplitudes and time durations must be evaluated.

After dwelling at one point, a lightning channel reattaches to a point farther aft on the aircraft by the mechanism illustrated in Fig. 7.15. During the dwell time, the aircraft is, of course, moving and the distance covered during the dwell time is equal to:

$$D = vt_d \qquad (7.1)$$

where

D = distance the channel is drawn along surface (m)

v = aircraft velocity (m/s)

t_d = dwell time (s)

Thus, at velocities of 67 m/s and 112 m/s, and with the dwell times of 2.0 and 4.8 ms reported by Brick, spacings between successive dwell points would be 0.13 m and 0.54 m, which are typical.

As a lightning channel sweeps across a surface the points at which the channel remained attached are marked by melted or pitted spots. The dwell time of the lightning channel at each spot can be estimated by comparing the distances between the spots with the aircraft's velocity at the time of the strike. The dwell times given in Table 7.3 are typical of those measured on actual aircraft and they confirm the dwell times predicted by the Brick tests.

Table 7.3
Typical Lightning Channel Dwell Times

Skin Material	**Surface Finish**	**Dwell Time**
Aluminum	Unpainted	≤ 2 ms
Aluminum	Anodized	≤ 5 ms
Aluminum	Painted	≤ 20 ms
CFC	Same as metal skins	

Actual dwell time for painted skins depends on paint thickness

The later work of Oh and Schneider [7.35] also confirms these results for uniform airflow conditions but shows that conditions which cause the airstream to leave the surface may force the arc to dwell longer at the last attachment point upstream of where the airflow is diverted. Oh and Schneider also demonstrated that higher aircraft velocities yield shorter arc dwell times, because the arc is stretched greater distances, allowing voltage to build up along its length and break down the insulation at its 'heel' at an earlier time.

Validity of wind tunnel tests

The validity of the wind tunnel test techniques that have been used for simulating swept flash attachments over metal surfaces has been questioned because the airstream used to blow the arc across the surface of the test object must have moved faster than the arc. This means that the air speed was only an imprecise indication of how fast the arc moved. In addition, the arc must have been cooled by the fast-moving air.

This cooling would have allowed the voltage to rise at a faster rate than it would in a natural lightning strike to an

aircraft, which probably caused the simulated lightning channel to reattach to subsequent spots sooner than it would in a natural event. Also, the behavior of the upper terminus of the arc, as it moved along the horizontal test electrode, probably had some effect on the behavior of its lower terminus at the surface of the test panel.

A more realistic simulation of a sweeping lightning channel would involve moving the test article (or test assembly), like an aircraft in flight, through a stationary arc. Plumer [7.36] attempted this by moving a wingtip fuel tank beneath a high-voltage electrode at a velocity of 15.5 m/s (35 mph), the fastest speed that could be safely maintained in the test area. A flash was triggered when the approaching tank, carried on top of a truck, sufficiently closed the air gap between the electrode and the earth.

The shortcomings of this experiment were the low velocity and the low (4 amperes) test current amplitude that was available from the high voltage generator utilized for these experiments. However, more recently, some actual, in-flight lightning strikes to two fuel tanks of the type used in Plumer's experiment have confirmed the simulated attachment points and breakdown paths. This points to the role of voltage along the channel in determining the next attachment spot and interrupting current flow into the original spot.

Despite the lower velocity and lower current amplitude, the arcs in Plumer's tests dwelled for times of between 1 and 4 ms on unpainted aluminum surfaces, results remarkably similar to those obtained in the wind tunnel work. These parallel results seem to indicate that the arcs in the wind tunnel tests may not have moved as fast as the wind itself and, also, that continuing current amplitude has relatively little to do with dwell time. It appears that the channel voltage is the primary factor. It is well known that the impedance of electric arcs varies inversely with arc current amplitude, so a low amplitude current in a long arc may produce the same voltage as a high amplitude current in a short arc.

Effects of exterior surface finishes

Robb, Stahmann, and Newman [7.37] utilized the wind tunnel technique to determine arc dwell times on various painted or coated surfaces. Most of the coatings were electrically insulating, requiring that the arc be further lengthened, until it produced the voltage necessary to puncture the insulation and form the next attachment point. Dwell times of up to 20 ms were recorded on painted surfaces. These times undoubtedly depended on the type and thickness of the paint, but precise details of those conditions were not recorded, as their importance had not yet been recognized.

Additional dwell time data has been obtained from the in-flight experience of the NASA F-106B research airplane during the period from 1981 – 1986 [7.38]. This airplane was instrumented as part of the NASA-Langley Research Center Storm Hazards Program to study lightning parameters and the effects of lightning on aircraft. Spacings between melted spots on surfaces of the aircraft showed that dwell times were less than 2 ms for unpainted skins and between 1 and 6 ms across the painted aluminum fuselage and wing surfaces. The dwell times were calculated by dividing the spacings between melted spots by the aircraft's air speed, 182 m/s (409 mph), during the thunderstorm penetrations.

A tabulation of laboratory and in-flight strike data is shown in Table 7.4 for several surfaces commonly found in swept channel zones.

The FAA User's Manual [7.39] for FAA AC 20 - 53A [7.40] recognizes that the coatings and paints on aircraft surfaces can affect dwell times.

Table 7.4
Lightning Dwell Times on Typical
Aircraft Surfaces in Zone 2A

	Aircraft Velocities		
Surface Type	15.5 m/s (35 mph)	58 m/s (130 mph)	103 m/s (230 mph)
Aluminum and titanium unpainted	1 to 4 ms	2.0 ms	1.0 ms
Aluminum anodized		4.8 ms	2.6 ms
Aluminum painted		Up to 20 ms	Up to 10 ms

The combined thicknesses of surface finishes including corrosion-resistant treatments, primers, and paints should be compared with data bases, such as those presented here, to establish anticipated lightning channel dwell times. New coatings for which little experience is available should be tested to establish dwell times and the time thresholds for melt-through or hot spot fuel vapor ignition. Guidance for performing such tests is given in [7.24]. Once the expected dwell times have been established, it is then necessary to assign the lightning current components applicable in each zone.

Ways to reduce dwell time

The preceding discussion makes clear the importance of lightning arc dwell time in establishing whether ignition is likely to result from a lightning strike to the skin. Dwell time is perhaps the only lightning characteristic over which the integral fuel tank designer has any control. The objectives, of course, should be to minimize the dwell time at any one point, thereby spreading the arc attachment among many different spots. The best way to achieve this is to provide a bare metal external finish, since most paints and coatings concentrate the lightning current density at more widely spaced points for correspondingly longer times.

If paint must be used, lightning dwell times may be reduced by making the paint partially conductive. Robb and others [7.37] have demonstrated that aluminum powder mixed within a polyurethane paint is effective in increasing the ability of sweeping electric arcs to puncture polyurethane paints and reattach to conductive surfaces beneath. This enhances the ability of the arc to reattach to new spots as the aircraft surface moves beneath it. Since no parametric data relating dwell time to the amount of conductive additive in a paint is available, it is advisable to make laboratory determinations of the degree of improvement afforded by specific paint compositions if this approach is to be considered for minimizing dwell times

McClenahan and Plumer [7.41] have shown that small-diameter metal wires, intermingled with the carbon yarns in CFC skins, split a single attachment spot into many spots within a nearby area, thereby reducing melting or other damage at each attachment spot. This effect, which has been termed *arc root dispersion* in §6.2.1, is due to the intensification of the local electric field above each of the exposed wire surfaces, resulting in multiple punctures of nonconductive finishes. The extent to which this treatment also shortens swept channel dwell times is not known to have been evaluated in wind-tunnel or flight tests but the ease with which the wires enable surface finishes to be punctures to allow the arc root dispersion would have to have a similar effect on reattachment of sweeping channels.

Role of current waveforms and amplitudes

These high amplitude strokes in the lightning flash are usually too short in duration to deliver appreciable charge and cause significant melting of metal skin materials. Most of the charge in a flash is delivered by long-duration continuing currents of several hundred amperes and by intermediate currents of several kiloamperes. In analyses of swept channel effects, emphasis should be placed on the intermediate and continuing currents, Components B and C, because these can deliver large amounts of charge that is capable of significant melting of aluminum skins.

For example, the aircraft lightning test standard [7.24] states that the lightning current environment that should be applied in tests of swept flash effects to surfaces in Zone 2A should be applied in the order shown in Fig. 7.16 Components B and C* are applied in the test current arc for whatever dwell time is expected, or for a total of 50 ms if the dwell time is unknown. For testing conventional painted skins, the standard recommends that the total dwell time be set at 20 ms, including 5 ms of Component B and 15 ms for Component C*. A square wave representation of this current is shown in Fig. 7.16. If a dwell time of less than 5 ms is expected, an average current of 2 kA should be applied for the actual dwell time only. It should be noted that even though the standard specifies that testing be conducted in this manner, nature is not restricted to the test environment and can deliver currents in any sequence.

Aircraft lightning strike experience since the test standard was first adopted shows that integral fuel tanks designed and tested with the environment described in Fig. 7.16 have been surviving the natural lightning environment without skin melt-throughs.

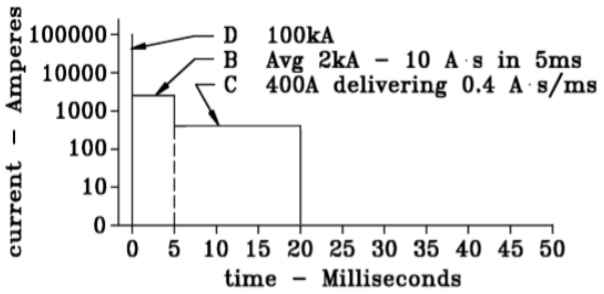

Fig. 7.16 Current and charge expected at a *Zone 2A* attachment spot.
C is C* since its time is only 15 ms.

The Zone 1A (or 1C) environment includes current Components A (or A_H) B and C*. Component A applies a higher action integral and more intense shock wave to the skin surface, which can puncture unprotected CFC and some thin metal skins, as described in Chapter 6. However, melt-through of metal skins is due primarily to charge transfer from inter-mediate and continuing currents. Thus, the likelihoods of melt-throughs in Zones 1A, 1C and *2A* are about the same. The more intense shock waves associated with Components A and A_H may crack or rupture metal skins that are less than 1 mm (0.040 in) thick.

Fuel tank skins in Zone 1B, such as external tanks on rotorcraft or the trailing edges of wingtip tanks on transport aircraft, must be able to tolerate all four current Components, A, B, C and D. It is assumed that these components may enter the skin at any spot on a Zone 1B surface. This usually precludes the use of integral tank skins in Zone 1B since the thickness of metal needed to resist melt-through would be excessive. The usual protection approach is to remove fuel from contact with tank skins in Zone 1B or provide a barrier between the fuel container and the exterior surface of the tank. This is done with some externally mounted helicopter tanks that must also meet crashworthiness requirements.

The standard lightning environment defined for physical effects protection design and verification purposes (described in the standards and in Chapter 5) is based on the known characteristics of cloud-to-earth flashes, described in Chapter 2. The standard environment also considers studies of in-flight damage reported by aircraft operators over the years. Tests based on the standard environment have generally replicated the observed in-flight lightning effects.

It is likely that other current waveforms appear, in the natural lightning environment, whose effects may not be fully represented by Components A, B, C and D. For example, there may be stroke currents whose amplitudes are lower than those of Components A and D but whose time durations may be significantly longer. An example might be a stroke with a peak amplitude of 50 kA and a time duration of 2 ms. Such a stroke might be a positive polarity cloud-to-earth stroke that delivers 50 coulombs to an aircraft surface during a sufficiently long time for melting to take place. Aluminum skins thicker than 1.5 mm (0.060) in) might be melted through by such a current. An example of a similar stroke current, recorded by Berger [7.42], is shown in Fig. 7.17. Due to the long time (11 ms) that elapsed between the initiation of the leader and arrival of the stroke, an aircraft struck by such a flash could receive this stroke in Zone 2A. Designers and lightning protection specialists should be aware of the possibility of 'non-standard' lightning characteristics and should try, wherever possible, to account for their possible effects by making their designs as tolerant as possible to a wide range of lightning parameters. This is not a requirement for certification, since, as has been described in Chapter 5, airplanes designed and certified to the standardized environment have survived natural lightning strikes without hazardous effects.

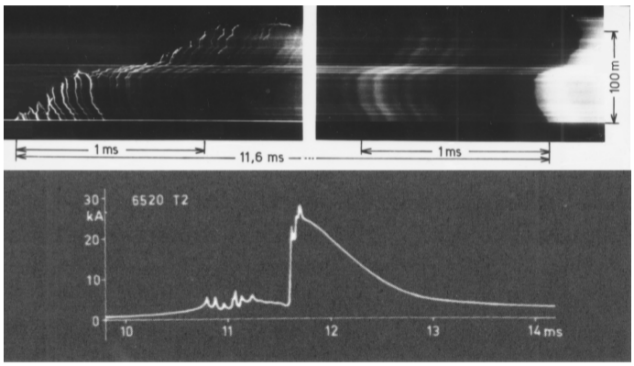

Fig. 7.17 Positive polarity flash with stroke arrival at 11.6 ms after flash formation. [Note that this was an upward-going flash, initiated from a tower. In such flashes the intensities of currents are expected to be greatest at the ground, and less at most flight altitudes].

The current waveform measurement shown in Fig. 7.17 was made at an instrument tower on the ground, and the long, upward-moving leader, which extended from this tower to the cloud base, accounted for most of the 11.5 ms delay which elapsed before the return stroke appeared at the ground. Not all of this delay would have occurred if the measurement had been made from an aircraft intercepting the flash (although similar delays are possible when an aircraft is contacted by a downward leader that originated in a cloud). Several milliseconds of delay still could have elapsed between initial leader attachment to a forward extremity of the aircraft and the occurrence of the stroke. The positive polarity stroke whose waveform is shown in Fig. 7.17 would have delivered about 20 C to its attachment point during the ~2 ms it would have dwelled there. According to the data in Fig. 7.12, a 1.6 mm (0.063 in) aluminum skin could have been melted through during that time.

There are reports of holes melted in 1 mm (0.040 in) skins from in-flight strikes in Zone 2A areas, but holes in 1.6 mm aluminum have not been reported. This demonstrates the apparent rarity of the high-energy positive polarity flash in Zone 2A areas.

More about Integral Fuel Tank Skins

Assuming that current amplitude, charge, and dwell time have been established, Figs. 7.12 and 7.13 show the designer how to estimate the thicknesses of aluminum or titanium skins required to ensure that lightning attachment will not melt through or overheat the skin (causing an incendiary hot spot). The important lightning parameters are charge transfer (coulombs) and rate of charge transfer (amperes). The combinations of amplitudes and current flow (dwell) times at a particular spot determine the thickness of aluminum skin that may be melted through, or the thickness of titanium skin that may reach an incendiary hot spot on the interior surface to ignite flammable vapors.

Since the data in Figs. 7.12 and 7.13 show melt-through or hot spot conditions, the plots (and the data points) show the ignition source threshold thicknesses. Thicker skins must be employed to prevent ignition sources. It should also be noted that the data apply to the metal alloys shown. Other alloys of either metal would be expected to behave in a similar fashion, although specific thresholds would vary somewhat from those presented in Figs. 7.12 and 7.13. No graphs of the type shown in Figs. 7.12 and 7.13 are known to have been generated for other alloys of aluminum or for other metals.

Aluminum integral tank skins

For example, assume that a bare aluminum skin is planned for an integral tank in Zone 2A. Further, assume that the aircraft is designed to fly at velocities as low as 58 m/s (130 mph), which is typical for descent and approach to landing.

From Table 7.3 the expected dwell time for this unpainted skin would be 2 ms. From Fig. 7.16, an average current of 2 kA would flow into the dwell point during this period, delivering 4 coulombs of charge. In Fig. 7.12, these parameters intersect at a point about half-way between the coulomb ignition threshold curves for 0.51 mm (0.020 in) and 1.02 mm (0.040 in) aluminum skins. This indicates that 0.81 mm (0.032 in) is the thinnest skin that should be considered. Since there would be little margin if a skin of this thickness were actually used, it would be prudent to select a greater thickness, such as 1.02 mm (0.040 in). Whatever alloy and thickness is being considered should be tested with the anticipated surface finish(s) to confirm absence of melt-through or hot spot ignition sources.

As previously noted, surface finishes, such as paint, increase dwell times. This increase is influenced by both the thickness and the composition of the surface finish. Generally, the thicker the coating, the longer the dwell time and the thicker the skin must be to avoid melt-through. Consider, for example, the longest dwell time, 20 ms, recorded by Robb, Stahmann, and Newman [7.37] for a painted surface. During this period, the current shown in Fig. 7.17 would deliver 16 C. These parameters intersect at a point just above the 2.29 mm (0.090 in) curve in Fig. 7.12, indicating that even the 2.03 mm (0.080 in) thickness advised by some design guidelines would be insufficient to prevent ignition where certain paints are used. Therefore, if paints are to be present, it is advisable limit their total thickness to 0.2 mm (8 mils) – a value known to limit dwell times to 20 ms or less or perform swept channel tests (or refer to applicable in-flight experience) in order to establish the actual dwell time and, therefore, the surface finish and aluminum skin thickness required to prevent melt-through. The data in Tables 7.3 and 7.4 may be used by reference for this purpose.

Additional coats of paint

Some transport airplanes, destined for lifetimes of 30 000 flight hours or more, should expect to receive additional coats of paint, or decals, due to maintenance requirements or owner name changes such that total surface finish becomes greater than original. Provision for this should be made, for integral fuel tank skins, by assuming longer dwell times, proportional to increases in finish thickness, and testing skin specimens with corresponding increased finishes, by applying the appropriate lightning test environment with component C* extended to represent the additional dwell time.

For example, an aluminum skin originally certified with 0.2 mm (8 mils) of surface finish by testing for Zone 2A with 15 ms of Component C* of 6 coulombs (15 ms x 400 A = 6 coulombs) would need to be retested with an additional 6 coulombs of charge added to component C* if the finish thickness were doubled to 0.4 mm (16 mils). Thus, the test requirements would be: Component B + Component C * at 12 coulombs (i.e., 400 A for 30 ms).

The analysis above assumes that the additional charge is applied by a continuing current (Component C*) that is conducted into the same spot during an overall dwell time of 22 ms + 12 ms = 34 ms, an unusually long time, but possible when surface finishes are thick. Survival of such a test without complete melt-through would necessitate a skin of over 3 mils (0.125 inch) thick. Therefore, other means of tolerating the lightning environment may have to be considered, such as those described in § 6.2.1 of Chapter 6. Of course, control of surface finish thickness over the lifetime of the aircraft may also be considered.

Titanium integral tank skins

From the data in Fig. 7.13, it is possible to determine titanium skin thicknesses required to prevent the formation of hot spots that could ignite fuel vapor. The method is similar to that used for determining aluminum skin thicknesses. The coulomb ignition threshold for titanium occurs when the interior surface of the skin reaches 900 °C (1 650 °F), a temperature Crouch found sufficient to ignite a fuel-air vapor from hot spot formation [7.43]. Because titanium will not melt at this temperature, no hole will be formed before the ignition threshold is reached. Melt-through or hot spot fuel vapor ignition thresholds should be determined for metals of interest by laboratory test.

CFC integral tank skins

The data in §6.5.1 can be utilized to determine the CFC thicknesses and protective treatments necessary to prevent punch-through by stroke currents (Components A or D). The data presented in this chapter indicates that incendiary hot spots are not likely to form on CFC skins. Studies by Lepetit et al [7.44] of the thermal and mechanical effects of stroke currents Component D on painted CFC surfaces have shown that explosive vaporization of resin between layers of paint and the CFC surface are responsible for the force exerted on the CFC. The paint confines the plasma associated with the heating effect of the stroke current. The resulting force causes the reinforcing carbon fibers to break, allowing arcing among broken fibers that are exposed to flammable vapors contained in integral CFC tanks. Chippendale et al [7.45] have studied the effects of continuing currents (Component C) on CFC skins and shown that pyrolysis of resin can be responsible for delamination that also can break the carbon fibers at the interior surface of thin CFC laminates, also resulting in fuel vapor ignition sources.

Edge Glow

Laboratory tests have also shown that currents being conducted through CFC laminates that have edges exposed to fuel vapors may produce a phenomenon called "edge glow" that is produced by minute arcs that develop among the cut ends of carbon fibers that are in casual contact with one another. There is not sufficient voltage developed among closely arranged fibers to cause electrical sparks, but arcs are easily formed among exposed fiber ends that are in contact. This edge glow has not always caused ignition of fuel vapors, but it should always be expected along exposed edges of laminates such as stiffeners, ribs, shear ties and spar caps made of CFC. Protection against fuel vapor ignition can be achieved by covering these edges with a wrap made of fiberglass or other non-electrically conductive material.

Specimens of CFC structures with protected edges should be tested with anticipated lightning currents and within a flammable vapor environment to confirm adequacy of protection against ignition sources.

External fuel tanks and trailing edge tanks

External fuel tanks on some aircraft are often attached to wing tips or pylons that are in lightning initial leader attachment and flash hang-on areas that are in Zones 1A or 1B, with intervening surfaces usually in Zone 2A. Thus, protection of these tanks from lightning strikes is necessary.

The design approach is the same as for integral tanks: Begin with consideration of necessary skin thicknesses and continue with attention to trailing edges where the lightning channel is expected to remain attached, and continue melting, for the duration of the flash.

At trailing edges, lightning flashes tend to remain attached at one spot long enough to melt through metal skins of almost any reasonable thickness. Fig. 7.12 shows that 200 coulombs, delivered in 1 second or less (as required by [7.24]) would melt through aluminum skins up to 8 mm (0.315 in) thick. A titanium skin 3.2 mm (0.125 in) thick would not be melted by such a charge, but Fig. 7.13 shows that it would be heated to 1 320 °C (2 400 °F), which exceeds the temperature necessary for fuel vapor ignition.

Therefore, it is hazardous to allow fuel or fuel vapor to accumulate in trailing edges located in Zones 1B or 2B.

It is possible that fuel vapor could exist at trailing edges of externally mounted fuel tanks or tip tanks, however. Such tanks must be protected by closing out and venting their aft-most volumes, as shown in Fig. 7.18, so that, if melt-through does occur, there will be no fuel vapor to be ignited.

The best way to prevent melt-through at a trailing edge (Zones 1B/2B) location will be to close out the fuel area some distance forward of the Zone 1B/2B surfaces so that the fuel is contained within Zone 2A surfaces where the dwell time is short and metal skins of traditional thicknesses can be used. The idea is shown in Fig. 7.18.

A second protection approach would be to consider using a thermal barrier to prevent a melt-through of the trailing edge metal skin from reaching a flammable vapor. Thermal barriers have consisted of layers of polysulfide type fuel tank sealants. Such materials prevent hot arc products or hot spots from contacting fuel vapors. Fuel

containers such as rubberized cloth bags (bladders) as used in helicopter fuel tanks may also be considered. Electric arcs in laboratory tests to melt holes in aluminum skins have not penetrated fuel bags next to melted holes.

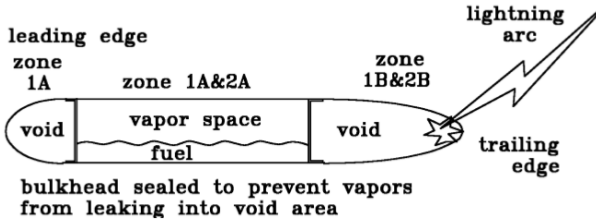

Fig. 7.18 Trailing edge construction to avoid fuel ignition from extended flash hang-on.

Candidate designs must always be tested to verify their effectiveness. Life cycle aspects, such as the durability of the thermal barrier and its chemical compatibility with fuels, must also be considered to ensure continued airworthiness.

7.3.4 Protection against Effects of Current in Tank Structures

In some of the aircraft accidents that have been attributed to lightning and that occurred because of in-flight explosion of fuel, the exact cause of fuel ignition has remained obscure. It is exceedingly difficult to find evidence of small arcs or sparks that have ignited fuel vapors in the presence of residual damage left in the wreckage of fuel tanks. In several other cases, the melt-through of an integral tank has caused ignition. Ignition of fuel vapors at vent outlets has also been the suspected cause of two accidents.

Another possible cause of these accidents is that lightning current, flowing through the fuel tank structure or fuel system components, could have caused sparking, or arcing inside the tanks which ignited the fuel vapor. No conclusive evidence of this has been found,

Much attention has been given to keeping lightning currents out of the interior of an aircraft by providing electrically conductive skins. However, even with highly conductive aluminum skins, some lightning current is going to *diffuse* or *redistribute* into the interior structural elements and system components, such as fuel transfer and vent pipes. Whenever current crosses joints and couplings, there exists the possibility of arcing. Since so little energy is needed to ignite fuel, the behavior of these internal currents is of great importance to fuel system safety.

Arcing can also occur when lightning currents in the skin encounter discontinuities, such as access panels and filler caps. Electrical wiring associated with the fuel quantity indicating system may experience induced voltages of sufficient magnitude to produce sparking if this wiring is not well protected. The processes of diffusion and redistribution of lightning currents to interior fuel tank elements are described in Chapters 11 and 12. The result of these processes is that significant amounts of lightning stroke and continuing currents can find their way into substructures like ribs, spars, and stringers, and into system components like fuel transfer and vent tubes and hydraulic tubes. There is no practical way to prevent this from happening in structures. It can be prevented by use of electrical insulation, as will be discussed later.

Fig. 7.19 shows the possible lightning current paths in a typical fuel tank and calls attention to some of the areas of concern. The following paragraphs discuss each of these areas in turn. Other possible sources of ignition, not shown in the figure, are also discussed.

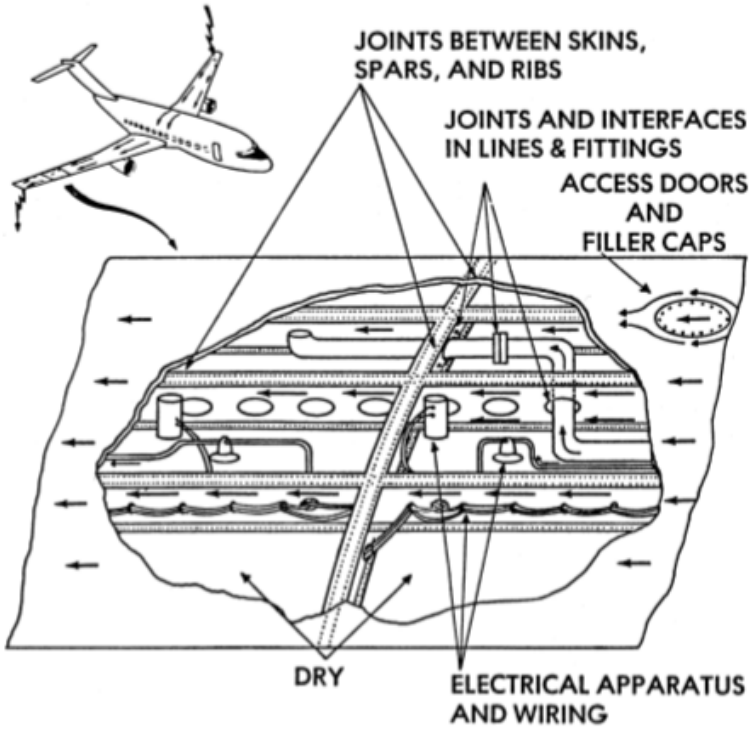

Fig. 7.19 Lightning current paths in a fuel tank and potential ignition sources.

Gravity Filler Caps

Fuel filler caps must be fitted with gaskets and seals between the removable cap and its adapter in the tank, but they must also make some mechanical contact, so that the cap is secured to the adapter. The seal is usually electrically nonconductive. However, if the mechanical connection is conductive, arcing may occur in this interface since the cap and its adapter are installed in a tank skin that must conduct lightning currents. Some of this current will try to flow into and out of the filler cap, even if it is not installed in a lightning attachment zone. If the arcing is sufficiently intense, the arc products may blow past the seal and into the fuel vapor space. Sometimes the cap must be installed in a strike zone, and at least one aircraft accident involving a military transport airplane has been caused by a lightning strike to a fuel filler cap that ignited fuel vapors.

Newman, Robb, and Stahmann [7.37] were among the first to evaluate lightning-related arcing at filler caps in a laboratory. They demonstrated that direct strikes to filler caps of the design then in common use would cause profuse showers of incendiary arc products inside the tank. They applied simulated strikes (ranging in energy from a very mild 35 kA, 0.006 x 10^6 A^2s stroke to a very severe 180 kA, 3 x 10^6 A^2s stroke) to typical fuel filler caps in use up to the 1980's The profuse arcing occurred under all lightning strike conditions. When an ignitable fuel vapor was placed in a test chamber on which the filler cap was installed, these arc products readily produced ignition. Caps of the type studied in [7.37] are illustrated in Fig. 7.20(a).

When the same filler caps were not struck directly but merely installed in a tank skin through which Zone 3 lightning current was flowing, Newman and his colleagues reported that neither arcing nor fuel vapor ignition occurred. Subsequent studies confirm these results, but the possibility of arcing at a fuel filler cap of the type shown in Fig. 7.20(a) even if it is not struck by lightning directly, cannot be entirely ruled out.

Protection techniques for filler caps

After observing the arcing from the direct strikes to the original filler caps, Newman evaluated several design modifications to prevent this. Fig. 7.20(a) shows where arcing can take place on the inside surfaces of an unprotected filler cap while Fig. 7.20(b) shows a design that has been successful in preventing arcing.

A "lightning-protected cap" typically has a plastic insert so that there are no mating metal surfaces across which lightning current might flow and cause arcing. If a lanyard is required, it is made of plastic, since one source of arcing on filler caps was found to be along the ball chain used to retain the cap. Such ball chains are still found on gravity filler caps (even ones that are otherwise safe from arcing). These should always be replaced with a nonconductive lanyard.

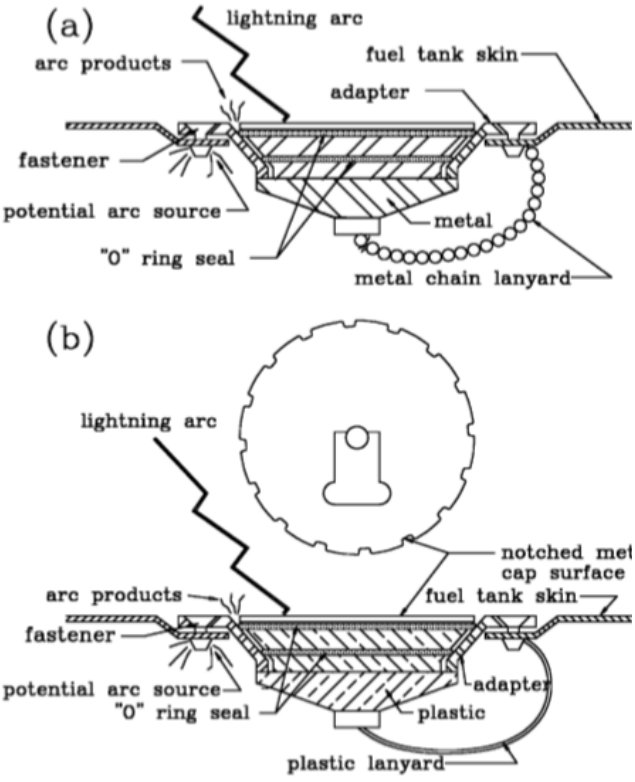

Fig. 7.20 Fuel filler cap designs.
(a) Unprotected
(b) Protected

An electrically nonconductive O-ring often provides a seal between the plastic insert and the mating adapter to prevent fuel leaks. When a strike to the cap occurs, the lightning currents are forced to arc from the cap to the adjacent adapter, since the O-ring seal prevents direct electrical contact between the two parts. This arcing creates a pressure buildup at the O-ring. If this pressure is too high, arc products could blow past the O-ring and into the fuel vapor. To minimize pressure buildup, a series of cutouts are made around the perimeter of the cap surface, so that arc products can vent to the outside of the tank.

An alternative protection design replaces all the metal parts of the cap with plastic, thus preventing direct arc attachment to the cap from taking place at all.

Lightning protected caps should always be used, even if it is installed in zone 3 since some current will pass by and through the cap installation. At least one specification, *MIL-C-38373B*, has been written describing a lightning protected cap. If there is any doubt about the protection capability of the design, the cap should be tested with its mating adapter installed in a specimen of the intended tank skin, according to the procedure described in [7.24].

Lightning protected caps are usually designed for use with mating adapters furnished by the cap manufacturer. These are intended to be installed in the tank skin. The interface between the filler cap adapter and the surrounding tank skin can also be a source of arcing, and care must be taken to prevent this arcing from contacting fuel vapors. Some design methods for installing fuel-filler cap adapters are described in Fig. 7.22.

Protection for access panels

Access panels (also known as access doors) are found in nearly all fuel tank designs to facilitate the installation and maintenance of system hardware. Some typical access panels are shown in Fig. 7.21. Since these panels are frequently installed in the external skins, they are usually exposed to sweeping lightning channels. Early tests showed that arcing could occur at access panels if they were subjected to simulated lightning strikes and if they were not specifically designed to tolerate lightning. This happens if strikes occur to the surface of the door, or to the fasteners.

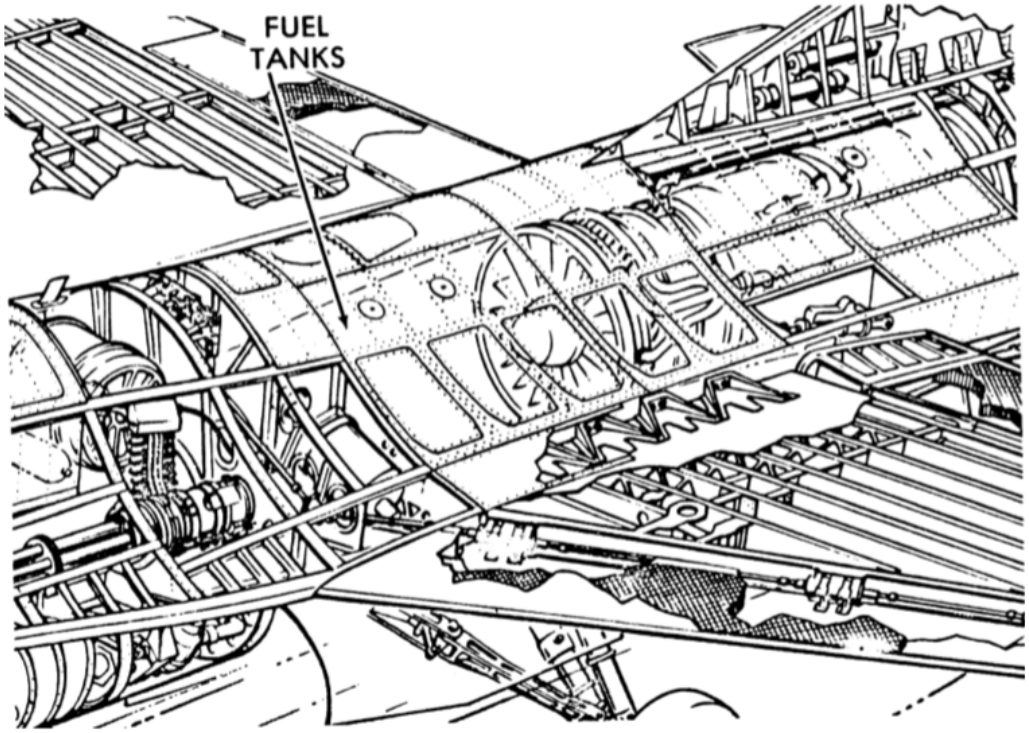

Fig. 7.21 Large access doors in *Zone 2A* over fuselage integral fuel tanks.

Modifications have been developed that prevented this arcing, even when the access panels were struck directly. Such modifications usually consist of some combination of the following features:

1. Avoidance of metal-to-metal contact between parts exposed to fuel vapor spaces.

2. Provision of adequate current conduction paths between panel and adapter and between adapter and surrounding skin, away from fuel vapors. These paths are usually provided by the fasteners, which are separated from vapor areas by O-rings, gaskets, or sealants.

3. Application of sealant to other potential arc or spark sources, to prevent contact with fuel vapors. Sealants are discussed in §7.3.5.

4. For transport airplanes, it is necessary to provide protection against possible failure conditions in the assembly from becoming and ignition source.

This means that whatever protection methods are considered need to be fault tolerant (not allowing ignition sources in the event of some failure or degradation of the protection feature). Usually a second protection feature ("layer') needs to be provided, and the two must not interfere with each other, such that a failure or degradation of one protection feature does not cause a failure in another feature. This usually requires that these features be independent of each other. In other words, two layers of sealant (for example) would not be expected to be sufficiently independent of each other to be considered as two independent protection features for the purposes of providing fault tolerance. A layer of tank sealant combined with a conductive, interference-fit fastener would likely provide two independent protection features since failure of the sealant would not cause the fastener installation to fail, and vice versa. While mentioned within the context of fuel access panels, the requirement to provide fault tolerance applies to all aspects of transport airplane fuel tanks and fuel systems.

Any design which allows the panel installation to tolerate the applicable lightning environment while meeting other performance and structural requirements is acceptable. A wide variety of designs have proven satisfactory. Some acceptable access panel designs are shown in Figs. 7.22(a) through 7.22(d). These same approaches are applicable to gravity-filler cap adapters, fuel-vent outlet installations, and any other assembly that is intended to be installed in integral tank skins.

O-rings and gaskets: Fig. 7.22(a) shows a common access panel design in which an O-ring, fitted in a slot in the doubler, prevents arc products around the fastener from entering the fuel vapor space. Instead of entering the space, the arc products escape to the outside. In addition, the access panel riveted nut plate (dome nut), doubler fastener, and the fillets have all been covered with polysulfide type fuel tank sealant to contain arc products at these locations, isolating them from exposure to fuel vapor. All the other variations shown in Fig. 7.22 employ an O-ring as a barrier to arc products that originate from around the fastener or rivets. Fig. 7.22(b) and (c) are variations on the design approach of Fig. 7.22(a). Variation (b) uses an integral nut plates or nut ring to eliminate the arc sources at the riveted nut plates. Variation (c) extends this concept further by eliminating the interface between the fuel tank skin and the doubler by making the doubler integral to the skin. Anywhere that interfaces between separate parts that comprise a fuel tank assembly can be eliminated is an opportunity to reduce the number of possible arcing sources and the number of places that protection against these possible ignition sources have to be provided. Further discussion about these alternatives follows.

Integral nut ring: In example (b) of Fig. 7.22, the riveted nut plate has been replaced with an integral nut ring. This configuration, in which either the captive nut is installed inside a casting or the ring has a tapped hole, allows higher currents to be conducted than the riveted nut plates. Current entering the integral nut ring diffuses to several fasteners that share the current carried to the doubler and the skin. Fuel tank sealant is applied around the fillets, nut-ring-to-doubler fasteners and skin-to-doubler fasteners (if present) to prevent arc products from entering the vapor space from these interfaces.

Elimination of fasteners: Two additional designs are shown in Figs. 7.22(c) and (d), in which the separate doublers in examples (a) and (b) have been removed and replaced with integral doublers machined or molded from one original block of metal. This eliminates the need for the skin-to-doubler fasteners used in the previous examples thus removing them as potential ignition sources.

Preferred fastener locations: In Fig. 7.22(d), the access-panel fastener head is in the surrounding skin panel so that a strike to the panel or to the fastener head would enable current to flow directly into the primary structure and not need to flow across the interface between access panel and surrounding skin. Achievement of this arrangement necessitates that the panel be oval shaped to allow its removal from the aircraft. In Fig. 7.22(d), the fastener head is countersunk into the skin rather than into the access panel. The current from a strike to this fastener would be mostly conducted directly into the skin, decreasing the current density in the panel-to-skin fastener. This configuration would minimize the intensity of arcing at the fastener/panel interface. The use of an integral nut ring would reduce current density in the panel-to-ring fasteners still further. Arc products would be contained by the O-ring seal as in the first example, Fig. 7.22(a).

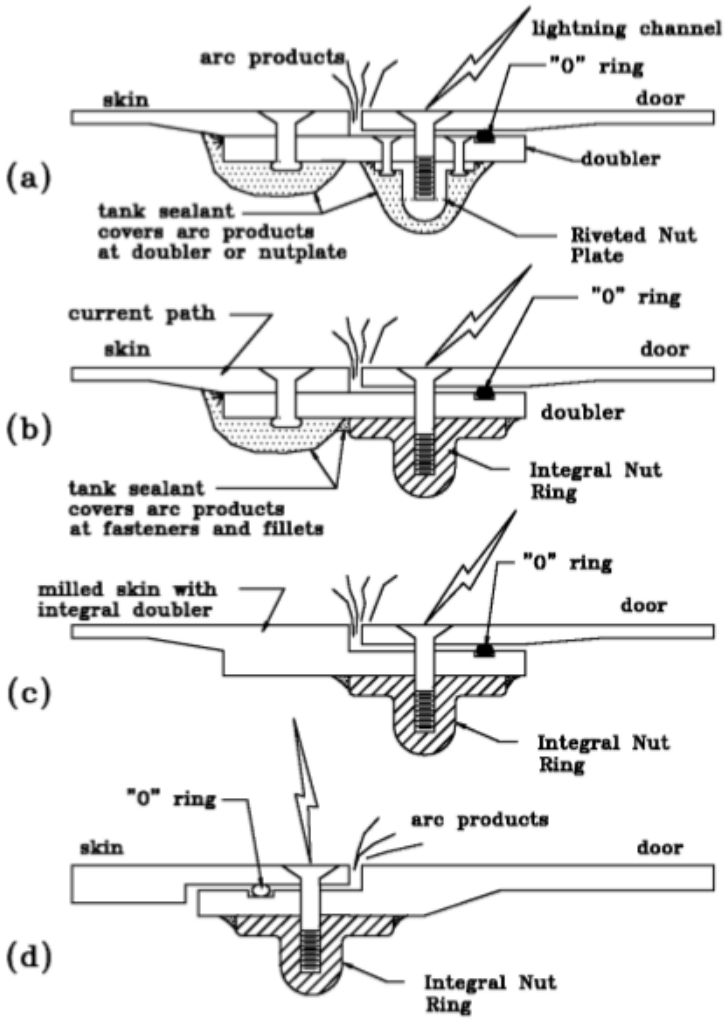

Fig. 7.22 Treatment of fasteners on access doors.
(a) O-ring
(b) Integral nut plate
(c) and (d) Elimination of doublers.

Nonconductive panels: Currents can be eliminated from the panel altogether if the panel is constructed of a nonconductive material, such as chopped glass fiber reinforced composite. A lightning channel attempting to attach to such a panel would simply flash over its surface to the adjacent conductive skin or to a fastener in the arrangements of Fig. 7.22 (b), (c) or (d). In this case all or most of the current would enter one or two fasteners so the per fastener current would be high and difficult to manage without arcing. Arrangement (d) has the fasteners installed in the fixed skin where it would presumably be shared among multiple fasteners.

Alternative gasket approaches: Figs. 7.23(a) and (b) show two access panel gasket designs. Example (a) has an O-ring, which fits into a groove in the doubler and prevents arc products from entering the vapor space within the fuel tank.

In Fig. 7.23(b), a flat gasket has been provided with slots, as shown, so that arc products originating at the panel-to-doubler (or panel-to-skin) fasteners can be vented to the external surface, away from the internal fuel/vapor space. If this installation is intended for a transport aircraft, fault tolerance has to be provided. This is possible by adding a second O-ring so that if one is damaged or omitted the second one is available to stop arc products. A consideration when using two similar protection features is whether the condition that resulted in the first failure (i.e. broken O-ring in this example) could also cause a failure in the second protection feature. If this is the case, the second feature would need to provide a different kind of protection, and not be susceptible to a common-mode failure condition. One approach would be to eliminate the source(s) of the arcing, which are typically around the fastener installations. This is not always practical

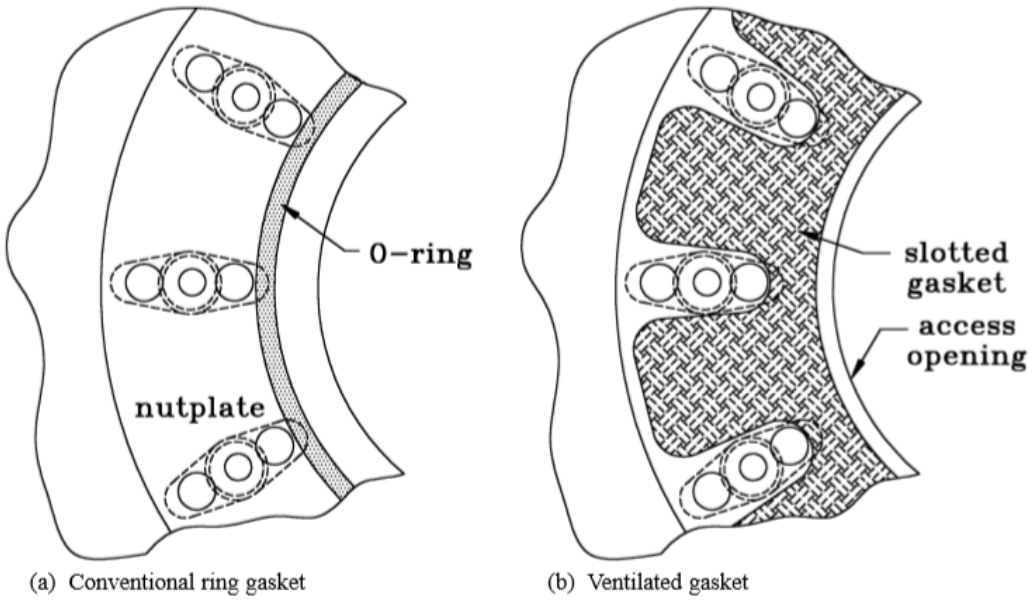

Fig. 7.23 O-ring and slotted gasket installations.

Other modifications: Other modifications to access panel seal design, not described here, have proven equally effective in preventing arcing.

In some cases, anodized clamp rings or insulating gaskets have proven acceptable merely by providing sufficient metal-to-metal conductivity through the bolts or fasteners alone. The panel for which the modification described in was developed, had only 23 fasteners. Some panels, held in place by more than 40 fasteners, have been found to resist arcing so successfully that insulating finishes or paints (such as anodizing or zinc chromate) could be left on the mating surfaces. Generally, the more fasteners available for current conduction, the lower the current density per fastener.

Guidelines for Access panels: Here are some guidelines for designing a lightning-protected access panel:

1. Provide as much electrical contact via screws or fasteners as possible and make the current paths through these fasteners as short as possible.
2. Isolate the fasteners from vapor areas with nonconductive gaskets or O-ring seals.
3. Thoroughly coat all exterior surfaces of fasteners and nuts with tank sealant.

The importance of eliminating ignition sources at access panel installations cannot be overemphasized, especially in designs where the access panel is, itself, a part of the aircraft skin that encloses fuel. An example of this on a small fighter aircraft is shown in Fig. 7.21. This airplane has large access panels covering its fuselage fuel tanks. The panels cover a large area and are exposed to lightning strikes sweeping aft from the nose. Panels of new design should be tested to be certain that their lightning protection is adequate.

Protection for water drains

Water drains are often installed near the low points in fuel tanks. These are usually in Zone 3 if installed in main wing tanks and in Zones 2A if located in exposed surfaces of center tanks. Many of these are small metal assemblies with a hexagonal exterior nut containing and open/shut screw and a similar retainer on the inside tank surface with openings for water flow when the screw is turned to the "open" position. Some of these devices are made of plastic and marketed as "Lightning Safe" but this claim must not be depended upon until the drain is tested in an intended installation. Aircraft skin finishes may play a significant role in whether the drain is free of ignition sources when tested in accordance with the lightning environment assigned to the zone that the drain is to be located in.

Resistance measurements: Adequate electrical conductivity between access panels, other adapters, and surrounding skins cannot be verified just by measuring the direct current (DC) resistance between the panel and the surrounding airframe and seeing that it is below some arbitrary value, such as 2.5 milliohms. Instead, the design emphasis should be focused on the ability of the panel-to-skin interfaces to conduct lightning currents without arcing that could be a potential ignition source. This must be evaluated by a lightning test. The DC resistance of a panel-to-skin interface may be easy to measure, and it may also be a result of a successful, arc-free design, but it is a result, not the driving design criterion.

Verification of protection: The only way to be certain that a protection design is adequate is to perform lightning tests on production-like installations. Details of the production assembly, such as mating surface finishes and fastener torque or tightness, also play a role in protection effectiveness. These details, with appropriate tolerances, should be accounted for in test planning and in the assessment of test results. Tests performed by equipment vendors usually do not include tests of the *installations* of fuel-filler cap adapters or access panel adapters into the airplane skin or structure. Vendor tests usually qualify only the vendor item, not its installation in the aircraft. The SAE aircraft lightning test standard [7.24] describes tests appropriate for all lightning strike zones.

7.3.5 Containment of Arc Products

As noted earlier, certain design methods can be employed to reduce the intensity of arcs at conductive interfaces. These methods may prevent ignitions at low to moderate current levels, but at higher levels the arc pressure buildup may be sufficient to blow arc products into the fuel vapor space. For this reason, it is generally necessary to employ barriers between arc sources and fuel vapor areas. The purpose of these barriers is to contain the arc products and prevent them from reaching flammable vapors. One approach to this has been to provide a measured amount of sealant into a plastic container of sufficient diameter to cover the nut and washer such that a consistent coverage is achieved. This reduces any variations in arc containment performance. The concept is shown in Fig. 7.24.

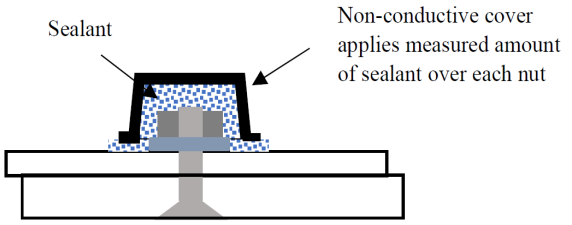

Fig. 7.24 Concept for achieving consistent sealant application

Containment with tank sealant

Sealant is used so often throughout fuel tanks and it can provide a barrier to prevent arc products from reaching fuel vapors.

In situations where it is not possible to prevent all the fasteners or other interfaces in a fuel tank from arcing, the arc products must be isolated from fuel vapors. This isolation is often accomplished by coating the fasteners with fuel tank sealant of the sort that is usually applied to prevent fuel leaks. Tank sealants are usually made from a polysulfide material, but other materials may also be used. These sealants must adhere well to structural surfaces, including the primers, paints, and resins that may coat those surfaces. The coverage thickness of a sealant should be at least 2.5 mm (0.100 in). While its intended purpose is usually prevention of fuel leaks at fasteners, sealant also contains the arcs arc products that occur at the fasteners during lightning strikes, preventing them from contacting fuel vapors. Typical areas that require sealant protection include structural interfaces, such as rib/spar/skin interfaces, fasteners which extend through the tank skin from the exterior surface, and internal fasteners and rivets which form part of the current path (especially if the structural members are of CFC material). This is the most common method of preventing fuel vapor ignition from arc sources at fasteners.

It must be emphasized that sealant does not eliminate arcs, but merely contains the incendiary products of arcs, so that they are not exposed to the flammable vapor space.

The effectiveness of tank sealant coatings increases with their thickness, although there are practical limits to the amount of sealant that can be applied because of the weight it adds to the aircraft, its cost and the labor involved in applying it. The effectiveness of sealants also depends upon the skill of the technician applying it. Fasteners must be thoroughly coated and there must be no voids or thinly coated areas.

Examples of acceptable and unacceptable sealant coverage for fasteners are shown in Fig. 7.26. Fig. 7.25(a) shows sealant applied at the sides of the fastener, but in an insufficient quantity to prevent arc pressure from bursting through the sealant or through the interfaces between the sealant and the fastener. This can be remedied by applying a thicker coating as shown in Fig. 7.26(b). Note that the sealant in Fig. 7.26(b) has been extended over the fastener head, thus reducing the possibility of arc products bursting through the sealant at this location as well.

Fig. 7.25(c) illustrates use of a nonconductive washer to prevent arc products from within the fastener hole from reaching the vapor space. This concept also insulates the nut from contact with the interior surface, thereby eliminating one source of arcing.

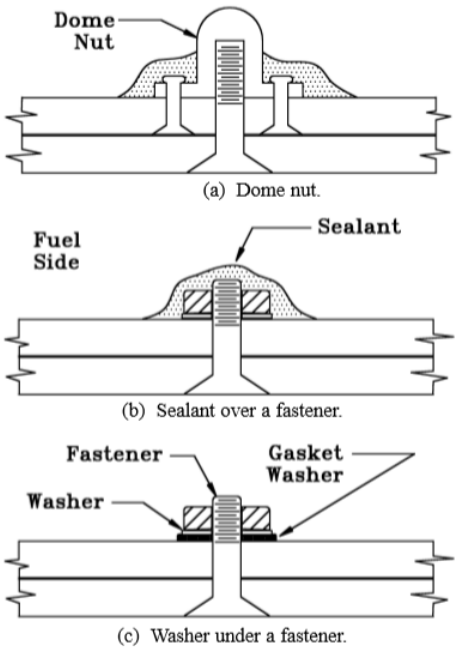

Fig. 7.25 Some fastener sealing concepts.

Overcoating of fasteners

Guidelines for overcoating of fastener nuts are shown in Fig. 7.26.

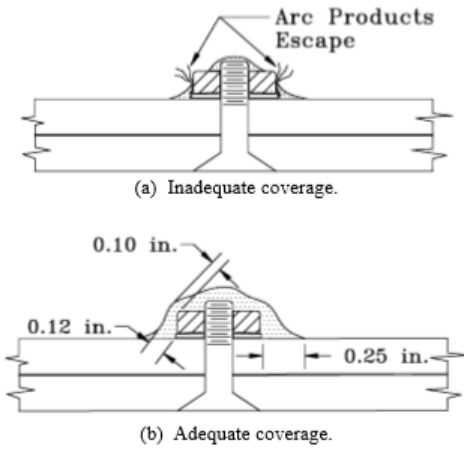

Fig. 7.26 Guidelines for coverage of fasteners

Although arcing can take place at any interface between a fastener and tank structure, the most significant arcing usually takes place between the shaft of the fastener and the inside surface(s) of the hole(s). The pressure that builds up in this area may vent under the fastener nut or washer into the fuel tank vapor space. One way to reduce this danger is to use a special type of fastener that provides a pressure seal. Examples of these fasteners are shown in Fig. 7.27. Each has a built-in gasket that contains arc products that form between the fastener and the structure. Arcing may occur between surfaces in proximity, such as between a fastener housing and an interior skin surface, but electrically nonconductive primers or finishes on the skin surface may help prevent this. Candidate installations that utilize these specialized fasteners should be tested to be certain they will perform as expected during a lightning strike.

The arcing threshold levels of self-sealing, rivet-less nut plates, Fig. 7.27(a), are generally higher than those of similar nut plate fasteners with rivets. This can be accredited to the combination of the rubber seal, which prevents blow-by of arc products into the fuel vapor space, and the elimination of the rivets, which are a source of arcing when currents of any appreciable amplitude are conducted through the nut plate fastener. While arcing threshold levels of typical fasteners have been demonstrated to be approximately 5 kA, the current amplitudes conducted without arcing by rivet-less nut plate fasteners have been three to four times this level.

Sealing of structural interfaces

Sealants must also be applied to structural interfaces, at least in the interior interfaces of exterior skins where lightning current densities are highest. In aluminum tanks, coatings of electrically nonconductive anti-corrosion finish on interfacing surfaces can cause arcing to occur between parts due to the poor electrical contact.

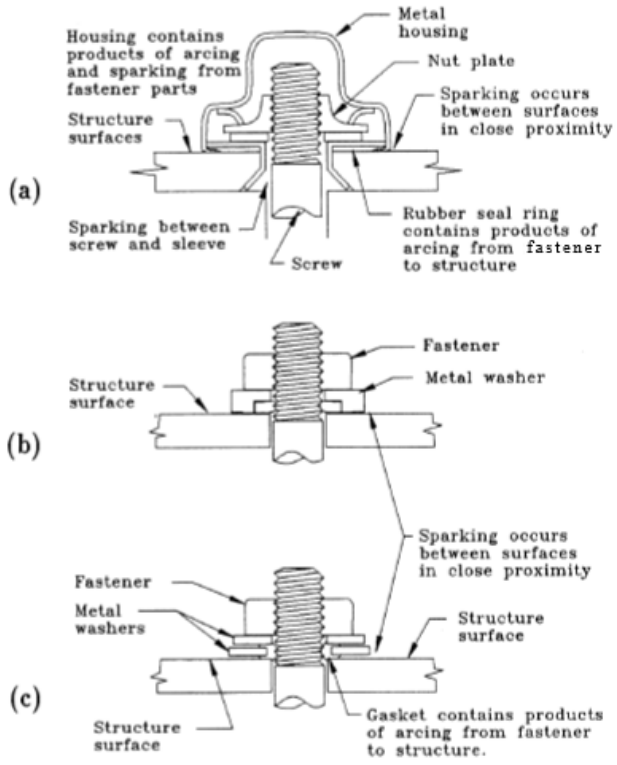

Fig. 7.27 Gasket sealed fasteners.
(a) Self-sealing rivet-less nut plate
(b) Washer with gasket
(c) NAS 1523 sealing washer

For CFC tanks, arcing can be caused by the inadequate electrical bonds due to nonconductive resins and adhesives used in the fabrication of the structures. Arcing may also occur due to insufficient electrical contact between fuel system components and sparking may occur due to voltage potential differences between those components or between the components and adjacent airframe structure. Fig. 7.28. [7.46] gives recommended dimensions for applying fuel tank sealant at structural interfaces. To provide protection against lightning-related arc products, sealant application must be thorough and of sufficient thickness, with no voids, or thinly applied areas.

Advantages of sealant for protection

The advantages of using sealant for lightning protection include the following:

1. Sealants applied to prevent leaks may provide containment of arc products. But not all leak prevention applications will be adequate barriers against electrical arc products. Containment of arcs and arc products may only require that the sealant, used anyway to prevent leakage, be applied more thickly, and/or over a wider area.

2. Sealants can usually be applied to existing designs and installations.

Disadvantages of sealant for protection

The disadvantages of sealant use in lightning protection include the following:

1. The effectiveness of the sealant application depends on the skill of the person and/or method of applying the sealant, especially in areas of the tank that are difficult to access. In these areas, even a skilled technician may have difficulty ensuring that sealant coverage is complete and without voids or thin spots. Some areas may receive excessive sealant while others may receive too little to contain energetic arc products. Protection effectiveness also depends on how closely the operator adheres to sealant guidelines.

2. Additional sealant may incur a weight and cost penalty. While application of thick layers of sealant improves lightning protection, it also adds to the weight of the aircraft which increases operating costs.

3. The effectiveness of fuel tank sealants for arc and arc product containment may deteriorate with age, temperature cycling, and the constant 'working' of the airframe. Sealants within the tanks must be given periodic visual inspections.

4. The development of fuel leaks may indicate that fuel tank sealants are cracking or disbanding.

5. Multiple layers of sealant applied to the same installation may not be considered as offering a fault tolerant design, since protection features must be independent of each other.

7.3.6 Structural Joints

High density patterns of rivets or fasteners, such as those commonly used to join fuel tank skins to stiffeners, ribs, and spars, have been found to be capable of conducting Zone 3 stroke currents even when nonconductive primers and sealants are present between the surfaces, as in Fig. 7.29. This is because there are usually sufficient random electrical contacts between fasteners and holes to provide adequate current paths. More of these incidental current paths are usually developed as current density increases. This situation should not be depended upon for protection purposes. Lightning current conduction tests should be applied to specimens of these designs to confirm ability to safely conduct lightning currents.

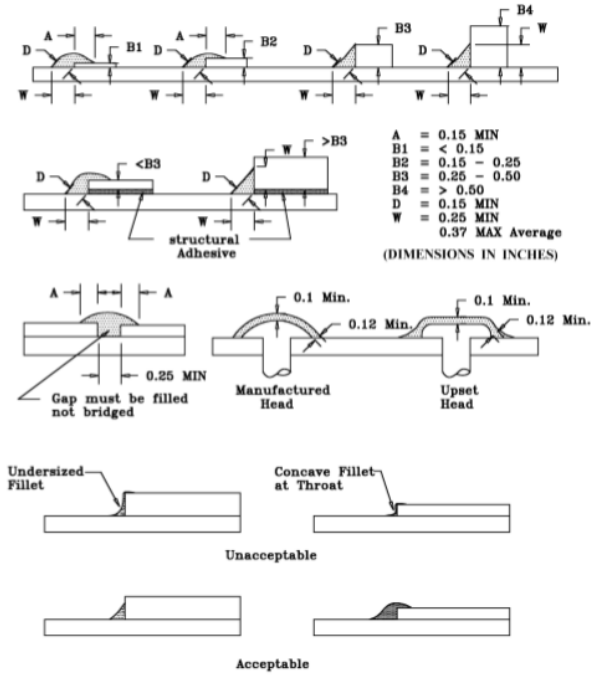

Fig. 7.28 Recommended fillet configurations. (based on less than 0.003-inch joint deflection) [7.46]

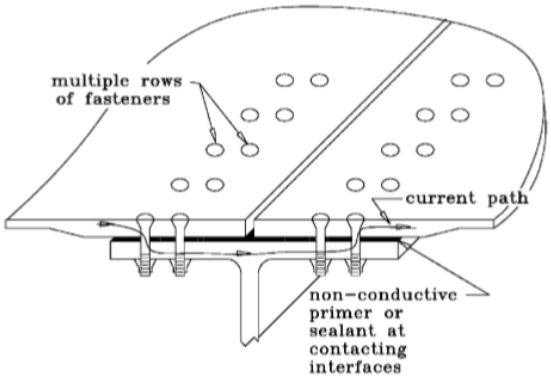

Fig. 7.29 Fasteners provide electrical bond paths where mating surfaces are coated with nonconductive finishes and sealers.

Short [7.47], for example, reports 200 kA stroke current tests of skin-to-stringer joint samples fastened with double rows of taper-lock fasteners, such as have been used in the wing structures of large transport category aircraft. The test samples had 16 fasteners on each end of the joint, and no arcing was detected in the joint. This represents an average of more than 10 kA of stroke current per fastener, even though the average current density in the same fasteners when installed in the wing structure would be far less than this.

At areas of high current density, ignition sources due to arcing usually occur at the interfaces between the fastener and surrounding metal, as shown in Fig. 7.30. The occurrence of this arcing depends on other physical characteristics, such as countersink and skin thicknesses, fastener installation details (i.e., whether clearance or interference fit), surface coatings, and fastener tightness. Fuel tank structural joint designs should always be subjected to tests in which simulated lightning currents are conducted through prototype joints to confirm absence of ignition sources or identify and address sources that are identified by these tests.

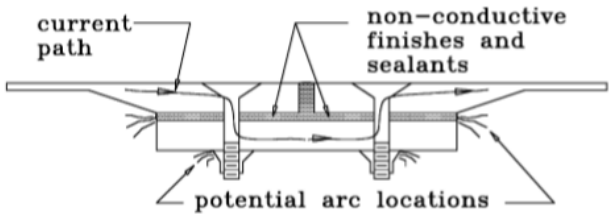

Fig. 7.30 Potential ignition source locations at structural interfaces coated with corrosion-resistant nonconductive finishes and sealants.

Numerical simulation of structures can be used to estimate the current densities (i.e., average current through each fastener) so that realistic test conditions can be defined.

There is no hard-and-fast rule for determining the number of fasteners per joint necessary to avoid arcing, but a rough guideline of 5 kA per fastener is useful for estimating the number of fasteners that may be required to transfer lightning currents through structural joints without arcing if these fastener installations have been designed to provide current conduction capability. This depends on the details of fastener installations. There must be dependable paths and interfaces for currents to flow among elements of the installation. If there are not conductive interfaces, arcing will occur. If the conductive interfaces are present, arcing may still happen if current per fastener exceeds the arc threshold(s) of the conductive interfaces in the installation.

Of course, fastened joints must be consistently able to safely conduct currents. For this to happen it may be necessary to provide a certain minimum number of fasteners with dependable conduction features, such as interference-fit installations that provide metal-to-metal contacts between fasteners and holes. Some designs include this feature.

The interior surfaces of most penetrating fastener nut installations are usually covered with sealant, so that the arc products may not reach the fuel vapor space. Sealant also prevents water from entering the joint and so inhibits corrosion. In general, it has been found that structural fastener configurations inside tanks whose fasteners are not exposed to lightning attachment can tolerate Zone 3 current densities without visible arcing or the need for over coating with sealant. This is because there are sufficient random electrical contacts between fasteners and holes, even with sealant included in 'wet' installations. This is especially true in large transport aircraft fuel tanks employing many fasteners.

Interior tank structural interfaces with only a few fasteners in which lightning strike Zone 3 current densities would be higher, may not have sufficient conductivity. These situations must be evaluated by test. Transport aircraft will need to show fault tolerance to effects from Zone 3 currents, so the sealant cannot be depended upon as a primary means of preventing ignition sources.

Fuel tank fasteners exposed on exterior surfaces of all aircraft in Zones 1A, 1C or 2A must usually be protected by overcoating of nut installations with fuel tank sealant, since fastener current densities are higher in these zones where lightning channels may directly contact the fasteners.

The ability of these sealant coatings to contain arc products should be verified by lightning test.

The points described above may be summarized as follows:

- The term "fastener", as used in this chapter, refers to rivets, screws or bolts, or any other device that penetrates from the exterior to the interior surfaces of the aircraft integral fuel tanks. These are mostly primary structural rivets and, sometimes, rivets or removable fasteners (screws) associated with removable access panels, gravity-fuel filler caps, or other installations.

- Lightning flash channels that 'sweep' across the exterior surface of a fuel tank tend to reattach to fasteners as defined above. When this happens, some of the lightning current is immediately conducted between countersunk rivet heads to countersunk holes and to

other fasteners in a row, the rest of the current flows through the fastener to interior structural surfaces. This is where the arcing that may become a fuel vapor ignition source occurs. It is the products of this arcing that must be contained by the fuel tank sealant or other barriers.

- Most fasteners that penetrate fuel tanks from exterior surfaces in lightning strike zones require fuel tank sealant overcoating or other barriers to prevent arc products from reaching fuel vapor areas. The traditional flow-on sealants require care in application to achieve a uniform coverage. Several commercial products are available to enable application of measured amounts of sealant over each fastener and/or provide an additional barrier to prevent escaping arc products from reaching fuel vapors.

- The current density in a fastener to which a lightning channel attaches directly is higher if the fastener is installed in a CFC skin (even if protected by expanded metal foil (EMF) than if the fastener is installed in an aluminum structure. For this reason, additional sealant and/or barriers must usually be provided for the interior surfaces of fasteners that penetrate CFC skins.

- It is advisable to provide a layer of EMF along rows of exterior fasteners in CFC tank structures to help distribute lightning currents into all the fasteners in the row and reduce the lightning current density in any single fastener. (It may also be necessary to protect the rest of the CFC with EMF to prevent punch-through due to lightning attachment to these surfaces as well).

- On large transport airplanes, the current densities in Zone 3 areas are usually sufficiently low (i.e., less than 5 kA of conducted stroke current per fastener, where the 'stroke current' is defined by the Component A waveform).

- Structural interfaces in which there are only a few fasteners available to share the conduction of Zone 3 currents, or where there may not be adequate sharing of stroke currents among neighboring fasteners, lightning tests of typical integral fuel tank structural elements are necessary. The test currents should be selected based on analysis of the complete tank structure to estimate the percentage of the total (200 kA, etc.). Zone 3 current that is expected to flow in the portion of the tank (i.e., wing) cross-section that is to be included in the test specimen.

Arc threshold of fasteners in Zone 3 areas

Under a program sponsored by NASA [7.48], tests were performed to determine the arc threshold current levels of typical fastener configurations used in aircraft.

For those tests, aluminum lap-joint specimens were adhesive-bonded with electrically nonconductive fuel tank sealant and were also fastened with a single rivet which had been 'wet-installed' with the same sealant. Currents were conducted directly into one end of these specimens and removed from the other end. All current was forced through the single fastener since the nonconductive sealant eliminated any direct electrical contact between the mating surfaces. No coatings of any kind were applied to the head or nut of the fastener.

The tests indicated that the arc threshold current level of the fastener was 5 kA. Thus, a door containing 40 fasteners could in theory conduct nearly 200 kA without arcing if the current were distributed evenly among the fasteners. In reality, lightning current does not divide uniformly, but is somewhat more concentrated in the fasteners closest to the point of lightning arc entry or current attachment or exit(s).

Lightning attachments to fasteners

The preceding discussion relates mostly to joints in Zone 3 that must conduct only a portion of the Zone 3 lightning current. Exterior fasteners located in Zones 1A, 1C, or 2A, trailing edge zones in fixed-wing aircraft or certain surface zones in hovering helicopters are in Zones 1B or 2B can experience the total lightning continuing current Since it is possible for the lightning arc to remain attached to a single fastener or rivet in these zones. When this happens, the continuing current arc can melt the fastener and the surrounding skin, and arcing may occur at interior fastener interfaces with interior surfaces of skins or structures. Generally, it is recommended that fuel vapors not be in direct contact with tank surfaces that are in lightning strike zones 1B or 2B since all the flash currents are expected to enter or exit there. Fuel bladders or other barriers should be used to separate fuel vapors from fuel tank interior surfaces where arcing and melting of metal skins may occur.

Some guidelines for fuel tank structural joints

Here are some basic guidelines for designing structural joints in integral fuel tanks:

1. Provide electrically conducting paths between structural elements, so that lightning currents can be conducted from one to the other without arcing and without having to spark across nonconductive adhesives or sealants. Often, this can be achieved by providing enough rivets or removable fasteners that make metal-to-metal contact with the joined parts. There must be sufficient areas of contact among all the fasteners in the current path to avoid arcing, damage to the fasteners or damage to surrounding structure.

2. Try not to put any insulating materials in places that would divert lightning current from straight and direct paths between entry and exit points on the aircraft. Otherwise, voltages may build up wherever such diversions occur, causing sparking. The diversions through the fasteners and stringer shown in Fig. 7.29 are acceptable, but more extended paths may not be.

3. Consider the possibility that aging and mechanical stress may reduce electrical conductivity in structural joints. Continued flexing of structures under flight load conditions may eventually loosen joints enough that arcing could occur. To evaluate this possibility, perform simulated lightning tests on joint samples that have been previously subjected to fatigue or environmental tests.

4. Coat all joints thoroughly with fuel tank sealant to contain any arcs or arc products that may occur. A discussion on sealing is found in §7.3.5.

5. Do not rely upon resistance measurements to confirm the adequacy of lightning current conductivity in a joint. The inductance of the current path provided by a joint plays an equally important part in this. Resistance measurements (ac or DC) may be useful as a production quality control tool, but they are not useful for establishing the adequacy of the lightning current path through a joint.

A variety of objects are installed in exterior skins. When these are in lightning strike zones, they are most susceptible to becoming ignition sources if exposed to a strike. These, and other objects that are in Zone 3 are also exposed to conducted lightning currents that may also be a cause of ignition sources.

7.3.7 Eliminating Ignition Sources in Tank Structures

The previous sections details of some of the most likely sources of ignition have been presented and some ways to prevent them. In the following sections, some overall design approaches are discussed that eliminate potential ignition sources associated with tank structures, so that some of these details may not have to be dealt with. These approaches involve selecting basic structural materials, modifying the airframe structural design, and preventing contact between any remaining ignition sources and fuel vapors. Successful implementation of these measures requires the lightning protection specialist to work closely with airframe and structures designers and manufacturing technologists beginning early in the design cycle. Structural design modifications that minimize lightning protection problems can result in substantial reductions in the weight and cost associated with lightning protection, but these benefits cannot be obtained unless the principles outlined here are incorporated into the design early in the program. Structural designs must satisfy many requirements, and some features that would alleviate potential lightning problems may not be compatible with these other requirements.

The following design approaches should be utilized, to the extent practical, to minimize potential ignition sources within aircraft fuel tanks.

1. Design the fuel tank structure to minimize the number of joints, fasteners and other potential arc and spark sources in fuel vapor areas. Structural materials, by themselves, whether metal or composite, are not likely to produce ignition sources. It is the structural interfaces that produce ignition sources, usually by arcing, but sometimes by sparking.

2. Provide adequate electrical conductivity between adjacent parts of fuel tank structures at places that are designated as current paths. This usually is best provided by utilizing rivets or fasteners with electrically conductive finishes unless parts can be welded or cocured together so that inherent paths exist for electric currents. Conductivity can also be provided by providing metal-to-metal contacts among structural members, and by not having edges of these conductive interfaces exposed to fuel vapors. This latter guideline is prompted by the fact that current densities at edges of electrical bonds are usually of higher density than they are in mid-sections of such bonds, and minute arcing that appears along edges may be sufficient to ignite flammable vapors.

3. Provide barriers to isolate arc or spark products from the fuel vapor.

4. Design the fuel system components that are to be installed within tanks so that they interrupt potential current paths and can withstand any potential differences that may occur across those interruptions during lightning strikes to the airframe.

Interfaces incorporating the features listed above are shown in Fig. 7.31.

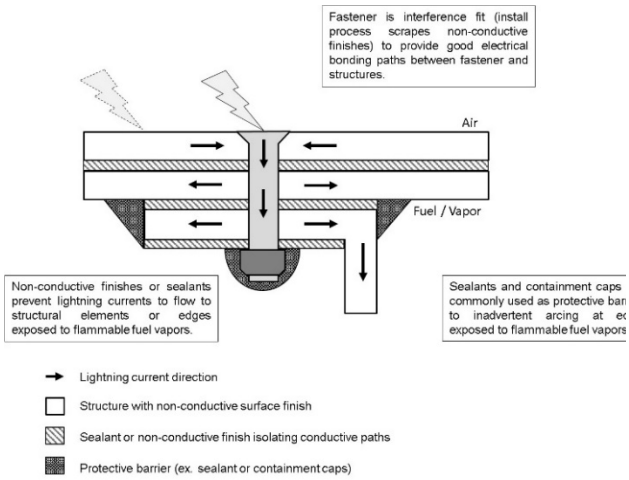

Fig. 7.31 Structural interfaces with protection design features

In summary, it might be stated that successful lightning protection designs for fuel tank structures have employed the following three features:

1. **Electrical bonding** to provide dependable current paths through the structural interface

2. **Electrical Insulation** to prevent currents from crossing interfaces that may cause arcing

3. **Barriers** against any arc products that may escape from a current conducting interface

7.3.8 Protection of Equipment Installed in Fuel Tanks

Couplings and Interfaces in Pipes

Fuel transfer and vent pipes within fuel tanks usually conduct some of the aircraft lightning currents, since they provide conducting paths in contact with conducting structures. The amount of current in plumbing depends on how the impedances of the current paths afforded by that plumbing compare with the impedances of the surrounding structural paths. Currents in plumbing within metal aircraft may be small (a few tens or hundreds of amperes) but current in metal pipes inside nonconductive or CFC structures may be high, reaching hundreds to several kiloamperes of stroke current, and similar proportions of continuing currents.

Potential ignition sources in pipes

Lightning current in fuel system plumbing may cause arcing at pipe couplings where there is intermittent or poor electrical contact. Many pipe couplings are designed to permit relative motion between the mating ends of a pipe to relieve mechanical stresses caused by wing flexure and vibration. Unfortunately, this feature precludes the tight metal-to-metal contact needed to carry lightning current. Also, electrically insulating coatings, such as anodized finishes, are often applied to the pipe ends and couplings to control corrosion. Relative motion and vibration may wear this insulation away, providing unintentional and intermittent conductive paths, but these situations lead to arcing even when small currents of 10's of amperes are involved. Therefore, particular attention should be given to the design of fuel system plumbing.

Lightning currents in pipes

The mechanism by which lightning currents diffuse to the interior of an aircraft is discussed in Chapter 11. There, it is pointed out that it can take many microseconds for lightning current to become distributed through the aircraft, because rapidly changing currents distribute primarily according to the inductance of the structural current paths, while slowly changing currents distribute according to resistances of those paths. The conductive paths in question include not only skins but also interior structures, such as floorboards, longerons, stringers, spars, ribs, frames, etc.

The early-time portions of lightning stroke currents do not spread very deeply into interior structural elements or other interior conductors because they are of short duration. Instead, they tend to remain in the metal skins. They diffuse much more rapidly to the interiors of CFC airframes.

During a NASA sponsored program [7.49], currents in the fuel lines within a fuel tank containing adhesively bonded aluminum structural elements were measured. In one example, with a current of 88 kA injected into the wing, the current in a small-diameter fuel line within the tank was 160 amperes.

The analytical procedures for determining how rapidly changing currents distribute are complex, but it can be assumed that short duration stroke currents intermediate and continuing currents have long enough durations that their distributions can be calculated on the basis of DC resistances.

For example, assume that, on a transport airplane, the leading and trailing edge sections of a wing containing integral fuel tanks are nonconductive (or sufficiently isolated to be unavailable for carrying lightning current) and that the remaining wing box is comprised of aluminum skins and spars having the dimensions shown in Fig. 7.32. Assume that the cross-sectional area of the spars and skins forming this box is 135 cm^2 (21 in^2). Assume also that the tank contains an aluminum vent pipe electrically bonded to the structure at each end of the tank. This pipe has an outside diameter of 10 cm (4 in), a wall thickness of 0.5 mm (0.02 in^2), and a cross sectional area of 1.56 cm^2 (0.24 in^2).

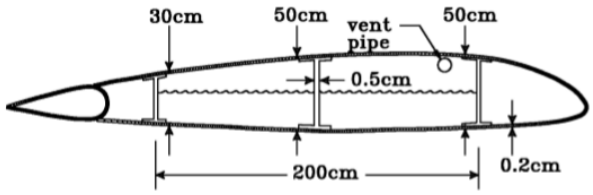

Fig. 7.32 Hypothetical wing box with integral fuel tank.

Assume further that an intermediate current with an average amplitude of 2 000 A for 5 ms, in accordance with the definition of Component B. The current in this pipe can be calculated by assuming a resistively governed distribution of current (i.e. assuming that the lightning current is unchanging) as follows,

$$I_{pipe} \approx \left[\frac{1.56\ cm^2}{135\ cm^2}\right] x\ 2\ 000A = 23.1\ A \qquad (7.2)$$

A current of this time duration has sufficient time to diffuse fully throughout the airframe and divide in accordance with the resistances of structural elements and other current paths, such as fuel pipes. Currents of this amplitude have produced incendiary arcs at poorly conducting interfaces in some fuel pipe flexible couplings. There is a fundamental incompatibility between requirements that an interface be capable of conducting electric currents and requirements that an interface be capable of continuous flexing.

Protection approaches for pipe couplings

Bond straps: Electrical bond straps or jumpers are sometimes installed across poorly conducting pipe couplings as shown in Fig. 7.33.

These bond straps should not be relied upon to prevent arcing at the couplings. Lightning currents divide between the coupling and the bond strap according to the impedances of each path. Tests of bonded couplings have shown that bond straps increase the total pipe current required to produce arcing at the coupling, but do not eliminate the possibility that some current in the coupling could lead to sparking even with the bond strap in place.

Electrical bond straps should be avoided in fuel tanks since intermittent contact internal to the braid and at the braid crimp can create ignition sources when subjected to lightning currents in the tank. Such straps also create unnecessary paths for lightning currents inside fuel tanks that can cause ignition sources at unexpected locations.

Bonded couplings: Coupling manufacturers have developed means to conduct currents across flexible couplings via spring-loaded wires included within the coupling. These, however, also employ moveable interfaces between these wires and conductive surfaces. Moveable interfaces are never consistent electrical bonds and so arcing may occur, at some current level. Added to this is the fact that the bonding wires usually make only point contacts with the moveable surfaces, so current densities at these places can become high. Tests of these bonded couplings have indicated capabilities to transfer up to several hundred amperes of lightning current, but the standard tests for fuel system equipment are necessarily conducted under stationary conditions, in room-temperature laboratory environments. Slight changes in the relative position of the mating surfaces, or introduction of dirt or residue might drastically change the current-carrying capability of a coupling. In fact, the current-carrying capability of a typical pipe coupling fluctuates continually during flight, because of the relative motion caused by structural vibrations and flexing. Tests would be difficult to conduct under simulated flight conditions where vibration and constant flexing are taking place. All of this makes safe use of these couplings a risky proposition.

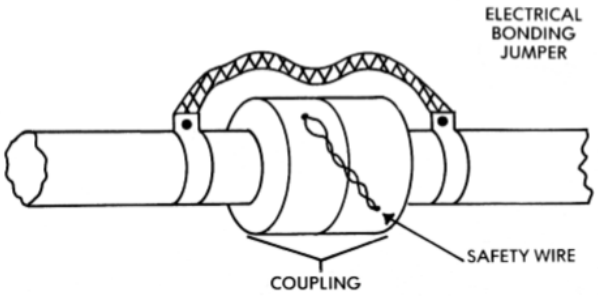

Fig. 7.33 Electrical bonding strap (‘jumper’) across A flexible coupling.

Some of the commercially available bonded couplings might be considered for use in metal fuel tanks where the amounts of lightning current that can appear in pipes are in the range of 10’s of amperes and the abilities of such couplings to conduct currents in the range of 100’s of amperes without igniting fuel vapors has been demonstrated by test. The wide margin between actual current levels and coupling successful test levels usually overcomes the instability in coupling performance.

Fuel tanks fabricated of CFC materials, however, are more highly resistive than aluminum. Currents on the exterior skin surfaces of CFC tanks diffuse more rapidly to internal conductive plumbing, where they can reach thousands of amperes. Few couplings have been able to tolerate several thousand amperes without arcing. Fig. 7.34 shows what can happen when lightning currents flow through flexible couplings. The couplings in this figure were not provided with internal bonding or external bond straps.

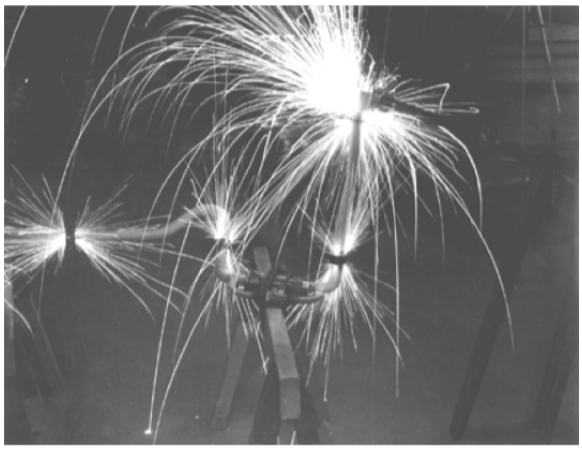

Fig. 7.34 Electrical arcing at flexible fuel pipe couplings

Fig. 7.29 shows a small arc at a typical ‘bonded’ coupling conducting 800 A of current. Light from the arc was hardly discernable on the camera film, yet the arc ignited the flammable gas atmosphere that surrounded the coupling. (Fuel pipe couplings should be tested within a chamber filled with flammable gas so that ignition sources appearing inside the pipe can be detected).

Fig. 7.35 Arcing at a bonded coupling. The larger spot of light is the optical fiber position light. The small spot is from arcing within the coupling.

The voltage measured across the coupling, shown in Fig. 7.36, also shows evidence of arcing. The test rep-resents the currents that appear in fuel tank plumbing during a lightning strike to the aircraft. This test, like most tests of couplings, was conducted with the coupling in a stationary position. Results from tests performed on couplings while they are being flexed have not been reported, but the results of such tests are likely to be even less stable.

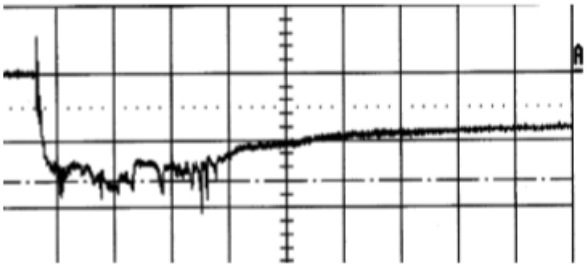

Fig. 7.36 Voltage across the bonded coupling tested in Fig. 7.35. Unstable voltage trace indicates arcing.

The fuel pipe currents are often recorded during full vehicle tests (FVTs) conducted to measure the lightning-induced transient levels in the aircraft’s electrical and avionic systems. A summary of the range of pipe currents measured by Lightning Technologies is given in Table 7.5.

Table 7.5 Summary of Fuel Pipe Currents Measured by Lightning Technologies

Applied Current Component (Per SAE ARP 5412 FIG 12A)	Pipe Current I_{peak} (A)	Rise and Decay Times T_r (µs) x T_d (µs)	Pipe V_{oc} (V)
A (Zone 3)	30 - 200	(30 – 100) x (80 – 400)	50 - 200
A (into exposed installation	500 – 10,000	(10 – 50_ x (100 – 200)	
B (Zone 3)	10 - 30	Similar to B	nil
C (Zone 3)	1 - 10	Similar to C	nil

The data in Table 7.5 comes from fuel pipes in a variety of conventional aluminum aircraft. The Zone 3 currents due to Component A were measured in pipes extending between wing tank ribs. The 'exposed installations' are pipes connected to fuel pumps or drains mounted in external tank skins in lightning strike zones where a lightning attachment to the exterior surface of a fuel pump or its adapter plate is possible. As shown in Table 7.5, tests were also made with lightning intermediate and continuing current Components B and C conducted through these tanks, instead of applying only the shorter duration stroke current Component A, as is usually done for avionics certification.

The pipe data of Table 7.5 shows that transfer of current from the airframe to the pipes is most efficient for the long duration lightning currents represented by Components B and C. The percentages of the total airframe current that appeared in fuel pipes due to each lightning current component are shown below.

From Component A: ~ 0.1%
From Component B: ~ 1.0%
From Component C: ~ 1.0%

This implies that a positive polarity stroke current with a time duration (i.e., to 50% on decay) like that of Component B (~ 2 000 µs) but with an amplitude in the 20 - 30 kA range (for example) could produce 200 - 300 amperes of current in pipes. Such a stroke would have an Action Integral (~ 0.6 x 10^6 A^2s), lower than that of Component A, and certainly well within the range of positive lightning flash characteristics.

Guidelines for use of bonded fuel-pipe couplings: In the absence of definitive data on the electrical conductivity of pipe couplings under in-flight conditions, it is advisable to take the following approach:

1. Determine, by analysis or airplane test, the amount of current that is expected to flow in a fuel system's pipes and then design and test candidate bonded couplings that can consistently tolerate at least three times this current amplitude without arcing. The standard for lightning testing of fuel tank and system components is in [7.24].

2. Verify the ability of the selected coupling(s) to tolerate the assigned current (as determined from Step 1) by injecting this current through samples of the selected couplings under simulated flight vibration and contamination conditions. The couplings should be wetted with liquid fuel and immersed in a flammable gas during the tests. The tests should be conducted on at least three (3) samples of each selected coupling. The test standard [7.24] does not call for conducting lightning tests of components under simulated flight environments and conditions. Such tests would likely by conducted as engineering or "company" tests.

3. Perform the tests described in steps 1 and 2 in a flammable gas within a darkened enclosure and observe whether any ignition sources occur. If inconsistent test results occur (i.e., there is a large scatter in the amplitudes of test current that result in ignitions), the cause(s) of this should be determined (if possible) and additional tests conducted to establish the minimum amplitude of current that will produce an incendiary arc in the coupling. This amplitude should still be at least 300% of the expected current in the installed pipe. One arrangement for conducting ignition-source threshold tests of fuel pipe couplings is shown in Fig. 7.37.

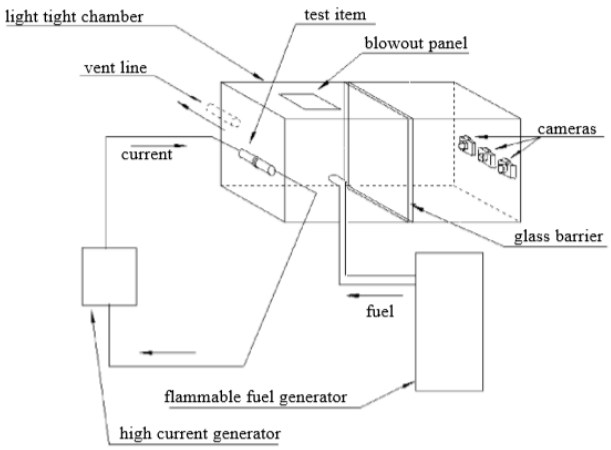

Fig. 7.37 Typical arrangement for fuel pipe coupling tests [7.24]

Current interruption: There is a wide range of variables associated with the arcing possibilities at pipe couplings that are required to conduct lightning currents. The best way to eliminate ignition sources at couplings is to prevent currents of any kind from flowing on fuel system plumbing. This means replacing bonding with insulation. There are three possible methods for doing this:

1. Make the fuel pipes of nonconductive material. This would allow conventional couplings without bonding

provisions to be used. Various solid polymers or fiber reinforced resins could be used for this purpose. However, due to static charge generation from fuel flow, the actual material used must provide dissipation of this static charge. Resistances in the kilohm to megaohm range have proven to dissipate charge while allowing only negligible lightning current flow.

2. Interrupt current paths through pipes by installing insulating pipe sections, as shown in Fig. 7.37. Use conventional pipes and couplings but provide insulating pipe sections to interrupt currents. These are called "pipe isolators" or "lightning isolators" and are available in a variety of sizes and configurations. Some include bulkhead attachments, and others are intended for in-line applications. Some commercially available insulating pipe sections are made of fiberglass composites whose resins contain some conductive particulate for static charge dissipation.

Method 1 is ultimately the least expensive, but certifiable nonconductive fuel pipes, with adequate flight experience, are not widely available. Fire and crashworthiness considerations also encourage the use of metal pipes. Method 2 permits use of couplings compatible with other system couplings. To assure the reliability of designs based on interruption of pipe currents it is important to provide a significant margin between the insulation withstand voltage and the expected actual voltage during a lightning strike. This is usually easy to do.

Structural potentials of several 10s of volts can occur in aluminum airframes, and thousands of volts can appear along carbon composite structures. At flight altitudes of 10 000 m (33 000 ft.), air gaps withstand only about 30 % of the voltage they withstand at sea level. Although the peak lightning stroke current amplitudes assigned in the standards rarely occur at flight altitudes above 3 000 m, it is prudent to assume that the peak currents exist throughout the flight envelope. There is no guidance in the regulations or advisory material for doing otherwise. Contaminants, including fungi, metal shavings from structural repairs or worn bearings, and condensates, may reduce the voltage withstand strength of insulating surfaces. Thus, insulating pipe sections or other insulating elements should be designed to operate at a minimum of three times the magnetically induced or structural *IR* voltages expected to appear across insulating pipe sections during lightning strikes, at flight altitudes.

Transport aircraft certification requirements stipulate that ignition-source protection designs for transport airplanes must be single fault tolerant. For an insulating pipe section, a single fault would most likely be impairment of the insulator with some electrically conducting contaminate. Analysis of this possibility would likely show that only a portion of an insulator surface could be contaminated in this manner. So, sizing of the insulator to withstand the expected voltage while contaminated would need to be demonstrated. This would be easily shown, since only a short length of such an insulator would have to be free of contamination to withstand the expected voltage. This is easily demonstrated with tests of contaminated insulators. For example, a 'clean' insulator that is 100 mm (4 in) long will withstand ~50 kV of impulse voltage. Maximum voltages appearing in tanks made of CFC are of the order of 10 000 volts. Structure voltages within aluminum tanks are much less; only 10s of volts.

An important point here is that it is fundamentally easier to maintain insulation in pipe isolators than it is to maintain electrical bonding in 'bonded' couplings. In other words: pipe isolators are inherently fault-tolerant whereas bonded couplings are not.

Compliance with the fault-tolerance and the continued airworthiness requirements for transport airplanes can be achieved with one insulating section (per typical pipe installation) as illustrated in Fig. 7.38, and the design is safer than would be a design that depends upon use of bonded couplings. It would not be necessary to employ two insulting sections ("isolators") in series, as shown in Fig. 7.39. The minimum voltage withstand capability of the insulating section in Fig. 7.39 should be at least three times the expected structure voltage, measured at the air pressure of flight altitude.

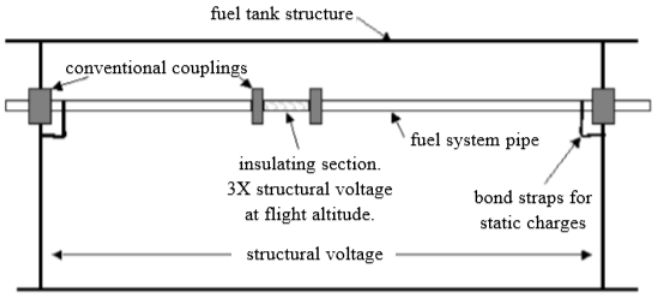

Fig. 7.38 Application of insulating pipe section.

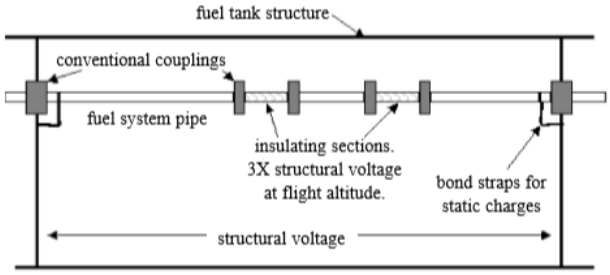

Fig. 7.39 Two isolators are not needed for fault tolerance.

Fuel pipe insulating sections should have sufficient conductivity to dissipate any static charges that are deposited on the insulating surface by incoming fuel. This may happen during the refueling process. Surface resistivities of 106 to 108 oms/square can dissipate these charges, yet not allow hazardous lightning currents to flow.

If the configuration shown in Fig. 7.39 were chosen, the pipe section between the two insulating sections would need to be electrically isolated from the tank structure. To prevent static charges from accumulating on this section, the insulators should have some electrical conductivity, in the range of 10^6 to 10^8 ohms. *This dual isolator approach is not needed, and not recommended.*

Insulated pipe sections have already been used successfully in carbon composite tanks where pipe currents would otherwise be very high and conventional couplings would certainly arc. Their use is also advisable in conventional aluminum fuel tanks, since even a few tens or hundreds of amperes may produce arcs in flexible couplings, and the electrical conductivity of such couplings is not stable. The simultaneous requirements of flexibility and arc-free electrical conductivity in the same coupling are fundamentally incompatible.

Some electrically conductive material must be provided in the interior linings of pipes transferring fuel to prevent frictional charge accumulation, but the resistivity of these materials can be on the order of 10^6 to 10^8 ohms.

Electrical wiring in fuel tanks

Lightning current in an aircraft can induce voltages in electrical wiring. If this wiring is not adequately protected the induced voltages may be high enough to cause a spark.

Electrical wires are usually installed in fuel tanks to service capacitance-type fuel quantity probes or to power electric motors that operate pumps or valves. If these wires are totally enclosed by metal skins and ribs or spars, the internal magnetic fields, and induced voltages in them can be kept low enough that they will not produce sparks across gaps like those between fuel probes and tank structures. However, if wires enter the tank from other less well shielded areas outside of the tanks the induced voltages may reach higher levels that are sufficient to cause sparks across unintentional gaps, such as between fuel quantity probes and adjacent tank structures or mount- ting brackets. Most electrical devices installed in fuel tanks have been intentionally designed to withstand voltages up to 600 volts or more without sparking. The fuel system designer, however, must be continually alerted to changes in material or structural design that might permit excessive induced voltages to appear in fuel tank electrical circuits.

Sparkover characteristics of small gaps

Several measurements have been made of the voltages that lightning currents can induce in fuel probe wiring. Measurements have also been made of the voltages required to cause a spark to occur between the elements of typical capacitance-type fuel quantity probes. These sparkover voltages are usually much higher than those typically induced in the wiring. As an example, Newman, Robb, and Stahmann [7.37] found that DC voltages of at least 3 000 V were required to cause a spark to jump between the active and grounded cylinders of the capacitance-type fuel probe installed in a KC135 aircraft wing.

Even higher voltages were needed to spark over the gaps between elements of this probe and the surrounding tank structure. Since the wires attached to the concentric tubes in the probe run close together, each experiences the same line-to-airframe (i.e., ‘common mode’) induced voltage and the voltage between them is small. Plumer [7.49] ran a similar test using impulse voltages and found that 12 kV was required to cause a spark to jump between the inner and outer cylinders of a typical probe. Small gaps like this can withstand more impulse than DC voltage, and the impulse test more realistically represents a lightning-induced voltage.

Effects of air pressure on gap sparkover voltages: The sparkover tests reported above were made in ambient, ground-level air-pressure conditions. At flight altitude, the same gap would break down at a lower voltage because of the lower air pressure. The expected reduction in impulse sparkover voltage at various altitudes can be determined from the Paschen curve shown in Fig. 7.40 [7.50].

To use this curve, one first calculates the product of the pressure and gap distance, *pd*. The pressure as a function of altitude can be obtained from the chart in Fig. 7.40(a).

For example, to find the sparkover voltage of a 5 mm (0.2 in) gap at a 10 000 m (33 000 ft.) altitude, one must first determine the pressure at that altitude, which is given in Fig. 7.40(a) as 198.16 mm Hg. Therefore, the product, *pd*, is 990.8 mm Hg. The Paschen curve, in Fig. 7.40(b), gives a sparkover voltage of approximately 5 500 V for this *pd* value. The Paschen curve is based on DC sparkover voltage. It usually requires a higher impulsive voltage than DC sparkover voltage to break down a gap of a given geometry, so the voltages predicted by the Paschen curve are somewhat lower than the corresponding breakdown voltages for typical lightning-induced transients.

Ignition energy vs altitude

The minimum spark energy necessary to ignite a flammable vapor rises as the pressure in the vapor area falls. This effect tends to offset the reduction in sparkover voltage with decreased pressure. Tests [7.8] have shown that 20 times as much spark energy is needed to cause ignition at 11 000 m (36 000 ft.) as at sea level. Within this range of altitudes, the ignition threshold might rise to between 4 and 10 millijoules instead of 0.2 to 0.5 millijoules. A spark due to a high lightning-induced voltage (3 000 - 10 000 volts) is likely to dissipate several joules of energy, which is sufficient to ignite most flammable vapors.

The sparkover voltages given by the Paschen curve in Fig. 7.40 are only approximate, since the curve assumes uniform electric field conditions, such as are found between parallel plane electrodes. Other electrode configurations, such as a sharp point-to-plane, would spark at lower voltages (perhaps 25% less). Since electrode shapes and surface treatments also influence sparkover voltage, more reliable measurements for specific gaps in a fuel system would be obtained from laboratory tests on actual hardware, preferably using impulse test voltage waveforms. The tests can be made at ground-level atmospheric pressure and then corrected for different flight altitudes.

Guidelines for design to eliminate sparks

In practice, the breakdown strengths of the smallest air gaps in fuel system hardware installations should provide a safety margin of 100% over the actual voltages expected during a lightning strike to the aircraft. This margin is needed to account for the tolerances of the mechanical installation, the effects of contaminants and statistical variations in small gap sparkover voltages themselves. In other words, a particular gap should be sized to withstand, at altitude, twice the anticipated actual induced transient voltage.

In some cases, particularly in installations within CFC tanks, this margin requires unacceptably large clearances between objects, for example, between fuel quantity probes and adjacent structure. In such cases, other means, such as coating adjacent surfaces with dielectric films, may be explored to enable smaller gaps to withstand twice the anticipated voltage. Designs like this must be given voltage withstand tests, as handbook-type data is not available to support specific designs. The test specimen would include the fuel probe, the bracket that secures the probe to adjacent structure, a sample of the fuel tank skin above and below the probe ends, any surface finishes, and the insulating pad. The test would have to be conducted in a chamber at the reduced pressure associated with flight altitudes, or else the test voltage could be adjusted upward to compensate for the altitude condition when test at sea level (standard conditions).

It is particularly important that sufficient insulation be provided between the active elements and the airframe because the highest induced voltages usually appear, for example, between a fuel quantity indicating system (FQIS) wire harness and the airframe. These voltages may be IR voltages related to lightning currents in the structural resistance of a wing or they may be magnetically induced voltages as illustrated in Fig. 7.41. Structural IR voltages may be only a few volts in a metal wing, but they may be several thousand volts in a composite wing.

Considerations for sparkover tests

When testing the sparkover voltages of small gaps, such as those at a fuel quantity probe, care must be taken to apply test voltages to all of the gaps in the fuel system, although these voltages do not need to be applied simultaneously. In most cases, both the ‘high’ and ‘low’ elements of a quantity probe are insulated from ‘ground’ (the airframe), but there is always a mounting bracket that holds the probe in proximity to the airframe. Fig. 7.42 shows a typical mounting for a fuel quantity probe. The test should evaluate both the sparkover voltage between the ‘low’ electrode and the structure upon which the probe is mounted.

Usually, the gaps between the probe and the mounting bracket or airframe are the largest and require the highest voltage to cause sparkover, but these gaps also experience the highest (common mode) induced voltages.

Fig. 7.41 illustrates that the proximity of a probe to the airframe structure on which it is mounted is especially important in determining breakdown voltages between the probe and the airframe. Because of this, the electrical insulation between the active elements of the probe and the airframe may not be entirely within the probe designer's control.

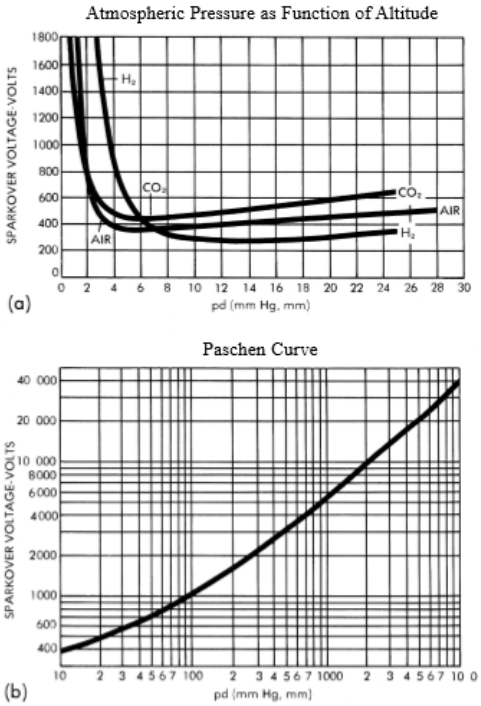

Altitude m	Pressure mm of Hg
0	760.00
500	716.02
1 000	674.09
1 500	634.18
2 000	596.23
2 500	560.11
3 000	525.79
4 000	462.26
5 000	405.09
6 000	353.77
7 000	307.87
8 000	266.89
9 000	230.45
10 000	198.29
11 000	169.66
12 000	145.05
14 000	106.02
16 000	77.48
18 000	56.65
20 000	41.41

Fig. 7.40 The relationship between sparkover voltage and altitude.

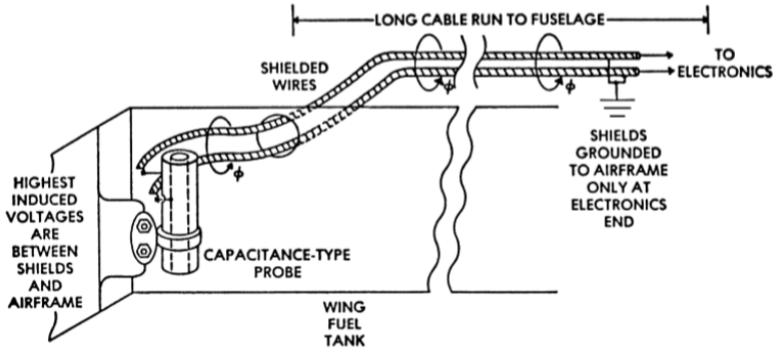

Fig. 7.41 Typical fuel probe wiring:

- Most magnetic flux and induced voltages appear between wire (or shield) and the airframe at probe end.
- Less magnetic flux and voltage appears between any two wires
- Even less flux or voltage appears between a wire and its shield
- Other voltages can occur between probe and airframe because of structural IR potentials

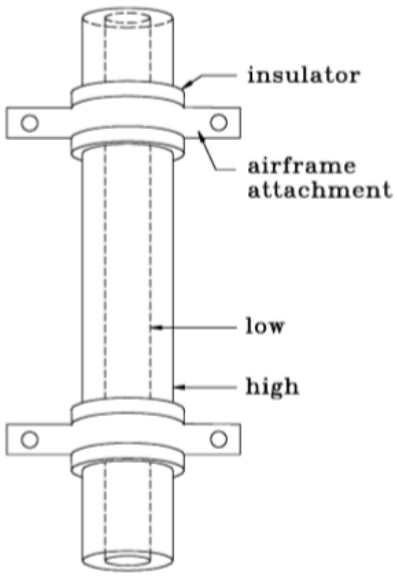

Fig. 7.42 Possible breakdown of gaps in capacitance type probe:
1. High to low
2. High to airframe
3. Low to airframe

Shielding of fuel probe wires

The wire harnesses for a fuel quantity indicating (measurement) system (FQIS, FQMS) are most close in potential to the airframe at the electronics end, which is usually in an avionics bay within the fuselage. FQIS harnesses are usually shielded, but, unlike most other shielded harnesses, only the ends connected to the fuel quantity indicating electronics unit are grounded, or at least electrically close to ground potential. The sensor ends of these harnesses are floating, although they may be connected to one of the probe's concentric tubes. This arrangement is necessary for the proper functioning of the indicating system, which operates at very low signal amplitudes. If both ends of the shields were grounded, small ac power currents (and other currents induced by fields from nearby circuits) would induce small voltages along the harness shields that would add to the signal voltages and cause erroneous fuel quantity indications.

Also, the grounding of an FQIS harness shield within a fuel tank would allow lightning-induced voltages to drive currents through shields and shield terminations that if allowed to become frayed, would cause arcing. This is one reason why FQIS harness shields are never grounded within fuel tanks. This is one of the few situations within aircraft wiring where it is not advisable to ground shields at both ends for lightning protection purposes.

A shield grounded at only one end does not reduce magnetically induced voltage between conductors and ground, although it may reduce induced voltages between conductors within the shield. This subject is treated at length in Chapter 15, but the important fact is that a shield can reduce voltages between conductors and ground only if it is grounded at both ends and allowed to carry current. If a shield is ungrounded at one end, magnetically induced voltages can develop between the conductors at that end and ground. Thus, most shields found on FQIS harnesses offer little or no protection from lightning induced effects. Since these harnesses are frequently routed within the fuel tanks, or within well-enclosed portions of the airframe, they often do not need shields for lightning protection purposes if the air gaps between the probes and the airframe are wide enough to tolerate lightning-induced voltages without sparkovers. However, if additional lightning protection is required, this can be provided by enclosing the exposed portion of a fuel quantity wire harness (located outside of fuel tanks) within an over braid, both ends of which are connected to the airframe or to equipment that is attached to the airframe.

The use of overbraids is described in Chapter 15. When an overbraid is used on a FQIS harness, the FQIS shield should remain ungrounded at the probe end and the overall shield (OAS) provides the lightning protection. The inner and OASs must be separated by insulation. It is necessary to include FQIS circuits in the FVT plan to ensure that induced transients are controlled and compatible with system protection requirements, as described in Chapters 5 and 13.

Measurements of induced voltages in fuel quantity circuits: Measurements of induced voltages and currents in FQMS circuits are typically included in aircraft tests to determine actual transient levels (ATLs) in circuits associated with electrical and avionics systems performing safety related functions. This test is described in Chapter 13. Wiring that is installed totally within conventional metal fuel tanks is well protected from induced effects and transient voltage levels are low, reaching only a few 10's of volts. However, some wiring, such as power circuits for electrically-driven pumps and valves, is also located outside of tanks, where exposure to lightning electromagnetic environments may be much higher, so that induced voltages of hundreds of volts are common.

Additionally, even the in-tank wiring installed within CFC fuel tanks is exposed to high voltage and current transients induced by the structural IR voltages that develop as lightning currents flow in CFC. This topic is discussed in Chapters 9 and 14.

Protection from excessive induced voltages is afforded by shielding of the interconnecting wiring, as discussed in Chapter 15. If this does not sufficiently control the voltages, alternate means of measuring fuel quantity may be considered.

Protection by routing of wiring

The routing of electrical wires in a fuel system can have a lot to do with how much induced voltage appears at apparatus inside fuel tanks. A comprehensive discussion of shielding airframe wiring and shielding practices is given in Chapters 15, 16 and 17. For the FQIS wiring, the benefits of routing will be most significant to the wiring located outside of the tanks. The tanks themselves usually are an electromagnetically well-shielded region.

7.4 Design of Tank Structures to Minimize Potential Ignition Sources

The fuel tank structure approaches described here must be considered and adopted before much of the detail tank and system designs are begun. These "global" designs will, if adopted early, eliminate many of the structural ignition sources described in earlier parts of this chapter and make the rest of the lightning protection process easier.

Most ignition sources are associated with structural joints and fasteners of various kinds. Therefore, as much as possible, joints and fasteners should be eliminated from fuel vapor areas. If they cannot be eliminated, they should be designed using the guidelines in §7.3.

Eliminating penetrating fasteners

Figs. 7.43 through 7.45 show how wing spars and ribs can be rearranged to eliminate penetrations of fasteners into fuel tanks. This approach may eliminate potential fuel leaks in addition to eliminating ignition sources. Care must be taken to ensure that the edges of spars and the rib-to-skin interfaces do not present arc or spark sources themselves. This can be accomplished by providing electrically insulating, corrosion-resistant finishes, as well as sealant materials between parts. Polysulfide type sealant is sometimes necessary at fillets and edges, as discussed in §7.3.5.

The design approaches illustrated in Figs. 7.43 and 7.44 are applicable to CFC as well as to metal structures. Lightning currents in fasteners within CFC structures may be higher than those in aluminum structures because diffusion times in CFC are much shorter than in aluminum. The concept of diffusion of lightning currents is explained in Chapter 11.

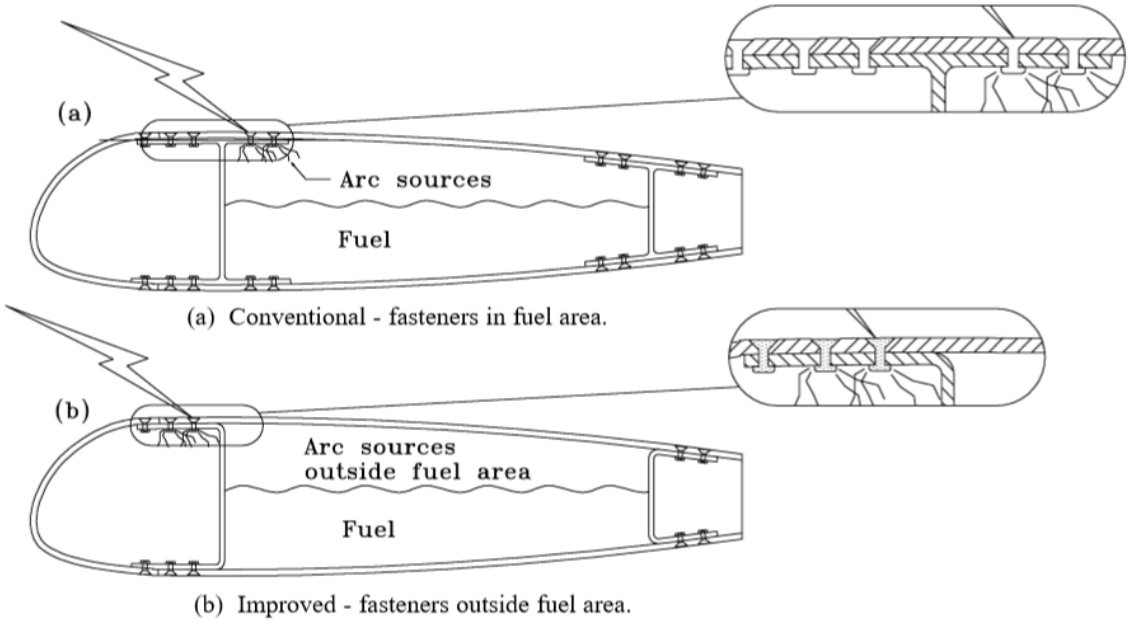

Fig. 7.43 Spar-skin interface design to reduce potential fuel vapor ignition sources.

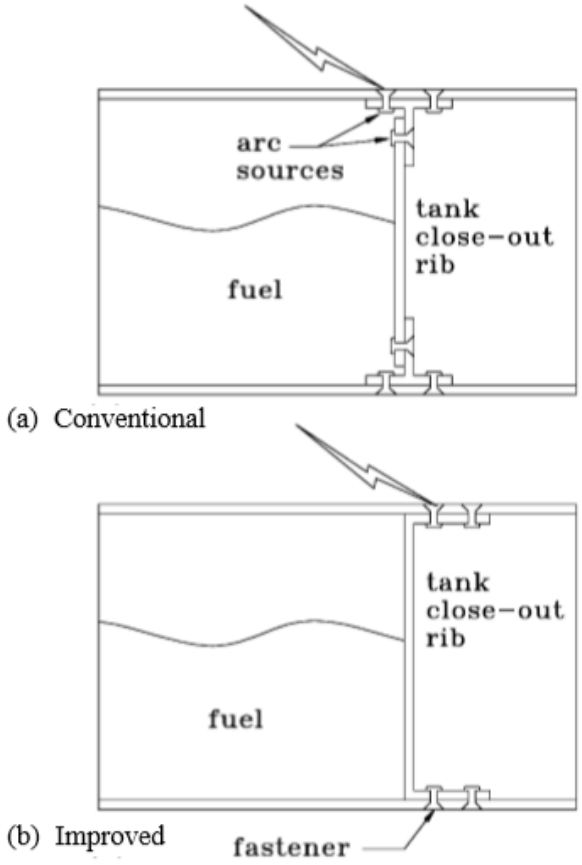

Fig. 7.44 Wing fuel tank closeout rib-skin interface design to reduce fuel vapor ignition sources.

Short diffusion times of lightning current in CFC structures allow more current to flow in interior structural elements, such as ribs and spars, in CFC structures than in aluminum structures. Also, it is usually more difficult to make arc-free electrical contact between CFC parts than between aluminum parts. Thus, these design concepts may be more necessary in CFC airframes than in aluminum airframes. Fasteners installed in exterior CFC or aluminum skins located in lightning attachment zones may be directly struck by sweeping lightning channels. If this happens, a higher percentage of the lightning current enters the struck fastener in a CFC structure than would be the case in a more conducive aluminum structure, which allows currents to be shared more uniformly by other fasteners in the same skin. The lightning current densities in small airframes, including general aviation aircraft and small rotorcraft, are proportionally higher than the current densities in larger transport category aircraft exposed to the same amount of lightning current. The design concepts illustrated in Figs. 7.44 through 7.49 are also appropriate for eliminating potential ignition sources in small, integral tank structures.

Co-curing of CFC tanks

The most elegant way to eliminate the ignition sources associated with structural fasteners in a fuel tank is to build the tank as a single monolithic structure that is electrically conductive throughout. In Figs. 7.45(a) and 7.46(a), fasteners penetrate the tank, as in conventional construction. In Fig 7.45(b), filament or tape winding is used to achieve an entirely co-cured structure. Practical limitations may prevent this method from being used to build complete wings of large aircraft, but the concept may be useful for building various substructures.

Co-cured joints in CFC structures provide the best possible electrical conductivity and usually produce no ignition sources. In co-cured joints, the pre-impregnated resin is used to bond yarns and plies together without the need for additional adhesives. Practical difficulties arise in co-curing large structures, but great improvements in the lightning protection of CFC structures can be achieved by co-curing simple interfaces, such as those between stiffeners and skins.

Nonconductive ribs

Another method, shown in Fig.7.47, illustrates the use of fiberglass or aramid fiber reinforced composites to fabricate spars within a wing fuel tank. In this case, lightning currents tend not to flow into fasteners because the fasteners are installed in non-conducting interior surfaces that do not constitute current paths. Mechanical strength considerations may preclude use of materials other than CFC for spars and ribs. If so, several other approaches can be used to interrupt current through fasteners. Some of these are illustrated in Figs. 7.48 and 7.49.

Nonconductive shear ties

Fig. 7.48 illustrates the use of a nonconductive shear tie, sometimes called a clip or shear clip, to interrupt electric current paths between skin and interior structures that are conductive. This allows these elements to remain conductive yet ensures that lightning currents remain in the tank skin and eliminates potential arc sources at interior fasteners.

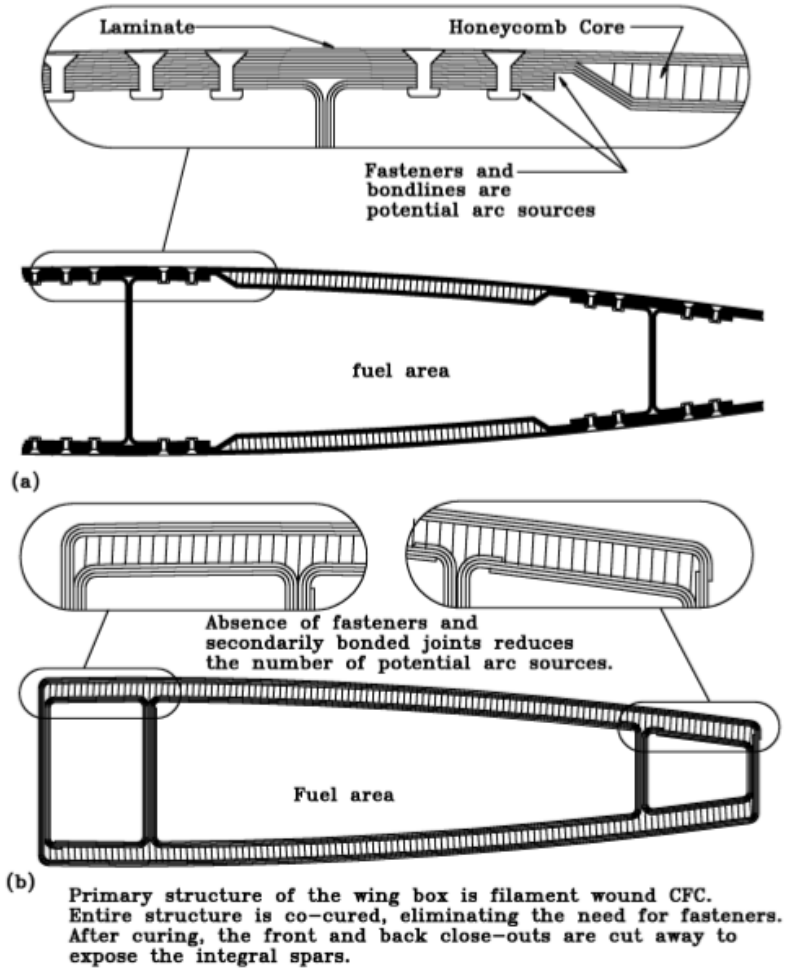

Fig. 7.45 Use of filament winding techniques to obtain co-cured, monolithic structure at eliminate fasteners.
(a) Conventional – penetrating fasteners.
(b) Improved – fasteners eliminated.

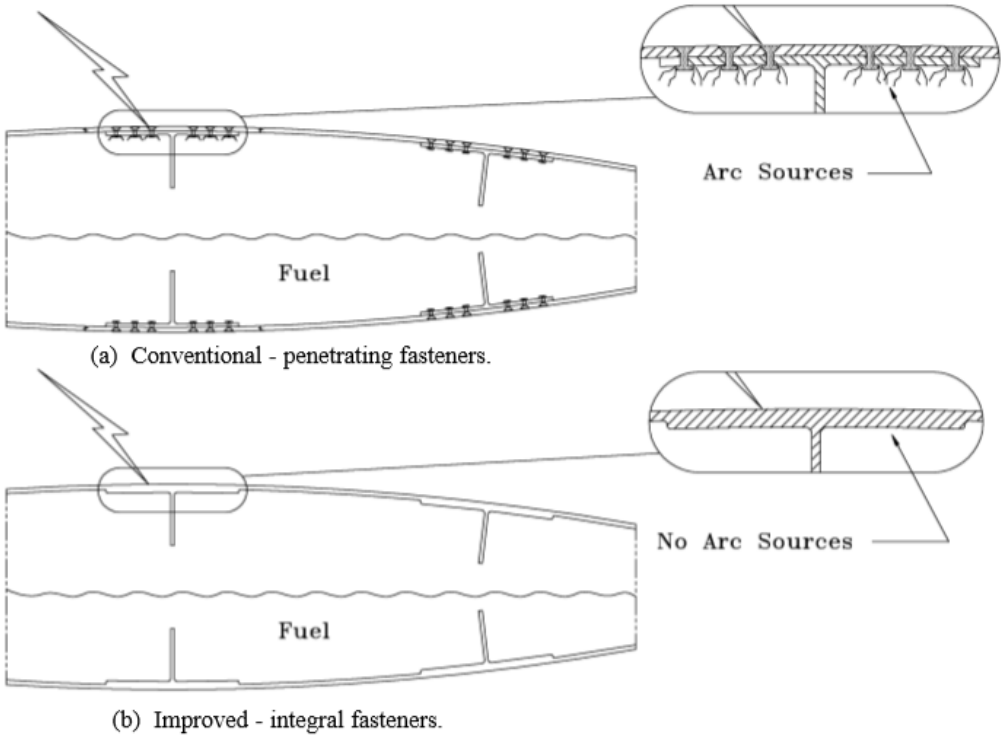

Fig. 7.46 Wing stiffener design to eliminate potential ignition sources

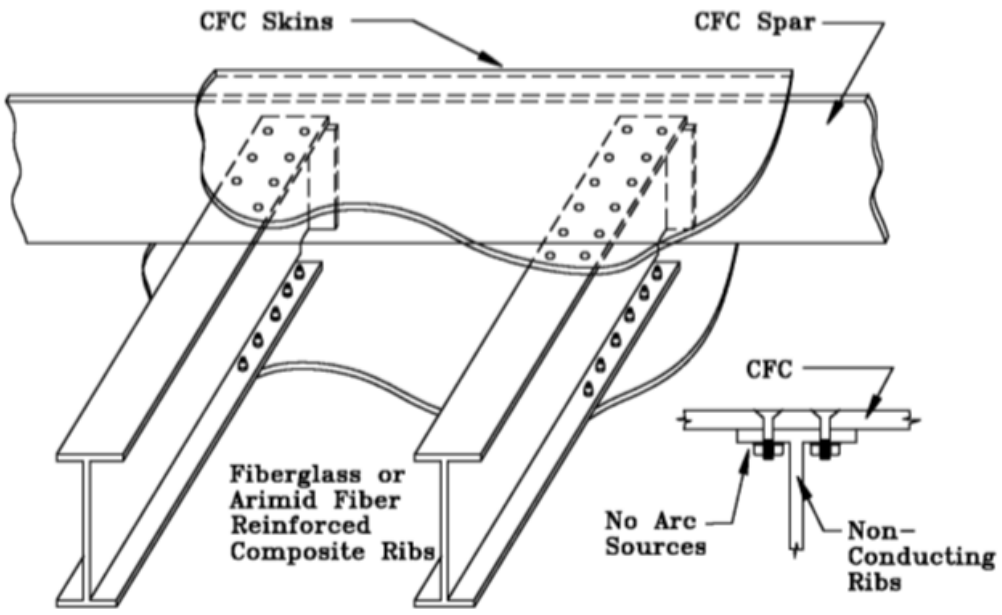

Fig. 7.47 Non-conducting ribs to eliminate potential arc and spark sources at fasteners.

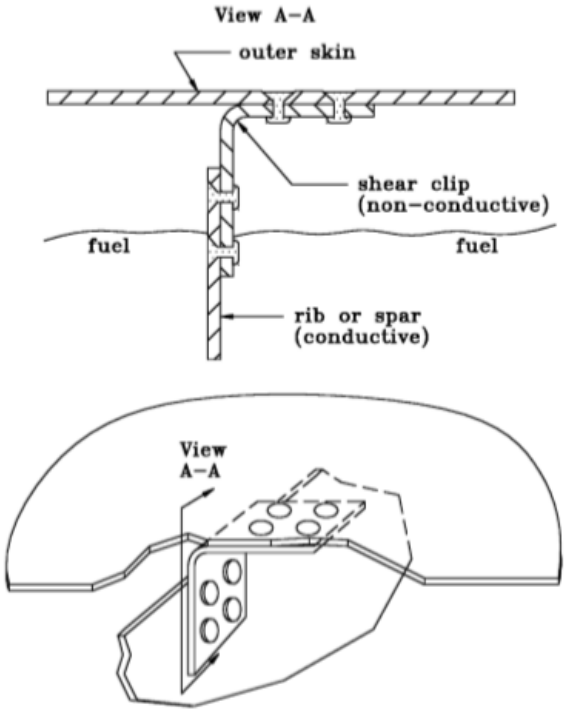

Fig. 7.48 Non-conducting shear clips to interrupt current paths and prevent ignition sources.

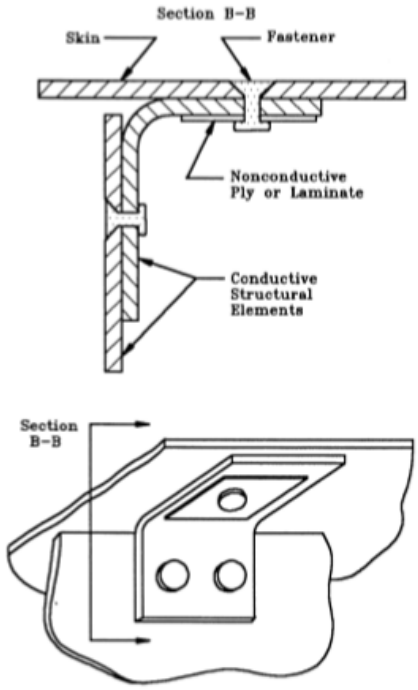

Fig. 7.49 Non-conducting ply or laminate to eliminate current paths and prevent ignition sources.

Prevention of arcs at fasteners

If it is not feasible to use a nonconductive shear tie (or clip), Fig. 7.49 illustrates another method of controlling internal arcing at shear tie fasteners. A nonconductive single or multi-ply laminate can be bonded to the interior surface of the shear tie or clip. This prevents current from arcing from the fastener to the inside surface of the shear tie. Arcing may occur beneath the nonconductive ply, but the incendiary products of those arcs would be contained by the nonconductive laminate.

The structural designs illustrated in Figs. 7.43 through 7.49 can eliminate potential fuel-vapor ignition sources and avoid the 'brute force' method of applying extensive sealant overcoat or other barriers. The unrestrained use of sealants imposes cost and weight penalties and raises concerns about lifecycle durability. Designers are encouraged to develop more efficient means of achieving the same ends. Since the success or failure of many of these concepts depends on factors such as dimensions, clearances and torques on fasteners, whose significance cannot always be predicted, candidate designs should always be evaluated by simulated lightning tests.

Some cautions

When employing electrically insulating structural materials to interrupt lightning current (as illustrated in Figs. 7.47 to 7.49) it must be remembered that current paths must be provided between extremities, such as nose, tail, wing and empennage tips, and control surfaces. Thus, the main current paths, such as wing tank skins and the main spars must be fabricated of materials capable of conducting lightning currents.

Structural requirements must be met for any tank design that utilizes any of the concepts described above, or any other tank design concepts for minimizing lightning hazards.

7.5 Considerations Regarding Lightning Current Densities in Structural Fasteners

As discussed in earlier sections, primary means of current transfer between fuel tank structural elements is through fasteners, but when current is conducted through fasteners, arcs and sparks may occur. These produce arc

products, consisting of plasmas of ionized air, vaporized and melted metals, and/or composite materials. Any of these arc products can be hot enough to ignite fuel vapor.

The basic mechanism is shown in Fig. 7.50. The lightning current is conducted from one part to another through the fastener, threaded nut, and washer.

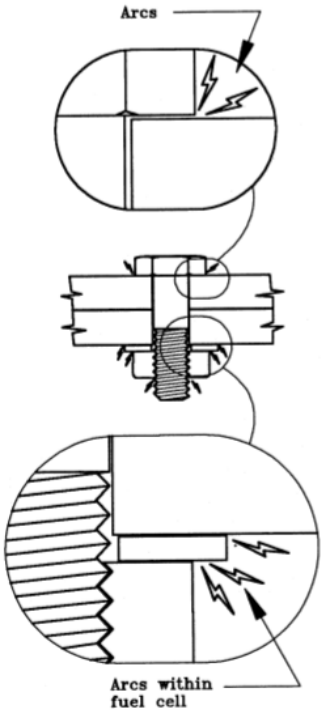

Fig. 7.50 Arcing and sparking at fastener interfaces.

Lightning current densities of hundreds or thousands of amperes per fastener would cause arcing at the points of contact between the fastener and fastened parts, as illustrated in Fig. 7.50. If the fastener could bear directly against bare metal, the arc threshold (amperes per fastener) could be increased. However, bare, uncoated parts are almost never tolerated within aircraft structures due to the possibility of corrosion. Most corrosion-resistant surface finishes are nonconductive, but Alodine is sufficiently conductive to transfer lightning currents, depending on the areas of contacting surfaces. The tightness of connections is important. Arcing due to excessive current densities at edges of contacting surfaces is a possibility, so edges may have to be provided with a barrier to prevent arc products from reaching flammable vapors.

Minimizing current densities

One way to minimize arcing at a fastener is to minimize the current in the fastener. This can be accomplished by using the largest diameter fasteners possible, to maximize the contact area between the fastener and the joined surfaces (see Fig. 7.51). The upper drawing shows arcing occurring at the fastener interface with the parts due to small cross-sectional contact area.

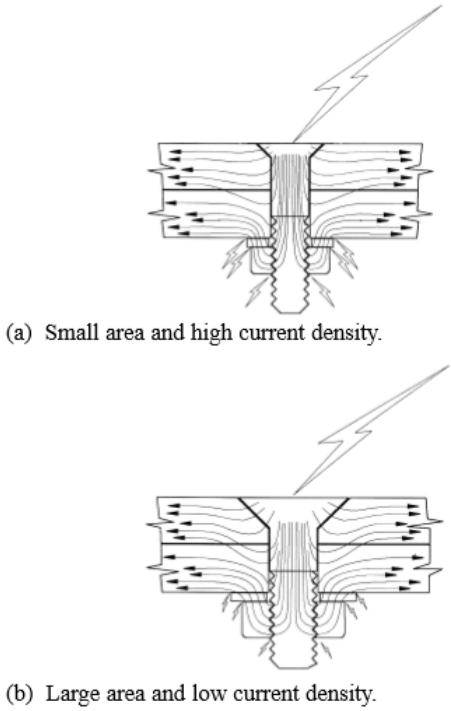

Fig. 7.51 Effect of fastener contact area on current density and arcing.

When the contact area is increased, as shown in the lower drawing, the current density through the fastener is reduced, which decreases the intensity of the arcing at the interfaces. This is provided that the fastener is making electrical contact with the hole. This is not always possible unless the fastener is a tight fit to the hole (i.e., 'interference fit'). If the fastener head can make electrical contact with the countersink this will permit good current transfer to surrounding exterior skins.

The intensity of arcs at fastener installations may also be reduced by allowing or encouraging the current to be shared among several fasteners. This concept is shown in Fig. 7.52. If there were many fasteners in a current path, the current in any one fastener would be low. In most structures, lightning currents do not divide evenly among all fasteners, since current varies with the conductivity of individual fastener installations, and the overall current densities diminish with distance from lightning entry and exit points. Analysis methods are available to calculate the current distribution among individual fasteners if realistic estimates of the conductivities among fasteners and the holes are unavailable.

Strikes to fasteners in a row: Analysis of current flow patterns in large aircraft fuel tank structures made of conventional aluminum materials has shown that, if one fastener in a row of fasteners is struck by lightning, as in Zones 1A, 1C or 2A, a significant percentage of the stroke current entering the struck fastener will flow back to the aluminum skin surface via the two neighboring fasteners, and sometimes via the next two fasteners. This is because short duration pulse currents want to flow near the exterior surfaces ("skin effect"). The concept is shown in Fig. 7.52.

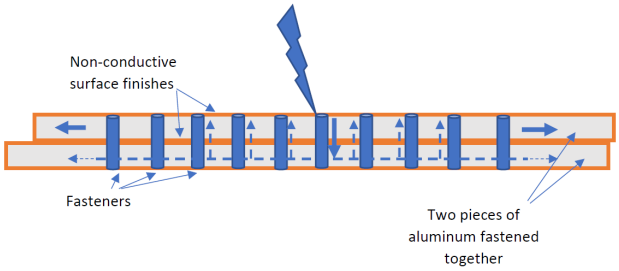

Fig. 7.52 Stroke to a fastener in aluminum skin causes currents in neighboring fasteners to return current to exterior part of structure

The overall flow of lightning current among tank skins and interior structures is shown in Fig. 7.53.

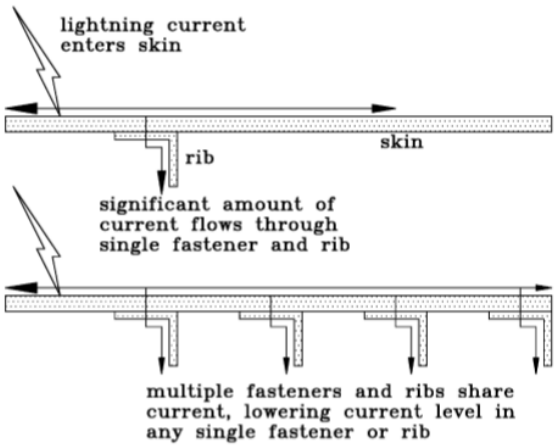

Fig. 7.53 Lightning current sharing among skins and interior structures.

The amount of current transitioning to interior structures is high when skins and interiors are made of CFC. Skin effect prevents current from diffusing rapidly to interior structures. Current densities in the exterior skins of integral fuel tanks and other boundaries, such as spars and ribs, can be inferred from measurements of magnetic fields at those boundaries. These magnetic field measurements can be obtained during the aircraft FVTs normally conducted to verify the transient levels in interconnecting wiring (see Chapter 13). Magnetic field measurements can also be taken during tests of aircraft wings, or other large structures, conducted solely for design/verification of fuel tank lightning protection.

References

7.1 L. J. Nestor, "Investigation of Turbine Fuel Flammability within Aircraft Fuel Tanks", *Final Report DS-67-7*, Aeronautical Engine Department, Naval Air Propulsion Test Center, July 1967.

7.2 Adapted from Nestor, "Investigation of Turbine Fuel Flammability", ibid, pp. 8.

7.3 Redrawn from Coordinating Research Council, Handbook of Aviation Fuel Properties, *CRC Report No. 530*, Second Printing May 1984, pp. 72.

7.4 Adapted from Nestor, "Investigation of Turbine Fuel Flammability", op cit, pp. 23.

7.5 Michael Zabetakis, Bureau of Mines Bulletin 627 "Flammability of Combustible Gases and Vapors".

7.6 W. Q. Brookley, "SAF C-141 and C-135 Fuel Tank Nitrogen Inerting Tests", *Report of the Second Conference on Fuel System Fire Safety*, 6 and 7 May 1970, Federal Aviation Administration, 1970, pp. 75.

7.7 Von Elbe, G., Lewis, B., et al., "Ignition of Explosive Gas Mixtures by Electric Sparks", *Third Symposium on Combustion & Flame & Explosion Phenomena*, Baltimore: Williams & Wilkins Co., 1949.

7.8 K. E. Crouch, "Aircraft Fuel System Lightning Protection Design and Qualification Test Procedures Development Investigation of Fuel Ignition Sources", NADC-86100-20, August 1986, Naval Air Development Center.

7.9 M. M. Newman and J. D. Robb, "Investigations of Minimum Corona Type Currents for Ignition of Fuel Vapor," *NASA Technical Note D-440*, June, 1960.

7.10 "Investigations of Mechanisms of Potential Aircraft Fuel Tank Vent Fires and Explosions Caused by Atmospheric Electricity", Final Report under Contract No. NA Sr-59, prepared by the Lockheed California Company, for the National Aeronautics and Space Administration, May 31, 1963.

7.11 Redrawn from "Investigations of Mechanisms of Potential Aircraft Fuel Tank Vent Fires", op cit, pp. 90.

7.12 Civil Aeronautics Board Aircraft Accident Report, Boeing 707-121, N709PA, Pan American World Airways, Inc., near Elkton, Maryland, December 8, 1963, File No. 1-0015, adopted February 25, 1965.

7.13 C. C. Bolta, R. Friedman, G. M. Griner, M. Markels, Jr., M. W. Tobriner, and G. von Elbe, "Lightning Protection Measures for Aircraft Fuel Systems, Phase II", *Technical Report ADS-18*, prepared by the Atlantic Research Corporation with the Lightning and Transients Research Institute for the Federal Aviation Agency, May 1964.

7.14 Based on Bolta et al, "Lightning Protection Measures", ibid, pp. 22 and B-3.

7.15 Bolta et al, "Lightning Protection Measures", excerpted from Proposal No. PS-139, Fenwal, Inc., Ashland, Massachusetts, pp. 70-79 and C-1 to C-3, January 23, 1964.

7.16 Bolta et al, "Lightning Protection Measures", ibid, pp. 116-149.

7.17 M. M. Newman, J.R. Stahmann, and J. D. Robb, "Airflow Velocity Effects on Lightning Ignition of Aircraft Fuel Vent Efflux", *FAA Final Report DS67-9*, prepared by the Lightning and Transients Research Institute, with Consultant Staff Cooperation of the Atlantic Research Corporation, for the Federal Aviation Administration, July 1967.

7.18 Newman, Stahmann, and Robb, "Airflow Velocity Effects", ibid, pp. 10-20.

7.19 Redrawn from F. L. Kester, M. Gerstein, and J. A. Plumer, "A Study of Aircraft Fire Hazards Related to Natural Electrical Phenomena", *NASA CR-1076*, prepared by Dynamic Science for the National Aeronautics and Space Administration, Department of Transportation, June 1968, pp. 75.

7.20 J. P. Gillis, "Study of Flame Propagation through Aircraft Vent Systems", *Final Report NA-69-32*, prepared by Fenwal, Inc. Walter Kidde and Co., for the National Aviation Facilities Experimental Center, Federal Aviation Administration, May 1969.

7.21 Redrawn from Gillis, "Study of Flame Propagation", ibid, pp. 21, 22.

7.22 Gillis, “Study of Flame Propagation”, ibid, pp. 23.

7.23 Gillis, “Study of Flame Propagation”, ibid, pp. 35.

7.24 *Aircraft Lightning Test Methods*, SAE ARP 5416, SAE International, Warrendale, PA (present edition).

7.25 Crouch, “Aircraft Fuel System Lightning Protection”, op cit, pp. 6-6 to 6-9.

7.26 Redrawn from L. Oh and S. Schneider, “Lightning Strike Performance,” op cit, pp. 12.

7.27 Kester, Gerstein, and Plumer, “A Study of Aircraft Fire Hazards,” op cit, pp. 39.

7.28 T. S. Lee, W. Y. Su, “Transient Spark-Arc Hot Heating on Metallic and Reinforced Composite Skins”, International *Aerospace and Ground Conference on Lightning and Static Electricity,* Orlando, FL, June 26-28, 1984, pp. 27-1 - 27-9

7.29 E. H. Schulte, W. T. Walker, “Rear Surface Temperature Measurement of Aircraft Materials Subjected to Zone 2A Lightning Strikes”, *International Aerospace and Ground Conference on Lightning and Static Electricity*, Orlando, FL, June 26-28, 1984, pp. 31-1 - 31-12.

7.30 K. G. Lovstrand, B. Olsson, B. Wahlgren and L. Anderson, “Lightning Test of a CFC Wing Skin”, *International Aerospace and Ground Conference on Lightning and Static Electricity*, Orlando, FL, June 26-28, 1984, pp. 30-1 - 30-9.

7.31 G. Olsen, R. Force, and J. Lauba, “Ignition Hazard Study of Advanced Composite Fuel Tank,” *Report D 180 - 25598 - 1*, Boeing Military Airplane Co. Seattle, WA, May 1980.

7.32 L. L. Oh and S. D. Schneider, “Lightning Strike Performance of Thin Metal Skin,” *Proceedings of the 1975 Conference on Lightning and Static Electricity,* 14-17 April 1975, at Culham Laboratory, England.

7.33 Federal Aviation Administration, *Advisory Circular AC 20-53A*, “Protection of Airplane Fuel Systems Against Fuel Vapor Ignition Due to Lightning”, April 12, 1985.

7.34 R. O. Brick, L. L. Oh, and S. D. Schneider, “The Effects of Lightning Attachment Phenomena on Aircraft Design”, 1970 *Lightning and Static Electricity Conference*, 9-11 December, pp. 139-156.

7.35 L. L. Oh and S. D. Schneider, “Lightning Strike Performance of Thin Metal Skin,” *Proceedings of the 1975 Conference on Lightning and Static Electricity*, 14-17 April 1975, at Culham La-boratory, England.

7.36 J. A. Plumer, “Lightning Effects on General Aviation Aircraft”, *FAA-RD-73-99*, Federal Aviation Administration, October 1973, pp. 21-44.

7.37 J. D. Robb, J. R. Stahmann, and M. M. Newman, “Recent Developments in Lightning Protection for *Aircraft and Helicopters,” 1970 Lightning and Static Electricity Conference*, pp. 25-35.

7.38 B. D. Fisher, G. L. Keyser, Jr., P. L. Deal, “Lightning Attachment Patterns and Flight Conditions for Storm Hazards, 1980”, *NASA Technical Paper 2087*, December 1982.

7.39 Federal Aviation Administration, User's Manual for *AC 20-53A*, “Protection of Airplane Fuel Systems Against Fuel Vapor Due to Lightning”, October 1984.

7.40 Federal Aviation Administration, *Advisory Circular AC 20-53A*, “Protection of Airplane Fuel Systems Against Fuel Vapor Ignition Due to Lightning”, April 12, 1985.

7.41 D. H. McClenahan and J. A. Plumer, “Protection of Advanced Composites Against the Direct Effects of Lightning Strikes”, *International Aerospace Conference on Lightning and Static Electricity*, Vol. II, Oxford, 23 - 25 March 1982, G3-1 - G3-9.

7.42 K. Berger, “Development and Properties of Positive Lightning Flashes at Mount S. Salvatore with a Short View to the Problem of Aviation Protection”, *Proceedings of the 1975 Conference on Lightning and Static Electricity*, 14-17 April 1975, at Culham Laboratory, England, pp. 7.

7.43 C. Crouch, “Aircraft Fuel System Lightning Protection”, op cit, pp. 6-6 to 6-9.

7.44 B. Lepetit, C. Escure, S. Guinard, I. Revel, G. Peres, and Y. Duval of EADS Innovation Works “Thermo-mechanical effects induced by lightning on carbon fiber composite materials” ICOLSE 2018 Proceedings.

7.45 R. Chippendale, I. Golosnoy, P. Lewin, Univ. of Southampton “Numerical Modelling of the Damage Caused by a Lightning Strike to Carbon Fibre Composites” ICOLSE 2018 Proceedings.

7.46 Mahoney, J W., Bush, C. A., and Dickerson, E. O., "Aircraft Integral Fuel Tank Design Handbook", Report AFFDL-TR-79-3047, Air Force Flight Dynamics Laboratory, pp. 3-11.

7. 47 L. E. Short, "Electrical Bonding of Advanced Airplane Structures", Lightning and Static Electricity Conference, 3-5 December 1968, pp. 425-441:433.

7.48 J. E. Pryzby and J. A. Plumer, "Lightning Protection Guidelines and Test Data for Adhesively Bonded Aircraft Structures", *NASA Contractor Report 3762*, January 1984, pp. 33-35.

7.49 J. A. Plumer, "Lightning-Induced Voltages in Electrical Circuits Associated with Aircraft Fuel Systems", *Report of Second Conference on Fuel System Fire Safety, 6 & 7* May 1970, Flight Standards Service, Engineering and Manufacturing Division, Federal Aviation Administration, Washington, D.C. (1970), pp. 171-191.

7.50 J. D. Cobine, Gaseous *Conductors: Theory and Engineering Application*, New York: Dover Publications, 1958, pp. 164.

Chapter 8

INTRODUCTION TO INDUCED EFFECTS

8.1 Introduction

The previous chapters have addressed issues related to the physical (also known as induced) effects of lightning. The remaining chapters of this book will deal with the induced (also known as indirect) effects. The term *induced* effects of lightning refers to the upset or damage to electrical and avionic equipment and systems that results from lightning strikes to an aircraft. These effects may include burnout of devices, and temporary or permanent upset of computerized functions, complete or partial include loss of an aircraft's electric power, loss of control by flight or engine computers, or display of hazardous misleading information. Included in this definition (and discussed here) are the transient voltages and currents induced by lightning on the electrical wiring of the aircraft, irrespective of whether such transients cause damage or upset of electrical and avionic equipment and systems.

This chapter is intended as a summary of typical lightning-induced transients and an introduction to the chapters that follow, which address more specific aspects of lightning induced effects. The chapter will explain, briefly, the basic physics involved in the coupling of induced transients into aircraft wiring. It will also describe procedural steps that must be taken to deal successfully with these effects. Examples of transient voltage and current measurements that have been made on aircraft wiring to determine the nature of induced effects will also be reviewed. Most of the subjects discussed here will be discussed in more detail in later chapters.

8.2 Background

Some overview of related background and related technologies is worthwhile.

Electromagnetic interference (EMI)/Electromagnetic compatibility (EMC)

The physics of coupling lightning energy into aircraft wiring are similar to that of EMI and many of the practices involved in the control of lightning induced effects are the same or similar to those utilized in control of classic electromagnetic interference via EMC and generally one can say that the practices that are good for control of lightning induced effects (i.e., grounding, bonding, and shielding) are also good for control of EMI. This is not to say that they are the same and certainly not to say that attention to control of EMI will also control the induced effects of lightning. One major difference in assessments of the effects of these environments is that, whereas both include effects of electric and magnetic fields, EMI is best understood via the electric field coupling mechanism, whereas lightning is best explained via its magnetic field coupling mechanism. This is of course a simplification since each source of interference includes both electric and magnetic fields. Other differences include:

Lightning is a time-domain source

EMI is a frequency domain source

In addition, EMI is usually a steady state environment that may be present for the duration of a flight, whereas lightning is an impulse environment that may happen once or twice during a flight, or within an even longer time period.

Finally, EMI is rarely capable of permanently damaging an item of equipment or system, whereas lightning may deliver sufficient energy to cause permanent failures.

Some of the practices and mythology that have been developed for control of EMI problems, in fact, may *not* help control lightning problems, and some may even make systems *more* susceptible to damaging lightning induced effects. The classic EMI practice of grounding wire shields at only one end is perhaps the best example of this. (This subject is discussed in Chapter 15. The replacement of analog with digital signal transmission has made it less necessary to have EMI shields ungrounded at one end). Another EMI control practice that may increase vulnerability to lightning induced transients is the indiscriminate use of

EMI filters which may experience short circuits when low voltage capacitors fail due to lightning-induced transients

Analytical tools and test techniques developed for EMI/EMC are not particularly applicable to lightning induced effect problems, principally because lightning is a time-domain phenomenon, and most EMI/EMC activities deal with the frequency domain. Practices related to narrow-band radio frequency (RF) emission and absorption may not adequately deal with time-domain voltages and currents of magnitude sufficient to burn out electrical components.

Nuclear electromagnetic pulse (NEMP)

Nuclear electromagnetic pulse (NEMP) protection activities have had an influence on lightning induced effects, partly because that activity has been well funded in the past and partly because, like lightning, NEMP is a time domain phenomenon. Some of the published analytical work on lightning induced effects has been influenced by the work done in the field of NEMP. Some computer codes of use for lightning analysis in aircraft were originally developed for NEMP and to deal with coupling through apertures. Perhaps the best single summary of that analytical work is [8.1]. It contains numerous references to the most important of the original works.

Some of the electronic component and equipment test techniques developed for evaluating the effects of NEMP-induced transients on equipment have also influenced those used for evaluation of lightning induced effects. This is particularly true of bench tests, in which currents and voltages are injected into electronic equipment and its interconnecting wiring. Some of the early work related to determining the voltage and current amplitudes necessary to damage semiconductors (i.e., 'Wünsch analysis') have also come from the NEMP community. Some of that work is reviewed in Chapter 17.

Atmospheric Electricity Hazard Program (AEHP)

A comprehensive review of work dealing with lightning induced effects was conducted under the Atmospheric Electricity Hazard Program (AEHP) organized in the 1980s by the United States Air Force (USAF) with Boeing Military Airplane Company as the prime contractor. In that program, reviews were conducted of the lightning environment presented to aircraft. Lightning protection concepts were reviewed, and protection specifications were prepared for two test bed aircraft, an F-14A fighter aircraft and a YUH-61 helicopter. The AEHP did not fund any research activities. Instead, it collected materials developed under other programs, sponsored various workshops to review the material and assembled the materials into a five-part series of reports [8.2 - 8.6]. There has not been a similar program since this period.

The AEHP dealt mostly with induced effects of lightning; physical effects having been excluded from its charter. Physical effects were understood to be important, and readers of the reports were cautioned to be aware of the necessity of dealing with these effects. A limited review of physical effects was made [8.7], but no attempt was made to develop engineering data relating to these effects. The user of this book is urged to consider all lightning effects together since there is often only a vague distinction among these two broad categories. A lightning-induced current transient in a wire harness is in fact just a small portion of the total lightning stroke current that is being conducted through the airplane after it has been struck by lightning. It is for this reason that we have set aside the familiar *direct* and *indirect* effects terminology for somewhat more useful *physical* and *induced* effects. Even these might better be combined to simply: *lightning effects.*

SAE and EUROCAE Lightning Committee activities

The groups that have been charged with reviewing lightning design and test practices and with developing lightning environment and test standards for use in the aircraft industry and by regulatory authorities are the SAE Committee AE-2 and the European Organizations for Electrical Equipment EUROCAE Working Group 31. Members of these committees have included representatives from the US and European aircraft industries; military services, certifying authorities, lightning specialist organizations and test laboratories. The SAE and EUROCAE lightning committees have worked together since 1988 to harmonize technical standards among US and Europe, thus promoting agreement between various certifying agencies. Many other countries, world-wide have joined these harmonizing efforts so that the environment and test standards used for addressing induced effects are in wide use.

Part of the SAE and EUROCAE lightning committee charters (also known as 'terms of reference') has been to provide inputs to advisory circulars (ACs) issued by the Federal Aviation Administration (FAA) and other certifying authorities as ACs or military standards. One such document [8.8] has previously been cited in connection with the aircraft lightning environment. Other documents include [8.9], which describes how the lightning environment is applied to an aircraft throughout the process of

aircraft lightning zoning and [8.10], which describes the process of certification for aircraft electrical and avionic systems. Much of the material resulting from the SAE and EUROCAE committee activities has also been incorporated into a Military Standard [8.11].

FAA and National Aeronautics and Space Administration (NASA) research

The United States (US) FAA and National Aeronautics and Space Administration (NASA) have sponsored original research to address lightning induced effects and develop test techniques to evaluate these effects in aircraft wiring. For example, NASA sponsored the initial development [8.12] of the Lightning Transient Analysis (LTA) test technique (now known more commonly as the 'Full Vehicle' test) to determine the transient voltages and currents induced in aircraft electrical circuits by lightning. The US FAA has sponsored tests [8.13] to compare results using several test techniques, including the full vehicle test (FVT) technique.

8.3 Steps in a Lightning Induced Effects Protection Design Program

Quantification of the induced effects of lightning in the wiring of a specific aircraft generally requires subjecting the aircraft's electrical and electronic systems to controlled tests in a laboratory. These tests include measuring the induced transients in electrical wiring to determine the actual transient levels (ATLs, as defined in Chapter 5). The amplitudes of these measurements (plus a margin to account for uncertainties in the measurements and in the certification test methods) are used to determine the amplitudes of the test waveforms used to test the susceptibility of electrical and avionic equipment and systems. The transient test levels applied to individual items of avionic equipment, and to complete systems, are known as the equipment transient design levels (ETDLs). The process of defining ETDLs is described generally in Chapter 5.

The lightning protection design for aircraft electrical and avionic systems, like protection against EMI/EMC problems, cannot be accomplished by analysis alone, nor merely by reliance on field experience.

The problem of analysis and control of induced effects is a complex one but, fortunately, it can be divided into several steps. These steps are listed below. Conduct the Lightning Safety Assessment to identify the systems and equipment that perform functions that are necessary for continued safe flight and landing of the aircraft after a lightning strike. Guidance for conducting this assessment is found in FAA ACs and other documents discussed in Chapter 5. The outcome of this assessment will be identification of the equipment, systems, and their interconnecting wiring and installations in the airplane.

1. Determine the external lightning environment applicable to the aircraft. The most important aspects of this environment are the lightning currents conducted through the airframe, and the associated external magnetic fields (see Chapter 10).

2. Determine the structural IR voltages and the internal magnetic fields that would result from the lightning currents in the airframe (see Chapters 11 and 12).

3. Determine the voltages and currents that would be induced on the aircraft wiring by the IR voltages and magnetic fields from steps 2 and 3 (see Chapters 13 and 14).

4. Establish requirements for the equipment and systems identified in step 1. These requirements include the pass/fail criteria, and the lightning-induced transient waveform sets and levels that are applicable to individual equipment and systems. These are called the ETDLs. They also include the interconnecting cable bundle transient waveforms and levels that are applicable to the system that contains the equipment.

5. Design and incorporate protective measures for the equipment and systems identified in step 1 (see Chapters 15 and 16).

6. Conduct laboratory tests to prove the success of protection designs (see Chapter 18).

The relationships between the actual transients induced in aircraft interconnecting wiring and the transients that need to be tolerated by equipment and systems are illustrated in Fig. 8.1.

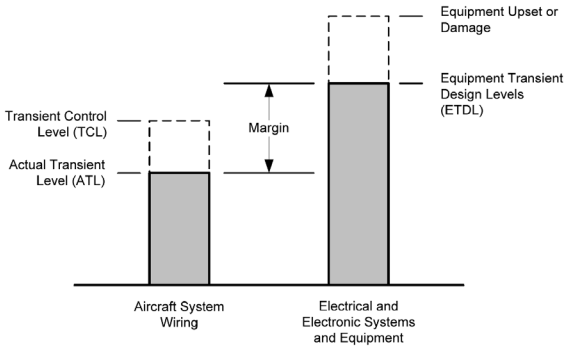

Fig. 8.1 Relationships of Transient Levels

Coupling physics

The basic scientific principles involved in analysis of the induced effects of lightning are reviewed in Chapter 9. Some of the points discussed there, particularly the mathematical operations, are included in this chapter as well, to illustrate the coupling mechanisms.

8.4 Lightning

Lightning current in an aircraft

Lightning strikes to aircraft occur often enough that a strike to any aircraft should be regarded as a certainty. A lightning strike involves a direct contact between the aircraft and the lightning channel. The currents on the surface of the aircraft may have an oscillatory component whose frequency is governed by the size of the aircraft, but the oscillation may also be influenced by the characteristics of the lightning channel. These oscillating currents are known as traveling wave currents, and their behavior is like that of the high intensity radiated fields (HIRF) induced currents, except that traveling wave currents induced by lightning are probably higher in amplitude than those induced by HIRF and NEMP.

The injected lightning current and the resulting traveling wave currents are also accompanied by electric (E, V/m) and magnetic (H, A/m) fields at the surface of the aircraft. These E and H fields are related by the characteristic impedance of the aircraft, which is typically of the order of 100 ohms. The forcing function, however, is the injected lightning current and the external electrical and magnetic fields are a consequence of that current. This much different from what happens when an airplane is exposed to electromagnetic fields produced by NEMP or other HIRF sources that analysis and test methods developed for evaluating these effects are not usually effective for evaluating effects of lightning. The concept of shielding effectiveness (SE), a ratio of field outside to field inside, is not a particularly helpful way to evaluate the response of an aircraft to lightning current. It is more straightforward to base analysis of the effects of lightning on the concept of transfer impedance (ratio of internal voltage to external current), a subject discussed in Chapters 9 and 10.

Frequency spectra: NEMP and lightning can also be compared according to their frequency spectra (see Fig. 8.2). NEMP contains more energy than lightning at high frequencies (50 MHz and above) while lightning contains more energy than NEMP at lower frequencies. The data presented in Fig. 8.2, should be viewed with caution, since the frequency spectrum calculated for lightning is based on simplified waveforms that may not truly represent the multi-pulse nature of lightning.

Some research is indicating that there are portions of lightning currents that change with time more rapidly than previously assumed, although these higher rate-of-change currents, if they exist, do not appear to have adversely affected aircraft avionic systems. Whereas the lightning environment for application to aircraft is presented in the time domain, it is possible to convert time domain current pulses into frequency domain via the Fourier transformation so that a series of sinusoid waveforms at varying frequencies and peak amplitudes are combinable to produce the time domain lightning current pulse. It is not useful to apply tests of systems and equipment using the series of frequency domain waveforms since the effects of these on electronic components are not going to be the same as would the time domain pulse.

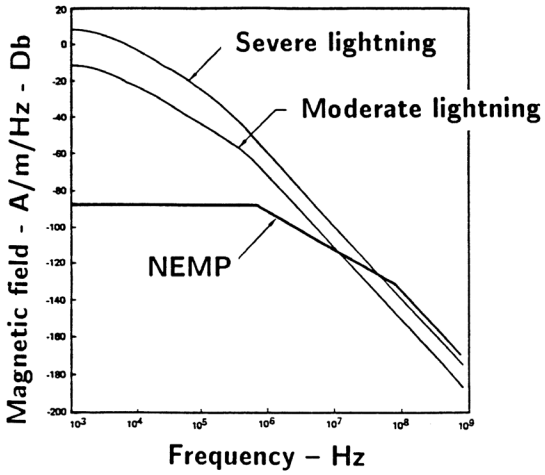

Fig. 8.2 Frequency spectra of lightning and NEMP (Range = 0.75 m).

8.5 Basic Coupling Mechanisms

The primary mechanism by which HIRF and NEMP fields induce signals in aircraft wiring is through field penetration of apertures. Aperture coupling is also significant in lightning interactions but, with lightning, coupling through resistive or diffusion mechanisms is also important, particularly for aircraft having large amounts of composite material in their structures. The other two coupling mechanisms are via structural IR voltages and electric fields. These coupling mechanisms are illustrated in Fig. 8.3 and discussed in more detail in Chapters 11 and 12.

A metal aircraft is often viewed as providing a 'Faraday shield' for the systems contained within. This is a concept from electrostatics that implies that the electrical environment inside the aircraft is separate and distinct from the environment outside. To some extent this is true; the lightning environment inside an aircraft is not nearly as high as the external environment.

There are three mechanisms by which electrical energy couples to the interior of an aircraft. The basic coupling methods are illustrated in Fig. 8.3. Chapter 9 describes the physics of each of them, and subsequent chapters discuss them in greater detail, with examples.

8.5.1 Structural Resistive Voltage

The first coupling mechanism relates to the electric field produced along the inner surface of the aircraft by the flow of current through the resistances of structural materials and joints. In some cases, an easily identifiable resistance is involved, although frequently that resistance is of a distributed nature that may depend upon the amplitudes and durations of the structure currents. It has been learned that resistances of aircraft structures generally decrease with current amplitudes. Due to improvements in joint conductivities as current is increased. The variability is due to the surface finishes and sealants included in the fastener installations. When tests of airplanes at low (i.e., 1-3 kA) current amplitudes are made to measure induced transients, it may be assumed that the IR coupling will result in somewhat higher amplitudes of induced transients than would be the case had the airplane been conducting a full threat (say 200 kA) stroke current, normalized for stroke amplitude.

Voltage rise: The term voltage rise is preferable to voltage drop since the product of current and resistance acts as a source (akin to a battery as a voltage source), which is then applied to an internal circuit, in this case the wiring of the aircraft.

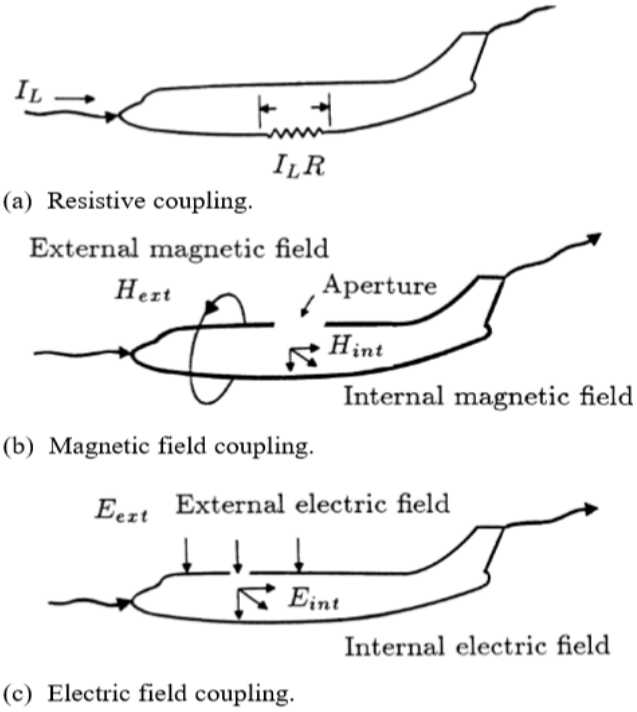

Fig. 8.3 Lightning coupling mechanisms.

Joint resistance

The most easily understood mechanism by which lightning induces voltages on aircraft electrical currents is that in which the current, flowing through airframe structure and joint resistances produces a voltage by the elementary IR (also shown as IxR) mechanism. A simple example of this mechanism is shown in Fig. 8.4, in which lightning current flows through the resistance of the mechanical mounting structure of a light. The resulting voltage rise across this resistance has the same waveform as the injected lightning current but, at some remote point, the waveform may be altered by oscillations between the inductance and capacitance of the wire supplying power to the filament of the light.

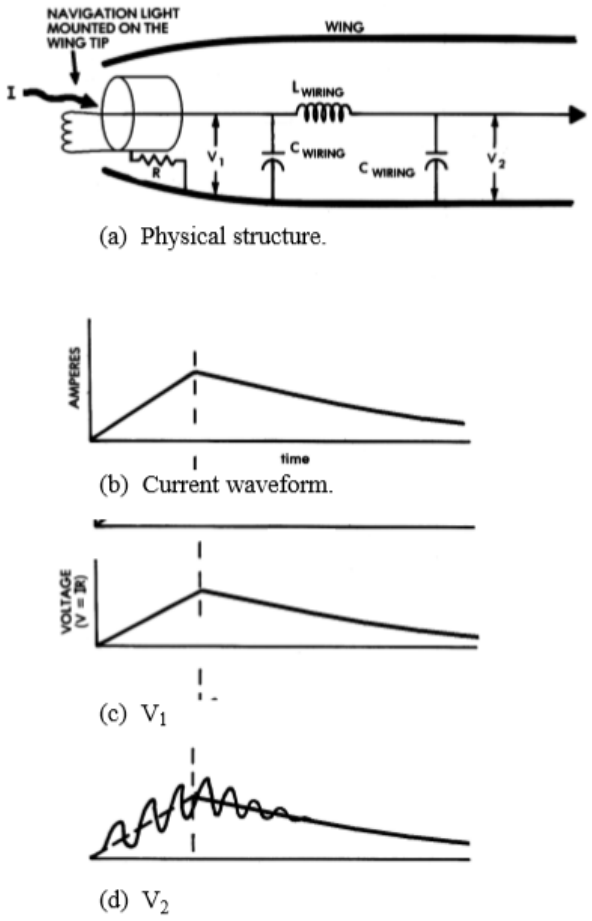

Fig. 8.4 Resistive voltages.

Fig 8.5 shows two other examples of situations in which resistive voltages might be encountered. Example (a) is at the interface between a pylon and external stores mounted on it (Fig. 8.5(a)). If lightning attaches to the external stores, it must flow through this interface to enter the aircraft. Since pylon interfaces are not primarily designed for carrying current and since the lightning current would be concentrated as it flowed through them, a voltage would be developed across the resistance of the pylon interface. This is particularly likely if the mounting bolts are made of steel, which has a higher resistance than aluminum. A bolt resistance of 10 milliohms, for example, would produce an IR voltage of 2 000 volts if exposed to a conducted stroke current of 200 kA. Similarly, IR voltages may also develop across the structural interfaces between large, adjoining sections of an airframe, such as that between the vertical stabilizer and tail section shown in Fig. 8.5(b).

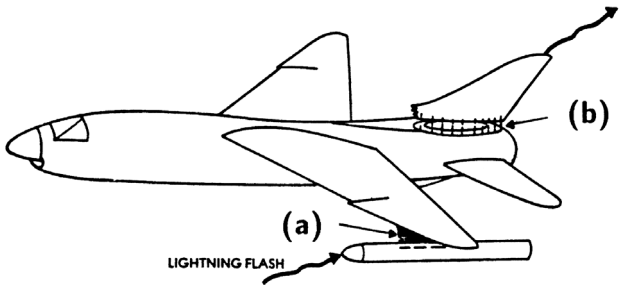

Fig. 8.5 Other examples of resistance.
(a) The pylons for external stores.
(b) Joints in structural members.

Effects of aircraft circuit return architecture

The effects of joint resistance on circuits are strongly influenced by the way electric power or signal circuits are returned or 'grounded'. In Fig. 8.6, current flowing across the joint resistance, R, produces a voltage, V = IR. Since the circuit across which V_1 is measured employs the structure as a ground-return path, it experiences all of this voltage; thus, V_1 is high. A circuit employing a single-point ground does not include this IR voltage rise; hence V_2 would be low, especially if the wires were twisted together so that the magnetically induced voltage was also low.

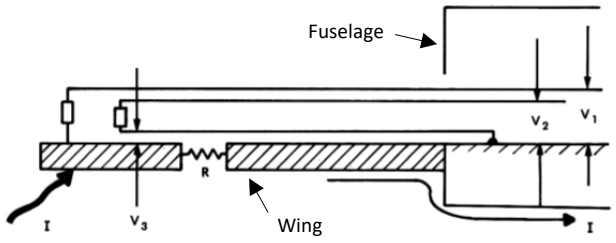

Fig. 8.6 Effects of aircraft circuit grounding.
(a) Structural return, $V_1 = IR$
(b) Single-point ground, V_2
(c) Single-point ground, $V_3 = IR$

The use of a single-point ground for the circuit would not eliminate the IR voltage because the voltage at the load end of the circuit, V_3, would be high and would include the IR voltage as well as any voltage induced by magnetic fields passing through the loop between the wire harness and the airframe.

Structural IR voltages are of particular concern in aircraft made from carbon fiber composite (CFC) materials because the structural resistances of such aircraft may be tens of milliohms. A 200 kA current flowing through a structural resistance of 60 milliohms would produce 12 000 volts. Equipment located at one end of such a structure that is referenced through an unprotected wire harness to a point at the opposite end of the structure may be subjected to the IR voltage of the entire structure. This voltage would appear in the loop formed by the wire harness and the adjacent airframe. The amount of it that reaches any item of equipment between the equipment and the local structure. Any voltages induced by magnetic fields would be superimposed on this IR voltage.

Limitations of structural resistance analyses

These descriptions of the effects of joint resistance should not be relied upon to predict coupling into circuits extending throughout the entire aircraft. Joint resistance effects only the IR component of induced voltage, not the magnetically induced component. Therefore, if joints are made more massive, reducing IR-induced effects, the effects of changing magnetic fields become proportionately more significant. These effects are discussed in more detail in other sections, but one common oversimplification, illustrated in Fig. 8.7, should be pointed out here.

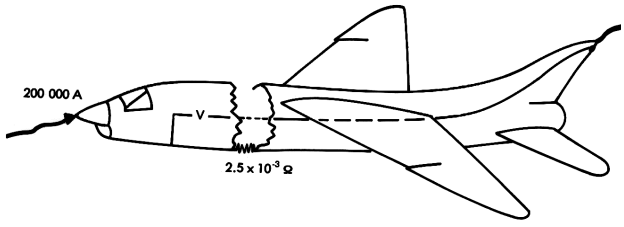

Fig. 8.7 An oversimplified model. Maximum Induced voltage is not determined solely by end-to-end resistance.

If the total end-to-end resistance of an aircraft is 2.5 mΩ and a lightning current of 200 kA flows through this resistance, the end-to-end voltage on any circuit cannot be depended upon to be less than 500 V (the product of the lightning current and the DC resistance). For more discussion about the relevance of bonding resistances to lightning protection, see §6.1.5., etc.

Resistances play a similar role in internal conduits and shields that are used to protect circuits, but the voltage rises that happen in these items are considered part of the performance of shields, which is the topic of Chapter 15.

8.5.2 Magnetically Induced Voltages

The second coupling mechanism (Fig. 8.8) is due to lightning magnetic fields in the interior volume of the aircraft.

Aperture coupling

The most common and important magnetic field interaction involves external magnetic fields passing through apertures to the interior of the aircraft, as illustrated in Fig. 8.8(b). These fields are due to the lightning current in the airframe. If windows and other apertures are present a portion of the exterior magnetic fields will pass into and out of the interior of the airplane via these apertures, so these are frequently called the *aperture fields*. A changing magnetic field passing through a loop (Fig. 8.8(c)) generates an open circuit voltage, usually expressed as Voc. This is the magnetic field coupling mechanism. It is also a combination of Faraday's law and Lenz's law. Specifically, Faraday's law is the magnitude of the voltage and Lenz's law is the polarity of the voltage, which, importantly, is so that current driven by the induced voltage will be to oppose the incident field that yields the induced voltage in the first place, a feature that is important for SE as discussed in Chapter 15). The loop mentioned above could be any circuit loop of interest, but most commonly it is the area between a wire harness and the nearest airframe surface, such as the interior surface of a fuselage skin along which the harness is routed, or perhaps a cabin floor beneath which the harness of interest is routed. Since wire harnesses are usually groups of individual wires, routed and tied together, it is the magnetic field passing through the common loop area between these wires, and the adjacent surface that is important, since the loop voltage induced by this field is common to all wires. This is usually a significantly higher voltage than is the voltage induced in the smaller spaced between individual wires. This common-mode loop voltage is given by,

$$V_{oc} = -\frac{d\varphi}{dt} \qquad (8.1)$$

or

$$V_{oc} = 4\pi \times 10^{-7} A \frac{dH}{dt} \qquad (8.2)$$

where H is the magnetic field strength and φ is the total magnetic flux passing through the common loop of area A. Eq. 8.2 is useful if the magnitude of the field intensity, H, can be assumed to be the same throughout a loop.

These numerical relationships are discussed further in Chapter 9. The most important point is that the voltages

are proportional to the rate of change of magnetic field, some-times referred to as dH/dt, or H-dot.

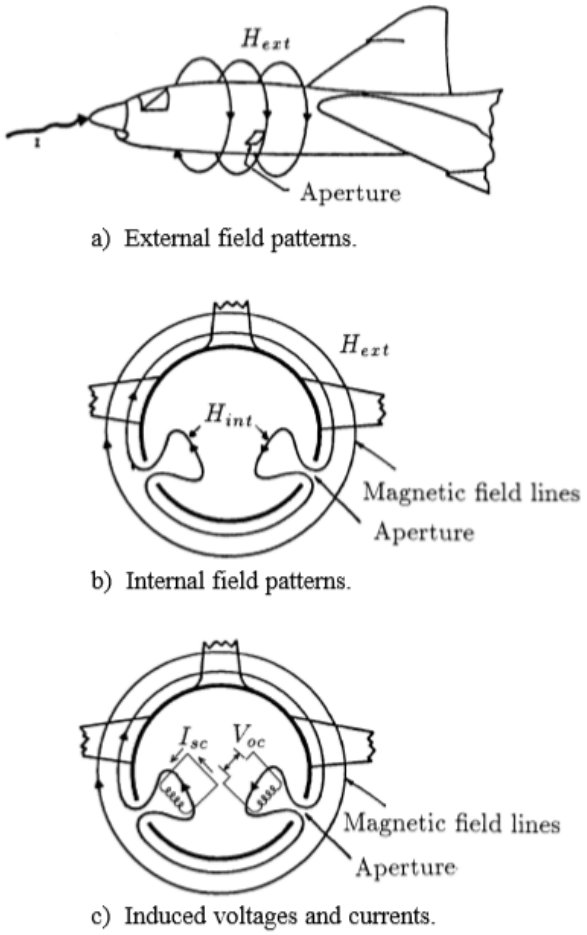

Fig. 8.8 Aperture-type magnetic field coupling.

Induced current

If the loop is short-circuited, a short circuit current, usually referred to as I_{sc}, is induced in the loop. The amplitude of I_{sc} is given by Eq. 8.3.

$$I_{sc} = \frac{1}{L}\int V_{oc}dt \qquad (8.3)$$

where *L* is the self-inductance of the loop.

The current in the short-circuit loop thus tends to have the same waveform as the inducing magnetic field, unlike the voltage, whose waveform corresponds to the rate of change of the magnetic field *(dφ/dt)*.

Diffusion coupling

Magnetic fields are also produced by the diffusion of lightning currents to the inside surfaces of the aircraft skins. These are referred to as the *diffusion fields*. The *diffusion fields* are also related to the frequency dependent properties of the resistively generated electric field. Because some of the concepts involved in the study of the *diffusion fields* are central to an understanding of other effects, particularly with respect to the response of shielded wires, they are discussed in detail in Chapter 11.

Composite aircraft Structures

Magnetic field effects are sometimes more severe in aircraft made from composites than in metal aircraft. Fiberglass and aramid fiber reinforced plastics provide no magnetic shielding. Carbon fiber composites provide some shielding against aperture fields, but not as much as metals provide. Not only are the magnetic fields higher inside nonconductive composite airframes, but they rise to peak faster than in either metal aircraft or aircraft fabricated of CFC. An effect of the increased magnetic fields is that much more of the total lightning current flows on internal metal objects in a composite aircraft than flows inside a comparable metal aircraft. Another way of phrasing this is to say that the current redistribution time constants in a composite aircraft (even one made from CFC) are much faster than in a metal aircraft. The phenomena of redistribution are discussed further in Chapter 11.

8.5.3 Capacitively-generated Currents

The third type of coupling, Fig. 8.9, involves electric fields passing directly through apertures, such as windows or canopies, to the interior of the aircraft. The displacement current, I_{disp}, induced in a conductor by a changing electric field (Fig. 8.9(c)) is

$$I_{disp} = 8.85 \times 10^{-12} A \frac{dE}{dt} \qquad (8.4)$$

where *A* is the area available to intercept the electric field and E is the intensity of the field, V/m.

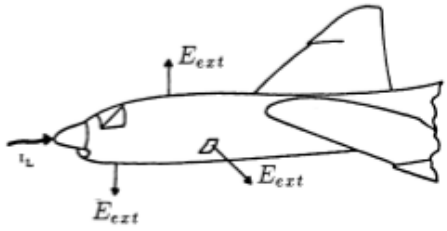

(a) External field patterns.

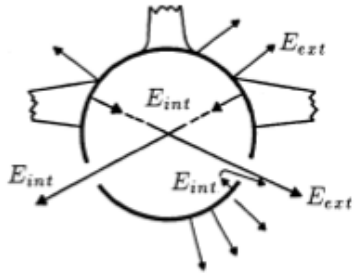

(b) Internal field patterns.

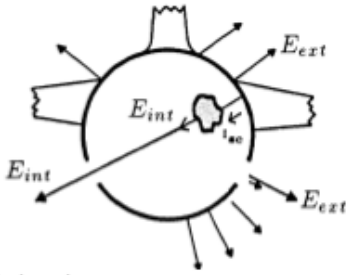

(c) Induced current.

Fig. 8.9 Aperture-type electric field coupling.

If the current flows through an impedance, a voltage appears across that impedance. Capacitively induced voltages and currents are proportional to the rate of change of electric field, frequently referred to as dE/dt or E-dot. Changing electric fields, and the displacement currents they induce, are discussed in detail in Chapter 9.

In metal aircraft, electric field coupling takes place entirely through apertures, since virtually any thickness of metal provides extremely good shielding against electric fields. In aircraft that have CFC instead of aluminum skins, this is usually also the case.

8.6 Approaches to Determining the Responses of Circuits

The two basic methods of determining how much voltage and current would be induced on aircraft wiring by lightning are numerical analysis and measurement.

Numerical analysis

Since an aircraft is a complex structure, it is difficult to determine, by purely analytical means, the voltages and currents that would be induced on aircraft wiring by lightning. Computer codes exist that have been verified by comparisons with aircraft test data. Such verification is required by airworthiness certifying authorities if the codes are to be utilized to compute induced transient waveforms and levels to set certification test conditions for equipment and systems. As of this writing, they are limited in the degree to which they can accurately predict the voltages and currents of actual aircraft wiring systems, as opposed to idealized and oversimplified geometries; however, computational power and codes are progressing to provide solutions to more complex situations.

The primary virtue of numerical analysis is that it enables one to predict the approximate responses of wiring on an aircraft that has not yet been built. Also, using simplified and idealized geometries, one can predict the order of magnitude of voltage and current on circuits too complex to analyze precisely. Frequently, an order of magnitude estimate of the voltages and current induced by lightning is enough to enable one to make useful decisions regarding protective measures.

Measurements

The experimental method for analyzing the response of an aircraft to lightning is to inject current into the aircraft and measure the resulting voltages and currents on internal wiring. This has been known as 'Lightning Transient Analysis' (LTA) or 'Full Vehicle' testing. There are three basic approaches to such tests:

1. Measure the aircraft's response to lightning currents through Fourier analysis of wiring responses to sinusoid currents of various frequencies.

2. Inject (full threat level) pulse currents into the aircraft and measure the response in the time domain.

3. Inject low level (much less than full threat level) currents into the aircraft, measure the response in the time domain, and extrapolate the results to full threat level.

These three methods are discussed further in Chapter 13. The method of injecting low level pulse currents into the aircraft is the one that has been used for most measurements of the response of aircraft electrical circuits. Full threat level tests are seldom made on aircraft, since test equipment capable of doing this is not readily available and the physical effects of multiple full threat tests on an

airplane are unknown, as are the possible effects on installed avionic equipment. Tests at full threat have been conducted occasionally on military airplanes.

Sometimes, a designer does not have access to an airplane to test when information on the induced transient levels is needed to prepare lightning induced transient tolerance specifications for the avionic equipment. In recognition of this common situation, Chapter 14 provides some simplified tools with which to estimate these levels. An engineer who needs to establish ETDLs for aircraft avionics may find this chapter helpful.

8.7 Examples of Induced Transients Measured on Aircraft Wiring

It is common to inject simulated lightning currents into an aircraft and measure the resultant voltages and currents on wiring inside the aircraft. A few examples of typical measurements will be given in the following sections, primarily to illustrate the general nature of voltages and currents induced by lightning. Where appropriate, reference will be made to the subsequent chapters where the phenomena are discussed in further detail.

8.7.1 Electrical Circuits in an Aircraft Wing

The first set of tests to be discussed [8.1] is one in which lightning-like currents with amplitudes up to 40 000 A were injected into one wing of an F-89J fighter aircraft. During these tests, represented in Fig. 8.10, the wing was fastened onto a screened instrument enclosure, which may be regarded as representing the fuselage of the aircraft. The current was injected either into the wing or into the external wing tip tank, allowed to flow along the wing to the outer wall of the screened instrument enclosure, and then to a ground plane from which it was returned to the opposite terminal of the current generator. Whereas this airplane is not of interest today, the transient measurements are typical of those measured in many airplanes. The wing and fuel tank were constructed of aluminum. An example of one type of current waveform injected into the wing is shown in Fig. 8.10(b). These tests were of an exploratory nature, prior to the adoption of industry standards for aircraft FVTs. The injected current for these examples had an amplitude of approximately 30 kA and an overall time duration of about 30 μs. Although this is not equivalent to the standard stroke current Component A, it is nevertheless somewhat typical of an 'average' negative cloud-to-earth stroke.

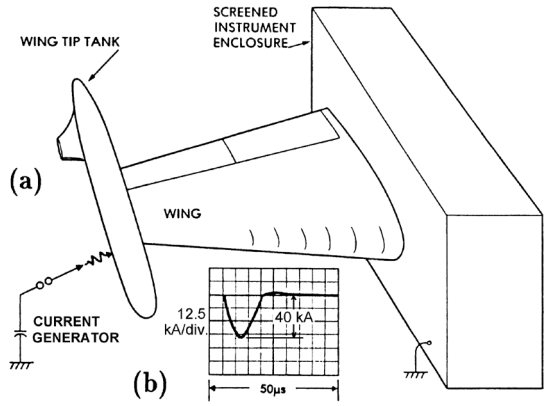

Fig. 8.10 High current injection tests on a wing.
(a) Test arrangement.
(b) Waveshape of injected current.

The test current differed from a typical lightning stroke current, which would usually rise rapidly to crest and then decay at a much slower rate. The shape of the test current waveform must be considered when observing the waveform of some of the measured induced voltages and currents illustrated in the following paragraphs. Note that at about 20 μs, a major discontinuity occurs in the test current waveform. This discontinuity is reflected in the induced voltages.

Within the wing there were several electrical circuits associated with navigation lights, fuel gauges, pumps, relays, switches indicating flap positions, etc. Some of these were in the leading edge of the wing and were well shielded from many electromagnetic effects, while others ran along the trailing edge, between the main body of the wing and the control surfaces. The latter circuits were the most exposed to the electromagnetic fields. All the circuits were relatively simple and independent from each other. They were not, as a rule, bundled together in one large cable bundle, a practice that provides maximum coupling from one circuit to another and makes analysis difficult. (The question of how the location of wiring affects the voltages induced in it by lightning is discussed in Chapter 16.)

Position light circuit

The schematic shown in Fig. 8.11 represents a circuit that supplied power to a position light mounted on the external fuel tank. The circuit consisted of one wire supplying power to the filament of the position light. The return circuit was provided by the structure of the wing itself. Accordingly, if a lightning flash attached to the external tank, that circuit would be influenced by the resistance R_1 of the

hangers fastening the tank to the wing, by R_2, the inherent resistance of the wing, and by magnetic flux arising from the flow of current.

Typical test results are given in Figs. 8.11(c) and 8.11(d). The open circuit voltage rose rapidly to its crest and decayed more rapidly than the injected current, shown in Fig. 8.10(b). This indicates that the open circuit voltage was responding primarily to the derivative of the magnetic flux.

When the conductor was shorted to ground at the measurement end, the short circuit current rose to its crest in approximately the same length of time as the injected current did and had essentially the same waveform. This example shows that "induced" short-circuit currents are simply a portion of the total lightning current conducted through the airplane. Fig. 8.11(e) shows an approximate equivalent circuit, in which L_1 and R_1 represent the transfer impedance that relates the induced transients to the lightning current. L_2 and R_2 represent the inherent inductance and resistance of the wires between the fuselage and the light. The transfer inductance and resistance are merely the empirical values that would produce the observed open circuit voltage when operated upon by the external lightning current. They do not necessarily represent any clearly definable resistance or inductance of the wing.

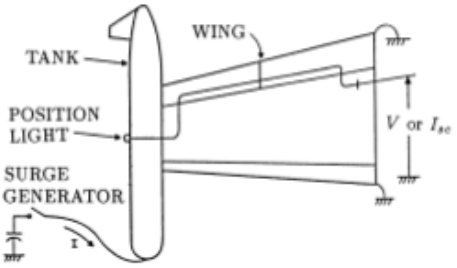

(a) Circuit orientation

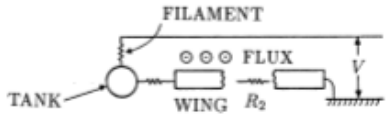

(b) Electrical details of circuit

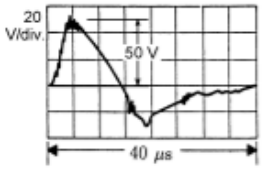

(c) Open circuit voltage

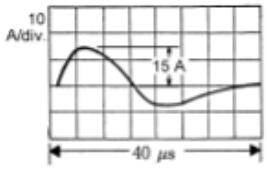

(d) Short circuit current

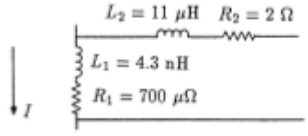

(e) Equivalent circuit

Fig. 8.11 A wing tip circuit and induced transients

Pylon circuit

In the circuit shown in Fig. 8.12, a conductor runs through the leading edge of the wing and terminates in an open circuit in a pylon mounted underneath a wing. In the electrical detail circuit shown in Fig. 8.12(b), this circuit would not respond to the voltage developed across the resistance between the external tank and the wing. However, the circuit would respond, in some measure, to IR rise through the resistance of the wing structure and to the magnetic field accompanying the flow of current in the wing, but, since the circuit was only capacitively coupled to the wing, the measured voltage, V was less than that in the circuit shown in Fig. 8.11.

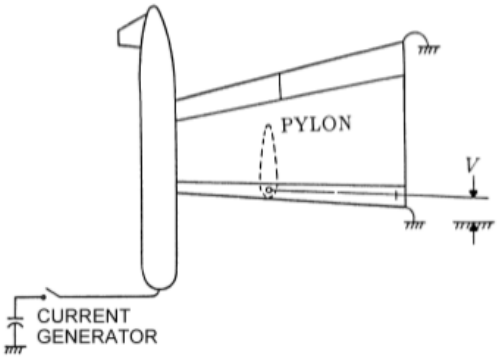

(a) Location of circuit.

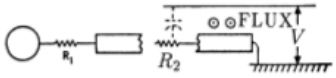

(b) Electrical details of circuit.

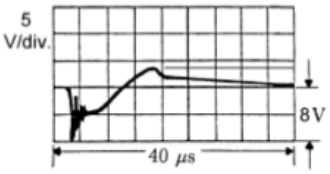

(c) Open circuit voltage.

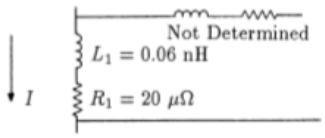

(d) Equivalent circuit

Fig. 8.12 A pylon circuit – open at pylon and induced voltage.

The conductor shown in Fig. 8.12 supplied power to a relay and to explosive bolts in the pylon used to hold an external store. In Fig. 8.12, the pylon was not installed, so there was no load on the conductor. Fig. 8.13 shows the results with the pylon installed and the conductor connected to a relay with a return through the aircraft structure. In this test, the simulated lightning stroke current was injected to the pylon. The combination of the circuit's structural path and the fact that the lightning strike terminated on the pylon (thus including in its path the resistive drop across R_3, the resistance between the pylon and the wing) produced a much higher voltage on the wire than when the conductor was open circuited. No attempt was made to completely analyze from which area the magnetic flux was coming or which component of that flux (φ_1, representing that in the pylon, or φ_2, representing that in the wing) was larger.

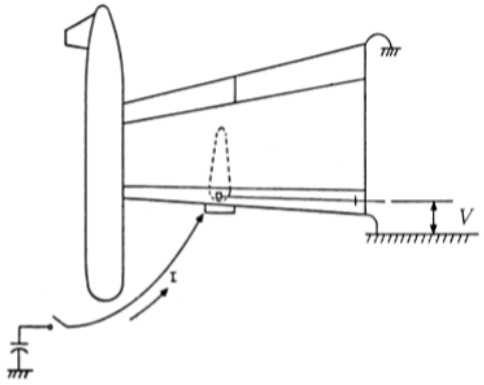

(a) Circuit location

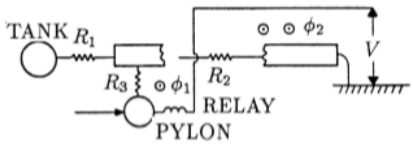

(b) Electrical details of circuit

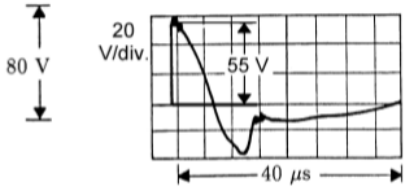

(c) Open circuit voltage

Fig. 8.13 A pylon circuit – loaded at pylon and induced voltage.

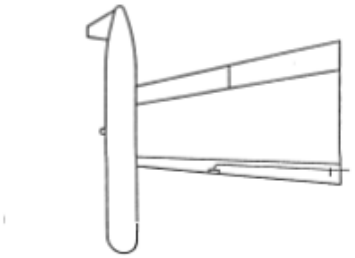

(a) Circuit orientation

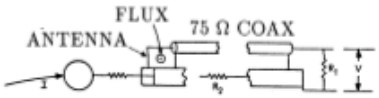

(b) Electrical details of circuit

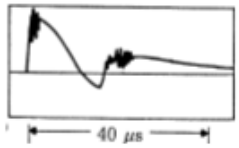

(c) Open circuit voltage - $R_1 = \infty$

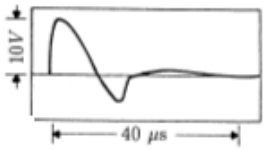

(d) Open circuit voltage - $R_1 = 75\Omega$

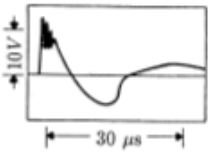

(e) Open circuit voltage - $R_1 = \infty$

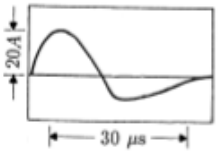

(f) Short circuit current - $R_1 = 0$

Fig. 8.14 An antenna circuit and induced transients.

Antenna circuit

The circuit shown in Fig. 8.14 illustrates the interaction between the lightning-induced voltage and the circuit response. In this circuit, a slot antenna, excited by a grounded stub and fed from a length of 75 Ω coaxial cable, was installed in the leading edge of the wing. The shorted stub that excited the slot antenna was the predominant area intercepting the magnetic flux produced by the lightning current in the wing.

The voltage developed in this antenna, whose waveform is shown in Figs. 8.14(c) and 8.14(e), followed the same pattern as that shown for the other circuits. The rapid transition on the leading edge of the voltage, however, was capable of exciting an oscillation within the coaxial cable feeding the antenna. When the antenna circuit was terminated through a resistor matching the surge impedance of the cable, the higher frequency ringing oscillation disappeared, leaving only the underlying response of the antenna to the magnetic field surrounding the wing.

Significant conclusions

Several significant things were learned during this test series. First, the voltages induced in a typical circuit within a wing consist of the sum of a magnetically induced component and a component proportional to the resistance of the current path. Second, the location at which the lightning flash contacts the wing has an important effect on the magnitude of voltage developed on different circuits.

Nearly all the voltages and currents measured on the circuits in the experiment described above could be explained in terms of simple equivalent circuits, such as those shown in Fig. 8.15. One way to view these equivalent circuits is in terms of the self-inductance of the wing, the self-inductance of the circuit within the wing, and the mutual impedance between the wing and the internal conductor, as shown in Figs. 8.15(a) and (b). Note that these equivalent circuits include the effects of mutual inductance. Without this, they would be incorrect.

Another approach to viewing equivalent circuits is based on transfer impedance, as illustrated in Fig. 8.15(c). In the approach based on self and mutual inductances, the self-inductance of the wing would be nearly equal to the mutual inductance between the wing and the internal conductor. The difference between the two would be equal to the transfer inductance in the latter approach.

Since the values for the transfer impedance are much smaller than the values representing the self-impedance of the circuit, the latter approach leads to an equivalent circuit that is easier to work with. It is also compatible with the concept of mutual inductance or transfer impedance discussed regarding shielded cables in Chapter 13.

There is no easy way to correlate the magnitudes of the transfer impedance with the physical geometry of the wing or with the location of the conductors within the wing.

However, it can be said that conductors located in the forward portion of the wing are better shielded, and consequently have lower transfer impedances, than those along the trailing edge. Likewise, it can be observed that circuits which do not have any electrical return through the wing structure have lower transfer impedances than circuits which do have a return through the wing structure.

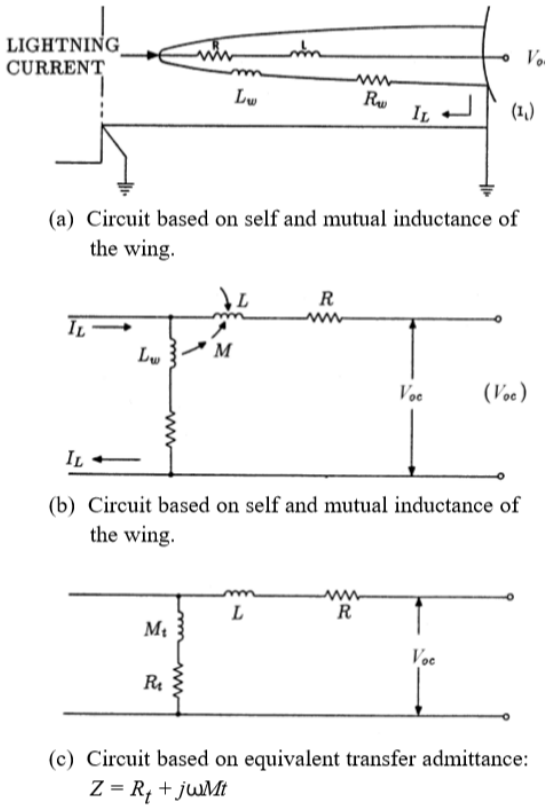

(a) Circuit based on self and mutual inductance of the wing.

(b) Circuit based on self and mutual inductance of the wing.

(c) Circuit based on equivalent transfer admittance: $Z = R_t + j\omega Mt$

Fig. 8.15 Equivalent circuits.

It is significant to note that the short-circuit currents have waveforms of longer duration than the open-circuit voltages. This occurs because the impedance of conductors is primarily inductive, not resistive. Some of the specifications now being placed on proof testing for aircraft avionic systems do not recognize this inductive nature of wiring systems. Rather, by design or by oversight, they treat the impedance as if it were resistive, which complicates test procedures and may lead to improper interpretation of test results. This matter is discussed further in Chapter 18.

8.7.2 Digital Fly-By-Wire Circuits

The following discussion is based on measurements made on an F-8 aircraft operated by NASA as a research platform for a digital fly-by-wire control system. The fly-by-wire controls, represented by Fig. 8.16, consisted of a primary digital system, a backup analog system, and a common set of power actuators operating the control surfaces. The major components of the control system were in three areas: the cockpit, where sensors coupled to the control stick provided signals for the control systems; an area behind the cockpit, where the digital computer was mounted; and a compartment behind and below the cockpit on the left side of the aircraft. This last compartment would formerly have been occupied by guns. Accordingly, it is referred to here as the 'gun bay', although in this research aircraft it was used to house interface and control assemblies, not guns.

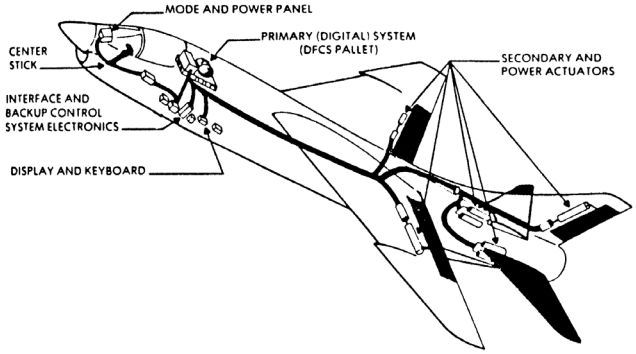

Fig. 8.16 Location of fly-by-wire control system hardware and wiring bundles in F-8 aircraft.

Several hydraulic actuators were located at each of the major surfaces. These were interconnected to the fly-by-wire control systems through wire bundles that ran under the wings. The control systems did not depend upon the aircraft structure as a return path; the system was considered to have a single-point ground, and that single-point ground was located at a panel in the gun bay. By and large, none of the control wiring in this aircraft was shielded.

Test techniques

In contrast to the tests on the wing of the F-89J aircraft, in which high amplitude currents were injected into the wing from a high-power surge generator, the tests on the complete F-8 aircraft were made using the LTA technique described briefly in §8.6 and more completely in Chapter 13. During the tests on the F-8, the injected current was on the order of 300 A. The measured transient amplitudes discussed here are the amplitudes induced by this injected current. To scale the results to what would be produced by atypical 30 kA lightning current, the measured amplitudes should be multiplied by 100. To scale the results to a design-level amplitude of 200 kA, they should be multiplied by 666.

It is important to measure common-mode (line to airframe) transients induced in individual circuits because these are needed to set damage tolerance tests of equipment, which need to be applied using the pin-injection test between individual equipment connector pins and chassis.

Several different current waveforms were applied. The waveform to which most frequent reference will be made in this abbreviated set of test results is that described as the 'fast waveform'; a current rising to crest in about 3 μs and decaying to half value in about 60 μs. These waveforms are shown in Fig. 8.17. The fast waveform is the most like the standard test current Component A recommended for such tests today and described in Chapter 5.

Fuselage circuit

The first set of measurements were made on a group of spare conductors that ran between an interface box in the gun bay and a disconnect panel located near the leading edge of the vertical stabilizer. The routing of the circuit is shown in Fig. 8.18(a) and the waveforms of the voltages that were measured are shown in Fig. 8.18(b). The voltage measured between the conductor and ground consisted of a high-amplitude oscillatory component and a second component of lower amplitude but longer duration. This is typical of voltages induced by lightning currents in unshielded wiring.

Voltages measured between the conductors, shown in Fig. 8.18(c), were much smaller than the voltages measured, *common mode,* between individual conductors and the airframe. Such results would be expected on a well-balanced circuit. The voltages were, however, not zero, and one should not assume that voltages on twin conductor circuits will be low enough to eliminate problems.

The oscillatory component of the voltage was excited by magnetic flux (and possibly electric fields) leaking inside the aircraft, while the longer duration component was produced by the flow of current through the structural resistance of the aircraft. Since voltages induced by the magnetic flux are proportional to the rate of change of that flux, the oscillatory component tends to be more pronounced for faster-changing (or rising) currents injected into the aircraft than for slower-changing (or rising) currents. This effect was noted in the tests under discussion and evidence of it can be seen in the oscillograms.

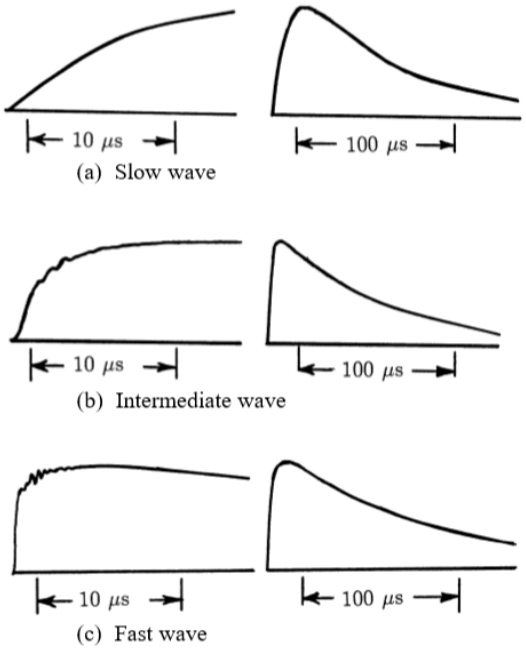

Fig. 8.17 Simulated lightning current test waveforms. Peak amplitudes were ~300 A

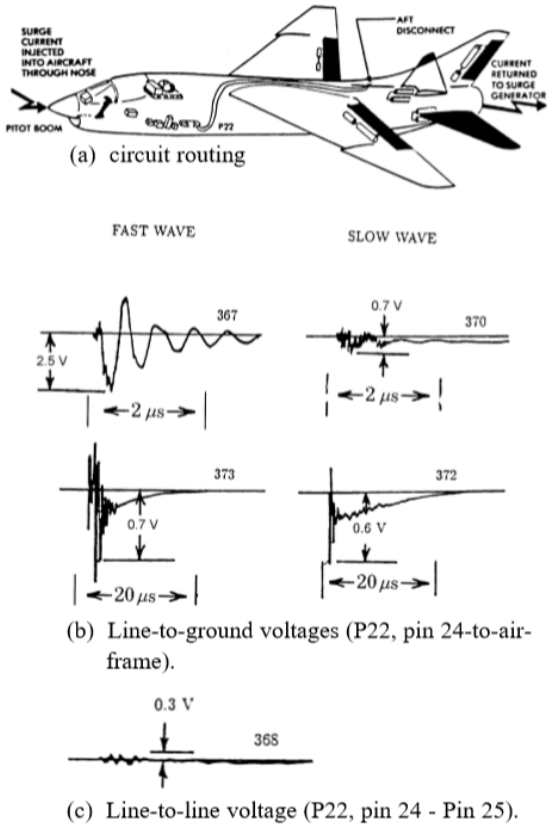

Fig. 8.18 Voltages induced in a fuselage circuit.

Circuit to wing position indicator

The second set of measurements was made on a circuit running from the interface control unit and the gun bay to a wing position indicator switch, located underneath the leading edge of the wing. The wing on the F-8 aircraft could be raised or lowered around a pivot point, towards its rear, to achieve a higher pitch angle during landing and takeoff. The purpose of the switch was to indicate the position of the wing.

The voltages induced on the wing-position indicator switch circuit are shown in Fig. 8.19. The voltages measured from 'line-to-airframe' (common mode) were higher than those measured 'line-to-line', but it is significant that the line-to-line voltages, while of a somewhat different waveform, were not much lower than the 'line-to-airframe' voltages.

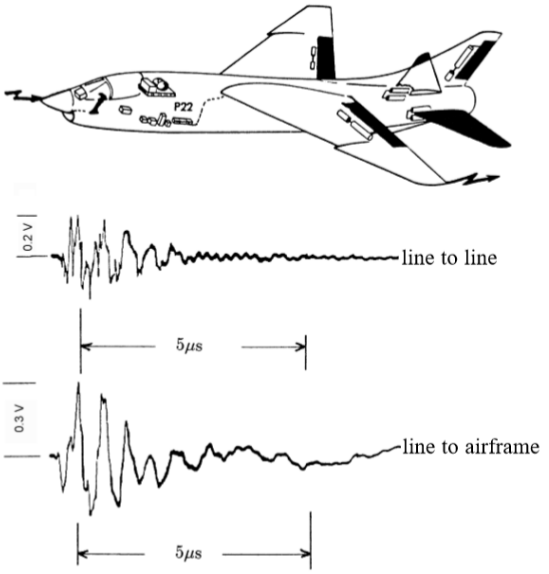

Fig. 8.19 Voltages induced in wing position indicator circuit at open plug P22.

The reason for this was that the load impedances of the two sides of the interface box in the gun bay differed. One side connected to a power supply bus, while the other side probably connected to an emitter follower. In standard tests, the wire plugs would be disconnected from equipment at the remote ends and the individual wires grounded locally to the equipment chassis or airframe ground, so that the entire loop voltage (V_{OC}) be recorded at the measurement end, as described in Chapter 13. The measurements reported here were taken prior to the advent of the FVT standard.

Note that these voltages were, again, of an oscillatory nature. They were apparently excited by the leakage of magnetic flux to the inside of the aircraft, not by the rise in potential along the structural resistance of the aircraft. The oscillatory responses are due to traveling wave currents in the aircraft, excited by the differences in characteristic impedances of the lightning channel (represented by the test current generator) and the airframe. This topic is explored further in Chapter 14.

Circuits to actuators

Figs. 8.20 and 8.21 show voltages measured on two different circuits going to actuators, one (Fig. 8.20) going to the left pitch actuator and the other (Fig. 8.21) going to the left roll actuator. In both cases, the voltages measured were the output of the driver amplifier used to control the servo valve in the actuator. Both were differential (i.e., line-to-line) measurements. Note, again, that the characteristic response was oscillatory and excited by the penetration of magnetic flux to the inside of the aircraft. The voltage depended somewhat on the path the current followed through the aircraft, but this dependence was not strong. Both lightning current paths produced transient voltages of about the same amplitude.

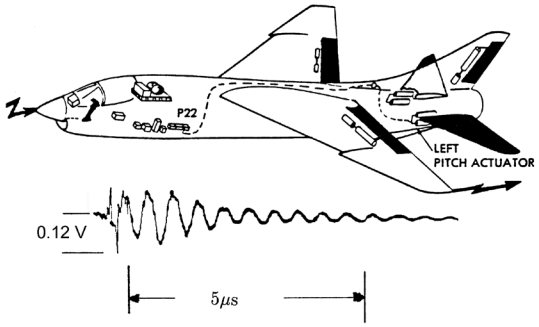

Fig. 8.20 Left pitch valve drive output (high to low) at plug P22.

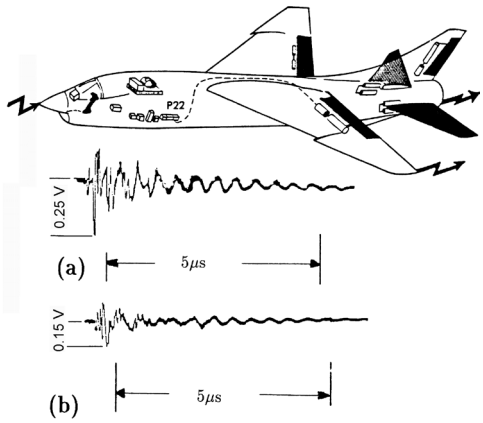

Fig. 8.21 Voltages induced in left roll valve drive output circuit (pins 44-45) at open plug P22.

Cable bundle currents

On the F-8, the control wires were laced together into large bundles, as is typical on most aircraft. The routing of some typical bundles in the gun bay, housing the backup and interface electronic control boxes is shown in Fig. 8.22. It is important to measure cable bundle currents because are needed to levels for performance of system functional upset tests of operating systems to verify adequacy of protection against system functional upsets, a topic discussed in Chapter 18. These tests are applied by injecting cable bundle transients into one or more cable bundles while a system is operating so that functional responses can be identified. This involves coupling current onto a cable bundle (usually through a transformer) and allowing the voltages and current on individual wires to develop as appropriate to the impedances of the circuits to which they connect. The technique of injecting current onto cables in this way is discussed in Chapter 18.

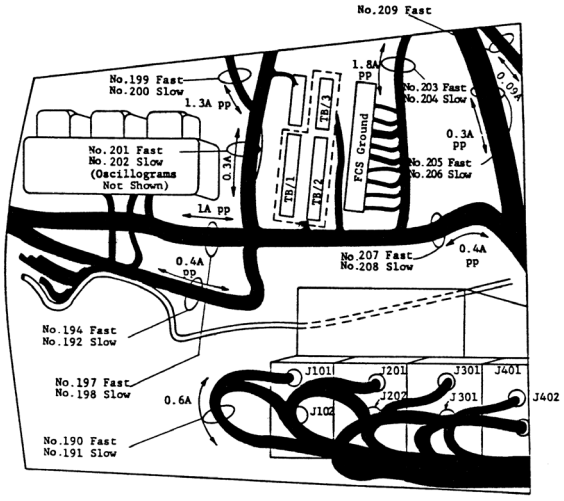

Fig. 8.22 Cable bundles within the gun bay.

Typical results of these cable measurements are shown in Figs. 8.23 and 8.24. The cable bundle currents were also found to be oscillatory, like the voltages on conductors, described earlier. Since the flight control wiring was not grounded at multiple points within the aircraft, none of the currents in these cable bundles exhibited any of the long-time response characteristic of multiple-grounded conductors.

Statistical distribution

Fig 8.25 shows a statistical distribution of the peak amplitude of currents in all the cable bundles upon which measurements were made. The distribution is shown for both the actual test current amplitudes injected into the aircraft and for currents extrapolated to represent the effects of actual lightning flashes. In terms of an average-amplitude lightning stroke (30 000 A), the total current on most cable bundles in this airplane would have been on the order of 20 to 100 A.

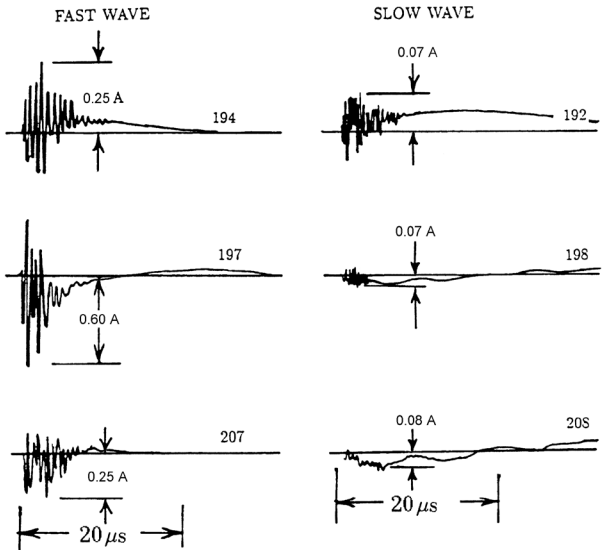

Fig. 8.23 Currents on cable bundles leading toward cockpit and left-hand instrument panel.

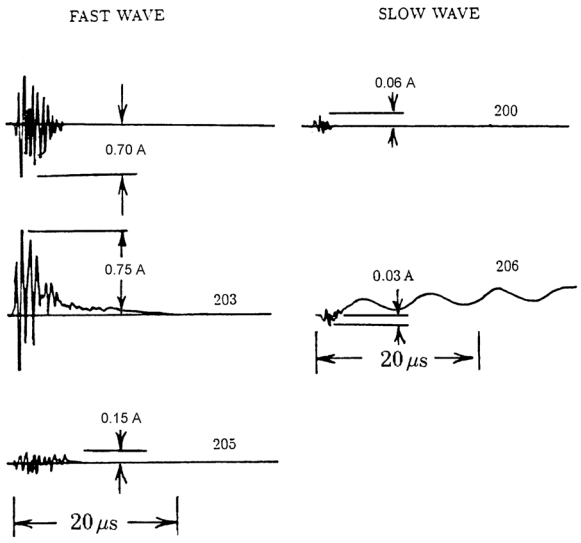

Fig. 8.24 Currents on cable bundles leading toward the area behind the cockpit.

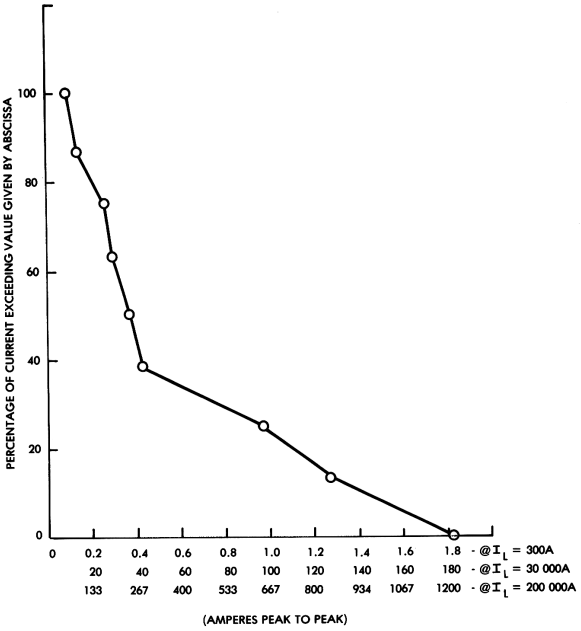

Fig. 8.25 Distribution of amplitudes of cable bundle currents (measured in left gun bay).

Magnetic fields

Measurements were made of the amplitude and waveform of the magnetic field at several points in and around the aircraft. One location upon which attention was concentrated was the cockpit, since the cockpit is an inherently unshielded region and one in which many control circuits can be subjected to changing magnetic fields.

The positions at which fields were measured, the peak amplitudes of the fields, and their predominant orientations are shown in Fig. 8.26. The magnetic fields were measured with a probe which had a characteristic time constant of about 4 μs. When exposed to fields changing in times less than 4 μs, it would respond to the absolute magnitude of the field intensity and, when exposed to fields changing in times longer than 4 μs, it would respond to the rate of change of the magnetic field.

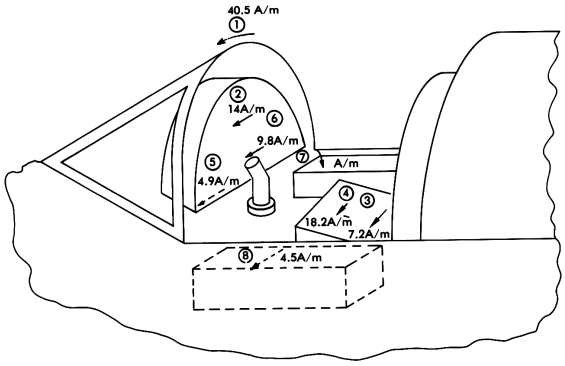

Fig. 8.26 Magnetic field measurements in the cockpit.

A few typical measurements of field waveform are shown in Fig. 8.27. The most significant feature of these measurements is that there was no orientation of the magnetic field probe that resulted in a zero output. This indicated that the orientation of the magnetic field was not uniform with respect to time. The field produced at any one point was the sum of the field produced by the total flow of current through the aircraft and that produced by oscillatory current in the various structural members, as the current in those members changed with time.

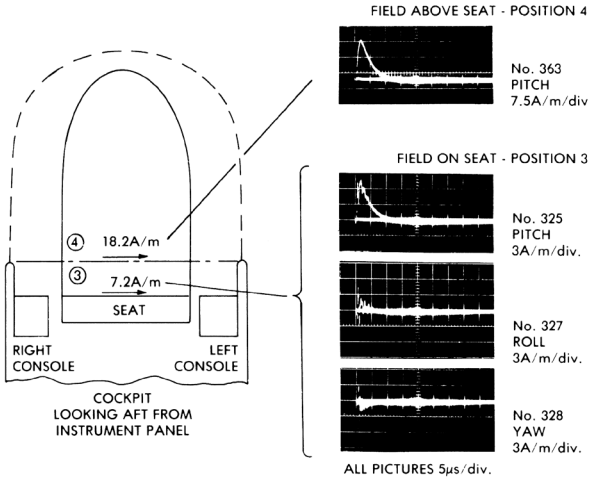

Fig. 8.27 Magnetic fields near pilot's seat.

When fields of high frequency are produced by oscillatory currents excited by an original transient field, the process is sometimes called re-radiation.

Also, it was noticed that the waveform of the magnetic field was quite oscillatory whenever the peak magnitude of the field was low. This behavior is common. It occurs because the low-level magnetic fields found within partially shielded structures arise either from re-radiation, due to circulating currents, or from coupling through apertures. It is noted in Chapter 12 that coupling through apertures is frequency-dependent, and that high frequencies (or the high-frequency portions of transient waveforms) are coupled more effectively than low frequencies.

Some measurements of the magnetic field within the gun bay are presented in Fig. 8.28. Clearly, the magnetic field inside the gun bay compartment was of lower amplitude than the magnetic field outside the gun bay. The waveforms of the fields are more difficult to understand. First of all, it must be kept in mind that the probe was responding to the rate of change in the magnetic field after about 4 μs and was responding to the field itself for times shorter than about 4 μs.

Accordingly, the oscillograms displaying the field inside the gun bay indicated an initial component of internal magnetic field that rose to its crest about as fast as the external field did.

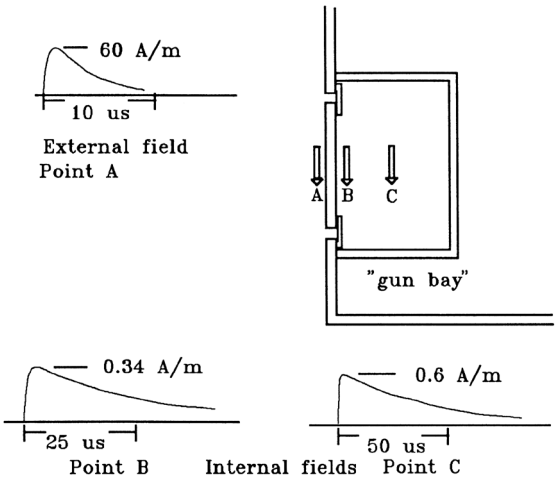

Fig. 8.28 Magnetic fields inside the gun bay.

From then on, the field continued to increase at a slower rate. (The final value of the field is not shown in the oscillograms). The fact that the field continued to rise, but at a slower rate, agrees with the behavior predicted in §11.3.5, Fig. 11.11 and §11.6, where it is shown that the magnetic field should increase with a time constant characteristic of the internal inductance and resistance of the cavity in which the fields are measured.

Magnetic Fields inside a battery compartment located aft of the gun bay are presented in Fig. 8.29. The measurements indicate some initial oscillatory magnetic fields, followed by a field that rose to crest at a time much longer than the crest time or even the duration of the simulated lightning current. Oscillogram (d), in Fig. 8.29, shows the rate of change of field falling to zero after approximately 400 μs. This indicates that the field itself reached its crest value in about that time.

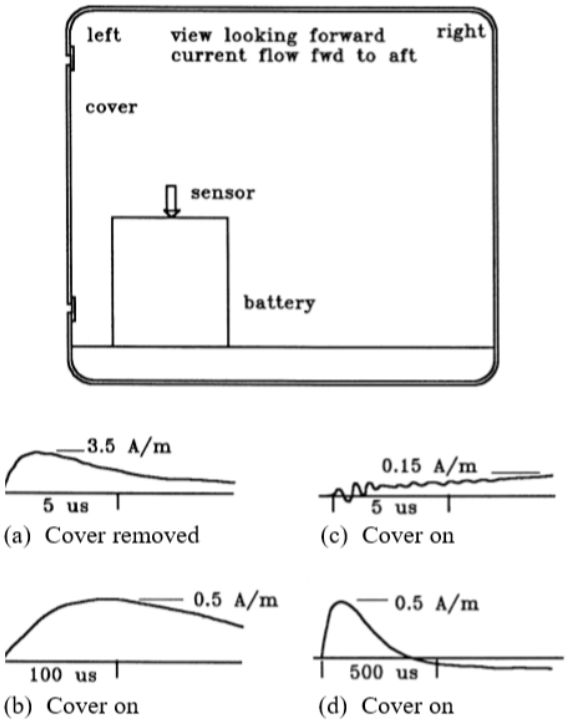

Fig. 8.29 Magnetic fields inside the battery compartment (probe time constant = 4 μs).

The differences between the responses of the magnetic fields inside the gun bay and those in the battery compartment can be attributed to differences between the types of covers and fasteners used on the two compartments. The cover over the battery compartment was held in place by fasteners spaced about every 3.8 cm, and thus made good contact to the rest of the airframe. The multiple fasteners provided many paths for circulating currents to flow in the walls of the battery compartment.

The gun bay covers, on the other hand, since they were originally designed for ease of access, had far fewer fasteners. These fasteners were spaced about every 30 cm. Accordingly, the cover on the gun bay afforded a much more severe constriction to circulating currents than the cover on the battery compartment. These differences allowed the magnetic field within the gun bay to reach its peak faster than the magnetic field within the battery compartment. The influence of fasteners on magnetic field penetration are discussed further in §11.6 and Fig. 11.19.

Simplified techniques for estimating magnitudes and waveforms of induced transients are discussed in Chapter 14.

Significant conclusions

Some significant points about the results of tests on this aircraft can be summarized here. The first is that the use of a single-point ground system did not eliminate all transient voltage produced by the flow of lightning current through the structure of the aircraft.

The second is that the characteristic response of the wiring, both for voltage and current, was a damped oscillation with a frequency in the range from 1 to 5 MHz. It should also be noted that the frequency of oscillation depended considerably on the length of the circuit involved, and also the length of the airplane within which the wiring is installed. The longer the physical length of the airplane, and of the wires installed within, the lower the oscillatory frequencies. This is not a clear-cut rule since the response of any one circuit can be greatly influenced by coupling between all of the different circuits.

The third significant point is that the total current on any cable bundle was of the order of 20 to 100 A for an average lightning stroke. This cable bundle current was again oscillatory, with a frequency tending to correspond to the length of the cable bundle.

The fourth point is that the equipment bays in this aircraft, not being designed for electromagnetic shielding, allowed significant amounts of magnetic flux to penetrate. This is particularly true of the bays intended for ease of access. As a rule of thumb, it can be expected that equipment bays housing electronic equipment are likely to be fitted with covers designed more with ease of access will provide less complete electromagnetic shielding, than will other access covers that are installed with many fasteners, especially if these provide some electrical bonding. Some access covers, not found on the F-8 airplane, are provided with continuous electrical bonding all around and this provided the best shielding.

Finally, the measurements of magnetic fields indicated that there is seldom any orientation of electrical wiring that can be expected to minimize its exposure to magnetic fields (and resulting induced voltages). It is best to assume that the magnetic field at any point will always have the worst-case orientation. Also, one should assume that internal magnetic fields are more oscillatory than external magnetic fields, because of re-radiation and the frequency-dependent transmission of magnetic fields through apertures.

No attempt was made to determine the degree to which circuit voltages could be reduced using shielded conductors in this aircraft. It was noted, however, that on circuits that had a shield grounded at more than one point, the waveform of the current on the shield resembled the slower, double exponential waveform of the external lightning current more than the high-frequency, oscillatory current that was excited on all the unshielded cable bundles.

8.7.3 Carbon Fiber Composite (CFC) Aircraft

Voltages and currents induced in the wiring of aircraft using CFC materials for structural members are very different from those induced in aircraft made entirely from aluminum. In a metal aircraft, the resistance of the structure is very low and the lightning stroke current flows mostly on the exterior metal surface. Only relatively small amounts of the current flow on internal wiring and internal structures and, in general, the duration of current flow in the interior is no longer than that on the exterior. In a CFC aircraft, however, the structure has a much higher resistance, and a much larger fraction of the lightning current eventually flows on the internal wiring and internal structure. Initially, the current may flow on the external structure but, at later times, it transfers to the inside, a process called redistribution. (Redistribution is discussed further in §11.4.)

The redistribution phenomenon also causes the internal currents to flow for much longer times, longer even than the duration of the lightning current. The overall result is that induced effects in a CFC aircraft can be more severe and harder to deal with than induced effects in a metal aircraft. Experiments performed on a test-bed fuselage for a CFC aircraft showed that, by the time an external injected current had decayed to half value (82 μs), 90% of the injected current was flowing on metal objects inside this fuselage.

A few examples of voltages and currents measured on CFC aircraft are given below, mostly to illustrate the redistribution effects and to illustrate the time scale over which they take place. Since the source of this data is proprietary, the illustrations are not as extensive as those in §8.7.1 and §8.7.2.

Aircraft structure

The general nature of the aircraft structure for which the following measurements were taken is shown in Fig. 8.30.

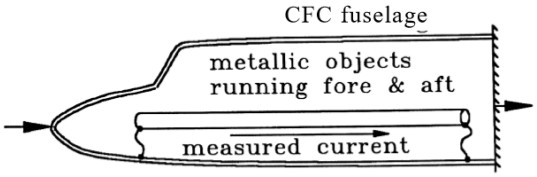

Fig. 8.30 General nature of a CFC fuselage upon which tests were conducted.

The main shell of the aircraft was made from CFC laminates. In the nose of the aircraft was an avionic equipment bay, built with aluminum shelves upon which the equipment was mounted. These shelves made good electrical contact with the CFC fuselage. In the main part of the fuselage were metal rails upon which seats were mounted, various electrical power wires and metal tubing.

Waveform of injected current

The aircraft was tested by injecting current pulses into the nose and taking the current off the tail. The injected current (Fig. 8.31) had a double exponential waveform with a time to peak of 6 μs and a decay to half value of 84 μs. Various peak amplitudes were used, ranging from 1 kA to 10 kA. Fig. 8.31 shows a current pulse with a peak of 1 kA. This waveform is nearly identical to current Component A.

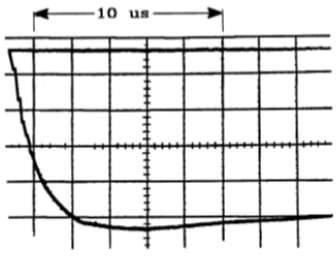

(a) Front of waveform.

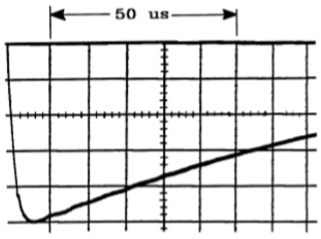

(b) Tail of waveform.

Fig. 8.31 Waveform of current injected into CFC aircraft.

Current on metal structural members

Fig. 8.32(a) is the waveform of the current measured on one of the metal tracks used to hold the seats and Fig. 8.32(b) was measured on an aluminum duct that carried air for heating. If the injected current were 200 kA, there would be 11 kA and 6.2 kA, respectively, on these members. These currents are much higher than would be encountered in a metal aircraft. They flow on these members because they are the ones that have a low resistance. The currents themselves present no hazard to the structures in which they flow, since the current flows for only a short time, but allowances must be made to ensure that the current can flow without any sparking. A remarkable feature of these currents is that they reach their peaks long after the injected current has begun to decay. This delay occurs because the inductive time constants, t, = L/R, are longer for the metal track and air duct than that for the fuselage of the aircraft.

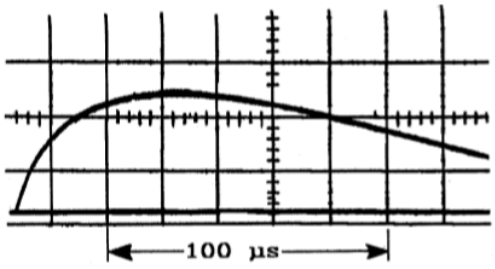

(a) Current on a seat rail.

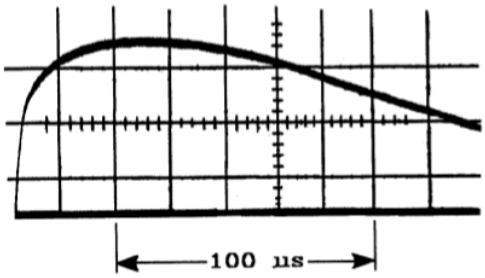

(b) Current on an air tube.

Fig. 8.32 Currents flowing through metal conductors within a CFC aircraft. Note longer time scales than the injected current.

Current on a power bus

Fig. 8.33 shows current on one of 28 V power return wires. If the current injected into the aircraft were 200 kA, there would be 2.04 kA flowing in this wire. This current amplitude is considerably higher than it would be in a

comparable circuit on a metal aircraft. It does not reach its peak until nearly 300 μs, by which time the injected current would have decayed to nearly zero. This long-time constant results from the low DC resistance of the copper power cable, and its relatively high inductance.

The tests showed that high voltages could be produced on power buses. However, with the addition of surge suppression devices between line and ground, bus voltages could be clamped to levels that would not present a hazard to equipment on the bus, but then currents like that shown in Fig. 8.33 would flow through the protective devices. The problem of current flowing through protective devices, and the analysis that must be made to be sure that the devices are properly rated, is discussed in Chapter 17.

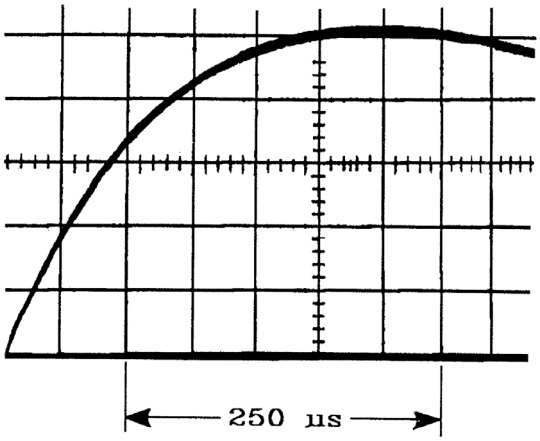

Fig. 8.33 Current flowing on a 28 V power return wire within a CFC aircraft.

Significant conclusions

The most important point revealed by tests on this CFC airframe is that large voltages can be developed on wiring and large currents can flow on metal objects inside such aircraft. Large currents also can flow through protective devices when they act to limit over-voltages, particularly if the protective devices are connected 'line-to-ground' (where 'ground', in this case, is aircraft structure). In other words, the surge impedance of the circuits in CFC aircraft may be very low.

References

8.1 K. S. H. Lee, Editor, "EMP Interaction: Principles, Techniques and Reference Data (A Compleat Concatenation of Technology from The EMP Interaction Notes) EMP Interaction 2-1", *AFWL-TR - 80 - 402,* Air Force Weapons Laboratory (NTMT), Albuquerque, NM, December 1980.

8.2 *Atmospheric Electricity Hazards Protection*, Part I. *Executive Summary*, AFWAL-TR-87-3025, Part I, AFWAL, Wright-Patterson Air Force Base, OH, June 1987.

8.3 *Atmospheric Electricity Hazards Protection, Part II. Assessment*, *Test and Analysis - F-14A, AFWAL-TR-87-3025*, Part II, AFWAL, Wright-Patterson Air Force Base, OH, June 1987.

8.4 *Atmospheric Electricity Hazards Protection, Part III. Assessment, Test and Analysis - ACAP Helicopter, AFWAL-TR-87-3025, Part III*, AFWAL, Wright-Patterson Air Force Base, OH, June 1987.

8.5 *Atmospheric Electricity Hazards Protection, Part IV, Design Guide for Air Vehicles AFWAL-TR-873025, Part IV*, AFWAL, Wright-Patterson Air Force Base, OH, June 1987.

8.6 *Atmospheric Electricity Hazards Protection, Part V. Qualification and Surveillance Tests and Analysis Procedures, AFWAL-TR-87-3025, Part V*, AFWAL, Wright-Patterson Air Force Base, OH, June 1987.

8.7 G. O. Olson and M. M. Simpson, *Atmospheric Electricity Hazards Direct Effects Protection Evaluation, D180 - 27423 - 43*, Flight Dynamics Laboratory, Wright Patterson Air Force Base, OH, September 1985.

8.8 *Aircraft Lightning Environment and Related Test Waveforms*, SAE ARP 5412B, SAE International, Warrendale, PA.

8.9 *Aircraft Lightning Zoning*, SAE ARP 5414B, SAE International, Warrendale, PA.

8.10 *Aircraft Electrical and Electronic System Lightning Protection FAA* AC 20-136B.

8.11 MIL-STD-464D Electromagnetic Effects Requirements for Systems.

8.12 L. C. Walko, *A Test Technique for Measuring Lightning Induced Voltages on Aircraft Electrical Circuits*, NASA Contractor Report NASACR-2348, National Aeronautics and Space Administration, February 1974.

8.13 W. W. Cooley, D. L. Shortess, "Lightning Simulation Test Technique Evaluation", *DOT/FAA/CT-87/38*, US Dept. of Transportation, Federal Aviation Administration, October 1988.

Chapter 9

THE PHYSICS OF INDUCED EFFECTS

9.1 Introduction

This chapter provides an overview of the fundamental concepts of electricity and magnetism that pertain to the induced effects of lightning on electrical and electronic circuits. These concepts lead to a deeper understanding of induced effects and facilitate predictions of the approximate magnitudes of transients that might be induced on wiring in different areas inside an aircraft that is struck by lightning. Important discussions in this chapter include:

a) Characteristics of Materials (§9.3)

b) Voltage and Current Concepts (§9.4)

c) Magnetic Field Effects (§9.5)

d) Electric Field Effects (§9.6).

9.2 Symbols and Units

In Chapters 9 - 18, dimensions are given in SI units with English equivalents in parentheses. The following symbols are used unless otherwise noted in the text.

A = amperes
A = area - m^2
B = Magnetic Flux Density – Webers/m^2 (or Tesla, T)
C = coulombs
C = capacitance - F
c = velocity of light - 3 x 10^8 m/s D = time derivative of E - V/m/sec
E = electric field intensity - V/m
e = 2.714 = the natural logarithm
F = farads
f = frequency - Hz
H = Henries
H = magnetic field intensity - A/m
I = current - A
j = current density - A/m^2
j = imaginary operator $\sqrt{-1}$
L = inductance - H
l = length - m
m = meters
φ = magnetic flux in Webers
R = resistance
r = radius – m
S = Siemens (unit of conductivity)
s = seconds
t = time - s
V = volts
V = voltage - V
v = velocity - m/s
γ = propagation constant
ε_o = permittivity of free space - F/m
ε_r = relative permittivity
η = wave impedance - ohms
μ_o = permeability of free space - H/m
μ_r = relative permeability
Ω = ohms
ω = angular frequency - 2πf
ρ = resistivity - Ω·m
σ = conductivity - S

9.3 Characteristics of Materials

9.3.1 Permittivity and Permeability

Permittivity is the property of a material, which measures the opposition offered against the formation of an electric field. Permeability is a measure of the extent to which a magnetic field may enter a material. So, permittivity relates to electric fields and permeability relates to magnetic fields.

The medium through which these fields couple voltages and currents to electric circuits is nearly always air, which has the permittivity and permeability close to those of space. The permeability, μ_0, and permittivity, ε_0, of free space are defined as:

$$\mu_0 = 4\pi \times 10^{-7} \text{ H/m} \qquad (9.1)$$

$$\varepsilon_0 = 8.854 \times 10^{-12} \text{ F/m} \qquad (9.2)$$

$$\varepsilon_0 = \frac{10^{-9}}{36\pi} \text{ F/m} \qquad (9.3)$$

Three numerical quantities involving μ_o and ε_0, (where ε_0 is as defined by Eq. 9.3) are:

$$\eta_0 = \left[\frac{\mu_0}{\varepsilon_0}\right]^{\frac{1}{2}} = 377 = \text{E/H} \qquad (9.4)$$

This is the plane wave impedance in free space; that is, the ratio between the electric and magnetic field intensities. The units are ohms, but this is not resistance, but rather, simply a ratio of the intensities of the E and H field components of an electromagnetic wave propagating in space. Another expression is,

$$\left[\frac{1}{\mu_0 \varepsilon_0}\right]^{\frac{1}{2}} = 3 \times 10^8 \text{ m/s} \qquad (9.5)$$

Eq. 9.5 defines the velocity with which electromagnetic waves propagate in free space. Useful engineering approximations for this velocity are 0.3 m/ns or 1 ft/ns. Eq. 9.6 defines the plane wave impedance of a coaxial cable.

$$\frac{1}{2\pi}\left[\frac{\mu_0}{\varepsilon_0}\right]^{\frac{1}{2}} = 60 \qquad (9.6)$$

Eq. 9.4 defines the wave impedance for plane waves propagating in free space.

9.3.2 Electromagnetic properties of other materials

Media other than free space have permeabilities, $\mu = \mu_o \mu_r$, where μ_r is a relative permeability factor that makes μ greater than μ_0 by some empirically derived amount. Similarly,

$$\varepsilon = \varepsilon_o \varepsilon_r$$

where ε_r is a relative permittivity factor. The materials dealt with in analysis of lightning effects on aircraft are almost always non-magnetic (aluminum, copper, composites, etc.) and therefore have relative permeabilities of unity. However, the relative *permittivities* of these materials are typically greater than one (see Table 9.1).

9.3.3 Resistivity of Materials

Some resistivities (the reciprocals of conductivities) of typical aircraft materials are given in Table 9.2. Metals are isotropic materials, which means that their resistivities do not depend on the direction of current flow, but composite materials, because they consist of plies bonded together with nonconductive resins, are *non*-isotropic. Thus, the resistivities of composites may depend on the direction of current flow and the current density. The value given in Table 9.2 is an average of resistivities measured in the plane of the reinforcing carbon fibers.

Table 9.1 Relative Permittivity of Some Common Materials

Material	Relative Permittivity
Air	1.0
Glass	3.0
Mica	6.0
Oil	2.3
Paper	1.5 - 4.0
Polycarbonate	2.6
Polyethelene	2.3
Polystyrene	2.7
Porcelain	5.4
Quartz	5.0
Teflon	2.0

Table 9.2 Resistivities of Typical Materials

Material	Resistivity Ω·m	Resistivity relative to copper
Copper	1.68×10^{-8}	1.0
Aluminum	2.69×10^{-8}	1.6
Magnesium	4.46×10^{-8}	2.7
Nickel	10×10^{-8}	6.0
Monel	42×10^{-8}	25
Stainless Steel	70×10^{-8}	42
Inconel	100×10^{-8}	60
Titanium	180×10^{-8}	107
Carbon	780×10^{-8}	464
CFC plain weave, x and y directions	$\sim 6 \times 10^{-5}$	~2 000

9.3.4 Good vs. Bad Conductors

If a unit cube (all sides = 1 m) of material is bounded on opposite faces by electrodes and a voltage is applied between the electrodes, a current will flow through the material. This current consists partly of resistive conduction (Eq. 9.7) and partly of capacitive displacement (Eq. 9.8).

For resistive conduction:

$$i = E\sigma \qquad (9.7)$$

For capacitance conduction:

$$i = j\omega E\varepsilon \qquad (9.8)$$

As used in this book, the term "good" conductor is one in which resistive conduction current predominates and the term "poor" conductor is one in which capacitive displacement current predominates. For oscillating voltages, this distinction may depend on frequency.

9.3.5 Skin Depth

If a voltage is applied across the surface of a conductive material, the current it produces penetrates the material a certain distance. The depth at which the relative current density drops to 1/*e* of the total current is defined as the skin depth, δ. Skin depth appears in the expressions for surface and transfer impedances of conductors, as discussed in §9.4.4 and §9.4.5. Its value is defined as:

$$\delta = \left[\frac{2}{\omega\mu\sigma}\right]^{\frac{1}{2}} \text{ m.} \qquad (9.9)$$

A numerically useful expression is:

$$\delta = \frac{50}{\pi}\left[\frac{1}{\sigma f_{kHz}}\right]^{\frac{1}{2}} \text{ m.} \qquad (9.10)$$

These expressions are in the frequency domain which means that higher frequency constituents of lightning stroke currents will take longer to penetrate the cross-sections of good conductors like copper and aluminum whereas lower frequency constituents will penetrate more deeply into the conductor. In more elementary terms, the fast-rising parts of stroke currents will not flow deeply into good conductors, whereas the longer duration parts of stroke currents will have time to appear deeper into good conductors. More resistive materials, like carbon and carbon fiber composite (CFC) will allow more of the rapidly changing parts of stroke currents to reach more deeply into these materials, and in the case of aircraft, which employ thin (i.e., 1 - 2 mm) skins of CFC, the stroke current density is practically the same throughout the skin cross-sections.

9.4 Voltage and Current Concepts

9.4.1 Lumped Constant Elements

The relationships between voltage and current for lumped constant circuit elements are well known.

Resistance

$$E = j\rho \text{ V/m} \qquad (9.11)$$

And for lumped parameters,

$$V = i \cdot r \quad \text{or, } IR$$

Inductance

$$i = V/j\omega L \quad \text{A} \qquad (9.12)$$

$$i = \frac{1}{L}\int V dt \quad \text{A} \qquad (9.13)$$

$$V = L\frac{di}{dt} \quad \text{V} \qquad (9.14)$$

Capacitance

$$i = j\omega C \qquad (9.15)$$

$$i = CdV \qquad (9.16)$$

$$V = \frac{1}{C}\int i\, dt \qquad (9.17)$$

9.4.2 Voltage as the Line Integral of Potential

The definition of voltage as the line integral of potential is less well appreciated. Voltage and potential are different concepts. For example, the charged sphere shown in

Fig. 9.1 establishes an electric field, E, in the space surrounding it. The potential of the sphere cannot be established independently; it can only be established by defining some separate point as a reference potential. Commonly 'ground' is assigned a reference potential of zero and the potential of the sphere relative to 'ground' is found by integrating the field along the same path, *S*, between the sphere and ground. Hypothetically, this integration could be accomplished experimentally by connecting a perfect voltmeter between the sphere and ground. The deflection of the meter would define the voltage of the sphere, although, to be more precise, one should say that the meter indicates the voltage of the sphere relative to the ground.

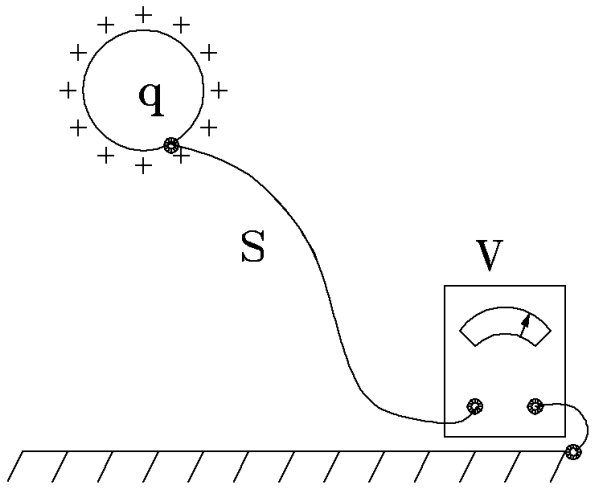

Fig. 9.1 Voltage as total difference of potential.

9.4.3 Importance of the Path of Integration

Does this voltage depend on the path of integration (i.e., the path taken by the leads connecting the voltmeter to the sphere and ground)? This is not a trivial question; it is of fundamental importance for understanding how voltages develop in objects carrying current, such as an aircraft carrying lightning current.

Direct current (DC) and lumped constant elements

For DC conditions, the answer is that the path taken by the measuring leads does not influence the voltage, but for ac or transient conditions this is true only if the measuring leads traverse a region free of electromagnetic fields. As a practical matter, this situation is found only when measuring the voltage across lumped constant elements; those in which the electromagnetic field is entirely enclosed within the element. An example of such an element is the core of a transformer. The ac voltage developed across the winding of a transformer can be measured without regard to where one places the measuring leads because the magnetic field inducing the voltage in the windings is entirely (or nearly entirely) contained in the core of the transformer. The external magnetic field is negligible (ideally zero) and thus no magnetically induced voltage appears in the measuring leads.

Distributed circuits

The effect of the electromagnetic fields on leads measuring voltages across distributed circuits is especially important, since the voltage does depend on the path taken by the measuring leads.

For example, consider Fig. 9.2, in which an alternating current is flowing through a metal cylinder. In an attempt to measure the voltage drop along the cylinder, an experimenter has connected four voltmeters and has observed that all four meters respond differently. They also respond differently from the meter measuring the voltage of the power supply used to circulate the current.

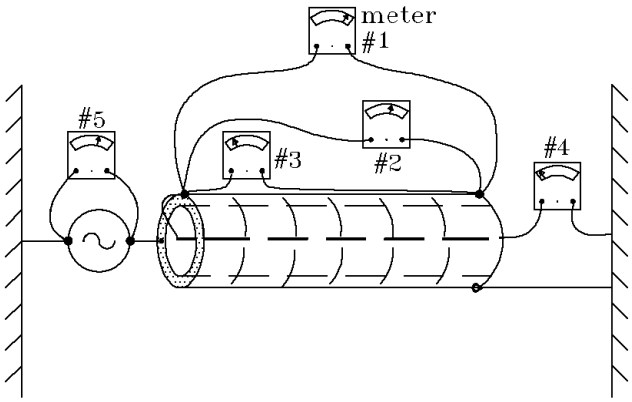

Fig. 9.2 Voltage as a function of path.

Which meter records the correct voltage or are any of them correct? The answer is that all of them respond correctly. Since there is no unique 'voltage drop' associated with the pipe; each of the meters responds according to the particular path along which the electric field is evaluated. The external voltmeters respond primarily to the magnetic field surrounding the cylinder. The leads connected to meter 1 enclose more magnetic flux than the leads connected to meter 2, and consequently there is more voltage induced in the leads of meter 1 than meter 2. (The amount of voltage induced in a loop exposed to a magnetic field is discussed in §9.5.4).

The leads for meter 3, which run flush with the exterior surface of the cylinder, intercept no magnetic flux. As a

result, meter 3 responds only to the voltage produced by the current flowing through the resistance of the cylinder.

Meter 4 responds in yet another way: Since there can be no magnetic field within the cylinder (see §9.5.2) there can be no voltage induced magnetically in the leads. However, the meter does respond to the voltage produced by the flow of current through the resistance of the cylinder, but it still indicates a different voltage from meter 3.

The reason is that meter 3 responds to the density of the current flowing on the outer surface of the cylinder while meter 4 responds to the density of the current flowing on the inner surface of the cylinder. These two current densities are different, as discussed in §9.3.5.

The concept of voltage as the line integral of the electric field around a particular path is of great importance. Anomalies in the voltage on circuit elements can generally be explained by careful attention to the path along which connecting wires are routed.

9.4.4 Internal vs. External Impedances

Consider Fig. 9.3, which shows voltage applied to series circuits composed of a conductor, a return path, and the gap between the two. The applied voltage, V, must be equal to the line integral of all the electric fields around the loop; that is, the sum of E_c, E_r and E_g, where E_c is the surface electric field of the conductor, E_r is the surface electric field of the return path and E_g is the electric field in the space between the conductor and the return path.

In Fig. 9.3(a), E_c is best described as the external surface electric field with external return since the return path is external to the conductor. In Fig. 9.3(b), E_c is best described as the internal surface electric field with internal return.

These electric fields can be related to the conductor current through impedances. Fig. 9.4 represents the internal impedance of the conductor, the internal impedance of the return path and the external impedance of the conductor. (i.e., the impedance of the gap between the conductor and return path). The internal impedances of the conductor and return path are determined by properties of the materials and by the sizes of the conductors. In the frequency domain, these impedances can be separated into real and imaginary components. The real component is a measure of resistance, and the imaginary components is a measure of the internal inductance (i.e., the magnetic flux within the conductor). Under DC conditions, the internal impedance of the conductor is simply its resistance.

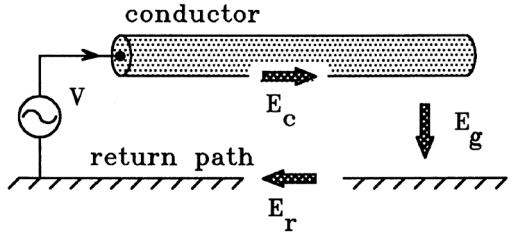

(a) Conductor over a ground plane

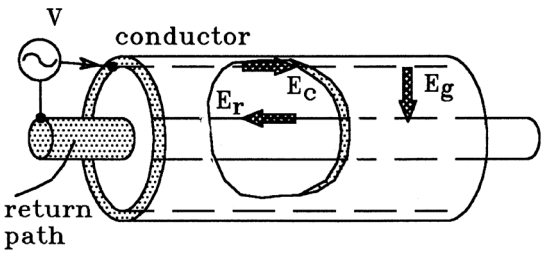

(b) Coaxial conductors

Fig. 9.3 Components of electric field.

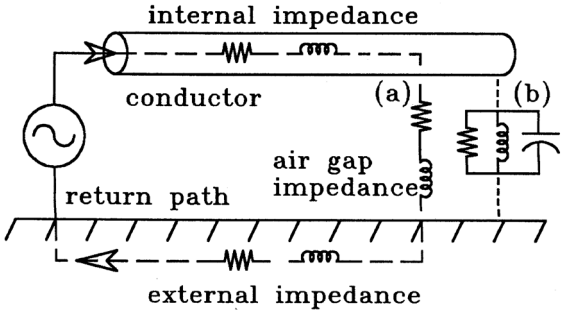

Fig. 9.4 Components of impedance.

The external impedance of a conductor is essentially a property of the space between a conductor and its return path. It is determined by the size and shape of the conductor, the separation from the return path, and of the material (insulation) between the two. With high frequencies, the capacitance of the insulation must be included in the insulation impedance, and it may become more appropriate to treat insulation losses as a shunt resistance. Fig. 9.4(a) shows the external impedance resolved into a series connection of resistance and inductance, while Fig. 9.4(b) shows it resolved into a set of parallel admittances.

9.4.5 Transfer Impedance

The electric fields on the inner and outer surfaces of a hollow tube conductor through which a current is flowing, Fig. 9.5, are generally not the same. The transfer impedance of a hollow tube conductor relates the current to the electric field along the inner surface of the conductor. This is distinct from external impedance, which relates the current to the electric field along the external surface.

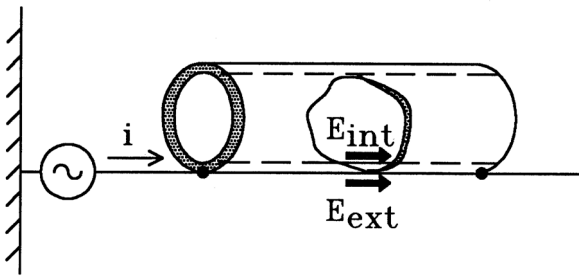

Fig. 9.5 Transfer impedance.

9.5 Magnetic Field Effects

Magnetic field effects are probably the main reason why voltages are induced on aircraft wiring by lightning currents flowing on the aircraft. Situations where shielding proves to be ineffective are usually those where magnetic field effects have been overlooked. Capacitive effects are also important, but those are discussed in §9.6.

9.5.1 Field External to a Conductor

Infinite conductor

In the space surrounding a conductor of infinite length, Fig. 9.6, the magnetic field is:

$$H = \frac{I}{2\pi r} \quad \text{A/m} \qquad (9.18)$$

In Eq. 9.18, the return path of the current is assumed to be so far away that it does not contribute to the magnetic field.

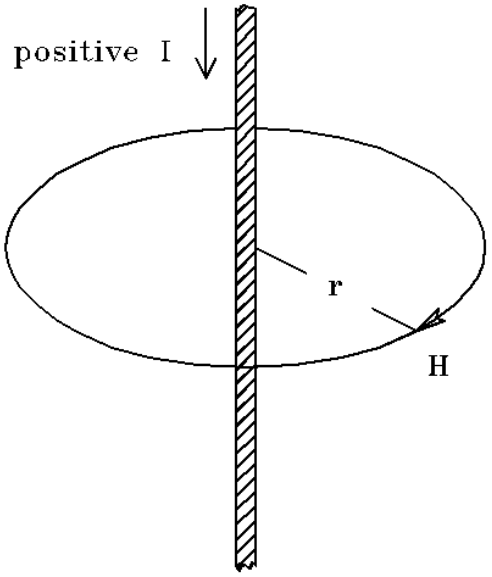

Fig. 9.6 Magnetic field of an infinite conductor.

Isolated filament

For an isolated filament (or circular conductor) carrying a current, I, over its entire length, l, as shown in Fig. 9.7, the flux density at a point, P, a distance, r, from the filament (or the axis of the conductor) is determined by Eq. 9.19.

$$B = \mu H = 4\pi \times 10^{-7} \frac{I}{4\pi r}(\sin\alpha + \sin\beta) \text{ Webers/m}^2 \qquad (9.19)$$

The return path for the current is assumed to be so far beyond r_3 that it does not influence the magnetic field.

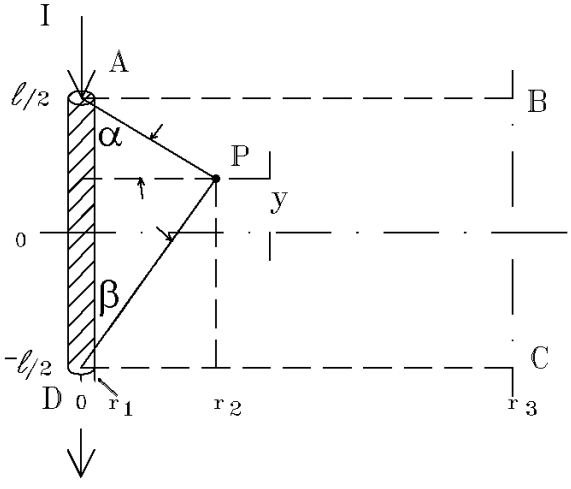

Fig. 9.7 Magnetic field of a finite conductor.

Dipole

For the limiting case of the short dipole represented by Fig. 9.8, the magnetic field intensity, H, is determined by Eq. 9.20.

$$H = \frac{Il}{4\pi} \cdot \sin\alpha \quad \text{A/m} \qquad (9.20)$$

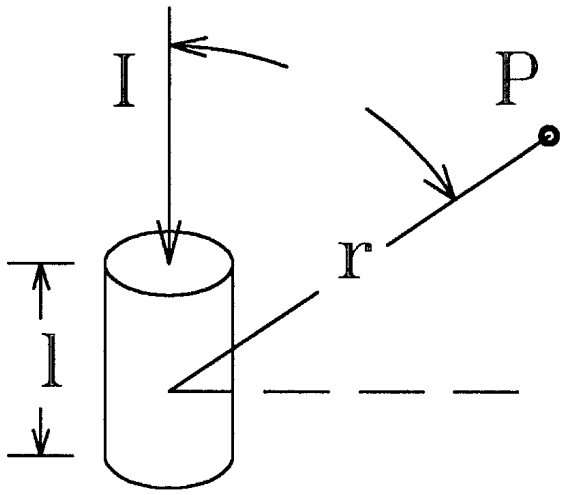

Fig. 9.8 Magnetic field of a short dipole.

The direction of the flux around a filament or a cylinder is given by the 'right hand rule' illustrated in Fig. 9.9. For all high frequency conditions, the magnetic flux lines are parallel to the surfaces of conductors, even if the conductors are of irregular shape. The magnitude of the field intensity is equal to the local surface current density, measured in amperes/meter. For circular conductors, the current density is uniform and equal to the total current divided by the peripheral distance around the conductor. For conductors of irregular shape, the current density depends on the local radius of curvature. This is discussed in Chapter 10.

The magnetic field external to a current-carrying tube is equivalent to the magnetic field that would surround an infinitesimal filament, carrying the same current, at the tube's axis.

9.5.2 Magnetic Fields within Hollow Conductors

If there are several conductors, the total magnetic field intensity is the sum of that produced by the individual conductors. If two parallel conductors each carry an equal current in the same direction, Fig. 9.9, the fields produced by the currents cancel along a line equidistant from the two conductors. The fields at other points do not cancel, but their sum is lower than in the space outside the conductors. If three equally spaced, parallel conductors carry equal currents, the field is reduced even more in the intervening space between the conductors. The more conductors of parallel current are arranged in a cylindrical configuration, the more magnetic field cancellation occurs within the cylinder. If an infinite number of parallel conductors are arranged in this configuration so that they merge, forming a solid tube, the magnetic field due to currents on the tube becomes zero everywhere inside the tube.

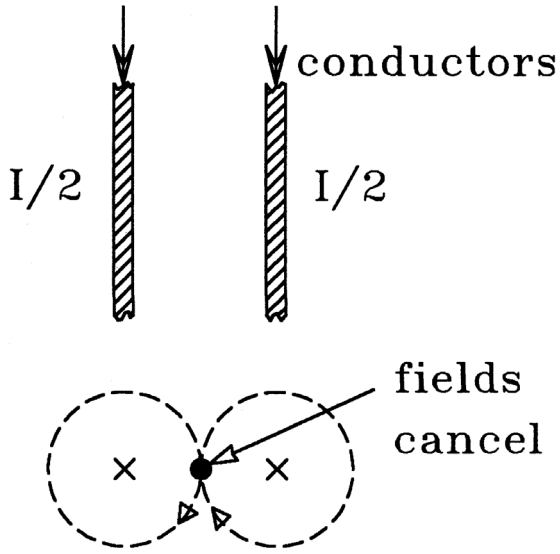

Fig. 9.9 Magnetic field between two conductors.

9.5.3 Inductance

Self-inductance

Self-inductance, L_{11}, is defined (see Eq. 9.21) as the amount of magnetic flux, φ_1, (in Webers/Ampere) that would be established around a conductor by a given amount of current, I_1, flowing through the same conductor.

$$L_{11} = \frac{\varphi_1}{I_1} \quad \text{Webers} \qquad (9.21)$$

Eq. 9.22 gives the self-inductive voltage on a conductor of self-inductance L, carrying a current that changes at a rate di/dt:

$$V_L = L\frac{di}{dt} \quad \text{Volts} \qquad (9.22)$$

Mutual inductance

The mutual inductance, M_{12}, of a conductor (conductor 1) with respect to another conductor (conductor 2) is defined as the amount of magnetic flux, φ_{12}, that would be established outside the space between both conductors per unit inducing current, I_2, flowing through conductor 2 (see Eq. 9.23). Of course, there can be many conductors of inducing current and many conductors of induced current in a given system.

$$M_{12} = \frac{\varphi_{12}}{I_2} \quad \text{Webers} \qquad (9.23)$$

Eq. 9.24 gives the voltage, V_1, induced in conductor 1 because of a changing current flowing through nearby conductor 2:

$$V_1 = -M_{12}\frac{di_2}{dt} \quad \text{Volts} \qquad (9.24)$$

Isolated linear conductors

Determining the inductance of a conductor requires integrating the magnetic field intensity over an area to determine the total flux set up by current in the conductor. An elementary case is shown in Fig. 9.6, which represents an isolated conductor of infinite length.

The return current path is assumed to be sufficiently far away that the magnetic field produced by the return current is negligible compared to that of the conductor under consideration. (For DC conditions this implies that the return path is at infinity).

The self-inductance is determined by the magnetic flux contained by the area A-B-C-D outside of a conductor of length l. Integrating Eq. 9.20 first over the limits from -l/2 to l/2 and then integrating the result over the limits from r_1 to r_3 gives:

$$\varphi = \frac{\mu I}{2\pi} l \left[\ln\left\{ \frac{1}{r} + \sqrt{1 + \frac{l^2}{r^2}} \right\} - \sqrt{1 + \frac{r^2}{l^2}} + \frac{r}{l} \right] \quad \text{Webers (9.25)}$$

from which the inductance can be determined using Eq. 9.21.

If there were two conductors of length l, as in Fig. 9.10, the mutual inductance between conductors 1 and 2 is determined by the flux between the limits r_2 and r_3; (the shaded area). The form of the equation is the same as that of Eq. 9.25; but the limits are r_3 and r_2, instead of r_2 and r_1. Note that the radii of the conductors are not involved, only their locations. This implies that mutual inductance can be defined for filaments as well as conductors. How one evaluates the flux, and thus the self or mutual inductance, depends on the relative values of r_2 and r_3:

Case 1: l » r_3: Under DC conditions, the magnetic field extends to infinity and so Eq. 9.25 must be evaluated over the limits r_3 and r_1. When $r_3 = \infty$, the sum of all the terms involving r_3 goes to zero and thus the self-inductance of conductor 1 becomes:

$$L_{11} = 2 \times 10^{-7} l \left[\ln\left\{ \frac{1}{r_i} + \sqrt{1 + \frac{l^2}{r_i^2}} \right\} - \sqrt{1 + \frac{r_i^2}{l^2}} + \frac{r_i}{l} \right] \text{H} \quad (9.26)$$

and the mutual inductance between conductors 1 and 2 is:

$$L_{12} = 2 \times 10^{-7} l \left[\ln\left\{ \frac{1}{r_2} + \sqrt{1 + \frac{l^2}{r_2^2}} \right\} - \sqrt{1 + \frac{r_2^2}{l^2}} + \frac{r_2}{l} \right] \text{H} \quad (9.27)$$

Case 2: r_3 » l and l » r_2 and l » r_1: For long conductors under DC conditions, the inductances are:

$$L_{11} = 2 \times 10^{-7} l \left[\ln\left\{ \frac{2l}{r_1} \right\} - 1 \right] \quad \text{H} \qquad (9.28)$$

$$L_{12} = 2 \times 10^{-7} l \left[\ln\left\{ \frac{2l}{r_2} \right\} - 1 \right] \quad \text{H} \qquad (9.29)$$

Note that these inductances are not directly proportional to the lengths of the conductors.

Case 3: l » r_3 and l » r_2 and l » r_1: Where the two conductors are parallel and of equal length:

$$L_{11} = 2 \times 10^{-7} l \left[\ln\frac{r_3}{r_1} \right] \quad \text{H} \qquad (9.30)$$

$$L_{12} = 2 \times 10^{-7} l \left[\ln\frac{r_3}{r_2} \right] \quad \text{H} \qquad (9.31)$$

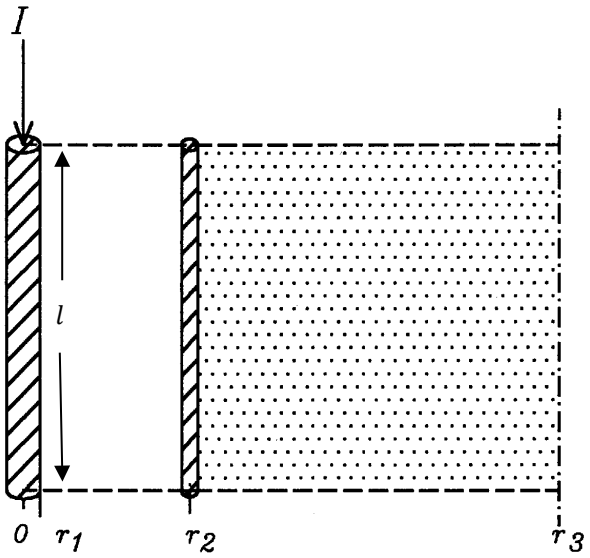

Fig. 9.10 Flux involved in mutual inductance.

The mutual inductance between two filaments of any arbitrary orientation is calculable and, while the expressions are too long to include here, they can be found in the literature [9.1 - 9.6].

While the inductance of an isolated conductor is an important concept, it must be used with care, since an isolated conductor cannot carry current. Current can only flow through a conductor that is part of a larger circuit. Thus, the inductance of an isolated conductor should be viewed as part of a larger problem, in which the self and mutual inductances must be considered together.

The formulae above yield only external (or high frequency) inductances. At low frequencies, magnetic fields also occur within conductors. This subject is treated in a later section.

Time dependence of inductance

Under transient conditions, one must also consider the retardation effects associated with the finite velocity of propagation of an electromagnetic field. If a current is suddenly applied to a conductor, the field does not initially extend to infinity. Instead, it propagates away from the conductor at the speed of light. Therefore, the total amount of magnetic flux established in the space around a conductor varies with time, becoming larger as the fields propagate farther from the conductor. The implication is that the inductance of a conductor is less for short duration transients (or high frequencies) than for long duration transients (or low frequencies). In an engineering sense, this effect is more important for long conductors than for short conductors.

For example, in 1 μs, a magnetic field propagates 300 m. Therefore, for a conductor one meter long, a 1 μs current pulse can be regarded as 'DC conditions". This is not the case when the same 1 μs pulse is applied on a conductor 1 000 meters long. For aircraft analyses, frequency dependence of external inductance due to this retardation effect does not normally need to be considered, since the various conductors on an airplane are, of necessity, close together.

Coaxial conductors

Usually, inductance is evaluated for a 'go-return' circuit. In a coaxial system, the center conductor (the 'go' conductor) is surrounded by a concentric 'return' conductor, Fig. 9.11(a), and the inductance is based on the magnetic field intensity between the limits r_1 and r_2. The current flowing on the cylindrical return path does not need to be considered, since it does not produce any internal magnetic field (see §9.5.2).

Since the lengths of practical conductors are long compared to their diameters; the magnetic fields may be evaluated using Eq. 9.32.

$$L_{11} = 2 \times 10^{-7}\, l \left[\ln \frac{r_2}{r_1}\right] \quad \text{H/m} \qquad (9.32)$$

For all practical cases, there are no end effects, and the inductance is directly proportional to length l.

Conductor pairs

Two parallel conductors can also be connected as a 'go-return' pair. The most common configuration is that in which current goes on one conductor and returns on the other, Fig. 9.11(a). The configuration shown in Fig. 9.11(b) is impractical for straight conductors, since the magnetic field of the connecting leads would influence the result, but it is practical for conductors bent into a circle, since that is the geometry of a helical coil.

The inductance of a pair of conductors involves four inductances: the two self-inductances and the two mutual inductances:

$$L_\tau = (L_{11} \pm L_{12}) + (L_{22} \pm L_{21}) \quad \text{H} \qquad (9.33)$$

If the conductors have about the same diameter, L_{12} and L_{21} are nearly equal, even when the spacing of the conductors is close. Also, L_{11} and L_{22} are equal if the diameters are the same. Thus:

$$L_\tau = 2(L_{11} \pm L_{12}) \quad \text{H} \qquad (9.34)$$

Evaluating the individual inductances, Eq. 9.34, gives:

$$L_\tau = 4 \times 10^{-7} l \left[\left(\ln\left(\frac{2l}{r}\right) - 1 \right) \pm \left\{ \ln\left(\frac{2l}{S}\right) - 1 \right\} \right] \text{ H} \quad (9.35)$$

The signs of the mutual inductance terms, L_{12} and L_{21}, depend on the way the conductors are connected at their ends (see Fig. 9.11). For the case illustrated in Fig. 9.11(a), the sign for the mutual terms would be negative. For the case illustrated in Fig. 9.11(b), the signs would be positive.

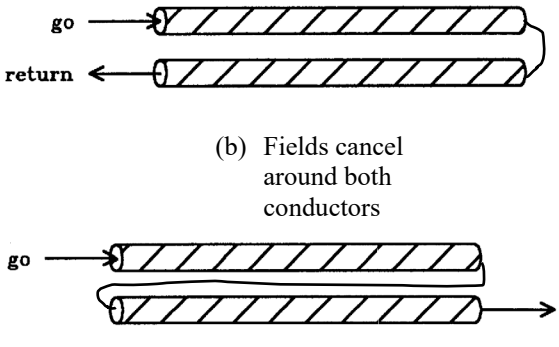

(b) Fields cancel around both conductors

(a) Fields add around both conductors

Fig. 9.11 Conductor pairs.

For the case illustrated in Fig. 9.11(a), the total inductance becomes:

$$L_\tau = 4 \times 10^{-7} \left[\ln\left\{ \frac{4l^2}{rS} \right\} - 2 \right] \text{ H/m} \quad (9.36)$$

$$L_\tau = 4 \times 10^{-7} \ln\left\{ \frac{S}{r} \right\} \text{ H/m} \quad (9.37)$$

Conductors over a ground plane

If current flows along a conductor and returns through a perfectly conducting ground plane, as illustrated in Fig. 9.12, the current in the ground plane becomes distributed so that it is most dense directly underneath the conductor and progressively less dense at points farther from the conductor. The effect is as if the return current were flowing on an image conductor underneath the ground plane. Therefore, the self-inductance of a conductor over a perfect ground plane can be regarded as the same as that of an imaginary pair of conductors with the ground plane lying in the plane of symmetry between them. Taking the individual inductances in Eqs. 9.36 and 9.37 and evaluating for the case where 1 » h gives:

$$L_\tau = 2 \times 10^{-7} \ln\left(\frac{2h}{r}\right) \text{ H/m} \quad (9.38)$$

This is the expression that is most commonly used in assessments of lightning-induced transients in aircraft wiring. The radius, r, is that of a single wire, or of a bundle of wires if the current in a cable bundle is being computed. Only one pair of inductances is involved; the image conductor does not actually carry current, and the concept of a perfect ground plane implies that it has no internal inductance of its own.

The ground plane shown in Fig. 9.12 is the airframe surface that is nearest to the individual wire or cable that is being analyzed.

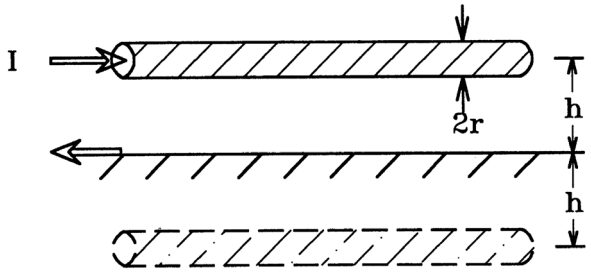

Fig. 9.12 Conductor over a ground plane.

Proximity effects

The formulas, above, for conductor pairs and conductors over ground planes, are only approximations, since they assume that the current is uniformly distributed over the surfaces of the conductors. This assumption becomes less accurate the closer the conductors are to each-other. The precise formulas involve hyperbolic functions. For example, the exact equation for the inductance of a conductor over a ground plane is [9.2, 9.7]:

$$L = \frac{\mu_0}{2\pi} \operatorname{arc\,cosh}\left[\frac{h}{r}\right] \text{ H/m} \quad (9.39)$$

The hyperbolic function in Eq. 9.39 can be written as:

$$L = \frac{\mu_0}{2\pi} \ln\left[\frac{h}{r} + \sqrt{\left(\frac{h}{r}\right)^2 + 1}\right] \text{ H/m} \quad (9.40)$$

Therefore, exact expressions for inductance can be written by substituting:

$$\frac{h}{r}+\sqrt{\left(\frac{h}{r}\right)^2+1} \quad \text{for } \frac{2h}{r} \qquad (9.41)$$

into Eq. 9.38.

Usually, the error that results from ignoring proximity effects is small. Even when h = d, Eq. 9.38 predicts an inductance only 5 % higher than that predicted by the exact formula, Eq. 9.39. These proximity effects do not arise on isolated or coaxial conductors.

Internal inductance of conductors

The formulas in §9.5.3 relate only to the fields external to the conductors. They are therefore valid only for high frequencies, at which skin effects confine current to the surfaces of conductors. At lower frequencies, current penetrates the conductors and magnetic fields are established within the conductor (see Fig. 9.13). The maximum internal flux for a given current occurs in solid conductors under conditions in which the current density is uniform. Under such conditions, the flux density varies directly with distance from the center of the conductor. The total flux within the conductor is:

$$\varphi = \frac{u_0\mu_r}{8\pi} I \quad \text{Webers} \qquad (9.42)$$

and the internal inductance is:

$$L_{int} = \frac{\varphi}{I} = \frac{\mu\times10^{-7}}{2} = 0.05 \quad \mu H/m \qquad (9.43)$$

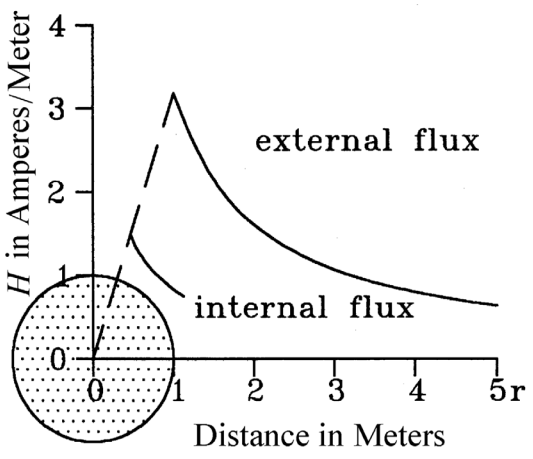

Fig. 9.13 Internal and external magnetic field density.

While the internal inductance is generally small compared to the external inductance, it is intimately linked with the transient resistance of conductors. The transient resistance and internal inductances of conducting bodies are of such importance in analyzing the penetration of lightning currents into aircraft that the subject of internal impedance is discussed in much more detail in Chapter 10.

For assessments of induced effects in aircraft electrical circuits, the self-inductance of typical circuits can be represented by Eq. 9.38 and the radius, r, is that of a single wire, or of a bundle of wires, depending on whether the induced current in a single wire, or in a bundle of wires, is being considered.

9.5.4 Magnetic Induction of Voltage and Current

Magnetically induced voltages and currents are probably the most common induced effects of lightning.

Open circuit voltage

A changing magnetic field passing through an open-circuited loop (Fig. 9.14) induces a voltage:

$$V = -\frac{d\varphi}{dt} \qquad (9.44)$$

where φ = μHA (H being the magnetic field intensity and A being the loop area). This voltage appears across the opening in the loop and has a waveform proportional to the derivative of the flux.

Short circuit current

If the loop is short-circuited, the voltage in Eq. 9.44 is applied across the impedance of the loop, inducing a circulating current, I:

$$I = \frac{1}{L}\int e\,dt = e\frac{\mu HA}{L} \qquad (9.45)$$

The waveform of this current resembles that of the incident magnetic field but differs from the open circuit voltage. This point is important: magnetically induced currents generally have longer rise and decay times than those of magnetically induced voltages. The reason that the inductance is the factor that limits the current is because the voltage, being a derivative, is not present for sufficient time to drive the current to a level that would be limited by the circuit resistance.

Field penetration of a loop

If a current loop enclosing a changing magnetic field had only inductance and no resistance, the current would have the same waveform as the incident magnetic field and would set up a magnetic field of its own, of equal amplitude and opposite polarity to the incident field. Therefore, a magnetic field cannot penetrate an ideal, short-circuited loop. If the loop had resistance, Fig. 9.14, the current would decay with a time constant proportional to L/R, and the magnetic field would gradually penetrate the loop.

Field penetration of a surface

A conductive surface, Fig. 9.15, may be viewed as an infinite assembly of conducting loops. A magnetic field line that attempts to penetrate the surface induces a circulating current (eddy current) that acts to oppose the penetrating field. The consequence is that, under high frequency conditions, a magnetic field incident on a surface can have only a tangential component. Any radial component is cancelled by an induced circulating current. Only as the circulating currents die away because of resistance can the magnetic field penetrate the surface. It is this property of eddy currents that allows non-magnetic materials to provide substantial amounts of shielding against transient magnetic fields. This subject is explored more fully in Chapter 15.

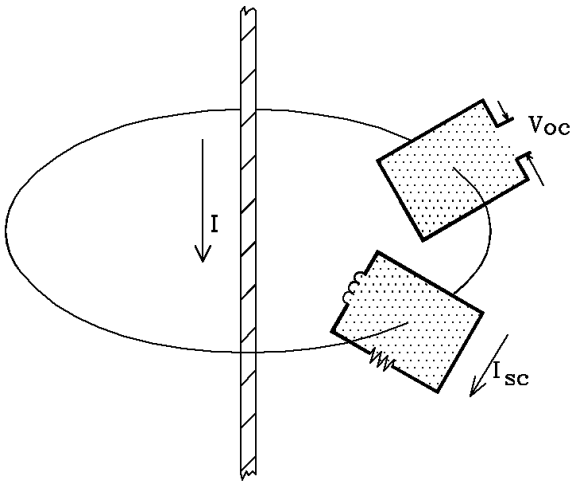

Fig. 9.14 Magnetic induction of voltage and current.

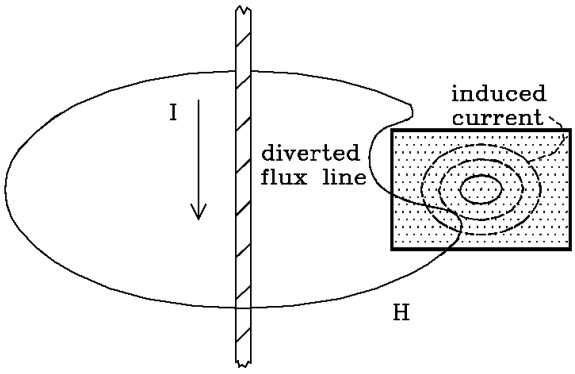

Fig. 9.15 Eddy currents in a conducting sheet.

9.6 Electric Field Effects

Changing electric fields also produce currents and voltages, particularly on unshielded conductors.

9.6.1 Evaluation of Capacitance

Point charge: In the space surrounding a charged point, an electric field, *E*, is established such that:

$$E = \frac{Q}{4\pi\varepsilon_0 r^2} \text{ V/m} \qquad (9.46)$$

This field is directed radially away from the point when *Q* is positive and is directed radially toward the point when *Q* is negative.

Isolated sphere (in air)

If the charge resides on a sphere of radius r, the electric field outside the sphere is as if all the charge were concentrated at the sphere's center. Integrating the electric field from the sphere to a remote point at which the electric field is negligible (as at infinity) gives the total voltage on the sphere:

$$V = \frac{Q}{4\pi\varepsilon_0} \cdot \frac{1}{r} \text{ volts} \qquad (9.47)$$

Capacitance is defined as:

$$C = \frac{Q}{V} \text{ F} \qquad (9.48)$$

By extending r_2 to infinity, the capacitance of an isolated sphere can be defined as:

$$C = 4\pi\varepsilon_0 r = \frac{10^{-9}}{9} r \quad \text{F} \qquad (9.49)$$

Similarly, the capacitance of an aircraft can be approximated by defining an equivalent sphere. For example, an aircraft with a surface area comparable to that of a sphere of radius 5 m would have a capacitance of about 556 pF.

Electric fields are different from magnetic fields in that an isolated object may have a charge and hence a finite capacitance, regardless of dimensions. Attempting to evaluate the inductance of an isolated conductor leads to conceptual and mathematical difficulties, as noted in §9.7, but no such problems arise with determining the capacitance of an isolated body.

Concentric Spheres

The capacitance between two concentric spheres, where the outer sphere is the 'ground' reference, Fig. 9.16, is calculated by integrating the electric field over the distance r_1 to r_2:

$$C = 4\pi\varepsilon_0 \left[\frac{1}{r_1} - \frac{1}{r_2}\right] \quad \text{F} \qquad (9.50)$$

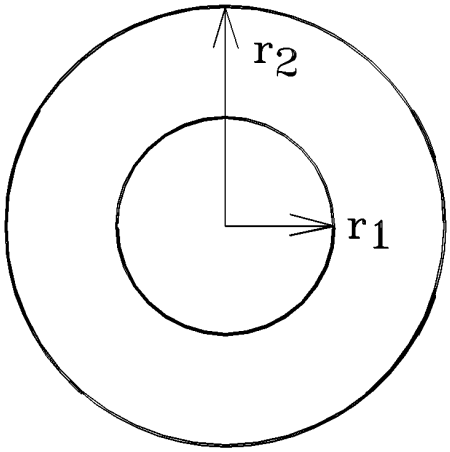

Fig. 9.16 Concentric spheres.

Sphere over a Ground Plane

If the charged sphere is located over a ground plane, a charge is induced in the ground and the effect is as if there were a sphere of equal and opposite charge below the ground, Fig. 9.17. The fields of the two charges combine to give the total electric field.

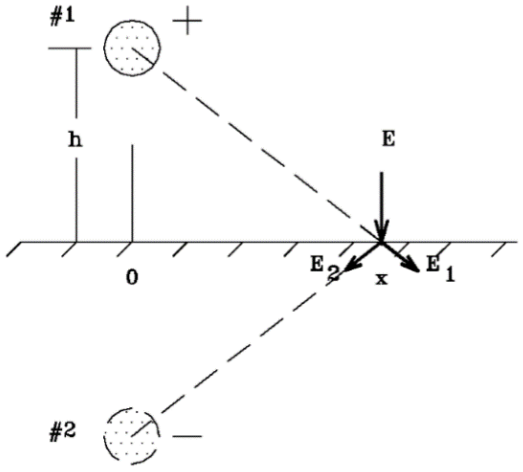

Fig. 9.17 Sphere over a ground plane showing imaginary sphere with equal charge of opposite polarity.

At the ground plane the horizontal components cancel, and the net electric field is oriented at right angles to the ground plane. Evaluating the electric field from the sphere to the ground plane gives the voltage between the sphere and the ground plane and hence the capacitance to ground, Fig. 9.18.

$$C = \frac{10^{-9}}{9\left[\frac{1}{(r-1)(r-2h)}\right]} \quad \text{F} \qquad (9.51)$$

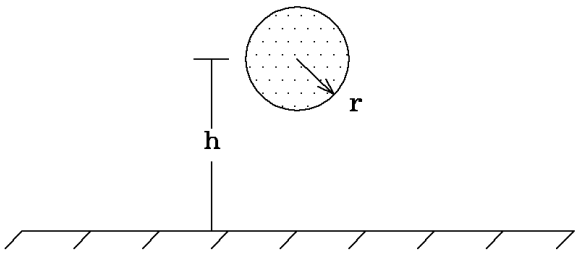

Fig 9.18 Sphere over a ground plane.

Isolated conductor

A charged conductor of infinite length and having a linear charge density of q_o coulombs per meter, may be regarded as an infinite number of charged points on a line. A rod of finite length, Fig. 9.19, presents mathematical difficulties, however, because the electric field intensity at its ends becomes infinite. These difficulties are overcome by approximating the rod as an ellipsoid, having major and minor axes *2a* and *2b*, respectively, with $c = \sqrt{a^2 + b^2}$.

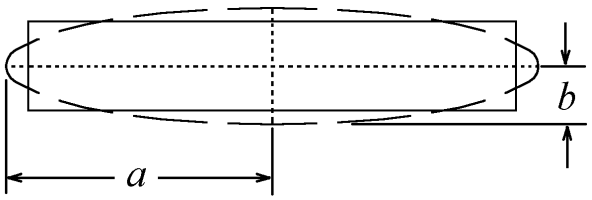

Fig. 9.19 Isolated conductor.

The capacitance is then:

$$C = 4\pi\varepsilon a = \frac{\frac{c}{a}}{\arctan\frac{c}{a}} \quad F \tag{9.52}$$

or

$$C = \frac{222c}{\ln\frac{1-\frac{c}{a}}{1+\frac{c}{a}}} \quad pF \tag{9.53}$$

Coaxial conductors

The electric field, as given by Eq. 9.50, between r_1 and r_2 gives the capacitance:

$$C = \frac{4\pi\varepsilon_0\varepsilon_r}{\ln(r_2/r_1)}r \quad F/m \tag{9.54}$$

or

$$C = \frac{55.56}{\ln(r_2/r_1)}r \quad pF/m \tag{9.55}$$

Conductor over a ground plane

The electric field is found by taking the vector sum of two fields: one due to the conductor and one due to its image in the ground plane. At the ground plane, Fig. 9.17, and for a conductor in air, the field is perpendicular to the ground plane and has a magnitude:

$$E = \frac{q_0}{\pi\varepsilon_0}\cdot\frac{h}{h^2+x^2} \quad V/m \tag{9.56}$$

From which the capacitance is:

$$C = \frac{2\pi\varepsilon_0}{\ln\left(\frac{2h}{r}\right)}r \quad F/m \tag{9.57}$$

Thus

$$C = \frac{55.6}{\ln\left(\frac{2h}{r}\right)} \quad pF/m \tag{9.58}$$

Symbolic similarities between inductance and capacitance

The above expressions show a good deal of similarity between the expressions for inductance and capacitance. This merely reflects the fact that the geometrical considerations that determine inductance also determine capacitance. In fact, it can be shown that:

$$LC = \mu\varepsilon \tag{9.59}$$

and that, if one knows one of the quantities (inductance or capacitance) of a structure, one can determine the other. In a medium of homogenous electric permittivity, one can determine the inductance of a structure or set of conductors simply by measuring the capacitances involved. In practical conductor systems, involving insulated conductors, the total dielectric space between conductors is not homogeneous.

9.6.2 Displacement Currents

If a capacitor is connected to a changing voltage, the current that flows through the capacitor is proportional to the derivative of the voltage:

$$i = Ej\omega C \quad A \tag{9.60}$$

or

$$i = C\frac{dE}{dt} \quad A \tag{9.61}$$

These currents, known as *displacement currents*, flow as the result of a changing electric field. Fig. 9.20, shows a surface exposed to a changing electric field that is assumed to be oriented perpendicular to the surface. A portion of the surface has been isolated and connected to the rest of the surface through a conductor. The current through that conductor would be:

$$i = \varepsilon_0 A\frac{dEa}{dt} \quad A \tag{9.62}$$

where

A = area of the surface - m^2

E_a = actual electric field intensity - V/m

E_u = undisturbed electric field intensity

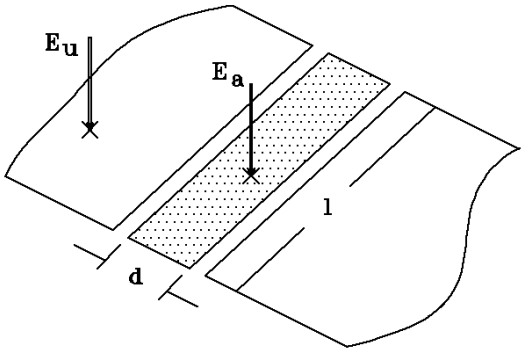

(a) Isometric view

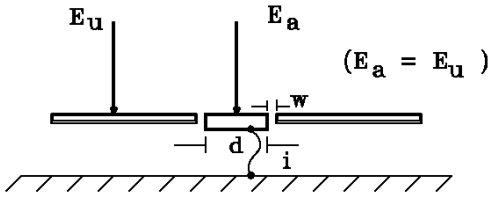

(b) End view

Fig. 9.20 A flush-mounted insulated surface exposed to an electric field.

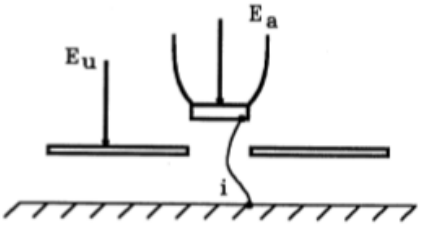

(a) Flat raised surface.

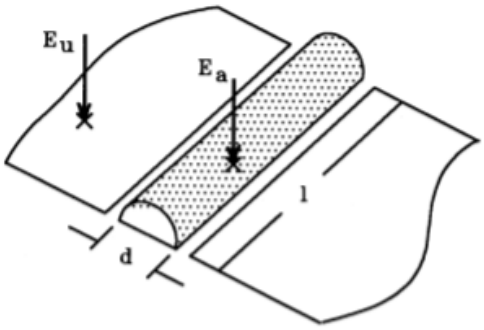

(b) Embedded hemicylinder.

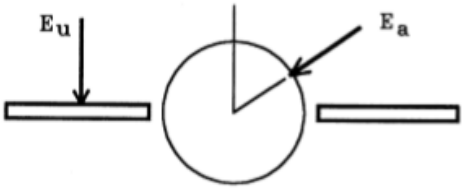

(b) End view.

Fig. 9.21 A raised insulated surface exposed to an electric field.

If the isolated surface is flat and flush with the surrounding surface, as shown in Fig. 9.20, the impinging electric field remains uniform over all the surfaces. However, if the isolated section is raised above the surrounding surface, as in Fig. 9.21, the electric field becomes concentrated around the isolated surface, so that its intensity is higher than that of the undisturbed electric field, E_u. Alternatively, one could say that the elevated surface has a capture area larger than its physically projected area, A. Displacement currents are also discussed in Chapter 14.

9.7 Analytical Descriptions of Waveforms

This section will discuss a few miscellaneous points about waveforms used for test and analysis of induced effects.

Difference of Two Exponentials

A waveform commonly used to represent unipolar induced current transients for analysis of effects is the double exponential:

$$I = I_1\left(\varepsilon^{-\alpha t} - \varepsilon^{-\beta t}\right) \qquad (9.63)$$

Reciprocal of the Sum of Two Exponentials

A characteristic of the double exponential wave is that it has a discontinuity at its highest rate of change at t = 0. Discontinuous waves do not exist in nature and are sometimes undesirable for numerical simulation because they stimulate spurious responses.

An alternative waveform [9.8] that avoids the discontinuity at $t = 0$, and thus deserves more attention, is plotted in Fig. 9.22.

The constant β governs the rise of the wave while α governs the decay but determining the values of these constants for a particular waveform is not straightforward.

$$I = \frac{I1}{\varepsilon^{-\beta(t-t_1)}+\varepsilon^{+\alpha(t-t_1)}} \qquad (9.64)$$

The rise time from (10% - 90%) would be 4.4/β and the time to decay (to 10%) would be $t_o + 2.3/\alpha$. This waveform is shown in Fig. 9.22, using the same values of α, β, and I_1 and with t_o = 10 μs.

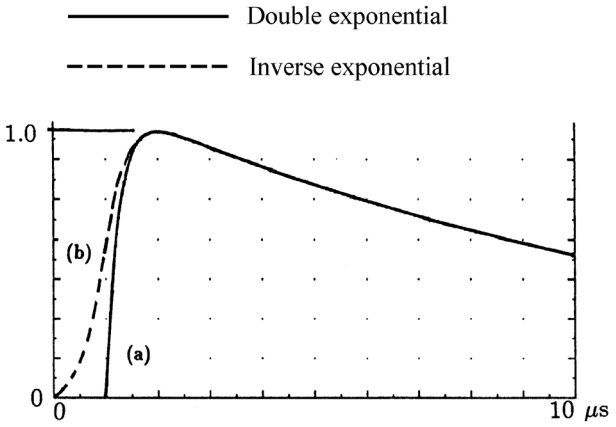

Fig.9.22 Exponential waveforms.

Decaying Sinusoids

Transients induced by lightning frequently are oscillatory (Fig. 9.23), with an exponential decay. An idealized decaying sinusoid is:

$$I = I_1 \sin(\omega t)\varepsilon^{-\alpha t} \qquad (9.65)$$

where

$$\omega = 2\pi f \qquad (9.66)$$

$$\alpha = \frac{\pi f}{Q} \qquad (9.67)$$

The damping factor, Q, determines how fast the wave decays. Typical damping factors called for by specifications range from 6 to 24. Fig. 9.23 shows a 1 MHz oscillatory wave with a damping factor of 10.

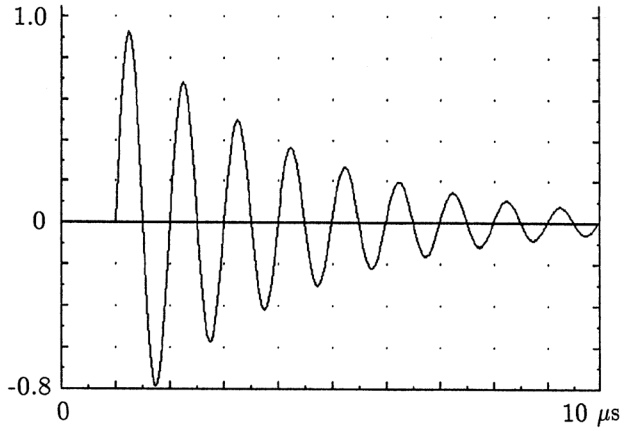

Fig. 9.23 Damped oscillatory waveform.

References

9.1 Grover, Inductance Calculations, Chapter 7.

9.2 F. A. Fisher, *Analysis and Calculations of Lightning Interactions with Aircraft Electrical Circuits*, AFFDL-TR-78-106, Air Force Flight Dynamics Laboratory, Wright Patterson Air Force Base, Ohio, 45433, pp. 196-201.

9.3 Grover, Inductance Calculations, Chapters 8, 13 and 16.

9.4 Transmission Line Reference Book, 345 kV and Above/Second Edition, Electric Power Research Institute, Palo Alto, CA, 1982.

9.5 E. R. Vance, *Coupling to Shielded Cables*, Chapter 3, John Wiley and Sons, New York, 1978.

9.6 J. R. Carson, *Wave Propagation in Overhead Wires with Ground Return*, Bell Syst. Tech. J., Vol. 5, 1926, pp. 539-554. Note that Carson's equations are also discussed in almost any elementary textbook on electrical power theory.

9.7 F. W. Grover, Inductance Calculations, Working Formulas and Tables, Dover, New York, 1962 or D. Van Nostrand, New York, 1946, Chapter 3.

9.8 A. Deri, G. Tevan, A. Semlyn and A. Castanheira, *The Complex Ground Plane, a Simplified Model for Homogeneous and Multi-layer Earth Return*, IEEE Transactions on Power Apparatus and Systems, Vol. PAS-100, No. 8, August 1981, pp. 3686-3693.

Chapter 10

THE EXTERNAL ELECTROMAGNETIC FIELD ENVIRONMENT

10.1 Introduction

To estimate the lightning induced transients in an aircraft, one must first determine the external electromagnetic fields. The internal environment is, after all, determined by the external environment and the degree to which the external environment couples to the inside of the aircraft.

The purpose of this chapter is to outline methods of determining the external environment. Elementary factors governing that environment will be discussed first, then various methods of calculation will be presented, ranging from simple approximations to more specialized techniques applicable to unique situations.

Detailed calculations are complex because an aircraft is a complex electromagnetic object. Its geometry is complex, requiring three-dimensional (3D) solutions. Also, its materials are varied, consisting of highly conducting metals (such as aluminum and copper), more resistive metals (such as titanium), carbon fiber composites (that are three orders of magnitude less conductive than metals), and insulators (such as glass, Kevlar, fiberglass, and plastic).

Finally, the lightning environment itself is complex. It is both a high frequency and low frequency phenomenon. Time scales on the order of tens of nanoseconds must be resolved, while some of the currents may persist for as long as a second. Also, different aspects of the lightning environment dominate at different times during the event. For example, during the initial lightning leader attachment phase, the electric field and its rate of change are of primary interest and, at later times, the current amplitude is of primary interest. For some periods, both are important. The interaction of the aircraft with the lightning channel is also a complex phenomenon, some features of which may not yet be well understood.

Fortunately, a mathematically rigorous treatment is not always necessary. The analysis procedure can often be taken in stages since the inside and outside of the aircraft are only loosely coupled. The term 'loose coupling' means that, while the lightning may produce electromagnetic effects that couple to the inside of the aircraft, there is little need to study the reverse coupling, i.e. the effects of currents appearing within an aircraft upon the currents on its exterior; the voltages and currents induced on wiring do not affect the lightning. It is this separation of interaction effects that allows the internal response of the aircraft to be reviewed by first determining the external electromagnetic fields, without consideration of how they couple to the interior, and then applying the coupling factors to those fields to determine the internal environment.

For many purposes, approximate methods of analysis provide coupling estimates that are satisfactory for lightning protection purposes, since lightning parameters themselves cover wide ranges of possibilities. The type of analytical method one uses depends upon financial considerations, vehicle complexity, design requirements, available computational tools, and known susceptibility and criticality of electrical and electronic systems in the aircraft.

10.2 Elementary Effects Governing Magnetic Fields

Units of Magnetic Field Intensity

In all cases the unit of magnetic field intensity, H, is amperes per meter if the radii are measured in meters. H is the magnetizing force per unit area of air through which the magnetic field exists. The density of magnetic flux, B, measured in Webbers per meter squared (Wb/m^2) is,

$$B = \mu H \qquad (10.1)$$

where μ the permeability for air, is $4\pi \times 10^{-7}$ H/m.

In Chapter 9 it was shown that if a long conductor is carrying a current, *i*, and the return path is far removed, the field intensity at a distance, *r*, from the conductor, as shown in Fig. 10.1(a), is:

$$H = \frac{i}{2\pi r} \quad \text{A/m} \qquad (10.2)$$

If instead of on a solid wire the current is carried on a hollow tube of radius r_0 as shown in Fig. 10.1(b), the field intensity, H, at the surface of the tube is,

$$H = 1/2\pi r \quad \text{A/m} \qquad (10.3)$$

It follows that the average field intensity at the surface of the tube is also equal to the total current divided by the circumference, *P:*

$$H = \frac{I}{P} \quad \text{A/m} \qquad (10.4)$$

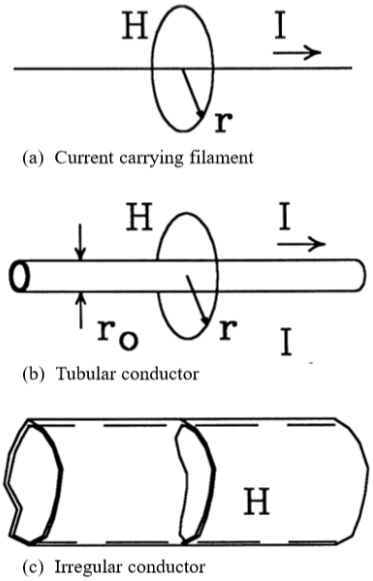

Fig. 10.1 Magnetic fields surrounding current-carrying conductors.

If the conductor is not cylindrical, as shown in Fig. 10.1(c), the field intensity at different points on its surface will be different. However, the average field intensity will still be equal to the total current divided by the circumference:

Radius of curvature

The actual surface magnetic field intensity on a conductor is greater than average at points where the conductor's radius of curvature is less than average and is less than average at points where the radius of curvature is greater than average (see Fig. 10.2). For example, the circumference of the fuselage of a typical fighter aircraft, at a location just forward of its wing, is about 5.5 m.

If a lightning stroke current of 30 kA flowed through such a fuselage, the average field intensity at the fuselage sur-face would be:

$$H_{avg} = \frac{I}{P} = \frac{30\,000}{5.5} = 5\,455 \text{ A/m} \qquad (10.5)$$

Since there are rarely any points of very sharp curvature radius on an aircraft fuselage, the field intensity around the fuselage would probably not vary greatly from the average value. If the fuselage cannot be approximated as an out-of-round cylinder, then the local field intensity at any particular location would have to be calculated by more sophisticated means.

The situation at the surface of a wing carrying lightning current is considerably different from that at the surface of a fuselage. The corners of a wing box and the leading and trailing edges of a wing have radii of curvature much less than the average, so the field intensities at those locations are much higher than they are at the center of the wing box where the radii of the curvature is much larger.

Thus, the field intensity along the leading and trailing edges would be quite high compared to the field intensity long the top and bottom surfaces.

Fig. 10.2 shows, in general, how the magnetic field strengths would vary with position on an aircraft if a lightning flash entered through the nose boom and left through the vertical stabilizer. The field intensity would be highest around the nose boom, lowest around the midsection of the fuselage, and high again around the vertical stabilizer. Near the nose equipment bays, the field would be of greater than average intensity. Since the field intensity is inversely proportional to the radius of curvature, it then follows that the field intensity outside the fuselage of a large transport aircraft would be considerably less than that outside the small fighter aircraft shown in Fig. 10.3.

Since both the average current density, J_{avg}, and the average field density, H_{avg}, are equal to the total current divided by the circumference, it follows that the tangential field intensity at the surface of a conducting object is equal to the current density at that point:

$$J_{avg} = H_{avg} = \frac{\mathrm{I}}{\mathrm{P}} \quad \text{A/m} \qquad (10.6)$$

While this relationship is true for transient currents, it is not true for direct currents (DCs) or transients sufficiently slow that appreciable portions of current and associated magnetic fields penetrate the skin.

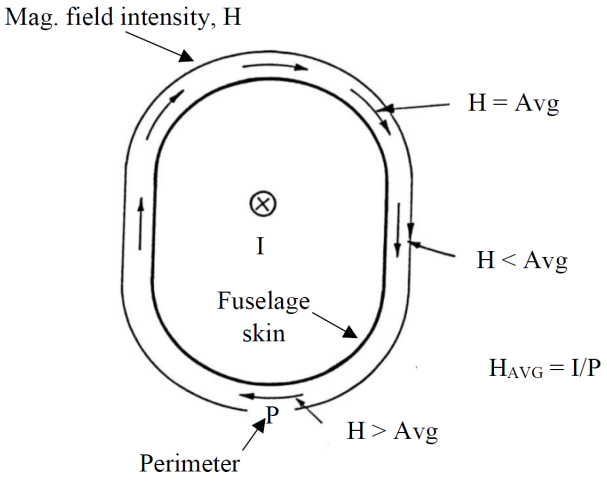

Fig. 10.2 Effect of the cross-sectional curvature radius of a current path on magnetic field intensity.

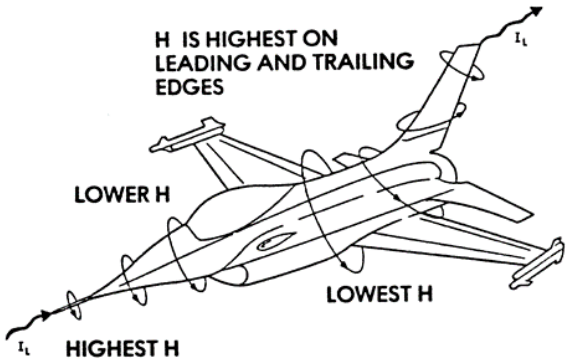

Fig. 10.3 Variation of magnetic field strength with aircraft radius of curvature.

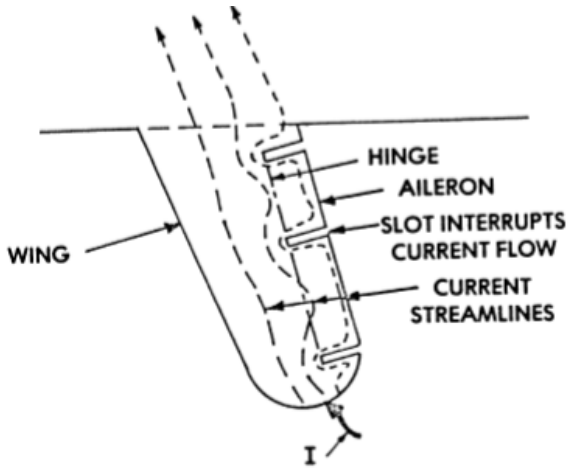

(a) Current entering typical wing.

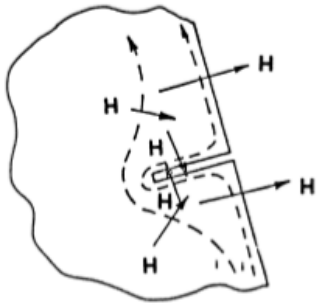

(b) resultant magnetic field virtually uneffected by slot interrupting flow of current.

Fig. 10.4 Current flow and magnetic field around structural gaps.

Orientation of magnetic field

The orientation of the H field vector is always at right angles to the direction of the current vector. While small gaps in the structure (Fig. 10.4) direct the current around the gap, the magnetic field is virtually unaffected, except directly on the surface and on a geometrical scale that is small compared to the dimensions of the gap interrupting the current flow.

While Eq. 10.4 suffices to show the average current density, and thus the average intensity of the magnetic field, it does not show how the current is distributed over the surface. This distribution must be known, since it affects both the resistive voltage rises inside a structure and the amounts of magnetic or electric field that penetrate through apertures.

Redistribution of current

Only for DCs is the current density at the surface of a conductor determined by the DC resistance of the conductor. For most transient conditions, the distribution is primarily controlled by magnetic field effects. The magnetic distribution of current density can be calculated for simple geometries. Around the periphery of a cylinder, for example, the current density, even for alternating currents, is uniform, at least as long as the return path for that current is coaxially arranged so that there is no appreciable flux in the vicinity of the cylinder. Such arrangements are often used to calibrate magnetic field probes used for measuring fields at points of interest on and within aircraft.

For anything other than a cylinder, the skin effect tends to crowd impulse currents of short duration (or high frequency alternating currents) toward edges, making the current density and magnetic field intensity higher than average at places with small radii of curvature (such as the leading and trailing edges of a wing) and less than average at places with a large radius of curvature. With impulse currents such as lightning leader pulses or stroke currents (i.e., as defined by current Components A and H), the skin effect forces the current to initially concentrate at edges in a manner that produces a magnetic field tangential to the surface, as illustrated in Fig. 10.5(a). After its initial high rate of change, as it decays to a slower rate of change, a stroke current gradually redistributes itself until its distribution is determined purely by the resistance of the structure. This resistive re-distribution permits some of the magnetic field to penetrate the surface (see Fig. 10.5(b)). The rate at which the current redistributes over the surface is governed by the ratio of inductance (a measure of magnetic fields) to resistance of the structure. It takes place faster for high resistance structures, such as those fabricated from carbon fiber composite (CFC), than it does for low resistance structures, such as those fabricated from aluminum.

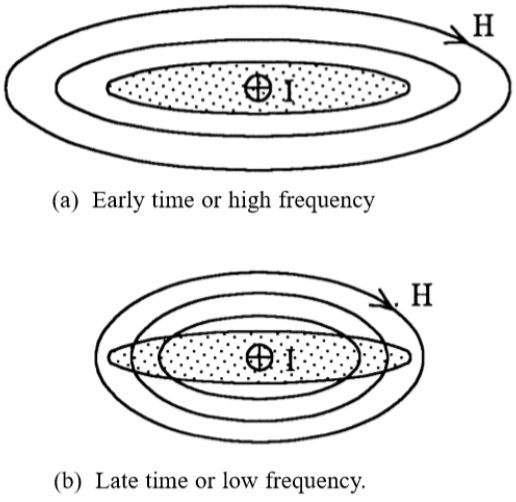

Fig. 10.5 Redistribution effects.

The time required for the current to redistribute from a pattern governed by magnetic field effects to one governed by resistive effects can be surprisingly long; hundreds or even thousands of microseconds. One geometry for which these effects can be calculated analytically is the elliptical cylinder shown in Fig. 10.6. Under high frequency conditions, the current density or magnetic field intensity at the center (X = 0, Y = ± d/2) is:

$$H = \frac{I}{\pi b} \text{ A/m} \qquad (10.7)$$

and at the edge ($X = \pm b/2,\ Y = 0$)

$$H = \frac{I}{\pi d} \text{ A/m} \qquad (10.8)$$

At intermediate points, the magnetic field intensity or current density [10.1, 10.2] is:

$$H_{surface} = \frac{I}{\pi} \frac{1}{\sqrt{b^2-(2x)^2[1-d^2/b^2]}} \qquad (10.9)$$

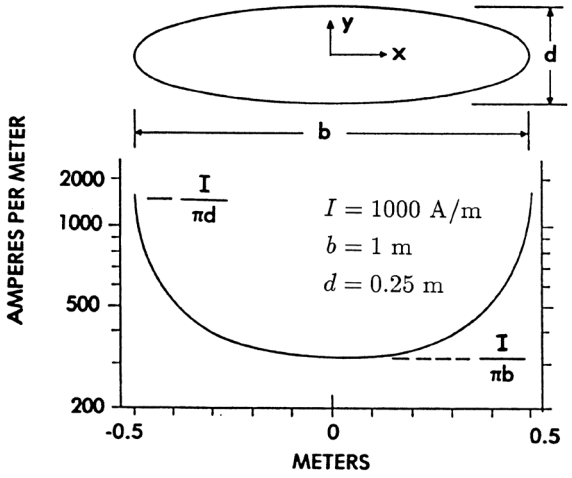

Fig. 10.6 Magnetic field intensity at the surface of an elliptical conductor.

This current distribution does not hold for DCs, for which the current density over the surface is determined by DC resistance. If the cylinder were of uniform thickness, the current density would be uniform. The time span or frequency range over which a transition takes place to the uniform distribution of current governed by resistance from the non-uniform distribution governed by magnetic fields (Fig. 10.6) can be defined in terms of a factor, *K*:

$$K = \sqrt{\frac{bd}{\delta}} \qquad (10.10)$$

where

b = width
d = depth
δ = skin depth

Traditionally, skin depth is given by

$$\delta = \sqrt{\frac{2\rho}{\mu\omega}} \qquad (10.11)$$

where

ρ = resistivity
μ = permeability
ω = angular frequency

This was discussed in greater detail in Chapter 9. For $K < 1$, the distribution of current is mostly controlled by resistance, while for $K > 10$, the distribution is controlled by magnetic field effects. The skin depth and value of *K* for aluminum, as functions of frequency, are given in Table 10.1.

Table 10.1
Skin Depth as a function of Frequency

F	δ	K
Frequency	Skin Depth	$\sqrt{bd/\delta}$
1 Hz	8.25 x 10^{-2} m	6.06
10 Hz	2.61 x 10^{-2} m	19.2
100 Hz	8.25 x 10^{-3} m	60.6
1 000 Hz	2.61 x 10^{-3} m	192
10 000 Hz	8.25 x 10^{-4} m	606

As an example of the frequency range over which the transition takes place, consider an elliptical cylinder made from aluminum (ρ = 2.69 x 108 Ω·m) with width, *b*, = 1 m, depth, *d*, = 0.25 m, and a wall thickness of 1 mm. Even at 10 Hz, $K = 19$, indicating that the current crowds to the edges of the ellipse and has a skin depth given by Eq. 10.11. At 1 Hz, $K = 6$, which is approximately the value at which resistive and magnetic effects have an equal effect on the current distribution. Thus, the frequency range over which the current density changes from its uniform DC value to the limiting ac distribution is perhaps 0.5 to 5 Hz. If a step function current were applied, it would take nearly a second before the current became uniformly distributed over the surface. The manner in which the currents redistribute over the surface affects the voltages developed on internal circuits, by the mechanism described in Chapter 11.

If an alternating current were injected onto the structure, the surface current density would remain distributed as described by Eq. 10.9, up to indefinitely high frequencies, unless the width of the ellipse were on the order of a tenth of a wavelength or less. The current density through the wall thickness of the elliptical cylinder would vary with the frequency, but it too would remain constant, until the skin depth became about the same as the wall thickness.

In many situations, external current densities may be determined with sufficient accuracy for practical purposes by assuming the surface under consideration to be an ellipse or ellipses. If such an approximation does not give sufficient accuracy, there are other techniques that may be used. Some of these are discussed in §10.5.

10.3 Elementary Effects Governing Electric Fields

The electric field around a conducting surface is also of importance, since a lightning flash produces rapidly changing electric fields that couple capacitively to the wiring in aircraft. The behavior of electric fields is, in many ways, like the behavior of magnetic fields, particularly in that electric charge crowds to the edges of conductors in the same way electric current does. A static charge on the elliptic cylinder shown in Fig. 10.7(a), for example, would distribute itself in the manner shown, where the current density is given by equations of the same form as Eq. 10.8.

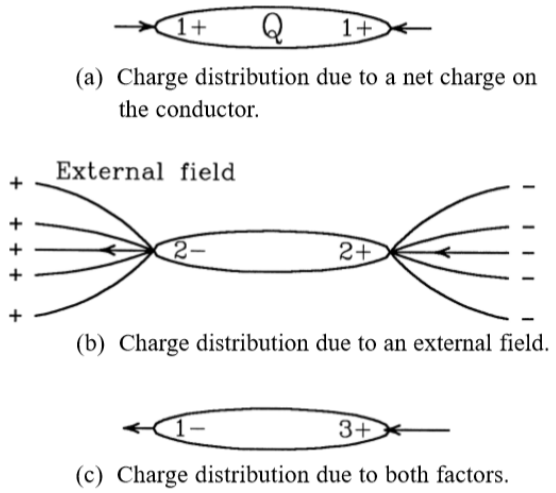

(a) Charge distribution due to a net charge on the conductor.

(b) Charge distribution due to an external field.

(c) Charge distribution due to both factors.

Fig. 10.7 Factors effecting the distribution of electric charge on conductors.

The electric field strength at the surface would be proportional to the charge density and directed at a right angle towards the surface, while the magnetic field would be tangential to the surface. The distribution of charge would not change with frequency; it would be the same for a DC static charge as it would be at high frequencies. Also, the distribution of charge would not be affected by the resistivity of the material (at least not under DC conditions).

A conductor placed in an electric field becomes polarized as shown in Fig. 10.7(a). The electric field draws electrons to one end of the conductor and leaves a deficiency of electrons, or positive charge, on the other end. The electric field strength at the end surfaces is thus greater than that of the undisturbed electric field. For the symmetrical conditions shown in Fig. 10.7(b), the electric field strength is equal at the two edges and opposite in polarity. A static charge produced by some mechanism other than induction would add to the induced charge at one edge and subtract from it at the other edge, as shown in Fig. 10.7(c), making the electric field strengths unequal. Since the field strength is proportional to the density of charge, the electric field strength is greatest at points having small radii of curvature (the nose boom of a fighter aircraft for example). If the electric field strength is sufficiently high, the air in the vicinity may become ionized, producing either corona, as described in Chapter 1, or aircraft-initiated ('triggered') lightning, as discussed in Chapter 3.

10.4 Combined Magnetic and Electric Fields

Under DC conditions, magnetic and electric fields can exist independently of each other (except for resistively-generated electric fields) and one or the other or both may be present around a current carrying conductor. Under transient and ac conditions, both are present and, while for some conditions the effects of one or the other may be predominant, usually they must be considered together. The reason both types of fields are present is that a changing magnetic field gives rise to a changing electric field and vice versa. This relationship is described by Maxwell's Laws, which are discussed in §10.6. In simple terms, the magnetic fields are the result of moving charges and are accompanied by electric fields. The changing electric and magnetic fields are oriented at right angles to each other and propagate in a direction at right angles to the plane determined by their vectors. For example, a lightning current propagating through an aircraft skin panel would produce magnetic and electric fields as shown in Fig. 10.8. The electric field is normal to the surface of the airplane and the magnetic field is tangential to it. The magnitudes of the E and H vectors are given by the impedance, Z, of the surface over which they pass.

$$E/H = Z \qquad (10.12)$$

(Surface impedance is discussed in Chapter 9).

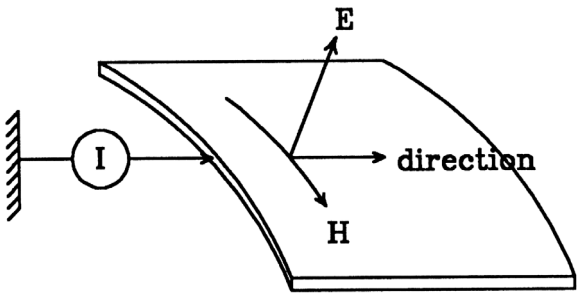

Fig. 10.8 Wave propagation over a surface.

For the initial wave propagating over the surface of a conductor in free space, Z is approximately 377 ohms. When the wave reaches a discontinuity, such as the end of the surface or a point where one surface joins another surface of different size or orientation, a reflected wave is generated, and the total field is the sum of the initial wave and the reflected wave. The reflected wave eventually reaches a discontinuity, at which point it generates another traveling wave. Note that the use of "ohms" to describe the ratio of *E* to *H* is not meant to imply resistance, but instead to indicate a ratio that, by convention, means characteristic impedance.

The fields at any point to which a wave propagates can be determined from the fields at the points previously traversed by the wave. Numerical techniques for doing this are given in §10.5 and §10.6. The phenomenon of waves propagating back and forth across the surface of an aircraft, or of aircraft resonances excited by an outside event, is discussed further in §10.7.

10.5 Evaluating Electromagnetic Fields

There are a number of ways that the electromagnetic field around a conductor may be evaluated. Three of the simpler methods are discussed here. Some of the results from the method described in §10.5.3 will be used to illustrate the way external and internal fields are influenced by the shape of the aircraft.

10.5.1 Numerical Solution of Laplace's Equation

Analytically, the solution of the field around a current carrying conductor may be determined by a solution of Laplace's equation:

$$\nabla^2 \varphi = 0 \qquad (10.13)$$

where φ = the potential.

In rectangular coordinates, Laplace's equation becomes:

$$\frac{\partial^2 \varphi}{\partial x^2} + \frac{\partial^2 \varphi}{\partial Y^2} + \frac{\partial^2 \varphi}{\partial Z^2} = 0 \qquad (10.14)$$

For some geometries, Laplace's equation can be solved analytically. Elliptical geometries are an example. The equations defining the field distribution over elliptical cylinders are not presented here, but Fig. 10.9 shows an example of the field around an elliptical cylinder of infinite length. If the field arises from current in the cylinder, the equipotential lines depict the magnetic field lines that are tangential to the cylinder's surface. If the field arises from static charge on the cylinder, the lines directed into the cylinder depict the electric field lines along which displacement currents flow.

The return path for either the voltage maintaining the charge or the current, is assumed to be sufficiently far away from the conductor that it does not influence the field around the indicated region.

The flow lines indicated in Fig. 10.9 divide the region into 44 sectors. At the surface of the conductor, the magnetic field strength is inversely proportional to the spacing between the flow lines. Since the average field strength around the surface is

$$H = \frac{I}{P} \qquad (10.15)$$

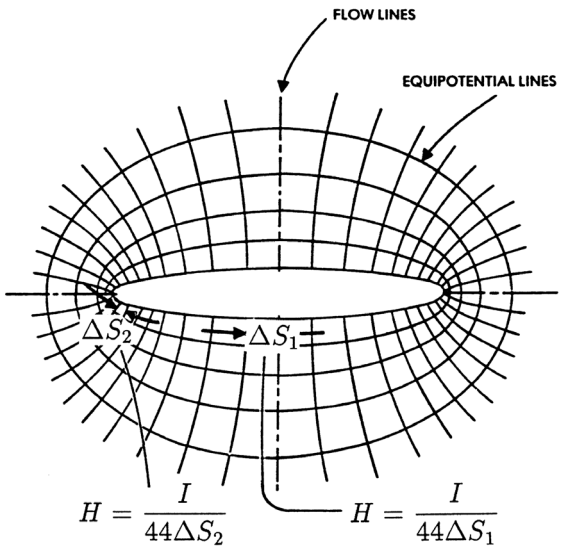

Fig. 10.9 The electromagnetic field around an elliptical conductor.

it follows that the field strength at the surface between any two flow lines is

$$H_{surface} = \frac{1}{44\Delta S} \qquad (10.16)$$

In Fig. 10.9, the flow lines indicate the directions that an electron would be caused to move by the electric field, so they are also known as electrostatic force lines. Likewise, the equipotential lines in the electric field are also the flux directions in the magnetic field.

It is only possible to calculate the field analytically in the simplest geometries. Usually, one must resort to a numerical or graphical method to determine the field. Numerically, the field may be determined by a numerical solution of Laplace's equations. Fig. 10.10 shows a conductor at potential *P* surrounded by a return conductor (a circle in this case) at potential zero. To this geometry is fitted a rectangular grid, shown here as a very coarse grid.

Initially, all grid points that lie on the conductor are assigned a potential, *P*, and all the grid points that lie on the return path are assigned a potential zero. Laplace's equation in two dimensions can be shown to be approximately:

$$\frac{\partial^2\varphi}{2X^2} + \frac{\partial^2\varphi}{2Y^2} = \frac{1}{k^2}[\varphi_1 + \varphi_2 + \varphi_3 + \varphi_4 - 4\varphi_4] \qquad (10.17)$$

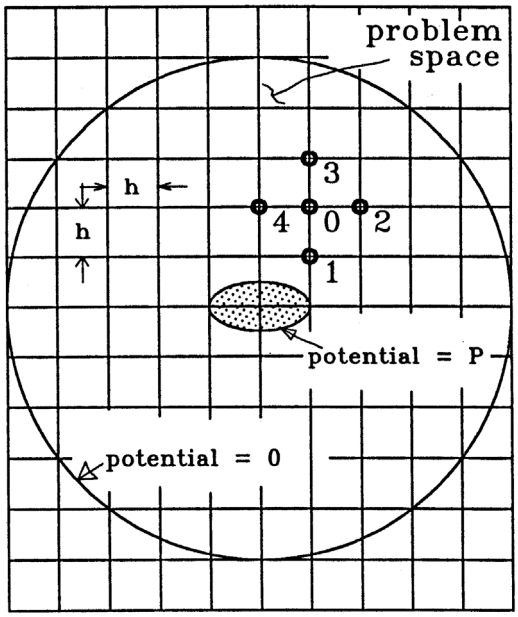

Fig. 10.10 A rectangular grid for evaluation of Laplace's equation.

From this, it follows that Laplace's equation is satisfied if the numeric values at four points surrounding a central point have values that satisfy the equation

$$\varphi_1 + \varphi_2 + \varphi_3 + \varphi_4 - 4\varphi_0 = 0 \qquad (10.18)$$

A determination of the field around the conductor then involves assigning field values at all the points between the conductor and its return path and adjusting those values until Eq. 10.17 is satisfied everywhere within the grid. The literature [10.3 - 10.4] indicates several numerical techniques by which the potentials at the points may be adjusted to their final values. While the process is tedious, it is not completely impractical to do by hand, as discussed briefly in §10.5.2. Usually, the process is done by computer routines that solve the field equations. In addition to tabulating the numerical values of the field at the grid points, such computer routines often allow one to plot the flow and equipotential lines.

Problem space and grid size

Fig. 10.10 illustrates two important aspects of numerical evaluation of electromagnetic fields. The first is that the solution can only take place in a defined problem space. For an isolated object, such as an aircraft in flight, the problem space, ideally, should extend very far in all directions since, in theory, the field intensity at even the most remote point affects the field at the surface of the aircraft. The second is that the grid size affects the precision and detail with which the field may be calculated. Ideally the grid size should be much smaller than the dimensions of the aircraft around which the field is to be determined.

The smaller the grid size and the larger the problem space, the greater the amount of computer memory and computer running time required to perform the analysis. This effect becomes more significant when calculations are performed in three dimensions. Computer resources are put to the ultimate test when time domain solutions are required, because the field must be calculated anew for each time step. Depending on the requirements of the analysis, problem space, grid size and the limitations of available computer resources may restrict the precision of the solutions.

Frequently one is only interested in the field in the immediate vicinity of the aircraft. If so, the problem space, and the amount of computer memory needed, can be made relatively small by setting field magnitudes at the outer boundary of the problem to an approximation of their

correct values, rather than zero, and concentrating the calculations on the field around the conductor under study. On an aircraft, similar techniques can be used to concentrate the calculation on those portions of most interest.

Apertures

Any solution of Laplace's equation also allows the pattern of low frequency coupling through an aperture to be calculated. Computer techniques are now commonly used for such solutions but, in the past, electrolytic tanks and resistive paper techniques were widely used. Fields were also mapped by hand. The technique of hand mapping is outlined in §10.5.2. The simplest computer routines deal either with two-dimensional (2D) problems or problems with rotational symmetry. In a 2D case, the aperture would run the length of the conductor being studied. This is not necessarily a disadvantage since some important geometries and apertures are basically 2D. An important aperture is that which may exist behind the rear spar of a wing when the flaps have been extended. Since it is a convenient region to reach, wiring is often placed in this region. Electrically it is a poor place since the aperture is near a region where the magnetic fields external to the wing are high. Another important set of apertures that may be approximated as a continuous opening is that formed by the windows in the fuselage of a transport aircraft.

Three-dimensional (3D) objects

In principle, the field around 3D objects may also be solved numerically by extending Eq. 10.19 to include eight points on a cube surrounding a central point. A solution of the field around a 3D object not involving rotational symmetry requires large amounts of computer storage and running time if the calculations are to define the field satisfactorily in all three dimensions.

10.5.2 Hand Plotting of Fields

The fields around any geometry may also be determined graphically by a cut-and-try process, in which flow lines and equipotential lines are drawn on the geometry and adjusted until repeated subdivision always yields small squares and the flow and equipotential lines intersect at all points at right angles. Cut-and-try field plotting, of which Fig. 10.11 is an imperfect example, may, with care, patience, and liberal use of a soft pencil and eraser, yield a field pattern of any desired accuracy. This approach has rarely been used since the advent of computer programs that quickly solve Maxwell's equations for more complex geometries such as the exteriors and interiors of aircraft. The example of a hand-plotted field that is shown in Fig. 10.11 is presented so that the directions of electric field lines of force and of magnetic field flux lines (or electric field equipotential) can be seen. This is not always practical with modern computational programs that show intensities as gradations of colors.

10.5.3 Calculation Using Wire Filaments

Another early approach to determining current density, shown in Fig. 10.12, is based on the premise that a 2D geometry can be represented as an array of parallel wires [10.5 - 10.6]. If the current in each wire is known, the average current density along the surface defined by any two wires is the average of the current on the two wires divided by the spacing between the wires.

If the wires are all of infinite length (so that no end effects need to be considered) and are all connected together at their ends, the manner in which current divides among the wires may be calculated with the aid of a simple computer program. The high frequency response of the wire models (i.e., the response due to lightning stroke currents) can be determined based upon the self and mutual inductances of the individual wires with respect to all the other wires in the model. If the current distribution due to slowly changing intermediate and continuing currents is desired the structure resistances can be represented by wire resistances and the currents in the wires determined by a simple network of resistors.

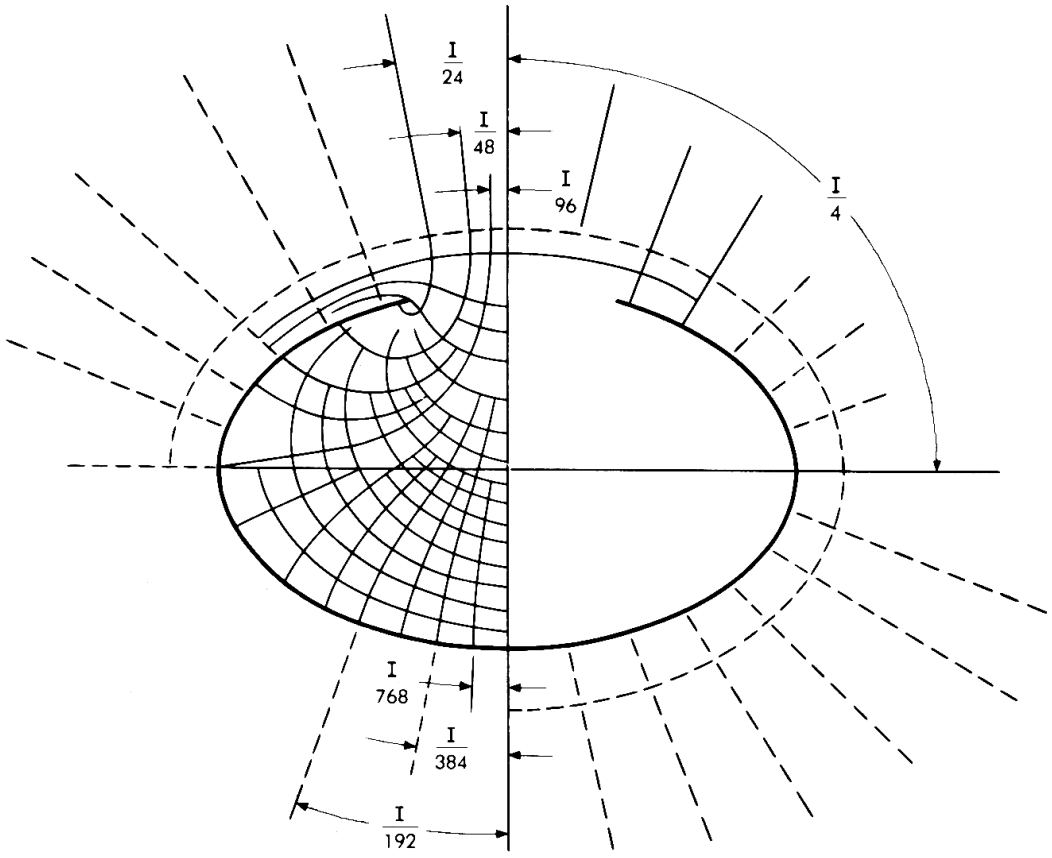

Fig. 10.11 Cut-and-try field plotting.

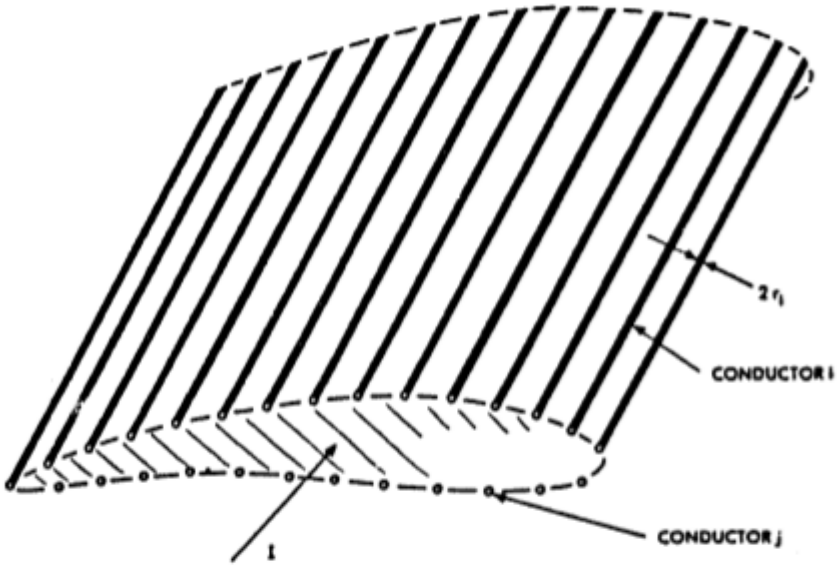

(a) The array.

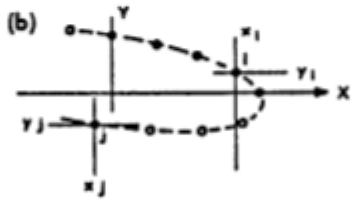

(b) Coordinates defining wire locations.

(c) Definition of the current return path.

Fig. 10.12 A structure defined as an array of wires.

Self and mutual inductances

Let the location of the wires be defined in terms of the rectangular coordinates x_i and y_i and let the radius of the conductors be r_1. The self-inductance per unit length of each wire is

$$L = 2 \times 10^{-7} \ln\left[\frac{R}{r_1}\right] \text{ Henrys per meter} \qquad (10.19)$$

In this equation R is defined as the distance from the conductor, or from the group of conductors, to an arbitrary return path. The numerical accuracy of the current distribution to be calculated does not depend critically upon the value assigned to R, but it should be on the order of 10 to 20 times the greatest dimension of the structure being modeled. Between any two conductors, i and j, there is a mutual inductance of:

$$M_{ij} = 2 \times 10^{-7} \ln\left[\frac{R}{r_{ij}}\right] \text{ Henrys per meter} \qquad (10.20)$$

The currents in each of the wires can be determined by solving the matrix equations that represent the self and mutual inductance effects, shown in Fig. 10.13, which control the currents during the fast-changing periods of the lightning stroke current when current distribution is determined by magnetic fields. These equations are not presented here. The currents will shift when the stroke current stops changing rapidly, and the wire resistances begin to control the currents.

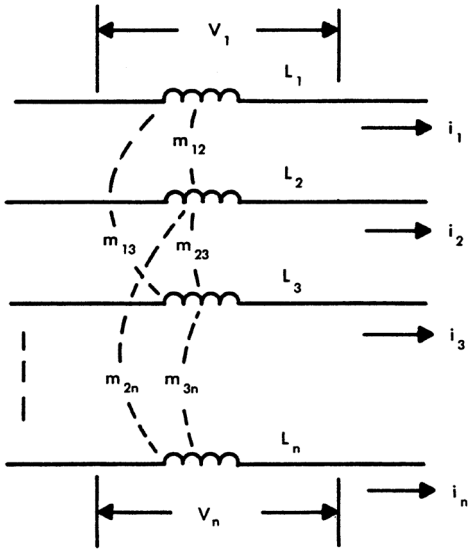

Fig. 10.13 Mutually coupled inductances.

10.5.4 Examples of Magnetic Fields

The magnetic field within and around the cluster of wires can be determined by taking the proper summation of the magnetic field produced by the current in each individual wire.

One computer program [10.7] that incorporates the above routines is MAGFLD. Some examples of calculations performed with MAGFLD will now be described, since they will serve to illustrate some of the points discussed in previous sections. The geometry chosen for analysis is the fuselage of the hypothetical aircraft shown in Fig. 10.14. The aircraft, whose airworthiness is not under discussion, has a fuselage of elliptical cross section, two meters along the major axis and one meter along the minor axis. The fuselage is considered long enough that no end effects need to be considered.

A lightning current of 1 000 A is assumed to enter the nose and to exit through the rear of the fuselage. This elliptical fuselage is represented by 48 parallel conductors distributed in the manner shown in Fig. 10.15. This figure also shows the current density, or magnetic field strength, at the surface of the cylinder, both as determined from the program MAGFLD and analytically, using Eq. 10.12. The field determined by a wire model is representative of the field that would exist outside the aircraft (and within the aircraft if diffusion time, i.e., skin effect, is neglected.) This is a good approximation for an aircraft made of CFC, but it is not applicable for a conventional aluminum aircraft, where diffusion times are long compared to the lifetime of a stroke current.

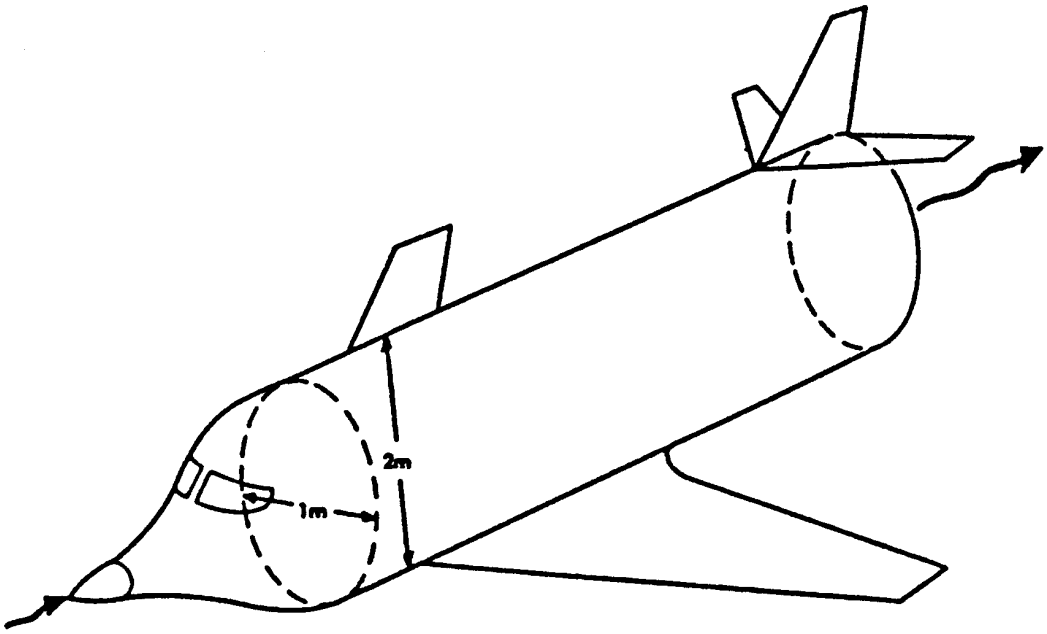

Fig. 10.14 A hypothetical fuselage to be modeled as a wire grid.

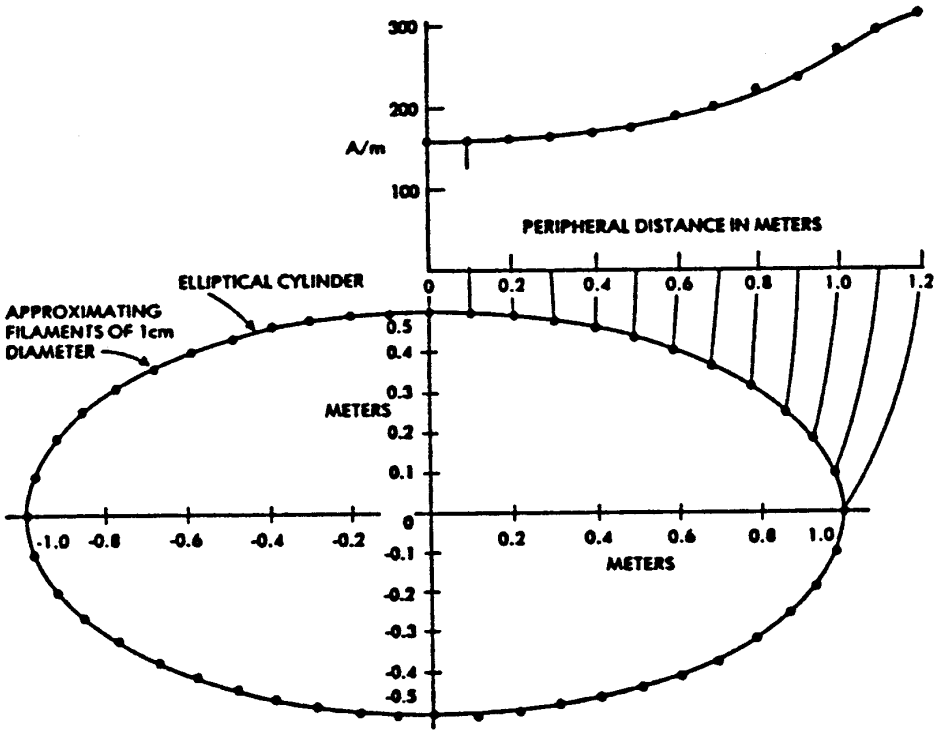

Fig. 10.15 Wire grid approximation of the elliptical fuselage.
Note that the axes in this figure are opposite from those of the fuselage in Fig. 10.14.

Magnetic distribution of current

One quadrant of the elliptical fuselage is shown in Fig. 10.16. This figure shows the magnetic field strength both within and around the wire grid as calculated by MAGFLD. The orientation of the magnetic field is shown by the direction of the arrows, and the strength both by the length of the arrows and by the indicated contour lines. Note that the field lines external to the surface are tangential to the cylinder.

The magnetic field strength inside the grid is much smaller than that outside, since, on the inside, the fields from each of the filaments tend to cancel, whereas outside the grid they tend to add. In Fig. 10.16, the fields inside the grid are largely the result of the finite number of wires defining the elliptic cylinder. If the cylinder were defined by more conductors, the fields inside would be smaller, but they would not be zero unless the shape of the fuselage were cylindrical.

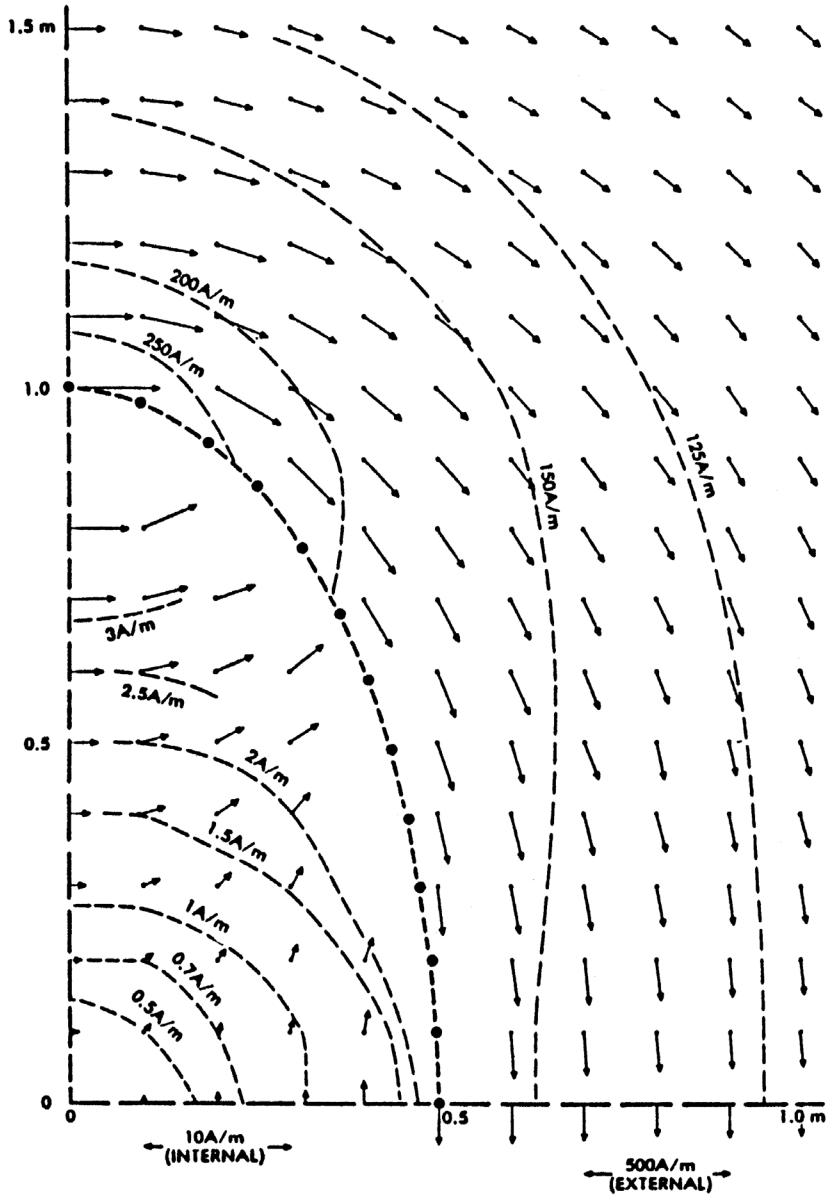

Fig. 10.16 Magnetic field produced by magnetically distributed current.

Resistive distribution of current

Fig. 10.17 shows a similar plot with one important difference: the current was forced to be equal in each wire. The magnetic field pattern produced here would be determined by the resistive current distribution, the pattern that represents the final stage after currents and current density have become uniform. The orientation of the field external to the grid shows only slight differences from the orientation in Fig. 10.16, but one important difference is that some of the field lines penetrate the surface, increasing the field intensity in the interior of the grid.

Recessed cavity

A third example of field distribution (shown in Figs. 10.18 and 10.19) assumes that on each side of the fuselage there is a recessed cavity. Such a cavity would be an approximation of the equipment bays for electronic equipment or baggage. The figures again assume that the current in each filament is governed by inductive, rather that resistive, distribution. The magnetic field patterns clearly show the field in the recessed cavity to be less than the field at other exterior points on the fuselage.

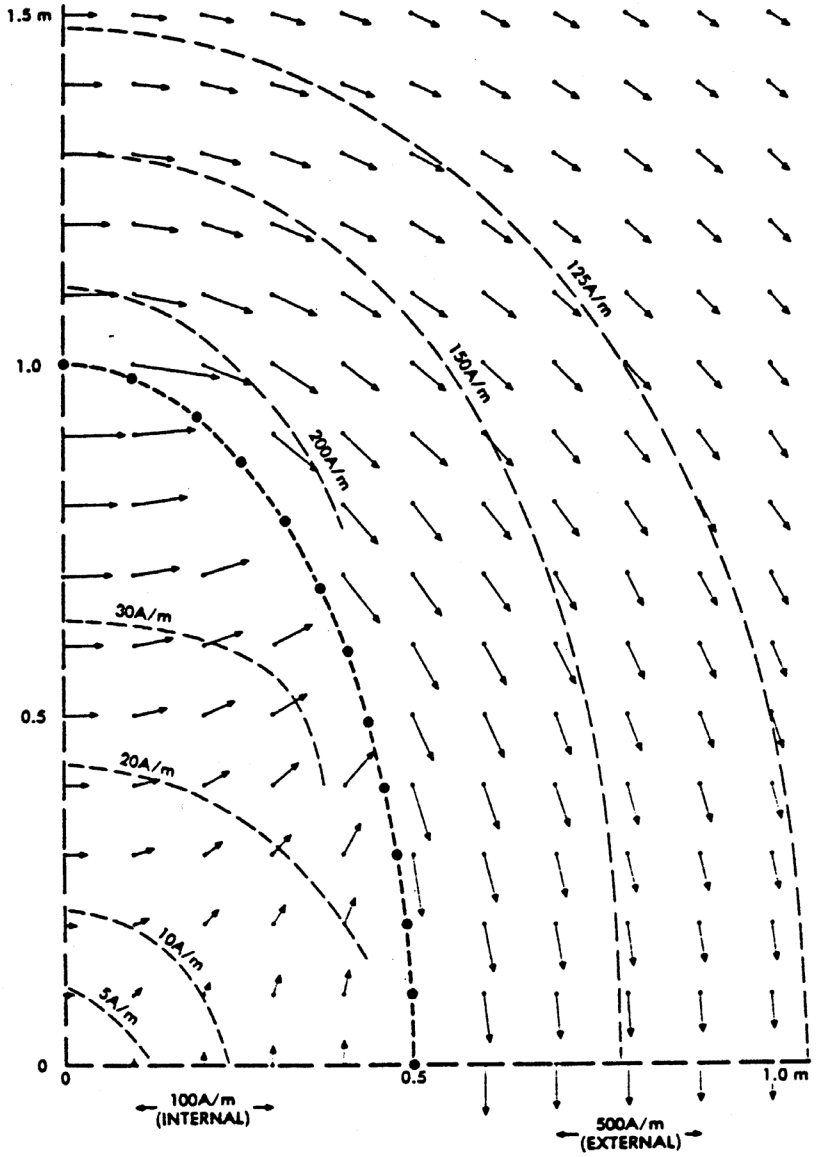

Fig. 10.17 Magnetic field produced by resistive current distribution.

The degree to which the MAGFLD program, or other programs, can calculate the magnetic field in the space surrounding the aircraft fuselage, while interesting, may not be of great use for aircraft studies, since it is usually only the field intensity at the surface of the structure that is of interest. Programs like these however, can calculate the field distribution in and around these simple geometries with sufficient accuracy for many purposes.

Redistribution

The filamentary method can be used to calculate redistribution effects by connecting a resistor of appropriate value in series with each of the inductors shown in Fig. 10.13. In the matrix operations the values of L and M must be replaced by R + jωL and jωM and the matrix operations must be carried out with complex number routines. Otherwise, the process is as indicated. Standard circuit analysis routines, such as SPICE, SCEPTRE, NET II and ECAP, can also be used to evaluate the current in each filament.

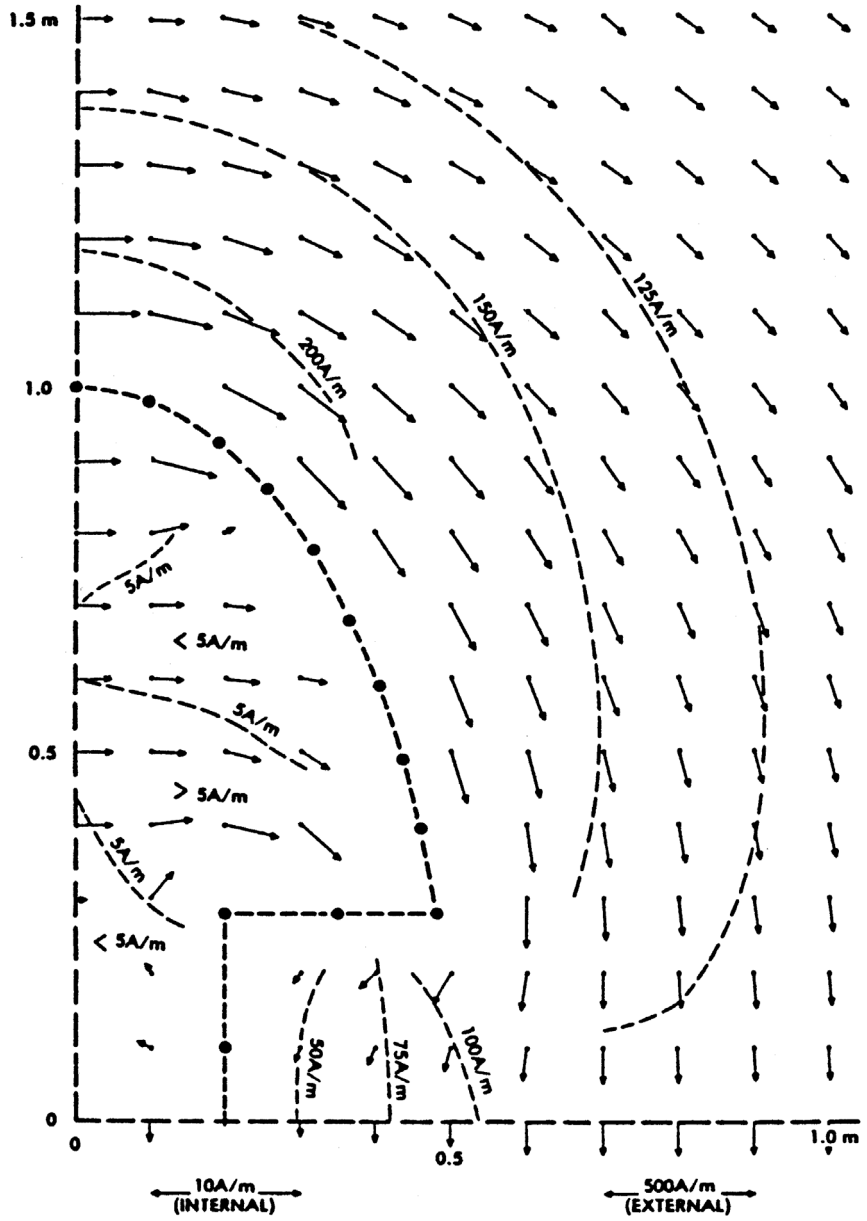

Fig. 10.18 Magnetic field intensities in a recessed bay.

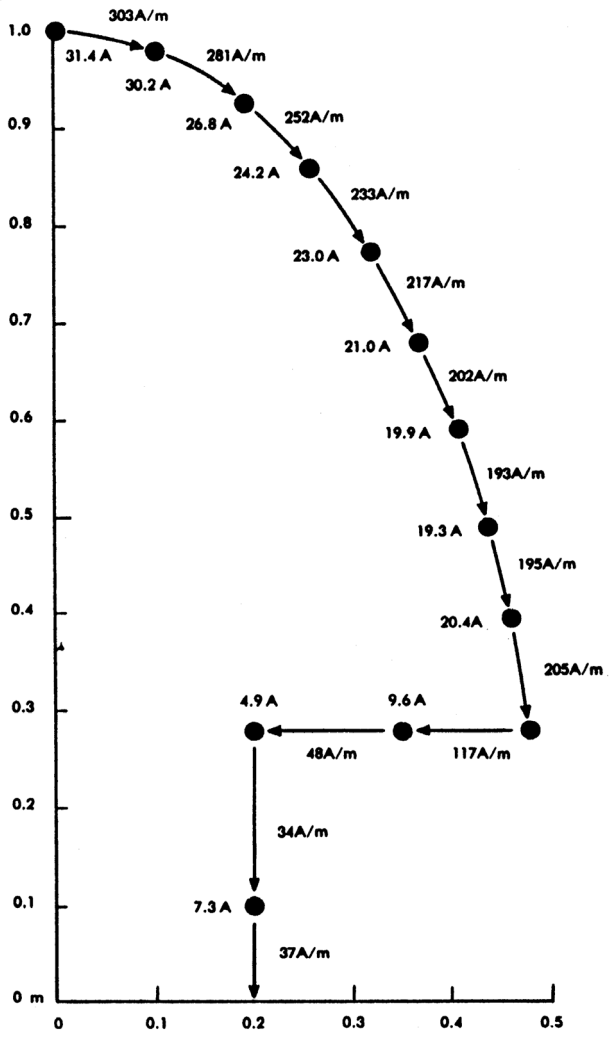

Fig. 10.19 Current distribution and magnetic field intensities at the surface (one quadrant shown).

Fourier transform techniques could then be used to evaluate the response as a function of time. Some of the circuit routines can, of course, evaluate the response directly as a function of time.

10.6 Maxwell's Equations

The foundation of all lightning interaction analysis is Maxwell's equations, given here in the time domain differential form.

$$\nabla \cdot E = \frac{q_{ev}}{\varepsilon_o} \qquad (10.21)$$

where q_{ev} is electric charge density in coulombs/cubic meter. Eq. 10.21 states that the number of lines of electric flux leaving a volume is equal to the amount of charge contained in that volume. This is Gauss's law.

$$\nabla \cdot B = 0 \qquad (10.22)$$

Eq. 10.22 states that the number of lines of magnetic flux entering a volume is equal to the number leaving it. This is Gauss's law for magnetism.

$$\nabla \, x \, E = -\frac{\partial B}{\partial t} \qquad (10.23)$$

Eq. 10.23 states that a changing magnetic field gives rise to an electric field. This is Faraday's law of induction.

$$\nabla \times H = \sigma E + J_s + \frac{\partial D}{\partial t} \quad (10.24)$$

Eq. 10.24 states that there are three sources of a magnetic field; conduction currents (σE), externally produced currents (J_s) and the displacement currents produced by a changing electric field.

If one assumes that the lightning interaction problem begins with the injection of an external lightning current into the aircraft, then the source term for the interaction is J_s in Eq. 10.23. In principle, electromagnetic fields can be calculated everywhere, based on a knowledge of J_s and the boundary conditions (that is, the aircraft geometry). However, sometimes the lightning interaction problem does not start with the injection of lightning current. This is true for analyses of aircraft initiated lightning. For that, the source term is the current, σE, conducted into the air from the aircraft.

Air conductivity

The conductivity of the air is, of course, non-linear. Air is poorly conductive until the electric field gets high enough to cause ionization, but very highly conductive as breakdown occurs. As a result, only a negligible current is conducted into the air before breakdown occurs, but considerable current afterwards. That current then transfers charge onto the aircraft, which affects the electric fields and may set in motion events that lead to a complete aircraft-initiated lightning flash. The response of the aircraft to the current is then calculated in the same way as it is for a naturally occurring lightning flash.

Various software programs are commercially available for solving Maxwell's equations for predicting lightning current distributions and induced transient characteristics in aircraft. A few of these are listed below:

COMSOL Multiphysics® is a general-purpose simulation software for modeling designs, devices, and processes in all fields of engineering, manufacturing, and scientific research. Add-ons can compute structural mechanics as well as temperature rises and some other effects of the lightning currents.

CST Studio Suite® is a high-performance 3D electromagnetic analysis software package for designing, analyzing, and optimizing electromagnetic components and systems. Electromagnetic field solvers for applications across the electromagnetic spectrum are contained within a single user interface.

EMA3D® is a 3D Finite-Difference Time-Domain solver with an integrated multiconductor transmission line solver. The two electromagnetic solvers co-simulate to allow for a complex cable harness to be accurately modeled inside complex geometry, such as an electronic device, a piece of machinery, an automobile, or an aircraft.

External environment

When used to compute lightning effects on or within an aircraft, the strike conditions must be decided and become inputs to the computation process. These include lightning strike entry and exit locations, and the waveforms and amplitudes of the lightning currents. Typically, the stroke currents are of greatest interest, since the amplitudes and waveforms of these cause the highest currents throughout an aircraft, and the highest induced transients in electrical wire harnesses. The intracloud current pulse is also used since its rate of change is higher than that of the cloud-to-earth stroke current. Both currents are standardized and described in Chapter 3.

Validation

If used as a tool for certification of aircraft, the authorities usually require that whatever program is proposed be validated for use on the aircraft to be certified. This is done by comparisons of computed lightning effects with measurements of these effects during simulated lightning current applications. These tests are discussed in Chapter 13. Calculated parameters should compare favorably with measurements. Favorable comparisons are needed between calculated and measured amplitudes, as well as waveforms, of the parameters to be computed by the software program.

The linear technique can be used for either aircraft-initiated or natural lightning. The distinction between the two is that aircraft-initiated lightning leaders begin at the aircraft and move away, in generally opposite directions, while natural lightning leaders begin away from the aircraft and move toward it. Typical geometries for each of these cases are shown in Fig. 10.20. The figure shows the channel attached to the nose of the aircraft, as often happened on the F106B storm hazards research airplane operated by National Aeronautics and Space Administration (NASA), but the analysis procedure allows attachment to any point on the aircraft.

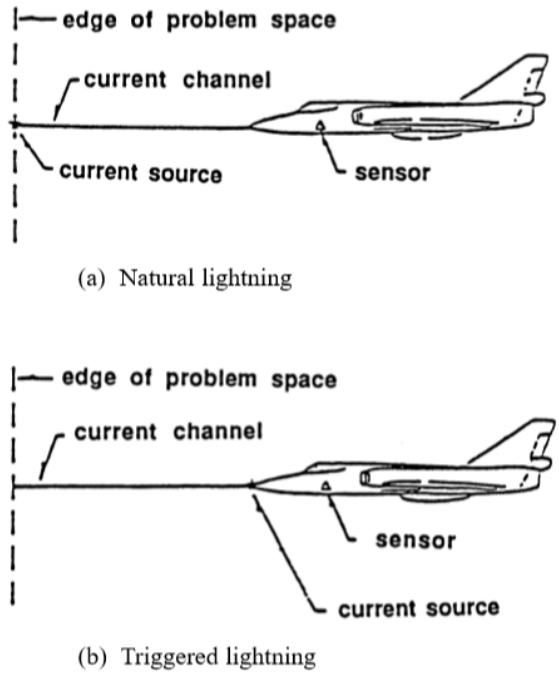

Fig. 10.20 Locations of current source used in a computer code.

The difference between Fig. 10.20(a) and Fig. 10.20(b) is the location of the current source. For calculations simulating natural lightning, the source is located at the edge of the problem space, as far from the aircraft as possible, reflecting the fact that the initiation and driving forces for a natural lightning flash occur away from the aircraft and the lightning propagates towards it. For aircraft-initiated lightning, the source is located near the point where the channel attaches to the aircraft, reflecting the fact that the lightning leaders originate at the aircraft and propagate away from it, generally in opposite directions.

Channel characteristics

The characteristics of the lightning channel must also be defined. The most important of these are the characteristic impedance (since interactions between the aircraft and the channel depend on the channel impedance) and the velocity of propagation. Elementary aspects of this interaction were discussed in Chapter 8. The characteristic impedance and velocity of propagation can be determined from the resistance, inductance, and capacitance of the channel, per unit length. The last two properties are determined by the physical diameter of the channel, as discussed in Chapter 2.

10.7 Aircraft Resonances

Traveling Waves

The magnitudes of electric and magnetic waves traveling together on a conductor are related by a characteristic impedance, Z, also known as a surge impedance, determined by the inductance and capacitance of the conductor.

$$Z = \sqrt{\frac{L}{C}} \qquad (10.25)$$

For a conductor in air, this impedance is usually in the range from 100 - 1 000 Ω, depending on the geometry of the conductor. If the traveling wave encounters another conductor of different impedance, part of the wave is transmitted onto the other conductor and part is reflected back along the conductor on which the incident wave was traveling. The magnitudes of the transmitted and incident waves are given by the relative surge impedances of the two conductors. The relevant equations for this are given in Fig. 10.21. If the wave on the second conductor encounters a third conductor, a second set of transmitted and reflected waves is produced. The reflected waves on the second conductor travel back towards the source, again encounter a change in impedance and set up a third set of traveling waves. This process repeats until all the energy is radiated away or lost in the resistance of the conductor. The result of this response is that an oscillatory wave is developed on the second conductor, the frequency of which is determined by length of the second conductor or, more properly, by its electrical transit time. For a conductor in air, where the velocity of propagation is 3 x 10^8 m/s, the ringing frequency would be

$$f = \frac{3\times10^8}{2l} \qquad (10.26)$$

where *l* is the length in meters. If, for example, the second conductor mentioned above is an airplane whose length (nose to tail) is 34 m (the length of a B737-700), the resonate frequency would be 4.4 MHz. Larger airplanes would exhibit a lower resonant frequency, and smaller airplanes a higher frequency of traveling wave oscillations. This is the reason for the assignment of 1 MHz and 10 MHz to certain test voltage and current waveforms included in the system and equipment test standards noted in Chapter 5. Airframe resonances are not the only source of traveling waves. Individual wire harnesses throughout the airplane usually have their own resonant frequencies. Since most of these are shorter than the overall length of the airplane, their resonant frequencies are higher. When measurements are made of voltages induced in wire harnesses such as shown in Chapter 8, the voltages often display a combination of frequencies, most of which are within the range of 1 - 10 MHz.

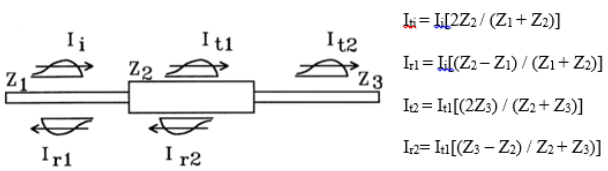

Fig. 10.21 Transmitted and reflected waves at junctions.

Influence of waveform

The nature of these oscillations is also influenced by the shape of the incident wave. Fig. 10.22 shows the two different current waveforms (i.e., rate of charge introduction to the aircraft). The geometry of the situation is shown in Fig. 10.22(a). There are two significant points to be noted about this figure. The first is that the input and output currents have different waveforms and that both are different from the current at the center of the second conductor (the airplane). The second point is that the oscillation on the second conductor is more pronounced for the incident current that rises to its peak the most rapidly. If the incident current had a sufficiently slow rise time, the oscillations on the conductor would become insignificant, since there would be time for the initially injected charge to exit from the second conductor.

Although not illustrated, the nature of the oscillations is also influenced by the relative characteristic impedances of the conductors. The more nearly equal the impedances, the less pronounced the reflections. If the characteristics of all three conductors were the same, there would be no reflections, and hence no oscillations, on the second conductor (i.e., the aircraft) at all.

Lattice diagrams

The nature of these oscillations can be calculated graphically, using the lattice diagrams described in the literature [10.8 - 10.9] or by time domain computer routines capable of representing distributed, constant transmission lines [10.10 - 10.11].

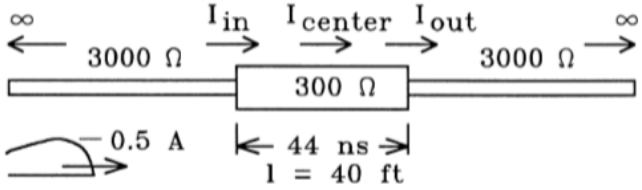

(a) Geometry

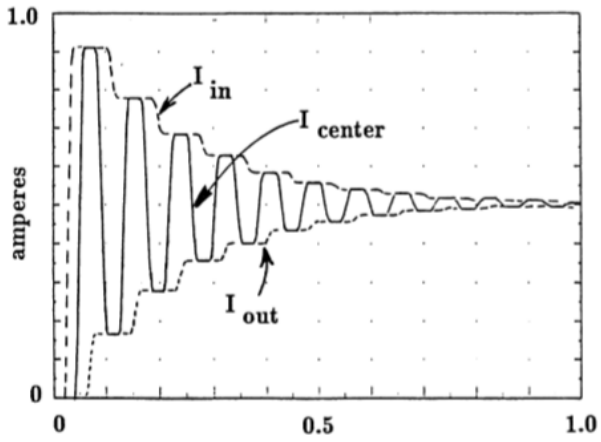

(b) Waves excited by a 10 ns rise time

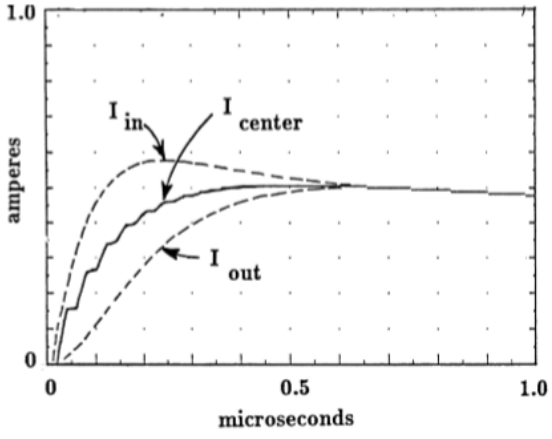

(c) Waves excited by a 0.5 μs rise time.

Fig. 10.22 Calculated response of a 12 m (40 ft.) aircraft to charge injection.

Oscillation modes on aircraft

Oscillations like those described in the preceding discussion can be excited on aircraft, although such oscillations are more complex. One reason for the complexity is that there are several modes of oscillation that can be excited, such as nose to tail and wing to wing, and these modes are not independent of each other either. For example, a wave traveling nose to tail would have two components, as shown in Fig. 10.23; one that propagated back and forth along the fuselage and one that reflected along the wings. The ringing frequencies of these oscillations are determined by the length of the paths involved. An aircraft with a nose to tail length of 20 meters would have a ringing frequency about 3 MHz.

The actual ringing frequencies can be determined by test or can be calculated by the 2D and 3D, time domain, analytical techniques described in the preceding sections. Aircraft full vehicle tests (FVTs) have shown evidence of traveling waves, especially when the aircraft was not terminated to the test current return conductor array through resistors approximately equal in value to the characteristic impedance of the aircraft and its return conductor array (typically ~100 Ω). This topic is discussed in Chapter 13. Induced voltages measured in many airplanes have showed oscillations that may have been due to airframe traveling waves, although the measured electric circuits inside the aircraft could also have been ringing. This possibility complicates the task of assessing the cause (or causes) of these responses.

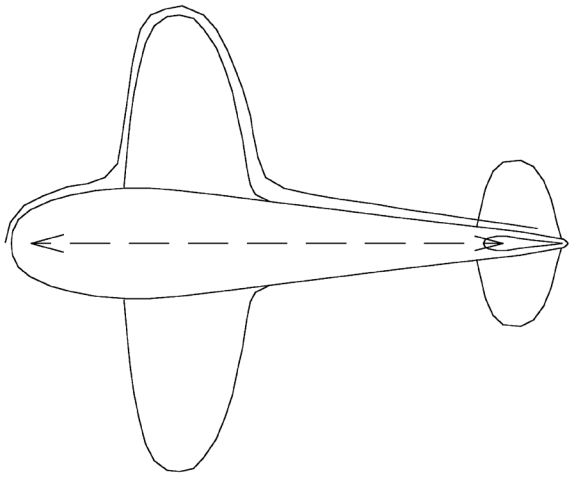

Fig. 10.23 Current paths for nose-to-tail traveling waves. Solid and dashed lines represent range of current paths.

Significance of oscillations

Aircraft traveling waves are important factors in induced effects protection design because they have faster rates of change than either the incident lightning leader or the stroke currents. This means that fields associated with these traveling waves and penetrating apertures can induce higher voltages in unshielded circuits inside the aircraft than the stroke or leader currents themselves. If the aircraft ringing (i.e., resonant) frequency happened to coincide with the ringing frequency of a wiring harness, the electrical energy on the exterior of the aircraft would couple more efficiently to the internal wiring. The natural ringing frequency of the wiring harness is determined more by the physical length of the harness than by the length of the aircraft. Transients induced in small aircraft tend to ring at higher frequencies than those induced in large aircraft. In part, this can be explained by the differences in the lengths of wiring harnesses in aircraft of different sizes. The way airframe traveling wave effects should be interpreted for aircraft certification purposes is discussed in Chapter 13.

Resonances with lightning:

The nature and importance of aircraft oscillations is less clear in the case of lightning, partly because the oscillations are damped by the attached conducting arc channel. Calculating the effects of lightning-induced aircraft resonance is difficult because the impedance of the arc channel is not constant; it changes with time and with the amount of current flowing in the arc. An assumed lightning channel impedance of 3 000 ohms (as used in Fig. 10.22 to illustrate traveling waves) would be more representative of the channel as it is conducting a stroke current than during the leader formation phase, when the leader is propagating from the aircraft. No measurements have been made of actual characteristic impedances of lightning channels attached to aircraft (nor would this be possible), although values of several thousand ohms have been inferred from measurements of aircraft responses.

Significance of aircraft initiated lightning

Current pulses associated with the initial development of an aircraft-initiated lightning flash are believed to have fast rise times. If this is true, the impedances shown in Fig. 10.22 are representative of the impedance of a developing lightning leader.

In view of the uncertainties associated with the impedance of a lightning arc, it may be appropriate to view calculations of the interaction of an aircraft with a lightning channel with caution.

Resonances with aircraft tests

One place where the oscillations associated with aircraft traveling waves are important is during the aircraft FVTs that are conducted to measure the voltages induced on aircraft wiring. Interactions between the aircraft and the test circuit govern the waveform of the current that can be injected into the aircraft. The currents associated with these oscillations may vary from one portion of the aircraft to another. Also, current in the aircraft may differ from the current measured at the generator's output terminal. This subject is discussed further in Chapter 13.

10.8 Composite Aircraft

The analyses in this chapter have focused on metal aircraft because, as far as the external electromagnetic field distribution is concerned, metal airframes can usually be accurately modeled as perfectly conducting. The distribution of current does change from an initial state, governed by magnetic fields, to a final state, governed by resistance, but the timescale over which that redistribution takes place is long compared to the duration of lightning currents. (The factors governing redistribution are discussed in more detail in Chapter 11).

However, some aircraft structures consist of significant amounts of CFC material. CFC is three orders of magnitude less conductive than aluminum. This is still a small resistance compared to the source impedance of a lightning stroke current so that the aircraft material, whether CFC or aluminum of some combination thereof, is not sufficient to influence the magnitude or waveshape of the stroke current.

CFC in the airframe will cause the stroke currents to redistribute throughout the aircraft over their lifetimes in a manner different than will be the case if the entire airframe is made of aluminum. The factors influencing current paths through the airplane are described in Chapter 11. Stroke current redistribution in aircraft structures consisting of a mixture of metal and composites takes place much more rapidly than on all-metal structures. This is due to the shorter L/R time constants associated with the CFC structure elements as compared with aluminum elements. As a result, the external current distribution and the internal coupling on CFC aircraft cannot be regarded as distinct issues. Current penetrates to the interiors of such aircraft on a timescale comparable to the duration of lightning stroke current. As a result, voltages coupled to internal circuits of CFC aircraft have higher magnitudes and larger resistive components than voltages on metal aircraft.

References

10.1 V. Belevitch, "The Lateral Skin Effect in a Flat Conductor," Philips Technical Review, 32, 6/7/8/ (1971): 221-231.

10.2 H. Kaden, "Über den Verlustwiderstand von Hochfrequenzleitern," (On the Resistance of High Frequency Conductors), *Archiv für Elektrotechnik*, 28 (1934): 81825.

10.3 J. B. Scarborough, *Numerical Mathematical Analysis*, 6th ed. (Baltimore: Johns Hopkins University Press, 1966).

10.4 G. E. Forsythe and W. R. Wasow, *Finite-Difference Methods for Partial Differential Equations* (New York: John Wiley and Sons, 1960).

10.5 K. J. Maxwell, F. A. Fisher, J. A. Plumer, and P. R. Rogers, "Computer Programs for Prediction of Lightning Induced Voltages in Aircraft Electrical Circuits," *AFFDL-TR-75-36,Vol 1*, April 1975.

10.6 F. A. Fisher, "Analysis and Calculations of Lightning Interactions with Aircraft Electrical Circuits," *AFFDL-TR-78-106*, August 1978.

10.7 F. A. Fisher and J. A. Plumer, *Lightning Protection of Aircraft*, NASA Reference Publication # 1008, October 1977.

10.8 P. L. Rustan and J. P. Moreau, *Aircraft lightning Attachment on Low Altitudes*, *10th Int. Aerospace and Ground Conf. On Lightning and Static Electricity*, Paris, France, June 1985.

10.9 W. Radasky, *An Examination of the Adequacy of the Three Species Air Chemistry Treatment for the Prediction of Surface Burst EMP*, *Defense Nuclear Agency, DNA 3880T*, December 1975.

10.10 L. V. Bewley, *Traveling Waves on Transmission Systems*, Dover, New York, 1963 or John Wiley and Sons, New York, 1933 and 9151, Chapter 4.

10.11 *Electrical Transmission and Distribution Reference Book*, Westinghouse Electric Corporation, East Pittsburg, PA, 1950, Chapter 15.

Chapter 11

THE INTERNAL FIELDS COUPLED BY DIFFUSION AND REDISTRIBUTION

11.1 Introduction

Lightning currents and electromagnetic fields on the outside of an aircraft reach the inside of the aircraft through apertures and also by the processes of diffusion and redistribution. Generally speaking, penetration through apertures, which is discussed in Chapter 12, is a high frequency mechanism, while coupling through diffusion and redistribution (the subjects of this chapter) are low frequency mechanisms. Thus, fields that penetrate through apertures have rise and decay times like the external fields, whereas fields that appear on the interior of an aircraft by diffusion or redistribution have much longer rise and decay times, associated with diffused and redistributed currents. Diffusion refers to the process by which electric and magnetic fields penetrate through conducting materials along with diffused currents. Redistribution refers to the process by which the overall pattern of current flow throughout an aircraft changes from an initial state, where current distribution is controlled by magnetic fields, to a final state, where current distribution is controlled by structural resistances. The factors that affect diffusion and redistribution on metal structures are the same factors that affect the electromagnetic shielding of such structures, although it might be better to say that diffusion and redistribution are the mechanisms by which electromagnetic shielding is obtained.

In the context of this book, diffusion primarily relates to the process by which electric fields build up on the inner surfaces of an aircraft in response to the diffusion of lightning current from exterior to interior surfaces of the aircraft's skin. In the most elementary terms, electric fields produced by diffusion arise from the passage of lightning current through the resistance of the aircraft. A more thorough discussion must be based on surface and transfer impedances, subjects that were introduced in Chapter 9.

Carbon fiber composite (CFC) materials have conductivities about three orders of magnitude less than that of aluminum. This means that, the concepts of redistribution and diffusion are especially significant for CFC aircraft.

When lightning strikes such an aircraft, the early time (or high frequency) portion of the lightning current distributes in the same manner as it would on an all-metal aircraft, but the late time (or low frequency) component distributes according to the relative resistances of the various structural parts. Thus, there is much more current in metal structural elements on or within a 'CFC' aircraft than there would be on a comparable, all metal aircraft.

Another way of viewing this subject is that CFC aircraft provide much less electromagnetic shielding than all-metal aircraft. Magnetic field shielding that might be inherent to, and taken for granted on, an all-metal aircraft may have to be intentionally provided on a CFC aircraft, usually with an unfavorable impact on weight and cost.

In the sections that follow, internal and external electromagnetic fields are discussed first, in order to differentiate somewhat between concepts used for lightning interactions and classic electromagnetic shielding problems. Concepts of circuit voltage are discussed next, first for a circular cylinder where only diffusion effects are encountered and then in terms of elliptical cylinders where redistribution effects must be considered. This portion also includes a discussion of the processes by which external current produces magnetic fields inside cavities such as equipment bays. Redistribution effects are then illustrated for the more complex structures, where recourse must be made to numerical analysis techniques.

11.2 Internal vs. External Fields

Fig. 11.1 shows a metal sheet defining an interior volume. For the following discussions, the sheet can be regarded either as flat and of infinite extent or as closed and having a radius of curvature that is large in comparison to the thickness of the sheet. On the outside of the sheet an electromagnetic field is impressed, this being associated with a current flowing in the sheet. Some portion of the external electromagnetic field penetrates through the sheet and couples to the interior volume defined by the sheet.

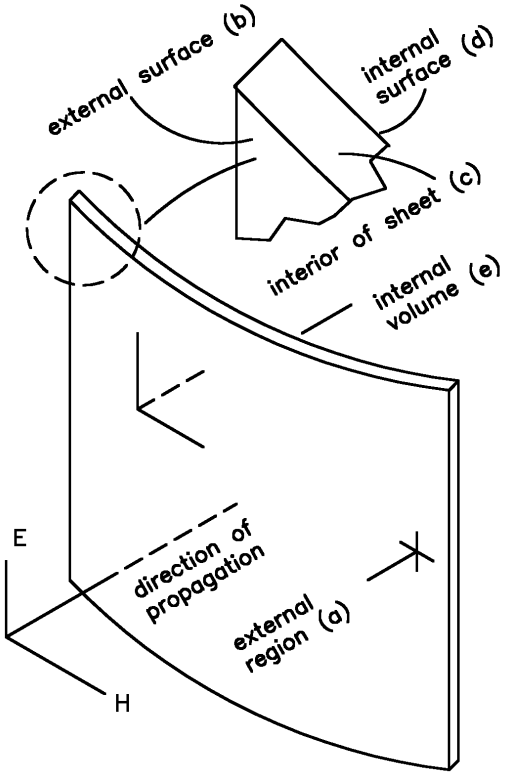

Fig. 11.1 A plane wave incident upon a shielding surface.

Five regions important to the interaction problem can be defined:

(a) The external region.
(b) The external surface ($z = 0$).
(c) The interior of the sheet.
(d) The internal surface ($z = d$).
(e) The internal volume.

Regions (a) and (b) are the main ones involved in the interaction between the sheet and any impinging electromagnetic field. Regions (b), (c) and (d) affect the way the fields penetrate the sheet while regions (d) and (e) affect the way fields build up in the interior volume.

The penetration of fields to the interior is often discussed in terms of "shielding effectiveness (SE)", but there are two different ways that the external electromagnetic fields may be visualized. They can give rise to two very different measures of the SE of a structure.

11.2.1 Impinging Electromagnetic Field

In the most common treatment of electromagnetic shielding, the field at the surface, region (b), above, is produced by some external source in region (a) that causes a field to propagate toward the surface. When the incident field arrives at the surface it is partially reflected, and the reflected wave propagates back, away from the surface. The sum of these incident and reflected waves, with proper regard for polarity, is what appears at the surface of the sheet. If the sheet were a perfect conductor, the polarities of the incident and reflected waves would be such that their resultant magnetic field would be tangential to the surface and the resultant electric field would be normal to the surface.

The magnitude of the resultant field depends on the shape of the conducting sheet and its orientation toward the incoming wave. With a flat conductor of infinite extent, oriented broadside to the incoming wave, the tangential magnetic field would have twice the amplitude of the incoming field and the electric field would become zero. For other angles of incidence, the tangential magnetic field would have less than twice the magnitude of the incoming field and a radial electric field would develop. The fields that develop at curved surfaces might have several times the magnitude of the incoming field. This condition is not representative of a lightning strike condition, in which the fields at the surface of an aircraft are determined by the lightning current in the airframe, not from some external source. (An externally originated field might occur from a nuclear electromagnetic pulse (NEMP) event, or from another radiated field source.)

Shielding effectiveness (SE)

For an impinging field, the SE is usually taken to be the ratio of the external impinging magnetic field to the internal magnetic field, expressed as

$$SE = 20 \log \left[\frac{H_e}{H_i}\right] \; dB \qquad (11.1)$$

An effectiveness of shielding against electric fields could be defined in a similar fashion but shielding against electric fields is usually an easier task than shielding against magnetic fields. The impinging magnetic or electric field is that which would exist in the absence of the sheet and should not be confused with that which appears at the surface of the sheet.

The SE can be taken to have three components; one due to reflection at the surface, one due to transmission of the field through the sheet, and one due to the way that the fields build up on the internal volume. As defined in Eq. 11.1, the SE is largely determined by how well the surface reflects the incident electromagnetic field.

11.2.2 Injected Current

In many lightning interaction problems, the magnetic field at the surface is the result of injecting current into a structure and can be determined directly from the current density. The SE is best defined in terms of the magnetic fields that appear at the exterior surface (H_s) due to the current in the structure, and the field that appears inside the structure (H_i), thus,

$$SE = 20 \log \left[\frac{H_S}{H_i}\right] \; dB \qquad (11.2)$$

This definition of SE deals only with the propagation of magnetic fields through the sheet and their appearance within to the interior volume. There is an external field produced by the conducted current as well, but any discussion of incident and reflected waves would be a roundabout way of determining the external field. Since the current is the independent variable in this discussion and the external field is the dependent one, the external 'surface reflection factor' is not a matter for consideration.

Thus, SE has a lower value than in the case where the current is produced by an impinging field. Most high intensity radiated fields (HIRF) and external electromagnetic interference (EMI) sources produce fields that originate at locations far from the airplane.

11.3 Diffusion Effects

The way that diffusion influences voltage on electrical circuits will first be illustrated for circular cylinders; partly because these effects are easiest to analyze for cylindrical geometries and partly because those or similar geometries are often encountered in lightning interaction problems.

11.3.1 Direct current (DC) Voltage on Circular Cylinders

Consider Fig. 11.2, in which a current, I, is entering a circular cylinder. This current is assumed to rise from zero to its peak in 0.25 μs. This is shorter than the rise times of most lightning stroke events but serves to accentuate the magnetically induced voltage to be described in this example.

The cylinder is considered long compared to other dimensions, so that end effects can be neglected, but short compared to the electrical wavelength of any of the frequency components of the current I. The return path for the current is not shown, but it is assumed to be sufficiently far away from the cylinder so that there are no proximity effects. Also shown are two conductors, one external (conductor 1) and one internal (conductor 2) to the cylinder. These are connected to an end cap having negligible resistance and, since the current is conducted through the cap uniformly, no electromagnetic fields penetrate it.

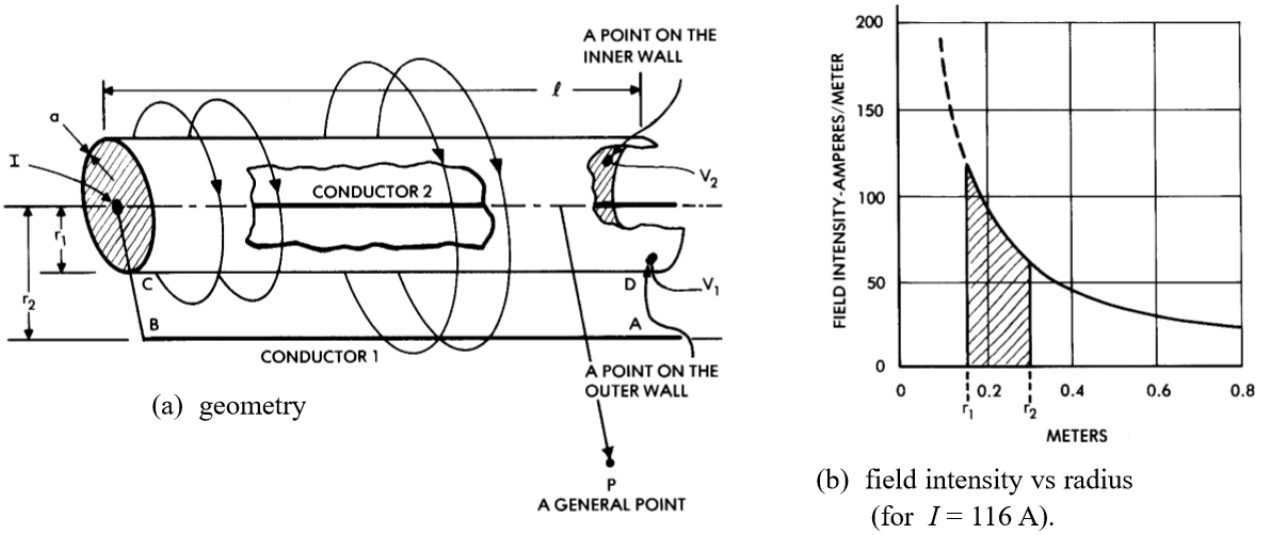

Fig, 11.2 Magnetic fields around a circular cylinder.

At the other end of the cylinder are shown two voltages; V_1 measured from conductor 1 to the external surface of the cylinder, and V_2 measured from conductor 2 to the inner surface of the cylinder.

DC resistance

The cylinder has a DC resistance:

$$R = \frac{\rho l}{A} = \frac{\rho l}{2\pi r a} \qquad (11.3)$$

where

ρ = volume resistivity
l = length
A = cross sectional area
r = radius
a = thickness (a « r).

If the cylinder has the following dimensions and is made from aluminum, (having a volume resistivity, ρ, of 2.69 x 10^{-8} Ω·m),

l = 2 m v
r = 15.7 cm
a = 0.381 mm (0.015 in)

then the DC resistance, R, will be 0.14 x 10^{-3} ohms.

If the input current is 116 amperes (a value chosen because it was used in an experimental verification of the concepts), a voltage

$$e = IR = 116 \times 0.14 \times 10^{-3} = 0.017 \text{ V} \qquad (11.4)$$

will be developed along the cylinder and this same voltage rise would be measured by a conductor either inside or outside the cylinder.

Transient conditions

V_1 is not equal to V_2 until steady-state conditions are established, and neither of these voltages is equal to the steady-state, DC resistive voltage rise. Let us first consider voltage V_1, which can be regarded as the line integral of the potential around the path ABCD in Fig. 11.2 (see Chapter 9).

This voltage has two components; a magnetically induced voltage due to the changing magnetic flux associated with the total current in the cylinder that passes through the loop ABCD and a voltage due to the surface impedance along the path CD. Under DC conditions, that surface impedance reduces to the DC resistance discussed above.

11.3.2 External Voltage on the Cylinders

On the outside surface of the cylinder the flow of current sets up a magnetic field of intensity

$$H = \frac{I}{2\pi r} \qquad (11.5)$$

where

I = current
r = radius
H = magnetic field intensity.

This field has a geometry like that shown in Fig 11.2(b). The magnetically induced component of V_1 is:

$$V_1 = \frac{d\varphi}{dt} = \mu_o l \ln\left|\frac{r_1}{r_2}\right| \frac{dI}{dt} \qquad (11.6)$$

while φ (the flux passing through the loop ABCD) is represented by the shaded area in Fig. 11.2(b). The flux, φ, is measured in Webbers. Remembering that

$$\mu_o = 4\pi \times 10^{-7} \text{ A/m} \qquad (11.7)$$

V_1 becomes

$$V_1 = 2 \times 10^{-7} l \ln\left(\frac{r_1}{r_2}\right) \frac{di}{dt} \qquad (11.8)$$

If r_2 were 31.4 cm and the indicated current of 116 A in Fig. 11.3 reached peak in 0.25 μs, then V_1 would reach an initial voltage of 129 V. As steady state conditions were reached, and the external magnetic field ceased to change with time, V_1 would decay to its steady state value of 0.017 V from Eq. 11.4.

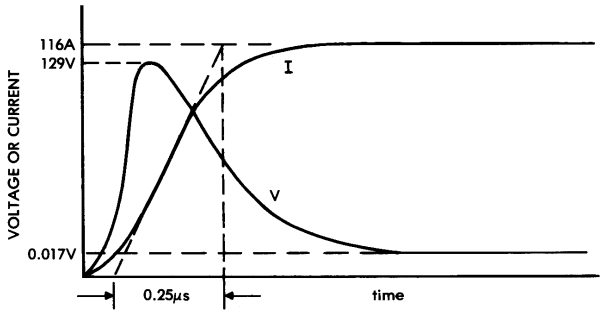

Fig. 11.3 External voltage (not to scale).

Influence of skin effect

This analysis ignores the skin effect, a phenomenon that causes the first part of lightning stroke currents to flow mostly on the exterior surfaces of metal airplane skins and other metal conductors. For electrical wiring outside the cylinder, the increased current density in the exterior of a conventional metal skin is of little consequence compared to the much larger voltage induced by the changing magnetic field that encircles the entire conductor (i.e., fuselage).

Example of external conductors

While it is unusual to locate conductors outside an aircraft fuselage, this is done on occasion. An example is the wire harness commonly installed on the exterior of a turboshaft or turbojet engine that is exposed to full threat lightning currents entering the engine, via a propeller or an exposed exhaust pipe. Another example might be external cables on a missile or rocket that run between an electronic control unit (ECU) in the nose and the engine controls mounted on the engine in the tail area. Of necessity, such cables must run outside the fuel and oxidizer tanks, as shown in Fig. 11.4. If the cables are not in a shielded cable tunnel, they will be exposed to the external magnetic field.

Simplified expression

If the spacing between the wires and the surface of the vehicle is not large, Eq. 11.8 may be somewhat simplified, since the magnetic flux density does not vary greatly with distance from the surface of the vehicle (within the context of the example) and may, therefore, be considered uniform.

$$V_1 = \frac{2\times10^{-7} ld}{r} \cdot \frac{di}{dt} \qquad (11.9)$$

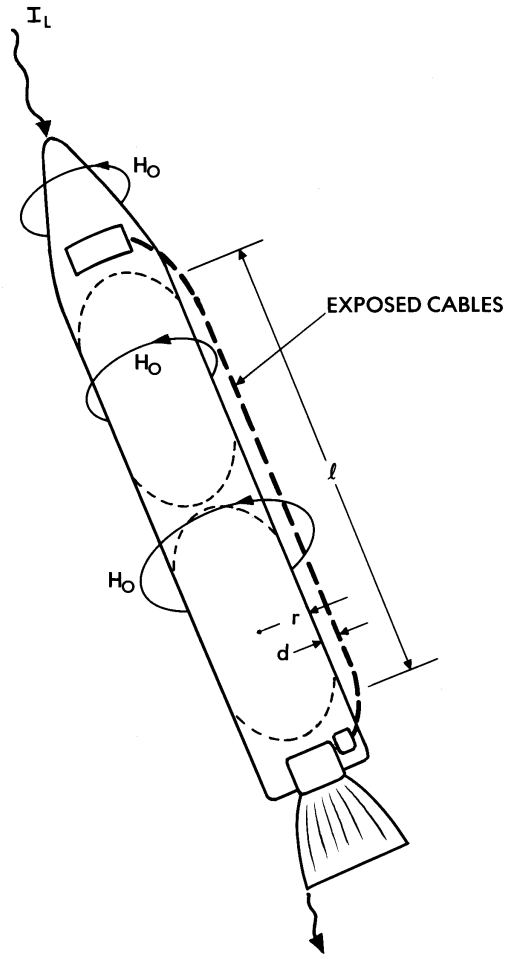

Fig. 11.4 Exposed cables

11.3.3 Internal Voltage on Circular Cylinders

Let us now consider the conditions inside the cylinder. As with the external voltage, the voltage, V_2, indicated in Fig. 11.5 can be defined as the line integral of potential around the path ABCD. The voltage, again, has two components, one due to the changing magnetic field passing through the loop ABCD and one due to the flow of current around that path. Conditions inside the cylinder, however, are very different from those on the outside.

First, the magnetic field inside the inner surface of the cylinder is zero, as explained in Chapter 9. If there is no magnetic field, there can be no magnetically induced voltage. Any voltage induced on internal wiring would be due to the flow of current through the resistance of the various portions of the circuit.

There would be no voltage along the path BC, since we have assumed a perfect conductor for the end cap, and there would be no resistive voltage along the path CD, since we have assumed an open circuit between points A and D, which implies no current along the path CD. Whatever voltage appears must be due to the resistive rise along the path AB.

Cause of skin effect

The voltage rise along the internal path AB, indicated in Fig. 11.5, would be completely different from that along the path CD, indicated in Fig. 11.2. This difference can be attributed to the skin effect, which delays the buildup of current on the inner surface of the cylinder. The origin of the skin effect phenomenon is illustrated in Fig. 11.5. If a magnetic field line is assumed to be suddenly established inside the wall of the conducting cylinder, eddy currents are induced around that field line. These eddy currents induce a magnetic field of opposite polarity to of the external magnetic field. Only as the eddy currents decay can the magnetic field, and associated current, penetrate the wall of the cylinder. Further analysis of the resistively generated voltages requires a discussion of surface and transfer impedances.

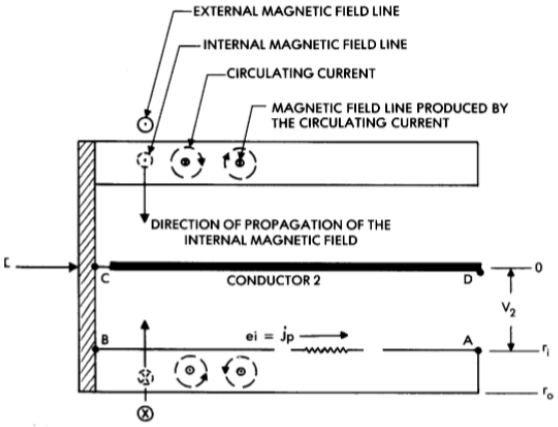

Geometry and decaying eddy currents.

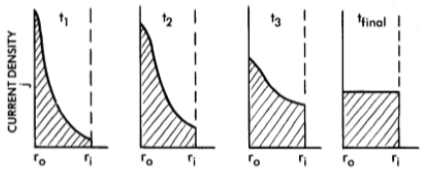

Current density at different times.

Fig. 11.5 Factors governing the internal voltage.

11.3.4 Surface and Transfer Impedances

The surface impedance Z_s, is the ratio of the electric field on the external surface to the current density on the external surface, while the transfer impedance, Z_t, is the ratio of the electric field on the internal surface to the current density on the external surface. Formulations can be given in either the frequency or the time domain.

Frequency domain formulation

Exact expressions for surface and transfer impedance of a flat sheet were given in Chapter 9 but, for most cases of practical interest, simplified expressions [11.1] are sufficiently accurate.

$$z_s(\omega) = \frac{jkm}{\sigma}\coth(jk_m d) \qquad (11.10)$$

$$Z_t(\omega) = \frac{\frac{k_m}{\sigma}}{\sin(k_m d)} \qquad (11.11)$$

where

$$k_m \approx \frac{1}{\sqrt{2}}(1-j)(\omega\mu_2\sigma)^{1/2} \qquad (11.12)$$

and

d = thickness
σ = conductivity.

While Eqs. 11.10 and 11.11 can be readily evaluated in the frequency domain, it is sometimes helpful to use series formulations. This can be done by expressing the coth(x) and sin(x) functions by their series expansions.

$$\coth(x) = \frac{1}{x} + \sum_{n=1}^{\infty}\frac{1}{(n\pi)^2+x^2} \qquad (11.13)$$

$$\sin(x) = x\prod_{n=1}^{\infty}\left(1-\frac{x^2}{n^2\pi^2}\right) \qquad (11.14)$$

Substituting these expressions into Eqs. 11.10 and 11.11 gives:

$$Z_Z(\omega) = \frac{1}{\sigma d} + j\omega\left(\frac{2}{\sigma d}\right)\sum_{n=1}^{\infty}\frac{1}{\omega_n + j\omega} \qquad (11.15)$$

$$Z_t(\omega) = \frac{2}{\sigma d}\sum_{n=1}^{\infty}\frac{(^{-}1)^{n+1}}{(1+j\omega/\omega_n)} \qquad (11.16)$$

where

$$\omega_n = \left(\frac{n\pi}{d}\right)^2 \frac{1}{\mu\sigma} \qquad (11.17)$$

These formulations [11.2] are applicable to flat sheets or to sheets having radii of curvature that are large in comparison to the thickness of the sheet. For other geometries, refer to the formulas in Chapter 9.

Variation with frequency

Figs. 11.6(a) and 11.6(b) show how surface and transfer impedance vary with frequency. Fig. 11.6(a) relates to a CFC sheet 6.35 mm (0.25 in) thick and having a resistivity 5 x 10^{-5} ohmmeters, a resistivity typical of some CFC materials, while Fig. 11.6(b) relates to an aluminum sheet 1.27 mm (0.05 in) thick and having a resistivity of (ρ = 2.69 x 10^{-8} ohm-meters). Note the differences in panel thicknesses.

Inspection of the equations and the figures show that at low frequencies both impedances reduce to a DC value:

$$Z_s = Z_t = \frac{1}{\sigma d} \qquad (11.18)$$

This low frequency (or DC) value has the units of ohms but is generally specified as 'ohms per square', that is, the impedance between opposite sides of a square of any size.

At higher frequencies, the surface impedance rises, and the transfer resistance falls. In the limit, the surface impedance approaches the value:

$$Z_s = \sqrt{\frac{j\omega\mu}{\sigma}} \qquad (11.19)$$

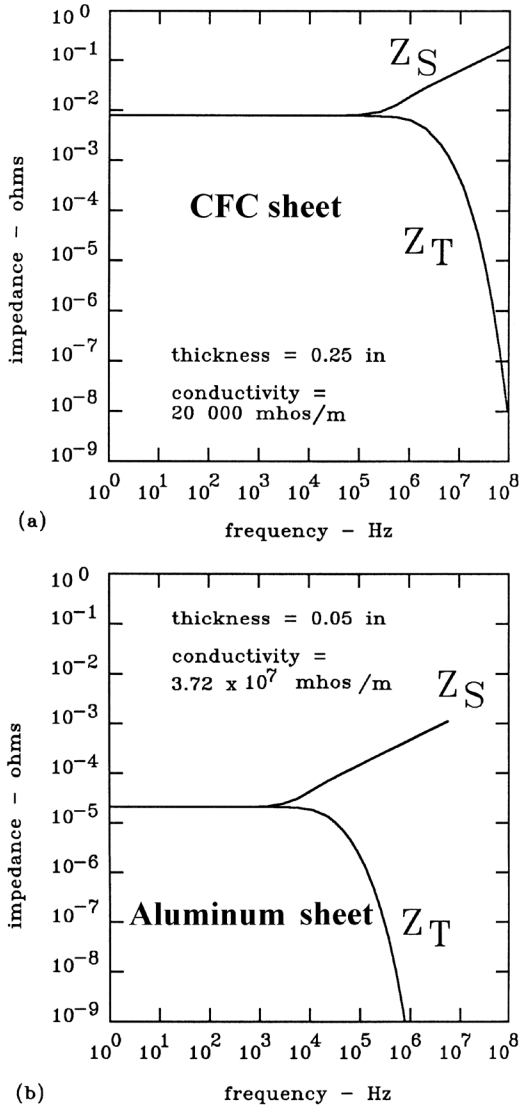

Fig. 11.6 Frequency dependence of surface and transfer impedance.

The surface impedance thus approaches the intrinsic impedance of the material, has equal resistive and reactive components, and has a magnitude that varies as the square root of frequency. This is the phenomenon frequently referred to as the 'skin effect'.

Time domain formulation

$Z_s(\omega)$ and $Z_t(\omega)$ are defined in Eqs. 11.15 and 11.16 by the poles, ω_n, given by Eq. 11.17. The first order pole, given by

$$\omega_1 = \left(\frac{\pi}{d}\right)^2 \frac{1}{\mu\sigma} \quad (11.20)$$

is used to define the diffusion or penetration time constant, τ, according to

$$\tau = \frac{1}{\omega_1} = \mu\sigma\left(\frac{d}{\pi}\right)^2 \quad (11.21)$$

The penetration time constant can also be given as

$$\tau = \frac{L}{\pi^2 R} \quad (11.22)$$

where R is the resistance of the surface and L is the internal inductance.

In response to a step function of injected current, I, the current density J at any point x in the sheet can then be given as [11.3]:

$$J(x) = I\left[1 + 2\sum_{n=1}^{\infty}(-1)^n\left(\varepsilon^{n^2 t/r}\right)\cos\left(n\pi\frac{x}{d}\right)\right] \quad (11.23)$$

In Eq. 11.24, x = 0 at the inner surface and $x = d$ at the surface where current is injected. The current density at the surface where current is injected is given by evaluating Eq. 11.23 for $x = d$.

$$J_s = \sigma I\left[1 + 2(\varepsilon^{t/r} + \varepsilon^{4t/r} - \varepsilon^{9t/r} - \varepsilon^{16t/r} + L)\right] \quad (11.24)$$

The current density at the other surface is given by evaluating Eq. 11.23 for $x = 0$.

$$Z_t(t) = \sigma I\left[1 - 2(\varepsilon^{t/r} - \varepsilon^{4t/r} - \varepsilon^{9t/r} - \varepsilon^{16t/r} - L)\right] \quad (11.25)$$

In response to a step function applied current, the current density along the inner surface builds up as shown in Fig. 11.7 and produces an incremental voltage, which is the product of the current density and the resistivity of the surface. The voltage along the interior surface path AB is then given by integrating these incremental voltages. Since the voltage along the path AB is the only component of voltage V_1, it follows that V_1 will eventually rise to a value equal to the product of the current and the DC resistance of the cylinder and the injected current.

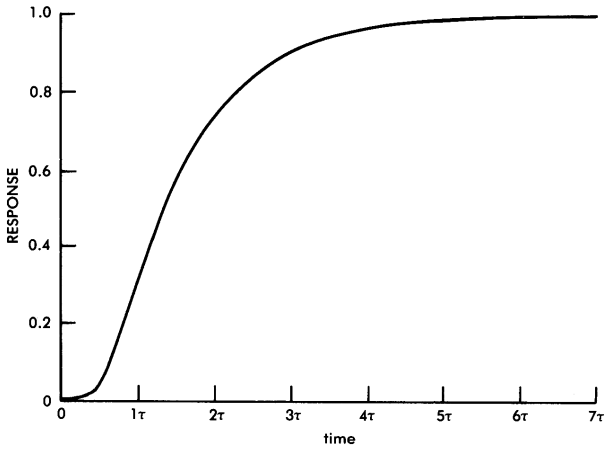

Fig. 11.7 Diffusion-type response to a step function.

11.3.5 Characteristic Diffusion Response

This response curve is called a *diffusion-type* response and is characteristic of many types of situations involving the transmission of energy through a distributed medium. Another example is the transfer of heat into a block of matter when a heat flux is suddenly applied to one face of the block. Another is the transmission of electrical energy through the *R/C* or *L/R* ladder network shown in Fig. 11.8. Fig. 11.8(b) is often used to illustrate the skin effect.

Diffusion response curve

Two important observations can be made about the shape of the response curve shown in Fig. 11.7. The first is that the response initially changes only slowly and thus has a zero first derivative, unlike a simple exponential response, which has a finite first derivative. The second is that the response approaches its final value much more slowly than simple exponential responses do. In three-time constants (as defined by Eq. 11.22), the response has reached 90% of its final value, but the rise to 99% of peak value takes nearly 20 time constants. In contrast, an exponential response reaches 95% of its final value in three time constants and reaches 99% in 4.65 time constants.

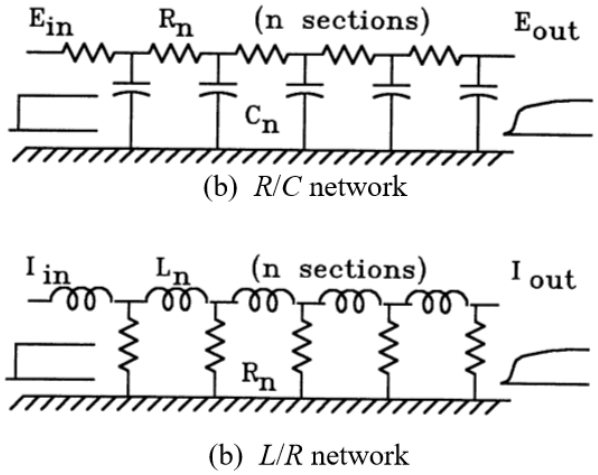

Fig. 11.8 Ladder networks displaying a diffusion-type response.

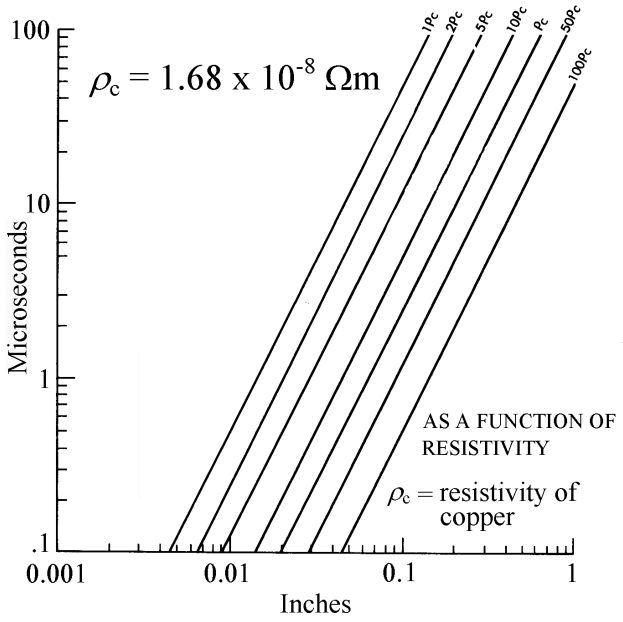

Fig. 11.9 Skin thickness vs penetration time constant.

Influence of material

With respect to Eq. 11.22, it should be noted that the penetration time constant is directly proportional to the permeability of the material, inversely proportional to the resistivity of the material and directly proportional to the square of the thickness of the material. The relative permeability of structural materials used in aircraft is always nearly unity (i.e., the permeabilities of aluminum and composite materials commonly used for aircraft skins are nearly the same as that of air) but thickness and resistivity can vary over wide ranges.

For reference, Eq. 11.21 is plotted in Fig. 11.9 as a function of material thickness and resistivity. (The resistivities of some typical metals are given in §9.3.3.) If we assume an aluminum alloy sheet with a resistivity of 2.69 x 10^{-8} ohmmeters and a skin thickness of 1.016 mm (0.040 in), the penetration time constant would be 3.9 μs. If a step function of current were established on the outside of this sheet of metal, it would take 11.7 μs for the current density on the other side to reach 90% of its final value. If the duration of the injected current pulse were short compared to 11.7 μs, the response would never reach the full *IR* voltage.

Responses to other waveforms

The response to other waveforms can be obtained by application of the convolution, or superposition, integral:

$$[f(t, I(t), \tau)] = \frac{d}{dt}\int_0^t E(t-\tau)I(t)d\tau \qquad (11.26)$$

Graphically, the elements of Eq. 11.26 are shown in Fig. 11.10. Just as an arbitrary waveform can be regarded as the summation of a series of elementary step functions, the response to that arbitrary waveform can also be regarded as the summation of a series of step function responses. This process is described in many textbooks on circuit theory, such as [11.1]. It is also described in [11.3], along with a computer routine for handling numerical data. Convolution assumes linear conditions, such as would prevail, for all practical purposes, in metals. The electrical properties of CFC materials *might* be sufficiently non-linear to render convolution calculations inaccurate.

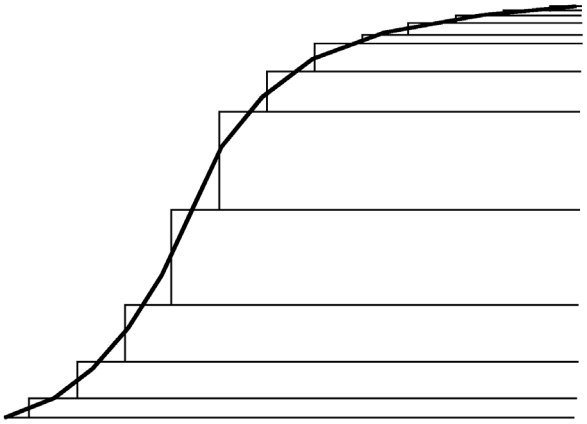

Fig. 11.10 A wave approximated as a superposition of step functions.

Equivalent circuits

The L/R network shown in Fig. 11.8(b) is a valuable model for representing diffusion effects, because it can be directly solved with a variety of network-analysis computer programs, most of which can utilize continuous driving functions, rather than step functions. The internal inductance of the surface is represented by *n* incremental inductors in series, while the DC resistance is represented by *n* +1 incremental resistors in parallel.

For example, consider the 2-meter-long circular cylinder treated in §11.3.1 and §11.3.2. The exact internal inductance of such a cylinder is

$$L_i = \frac{\mu}{2\pi} \ln\left[\frac{r_o}{r_i}\right] \text{ henrys} \qquad (11.27)$$

or, for nonmagnetic materials, such as aluminum

$$L_i = 2 \times 10^7 \ln\left[\frac{r_o}{r_i}\right] \text{ henrys} \qquad (11.28)$$

An approximate expression applicable to thin tubes is

$$L_i = \frac{\mu l d}{2\pi r} \qquad (11.29)$$

For a flat sheet of 1-meter width, length *l* and thickness *d*, the internal inductance would be simply

$$L_i = \mu l d \qquad (11.30)]$$

Using the dimensions of the 2-meter-long cylinder discussed in §11.3.1 and §11.3.2,

$r_i = 0.157$ m
$r_o = 0.157$ m + 0.000381 m
$L_i = 9.695 \times 10^{-10}$ H

An equivalent circuit can be obtained by dividing this series inductance into four equal parts, L, each 2.424×10^{-10} henrys, as noted on Fig. 11.11. The incremental resistance, R, in the figure is the 1.43×10^{-4} ohms calculated in §11.3.1 and divided into five parallel sections.

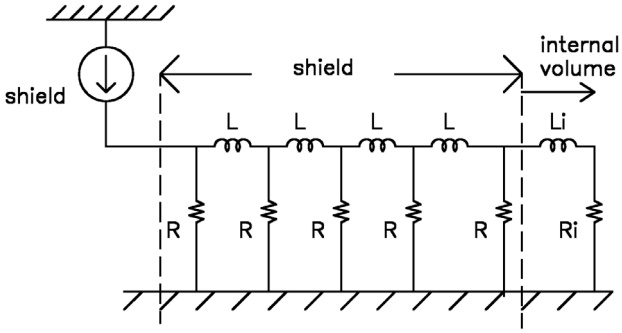

Fig. 11.11 Equivalent circuit representing a propagation through solid wall cylinder.

where

$L = 2.424 \times 10^{-4}$ henrys
$R = 2.860 \times 10^{-5}$ ohms
$L_i = 1 \times 10^{-6}$ henrys
$R_i = 1 \times 10^{-3}$ ohms

The response of this 2-meter-long tube to two different driving function waveforms is shown in Fig. 11.12. The figure shows how the waveform of the internal response may be almost independent of the waveform of the external driving current, a situation that occurs if the duration of the external current is short compared to the pulse penetration time. The amplitude of the internal response depends on the external driving current.

Internal cavity impedance

The equivalent circuit in Fig. 11.11 can be extended by incorporating the internal impedance, R_i and L_i of the volume bounded by the shielding surface. In general, the internal impedance bounded by the surface is dominated by the internal inductance. This leads to the observation that the internal current is:

$$I_i = \frac{1}{L_i}\int E_i dt \qquad (11.31)$$

The magnetic field will have the same shape as that predicted by Eq. 11.31, which is to say that the derivative of the internal magnetic field will have essentially the same shape as the current I_i shown on Fig. 11.12.

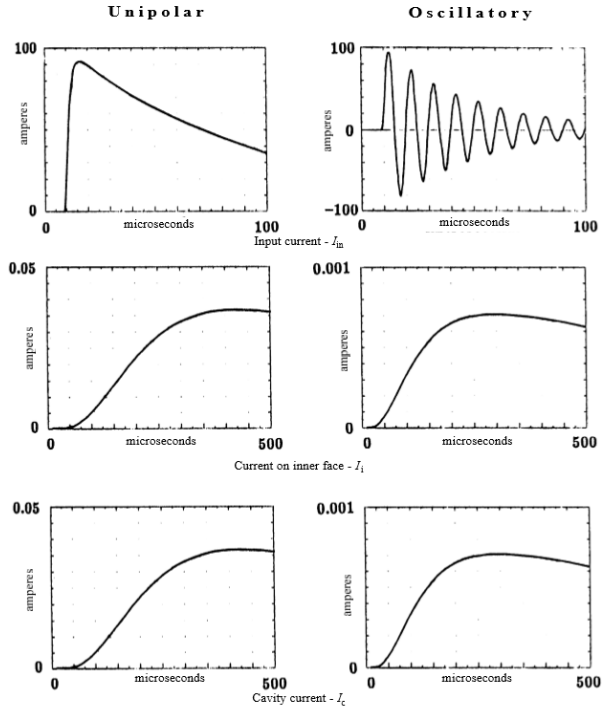

Fig. 11.12 Internal and external waveforms

The question of the fields within cavities is discussed further in §11.6.

11.4 Redistribution

In many cases, analysis of lightning interactions must account for the phenomenon of redistribution, the process by which the division of current changes from an initial state, governed mostly by inductive effects, to one governed by resistive effects. Lightning currents redistribute from the skins of the aircraft to interior structural elements and other interior conductors. An elementary example of redistribution can be illustrated using the *RL* circuit shown in Fig. 11.13. The figure also shows the waveform of the current in each of the two branches.

A current pulse of short duration that enters the network divides between the two branches in inverse proportion to their respective inductances, but a pulse with a long rise time and decay time divides more according to the resistances of the branches. A pulse with a short rise time and a long decay time initially divides according to inductance, but then, as the current begins to change less rapidly and di/dt becomes smaller, the distribution ultimately becomes governed more by resistance.

Redistribution as a sum of components

One way of viewing the phenomenon is to consider the current in the two branches to be composed of the sum of two components; a steady state component, governed by the resistances, and a transient circulating current, governed by the *L/R* time constants of the circuit. One branch represents the current in the CFC airframe, and the other branches represent metal conductors within the airframe. The CFC airframe path has a low inductance and a high resistance, while current paths through metal wires installed within the airframe have higher inductances and low resistances. Thus, the rise and decay times of the airframe and internal wire currents behave in accordance with different *L/R* time constants. The CFC airframe path has the shortest time constant, and the internal wire path has the longest time constant. The transient circulating current in the metal conductors within the CFC airframe eventually die away, as the energy associated with the circulating current, and stored in the magnetic field surrounding the metal conductors, is consumed by the resistance of the wire circuit return path through the airframe.

If the injected pulse has a finite duration, the circulating component of current in the internal, metal conductors lasts longer than the injected current. It must therefore return through the airframe in a direction opposite to that of the injected current. This current is propelled by the magnetic field that surrounds the circulating current conductor. The redistribution process can be described in terms of simple equivalent circuits, such as Fig 11.13. In this circuit, the airframe and one or more internal current paths are represented by parallel circuit branches with appropriate resistances and inductances. Comparisons of the results of computations in this manner with measurements of currents within CFC airplanes have been good.

The redistribution process also causes the current paths *inside* the airframe to change, between the time the stroke current first begins to flow in the structure and the time after the stroke has reached its peak and the current is decaying at a slower rate. Current redistribution within an airframe is illustrated, first, for an elliptical cylinder and then for more complex structures, in which the redistribution responses must be calculated by numerical means.

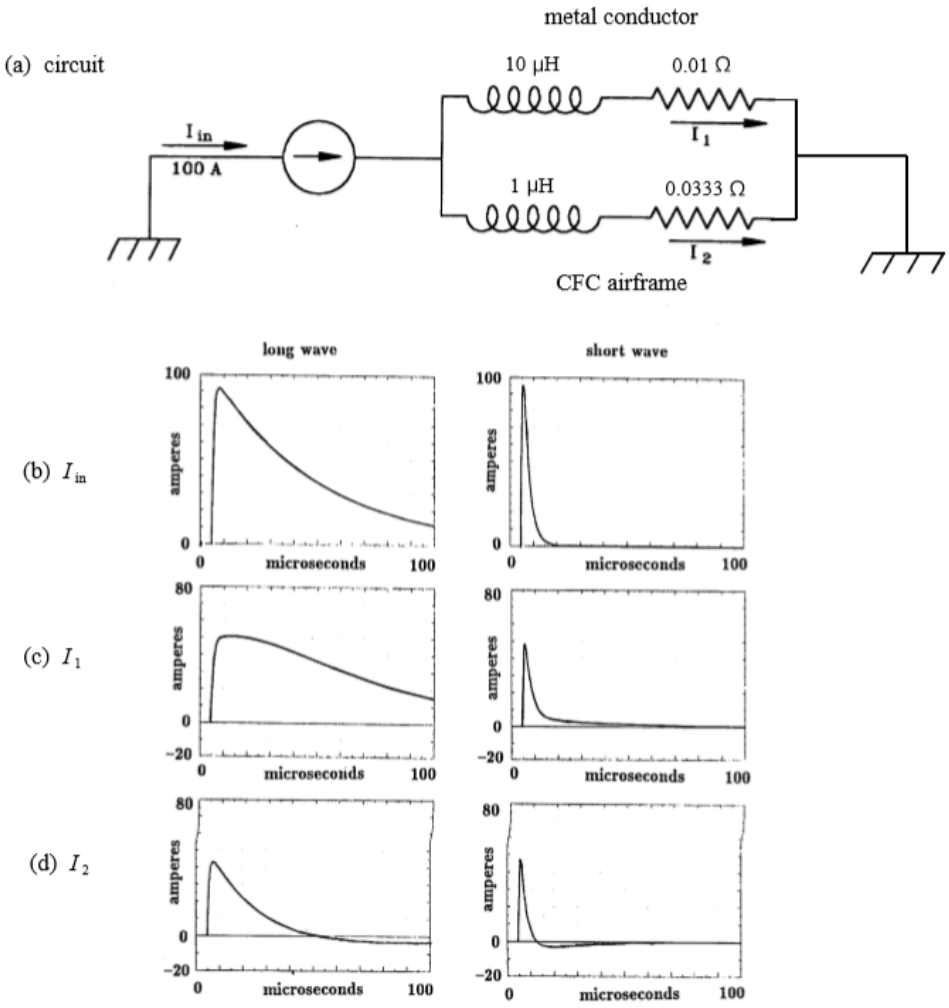

Fig. 11.13 Lumped constant circuit exhibiting redistribution effects.

11.4.1 Elliptical Cylinders

Fig. 11.14 shows an elliptical cylinder into which a step-function current is injected. As in §11.3.1, the cylinder is assumed to be long enough that all end effects may be neglected. It is also assumed that the cylinder is short compared to the wavelengths of any frequency components of the injected current, and that the return path for the current is far enough removed that no proximity effects need to be considered.

The instantaneous current in the cylinder is regarded as being composed of the sum of two components: a steady state component and a transient component. The transient component takes the form of a circulating eddy current. In the following discussions, it should be kept in mind that the eddy currents described represent only the transient component of current. The total current at any point or time is always the sum of the two components.

Steady state conditions

Under steady state, DC conditions, the current density along the wall of the cylinder is governed by the DC resistance and, if uniform wall thickness is assumed, the current density is uniform. The current in the cylinder produces a magnetic field. Most of the field lines completely encircle the cylinder, as shown in Fig. 11.14(a), but some (because of the uniform current density) pass *through* the cylinder.

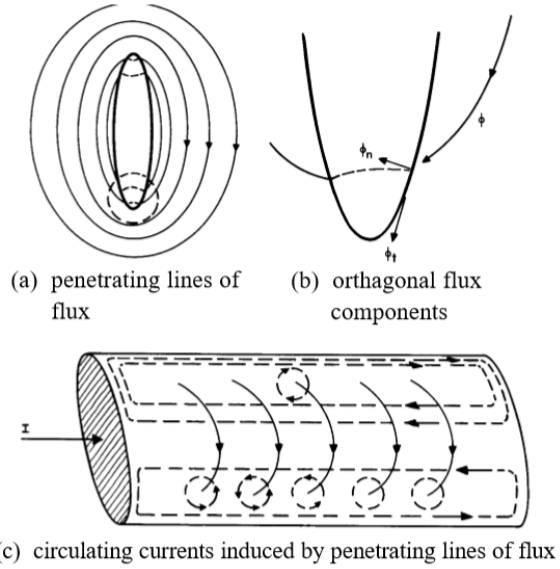

Fig. 11.14 Magnetic fields around an elliptical cylinder.

The greater the eccentricity of the cylinder, the greater the number of lines of flux passing through it. This is because the magnetic field intensity is the highest where the local radii of curvature are the smallest.

Transient conditions

A penetrating flux line is shown in Fig. 11.14(b). The vector defining that line can be resolved into two vector components at the point of entry, one, φ_n, normal to the surface, and another, φ_t, tangential to the surface. If the field line, φ, is established abruptly, it induces a circulating (or eddy) current in the conducting sheet as it attempts to penetrate. The eddy current produces a magnetic field of its own, and, initially, the intensity of that eddy current is such that the magnetic field it produces is exactly that required to cancel the normal component of the exterior field.

Circulating component

If, as shown in Fig. 11.14(c), a number of lines of magnetic flux attempt to penetrate the surface of the elliptical cylinder, the eddy currents produced by each line of flux combine to produce a circulating component of current. In an elliptical cylinder, this circulating current can be divided into four regions, two on each of the two sides of the cylinder, each contributing a component of the cancelling magnetic field.

The current density of these circulating current components increases at the edges of the cylinder and decreases along toward the center of the cylinder. The magnetic field these currents produce cancels any penetrating magnetic field, forcing the field around the cylinder to be entirely tangential to the surface, at least initially.

From the viewpoint of component currents, the circulating currents produce an internal magnetic field that, initially, has the same pattern as that produced by the DC current, but of opposite polarity. This reduces the initial internal magnetic field to zero.

Transition to DC conditions

The eddy currents cannot exist forever since their energy is lost as the currents circulate through the resistance of the metal sheet. Accordingly, the current density at all points varies with time, eventually becoming uniformly distributed, at least in structures of uniform thickness and resistivity. Fig. 11.15 shows the manner in which the current density varies. As the circulating current shown in Fig. 11.15 (c) decays to zero, the current at the edge decays from its initial high value to the final resistively determined value, and the current at the center increases from its initially low value also to its resistively derived value. The current densities change according to an essentially exponential pattern, although the transient increase in surface resistance produced by diffusion effects prevents the circulating current from following a true exponential decay.

Redistribution time constant

The approximate redistribution time constant, τ, is defined in Eq. 11.32 [11.4] as:

$$\tau = \frac{\mu A a}{\pi P} \qquad (11.32)$$

where

A = enclosed area of structure
P = peripheral distance around the structure.

The thickness of the wall, a, is assumed to be very small compared to other dimensions. For a rectangular box of height h and width d, Eq. 11.32 becomes

$$\tau = \frac{\mu h d a}{2\rho(h+d)} \qquad (11.33)$$

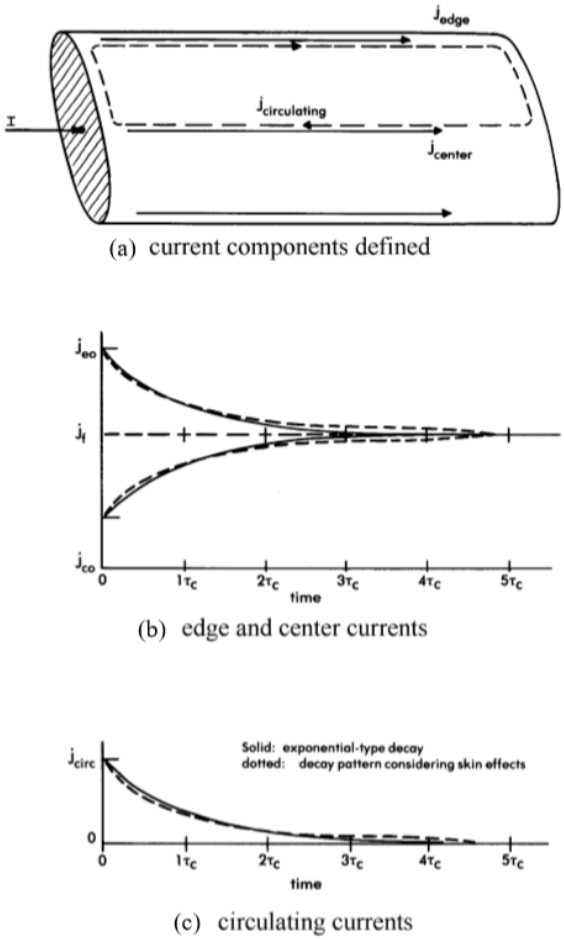

Fig. 11.15 Variation of current density with time.

These equations define the approximate redistribution times, but the actual time constants depend on geometry and are somewhat different for different portions of a structure.

For an elliptical cylinder made from aluminum of thickness 0.0381 cm, having a major axis of 47 cm, a minor axis of 9.4 cm, and a perimeter of 98.7 cm (essentially a flattened version of the circular cylinder discussed in §11.2) the redistribution time constant predicted by Eq. 11.32 would be 745 μs. As is always the case, the redistribution time constant is much longer than the pulse penetration (i.e., diffusion) time constant.

11.4.2 Eddy Currents and Internal Magnetic Field

As the circulating component of current dies out and the external lines of flux penetrate the walls of the cylinders, an internal magnetic field is set up, oriented as shown in Fig. 11.16. In its latter stages, the rate at which this internal field builds up is dependent upon the rate at which the externally induced circulating currents die away. The time constant for the internal field build-up is about equal to the redistribution time constant.

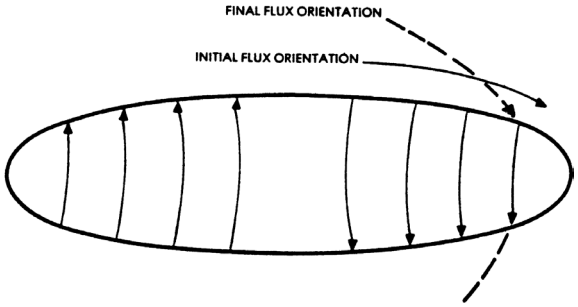

Fig. 11.16 The internal magnetic field that results From flux penetration.

The early-time build-up of the internal magnetic field depends on the rate at which the eddy currents build up along the inner surface. The eddy currents build up in response to the electric field on the inner surface, but are also governed by the inductance of the path through which they circulate, according to the elementary formula:

$$I = \frac{1}{L}\int_o^t E dt \qquad (11.34)$$

Since the internal surface voltages are retarded by the diffusion effect, it follows that the internal circulating currents (and therefore the internal magnetic field) build up even more slowly.

11.4.3 Internal Loop Voltages

We are now able to evaluate the voltages on conductors contained in a cylinder of non-circular geometry. Fig. 11.17(a) shows an elliptical cylinder with two internal conductors, one adjacent to the surface, and one in the center. Both are connected, at one end, to an end cap sufficiently massive that no voltage drops will appear along its inner surface. The other ends are open circuited. The usual assumptions about the length of the cylinder and the return path for the injected current apply.

Voltages V_1 and V_2 are shown, both measured between their respective conductors and a point on the inner wall of the cylinder. Fig. 11.17(b) shows that all of the internal flux passes between conductor 2 and the inner wall of the cylinder, while only a small amount will pass between conductor 1 and the inner wall. Correspondingly, a large fraction of the internal flux passes through the plane defined by conductors 1 and 2.

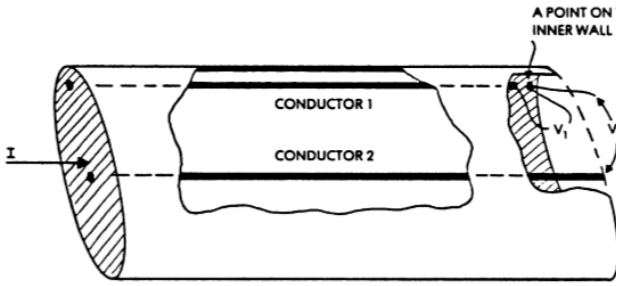

(a) geometry

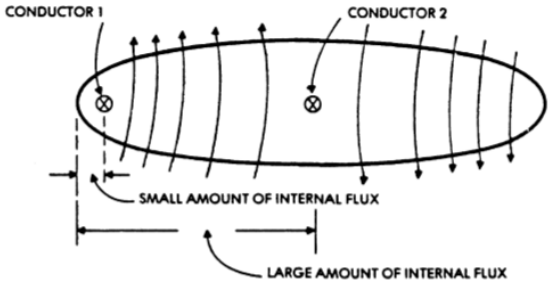

(b) internal flux linkages

Fig. 11.17 Factors governing internal voltage.

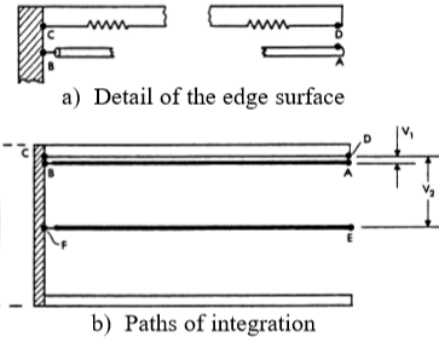

a) Detail of the edge surface

b) Paths of integration

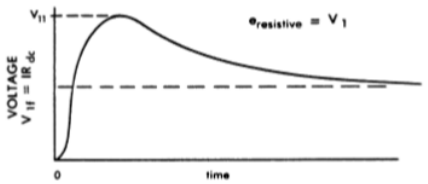

c) Components of V_1

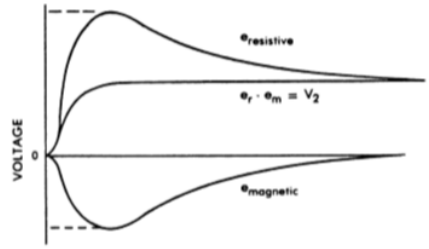

d) Components of V_2

Fig. 11.18 The internal voltages.

Voltage as line integral of potential

The voltage between any two points is defined again as the line integral of the potentials around a closed path. Figs. 11.18(a) and (b) show the simplest paths to consider. V_1 would be the sum of the potentials developed around the loop *ABCD*. If there is no current along conductor 1, the potential along path *AB* is zero. The potential drop along the path *BC* is also zero because of the assumptions regarding the end cap. The potential along path *CD* is thus the voltage drop produced by the inner current density multiplied by the resistivity of the material along the path *CD*.

To these potentials must be added the voltage induced magnetically by the changing magnetic flux passing through the loop defined by the points *A, B, C*, and *D*. If the spacing of the conductor to the wall were made vanishingly small, so that *C* - *B* and *D* - *A* became zero, there would be no magnetic flux; hence the voltage V_1 between points *A* and *D* would be only the resistive voltage drop along the path *CD*.

As in the cylindrical geometry case, the voltage for a step function current injected into the exterior of the tube builds up according to the diffusion pattern shown in Fig. 11.7. Its magnitude is greater than the DC resistance rise by the same ratio as that of the initial current density along the end of the ellipse to the steady state current density.

V_2 is, again, the sum of a resistive voltage rise and a magnetically induced voltage, this time along the path *EFDC*. The resistive component is identical to the resistive component of V_1, which is the resistive voltage rise along the path *CD*. For V_2, however, there is a non-zero magnetic component of voltage produced by the passage of a finite amount of magnetic flux through the finite loop *EFDC*. The magnetically induced component of voltage is given by

$$e_m = \frac{d\varphi}{dt} = K\frac{d}{dt}(I_{circ}) \qquad (11.35)$$

where *K* is a proportionality constant relating the flux produced in the loop *EFDC* to the internal current. In Eq. 11.34, however, it was shown that the internal current was proportional to the integral of the internal resistance rise. This leads to the rather unusual observation that the magnetically induced component of voltage has, initially at least, the same waveform as the component of voltage produced by the flow of internal current through the resistance of the material.

The long-term response of the magnetically induced voltage is different from the resistively generated component, since, as steady state conditions are reached and the internal magnetic field reaches its final value, its rate of change decreases to zero.

Influence of physical shape

The amount of the magnetically induced voltage depends upon the location of the conductor and upon the degree to which the initial distribution of magnetic flux around the outside of the cylinder differs from the final distribution. Since the difference between the initial and final flux patterns is greater for cylinders of high eccentricity than for cylinders of low eccentricity, it follows that the flatter the cylinder, the greater the influence of the magnetic component.

11.4.4 Redistribution with Both Metal and Composite Materials

A so-called 'composite aircraft', having large amounts of CFC material in its structure, is really a mixture of metal and CFC materials. The structures are sufficiently complex that there are no simple analytic formulas to estimate the redistribution time constants. Three-dimensional (3D) solutions of Maxwell's equations can be used to solve this type of problem, but engineering estimates can frequently be made based on test experience.

11.5 Diffusion and Redistribution on CFC Structures

Electrical properties

Previous discussions in this chapter have been related to materials which are lossy, but isotropic. Carbon fiber composite, CFC, materials are, in general, anisotropic. The CFC materials commonly used in aircraft construction typically have resistivities of the order of $3 - 5 \times 10^{-3}$ ohm-cm in directions tangential to the surface. This conductivity may vary with different orientations on the surface since graphite fibers in a composite are primarily woven in the orientation in which the greatest physical strength is needed. Plain weave fabrics have the most uniformity of resistivity in all directions, whereas unidirectional (UD) plies have lowest resistivities in the direction of the fibers and considerably higher resistances in other directions. When laid up and cured into laminates, the resistivities in the directions of most fibers are the lowest. The plane of the laminate is usually termed the x-y direction, whereas the direction normal to the laminate is usually the z direction. Resistivities in the z direction are usually much higher than in the plane of the laminate; sometimes reaching open circuit.

Resins used in composites usually have no conductivity and so behave as insulators until the interlaminar resin breaks down and becomes conductive. Attempts to add conductivity to resins have not proved successful either in improving ability of CFC to conduct electric currents including in the z direction, or in maintaining laminate mechanical properties. This is because conductive adders degrade the mechanical properties of the resin and of the laminates.

There have been many studies of CFC materials and their electrical properties [11.5 - 11.12]. The general conclusion of these studies is that, for conditions of uniform current flow on CFC surfaces, the only conductivity that really matters is that provided by the carbon fibers that is tangential to the composite surface.

The example of §11.3.5 may not apply to anisotropic CFC materials, because in that example there was a significant conduction of current normal to the surface. The usual definitions of surface and transfer impedances (Eqs. 11.10 and 11.12) may also not apply, since they are based on current being able to flow normal to the surface. The reason the word 'may' is used is that the conductivity of CFC materials in the direction normal to their surfaces can depend on current density. For low level currents, the

epoxy resin may insulate one surface from another but, for high level currents, the voltage gradients may be high enough to cause breakdown of the resin insulation and more uniform current transfer between layers. This would tend to increase the conductivity between the layers, both during the time when lightning current is flowing and afterwards. Composites that are cured under high temperature and high vacuum conditions have more isotropic conductivities than those cured under room temperature and low (or no) vacuum conditions. In the latter case, more resin may be left between adjacent plies.

11.6 Fields within Cavities

In §11.3.5 it was observed that the electric field developed along the inside of a shielding surface, in response to a current or magnetic field on the outside, excites a current around the cavity enclosed by the shielding surface. In the fuselage of an aircraft, it is common to find a cavity that is effectively exposed to the external field on only one face, either because the inner walls of the cavity are thick enough to provide more shielding from the other parts of the external field or because the cavity is much closer to one of the external surfaces than it is to any of the other external surfaces. An example of such a cavity would be a baggage compartment or an electronic equipment bay located along the fuselage of the aircraft and accessible through access panels. Some cavities are covered by non-electrically conductive doors or panels and so will provide to shielding of contents from external magnetic fields originating outside the airframe.

Covers and fasteners

If the cavity is provided with a removable cover and it is made of conductive material such as aluminum or CFC, it will conduct some of the lightning current and provide some protection of contents within.

If this cover is in the external current flow, it will seldom make good or dependable electrical contact to the surrounding structure to upon which it is mounted, so the current flow onto and off of the cover is due to the fasteners and the resistance of the fastener installations. It will be seen, then, that the greater the number of fasteners, the less the restriction of current flow due to the resistance of the fasteners. The resistance introduced by the fasteners is important because it is frequently much higher than the intrinsic resistance of the metal surface and because the resistance is not subjected to the skin effects that retard the buildup of current density on the inner surface. The situation is shown in Fig. 11.19.

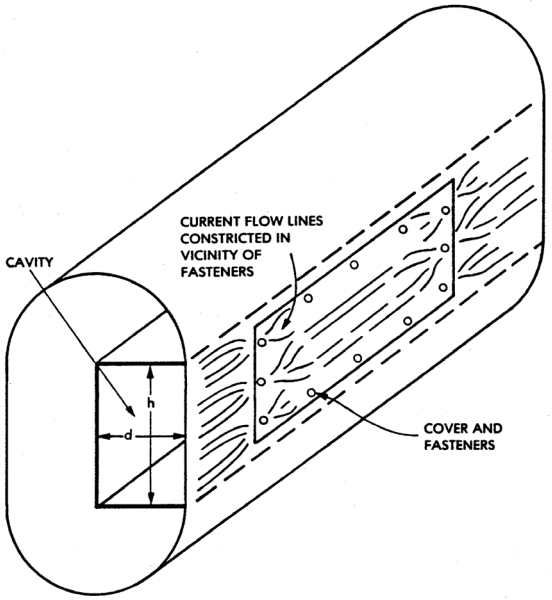

Fig. 11.19 Effects of covers and fasteners.

References

11.1 S. Goldman, *Transformation Calculus and Electrical Transients*, Prentice-Hall, Inc. Englewood Cliffs, NJ, 1949, 1955, pp. 112-120.

11.2 P. M. McKenna, T. H. Rudolph, and R. A. Perala, "A Time Domain Representation of Surface and Transfer Impedances Useful for Analysis of Advanced Composite Aircraft," "*Proceedings of International Aerospace and Ground Conference on Lightning and Static Electricity*," held in Orlando, FL, June 26-28, 1984.

11.3 F. A. Fisher, "Analysis and Calculations of Lightning Interactions with Aircraft Electrical Circuits", *Air Force Flight Dynamics Laboratory, AFFDL - TR - 78 - 106*, August 1978, pp. 307-324.

11.4 K. Khalaf-Allah, "Time Constant for Magnetic Field Diffusion into a Hollow Cylindrical Conductor," *UKAEA (United Kingdom Atomic Energy Authority) Research Group Report CL-1414*, Culham Laboratory, Abingdon, Oxfordshire, England, 1974.

11.5 D. A. Bull, and G. A. Jackson, "Assessment of the Electromagnetic Screening Characteristics of Carbon Fibre Composite Materials," *IEEE Conference Proceedings*, No. 47, Vol. 1, pp. 1-198, 16-18th September 1980.

11.6 B. W. Smithers, "RF Resistivity of Carbon Fibre Composite Materials," *Conf. on Electromagnetic Compatibility*, Vol. 1, pp. 1-198, Univ. of Southampton, UK, 16-18 September 1980.

11.7 F. A. Fisher and W. M. Fassell, "Lightning Effects Relating to Aircraft: Part 1 - Lightning Effects On 11.26 B. J. C. Burrows and W. Walker, "Electromagnetic Shielding Properties of Graphite Epoxy Panels to Lightning," *Final Report No. NADC-80237-20*, Jan.-Sept. 1980.

11.8 "Composite forward Fuselage Systems Integration," Vol. 1, *AFFDL-TR-78-110*, General Dynamics, September 1978.

11.9 F. W. Grover, *Inductance Calculations: Working Formulas and Tables*, New York: Dover, 1962.

11.10 D. M. Kalyon, E. Birinci, R. Yazici, B. Karuv, and. Walsh, *Electrical Properties of Composites as Affected by the Degree of Mixedness of the Conductive Filler in the Polymer Matrix*, Stevens Institute of Technology.

11.11 G. Boguki, W. McCarvill, S. Ward, J. Tomblin, *Guidelines for the development of Process Specifications, Instructions and Controls for the Fabrication of Fiber-Reinforced Polymer Composites*; National Institute for Atmospheric Research.

11.12 MIL-Handbook 17-3F Volume 3 of 5, 17 June 2.

Chapter 12

PENETRATION OF EXTERNAL FIELDS THROUGH APERTURES

12.1 Introduction

The most important mode by which electric and magnetic fields appear inside conventional aluminum aircraft is through apertures, such as cockpit and cabin windows, nonconductive access panels, wheel wells, wing aft spar cavities and weather-sealed joints. There are several reasons for the importance of aperture coupled fields. One is that apertures are the only direct means by which external electric and magnetic fields can penetrate to the interior of an aircraft. Another is that some apertures, especially windows, are quite large. Also, unlike the electric and magnetic fields that arise through the gradual diffusion of lightning currents to the interior surfaces of an airframe, the waveforms of aperture fields are not retarded, but tend to be the same as those of the external electric and magnetic fields. The most important consequence of the internal fields are voltages induced by changing magnetic fields in loops between the aircraft wire harnesses and airframe reference planes, such as skins, floor boards and bulkheads and, to a smaller extent, currents induced on internal conductors by penetrating electric fields. A magnetic or electric field of given peak intensity is more likely to cause trouble if it rises to its peak quickly than if it is delayed or distorted. Small apertures, in fact, tend to accentuate the rates-of-change of penetrating fields, because they are more efficient at coupling the short time duration (i.e., nanoseconds, ns) (also known as high frequency) components of the external electromagnetic field to internal wiring than at coupling the longer duration (low frequency) components.

The subject of aperture coupling has been of considerable theoretical interest since the time of Lord Rayleigh [12.1]. Since literally hundreds of papers and articles have been written on the subject, no attempt will be made to give a complete review. Instead, this chapter will discuss the basic points of aperture coupling and refer to the literature for additional details. It will also describe some simple techniques for estimating (or finding bounds for) expected responses of internal circuits to aperture fields. Numerical methods are available for computing intensities of fields inside airplanes, but these will not be discussed in this book. For a more complete treatment of the mathematical aspects of aperture coupling, the reader is referred to some of the review articles that have appeared in [12.2 - 12.4]. Ref. [12.2] is particularly recommended.

A distinction was made, above, between 'large' and 'small' apertures. One way to distinguish between 'large' and 'small' apertures is to relate the physical size of the aperture to the wavelength of the frequencies of interest. Since most of the energy in a lightning flash is manifested in frequencies below 50 MHz ($\lambda = 6$ m), it follows that most apertures on aircraft are 'small' with respect to the impinging wavelength.

Another way to distinguish between 'large' and 'small' apertures is to relate them to the size of the aircraft on which they are found. In dealing with 'small' apertures, it is acceptable to treat calculations of the external response of the aircraft (Chapter 10) separately from calculations of how much energy propagates through the aperture. However, if an aperture is large enough that it effects the external response of the aircraft, then the external and internal responses must be calculated together. Examples of such large apertures may include the windows in a cockpit or open landing gear doors. Methods of computation of lightning electromagnetic fields within aircraft are available via computerized modeling programs. These are not presented in this book. A qualitative discussion is presented to give the user a view of the nature of these fields.

12.2 Basic Concepts

Both electric and magnetic fields penetrate through apertures. For small apertures, it is convenient to determine this penetration in terms of hypothetical external electric and magnetic fields that would be present at the aperture if the aperture were closed by a perfectly conducting surface. These hypothetical fields are referred to as "short-circuit" fields, E_{sc} and H_{sc}. These short-circuit fields, together with the geometry of the aperture, are used to estimate the magnitude of hypothetical electric and magnetic dipoles (equivalent antennas) which are placed just inside the closed (shorted) aperture. This process is illustrated in Figs. 12.1 and 12.2.

Analytically, the interior fields can be visualized in two steps; first, by finding the strength of each field at the apertures, and second, by visualizing the fields inboard of the apertures, where the wire harnesses are located.

Magnetic fields must pass through loops between the harnesses and the airframe to induce voltages in these loops, and electric fields must impinge on surfaces of the harnesses to induce currents on them.

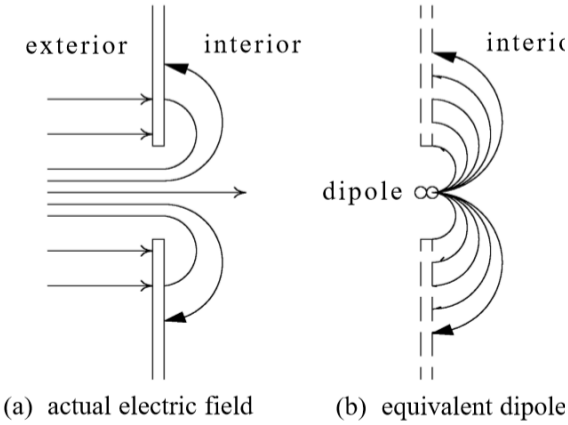

Fig. 12.1 Development of equivalent electric field dipole.

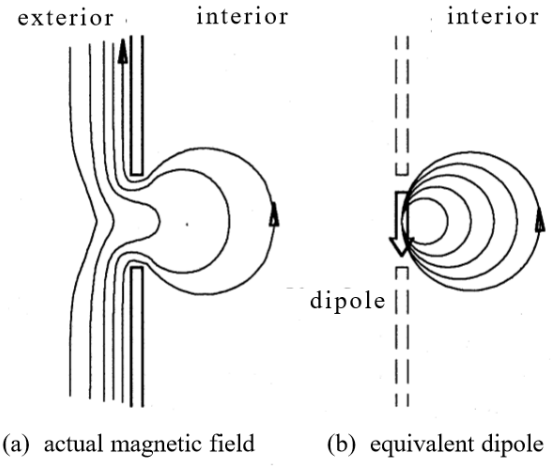

Fig. 12.2 Development of equivalent magnetic field dipole.

Waveshapes: The geometry of the aperture is shown in Fig. 12.3. The origin of these fields is the C-G stroke current (Component A or D), or one of the intracloud current pulses represented by Component H, all as defined in [12.3] and reviewed in Chapter 5. When these currents are conducted through the aircraft, between entry and exit locations, the waveshapes of the magnetic fields that accompany the currents are like the waveshapes of the currents themselves. Thus, for example, the waveshape of the magnetic field associated with the first stroke current is that of current Component A, which has a rise time of 6.4 μs and a decay time (to 50% of peak amplitude) of 69 μs. Where some of this magnetic field penetrates an aperture, the portion of the field that reaches inside the aircraft also has a similar waveshape. This is one of the reasons for the appearance of damped sinusoid voltages and currents in aircraft wire harnesses, as voltage or current Waveform 3, defined in SAE ARP 5412B [12.3].

Because the aircraft surface is conductive, the electric (E) field component of the traveling electromagnetic wave must be oriented at right angles to the aircraft surface. The magnetic (H) field component must be tangent to the surface, and perpendicular to the direction of current (charge) flow. When viewed at a particular spot on the aircraft surface, this appears as a damped sinusoid waveform. This has not been defined in the standards because its amplitude and frequency depend on the geometry of the particular aircraft and the mismatch in characteristic impedances of the lightning channel and the aircraft. Evidence of these traveling waves can be seen in the intracloud current pulses in the research aircraft described in Chapter 10, and in test currents that appear on airplanes undergoing the full vehicle tests (FVTs) described in Chapter 13. When this traveling wave (which propagates along the aircraft at the speed of light) passes by an aperture, some of both fields pass through the aperture and appear inside the aircraft. The subject of how to deal with the induced transients due to the traveling waves is discussed in Chapter 13.

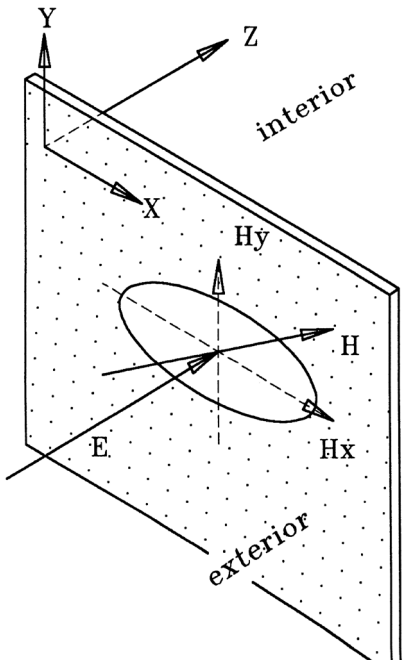

Fig. 12.3 External electric and magnetic fields impinging on an aperture.

Aperture: An elliptical aperture is considered because it is the most general of the elementary geometries. For this description, the major axis of the ellipse will lie on the *X* axis so that the origin of the axes is at the center of the ellipse.

On the interior of the airplane surface (Fig. 12.4) one equivalent electric field dipole, *P*, and two equivalent magnetic field dipoles, M_x and M_y, can be defined such that they represent the normal electric field and the *x* and *y* components of the tangential magnetic field, respectively. The magnitudes depend on the size and shape of the aperture.

The waveshapes of the electric and magnetic fields should be assumed to be the same as those on the exterior of the aircraft, which in turn are related to the waveshapes of the external lightning environment. For assessments of lightning effects and protection design, these waveshapes should be the same as those of the standard environment defined in SAE ARP 5412B [12.3].

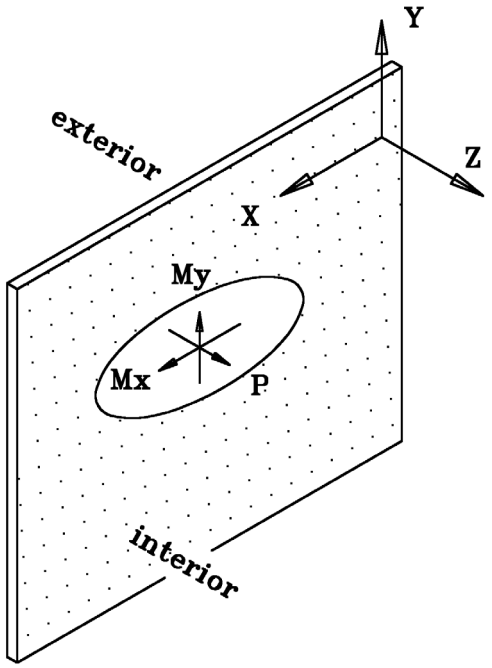

Fig. 12.4 Equivalent dipoles illuminating an interior volume.

The dipole field strength is proportional to the cube of the length of the major axis of the aperture, so it follows that large apertures allow much more energy to reach an inner volume than do small apertures. This approach of representing fields at apertures is explained more fully by Taylor in [12.4 - 12.5].

Using the magnetic dipole along the *X* axis (M_x) as an example, the pattern of the magnetic fields in the interior region consists of concentric closed loops lying in planes that pass through the *X* axis (Fig. 12.5). At any point, P, the total magnetic field can be represented as a vector normal to the radius vector, *r*, between the dipole and P and lying in the plane defined by point, P, and the *X* axis.

Likewise, the magnetic field due to the M_y dipole can be defined as a vector lying in the plane defined by P and the *Y* axis.

The pattern of the electric field due to the dipole will consist of concentric loops, originating at the dipole and terminating on the skin containing the aperture.

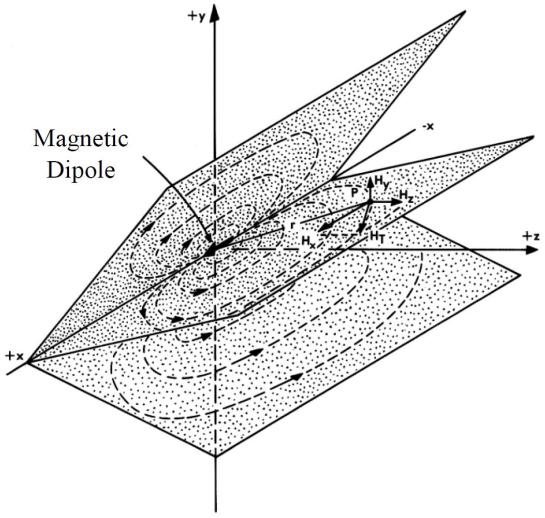

Fig. 12.5 Magnetic field patterns produced by a dipole lying along the X axis.

If the aperture under consideration is not elliptical, a corresponding elliptical aperture can generally be specified, as shown in Fig. 12.6. The equivalent aperture would have the same area and the same eccentricity as the aperture under study.

12.3 Treatment of Surface Containing the Aperture

The location of the surface containing the aperture is used as a boundary between an exterior and interior region. The fields of interest are in the interior region, but these "begin" with current flowing on the exterior surfaces of aircraft and then some of them propagating "coupling" to the interior, via apertures.

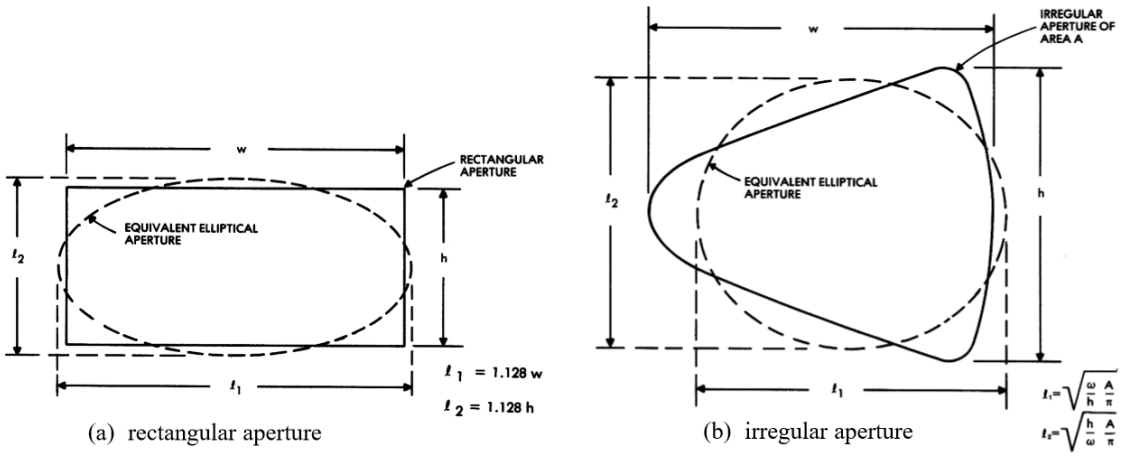

(a) rectangular aperture (b) irregular aperture

Fig. 12.6 Equivalent apertures

12.4 Fields Produced by the Dipoles

The complete formulation [12.4 - 12.5] of the fields produced by the dipoles (neglecting the far field radiation component) is, in the frequency domain:

$$H_x = H_{xx} + H_{xy} \qquad (12.1)$$

$$H_y = H_{yx} + H_{yy} \qquad (12.2)$$

$$H_z = H_{zx} + H_{zy} \qquad (12.3)$$

The x, y and z components of the total magnetic field strength at P would be the sum of the components produced by dipoles lying along the X and Y axes:

The total magnetic field at point P in Fig. 12.5 would be:

$$H_T = \sqrt{H_x^2 + H_y^2 + H_z^2} \qquad (12.4)$$

An example of an aperture-coupled field intensity is shown in Fig. 12.7, in which the elliptical fuselage described in § 10.5.4 has been approximated by two sheets of infinite size. One of the sheets contains the aperture and the other serves as a reflecting surface. The figure shows only the top half of the field pattern since the field is symmetrical across the minor axis of the aperture. The aperture assumed in this example was 0.2 m high by 0.1 m wide, the long axis of the ellipse being oriented at right angles to the plane of the figure.

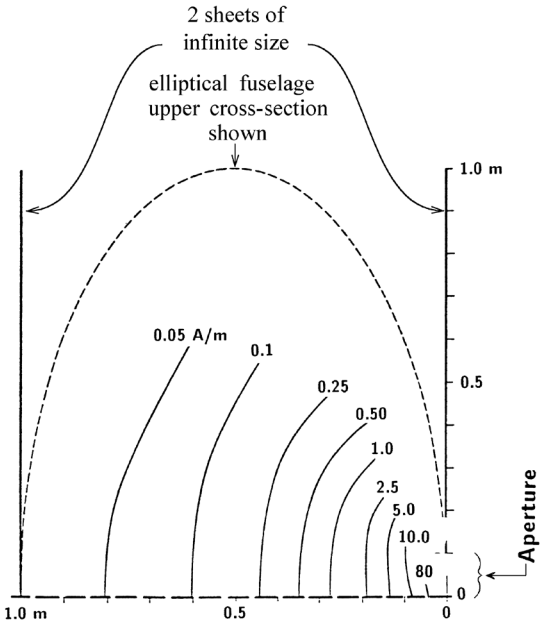

Fig. 12.7 Field intensity penetrating through a 0.4 x 0.1 meter, vertical aperture in a fuselage of elliptical cross-section conducting 1 000 A of stroke current.

The magnetic field intensity that would exist if the aperture were not there was taken to be 160A/m, which is the field strength that would be produced by a lightning current of 1 000 A flowing axially on the exterior surface of the elliptical fuselage. Based on this current, the magnetic field intensity at the aperture would be 80 A/m, or half of the short-circuit field. This is a convenient assumption to use for estimating magnetic field intensities at the interior of cabin windows and similar apertures.

This field intensity inside the aperture varies inversely with the cube of distance from the aperture. Accordingly, the fields that penetrate apertures such as this are very localized; confined to a small space close to the aperture. 'Small' apertures are thus less troublesome than 'large' apertures, both because of the decreased magnetic field strength associated with the corresponding equivalent dipole and because of the relatively small distance from the aperture at which the field strength becomes negligible. A simple rule of thumb is to recognize that the field at the plane of the aperture cannot be greater than half the magnitude of the short circuit field. One can simply ignore numerical answers that exceed this limit.

12.5 Reflecting Surfaces

Estimations of the intensities of fields penetrating through apertures ("aperture fields") sometimes have considered the presence of reflecting surfaces. The simplest example of this, shown in Fig. 12.8, addresses the situation where an infinite reflecting plane is parallel to the surface containing the aperture.

The total field at any point between these two surfaces is the sum of the fields produced by the infinite array of images and can be determined from equations reported in [12.4 - 12.5]. Fortunately, in most cases, only a few of the images need be considered because the field strength falls with the cube of the distance from the aperture. The presence of reflecting surfaces never causes the fields to be more than twice the intensity contributed by the aperture itself. This fact may render calculations of the effects of reflecting surfaces unnecessary in some cases.

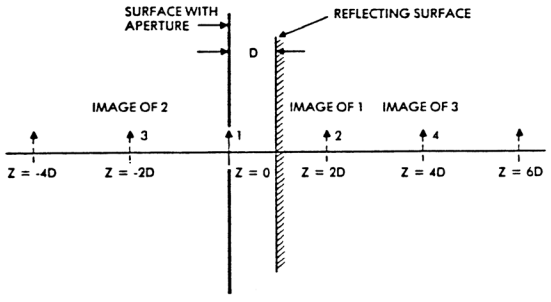

Fig. 12.8 Surface with aperture and reflecting surface.

In principle, one could include enough additional reflecting surfaces in one's analysis to completely define an interior volume. An example of this level of detail is shown in Fig. 12.9.

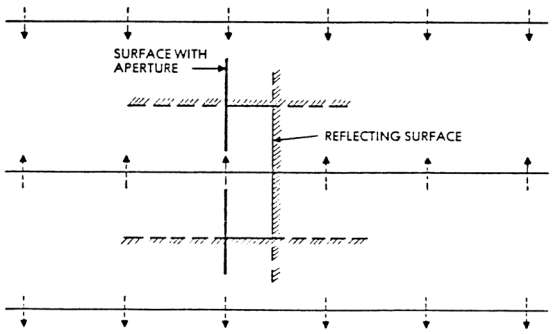

Fig. 12.9 Multiple reflecting surfaces.

Field reflections: The interior surfaces can allow fields to reflect among themselves, but this is not going to happen unless the time duration of the fields is as short as or shorter than the transit time (speed of light) through the air between the surfaces. At $3x10^8$ m/s a field would need to have a time duration of less than 10^{-8} s (0.01 μs) for an electromagnetic field to have time to propagate across a 1 m distance and begin a reflection back. Such fields may arise from a nuclear electromagnetic pulse (NEMP) event or a local discharge of static electricity across a nearby windowpane, but fields produced by lightning leaders and stroke currents (Voltage Waveform A, Current Component A) exist for 10's and hundreds of microseconds and so would not entirely reflect. Some field waveform distortion should be expected, but not reflecting, and resonating fields. There is evidence of reflecting fields in measured lightning-induced voltage measurements in aircraft electrical circuits, but these are attributed to traveling wave currents on the aircraft, whose speeds are on the order of 0.3 m/ns. Even the largest airplanes are not sufficiently long for a stroke current to be reflected down and back. It is instead the initial injection of charge (+ or -) at junction leader inception that is of sufficiently short duration to be reflected, and there is evidence of this in in-flight measurements of airplane skin currents, as described in Chapter 10.

12.6 Exposure of a wire to electric and magnetic fields

If there were a wire (or cable) in the space illuminated by the aperture, voltages could be induced in the loop formed between the wire and the airframe reference plane, and these voltages would induce current on the wire. Estimates of the magnitudes of these induced voltages and currents can be determined by substituting equivalent circuits for the actual magnetic and electric aperture field coupling mechanisms and solving for the cable's response to these equivalent voltage and current sources. For example, consider the circular aperture shown in Fig. 12.10. A wire with a characteristic surge impedance, *Z*, is located at height, *h*, above the surface containing the aperture, and at a distance, w, from the aperture.

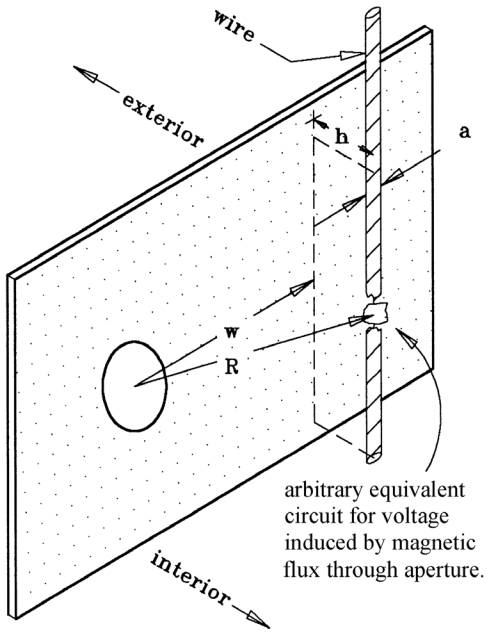

Fig. 12.10 Coupling from an aperture to a wire.

The characteristic impedance (sometimes also called *surge impedance*) is:

$$Z = \sqrt{L/C} \qquad (12.5)$$

$$\approx 60 \ln(2h/a) \qquad (12.6)$$

An equivalent circuit including the aperture-coupled voltage is shown in Fig. 12.11. There are two aspects of this equivalent circuit that must be considered. The first is to define the equivalent induced voltage and current sources, V_{eq} and I_{eq}. The second is to determine the effect of the aperture on the inductance and capacitance of the cable. In an elementary geometry, the inductance, capacitance, and characteristic impedance of the cable is governed by the spacing between the cable and the adjacent ground plane. The ground plane may consist of the conductive surface containing the aperture or whatever other conducive surface is nearest to the cable installation. In the region near the aperture, the cables effective distance from the ground plane is increased, yielding a somewhat larger inductance and a somewhat smaller capacitance. However, since cables are rarely installed directly across apertures, the influence of the aperture on the cable inductance and capacitance can be ignored.

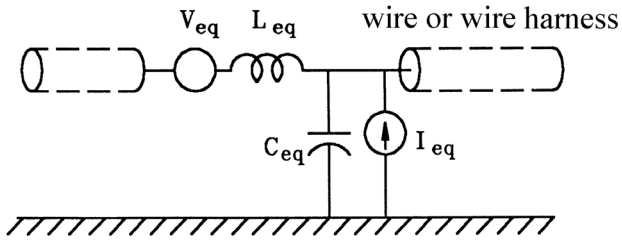

Fig. 12.11 Equivalent circuit of an aperture.
V_{eq} = voltage source due to magnetic fields.
I_{eq} = current source due to electric fields.

It should be noted that these approximations are valid only if the aperture is small with respect to wavelength, and if the distance between the plane of the aperture and the cable is several times the length of the aperture. This is the case with fields due to lightning stroke currents.

Seams: On an aircraft, seams are formed where sections of skin are joined together by rivets or other fasteners. Other seams may be formed by wheel-well or bomb bay doors, which form slots in an aircraft's inherent electromagnetic shielding. The penetration mechanism due to seams is the result of skin current (J_S) flowing across the impedances of seams and creating voltages that drive currents into circuits that are installed across the seams. Such currents are often influenced by diffusion of skin currents to the interior surfaces of the seams as discussed in Chapter 11.

The seam situation is shown in Fig. 12.12, which shows a lightning current of density J_S flowing across a seam. The current, flowing through the impedance of the seam creates a voltage rise on the interior surface.

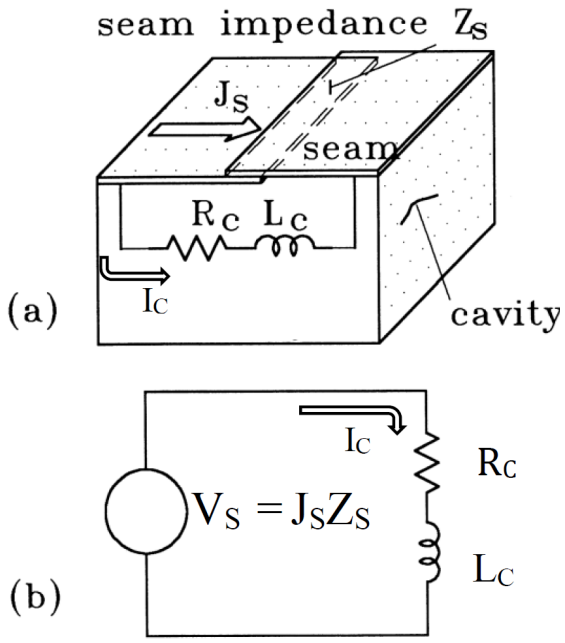

Fig. 12.12 Seams and joints.
(a) Typical seam and enclosed conductor
(b) Equivalent circuit

This can also be called a *transfer impedance.* Seam transfer impedance typically has two components: a resistive component, due to the flow of current through resistive films or through resistive fasteners, and an inductive component, due to penetration of magnetic fields. The resistive component generally predominates where overlapping metal surfaces are joined permanently with rivets or bolts.

The inductive component tends to predominate where surfaces are easily separable, as in the case of access panels that provide entry to equipment bays, and current must neck-down to pass through individual hinges or quick-release fasteners. Both the inductive and resistive components will be low if the faying surfaces make good metal-to-metal contact, and the seam is fastened with multiple tightly fitting rivets. Such an impedance is characteristic of the diffusion coupling mechanism discussed in Chapter 11.

The impedances-per-unit-length of seams can range from 10^{-4} to 10^{-2} Ω/m, with typical values on the order of 10^{-3} Ω/m. The lowest resistance is, of course, associated with the most tightly joined contacts.

Chapter 13 presents experimental means of determining the waveforms and magnitudes of induced transients in aircraft electrical wiring, and Chapter 14 presents analytical examples of the three coupling mechanisms (Structural IxR, magnetic field, and electric field) in typical electrical wire harnesses.

References

12.1 Lord Rayleigh, "On the Incidence of Aerial and Electrical Waves on Small Obstacles in the Form of Ellipsoids or Elliptic Cylinders, on the Passage of Electric Waves Through a Circular Aperture in a Conducting Screen," *Phil*. *Mag*., Vol. 44, pp. 28, 1897.

12.2 K.S. Lee, Editor, "EMP Interaction: Principles, Techniques, and Reference Data (A Compleat Concatenation of Technology from the EMP Interaction Notes)," *AFWL-TR-80-402*, December 1980.

12.3 *Aircraft Lightning Environment and Related Test Waveforms,* SAE ARP 5412B, 11 January 2013.

12.4 C. D. Taylor, "Electromagnetic Pulse Penetration Through Small Apertures", *IEEE Transactions on Electromagnetic Capability*, Vol. EMC-15, No. 1, February 1973, pp. 17-26.

12.5 C. D. Taylor, "Electromagnetic Pulse Penetration Through Small Apertures", Interaction Note 74, *Electromagnetic Pulse Interaction Notes*, 5, March 1973.

Chapter 13

AIRCRAFT FULL VEHICLE TESTS

13.1 Introduction

This chapter discusses 'full vehicle' test methods. This is one of the tests that are frequently included in aircraft certification programs. Sometimes it is (mistakenly) applied as a certification test, but since it is usually conducted at low, non-destructive levels and does not, by itself, verify system safety, it more properly should be an considered an engineering test that is used to provide data from which full-scale certification tests of avionic equipment and systems can be planned. In particular, the full vehicle test (FVT) is for determining the lightning-induced transient voltage and current waveforms and levels throughout aircraft interconnecting wiring. If not being performed as a certification test, it is usually conducted after conformity of the aircraft and installed wiring to be measured to type design has been assured. In either case it is a part of the certification *process*. After extrapolation to correspond with the full-threat lightning environment, the data from the FVT is used to establish the certification test conditions for electrical and avionic systems. Those certification tests are bench level tests and are described in Chapter 18, and in the applicable standards.

Analytical techniques are available that can also predict lightning-induced transient levels in aircraft wiring, but these can seldom be relied upon as the sole method for determining these voltages and currents. Most avionics certification programs include tests of a complete aircraft, containing the interconnecting wiring, to verify that the actual transient levels (ATLs) in interconnecting wiring do not exceed the transient control levels (TCLs) assigned to this wiring, and especially the equipment transient design levels (ETDLs) that the equipment must tolerate, in accordance with the certification process described in Chapter 5. This is known as an aircraft 'full vehicle' test that is described in [13.1]. Sometimes, this verification is accomplished by numerical analysis, but the analysis must, at some time, be verified by a FVT. FVTs are also employed to evaluate the effects of changes in structural materials, or in wiring designs. The FVT deals only with the response of the aircraft and its wiring. It does not include tests of avionic equipment and systems.

There are several different approaches to performing FVTs. Five of these are listed below. Each method has its own advantages and disadvantages. As a practical matter, only methods 3, 4 and 5 are used to support aircraft protection design.

1. High level unipolar pulses
2. High level oscillatory pulses
3. Intermediate level unipolar pulses
4. Low level unipolar pulses
5. Low level swept continuous wave (CW)

The 'unipolar pulses', mentioned above, refer to current waveforms similar or identical to the defined lightning environment waveforms, Components A and H that are described in Chapter 5.

'Oscillatory pulses' refers to the damped sinusoidal waveforms that often result when series resistance is removed from a test current generator to allow higher currents (up to full threat amplitudes) to be reached. These damped sinusoids do not represent the important characteristics of the defined lightning currents and means must be provided to assess the resulting test data in terms of the defined environments. This is not a simple task.

Techniques 1 through 4 apply current impulses in the time domain, whereas technique 5 is a frequency domain technique that applies CW sinusoid currents at enough frequencies throughout the frequency range of the defined lightning environment waveforms. Corresponding induced voltages are recorded and inverse-transformed to get the equivalent time-domain pulse transients. High level, time domain test procedures could in principle be used as proof or verification tests (i.e., 'Go/No-Go' tests) to make an overall evaluation of the effectiveness of protective measures. However, these may cause unseen and undetectable effects throughout the airframe and systems and so should not be applied to an airplane that is eventually to be operated either for flight test or commercial purposes.

The following sections discuss the various approaches to testing.

The low level, unidirectional (UD) pulse test procedure is discussed further in §13.4. This is often the most appropriate test procedure since it applies the defined environment current waveforms and therefore yields the most direct results, without damaging the test airplane or equipment within. By applying the test currents at low levels, damage to onboard equipment and to the airframe is eliminated. The measured transients must then be extrapolated to find the values that occur when the aircraft is exposed to the full threat lightning environment.

While this chapter concentrates on techniques for performing low-level pulse tests, much of the discussion is equally applicable to any of the FVT procedures.

13.2 Basic Assumptions

All the experimental techniques are based, to one degree or another, on the following premises:

13.2.1 Defined Environment

Lightning testing is approached in terms of a standardized lightning environment. This environment is defined in standards documents, rather than in terms of what is most produced by lightning. The standardized lightning environment, described in Chapter 5, is intended to represent a very severe lightning flash, although not necessarily the most severe. One of the aims of testing, therefore, should be to determine the response of the aircraft to waveforms defined in that environment. A test program may involve using or discussing waveforms other than those described in the standard environment, but it should, as a minimum, deal with the lightning current waveforms of the defined threat.

13.2.2 Linearity

The intermediate level and the low-level test methods assume that the response of the aircraft to a low-level test can reasonably be linearly extrapolated to estimate the response to full-threat lightning. This linearity of induced transient responses to the injected test current has been demonstrated on numerous occasions. There are some situations where linearity plainly cannot be expected. These exist where the current flow paths through an airframe change as the amplitude of current increases. Such a situation may exist when a current is prevented from taking one path due to an interface comprised of non-conducting materials, whose electrical properties change with applied voltage. One example is an empennage section that is attached to primary structure with a hinged bolt that is lubricated with a solid material. As test current through this section is increased sufficient voltage is developed to cause the lubricant to become conductive, thereby changing current flow paths. Another example is a control surface that is operated by a linear actuator that includes a lubricated piston and cylinder which does not allow current flow until sufficient voltage is developed in the impedances of alternate paths to cause the actuator insulating material to become conductive thereby changing basic current flow paths and induced effects. Most of these situations are known to those conducting the tests and can be accounted for by use of temporary jumpers or other means to assure stability of current paths.

The role of mechanical fasteners in conduction of lightning currents has been studied thoroughly. Fasteners installed using ‘interference-fit’ methods usually provide metal-to-metal contacts within the holes that results is low and stable resistances. These are often found in integral fuel tank structures. This is in contrast with fuselage fasteners that are often installed ‘clearance-fit’ so that metal-to-metal contacts are less common, until current densities increase sufficiently to build sufficient voltage to cause more of these fasteners to conduct currents resulting in lower overall structure resistances.

Resistive effects

Most of the test methods listed in §13.1 provide good simulation of the effects of resistance in the aircraft structure and, for these effects, the assumption of linearity is generally valid except as noted above. This is true even for aircraft made from large amounts of carbon fiber composite (CFC) materials. Studies documented in [13.2] and [13.3] have invariably shown that resistively coupled voltages predicted under an assumption of linearity are, if anything, somewhat higher than any likely to be encountered in actual service.

Magnetic field effects

These test methods also provide reasonable estimates of the magnetic field effects produced by lightning current. This means that the response produced by a low-level pulse of current can be scaled linearly to give the response to a high-level pulse of current, provided that the waveforms of the currents are the same. This point is discussed further in §13.3.3.

Electric field effects

Whether or not any of the test methods provide good simulation of the electric field effects is less clear. Electric field coupling is determined by the strength of the electric field at the surface of the aircraft, but this can be influenced very greatly by the corona and streamers that appear around the aircraft when it is struck. Both of these are very

non-linear phenomena. The corona and streamers limit the electric field at the surface and may limit the electric field coupling. Also, the circuits used for ground-based aircraft tests probably do not give the same ratio of magnetic to electric field effects as is found in flight. This chapter will not attempt to address the question of whether electric field effects are correctly simulated; all it will do is alert the reader to the fact that there are questions about the simulation of electric field coupling. As will be shown in Chapter 14, when considered separately, electric field coupled transients tend to be significantly lower than those due the other two coupling mechanisms.

Another basic premise of all the test approaches is that the response of an aircraft in flight to natural lightning can, in fact, be predicted by performing tests with the aircraft parked on the ground. There is always some question as to whether this is valid, and some investigators, recognizing the complicated interactions of the electromagnetic fields surrounding an aircraft in flight during a lightning strike, have referred to ground tests as 'stimulations' rather than 'simulations'. It is true that the electromagnetic environment of an aircraft parked on a hangar floor is different from that of one in flight, but the test current generator and current return conductors can be arranged to make the aircraft appear electromagnetically (to some extent) as if it were being struck by lightning in flight.

Some of these issues will be discussed in the following paragraphs, along with methods of obtaining an electromagnetic environment that is as representative as possible of that produced by natural lightning.

13.3 Time domain pulse tests

All full vehicle testing involves charging capacitors and then discharging them, through wave shaping elements, into the aircraft to produce currents that are as defined in the standards. Differences between various techniques relate mostly to the energy levels of the surge generators and the techniques and degree of extrapolation needed to estimate full threat responses from tests made at less than full threat. Before discussing the various approaches to testing, the basic response of an aircraft in a pulse test circuit must be discussed, since that response is essentially the same, whatever the test level.

13.3.1 Basic Test Circuit

As reduced to lumped constants, the basic pulse test circuit is shown in Fig. 13.1. Energy is stored in a capacitor, conducted into the aircraft, and returned to the capacitor along a return circuit. Time duration of test current is controlled by the capacitance and series resistance, while current rise ('front time') is controlled by resistance and series inductance, some of which may be intentionally added to the surge generator and some of which is intrinsic to the aircraft and the return circuit. If single wires are used for the connections between the generator and the aircraft, the inductance of the circuit can be approximated as 1 μH/m or 0.3 μH/ft times the total distance around the circuit.

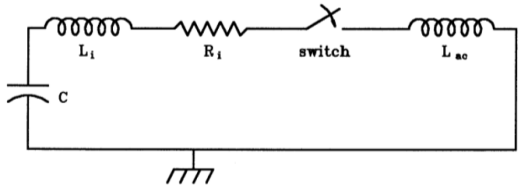

(a) Generic test circuit

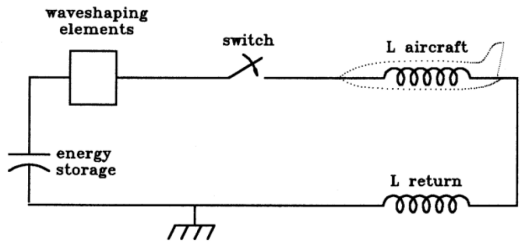

(b) An actual test circuit

Fig. 13.1 Basic aircraft test circuit

The test current rise and decay times can be approximated by the following two expressions:

$$T1 = \text{Current rise time} = 3L/r \qquad (13.1)$$

$$T2 = \text{Current decay time} = 0.7RC \qquad (13.2)$$

In these expressions, T1 is the time to peak of the test current. T2 is the decay time from T=0+ to 50%. C is the capacitance of the energy storage capacitor. L and R are the totals of series resistance and inductance. If the μ is removed from the values of L and C, the times are computed in microseconds.

Coaxial return circuits

It is not recommended that the current return path to the generator be made simply by using a single wire adjacent to the aircraft (Fig. 13.2(a)), because the aircraft would respond to the electric and magnetic fields produced by current in the wire, yielding an unrealistic test.

Instead, a coaxial geometry should be used for the return path, with the aircraft as the center conductor and the return path as the outer conductor (see Fig. 13.2 (b)). As indicated in §9.5.2, current on a cylindrical conductor produces no magnetic field inside the conductor. In practice, the return circuit is usually formed from an array of wires surrounding the aircraft, as shown in Fig. 13.2(c), although metal sheets may also be used. The magnitude of the magnetic field due to return current is reduced, but not eliminated, within the return conductors in the vicinity of the aircraft. Expressed another way, the effects, on the aircraft, of the magnetic field from one return wire are cancelled (approximately) by the effects from all the other wires. The more wires are available, the more complete is this cancellation. Thus, in theory, the more wires in the return path, the better. Studies [13.3] have shown that about twelve conductors, arranged more or less uniformly around the aircraft, are adequate. The more wires, the more like a true coaxial arrangement the setup looks like. Many wires will render access to the aircraft difficult.

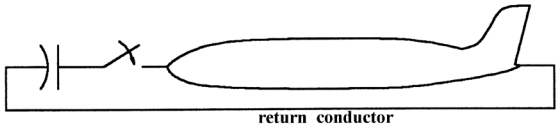

(a) Signal wire - bad

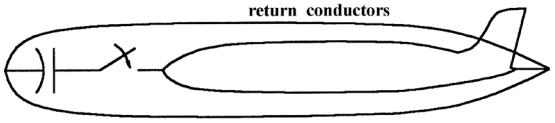

(b) Coaxial wire - good

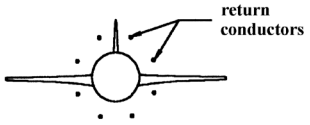

(c) End view

Fig. 13.2 Test current return circuits.

Diameter

In theory the farther the return wires are from the surfaces of the airplane the better. It is important that the wires be separated from the aircraft surfaces the same or nearly the same distances uniformly around the fuselage, so the distance between the airplane and the floor of the test area may establish the maximum separations of all the wires from the airplane surfaces.

In theory, the further the return conductor array is from the surface of the aircraft, the better, but wider spacing increases the impedance of the test circuit and reduces the ability of the generator to drive the desired currents through the aircraft. Because of these practical limitations, the spacing between the wires and the aircraft's skin cannot be more than the one or two meters that the landing gear support a large aircraft above the ground. This usually requires that the wheel well doors be open for the tests, which may expose any circuits that run through the wheel wells to fields more intense than those that would be present in flight, when the doors are closed. (Though lightning strikes to aircraft during approach or climb out, when the doors are open, have occurred.)

Impedance

Inductance and characteristic impedance (also known as surge impedance) can be estimated by calculation. Treating the aircraft and the return circuit as coaxial cylinders of the dimensions shown in Fig. 13.3 gives an inductance of 0.18 μH/m or 2.7 μH for the indicated length. The inductance of an actual installation is larger, because the outer conductor is a cage of wires. A typical inductance per unit length for an actual aircraft and return array might be approximately 0.5 μH/m. One way to measure this would be to discharge a known capacitance into the circuit and observe the ringing frequency.

The characteristic impedance of the transmission line formed by the aircraft and return circuit represented in Fig. 13.3 would be about 55 ohms, but the impedance of an actual installation varies, over its length, with corresponding changes in the aircraft's cross-sectional geometry. Typically, characteristic impedances lie in the range from 75 to 125 Ω and are best evaluated by time-domain reflectometry techniques.

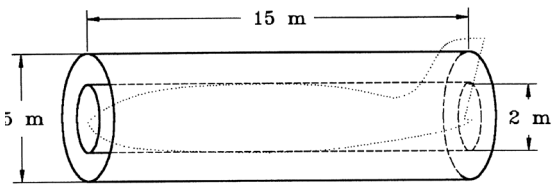

Fig. 13.3 Coaxial approximation of the test circuit.

Lumped constant example

Fig. 13.4 shows typical waveforms that might be expected when treating all elements as lumped constants. The generator circuit shown was one used in an actual test of an aircraft [13.3] and the waveforms shown in Figs. 13.4(b) and (c) closely match those obtained in the actual test, as shown in Fig. 13.7. The inductance of the aircraft and its return circuit was not measured during the tests, but the 8 μH estimated by matching calculated and measured current waveforms is typical of actual circuits.

The intent of that particular test was to obtain a current having a front time of several microseconds and a decay time of several tens of microseconds. These dimensions are typical of standard lightning stroke current definitions, such as current Component A, although the waveforms shown in Figs. 13.4 and 13.7 are not the same as Component A. The inductance of the aircraft and return conductor circuit was not critical since additional inductance had to be added to the generator to obtain the desired waveform. The rise time of the test current (to actual peak) was approximately three L/R time constants, whereas the decay time (to 50% of peak current) was approximately 0.7 RC. R and C are the resistance and capacitance of the test current generator, respectively, and L is the inductance of the aircraft and return conductors, plus any additional lumped inductance that must be included in the test current generator to obtain the desired current rise time.

Lumped constant circuits are sufficient for estimating the peak current obtainable from a particular test circuit. For the circuit shown in Fig. 13.4, and during the tests of [13.3], a current of 500 A was obtained with a generator capacitor charged to 25 kV. Obtaining a full threat current of 200 kiloamperes with this same circuit would have required a capacitor charged to 10 megavolts (a highly impractical condition) or some other combination of circuit R, L, and C. The circuit shown in Fig. 13.4 is a simple series R-L-C circuit operated in an over-damped condition, which requires a significant amount of series resistance. This resistance limits the available test current amplitude. Other circuits that include less R and L and more C can produce higher amplitude currents per kV of capacitor charge voltage, but the reduction of L necessary for this means that the return conductors must be placed close to the aircraft surface, a condition that may aggravate increasing traveling wave intensities and produce unrealistic test results.

The circuit can also be configured to obtain higher currents by reducing the series impedance but doing so precludes obtaining the desired double exponential current wave. Reducing the series resistance increases the time required for the current to reach its peak. If the series resistance is reduced sufficiently, the current becomes oscillatory. Figs. 13.4(d) and (e) show the effect of reduced series resistance on the current waveforms.

13.3.2 Traveling Wave Effects

It is not sufficient to analyze interactions between aircraft and test current generators using lumped constant circuits, since the aircraft structure is large enough that traveling wave effects will normally arise and must be considered. The aircraft and the return circuit form a short transmission line and, when the switch in the generator is closed, steep-fronted voltage and current waves are injected onto the aircraft. These are in phase with each other and comprise a traveling wave that passes between the airplane and the return wires, moving at nearly the speed of light and reflecting to the switch location at an amplitude that depends on the impedance between the airplane and the return conductors at the 'exit' end of the airplane. If, as is sometimes the case, this is a short circuit because no consideration has been given to controlling or eliminating these traveling waves, the wave will be reflected to whence it originated at the opposite polarity from what it started as. These reflections will continue for several cycles, until losses will have absorbed all the energy in the traveling wave. These are called the traveling wave voltage and current, and the amplitudes of each are related by the characteristic impedance of the transmission line bounded by the aircraft and the return conductor array.

Specifically, at the opposite end of this transmission line formed by the airplane and the current return conductor array from the test current generator, reflected voltage and current waves are launched. The polarities of the reflected waves are such that the voltage wave at that end of the transmission line goes to zero and the current doubles. When a reflected wave returns to the generator end of the aircraft, another reflected wave is generated. These waves combine to produce a current that increases in a series of steps and a voltage that oscillates, as illustrated in Fig. 13.5. In that figure, the aircraft is represented by two transmission lines, each 6.1 m (20 ft.) in length and having a characteristic impedance of 100 ohms and a propagation velocity 80% that of the speed of light. This representation is an oversimplification because it makes no allowance for the non-uniform geometry of the aircraft, but it does illustrate the basic effects.

The first effect is that the current in the aircraft builds up, not in an exponential manner, but in a series of steps as current propagates back and forth along the aircraft,

reflecting at the discontinuities at the ends. The second is that the current is different at different points on the airplane and the steps are least noted at the point of connection to the surge generator. This means that if, as is typical, the test current is measured at this point; the traveling waves may go unnoticed.

The presence of these complex traveling waves may prevent actual current waveforms in the aircraft from having the idealized shapes of the waveforms defined in the test standards reviewed in Chapter 5. They also influence the coupling of voltages and currents into the aircraft wiring. During an actual in-flight lightning strike, traveling waves may also be launched, but the traveling waves that occur on an aircraft in flight are almost certain to differ from those that occur on an airplane undergoing a FVT. These differences arise because the source impedance of a lightning channel is different (and probably higher) than the source impedance of a laboratory surge generator, and the characteristic impedance of the aircraft in flight is also probably higher too since no return conductors are present. Given that the intent of a laboratory test (one of them at least) is to duplicate, as closely as possible, the standardized lightning environment, these oscillations are undesirable and should be suppressed, as described in §13.4.

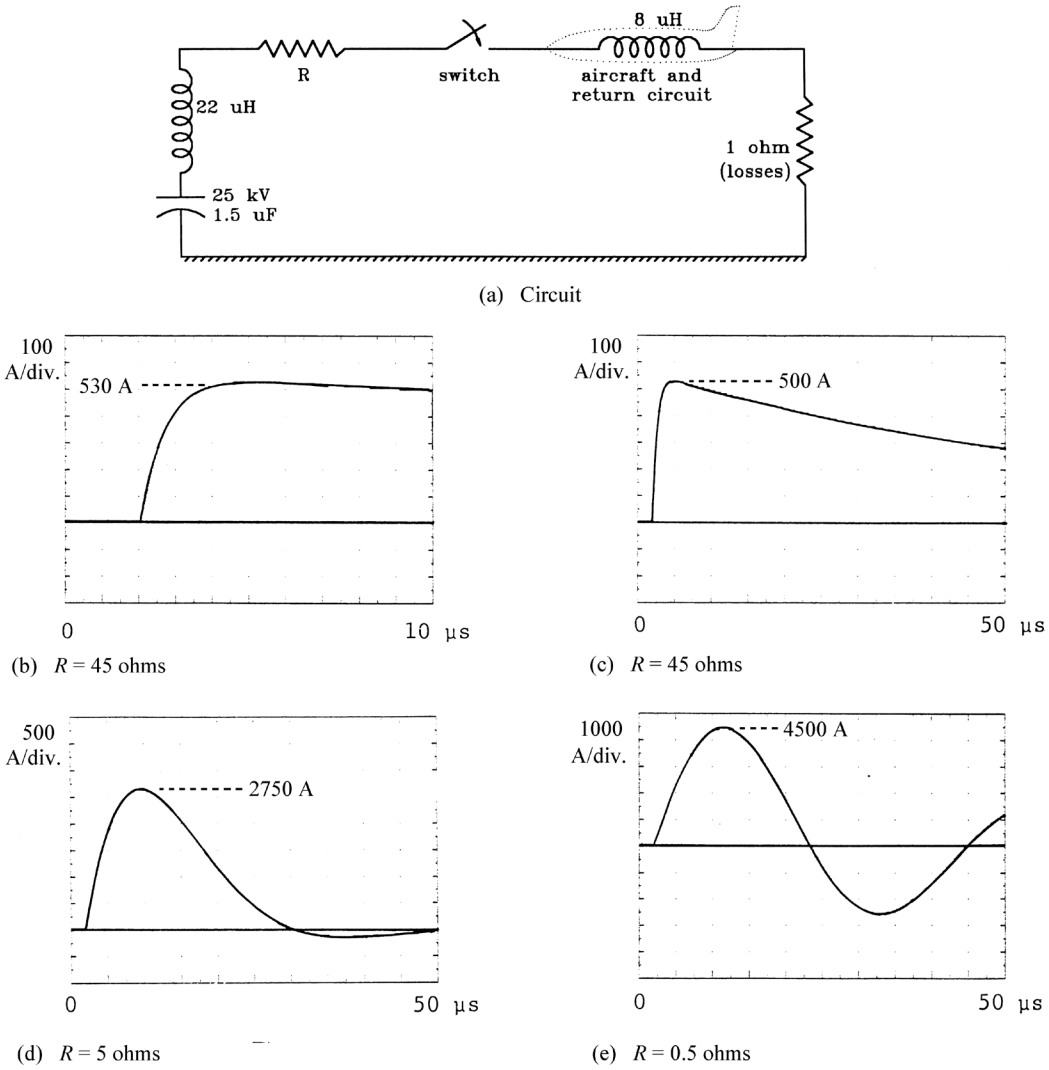

Fig. 13.4 Lumped constant representation of the test circuit. Waveforms (b) and (c) most closely represent standard current Component A. Waveforms (d) and (e) are not standard waveshapes and should not be used.

More importantly, the contributions of the traveling waves to aircraft lightning environment have already been accounted for in the standardization progress that led to the definitions of current Components A and H in the standards. This latter point has sometimes been lost to those conducting aircraft tests, resulting in test plans that provide for allowing traveling waves to appear on the tested aircraft. Steps should be taken to eliminate or minimize traveling waves. If this is not possible, adjustment must be made in the extrapolation of induced test data that is due to the rate-of-rise of the current in the aircraft, as will be discussed in subsequent sections of this chapter.

Detecting traveling waves

Traveling waves on the aircraft are difficult to detect if the test current is measured only at the input and exit points. Measuring the current at the midpoint of the aircraft is, of course, not feasible, although one could measure the magnetic field at the center and thus estimate the current. Traveling waves can best be detected by measuring the *voltage* between the aircraft and the return conductors, preferably at the midpoint of the aircraft. Fig. 13.5(e) shows a calculation of what this voltage might look like. The amplitude of the generator charging voltage can be reduced to a level that can be tolerated by the voltage probe used to view the airplane traveling voltages.

Controlling traveling waves

These traveling waves can be eliminated or controlled, so that a current wavefront with a relatively smooth double exponential rise obtained, by proper termination of the transmission line formed by the aircraft and the return circuit. One type of termination uses a resistor connected in shunt with the aircraft at the current input end. Another uses a resistor connected in series between the exit point on the aircraft and the return lines. Theoretically, both types of termination are effective, as shown in Figs. 13.6(b) through (e) but, in actual practice, neither is completely effective, since the characteristic impedance per unit length of the aircraft is not uniform from nose to tail and because actual resistors have inductances that degrade their performance.

One draw-back to a series resistor is that it reduces the maximum current available from a surge generator of a given size (see Figs. 13.6(d) and (e)). Another drawback is that considerable voltage develops between the aircraft and the return circuit. For safety reasons, it is preferable that the return circuit be grounded. Thus, the aircraft's potential rises, and insulation becomes necessary under the wheels. Insulation capable of withstanding up to 100 kV can usually be provided between the aircraft wheels and the test hangar floor without difficulty. This dielectric strength is sufficient for tests at current levels up to several thousand amperes.

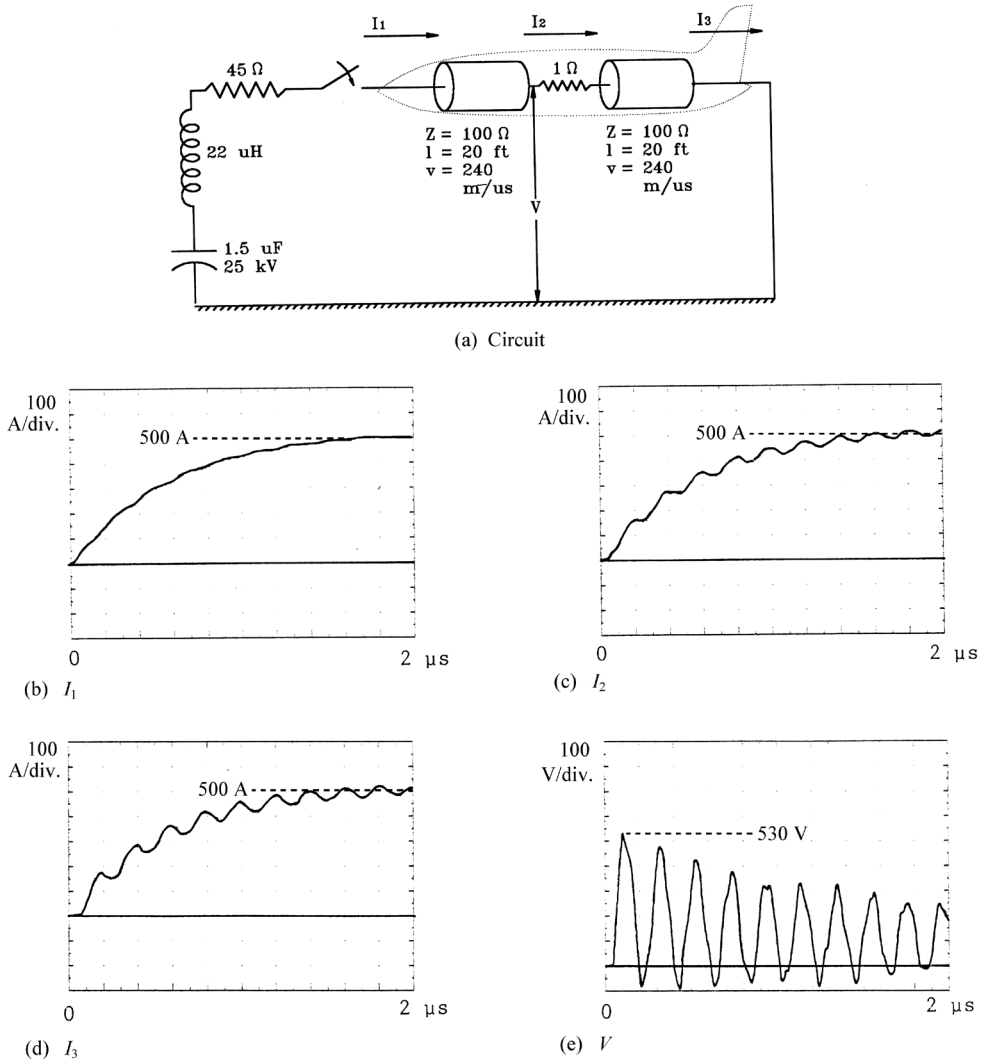

Fig. 13.5 Transmission line representation of the test circuit.

The traveling wave currents have a higher rate-of-rise than those defined for current Components A or H. No guidance is given in the aircraft lightning environment or test standards [13.1] or [13.4] on how to account for or simulate these effects in FVT tests, since the authors of those standards did not anticipate the existence of traveling waves. Thus, it is best, first, to take steps to minimize traveling wave currents, so that only the defined test currents are responsible for the measured induced effects.

If this cannot be achieved, then two extrapolation factors can be defined; one for transient voltages and currents that are related to airframe current, and another for voltages that are proportional to airframe current rate-of-rise.

This is proper since the definitions of lightning current components A, D, and H already account for the likelihood of traveling waves existing on airplanes that are struck by lightning. That is, the current rise times, and rates of rise, that are part of these waveform definitions are incorporated in the waveform definitions.

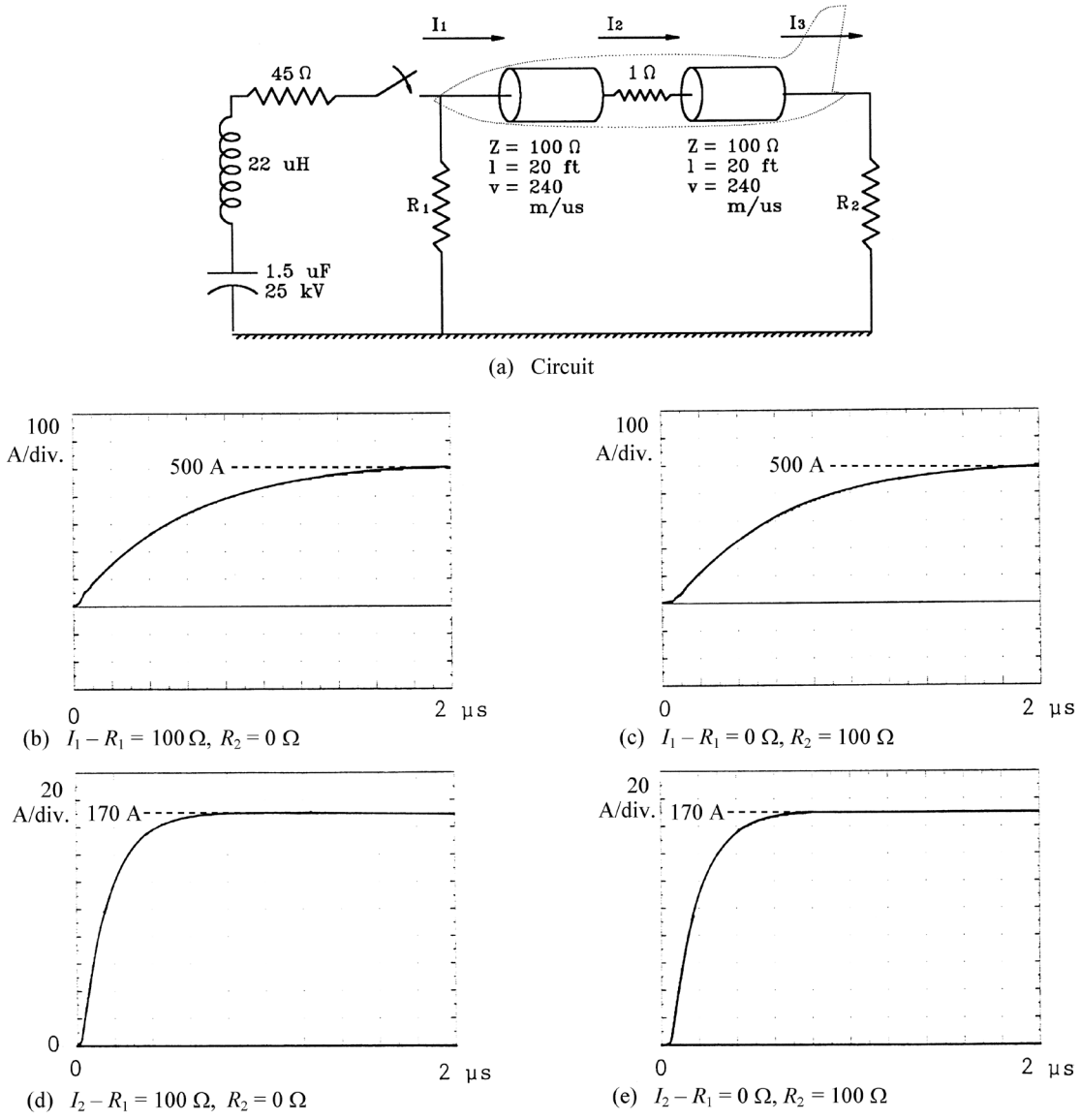

(a) Circuit

(b) $I_1 - R_1 = 100\,\Omega,\ R_2 = 0\,\Omega$

(c) $I_1 - R_1 = 0\,\Omega,\ R_2 = 100\,\Omega$

(d) $I_2 - R_1 = 100\,\Omega,\ R_2 = 0\,\Omega$

(e) $I_2 - R_1 = 0\,\Omega,\ R_2 = 100\,\Omega$

Fig. 13.6 Methods of termination.

With respect to Fig. 13.6(a), traveling wave current amplitudes are proportional to generator charging voltage, (kV), divided by the characteristic impedance, Z (shown at 100 ohms in the example of Fig. 13.6(a)). Generators producing ~1 000 A of Component A typically require a V of about 25 - 50 kV, and the transmission line arrangement typically has a characteristic impedance of ~100 ohms, so traveling wave currents of ~250 A to 500 A are possible. The rates of rise of these traveling wave current steps are determined by factors in the test circuit that influence d^2i/dt^2 (i.e., the rate-of-rise of the rate-of-rise) and they are always faster than the di/dt of the defined test current. This means that the traveling waves induce higher transient voltages, in aircraft circuits that are exposed to magnetic fields, than the applied test waveform does. This is the reason that attempts must be made to eliminate the traveling waves from the test current.

External oscillations on the return wires

Since the aircraft cannot be completely enclosed by a cylindrical return conductor, magnetic and electric fields leak through the cage of return wires and are bounded by other conductors outside, such as steel in the hangar floor and walls. Energy coupled to these systems causes a secondary set of traveling waves to propagate between the return wires and the facility structural conductors, as well as the primary set of traveling waves that propagates between the aircraft and the return wires. Reflections and refractions in the external systems may show up in the measurements made in the primary circuit.

These oscillations can be controlled by connecting both ends of the return conductor array to building ground through resistors, R_F and R_R, as shown in Fig. 13.7. Values of 100 to 150 ohms are usually sufficient. Fig. 13.7 also shows the current waveforms obtained in the actual test for which Fig. 13.4 showed calculations.

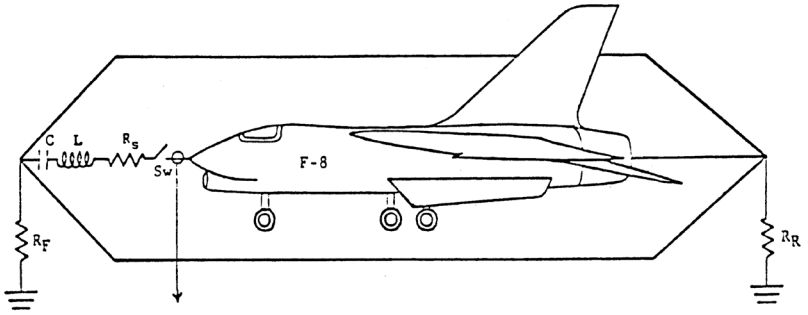

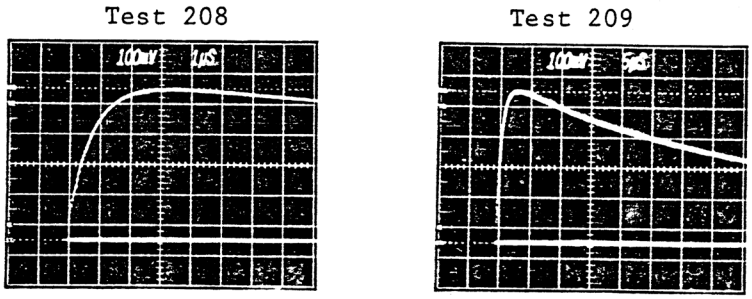

$L = 18\ \mu H$
$C = 1.5\ \mu F$
$R_s = 45\ \Omega$
$E = 25$ kV
$R_f = 120\ \Omega$
$R_R = 130\ \Omega$

Fig. 13.7 Termination resistors on the test current return array.

13.3.3 Extrapolation of Measured Transients

The low-level pulse test is applied by conducting a defined test current through the aircraft and measuring the corresponding induced transient voltages and currents in selected interconnecting wire harnesses. The tests are conducted with the same current waveforms, but at amplitudes significantly lower than the defined full-threat lightning currents. The current waveforms represent the cloud-to-earth stroke (Component A) and intracloud current pulses (Component H). The bases for extrapolation are:

- Aircraft are manufactured from non-electromagnetically saturable materials, whose properties do not change when exposed to current amplitudes and electric and magnetic fields of varying amplitudes.

- Experiments have confirmed the linear relationship between induced transients and conducted airframe current. This relationship is not strictly linear, since structural joint resistances may decrease with increased structural current density, decreasing the structural *IR* component of most induced voltage transients.

- It is rarely possible to have a fully equipped airplane available for a full threat (i.e., 200 kA) test, since test aircraft are nearly always destined to be delivered to a purchaser. Only government-owned, military aircraft, or airplanes that have been retired from service, have been tested at full threat current amplitudes.

The principle of linear extrapolation is illustrated in Fig. 13.8. Transients induced by changing magnetic fields are mostly proportional to the rate-of-rise of the test current (di/dt), and transients generated by magnetically induced or structural IxR voltages are proportional to structural current amplitudes. If the test current waveform is the same at all amplitudes, the di/dt and IxR - induced transients increase by the same extrapolation ratio. It is largely for this reason that the standardized lightning currents described in Chapter 5 are described in such detail.

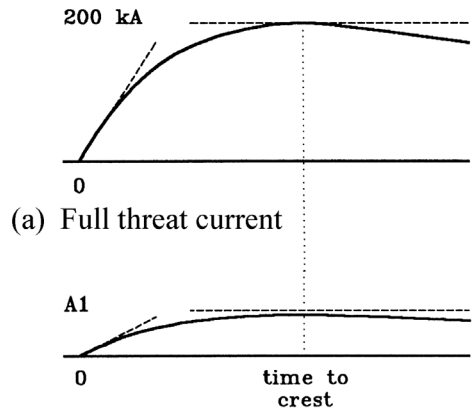

Fig. 13.8 Justifiable extrapolation.

13.3.4 Typical Test Arrangements

For the induced transients to be relatable to the conducted test current, it is necessary that influences of the magnetic fields associated with test current return conductors be minimized. This is done by positioning the test current return conductors in coaxial arrangement around the test airplane, so that the magnetic field produced by each return conductor in the vicinity of the airplane is more or less cancelled ('minimized' would be a better word.) This arrangement is shown, for example, in Fig. 13.9.

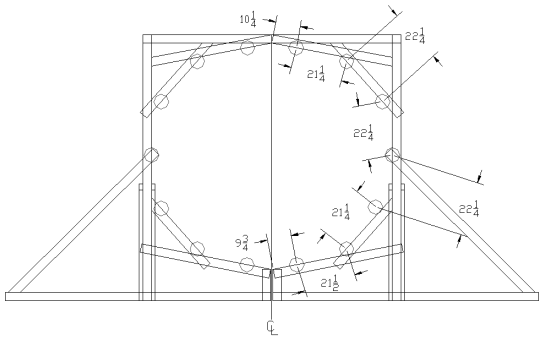

Fig. 13.9 Typical arrangement of test current conductors.

The return conductors are usually about 12 - 20 small-diameter copper wires, or sometimes a smaller number of metal foils. These can be supported rather easily from insulating stanchions made of wood or fiberglass (see Fig. 13.10)

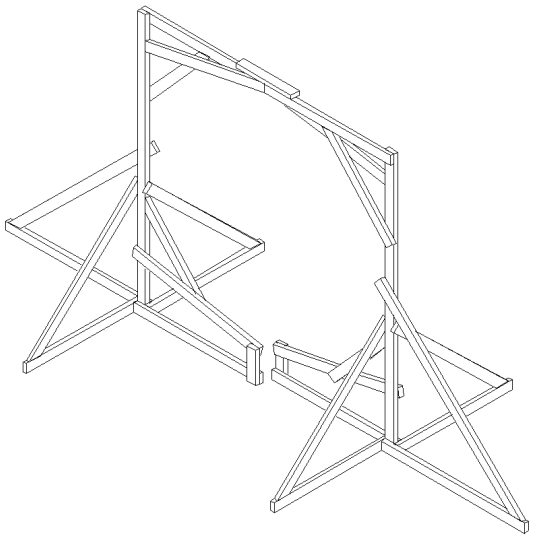

Fig. 13.10 Physical arrangement of a return conductor stanchion.

A fully assembled return array is illustrated in Fig. 13.11.

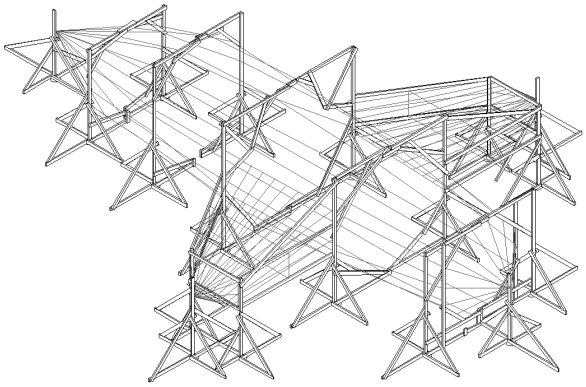

Fig. 13.11 Typical stanchion support of return conductors.

An alternate arrangement that can be used when circuits in only one wing are to be measured (on the assumption that transients in the opposite wing will be similar) is shown in Fig. 13.12.

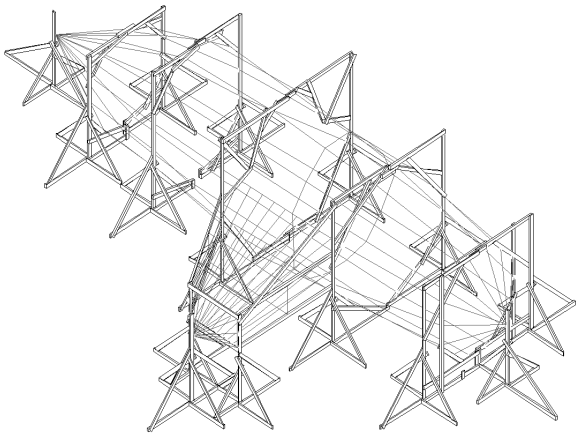

Fig. 13.12 A return conductor arrangement covering the fuselage and only one wing.

The spacing between return conductors is not critical, but the following guidelines have been shown to reduce the influence of return wires on test data:

1. Maximize the distance between the return conductors and the airplane. This is usually limited to the distance between the lower surface of the fuselage and the test facility door. Some return arrays have been supported by foam blocks that conform to the contours of the airplane major structures as shown in Fig. 13.13.

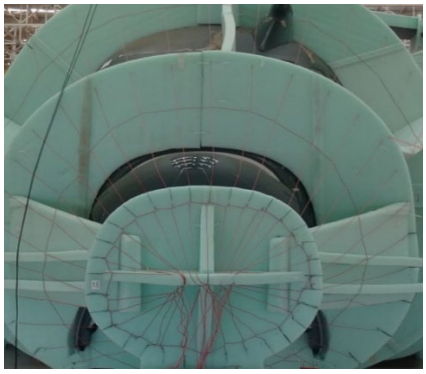

Fig. 13.13 Return wires supported by foam blocks. Close proximity of wires to airplane and large number of wires decreases characteristic impedance

Many wires can be supported at uniform spacing from the airplane surfaces using this method. A frequent pitfall is that this results in a low characteristic impedance which can increase the amplitudes of traveling waves since, as previously explained, the amplitudes of these are proportional to the generator charging voltage divided by the characteristic impedance. It is therefore desirable to place the return conductors as far from the aircraft surfaces as possible. Consideration should be given to having test current returned to the generator via a ground plane placed upon the floor beneath the airplane. This can be made of wire screens or thin metal foils.

2. Space the return conductors equally from each other.

3. Place nonconductive pads under the landing gear to provide electrical isolation between the aircraft and the floor.

Some users of wire return arrays have recommended that placing the return conductors in a profile that represents magnetic flux lines (or electric field equipotential surfaces) surrounding a charged, current-carrying airframe makes an ideal configuration.

This requires that the locations of the return conductors be generated by an electromagnetic field computational pro-gram, a process that requires an airframe configuration data file. These tools are not readily available to many users of this test method. The design of a precise return conductor array, based on computation of the electromagnetic fields around the airplane, is likely to be too expensive to be worthwhile.

Moreover, an ideal arrangement of test return current conductors would probably simulate the natural lightning environment no more accurately than the arrangement described in the simple guidelines above. Lightning inter-actions with airplanes in flight include the uncertainties associated with sweeping lightning leaders and with channels that can appear in any imaginable orientation. Thus, the 'entry' current to the nose of an airplane may in fact originate from a lightning channel that has swept along one side of the forward fuselage and then reattached to some other location. Since an infinite number of possibilities exist, a more practical approach would be to adopt a set of simple, easily implemented guidelines for test current return conductor arrangements. That way, test results obtained by different certification test facilities or organizations could be compared on a reasonably consistent basis. Another return conductor arrangement commonly used by manufacturers of large transport airplanes consists of a large ground plane, in the form of a large wire net (i.e., 'chicken wire') on the floor beneath the airplane, rather than a coaxial arrangement. This ground plane arrangement also minimizes the influence of return current, because the current density anywhere in the large ground plane is small.

13.3.5 Typical Test Currents

The test waveforms typically applied in FVTs are Current Components A and H. They are usually applied one after the other, so that measurements can be made of induced transients at each circuit identified for measurement in the test plan. Typically, records are made of the test current injection ('entry') location at recording oscillograph sweep speeds capable of viewing the wavefront and complete current waveform. Some examples of Components A and H test currents applied in FVTs by Lightning Technologies, an NTS Company, are shown in Figs. 13.14 through 13.17. The rise and decay times shown are within the allowable tolerances for testing with Components A and H.

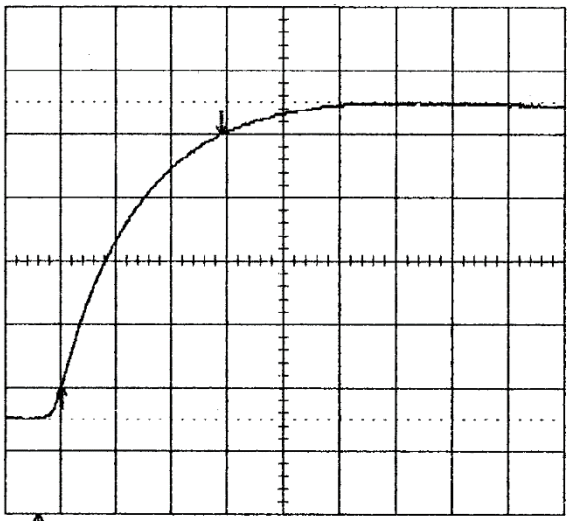

Fig. 13.14 Current Component A wavefront.
rise time (10-90%): 2.89 μs
peak: 1 000 A.

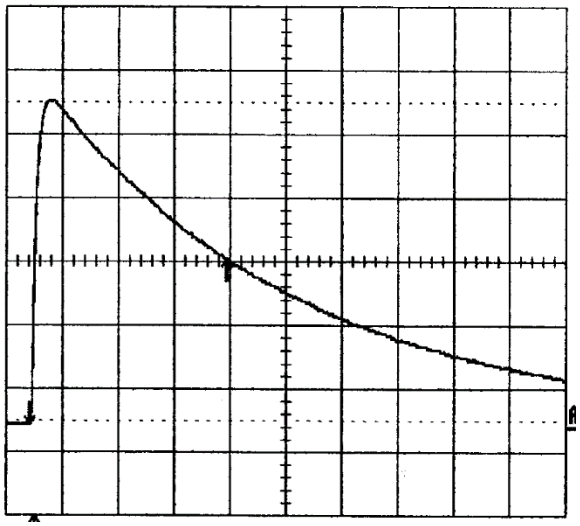

Fig. 13.15 Current Component A waveform
50% decay: 70 µs, peak: 1 000 A

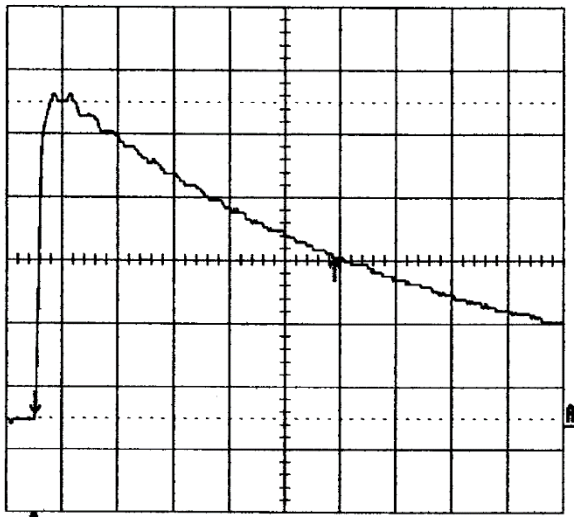

Fig. 13.17 Current Component H waveform.
50% decay: 5.3 µs peak: 135 A. Note that traveling waves cannot be seen in this view of the full waveform.

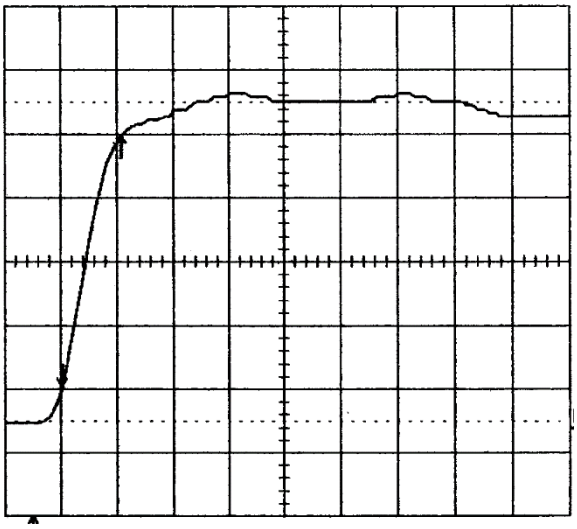

Fig. 13.16 Current Component H wavefront.
rise time (10-90%): 106 ns, peak: 135 A.

An example of a Component H waveform with more pronounced traveling waves is shown in Fig. 13.18.

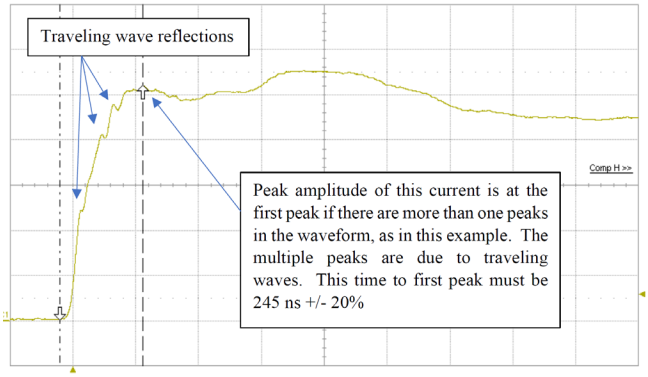

30 A/div 200 ns/div

Fig. 13.18 Component H wavefront showing traveling waves

Accommodating traveling wave effects

The peak rate of change (rise) of the traveling wave currents is always higher than the rate-of-rise of the defined Component H. Attempts should always be made to eliminate the traveling waves and achieve the correct wavefront. If this is not possible, any measurements of voltages, V_{oc}, that are due to magnetic field rate of change (and not to structural IR voltages) should be extrapolated by the ratio of 200 kA/μs divided by the actual traveling wave current rate-of-rise. This will yield an extrapolation factor that is lower than one that is based on the ratio of 10 000 A divided by the test current peak amplitude.

Measured short circuit currents, I_{sc}, are not sensitive to Component H rates of rise, and should always be extrapolated by the ratio of amplitudes.

Many low-level tests have been made with test currents as low as 300 to 1 000 amperes. The practice of estimating aircraft response from tests with lower-level UD current pulses was initially described as the 'Lightning Transient Analysis (LTA) Technique', and its development is traced in [13.2 - 13.3, and 13.5 - 13.8]. Usually, these tests are performed with currents on the order of 1 000 amperes, having waveforms as similar as possible to those in the standardized lightning environment. Some virtues of the technique are that test equipment can be transported in one package, without the need to rebuild surge generators on site, and that a large amount of testing can be done in a short time, since the equipment is easy to operate. In addition, the test current generator can be well shielded so that incidental radiation from switching spark gaps can be suppressed using small components, such as would fit inside the package that houses the energy storage capacitors. Finally, since all high voltage components can be contained in a shielded enclosure, exposure of operators to dangerously high voltages is minimized.

The main drawback to low level pulse testing is that measured results must be extrapolated by large factors. Extrapolating data from a test performed at 1 kA to a full threat, Component A current of 200 kA, requires that results be extrapolated by a factor of 200. Concerns about non-linearities associated with conducting tests at low test current levels are largely overstated. Most non-linearities result in the extrapolated transient amplitudes being somewhat (i.e., 20% or so) higher than the actual transients that would appear in the same circuits if the aircraft were tested with higher amplitude test currents. There are some situations in which actual transients would be higher at full threat than the extrapolated values predicted based on low level test currents. This usually happens with circuits that cross actuators, joints or hinges that do not conduct lightning current at low currents but do conduct at full-threat amplitudes. These situations can be identified, however, and corrected in advance of the testing, as part of the test planning process, by persons knowledgeable of lightning induced transient coupling mechanisms and experienced with this test method.

Measurement techniques for low-level tests are described in §13.4. They are, of course, also applicable to tests made at higher current levels.

13.3.6 Other Test Approaches

Full threat verification tests

One approach to testing is to subject a complete aircraft, fully configured, with all systems operating, to a full threat lightning current and note any harmful effects. Although this approach, when treated as a 'go/no-go' test, has the virtues of simplicity and rapid preparation time, it is seldom used, for the following reasons.

1. The cost and complexity of a generator capable of generating 200 kA peak current (for Current Component A) with the required waveform is excessive.

2. There would be less flexibility for controlling traveling waves, and other facility effects, than is afforded by the low-level pulse test approach.

3. Since the test program would not be aimed at gathering information on voltages and currents, there would be no immediate information with which to correct problems, should they be found.

4. This approach has the potential to damage the test vehicle. Equipment has been built to perform full threat tests, on small aircraft at least [13.9], but such equipment is not readily available for certification tests of most aircraft. Therefore, this approach has been limited to tests of military aircraft.

High amplitude tests with damped oscillatory current waveforms

Unipolar current waveforms are produced either by crowbarring, which increases the complexity of the circuit, or by using enough circuit resistance to damp oscillations, leading to inefficient use of the energy stored in the surge generator. An alternative approach to applying test current

waveforms is to accept oscillatory test currents when evaluating induced effects, just as they are accepted during tests of physical damage effects. Oscillatory currents of high amplitude can be produced by simple capacitor banks, but the waveforms are totally unlike those produced by natural lightning, or the test current waveforms defined for FVTs. Oscillatory currents have the following advantages and disadvantages.

Advantages of the high amplitude oscillatory waveform

During the period before the present standards became available, it was sometimes considered valuable to have applied "full threat" currents in FVT tests for some "added assurance" of the safety of an airplane in the lightning environment. This reason no longer makes sense in the light of the complete family of aircraft, system, and equipment tests now available and included in certification programs, which include full threat tests of everything that might respond differently to full threat test conditions as compared to low level testing. Everything on or inside an airplane that needs a full threat test for verifying its safety is assigned such tests. The fuel tanks and system equipment are examples.

Disadvantages

1. Oscillating test currents over-emphasize a particular frequency component of lightning current.

2. Tests of unique oscillating frequencies may not correctly simulate diffusion penetration of magnetic fields.

3. Oscillatory currents applied at high amplitudes are potentially damaging to the airframe and electrical or avionic equipment on the aircraft under test.

Moderate level pulse testing

A moderate level Component A test current waveform would appear as shown in Fig. 13.19.

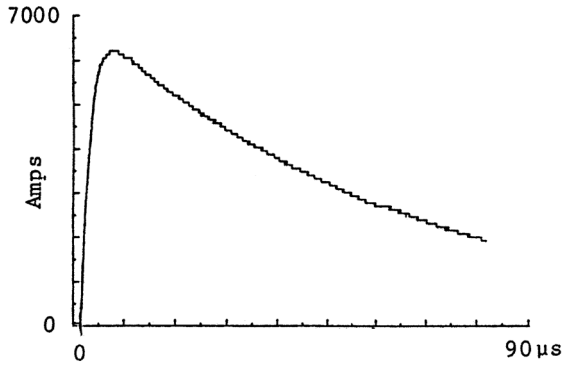

Fig. 13.19 Current waveform through an airframe.

There are two advantages to performing aircraft tests with such levels. One is that, when testing with moderate level generators (say, up to 30 kA), the stress imposed on the aircraft is comparable to that imposed by the lower amplitude (and more common than full threat) natural lightning flashes. Another, and more important advantage, is that the extent of extrapolation required to estimate full threat level responses is not great. Scaling to 200 kA from 1 kA tests involves an extrapolation of 200:1, while scaling to 200 kA from 30 kA tests involves an extrapolation of 6.7:1.

One drawback to testing with higher amplitude generators is that they are not easy to transport to remote locations for tests on aircraft. They may have to be disassembled before transit and then re-assembled at the test site. Another disadvantage is that (as experience has shown) radiation from the spark gap switches in such generators tends to couple into the aircraft under test, and into the measuring instruments, partially obscuring the voltages and currents under observation. The larger the test current generator, the more difficult it is to shield against or suppress this undesirable radiation, or to employ solid state switches that can minimize switching noise.

Then there is the ever-present need for maintaining safety of test personnel. Lightning tests at any level are potentially hazardous, but the higher the generator voltage, the higher the safety risk.

The pulse techniques described above involve direct, metal-to-metal connection of the current generator to the aircraft, for the purpose of assessing the effects of resistively and magnetically generated voltages.

These techniques are concerned exclusively with injecting current into the aircraft, without making any attempt to duplicate electric field levels at the surface of the aircraft. For safety reasons, the aircraft is at or near facility ground potential during these tests, and attempts are made to minimize voltages between the aircraft and the return circuit. Both provisions provide the vicarious benefit of keeping the electric field intensity low.

The fact that electric field coupling accompanies resistive and magnetic field coupling has been recognized, but the standardized lightning environment, as it relates to induced effects, makes no recognition of electric fields, and imposes no specifications regarding them. This is partly because electric field effects have been considered of less consequence than other effects and partly because there is little firm data available on which to base specifications regarding electric fields.

Shock-excited pulse technique

Questions surrounding some of the early full-vehicle tests led to the development of the shock-excited test technique, (Fig. 13.20), [13.10], in which the vehicle under test is insulated and excited at one point by an electrical arc. This suddenly raises the vehicle to a high voltage relative to its surroundings and establishes a high electric field at its surface. Once the vehicle becomes fully charged, a few microseconds later, a second arc is established from the vehicle to the generator return terminal (or facility ground) ground, suddenly completing the circuit and allowing current to flow, reducing the electric field to a low level.

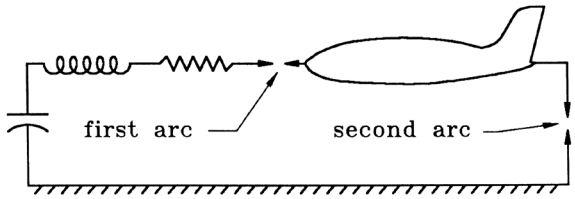

Fig. 13.20 Shock excited pulse technique.

There have been those who believed that lightning tests should be applied via electric sparks. This has been a reason for current entries and exits via sparks.

These sparks produce changes in electric fields at the aircraft extremities and thereby induce displacement currents on the airframe and (presumably) in internal circuits, presumably in a manner like that which occurs when the aircraft is struck by natural lightning.

Studies have shown that these displacement currents are much lower than those due to magnetic fields or structural IxR voltages associated with the flow of stroke current through the aircraft. For this reason, electric field tests have not been included in the family of tests applicable to certification of aircraft electrical and avionic systems.

Testing of this nature, if attempted at all, should be done with a high voltage generator that is well shielded to minimize interference coupling from its spark gaps. The pulses should be applied at voltages sufficiently high that corona forms and limits the electric field at the surface of the vehicle. This would probably require voltages more than 10^6 volts. Such tests are not necessary to demonstrate compliance of electrical and avionics systems with airworthiness regulations.

Some tests have shown that electric field coupling is the primary coupling method for some high impedance signal circuits exposed to electric fields external to the aircraft. The opposite is true for low impedance circuits, for which magnetic field coupling predominates. Electric field effects are not covered by the standardized lightning environment and there is, so far, no clear consensus as to how electric fields should be treated or what test techniques would be best for simulating them.

13.4 Measurements

This section will discuss some of the objectives of full vehicle pulse tests, particularly the techniques used in making satisfactory measurements. These objectives are applicable at whatever current level the tests are being made. They are also applicable for tests made using the Swept CW test technique that is discussed in §13.5.

13.4.1 Objectives

The main purpose of the FVTs described in the preceding sections, is to determine the magnitudes of electrical transients appearing in aircraft interconnecting wiring. This data is needed to verify that actual transients do not exceed the TCLs established for specific systems and circuits. Collecting this data is part of the certification process described in Chapter 5.

Open circuit voltages and short circuit current

The most important type of data to be collected is that on open circuit voltages and short circuit currents. There are two reasons for this:

1. They represent the total voltage induced in the circuits, and the maximum currents that may be driven by these voltages.

2. ETDLs are defined in terms of the open circuit voltage and short circuit currents that appear at the interfaces between wiring and equipment.

The open circuit voltage is the voltage appearing at the equipment interface with the equipment disconnected from the ends of the circuit. This is the wire-to-airframe ground voltage. The short circuit current is the current flowing in a short circuit between two wires, or (more commonly) between a wire and the airframe ground, also at the equipment interface, with both ends of the wire grounded.

The open circuit voltage and short circuit current suffice to define a Thevenin equivalent of the circuit. They also define the capabilities needed in a test generator used to evaluate the ability of the equipment to withstand ETDL. This latter process is the second part of the verification process described in Chapter 5. Methods for conducting equipment tests are described in Chapter 18.

Other measurements

Other measurements to be made during FVTs include cable bundle currents, currents on shields of cables, magnetic fields within structures and structural *IR* voltages.

Another purpose of FVTs is to obtain data from which TCLs and ETDLs can be established. This, of course, is only possible if a suitable airframe is available at an early stage in the design cycle, when protection criteria are being established. Sometimes, an earlier version of a derivative aircraft is available, with physical dimensions and materials of sufficient similarity to enable representative 'ballpark' transients to be measured in typical circuits and circuit routes. Occasionally, useful data can be obtained from testing major sub-assemblies of such aircraft, such as wings, fuselages, or empennage sections. In these cases, test currents are circulated through the subassembly and measurements are made of transients induced in wires that have been installed in the subassembly specifically for test purposes.

More about induced transient measurements

Aircraft FVTs conducted in support of certification are usually performed according to a test plan. The plan usually provides for measurement of the open circuit voltages and short circuit currents in individual harness conductors, as well as cable bundle voltages and currents, since this data is needed to set cable bundle ETDLs and establish the test conditions for system tests, as discussed in Chapter 5.

Lightning current entry and exit points (attachment points) on the aircraft, determine the test current paths through the airframe. These entry and exit points are selected to represent the worst case for each circuit listed for measurement in the test plan. Open circuit voltage (V_{oc}) measurements at individual circuit pins and harness connectors are made with the harness disconnected from the equipment at both the measurement and remote ends. At the remote end, the shields (if any) and the wire being measured are grounded to the equipment connector or nearby airframe structure using short jumper wires. The

lengths of these jumper wires must be kept to a minimum to prevent significant magnetic coupling from occurring and influencing test results. By grounding the measured conductor at the remote equipment end, all of the voltage induced in the conductor appears at the measurement end. When all the shields and ground wires in a harness are grounded at both ends, all signal conductors (including the one being measured) benefit from the shielding effect of the nearby shields and ground wires, just as when the harness is connected to equipment and functioning. Transient voltages are measured with high-input impedance voltage probes.

Short circuit current measurements are made by installing a short grounding jumper between the measured harness conductor pin and the local equipment connector (or other local ground point) at the measurement end of the conductor. In this case, both ends of the wire being measured are shorted to the aircraft structure or to equipment chassis that is itself grounded to the airframe. Currents flowing in the harness conductor are measured by a current transformer, placed around the grounding jumper at the measurement end of the measured conductor. These configurations are illustrated in Fig. 13.21, which shows a typical open circuit voltage measurement and a short circuit current measurement.

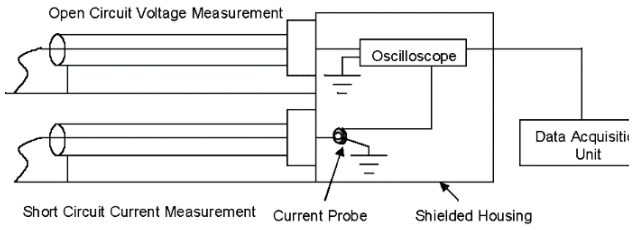

Fig. 13.21 Typical harness conductor open circuit voltage and short circuit current measurements.

For harness conductor measurements, a recording oscilloscope is often placed inside the aircraft, with the oscilloscope's inputs connected to voltage and/or current probes. A fiber optic transceiver sends the measured waveforms to the data acquisition unit for electronic storage. The oscilloscope and the fiber optic transceiver are placed in a shielded enclosure to minimize the coupling of extraneous noise into the instrumentation.

Instrument noise measurements

Voltages and currents induced in the aircraft wiring are several orders of magnitude lower than test current generator voltages and currents. This means that the oscilloscope, recording the data, must be sensitive enough to measure relatively low-level probe output voltages in areas where significant electrical and magnetic fields are present. Care needs to be taken to shield the measurement system from this radiated and conducted noise. Instrumentation noise measurements should be made periodically at each of the measurement locations, to ensure that noise levels are minimized. Signal-to-noise ratios for both voltage and current measurements more than 19:1 are always possible. (It is wrong to assume that the signal-to-noise ratio gets lower at low test current amplitudes, since both the noise and the signal are in proportion to the test current, or generator charging voltage.) Test experience confirms this.

Cable bundle currents are measured on complete aircraft harnesses using split core pulse current transformers that can fit around installed and connected harnesses.

The current probes (pulse current transformers) are connected to the shielded oscilloscope in the aircraft and a fiber optic transceiver sends the measured waveforms to the data acquisitions unit for electronic storage.

Magnetic field Measurements

Two-axis magnetic field probes have been used to measure magnetic field intensities at various locations inside the test aircraft. Data from such measurements has been used to establish data bases for use in computing anticipated induced transient levels. Magnetic field sensor outputs are fed to a digital storage oscilloscope, such as is used for the induced transient measurements. Measurements are usually made with the probe in three orientations, to measure the three, orthogonal components of the magnetic field.

Typical measured transients

Voltages and Currents in Individual Conductors: Some typical induced voltage and current transients recorded in an aircraft digital fly-by-wire flight control system harness conductors due to Components A and H test currents are shown in Figs. 13.22 - 13.24. Tests like this provide opportunities to evaluate the protective effects of shielding on induced transients. Note the different voltage scales on Figs. 13.23 and 13.24.

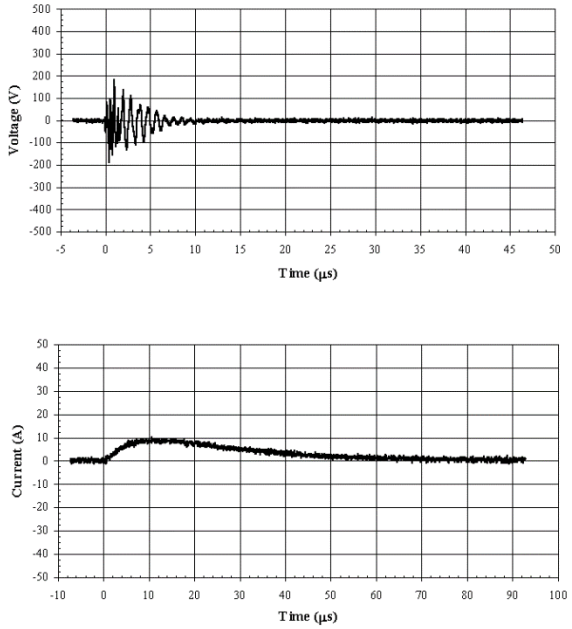

Fig. 13.22: Typical V_{oc} and I_{sc} transients with shield ungrounded at one end.

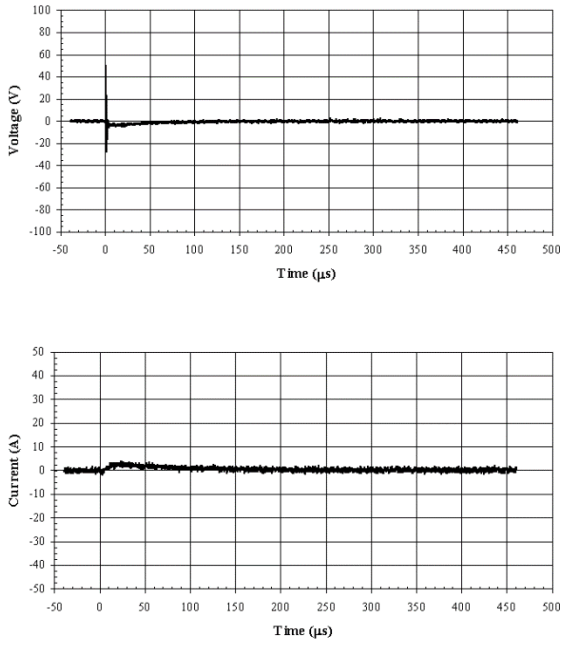

Fig. 13.23 Typical V_{oc} and I_{sc} transients with shield grounded at both ends.

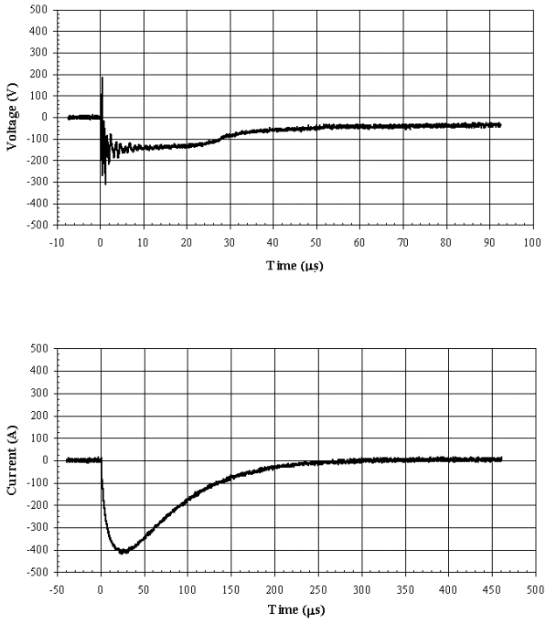

Fig. 13.24 Typical V_{oc} and I_{sc} transients with shield installed in a CFC structure with shield grounded at both ends. Note V and I scales.

The amplitude scales of all the induced voltage, cur-rent and magnetic field transients displayed in the figures have been extrapolated to full-threat (i.e., 200 kA for Component A). The oscilloscope displays are as they were recorded during the tests, which were usually conducted with 1 000 A of Component A current, conducted through the airplane. The airplane test circuit was terminated as described in §13.3.2, to minimize traveling wave effects.

When the shield was grounded at both ends (which is recommended for most aircraft signal circuits) the induced transients were reduced but not eliminated, as shown by the measurements presented in Fig. 13.23.

Fig. 13.24 shows examples of conductor V_{oc} and I_{sc} transients inside an over braided harness installed in a CFC structure. The current in the harness shield was very high, driven by the structural IxR voltage. This yields an IxR voltage in the shielded conductor, and a portion of the harness shield current is shared by the shielded short conductor, when both ends of this conductor are ‘grounded’ (i.e., connected to the shield).

Magnetic field measurements: It is useful to measure the magnetic fields present within areas where the wiring harnesses are installed for two reasons:

- For correlation with induced transients measured in circuits in the same region of the aircraft.
- To generate a database that can be used for future computations of induced transients in circuits installed in similar areas within the tested aircraft, or aircraft of similar construction.

Fig. 13.25 presents some magnetic field measurements that were taken inside a cockpit windscreen (adjacent to the glare shield) during a FVT. These measurements are typical examples of their kind. They were made using a magnetic flux probe that produced an output voltage induced by the changing magnetic field that penetrated the windscreen. This voltage was integrated to produce the magnetic field (H). Note that the waveform of the magnetic field approximates the waveform of Current Component A, and that its amplitude relates to the total test current in the airframe. This is as it should be.

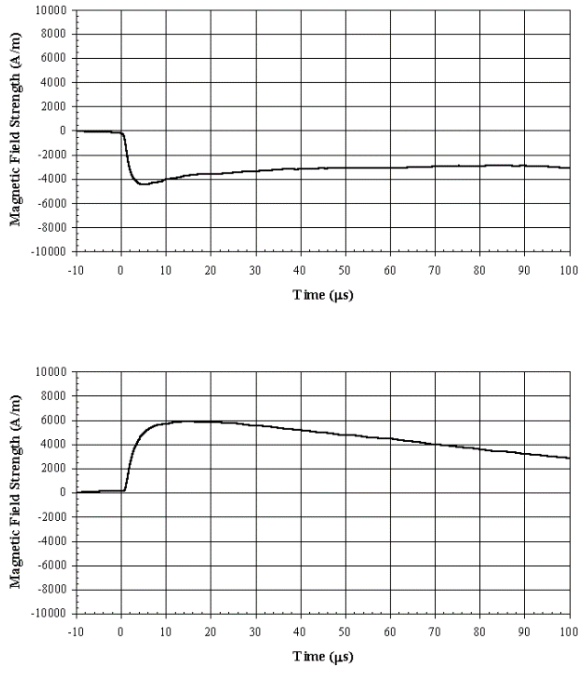

Fig. 13.25 Typical magnetic field waveforms recorded near cockpit windscreen, shown in roll axis (upper) and pitch axis (lower). Amplitudes extrapolated to correspond to 200 kA lightning stroke.

Test plans

Since it is never practical to measure transients in all wires of an aircraft, or even all wires of a flight critical system, measurements are usually made only on representative wires. The choice of where to make measurements is made based on wire routing, degree of shielding and circuit function, so as to be typical of other wires of similar description. The process of selecting the circuits and wires to be measured is a very important part of the certification process and, together with selection of test conditions (that is, current entry and exit points), constitutes the test plan.

Proposed certification plans should be reviewed with certifying authorities for concurrence prior to the start of tests if the tests are planned as certification tests.

13.4.2 Measurement Transducers

Lightning induced voltages are usually measured with commercially available, wide-band, voltage, and current probes and recorded by digitizing storage oscilloscopes (DSOs) located inside the aircraft under test. Data is usually transmitted on optical fibers to additional recording equipment located away from the aircraft.

High impedance voltage probes

Measurement of lightning-induced voltages requires sensitive DSOs, with bandwidths up to 100 MHz and dynamic ranges of at least 3 orders of magnitude. Measurements of lightning-induced voltages and currents require that digital oscilloscopes have a wide bandwidth, on the order of 100 MHz. When reviewing the specifications of digital oscilloscopes, care should be taken not to confuse the bandwidth of the analogue input circuits with that of the sampled data. Accurate measurement of an oscillatory waveform requires that the waveform be sampled several times per cycle. For example, sampling a 20 MHz oscillatory waveform 5 times per cycle requires a sampling rate of 100 MHz. Other discussions of requirements for digital measuring equipment are presented in [13.1].

Most of the DSOs available today are at least as susceptible to electric and magnetic fields as the aircraft equipment. Therefore, DSOs must be placed in shielded enclosures and, preferably, powered from independent battery packs.

If the DSO can be placed close enough to the circuit interface being tested, conventional, high impedance voltage probes can be used to transmit the signal to the DSO. Probes with leads 2 to 3 m long are commercially available.

Resistive probes

If the oscilloscope must be placed further away, then the probe signals may have to be transmitted through low impedance, coaxial cables. Connection through un-terminated coaxial cables is only satisfactory for measurements of long duration transients, such as short circuit currents and structural or shield IxR voltages. If higher frequencies are involved, the cables must be terminated with a resistance equal to the characteristic impedance of the cable (usually 50 ohms), but then the circuit being measured may be loaded excessively.

Loading can be reduced by connecting a resistor in series with the measurement cable, but this has the drawback that the voltage delivered to the measurement oscilloscope is only a fraction of the original signal voltage and is more easily contaminated by noise pickup. The higher the series resistance, the lower the loading, but the smaller the signal transmitted to the oscilloscope. If a 4 950-ohm series resistor were added to the measurement lead connected to a DSO 50-ohm input (total circuit loading of 5 000 ohms), only 1% of the induced voltage would reach the oscilloscope. If the unloaded, induced voltage signal were on the order of 1 V, the signal to the scope would be 10 mV. This would be a signal noise level of only 10:1, even without any margin for noise pickup on the measurement cables.

Active probes

Active probes may be required in some instances when small signals must be measured. Both single-ended and differential probes are commercially available, but experience with some of them has indicated that their shielding may not be sufficient to eliminate problems of noise pickup. They must be checked to ensure that the shielding is adequate.

Current measurements

Most current measurements are made using pulse current transformers that can be transmitted through a 50 Ω cable to the measuring oscilloscope. Spacing between the oscilloscope and the point being measured is seldom a problem. Currents on individual wires and small bundles can be measured with clamp-on current probes. Some clamp-on probes are available with large window openings through which large cable bundles may be passed. Other current transformers have solid cores that cannot be opened. To make a measurement with the latter type of current transformer, the conductor must be disconnected at one end, threaded through the transformer, and then reconnected. This is usually feasible for cable bundles, provided that the cable terminates in a removable connector. In order to use such transformers on single conductors, it may be necessary to cut and resplice the conductor.

Response of current transformers

Current transformers are subject to limitations in their low frequency and high frequency responses. In the time domain, these limitations are characterized by output droop during long-duration pulses and roll-off and oscillations during short-duration pulses. Care must be taken to ensure that the response at low frequencies is adequate, particularly when making measurements of short circuit currents induced by resistive effects.

Power system and radio frequency (RF) interference transforms

Current transformers operate by passing the secondary current through a burden resistor to develop an output voltage. A high burden resistor provides better low frequency response, but lower sensitivity. No transformer should be used without a burden resistor. Current trans-formers made for power frequency metering and relaying are not provided with burden resistors and, therefore, are not satisfactory for use in making measurements. They may be rendered satisfactory, however, if they are fitted with non-inductive burden resistors. (It would be best to prove such a modification by making some response measurements.) Current transformers made for electromagnetic interference and compatibility (EMI/EMC) measurements are not usually satisfactory either since they do not have adequate low frequency responses or they are meant to be loaded with the 50 Ω input impedance of a measuring instrument.

Optical coupling of probes to recording oscilloscopes

Some of the noise problems encountered during surge testing can be overcome by using optical links to couple the outputs from voltage and current probes to the measuring oscilloscope, but optical links have problems of their own. Analog (not digital) optical links are required, with bandwidths as wide as that of the measuring oscilloscope. Wide bandwidth optical links tend to have high noise levels and limited dynamic range. The sensitivities of analog optical links are more prone to deterioration than the sensitivities of conventional, hard-wired links. Care must be taken not to overload the transmitters and the sensitivity of the link must be checked frequently.

Noise induced in measurement circuits

Noise can be induced in the measurement system in several ways, as shown in Fig. 13.26. Electric and magnetic fields can impinge on the recording DSO and induce noise directly into the internal circuits. Experience indicates that the best way to avoid this is to install the DSO in a shielded enclosure.

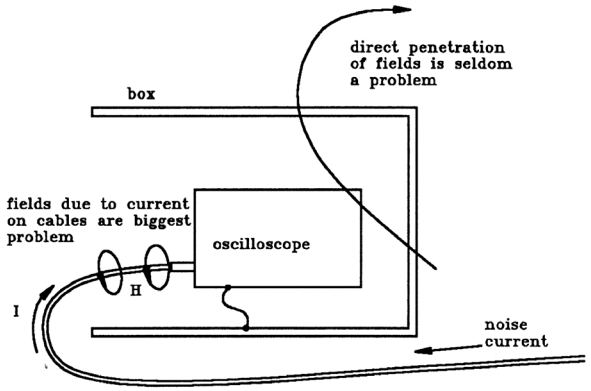

Fig. 13.26 Mechanism by which noise is induced into measuring circuits.

A more common source of noise is current induced in the shields of the measurement cables. Such currents may be caused by differences in potential between the point of measurement and the oscilloscope, or they may be caused by electric and magnetic field induction into the measuring cable. As the currents flow through the resistance of the cable shield, they produce a voltage rise that appears at the terminals of the cable, as described in Chapter 15. Minute amounts of magnetic and electric flux also leak through the holes in the shield and induce voltages. As the current on the cable flows through the connectors at the oscilloscope, additional voltages are introduced. The way to eliminate these voltages is to shield the measurement cables well and to keep the noise currents out of the measurement cable and away from the oscilloscope. This is usually achieved by insulating the cable shield and DSO enclosure from the airframe and by keeping the cables as short as possible.

Shielding for oscilloscopes

The primary means of minimizing noise problems during FVTs is to shield the oscilloscope and the measuring leads. Some reference to such shielding has already been made in the preceding section, but more discussion is in order, since accumulated experience has yielded insight into which techniques are useful and which are not.

There are two main concerns. The first is preventing incoming probe leads from carrying noise current into the oscilloscope. The second is preventing ambient fields from interacting directly with the oscilloscope.

These problems can be mitigated by placing the scope within an aluminum box and having the probe leads shielded, with those shields terminated at connectors on the box, and the box grounded to the airframe near to where the measurements are to be made. To be effective against electric fields the shields need only be grounded at one end (see Chapter 15) but for protection against magnetic fields the shields must be grounded at both ends. This can allow induced currents to circulate in the shields, sometimes introducing noise into the probe leads.

Sometimes it has been possible to place a small battery-powered oscilloscope within an empty equipment enclosure. Then the voltage or current probes may also be positioned within this enclosure and the cables are plugged in to the connectors on the enclosure in the normal way. An example of this is shown in Fig. 13.27. This works for measurements to be made at this equipment, but not for other measurements needed in the same or other areas within the airplane. A view within such an enclosure is shown in Fig. 13.27.

Fig. 13.27. Empty equipment enclosure with oscilloscope, modem, and optical fiber link to a display outside of the airplane.

Measurement system sensitivity and response times

The primary means of minimizing noise problems during FVTs is to shield the oscilloscope and the measuring leads. Some reference to such shielding has already been made in the preceding section, but more discussion is in order since accumulated experience has yielded insight into which techniques are useful and which are not. For the applied Components A and H test currents, a conventional DSO was used to capture the currents using a Pearson 110 current probe. Measurement Equipment Sensitivity, Bandwidth, and Response Times are shown in Table 13.1.

Table 13.1 – Typical Measurement Equipment, Sensitivity and Response Times

Equipment	Sensitivity	Lower Bandwidth Limit	Upper Bandwidth Limit	Response Time Limit
LeCroy Model WS24XS	2 mV to 10 V/div (±2%)	DC	200 MHz Can be limited to 20 MHz	1.75 ns
Agilent Technologies Model U2702A	2 mV (±4%)	DC	200 MHz	1.75 ns
Pearson Model 110 CT	0.1 Volt/Amp (+1/-0%)	1 Hz (-3dB)	20 MHz (-3dB)	20 ns
Pearson Model 150 CT**	0.5 Volt/Amp (+1/-0%)	40 Hz (-3dB)	20 MHz (-3dB)	20 ns
Pearson Model 3525 CT*	0.1 Volt/Amp (±1%)	5 Hz (-3dB)	15 MHz (-3dB)	25 ns
Pearson Model 411 CT	0.1 Volt/Amp (±1%)	1 Hz (-3dB)	20 MHz (-3dB)	20 ns
Pearson Model 5523 CT	0.1 Volt/Amp (±1%)	7.5 Hz (-3 dB)	12 MHz (-3 dB)	30 ns
Pearson Model 7795 CT	0.1 Volt/Amp (±1%)	25 Hz (-3dB)	15 MHz (-3dB)	25 ns
Pomona 1:1 6491 Voltage Probe	1 Volt/Volt	DC	30 MHz at -3dB for Pomona 6491 probe	N/A

Additional noise Considerations

The above considerations do not include the effects of instrumentation noise being mixed in with the data measurements. Noise could be coupled from various sources: generator switch noise, the return array, adjacent harnesses, or airframe structures.

Voltages and currents induced in shielded aircraft wiring are several orders of magnitude lower than test current generator voltages and currents. This means that the measurement oscilloscope must be sensitive enough to measure relatively low-level probe output voltages in areas where significant electrical and magnetic fields are present due to conducted currents on return arrays and noise from generator high voltage switches. Care must be taken to shield the measurement system from this radiated and conducted noise.

In some cases, instrumentation noise results in a noticeable response added to an individual wire measurement. In some instances where the wire measurements are very low, it is necessary to distinguish the difference between real signal and noise induced on the instrumentation. Voltage probe noise is measured by shorting both leads of the voltage probe to its ground reference point. Current probes should be placed nearby the wire or cable whose current is to be measured.

If noise is measured by either the voltage or current probes, the probe may be removed and a shorting plug installed on the probe cable to see if the noise has originated in the probe, or in the cable.

If noise is excessive, the offending probe or cable can be wrapped in aluminum cooking foil that is connected to existing cable shields with hose clamps and the noise measurements repeated.

Shielding for measurement cables

The best way to avoid measurement noise problems is to prevent noise currents from flowing on the shields of the measuring cables. This can be achieved by making sure that the instrument cable shield and the DSO enclosure are isolated the airframe, and by fitting all incoming measurement cables with an external braided shield. This external shield should be terminated to the DSO enclosure, not to the input connectors of the DSO. Triaxial cable is good, but it is also easy to slide woven copper braid or aluminum cooking foil over the surface of ordinary coaxial cable. For best results this additional shield should be insulated from the original shield (see Chapter 15).

The objective of tis external shield is to keep noise currents off the measuring cable and away from the DSO, particularly away from the input connectors, where the DSO

is most vulnerable to noise pickup. It is best to terminate the external shield to the exterior of the box and as far from the input of the DSO as possible. The inconvenience of having to open the box to make connections is part of the price of getting good shielding performance. It is preferable to bring the measurement cable (but not the external shield) through a hole in the box (Fig. 13.28(a)) but a bulkhead connector for the signal carrying cable is often satisfactory (Fig. 13.28(b)). If a bulkhead connector is used, the overall shield (OAS) should terminate on a shell around the connector, not on the connector itself (Fig. 13.28(c)). The OAS should *not* be terminated to the box through a pigtail (Fig. 13.28(d)). The OAS on the measuring cable must be connected to the probe and the DSO enclosure to protect against magnetic fields, as discussed in Chapter 15.

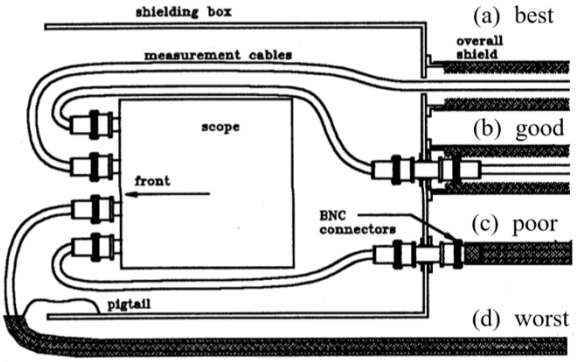

Fig. 13.28 OASs for reduction of noise

Noise checks

Tests should be performed to verify the effectiveness of the shielding on the measurement system. This is accomplished by disconnecting the measurement leads from the aircraft wiring, connecting them to a local airframe ground point close to where the transient measurements will be made, and discharging the surge generator. If no noise is picked up by the measuring system, then one can have good confidence that the signal displayed on the oscilloscope truly represents the response of the aircraft wiring.

13.5 Low-level, Swept Continuous Wave (CW)

The low-level, swept CW technique is a frequency-domain method that involves exciting the aircraft with very low amplitude (< 1 A), continuous sinusoidal currents, rather than time-domain pulses. A network analyzer is used to measure transfer functions that relate the multiple-frequency, sinusoidal signals recorded in the aircraft's internal wiring to the sinusoidal currents conducted through the airframe. These transfer functions, if measured over a suitably wide frequency-range, may then be multiplied by the frequency spectrum of a lightning pulse to determine the overall spectral response at the test point. Fourier transforms can then be taken to evaluate the time-domain response.

Advantages and disadvantages of the swept CW technique are outlined below:

Advantages

1. Standard low-level oscillators and network analyzers may be used. These are commercially available and operate at levels sufficiently low that there are no safety problems, either to personnel or the aircraft.

2. Measuring instruments are not exposed to the effects of spark-gap switches.

3. Aircraft and wiring system resonances are clearly displayed and quantified.

4. System responses may be quantified by tabular listings of amplitude and phase without need for developing equivalent circuits.

5. Many users are more used to working with frequency domain data than with time domain data.

Disadvantages

1. There is no way to evaluate non-linearities in the aircraft response.

2. Interpretation of test results in terms of time domain waveforms requires inverse Fourier transformations.

3. Scaling to full threat levels requires very large extrapolation factors.

Since very large extrapolation factors are necessary and there is no way to evaluate possible non-linearities in the response of a tested aircraft, the swept CW method is not recommended for tests of aircraft whose electrical circuits span composite airframe materials. The reason for this is that composite airframes often display greater non-linearities than conventional aluminum airframes.

When the swept CW technique is applied to a composite aircraft, the test results should be compared with results using higher amplitude pulse currents representing Component A (i.e., 1 000 - 3 000 A) for authenticity.

Methods for conducting both the time domain impulse and the frequency domain swept frequency sinusoid wave tests are included in the test standard [13.1].

13.6 Safety

During simulated lightning testing, even at reduced levels, lethal levels of electrical energy are present at the terminals of capacitors, spark gap switches and other high voltage equipment. Thus, safety precautions must be taken and test procedures must be designed (and followed) that ensure that, during the test applications, personnel will not accidentally come in contact with any electrically energized parts of the test circuit.

A secondary concern is the inherent danger of passing substantial currents through an aircraft fuselage containing fuel. This concern includes the problems associated with electrical arcing taking place in an area where fuel vapors may be present.

13.6.1 Personnel Safety

Personnel actively involved with operating surge generators, RF equipment, and measuring equipment may need to be physically close to or inside the aircraft during the test. This is particularly true for personnel operating measurement instruments. The safe operation of measurement instruments requires that safety procedures be developed and well understood, not only by those directly involved in the tests, but by those witnessing the tests. Appropriate licenses for use of RF equipment will likely be required.

Safety briefings

Prior to the start of active testing, all personnel working in the area, both those assigned to the test and those normally working in adjacent areas, should be assembled for a safety briefing and familiarization with the project. Written safety procedures are advisable.

Test area

The aircraft, test generators, wave shaping circuits, high voltage power supply, and capacitors involved in full vehicle testing are, periodically, energized to dangerous voltages. Therefore, a clearly defined test area should be fenced or roped off, in such a manner as to preclude any person standing outside of the area from coming into accidental contact with these dangerous voltages. No one should enter the test area without the permission of the test operator.

Safety ground point

A safety ground point should be established, to which the facility ground, test circuit power supplies, low voltage side of the generator and safety grounding sticks can be connected. This ground point must be attached to the building structural steel, preferably in the floor. This point may also serve as an instrumentation ground reference-point, although that is not its major function. The grounding stick can be in the form of a metal hook fastened to an insulating handle and connected to a flexible grounding wire. Another grounding hook should be provided for the surge generator.

Testing procedures

High voltage test equipment should be operated only by qualified personnel specifically designated to do so.

During a test, observers should not remain within the test area. Those who are working on the aircraft or assisting with the test should approach or enter the aircraft only when test equipment is de-energized and grounded and after entry has been authorized by test personnel. The test personnel should ensure that equipment is de-energized and safety grounds are applied before observers are permitted to enter the test area or the aircraft under test.

Personnel who are operating the surge generator or measuring equipment should repair to their designated stations before the safety grounds are removed. Those operating measuring instruments may be in physical contact with the aircraft (in it or alongside it) during the test, but only if they are not in simultaneous contact with ground and return wires.

Except for those operating measuring instruments, no one should contact the aircraft or return lines when a pulse from the surge generator is being applied.

Those who must make physical contact with the aircraft or test equipment during the tests have a special responsibility to ensure that they understand where and when such contact is safe and what procedures are necessary to avoid unsafe contact.

Once the test area has been cleared of personnel, (with the exception of those operating measuring instruments) the test operator should enter, remove the grounding

sticks, return to his station, and perform the test. At the completion of a test or a series of tests, the operator should shut down the high voltage power supplies, enter the area, and ground all potentially energized points before allowing any others to enter. The ground stick should be hung on the aircraft pitot boom or other current injection points between tests.

13.6.2 Fuel System Safety

Since the aircraft under test is usually operational, residual fuels may be present in the tanks, fuel lines, and vents. Since a fuel vapor mixture may be flammable, it is recommended that the tanks be drained of fuel and filled with dry nitrogen at positive pressure during the test period. Alternatively, the fuel tanks may be filled with fuel to eliminate as many vapor spaces as possible and the remaining spaces (such as fuel and vent lines) can be filled with dry nitrogen at positive pressure, to ensure a nonflammable atmosphere during the test period. Local fire marshal requirements may also be applicable.

Exposed electrical arcs

Some effort should be made to ensure that all switching arcs in the aircraft test circuit (including the switching gap of the surge generator) are restricted or enclosed. However, some tests may require (or produce) exposed arcs, which could become ignition sources. Consequently, it is very important that all personnel be aware of (and on the alert for) fuel spills or fuel vapors in the test area. No test should be conducted with fuel leaks or spills in the area. Testing can resume only after the leaks or spills have been repaired and/or cleaned up. The source of any fuel vapors in the area must be identified and dealt with prior to proceeding with the tests.

References

13.1 *Aircraft Lightning Test Methods*, SAE ARP 5416, Section 6.1, *Aircraft Tests,* SAE International, Warrendale, PA.

13.2 J. E. Pryzby and J. A. Plumer, "Lightning Protection Guidelines and Test Data for Adhesively Bonded Aircraft Structures", *NASA CR3762*, NASA, Langley Research Center, January, 1984.

13.3 K. E. Crouch, "Aircraft Lightning-Induced Voltage Test Technique Developments", *NASA CR 170403*, June 1983.

13.4 SAE Aerospace Recommended Practice: *Aircraft Lightning Environment and Related Test waveforms*, ARP 5412, November 1999.

13.5 W. W. Cooley, D. L. Shortess, "Lightning Simulation Test Technique Evaluation", *DOT/FAA/CT87/38*, U.S. Dept. of Transportation, Federal Aviation Administration, October 1988.

13.6 L. C. Walko, "A Test Technique for Measuring Lightning-Induced Voltages on Aircraft Electrical Circuits", *NASA CR2348*, NASA Lewis Research Center, February 1974.

13.7 K. J. Lloyd, J. A. Plumer and L. C. Walko, "Measurements and Analysis of Lightning-induced Voltages in Aircraft Electrical Circuits", NASA CR-1744, February 1971.

13.8 J. A. Plumer, "Lightning Effects Relating to Aircraft, Part III-Measurements of Lightning-Induced Voltages in an F4H1", *AFAL-TR-72-5, Part III*, Air Force Avionics Laboratory, Wright Patterson AFB, Ohio, March 1973.

13.9 J. A. Plumer, F. A. Fisher and L. C. Walko, "Lightning Effects on the NASA F8 Digital Fly-by-Wire Airplane*", NASA CR-2524*, 1975.

13.10 J. W. G. Butters, D. W. Clifford, K. P. Murphy, K. S. Zeisel and B. P. Zuhlman, "Assessment of Lightning Simulation Test Techniques", *Proceedings of IAGC on Lightning and Static Electricity*, March 1982.

.

Chapter 14

THE RESPONSE OF AIRCRAFT WIRING

14.1 Introduction

The primary means of verifying that an aircraft will not be harmed by the induced effects of lightning are equipment and systems tests, in combination with the aircraft full vehicle tests (FVTs) described in Chapter 13. These are tests in which transient voltages and currents are injected into the terminals and wiring of aircraft systems. The specifics of these tests are described in Chapter 18. The roles that each of these tests play in the certification process are described in Chapter 5, together with the standards that describe how to conduct each of these tests.

The standards present the aircraft lightning environment and menus of transient waveforms that this environment is likely to induce in the interconnecting wiring. Chapters 9 through 13 of this book have described the physics that leads to the transients appearing in the wiring, depending on the aircraft structure characteristics and the amount of protection incorporated in the wiring. We have referenced some of the programs that are available to apply the physics and compute transient waveforms and levels.

Some have called the process of determining voltages and currents on individual components a 'flow-down' process, implying that it involves determining how much of the external lightning environment 'flows down' onto individual components. Ideally, the performance of 'flow-down' calculations to determine the most likely voltages and currents on the wiring of an aircraft would be clearly identified as one of the necessary engineering tasks, and would be allocated suitable staff, time, and funding. This will lead to improved safety. Planners that overlook this part of the process and jump directly to testing invite risks of lightning strikes compromising system performance.

In principle, the voltages and currents on the aircraft wiring may be calculated based on the geometry of the wiring and a knowledge of the strength and orientation of the internal magnetic and electric fields, as discussed in Chapters 10, 11, and 12 and this is what the computer programs are best suited for. Alternatively, these voltages and currents may be measured experimentally, as discussed in Chapter 13.

Since staff and funding are not always available to perform the necessary measurements and calculations, it is usually best to use simplified techniques that are at least accurate enough to determine the order of magnitude of the voltages and currents induced by lightning effects. The following material will describe such techniques. The estimates that result from them may not be very precise, but they can at least indicate the general magnitude and nature of the induced voltages and currents, and that may be sufficient for preliminary designs or equipment specifications.

This chapter treats both the open circuit voltage and the short circuit current induced on these circuits. Knowing the open circuit voltage is important because it represents the maximum voltage to which a circuit or electrical insulation might be exposed during a lightning strike. Short circuit current is important because it represents the maximum current that might flow through an element designed to carry current, such as a protective spark gap or diode. The two factors together define the source impedance of the surge, a quantity needed to conduct rational bench testing of equipment.

14.2 Impedances of wires

Inductances and capacitances of conductors were discussed in §9.5.3 and §9.6.1. The situation is shown in Fig. 14.1. Simplified expressions for calculating the self-inductances and capacitances per unit length of wires suspended in air above a ground plane are:

$$L = 2 \times 10^{-7} \ln \left| \frac{2h}{r} \right| \qquad (14.1)$$

$$C = \frac{55.56}{\ln(2h/r)} \quad \text{pF/m} \qquad (14.2)$$

where

h = height above a ground plane
r = radius of conductor

Self-inductance and capacitance may also be estimated from Figs. 14.2 and 14.3. Inductance and capacitance also define the surge impedance of a conductor.

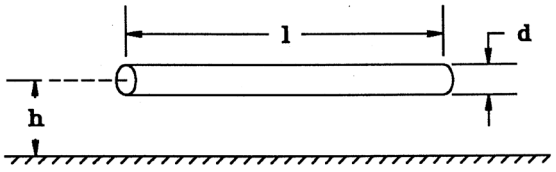

Fig. 14.1 Wire above ground plane.
Note that r = d/2

$$Z = 60 \ln\left(\frac{4h}{d}\right) \text{ ohms} \qquad (14.3)$$

The velocity of propagation on such conductors is 300 m/μs (the speed of light).

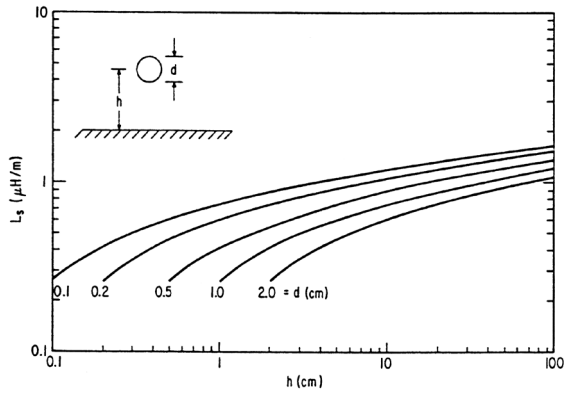

Fig. 14.2 Inductance of wires.

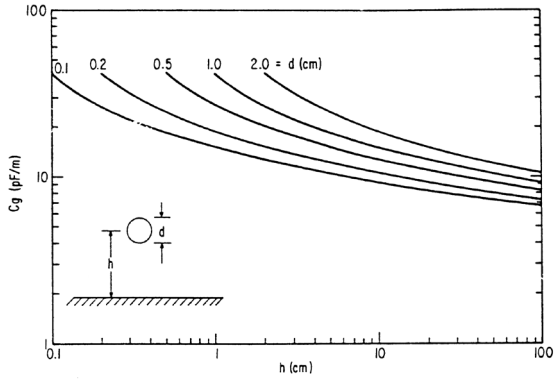

Fig. 14.3 Capacitance of wires.

14.3 Response Mechanisms – Short Wires

The response mechanisms will be reviewed first for conductors short enough that their responses can be treated in terms of lumped constant elements. Many wiring systems in aircraft do not strictly qualify for this treatment, since they are long enough to be treated as transmission lines, but the lumped constant approach does illustrate the general nature of the response. Transmission line or distributed constant considerations are discussed further in §14.4.

14.3.1 Response to Resistive Voltage Rises

The elementary equivalent circuits are shown in Fig. 14.4.

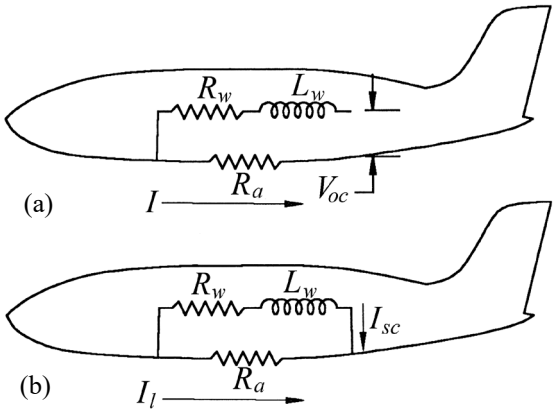

Fig. 14.4 Open circuit voltage and short circuit current responses to resistive voltage.

R_a represents the resistance of the aircraft or, more precisely, of the portion of the aircraft under consideration, while R_w and L_w represent the resistance and inductance of the wire. The most severe case involves conductors that are referenced to the airframe at one or more points. Power distribution systems are frequently so arranged. If the conductor is grounded at only one end (Fig. 14.4(a)), the quantity of most interest is the open circuit voltage developed at the other end. If both ends of the wire are grounded (Fig. 14.4(b)) the quantity of interest is the short circuit current.

Open circuit voltage

A lightning current, I_l, produces an open circuit voltage:

$$V_{oc} = I_l R_a \qquad (14.4)$$

Wire routing and wire resistance do not affect this voltage.

Short circuit current:

If the wire is connected to the airframe structure at both ends, the current through it depends on its resistance, its inductance, and the waveform of the lightning current. The relevance of the waveform is, perhaps, not obvious, but it becomes a limiting factor where surge arresters are employed to limit the voltage appearing between a conductor and the airframe. Assuming $R_a < R_w$, the wire current for lightning currents of long duration is,

$$I_{sc} = I_l \frac{R_a}{R_w} \qquad (14.5)$$

while, for lightning current of short duration, the wire current is

$$I_{sc} = \frac{1}{L_w} \int V_{oc} dt \qquad (14.6)$$

where

I_{sc} = amperes, A
L = self-inductance of wire or cable, H
V_{oc} = open circuit induced voltage, V
t = time, s

Multiple conductors

If there are several conductors in a bundle, all of them are subjected to the same open circuit voltage and short circuit current.

Wire shields

If a shield around the wire, is grounded at only one end, as shown in Fig. 14.5(a), it does not reduce the voltage or current to which the wire is subjected. However, if the shield is grounded at both ends, as shown in Fig. 14.5(b), it does reduce the induced voltage or current, but the amount of reduction depends primarily on the resistance of the shield, rather than the resistance of the aircraft and the wire.

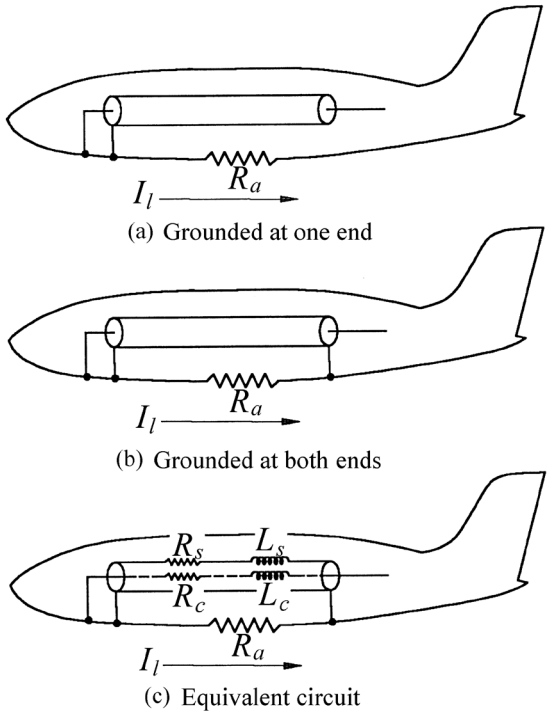

Fig. 14.5 Effects of a shield.

Example

The #6 AWG wire represented in Fig. 14.6(a) is typical of a power distribution bus on an aircraft. The 10 mΩ resistive path, to which the wire is connected at one end by a ground lead, represents aircraft structure. The circuit is exposed to the IxR voltage due to 50 kA of lightning current Component A in the airframe.

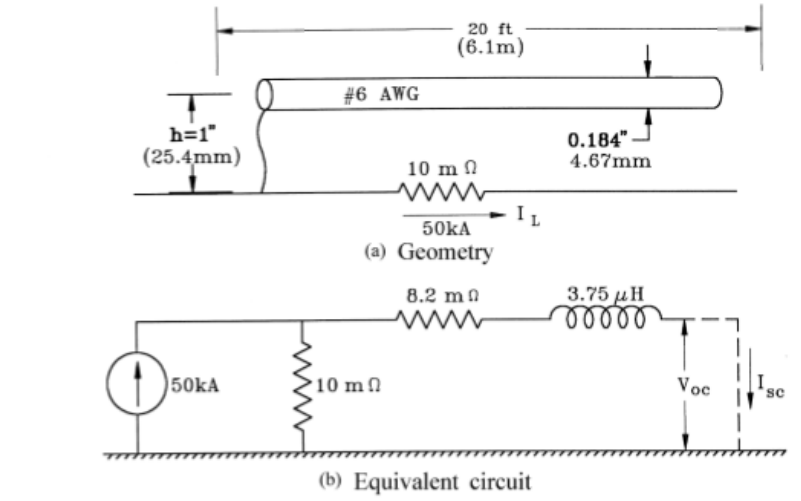

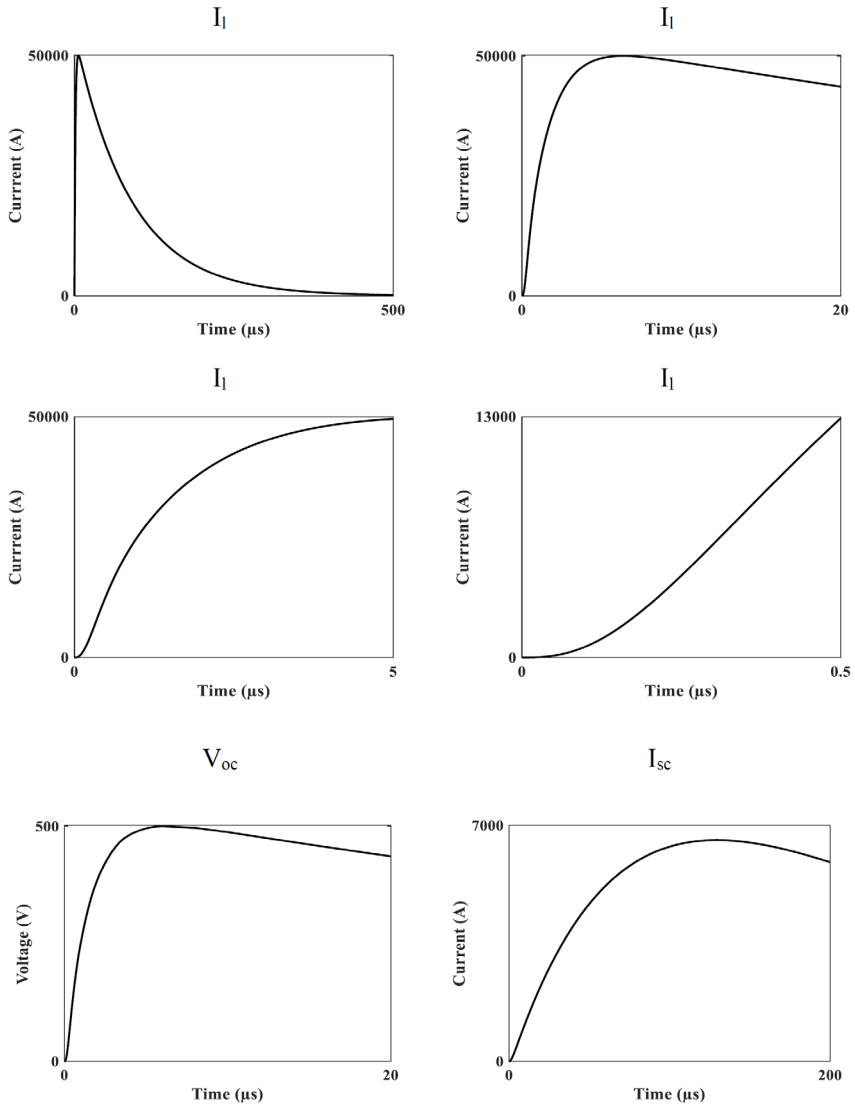

Fig. 14.6 Resistively coupled voltage and Current.

Fig. 14.6 shows the 50 kA lightning current source as a complete waveform within 500 μs and then the wavefront is displayed on 20 μs, 5 μs and 0.5 μs time bases, the latter to show the asymptotic startup of the current waveform, which is that of Component A shown in Fig. 5.7.

For the designated lightning current in Fig. 14.6 an open circuit voltage or short-circuit current, V_{oc} or I_{sc}, would by induced in the loop between the wire and the ground plane. The point of most importance is that this short-circuit current is controlled more by the inductance of the wire than by its resistance and reaches its peak long after the aircraft current has begun to decay.

Source impedance

Strictly speaking, source impedance is the ratio of the instantaneous voltage to the instantaneous current, and

$$Z = \frac{V_{oc}}{I_{sc}} \qquad (14.7)$$

it is time and frequency dependent. Often, however, this ratio is used to determine the source impedance. For the above example, this would be 0.08 ohms. This quantity is a useful measure of the impedance of the circuit, but it should be used with caution since it pertains only to the specific driving current waveform.

The illustration in Fig. 14.6 is somewhat oversimplified, but it does illustrate the point that source impedance for resistively generated voltage is quite low. This low source impedance is an important point that must be considered when applying surge protective devices, as discussed further in Chapter 16.

14.3.2 Response to Magnetic Fields

The simplest geometry to consider (Fig. 14.7) is that of a conductor placed adjacent to a metal surface and exposed to a uniform magnetic field that is oriented to produce the maximum voltage in the conductor. Of course, signal conductors are rarely found in an aircraft. Conductors in aircraft are usually part of a bundle of wires, or one of the wires is a multiconductor cable. For the analyses to follow, the loop voltages for a single wire are about the same as they would be for a group of wires comprising a cable or bundle. If the cable is fitted with a shield, the shield can be treated as just another conductor.

Open circuit voltage

The open circuit voltage induced between the wire and the nearest ground plane (called the common mode voltage of wires in a cable) is given by

$$V_{oc} = \frac{d\varphi}{dt} = \mu_o A \frac{dH}{dt} \qquad (14.8)$$

where

A = area of the loop involved - m^2
A = *lh* in Fig. 14.7.
$\mu_o = 4\pi \times 10^{-7}$ H/m
φ = total flux linked - webers
H = magnetic field intensity - A/m
t = time - s

If *l* and *h* are measured in inches:

$$V_{oc} = 8.11 \times 10^{-10} lh \frac{dH}{dt} \qquad (14.9)$$

where

l = length - in
h = height above ground plane - in
H = magnetic field intensity - A/m
t = time - s

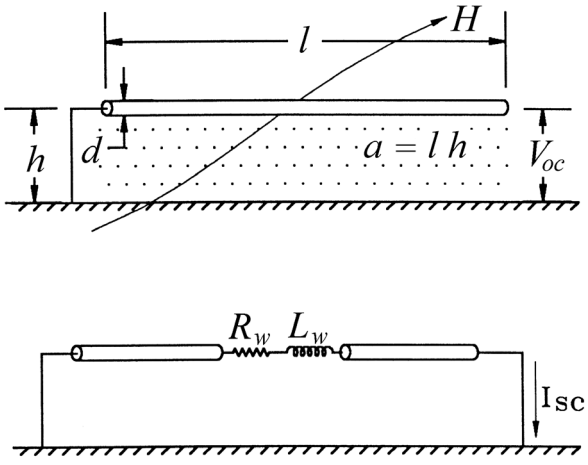

Fig. 14.7 Response to magnetic field.

The induced voltage is thus proportional to the length of the wire, its height above ground and the strength of the magnetic field. This voltage can be reduced by keeping wires or cables close to the ground plane and by routing them along a path where the magnetic field strength is low. (These points are discussed further in Chapter 15.)

An elementary model for voltage induced in a loop formed by a wire and a ground plane consists of an ideal voltage source placed at the center or at one end of the wire. If the actual circuit load impedances are included, the induced voltage divides between the loads at the ends of the wire. The largest voltage appears across the load with highest impedance. For worst-case analysis, one can consider one end of the wire to be grounded and the other end to be open circuited. All the voltage, then, appears at the open circuit end of the wire.

Short circuit current

The maximum induced current for a given circuit geometry is that which would flow if both ends of the wire or cable were connected to the vehicle structure through a low or zero impedance (Fig. 14.7). The short-circuit current is then mostly affected by the wire inductance and (considering inductance only) is:

$$I_{sc} = \frac{1}{L}\int V_{oc}\,dt \qquad (14.10)$$

where

I_{sc} = amperes
L = self-inductance of wire or cable - H
V_{oc} = open circuit induced voltage - V
t = time - s

The induced voltage, V_{oc}, that drives the current, is directly proportional to the height of the cable above the ground plane, but the cable inductance, L, that impedes the flow of current, is proportional to the logarithm of that dimension. Both V_{oc} and L are proportional to cable length. The result is that short circuit current is practically independent of the length of the cable and only moderately dependent on the height of the cable above ground.

An individual wire might have a low impedance load if it is connected to a semiconductor, in which case the short-circuit current would flow directly through the semiconductor and its bias source. If the circuit is intentionally designed to have a low input impedance, there may be no damage, if the current is not too large. Maximum available short circuit current is an important point to consider when selecting surge protective devices.

Multiple wires

If a group of wires is involved (Fig. 14.8) the induced voltage, calculated using Eq. 14.8, represents the voltage between the entire group of conductors (comprising the bundle or cable) and the vehicle structure. If the load impedances at the ends of the wires are equal, the voltage on each of the wires is about the same and does not depend on the location of the wire within the bundle or cable.

Line-to-line voltages

Line-to-line voltages (also called differential or circuit voltages) are generally lower than line-to-ground voltages by a factor of between 10 and 200 (or between 20 and 46 dB), because individual conductors are usually closely grouped and are often twisted together, which reduces the total loop areas of their circuits.

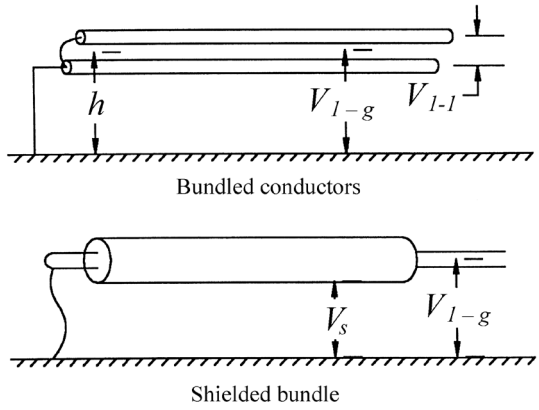

Fig. 14.8 Multiple conductors.

Analytically determining the voltages between wires, or the dB differences between line-to-ground and line-to-line voltages in terms of wire locations, requires modal analysis techniques, but that subject is beyond the scope of this book. Empirical estimates are often about the best that can be hoped for.

The actual magnitude of the circuit voltage is determined as much, or more, by the impedances of the circuits to which the wires connect as it is by the characteristics of the wire. Prudence suggests that one should not rely on line-to-line voltages being less than line-to-ground voltages by more than 10%, unless the circuits have been carefully designed to have balanced impedances at both ends of their cables.

Effect of a shield

If a wire is enclosed in a shield that is grounded at only one end (Fig. 14.8) the magnetically induced voltage between the conductor and ground is not much reduced. The magnetic field outside the shield induces as much voltage between the end of the shield and ground as it does between the conductor inside it and ground. A shield grounded at both ends does reduce the induced voltage, but a description of how this happens is deferred to Chapter 15.

Orientation of the field

Eqs. 14.8 and 14.9 assume that the magnetic field is oriented at right angles to the plane of the loop. If the field were oriented differently, the induced voltage would be less but, for simplified calculations such as these, it is probably prudent to consider only worst-case orientation of the field.

Example

Fig. 14.9(a) shows the same conductor that was shown in Fig. 14.6(a), but this time it is subjected to a changing magnetic field having the waveform also shown in Fig. 14.9, which is the same waveform as current Component A. The amplitude of 1 000 A/m is typical of a field that might penetrate a cabin window. In the equivalent circuit in Fig. 4.7 the voltage source would have an amplitude and waveform as calculated by Eq. 14.9. For this elementary circuit, the driving voltage is the same as V_{oc} in Fig. 14.9, and its waveform is the derivative of the magnetic field. The short circuit current is proportional to the integral of the open circuit voltage and has nearly the same waveform as the magnetic field driving the circuit.

Source impedance

The ratio of open circuit voltage to short circuit current for Fig. 14.9 is 2.9 ohms, a value much higher than in the resistively coupled example shown in Fig. 14.6. As in §14.3.1, this source impedance only applies when the magnetic field has the specific waveform indicated in this example.

14.3.3 Response to Electric Fields

Equivalent circuits for objects exposed to electric fields are not as intuitively obvious as equivalent circuits for conductors exposed to *IxR* rises or changing magnetic fields. They are best developed by discussing the short circuit current (also known as the displacement current) before discussing open circuit voltage.

Displacement current

Theoretically, magnetically induced voltages and currents can be eliminated from conductors by placing the conductors flush with a ground plane. This does not apply to conductors exposed to a changing electric field, however. Fig. 14.10 shows a surface exposed to a changing electric field, E_u, which is assumed to be oriented perpendicular to this surface. The changing electric field produces a displacement current, I_{disp}. If a portion of the surface is isolated and connected to the rest of the surface through a conductor, then this displacement current flows through the conductor and has an amplitude given by Eq. 14.11.

$$I_{disp} = \varepsilon_o A \frac{dE_a}{dt} \qquad (14.11)$$

where

A = area of the surface - m^2
$\varepsilon_o = 8.854 \times 10^{-12}$ F/m
E_o = actual electric field - V/m
t = time - seconds
I_{disp}= displacement current - amperes

The capacitance of the plate depends on its geometry and that of the surroundings surfaces and can be either calculated or measured. The capacitance does not affect the short circuit current, but it does affect the open circuit voltage, as will be explained shortly.

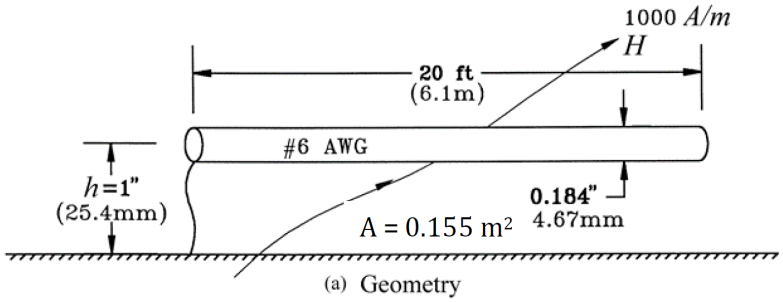

(a) Geometry

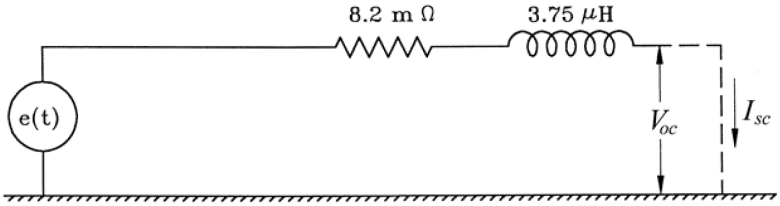

(b) Equivalent circuit

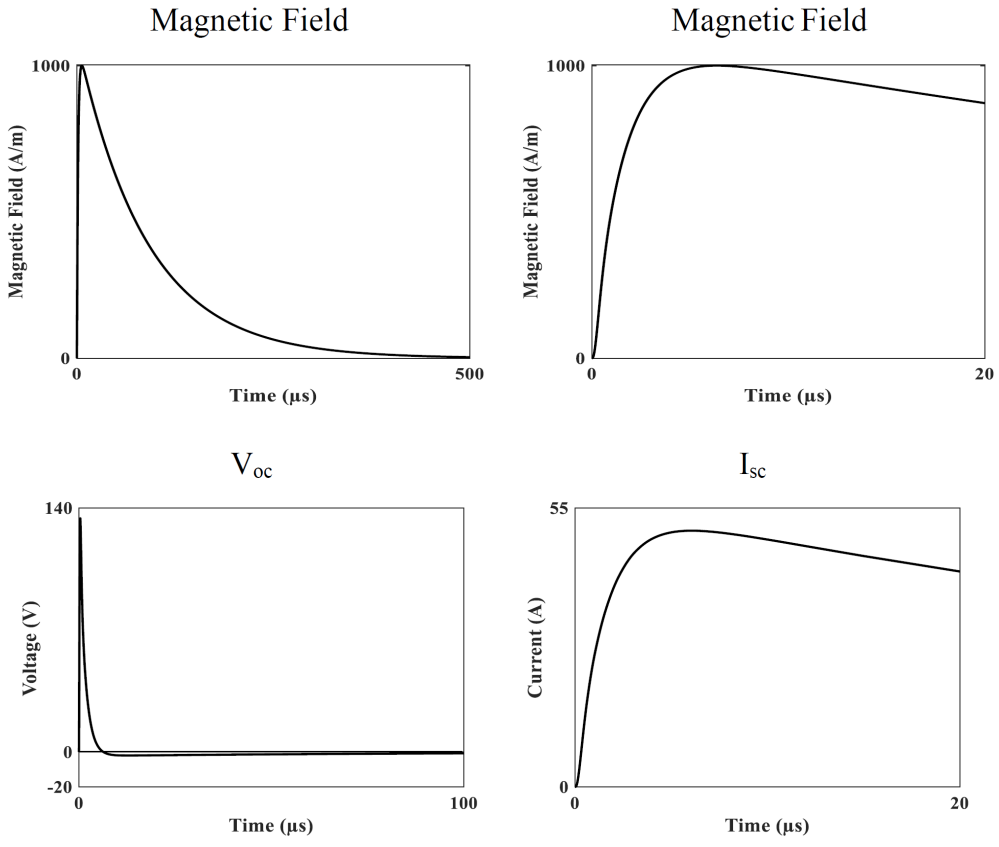

Fig. 14.9 Magnetically induced voltage and current.

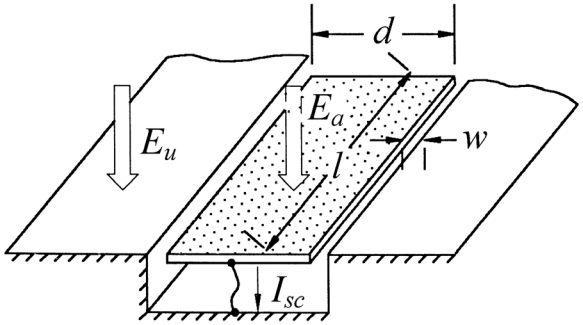

(a) Geometry

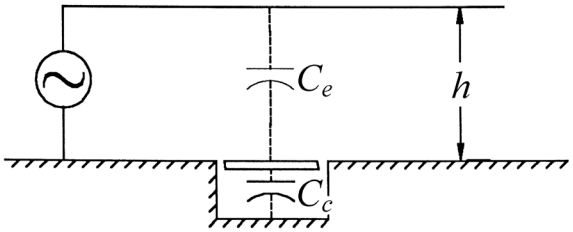

(b) Equivalent circuit

Fig. 14.10 Elevated surface.

An alternative view, more readily adapted to numerical analysis, treats the problem of displacement current in terms of the equivalent circuit shown in Fig. 14.10(b). This circuit involves an equivalent capacitance, C_h, connected to a hypothetical plate at a height h_e. The plate is energized by a hypothetical voltage source, V_e.

$$I_{disp} = C_h \frac{dV_e}{dt} \qquad (14.12)$$

where

$$V_e = h_e E \qquad (14.13)$$

$$C_h = \frac{\varepsilon_o l d}{h_e} \qquad (14.14)$$

h_e cancels out because it appears in both V_e and C_h (in both numerator and denominator of Eq. 14.12).

The current depends on the intensity of the electric field E_a incident to the isolated section. If the isolated section were set flush with the rest of the surface and the spacing, w, between the two sections were negligible, then the actual field E_a would be equal to the undisturbed field E_u.

If, as shown in Fig. 14.11, the isolated surface were raised above the surrounding surface, the actual electric field intensity E_a would be greater than the undisturbed field, E_u. Consequently, such a surface would intercept more displacement current. Calculating the current intercepted (or evaluating the factor, K, in Eq. 14.11) would require evaluating the electric field intensity at all points on the surface. This would involve either cut-and-try field plotting or one of the various two-dimensional (2D) and three-dimensional (3D) modeling techniques referenced in Chapters 10 - 12.

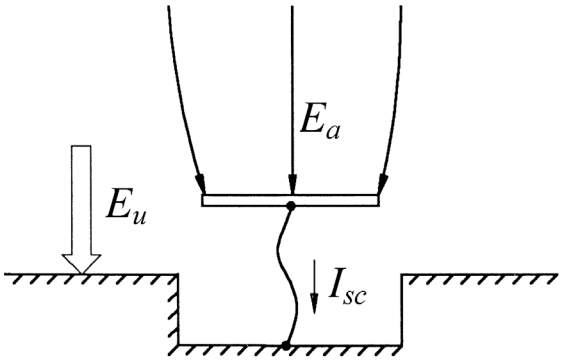

Fig. 14.11 Elevated surface.

A simple geometry for which K or E_a can be calculated is the hemicylinder shown in Figs. 14.12(a) and (b).

$$E_a = 2E_\mu \cos\varphi \qquad (14.15)$$

Integrating this electric field over the surface of the hemicylinder shows that it intercepts twice the displacement current of a flush surface having the same projected area.

Thus, the factor, K, for the hemicylinder is equal to 2. The current intercepted by several other geometries is shown in Table 9.5, and values of K can be calculated. (Values of K for conductors above ground planes can easily be calculated.)

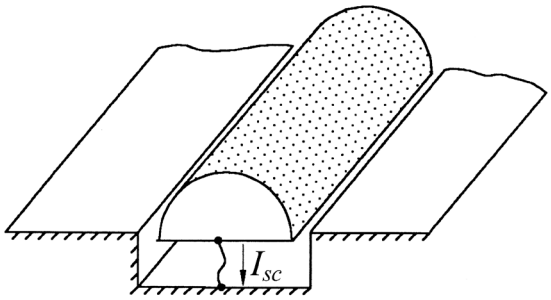

(a) Geometry

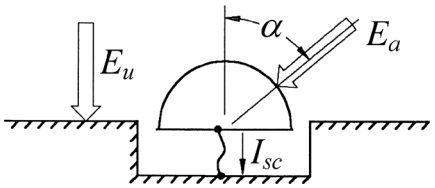

(b) End view

Fig. 14.12 Hemicylinder

Figs. 14.11 and 14.12 are examples of how some antennas are designed to be effective receivers and transmitters of modulated electric fields. They also remind us of why it is that projections from aircraft surfaces may sufficiently intensify electric fields to initiate streamers, leaders, and lightning attachments.

Open circuit voltage

The open circuit voltage is most easily obtained by integrating the displacement current in the known (by measurement or calculation) capacitance of the conductor.

$$V_{oc} = \frac{1}{C}\int I_{sc}dt \qquad (14.16)$$

Recognizing that I_{disp} is proportional to the rate-of-change of electric field, the open circuit voltage of the isolated plate of Fig. 14.10(b), for example, is

$$V_{oc} = \frac{\varepsilon_o ld}{C}E \qquad (14.17)$$

where C is the capacitance of the plate with respect to its immediate surroundings.

Conductors above ground

For the case of an isolated conductor above ground (Fig. 14.13(a)), the open circuit voltage would be

$$V_{oc} = hE_a \qquad (14.18)$$

The equivalent circuit in Fig. 14.13(b) treats this open circuit voltage as if it were connected to a load through the capacitance of the conductor. The capacitance being as given by Eq. 14.2. The short circuit current is then

$$I_{disp} = C_c\frac{dV_{oc}}{dt} \qquad (14.19)$$

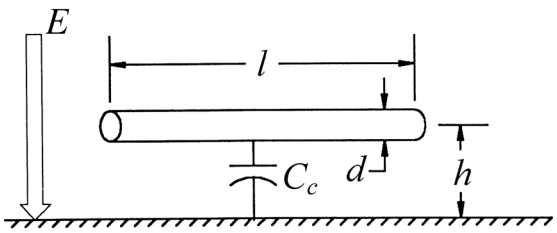

(a) Geometry

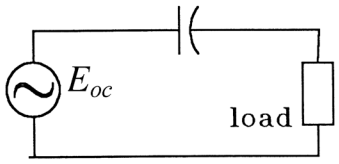

(b) Equivalent in terms of V_{oc} and C_c

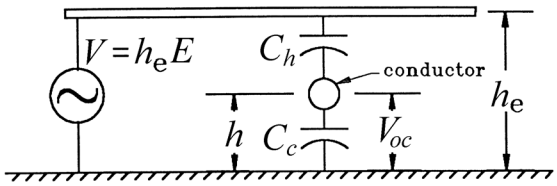

(c) Equivalent in terms of V and C_h

Fig. 14.13 Equivalent circuits for electric field coupling to elevated conductors.

Note that E_{oc} is the electric field (V/m) presented by the electric field to an open-ended wire suspended in the air as shown in Fig. 14.13. The transient voltage of interest, V_{oc} is shown in Fig. 14.15.

The equivalent circuit in Fig. 14.13(c) is more convenient for analysis purposes. The electric field is replaced by a fictitious surface at a height, h_e, connected to a voltage, $V_e = h_e E$. The open circuit voltage can then be defined in terms of the actual, physical capacitance, C_c, and an equivalent coupling capacitance, C_e:

$$V_{oc} = V_e \frac{C_h}{C_h + C_c} \tag{14.20}$$

If h < 1, h_e may be regarded as unity, in which case

$$C_h = C_2 \left(\frac{h}{1-h}\right) \tag{14.21}$$

K factors

For isolated conductors, the factor, *K*, (as used in Eq. 1.11) can be calculated by equating short-circuit currents as expressed by Eqs. 14.11 and 14.19

$$K = \frac{d}{h} \cdot \frac{2\pi}{\ln(4h/d)} \tag{14.22}$$

A graph of *K* as a function of h/d is shown in Fig. 14.14.

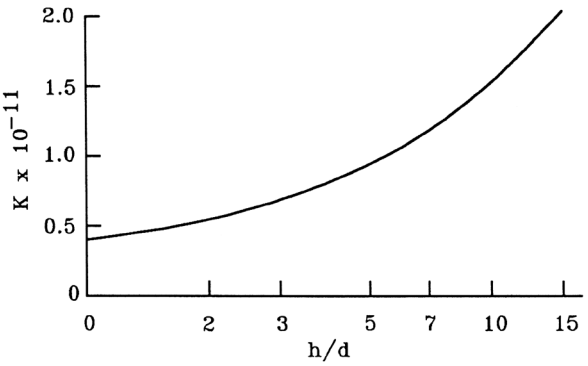

Fig. 14.14 Factor *K* for elevated conductors.

Example

Fig. 14.15(a) shows the conductor from Fig. 14.6 exposed to the electric field whose waveform is shown in Fig. 14.15(c). The equivalent circuit of Fig. 14.13(b) was derived as shown in Fig. 14.13(c) and Eq. 14.21, where h_e is regarded as unity. The open circuit voltage and short circuit current for this circuit shown in Fig. 14.15(d).

Source impedance

The source impedance of the circuit in Fig. 14.15, defined by the ratio of the peak voltage to the peak current, is 12 500 ohms. This impedance is much higher than it would be for an equivalent conductor exposed to *IR* voltage rises or a magnetic field. Note that this impedance pertains only to the electric field waveform shown in Fig. 14.15(c). This high source impedance partially explains why it is easier to provide effective shielding against electric fields than against magnetic fields or resistively generated voltages.

Multiple conductors

Electric fields impinging on conductors in a bundle are intercepted primarily by the outer conductors in the bundle. Thus, the location of a conductor in a bundle does make a difference in the displacement currents that can be expected to flow on it. This is not true of resistively or magnetically induced currents.

Effect of a shield

Since displacement currents are primarily intercepted by the outermost conductor, a shield reduces capacitively coupled currents, even if it is grounded at only one end. This observation assumes that the shield is short enough that its impedance is negligible; an assumption typically made (although often unstated) in discussions of shielding practices.

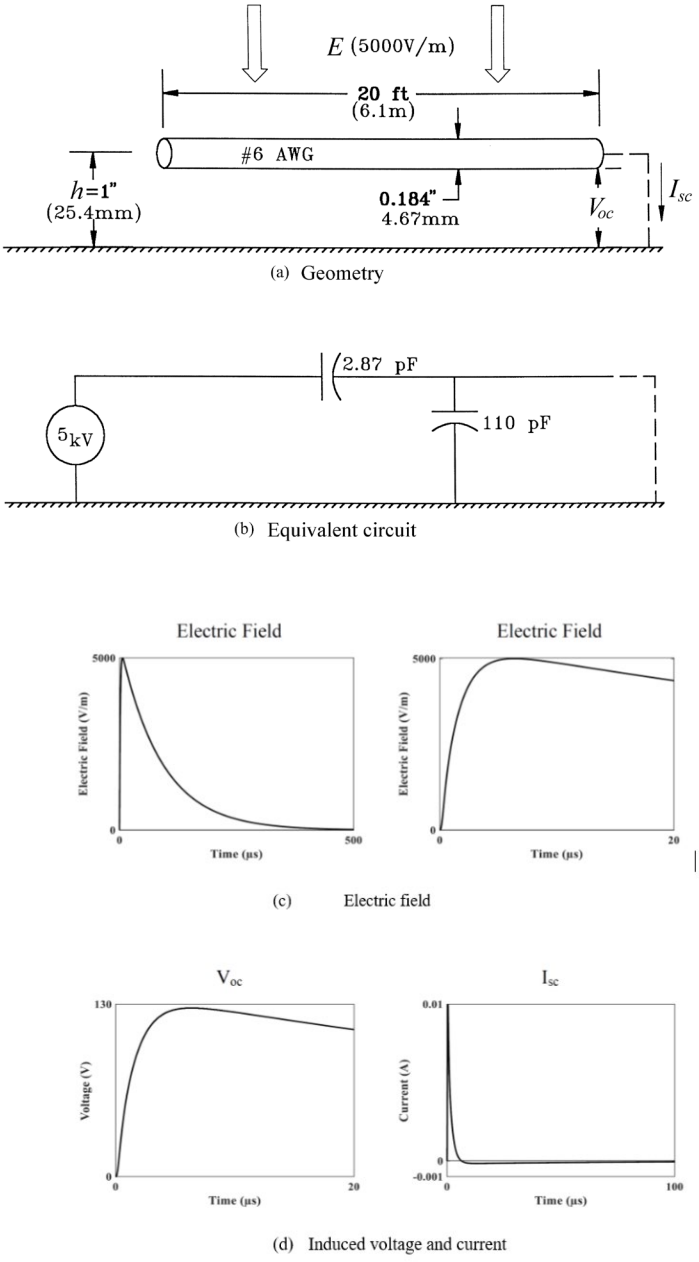

Fig. 14.15 Capacitively induced voltage and current.

14.4 Transmission Line Effects

Conductors always have, associated with them, some distributed capacitance and inductance, the values of which are determined by the size of the conductors and the distance of the conductors from adjacent ground planes and other conductors. Considering these inherent properties of conductors, it is not surprising that changing electric and magnetic fields produce oscillatory voltages and currents.

Example

Fig. 14.16 shows an example of how these oscillatory voltages and currents occur. The wire of Fig. 14.9 can be regarded as a transmission line of 185 ohms surge impedance (Eq. 14.3). The induced voltage is represented Fig. 14.16(c) as an ideal voltage source connected at the center. The calculations pertain to a magnetic field with a faster rate-of-rise than was used for Fig. 14.9. The distributed nature of the wire gives rise to traveling waves or oscillations

that persist longer than the induced voltage. The more rapid the rate of change of the inducing field, the more pronounced the oscillations. Losses dampen the oscillations, and may eliminate them entirely, at least as calculated for simple circuits.

The oscillations do not occur in the short circuit current, since I_{sc} responds to the integral of the induced voltage. The source impedance of the circuit shown in Fig. 14.16 was 62 ohms, which is several times higher than that of the circuit shown in Fig. 14.9. This difference in impedance is mostly due to the difference in the waveform of the inducing magnetic field.

Complex oscillations

When the internal magnetic field has a complex waveform (as is typical), instead of the idealized, inverse exponential waveform shown in the preceding figures, the waveform of the open circuit voltage it induces may also be complex. A few examples of such waveforms were shown in Chapter 8. While the maximum voltage may be difficult to predict, given the complex nature of the superimposed oscillations, the amplitude of the envelope can at least be approximated, using the elementary techniques described above.

Frequency

The frequency of superimposed oscillations tends to be inversely proportional to conductor length. Conductors (such as shields) grounded at one end tend to ring as quarter-wave dipoles. For example, a conductor 10 m long tends to ring at 7.5 MHz. Even this simple relationship is difficult to apply to actual situations, since one conductor is seldom free of the influences of adjacent conductors. Capacitance and inductance at the ends of conductors reduce their oscillatory frequencies. As a result, oscillations may be excited in a complete circuit, which would not happen if only the distributed inductance and capacitance of the conductors were involved.

Aircraft wiring is usually grouped into bundles that contain both short and long conductors. These assemblies, even if exposed to magnetic fields with simple waveforms, oscillate in a complex manner. Generally, there is one dominant frequency with several other (usually higher) frequencies superimposed. Each conductor has its own characteristic decrement. Generally speaking, bundles in large aircraft are longer than bundles in smaller aircraft and oscillate at lower frequencies. Induced voltages measured on large transport aircraft have oscillatory frequencies around 1 MHz and frequencies observed on small recreational or military fighter aircraft have had oscillatory frequencies ranging from 5 to 10 MHz.

Currents measured on bundles of conductors, like the voltages, tend to be oscillatory, if the conductors are part of a wiring group employing a single-point ground concept. Currents on conductors contained in a shield grounded at both ends tend not to be oscillatory, having, instead, the approximate waveform of the internal magnetic field.

14.5 Analyses Using First Principles

Numerical simulations of wiring exposure to lightning electromagnetic fields can be carried out with one or another of the modeling programs referenced in Chapter 10. This approach is recommended in situations where expertise in use of such modeling is available, and the aircraft and physical aspects of systems installations are sufficiently well defined so that useful computations of induced effects can be made.

In other situations, including for preliminary estimates before a design is sufficiently mature as to be worth the effort and cost of modeling. A more simplified approach that employs the coupling physics and basic geometries can be used to obtain estimates of the transient waveforms and amplitude to be expected. Such an approach is useful in the following situations:

- Preliminary designs for new aircraft
- Unoccupied air vehicles
- Additions and modifications to existing aircraft
- Protection design studies and comparisons

Hand computations and/or circuit analysis tools such as SPICE circuit simulation programs [14.1] can be used inexpensively to achieve estimates of induced transients in various types of circuits located in various regions within an aircraft, and from these estimates design decisions can be made and requirements applicable to equipment can be established.

Both the IxR and magnetically induced transients depend on the structural materials and basic geometries of the aircraft regions where the wiring of interest is located. This lends itself to solution of the transients in various regions (sections) of an aircraft or other air vehicle.

These *regions* should not be confused with the lightning strike *zones* discussed in the chapters dealing with physical effects of lightning.

As an example of a magnetic field region, consider the cockpit of an aircraft, or more especially, a helicopter. It can be regarded as a magnetically open region, exposed primarily to aperture-coupled magnetic fields. All manned aircraft have strong aperture magnetic fields in their cockpits.

Another type of magnetic region would be the fixed trailing edge area behind most airplane wings. This is similar to a three-sided channel, with the fourth side mostly open. Wire harnesses are usually installed within this area.

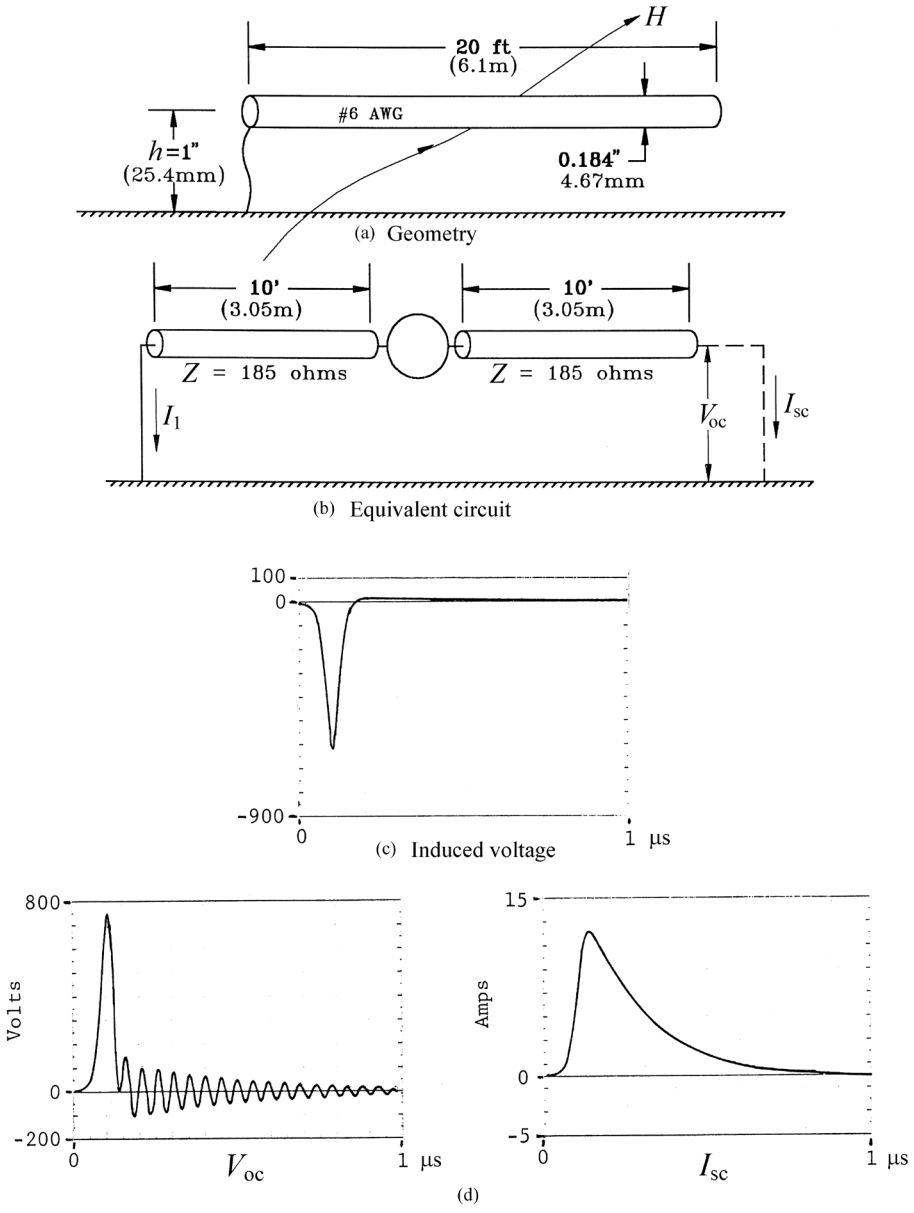

Fig. 14.16 Traveling wave effects.

Accordingly, one can divide an aircraft into a relatively small number of typical magnetic regions, assign a characteristic magnetic field intensity to each region, and provide rather simplified tables or nomograms, listing the characteristic transients likely to be induced in wiring of a given length. Other categories would be whether or not the wiring in these areas is shielded.

14.5.1 Predicting Magnetically Induced Voltage and Current

Conductor length does not influence short circuit current. The waveform of the short circuit current tends to be the same as that of the incident magnetic field.

The height, *h*, of the cable bundle above a ground plane is difficult to specify, partly because the ground plane is seldom purely a plane surface and partly because cable bundles are often strapped, at intervals, directly to a supporting structure.

For purposes of analysis, it was assumed:

1. That height *h* was measured to the nearest substantial metallic structural member.

2. That if the cable bundle was laid directly on that member, *h* equaled one-half the cable diameter.

3. That if the cable bundle was elevated above the metallic structural member, *h* equaled the clear height above the member plus one-half the cable diameter. If the cable's height varied along its length, an average height was used.

Screening calculations

Analyses of this type can be made for wiring in major regions of an aircraft and used for preliminary assignments of lightning-induced transient levels in critical circuits. The expected open circuit voltage and short circuit currents are computed then preliminary analyses can be conducted to see if the electrical and electronic components to which that circuit connected could reasonably be expected to withstand those voltages and currents. If so, specifications can be prepared for the equipment. If not, additional protection in the form of shielding can be considered.

Part of this process includes estimating the margin between what the equipment can reasonably withstand, and the voltages and currents estimated by these simple techniques. For the circuits exposed to excessive voltages or where the margin is too small for comfort, additional protection can be considered.

14.6 Calculating Circuit Responses

This section discusses the art of calculating circuit responses, either by hand calculations or with the aid of numerical circuit analysis routines. All the following discussion is based on the time domain. Frequency-domain calculations are not readily adapted to analysis of non-linear surge protective devices. In addition, conversion to the time domain requires time-consuming Fourier transforms.

14.6.1 Steps in the Modeling Process

Some of the steps involved in modeling the response of a circuit are the following:

1. Break the aircraft geometry into manageable sections, such as the magnetic field regions discussed above.

2. Simplify the cable geometry by determining average cable diameters and average heights relative to the surrounding ground structure.

3. Determine the electric and magnetic fields for the regions discussed in Step 1.

4. Determine the voltages and currents developed by the fields. These will be used to drive the equivalent circuits.

5. Develop equivalent circuits of cable (wire harness) sections.

6. Identify end impedances, perhaps simplified to opens and shorts.

7. Develop complete equivalent circuits.

8. Calculate response.

14.6.2 Example of Computation

This section demonstrates how these steps would be applied to the aircraft illustrated in Fig. 14.17. This demonstration should not be regarded as a representation of an actual circuit in any realistic aircraft. Its purpose is to develop an equivalent circuit that can be solved with a time-domain circuit analysis program that accepts a description of the circuit in terms of its nodes and branches. Some programs that could be used for this purpose include ECAP,

SPICE and EMTP. The principles of these analysis programs are described in [14.2 - 14.6].

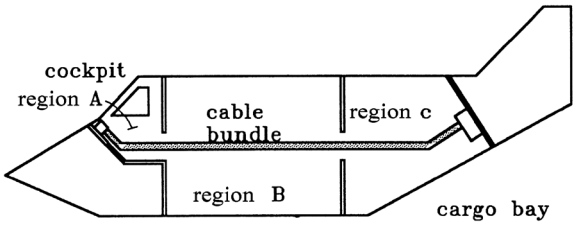

Fig. 14.17 Hypothetical aircraft.

The following illustrations used a program [14.7] based on the principles described in [14.4].

Breaking the model into sections

For this illustration, the aircraft will be divided into the three indicated magnetic regions. A cable runs from the cockpit to the cargo bay, with no intermediate branches.

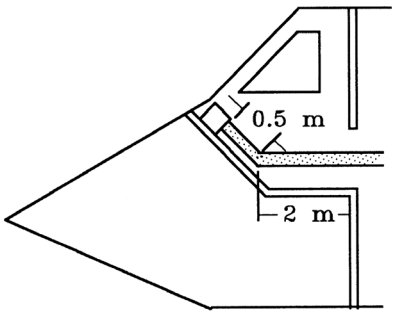

Cable lengths

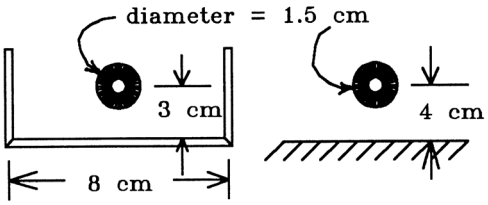

Position for run A Position for run B

Fig. 14.18 Cable in magnetic region A *Containing Run A and Run B*.

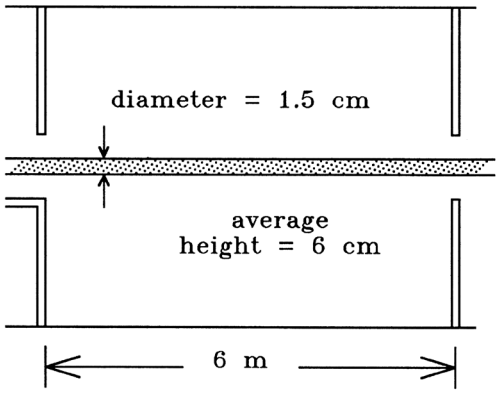

Fig. 14.19 Cable in magnetic region *B*.

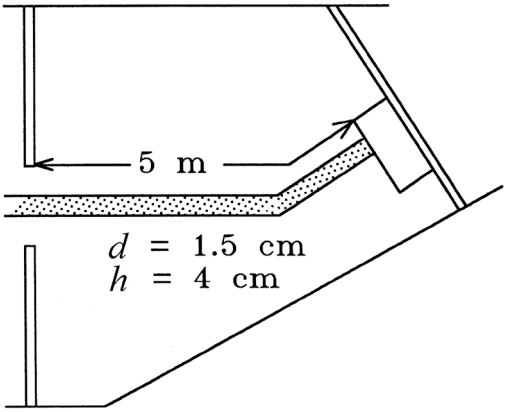

Fig. 14.20 Cable in magnetic region *C*.

Cable geometry

The cable geometry and distances from ground planes are shown in Figs. 14.18 - 14.20.

E and *H* fields

The electric and magnetic fields in the different magnetic regions are as shown in Figs. 14.24 - 14.27. The figures also show the currents and voltages that would be developed in the various cable sections by those fields. For simplicity, only the electric field induced current, and the magnetically induced voltage shown in Figs. 14.21 and 14.22 will be considered.

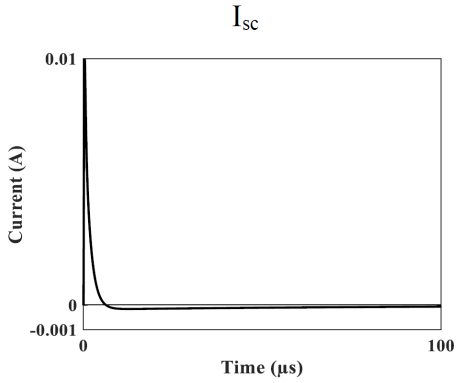

Fig. 14.21 Electric field effects in region *A*. (From Fig. 14.15)

The induced current and voltage are assumed to be the same as those appearing in Figs. 14.15 and 14.9, respectively. The induced voltage is due to a 1 000 A/m magnetic field from current Component A in the fuselage. The induced current is due to an electric field pulse originating somewhere outside of the aircraft. (Note that there is not a standard external electric field environment due to lightning).

Some circuit analysis programs require that voltage sources be described as being in series with a branch of some sort, rather than existing independently. For these illustrations the voltage source will be in series with a 1-ohm resistors, although it could equally well have been in series with one of the inductors comprising a lumped parameter representation of a transmission line.

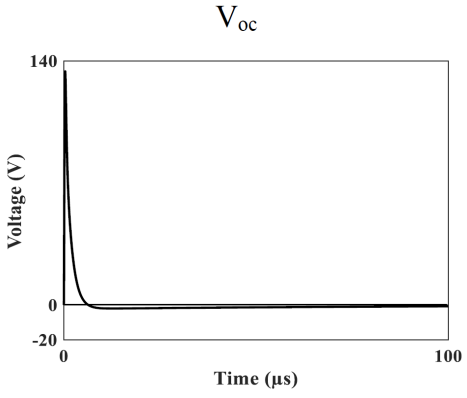

Fig. 14.22 Magnetic field effects in magnetic region A.

The induced current could be regarded as current sources in shunt with a circuit branch, although some circuit analysis programs allow a current source to be connected directly to a node. The circuits shown below include such a connection, but the induced voltages in magnetic regions B and C were not included in the simulations since they were small. Further discussion of methods of treating sources, including the use of dependent sources to treat coupling between circuits, is given in [14.8].

Equivalents of cable sections

If the circuit analysis program allows, it is simplest to regard conductors in Figs. 14.17 - 14.20 as transmission lines having specific surge impedances and propagation velocities. Otherwise, conductors should be represented as ladder networks of series inductors and shunt capacitors. For the following analyses, the cable sections are treated as two inductors in series, with the shunt capacitance distributed 1/6 at each end and 2/3 at the junction of the two inductors, these fractions being based on engineering judgement.

The appropriate electric field induced current source and the magnetic field induced voltage source for the cable sections in the cockpit (Region A) are connected between the two inductors. The appropriate impedances for the various sections of cable are as indicated in Figs. 14.23 - 14.27.

The number of lumps into which a distributed transmission line is broken depends on the accuracy desired of the solution. The more 'lumps', the greater the accuracy (and the broader the valid frequency range), but the use of large numbers of 'lumps' increases computation time. Discussion of the merits of various modeling alternatives is beyond the scope of this section.

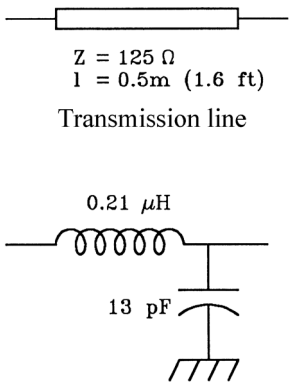

Fig. 14.23 Equivalent impedance for run *A* in magnetic region *A*.

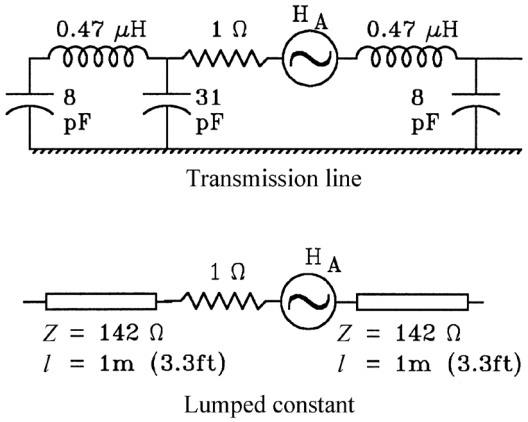

Fig. 14.24 Equivalent impedances for run *B* in cockpit magnetic field Region *A*.

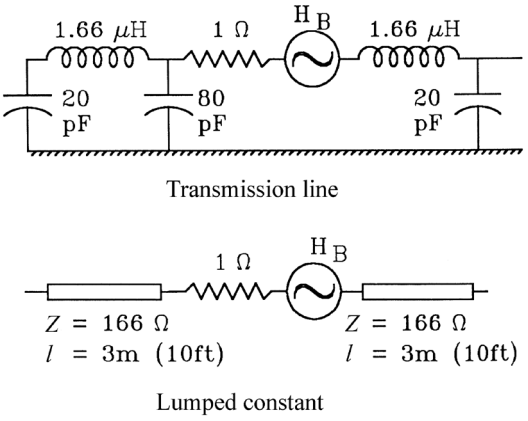

Fig. 14.25 Equivalent impedance for Run *C* in magnetic Region *B*. For this example, H_B is set to zero.

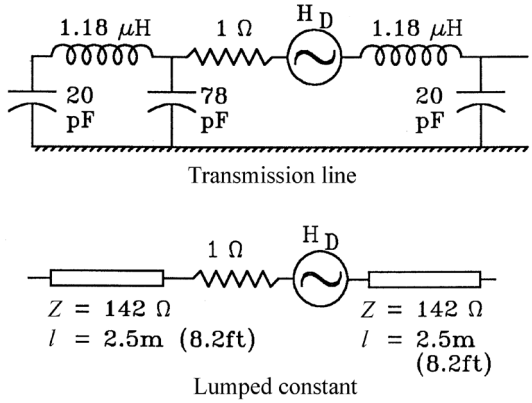

Fig. 14.26 Equivalent impedance for run *D* in magnetic field Region *C*. For this example, H_D is set to zero.

Any discussion of the merits of different modeling approaches must, of course, recognize that the wiring system of any real aircraft is probably too complex to model with complete precision whichever approach is used.

End impedances

For these illustrations, the cable will be assumed to be grounded through a low impedance (1 ohm) in the cockpit and to be grounded in the cargo bay through a 500 pF capacitor shunted by a resistor. 100 kilohms will be used for calculating the open circuit voltage and 1 ohm for calculating the short-circuit capacitance. In any actual calculation, the terminal impedances would have to be determined by inspection of the circuit, perhaps supplemented by measurements of stray capacitance. In reality, a lower resistance should be used for computation of the short circuit current (I_{SC}).

Complete equivalent circuit

Fig. 14.27 shows a representation based on transmission lines. This circuit includes one current source (E_A) and three voltage sources (H_A, H_B and H_C) but only E_A and H_A were used in these calculations. H_B and H_C were too small to significantly affect the response of the circuit.

Calculated response

Fig. 14.27 also shows the amplitude and waveform of the current predicted at the grounded end of the conductor, in the cockpit, and the voltage predicted at the open end, in the cargo bay. Each of these responses is oscillatory. This is typical of real circuits in actual aircraft, where the response is excited by changing electric and magnetic fields. The current at the grounded end shows higher frequency components superimposed on a lower frequency fundamental oscillation. At the ungrounded end, in the cargo bay, the higher frequency oscillations are filtered out by the 500 pF shunt capacitor.

Voltages and currents at intermediate points tend to retain their high frequency components. Fig. 14.27, for example, shows the voltage at the junction of cable runs *C* and *D*.

Fig. 14.27 shows the short circuit current calculated when the cable is grounded through a low impedance (1ohm) at the cargo bay end. As predicted by elementary theory, the current is less oscillatory than the open circuit voltage.

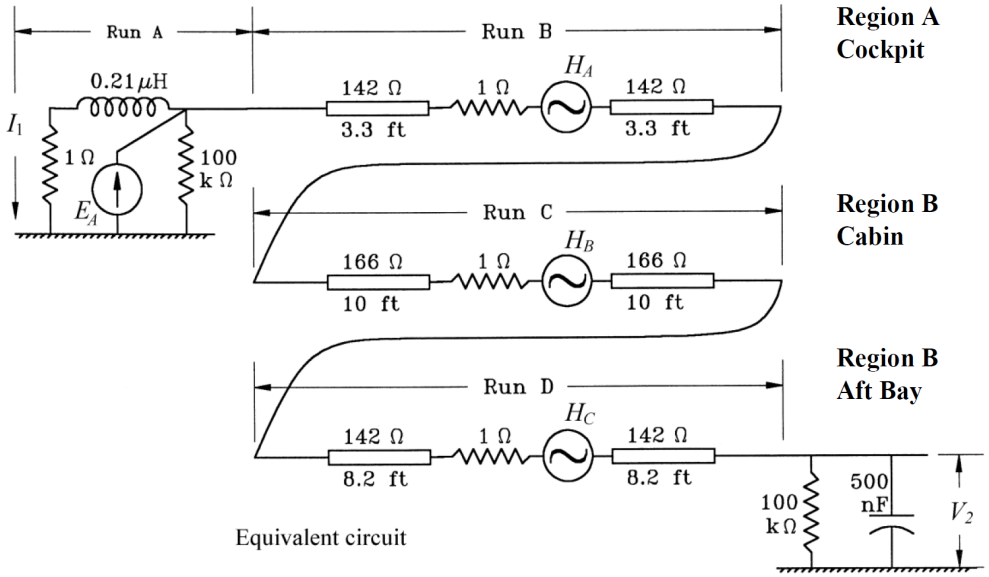

I_1 - Cockpit	V_2 - Aft Bay	Voltage at junction of Runs C and D
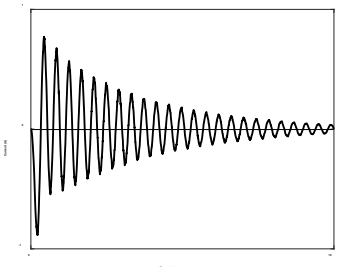	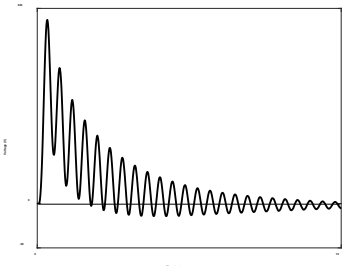	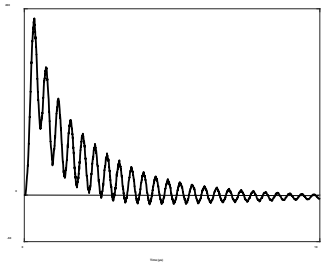

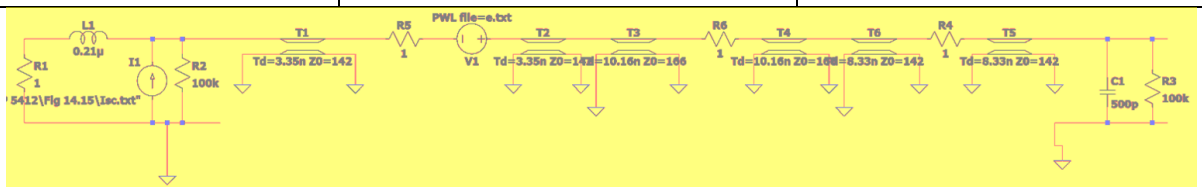

Voltage at junction of C and D is the between T4 and T6

Fig. 14.27 Circuit modeled as transmission lines.
Electric field induced current E_A is from Fig. 14.21 and Magnetic induced voltage H_A is from Fig. 14.22.

Discussion

The above calculations were made in 2021 using the PSPICE program [14.7].

Similar calculations using the lumped parameters upon which the Transmission lime model was based showed no significant differences from the results of the transmission line model shown in Figs. 14.23 – 14.27.

14.6.3 Extensions and Limitations of Modeling

The equivalent circuits above are probably of about the minimum complexity that should be used for practical calculations. More sophisticated modeling should take account of losses in the circuit, coupling between different cable systems and conductors, and multi-mode propagation between conductors in a cable bundle.

Losses

No attempt has been made to model losses in the circuits shown in Figs. 14.23 and 14.27. If losses had been considered, the amplitudes and durations of the oscillations would have been reduced. A first order approximation to these losses could be made by including series resistance in the circuit, either by invoking the resistive option provided by [14.4] and [14.7] for transmission lines, or by including the lumped resistances in series with the inductors shown in Fig. 14.27. Losses in actual circuits are frequency dependent and difficult to incorporate in circuit analysis programs, although considerable work has been done to develop methods of doing so [14.9 - 14.11].

Circuit-to-circuit coupling

Many problems of coupling between circuits can probably be modeled based on mutual impedance and mutual capacitance between circuits. Some of the considerations involved in calculating coupling by this means are given in [14.8]. Almost all circuit analysis programs include mutual inductors as permissible circuit elements. Some of them can even model coupled transmission lines.

Multi-mode propagation

Realistic calculations of voltages and currents on closely coupled conductors requires recognition that waves generally propagate at slower speeds between conductors than in the space between the conductors and ground.

This is particularly true for waves propagating inside shielded conductors, the analysis of which involves determining the voltages and currents induced on the conductors inside the shield on the basis of the currents propagating on the outside of the shield. Multi-mode propagation is discussed in the literature [14.12 - 14.15] and can be analyzed, to some degree, using circuit analysis programs [14.16- 14.17]. Taking close coupling effects into account greatly complicates calculations and probably should be considered at the edge of the modeling art.

Some discussions of equivalent circuits for shielded conductors are given in Chapter 16. Those circuits can be used with dependent current sources to model coupling into shielded circuits.

References

14.1 *Space Shuttle Program Lightning Protection Criteria Document*, JSC-07636, Revision A, National Aeronautics and Space Administration, Lyndon B. Johnson Space Center, Houston, Texas (November 4, 1975), pp. F-6.

14.2 F. H. Branin, Jr., "Computer Methods of NetworkAnalysis", *Proc. IEEE*, Vol. 55, November 1967, pp. 1787-1801.

14.3 L. O. Chua, Pen-Min Lin, *Computer Aided Analysis of Electronic Circuits*, Prentice-Hall, Englewood Cliffs, NJ.

14.4 H. Dommel, "Digital Computer Solution of Electromagnetic Transients in Single and Multiphase Networks", *IEEE Trans. on Power Apparatus and Systems*, Vol. PAS-88, April, 1969, pp. 388-399.

14.5 H. Dommel, W. S. Meyer, "Computation of Electromagnetic Transients", *Proc. IEEE*, Vol. 62, July 1974, pp. 983-993.

14.6 *Alternative Transients Program (ATP) Rule Book*, K. U. Lwuven EMTP Center, KARD. Mercier-laan 94, B-3030 Heverlee, Belgium or Tsu-huei Liu, 3179 Oak Grove Court, West Linn, Oregon, 97086.

14.7 ORCAD PSpice A/D.

14.8 F. A. Fisher, *Analysis and Calculation of Lightning Interactions with Aircraft Electrical Circuits*, AFFDL-TR-78-106, Aug. 1978, Air Force Flight Dynamics Laboratory, Wright Patterson Air Force Base, Ohio, 45433.

14.9 A. Semlyn, A. Dabuleanu, "Fast and Accurate Switching Transient Calculations on Transmission Lines with Ground Return Using Recursive Calculations", *IEEE Trans. on Power Apparatus and Systems*, Vol. PAS-94, March/April 1975, pp. 561-571.

14.10 A. Semly, A. Roth, "Calculation of Exponential Propagation Step Responses- Accurately for Three Base Frequencies", *IEEE Trans. on Power Apparatus and Systems*, Vol. PAS-96, March/April 1977, pp. 667-673.

14.11 A. Semlyn, M. H. Abdel-Rahman, *Transmission Line Modeling by Rational Transfer Functions, IEEE Trans. on Power Apparatus and Systems*, Vol. PAS-101, September 1982, pp. 3576-3583.

14.12 D. E. Hedman, "Propagation on Overhead Transmission Lines, I-Theory of Modal Analysis," *IEEE Trans. on Power Apparatus and Systems*, March 1965, pp. 200-205.

14.13 L. M. Wedepohl, "Application of Matrix Methods to the Solution of Traveling-wave Phenomena in Polyphase Systems", *IEEE Proceedings, Vol. 110*, December 1963.

14.14 T. K. Liu, "Coupling and Propagation in Multiconductor Transmission Lines", *International Conference on Electromagnetic Compatibility*, May 19-21, 1987, San Diego, CA, pp. T21.12-14.

14.15 R. F. Harrington, "Time-Domain Response of Multiconductor Transmission Lines".

14.16 A. R. Djordevic, R. F. Harrington, T. K. Sarkar, M. B. Bazdar, *Matrix Parameters of Multiconductor Transmission Lines*, Artech House Books, Norwood, MA. 1988.

14.17 A. R. Djordevic, R. F. Harrington, T. K. Sarkar, M. B. Bazdar, *Time Domain Response of Multiconductor Transmission Lines*, Artech House Books, Norwood, MA. 1988.

Chapter 15

SHIELDING

15.1 Introduction

If electronic equipment is to be operated in a region where there are changing electro-magnetic fields, and if experience or analysis indicates that the currents and voltages induced by those fields may be harmful, the most straight- forward way to achieve transient compatibility is to shield both the electronic equipment and its interconnecting wiring. Often, electronic equipment is inherently shielded by its enclosures, although there are practices that can defeat the inherent shielding of metal enclosures and there are non-metal enclosures that offer little shielding. The discussions that follow will comment on the shielding provided by enclosures, but they will focus primarily on shields on conductors.

15.2 Shielding Effectiveness (SE)

The degree to which a cable shield reduces the voltage induced on a conductor depends on the construction of the shield (solid tubular, braided, tape wound, diameter, thickness, material resistivity etc.) The type of construction effects the resistance of the shield. Braided shields for cables are almost universally made from copper but solid shields, such as conduits and enclosures, are usually made from aluminum. Aluminum offers the advantage of light weight, but copper has the virtue that it is solderable and that it resists cold flow at pressure points. Shields made from magnetic materials, such as iron and steel, have higher resistances, and therefore usually produce higher *IxR* voltages when lightning-induced currents flow in them. While these materials can provide more SE against impinging fields than either copper or aluminum, they are seldom either needed or used in aircraft.

Shield construction also effects transfer impedance, which is a measure of how the amplitude of shield current is related to the amplitudes of transients induced on signal conductors inside the shield.

The concept of transfer impedance was previously discussed in §9.6. Transfer impedance of cable shields is also discussed in §15.6. The coupled voltages are also affected by the way that the shield and conductors are terminated to ground and to loads. The effects of these terminations, discussed in §15.3, are often of more importance than the construction of the shield.

In this chapter, transfer impedances are discussed in §15.6, while the effects of different types of shield termination are discussed in §15.3. The ultimate aim of the discussion is to develop equivalent circuits relating the voltage on shielded conductors to the magnitude of the shield current. Section 15.7 provides tabular data on the transfer impedance of various types of cable.

In steady state or frequency domain analyses of radio frequency (RF) interference, shields are generally rated in terms of their SE, a quantity that relates the voltages or currents on shielded conductors to the voltages and currents that would be induced on those same conductors without a shield. SE is defined as:

$$SE = 20 \log \left[\frac{\text{voltage(or current) without shield}}{\text{voltage (or current) with shield}} \right] \quad (15.1)$$

When discussing transient or time-domain analyses, the above definition of SE may not be the most valuable concept, because shields not only reduce the amplitude of interfering voltages and currents, they change their waveform as well. The SE does not account for the changes of amplitude. It is better to keep all analyses in the time domain and to discuss shielding in terms of transfer impedances. This approach is taken throughout most of the following material.

15.3 Cable Grounding Effects

In aircraft, shielded conductors are typically used to control low-level and low-frequency interference signals. The question of how shields are to be grounded is often a controversial matter. There are two predominant schools of thought on this subject; one that recommends that shields be grounded at only *one* end and another that recommends they be grounded at *both* ends.

Single point grounding

The aim of the single-point ground concept is to minimize current flow on shields, with the intent of minimizing voltage rise along the interiors of the shields. The assumptions behind this concept (often unstated) are that the shields are short and that their function is to intercept low frequency electric field displacement currents and keep those currents from flowing on signal circuits. 'Short' implies that the shield must be a small fraction of the wavelength of the interfering signal (perhaps $L/20$). For example, the wavelength of a 30 kHz electromagnetic wave is approximately 10 km. At this frequency, any shield on an aircraft would be 'short'.

The single-point ground concept is most applicable in a situation such as that shown in Fig. 15.1(a), in which a source feeds a load that is contained in a grounded enclosure. If the source is electrically ungrounded, noise voltages between the source and ground, V_1, and between the source end of the shield and ground, V_2, do not couple to the interior of the shield and are of no consequence.

Shield current is most objectionable if the shield is used as return for the source (Fig. 15.1(a)) since any shield voltage is directly added to the signal from the source. Shield voltages are of less concern if two-wire transmission (Fig. 15.1(b)) is used since the shield voltages then couple only through the capacitance between the shield and the signal conductors. Shield voltages are of least concern if true, balanced transmission is used, with the output taken from a differential amplifier (Fig. 15.1(c)).

If the source is connected to ground through an impedance (Fig. 15.1(d)), the effectiveness of the single-point ground concept is reduced, regardless of the type of transmission, since this configuration does allow some of the voltage on the source (or ungrounded) end of the shield to couple to conductors and the load.

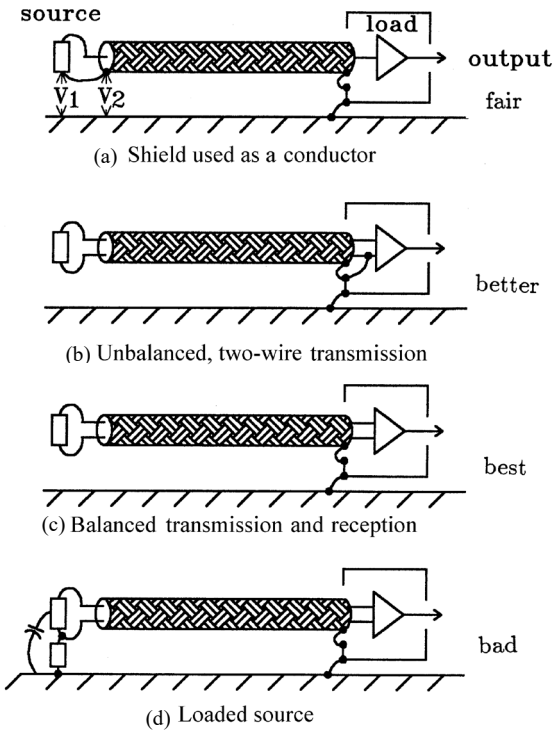

Fig. 15.1 Single point ground of shield.

An impedance often unrecognized is that provided by the stray capacitance of the source to ground. With rapidly changing electromagnetic fields, the effects of this capacitance can be of more importance than the performance of the shield.

Multiple point grounding

In an aircraft subjected to the rapidly changing electromagnetic fields associated with lightning, interference frequencies can extend higher than 30 MHz (L= 10 m). At these frequencies, a shield 1 m long would no longer be 'short'. Under such conditions, shields grounded at only one end may not be effective and, in some cases, may even act as antennas. This can induce higher amplitude surge voltages than would be induced if the conductors were not shielded at all.

In such cases, a multiple-point ground concept is more appropriate. That concept aims to ensure that noise currents do flow on shields (the opposite of the single-point ground concept).

Illustration of grounding effects

Some of these connection effects were illustrated by a series of tests [15.1] made on a 5 m long length of RG-58 / U coaxial cable. The cable was placed adjacent to a metal ground plane and a magnetic field was passed between the cable and the ground plane to generate 'interference'. During the tests, measurements could be made of the common-mode voltage between the center conductor and ground at each end of the cable or of the current flowing in the shield of the cable. The magnetic field was not a distributed field but was confined to the core of a pulse injection transformer in the manner shown in Chapter 18. The 'interference' was thus magnetically induced, the induced voltages being proportional to the rate of change of magnetic flux. In actual practice, interference can also be induced by electric field coupling and, with high frequencies, one will never exist without the other.

The shields shown in Figs. 15.4 through 15.10 appear as if terminated with pigtails. This is just for illustrating the effects of connections. The shields were actually terminated via connectors to aluminum boxes within which the conductor measurements were made.

Unshielded conductor

Figs. 15.2 and 15.3 show conditions on an unshielded conductor, or one in which the shield is not used.

Balanced loads

In Fig. 15.2, the conductor has equal (open) load impedances at both ends. The changing magnetic field induces a total voltage of 64 volts. How that voltage divides between the ends of the conductor depends on the impedances from the ends to ground. Since these impedances are equal in Fig. 15.2, half of the voltage appears at each end of the conductor and the voltages are of opposite polarity, as they would be if the conductor had an equivalent voltage generator at its center (Fig. 15.2(d)).

Unbalanced loads

Fig. 15.3 shows what would happen if the load impedances at the ends were unbalanced by the addition of a 50-ohm resistor at one end. The voltage at the loaded end is reduced but, since the *total* voltage induced around the loop remains unchanged, the remaining voltage is simply shifted to the end with the highest impedance.

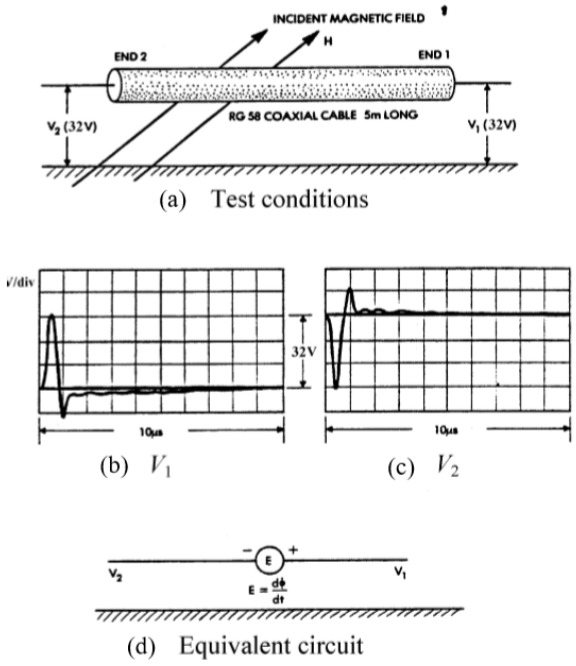

Fig. 15.2 Shield not grounded at either end.

With reference to the equivalent circuit shown in Fig. 15.3(c), the fact that there is any voltage at V_2 implies that there is some capacitive loading, in addition to the indicated resistive load. Otherwise, there would be no voltage across V_2.

Shield grounded at one end

Adding a shield but grounding the shield at only one end (Figs. 15.4 and 15.5) lowers the voltage at the end where the shield is grounded but raises it at the opposite end. This phenomenon can be explained using the equivalent circuit shown in Fig. 15.4(c). The changing magnetic field induces a voltage between the ends of the shield and, since one end of the shield is grounded, all the voltage must appear between the open end of the shield and ground.

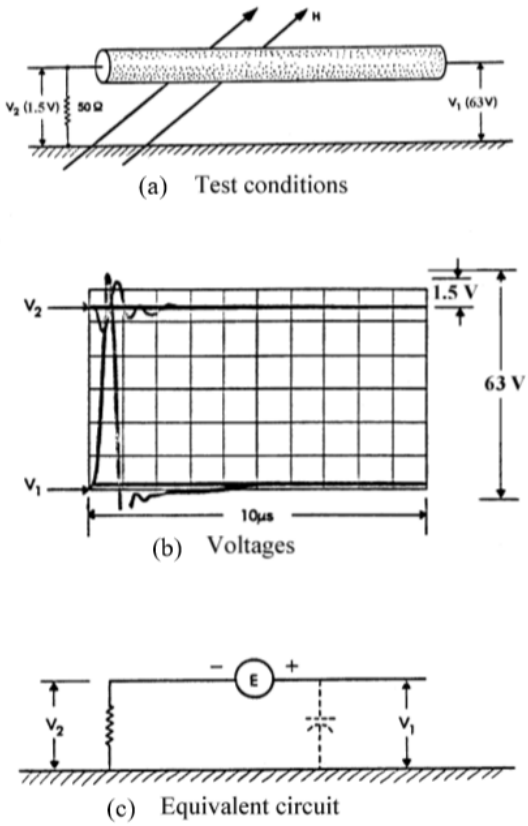

Fig. 15.3 Unequal load impedances.

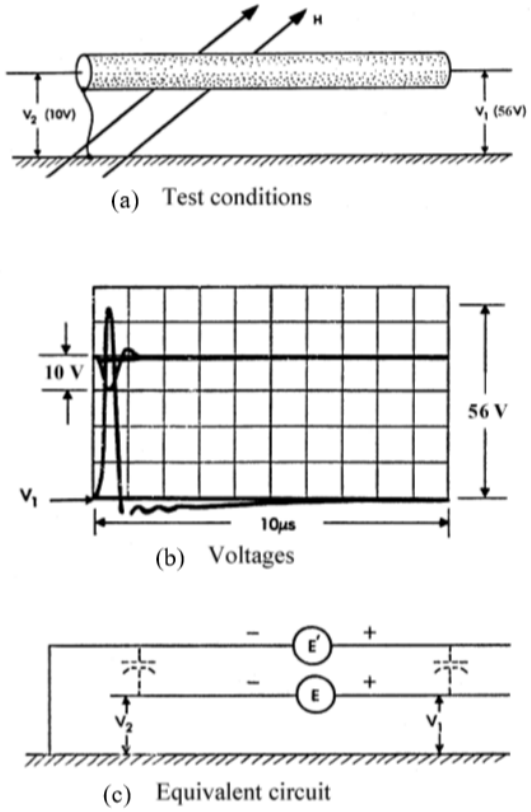

Fig. 15.4 Shield grounded at one end.

Since the conductor *inside* the shield has the same field between itself and ground as the shield, the same voltage is developed between the ends of the conductor as between the ends of the shield.

How this voltage divides between the ends of the conductor depends both on the grounding of the shield and on the load impedances on the conductor. With unloaded conductors (Fig. 15.4) the voltage at end 2 is reduced by the capacitance between the conductor and the grounded end of the shield, but the remainder of the total loop voltage simply appears at the other end. With a loaded conductor (Fig. 15.5) the division of voltage is primarily governed by the load impedances. Connecting the shield makes practically no difference in the voltage.

Shield grounded at both ends

Grounding the shield at both ends and allowing it to carry current, as shown in Figs. 15.6 through 15.8, produces an entirely different response. The induced voltages are reduced in amplitude and their waveforms are changed. If the shield is grounded at both ends, the voltage induced by the changing magnetic field appears in the loop formed by the shield and ground plane. The result is a current through the shield (Fig. 15.6) that has a waveform like that of the magnetic field.

$$V = \frac{d\varphi}{dt} = \mu A \frac{dH}{dt} \qquad (15.2)$$

$$I = \frac{1}{L_s} \int V dt = \frac{\mu A}{L} H \qquad (15.3)$$

where,

μ_o = the permeability of free space, $4\pi x10^{-7}$ Henries per meter.

φ = the magnetic flux through a loop, Webers/m^2

H = Magnetic flux density, Webers/m^2

A = Loop area between shielded cable and airframe, m^2

L = inductance of the loop, Henries

V = voltage in the loop, Volts

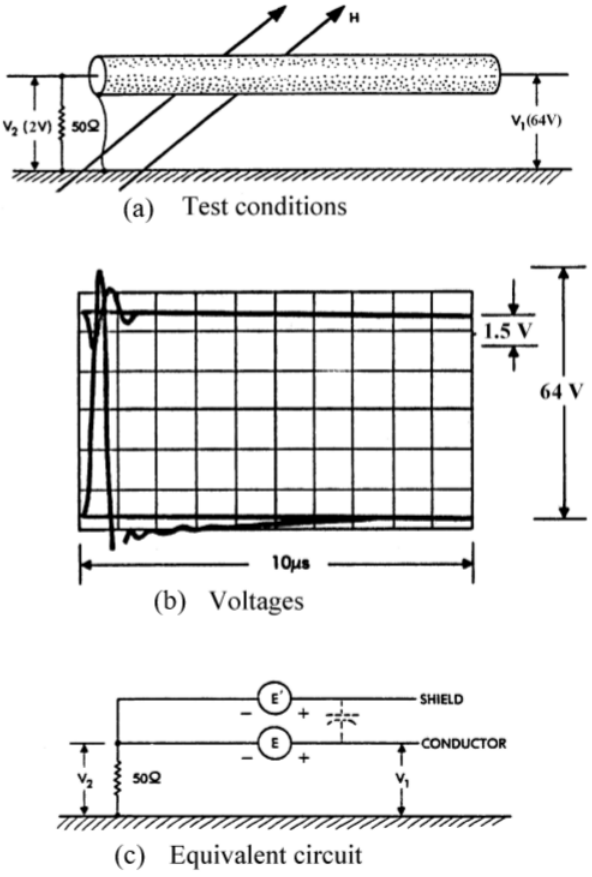

Fig. 15.5 Shield grounded at one end.

How shield current reduces voltage

This shield current reduces the voltage induced between the signal conductor and ground, as shown in Fig. 15.7. The reduction in voltage can be viewed equally well from two different viewpoints.

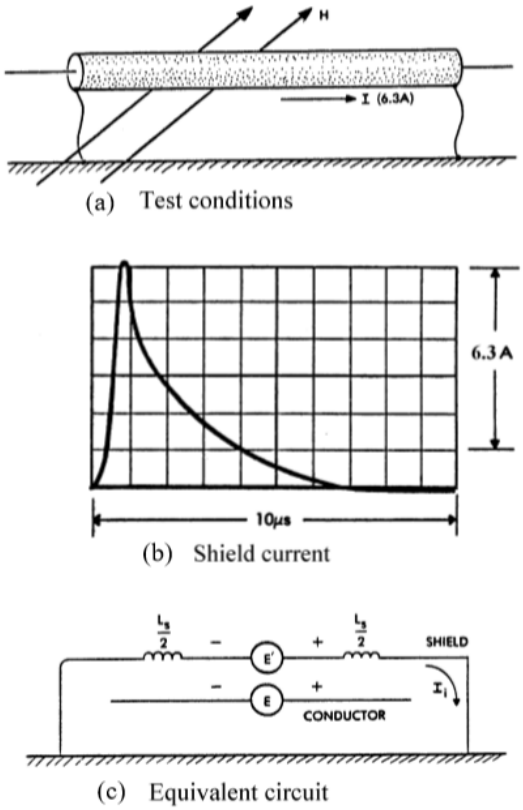

Fig. 15.6 Shield grounded at both ends.

where,

E = voltage induced in loop between the shield and ground plane
I = current on the shield
L = self-inductance of the shield and ground plane return loop

Cancellation of incident field

The first viewpoint is that the shield current flows in such a way as to produce a magnetic field that tends to cancel the incident field (Fig. 15.7(a)). From this viewpoint, the voltages between the signal conductor and ground depend on the difference between the incident and the cancelling fields.

Transformer coupling

Alternatively, the reduction in voltage can be regarded as the effect of the mutual inductive coupling between the shield and the signal conductor. This approach is illustrated by the equivalent circuit shown in Fig. 15.7(c). The shield is regarded as the primary of a transformer and the

conductor as the secondary. Since the shield is grounded at both ends, all the voltage developed on the shield appears across the primaries of the transformers.

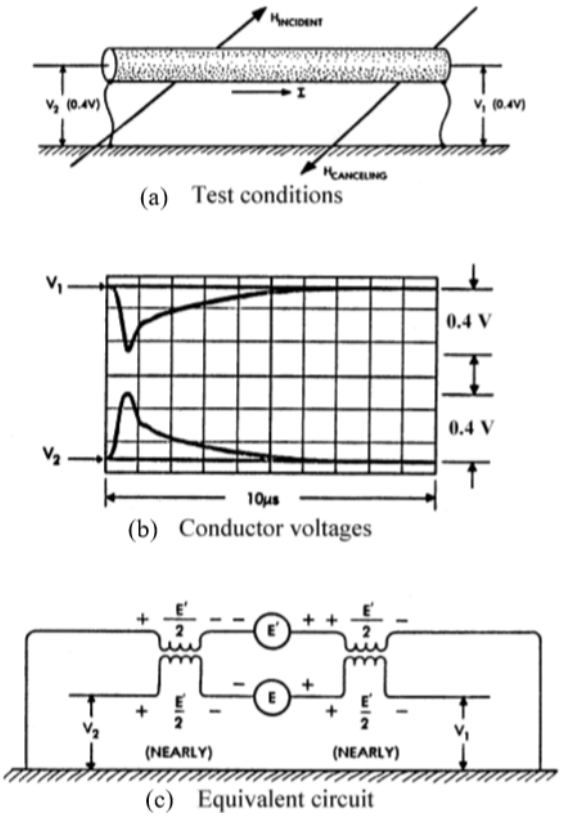

Fig. 15.7 Shield grounded at both ends.

The mutual coupling between the shield and the signal conductor is very nearly unity, since there is only a small (ideally zero) magnetic field inside the shield and so the voltage induced in the secondary (or signal conductor) side of the equivalent transformer is about equal to the voltage originally induced in the shield. The voltage appearing between the ends of the conductor is the sum of that induced in the conductor and that coupled through the transformer from the shield. Accordingly, the voltages appearing at the ends of the conductor are lower than they would be if the shield could not carry current.

Transfer impedance

The transformer equivalent circuit shown in Fig. 15.7(c) is not well suited to numerical calculation, since it requires that the self and mutual inductances be evaluated with high precision. The transfer impedance model shown in Fig. 15.8 is more manageable since it only requires calculating the resistance of the shield and the magnetic flux that leaks through it and appears between the shielded conductors and the shield.

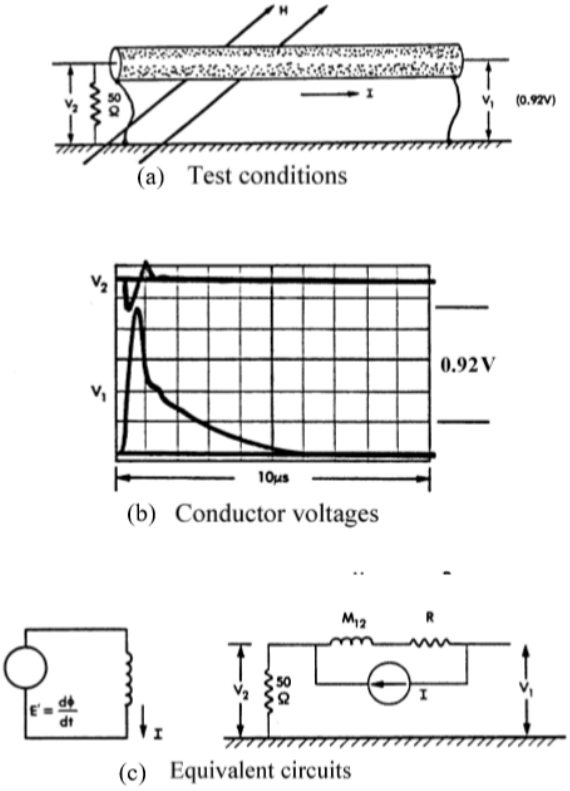

Fig. 15.8 Shield grounded at both ends.

This flux can be expressed as an equivalent transfer inductance L_{12}. When multiplied by the rate of change (di/dt) of the current in the shield, this transfer inductance produces the voltage that is induced by the field that penetrates the shield. The voltage induced on the conductor then depends on the shield current, shield resistance, R, and L_{12}. How the voltage distributes depends on the loads at the ends of the cable. In Fig. 15.8 most of the voltage develops on the open end.

15.4 Multiple Conductors in Cable Shields

If there are multiple conductors in the cable, all of them are exposed to nearly the same amount of shield IR voltage and leakage magnetic flux, and therefore have nearly equal voltages induced between them and the interior of the shield. This holds true whether the conductor is located adjacent to the interior of the shield or in the center of the bundle of conductors. In other words, the position of a wire within its shield has little effect on its magnetically induced voltage. Accordingly, the voltage induced between any pair of conductors within the same shield is small.

It is best to determine the amplitudes of conductor-to-conductor (also known as 'line-to-line') voltages by actual measurement. Line-to-line voltages are much more strongly influenced by the load impedances to which the conductors are connected than by the position of the conductors within their shield.

15.5 Multiple Shields on Cables

Occasionally, shielded conductors are contained in an additional, overall shield (OAS). Fig. 15.9 shows such a configuration and illustrates some of the factors that must be considered when predicting the response of this doubly shielded configuration. These factors include the currents on the outer shield, the internal field of the outer shield, the current induced on the inner shield, the internal field of the inner shield and the coupling from the inner shield to the signal conductor. The internal field of the outer shield is the product of the shield current and the transfer impedance of the outer shield. The 'field' as used above means the voltage per unit length along the interior surface of the shields.

Note that this is called a *double shield.* There is another situation where two shields are employed, but in this case the second shield is simply applied directly over the first (inner) shield. This is called an *overbraid.* It is important to avoid confusing the two terms. The performance of the overbraid is just as if a single shield has been made of a heavier, thicker braid. In fact, a common version has a second layer of copper (usually) braid woven directly over the first layer, so that the two layers are continuous electrical contact along the entire length. The factors in the transfer impedance are reduced by the additional copper and increased optical coverage.

In contrast, a double shield takes advantage of the inductance between the two, separate shields, and the reduced resistance afforded by the two shields. The protection effectiveness of the double shield is usually greater than that of an overbraid shield, but the weight of the double shield is usually greater since a layer of insulation is needed between the two shields. Further discussion of these shields follows.

Inner shield grounded at only one end

If the inner shield were ungrounded at its right-hand end (switch S of Fig. 15.9(b) open), the internal field of the outer shield, $E_{i\text{-}os}$, would produce a voltage difference, $V_{is\text{-}os}$, at the right-hand end of the cable. Neglecting the distributed capacitance between the inner and outer shields, the noise current on the inner shield, I_{is}, is zero.

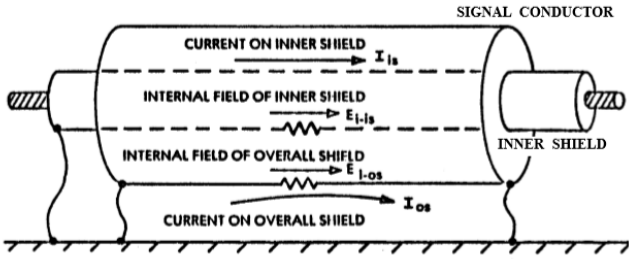

(a) Current and field polarities

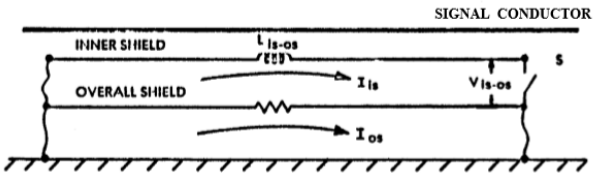

(b) Current on inner shield and forced through $I_{is\text{-}os}$

Fig. 15.9 Double shielded cable.

The total voltage to which the conductor is exposed is also $V_{is\text{-}os}$. Under such conditions, the inner shield does not significantly reduce the voltage.

Inner shield grounded at both ends

If the inner shield were connected to the outer shield at both ends (switch S closed), the current on the shield would be shared between the inner and outer shields, but the conductor would respond only to the field (i.e., V/m) along the inner surface of the inner shield. Initially, all the current would be confined to the outer shield, and, under direct current (DC) conditions, the currents would be divided according to the relative resistances of the shields. Between these two conditions, there would be a transient state, during which the division of current would be determined primarily by the inductance between the inner and outer shields.

Treatment as component currents

One way to visualize this phenomenon is to consider the current to have two components, the total shield current, induced by an outside source, and a current component circulating between the inner and outer shields. From this viewpoint, the current on the inner shield would be equal to the circulating component, while the current on the outer shield would be the sum of the two current components. The voltage driving the current on the inner shield would be the voltage produced by the flow of current through the transfer impedance of the outer shield. This voltage, when applied across the impedance between the inner and outer shields, would determine the current on the inner shield. For well shielded cables, this impedance is

predominantly inductive. The waveform of the current on the inner shield, I_{is}, would therefore be proportional to the time integral of the voltage developed along the inner surface of the outer shield. The current on the inner shield thus typically has a slower rise time and a longer duration than the voltage along the inner surface of the outer shield. This current on the internal shield, I_{is}, then produces an electric field along the surface of the inner shield, $E_{i\text{-}is}$. The conductor responds primarily to the electric field along the inner shield.

Example of multiple shielding

It is apparent that there are several possible combinations of shield connections and termination impedances, all of which can affect the overall response of a cable system. Some of these effects have been demonstrated during an extension of the tests illustrated in Figs. 15.2 through 15.8. The piece of RG-58/U coaxial cable used for those tests was modified by pulling another length of flexible copper braid over the outer jacket, forming a triaxial cable. (Triaxial cable is, of course, commercially available.)

The test connections and results are shown in Fig. 15.10. The equivalent circuit has three separate components; separate in the sense that each, for all practical purposes, may be treated independently. The first part of the circuit determines the voltage induced along the inner surface of the outer shield. This is governed by the outer current, flowing through the transfer impedance (see §15.10) of the outer shield, R_1 and M_1.

In the second stage of the problem, this inner shield voltage was applied across the inductance produced by the magnetic field between the inner and outer shields, $L_{is\text{-}os}$, to determine the current flowing on the inner shield.

In the third stage, the current on the inner shield was passed through the transfer impedance of the inner shield, R_2 and M_2. The product of current and transfer impedance gives the voltages that appear between line and shield on the central signal conductor. The amplitudes and shapes of these voltages, shown in Fig. 15.10(b), are much less than those developed on the singly shielded conductor shown in Fig. 15.7.

15.6 Transfer Impedance of Cable Shields

The equivalent circuit shown in Fig. 15.7 uses transformers to simulate the self-inductance of the conductor/shield combination and the mutual inductance between the conductor and the shield. The self and mutual inductances must be known with great precision if results are to be calculated accurately. This requirement can be relaxed if the circuit is split into two parts, as shown in Fig. 15.8. One part of the circuit relates the magnetic field to the current flowing on the shield. The other part relates the current on the shield to the voltage developed on the conductor using a transfer impedance, L_{12}, and R. The values of these components depend upon the type of shield.

Transfer inductance vs. mutual inductance

The transfer inductance L_{12} should not be confused with the mutual inductance M_{12} between the shield and the conductor.

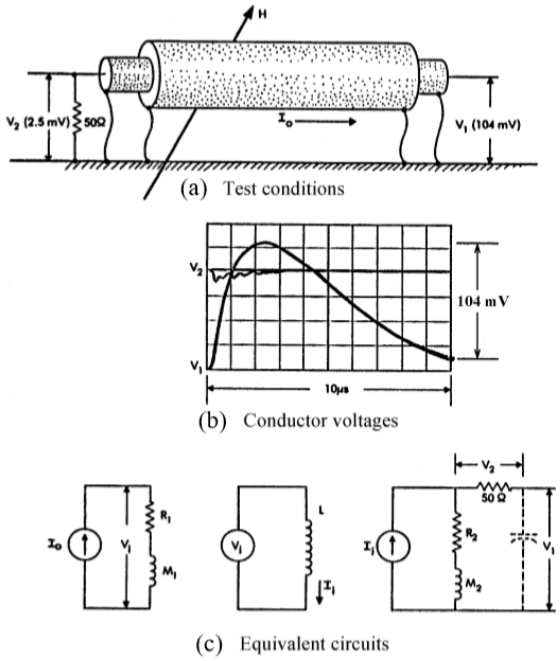

Fig. 15.10 Multiple-shielded cable.

For the two-conductor system that was described in §9.5.3 and Fig. 9.10, mutual inductance is controlled by the magnetic flux in the shaded area between r_2 and r_3, while transfer inductance is governed by the magnetic flux between $r_1$and r_2.

Handbook data (see end of this chapter) on shielded conductors often uses the term M_{12} for transfer inductance, but this usage is unfortunate since M is usually the symbol for a mutual inductance, which the transfer inductance is not.

If the resistance of the shield were zero and if the mutual inductance between the shield and the signal conductor were equal to the self-inductance (i.e., unity coupling) the flow of current on the shield of the cable would not cause any voltage to be developed between the shield and the

signal conductor. This section of this chapter will now discuss the factors that prevent the coupling between shield and signal conductor from being perfect.

15.6.1 Tubular Shields

Consider, first, a tubular shield with no openings, like that shown in Fig. 15.11. A current flowing through the resistance of the shield produces an electric field (i.e., voltage) along the internal surface of the shield.

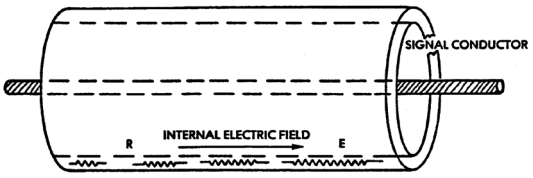

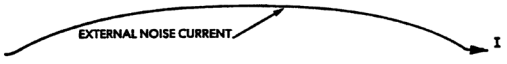

Current and field polarities

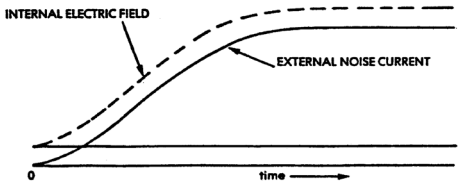

Current and field waveshapes

Fig. 15.11 Coupling resulting from resistance effects.

The internal and external electric fields are equal and, since there are no openings through which a magnetic field can leak, the transfer inductance is zero.

The transfer impedance of a tubular shield was previously discussed in §9.4.5. For thin tubes and low frequencies, transfer impedance is simply the DC resistance of the shield.

$$R_o = \frac{1}{2\pi r \sigma a} \qquad (15.4)$$

where

r = radius of the shield (m)
a = wall thickness (m)
σ = conductivity of the shield ($1/\Omega \cdot m$)

The waveform of the internal electric field is the same as that of the external shield current.

Eq. 15.4 would hold at any frequency for which the skin depth, δ, was large compared to the thickness of the shield. A numerically convenient expression for skin depth, provided in §9.3.5, is:

$$\delta = \frac{\pi}{50}\sqrt{\frac{1}{\sigma f_{kHz}}} \text{ meters} \qquad (15.5)$$

In the time domain, the shield may also be considered 'thin' if the pulse penetration time, §11.3.4, Eq. 11.21, is small compared to the rise time and duration of the interfering noise currents.

Thick tubular shields

If the shield is not thin (Fig. 15.12), the internal electric field depends upon the product of the resistivity of the shield material and the density of the current on the internal surface of the shield. As discussed in §11.3.3, this internal current density, J_i, is not generally the same as the current density on the external surface of the cylinder.

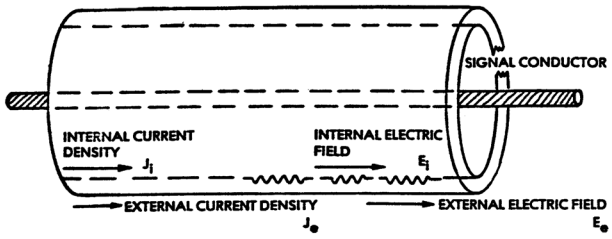

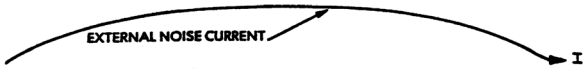

Current and field polarities

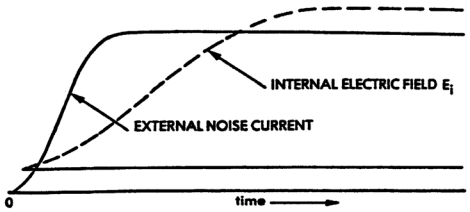

Current and field waveshapes

Fig. 15.12 coupling via diffusion through a solid wall.

Because of the skin effect, the current density on the inner surface of the shield rises more slowly than the current density on the exterior surface. The rate at which the internal current density increases is directly proportional to the permeability of the shield material and to the square of the wall thickness and inversely proportional to the resistivity of the wall material. Cables with solid wall shield and cable trays of solid metal with tightly fitting covers typically exhibit this behavior.

The maximum transfer impedance of a solid-walled tube, as expressed in [15.2], occurs under DC (or low frequency) conditions and decreases with increasing frequency to,

$$R_0 = \frac{1}{2\pi r \sigma a} \qquad (15.6)$$

The expressions above assume that the wall thickness of the shield is small compared to its radius and that the radius is small compared to the smallest wavelength of interest. They also assume that the shield is made from a good conductor, so that the displacement current in the shield material is negligible compared to the conduction current. Such is the case for any practical metal shield.

The time-domain response was previously given in §11.3.4 and §11.3.5. In response to a step-function current, the internal electric field increases according to the pulse penetration time-constant predicted by Eq. 11.21 and shown in Fig. 11.7. An equivalent circuit applicable to both frequency and time domains would be a ladder network of two or more terms, as shown in Figs. 11.8 and 11.11.

15.6.2 Braided Shields

Braided shields (Fig. 15.13) do not provide a perfect conducting cylinder since they have small holes (Fig. 15.14) that permit leakage of electric and magnetic fields. The weaving of the braided-wire shield is described in terms of the number of bands of wires (carriers) that make up the shield, the number of wires in each carrier (ends) and the number of carrier crossings per unit length (picks). These characteristics, along with the radius of the shield, define the volume of metal in the shield, the optical coverage, and the weave angle. A large volume of metal implies low resistance and good shielding, but also a high weight, which is a drawback for aircraft applications.

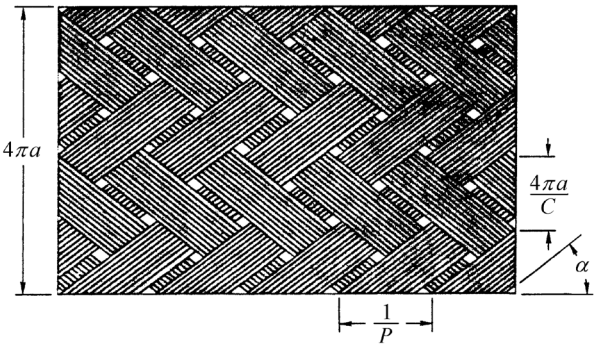

Fig. 15.13 Pattern of a braided shield [15.3]

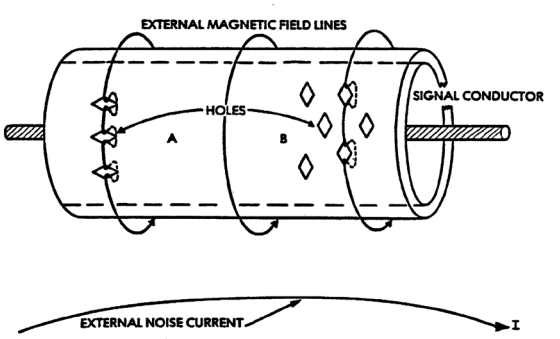

(a) Current and field polarities

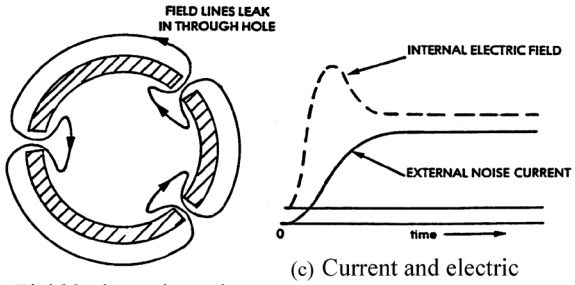

(b) Field leakage through holes: end view

(c) Current and electric field waveshapes

Fig 15.14 Coupling via magnetic leakage through holes.

Optical coverage and weave angle

The optical coverage of a shield is a measure of the number and size of the holes in the shield. The greater the optical coverage, the smaller the combined area of the holes and the better the shielding. The holes between the

individual bundles of wire forming the shield can be approximated as a group of diamonds, the size and orientation of which depends upon the weave angle. If the weave angle is small, the long axes of the diamonds are oriented lengthwise (parallel to the axis of the shield, as at end A of the cable shown in Fig. 15.14(a)). If the weave angle is large, the long axes of the diamonds are oriented *circumferentially* (or *perpendicular* to the axis of the cable, as at end *B* of the cable in Fig. 15.14(a)). Other things being equal, a shield with a small weave angle provides better shielding performance than one with a large weave angle.

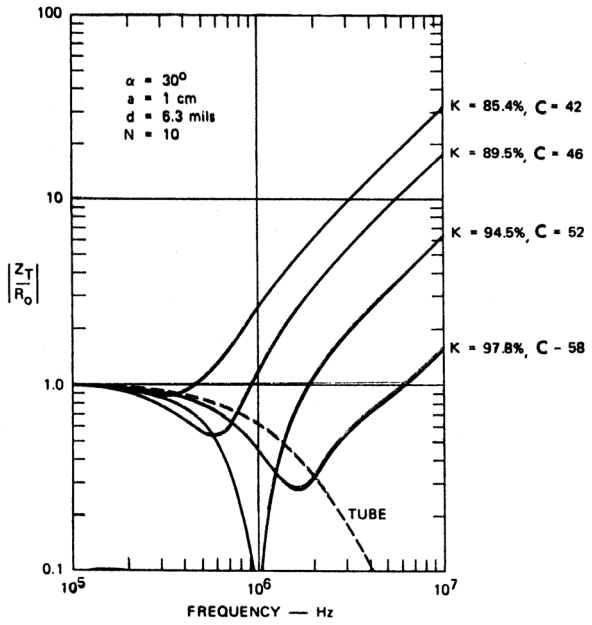

Fig. 15.15 Transfer impedance of a braided wire shield as a function of frequency.
k = Percent coverage
C = Number of carries

In Fig. 15.15 the transfer impedance has been normalized to permit comparison of the influence of various optical coverages on transfer impedance. It will be seen that, within the equivalent frequency range of current Component A, sinusoid components higher than 1 MHz reach only a few percent of the peak amplitude frequencies, which are of the order of 1 kHz. This means that shields like those described in Fig. 15.15 with 85% optical coverage will provide adequate protection against the Component A lightning environment, the frequency spectrum of which is shown in Fig. 15.16. Below 1 MHz, the shield DC resistance is the most important factor in the transfer impedance, Z_T.

Shields, of course, are provided also for protection of circuits against other environments, including electromagnetic interference (EMI) and high intensity radiated fields (HIRF), which include much higher frequency radiated field environments. For this reason, specifications for shields of aircraft wiring often include optical coverages, K, of over 90%. For lightning protection, it is important to employ shields.

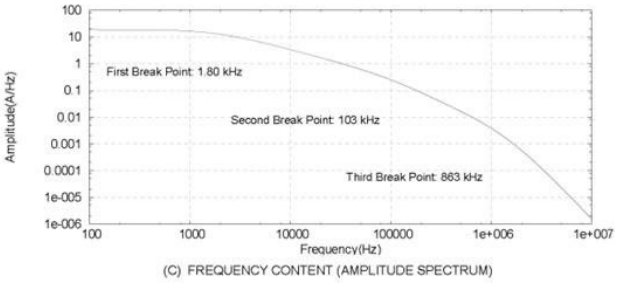

FIGURE 12 - CURRENT COMPONENT A FOR ANALYSIS AND INDIRECT EFFECTS TEST PURPOSES

Fig. 15.16 Frequency spectrum of current Component A [15.4]

Mechanism of magnetic field leakage

Current in a shield produces a circumferential magnetic field around the outside of the shield. If the shield is of a braided construction, one may visualize the flux lines of this magnetic field looping in and out of the holes in the braid. There is more magnetic field leakage through holes whose long axes are oriented circumferentially than through holes whose axes are lengthwise. Viewed from the end of the cable, as in Fig. 15.14, the field that leaks into the cables produces a net magnetic field circumferentially around the inside surface of the shield.

This magnetic field produces an internal electric field whose amplitude is dependent upon the amount of flux leaking into the shield and upon the rate of change of that flux (and of the external shield current producing it). Thus, the total internal electric field is proportional to the resistance of the cable shield, to the rate of change of the shield current, and to the size and number of the holes in the shield.

Transfer impedance vs. frequency

Some examples, from [15.3 and 15.5 - 15.6], showing the variation of transfer impedance with frequency for various amounts of shielding are shown in Fig. 15.15.

Equivalent circuit

An equivalent circuit for a braided shield is shown in Fig. 15.17. The resistance can frequently be regarded as the DC resistance of the shield, although the effective resistances of some shields are less because of skin effects. The *transfer inductance,* L_{12}, is approximately 0.5 nH/m

for small diameter cables with small weave angles and several nH/m for large diameter cables with large weave angles. Note that this is not mutual inductance, nor a self-inductance.

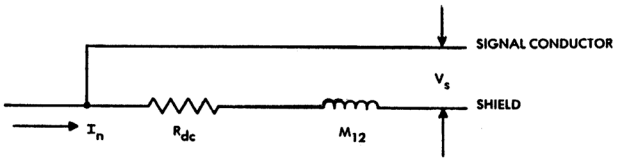

Fig. 15.17 Equivalent circuit of a shielded conductor.

Calculation of shield performance

Vance [15.6] gives equations relating resistance and transfer inductance to the construction of shields. Fig. 15.17 shows one example of how transfer inductance depends on weave angle. In the frequency domain, the transfer impedance is generally dominated by the resistance at frequencies below about 1 MHz and by the transfer inductance at frequencies above 1 MHz. The reference to mutual capacitance in Fig. 15.17 is addressed below, under the heading; 'electric field leakage'.

Flexibility vs. weave angle

The SE of a braided shield can be improved by increasing the density of the braid, but this also reduces the flexibility of the shield. Small diameter shields can be made with a small weave angle, but on large diameter cables the weave angle must be large to maintain physical flexibility.

Overlapping layers of braid

An alternative construction involves two overlapping layers of braid (Fig. 15.18). Using two similar layers of braid reduces the resistance by a factor of two (and doubles the weight of the shield) but can reduce the transfer inductance even more, often to less than 0.1 nH/m.

The resistances of doubly shielded cables can be calculated, but it is best to measure the transfer inductances.

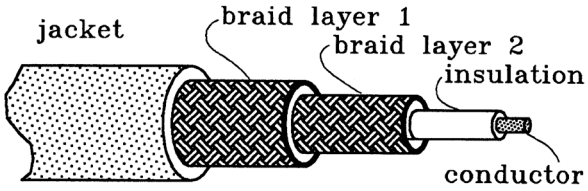

Fig. 15.18 Doubly shielded cable.

Porpoising

Sometimes cables exhibit a phenomenon called 'porpoising' (illustrated in Fig. 15.19), in which a change in shield current path induces an internal electric field of the opposite polarity. Porpoising occurs because braid wires loop back and forth between the inner and outer surfaces of the shield, carrying current to the inner surface by conduction rather than by diffusion. As shown in Fig. 15.19(c), wires carrying axial current on the inside surface of the shield produce a magnetic field whose orientation opposes the field leaking in through holes. Measurements in the frequency domain would not show this effect unless they also included a measurement of phase as well as of amplitude.

Electric field leakage

Another source of coupling through braided shields is capacitive leakage through the holes in the shield, as shown in Fig. 15.20. If the shielded cable is subjected to a changing external electric field, electric flux passes through the holes in the cable and shines on the signal conductor.

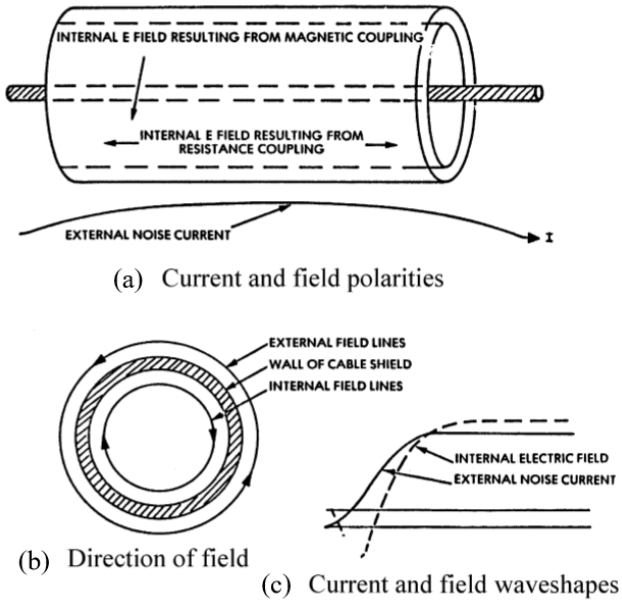

Fig. 15.19 Magnetic coupling giving effect of a negative coupling inductance.

The flow of the resulting displacement currents through the load impedances of the wires inside the shield produces

a voltage between the signal conductor and the shield. An alternate source of coupling, shown in Fig. 15.20(b), involves the voltage on the shield itself. Currents flowing through the external impedance of an imperfectly grounded shield produce a voltage between the shield and any external ground structure.

Leakage due to shield voltage

External impedances between the signal conductor and the shield, as well as the inherent capacitance between the shield and the signal conductor, force the signal conductor to assume nearly the same potential as the shield. Because the signal conductor is then at a potential different from the surrounding ground, electric flux can pass from the signal conductor through the holes in the shield and to ground. The displacement currents, again, produce a voltage between the signal conductor and the shield.

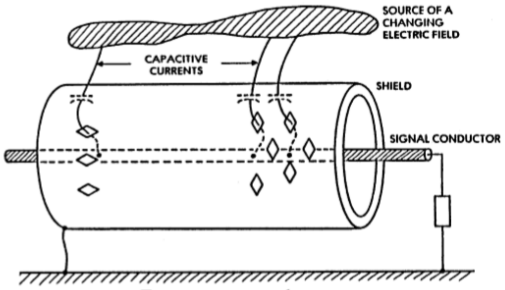

(a) From an external source

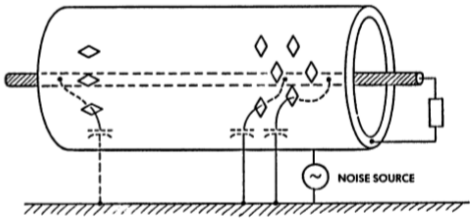

(b) From voltage on the shield

Fig. 15.20 Coupling via capacitive leakage through holes.

Equivalent circuit for capacitive leakage

An equivalent circuit for capacitive leakage (Fig. 15.21) is simply a transfer capacitance, C_{12}, (or transfer admittance, $j\omega C_{12}$, in the frequency domain). The constants for this equivalent circuit depend on the total area of the holes in the shield and on the capacitances between the shield and the conductor (C_{12}) and between the shield and the ground return path (C_2). The transfer capacitance is not very sensitive to weave angle, as was shown in Fig. 15.13.

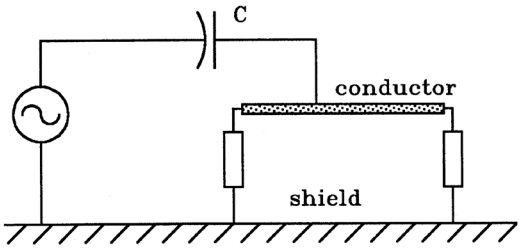

Fig. 15.21 Equivalent circuit for capacitive leakage.

Determination of leakage capacitance

Vance [15.6] also gives expressions relating transfer capacitance to various parameters associated with shield construction. Some cables have a layer of metal foil or a layer of metallized Mylar under the braid to improve the optical coverage and to reduce the transfer admittance. The transfer properties of such shields are best determined by measurement. Some software programs are available that purport to compute SE. To be acceptable for aircraft certification purposes, these programs must be validated for the application that they will be used for by successful comparison with measurements from tests.

Relative order of importance

In most cases, the effects of magnetic field leakage are probably more important than the effects of capacitive (electric field) leakage. Magnetic fields occupy the loop areas between shielded conductors, whereas electric field leakage affects only the surface areas of the shielded conductors. The coupling physics of magnetic and electric fields are explained in Chapter 9.

15.6.3 Tape Wound Shields

Tape-wound shields, like that shown in Fig. 15.22, are often used where an especially flexible shielded cable is required. The shield may be formed either from a narrow metal sheet, spiraled around the bundle, or from a carrier of fine wires, again spiraled around the bundle. Flexible armor and flexible conduit, which is normally used primarily for mechanical protection, may also be analyzed as a tape-wound shield. Tape-wound (or spiral-wound) shields perform rather poorly because the spiral winding tends to behave like a solenoid, wound about the internal conductors. This results in a rather large transfer coupling term, relating the internal voltage to the shield current. The solenoid effect is particularly prevalent if the tape is wound without any overlap because the gaps in the turns force the entire cable current to spiral around the core.

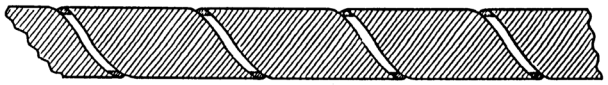

Fig. 15.22 Tape-wound shield.

Vance [15.6] analyzes a 1 cm-radius cable wound with 0.25 mm thick, 1 cm wide, copper tape. The tape is assumed to be wound without any overlap.

The transfer inductance of the tape-wound shield was calculated as 3.9 μH/m, which is four orders of magnitude greater than the transfer inductance obtains for a braided wire shield.

15.6.4 Cable Trays

Cable trays are most often used to provide mechanical protection for wires. They may also provide some electrical protection. The characteristics of a cable tray that determine its effectiveness as electromagnetic shields are the same as for any other shield:

1. It must be able to carry current along its axis.

2. It should be of low-resistance material.

3. It should surround the wires it is protecting. This implies that the tray should be fitted with a conducting cover that makes good electrical contact with the tray along its entire length.

4. It should have a minimum number of openings through which magnetic fields may leak.

5. It should have as few joints as possible, and any joints that are provided should contribute minimum resistance and provide minimum magnetic field leakage.

The transfer characteristics of the tray are about the same as those of the solid tubular shields discussed previously. This comparison assumes the tray is made of solid metal and is fitted with a well-sealed cover. Since covers never form perfect seals, the pulse penetration time constant would probably not be as long as predicted by Eq. 11.21. Even with an imperfect cover, the transfer impedance Z_T would not be greater than the DC resistance.

Trays are usually built-in short sections joined by splices or transition sections. The transition sections are often designed to allow thermal expansion, which precludes their having good electrical continuity or much ability to protect against magnetic leakage. The transfer characteristic of a cable tray formed from multiple sections is typically found to depend almost entirely on the treatment of the joints between the sections. Leakage at joints can be reduced by covering them with flexible tape or metal braid. The transfer characteristics can seldom be determined by calculation; they must be determined experimentally.

Conduits

Conduits used in aircraft are sometimes intended only to provide mechanical protection for wires. They should not be relied upon for electromagnetic shielding unless it has been verified that the conduit is electrically continuous and is grounded to the airframe at intervals and at each end. Sometimes conduits are supported by nonconductive shock mounts and thus are not inherently grounded.

15.7 Transfer Impedance Characteristics of Actual Cables

The transfer impedance of a shielded cable relates the voltage (typically) or the current to the current that is in the shield. Therefore, the impedance can be expressed as a ratio of either shielded conductor voltage, or current, to the shield current. This ratio is predominantly the resistance, R_{DC} of the shield, but it also includes the transfer inductance, M_{12}, as shown in Fig. 15.17. It sometimes also includes a transfer capacitance, but this is not a significant factor in most shields found in aircraft applications.

Transfer impedance is not a factor commonly specified either by the manufacturer or by procurement specifications, although sometimes the DC resistance is specified. Even among cables of the same nominal type, transfer impedance may vary considerably between cables supplied by different manufacturers. The most straightforward method of determining the transfer characteristic of a shielded cable (particularly if multiple shields are involved and if the wires are terminated to a variety of load impedances) is to make actual measurements of the conductor voltages produced by currents circulating through the shield. The techniques by which experimental transient currents may be injected into the shields of cables through coupling transformers are described in Chapter 18.

If actual measurements of coupling effects are not available, the transfer characteristics of many cables can be estimated from other published literature. One such summary, giving the parameters of coaxial cable shields, is shown in Table 15.1 [15.7].

15.8 Connectors

Transfer impedance

The transfer impedance of a cable connector or splice can be represented by

$$Z_\tau = R_o + j\omega L_{12} \qquad (15.7)$$

where R_o is the resistance measured across the connector and L_{12} is a transfer inductance between the external shield circuit and the internal conductors of the cable. The value of $Z\tau$ is usually not calculable, but it can be measured by passing current through a cable sample containing the connector and measuring the open circuit voltage induced on conductors inside the shield. Some typical values of R_o and L_{12} have been measured on cable connectors and are listed in Table 15.2.

The transfer impedance of a connector can be regarded as a lumped element in the cable circuit (as distinct from the distributed nature of the transfer impedance of a cable shield). Thus, the effect of leakage through a connector can be simply represented by a discrete voltage source

$$V = IZ_\tau \qquad (15.8)$$

where I is the shield current.

Transfer admittance

Since most connectors available for use with shielded cables have essentially 100% optical coverage, their transfer admittance is usually negligible. In addition, most bulkhead or panel-mounting connectors are located at points where the shield voltage is minimal, so that excitation of the internal conductors by the transfer admittance is small, even when the transfer admittance itself is not small.

15.9 Ground Connections for Shields

The transfer parameters of Table 15.2 refer only to the properties of the connector itself. Transfer impedances are also influenced by the way cable shields are bonded to their connectors, and by the way the jacks (to which the connectors mate) are mounted to bulkheads. Even slight inattention to these details may introduce transfer impedances into circuits far greater than the impedances of the connectors or, possibly, far greater than that of the entire cable shield.

Pigtail grounding

A common treatment of shields at connectors is to insulate the shield with tape and connect it to the connector back-shell through a pigtail (Fig. 15.23(a)). Another practice, often used in the past, was to insulate a panel connector from its panel with an insulating block and to ground the connector either to the panel through a pigtail or (more commonly) to an internal ground bus, also as illustrated in Fig. 15.23(a).

Another typical shield-to-connector termination, shown in Fig. 15.23(b), involves connecting the shield to one of the connector pins and grounding it internally (through a pigtail) either to the panel or to an internal ground bus. This arrangement allows some magnetic flux from the shield current to originate inside the enclosure, not a healthy situation. The rationale for this arrangement seemed to be that the ground inside the enclosure was "cleaner" than a ground point on the exterior of the enclosure. This is not correct. There is no such thing as a "clean" or "noisy" ground. "Noise" comes from the voltages or currents induced in loops between pigtails and nearby references, such as cable trays, airframe structures, and any other nearby references.

Grounding to remote point

Sometimes shields are not connected at all to the panel on which the connector is mounted, but are connected, instead, to some remote 'system ground' point (Fig. 15.23(c)). This practice should always be avoided because it introduces enough loop area to completely undermine the effectiveness of the shield. Remote grounding of shields reflects a fundamental misunderstanding of the role of 'ground' connections on shields.

Calculation of effects

The coupling introduced by any of these configurations can be studied in terms of the self-impedance of the conductor used for the pigtail and the inductance (magnetic field) between the pigtail and the conductors in the connector. The flow of current through the self-inductance of the pigtail produces a voltage.

$$V = j\omega L \qquad (15.9)$$

Or in the time domain,

$$V = L\left[\frac{di}{dt}\right] \qquad (15.10)$$

Where L is the inductance that represents the magnetic field between the shielded conductor(s) and the pigtail. This voltage adds directly to the voltage produced by the flow of current along the shield. The self-inductance of conductors was discussed in §9.5.3, in which Eq. 9.28 shows that the inductance of a straight conductor of non-magnetic material is:

$$L = 2 \times 10^{-7} l \left[\ln \frac{2l}{r} - 1 \right], \qquad (15.11)$$

where l = length and r = radius of the wire.

The inductance of a typical pigtail does not differ significantly from this, even if it is curved or bent.

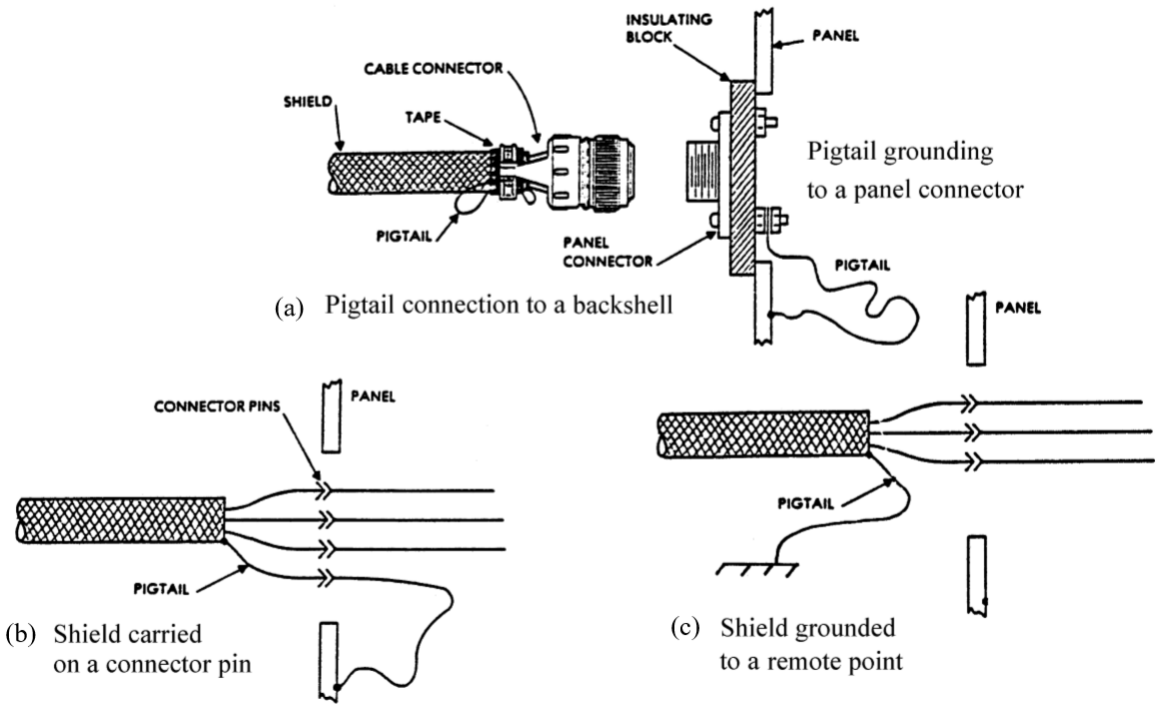

Fig. 15.23 Termination of shields at connectors.

Measured example

This point is illustrated in Fig. 15.24, which is taken from an extension of the test series previously discussed in reference to Figs. 15.2 through 15.8. One end of the cable was grounded through a 33-inch length of wire, while the other end was connected to the ground plane directly. Note that the voltage, V_1, increased from 0.4 volts (Fig. 15.24) to 3.5 volts, solely because of the inductive voltage rise in the loop formed by the ground lead.

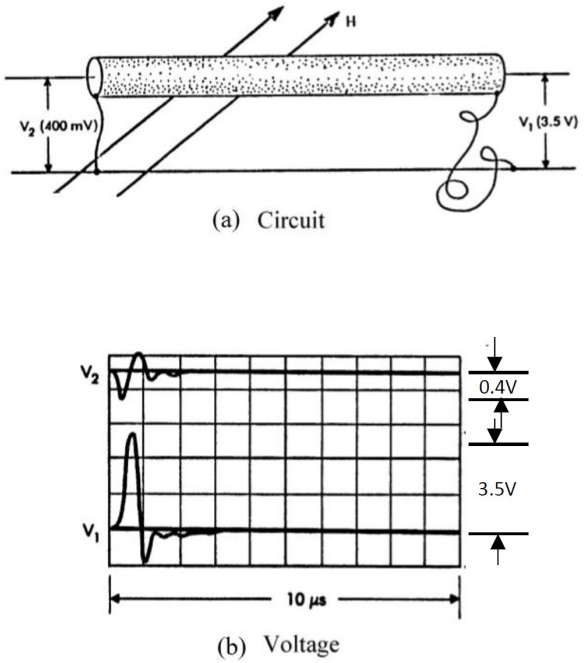

Fig. 15.24 Effect of inductance in a shield pigtail ground connection.

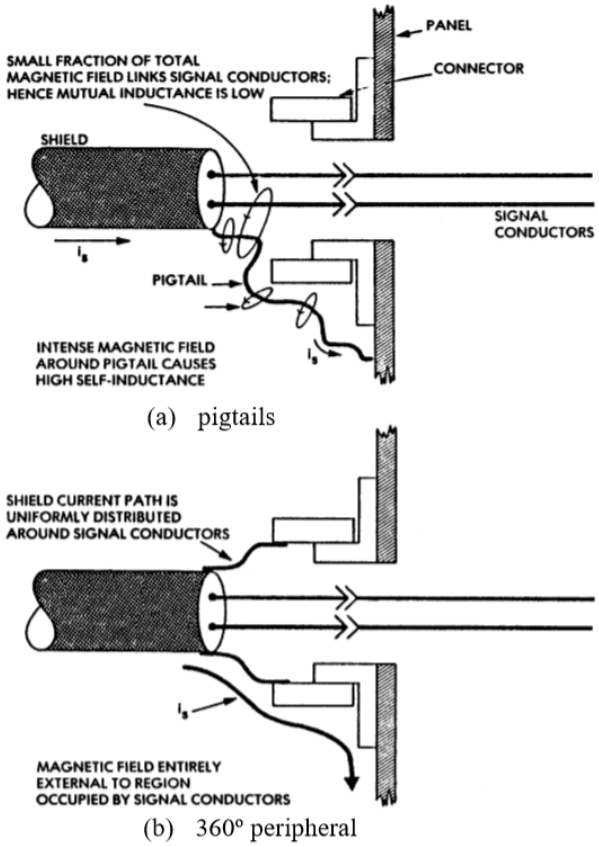

Fig. 15.25 Grounding of shields.

Peripheral grounding

The best type of connector for minimizing transfer impedance is one in which the shield currents pass from the shield to the connector through a path that surrounds the shielded conductors, as shown in Fig. 15.25(b). A wide variety of connectors provided with a means of bonding shields directly to them are commercially available.

Such connectors introduce much less voltage into the conductors for the following reasons:

1. The length of the path through which the shield current must flow is short.

2. The field intensity outside the shield is reduced by the inherently large diameter of the path upon which the current flows.

3. The field intensity inside the shield is low, nearly zero, because of magnetic field cancellation described in §9.5.3.

The shortness, and large diameter of the current path implies low self-inductance. The absence of magnetic flux within the shield implies that the signal conductors are exposed to as much flux as the shield. In other words, the transfer inductance is zero.

15.10 Shielding of Enclosures

The effects of the structural details of enclosures on their shielding performance are usually discussed in terms of the frequency-domain. This topic is thoroughly addressed in many sources and will not be repeated here. Instead, this section is limited to a qualitative discussion of the responses of shielding enclosures to time-domain magnetic fields. It highlights some of the more rigorous discussions found in Chapters 11 and 12.

Origin of magnetic shielding by non-magnetic materials

A magnetic field line that attempts to penetrate a conductive sheet (Fig. 15.26(a)) induces circulating currents that set up an opposing magnetic field. The result is that a transient magnetic field initially surrounds the sheet (Fig. 15.26(b)) and only as time progresses does a portion of the field penetrate the sheet. This is true even if the sheet is made from a non-magnetic material, such as aluminum.

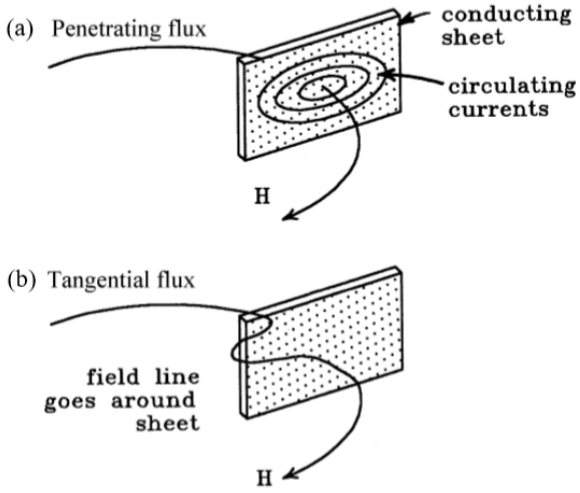

Fig. 15.26 Magnetic field intersecting a conducting sheet.

Response of an enclosure

If a metal box is exposed to the field (Fig. 15.27), circulating currents are induced on the surface of the box. In cross-section, the field patterns resemble Fig. 15.28. As time progresses, the field begins to penetrate the box, starting at the corners and eventually passing directly through.

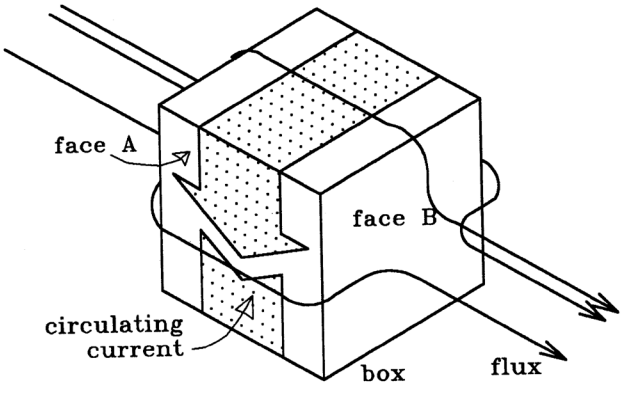

Fig. 15.27 Circulating current induced by a changing magnetic field.

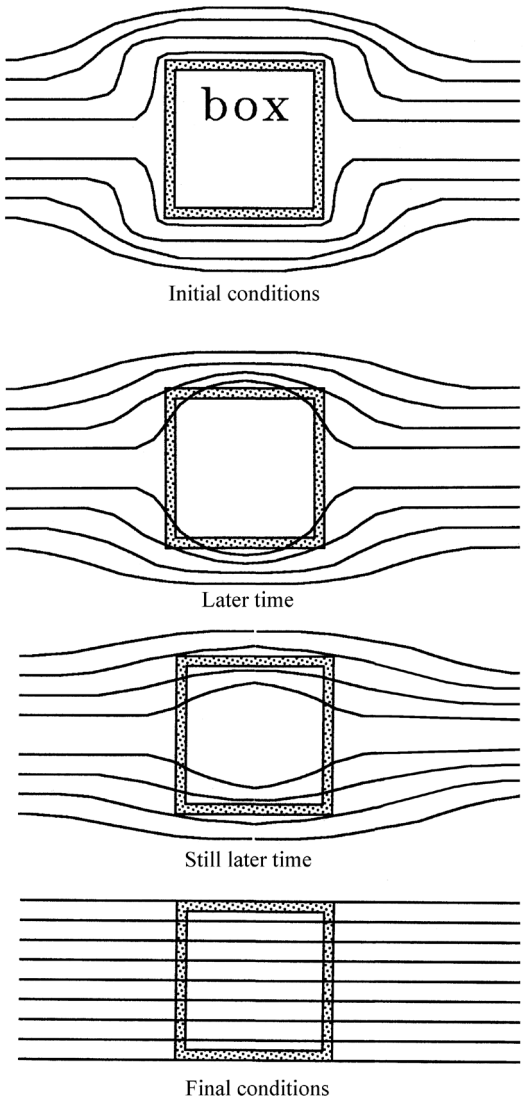

Fig. 15.28 Paths of the magnetic field.

Interestingly, there are no tests included in the family of lightning tests (e.g., RTCA DO-160 Section 22 - 23, and SAE ARP5416) that examine lightning originated electromagnetic field-immersion effects on equipment, as there are for EMI and HIRF. Lightning bench tests of equipment are limited to either cable bundle injection or individual connector pin injection.

Induced Current

Equipment installed in location where it is exposed to lightning magnetic fields, such as within nonconductive parts of an airframe, wheel wells, or engine nacelles may be exposed to high magnetic field intensities that may induce significant currents into the equipment enclosures as illustrated in Fig. 15.29.

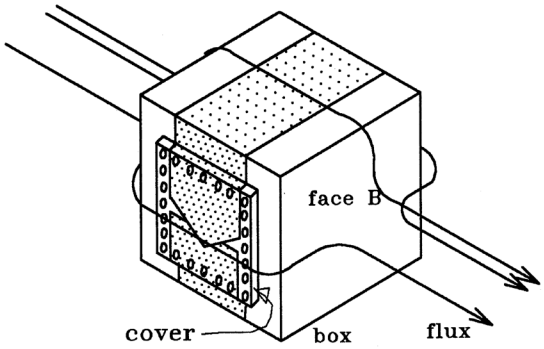

Fig. 15.29 Magnetic field induction of circulating current.

Internal current

In response to a step function magnetic field, the induced current density on the inside surface of the box acquires the diffusion waveform discussed in §11.3.5 and illustrated in Fig. 15.30(d).

The current density, multiplied by the resistivity of the metal, gives the internal voltage rise. The sum of all the internal voltages (Fig. 15.30(a)) induced across the internal inductance of the box (Fig. 15.31) drives an internal circulating current, which, in turn, produces the net internal magnetic field.

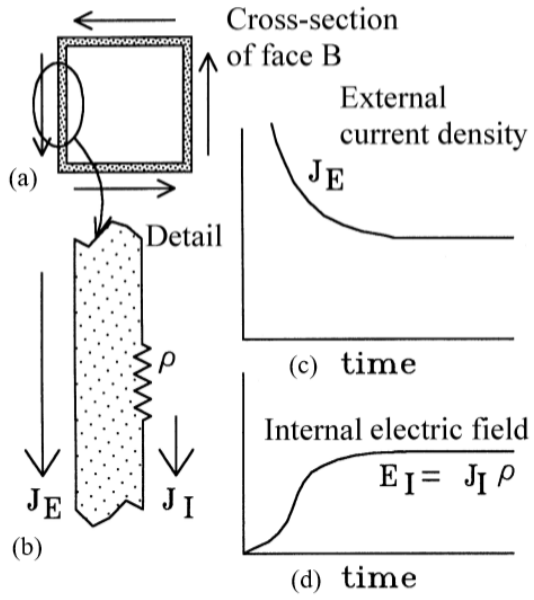

Fig. 15.30 Current densities.

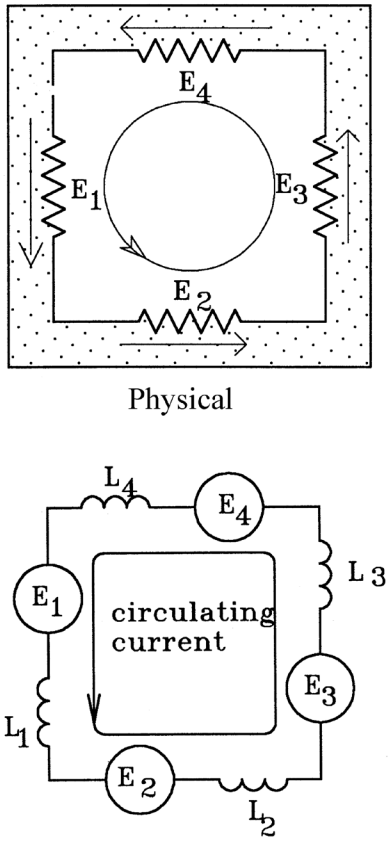

Fig. 15.31 The internal circulating current.

Injected current

Exposure to a magnetic field is not the only means by which a current can be induced on the surface of the box. It is more common for current induced on a cable shield to be *transferred* to the box at a termination point, from which it distributes over the surface of the box, as illustrated in Fig. 15.32. Designers need to know the amplitudes of shield currents so that the connectors and interfaces with the boxes can be built to tolerate physical effects of shield currents. Some lightning induced currents can be as high as several kiloamperes. Traditional metal connectors can usually tolerate such currents without damage. Plastic or composite connectors usually cannot tolerate currents higher than several hundred amperes, since the conductivity is provided by thin layers of conductive material.

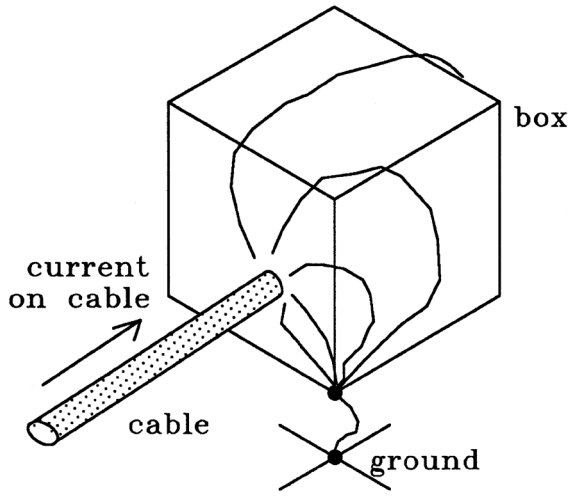

Fig. 15.32 Direct injection of current.

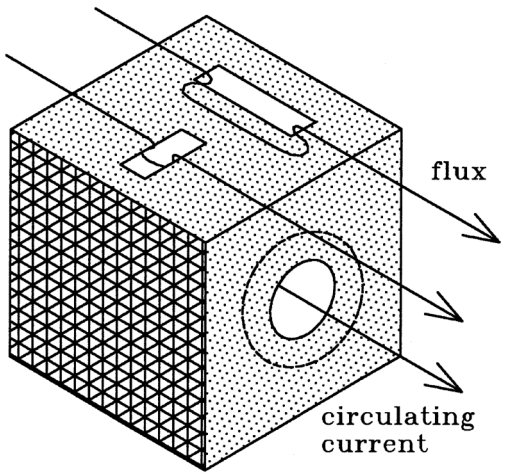

Fig. 15.33 Leakage through apertures.

Factors that degrade shielding

One factor that can degrade the shielding of the box is the presence of removable covers, like the one illustrated in Fig. 15.33. Covers always present a higher impedance path than continuous metal. Circulating current that flows through cover joints produces a resistive voltage that is not retarded by diffusion effects. Louvres, screens, and cooling vents may allow fields to directly penetrate enclosures and interact with circuits and devices. Another factor is the presence of apertures, like the one illustrated in Fig. 15.33. External magnetic fields loop in and out of such apertures, producing net internal magnetic fields.

An aperture whose longest dimension is oriented parallel to the impinging magnetic field admits more flux to the interior of the box than an aperture oriented perpendicular to the field.

Table 15.1 Design data for braided wire shields

Cable Type (RG-)		Strand Diameter d (inches)	Outside Diameter (inch)	Carriers, C	Ends, N	Picks, P (inch^{-1})	Weave Angle, α (degrees)	Fill, F	Coverage K (%)	Weight per Foot (lbs)	Stranding Factor	DC Resistance, R_o (mΩ/m)	Leakage Inductance, M_{12}(nH/m)	Leakage Capacitance C_{12}/C_1C_2(m/F)
6	I	0.0063	0.189	16	9	5.90	25.0	0.790	95.61	0.019	1.54	6.6	0.42	2.9×10^7
6	AI	0.0063	0.189	24	6	8.80	24.9	0.790	95.58	0.019	1.54	6.6	0.28	1.9
6	O	0.0063	0.214	16	9	8.79	37.7	0.886	96.23	0.022	1.98	7.5	0.36	1.9
6	AO	0.0063	0.214	24	6	13.00	37.6	0.885	96.18	0.022	1.98	7.5	0.25	1.3
11		0.0071	0.292	24	8	6.50	27.5	0.799	95.96	0.033	1.59	4.0	0.25	1.6
22	I	0.0063	0.291	24	8	9.10	35.9	0.763	95.27	0.028	1.95	5.5	0.34	1.9
22	0	0.0063	0.316	24	8	12.00	45.9	0.842	97.50	0.033	2.45	6.4	0.14	0.6
23	I	0.0063	0.394	24	9	10.50	48.2	0.799	95.95	0.039	2.82	5.9	0.29	1.2
25	I	0.0063	0.298	16	13	5.00	31.4	0.786	95.44	0.029	1.74	4.8	0.46	2.8
25	AI	0.0063	0.298	24	9	6.00	26.0	0.776	94.98	0.029	1.60	4.4	0.34	2.3
25	O	0.0063	0.355	16	15	5.00	35.8	0.887	96.29	0.036	1.88	4.4	0.35	1.9
25	AO	0.0063	0.355	24	11	5.00	25.7	0.799	95.96	0.035	1.54	3.7	0.25	1.6
35		0.0071	0.470	24	10	9.00	48.8	0.850	97.74	0.056	2.71	4.3	0.12	0.5
58		0.0050	0.120	12	9	7.70	27.7	0.746	93.57	0.089	1.71	14.2	1.0	6.6
58	A	0.0050	0.120	16	7	10.30	27.7	0.775	94.92	0.018	1.65	13.7	0.53	3.5
59		0.0063	0.150	16	7	8.20	27.6	0.780	95.14	0.015	1.63	8.6	0.49	3.2
59	A	0.0063	0.150	24	5	12.30	27.6	0.835	97.29	0.016	1.53	8.1	0.14	0.9
62		0.0063	0.151	16	7	8.20	27.8	0.776	94.98	0.015	1.65	8.7	0.52	3.4
62	A	0.0063	0.151	24	5	12.30	27.8	0.831	97.15	0.016	1.54	8.1	0.15	1.0
63		0.0071	0.295	16	12	4.30	27.6	0.792	95.66	0.033	1.61	4.0	0.42	2.7
63	A	0.0071	0.295	24	8	6.50	27.8	0.793	95.71	0.033	1.61	4.0	0.27	1.8

A – Alternate
A1 – First Alternate
A2 – First Alternate

I - Inner
O - Outer
S –Shield (insulated from braid)

- Braid actually consists of flat tape conductors. Strand diameter and ends are estimated for the equivalent cross-sectional area of the tape conductor, therefore, F, K and stranding factor are approximate.

Table 15.1 (continued) Design data for braided wire shields

Cable Type (RG-)		Strand Diameter d (inches)	Outside Diameter (inch)	Carriers, C	Ends, N	Picks, P (inch^{-1})	Weave Angle, α (degrees)	Fill, F	Coverage K (%)	Weight per Foot (lbs)	Stranding Factor	DC Resistance, R_0 (mΩ/m)	Leakage Inductance, M_{12}(nH/m)	Leakage Capacitance C_{12}/C_1C_2(m/F)
65		0.0071	0.295	24	8	6.50	27.8	.793	95.71	0.033	1.61	4.0	0.27	1.8
108		0.0050	0.164	16	6	10.80	36.4	.546	79.36	0.009	2.83	17.6	4.6	25.0
114		0.0063	0.295	24	8	7.00	29.4	.718	92.07	0.020	1.83	5.1	0.70	4.4
119	I	0.0071	0.337	24	10	5.40	26.4	.862	98.10	0.041	1.45	3.1	0.08	0.5
119	O	0.0063	0.367	24	8	10.60	46.5	.737	93.06	0.033	2.86	6.5	0.65	2.8
122		0.0050	0.099	16	6	12.90	28.9	.801	96.02	0.008	1.63	16.2	0.37	2.4
122	A	0.0050	0.099	24	5	12.20	19.2	.928	99.48	0.010	1.211	12.0	0.01	0.08
130		0.0100	0.487	24	8	6.30	39.9	.786	95.41	0.076	2.16	2.3	0.33	1.7
142	I	0.0050	0.121	16	7	11.50	30.6	.791	95.61	0.010	7.71	14.1	0.43	2.7
142	O	0.0100	0.141	16	7	14.50	40.7	.778	95.09	0.011	2.23	16.0	0.55	2.8
144		0.0063	0.290	24	8	9.20	36.1	.787	95.47	0.029	1.95	5.5	0.32	1.7
156	I	0.0063	0.290	24	8	11.20	41.6	.851	97.77	0.031	2.10	6.0	0.11	0.55
156	O	0.0070	0.333	24	8	9.20	39.9	.803	96.13	0.034	2.11	4.7	0.26	1.3
156	S	0.0063	0.413	24	8	14.00	57.3	.838	97.38	0.043	4.10	8.3	0.17	0.51
157	I	0.0063	0.465	24	9	12.80	58.0	.856	97.92	0.049	4.16	7.5	0.12	0.36
157	O	0.0070	0.500	24	10	7.30	44.5	.729	92.67	0.046	2.69	4.1	0.70	3.1
157	S	0.0063	0.580	24	9	13.50	64.5	.848	97.70	0.060	6.35	9.2	0.16	0.34
174		0.0040	0.063	16	4	16.30	24.4	.630	86.33	0.003	1.91	36.5	2.3	15.8
179		0.0040	0.066	16	5	12.00	19.2	.729	92.65	0.004	1.54	28.1	0.88	6.6
181	I	0.0063	0.215	24	7	8.80	27.7	.836	97.30	0.023	1.53	5.7	0.14	0.9
181	O	0.0100	0.490	24	8	7.00	19.2	.820	96.76	0.080	2.28	2.4	0.20	0.95
189	I	0.0100	0.635	48	7	6.00	27.7	.918	99.33	0.114	1.38	1.1	0.008	0.06
189	O	0.0100	0.680	48	6	7.00	32.7	.778	95.07	0.104	1.81	1.4	0.17	1.0
192	I	0.0100	1.725	48	11	5.87	53.3	.806	96.22	0.265	3.47	1.1	0.14	0.49
192	O	0.0095	1.780	48	11	5.95	54.5	.764	94.43	0.182	3.88	1.1	0.25	0.85
192	S	0.0100	1.890	48	11	6.03	56.4	.796	95.84	0.289	4.11	1.2	0.17	0.53
193	I	0.0100	1.725	48	11	4.15	43.5	.664	88.68	0.220	2.86	0.89	0.66	3.1
193	O	0.0095	1.780	48	11	5.50	52.3	.726	92.50	0.225	3.69	1.2	0.39	1.4
193	S	0.0100	1.890	48	9	7.70	62.6	.781	95.20	0.284	6.83	1.7	0.23	0.54

Table 15.1 (continued) Design data for braided wire shields

Cable (RG-)	Type	Strand Diameter d (inches)	Outside Diameter (inch)	Carriers, C	Ends, N	Picks, P (inch^{-1})	Weave Angle, α (degrees)	Fill, F	Coverage K (%)	Weight per Foot (lbs)	Stranding Factor	DC Resistance, R_0 (mΩ/m)	Leakage Inductance, M_{12}(nH/m)	Leakage Capacitance C_{12}/C_1C_2(m/F)
194	I	0.0100	1.725	48	11	4.15	43.5	0.664	88.68	0.220	2.86	0.89	0.66	3.1
194	O	0.0095	1.780	48	11	5.50	52.3	0.726	92.50	0.225	3.69	1.2	0.11	0.38
210		0.0063	0.151	16	7	8.20	27.8	0.776	94.98	0.015	1.65	8.7	0.52	3.4
210	A	0.0063	0.151	24	5	12.30	27.8	0.831	97.15	0.016	1.54	8.1	0.15	0.96
211		0.0080	0.625	36	10	5.60	32.1	0.844	97.56	0.082	1.65	1.7	0.09	0.48
211	A	0.0080	0.625	48	8	5.60	25.2	0.843	97.53	0.082	1.45	1.5	0.06	0.40
212	I	0.0063	0.189	16	9	5.90	25.0	0.790	95.61	0.019	1.54	6.6	0.452	2.9
212	AI	0.0063	0.189	24	6	8.80	24.9	0.790	95.58	0.019	1.54	6.6	0.28	1.9
212	O	0.0063	0.214	16	9	8.70	37.7	0.806	96.23	0.022	1.98	7.5	0.36	1.9
212	AO	0.0063	0.214	24	6	13.00	37.6	0.805	96.18	0.022	1.98	7.5	0.25	1.3
213		0.0071	0.292	24	8	6.50	27.5	0.799	95.96	0.033	1.59	4.0	0.25	1.6
214	I	0.0063	0.292	24	6	16.60	52.9	0.786	95.44	0.029	3.50	9.9	0.37	1.3
214	O	0.0063	0.317	24	7	15.40	53.0	0.850	97.75	0.034	3.25	8.5	0.13	0.45
217	I	0.0071	0.380	24	10	5.40	29.1	0.788	95.49	0.042	1.66	3.2	0.30	1.9
217	O	0.0071	0.405	24	8	10.60	49.3	0.794	95.75	0.045	2.96	5.4	0.32	1.3
218		0.0100	0.690	24	14	3.10	30.0	0.869	98.29	0.118	1.53	1.2	0.07	0.44
218	A1	0.0100	0.690	36	9	4.00	26.4	0.811	96.41	0.110	1.54	1.2	0.14	0.92
218	A2	0.0100	0.690	48	7	5.60	27.5	0.849	97.72	0.115	1.50	1.1	0.05	0.35
220		0.0100	0.925	36	12	3.50	30.0	0.840	97.44	0.151	1.59	0.91	0.09	0.53
220	A	0.0100	0.925	48	9	4.20	27.5	0.820	96.76	0.148	1.55	0.89	0.09	0.59
222	I	0.0063	0.189	16	9	5.90	25.0	0.790	95.61	0.019	1.54	6.6	0.42	2.9
222	AI	0.0063	0.189	24	6	8.80	24.9	0.790	95.58	0.019	1.54	6.6	0.28	1.9
222	O	0.0063	0.214	16	9	8.70	37.7	0.806	96.23	0.022	1.98	7.5	0.36	1.9
222	AO	0.0063	0.214	24	6	13.00	37.6	0.805	96.18	0.022	1.98	7.5	0.25	1.3
223	I	0.0050	0.120	12	9	9.00	31.5	0.775	94.95	0.010	1.77	14.8	0.72	4.4
223	AI	0.0050	0.150	16	7	11.50	30.4	0.795	95.80	0.010	1.69	15.5	0.43	2.3
223	O	0.0050	0.140	12	9	10.00	38.1	0.729	92.63	0.010	2.22	16.0	1.3	7.0
223	AO	0.0050	0.140	16	7	15.00	41.5	0.793	95.71	0.011	2.25	16.2	0.45	2.2
225	I	0.0063	0.290	24	6	16.60	52.7	0.788	95.52	0.029	3.46	9.8	0.36	1.3

Table 15.1 (continued) Design data for braided wire shields

Cable Type (RG-)		Strand Diameter d (inches)	Outside Diameter (inch)	Carriers, C	Ends, N	Picks, P ($inch^{-1}$)	Weave Angle, α (degrees)	Fill, F	Coverage K (%)	Weight per Foot (lbs)	Stranding Factor	DC Resistance, R_0 (mΩ/m)	Leakage Inductance, M_{12}(nH/m)	Leakage Capacitance C_{12}/C_1C_2(m/F)
225	O	0.0063	0.315	24	7	15.40	52.9	0.852	97.80	0.033	3.22	8.5	0.12	0.44
226	I	0.0063	0.375	24	10	10.50	46.8	0.907	99.14	0.042	2.35	5.2	0.03	0.12
226	O	0.0063	0.400	24	8	10.50	48.6	0.706	91.33	0.035	3.24	6.6	0.92	3.7
301		0.0050	0.190	16	10	8.00	32.1	0.752	93.84	0.014	1.86	10.0	0.73	4.4
302		0.0050	0.151	16	7	11.50	36.0	0.684	90.04	0.010	2.23	15.0	1.5	8.4
303		0.0050	0.121	16	7	11.50	30.6	0.791	95.61	0.010	1.71	14.1	0.43	2.7
304	I	0.0063	0.190	24	5	14.50	37.6	0.749	93.71	0.213	2.12	9.0	0.52	2.8
304	O	0.0063	0.215	24	6	11.50	34.4	0.769	94.57	0.021	1.91	7.2	0.40	2.3
316		0.0040	0.063	16	5	4.50	7.2	0.723	92.32	0.004	1.41	26.8	0.88	7.7
326	I	0.0035	0.550	24	27	6.46	43.3	0.890	98.80	0.042	2.12	5.9	0.05	0.22
326	O	0.0035	0.566	24	27	6.46	44.1	0.877	98.49	0.043	2.21	6.0	0.06	0.30
328	I	0.0100	1.085	48	9	5.50	38.5	0.795	95.80	0.167	2.05	1.0	0.14	0.75
328	O	0.0070	1.125	48	12	6.70	45.0	0.796	95.85	0.111	2.51	1.7	0.15	0.66
328	S	0.0100	1.225	48	9	5.60	42.4	0.748	93.63	0.177	2.45	1.1	0.28	1.3
329	I	0.0100	0.390	24	7	5.90	32.3	0.772	94.80	0.060	1.82	2.4	0.38	2.3
329	O	0.0070	0.430	24	9	9.20	46.9	0.794	95.74	0.043	2.70	4.7	0.31	1.3
391		0.0063	0.307	24	7	16.30	53.8	0.891	98.82	0.034	3.21	8.1	0.05	0.17

Table 15.2 Transfer Impedance of Typical Cable Connectors [15.7]

Connector	**Identification**	**R_o (ohms)**	**M_{12} (H)**
Multipin	Burndy NA5-15863	0.0033	5.7×10^{-11}
Aerospace	Deutsch 38068-10-5PN	0.15	2.5×10^{-11}
Connectors	Deutsch 38068-18-31SN	0.005	1.6×10^{-10}
(Threaded)	Deutsch 38068-22-55SN	0.023	1.1×10^{-10}
	Deutsch 38068-14-7SN	0.046	5.0×10^{-11}
	Deutsch 38060-14-7SN	0.10	8.2×10^{-11}
	Deutsch 38068-14-7SN	0.023	6.7×10^{-11}
	Deutsch 38068-12-12SN	0.0033	3.0×10^{-11}
	Deutsch 38068-12-12SN	0.012	1.3×10^{-11}
	Deutsch 38068-12-12SN	0.012	1.3×10^{-11}
	Deutsch 38060-12-12SN	<0.001	2.5×10^{-12}
	Deutsch 38068-12-12SN	0.014	3.5×10^{-11}
	AMP	0.0067	1.6×10^{-11}
	AMP	0.0067	1.5×10^{-11}
	AMP	0.003	1.9×10^{-11}
Type N	UG 21B/U-U58A/U	*	*
Type BNC (Bayonet)	UG 88C/U-UG1094/U	0.002	$4\text{-}8 \times 10^{-11}$
Anodized	MS 24266R-22B-55	$5\ 10^4$	$\omega M < R_O$@ 20 MHz
Open Shell	MS 3126-22-55	0.5^{-1}	$\omega M < R_O$@ 20 MHz
Split Shell	MS 3100-165-1P	0.001	$\approx 20 \times 10^{-11}$
	MS 3106A-		

*Too small to measure in present of 4 inches of copper tube used to mount connector.

References

15.1 F. A. Fisher, “Effects of a Changing Magnetic Field on Shielded Conductors”, *Lightning Protection Note 75-2*, Internal General Electric Memorandum, High Voltage Laboratory, Corporate Research and Development, General Electric Company, Pittsfield, Massachusetts, June 2, 1975.

15.2 S. A. Shelkunoff, “Electromagnetic Theory of Coaxial Transmission Lines and Cylindrical Shields”, *Bell System Technical Journal*, 13, 1934, pp. 532-579.

15.3 E. F. Vance, H. Chang, “Shielding Effectiveness of Braided Wire Shields”, Stanford Research Technical Memorandum 16, November 1971.

15.4 SAE ARP5412B Aircraft Lightning Environment and Related Test Waveforms January 2013.

15.5 E. F. Vance, “Comparison of Electric and Magnetic Coupling through Braided-Wire Shields”, *Stanford Research Technical Memorandum 18*, February 1972.

15.6 E. F. Vance, “Coupling to Cables”, *DNA Handbook Revision*, Chapter 11, Stanford Research Institute, Menlo Park, California, December 1974.

15.7 E. F. Vance, “Comparison of Electric and Magnetic Coupling through Braided-Wire Shields”, Stanford Research Technical Memorandum 18, February 1972, pp. 1-133 to 11-166.

Chapter 16

DESIGN AND COORDINATION OF PROTECTION FROM INDUCED EFFECTS

16.1 Introduction

This chapter discusses methods for controlling lightning induced effects. It focuses on the larger issues, involving the aircraft, such as the location of equipment and the selection of appropriate types of wiring. In other words, this chapter primarily addresses systems integration and basic policy regarding lightning protection. The chapter also presents the evolution of the lightning-induced transient standards, the definitions, and applications of the standards.

Some of the policy steps involved in controlling induced effects are:

1. Induced effects should not cause damage or upset to electronic equipment and systems.

2. Consider options for the airframe materials and construction. These have a very significant influence upon susceptibility of systems and equipment to lightning effects. There are tradeoffs to be made that impact cost and weight.

3. Consider options for control of induced transients and for protection of equipment. There are tradeoffs to be made.

4. Remember that it is primarily the interconnecting wiring that determines equipment susceptibility. Take as much advantage as possible of inherent shielding provided by the airframe.

5. Coordinate equipment transient withstand specifications with actual transients expected to be induced in wiring.

6. Prepare specifications that apply both to the airframe protection and to protection of the equipment and systems. Require that transient tolerance of equipment and systems be verified by test.

7. Require that equipment withstand equipment transient design levels (ETDLs) and that these be applied to individual equipment connector pins.

The points outlined above are discussed in the following sections. The 'goals' for design described in §16.2 may seem self-evident to some readers, but sometimes these issues are not adequately addressed. The sections entitled 'Location of equipment' (§16.3) and 'Locations for wiring' (§16.4) discuss general good practice. Section 16.5 discusses shielding of interconnecting wiring, continuing a discussion begun in Chapters 9 and 15. Determining the actual transient levels (ATLs) to be expected in aircraft wiring was the subject of Chapters 9 - 14. Design of equipment is discussed further in Chapter 17 and verification testing is discussed in Chapter 18.

The transient control level (TCL) and ETDL concept first described in Chapter 5, under the encouragement of airworthiness certification guidelines like [16.1], has become widespread in its application to aircraft design. This is especially true for aircraft designs undergoing civil certifications. The practice seems to have been less well understood and applied in military aircraft, where adherence to earlier electromagnetic interference (EMI) specifications has sometimes gotten in the way of adoption of the more logical TCL/ETDL procedure. Therefore, since this logical concept is still not widely understood, it is explained in some detail in this chapter and some discussion of its historical development is included.

16.2 Requirements and Goals

The requirements regarding induced effects are:

1. Induced effects should not cause physical damage to electrical or electronic equipment.

2. Induced effects should not cause interference that presents an imminent hazard to the safety of the vehicle or its crew. This includes interferences that could convey misleading information to the crew that would pose a severe risk to the completion of the aircraft's safe flight or mission.

Other interference, although undesirable, might be tolerated. For example, induced effects that cause warning lights to be illuminated might be considered acceptable,

whereas induced effects that lead to unwanted flight or engine control inputs, or hazardous, misleading information on cockpit displays would be considered unacceptable. The tripping of circuit breakers or solid-state power controllers in the electric power distribution system might be unacceptable, even if it were possible to re-initialize or reset the displays or circuit breakers. Acceptance criteria for any lightning effects should be determined by the lightning safety assessment described in Chapter 5.

Interference that leads to the scrambling of one channel of a redundant digital control system is probably acceptable if this can be depended upon to happen only in one channel of a two independent and dissimilar channel system (for example), but interference that causes all computers to shut down, with loss of display or control function, is unacceptable. At least one channel must be shown, either through test or analysis, to maintain the function during and after the lightning event.

Some general premises that go along with these goals might be:

1. It is more productive to design electronic equipment so that it can accept lightning induced transients on input and output leads than it is to initiate a retrofit program to provide protection to an existing system, found susceptible to hazardous lightning induced effects during service.

2. It is more practical to design an electronic system around the capabilities of existing and proven protective devices, such as shields, transient protectors, or circuit design approaches, than it is to develop and retrofit new and improved protective techniques to an electronic system designed without consideration of the transients that might be produced by lightning.

3. Trade-offs must be made between the cost of providing electronic equipment capable of withstanding lightning induced transients and the cost of shielding equipment and interconnecting wiring from the electromagnetic effects of lightning.

4. Designers should take as much advantage as possible of the inherent shielding that aircraft structures can supply and should avoid placing equipment and wiring in locations that are most exposed to the electromagnetic fields produced by lightning. Frequently, decisions regarding the location and installation of avionic equipment and interconnecting wiring are made by persons with no knowledge of the implications of these installations on susceptibility to lightning effects. The selection of materials for use in instrument panel and glare shield construction is made with weight, manufacturability, and cost in mind but without regard for the need to protect against lightning and other electromagnetic effects.

16.3 Importance of the Airframe

As discussed in earlier chapters, the materials of which the airframe is made have a significant impact on the magnitudes of induced transients in aircraft systems. An all-aluminum airframe, especially fuselage and wings, can provide significant protection of the interconnecting wiring, both by prevention of direct contact of lightning channels with the installed wiring and by providing electromagnetic shielding. Airframes constructed either partially or fully of composite materials do not provide as much protection of installed electronics, and other systems. Brief discussions of the situations with all-aluminum, carbon fiber composite (CFC), and combinations of these structural materials, and of non-electrically conductive composites, like glass fiber reinforced composites are presented in the following subsections.

In the discussions that follow, the transient voltages and currents mentioned are those appearing between the individual conductors or cable bundles and the local airframe. These are called *common-mode* transients. Whether or not this is how the system voltages are utilized, there are always common-mode voltages and currents, and these cause the most damage. Lightning-induced transient specifications are typically specified as common-mode.

16.3.1 Aluminum airframes

Wiring installed within all-aluminum fuselages and wings is protected from direct strikes and will experience only transients that are induced by magnetic fields and (to a lesser extent) structural IR voltage rises. The resistance of a conventional metal fuselage or wing is in the order of 3×10^{-6} ohm-cm so IR voltages along metal airframes are low. Most of this resistance is in the (usually) fastened joints. Exceptions to this might be circuits that are connected to externally mounted electrical devices. Induced voltages should be expected to be in the range of 50 - 600 volts and 4 - 60 amperes, or not exceed TCL Level 3 in Table 5 of [16.2], depending on location within the airframe and degree of additional shielding provided on the wires. Similarly, cable bundle currents will be in the range 20 A - 600 A or Level 3 in Table 6 of the above reference.

Some wire harnesses that run to outlying areas such as engines, flight control actuators and landing gear may experience transients up to and including Level 5 of both tables in [16.2]. The reasons or these higher ranges is because these harnesses often are routed across or through less well shielded parts of an airframe, such as along an aft

spar, an engine/pylon interface, or deployed landing gear that is open to the outside. Landing gear harnesses may share lightning zone 3 currents and experience 10's of kiloamperes of cable bundle current.

Designers should beware of guidance in some references [16.1, 16.3] that suggest that systems performing less critical functions (i.e., lightning criticality levels B, C) need not be required to tolerate transient levels as high as those performing more critical level A functions. Assignment of test levels based upon criticality makes no technical sense. Wiring susceptibility is determined by location within an airframe, not by criticality. Equally, the widespread integration of aircraft systems leaves all systems exposed to the same or similar transient levels and allows for propagation of damaging transients among systems performing all criticality of functions.

16.3.2 CFC Airframes

CFC structural materials have volume resistivities ranging around 6 x 10^{-3} ohm-cm in the plane of the laminates which is where the lightning current will predominantly flow. This is also the general direction of the interconnecting wiring, so the IxR voltages appear in wiring that runs along the airframe, in the common mode with respect to the local airframe. Since the CFC material is much more resistive than is aluminum, the IxR voltages are high. Magnetically induced transient voltages and currents are similar to those in an aluminum airframe of similar size and configuration.

The result of all this is that the ranges of induced voltages and currents in CFC airframes is typically between Levels 2 and 5 in Tables 5 and 6 of [16.4]. Cable bundle currents can often exceed Level 5 if installed in more exposed locations. This can increase the amounts and weights of shields required to control transients to levels (i.e., Levels 2, 3) that can be tolerated by off-the-shelf equipment.

Here the designer must consider the needs of protecting the CFC airframe against physical damage from lightning strikes (Chapter 6) which can be accomplished by adding a layer of expanded copper foil, the heaviest option, or by protecting the airframe with interwoven wire fabric (IWWF) – the lightest option.

The amount of reduction of the airframe IxR voltage is much greater with the expanded copper foil than airframe resistance is much greater with the expanded copper foil than with the IWWF. The tradeoff is between metalizing large surfaces of CFC skin or providing heavier shielding on individual cables. Designers sometimes incorporated a compromise in the form of various arrangements of copper (usually) conductors installed throughout a CFC airframe, together with IWWF on the exterior surfaces. This has had the benefit of providing a ground return for electric power distribution, and some degree of lightning IxR voltage reduction, thus reducing the weight of shields needed for individual wire harnesses. These copper conductors have been given various names. One such arrangement has been called a ground return network (GRN). The idea is illustrated in Fig. 16.1.

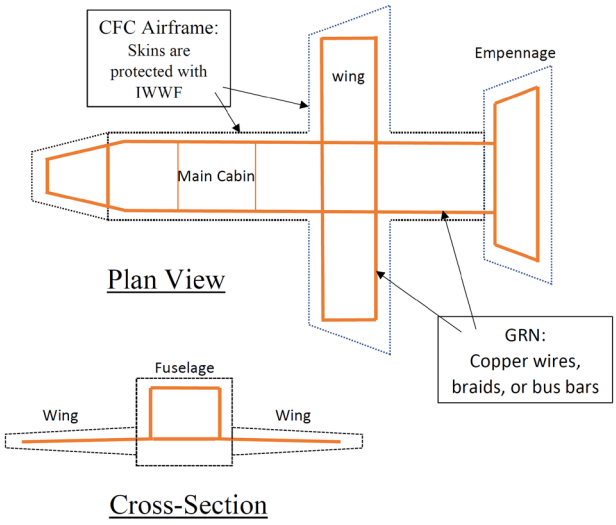

Fig. 16.1 Conductor network within a CFC airframe

The purpose of the conductor network of Fig. 16.1 is to provide an equipment ground and electric power return network. The concept for use of the GRN is illustrated in Fig. 16.2.

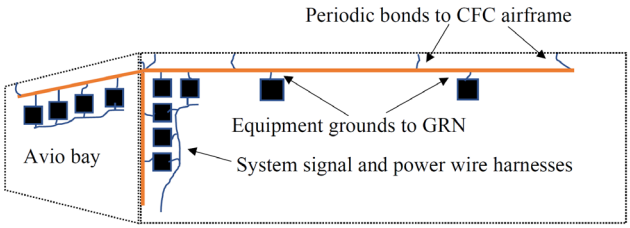

Examples of equipment ground to GRN
and
Connections of GRN to CFC airframe

Fig. 16.2 Concept for utilization of a GRN

The individual items of equipment are to be grounded to the GRN as shown in Fig. 16.2. The impedance of the GRN at the power and signal frequencies of most aircraft systems is sufficiently low as to enable the systems to have a common ground.

Other aspects of the GRN

Other aspects of the GRN and its installation in a CFC airframe are as follows:

1. **The cross-sectional area of the GRN conductors** must be able to conduct portions of the lightning current. This is the *redistributed current* that is discussed in Chapter 11. Typically, the rise times are in the 10s of microseconds and the decay times are in the 100s of microseconds – significantly longer than the waveform of the lightning stroke current Component A. The amplitudes of GRN conductor currents should be expected in the range between 10 kA and 100 kA. The lower amplitudes should be found in large transport airplanes. Higher amplitudes are found in GRNs within small aircraft fabricated of CFC. Any conductors considered for GRN should be tested at anticipated current waveforms and amplitudes. Specific details can be computed by commonly available programs such as EMA3D [16.5] COMSOL [16.6] and, and even circuit analysis programs like SPICE [16.7]. American Wire Gauge (AWG) sizes from AWG#6 (15 mm^2) to AWG#2 (35 mm^2) should be adequate to conduct redistributed stroke currents if made of copper. Other requirements like flexing, accessibility, and mechanical strength may necessitate larger cross-sections. Since lightning stroke currents are transients, the inductances of GRN conductors are as important as DC resistances. Flat conductors offer lower inductances than do round wires.

2. **Bonding of the GRN to the CFC airframe** should be provided periodically to equalize the potential between the adjacent CFC and the GRN. If this is not done, high transient voltages will develop between the airframe and the GRN which will be hazardous. A guideline would be to bond the GRN conductors to the CFC airframe a minimum of every 3 m.

3. **If the airframe includes metal and CFC** a GRN is not usually needed in the metal (i.e., aluminum) sections but the GRN in the CFC structures needs to be connected to the metal structures.

4. **Utilization of other hardware** in the airplane for part of the GRN is possible and to be encouraged. For example, metal instrument panels, floor Isoboards, quadrant assemblies, seat tracks, and engine mounts if electrically connected together can comprise part of a GRN. This approach has been especially useful in small airplanes, where weight budgets and space are at a premium.

5. **Insulating the GRN** from some other system components such as hydraulic tubes, wire harnesses, cabin entertainment systems, and personnel accommodations should be provided where needed. Engineering analysis needs to be applied to determine which systems should be bonded to the GRN, and which others need not be.

6. **Isolating the GRN from the airframe** has been considered but this should not be attempted, for the following reasons:

   - Isolation is not necessary. Doing so would introduce many problems, a few anticipated, and many unforeseen.

   - Sharing of current paths, both system and lightning, is always best. This minimizes high transient voltages and currents throughout the airplane.

   - Isolating features would be a design challenge and be difficult to monitor and maintain.

16.4 Location of Electronic Equipment

Because of other constraints, the designer may not have much choice in the matter, but it is often possible to make improvements in the protection against lightning induced effects by locating electronic equipment in regions where the electromagnetic fields produced by lightning current are lowest and by avoiding the placement of equipment in the region where the electromagnetic fields are highest. For example, since the most important type of coupling from the external electromagnetic environment to the inside of a metal aircraft is through apertures (Chapter 12), it follows that wiring (especially) and equipment should be located as far from major apertures as possible. Equipment installed within aircraft constructed of CFC is also exposed to significant transients driven by structural IxR voltages.

Wiring locations are of most importance (see §16.5) since the major source of lightning-induced transients is via the interconnecting wiring. Equipment is usually provided with metal enclosures that protect electronic circuit elements within. Equipment with displays may be susceptible to electromagnetic fields coming through nearby windows. Most of these displays have been subjected to EMI and high intensity radiated fields (HIRF) field tests but these fields are usually much higher in frequency and lower in intensity than those presented by lightning strikes. Other equipment that might be vulnerable to lightning fields would be that within nonconductive enclosures.

Vulnerable equipment should be located as far away from windows, access doors, or panels as practicable since these often are a major source of electromagnetic field leakage. In practice this may be more easily said than done, because the purpose of these doors and panels is to provide ready access to electronic equipment. These issues are always more acute for small general aviation and business class aircraft than for large transport aircraft, where there is usually, overall, more surrounding structure, and greater distances available between equipment racks and access panels. Of course, field intensities at apertures on large airplanes are lower than those on smaller airplanes simply because fuselage diameters and other major dimensions are smaller. This topic is discussed in Chapter 10.

An overall goal should be to locate electronic equipment toward the center of the aircraft structure, rather than at its extremities since the electromagnetic fields tend to cancel toward the center of any structure. Interconnecting wiring should also be further away from the sources of internal electromagnetic fields. Doing this may not always be practical.

Shielded compartments can be provided for vulnerable equipment. Some airframe manufacturers have begun to enclose groups of avionics within well-shielded aluminum enclosures that are installed within less well shielded airframes. The equipment within these enclosures is installed in the conventional manner, with minimum attention given to special protection measures within. Shields of cable bundles can be grounded to the equipment enclosures, and circuits among equipment inside can be left unshielded.

The shielded enclosure is treated as a single item of equipment and wiring between itself and other avionic equipment is protected from lightning electromagnetic field effects. This approach minimizes the need to apply special protection features to off-the-shelf equipment that can be located within a protection enclosure. Care needs to be taken to protect the wire harnesses that connect to this enclosure.

Shelves and ground planes

One important factor that is usually under the designers control is the type of shelf upon which electronic equipment is mounted. This is of particular importance in airframes made from large amounts of composite material. These shelves are intended to provide ground planes or reference surfaces for electronic equipment, and thus it is essential that they be electrically conductive and be well bonded to the aircraft structure. They should either be made of metal or, if made from composite materials, they should be covered with expanded copper foil or some other metal surface that has a low resistance and is well bonded to the aircraft structure. These conductive shelves can become a part of a GRN.

16.5 Location of Wiring

Designers have somewhat more control over the routing of wiring used to interconnect equipment than over the location of the equipment itself. Wiring should be located away from apertures and away from regions where the radius of curvature of structural members or the outer skin is smallest. Moreover, wiring should be located as close to a ground plane or structural member as possible, to minimize the amount of magnetic flux that may penetrate the loops between the wire harnesses and the nearest airframe references, like floor panels, bulkheads, and exterior surface skins. If a structural reinforcing member, such as an integral stiffener, longeron, or fuselage frame, is shaped or can be shaped to provide a trough into which the wiring may be placed, the member will provide more inherent shielding than if the wiring must be placed on the edge of the member. The suspension of wiring from fuselage frames is a common practice and has the disadvantage that the wiring must be spaced from the fuselage skin by a wide margin as it ‘bridges’ the distances between frames. Some examples of the best locations for bundles of wiring with respect to some typical structural members are shown in Fig. 16.3. In each case, the structural member is assumed to be carrying lightning current along its axis.

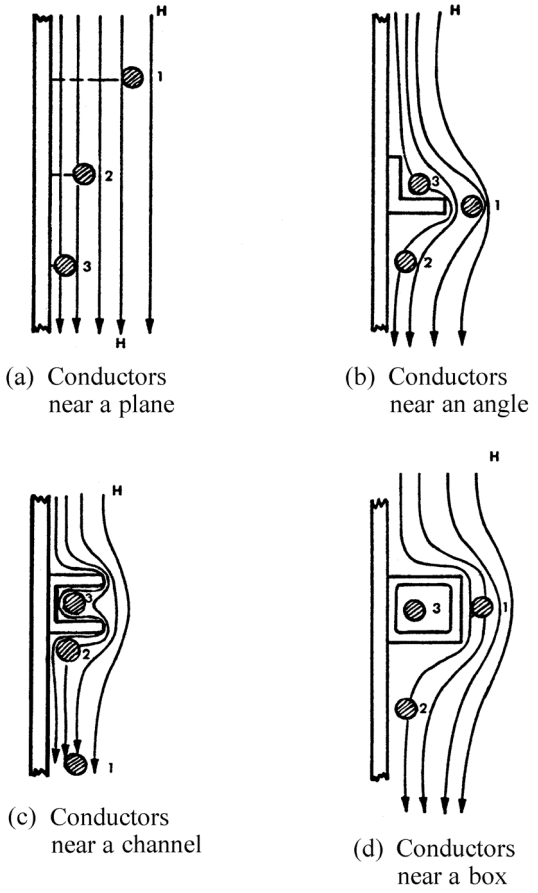

Fig. 16.3 Magnetic flux linkages vs conductor position.
In each case pictured:
Conductor 1 - highest number of flux linkages: worst.
Conductor 2 - intermediate number of linkages: better.
Conductor 3 - lowest number of linkages: best

Some basic principles to follow regarding the location or wiring are:

1. The closer a wire harness is placed to a metal ground plane; the less flux can pass between that wire harness and the ground plane and the lower the common-mode voltage induced. (The current driven by such voltage may be somewhat higher but not by as much as the voltage is reduced, since the current is limited by the inductance which is a function of the natural logarithm of the loop area (Eq. 9.38)).

2. Magnetic fields are concentrated around protruding structural members and diverge in inside corners. Hence, wires located on the projected surfaces of protruding members intercept more magnetic flux than wires placed within corners, where the field intensity is weaker.

3. Magnetic fields are weaker on the interior of a 3-sided channel than on the edges of such a member.

4. Magnetic fields are lowest inside a closed member.

The above points are illustrated in Fig. 16.3.

Stiffeners, Frames and Channels

Along the interior of a structure, a wire harness clamped to frames or stiffeners, as at position 1 in Fig. 16.4(a), is effectively separated from the metal skin by the height of the stiffeners. A conductor along the outside edge of the 3-sided channel, as shown by conductor 2 in Fig. 16.4(a), may or may not be better placed than conductor 1.

The effectiveness of such a configuration depends on how closely the conductor is attached to the side of the 3-sided channel. Conductor 3, placed along the lower corner of the 3-sided channel, where the channel is attached to the stiffeners, would probably be in a lower field environment than either conductor 1 or conductor 2. Conductor 4, located on the interior of the channel, would be in the lowest field region and, hence, in the most effective position. Similar considerations apply to conductors located in structures like wings or stabilizers.

Fuel Tanks

Wire harnesses installed within fuel tanks as shown in Fig. 16.4(b), locations 2 through 4 enjoy the best possible protection from magnetically induced transients afforded anywhere in an aircraft due the absence of windows and other apertures. Location 5 is assumed to be in the fixed leading edge that is not part of the fuel tank). This is true for CFC tanks as well as aluminum tanks. This applies to wire harnesses that are insulated from electrical contact with the airframe, which should be the case for protection from ignition sources as described in Chapter 7. In an aluminum tank it matters little whether the wiring is in location 2, 3, or 4, although in theory location 4 would experience the lowest amount of magnetic flux from diffused lightning currents as explained in Chapter 11. Even with shielding, ATLs in shielded conductors in fuel tanks may be assigned TCL Level 1 or 2 and ETDL Level 2 or 3 as defined in [16.2]. This is usually the fuel tank wiring that interfaces with the fuel quantity system remote data concentrators. Shields on fuel tank wiring do not provide protection from magnetic fields since only one end of these shields can be grounded. The theory for this is described in Chapter 15.

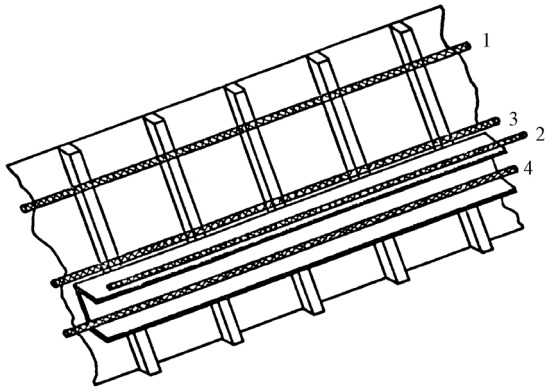

(a) A fuselage structure

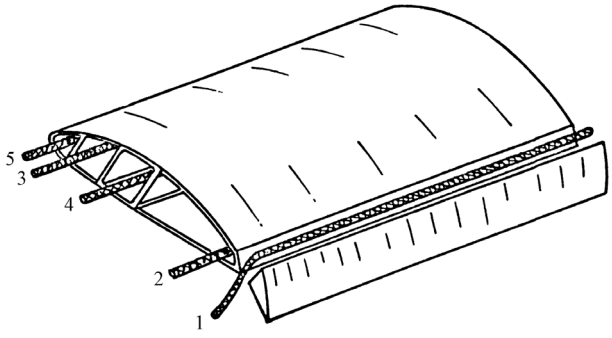

(b) A Wing structure

Fig. 16.4 Wire harness routing.

In each case pictured,
Harness 1 - highest number of flux linkages: worst.
Harness 4 - lowest number of linkages: best.

Leading and Trailing edges

A wire harness located along leading or trailing edge of the wing as represented by conductor 5 or conductor 1 in Fig. 16.4(b) would pick up much more flux than any conductor located inside the wing, probably by several orders of magnitude. Harness 5, located in the leading edge of the wing, would usually be in a well shielded region if the leading edge of the wing were metal, but it would be in a higher field region if the leading edge were made of CFC or (especially) a nonconductive enclosure.

Wire harnesses installed in location are exposed to much higher fields than any of the other harnesses due to its exposure to the external lightning environment. The control surfaces and flaps make only cursory contact with the fixed airframe and for no real enclosure to protect the wire harnesses and other systems that are commonly installed along the wing and empennage trailing edges. Lightning-induced currents of the same magnitude as measured in wiring harnesses will be also induced in hydraulic tubes and control surface cables. Even with shielding, ATLs in shielded conductors may have to be assigned TCL Level 3 and ETDL Level 4 as defined in [16.2].

Windshield frames and center posts

Windshield posts (Fig. 16.5) tend to concentrate lightning current flowing on the exterior surface of an aircraft, particularly if a flash is swept back, so that it attaches to the windshield post directly or to the eyebrow region above the windshield. Since the current is concentrated, the magnetic field intensity inside the crew compartment tends to be very high. This situation is aggravated by the fact that the windshields, unlike other regions where the field might have to diffuse through the metal surfaces, act as large apertures, allowing the internal magnetic flux to build to its peak very rapidly.

Instruments and wiring on control panels are thus in a region of inherently high magnetic field strength. To make matters worse, wiring that runs from overhead control panels (Fig. 16.5, position A) to other instruments (Fig. 16.5, position B) is often routed along the windshield center post. Such wiring experiences the most concentrated magnetic fields likely to be found on an aircraft and, accordingly, it has some of the highest voltages induced in it during a lightning strike.

Wire harnesses installed in these locations nearly always must be shielded unless covered cable trays or raceways are provided for protection of this wiring. Even with shielding, ATLs in shielded conductors may have to be assigned TCL Level 3 and ETDL Level 4 as defined in [16.2].

16.6 Basic Wiring and Grounding Practices

Wiring and grounding practices should be chosen with forethought, properly illustrated, and implemented, and should not be left to develop by chance. The design office should make sure that everyone knows what the design practices are, and all designs should be checked to ensure that they follow practices that are conducive to lightning protection.

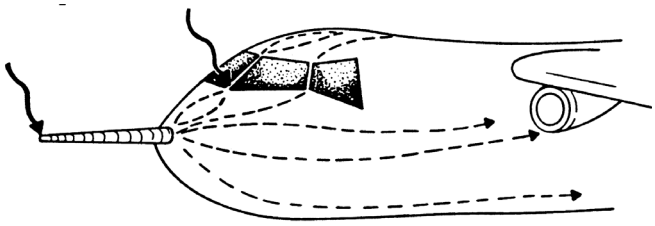

(a) External current flow

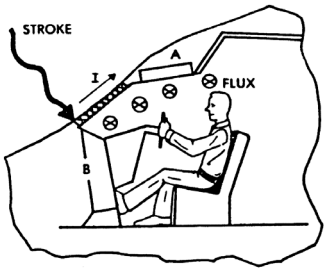

(b) Internal magnetic fields

Fig. 16.5 Current flow along windshield posts.

Proper grounding of equipment is a necessary part of controlling induced effects, but there are many factors to be considered. There is no single point on an aircraft that can be called 'ground' and compatibility problems are not resolved just by making a wire connection to an 'equipotential ground plane'. The closest approximation to an equipotential surface is found on the inner surface of a shielding enclosure or the inner surface of a properly terminated wire shield, places where the density of lightning induced currents is low.

Some basic considerations regarding grounding practices are as follows:

Aircraft structure as return path

Lightning current flowing through the structure of an aircraft produces structural voltage rises that can couple to internal circuits through 'ground' connections. Historically, experience has shown that the structure of metal aircraft can be used successfully as a return circuit for power distribution, but aircraft structure should never be used as a return path for signal or control circuits, since lightning-induced voltages in loops between wiring and the airframe would appear in these circuits and be added to the signal voltages in the system. Aircraft having large amounts of composite material in their structure should use separate, dedicated return wires for both signal *and* power circuits. This is one of the purposes of a GRN.

Single point grounding

Single point grounding, employing dedicated signal return conductors (as in twisted-pair circuits shown in Fig. 16.6) prevents the loop voltages described above from appearing in the system. This design approach is especially useful and practical for systems (or subsystems) comprised of one item of active electronics that drives or interfaces with other items, such as sensors or actuators (called 'remote equipment' in this discussion) whose functions do not require connections to local grounds. Electronic flight and engine controls are good examples of systems that lend themselves to this design approach. Care must be given to assuring that the insulation between remote end circuit elements and local case grounds is sufficient to withstand the ETDL assigned to these circuits. All of the induced voltage in the loop appears at the remote end.

Care also needs to be given to the use, if necessary, of EMI filters at remote equipment, since the dielectric strength of typical filter capacitors is often low (in the range of 50 - 100 volts). Since most of the common-mode voltages developed by EMI or lightning sources appear harmlessly across remote element insulation, and not at the active electronics, EMI filters may not, in fact, be needed at the remote equipment. The exception is when the remote equipment includes some generator of EMI voltages, such as a DC motor, or relay. In these situations, transient protection devices are sometimes placed across the EMI source to control inductive voltages produced by relay coil switching. Care should be taken to ensure that these protectors are installed across the coil, and not between coil terminals and case grounds.

The single point signal ground approach is most easily implemented for circuits associated with simple electromechanical devices, such as motors, servos, position sensors, rate gyros, solenoids, potentiometers, lights, and switches. These devices can usually withstand up to a few thousand volts between their internal circuits and their cases.

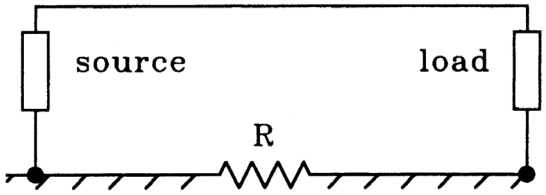

(a) Coupling of structural *IR* voltage.

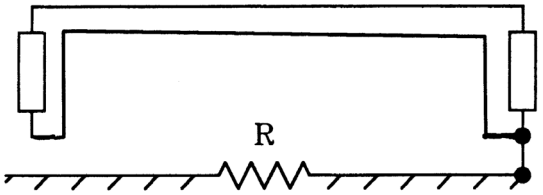

(b) Elimination of structural *IR* voltage.

Fig. 16.6 Grounding of electric circuits

Problems with single-point grounding

While the single point ground concept avoids coupling of structural voltage rises and magnetically induced voltages that are directly related to the lightning environment Components A and H, it does not entirely eliminate lightning-related interference, particularly interference with low-level electronic circuits. Specifically:

1. Single point grounding does not eliminate the traveling waves initiated by lightning-induced transients in long circuits. These transients are reflected back and forth, along the lengths of circuits, and are represented by transient Voltage Waveform 3 as defined in [16.2]. The voltage and current associated with these traveling wave transients are related by the characteristic impedance of the circuit, which is typically about 100 ohms. Thus, if a 600-volt traveling wave voltage is initiated, it is accompanied by a 6-ampere traveling wave current. This current may or may not be sufficient to damage the active electronics. An example of the traveling wave voltage and current in a long circuit is described in Chapter 14, Fig. 14.16. The ability of the active electronics to tolerate the waveform 3 traveling wave transients should be verified by equipment test.
2. It eliminates the low frequency component of voltage rises only by subjecting the remote equipment to a common mode voltage. The common mode voltages may be excessive for some electronic equipment, such as temperature probes, that typically have limited dielectric strength.

Multiple point grounding

Shielding against electromagnetic effects usually requires that equipment cases be grounded to the airframe, since the equipment must be physically mounted to the airframe. When shields are employed for protecting interconnecting circuits, the shields must be grounded ('terminated') to the equipment at each end of the shield if they are to be effective (as described in Chapter 15). This requires that the equipment and shields be grounded at multiple points. When it is necessary for circuits within equipment to be grounded locally (as illustrated in Fig. 16.7) each equipment case usually becomes the single point reference for all internal circuitry that must be grounded, and this is usually necessary for equipment that requires aircraft power.

Opinions vary regarding how best to make these ground connections but, from an EMI and lightning protection standpoint, the best approach is to make the ground connections to local reference planes (or circuit board ground tapes). Each reference plane is then terminated to the chassis and the chassis is grounded to the nearest airframe ground point, ideally through the equipment mounts.

Separate Grounds

There has been a perception that it is best to establish purposeful grounds that are dedicated to specific parts of an equipment or system. For example, "radio frequency (RF) Ground". "Digital Ground" "Signal Ground" "Power Ground" etc. and to isolate these grounds one from another. Aside from greatly complicating the overall design task, logical reasons for these separate grounds are rarely given.

The best practice is to combine all grounds into one, low inductance ground connection to the equipment chassis (enclosure) and from chassis to structure ground or a GRN.

A similar concept has been to isolate the "electronics" ground from the chassis ground, on the basis that the electronics ground is somehow 'cleaner' than the chassis ground would be. This concept is illustrated in Fig. 16.7(b). The problem is that there can be large voltage differences between these grounds, due to the remote

connection of the electronics ground ("E-ground") to a point far from the equipment. The situation is shown in Fig. 16.7(b).

Some designers prefer to carry circuit grounds through connector pins to airframe ground points outside the equipment, presumably on the premise that such grounds are (somehow) 'cleaner' than grounds within equipment cases. This practice requires longer ground leads, which, when exposed to lightning and EMI fields, couple induced voltages into the electronic equipment. The best practice is to make all grounds together, at each item of equipment, as shown in Fig. 16.7(a). This should be the case for all grounds, no matter what the purpose.

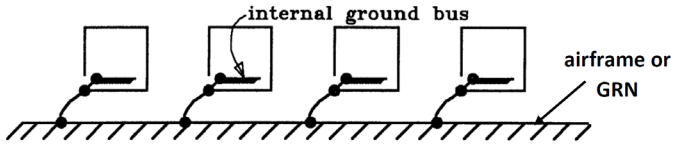

(a) Good

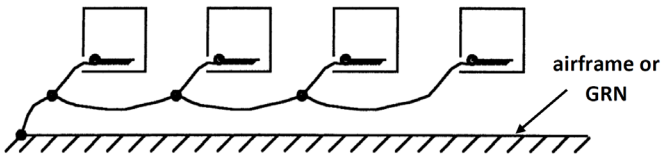

(b) Bad

Fig. 16.7 Multiple and single point grounding.

16.6.1 Shielding of Interconnecting Wiring

In order to make an electronic system immune to the effects of lightning, it is almost always necessary to make judicious use of shielding on interconnecting wiring and to provide proper grounding for these shields. Factors governing the performance of cable shields were discussed in detail in Chapter 15 but will be reviewed here. Fig. 16.8 shows some of the basic considerations.

Unshielded conductors

If an unshielded conductor, like that shown in Fig. 16.8(a), were subjected to structural IR and magnetic-field-induced voltages between itself and adjacent structure, most of these induced voltages would appear across high impedance terminations at the ends of the conductor.

Types of shield

Of the different types of shields, shown in Fig. 16.8(c), the solid shield inherently provides better shielding than the braided shield, and the tape-wound shield can be far inferior to a braided shield in performance. In severe environments, braided shields consisting of two overlapping courses of braid may give shielding performance approaching that of a solid-walled shield.

Conduits

Conduits (Fig. 16.8(d)) should not be relied upon for protection against induced effects since they may or may not provide electromagnetic shielding.

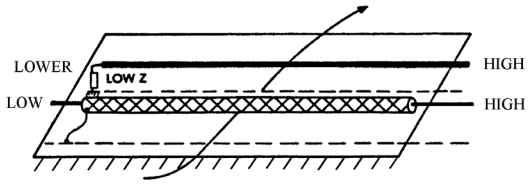

(a) Unshielded vs. shielded

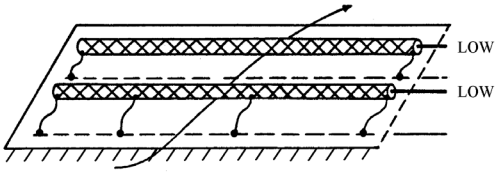

(b) Multiple-grounded

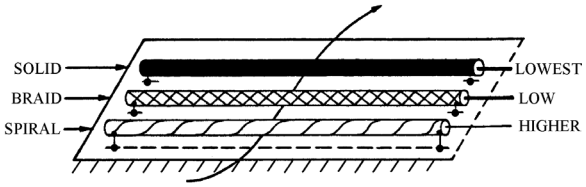

(c) Solid vs. braided vs. spiral wrapped

(d) Conduits

Fig. 16.8 Multiple point grounding.

Conduits in aircraft tend to be used more for mechanical protection than for electrical protection of conductors. Only if the conduit is electrically connected to the aircraft structure at regular spatial intervals, and especially at its ends, will it be able to carry current and thus provide shielding for the conductors within. Clearly, nonmetallic conduits do not provide electromagnetic shielding.

16.6.2 Grounding of Shields

Shield grounded at one end

As discussed in Chapter 15, the presence of a shield grounded at only one end does not significantly affect the voltage induced by changing magnetic fields, although it may protect against changing *electric* fields. While such a shield may keep the voltage at the grounded end low, common mode voltages at the ungrounded end can, nevertheless, be high.

Fuel quantity indicating systems (FQIS) are perhaps the last type of system that still needs to have its shields ungrounded at one end. The individual, ungrounded shields (usually of twisted shielded pairs or triplets) of the FQIS system can be enclosed in overall shields (OASs) that are grounded at both ends to provide shielding for the FQIS outside the fuel tanks. Within the fuel tanks, it is permissible to have unshielded circuits, since the tanks themselves are usually very good, shielded enclosures. In fact, it is not desirable to have shields grounded within fuel tanks, since this invites lightning currents to flow in shields within the tanks with the attendant risk of arcing at shield ground connections inside the tanks.

Shield grounded at both ends

If a shield is intended to protect against magnetic fields, it must be grounded at both ends, as shown in Fig. 16.8(b), in order that it may carry a circulating current. It is the circulating current that cancels the magnetic fields that would otherwise induce common mode voltages on the wires inside the shield.

Multiple ground points

It is usually advisable to ground long shields at multiple points. When a shield is grounded at multiple points, circulating currents tend to flow along only a portion of the shield, whereas, if the shield is grounded only at the ends, current is forced to flow the entire length of the shield. The locations of shield ground terminations should be chosen so that they divide the shield currents induced in regions of high-level magnetic field and structural IxR coupling from those induced in regions of lower-level coupling. This confines the high amplitude shield currents to the higher-threat regions, so that the contribution of that current to the total induced voltage on the shielded wiring is minimized. This approach is especially recommended for electronic engine control systems, where the highest lightning induced voltages usually occur close to the engines; either on the engines themselves or in the pylons between the engines and the wing. The circuit segments between wing/pylon disconnects and wing/fuselage disconnects usually experience lower induced voltages and lower resultant shield currents. Thus, the engine control-system circuit shields should, ideally, be grounded to the airframe at the locations described in Table 16.1

Theoretically, there is some virtue in varying the spacing between multiple ground points on a cable shield since uniform spacing could reinforce a particular resonant frequency in the cable. This frequency might become excited, leading to troublesome standing wave interference, if the shield were illuminated by a sustained frequency interference source (such as an onboard EMI source or an external source of HIRF).

Multiple point grounding of shields is sometimes objected to on the basis that it creates ‘ground loops’ that allow EMI current to flow in the shields, producing small EMI voltages in the shielded conductors. This was a serious problem for analogue circuits operating at very low signal voltages, but it is usually not a problem for digital circuits that have higher noise thresholds and are, thus, inherently immune to low-level interference voltages.

Table 16.1: Appropriate Places to Ground System Shields to the Airframe

System Circuit Segment	Locations for Shield Grounds to the Airframe	Comments
Between engine equipment and engine-mounted electronic control units (ECUs)	At engine-mounted equipment and at the engine ECUs	This is the highest magnetic field region.
Between the engine-mounted ECUs and the engine/pylon disconnects	At the engine ECUs and at the engine side of the pylon disconnects.	This is usually also a high field region.
Between the wing disconnects and the fuselage pressure hull disconnects (if present)	At the pylon/wing disconnect and at the fuselage disconnects, or at whatever fuselage structure the circuit shield interfaces with.	This is not as high a field region as the engine and engine/pylon region, or the pylon/wing region.
Inside the fuselage pressure hull	Requirements for shielding of circuits within the fuselage may allow some circuits to be unshielded if system-to-system effects can be controlled.	Shielded requirements inside an all-metal fuselage usually depend more on intra-system EMI requirements than upon lightning protection requirements.

Potential conflicts

As noted before, the necessity that a shield intended for protection against lightning effects be grounded at both ends raises a perennial controversy about grounding shields at one-end vs. grounding them at both ends. For many reasons, usually legitimate ones, low signal amplitude circuits are shielded against low frequency interference that originates on the aircraft, such as that produced by 115 Vac 400 Hz electric power distribution circuits and other onboard interference sources. Usually, the shields intended for this low frequency interference protection are grounded at only one end.

A fundamental concept often overlooked is that the physical length of such shields must be short compared to the wavelength of the interfering signals. Lightning interference, however, is broad-band, and includes significant amounts of energy at quite high frequencies, frequencies higher than those the typical low frequency shields are intended to handle.

Resolution of conflict

The conflict between the practices best for shielding against high frequency, lightning-produced interference and those best for shielding against every day, low frequency interference is sometimes too great for both sets of requirements to be satisfied by one shield system.

Usually, both sets of requirements can be met only by having two shield systems; one to protect against low frequency interference, and a second to protect against lightning-induced interference. The lightning shield can usually consist of an overall braided shield that encloses a group of conductors. This OAS is grounded to the aircraft structure at least at the ends. Alternately, the lightning shield can be a shielded enclosure, a conduit, or a cable tray (as described earlier in this chapter and in Chapter 15). Circuits routed within this OAS may be provided with additional, inner shielding as needed.

In a coordinated shielding system design effort, the designers of individual circuits should have the option of grounding these inner shields as their own requirements dictate, but they should not have the authority to dictate the treatment of the OAS. An OAS is illustrated in Fig. 16.9. This illustrates a double-shielded cable because the outer shield is insulated from the inner shield. The difference between the double shield and an overbraid shield is explained in Chapter 15.

16.6.3 Ground Connections for Shields

The way an OAS is grounded can have a great impact on its effectiveness against lightning-induced transients. Figs. 16.10(a) through 16.10(e) show several grounding methods for shields enclosing groups of conductors that are routed into an equipment case.

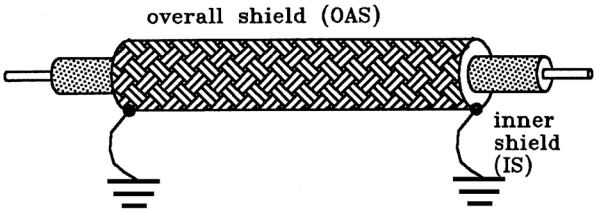

Fig. 16.9 OAS on double-shielded cable.

360-degree grounding

For best performance, the OAS should be terminated (i.e., 'grounded') on the back shell of a connector specifically designed for such termination. The overbraid shield, if there is one, should make a 360-degree circumferential connection to the back shell of the connector, and the connector shell itself should be designed to have low DC resistance to its mating panel connector.

Sometimes, such low resistance mating requires the use of grounding fingers or other provisions to establish good electrical bonding within the connector shell. Connectors that lack grounding fingers sometimes have high resistances between their mating shells, since the shells frequently have a nonconductive, anti-corrosion coating. The shell of the panel connector should also provide a 360-degree peripheral connection to the metal equipment case. This often means that paint or other coatings on the equipment case must be removed to expose bare metal.

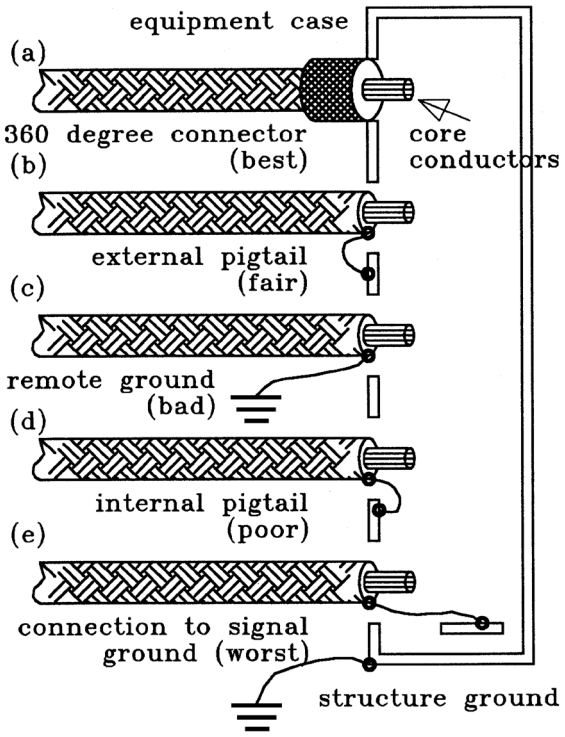

Fig. 16.10 Types of grounding for shields.

Sometimes, by paying careful attention to the maintenance of adequate connectors, one can eliminate all aspects of field effects.

Pigtail grounding

If a connector that can be bonded to a shield through a '360 degree' connection is unavailable, an external pigtail is often used for grounding the OAS, as shown in Fig. 16.10(b). Such pigtails are inferior to a 360-degree connector, because shield currents become concentrated as they flow through the pigtail. This concentrated current magnetically couples to the shielded conductors much more readily than the distributed current on a properly designed connector back shell. If such a pigtail is used, it should be kept as short as possible and should terminate on the connector, not be carried to the interior of the equipment through a connector pin, or to the connector back shell through a pigtail longer than 50 mm (2 in). A pigtail of only a few inches' length can introduce more voltage to the shielded conductors than a section of the shield measuring several feet.

Grounding to a remote point

Cable shields should be grounded to the equipment case (chassis) upon which the connector is mounted, not to a remote 'low noise' ground point, as shown in Fig. 16.10(c). There is no such thing.

Grounding to an inside surface

It is better to ground a shield to the exterior of an equipment case with an external pigtail than to the inside surface of the case as in Fig. 16.10(d) through an internal pigtail or through a set of contacts in the connector. One reason for this is that an internally grounded pigtail inherently has a longer electrical length than an external one. In addition, an internal pigtail brings currents and associated magnetic fields directly to the inside of the equipment case. Such grounding of an OAS should be avoided wherever possible, particularly when the OAS runs through a region where it will intercept a significant amount of energy from the external electromagnetic field.

Grounding to a single bus

In no case should an OAS (or any shield) be connected to a signal ground bus as shown in Fig. 16.10(e).

Daisy chain grounding

Daisy chain grounding of cable shields (illustrated in Fig. 16.11) should never be used. It constrains current intercepted by all the shields to flow through a common path, allowing shield currents to produce inductive voltages that appear at all items of equipment. Such a configuration has the greatest potential to defeat the purpose of the shields.

16.7 Transients and Standards

Section 5.7 discusses pass/fail criteria in terms of TCLs and ETDLs while [16.2] suggests possible levels. The following material discusses the TCL/ETDL concepts in more detail.

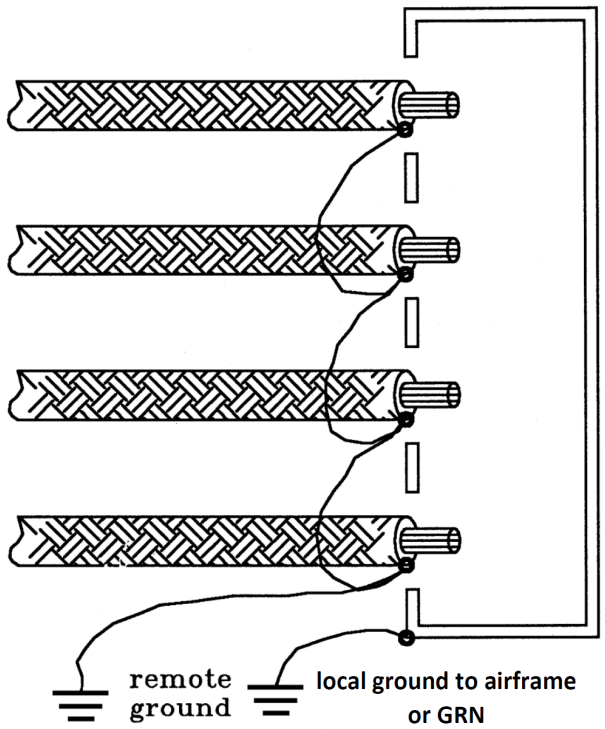

Fig. 16.11 Daisy chain grounding.

Alternatives regarding protection against transients

Three possible approaches to dealing with lightning induced transients are:

1. Designers of aircraft equipment might be responsible for providing equipment that will withstand standardized voltage and current levels, and the airframe designer would have to design to control the transients to levels that are lower (by a standard margin) than the equipment tolerance levels. **i.e., equipment dominates.**

2. Designers of aircraft interconnecting wiring might be responsible for designing to control the transients to a set of standard levels, and equipment manufacturers would have to design to tolerate those levels, plus a standard margin. **i.e., airframe dominates.**

3. Design efforts should be coordinated so that equipment designers verify that their equipment can withstand transients of one level and designers of wiring systems would verify that the transients would not exceed another, lower, level. This approach is called **transient coordination**.

16.7.1 Evolution of Transient Standards for Aircraft

ETDL standards now in common use for commercial aircraft protection design and certification have evolved from several sources; aircraft, military and industrial.

Basic insulation levels (BILs)

The TCL philosophy was originally inspired by the basic insulation level (BIL) or transient coordination philosophy used in the electric power field for many years [16.8]. It developed in recognition that power equipment, such as transformers, would always be subjected to surges produced by lightning and that the magnitude of the surges could be known only in statistical terms. Experience had shown, however, that these surges could destroy equipment and that equipment would have to be protected by surge arresters. It was also taken as axiomatic that the insulation built into equipment would have to be coordinated with the abilities of the protection devices (lightning arresters) used to protect equipment from damage due to lightning-induced transients. Also, it was taken as axiomatic that it would be preferable to coordinate the standard ratings for surge arresters with the limited number of standard ratings for power system operating voltages.

The transient coordination system that evolved [16.4] provided for a limited number of insulation levels, such as a 150 kV BIL level for power system equipment operating on a 23 kV system and 550 kV BIL for 115 kV equipment. Equipment designed to operate at 115 kV was provided with insulation sufficient to withstand a 550 kV lightning-induced transient impulse voltage. (This voltage would appear when an exposed power line was directly struck by lightning). The ability of the power system equipment to tolerate this voltage is verified by test on each major piece of equipment before it is shipped.

The BILs represented the levels to which the designer knew the equipment would be tested in the factory. This voltage was established by technical committees, acting on the basis of research studies that had included measurements of actual lightning-induced voltages on power transmission lines operating at various system operating voltages. All the designer needed was assurance that protective equipment was available and would be used to ensure that naturally occurring surges would be less than the assigned BIL by a suitable margin.

The essential elements of the BIL system thus consisted of:

1. Availability of equipment to control natural transients.

2. Standards covering equipment and practices for performing tests.

3. A limited number of standard voltage test levels.

4. Availability of equipment capable of withstanding those levels.

5. Standard tests, capable of being performed by equipment in many laboratories.

6. Agreement among users and builders of equipment to follow this system.

The BIL system has been in place for many years, is recognized world-wide and has resulted in electrical power equipment that is very seldom damaged by the effects of lightning.

American National Standards Institute (ANSI) Surge Withstand Capability (SWC) Test

Another specification that influenced development of the TCL philosophy was the ANSI Surge Withstand Capability (SWC) test [16.9 - 16.10]. This test was intended to simulate the transients that occurred in high voltage electrical substations when circuit breakers and disconnect switches were operated. Tests had shown that equipment in such substations might be exposed to oscillatory transient voltages of several kV in magnitude. To some extent, this specification was applied to equipment of types other than those for which it was originally intended, largely because it was already in existence and was recognized by standardizing agencies.

The SWC test standard called for open circuit voltages of between 2.5 and 3 kV, with the oscillatory frequency between 1.0 and 1.5 MHz. Decrement was specified by requiring that the envelope decay to 50% in no less than 6 μs, although this implies a lower-loss test circuit than is likely in practice. The voltage range specified was reasonable for apparatus in high voltage substations but might be high for electronic equipment located in shielded locations.

The standard recognized the importance of defining short circuit current as well as open circuit voltage. (Open circuit voltage refers to the voltage available at the open terminals of the test transient generator (TG) when not connected to the load impedance of an item of equipment being tested. Short circuit current refers to the current available when the test generator terminals are short circuited.) This test standard was based on the idea that the test generator would have a source impedance of 150 Ω. The SWC standard also provided construction details for a surge generator to produce the specified open circuit voltage and short circuit current waveforms and amplitudes, although the waveform itself does not imply any generator test circuit.

Transients in residential wiring

Martzloff and Howell [16.11] proposed a transient voltage test for residential equipment. Martzloff and Howell show a test circuit capable of injecting a typical lightning-induced transient onto 120 V ac lines where, since the output impedance of the circuit is basically 150 Ω resistive, the shape of the short circuit current would be about the same as that of the open circuit voltage. This waveform and this test circuit have been widely accepted in some fields. One example is in relation to ground fault interrupters [16.12].

Nuclear Electromagnetic Pulse (NEMP):

Test practices for simulation of nuclear electromagnetic pulse (NEMP) effects were being developed about the time the TCL philosophy was evolving. Particularly valuable was the practice of injecting transients into interconnecting wiring using transformer coupling. The waveforms in use were most commonly oscillatory, with frequencies of several MHz.

National Aeronautics and Space Administration (NASA) Space Shuttle

The present TCL/ETDL philosophy was first proposed in [16.13] and later presented in [16.14].

At one stage in the development of the Space Shuttle Lightning Criteria Document, there was an allowance made for two, essentially unipolar transient test waveforms. While those waveforms had some deficiencies, and have been largely superseded, some discussion of them will illustrate some of the problems inherent in transient test waveform specifications.

Waveforms for simulating aperture field effects

The first of these specifications dealt with a transient rising to crest in 2 μs and decaying to zero in 100 μs. The intent of this test waveform was to duplicate, in some manner, the effects produced by magnetic flux penetrating apertures.

The second specification was for a long-duration transient representing the effects produced by magnetic flux diffusing through the walls of cavities. Such flux has rise and decay times much longer than those of the lightning current. The specification called for a short circuit current of 5 amperes and an open circuit voltage of 50 volts, both taking 300 μs to reach crest and another 300 μs to decay to zero. The specification of equal times to crest and from crest back to zero is incompatible with the response of real physical elements. In practice, any waveform with a rise time of 300 μs would have a decay time longer than 600 μs.

One common deficiency of the above specification was that it did not clearly distinguish between transient voltages and transient currents and did not satisfactorily account for the effects of transient source impedance. Both the short circuit current and open circuit voltage had the same waveform. In practice the open circuit voltage would be of a duration shorter than that of the short circuit current, as discussed in Chapters 9 through 14.

Original TCL proposals

In the paper in which the concept of TCLs was first presented [16.15], Fisher and Martzloff proposed a test waveform that was primarily unipolar.

The open circuit voltage was characterized by a fast rise to crest and then a decay to zero in 5 μs, or greater. To allow for transformer coupling of the transient, an undershoot was allowed after the transient had decayed to zero. The only specification for this undershoot was that its amplitude be less than 50% of the waveform's peak amplitude.

The rationale behind this voltage waveform concept included the following aspects:

1. The test transient should be, in some measure, proportional to the derivative of the magnetic field produced by a lightning current.

2. The duration of the test transient should be long enough that failures of semiconductors would not be strongly affected by experimental variations in the waveform of the transient. (For test transients shorter than about a microsecond, the failure levels of semiconductors are strongly affected by waveform.

3. The duration of the transient should be roughly comparable to the (then existing) duration of clock cycles in digital equipment.

4. The transient should include a rapidly changing phase to excite inductively coupled circuit elements.

5. The transient should be one that could be produced by, and coupled to, the equipment being tested using relatively simple test apparatus.

Directly associated with the open circuit voltage transient, was a short circuit current transient. The short circuit current transient was defined as the current that would flow from a source whose internal impedance consisted of 50 Ω of resistance in parallel with 50 μH of inductance (Fig. 16.12(a)).

Taken together as a set, these test waveforms were thus more consistent than those relating to the Space Shuttle. Amplitudes were not specified for either the voltage or the current since the test levels would be part of TCL specification.

In answer to response from readers and users of the original Fisher and Martzloff paper [16.15] on the TCL philosophy, Crouch, Fisher, and Martzloff [16.16] proposed a test waveform somewhat different from the original one. The revised voltage waveform, shown in Fig. 16.12(b), emphasized the oscillatory nature of the waveform, rather than de-emphasizing it, as the original test waveform had. The front time was raised to 0.5 μs. The characteristics of the waveform after crest were defined in terms of its oscillatory frequency (100 kHz) and decrement (i.e., the ratio of successive half-cycles had to be greater than 0.6). The voltage waveform thus became nearly identical to that proposed by Martzloff and Howell.

These papers seem to have been the first to explicitly deal with the question of source impedance in transient specifications.

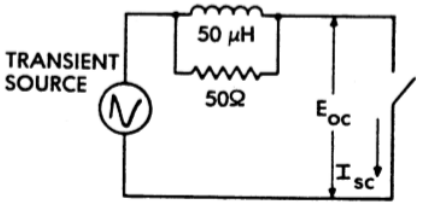

(a) Source impedance

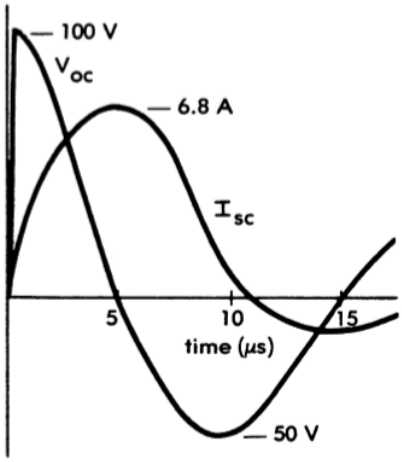

(b) Voltage and current

Fig. 16.12 Original TCL Proposals [16.15]

Transient Control Level (TCL) Philosophy

The TCL philosophy [16.17 - 16.18] follows the basic concepts of the BIL approach to transient coordination, in that it assigns transient specifications both to those who design electronic equipment ('black boxes') and to those who design wiring to interconnect those black boxes (rather than letting these responsibilities develop by chance).

The levels would be assigned by a transient coordinator (system integrator) and tests would be performed to verify that the goals had been met; tests on equipment to verify that it can withstand the assigned ETDL's transients and tests on the aircraft to verify that the specified TCLs in interconnecting wiring have not been exceeded. The TCL concept is illustrated in Fig. 16.13 and encompasses the following:

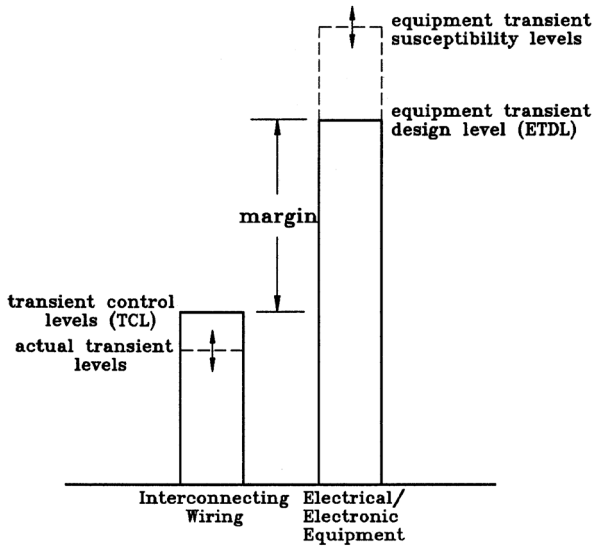

Fig. 16.13 The transient coordination philosophy.

Actual transient level (ATL)

The TCL philosophy involves ensuring that the ATL produced by lightning (or any other source of transient) is less than that associated with the TCL assigned to the interconnecting wiring (i.e., 'cable') designer. The cable designer's job is to analyze the electro-magnetic threat that lightning would present and to use whatever techniques of circuit routing or shielding are necessary to ensure that the actual transients produced by lightning do not exceed the values specified for that particular type of circuit. Some designers ignore the concept of the TCL and simply design to assure that the actual transients induced in the wiring (i.e., ATL) are less than the ETDL by the assigned margins. This approach is equally effective, though somewhat less formal.

Equipment transient design level (ETDL)

The ETDL level assigned to the avionics designer is higher than the TCL by a margin reflecting how important it is that lightning not interfere with the piece of equipment under design. A margin is necessary to account for uncertainties in determination and verification of the induced transient levels in the interconnecting wiring. Whereas there is always a possibility that any single lightning flash might produce an ATL higher than the assigned transient control level, this possibility is not the reason for the margin since the external lightning certification activities (for commercial aircraft at least) are based on the standardized lightning environment.

Thus prediction of ATLs induced by standard lighting environments, while an imperfect art, is nevertheless an important part of the protection design and certification process.

Vulnerability and susceptibility levels

The job of the avionics designer is to ensure that the damage tolerance level of the equipment being designed is higher than the assigned ETDL. The vulnerability level is that level of the transient which, if applied to the input or output circuit under question, would cause the equipment to be permanently damaged or experience functional upset. The tolerance level is defined as that level of transient that can be tolerated by the equipment without functional upset or component damage that would result in interference with or malfunction of the equipment.

Ways of setting ETDL's

There are several ways in which the levels might be set. In the first, the system integrator would set the desired transient level, then set the required margin, which, in turn, would set the TCL. Whatever the rationale by which the system integrator sets the transient design level, that level would become a part of the purchase specifications and would, presumably, not be subject to variation by the vendor of the avionics.

Alternatively, the avionics designer might determine the vulnerability and tolerance levels of his equipment through suitable testing. The tolerance level would then become the ETDL. After the system integrator had set the desired margin, the appropriate TCL for the cable designer would have been established. One approach to the setting of margins is described in [16.1].

Open circuit voltage and short circuit current

The amplitude assigned to the transient design level should probably be expressed in terms of the maximum acceptable voltage appropriate for a high impedance circuit (open circuit voltage) or the maximum acceptable current for a low impedance circuit (short circuit current).

Test levels

For the TCL philosophy to be of practical use, there should be a limited number of levels. An example of the set of levels due to stroke current Component A is presented in [16.18] and in Table 16.2. With each level, there is an associated open circuit voltage and short circuit current, related to one-another through an implied, transient source impedance (see Fig. 16.12).

Source impedance

If transient test generator source impedance is not included in transient specifications, there is a risk of confusion and wasted design and test effort. For example, a specification might require that a test voltage of 1 000 V be developed across a circuit protected by a spark gap with a 500-volt breakdown level. In order to meet such a requirement, designers would be forced to take extraordinary measures, such as adding impedance in series with the spark gap so that, by brute force and the application of an enormous amount of current, a specified voltage could be developed across the protected circuit. Such an effort would accomplish nothing and would reflect a basic misunderstanding of the motivation for using the spark gap in the first place. Similar confusion could occur if a specification required that a specified *current* be developed, regardless of impedance.

Transient test specifications for aircraft and electronic equipment usually avoid such problems by defining both open circuit voltage and short circuit current. The intent is that, if a circuit has a high impedance, it is appropriate to define the voltage that should be developed and if the circuit is low impedance, it is appropriate to define the maximum surge current.

Implementation of the TCL Philosophy

The TCL philosophy has become ingrained in the transient protection design and certification practices for aircraft avionics. Industry standards [16.3] include standards for TCL and ETDL testing.

Levels appropriate for aircraft

Some test levels that have been suggested for aircraft use are shown in Tables 16.2, 16.3 and 16.4, which are reproduced from [16.18]. Table 16.2 lists the transients that arise from the external lightning environment Component A and are applicable to individual circuit conductors (as TCLs) or to equipment connector pins (as ETDLs). Table 16.3 lists the transients to be applied to cable bundles due to Component A. Table 16.4 shows transients that are applicable to cable bundles due to Waveform H currents that comprise the Multiple Burst (MB) environment. Other details of the transient environment in use for aircraft avionics certification are contained in [16.3] and [16.18].

Waveforms

The waveforms of voltage and current actually coupled to the internal structure and wiring of an aircraft are complex and depend on both the coupling mechanism and the type of circuit. However, the TCL philosophy recognizes that these waveforms can be separated into several distinct categories, and that their amplitudes and impedance relationships depend on the coupling mechanism. The waveforms specified in international test standards [16.18] are shown in Fig. 16.14. All are induced by Current Component A.

Table 16.2 Individual conductor TCL, ETDL, or test levels due to *Current Component A.* [16.18]

Level	Waveform 3 V/I	Waveform 4 V/I	Waveform 5 V/I
1	100/4	50/10	50/50
2	250/4	125/25	125/125
3	600/24	300/60	300/300
4	1 500/60	750/150	750/750
5	3 200/128	1 600/320	1 600/1 600

Table 16.3 Cable bundle TCL, ETDL test levels due to *Current Component A*

Level	Waveform 1 V/I	Waveform 2 V/I	Waveform 3 V/I	Waveform 4 V/I	Waveform 5 V/I
1	50/100	50/100	100/20	50/100	50/150
2	125/500	125/250	250/50	125/250	125/400
3	300/600	300/600	600/120	300/600	300/1 000
4	750/1 500	750/1 500	1 500/300	750/1 500	750/2 000
5	1 600/3 200	1 600/3 200	3 200/640	1 600/3 200	1 600/5 000

Table 16.4 Cable bundle TCL, ETDL or MB test levels due to *Current Component H*

Level	Waveform 3_H V/I	Waveform 6_H V/I
1	60/1	100/5
2	150/2.5	250/12.5
3	360/6	600/30
4	900/15	1 500/75
5	1 920/32	3 200/160

Waveform 1 is a double exponential, unipolar current waveform, similar in shape to the defined lightning return stroke current Component A. This waveform represents that portion of the lightning current that would flow in internal conductors, such as cable shields and conduits. Within certain structures, this waveform slows down and acquires the appearance of current Waveform 5, described below.

Waveform 2 is a double exponential derivation voltage waveform and is the classic open circuit response to the magnetic field produced in and around an aircraft due to current Component A. This waveform is similar to the derivative of current Component A, and thus its time-to zero-crossing is equal to the time-to-peak of Component A. Waveform 2 predominates in unshielded circuits with high impedance loads, where magnetic field coupling is the major contributor.

Derivative voltage waveforms can also appear in some shielded circuits, but their times-to-zero-crossing are controlled by the times to peak of the shield currents inducing them, not by the external lightning current. The short circuit current related to this voltage waveform is similar to Waveform 1, or to the waveform of the related shield current.

Waveform 3 is a damped sinusoidal voltage waveform and is one of the responses to the lightning stroke currents, Components A and D. Also, it is the only response to the MB current, Component H. The predominant frequencies are often associated with the natural resonances of the aircraft, but may also be associated with resonances of aircraft apertures, aircraft wiring, shield terminations (pigtails), or circuit interfaces. The defined frequencies for this waveform lie in the range of 1 to 10 MHz. Short circuit currents are typically related to Waveform 3 by the surge impedance of the aircraft circuit in question.

Waveform 4 is a double-exponential, unipolar voltage waveform, and represents the potential differences that can appear between interconnected equipment ground references when lightning current flows through the intervening resistance of the airframe structure.

This waveform has the same shape as the lightning stroke current, Component A, and predominates in high resistance airframe structures where circuits use the airframe as return.

Waveform 4 is also typical of voltages that appear in shielded conductors because of current flowing through shield resistance. The short circuit current related to this voltage waveform is Waveform 1. However, as the line-to-ground impedances of wiring and its loads approach short circuit conditions, wiring inductance and diffusion and redistribution currents tend to produce the longer duration current Waveform 5.

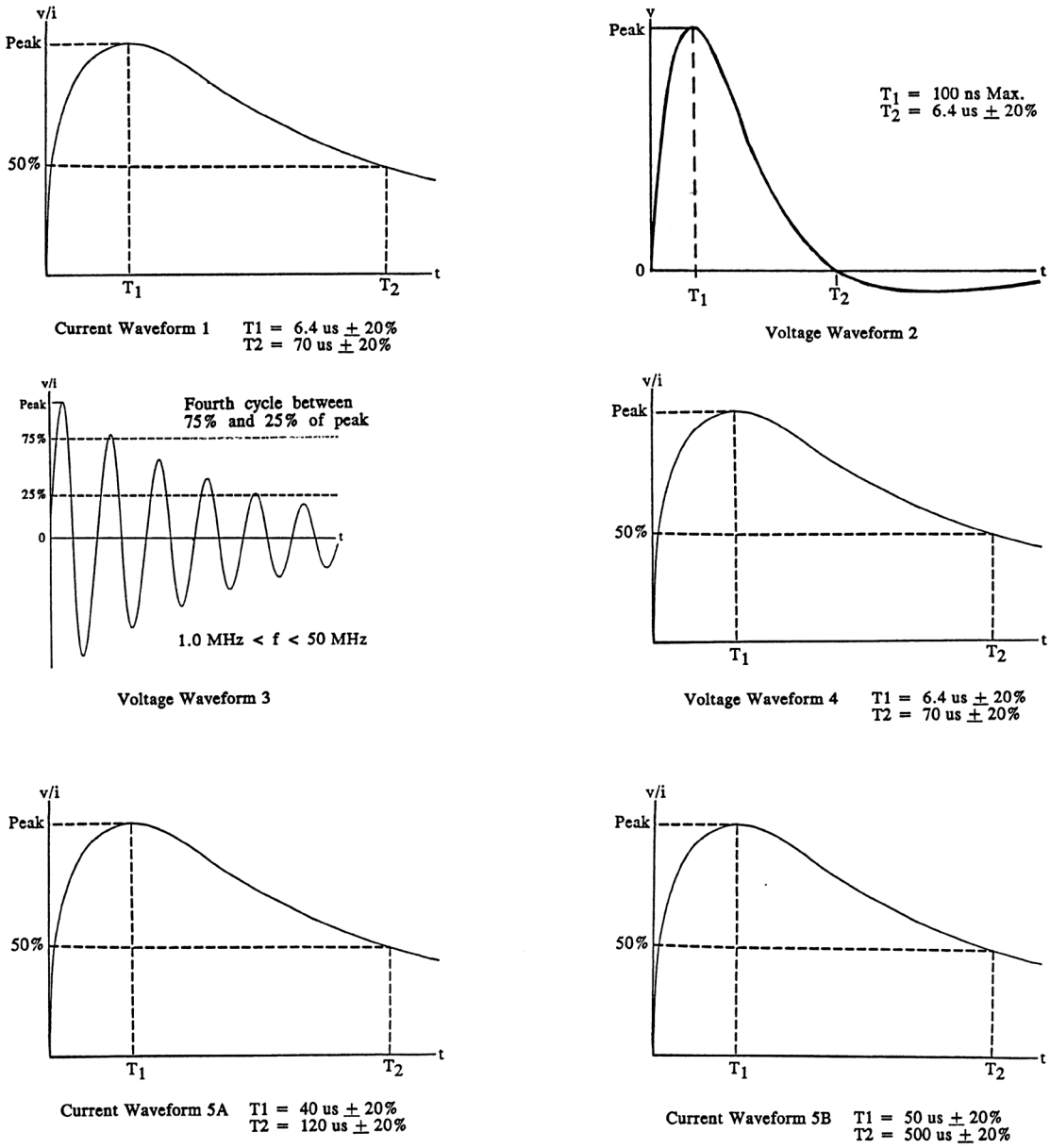

Fig. 16.14 Transient waveforms for aircraft electrical wiring and equipment.

Waveform 5 is a long-duration, double-exponential, unipolar current waveform of the type found on most low-impedance conductors within an airframe. This waveform arises from the diffusion and redistribution of currents through shield boundaries formed by the surrounding airframe structure, shields and nearby conductors. It is particularly prevalent when the airframe is constructed primarily of CFC. Because of the long duration of this waveform, the distribution of Waveform 5 currents among airframe conductors is primarily governed by the resistances of those conductors, rather than by their inductances.

The source impedance associated with Waveform 5 tends to approach the DC resistance of the structure or shield across which the driving voltage is developed and may be as low as a few milliohms. Aside from its high energy content, the major concern in airframe wiring with regard to *Waveform 5* is that the accompanying voltages are sometimes too low to activate suppression devices. Thus, suppression devices may fail to divert Waveform 5 currents from paths where it can cause damage.

Waveform 5A is typical of the currents developed in low impedance conductors (< 5 ohms), such as shields, power wires or other circuits with suppression devices at both ends. Current amplitudes associated with Waveform 5A tend to be low to non-existent inside all metal fuselages but can be quite high on equipment whose interfaces are vulnerable to direct lightning strikes. Examples of such equipment include lights, antennas, and various pressure and temperature probes.

Waveform 5B is produced by the same mechanism as Waveform 5A but is observed more often in conductors within CFC structures because of the higher internal currents that result from resistive sharing with the structure. Waveform 5B currents tend to be very high in CFC structures; hundreds of amperes in small gauge conductors (such as power and low impedance signal wires) and thousands of amperes in larger gauge conductors (such as shields and power buses).

Waveform 6 is a double-exponential, unipolar current waveform, and represents the short circuit current that follows is induced by current component H. This is shown in Fig. 16.15.

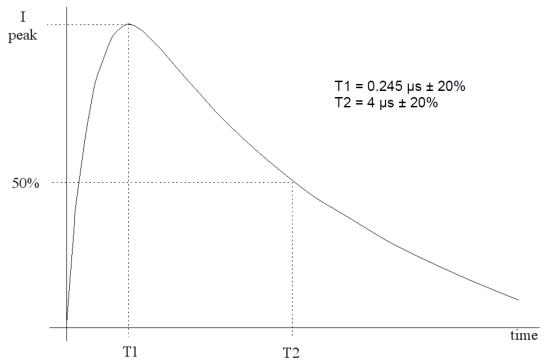

Fig. 16.15 Waveform 6_H
(also sometimes labeled 6, 6_h and 6_H)

Multiple stroke (MS) waveforms

The effects of MS lightning currents (defined in Chapter 5) are simulated by applying repeated pulses of one of the standard internal airframe waveforms to the system under test, while the system is functioning.

Each pulse of the selected standard internal waveform is scaled to represent the peak amplitude induced by the appropriate lightning components, D, D/2 and D/2.5. In some situations, more than one of the transient waveforms may be required to represent each of the important coupling mechanisms applicable to the system being tested.

Multiple burst (MB) waveforms

Practices regarding simulation of the effects of the MB lightning currents are defined in Chapter 5. The damped oscillatory Waveform 3, but Waveform 6H has also been defined to represent currents induced in shields by Component H.

Categories of equipment for various levels

Deciding what transient test level is appropriate for various types of equipment is a task for the system integrator. Guidance is offered in [16.1 and 16.18].

References

16.1 FAA Advisory Circular 20-136B Aircraft *Electrical and Electronic System Lightning Protection*.

16.2 *Aircraft Lightning Environment and Related Test Waveforms*, SAE ARP 5412, SAE International, Warrendale, PA, 1999.

16.3 *Lightning Indirect Effects* RTCA DO-160 Section 22.

16.4 *Standard Basic Impulse Insulation Levels, A Report of the Joint Committee of Insulation*, AIEE, EEI and NEMA Publication No. H8 or NEMA Publication No. 109, AIEE Transactions, 1941.

16.5 https://www.ema3d.com/ema3d-is-a-general-em-solver-for-system-level-3d-modeling

16.6 https://www.comsol.com

16.7 https://nanohub.org/app/site/archive/Spice3F4_Manual.pdf

16.8 A. C. Monteith, H. R. Vaughan and A. A. Johnson, "Chapter 18 - Insulation Coordination", *Electrical Transmission and Distribution Reference Book*, Westinghouse Electric Corp., East Pittsburgh, PA, 1950.

16.9 ANSI C37.90a-1974 (IEEE Std 472-1974), "Guide for Surge Withstand Capability".

16.10 IEEE Static Relay Surge Protection Working Linebreak Group, "Interim Report Static Relay Surge Protection", *IEEE Conference Paper C72 0334.*

16.11 F. D. Martzloff and E. K Howell, "Hi-Voltage Impulse Tester", 75 CRD 039, Corporate Research and Development Center, General Electric Company, Schenectady, NY, March 1975.

16.12 Proposed Requirements for Surge Tests on Ground Fault Circuit Interrupters, Underwriters Laboratories Inc., Melville, NY, July 1975.

16.13 Space Shuttle Lightning Criteria Document, JSC-07636, Revision A, NASA, Johnson Space Center, Houston, TX, November 4, 1975.

16.14 M. S. Amsbary, G. R. Read and B. L Giffin, "Lightning Protection Design of the Space Shuttle", *Workshop on Grounding and Lightning Protection*, Florida Institute of Technology and Federal Aviation Administration, Melbourne, FL, 68 March 1979.

16.15 F. D. Martzloff, F. A. Fisher, "Transient Control Level Philosophy and Implementation: I The Reasoning Behind the Philosophy, II Techniques and Equipment for Making TCL Tests", Second EMC Symposium, Montreux, June 1977.

16.16 K. E. Crouch, F. A. Fisher, F. D. Martzloff, "Transient Control Levels: A Better Way to Voltage Ratings in Power Converter Applications", *76CRD154*, Corporate Research and Development Center, General Electric Company, Schenectady, NY, July 1976.

16.17 F. A. Fisher, F. D. Martzloff, "Transient Control Levels: A Proposal for Insulation Coordination in Low Voltage Systems", *IEEE Transactions on Power Apparatus and Systems*, PAS95, No. 1, pp. 120-129, Jan/Feb. 1976.

16.18 *Aircraft Lightning Test Methods* SAE ARP5416.

Chapter 17

CIRCUIT DESIGN AND PROTECTION

17.1 Introduction

This chapter deals, on a circuit level, with some of the factors related to minimizing damage and upset of electrical and electronic equipment due to lightning strikes. Where possible, examples will be given of good and bad practice. The subjects of methods to make equipment less likely to be damaged, and, where this is impractical, the use of surge protective devices and of the mechanisms by which components are damaged will be discussed in some detail.

In general, the design practices that are effective for controlling lightning induced effects are also effective for controlling steady-state electromagnetic interference and compatibility (EMI/EMC). There are sometimes conflicts but, since the advent of digital avionics, most conflicts related to the grounding of shields no longer exist. Conversely, while most EMI/EMC design conventions are *compatible* with lightning protection requirements, the protection they provide from lightning-induced transients is generally inadequate. This is because the amplitudes and time durations of lightning-induced transients and higher than those induced by EMI sources.

17.2 Signal Transmission

Most problems involving lightning induced effects on aircraft systems originate with the coupling of lightning energy into the wiring of the aircraft. (There are few situations in which lightning induces effects directly into equipment cases unless the equipment is housed within nonconductive enclosures.) Proper choices regarding signal transmission can reduce or even eliminate these problems. Basic considerations about circuit design and signal transmission are shown in Figs. 17.1 – 17.7.

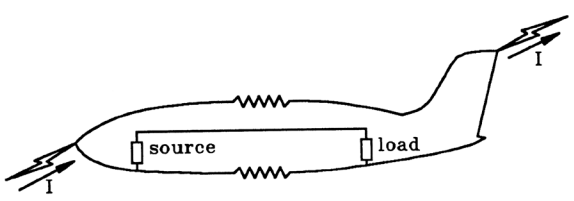

Fig. 17.1 Structural IR voltage.

Airframe structure as a signal return

First, as shown in Fig. 17.1, signal circuits should avoid the use of the aircraft structure as a return path, since this would include, in the path between transmitting and receiving devices, all of the resistively generated voltage rises and the magnetically induced voltages in the loops between circuit conductors and the airframe returns. Also loops between wire harnesses and the airframe are usually longer than loops between circuit independent 'go' and 'return' conductors.

It is common for power circuits to use the airframe as a return path. With metal aircraft, experience has shown this to be generally satisfactory, but provisions should still be taken to ensure that lightning induced voltages in the power circuits are controlled within acceptable limits, possibly with the aid of voltage limiting devices, as discussed in §17.4.

On aircraft fabricated with carbon fiber composite (CFC) or other materials with higher resistivities than aluminum, power return through the airframe should be avoided. Instead, separate return conductors should be used.

Single ended transmission

In single ended signal transmission over a shielded wire, where the shield functions as the return path (Fig. 17.2), any noise current flowing in the shield produces a corresponding voltage that adds to the signal voltage. Thus, if the shield were grounded at both ends, currents could flow in the shield and the resulting voltage would show up as noise on the signal wires. This is why shields for single-ended signal transmission are sometimes grounded at only one end. Lightning current in the structure of an aircraft is another source of noise current that can induce large voltages in signal circuits in the event of a lightning strike.

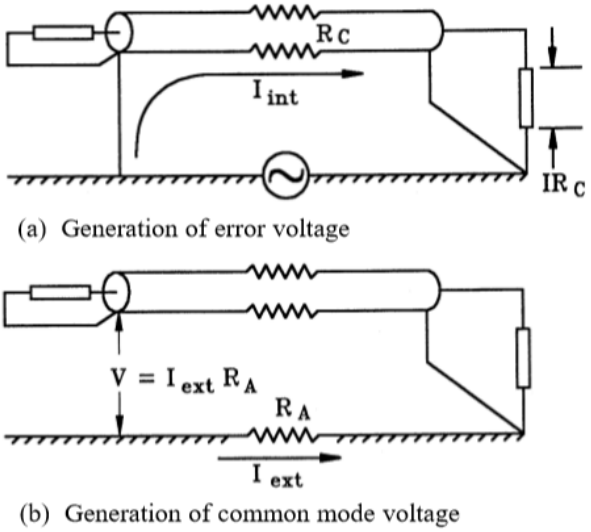

Fig. 17.2 Single-ended transmission.
Shielded circuit voltages are very low.
Common mode voltages are high.

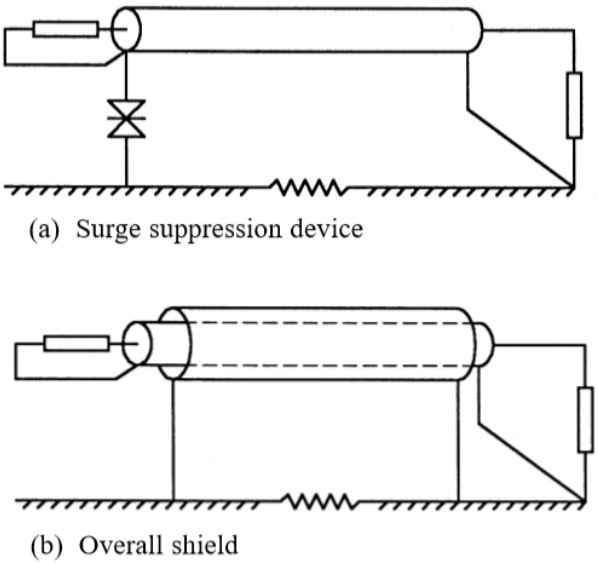

Fig. 17.3 Elimination of common mode voltage.

However, grounding shields at only one end does not solve most lightning problems, because excessive voltage can still appear between the ungrounded end of the shield (and the circuit conductors it encloses) and the local ground system, as described in Chapter 15. Grounding shields at both ends removes this voltage but allows lightning-induced currents to flow in the shield and allows circuit voltages to develop.

If shields must be left ungrounded at one end, for EMI control purposes, there are two methods for allowing this without defeating the ability of the shields to provide lightning protection. These methods are illustrated in Fig. 17.3. One of them is to limit the voltage on the ungrounded end with a surge protective device, leaving the shield, in effect, grounded at only one end for normal operation and grounded at *both* ends when lightning current flows. This may allow an EMI effect to occur during the passage of the lightning stroke current, but this can be addressed using surge suppression devices. At least the greater risk of permanent damage from high common-mode lightning-induced transients is reduced. This approach imposes the practical problem of having to find a location for the surge protective devices. Protective devices selected for this application may be diodes or metal oxide varistors (MOVs). If the common-mode EMI voltages are lower than the forward conduction voltages of available diodes, two diodes, side-by-side in reverse directions may be used to ground the shield in response to lightning-induced transients of either polarity.

If the EMI voltage is higher, diodes in the reverse direction (or MOVs) may be used to ground the shield. Whatever combination of devices is selected, it should have sufficient impulse current conduction capability to tolerate the expected induced shield current.

A second method of providing lightning protection, while permitting shields to be ungrounded, is to cover the signal shield with an overall shield (OAS) that is grounded at both ends. This minimizes both circuit and common mode voltages. It also separates the functions of providing for lightning protection and providing noise-free transmission under normal circumstances. The OAS must, of course, be grounded at both ends. This arrangement is frequently used to protect fuel-quantity indicating systems (FQIS) since the in-tank portion of the wiring that connects with the FQIS sensor units must not have shields that are grounded at both ends. In-tank shield grounds should not be made since doing so would run the risk of arcing at the ground connections. The exterior wire harnesses are double shielded to the tank wall. The inner shield is carried through to the in-tank sensors, but not grounded to the in-tank structure.

Twisted pairs

Signal transmission over a twisted-pair circuit with signal grounds isolated from the aircraft structure (Fig. 17.4) tends to couple lower voltages because the resistive rise in the shield is not in the signal path. It must not be forgotten,

however, that the use of twisted-pair transmission lines does not eliminate the common-mode voltage that appears between each conductors and the shield or equipment chassis. That voltage is minimized only by grounding the shield at both ends.

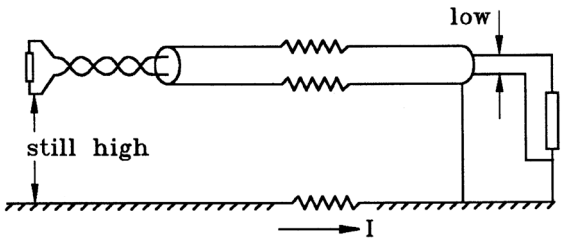

Fig. 17.4 Twisted pair transmission.

Differential transmission and reception

Differential transmission and reception devices (used along with twisted pair wires, as shown in Fig. 17.5) allow the shield to be grounded at both ends because residual noise voltages produced by current in the shield are rejected.

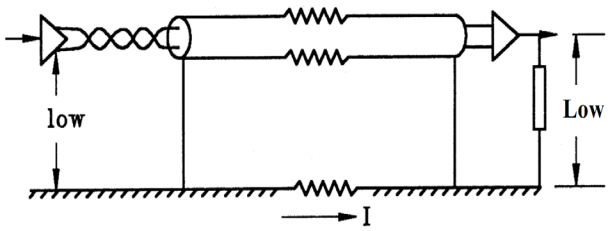

Fig. 17.5 Differential transmission and reception.

Junctions with semiconductors

In general, it is preferable that wiring interconnecting two different pieces of electronic equipment not interface directly with the junctions of semiconductors (see Fig. 17.6(a)).

Resistance in series with semiconductors

Where possible, resistors should be used to limit the surge current into semiconductor junctions from input and output conductors. Even modest amounts of resistance connected between the junctions and the interfacing wires (shown in Fig. 17.6(b)) can greatly improve the ability of semiconductors to resist the transient voltages and currents.

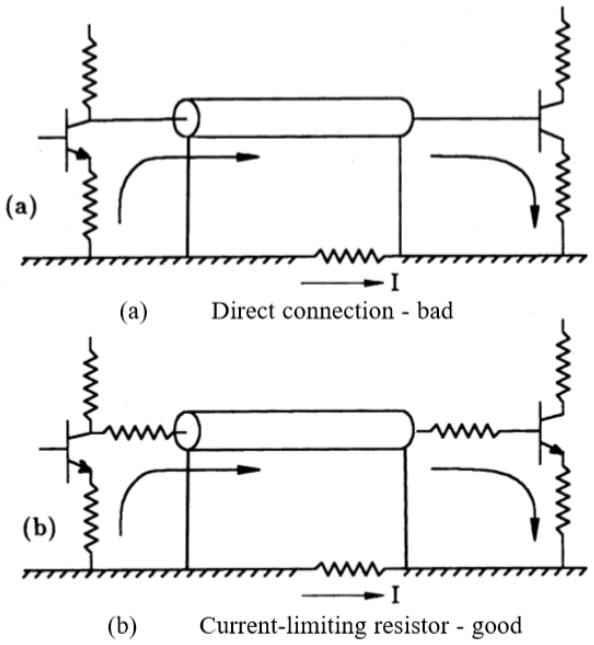

Fig. 17.6 Connection to semiconductor junctions.

Section 17.5, on component damage mechanisms, gives examples that demonstrate the protection offered by the addition of series resistance at semiconductor junctions. The resistors should be physically as large as possible. Half-watt resistors are better than one-quarter-watt or one-eighth watt resistors, which may not be able to tolerate the voltage that drops across them when the induced transient current flows.

Transmission through balanced transmission lines and transformers, combined with input protection for semiconductors, usually provides the greatest amount of protection against the transients induced on control wiring.

Direct current (DC) coupling

Where possible, coupling that can pass DC voltages and currents should be avoided, since lightning-induced voltages and currents have sufficiently long-time durations to be efficiently transmitted through DC coupling paths.

AC transmission through isolation transformers offers one means of avoiding DC coupling paths and the use of optical isolators offers another. Of course, optical isolation is particularly appropriate for digital circuits, but even analogue signals can be transmitted through optically isolated operational amplifiers.

DC coupling paths in power supply circuits can employ DC-DC converters using an intermediate isolation transformer, or an opto-isolator, although surge suppressors (such as MOVs) usually provide a simpler and less expensive way to protect power inputs from damaging, lightning-induced transients.

Fiber optic transmission

Fiber optic transmission lines do not conduct lightning-induced voltages or currents, but the transmitting and receiving devices at the ends of the optical fibers could still be susceptible to interference or damage from local electromagnetic fields. The power sources for these optical couplers may also experience effects from lightning-induced transients.

17.3 Circuit Bandwidth

One of the most important circuit design considerations related to lightning interference is the fact that devices with broad bandwidths can receive and transfer more noise energy than devices with narrow bandwidths. Some of the practical implications of this observation are illustrated in Fig. 17.7.

The induced transients produced by lightning have a broad frequency spectrum. It is often said that most of the energy associated with lightning current falls in the frequency range below 10 or 20 kHz. Before any sense of security is derived from that observation, it should be remembered that the amount of damage or malfunction sustained by equipment is a function of the total amount of energy intercepted by the aircraft. The total energy in a lightning flash is so large that there may, nevertheless, be more than enough energy in the megahertz and multi-megahertz range to cause interference. In addition, this energy may become concentrated in certain frequency bands by the characteristic response of the aircraft or the wiring within the aircraft.

Without reference to any specific frequency ranges, however, the energy spectrum of lightning-generated interference on aircraft electrical wiring still has a broad frequency range.

A receptor with a broad passband (Fig. 17.7(a)) inherently collects more energy than a receptor with a narrow passband (Fig. 17.7(b)). Thus, regarding lightning protection, the narrower the passband, the better. In this respect,

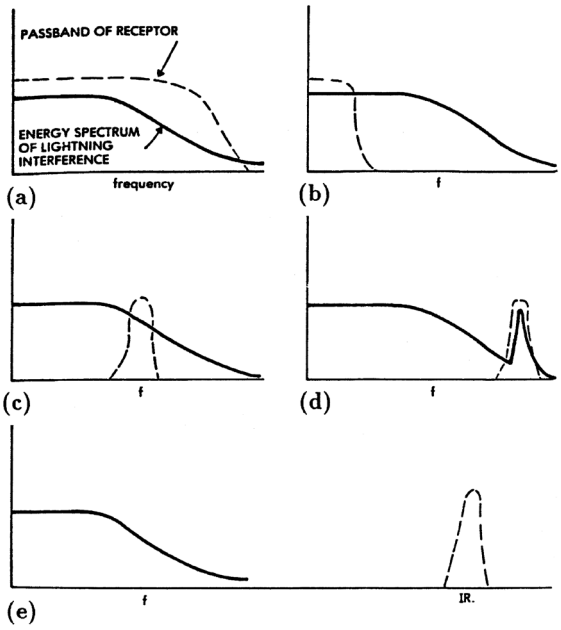

Fig. 17.7 Frequency considerations.

analog circuits have an inherent advantage over digital circuits, since a narrow passband digital circuit is almost a contradiction in terms. If possible, circuits should not have a passband that includes DC (Fig. 17.7(c)), since, when DC is excluded, the circuits reject more of the energy associated with the flow of current through resistance of the structure.

Typical oscillatory frequencies

Studies of the types of interference produced by the flow of lightning current through aircraft have shown that lightning energy excites oscillatory frequencies on aircraft wiring, particularly if the wiring is based on a single-point ground concept. The characteristic frequencies of this oscillation have tended to range from several hundred kilohertz to a few megahertz. If possible, the passbands of electronic equipment should not, like the hypothetical passband shown in Fig. 17.7(d), include these frequencies. Higher or lower passbands are better than the one shown in this figure.

To take an extreme example, the fiber-optic signal trans-mission system represented in Fig. 17.7(e) operates in the infrared region, thereby avoiding the frequency spectrum associated with lightning-generated interference almost completely.

17.4 Protective Devices

Circuit protective devices can sometimes be used to limit the amount of electrical energy that can be conducted into a piece of electronic equipment. While one can seldom eliminate interference through the use of the circuit protective devices, judicious use of these devices can virtually eliminate physical damage to electronics. 'Judicious use' means that the protective devices are incorporated into the basic design of the electronic equipment, not added later, when a transient specification is applied, or trouble is experienced.

Some cautions: When considering protective devices, it should be remembered that when these fail, due to overstress, they often "fail short" which means that they apply a short circuit across the equipment interface that they are supposed to protect. This disables the function of that interface. Additionally, continued operation of the equipment sometimes causes the protective device to "fail open" either immediately, or after some time period. If this happens, the interface may continue to operate satisfactorily, but there is no way to know that protection is no longer available. Life-cycle environments may also cause protective devices to fail (literally: break apart) and remove the protection from the interface. No practical ways to detect and announce this loss of protection have been found. Post-strike inspections of equipment incorporating these devices may be necessary to confirm absence of damage to protection devices. This makes use of protection devices (line-to-ground devices especially) difficult in equipment that has been assigned lightning criticality level A or B difficult if the certification basis includes requirements for fault tolerance.

It should also be noted that most of the available surge protective devices (also known as terminal protective devices, etc.) have been intended for industrial and commercial ground-based applications where environmental tolerances and failures are not critical and low cost is essential. These are much larger markets than is the aircraft market. When considered for aircraft equipment applications the user needs to qualify the devices for such applications.

Basic types of protector

There are two basic types of over-voltage or transient protection device: switching devices and non-linear devices. Their respective V-I characteristics are characterized in Fig. 17.8.

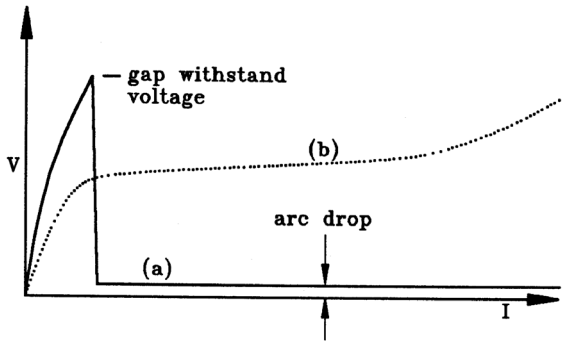

Fig. 17.8 Frequency considerations.
(a) Switching device
(b) Non-linear resistance device

Switching devices

Switching devices (Fig. 17.8(a)) conduct essentially no current until the voltage across them reaches a critical value. When the critical voltage is attained, current flows through the device to ground and the voltage collapses to nearly zero. The current is controlled by the properties of the external circuit. (Spark gaps and controlled rectifiers are examples of switching devices.)

The instantaneous power dissipated in a transient protective device is the product of the surge current flowing through the device and the voltage across the device. Thus, even if the surge current through a conducting spark gap is high, the power dissipated in the gap is small.

Spark gaps and other switching devices limit the voltage that can appear at equipment to the sparkover or turn-on voltage of the device. These devices do not control surges by absorbing the energy of the surge. Primarily, they operate by limiting let-through voltages to the sparkover voltage of the device and reflecting surge energy back toward its source, where it is dissipated in the resistance of the conductors. Sometimes these reflections continue for few cycles until all the surge energy is used up.

Non-linear devices

Non-linear devices have V-I characteristics as shown in Fig. 17.8(b). They conduct very little current at low voltage levels but, once conduction begins, the voltage across the device remains nearly constant. Because the voltage does not collapse to zero, energy is released in the device.

The rating of the device is a function of the amount of energy it can dissipate, which is related to its thermal mass and its ability to tolerate temperature rise. Non-linear devices control surges partly by turning electrical energy into heat and partly by reflecting it back towards its source. (Zener-type surge suppression diodes and MOVs are examples of non-linear devices.)

Note: Since non-linear devices absorb more energy than switching devices, a spark gap is physically smaller than a non-linear device for a given surge-power handling capability.

Recovery characteristics

Another fundamental difference between switching devices (e.g., spark gaps) and non-switching devices (e.g., surge suppression diodes or varistors) relates to their recovery characteristics after a surge has passed. If a line protected by a spark gap is connected to an energy source (a power bus, for example), the spark gap remains in its low-impedance conductive state as long as the energy source is present. Only when the energy source is disconnected from the line can the spark gap return to its initial, high-impedance, nonconductive state. Bringing this transition about generally requires opening a circuit breaker on the line. By contrast, non-linear devices cease to conduct as soon as the voltage returns to its normal value. Thus, remote circuit breakers are not required on circuits protected by non-linear devices.

Circuit interrupters

Some devices are designed to sense an overvoltage and, on sensing the overvoltage, to interrupt power flow to the load. Devices that accomplish this interruption by electromechanical means should not be regarded as transient protection devices, because the response of a mechanical device is inherently too slow to be effective against lightning-induced transients. Such devices are not used for lightning protection of avionics and none of them will be discussed in this chapter.

Energy reflection

All types of overvoltage protection devices inherently operate by reflecting a portion of the surge energy to its source and by diverting the rest into another path. The intention is always to dissipate the surge energy into the resistance of the interconnecting leads and ground leads. The alternative to reflecting the energy is to divert and absorb it in an unprotected load, specially provided. This approach has the following hazards associated with it:

1. The reflected energy could appear on other unprotected circuits.

2. Multiple reflections could cause a transient to last longer than it would otherwise.

3. The spectral density of the energy in a surge could be changed, so that either high or low frequencies were enhanced. This could increase interference problems on other circuits, even though the risk of damage to the protected circuit is reduced.

Choosing locations for protective devices

Usually, the selection of a transient protective device depends on the amount of surge energy that must be dealt with. Generally, this energy decreases the further away one gets from the source of the transient. The surge energy to be expected can also be related, crudely, to the normal operating power of the circuit involved. One would normally expect lower surge levels on low voltage signal circuits than on medium-power control circuits, and one would expect the highest surge levels on main power distribution buses. This is because better shielding is usually provided for low voltage signal circuits than is typical for higher voltage circuits, including power distribution circuits. Thus, one might logically use surge suppression diodes and small varistors on individual circuit boards within equipment, larger varistors on terminal boards, even larger varistors at power distribution busses and spark gaps on radio frequency (RF) cables from antennas located in lightning strike zones.

Commercially available circuit protective devices that may be considered for aircraft applications include gas-filled spark gaps, specially fabricated Zener diodes, and varistors. Each has its advantages and disadvantages.

17.4.1 Spark Gaps

Incidental spark gaps

Sometimes spark gaps are incidental to the construction of some other device, such as a terminal board or a cable connector. Whenever the voltage on the ‘terminals’ of a spark gap becomes sufficiently high, there is a spark across or through the dielectric, and the voltage on connected devices is limited to that which produces this spark. Usually, sparkover of incidental gaps is unplanned and undesirable, particularly if it causes puncture and permanent failure of solid dielectric or tracking across insulating surfaces. Whether planned or not, the existence of incidental spark gaps should be recognized. Sparkover across the surface

of a dielectric might be tolerable in some cases, and sometimes can be made to provide perfectly acceptable surge protection at minimal extra cost.

Intentional spark gaps

Spark gaps intentionally provided for circuit protection are usually composed of two metal electrodes, held at a fixed distance from each other, separated by a dielectric, and sealed in a container. The electrodes may be spherical but in more sophisticated devices they are not. Not all spark gaps use metal electrodes and not all are sealed. Ground-based telephone circuits, for example, are often protected by gaps using carbon electrodes. (Examples of spark gaps are shown in Fig. 17.9.). One manufacturer's literature on spark gap product is in [17.1].

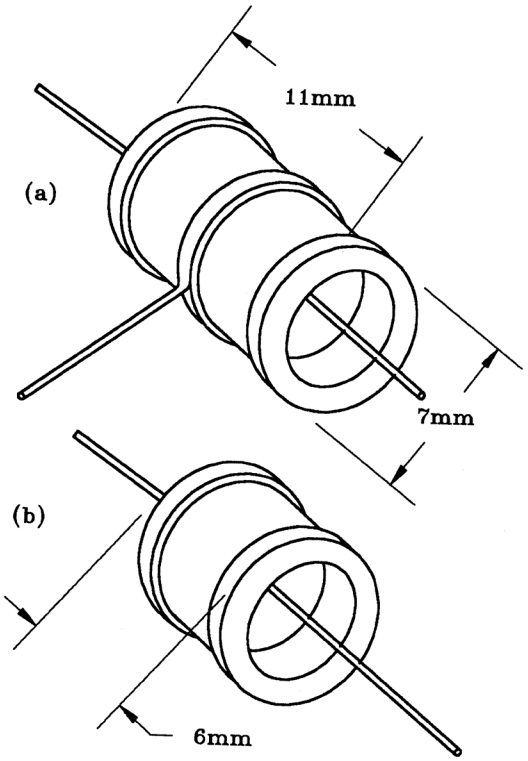

Fig. 17.9 Outline sketches of spark gaps.

Electron avalanche

Conduction through a spark gap involves an electron avalanche process, as discussed in Chapter 1. Dielectric composition, gas density and electrode geometry all affect the breakdown voltage of a spark gap and the speed with which the avalanche develops. Breakdown voltage depends on the waveform of the applied voltage.

A voltage waveform with a fast rate-of-change produces breakdown at a higher voltage than a more slowly increasing voltage transient would. A low-pressure gap (or, more precisely, a low gas density) breaks down at a lower voltage than a similar high-pressure gap, but the avalanche develops more slowly in the high pressure gap and the dependence of breakdown voltage on waveform is greater.

The dependence of breakdown voltage on rate of change of voltage partly relates to how long it takes, on average, for a free electron to appear and start the avalanche process. Commercially available spark gaps frequently contain minute amounts of tritium or other radioactive elements to reduce the dependence of break-down voltage on voltage waveform.

Breakdown voltage

Impulse breakdown voltages for gaps with metal electrodes operating in air at standard atmospheric pressure are seldom less than 1 - 2 kV, even with very small spacings between the electrodes. For commercial spark gaps, curves, such as Fig. 17.10, are generally supplied to relate breakdown voltage to rate-of-change of voltage. Catalog specification sheets generally cite the breakdown voltage for very slowly changing voltages or for DC voltages. Rated breakdown voltages for small gaps range upwards from a minimum of about 100 volts. The actual breakdown voltages for the same gaps, when subjected to rapidly changing applied voltage waveforms, may be substantially higher.

Normally, one should not regard spark gaps as the primary means for controlling surges, unless the equipment to be protected can withstand several hundreds of volts. (Radio receivers and other RF equipment often *can* tolerate such voltages.)

Recovery

Once a gap has sparked over, the current in the gap is governed by the impedance of the circuit and the normal operating voltage. Current continues to flow as long as the circuit is energized at a voltage less than a hundred volt. Gaps used for industrial machinery and commercial power systems can be made self-extinguishing (for applied voltages up to about 100 V) by using magnetic fields to activate ventilation systems that cool the arc, but such devices are not applicable for aircraft use.

Current rating

Small spark gaps can carry peak currents of several thousand amperes for a few tens of microseconds and they can carry several hundreds of amperes for a few milliseconds. Catalog sheets do not always clearly state the duration of surge current for which the specified peak current applies but, for aircraft protection, the matter is of little importance, since almost any gap can carry all the surge current likely to appear on internal aircraft wiring.

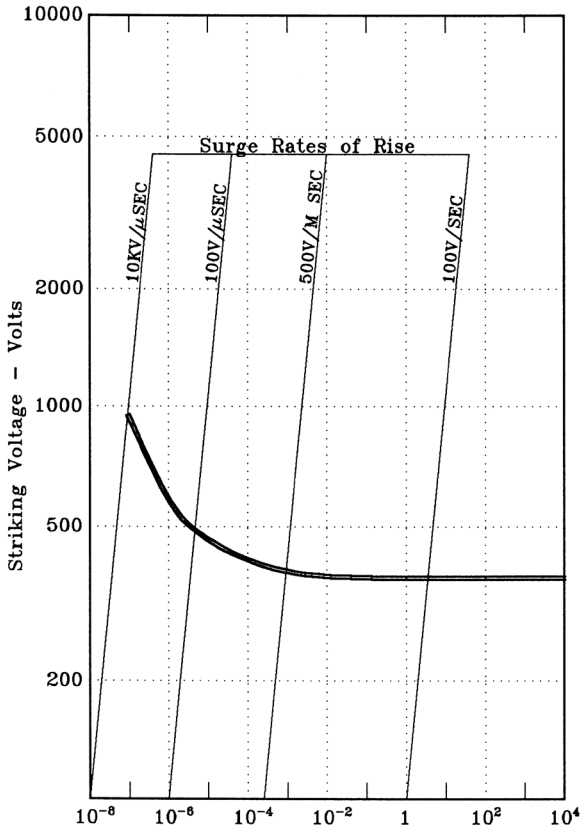

Fig. 17.10 Volt-time curve of a spark gap.

'Let-through' voltages

Until a spark gap ionizes, it has no effect on circuit voltage. Thus, the surge voltage on the protected line must rise enough to ionize the gap before the gap can provide any protective benefit. This voltage is sometimes referred to as the 'let-through' voltage. Some of this 'let-through' voltage (see Fig. 17.11) can be passed onto the rest of the circuit. If this residual surge voltage poses a problem, it can often be suppressed using MOV or Zener diode devices.

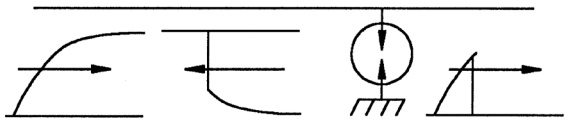

Fig. 17.11 'Let-through' voltage.

Sometimes spark gaps are installed on a pair of conductors, as shown in Fig. 17.12(a). Ideally, in response to a common mode surge, the two spark gaps should ionize at the same time but, in reality, one of them invariably ionizes before the other, so that a high voltage appears between the conductors. To alleviate this problem, three-electrode spark gaps are available (Fig. 17.12 (b)). Ionization between any two electrodes spreads almost instantaneously to the third, simultaneously shorting the two conductors together and to ground.

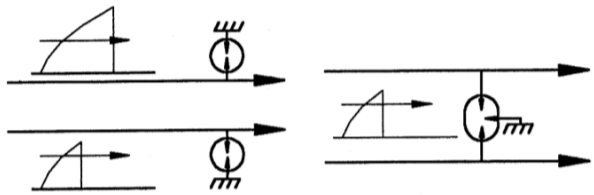

(a) Two separate gaps give high common mode voltage.

(b) Three terminal gap.

Fig. 17.12 Spark gaps on a conductor pair.

Application considerations

Spark gaps are attractive for protection of antenna interfaces with RF transmitter/receiver units due to their low capacitance. Other types of protectors typically have higher capacitances that apply unacceptable loads to RF circuits. In RF circuit applications the electric arc will self-extinguish since these are not electric power sources.

Spark gaps (and any other voltage-limiting device, for that matter) must be rated so that they will not ionize and conduct at the normal peak operating voltage of the circuit being protected. For this reason, they are not applicable for protecting electric power circuits since they apply a short circuit when they spark. This would be unacceptable in an aircraft power system, where power current might damage the gap and/or get interrupted.

Spark gaps are also not applicable for protection of semiconductors and electronic circuit boards since their voltage suppression levels would be too high.

Another use of spark gaps is for protecting against high energy surges, such as arise from lightning strikes to externally mounted equipment. External lights are an example. The gaps should be placed far from the most sensitive equipment and should be used in conjunction with other protective devices that have lower voltage clamping levels but less ability to carry high surge currents. Examples of this arrangement are shown in Fig. 17.23.

Failure modes of spark gap protectors

Usually, a spark gap fails when it is required to carry excessive surge current or excessive power system current following sparkover. This either shatters the case or burns away the connecting leads. In either case, the gap usually fails open circuit. Once in a while, a spark gap rated for low sparkover voltages (where the electrode gaps need to be small) will fail short, because electrode material melts and comes together, eliminating the gap.

Advantages of spark gaps:

1. Spark gaps have a large current-handling capability. In fact, gas-filled spark gaps have the highest peak current handling capabilities of any transient protection device, and almost any gap can handle the maximum surge currents induced by lightning.

2. Spark gaps have high open impedances and low capacitances. The low shunt capacitance and leakage current characteristics of gas-filled spark gaps minimize insertion problems for operating frequencies below 1 GHz. Therefore, spark gaps are applicable for RF circuits.

3. Spark gaps have bipolar properties. In other words, they exhibit the same response to both positive and negative polarity surges.

Disadvantages

1. Spark gaps have relatively high sparkover voltages and therefore high let-through voltages. They are not useful for protection of low voltage circuits, such as digital I/O. Minimum let-through voltages are rarely less than 100 V.

2. Power system follow current through spark gaps must be extinguished by removing the voltage (with a circuit breaker or fuse) or by inserting resistance rapidly into the circuit by means of an additional element, such as an MOV. Thus, they are not practical for protection of aircraft power circuits.

3. The performance of spark gaps is heavily dependent upon sparkover voltage and on the waveform of the voltage applied to them.

4. Spark gaps reflect more energy than they absorb.

5. The rapid change of voltage associated with the sparkover of a gap may excite circuit ringing.

17.4.2 Non-Linear Resistors (NLRs)

NLRs (or varistors) may be characterized by the expression

$$I = KV^N \qquad (17.1)$$

where N and K are device constants that depend on the varistors physical dimensions and material of which it is composed. One manufacturer's literature on MOVs is found in [17.2].

Varistors may be constructed of silicon carbide, selenium, or a metal oxide (usually zinc oxide). This section concentrates on MOVs [17.2]. Zener diode type protectors can be classified as NLRs, since their volt-ampere characteristics also follow Eq. 17.1, but, since their construction differs consider-able from that of MOVs, they will be treated separately in §17.4.3.

Formulation

MOVs are formed from zinc oxide grains (Fig. 17.13) that are pressed together and sintered into ceramic parts. The grains behave as if they had non-linear semiconductor junctions at their boundaries. The volt-ampere characteristics of a fully fabricated MOV depend both on the size of its zinc oxide grains and on how many grains in series are included in the thickness of the unit. Thus, for a given formulation of zinc oxide grains, the clamping voltage of an MOV is directly proportional to its thickness. Current handling capability depends on how many grains in parallel fit in the cross-sectional area of the unit. Thus, the volt-ampere characteristics of MOVs are derived from the bulk characteristics of multiple, parallel current paths, which accounts for their large power-handling capability.

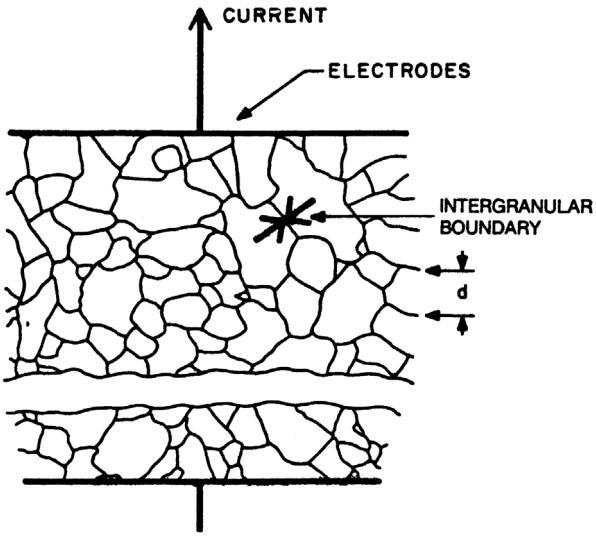

Fig. 17.13 Intergranular structure of MOV [17.2].
d is the average grain size.

Volt-ampere characteristic

A graph of the volt-ampere characteristic of a typical MOV device is shown in Fig. 17.14 and an equivalent circuit is shown in Fig. 17.15. The V-I characteristic is divided into three current ranges:

(1) **The Leakage Region:** Very low current levels, at which capacitance, C, and leakage resistance, R_{off}, dominate.

(2) **The Normal Region:** This is the region where the varistor is intended to operate.

(3) **The Upturn Region:** Very high current levels, at which bulk resistance, R_{on}, becomes important.

Leakage region

At low current levels (Fig. 17.14), the leakage resistance is high enough (on the order of 10^9 ohms) that leakage current is often insignificant for DC circuits. Leakage current is strongly dependent on temperature, as shown in Fig. 17.16.

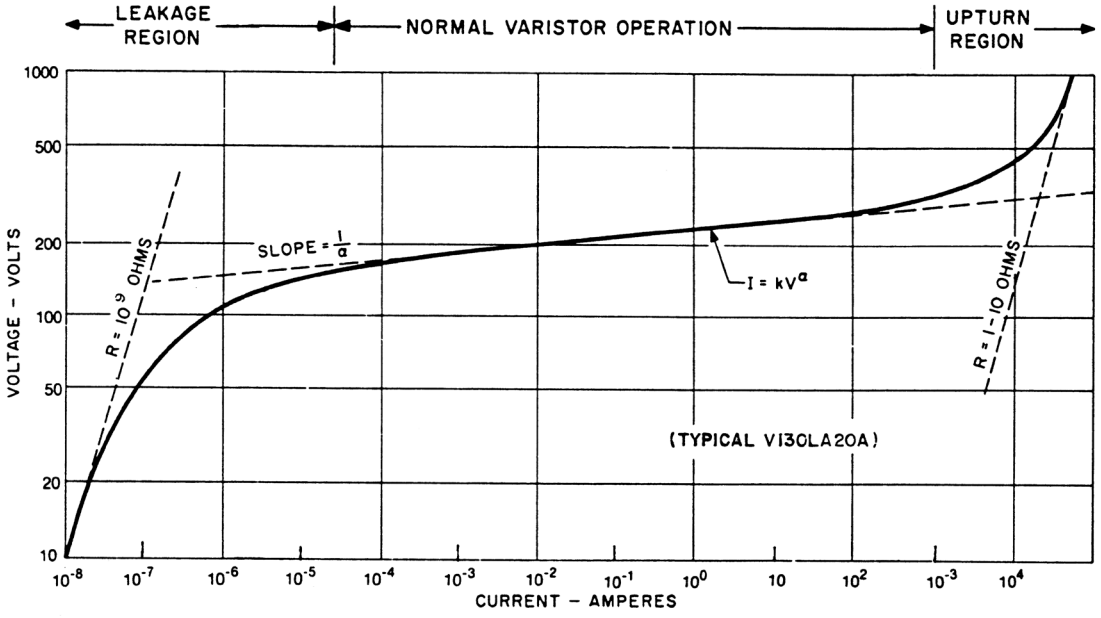

Fig. 17.14 V-I characteristic of MOV [17.2]

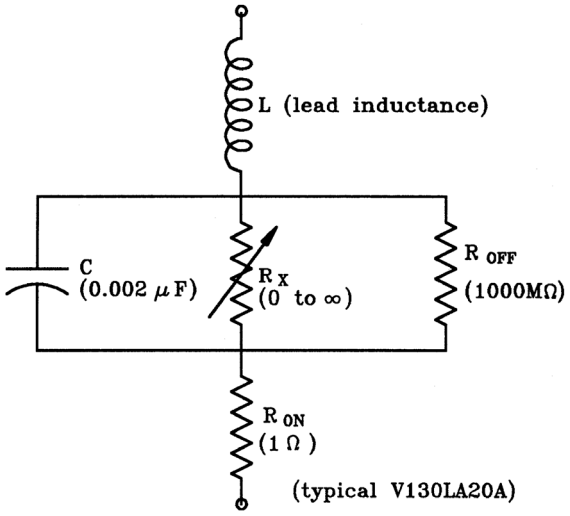

Fig. 17.15 Equivalent circuit of MOV [17.2]

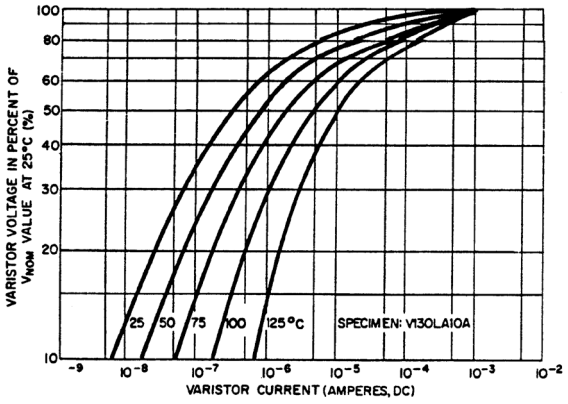

Fig. 17.16 Leakage current vs. temperature [17.2]

For ac circuits, the effects of leakage resistance are overshadowed by the effects of parallel capacitance. The capacitance of MOV devices is high (on the order of 1 - 10 nF), is nearly constant with frequency up to 100 kHz and is little affected by temperature. Capacitance is not usually a problem for circuits operating at power frequencies and may even be valuable, in that it helps to shunt high frequency noise currents to ground. The effects of MOV capacitance must be considered on circuits that operate at high frequencies or that react to rapidly changing pulses.

The capacitance of any particular MOV device may be measured with conventional bridges, provided that the bridge voltage is not high enough to cause non-linear conduction.

Normal varistor region

In the normal range of current (Fig. 17.14), the performance of an MOV resembles that of a NLR, R_x, having the characteristic

$$I = KV^{\alpha} \qquad (17.2)$$

The exponent, α, is on the order of 20 - 50, implying that a current that changes by four orders of magnitude would result in a change in voltage of 25% or less.

Upturn region

At high current levels (i.e., several hundreds to several thousands of amperes), bulk resistance becomes important and MOV performance deteriorates (see Fig. 17.14). The expected current through MOV installations should be kept below this range, either by limiting the surge current with series resistance, by using larger MOV packages. It is not a good idea to use MOVs in parallel since, due to their non-linear V-I characteristic they are unlikely to share surge current equitable and one may end up being overloaded (see Fig. 17.20).

Waveform dependence

Varistor performance is best analyzed by treating the surge current as the independent variable. Varistors are sometimes denigrated as having poor pulse response or being subject to overshoot (i.e., having excessive clamping voltage) in response to rapidly changing surge currents. If a half-sinusoidal current pulse (Fig. 17.17) is passed through a varistor, the waveform of the voltage developed is practically rectangular. A faster-rising, sinusoidal pulse also produces a rectangular pulse voltage, but of somewhat higher amplitude. The difference in voltage for slowly rising current pulses (> 10 μs) and for rapidly rising pulses (~ 0.5 μs) is seldom more than 10 - 20%. This is more noticeable with large disks of MOV material than with small disks.

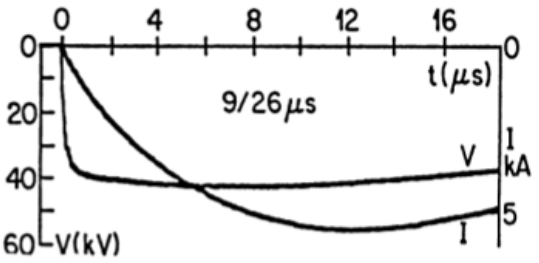

(a) Slowly changing current.

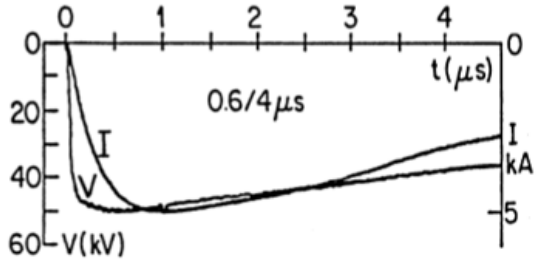

(b) Rapidly changing current. Adapted from [17.4].

Fig. 17.17 Time dependence of MOV voltage.

Studies of large MOV disks, such as are used in power transmission systems [17.3 - 17.4], have shown that overshoot is primarily caused by the diffusion of current into the varistor material. Studies of small disks, such as those used for protection of low voltage equipment [17.2], have shown that the time dependence of voltage is only a few tens of percent, even for surge currents having fronts of a few nanoseconds.

The fact that surge currents of moderate steepness produce rapidly changing MOV voltages should be recognized in circuit design. Circuit oscillations resulting from the rapid change in voltage may give rise to unexpected interference problems.

Lead effects

Most instances of MOV overshoot are due to lead inductance effects and are not intrinsic to the MOV itself. When specifying MOVs, or any other surge protective device, care should be taken to keep short any leads through which high or rapidly changing currents might flow. Voltage developed across the inductance of such leads adds to the voltage developed across the varistor material. For example, Fig. 17.18 shows two MOV installations (such as might be used on a 115 Vac power circuit) and the voltages that would be developed across them by half-sinusoidal current waveforms. One of the installations uses the minimum practical lead length and the other uses leads about 15 cm (6 in) long. For an applied current waveform with a 10 μs front (rise) time, the voltage is about the same, regardless of lead length, but for a current with a 0.5 μs front time, the voltage across the long leads is nearly twice that across the short leads.

Excessively long leads between protectors and the equipment they are protecting create large inductive loop areas. Leads should always be kept as short as possible. And, wherever practical, the protected circuit should be brought to the protector. Fig. 17.19 shows examples of good and bad practice. Arrangement (a) has excessive leads and will provide little protection. Arrangements (b) and (c) are more effective.

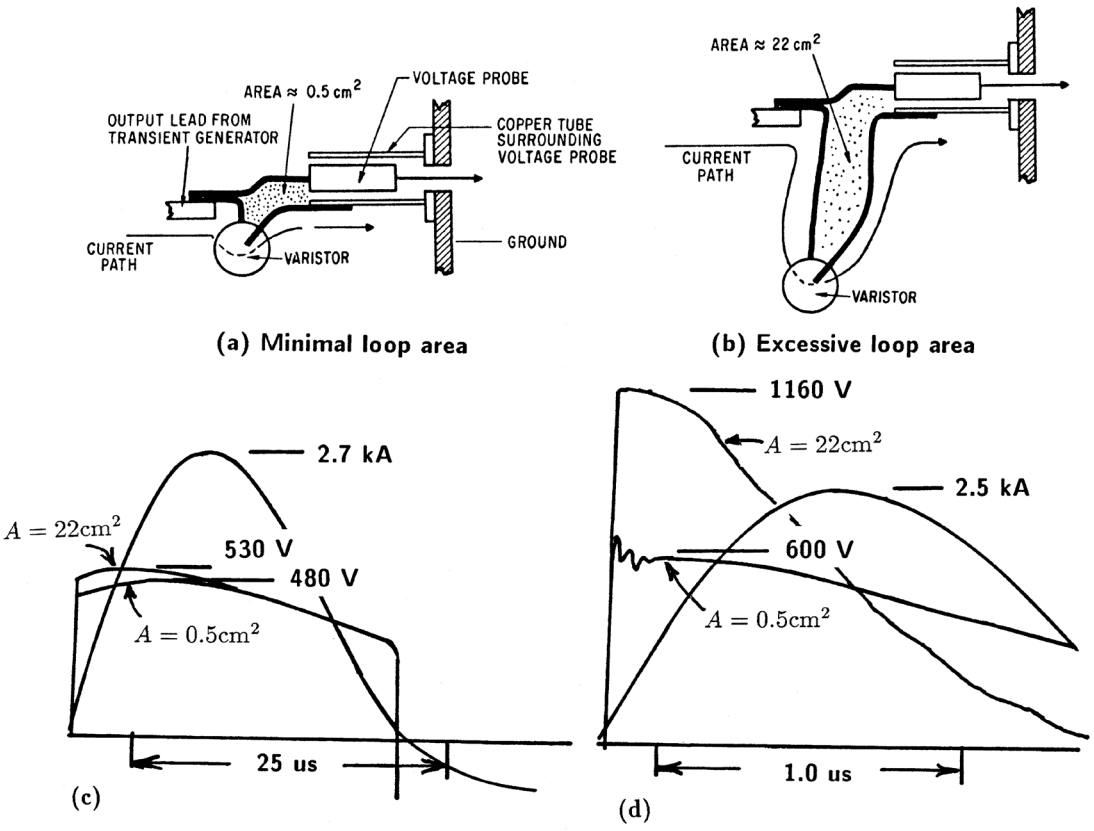

Fig. 17.18 Lead effects [17.5].

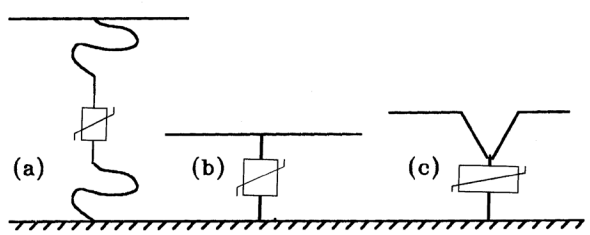

Fig. 17.19 Connections to a protection device.

Rating of MOVs

The several factors that are involved in the rating of a MOV device are illustrated below, using the Harris semiconductor V130LA series device (whose characteristics of are shown in Tables 17.1 and 17.2 [17.5]) as an example. Similar devices are available from other vendors and the illustration should not be taken an endorsement of any brand of device. MOVs should be selected based on the manufacturer's catalog data.

Device size

The most common packaging configuration for MOV devices is a disk with wire leads. The column in the manufacturer's data table that lists the device size refers to the diameter of the disk. The voltage rating of the device depends on its thickness, which is given in outline drawings but not in specification tables. Larger diameter disks have greater current-carrying capability than smaller disks.

Maximum continuous operating voltage

A fundamental consideration in the application of any surge protective device is that it does not conduct excessively under normal operating conditions, since the heat produced by continuous conduction is likely to destroy the device. Conduction must not take place even under the normally allowed excursions of operating voltage. For example, some aircraft power systems operate at a nominal DC voltage of 28 volts but, if a regulator were to fail, voltage on the bus could rise as high as 80 volts.

Table 17.1
Maximum Ratings for Typical 130 V MOVs [17.5]

Model Number	Model Size Disc Dia. (mm)	Device Marking	Maximum Ratings (85°C)			
			Continuous		Transient	
			RMS Voltage	DC Voltage	Energy (10/1 000μs)	Peak Current (8/20μs)
			$V_{m(ac)}$	$V_{m(dc)}$	W_{tm}	I_{tm}
			Volts	Volts	Joules	Amps
V130LA1	7	1301	130	175	11	1 200
V130LA2	7	1302	130	175	11	1 200
V130LA5	10	1305	130	175	20	2 500
V130LA10A	14	130L10	130	175	38	4 500
V130LA20A	20	130L20	130	175	70	6 500
V130LA20B	20	130L20B	130	175	70	6 500

Table 17.2
Specifications for Typical 130 V MOVs [17.5]

Model Number	Characteristics (25°C)					
	Varistor Voltage @ 1mA DC Test Current			Maximum Clamping Voltage V_C @ Test Current (8/20μs)		Typical Capacitance
	Min.	$V_{N(dc)}$	Max.	V_C	I_p	f = 1MHz
	Volts	Volts	Volts	Volts	Amps	Picofarads
V130LA1	184	200	255	390	10	180
V130LA2	184	200	228	340	10	180
V130LA5	184	200	228	340	25	450
V130LA10A	184	200	228	340	50	1 000
V130LA20A	184	200	228	340	100	1 900
V130LA20B	184	200	220	325	100	1 900

An MOV on such a circuit would have to either be rated higher than 80 volts or would have to be fitted with a fuse or circuit breaker to disconnect it from the bus.

The V130LA devices are rated to withstand 130 V-rms (184 V peak) or 175 V-DC continuously without excessive conduction. Such a device would most likely be used on a nominal 115 V-rms ac power system. Lower voltage ratings would not be appropriate, because the operating voltage on a power system can temporarily rise to levels significantly higher than nominal.

RMS vs. peak or DC voltage:

Because MOV devices are frequently used on ac power systems, the reference to rms quantities should be noted. Other protective devices, notably Zener diode-based devices, are more commonly used on electronic systems and are usually rated for a nominal DC or peak ac voltage.

50/60 Hz applications:

Experience has shown that some MOV devices marketed for industrial and commercial applications on 115 V-rms 50 or 60 Hz power voltages fail when installed on 400 Hz aircraft power systems. The cause of this failure is unclear since the matter has not been studied fully. Nevertheless, it is recommended that commercial MOV devices rated for ~240 V-rms applications at 50/60 Hz be used to protect 115 V-rms 400 Hz aircraft power circuits. This provides clamping levels about twice as high are afforded by the 115 V-rms rated devices but reduces the likelihood of failures that could short-circuit the protected power supply or create a fire hazard from the conduction of circuit currents through a failed device. Similarly, MOV devices intended for protection of circuits operating at other 400 Hz voltages should have higher operating voltage rating than would be selected for 50/60 Hz operation.

Transients

The manufacturers of MOV devices typically provide two types of maximum pulse rating: the *maximum allowable energy* and the *maximum peak current*. The *maximum peak current* ratings of commercial MOVs are usually defined for a surge having an 8 x 20 μs waveform (a surge of the type generally used for testing of ac power equipment, as discussed in §1.5.2). This waveform is neither representative of lightning stroke currents nor of the currents induced by them. It is an antiquated definition, which probably should be updated by the electric power industry, where it is most commonly used. The *maximum allowable energy* rating, on the other hand, is defined for a longer, 10 x 1 000 μs waveform that is commonly used for testing telecommunications equipment. There is no rationale for the difference between surge current and energy dissipation specifications for commercial MOVs. The use of both waveforms happened out of convenience, rather than from any engineering review of the matter.

As a practical matter, it is best to have transient protection devices rated in terms of maximum peak current (i.e., I_{SC}) since this is included in the definitions and standards for lightning-induced transients. Transient energy, on the other hand, is not quantifiable since there is no energy storage or dissipation factor in the transient definitions.

Since clamping voltage is relatively independent of surge current, instantaneous power dissipation in an MOV is the product of the instantaneous surge current and the clamping voltage. Thus, a rectangular surge current of 100 amperes, passing through a varistor clamping to 340 volts, would deliver a power of 34 000 watts. If the device were rated to withstand 70 joules (watt-seconds), then the surge could flow for 2.06 milliseconds. MOV specification sheets provide curves relating voltage and current across a device. More precise estimates of dissipated surge energy could be made by relating instantaneous surge current to surge voltage and numerically integrating the result.

Voltage at 1 mA

Varistor voltage is commonly specified at 1 mA test current, partly because a leakage current of 1 mA is seldom cause for concern and partly because it is a convenient and easily measurable reference point for V-I curves. Usually, this is a DC current but sometimes MOVs are tested with 50 or 60 Hz alternating currents. The specifications of the test current waveform should be included with varistor voltage specifications. Usually, the test current is set and the varistor voltage (sometimes called V_1) is read and recorded. The V_1 voltage should be on the device label, especially on the large-diameter devices used to protect aircraft power distribution busses.

After an MOV device has been exposed to a high amplitude surge current, as from a lightning strike, its condition may be determined by measuring its varistor voltage. Usually, a high-amplitude surge current, somewhat above the peak current rating for the device, is sufficient to permanently reduce the varistor voltage. If the varistor voltage is found to be lower than the originally recorded V_1 by 5% or more, the MOV should be replaced. MOVs whose V_1's have not changed significantly following exposure to lightning-induced transients, and which show no other indications of damage, need not be replaced and will continue to provide protection for the life of the airplane or system.

Maximum clamping voltage

Catalog data commonly cites the maximum clamping voltage at a surge current appropriate to the size of the device.

For more complete information on V-I characteristics, curves like Fig. 17.14 must be reviewed. Device manufacturers do not always include this data in service specifications, but it often exists and can be obtained upon request

from the manufacturers. If this data is not available, devices should be tested independently, before they are selected for use in protecting aircraft electronics.

Large diameter (typically 300 mm), high energy MOV devices used for ac power systems are often rated in terms of their clamping voltages when carrying peak surge currents of 10 000 amperes. Similar, but not as large devices are now becoming available for aircraft use. Devices of ~50 mm diameter have been able to tolerate transient current Waveform 1 (6.4 x 69 μs) surge currents as high as 50 kA.

Tolerance for multiple pulses

When selecting MOVs (or diodes) for use on aircraft power circuits, the ability of these devices to tolerate induced transient currents applied as multiple stroke (MS) waveform sets (as defined in Chapter 5) should be confirmed, because the energy deposited by such closely spaced pulses cannot be expected to be dissipated from the device between one pulse and the next. In fact, the cumulative dissipated energy from the pulses in the MS waveform set may fail a device that could have tolerated a single pulse without failure.

MOVs in series

MOV devices of the same cross-sectional area can be connected in series without difficulty. The individual units need not even have the same thicknesses or voltage ratings. This is sometimes done to achieve a higher operating voltage where a low maximum current requirement exists.

MOVs in parallel

MOVs are sometimes connected in parallel to suppress high current surges, but care must be taken to match the V-I characteristics of the parallel branches (see Fig. 17.20). If the V-I characteristics are not carefully balanced, one device may carry most of the surge current, which would defeat the purpose of using the devices in parallel. Exact matching is probably not necessary, however, since by the time current becomes high enough to require parallel devices, bulk resistance probably dominates the performance of the circuit, forcing more equal current sharing. In general, it is better to use one, larger-diameter disk than several small disks in parallel.

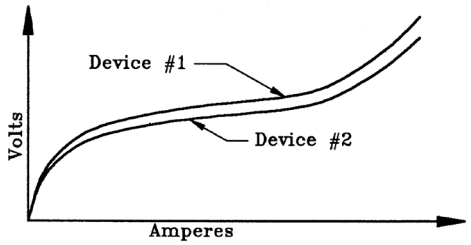

Fig. 17.20 Parallel operation of MOVs.

Wear-out

Specifications for MOV devices sometimes list a maximum allowable number of surges of a specific amplitude. This seems to imply that MOVs become 'worn out' and lose their non-linear properties so that they are no longer capable of protecting against surges. This is not the reason for this specification. The parameter that changes is the leakage current at operating voltage, which begins to increase after many surges. However, the MOV still retains its non-linear characteristic and its ability to protect against surges.

Turn-on voltage

Sometimes the V-I characteristics of MOVs are presented in linear plots, and discussions arise about the 'knee' of the curve or the voltage at which the MOV 'turns on'. Such discussions are misleading, since the so-called 'knee' is an artifact of the scale used for plotting current. The current is an exponential function of voltage and plotting the same function to a different current scale would indicate a different 'knee'. Also, discussions of 'turn-on' imply a switching function, by which the mechanism of conduction changes abruptly from one state to another. There is no more a 'switching' mechanism for an MOV device than there is for a semiconductor diode.

Failure Mode

If subjected to an excessively high-amplitude surge current, MOV disks may shatter and fail open circuit. However, it is more typical for MOVs to fail because of exposure to an excessive continuous voltage and current. When this happens, the disk usually fuses and fails shorted, but sometimes the heat is sufficient to melt the solder holding the leads to the MOV disk, and the device fails open circuit.

If a protector fails open, it may not degrade the operation of the circuit, but its continued protection effectiveness will be lost, and this may not be easily detected. If the failure is short, the circuit will cease functioning. In many cases this would be detected, but the circuit function will have been lost. Designers should take care to determine and verify the possible maximum I_{SC} environment and select protectors whose maximum current rating includes the circuit I_{SC} plus a margin and then make sure that the protectors they select can tolerate this current without degradation.

Advantage of MOVs

1. MOVs are bilateral devices.

2. MOVs are small as compared with their surge current capability.

3. MOVs are self-extinguishing. When applied voltage drops below the voltage for which the device is rated, they conduct very little current.

4. MOVs have inherently fast response times.

5. MOVs have high surge current-handling capabilities, second only to certain types of spark gap. MOVs give a higher ratio of energy absorbed to energy reflected than conventional spark gaps. Moreover, the energy is absorbed throughout the bulk of the material, rather than being concentrated in a narrow P - N junction

Disadvantages:

1. MOVs have high capacitances, which may make them unusable for protecting RF circuits.

2. MOVs are not very suitable for protecting circuits that operate below about 10 volts. Minimum clamping voltages are on the order of 30 volts. Most MOV clamping voltage applications are over 100 volts, applicable to 28 volt and 115-volt power circuits.

17.4.3 Zener-Type Diodes

This category includes all single-junction semiconductor devices (such as rectifiers) in addition to the Zener-type diodes. While other semiconductor devices, such as PNPN devices and bipolar transistors, may have application as surge arresters, they will not be covered here.

Zener diodes are polarized devices in which an avalanche breakdown occurs when the applied voltage in the reverse-biased direction exceeds the device's specified breakdown (or Zener) voltage. Voltage regulating diodes can be used for surge suppression, but it is better to use diodes specially designed for that purpose, because they have bigger silicon junctions and more massive end caps, which are better for dissipating heat. Some surge suppression diodes are intended only for protecting against surges of one polarity, and act as conventional forward-biased diodes in the other direction. Others are intended for dual polarity, and are, effectively, two diodes connected back-to-back.

The voltage across a diode does not switch to a low value when the diode is conducting but remains at the Zener voltage. This characteristic accounts for a Zener diode’s ability to cease conduction when the voltage falls below the Zener level, but it has a thermal disadvantage. During conduction, the power absorbed by the diode is the product of the current through the diode and the voltage across the diode. The power absorbed for constant current is thus directly proportional to the diode voltage.

Partially offsetting this disadvantage, however, is the fact that surge energy absorbed in the diode cannot be reflected back into the system to cause trouble elsewhere.

Depletion layer

The voltage drop across a diode is concentrated across the narrow depletion layer, and the mass available for absorbing energy is thus very small. Heat must be conducted into the metal end caps and then dissipated through the leads of the diode. For these reasons, diodes have less energy-handling capability than spark gaps and MOVs. As a result, diodes are not the preferable protective device where high transient current, or energy is predicted. For most lightning hardening applications in aircraft, this is not a serious limitation, since the induced surge current levels are in the 1 to 100 A range at those locations where surge suppression diodes are most likely to be used.

Ratings of Zener diodes

Ratings of Zener-type diodes follow a pattern like that used for MOVs. The discussion that follows is illustrated by reference to Bourns diodes [17.6].

Table 17.3 refers to a line of 1 500-watt, bipolar devices in a DO-13 hermetically sealed package [17.6]. (Similar devices are available from other sources and the discussion should not be taken as an endorsement of any particular product. For purposes of design, the manufacturer’s literature should be consulted).

Additional lines of transient voltage suppressor diodes are found at [17.7].

Rated standoff voltage

The *rated standoff voltage* of a Zener diode specifies the voltage below which leakage current is negligible. It corresponds to the *leakage region* discussed for MOVs. One difference between diode rated *standoff voltage* and MOV *leakage region* is that the former is a DC voltage, while the latter is typically rated in terms of Volts-rms for sine-wave excitation.

Breakdown voltage

As with MOVs, the *breakdown voltage* of a Zener diode is the voltage that develops across the device in response to a standard test current (usually 10 mA or 1 mA, DC). The term 'breakdown' does not imply that the device is expected to fail at this voltage but, rather, that conduction through the diode increases significantly above this voltage.

Clamping voltage and peak pulse current

The allowable surges for protective diodes and MOVs are stated somewhat differently. Diodes are specified in terms of a clamping voltage, V_{cc}, at a specified current, I_{pp}. The product of V_{cc} and I_{pp} yields the instantaneous peak power for which the device is rated. One protective diode, commonly used on circuit boards within avionic equipment, is rated at 1 500 watts, based on a surge current of double-exponential waveform that rises to peak in 10 µs and decays to 50% of peak at 1 000 µs. (This is a more conservative rating basis than the 8 x 20 µs surge current waveform used for commercial MOVs.) By comparison, MOVs are rated in terms of total deposited energy. For both protective diodes and MOVs, the specified current waveform used to compute energy dissipation has the 10 x 1 000 µs waveform [17.5].

Instantaneous powers higher than 1 500 watts may be dissipated in a 1 500-watt rated diode if the duration of the surge current is less than 1 ms. Protective diodes are readily available with power dissipation ratings up to 15 000 watts. However, if surge energies of this magnitude are anticipated, it is often better to use MOVs, because they are usually cheaper and physically smaller than equivalently rated diodes. When a protective diode is in its conductive state, the voltage and current through it are related in the same manner as with MOVs:

$$I = kV^{\alpha} \qquad (17.3)$$

The exponent, α, for protective diodes is in the range from 100 - 500, which is higher than for comparable MOVs. Thus, the clamping voltages of protective diodes are more nearly constant with surge current than the clamping voltages of MOVs.

Capacitance

Surge suppression diodes have high capacitances (ranging from several hundred pF to several nF). These values are on the same order as the capacitances of MOVs of comparable current and energy ratings.

Speed of response

Since the non-linear action of protective diodes takes place in the very thin depletion region, the clamping voltage exhibits little dependence on the waveform of the surge current. Theoretical response times of 1 - 5 picoseconds (1 - 5 x 10^{-12} seconds) have been cited, but such times have little meaning, since the performance of protective diodes is governed by inductance of leads, just as with MOVs. Excessive lead length degrades the performance of any protective device. For all practical purposes, MOVs and diodes have the same response time, nearly instantaneous upon arrival of the transient at the device terminals. Overshoots of transient voltage before clamping are the result of lead lengths, and not due to any characteristic of a diode or MOV.

Table 17.3
Specifications for Typical Transient Voltage Suppressor Diodes [17.6]

MAXIMUM RATINGS

Rating	Value
Power dissipation	1500 Watts @ 25°C
$T_{clamping}$ (0 volts to $V_{(BR)}$ min)	Less than 100 picoseconds
Operating temperature	-65°C to +175°C
Steady state power dissipation	1.0 Watts @ T_L = 25°C, ⅜" from body
Repetition rate (duty cycle)	.01%

ELECTRICAL CHARACTERISTICS (T_A = 25°C unless otherwise specified)

Part number	Rated Standoff Voltage	Breakdown Voltage			Maximum Clamping Voltage @ I_{pp} (1 mSEC)	Maximum Reverse Leakage @ V_{RM}	Maximum Peak Pulse Current	Maximum Temperature Coefficient of $V_{(BR)}$
	V_{WM}	$V_{(BR)}$ @ I_T			V_C	I_{RM}	I_{pp}	αV_Z
	Volts	Volts		mA	Volts	µA	Amps	%/°C
		Min	Max					
1N6036	5.5	6.75	8.25	10	11.7	1000	128	0.061
1N6036A	6.0	7.13	7.88	10	11.3	1000	132	0.061
1N6037	6.5	7.38	9.02	10	12.5	500	120	0.065
1N6037A	7.0	7.79	8.61	10	12.1	500	124	0.065
1N6038	7.0	8.19	10.00	10	13.8	200	109	0.068
1N6038A	7.5	8.65	9.55	10	13.4	200	112	0.068
1N6039	8.0	9.0	11.0	1	15.0	50	100	0.073
1N6039A	8.5	9.5	10.5	1	14.5	50	103	0.073
1N6040	8.5	9.9	12.1	1	16.2	10	93	0.075
1N6040A	9.0	10.5	11.6	1	15.6	10	96	0.075
1N6041	9.0	10.8	13.2	1	17.3	5	87	0.078
1N6041A	10.0	11.4	12.6	1	16.7	5	90	0.078
1N6042	10.0	11.7	14.3	1	19.0	5	79	0.081
1N6042A	11.0	12.4	13.7	1	18.2	5	82	0.081
1N6043	11.0	13.5	16.5	1	22.0	5	68	0.084
1N6043A	12.0	14.3	15.8	1	21.2	5	71	0.084
1N6044	12.0	14.4	17.5	1	23.5	5	64	0.086
1N6044A	13.0	15.2	16.8	1	22.5	5	67	0.086
1N6045	14.0	16.2	19.8	1	26.5	5	56.5	0.088
1N6045A	15.0	17.1	18.9	1	25.2	5	59.5	0.088
1N6046	16.0	18.0	22.0	1	29.1	5	51.5	0.090

Series and parallel connection of diodes

Protective diodes may be placed in series with no problems. Diodes in parallel must be carefully matched for voltage, just as with MOVs.

Failure mode

Usually, excessive surge energy causes the semiconducting junction of a diode to melt, so that the device fails shorted.

Advantages of Zener-type diodes:

1. Zener-type diodes are small in size.
2. Zener-type diodes are easy to install.
3. Zener-type diodes have low clamping voltages.
4. Zener-type diodes have low dynamic impedances when they are conducting current.
5. Zener-type diodes are self-extinguishing. When the applied voltage drops below the Zener level, they cease to be conductive.
6. Zener-type diodes have low volt-time turn-ups (impulse ratios).

Disadvantages of Zener-type diodes:

1. Zener-type diodes are not bilateral. To protect against both polarities, two diodes must be connect-ed in a series, back-to-back configuration. Bipolar packages are available.
2. Zener-type diodes have high junction capacitances, which may cause significant signal loss at operating frequencies above 1 MHz Special diode assemblies may extend the useful frequency to approximately 50 MHz
3. Zener-type diodes do not switch between a conducting and a non-conducting state.
4. Zener-type diodes have lower energy capabilities than spark gaps.
5. Zener-type diodes are not available for voltages below about 5 V.
6. Zener-type diodes are not normally available for voltages above a few hundred volts.

17.4.4 Forward-Conducting Diodes

In its forward-conducting state, a germanium diode conducts little current below about 0.3 V, and a silicon diode ceases to conduct below about 0.6 V. Thus, diodes can provide substantial protection if they are placed directly across a low-voltage line. To extend this capability to higher voltage circuits, forward conducting diodes can be connected in series. Forward-conducting diodes in parallel, side-by-side in both directions, would be needed for bipolar protection.

Advantages of forward-conducting diodes:

1. Forward-conducting diodes are small in size.
2. Forward-conducting diodes are inexpensive.
3. Forward-conducting diodes provide protection at very low-voltage levels.
4. Forward-conducting diodes have excellent surge-current ratings because the voltage factor in the power equation is very low.

Disadvantages of forward-conducting diodes:

1. Forward-conducting diodes are not bilateral. For protection of both polarities, two diodes in parallel must be used.
2. Forward-conducting diodes sometimes conduct at normal signal voltages, causing signal-clipping and frequency multiplication effects. Multiple forward conducting diodes must be connected in series to raise voltage levels.
3. Forward-conducting diodes have high capacitances.

17.4.5 Reverse-Biased Diodes

Reverse-biased diodes (as shown in Fig. 17.21) offer excellent protection for signal circuits. Under normal operation the diodes are reverse biased and effectively disconnected from the circuit, but whenever the voltage on the signal line exceeds the power supply voltage the diodes become forward biased (i.e., forward conducting) and allow the surge to be conducted into the capacitors. Since no circuit operates correctly for normal signals exceeding the supply voltage for the input semiconductor circuits, the supply voltage for the protective diodes is automatically of the correct level.

Since reverse-biased diodes have very low capacitance, this configuration is ideal for protecting high-frequency circuits, for which the capacitances of MOVs and Zener-type diodes present problems. When called upon to provide protection, the diodes operate forward biased and even small signal diodes can carry very large surge currents. Some CMOS devices have similar diodes built in, but they are only intended to guard against static electricity and should not be relied on to offer protection against surges. Data supplied by the manufacturers of these devices usually refers to a 'clamping voltage', with no reference to the device's tolerance for surge current. Since the built-in diodes must, of necessity, be very small, only very small currents, of less than 1 A, can usually be tolerated.

Resistors can be used to prevent excessive surge energy from being conducted into the circuit power supply and surge protective diodes can be used to shunt excessive surge energy to ground if the surge charges the capacitors to an excessive voltage.

Advantages of reverse-biased diodes:

1. Reverse-biased diodes have low capacitance.

2. Reverse-biased diodes have excellent surge handling capability.

Disadvantages:

1. Reverse-biased diodes must be included in the initial designs of the circuits in which they are used.

2. It is seldom practical to add reverse-biased diodes to existing circuit boards.

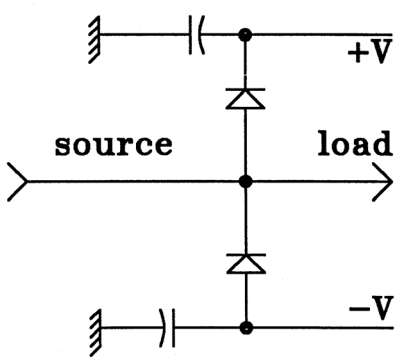

Fig. 17.21 Reverse-biased diodes.

17.4.6 Hybrid Protection

It is common to use a spark gap and an MOV, or an MOV and a surge-protecting diode, together to provide added protection (see Fig. 17.22.). When these combinations are used, the higher energy device should be connected close to the point where the surge enters the system, and the lower energy device should be connected close to the more sensitive components. The principal is that the high energy device provides the primary protection and diverts the major portion of the surge energy while the lower energy device provides protection for the residual transients.

Isolation of protective devices

Protective devices cannot be operated directly in parallel since the device with the lowest clamping voltage would carry all the surge current. Impedance must be added between parallel devices to limit the surge current in the lower energy device and to allow enough voltage to develop to initiate conduction in the high energy device.

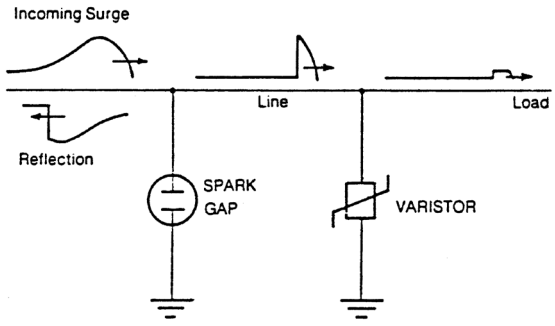

Fig. 17.22 Parallel protectors physically separated.

Physical separation

When an MOV is used in conjunction with a spark gap or a diode, the best protection is obtained if the two devices are physically separated by a considerable distance. For example, large MOVs or spark gaps should be located near exposed electrical apparatus (such as lights and air data probe heaters) and smaller MOVs or diodes installed closer to solid state power controllers or other electronic equipment. This separation is needed so that the interconnecting wires can provide the requisite impedance between the high and low energy devices. Physical separation also minimizes problems associated with inductive voltage rises in grounding connections.

Resistive or inductive isolation

Physical separation is not always possible in aircraft applications. Instead, it may be necessary to add resistance or inductance between the high and low energy devices, as shown in the three-element arrangement of Fig. 17.23. Added inductance may be more appropriate for power circuits, but it has the disadvantage that slowly changing surge currents can still pass into the low energy device without ever developing enough voltage to 'clamp' the high energy device. Resistors are preferable, because the current through the low energy protector can be controlled, irrespective of the surge waveform. However, added resistances higher than one or two ohms may be too high for electric power circuits. (This three-element arrangement is often seen in protectors for ground-based applications but not in aircraft due to component space limitations).

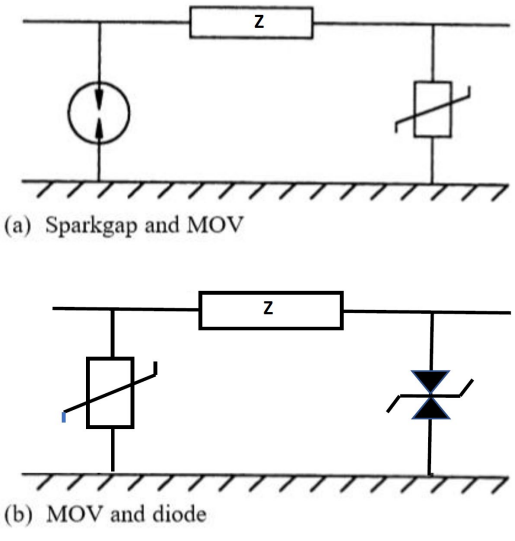

Fig. 17.23 Hybrid protectors.

Commercial availability

Hybrid protectors are commercially available with high and low energy protective devices incorporated into a single package but most (if not all) of these packages are unsuitable for aircraft applications, since they have not been qualified to operate in aircraft environments, or on 115 V-rms, 400 Hz aircraft power circuits.

17.4.7 Surge Protecting Connectors

Several manufacturers of avionics equipment multi-pin connectors offer transient voltage suppression connectors, usually incorporating transient voltage suppression diodes. These are available at wattages of up to 2 500 watts and capable of meeting the environmental requirements for applicable military specifications [17.8 - 17.9]. Some have been originally developed for protection of military electronics from nuclear electromagnetic pulse (NEMP) induced transients which are of shorter duration and lower amplitude than are typical lightning-induced transients.

A disadvantage of these is that if failure of the protection devices for some pins happens, the entire connector may have to be replaced. Some manufacturers offer connectors that allow individual pin/protectors to be replaced.

17.5 Damage Analysis - Semiconductors

The energy coupled into a system by lightning produces large current pulses in wiring and voltage pulses across equipment loads. Determining whether these voltages and currents cause upset or damage to active or passive components requires a knowledge of the failure thresholds of devices. These failure thresholds have been investigated extensively during studies of NEMP effects on electronic equipment. The following sections discuss some of the methods by which damage analysis has sometimes been performed. Typically, this has involved applying transients of increasing amplitude to the device's terminals until failure occurred. Most of these studies involved the discrete semiconductors in use during the cold-war years through the 1980s, when NEMP was of interest to military users.

Since then, the electronics component suppliers have mostly been motivated by ground-based industrial and commercial applications, so there have not been similar investigations of failure modes of more modern integrated circuit devices. For this reason, most of the discussions that follow are based on discrete semiconductors.

For the failure analysis of devices sensitive to thermal effects, one difference between NEMP and lightning analyses must be noted. NEMP vulnerability assessments are mostly made for a single pulse, often of very short duration. However, lightning usually subjects equipment to multiple transients, usually of longer duration, and there is usually more than one transient corresponding to the lightning MS and multiple burst (MB) waveform sets.

Generally speaking, semiconductor devices are more vulnerable to damage under pulse conditions due to permanent failures, than are non-semiconductor devices. This section discusses semiconductor devices. Capacitors and some other components are discussed in §17.6 and §17.7.

It is not necessary for aircraft and equipment designers to conduct analyses of the type described in the following paragraphs as part of the certification process. Instead, these discussions are presented to enable designers to understand basic lightning-induced failure mechanisms. In this manner the need for, and methods of assuring that modern avionics failure possibilities and certification tests are better understood.

17.5.1 Theoretical Models

Theoretical models have been developed that relate significant changes in the properties of a semiconductor PN-junction to the high temperatures generated in the junction region when a high voltage pulse is applied. Theoretical models, based on thermal analysis of the junction region, have been used to define a mathematical relationship between junction temperature and power dissipation in the junction. This relation can be used to define a constant that characterizes the performance of a device in each time domain.

Empirical Models

In addition to the theoretical correlations just described, the experimental data have been used to define empirical relationships based on two models of semiconductor junction device: the junction capacitance model and the thermal resistance model. These models provide a framework from which the power failure threshold of an untested diode or transistor can be estimated from the quantities listed in a data sheet provided by the manufacturer.

17.5.2. Limitations

The assumptions made about junction heating and transfer of heat in the derivation of the models limit their applicability to the region of pulse durations of approximately 0.1 to 20 μs. For longer times, appreciable heat transfer may take place away from the function area during the pulse input. For short pulses, the power levels are so high (1 to 10 kW) that very large currents flow; consequently, the joule heating in the bulk material is appreciable. The transition behavior between these three regions of pulse duration (regions that will be more precisely described later in this section) is not well defined and may vary from one device type to another. Examination of available data indicates the transition region generally occurs between 100 ns and 1 μs.

Still another limitation is fundamental to the work summarized in this section: it applies only to junction burnout. Other modes of device failure, such as metallization burnout and internal arcing, are not treated. Based on the results obtained in studies of junction burnout, other effects, such as metallization burnout, occur at higher power input levels than those input levels sufficient to damage the junction.

17.5.3 Failure Mechanisms-Semiconductors

The two principal breakdown modes for semiconductor PN junctions are the following:

1. Surface damage around the junction because of arcing.

2. Internal damage to the junction region because of elevated temperature.

'Surface damage' is the formation of a high-leakage path around the junction, which effectively prevents the junction from operating. The junction itself is not necessarily destroyed, since, if it were possible to etch the conductive material away from its surface, the device might still be able to operate. Such surface 'etching' is not practical, of course, in a practical semiconductor. In any case, the formation of a surface leakage path implies an operating condition that produces excessive heating in the bulk of the semiconductor material. No amount of cleaning or surface 'etching' would change this.

It is very difficult to make theoretical predictions about the conditions that would lead to surface damage on semi-

conductors because such damage depends on many variables, including physical geometry and details of the crystalline structure of the surface. Also, it is not practical to make predictions about surface arcing under pulse conditions [17.9]. Therefore, it should be cautioned that surface damage on semiconductor devices may occur at power levels that are orders of magnitude below those at which bulk devices (such as MOVs) are damaged [17.10].

Bulk damage, which produces permanent alterations in the electrical characteristics of a junction, is caused by physical changes in the structure of the semiconductor crystal in the region of the junction. The most severe of such changes involves the melting of the junction from excessive temperature rise. Other changes may involve the formation of impurities, the formation of alloys of the crystal materials, or large increases in the number of lattice imperfections (either crystal dislocations or point defects).

Example:

The simplest structure to analyze is a diode, like the one shown in Fig. 17.24. In this diode, a current is assumed to flow because of some outside stimulus. As this current flows, it produces a voltage across the diode, which may be either the forward bias voltage (0.5 to 1.5 V) or the reverse breakdown voltage, depending on whether the outside stimulus biases the diode in the forward or reverse direction. If one assumes that I is a square wave and V is independent of time (which would not be the case if V depended upon the junction temperature), then the instantaneous power dissipated in the diode, as a function of time, would also be a square pulse with a magnitude equal to:

$$P = IV \qquad (17.4)$$

and the total energy dissipated in the diode would be

$$W = \int_o^t P dt = IVt \qquad (17.5)$$

Assume that the power level is sufficient that the device fails at the end of the pulse. Both experimental and theoretical analyses indicate that the power required to cause failure depends on pulse width. The narrower the pulse, the greater the power required to cause failure. Over a broad range of times, typically between 0.1 μs and 100 μs, the power required to cause failure is inversely proportional to the square root of time. For very short pulse durations the power required to cause failure is inversely proportional to time, and for very long pulse durations the power required to cause failure is a constant.

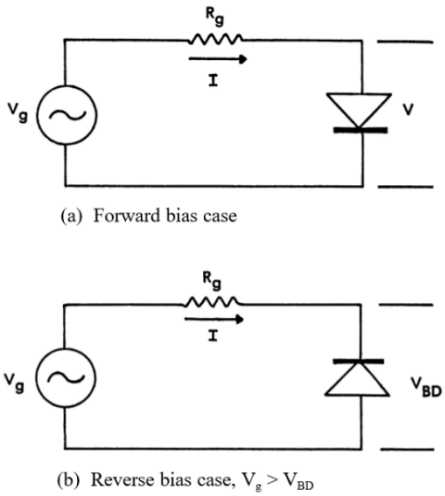

Fig. 17.24 Voltage and current through a diode junction.

These relationships may be expressed by the following equations:

$$Pt = C \qquad t < T_o \qquad (17.6)$$

$$pt^{1/2} = K \quad T_o < t < 100\ \mu s \qquad (17.7)$$

$$P = \text{Constant} \quad t > 100\ \mu s \qquad (17.8)$$

where T_o generally lies between 10 ns and 1 μs. Fig. 17.25 shows an example for a 10 W diode. The most important range or durations is the center range, for which

$$P = Kt^{-1/2} \qquad (17.9)$$

Effects of bias

Junctions are less susceptible to burnout when operated with forward bias. The primary reason for this is that the power dissipated by a given current in the reverse direction is greater than the power dissipated by the same current in the forward direction. An example of failure data for an actual device is shown in Fig. 17.25. The 2N2222 transistor is a 0.5 W NPN silicon high-speed switch.

17.5.4 Damage constants

From curves like those in Figs. 17.25 and 17.26, device-specific damage constants, K, can be defined and tabulated for a range of devices. The K value for a particular device can then be used to plot the damage power threshold-curve of that device.

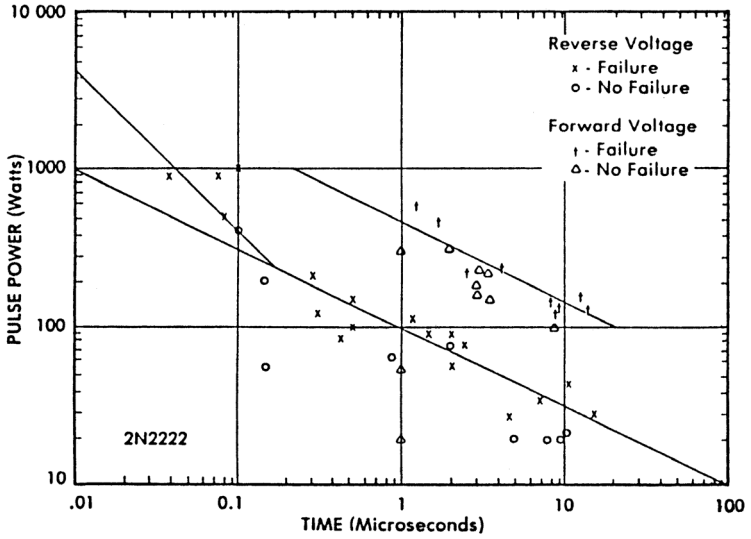

Fig. 17.25 Time dependence of pulse power failure for a 2N2222 transistor [17.11]

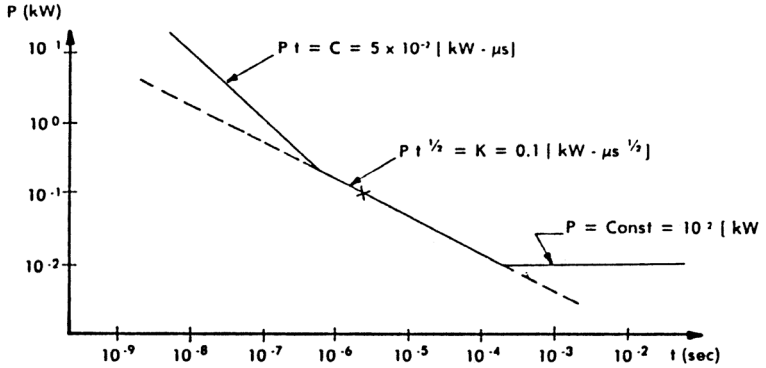

Fig. 17.26 Time dependence of pulse power failure threshold for a 10 W diode [17.9].

It is convenient to derive K in such a way that it is dimensionally equivalent to energy in kW. μs. This sets K equal to the minimum energy a square pulse of 1 μs duration would need to fail the device.

To plot the damage power threshold for a device, simply plot K as a single point on a log-log graph of damage power threshold as a function of duration (Fig. 17.25). Then, draw a straight line with a slope of -0.5 through this point. This line extrapolates the damage power threshold-data for the device. Ideally, the K factor should be known for both the forward-biased and the reverse-biased conditions but, usually, only the K factor for the reverse-biased condition is known. Thus, K factors give conservative of failure thresholds since K for the reverse-biased condition would almost always be lower than K for the forward-biased condition.

The magnitude of the damage constant depends upon the type of junction under consideration. K tends to have a higher value for large junctions than for smaller junctions. Figs. 17.27 and 17.28 show the ranges of the damage constants for some typical diodes and transistors.

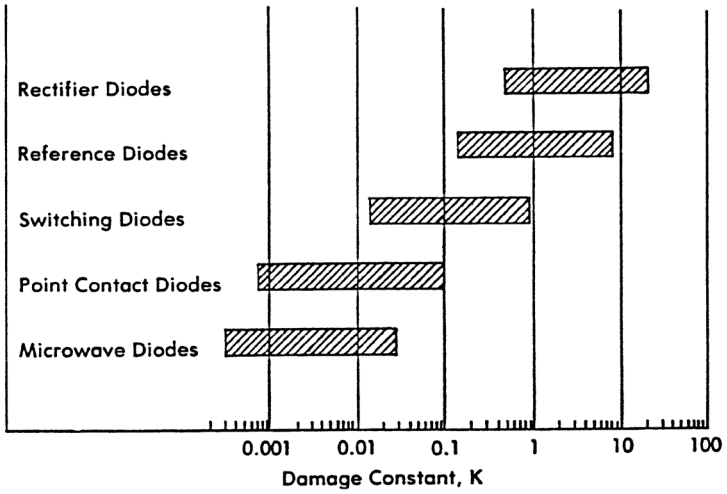

Fig. 17.27 Range of pulse power damage constants for representative diodes [17.12].

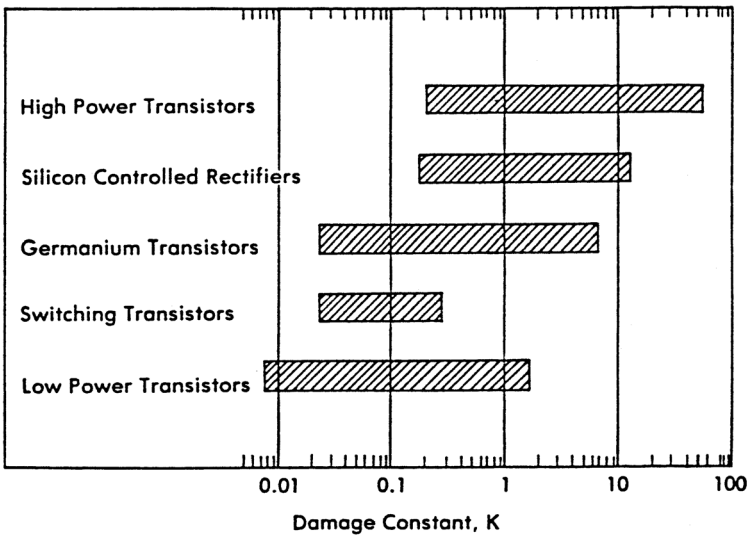

Fig. 17.28 Range of pulse power damage constants for representative transistors [17.13].

17.5.5 Experimental Determination of *K* Factor

K factors can be determined experimentally by injecting current pulses of specific power levels into semiconductor junctions, starting at low power levels and increasing the power until the junction either fails or is significantly degraded. These pulses are normally applied in both the forward and reverse directions.

K factors and breakdown voltages for some representative semiconductors are given in Tables 17.4 and 17.5. The tables are presented as general examples and are not complete.

While such data is available for discrete semiconductor devices and small-scale integrated circuits, it is less likely to be available for large-scale integrated circuits designed for specific commercial applications. The *K* factors listed for transistors generally refer to the failure threshold of the base-emitter junction, since this tends to be the junction most susceptible to burnout. All published *K* factors, whether for diodes or transistors, refer to the reverse-biased condition.

Table 17.4: Typical Diode Damage Data [17.12, 17.14 - 17.16]

Device Number	K	V_{BD}
IN483, A	.3	70.
IN483, B	.3	80.
IN484A	.45	130.
IN484B	.3	130.
IN485	.3	180.
IN486, B	.29	225.
IN487, Z	.3	300.
IN488	.3	380.
IN536	1.	50.
IN537	.51	100.
IN538, M	1.	200.
IN539	1.	300.
IN540	.93	400.
IN547	12.1	600.
IN560	.625	800.
IN561	.625	1 000.
IN562	1.8	800.
IN619	.36	10.
IN622	.347	150.
IN625	.164	30.
IN625A	.045	20.
IN643	.44	200.
IN643A	.1	200.
IN645	2.8	225.
IN646	2.29	300.

Device Number	K	V_{BD}
IN3157	.625	8.4
IN3189	10.	200.
IN3190	4.1	600.
IN3560	.038	.475
IN3561	.038	.475
IN3582A	.35	11.7
IN3600	.18	50.
IN3821	1.947	3.3
IN3828A	1.95	6.2
IN3893	6.41	400.
IN3976	132.	200.
IN4241	33.84	6.
IN4245	2.4	200.
IN4249	2.4	1 000.
IN4312	.116	150.
IN4370A	6.25	2.4
IN4816	6.8	50.
IN4817	6.8	100.
IN4820	10.	400.
IN4823	.208	100V
IN4989	14.33	200.
AM2	1.4	50.
D4330	.001	
FD300	.18	1.25
SG22	.23	
SLD10EC		10 000.

Table 17.5 Typical Transistor Damage Data [17.12, 17.14 - 17.16]

Device Number	K	BV EBO	BV CBO	BV CEO
2N43,A	.28	5.	45.	30.
2N117	.15	1.	45.	45.
2N118	.15	1.	45.	45.
2N128	.017	10.	10.	4.5
2N158	.499	30.	60.	60.
2N176	.46		40.	30.
2N189	.17		25.	25.
2N190	.58		25.	25.
2N243	.05	1.	60.	60.
2N244	.05	1.	60.	60.
2N263	.38	1.	45.	30.
2N264	.36		45.	30.
2N274	.0076	.5	35.	40.
2N279	.047		45.	40.
2N279A	.499	40.	60.	30.
2N329,A	.21	20.	50.	40.
2N332	.45	1.	45.	30.
2N333	.32	1.	45.	30.
2N335, A	.55	1.	45.	30.
2N336	.55	1.	45.	30.
2N337	.12	1.	45.	30.
2N338	.12	1.	45.	30.
2N339	2.0	1.	55.	55.
2N341	1.0	1.	125.	85.

17.5.6 Theoretical *K* Factors, as Determined from Junction Area

K factors may also be calculated [17.13, 17.17]. There are three methods for doing this, the most accurate of which is based on the surface area of the junction. If the surface area of the junction is known, the *K* factor may be estimated from the following equations:

$$\text{Diodes} - K = 0.056\,\text{A} \qquad (17.10)$$

$$\text{Transistors} - K = 0.47\text{A} \qquad (17.11)$$

where *K* is in kW/μs, and *A* is the surface area of the junction in cm^2.

For transistors, *A* should be the area of the base-emitter region because this is generally the weakest junction (lower breakdown voltage) and is, therefore, the junction from which experimental *K* values are determined.

This method described above yields damage constants accurate to within a factor of two, but it requires information about the junction area that may not always be available. For planar devices, the junction area can often be measured directly on the silicon chip.

17.5.7 K Factor as Determined from Junction Capacitance

Another method of calculating damage constants is based on the capacitance C_j and breakdown voltage V_{BD} of the junction. For silicon diodes and all silicon transistors (except for planar and mesa devices) the relationship between these constants is:

$$K = 4.97 \times 10^{-3} C_j V_{BD}^{0.57} \qquad (17.12)$$

For silicon planar and mesa transistors, the equation is

$$K = 1.66 \times 10^{-4} C_j V_{BD}^{0.992} \qquad (17.13)$$

For a base-emitter junction, the capacitance used should be taken at a reverse bias of approximately 1 V. For a collector-base junction or diode junction, the value should be taken at the reverse bias of approximately 5 to 10 V.

17.5.8 K Factor as Determined from Thermal Resistance

The least reliable, way of estimating the damage constant is from a knowledge of the thermal resistance of the junction, either the thermal resistance from junction to case (θ_{jc}) or from junction to ambient (θ_{ja}). For silicon diodes and all silicon transistors (except for planar and mesa devices) empirical equations are:

$$K = 707\theta_{jc}^{-1.93} \left(\theta_{jc} > 10.0\right) \qquad (17.14)$$

$$K = 4.11 \times 10^{4} \theta_{ja}^{-1.7} \qquad (17.15)$$

For silicon planar and mesa transistors, the equations are

$$K = 707\theta_{jc}^{-1.93} \qquad (17.16)$$

$$K = 2.47 \times 10^{5} \theta_{ja}^{-2.55} \qquad (17.17)$$

Normally, θ_{jc} and θ_{ja} are not provided in transistor data sheets. They must be calculated from the maximum operating junction temperature, (T_{jmax}), the total power dissipation (P_d), case temperature (T_c), and ambient temperature (T_{amb}).

$$\theta_{jc} = \left(T_{jmax} - T_c\right)/P_d \qquad (17.18)$$

$$\theta_{ja} = \left(T_{jmax} - T_{amb}\right) \qquad (17.19)$$

Usually, at least one of these thermal resistances can be determined from the manufacturer's data sheet.

The accuracy of the damage constant as determined from either the junction capacitance or the junction thermal resistance is somewhat limited. Table 17.6 gives some estimate of the accuracy within which the damage constant can be calculated.

Table 17.6 Accuracy of K Factors Determined by indirect Methods [17.5]

Device Number	K	BV EBO	BV CBO	BV CEO	Reference Source
T1487	4.5	6.	80.	60.	SP
TIXM101	.01	.3	15.	7.	SP
SW3042	.1	--	--		DX

SP - SAP-1 Computer listing from *SAP-1 Computer Code Manual*, U.S. Air Force Weapons Laboratory, 1972.

DX - Experimental data from DASA (Defense Atomic Support Agency) *Handbook* [17.9]

	Conditions	Accuracy
K_{amb}	$50 < \Theta_{ja} < 200$	Factor of 2
	$200 < \Theta_{ja} < 500$	Factor of 10
	$\Theta_{ja} < 500$	Factor of 30
K_{case}		Factor of 3
K_{cj}	$V_{bd} < 10$	Factor of 30
	$10 < V_{bd} < 200$	Factor of 10
	$200 < V_{bd} < 2\,000$	Factor of 2

K_{amb} = K as determined from Θ_{ja}.
K_{case} = K as determined from Θ_{jc}.
K_{cj} = K as determined from junction capacitance.

17.5.9 Oscillatory Waveforms

Eq. 17.9 assumes that the applied voltage, current, and power waveforms are rectangular. Actual transients are seldom rectangular, but it is possible to derive equivalent rectangular pulses for common transient waveforms.

One common transient waveform is the damped oscillatory wave. Based on multiple pulse studies by Wünsch and others [17.18 - 17.19], it can be assumed that device damage will occur, if at all, during the first cycle of the damped sine wave. Therefore, the lower amplitude cycles may be neglected.

In deriving an equivalent square waveform for a damped sinusoid, two cases should be considered: one in which one of the half cycles of the transient does *not* exceed the reverse breakdown voltage of the junction

(Fig. 17.29) and another in which the reverse breakdown voltage is exceeded (Fig. 17.30). In either case, one of the half cycles biases the junction in a forward direction.

Reverse breakdown not exceeded

Treating first the case in which the reverse breakdown voltage is *not* exceeded (Fig. 17.29) a rectangular waveform of the same peak amplitude, V_0 , and producing the same probability of damage as the sine wave, would have a duration, τ_p , such that

$$\tau_p = \frac{\tau_s}{5} \qquad (17.20)$$

where τ_s is the duration of the first cycle of the sine wave.

Reverse breakdown exceeded

If the transient *does* exceed the reverse breakdown voltage (Fig. 17.30), the duration, τ_p, of the equivalent transient is determined by the time interval during which the oscillatory transient exceeds the reverse breakdown voltage. τ_p is given by the equation

$$\tau_p = \frac{1-(V_{BD}/V_0)^2}{\pi\cos^{-1}(V_{BD}/V_0)}\tau_s \qquad (17.21)$$

This equation is plotted in Figs. 17.31 and 17.32. For oscillatory transients whose initial amplitude considerably exceeds the reverse breakdown voltage of the junction, Eq. 17.15 approaches a limiting value of 0.2, and thus becomes identical to the forward-biased case, Eq. 17.14.

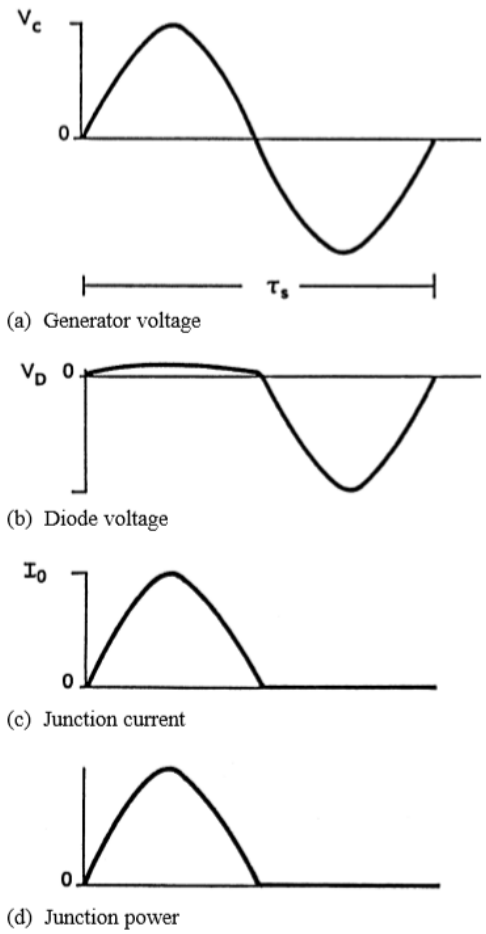

Fig. 17.29 Device waveforms for $V_g < V_{BD}$ [17.20].

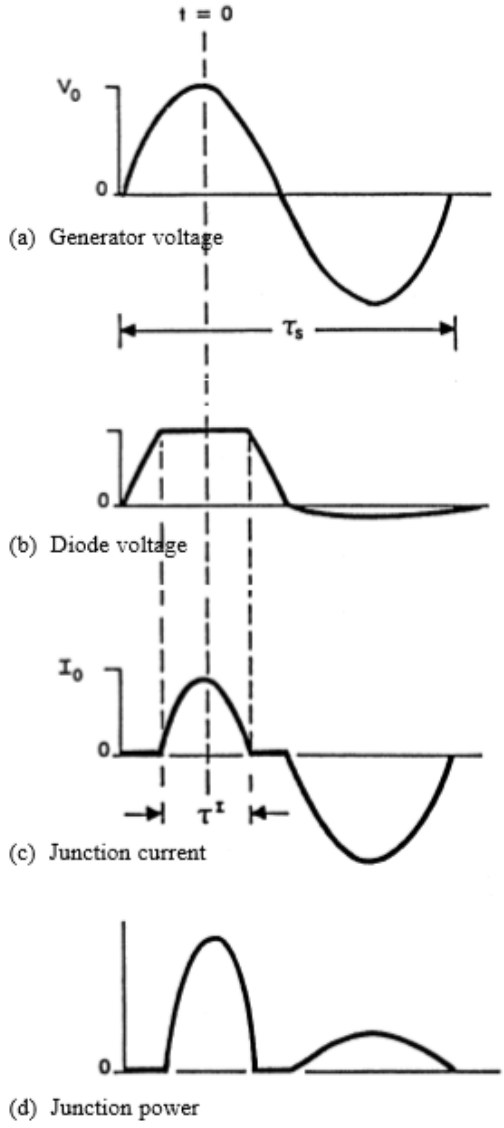

Fig. 17.30 Device waveforms for $V_g > V_{BD}$ [17.21].

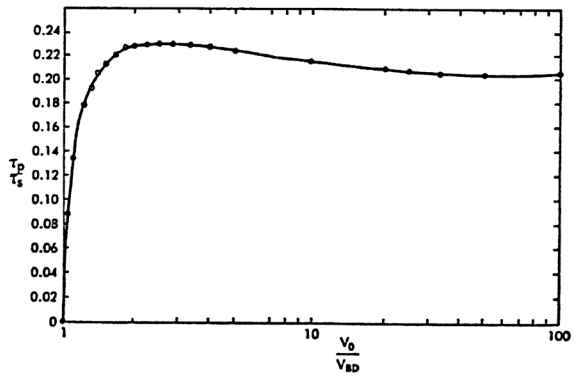

Fig. 17.31 Plot of τ_p/τ_s versus V_0 / V_{BD} [17.22]

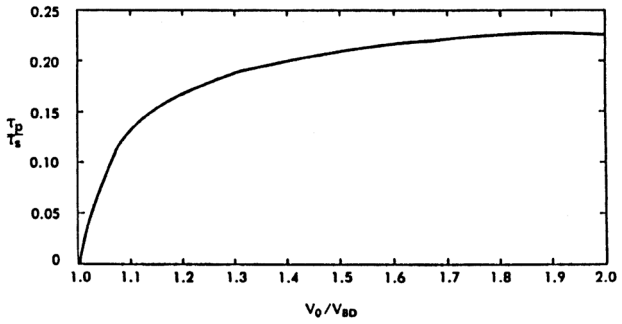

Fig. 17.32 Plot of τ_p/τ_s versus V_0 / V_{BD} for values of V_0 / V_{BD} less than 2 [17.23].

Integrated circuits

A limited amount of data relating voltage and current durations to the breakdown of integrated circuits is shown in Figs. 17.33, 17.34, and 17.35. Figs. 17.33-35 show the results of measurements on SN55107 line receivers, SN55109 line drivers, and CD4050 AE hex buffers, respectively.

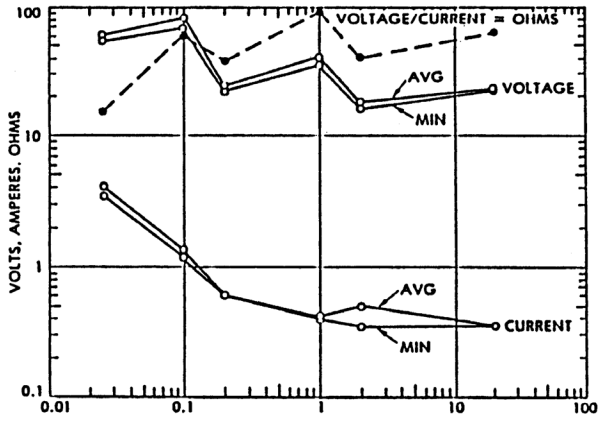

Fig. 17.33 Damage thresholds of SN 55107 line receivers [17.24].

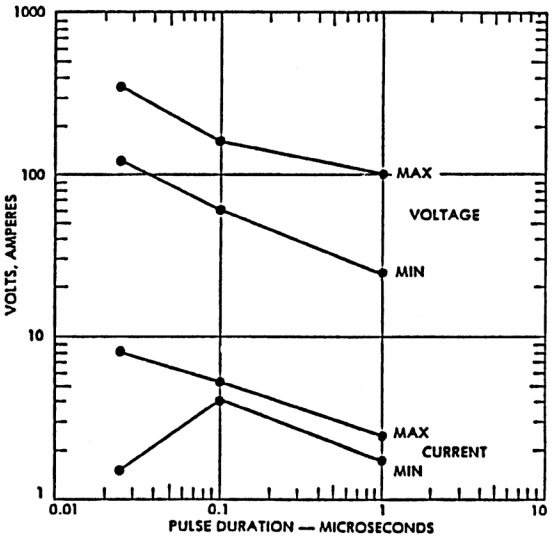

Fig. 17.34 Damage thresholds of SN 55109 line drivers [17.25].

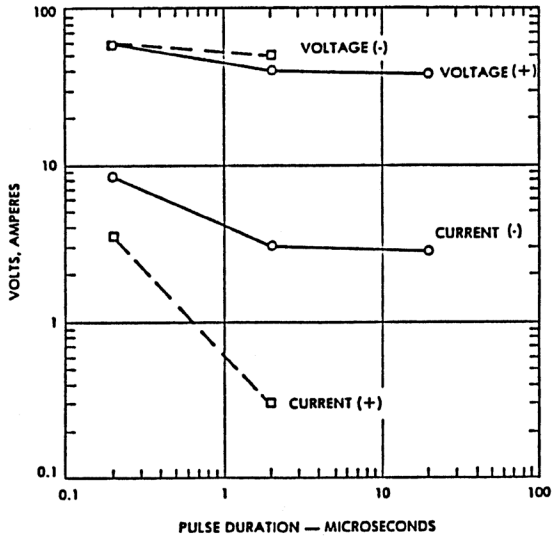

Fig. 17.35 Damage thresholds of CD 4050 AE hex buffers [17.26].

17.6 Failure Mechanisms-Capacitors

Capacitors fail by a different mechanism from that by which semiconductors fail. The failure mechanism of a capacitor depends upon the type of dielectric with which it is made.

Solid dielectrics

The failure of capacitors with solid dielectrics (such as paper, mylar or ceramics) when subjected to a single pulse, is caused by puncture of the dielectric. Some capacitors can withstand short-duration transient voltages of *higher* amplitude than the DC ratings of their insulation, while other capacitors break down at transient voltages *lower* than their DC voltage rating. This inconsistency arises from differences in the distribution of voltage throughout the windings of different capacitors. The pulse-breakdown rating of a capacitor is not directly related to the DC voltage rating, nor is it normally part of any manufacturer's specification. Accordingly, it is safest to assume that a capacitor is in danger of failure if the pulse voltage is close to or exceeds the DC voltage rating. Filter capacitors, and other capacitors that are exposed to lightning-induced transients, should be tested with the applicable standard lightning test waveforms and levels to confirm their ability to tolerate lightning transients.

Electrolytic capacitors

Electrolytic capacitors are not subject to abrupt failure when exposed to short-duration transients. When the voltage across an electrolytic capacitor exceeds that used to form its dielectric film, the dielectric film begins to conduct. Once the pulse has passed, the dielectric returns nearly to its normal state. In fact, the dielectric film can carry substantial transient current without permanent degradation.

However, transients may cause leakage currents through electrolytic capacitors to increase over time. Data is available from a series of tests that were made on tantalum electrolytic capacitors with values of 0.47 μF, 0.047 μF, and 0.0047 μF and DC voltage ratings of 350 V [17.27].

The data indicate that there was a connection between the severity of failure (defined as a substantial increase in the leakage current at voltages of less than 350 V) and the length of the time internal conduction was allowed to persist. For these particular capacitors, leakage began at voltages that were 3 to 4 times the dc voltage ratings. The leakage current increased continuously with time, beginning at a few nanoamperes and increasing to milliamperes.

Of course, the value of the capacitor determined how quickly the applied voltage reached the breakdown level (90 to 140 V), which, in turn, determined the duration of the conduction and the extent of the damage. Fig. 17.36 shows the data for the nine 0.0047 μF capacitors that were tested. Voltage pulses of 100 to 150 V with 5 μs durations produced leakage current. If the amplitudes of these pulses were increased to between 150 and 200 V, leakage currents in the milliampere range were measured. It should be noted that these results may not be readily extended to capacitors of different materials or construction.

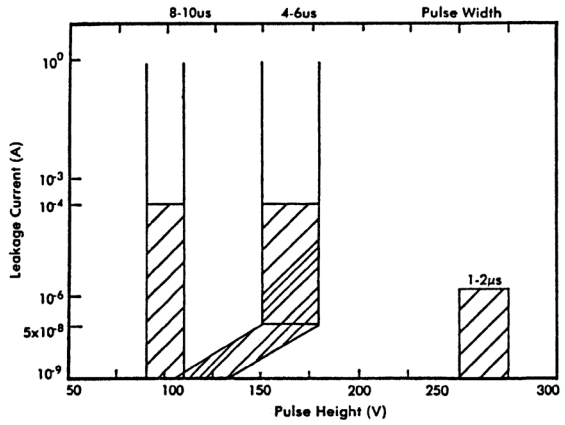

Fig. 17.36 Pulse data for 0.0047 mF tantalum electrolytic capacitors [17.28].

17.7 Failure Mechanisms-Other Components

A limited amount of pulse test data is available for various non-semiconductor electronic circuit components. These data were mostly obtained by tests that utilized square-wave pulses of 1 to 10 μs duration with amplitudes that ranged up to 1 kV. As would be expected, not all components are invulnerable to pulses of this shape. Sample test results for several types of components are given in Table 17.7. These data were obtained by applying a 8 μs, 1 kV pulse 10 times to each device. In the case of multi-terminal components, several pairs of terminals were tested in this manner.

Table 17.7 Damage Test Results for Non-semiconductors [17.14]

Device Type	Manufacturer	Manufacturer's Part Number	Properties	Test Results
Capacitor	Cornell-Dubier	C100K	10 pF	No change in capacity or leakage resistance
Capacitor	Cornell-Dubier	CK62 Series	470 pF, 500 Vdc	
Capacitor	Sprague	96P Series	1 μF, 200 Vdc	
Capacitor	WES CAP	KF223KM	0.022 μF, 600 Vdc	
Coil	Collins	240-2524-00	220 μH	No change in inductance or resistance
Coil	Collins	542-0916-002	2 μH 10^3 Hz	
Filter	Bundy	21-0526-00	Notch 400 and 1200 Hz	No change in frequency response.
Filter	Varo	954-0429-400	Bandpass 400 Hz	
Potentiometer	Computer Insts.	M18-178105	400 Ω	No changes
Potentiometer	Ohmite	51927-1	250 Ω	
Potentiometer	Ohmite	51927-3	25 Ω	
Relay	Babcock	RP11573-G2	Armature	Resistance increase:
				625 Ω > 629 Ω
Relay	C.P. Clare	A5245-1	Armature	Resistance increase:
				418 Ω > 524 Ω
Relay	Hathaway	63862	Magnetic Reed	Resistance increase: 25%
Relay	Potter Brumfield	FLB4002	Magnetic Latching	Resistance decrease: < 1%
Relay	Struthers Dunn	FC6-365	Armature	No changes
Transformer	Dektronics	D78Z222	Audio Frequency	No changes in resistance or voltages, no arcing during pulse
Transformer	Dektronics	D78Z225	Power, Isolation	
Transformer	Freed	667-0386-00	Audio Frequency	
Transformer	Varo	950-1622-200	Power, Isolation	
Transformer	Varo	999-0197-200	Power, Isolation, Stepdown	

17.8 Examples of Use of Damage Constants

This section describes some examples of semiconductor installations in practical circuits. Each example will be used to demonstrate how the damage susceptibilities of semiconductors can be assessed.

Relay

The first example (Fig. 17.37) is a simple remote-controlled relay. Across the terminals of the relay coil there is a diode that would be exposed to the same transients as those to which the coil is exposed.

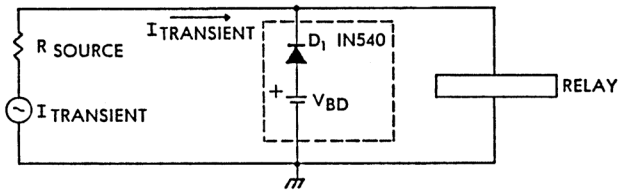

Fig. 17.37 Simple remote-controlled relay [17.15].

Analyzing the susceptibility of this diode to damage involves, first, calculating the current level that would cause the diode to fail and, second, assessing whether or not the transient voltage source could supply that current. It will be assumed that the transient voltage is an oscillatory pulse with a frequency of 1 MHz ($\tau_s = 1$ μs). At this frequency, the inductive reactance of the relay coil is large enough that the relay can be neglected.

The current required to fail the diode at time, *t*, would be

$$I_f = \frac{P_f}{V_{BD}} = \frac{Kt^{-1/2}}{V_{BD}} \qquad (17.22)$$

For a 1N540 diode, the reverse breakdown voltage, V_{BD}, is 400 V and the damage constant, *K*, is 0.93 (see Table 17.4). If a 200 ns pulse is used to approximate the 1 MHz voltage transient, the failure current for the diode would be

$$I_F = \frac{0.93(2\times10^{-7})^{-1/2}}{400} = 5.2A \qquad (17.23)$$

Assume, now, that the impedance of the source from which the voltage transient was generated is 10 ohms. The voltage required to drive a current of 5.2 A through the diode would be

$$V_{Transient} = V_{BD} + I_{Transient}R_{Source}$$
$$V_{Transient} = 452\ V \qquad (17.24)$$

Therefore, a single, square, 452 V pulse, 200 ns wide (or a 1 MHz damped sine wave with a peak amplitude of 452 V) would cause the diode to fail.

Phase splitter

The second example is the simple phase-splitter amplifier shown in Fig. 17.38. The first step in determining the input current required to damage this amplifier is to simplify the circuit. Again, assume that the transient voltage is a 1 MHz damped sine wave. At such a frequency, the reactances of capacitors C_1 and C_2 are so small that they may be neglected. Likewise, the 12-V operating voltage of the power line can be assigned a zero-reference potential.

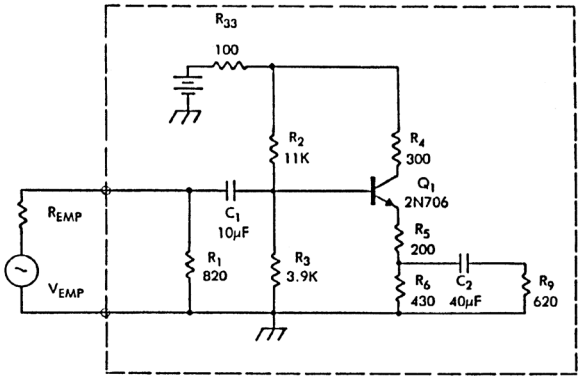

Fig. 17.38 Phase-splitter circuit [17.16].

After simplification, the circuit looks like Fig. 17.39.

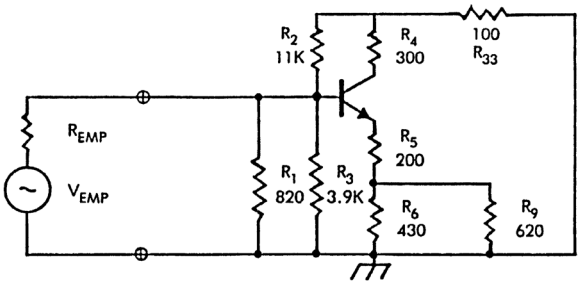

Fig. 17.39 Simplified phase-splitter circuit [17.29].

It can be further simplified by determining the equivalent resistances for the base and collector circuits. The base-emitter junction and the base-collector junction can also be replaced by their diode equivalents, to represent operation at breakdown voltages. This further simplification of the circuit is shown in Fig. 17.40 which also shows the breakdown voltages and damage constants for the 2N706B. Note that, for this transistor, a damage constant has been provided for the collector-base junction, although this constant is not listed in Table 17.5.

The circuit is now simplified enough that it lends itself easily to hand analysis. The next step is to predict which junction will fail and what the failure mode will be. Passive components are generally able to withstand higher energies from short-duration pulses than transistors can. It makes sense, therefore, that the transistor is the element under consideration. For this analysis, it will be assumed that failure of the transistor will occur in the reverse-biased direction.

Using the Wünsch damage model ($P = Kt^{-1/2}$), a calculation is made to see whether the emitter-base junction or the collector-base junction would fail first.

$$P_{EB} = K_{EB}t^{-1/2} = 17W \qquad (17.25)$$

$$P_{CB} = K_{CB}t^{-1/2} = 130W \qquad (17.26)$$

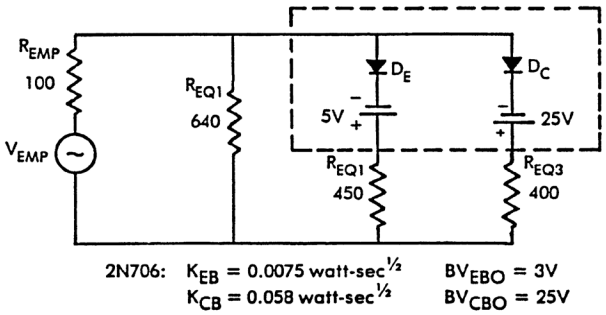

Fig. 17.40 Further simplification of phase-splitter circuit [17.29].

This calculation shows that the emitter-base junction is the more susceptible of the two. The current required to fail the emitter-base junction would be:

$$I_jF = \frac{P_{EB}}{V_{ED}} = 3.4A \qquad (17.27)$$

The voltage from the base to the zero-reference potential is

$$V_{BASE} = BV_{EBO} + I_{jF}R_{EQ2} = 1.5\text{ kV} \qquad (17.28)$$

The current through the collector-base junction is

$$I_{CD} = \frac{V_{BASE} - BV_{CBO}}{R_{EQ3}} = 3.7\text{ A} \qquad (17.29)$$

The power dissipated in the collector-base junction is

$$P_{CB} = BV_{CBO}I_{CB} = 93W \qquad (17.30)$$

which is below its failure-threshold power. The total current into the circuit is then

$$I_{Transient} = I_jF + I_{CB} + \frac{V_{base}}{R_{eq1}} \qquad (17.31)$$

and the $I_{Transient}$ voltage required to cause failure is

$$V_{Transient} = V_{BASE} + I_{Transient}R_{Source} = 2.5\text{ kV} \qquad (17.32)$$

Therefore (assuming a 100 Ω source impedance) a 2.5 kV 200 ns pulse, would cause the transistor to fail.

References

17.1 http://www.novaris.com.au/images/stories/Sales%20Kit/SK10/Spark%20Gap%20Surge%20Protectors.pdf

17.2 *Littlefuse™ Varistors - Basic Properties, Terminology and Theory* Application Note July 1999 N9767.1,https://www.galco.com/techdoc/lf/tmov20rp200m_inf.pdf

17.3 W. Schmidt et al, "Behavior of MO-Surge Arrester Blocks to Fast Transients", *IEEE Trans. on Power Delivery*, Vol. 4, No. 1, January 1989, pp. 292-300.

17.4 C. Dang, T. M. Parnell, P. J. Price, "The Response of Metal Oxide Surge Arresters to Steep Fronted Current Impulses", *IEEE Trans. on Power Delivery*, Vol. PWRD-1, No. 1, January 1986, pp. 157-163.

17.5 *Transient Voltage Suppression Manual, Fifth Edition*, Semiconductor Business Division, General Electric Company, Electronics Park, Syracuse, New York (1987).

17.6 Digitron Semiconductors 1N6036-1N6072 *Transient Voltage Suppressors* Rev 20161228.

17.7 Vishay Product Pages https://www.vishay.com/transzorb

17.8 Carlyle Transient Protection Connectors https://www.carlisleit.com/products/connectors-accessories/transient-voltage-suppression/

17.9 *DNA EMP (Electromagnetic Pulse Handbook, Vol. 2, Section 13: Analysis and Testing,* DNA 2114 H-2, Defense Nuclear Agency, Washington, D.C. (November 1971).

17.10 H. S. Velorie and M.P. Prince, "High-Voltage Conductivity-Modulated Silicon Rectifier", *Bell System Technical Journal*, July 1957, pp. 975-1004.

17.11 DNA EMP Handbook, ibid. pp. 13-34.

17.12 DNA EMP Handbook, op. cit., pp. 13-53.

17.13 *EMP Susceptibility Threshold Handbook, (Appendix D)*, prepared by the Boeing Company for the U.S. Air Force Weapons Laboratory, Kirtland Air Force Base, Albuquerque, New Mexico (July 21, 1972).

17.14 DNA EMP Handbook, op. cit., pp. 13-100.

17.15 EMP Susceptibility Threshold Handbook, *op. cit*., pp. 144.

17.16 EMP Susceptibility Threshold Handbook, *op. cit*., pp. 146.

17.17 *EC-135 Pretest EMP Analysis*, I, BDM/A-701-705, prepared by Braddock, Dunn and McDonald, Inc., for the Air Force Special Weapons Center, Albuquerque, New Mexico (March 1971).

17.18 J. B. Singletary and D.C., "BDM Final Report, Semiconductor Damage Study, Phase II", Report BDM/A-66-70-TR, prepared by Braddock, Dunn and McDonald, Inc., for the U.S. Army Mobility Equipment Research and Development Center, Fort Belvoir, Virginia (April 1969).

17.19 D.C. Wünsch and L. Marzitelli, "BDM Final Report, Semiconductor and Non-semiconductor Damage Study, I", Report BDM-375-69-F-0168, prepared by Braddock, Dunn and McDonald, Inc., for the US Army Mobility Equipment Research and Development Center, Fort Belvoir, Virginia (April 1969).

17.20 EMP Susceptibility Threshold Handbook, *op. cit*., pp. 212.

17.21 EMP Susceptibility Threshold Handbook, *op. cit*., pp.2.

17.22 EMP Susceptibility Threshold Handbook, *op. cit.*, pp. 223.

17.23 EMP Susceptibility Threshold Handbook, *op. cit*., pp. 224.

17.24 E. Keuren, R. Hendrickson, and R. Magyarics, "Circuit Failure Due to Transient-Induced Stresses", *First Symposium on Electromagnetic Compatibility*, Montreux, Switzerland, May 20-22, 1975, IEEE EMC Conference Record 75 CH10124, Institute of Electronic and Electrical Engineers, New York, New York (1975), pp. 500-505.

17.25 Keuren, Hendrickson, and Magyarics, "Circuit Failure", *ibid*., pp. 504.

17.26 Keuren, Hendrickson, and Magyarics, "Circuit Failure", *op. cit.*

17.27 DNA EMP Handbook, *op. cit*., pp. 13-19 to 13-101.

17.28 DNA EMP Handbook, *op. cit*., pp. 13-101.

17.29 EMP Susceptibility Threshold Handbook, *op. cit.,* pp. 148.

Chapter 18

TEST TECHNIQUES FOR EVALUATING INDUCED EFFECTS

18.1 Introduction

Since the introduction of digital 'Fly by Wire' flight and engine control systems into commercial transport aircraft in the early 1980's, there has been a need to ensure reliable operation of these systems in the lightning environment. Lightning-induced transients may damage electronic devices that operate on low power signal voltages. The multiple stroke (MS) and multiple burst (MB) environments have the potential of introducing error signals into data processing and control functions. Similar concerns apply to integrated cockpit displays that depend upon digitally processed data.

Engineering definitions of the MS and MB environments were introduced into the airworthiness certification standards in 1985 and updated in the 1990s, and methods of generating and injecting MS and MB – induced transients into control and display systems have been developed. These tests must be applied to an operating system, so the test involves transformer coupling or direct injection of the transients into the case(s) of one item of equipment, so the transients can flow throughout an interconnected system. Standard methods for injecting single-pulse transients have been incorporated in Section 22 of RTCA DO-160 and EUROCAE ED-14 [18.1] for some years and, in 2002, a procedure for injecting multiple pulse transients corresponding to the MS and MB environments was added to these standards. However, these standards apply only to tests of a single cable connected to a single item of equipment, and so do not provide guidance for applying MS and MB transients to a complete system comprised of multiple "boxes" and cables. Since the lightning environment induces transients into all cables of a system simultaneously, ways must be found to induce test transients for system lightning tests in a similar manner, or to otherwise account for the effects of simultaneously induced transients. The standards for these tests are SAE Aerospace Recommended Practice (ARP) 5416 [18.2] and EUROCAE ED 105 [18.3]. The US and European standards are identical. Reference 18.1 contains *equipment* test standards and therefore does not include standards for testing systems – a fact that is often lost to users, who sometimes try to use instructions in these standards for testing of systems. Manufacturers of aircraft equipment are sometimes not aware of the existence of the aircraft lightning standards [18.2] that contain the standards for lightning tests of aircraft systems. All of the test standards employ the standard voltage and current waveforms [18.3].

This chapter describes the general test techniques for the evaluation of lightning induced effects on electrical and electronic equipment and systems. Tests that are performed on individual pieces of electronic equipment or upon interconnected electronic systems are described. There are standards that provide detailed instructions for tests of individual equipment and systems. It is not the purpose of this chapter to repeat these instructions. Users should always follow the latest versions of the standards when conducting these tests. Rather, this chapter explains some of the commonly misunderstood aspects of the tests, and (especially for system testing) describes how the tests may be extended or modified to achieve objectives or conditions not fully covered by the standards. As always, test plans should be prepared for individual tests, and reviewed and approved by certifying authorities or their representatives.

In the paragraphs that follow, and in some of the standards, the term *equipment* is replaced *by* EUT (equipment under test).

18.2 Equipment Damage Tolerance Tests

Equipment-damage tolerance tests should be conducted using the pin-injection method, wherein transients are injected directly into equipment connector pins, one by one to verify ability of the equipment to tolerate the specified transient voltages and currents, in accordance with the equipment transient design levels (ETDLs) that have been assigned to the equipment. Therefore, most of this section is a discussion of this test method. The equipment test standards include a cable bundle test that is sometimes used for assessing damage tolerance, but this is not a reliable method of verifying ability of equipment to tolerate lightning-induced transients without damage. The equipment cable bundle test is more appropriate for evaluating equipment upset possibilities, as will be discussed later in this section.

Direct injection of induced voltages and currents transients into the input and output terminals of equipment (Fig. 18.1), is an appropriate way of determining whether the equipment will be damaged by transients, but it is generally not an appropriate method of testing for equipment (or system) upset, since only one pin of an equipment connector is tested at a time. The standards for conducting *damage tolerance tests*, also known as *pin injection tests*, are [18.1]. In other words, the damage tolerance tests verify the ability of equipment to tolerate the assigned ETDLs, as defined in Chapters 5 and 16.

As noted above, a second kind of test, also included in [18.1] has the transients directly injected or transformer coupled into a section of interconnecting cable (also called cable bundle) that is plugged into an equipment connector. The idea is that transients are caused to appear simultaneously in all conductors within a cable and therefore more closely represent what happens to equipment when installed in a system within an airplane that is struck by lightning. The problem with this approach is that no attempt is (or practically can be) made to control the amount of voltage or current that appears in any single conductor or equipment connector pin. The total cable bundle current (or voltage) is specified in the test standard and controlled. Accordingly, no assurance can be gained from this test that the circuitry within the equipment can withstand any specific amount of transient voltage and or current. This test approach, called the *equipment cable bundle test* is often preferred over the pin injection test because it can be more easily withstood (i.e., passed) than can the pin injection test. ETDLs may also be assigned to cables plugged in to equipment connectors. In some cases, the cable bundle ETDL voltages will be the same as the individual pin ETDLs, but the cable bundle ETDL currents will always be higher than the pin ETDL currents since the cable is expected to contain more than one conductor.

Cable bundle tests are useful for the *equipment upset test* which is applied to evaluate the susceptibility of an operating piece of *equipment* to tolerate the induced effects of the lightning MS and MB environments without system functional upset. Discussion of this test is the subject of §18.3.

For the equipment damage tolerance test the pin injection method is used. A simple illustration of this method is shown in Fig. 18.1.

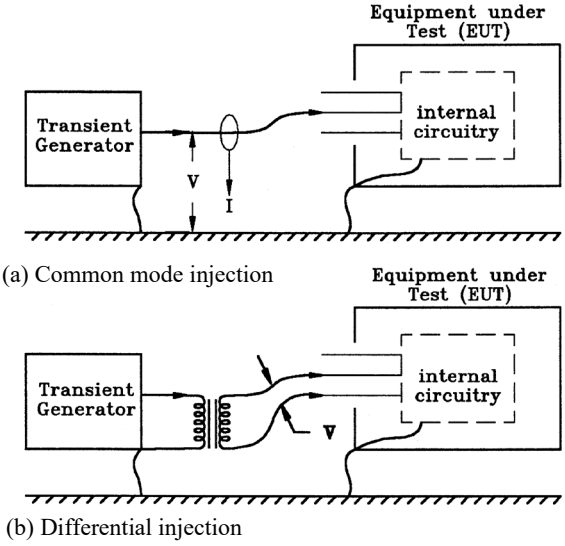

(a) Common mode injection

(b) Differential injection

Fig. 18.1 Pin injection tests

The 'pin test' (as it is commonly called) is most commonly applied between individual equipment connector pins, one by one, and equipment chassis ground (Fig. 18.1(a)). The reason for this is that the highest amplitudes of voltage and current transients are almost always appearing between cable conductors and airframe ground. This is known as the common-mode condition. The test standards assume that this is how the tests are to be applied, however in some less frequent situations, where conductors reaching a pair of connector pins are coming from different parts of an airplane, it is more appropriate to apply the test differentially, as shown in Fig. 18.1(b). It is therefore important for those preparing pin test plans to be aware of the routing of wires to/from the equipment to be tested. A simple example of differential wiring would be 28 VDC wires routed from a power control-unit connector to position lights on opposite wing tips.

Pin injection tests involve injection of transients defined by the open circuit voltage (V_{oc}) and short circuit current (I_{sc}) available at the output terminals of the transient generator. Care must be taken in equipment test specifications to avoid wording that can be interpreted as requiring a specified voltage to be developed across an equipment connector pin that is shorted to ground or requiring a specified current to flow into a pin that presents an open circuit or high impedance.

The voltage and current that actually appears at a tested pin depends on the equipment impedance (usually to ground) at that pin. Low impedances (typically less than 50 ohms at 1 MHz) will allow some measurable current to enter the tested pin, whereas higher impedances will allow most of the applied voltages to appear between the pin and chassis ground.

The pin test generator is intended to behave like a voltage circuit, where the source impedance is either 5 ohms, 25 ohms, or 100 ohms. These impedances are intended to represent typical aircraft circuit impedances, as viewed from an equipment pin looking out into the aircraft conductor with the remote end of the aircraft circuit imagined to be shorted to airframe ground. The remote end grounded condition is set to imagine a worst case in which the remote end equipment is equipped with line-to-chassis ground protection devices that switch to a near-zero impedance state when a lightning-induced transient is present.

The 5 ohm generator source impedance represents the combination of loop inductance and resistance under low frequency conditions (<1 MHz) of an aircraft conductor. This impedance relates unipolar voltage and current transients (i.e., transient Waveforms 2 and 1, and Waveforms 4 and 5, as defined in Chapter 5).

The 25-ohm and 100-ohm impedances represent the range of characteristic impedances of the transmission line formed between a cable bundle (or an individual conductor in a cable bundle) and the airframe. This impedance relates the traveling wave voltages and currents (i.e., voltage waveform 3 and current waveform 3).

Equipment Conditions

Pin injection tests are performed to verify the ability of equipment to tolerate the ETDLs assigned to them. How the tests stress internal components depends on several factors, but two generic configurations predominate: ungrounded equipment and grounded equipment.

Ungrounded equipment: An ungrounded pin test configuration is illustrated in Fig. 18.2. The case of the EUT is grounded to the test bench, but the electrical circuits inside are not grounded to the chassis. Usually, the circuitry is grounded at some other location within the airplane. The standards recommend that if an EUT is configured as in Fig. 18.2 and the ground pin is to be connected to an airframe ground within 1 m from where the EUT is to be installed, then the EUT ground pin is to be grounded locally to the test bench and the EUT is to be tested as if it were internally grounded. Otherwise, the standards say to ground the case of the EUT to the test bench locally. The

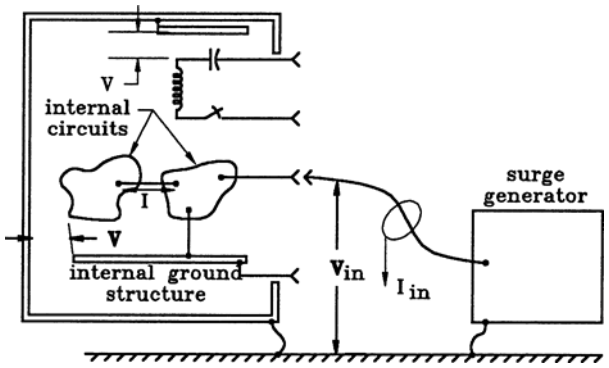

Fig. 18.2 Pin injection on an ungrounded equipment

EUT is to have all cables disconnected except the pin that receives power.

The EUT should be powered if it contains any devices that change state when powered as in flight. In other words, the EUT should be in as close as possible a state as when in flight.

Equipment such mechanical switches that do not require power to operate and will not itself receive power in flight, can be tested with no power applied. If signal or operating voltages at this EUT exceed 10% of the pin test voltage this signal voltage should be applied since it could influence whether or not the EUT passes the test.

The standards state that the pin test generator must be verified to produce the specified open circuit voltage (V_{oc}) and short circuit current (I_{sc}), waveforms, and amplitudes that are specified for the test. These are to be achieved with the same generator settings, without the EUT connected to the generator. Then, without changing the generator settings, the generator is to be connected between the designated pin and the chassis. The test is to be applied at the same generator settings. Since the EUT circuitry is ungrounded, the open circuit voltage will be recorded between the pin and chassis. If a pin-to-chassis failure happens the voltage will collapse, and the short circuit current will flow. This will be indicated on oscillograms of the applied voltage and current. Fig. 18.1 shows two situations within an EUT where breakdowns might occur.

Each application of a pin test represents the effects of one lightning stroke to the aircraft arriving at the tested connector pin on the EUT.

If no breakdown happens the usual test plan requires that ten positive polarity transients be applied followed by the same number of negative polarity tests. Once set, the charging voltage level of the generator should remain

fixed for all tests at that nominal level. These multiple tests are usually to be applied within one minute of each other and are not to be confused with the MS environment, where fourteen transients would have to be applied within 1.6 seconds.

Familiarity with EUTs

It is always important for test technicians to become familiar with the nature of the circuits and devices within the EUT. It is sometimes necessary to close switches or relays to connect internal circuit components to the pins of the connector under test. Temporary wiring across relays and switches that are open when the equipment is tested alone but closed when the equipment is operating in the aircraft is allowable.

It is also important to know what voltages may be present at each connector pin since some test generators have low source impedances that may draw excessive current from such pins and cause damage to the EUT. Pin injection tests should never be applied to equipment without knowing the functions and voltage status of each pin to be tested.

Internal connections between some connector pins may make some of the tests redundant but connecting all pins together and applying the transients to all pins simultaneously is not generally permissible, except for very simple circuits.

The applied voltage and current are to be applied to each pin, one at a time. Voltage at the tested pin should be recorded at least once during each series of ten tests. Some test plans require that the transients be recorded twice, so the first and last of each series of 10 transients are recorded. All the applied voltages and currents at each tested pin are to be monitored by the test technician for signs of changes in waveshape that may be due to partial or full breakdown. Fig. 18.3 shows examples of pass and fail pin tests where applied voltages and currents were monitored and recorded.

For ungrounded EUTs, current should be small unless breakdown of insulation takes place, and voltages should not be greatly different from the generator open circuit voltage. This observation does not apply to circuits fitted with protective devices or filters.

Permanent records should be made of the initial magnitudes and waveforms but making permanent records to document each applied pulse would probably be superfluous unless breakdown is observed.

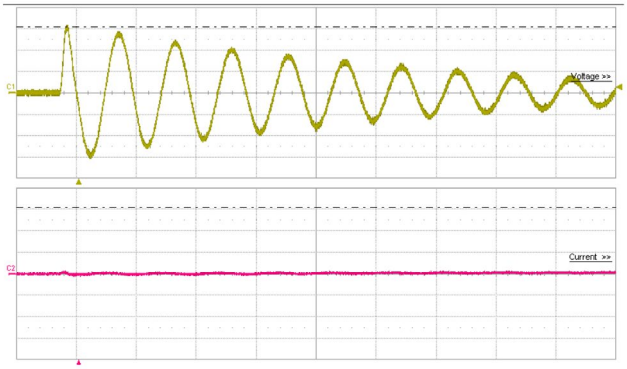

Upper Trace: Voltage. Lower Trace: Current. Pin has withstood the voltage

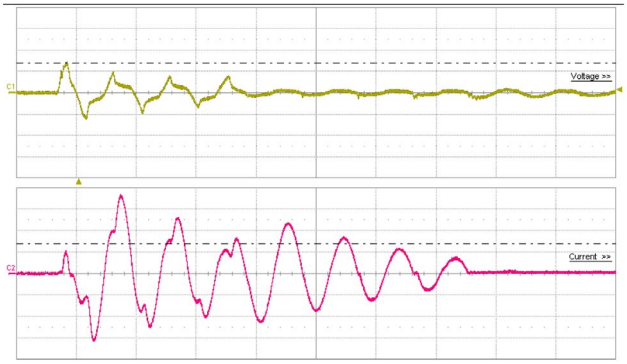

Upper Trace: Voltage. Lower Trace: Current. Pin has failed

Fig. 18.3 Examples of Pin test 'Pass' and 'Fail'. EUT was grounded to chassis

After the test has been completed, performance checks are to be conducted on the EUT to confirm that operation is normal and, if not, any abnormalities are to be recorded.

Number and polarity of applied transients

The number and polarity of the pulses applied in a pin test should be stated in the test plan. For example, [18.1] requires that each pin receive 10 pulses of each polarity for each of the specified test waveforms. This is the consensus of testing laboratories and certifying authorities.

Ungrounded system pin tests are most commonly conducted by applying common mode voltages. This simulates the condition where all wires entering the EUT originate at a common point. Essentially, this stresses the insulation between circuit elements and the case with the voltage, V, illustrated in Fig. 18.2. Some capacitive current (I_{IN} in the same figure) may flow through internal circuit components, but this current is small because there is no direct connection to the EUT chassis and the return terminal of the generator.

Direct current (DC) and low frequency hi-pot testing

Before conducting pin testing, an evaluation should be made of the possible failure modes of the EUT. In many cases, it may be unnecessary to test the EUT with all the waveforms specified in the test standard. Eliminating some of these waveforms may save unnecessary work and expense. In some cases, conventional DC, and low frequency high potential ('hi-pot') tests may be all that is actually needed, particularly if only electro-mechanical devices are involved. This option is useful and acceptable for simple electrical devices like switches and lamps. However, it is not applicable for other EUTs that include inductive components like motors, generators, and relays. The high inductances and capacitances of these devices will assure that the responses of them to lightning-induced transients will be different than their responses to DC and power frequency voltages. In particular, transient voltages may excite traveling wave oscillations with the inductive devices that may reach twice the amplitude of the applied test voltage. EUTs that have passed DC hi-pot tests have often failed transient tests.

Grounded Equipment: The grounded system pin-test configuration is illustrated in Fig. 18.4. Note that the internal ground circuits are grounded as well as the case. The ground connection may either be made internally (path A) if that is the normal mode of connection, or externally (path B). If path A is normally the only ground path, then the tests should include injecting transients onto the ground pin, to determine whether the internal ground path is capable of carrying the transient current. An external ground connection from the ground pin to the test bench as in path B should be applied only after tests on the ground pin have been made.

An external ground connection should normally be made directly from the EUT chassis (or from the EUT rack if that has been provided) to the test bench as shown in Fig. 18.4.

If the EUT is not intended to be grounded locally to the airframe (a condition that may exist when the airframe is fabricated of composite material) a grounded pin is provided for connection to a remote ground point. In such situations the EUT is usually tested as an ungrounded unit and the ground pin is tested as if it were like any other pin.

The test procedure is basically the same as for ungrounded equipment. Tests should be applied to each pin, one pin at a time, with the possible exception of any pin connecting the internal ground bus to an external local ground. If the ground bus is grounded internally, pulses should still be applied to grounded pins, to verify that ground wiring can carry the transient currents.

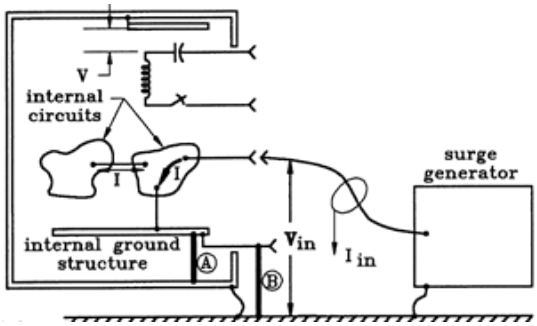

Fig. 18.4 Pin injection on a grounded system.

Type of stress applied to the EUT

Grounded equipment pin tests, in addition to stressing the insulation between the components and the chassis, also allow current to flow (shown as I in Fig. 18.4) to flow through circuit elements to the ground bus. Thus, this type of pin test applies some additional stress to circuit components as compared with the ungrounded condition. Whether or not this current flow depends on the type of circuit and *may* depend on whether the equipment is powered or not. Therefore, it is necessary to have the EUT powered during the tests.

For some circuit elements, it may make little difference whether the internal ground buses are grounded or not. This is true for the inductive devices shown at the tops of Figs. 18.2 and 18.4. If an EUT is to be tested under both conditions it is probably simpler to repeat the tests, than to spend time trying to analyze whether or not the tests are redundant. There might be some internal circuit paths not readily visible.

Effects of circuit loading

Circuit loading may reduce the voltage actually developed on a pin to a lower amplitude than that observed under open circuit conditions. This is a normal response, and the power level of the transient generator (TG) should not be adjusted to compensate for it. It is precisely because tested circuits may load test TGs that the impedances of generators are defined in the first place.

Protected Circuits

Some circuits may be fitted with filters and others may be fitted with circuit protective devices (Fig. 18.5), such as spark gaps, metal oxide varistors (MOVs), or protective diodes.

Generally, filters and protective devices should be left connected during tests, since one of the purposes of the tests is to verify that the protective devices can withstand the transient currents that flow when the devices operate to clamp the overvoltage transient.

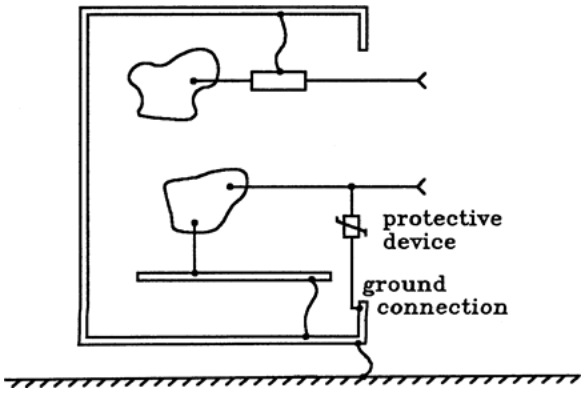

Fig. 18.5 Protected circuit.

Status of protective devices

Even if the EUT appears to function normally after the test, it should nevertheless be inspected to verify that its protective devices have not been damaged. A visual inspection may be sufficient, but if the test currents are known to have approached the design limits of the protective devices, a more detailed inspection may be appropriate. Diode and varistor-type devices usually fail 'short' and this will often disable the function of the connected circuit, but if these devices are protecting power pins the power current will usually follow the transient current and this may cause the protective device to burn open, leaving the circuit unprotected. This damage to the device may or may not be visible.

Since the circuit will continue to perform its intended function, the failure condition would not be detected during a functional test. For this reason, some equipment manufacturers install the protective devices on a separate circuit board that can be removed, and performance checked before re-installation.

Protective margin

If the EUT functions normally after the test, it is probably safe to assume the protection was adequate, but there may remain a question about how much protective margin the protective devices offer. Possibly, the circuit was just on the edge of failure and a slightly less effective protector would have allowed failure. During engineering development, it might be appropriate to determine whether the protective margin is satisfactory. The certification requirements and test standards do not require a margin beyond the passing of the test (there is of the course the margin between the ATLs and the ETDL that is described in Chapter 16). Any additional margin would be incorporated by equipment manufacturers for economic reasons.

Equipment Cable Bundle Tests: Individual pieces of equipment can also be tested by injecting the transients into a section of cable that is plugged into one of the equipment connectors. Instructions for this are also contained in [18.1].

One reason for this has been to verify equipment damage tolerance, although the standards do not recommend this. The second reason for an equipment cable-bundle test is to evaluate equipment upset possibilities. However, this cannot usually be depended upon to fully evaluate upset possibilities since only one cable is tested at a time, and usually that cable is not a replica of the aircraft cable. In fact, that standard describes only a 3.3 m section of cable. The most recent editions of these standards include application of MS and MB waveform sets of the applicable transients. This is necessary for any evaluation of upset of equipment performance.

In situations where the EUT, together with one cable is a complete system, the equipment cable-bundle test in the equipment test standards [18.1] will suffice for verification of system upset tolerance. In other situations, where the EUT is but one of several "boxes" and interconnecting cables comprising a system, it is probably best to omit the equipment cable-bundle test and rely on the system test to verify the upset tolerance.

It needs to be remembered that the standards provide a selection of tests. It is the responsibility of those managing the aircraft certification process to decide which tests are needed, and by whom they should be applied.

18.3 System Testing

The object of the tests is to apply test voltages and/or currents into the interconnecting wire harnesses of a system. These are injected as trains of voltage or current pulses that make up the MS and MB waveform sets that are included in cloud-to-earth lightning flashes (MS) and in intra-cloud flashes (MB). The standards for these system tests are included in the SAE and EUROCAE lightning test standards [18.2, 18.3]. The system tests are applied to complete systems, or to partial systems performing a single function, for the following purposes:

- To verify the ability of a system to resist damage or functional upset due to the Single stroke, MS and

MB aspects of the lightning environment. The MS and MB transients may induce "noise" in system data trains that can interfere with the proper functioning of the system. This may manifest itself as an error on a cockpit display, or an unwanted command to an electronic engine or flight control.

- To evaluate synergistic effects that may occur when transients appear at all pins of equipment connectors, and all cables, instead of at one pin at a time as in the equipment damage tolerance (pin injection) test.

- To verify the protection effectiveness of interconnecting cable shields (including shield terminations) that are not present during individual equipment tests. As has been explained in Chapter 15, shielding is perhaps the most important protection method, and this cannot be evaluated in the pin injection test.

Reasons for injecting multiple pulses, rather than just single pulses or single pulses repeated slowly, include the following:

1. The multiple pulse environments best represent natural lightning.

2. Data transfers throughout systems happen via digital streams of pulses that are arranged in time sequences to convey information. The lightning MS and MB pulse sets can intermingle with this digital data to cause errors and upsets.

3. Multiple test pulses are better for evaluating the thermal duty on objects under test. Multiple pulses of actual lightning occur sufficiently fast that objects do not cool off between pulses.

4. Some types of system (analog systems in particular) respond to the cumulative effect of rapidly applied disturbances.

5. Some types of devices are most susceptible to physical damage at certain points in their operating cycles. Semiconductors are most susceptible to damage when they are in the process of changing from one state to another.

6. Some types of devices are more susceptible to momentary upset at certain points in a cycle. Digital devices are most susceptible to upset when they are changing state.

7. Some types of systems are more susceptible to upset at certain points in a cycle when interface circuits are sampled or refreshed at periodic intervals.

The system tests are applied as cable bundle tests, so that all interconnecting wires and cables in the tested system or subsystem experience the induced effects of the applied transient waveform sets simultaneously, as happens when an aircraft is struck by lightning. The external MB and MS environments together with a menu of transients induced by them in typical interconnecting wiring are described in Chapters 5 and 16 along with typical transient waveforms and levels that correspond to these environments.

18.3.1 System Test Approaches

Extent of the tested system. The MS and MB tests satisfy the regulatory guidance in [18.4] to verify system functional upset tolerance of systems performing Level A, B, and C functions, the multiple pulse aspects of the lightning environment. Systems and equipment that perform less critical functions have only to be tested as individual items of equipment, although often these less critical items are connected to systems performing higher level functions and so should be included in setups of systems performing higher level functions.

Cable currents and loop voltages: Many systems that perform critical functions are protected from lightning and other electromagnetic effects by having their interconnecting circuits enclosed within flexible copper braid shields. The shields are connected to the EUTs through the cable connectors. When all the interconnecting cables are shielded in this manner the specified transient needs to be a shield current since this is responsible for inducing transients in the shielded circuits. However, when some, or all, of the circuits within a cable are not enclosed within shields, both a voltage and a current need to be specified. Usually this is a current test level, I_T, (when there are some shields) together with a voltage limit V_L. There are other situations (when none of the circuits are shielded) in which the reverse is true, with a V_T and I_L being specified. The following guidelines apply for three cases:

1. When all conductors are shielded only an I_T applies. A V_L is not applicable. The test current must be reached in the cable regardless of the loop voltage.

2. When some conductors in a cable are shielded and others are not, an I_T is applicable together with a V_L. If the test current level in the cable cannot be reached when the loop voltage reaches V_L, the test is stopped and considered successful.

3. When all conductors are unshielded and terminated in high impedance loads to ground, only a V_T may be necessary.

The locations of the cable currents and the loop voltage are illustrated in Fig. 18.6.

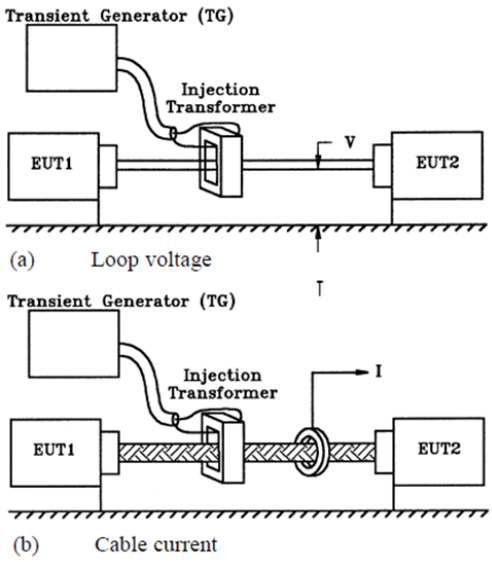

Fig. 18.6 Cable current, I, and loop voltage, V.

Voltage limit for testing hybrid cables

When an EUT is to be tested with a cable bundle comprised of a mixture of shielded and unshielded conductors using the transformer-injection method, as in Case 2 where a voltage limit (V_L) is to be observed. There is an important error in the test standard [18.1] where the loop voltage V_L is to be measured in a single turn around the injection transformer and the test stopped if V_L exceeds the value of given for V_L in Table 22-3 of [18.1]. This limit voltage method is shown in Fig. 18.7 [18.1].

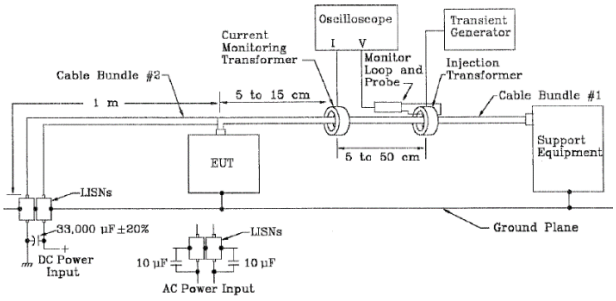

Fig. 18.7 Hybrid cable bundle test limit voltage measurement (Fig. 22-17 from [18.1])

The error is that if there is any current in the hybrid cable, the loop voltage is lower than the voltage that is measured in the injection transformer core. The difference is usually considerable [18.5]. Fig. 18.8 shows a typical comparison with the voltage measured between an unshielded wire run together with the hybrid cable and the ground plane.

The reason for the difference in these measurements is that the total voltage in the loop between the cable and the ground plane (test bench) is the sum of the voltages induced by the flux in the injection core and the flux produced by the current in the cable shields. These fluxes must always oppose each other in accordance with Lenz's law.

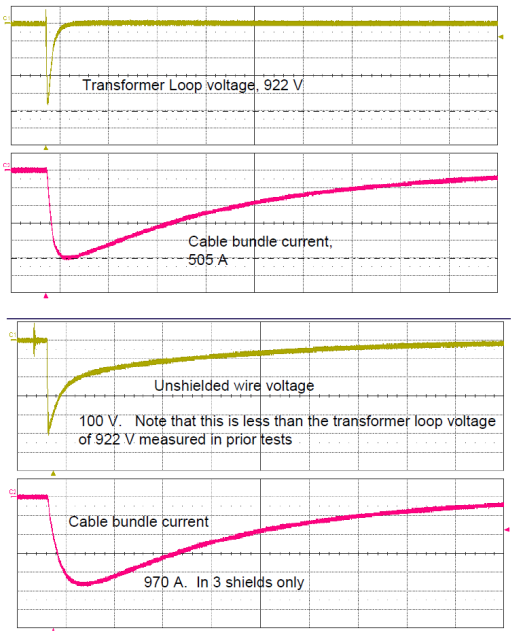

Fig. 18.8 Comparison of V_L measured in a one turn loop through the injection transformer per Fig. 22-17 from [18.1] with the loop voltage measured between an unshielded wire and the test bench [18.5].

This disparity of course does not exist if the test voltage and current are directly injected into the cable loop.

This disparity has been brought to the attention of the standards committees but as of the date of publication of this book no changes have been implemented in [18.1] to correct the error. The solution is of course, to measure V_L with a single sense wire run alongside the tested cable.

The usual reason given for not making the correction to the standard has been that the sense wire method of monitoring V_L is subject to variations in measurements, depending on location of the wire in (on) the cable. Such variations are in the range +/- 20 %. But this is far less than the 5X–10X error that exists in the present standard. Perhaps equipment suppliers are concerned about having to repeat earlier tests. Certifying authorities realize that technical progress happens gradually, and, unless past practice has knowingly

resulted in catastrophic consequences (this situation has not), standards should evolve along with advances in science.

Additional information including details of use of sense wire to measure V_L can be found in the most applicable method depends on test facility capabilities.

Direct injection (also called ground injection)

The injection principle is illustrated in Fig. 18.9. This example is of a simple system where a test TG injects current into one EUT that can be operated successfully without being mounted (and grounded directly) to the test bench. Test current flows through the chassis of EUT1 to several other EUTs that are grounded to the test bench.

The magnitudes of the cable currents I_1 and I_2 are controlled by the setting of the test current generator and impedances (not shown) that are inserted in the ground connections of EUTs 1 and 2.

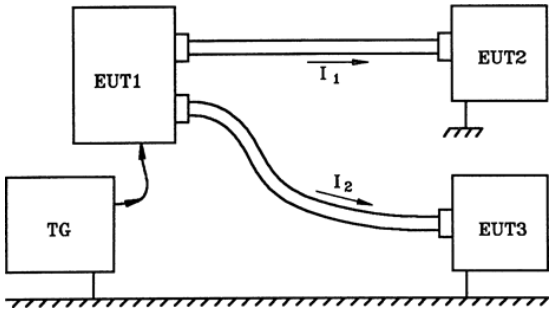

Fig. 18.9 Direct injection of test currents using parallel current paths.
(Also called *ground injection*)

The numbers of cables that can be injected by one generator via one ungrounded EUT are limited by the number of cables that are connected to the ungrounded EUT, and of course by the capability of the test current generator. Some further notes are:

1. Commercially available TGs, even if capable of producing MS and MB waveform sets, are not generally powerful enough to drive more than one or two cables. Generators for MS and MB testing of systems are available commercially. Also, they are sometimes built up by the laboratories conducting the system tests.

2. The system test standards generally require that *either* the injected current (in the cables) or the loop voltage (in the loop between the cable and the ground plane) be achieved as specified in the test plan or recorded when the other one is specified. Since most systems performing Level A, B, or C functions are interconnected with shielded cables, the cable shield current (i.e., cable bundle current) is the test parameter to be specified in the test plan. The loop voltage need not (and should not) be specified. In a fully shielded system, it is the shield currents that are responsible for the induced transients that appear at the EUTs.

3. The standards provide both current and voltage amplitudes and waveforms to be applied. This is because some systems are interconnected with mixtures of unshielded and shielded wires. In these cases, it is still usually appropriate to specify the current as the test level (I_T) and assign the voltage as the limit (V_L) that is not to be exceeded in the loop bounded by the cable and test bench. The subject of measurement of this limit voltage is one that is not adequately explained in the test standards, nor well understood by persons conducting these tests. The topic is addressed in [18.5].

A second example of a direct injection of test current into a shielded system is shown in Fig. 18.10.

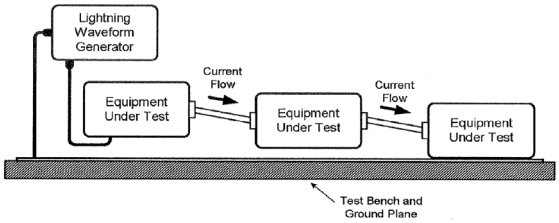

Fig. 18.10 Direct injection of test currents using series current paths.
(Also called *ground injection*)

In the arrangement of Fig. 18.10 the same current is in all cables. This is acceptable if the specified cable currents are the same or similar amplitudes.

The functional grounding of the 'elevated' EUTs is achieved via the cable shields.

The magnitudes of cable currents also depend upon cable impedances and EUT to test bench ground impedances, which can be adjusted. Cable impedances can be varied by inserting steel or ferrite cores around shielded cables.

Power to the EUTs can be furnished through one of the tested cables, or from an independent source that does not need to be grounded to the test bench.

Some topics like the role of limit voltages and waveform tolerances that need further explanation are discussed in subsequent paragraphs.

The other test arrangements for system lightning tests are generally in accordance with the housekeeping re-

quirements of [18.1] for tests of individual items of equipment, although some variations from the test bench grounding requirements may be taken for the system tests. More will be said about these topics in subsequent sections of this chapter.

Transformer injection

This principle is illustrated in Fig. 18.11. The objectives of the transformer injection and the direct injection methods are the same: to inject transients (usually currents) in as many cables as possible, simultaneously.

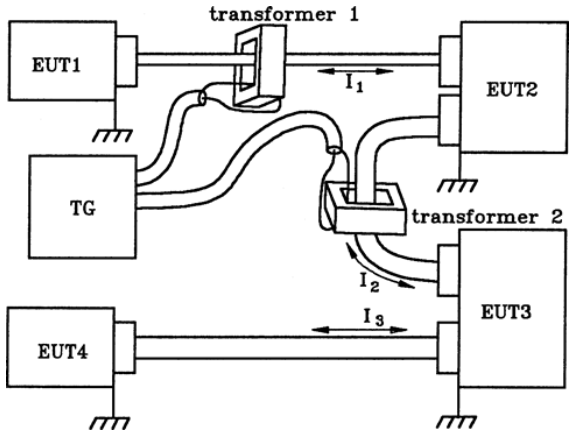

Fig. 18.11 Transformer injection of test currents (also called *transformer coupling*)

Fig. 18.11 shows transformer injection being applied at two locations in a system comprised of four EUTs and three interconnecting cables.

The TG in Fig. 18.11 drives current into the primary turns of each of the injection transformers simultaneously (in fact, the same primary conductor is sometimes routed through all the injection transformers).

The following means can be used to achieve the desired test current (or voltage) amplitudes between the different injection points:

- Varying the numbers of turns in the primary windings (one or two turns is most common).

- Adding different impedances between each EUT and the test bench ground plane. This approach would seem at variance with usual test housekeeping rules that include grounding of all equipment to test benches, but experience shows that the equipment and system will perform satisfactorily with some impedance between the chassis and the ground plane, or (especially for a fully shielded system) complete isolation from the ground plane.

- Changing cable impedances by adjusting the distances between the cables and the ground plane.

System power. Systems are powered up and operating during tests. The power is usually supplied through power line impedance stabilization networks that:

a) represent a typical aircraft power distribution bus impedance to ground.

b) provide some series impedance that isolates the power source from the injected transient when the system power supply harnesses are tested.

Sometimes additional DC and/or transient blocking needs to be installed in the power supply circuits to ensure that the injected transients do not damage the power sources.

18.3.2 Lightning-induced Transient Waveforms and Levels

The MS test levels are based on transients induced by current Components A and D/2 of the external lightning environment, whereas the MB test levels are based on Component H of the external environment, all defined in [18.3].

Airworthiness certification procedures require that the characteristics of lightning-induced transients in interconnecting wire harnesses be determined, either by measuring these transients in the harnesses inside an airplane that is being subjected to lightning tests, or by verifiable analysis. Sometimes, the test levels must be set before an airplane is available for testing, in which case the levels are determined by analysis and verified later by aircraft full vehicle tests (FVTs). By whatever means, lightning-induced transient levels for system and equipment connector pins and interconnecting cables should be established for protection design and certification test purposes. These levels are known as the ETDLs as defined in Chapter 5 and [18.4]. The selected ETDLs should be higher than the levels determined by test or analysis by at least a 2:1 margin. This 2:1 margin (sometimes expressed as 6 dB) is intended to account for uncertainty in the tests or analysis by which the actual transient levels (ATLs) in the interconnecting wiring are determined. (It is better to describe margins between EDTLs and transient control levels (TCLs) in terms of direct ratios, rather than in terms of dBs). Once the actual transient waveforms and levels are known (or have been estimated) standard waveforms and levels most closely approximating actual levels (plus the margin) are selected from the menu of waveforms and levels published in the test standards [18.6] and Chapter 5.

Applicability of the standard test levels: It should be noted that the standard transient waveforms and levels do not always cover the actual levels present in the wiring of an aircraft system. The transient waveforms (designated 1 through 6) defined in these standards are typical of transients measured in aircraft wiring, but amplitude levels 1 through 5, defined in these standards, represent only the 'middle range' of possible transient amplitudes. The standard levels defined for individual conductors or equipment connector pins presented in [18.6] are reproduced below in Fig. 18.12. It is often overlooked that the levels in these tables may be selected as either TCLs or ETDLs. In the former case, an ETDL associated with Level 5 for Waveform 4 could be 3 200 volts. In fact, the maximum voltage amplitude of 3 200 volts was originally selected because this is the approximate sparkover voltage of most harness termination devices, which impose a natural limit on the maximum ATL that could appear within equipment.

Table 5 from *ARP 5412*: "Individual Conductor TCL, ETDL or Test Levels Due to Current Component A"

Level	Waveform 3 V/I	Waveform 4 V/I	Waveform 5 V/I
1	100/4	50/10	50/50
2	250/10	125/25	125/125
3	600/24	300/60	300/300
4	1500/60	750/150	750/750
5	3200/128	1600/320	1600/1600

Table 6 from ARP 5412: "Cable Bundle TCL, ETDL or Test Levels Due to Current Component A"

Level	Waveform 1 V/I	Waveform 2 V/I	Waveform 3 V/I	Waveform 4 V/I	Waveform 5 V/I
1	50/100	50/100	100/20	50/100	50/150
2	125/250	125/250	250/50	125/250	125/400
3	300/600	300/600	600/120	300/600	300/1000
4	750/1500	750/1500	1500/300	750/1500	750/2000
5	1600/3200	1600/3200	3200/640	1600/3200	1600/5000

Fig. 18.12 Tables 5 & 6 from SAE ARP 5412 [18.6].

In fact, peak voltages and (especially) currents higher than those listed in Fig. 18.12 are frequently measured in aircraft circuits that extend between fuselage locations and equipment installed in the wings, empennage, landing gear, or engine nacelles. The brief captions assigned to each of the five transient levels in §22.3.2 of [18.1] can be misleading. Transients induced in wiring exposed to "severe electromagnetic environments" may not be represented by Levels 4 and 5. Such environments often induce transient levels higher than those defined by levels 4 and 5 in Fig. 18.12. The magnitudes of induced transients in wiring in severe environments depend on how well the wiring is protected. Some wiring in severe environments may experience transients within Levels 2 or 3, but less well-protected wiring may experience much higher transients. The menu of transient levels in Fig. 18.12 is intended for application to a large portion of the systems destined for installation in conventional aluminum transport aircraft.

Establishing ETDLs: ETDLs should be set for damage tolerance as well as system functional upset testing. The damage tolerance (i.e., pin injection) test levels should be based on individual conductor transients, and the ETDLs applicable for system functional upset testing should normally be cable bundle transients. If the cable is fully shielded, as in most engine and flight control systems, the cable bundle ETDL is a cable bundle current only. No cable loop voltage limit should apply since the voltage in the loop between the shielded cable and the test bench has no influence on the amplitude of transients induced in the shielded conductors, and the voltage necessary to drive the desired shield current in the tested harnesses will not be the same as the loop voltage that would have existed in the aircraft installations (this is because the coupling method chosen for the system test may not be the same as the coupling mechanisms in the aircraft, and the cable – airframe impedances are usually not the same as those existing on the test bench).

Damage tolerance levels imply a specific voltage and current combination that individual equipment pin interface circuit elements should be capable of withstanding without burnout or degradation. Cable bundle tests usually cannot provide damage tolerance assessments because they yield no information about the amplitudes of the transients applied to individual equipment connector pins. Even if that information were available, it is unlikely that the transients on the individual conductors in the test bundle would be the same as those that would appear in the actual aircraft installation.

The motivation behind system tests is to assess the susceptibility of the system to functional upset, but system tests may also cause component failure. This is most often true of cable bundles that include equipment power lines. Power lines may be protected with diodes or MOVs, which may fail if they are unable to tolerate the induced conductor currents.

Table 18.1 lists typical ETDLs applicable to systems intended for installation within an all-aluminum aircraft. The Component A related test levels used in pin injection and MS tests should be based on the ATLs determined during the FVTs or numerical analyses. These ETDLs are based on measurements (or numerical predictions) of the transients in the aircraft's wiring when Current Component A is being conducted through the aircraft, and for the MB levels, when an intracloud current pulse is flowing in the airframe. This table is an example of how a complete set of ETDL might be presented in system or equipment specifications.

Table 18.1 Typical ETDLs for Pin Injection, MS, and MB testing. (For equipment connected with fully shielded cables).

Test	Level[1]	Based on Component	WF 3[2] (V/I)	WF 4/5A (V/I)	Comments
Pin Injection	3	A	600/24	300/60	Tests per Ref 18.9 Section 22.5.1
Cable Bundle Multiple Stroke			WF 3 (I)	WF 1 (I)	only current is specified since the cables are fully shielded
first pulse	3	A	24[3]	600[3]	Test setup per Ref 18.9 Section 22.5.2
subsequent pulses	3	D/2	12[3]	150[3]	
Cable Bundle Multiple Burst	3	H	WF 3_H (I)	WF 6_H (I)	only current is specified since the cables are fully shielded
			6[3]	30[3]	Test setup per Ref 18.9 Section 22.5.2
Note 1: As defined in Reference 3 if applicable					
Note 2: 1 and 10 MHz					
Note 3: The current amplitude should be achieved in the tested cable bundle shields.					

MB Test Waveforms: The MB test levels are based on the guidelines of Fig. 18.13 in which test voltages and currents recommended for MB applications are set as fractions of the corresponding MS test voltages and currents for the same assigned ETDL level. Since the Waveform 6_H currents in Fig. 18.13 are applicable only to systems interconnected with fully shielded cables, only current levels are given. Other, partially shielded, or unshielded cables are exposed to both cable to airframe loop voltages and currents, so both are included. Whichever level (voltage or current) is reached first during the test established the test condition. Both do not have to be reached in the test.

Level	Waveform 3_H V/I	Waveform 6_H I
1	60/1	5
2	150/2.5	12.5
3	360/6	30
4	900/15	75
5	1920/32	160

Fig. 18.13 Table 7 from ARP 5412 [18.6]: "Cable Bundle TCL, ETDL or MB Test Levels Due to Current Component H".

MS test levels: The first pulse in the MS waveform set is always higher than the 13 subsequent pulses, reflecting the usual cloud-to-earth lightning flash wherein the first stroke is higher than the subsequent strokes. The MS levels in the example of Table 18.1 follows the 2:1 or 4:1 first pulse/subsequent pulse amplitude relationship for MS waveform sets specified in Table 4 of [18.6] reproduced in Fig. 18.14. The amplitude of the Waveform 1 subsequent stroke current is therefore 1/4 of initial Level 3 pulse amplitude 600 A (or 150 A). Similarly, the Waveform 3 the subsequent stroke current of 12 A follows the 2:1 amplitude relationship, also specified in Table 4 of [18.6]. There is a different relationship between first and subsequent pulses for Waveform 5 that comes from aircraft transient measurements.

These different first stroke/subsequent stroke relationships reflect differences between the coupling mechanisms that produce Waveform 1 and Waveform 2 and 3 transients on aircraft wiring.

It will be noted that the first waveform 1 current pulse in the MS waveform set is always one half of the single waveform 1 current pulse that is applied for single pulse cable bundle testing. This is because MS waveform sets are always due the negative polarity lightning flashes, whose peak amplitude does not exceed 100 kA (Current Component D), whereas the damage tolerance tests are always based upon the positive stroke amplitude of 200 kA (Current Component A). In practice, most MS test plans will have the MS waveform set begin with a current pulse that is derived from Component A, since systems and equipment must be designed and certified to tolerate both positive and negative flashes.

MB test levels: Transients induced by Component H are applied in the MB sequence. All of these transients are the same amplitude. The predominant response is either voltage Waveform 3_H, in a frequency range between 1 and 10 MHz, or current Waveform 6_H, which has the same shape as the external environment Component H.

Relationship between MS and MB levels: The relationships between the MS and MB test levels are also based on lightning-induced transient data from measurements made on the internal wiring of many aircraft, and upon the coupling physics. The MS and MB test amplitudes for each ETDL level are shown for MS in Fig. 18.12 and for MB in Fig. 18.13. These relationships are reflected in the examples in Table 18.1.

Note that, in Fig. 18.13 the Waveform 6_H level of 30 A, listed for MB testing, is 5% of the corresponding 600 A, MS, Waveform 1 level in Fig. 18.12. This reflects the relationship between the amplitudes of current Component A and Component H as they appear in the external environment. The amplitudes of induced currents on wiring are always proportional to the amplitudes of the inducing currents in the airframe.

The levels for Waveform 6_H shown in Fig. 18.13 are currents because unipolar transients induced by Component H have appeared in short, highly exposed cables such as those found in engine controls. These cables are always fully shielded. The Waveform 6_H levels in Table 18.1 apply only to fully shielded cables and so need only be tested by transient currents. Test levels for a system with unshielded wire harnesses include voltage Waveform 3_H, which would be applicable to unshielded circuits, typically have an amplitude of 60% of the Waveform 3 voltage response to Component A.

Transient Responses	Waveform 1	Waveform 2	Waveform 3	Waveform 4	Waveform 5
Response to D	1/2	1	1	1/2	2/5
Response to D/2	1/4	1/2	1/2	1/4	1/5

Fig. 18.14 Table 4 from ARP 5412: "Response to D and D/2 as Fraction in Response to A" [18.6]

18.3.3 Test Current and Voltage Waveform and Amplitude Tolerances

Although there is often a large variation in the currents induced in individual harness branches within a system, usually no attempt is made to replicate these specific currents in the system tests. Since the damage tolerance of system equipment will have been verified by pin injection tests (at transient levels based on the induced transients in the wiring of each circuit), it is not necessary to reach actual induced transient amplitudes in all branches of a tested system. Rather, the intent is to produce harness currents of amplitudes sufficient to induce conductor transients that might be 'read' along with system signals. Unlike pin-injection tests of equipment, it is simply not practical to achieve the standard voltage or current waveforms in each of the cables in a complex system. A typical cable bundle test current is shown in Figure 18.15.

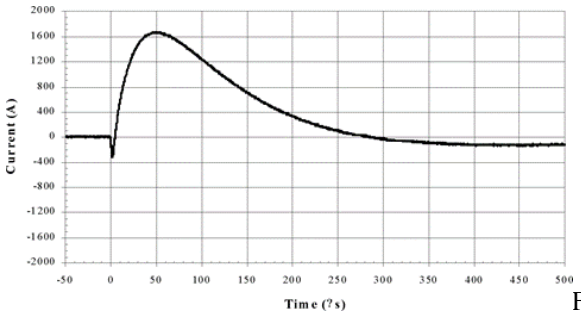

Fig. 18.15 Typical cable bundle current approximates waveform 5A due to external environment Component A.

However, since system upset is related to the amplitudes as well as the multiplicity of induced transients, attempts should be made to approximate the waveforms and levels assigned to each cable within a system. Since "approximate" implies non-precise conditions, here are some guidelines that have resulted in acceptable tests:

Transient Waveforms: It is rarely possible to achieve in actual aircraft cables voltage or current waveforms complying with the standard definitions. Typical loop voltages will be of lower frequency or longer rise times than the standards. Typical cable currents will have longer rise and decay times than the standard currents. These results are due to the inductance of the cable-test bench loop.

– Reduce cable inductance by reducing loop area. For lightning tests, it is not necessary to maintain 5 cm clearance between cables and the test bench.

– It is important to achieve unipolar loop voltages when Waveforms 2 or 4 are specified. Oscillatory voltage waveforms should be achieved when Waveform 3 has been specified.

– Unipolar currents should be achieved when Waveform Waveforms 1 or 5 are specified. It is best if decay times can be the same or longer than the specified times.

Transient amplitudes: It is also not practical to achieve specified amplitudes in all cables of a system, especially when simultaneous injection is desired. The best way to approach this is to arrange injection points (for ground injections) or transformer locations (for transformer injections) to achieve close to the desired amplitudes in the larger diameter cables ("trunk cables") and to accept lower than specified amplitudes in other, smaller diameter cables. It is acceptable if at least 50% of the desired (specified) amplitudes are achieved everywhere. If some cables have received less than 50%, then it is best to test that single cable at the specified level, after the simultaneous tests have been completed.

If a cable bundle test has been conducted for damage tolerance purposes: it is not necessary to reach the cable bundle ETDL in each cable during the system functional upset test.

18.3.4 Cables with Intermediate Connectors

If the shielding on an aircraft's wiring is grounded at intermediate locations, as shown in Fig. 18.16, the shields should be in this configuration when the individual circuit conductor V_{OC} and I_{SC} are measured during the FVT. (Engine and flight control circuit shields are often grounded in this manner). The measured voltage/current ratio should be used to verify or establish the EDTLs for the

equipment, and the damage tolerance should be verified by a pin injection test at the corresponding ETDL V_{oc} and I_{sc} levels.

If a cable is part of a system for which functional upset tolerance must also be verified, cable bundle currents should be measured during the FVT (or determined by analysis). Since the conductor voltages and shield currents in each section of the cable (labelled 'A', 'B', 'C' in Fig. 18.16) are confined within separate loops, they are likely to differ from one-another.

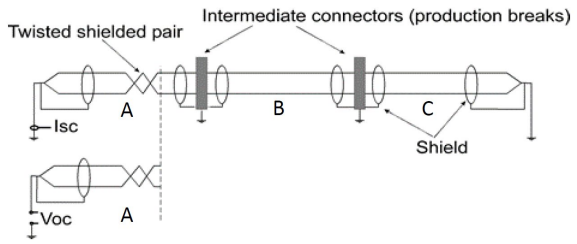

Fig. 18.16 Segmented cable. Each section is shielded.

Currents in each cable segment should be measured during the FVT (or computed). Sometimes the cable shield current can be much higher in one segment (such as a pylon or wing circuit) than in the others (such as a fuselage circuit). Nevertheless, the other segments should not be ignored. For example, cable segments that experience lower shield currents could be longer than the segments that experience the highest shield currents; and conductor voltage is proportional to cable length as well as shield current.

For the functional upset test of the system utilizing the cable in Fig. 18.16, it may not be practical to have all three segments of the cable (A, B, and C) present during the test, or to inject three currents of three different amplitudes, simultaneously, into the three cables with the intermediate connectors grounded to the test bench. However, the currents on the cable shields should induce transients in the shielded conductors that resemble the transients that would appear on the same conductors when they are installed the aircraft. This can be done by assuming that the conductor induced voltage (V_{oc}) is the sum of the voltages induced in each segment of the circuit, as follows:

$$V_{oc}(\text{total}) = \left(I_A \times Z_A\right) + \left(I_B \times Z_B\right) + \left(I_C \times Z_C\right) \quad (18.1)$$

where I_A, I_B and I_C are the cable shield currents in the three sections, and Z_A, Z_B and Z_C are the transfer impedances of each cable segment.

The transfer impedances, Z, of many cables are the same as the DC resistances of their shields. If the shield transfer impedances and currents are known, the characteristics of a single 'equivalent' cable and a single uniform cable bundle (shield) current can be defined. Then a representative cable can be provided for the system test, and sufficient current can be injected in it to produce the appropriate conductor voltages.

Sometimes, the combined length of cables A, B, and C is great, and it becomes impractical to inject enough current into the 'equivalent' cable shield to attain the equivalent conductor voltages. In such cases, a sufficient voltage (albeit with a different waveform) can often be achieved by ungrounding the test cable shield at one end and inducing voltage (and current) directly into the shielded conductors. If this is done, it should be remembered that the performance of one of the most important protection features (the shields) is no longer being evaluated by the test.

For testing cables that extend beyond the fuselage avionics bays to other locations in an aircraft, the transients listed in Fig. 18.12 may be chosen. Waveform 2 is the dominant voltage in the loops between shielded cables and the airframe since such cables are most likely to be exposed to magnetic fields penetrating apertures such as windows, vents, and engine nacelles. This voltage drives current Waveform 1 in the shields, which in turn produces Waveform 4 voltages in the shielded conductors. The conductor voltages drive currents of somewhat longer duration in the shorted conductors, which are best represented by Waveform 5A.

18.3.5 Notes about Simultaneous Injections

Injection transformer locations: Techniques for injecting transients into simple systems comprised of one item of EUT, one cable, and some dummy loads representing remote equipment (or a second box) are described in [18.1]. These include transformer injection and ground injection methods. Either method is potentially capable of injecting the required transients into the system. If the system is comprised of several EUTs and more than one interconnecting cable, it may be necessary to inject the transients simultaneously into more than one location in the system.

The physical location of the injection transformer(s) (or of the injection location(s) in the direct injection method) is not important. Neither is the distance between a transformer and the nearest equipment connector important. What is important is achievement of the desired test conditions in the cables.

Achieving the specified test current levels in shielded systems: When high currents must be injected into multiple cables, as is often required for electronic engine controls, TG limitations may prevent reaching the specified levels. Two approaches may sometimes be followed to surmount this problem:

1. Use the same current injection point to drive currents in multiple locations. This is accomplished by isolating some of the EUT's from the bench ground, so that test current is forced through additional cables.

2. Test all cables simultaneously at the highest possible levels (being careful not to exceed established ETDLs), then individually re-test at assigned ETDLs the cables that did not experience the full level in the initial test.

The first approach is illustrated in Fig. 18.17. The figure shows test current being injected into two cables on the left side of the Electronic Control Unit (ECU). Because the ECU is not grounded, the test current is forced to flow through the ECU case and into four other cables between the ECU and 'other EUTs'. The sum of $I_1 + I_2 + I_3 + I_4$ is equal to the injected current.

In an electronic engine control system, the cables on the left side of The ECU in Fig. 18.17 would go to the aircraft interfaces, and the cables on the right side of the ECU would go to engine-mounted accessories. The ECU receives its electric power through one of the aircraft cables, or through an engine mounted generator, which is one of the "other EUTs" in the figure.

The ECU does not have to be grounded to the test bench to function. These tests are also sometimes conducted with the bulkhead connector brackets (normally grounded to the airframe or engine) ungrounded, so that the injected test currents flow through the complete system.

The second approach is a combination of simultaneous application of currents in all branches of the system of sufficient amplitude to induce 'readable' signals in interconnecting circuit conductors, followed by application of full threat currents in those cables/branches where the specified currents were not reached during the simultaneous injections. This is not a perfect solution, since it leaves untested the condition in which all cables receive the specified currents simultaneously. However, systems tested in this manner are not known to have experienced functional upsets during in-flight lightning strikes.

Relationships among test currents and voltages: When a limit voltage (V_L) is applicable, as when the tested cables contain unshielded as well as shielded circuits, it should be verified that the relationships between test current and voltage limit resemble the voltage/current relationships that exist in the aircraft installation. This requires some knowledge of the coupling mechanism(s) that give rise to the transients being applied. [18.6] and give little guidance in this area, but the Table 18.2 (from SAE ARP 5412 [18.6]) give the proper relationships between the voltage and current waveforms induced by lightning in aircraft circuits.

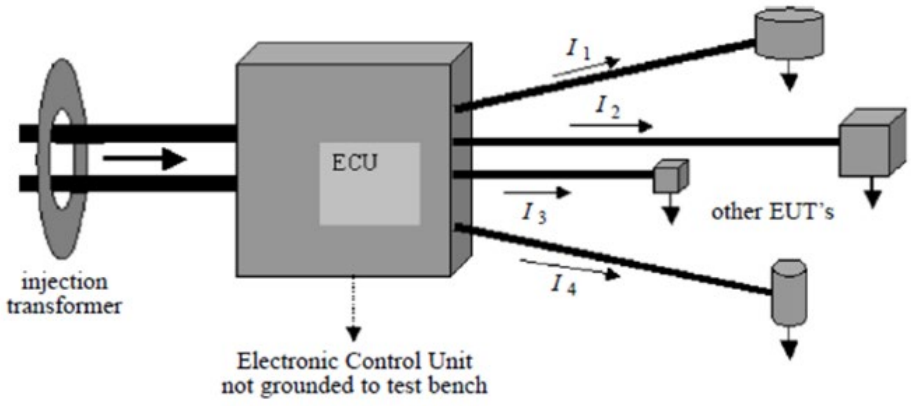

Fig. 18.17 Simultaneous test currents through ungrounded EUT.

Table 18.2. Relationships between Test Voltages and Currents

Voltage Waveform	Current Waveform	Coupling Mechanism
Due to Lightning Current Component A		
2	1	dϕ/dt
3	3	dϕ/dt, traveling waves
4	5A	IR
4	5B	IR and redistribution
5A	5A	Shield IR*
Due to Lightning Current Component H		
3_H	3_H	dϕ/dt, traveling waves
Not defined	6_H	dϕ/dt
*Here, WF 5A is the voltage inside a shield due to WF 5A current in the shield		

The waveforms noted in Table 18.2 are defined in [18.4]. The relationships between voltage and current waveforms listed in Table 18.2 are approximate and depend on the impedances of specific cables, and other factors. Thus, for example:

- When applying I_T as Waveform 1, V_L should look like Waveform 2
- When applying V_T as Waveform 4, I_L should look like Waveform 5A. Stopping the test when the I_L current amplitude is reached by a short-duration current waveform (i.e., a 'spike') may not sufficiently stress the system.

Existing test standards provide only minimal guidance in this area.

Traveling Wave Effects: The voltage/current relationships of traveling waves (represented by Waveform 3) are related to one-another by characteristic impedances. When performing tests with Waveform 3 on unshielded or hybrid cable bundles, the characteristic impedance should be assumed to be around 100 ohms. (A lower impedance of 25 ohms is specified for damage tolerance or 'pin' tests). The 5-ohm relationship implied in Fig. 18.12 is only realistic for bench test setups, where the Waveform 3 transients are the result of tank circuit oscillations between lumped L and C elements at circuit terminations. For a system installed in an aircraft, the cable-airframe transmission line characteristic impedance is typically about 100 ohms.

Generator performance verification: The ability of the TG to circulate specified test currents in the system cables should be verified prior to test. When a system with particularly long cables is tested, it is not sufficient to calibrate the TG by having it inject the specified current into a short circuit (e.g., a calibration jig). The ability of the generator (and intended injection method) to produce current waveforms in the system cables like the waveforms specified for the test (i.e., Waveform 1, 5A, 5B or 6_H) should be verified. This can usually be done by trying out the generator and injection method on the system cables themselves, at low levels.

Waveforms in Tested Cables: It is not necessary to exactly reproduce the specified current waveforms in the system cables, but it *is* necessary to inject waveforms that are able to couple realistic transients into the cable circuits. Such coupling usually depends on rate-of-rise (di/dt), as well as on the amplitude of the injected shield current. If the rates-of- rise, amplitudes, or durations of the injected currents are insufficient, a different test current generator should be used. Alternatively, the transfer impedances can be determined and based on these values, conductor transients that correspond to the specified shield current can be injected directly into system wiring, with the shields disconnected.

The generator performance verification tests described in [18.1] for cable bundle tests are usually adequate for the short (3.3 m) cables commonly used in cable bundle tests of individual EUTs, but not for systems employing longer cables.

MS waveform sets: The MS waveform set is defined as a single transient induced by Component D of the external environment followed by thirteen transients induced by Component D/2, as shown in Fig. 18.18.

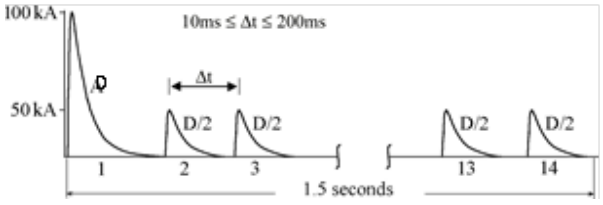

Fig. 18.18 MS waveform set.

In the MS application Component D represents a severe first stroke in a negative flash to earth, since only the negative flashes contain MSs. Since systems must also tolerate the induced effects of single, positive strokes, most MS waveform sets begin with a transient induced by Component A, instead of Component D. The minimum time separation between individual transients in the MS waveform set is 10 ms and the maximum is 200 ms.

A random number generator, set to produce times within this range, is often used to control the timing of the transients. Sometimes the generator control system is set to repeat a specific waveform set application in order to evaluate the sources of upsets or other responses in systems being tested.

MB Tests: Most of the examples in the preceding sections have referred to MS tests. MB tests are usually applied prior to the MS tests, since the chances of damage to the tested system from the MB transients are usually less than from the higher amplitude and longer duration transients induced by the MS environment. The same considerations regarding simultaneous applications and transient amplitudes apply to MB tests. The transient amplitudes are lower than those applied for the MS tests, as shown in Fig. 18.14. A typical MB waveform set comprised of Waveform 3_H transients is shown in Fig. 18.19.

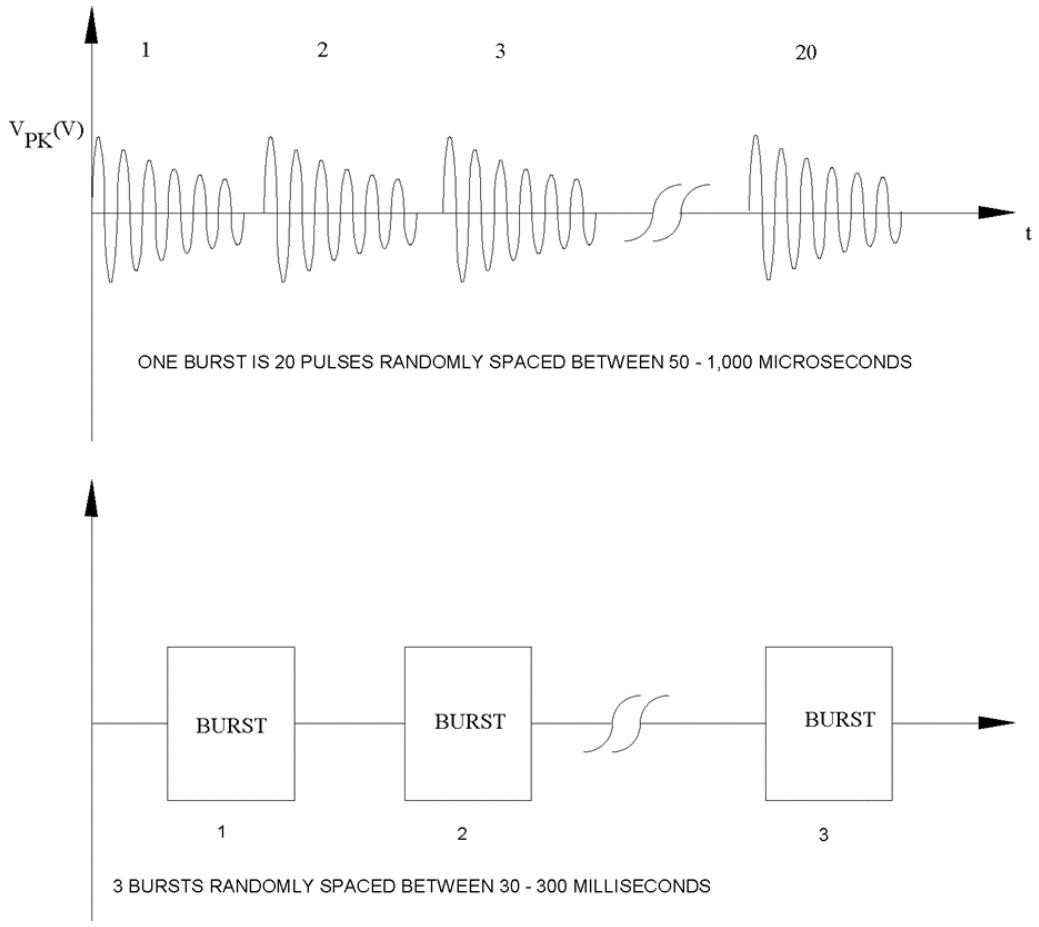

Fig. 18.19 MB transient waveform set.

For systems, such as engine controls, that are interconnected with short cables exposed to strong lightning magnetic fields, Waveform 6_H currents are applicable. A typical cable bundle current induced by current Component H in an aircraft is shown in Fig. 18.20. Current Waveform 6_H provides a good simulation of both the fast rate-of-rise and decay time aspects of the induced current shown in Fig. 18.20.

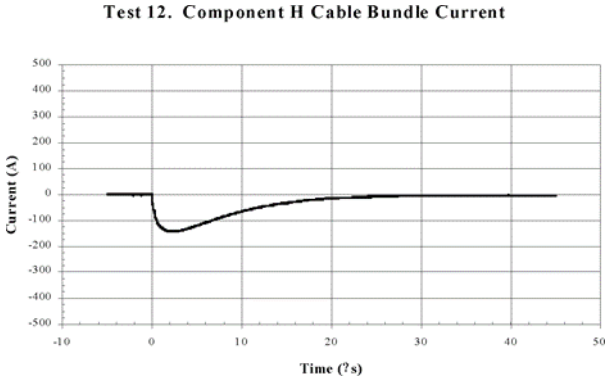

Fig. 18.20 Typical cable bundle current induced by Component H.

A typical burst pattern of 20 Waveform 3 transients is shown in Fig. 18.21.

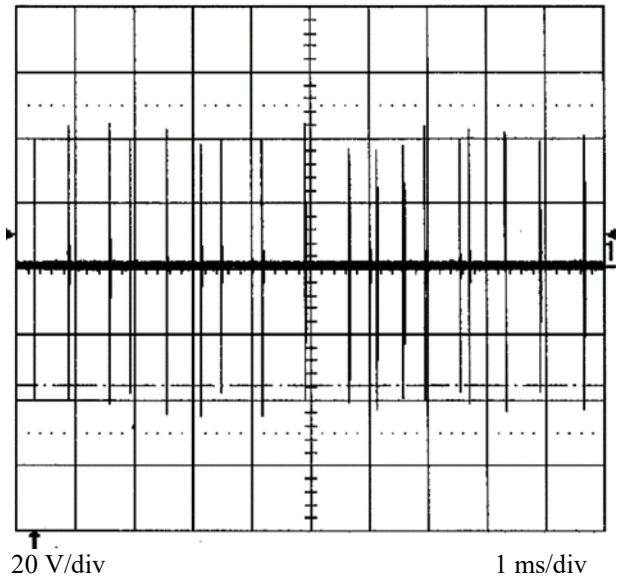

Fig. 18.21 Typical pattern of 20 transients in a burst.

A pattern of four bursts is shown in Fig. 18.22.

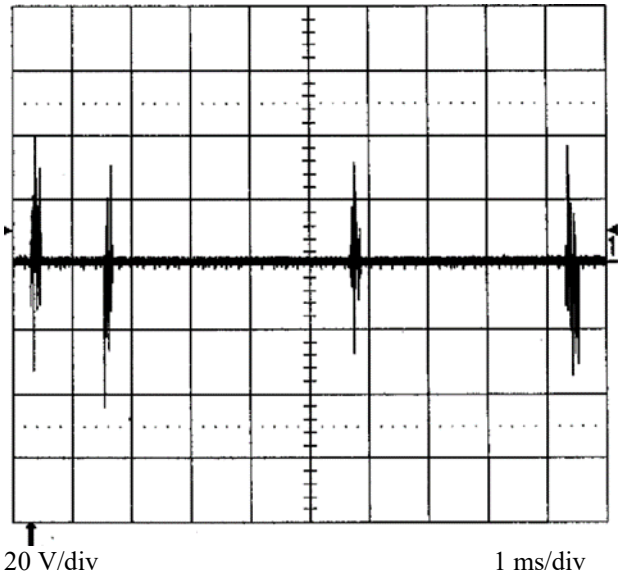

Fig. 18.22 Typical MB waveform set.

The transients in a burst are to be applied randomly at time spacings between 50 and 1 000 µs. The start of each burst is to be between 30 and 300 ms from the previous burst, and there must be a minimum of three bursts applied in each waveform set. Since a finite time period is usually needed to monitor system performance and the MB transients are usually not damaging to system components, the MB waveform sets are often run continuously for periods of several minutes, although this is not required by either the environment or the test standards.

Caution: *System upsets have happened during continuous applications of MB pulse trains without pauses after three bursts. It has been found that some of the system upsets have happened long after one waveform set of pulses (60 pulses) has been applied. If this should happen, the test should be re-run, with the MB waveform sets applied, one by one, with a period of several seconds between each application. It is possible that the original upset will not be repeated. (10 seconds of time spacing between individual waveform set applications would be reasonable). Intracloud flash strikes to airplanes are known to have happened in rapid succession, but that means a time period of typically 10 or more seconds between strikes.*

MB Waveform 3 transients at amplitudes up to 15 A (Level 4) can usually be produced by a signal generator and amplifier with a pulse power capability of 10 kW or so. Waveform 6_H transients above Level 2 usually must be generated by capacitor discharge circuits.

18.3.6 Experience with System Tests

Tests have been conducted on many types of systems since the MS and MB environments were first defined in the early 1980's. In some of these tests, the system has not been affected, but in others the system has experienced some type of response during the tests and occasionally some component damage has been experienced. The damage usually occurred when an MS test was applied to power inputs. Such damage can occur when a transient protection device at a power input has been selected to handle only a single transient, but not the additional 13 transients of the MS waveform set. It is usually the transient *currents* that have been responsible for the component damage.

Systems tested with the MS and MB waveform sets have included engine and flight controls and a wide variety of cockpit displays. Responses of the systems to these tests have included:

- Changes in fuel flow and engine thrust
- Changes in control surface position
- Momentary loss of a display, with automatic recovery
- Loss of display with pilot input necessary for recovery
- Changes in color of a display

These responses have sometimes occurred upon application of the first pulse in a waveform set but, more often, they have occurred after some later transient has been applied within a waveform set. These responses have prompted changes in system hardware or software, followed by retests to verify that the problem has been corrected.

In-flight experience: Whereas meaningful statistics are not available, the flight experience of systems that were certified using MS and MB system tests, in conjunction with damage tolerance tests of the individual system components, appears to have been very good. These systems do not appear to be being upset or damaged by the in-flight lightning environment.

Degraded protection tests: System tests have facilitated the evaluation of protection designs under deliberately degraded conditions, such as increased cable shield termination resistance (accomplished by inserting resistive gaskets between connectors and cases) or by interruption of cable shield continuity. Typically, these tests show that a significant amount of degradation needs to be introduced before system upsets happen. An example of a 'significant' degradation in protection might be a corroded cable shield termination that increases the resistance from a few milliohms to a few ohms. Another might be a broken lead connection on a protection device such as a Zener diode, or a MOV device.

The likely reason for this tolerance is the usual redundancy of protection features: i.e., shielded interconnect circuits combined with 'single-point ground' circuit design.

18.3.7 Configurations of Systems for System Test

The planner of system functional upset tests must consider how best to arrange the tested system (or subsystem) to best allow functional upsets and other responses to be detected.

The two most common options are:

"Open Loop" wherein the system is set up with as much of the electronics, interconnect cables, displays and actuators included so that responses can be observed (and recorded by visual or electronic data collecting means) as would happen in flight. An 'open loop' configuration usually means that the system receives crew input and sensor feedback but *cannot* adjust its outputs based upon sensor feedback. Thus, no feedback links are provided to adjust system operating parameters to compensate for the responses due to the lightning environment. This arrangement has the advantage that the responses can more readily be observed and recorded during the test.

"Closed Loop" wherein feedback links are provided on the test bench to allow the system to respond and correct itself from upset due to the lightning environment. For example, sensor feed-back (e.g., turbine speeds, temperatures, and adjust performance accordingly. This arrangement has the advantage of including performance of upset mitigation software but sometimes has the disadvantage of not easily permitting the upsetting events during the test to be identified and recorded. Diagnostic software and recording hardware have usually to be provided.

Certifying authorities have accepted test plans based on both 'open loop' and 'closed loop' configurations. 'Closed loop' configurations have the benefits of providing natural system filtering (because system reaction times may filter out short perturbations), and instantaneous pass/fail assessment of the overall system. 'Open loop' configuration tests are typically conducted in order to assess perturbations in system data signals and to establish whether they are acceptable (i.e., benign) or not. 'Open loop' configurations have the benefit of facilitating post-test, system evaluations. If the data from an 'open loop' test is re-played with a 'closed loop' software model control law changes can be evaluated without the need for a re-test. The 'closed loop' arrangement involves a more elaborate test setup, but the 'open loop' arrangement usually requires that more parameters be recorded during the tests, so that the assessment of the data becomes a more painstaking process.

Then there is always the question of how much of a system can be included on the test bench in in the test. This topic has been discussed in earlier paragraphs and will not be discussed further here. The principle is to include whatever computers, accessories and interconnecting cables are needed for the system to perform the function that is being tested. For an electronic engine control this is usually the entire system, or sometimes only one channel (of the usual two). For a landing gear control system, which performs three separate functions (Nose wheel steering, braking, and retraction) only the parts needed to perform one function might be tested at once.

These decisions are made based upon system availability, test bench space available, and lightning test equipment capability.

Field Immersion Tests

Most lightning transient problems are caused by electromagnetic field coupling of lightning energy into interconnecting wires. While the injection tests described in the previous paragraphs are appropriate for assessing this interaction, they do not directly check for leakage of electromagnetic fields into the cases (chassis) housing electronic equipment. Field leakage can be checked by immersing equipment in an electromagnetic field simulator. The elements of such a test are shown in Fig. 18.23. Checking for electric field effects involves placing the EUT between two plates between which a voltage is applied of a magnitude sufficient to develop the required electric field. Checking for magnetic field effects, requires circulating a current around the case of a magnitude sufficient to generate the required magnetic field.

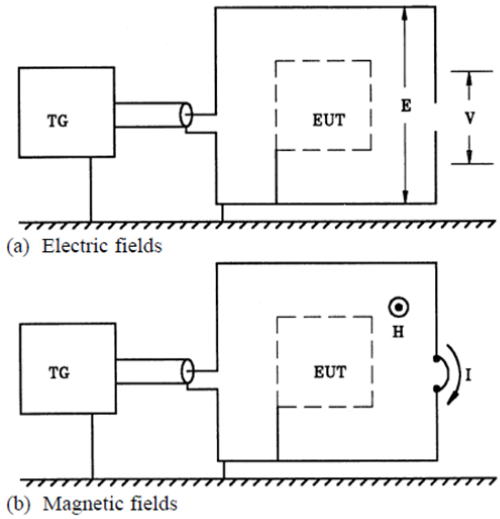

Fig. 18.23 Field immersion.

Some tests require that electric and magnetic fields be developed simultaneously, often with the ratio E/H = 377 ohms, associated with waves propagating in free space. Such tests can be made with strip-line test cells, as illustrated in Fig. 18.24. The test cells can be made large enough to hold several pieces of equipment, along with the necessary interconnecting cables.

'Strip line' test cells are most appropriate for evaluating coupling to conductors in free space and are not widely used to evaluate lightning induced effects inside aircraft, where E/H is, in general, not 377 Ω.

There are no standards for lightning field immersion tests, and they are generally not required for certification of aircraft systems. Occasionally they are used to diagnose in-flight responses which seem to have resulted from direct penetration of lightning electromagnetic fields into non-conducting apertures, such as cockpit equipment displays.

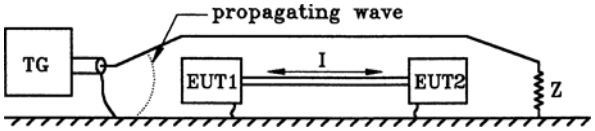

Fig. 18.24 Combined electric and magnetic fields.

18.4 Tests on Circuit Elements

Tests are sometimes necessary to evaluate breakdown voltages and currents of individual circuit elements (such as resistors, capacitors, and electro-mechanical components) or to evaluate interface protection for more complex circuits. Such tests can also be used to study how active circuits respond to various transients. Fig. 18.25 shows some general configurations for circuit element tests, but detailed discussion of the techniques for these tests is beyond the scope of this book.

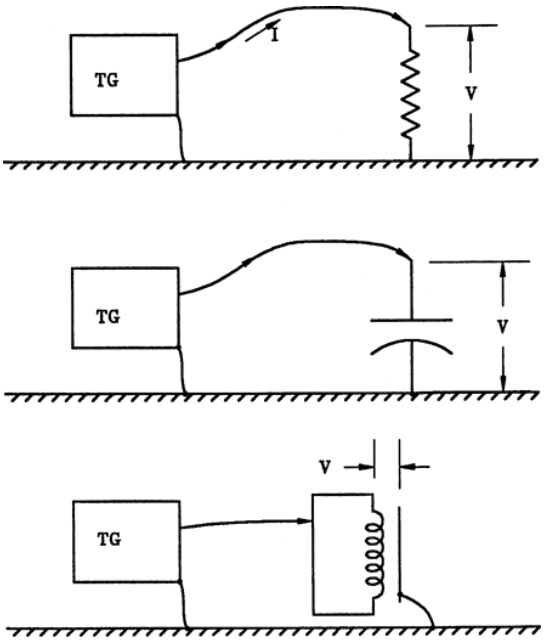

Fig. 18.25 Tests on circuit elements.

18.5 Transient Generators (TGs)

Most TGs used for evaluating induced direct effects employ charged capacitors that are discharged into wave shaping circuits. Much of the technology is basically like that used in the 1940s and 1950s for radar modulators and described in [18.7]. Sometimes complex waveforms can be generated by feeding the signals from waveform synthesizers into power amplifiers. Some generators are designed for only single-shot operation, while others are designed to produce sequences of similar pulses. Very few TGs operate continuously, but almost all operate at power levels that greatly exceed those of normal laboratory signal generators.

18.5.1 Capacitor Discharge Generators

Generators may be designed either for unipolar output with a waveform approximating.

$$V = V_0\left(\varepsilon^{-\alpha t} - \varepsilon^{-\beta t}\right) \qquad (18.2)$$

or for oscillatory output, with a waveform approximating

$$V = V_0\left(\varepsilon^{-\alpha t}\right)\sin\left(2\pi f t\right) \qquad (18.3)$$

Specifications for oscillatory waves sometimes express the waveform as

$$V = V_0\left[\varepsilon^{-\pi f t/Q}\right]\sin\left(2\pi f t\right) \qquad (18.4)$$

where Q governs the rate of decay of the oscillations. Specifications commonly cite values for Q ranging from 6 to 24.

Unipolar Transients: Basic unipolar circuits are shown in Fig. 18.26. Circuit (a) uses series R and C to shape the front of the wave and has a primarily capacitive output impedance circuit (b) uses series L and R to shape the front and has a primarily resistive output impedance. The values of R, C and L are approximately those required to produce the long-duration voltage waveform discussed in §16.7.1. Additional factors governing waveform were discussed in §5.5.4.

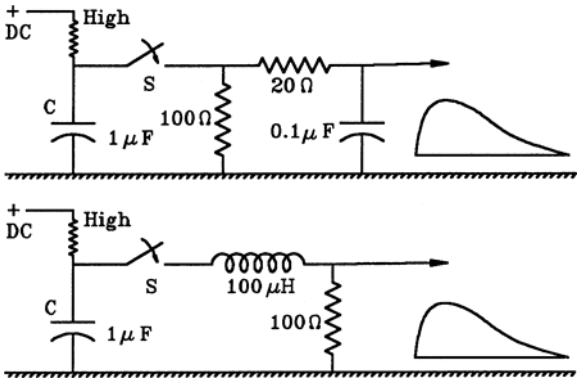

Fig. 18.26 Generators for unipolar transients.
(Element values shown are approximate and should not be used without validation).

Both circuits assume the energy storage capacitor, C, to be connected to a charging power supply through a resistance high enough to prevent the characteristics of the charging supply from effecting the waveform. Both use a series switch, S, to connect C to the wave shaping circuit, producing a positive output for a positive charging voltage. Reversing the positions of C and S (Fig. 18.27) results in a negative output for a positive input.

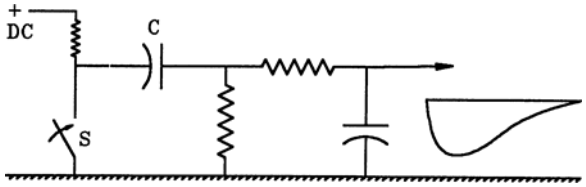

Fig. 18.27 Grounded switch configuration

Oscillatory Transient: Some basic oscillatory generators and their output waveforms are shown in Fig. 18.28. The frequency of oscillation is related to the capacitance and inductance of the circuit according to Eq. 18.5.

$$f = \frac{1}{2\pi\sqrt{LC}} \qquad (18.5)$$

The decrement of the wave may be controlled either by adding series or parallel resistance or by the residual losses of the circuit and the load to which the generator is connected. Most commonly the intrinsic losses are enough to give $Q \approx 6$ and high enough to make it difficult to achieve $Q = 24$.

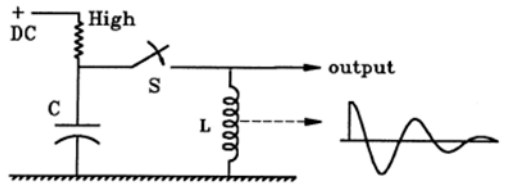

(a) Cosine front

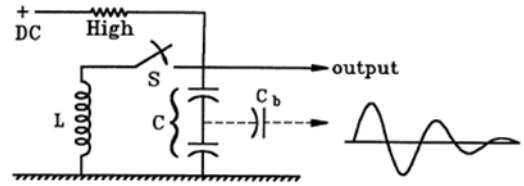

(b) Sine front

Fig. 18.28 Oscillatory TGs.

Taking the output from only a portion of *L* results in a lower output impedance and makes the effect of load resistance less noticeable but is achieved at the cost of reduced output amplitude.

The intrinsic output of Fig. 18.28(a) is a cosine wave, not the sine wave commonly cited in specifications. A sinusoidal output can be obtained by taking the output from the energy storage capacitor, Fig. 18.28(b), using a blocking capacitor C_b, to avoid coupling the DC charging voltage to the output circuit.

Questions regarding waveforms: Specifications for oscillatory waveforms commonly call for damped sine waves (Eq. 18.3 or 18.4), but actually obtaining a true sinusoidal front can be difficult. Sometimes, second order effects come into play, particularly with high frequency generators, and result in waveforms whose highest amplitudes occur not on the initial half-cycle, but on a subsequent half-cycle.

A common deficiency of oscillatory waveform specifications is that they do not give tolerances on allowable waveform distortion. From an engineering viewpoint, the most important parameters are probably:

1. The minimum peak amplitude needed to sufficiently stress the components under test.
2. The optimum decrement of the oscillation, over its first few cycles, so that stress is sustained for a sufficient time.
3. The frequency (or frequencies) most likely to excite internal resonances.

Those preparing specifications or requiring tests should ask the following questions:

1. Does the exact shape of the first quarter-cycle make any practical engineering difference?
2. Does the exact shape of the first few cycles make any practical engineering difference?
3. Does a test waveform with a front that approximates a cosine wave satisfy a test requirement that calls for a sine wave defined by Eq. 18.3?
4. If an oscillatory test waveform achieves its maximum amplitude after the first half-cycle, does this make any practical, engineering difference?

18.5.2 Switches for Generators

Several types of switches can be used for capacitor discharge generators. The best discussions of various types of switches are apt to be found in the older literature, such as [18.6]. In oscillatory circuits, losses associated with switches are one of the major factors governing the *Q* of the circuit.

Spark gaps: Higher power generators (i.e., those that operate at voltages greater than 35 kV) commonly use spark gaps as switches. These may be triggered gaps, fired by applying a pulse to a lower voltage, secondary 'trigger' gap, self-firing gaps, that discharge when the gap voltage exceeds the gap breakdown strength, or mechanically closed gaps, that move closer to one-another until sparkover takes place.

Gaps in air are the simplest to build but, with high power generators, air gaps may produce enough audible noise to be disturbing to those nearby. Commercially available triggered gaps are usually contained in enclosures, which reduce the noise somewhat. Spark gaps also emit broadband radiation which can interfere with operation of instrumentation and even with system performance (it should not be forgotten that a lightning strike is also an emitter of significant radio frequency (RF) energy).

Mechanically closed switches: The easiest method of switching is simply to bring two contacts together mechanically, until they are close enough for a spark to form between the contacts. When used in high-power generators, the contacts of these switches may burn and become roughened. However, since they are operated only intermittently, it is practical to maintain these switches by periodically cleaning them with sandpaper or a file. Immersing contacts in an insulating oil can reduce the arcing that takes place as the contacts close.

Mercury switches: Switches with mercury-wetted contacts are useful for low power generators, operating at a few hundred volts. The advantage of mercury switches is that the contacts switch cleanly, without bouncing.

Hydrogen thyratrons is a high peak power electrical switch which uses hydrogen gas as the switching medium. The switching action is achieved by a transfer from the insulating properties of neutral gas to the conducting properties of ionized gas. Tubes such as the 5C22, are suitable for operation up to about 10 - 15 kV and peak currents of several hundred amperes. The miniature 2D21 is suitable up to about 1 000 V and peak currents of several tens of amperes. Both devices switch in about 20 ns. When used in an oscillatory generator, a thyratron must be installed in parallel with a free-wheeling diode (see Fig. 18.29).

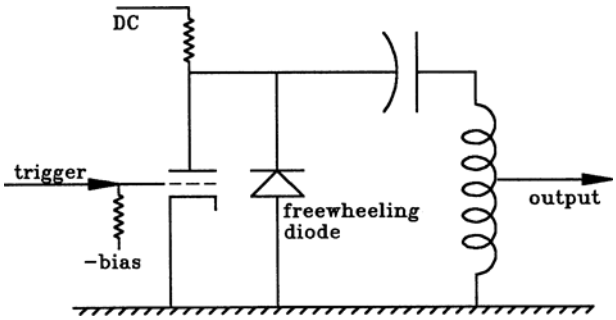

Fig. 18.29 Thyratron switch with free-wheeling diode.

Thyristors: Low power, sensitive gate thyristors are suitable for charging voltages up to about 1 000 V and discharge currents of several tens of amperes. For use at higher charging voltages, multiple thyristors may be operated in series. The switching time of a thyristor can be on the order of 100 ns, although care must be taken to provide sufficient gate drive. Free-wheeling diodes should be installed in parallel with thyristors in oscillatory circuits.

18.5.3 Generators Using Power Amplifiers

Some waveforms are difficult to produce using capacitive discharge circuits, particularly the higher frequency oscillatory waveforms. Capacitors must be small to obtain a high frequency, and small capacitors store little energy. Also, switches may not change state fast enough to support high frequency applications and circuit losses tend to increase with frequency, making it impossible to generate transients that ring well (i.e., have a high Q). Some of these problems can be overcome by generating the waveforms at low levels and using power amplifiers to step up the signal before it is coupled to the circuit under test. Amplifier-aided circuits are also useful for generating square waves or complex waveforms that differ greatly from the double exponential or damped oscillatory waveforms most naturally produced by simple circuits.

Waveform generation

Fig. 18.30 illustrates the two basic approaches to amplifier-aided waveform generation: (a) involves direct generation of the desired waveform, followed by linear amplification; (b) involves modulation of a sinusoidal input, followed by amplification. Waveforms for (a) may be generated by switching *R*, *L* and *C* circuits or by digital synthesis with arbitrary waveform generators. Modulation may be accomplished either by direct amplitude modulation or by multiplication of a sinusoidal wave by an appropriately chosen modulating pulse.

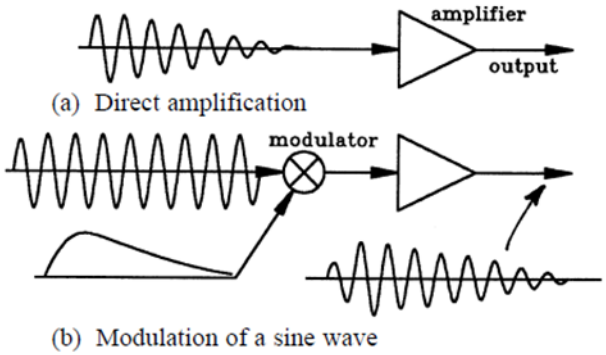

Fig. 18.30 Transient generation with amplifiers.

Amplifiers

Most induced effects testing calls for high voltage and high current output from the amplifier. While average power levels may be low, the peak power levels may be several tens of kilowatts. Amplifiers generally use high voltage vacuum tubes of the type used for broadcast transmitters. Vacuum tube amplifiers are well adapted to delivering high voltages, but many designs are not capable of delivering high short-circuit currents.

18.5.4 Multiple Pulse Generators

System tests require injection of a groups of pulses to simulate the effects of the MS and MB portions of the lightning environment. Sometimes these multiple pulses can be generated using low impedance charging networks that permit a single energy storage capacitor to be charged and discharged rapidly. This may be difficult to do, particularly at high power levels, since instantaneous charging currents of hundreds or thousands of amperes may be drawn from the power mains feeding the transient generator.

An alternative technique is to use many energy storage capacitors, charge them slowly, and then discharge them one by one into the circuit under test.

The transients in the MS and MB waveform sets should be applied randomly within the minimum and maximum separation times defined for them in [18.2]. This may require that 14 pulse generators be pre-charged and discharged by a random number generator, especially for the higher amplitude transients specified for some MS tests. MB transients can sometimes be produced repeatedly by a signal a generator and amplifier or by charging and discharging a single capacitor.

18.6 Injection Transformers

One of the common methods of injecting test transients into cables for system functional upset testing involves the use of injection transformers. Two basic modes of injection transformer operation are shown in Fig. 18.31: (a) involves magnetically injecting current into a short-circuited conductor and (b) involves magnetically injecting voltage into an open-circuited wire. In practice, the short- circuited conductor is usually an overall cable shield grounded at both ends.

The operation of an injection transformer follows the same physical laws that govern any magnetic circuit, but the normal mode of operation of an injection transformer differs in two respects from that normally associated with transformers. First, since the purpose of an injection transformer is to inject transients into interconnecting wire bundles, those wire bundles function as the secondary winding of the transformer. Thus, there is a practical limit to the number of secondary turns that can be wound around the core.

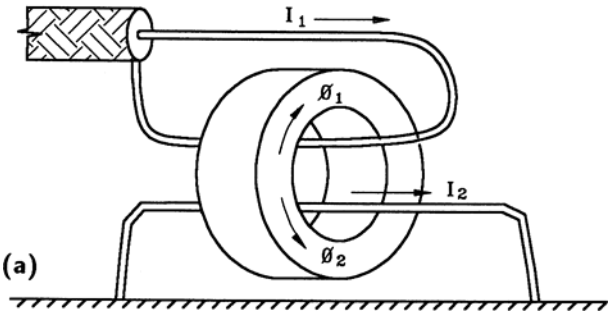

(a) Injection of current

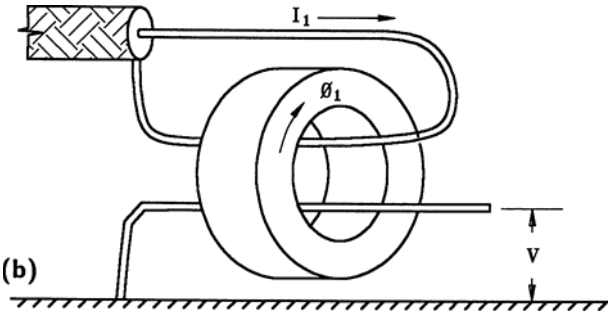

(b) Injection of voltage

Fig. 18.31 Transformer injection of transients.

Most magnetic injection configurations involve passing the bundle through the core only once or, at most, a very few times (unlike conventional transformers which employ windings of many turns). Second, the transformer is generally energized with a driving current, unlike conventional transformers, which are usually energized by voltage sources. A typical circuit is in Fig. 18.32.

Each current-carrying conductor that passes through the core sets up a magnetic flux. When injecting current into a short-circuited conductor, the induced current tends to have the same waveform as the driving current, so that the two components of flux tend to cancel, leaving a small net magnetic flux in the core. However, when injecting voltage into an open-circuited conductor, there is no canceling flux and the amount of voltage that can be induced is limited by the amount of flux that can be supported by the core.

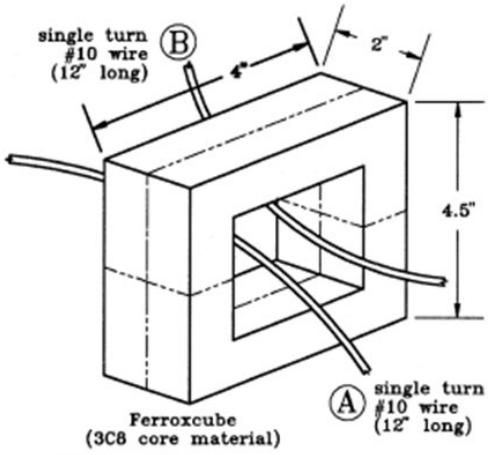

(a) Core dimensions

$L_P = L_S = 8.3\ \mu H$
$L_A = 28\ \mu H$
$L_B = 0.3\ \mu H$
$M = 6.93\ \mu H$
$K = 0.83$
$L_P(1-K) = L_{P_s}(1-K) = 1.38\ \mu H$
$KL_P = 6.93\ \mu H$

(b) Measured and derived quantities

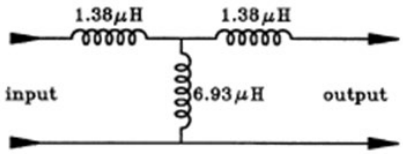

(c) Equivalent circuit

Fig. 18.32 Equivalent circuit of a typical transformer.

18.6.1 Basic Principles of Magnetic Circuits

An elementary magnetic circuit is shown in Fig. 18.33. The constants that define the core include the length of its magnetic path, l, its cross sectional area, A, and its relative permeability, μ_r. If the core has a large cross section, the magnetic path length is the average length measured around its center.

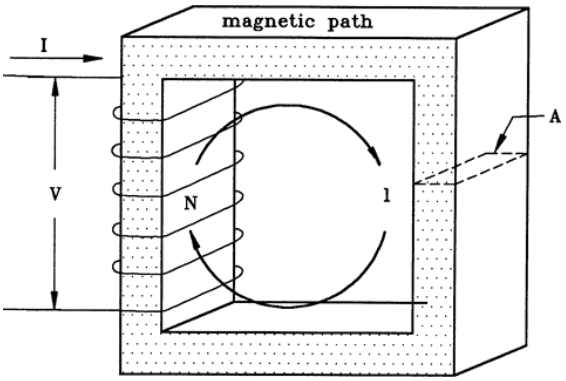

Fig. 18.33 Factors governing magnetic circuits.

Total magnetizing force: The total magnetizing force around the length of the core (MMF) is expressed in ampere-turns, NI or in gilberts, 0.4 NI. If there is an air gap in the magnetic circuit, a large portion of the total magnetizing force may be needed to force magnetic flux across the gap, even though the length of the gap is very small compared to the total magnetic path length.

Magnetizing force per unit length: The magnetizing force acting on the magnetic material is

$$H = \frac{NI}{L} \quad \text{Gilberts/cm} \qquad (18.6)$$

This quantity may be also expressed in ampere-turns per meter, ampere-turns per centimeter or in ampere-turns per inch.

In material specifications, it is commonly expressed in oersteds or gilberts per centimeter.

$$H_{\text{gilberts/cm}} = \frac{0.4\,\pi NI}{l} \qquad (18.7)$$

Total magnetic flux: Total magnetic flux may be expressed in webers, lines (maxwells) or kilolines.

$$1 \text{ weber} = 10^8 \text{ lines} = 10^5 \text{ kilolines} \qquad (18.8)$$

Flux density: Flux density may be expressed in teslas (webers per square meter), gauss (or lines per square centimeter) or in lines (or kilolines) per square inch. In round numbers, a core made of grain-oriented silicon steel can support a maximum flux density of about 100 kilolines per square inch (or 16 000 gauss). A ferrite core can sustain a maximum flux density of about 4 000 gauss.

Relations between units:

1 gilbert = 1.257 ampere-turns
1 oersted = 1 gilbert/cm
1 oersted = 0.495 ampere-turns/in
1 oersted = 1.257 x 10^{-2} ampere-turns/m
1 tesla = 1 weber per meter^2
1 tesla = 10^4 gauss
1 tesla = 1.550 x 10^{-5} lines/in^2
1 tesla = 1.550 x 10^{-2} kilolines/in^2
1 kiloline/in^2 = 1.55 gauss

Voltage vs. flux: The relations between voltage, V, and flux, ϕ, are

$$\Delta\phi = \frac{1}{N}\int V\,dt \quad webers \qquad (18.9)$$

$$\Delta\Phi = \frac{10^8}{N}\int V\,dt \quad lines \qquad (18.10)$$

Thus, it requires a given net change in magnetic flux to develop a transient voltage of a given volt-second product in a transformer. If the core cannot sustain the requisite flux, the voltage cannot be generated. For example, a rectangular pulse of voltage (Fig. 18.34(a)) with an amplitude of 100 volts and a duration of 10 μs would have a volt-second product of 10^{-3}. Developing this voltage on a wire that passes once through an injection transformer would require the flux in the core to change by 10^5 lines, or 100 kilolines. If the core were of a ferrite material with minimal residual flux from previous pulses, the cross-sectional area would have to be about 25 square centimeters.

For a double exponential waveform defined as

$$V = V\left[\varepsilon^{-\alpha t} - \varepsilon^{-\beta t}\right] \qquad (18.11)$$

the total volt-second product is

$$\int_0^\infty V = V_0\left[\frac{1}{\alpha} - \frac{1}{\beta}\right] \qquad (18.12)$$

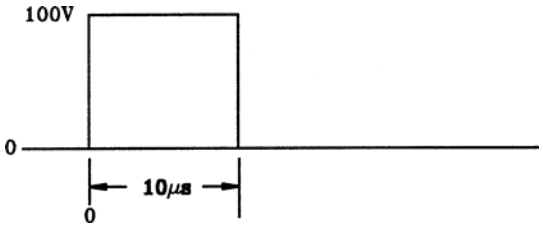

(a) $V \cdot t = 10^{-3}$ volt-seconds

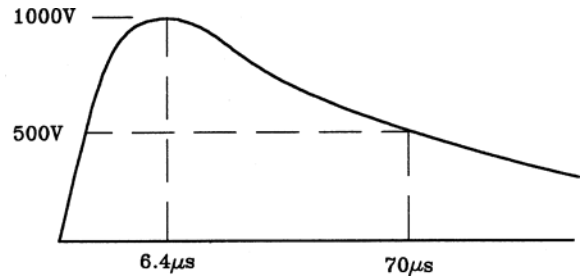

(b) $V \cdot t = 9.47 \times 10^{-2}$ volt-seconds

Fig. 18.34 Representative transient voltages.

To develop, on a single turn, a voltage pulse with a peak amplitude of 1 000 V, a front time of 6.4 μs and a time to half-value of 69 μs ($V_0 = 1\ 093$, $\alpha = 11\ 354$, $\beta = 647\ 265$, volt-second product of 0.0947) would require the flux to change by 9 466 kilolines. This would require a ferrite core with a cross-sectional area of about 2 400 square centimeters (350 square inches); a large core indeed!

Voltage vs. current: A given magnetic flux in a transformer core is associated with a given magnetizing force or, for a fixed number of turns, a given magnetizing current. Therefore, to develop a pulse of voltage, (Fig. 18.35(a)) with a certain volt-second product, the current must change from an initial value (zero in Fig. 18.35(b)) to a final value. Which comes first, voltage or current, is a matter of semantics. One could say that a magnetic core is 'carried to saturation' by excessive magnetizing current, but it is generally more helpful to say that the core has been carried to saturation by an excessive product of voltage and time.

Since most exciting current pulses applied to injection transformers eventually decay back to zero, it follows that a collapsing current is associated with a voltage of polarity opposite to that which was associated with the rise of current. Fig. 18.36 illustrates this point. The voltage pulse is under-damped so that the positive (A_1) and negative (A_2) lobes have equal volt-second products.

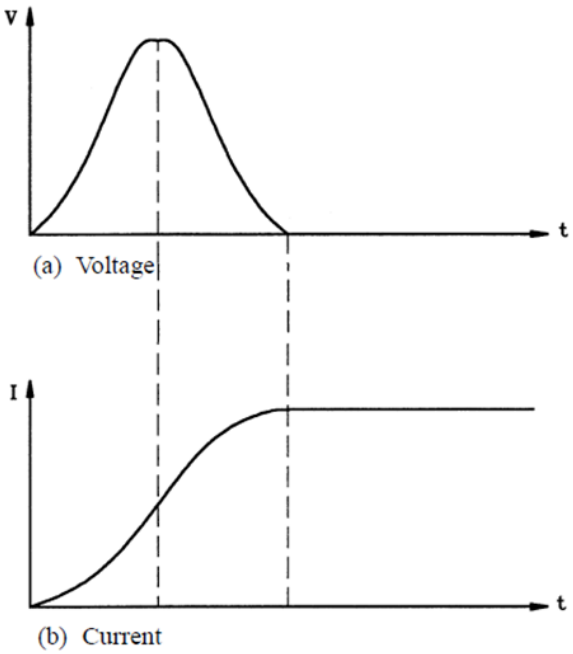

Fig. 18.35 Current as the integral of voltage.

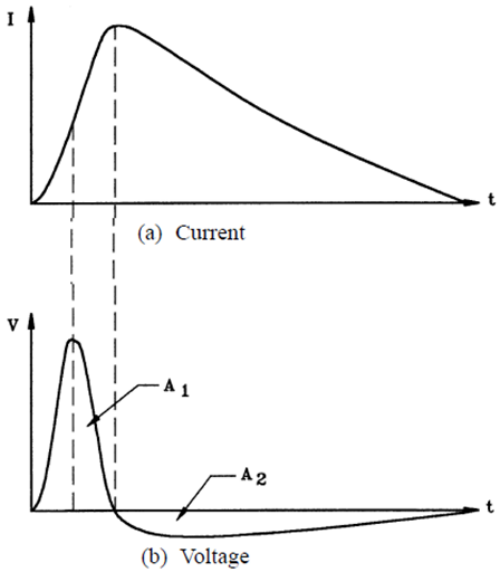

Fig. 18.36 Voltage as the derivative of current.

In other words, a double exponential current pulse passed through the primary of a pulse injection transformer cannot induce a unidirectional (UD) voltage pulse of the same waveform in a secondary winding.

B-H Loops: The magnetic characteristics of a magnetic material can be defined by its *B-H* loop (see Fig. 18.37). B and H are, respectively, flux per unit cross-sectional area and magnetizing force per unit length of path. For a transformer core of specific dimensions, the loop could be defined in terms of ϕ and NI.

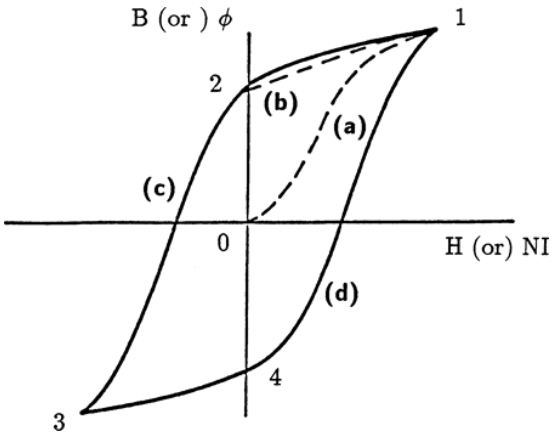

Fig. 18.37 B - H loop.

For an initially unmagnetized core, a current pulse might carry the magnetic state along path (a) from point 0 to point 1. Removing the current would allow the magnetic state to follow path (b) to point 2. Assuming that point 1 represents a flux density of 16 kilolines per square centimeter (16 000 gauss), a core cross-sectional area of 592 cm^2 (92 in^2) would be needed to support the 1 000 V, double exponential pulse. In the context of induced effects testing, that represents a very large transformer core and explains why it is difficult to use transformer coupling techniques to develop high amplitude, long duration voltages on open-circuited wires or cables.

Multiple pulses: The problems of core size are compounded when multiple pulses are involved. If the first pulse carried the core along path (a) to point 1, a second pulse of the same magnitude and polarity would have to carry the flux along path (b) to a point far higher than point 1. The core would become saturated, the magnetizing current would become limited by the characteristics of the pulse generator, and the desired voltage pulse would never be developed.

Full use of a transformer core for injecting multiple pulses would require pulses of opposite polarity and volt-second product, though not necessarily of equal magnitude or waveform. The first pulse in a series would carry the flux to point 1, the second would carry it to point 3, and the third would again carry it to point 1.

Measurement of B-H loops: B-H loops may be measured by exciting N_1 turns on a primary winding and allowing voltage to be induced in a second winding of N_2 turns, as shown in Fig. 18.38. A signal proportional to I (and hence to N_1I) is applied to the horizontal input of an oscilloscope and a signal proportional to the integral of e_1 applied to the vertical input.

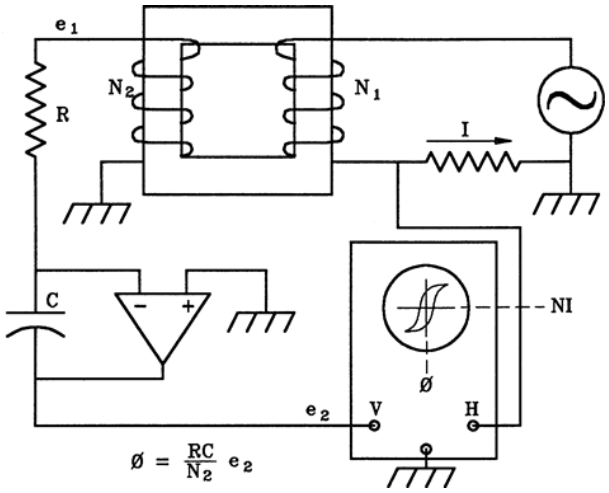

Fig. 18.38 Measurement of B-H loop.

Examples of B-H loops: Figs. 18.39 and 18.40 show examples of B-H loops as measured with the above technique. Fig. 18.39 refers to an un-gapped toroidal core wound from grain-oriented silicon steel of 0.36 mm (0.014 in) thickness. Fig. 18.40 refers to a core made from U-shaped ferrite blocks joined with no intentional air gap. The ferrite core provides a more linear B-H characteristic than the steel core and has lower residual flux at zero magnetizing force. Other things being equal, a ferrite core is better than a steel core at transforming multiple pulses.

Un-gapped steel cores tend to have large B-H loops and a large remnant fluxes. A gap in the core reduces the remnant flux and makes the B-H loop more like that of Fig. 18.40. Some ferrite cores have a large remnant flux and some do not; it depends on the type of core material. Powdered iron cores have a small remnant flux.

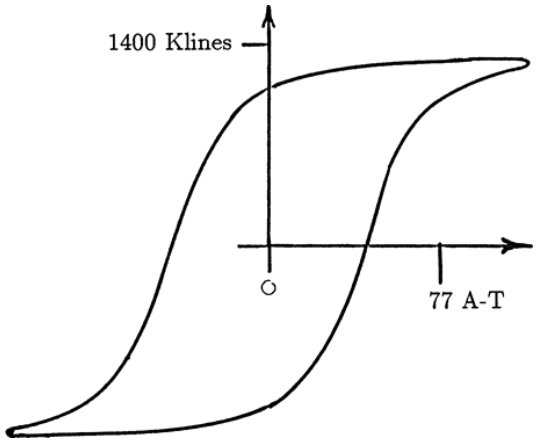

Fig. 18.39 B-H loop of an un-gapped steel core.

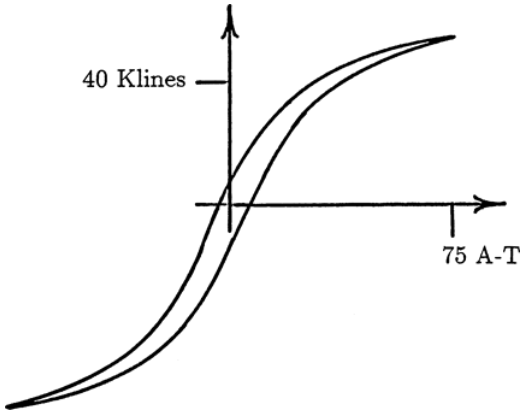

Fig. 18.40 B-H loop of a gapped, ferrite core.

Saturation effects when injecting current: In an ideal situation, the induced current would be equal to the injected current (equal turns assumed) and have the same waveform. Under these ideal conditions there would be no limit to the amount of current that could be injected by a core.

In practice, two factors, illustrated in Fig. 18.41, limit the amount of current that may be transformed. One of these is the resistance of the conductor upon which current is induced. Current through that resistance develops a voltage that increases the flux in the core, even though the induced voltage may be distributed along the conductor and may not be measurable. (Since long conductors have more resistance than short conductors, it is harder to induce current on long conductors than on short ones). The other factor is that the magnitude of the induced current is less, by virtue of leakage inductance, than the inducing current, irrespective of the resistance of the conductor. The net result is that I_2 is always less than I_1, and eventually decays to zero. For sufficient I_1, the net flux in the core can increase until the core is saturated, at which point transformer action ceases.

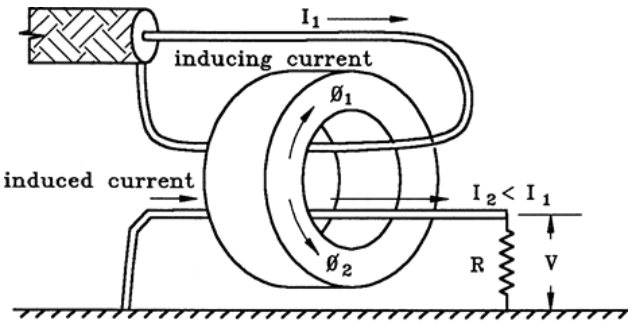

Fig. 18.41 Effect of conductor resistance on core flux.

18.6.2 Equivalent Circuits of Injection Transformers

Some of the parameters affecting the response of a complete current injection system are illustrated in Fig. 18.42.

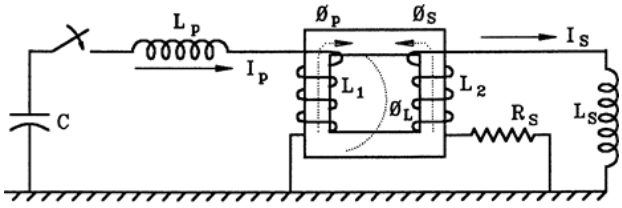

Fig. 18.42 Factors affecting performance of an injection transformer.

These parameters include:

1. The capacitance of the storage capacitor.
2. The inductance of the leads connecting the storage capacitor to the transformer.
3. The primary, secondary, and leakage inductances of the transformer.
4. The inductance and resistance of the conductor under test.

The characteristics of the injection transformer (item 3, above) are among the most important parameters. They effect the primary and secondary inductances, the flux in the transformer core and the proportion of flux produced by current in the primary that links the secondary winding. The difference between these two fluxes is the leakage flux, and it is the leakage flux that prevents the secondary current from being as large as the primary current.

Determining inductance: For a given transformer, the primary and secondary magnetizing inductances may either be measured on an inductance bridge or be determined by discharging a known capacitor through the winding and observing the frequency of oscillation. The magnetizing inductance can also be determined from the average slope of the B-H curve:

$$H = \frac{NI}{l} \qquad (18.13)$$

Mutual inductance, which determines the degree of coupling between windings, can be determined by connecting the primary and secondary windings in series, first so that the two magnetic fields set up are in the same direction (series aiding) and then, so the magnetic fields are in opposite directions (series bucking), as shown in Fig. 18.43(a).

Equivalent circuit of transformer: Knowing the primary, secondary, and mutual inductances, one can produce an equivalent circuit of an injection transformer. An example of such a circuit is the Pi circuit shown in Fig. 18.43(b).

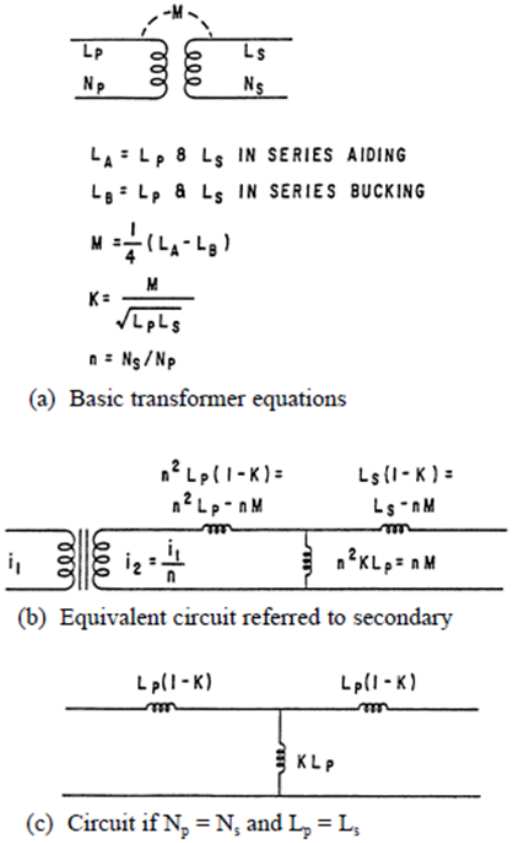

Fig. 18.43 Development of equivalent circuits.

If the number of turns on the primary winding is equal to the number on the secondary winding (the usual case), the circuit can be simplified as shown in Fig. 18.43(c). The basic factor governing the current that can be induced is the ratio of the series leakage inductance to the shunt magnetizing inductance. Leakage inductance is not particularly affected by saturation of the transformer, but saturation does affect the magnetizing inductance. When the core saturates, the shunt impedance drops to a low value and diverts current from the conductor under test.

Complete equivalent circuit: A complete equivalent circuit (Fig. 18.44) includes the parameters of the TG and the conductor under test, and possibly the stray capacitance of the injection transformer.

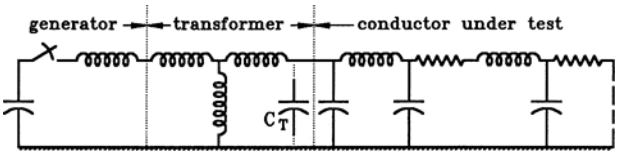

Fig. 18.44 Complete equivalent circuit of a conductor under test.

Effects of multiple turns: Injection transformers are not constrained to be operated with equal numbers of turns on the two windings. For instance, if the conductor under test is looped through the core several times, as illustrated in Fig. 18.45, a given excitation on the transformer produces less short circuit current, more open circuit voltage, and a decrease in the frequency of the natural oscillatory mode of the cable under test. If there are more turns on the primary, the result is more short circuit current, less open circuit voltage, and a decrease in the oscillatory frequency of the pulse generator. The rise time of the current and voltage pulses also increases.

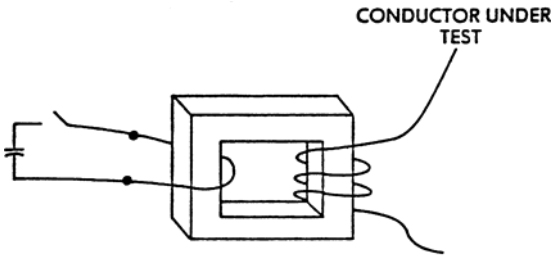

Fig. 18.45 Effect of more turns on secondary.

- Less short circuit current.

- Longer current pulse rise time.

- More open circuit voltage.

- A decrease in the frequency of the natural oscillatory mode of the cable under test.

18.7 Measurements

System testing involves high frequencies, high voltage, and high current. A few notes on measurement techniques follow. Additional notes on measurement techniques are given in [18.8].

Oscilloscopes: Oscilloscopes used should have bandwidths ranging up to of 100 MHz or greater. The oscilloscopes should also be well shielded against interference from the test TGs and from the circuit under test. This often requires that they be housed in a shielding enclosure and physically as far from the test setup as possible.

Voltage probes: Conventional, high-impedance voltage probes are somewhat susceptible to noise voltages and cannot tolerate input voltages higher than about 1 500 V. Since the impedances of the circuits under test are generally low, suitable voltage probes can be made from carbon resistors (Fig. 18.46). Wire wound resistors should be avoided because of their excessive inductance. Total resistances of several thousands of ohms are satisfactory and can be distributed among several resistors, if the voltage on individual, 1-watt carbon resistors is limited to about 1 000 volts. Instantaneous power dissipated in these resistors may be high, but the average power is low.

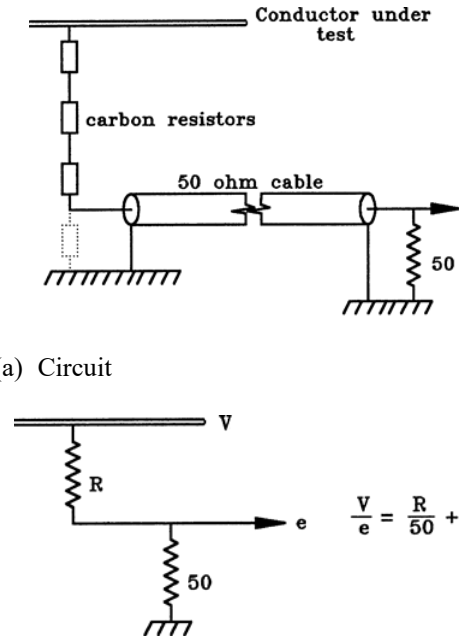

Fig. 18.46 Resistive divider for measurement of voltage.

Current transformers: Current measurements are usually made with a current transformer. Current transformers that are well shielded and that have wide bandwidths are commercially available. However, suitable current transformers for many purposes can also be custom wound on toroidal magnetic cores, as shown in Fig. 18.47. The secondary winding of a current transformer should be uniformly wound around the core and the conductor upon which measurements are made should be kept near the center of the core. Transformers can also be made using split cores, which are easier to place around conductors but have poorer low frequency response. A good discussion of the factors affecting the responses of current transformers appears in [18.9].

Low frequency response: An equivalent circuit of a current transformer is shown in Fig. 18.48(a). Primary current induces a voltage in the windings proportional to the derivative of the current. Because of the inductance, L, of the transformer windings, the current applied to the viewing resistor, R, is initially proportional to the integral of the voltage, and hence to the input current.

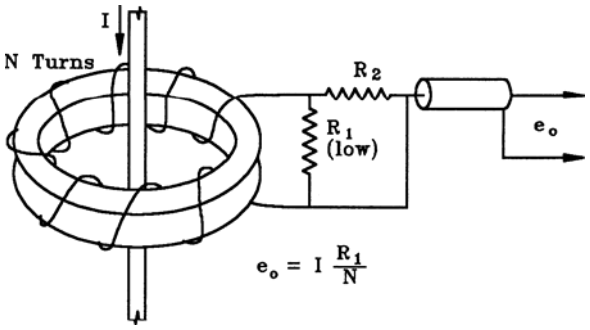

Fig. 18.47 Current transformer.

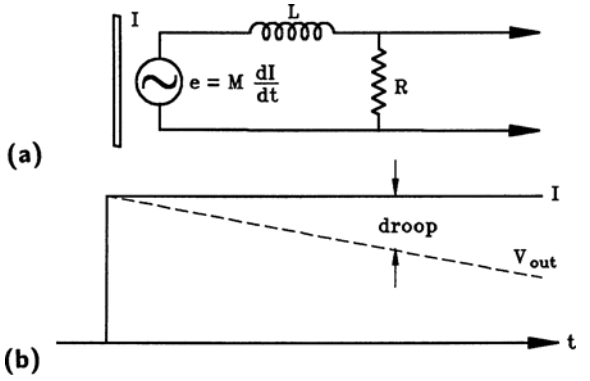

Fig. 18.48 'Droop' in a current transformer.

The resistance, however, prevents perfect integration, so that the output voltage gradually departs from the true waveform of the input current. Transformer specifications list this departure as the 'droop' of the current transformer, illustrated in Fig. 18.48(b). Care must be taken that this 'droop' is not excessive for the pulse waveform being observed. Split core transformers are prone to excessive 'droop'.

Rogowski coils: Rogowski coils can be used when the durations and amplitudes of the pulses exceed that which can be measured by conventional current transformers. A Rogowski coil (Fig. 18.49) consists of a helical coil of wire surrounding the current being measured.

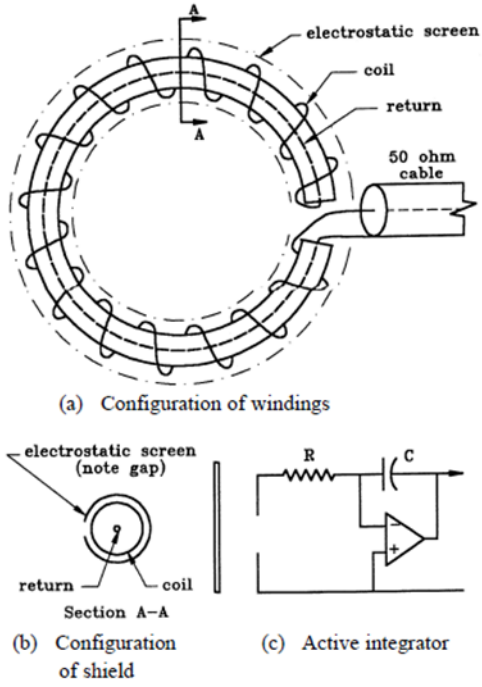

Fig. 18.49 Rogowski coil.

The output from a Rogowski coil is proportional to the derivative of current and must be integrated to yield the true waveform. Passive RC integrators are sometimes suitable, particularly for rapidly changing transients, but in general, active integrators, Fig. 18.49 (c), are better.

Rogowski coils are characterized by a mutual inductance, M, related to the dimensions of the coil.

$$M = n\left(\frac{\pi d}{a}\right)^2 \quad H \qquad (18.14)$$

where

n = turns per unit length
a = radius of coil
d = diameter of coil form

The output of a given Rogowski coil having an integrator time constant of RC would be:

$$e_o = \frac{M}{RC} I \qquad (18.15)$$

Resistive shunts: Resistive shunts, particularly those having a coaxial geometry, are useful for measuring the short circuit current from a generator and for calibrating current transformers and Rogowski coils. However, resistive shunts can seldom be used for measuring the current induced in conductors under test, because they must usually be operated with one terminal connected to ground.

18.8 Precautions Regarding Support Equipment

Most tests require the equipment or system under test to be supported (i.e., powered) and monitored by equipment that is not normally installed in the aircraft. Experience has shown that some of the problems encountered in conducting system functional upset tests involve the support equipment. It has also been found that some supposed 'failures' of the EUT have really been caused by the support equipment. These problems can arise either from malfunction of the support and monitoring equipment or because the leads to that equipment provide extraneous coupling paths into the EUT.

The support equipment and its connecting leads should be as well protected against lightning induced effects as the equipment being tested. As a minimum, all leads connecting the support equipment to the EUT should be shielded. Often, it is appropriate to use copper tubing for these shields. Optical isolation devices are appropriate where monitoring equipment must be connected to internal circuits of the EUT. Also, the monitoring equipment should be as far from the EUT as possible, to minimize direct radiation from the test circuit and EUT into the monitoring equipment.

18.9 Safety

Equipment and system testing, particularly at high power levels, involves the use of test equipment that operates at lethal voltages. Safety precautions are essential and should be addressed in test plans or laboratory procedures. At minimum, these precautions should include the following:

1. Restrict access to the test area to all personnel except those operating the test equipment.

2. Assure that all people that are assigned to set up and operate the tested system and equipment and the lightning TGs are trained in setting up the equipment and generators and in the operation of same.

3. Provide all capacitor banks with grounding sticks and ground dump switches. Never touch a capacitor until it has been verified that the grounding stick is in place, or the switch is closed.

4. Consider placing all high voltage equipment into a test cage fitted with interlocks that prevent the equipment from being energized when access doors are open.

5. Ground all shields on measurement leads and support equipment leads.

6. If a test might cause an item to explode or shatter, use barriers to confine flying fragments to the test area.

References

18.1 *Environmental Conditions and Test Procedures for Airborne Equipment*, RTCA DO 160 Section 22/ EUROCAE ED 14 Section 22, Washington DC 1997 and Paris.

18.2 *Aircraft Lightning Test Methods* SAE ARP 5416A, 1 July 2013.

18.3 Aircraft Lightning Test Methods EUROCAE ED 105, 1 July 2013.

18.4 *Aircraft Electrical and Electronic System Lightning Protection* FAA AC20-136B, 7 September 2011.

18.5 J. A. Plumer, "A Significant Error in Sensing of Limit Voltages in Cable Bundle Tests with the Cable Induction Method of RTCA DO160/EUROCAE ED 14 Section 22 and a Proposal to Correct this Error" International Conference on Lightning and Static Electricity, 2007.

18.6 *Aircraft Lightning Environment and Related Test Waveforms,* SAE ARP 5412/EUROCAE ED 84, SAE International, Warrendale, PA, 1999 and EUROCAE, Paris, 1997.

18.7 *Pulse Generators*, E. D. Glasoe and J. V. Lebacqz, McGraw-Hill, New York, 1948.

18.8 *High-Voltage Measurement Techniques*, A. J. Schwab, The M.I.T. Press, Cambridge, MA. and London, England, 1972.

18.9 J. M. Anderson, "Wide Frequency Range Current Transformers," *Review of Scientific Instruments*, Vol. 42, No. 7, July 1971, pp. 915-926.